DEVONIAN REEF COMPLEXES
OF THE CANNING BASIN, WESTERN AUSTRALIA

Geological Survey of Western Australia
Bulletin 145

Phillip E Playford, Roger M Hocking and Anthony E Cockbain



Government of **Western Australia**
Department of **Mines and Petroleum**

Geological Survey of
Western Australia

DEVONIAN REEF COMPLEXES
OF THE CANNING BASIN, WESTERN AUSTRALIA

Geological Survey of Western Australia
Bulletin 145

Phillip E Playford, Roger M Hocking, and Anthony E Cockbain



Government of Western Australia
Department of Mines and Petroleum

Geological Survey of
Western Australia

Government of Western Australia
Department of Mines and Petroleum

BULLETIN 145

DEVONIAN REEF COMPLEXES OF THE CANNING BASIN, WESTERN AUSTRALIA

by
Phillip E Playford, Roger M Hocking, and Anthony E Cockbain

Geological Survey of Western Australia

MINISTER FOR MINES AND PETROLEUM
Hon. Norman Moore MLC

DIRECTOR GENERAL, DEPARTMENT OF MINES AND PETROLEUM
Richard Sellers

EXECUTIVE DIRECTOR, GEOLOGICAL SURVEY OF WESTERN AUSTRALIA
Tim Griffin

REFERENCE
The recommended reference for this publication is:
Playford, P E, Hocking, R M and Cockbain, A E 2009, Devonian reef complexes of the Canning Basin, Western Australia: Geological Survey of Western Australia, Bulletin 145, 444p.

National Library of Australia
Cataloguing-in-publication entry

Playford, Phillip E (Phillip Elliott)
Devonian reef complexes of the Canning Basin, Western Australia / P E Playford, R M Hocking, A E Cockbain

Other authors/contributions:
Hocking R M (Roger Malcolm)
Cockbain, A E (Anthony Edward)
Geological Survey of Western Australia

Bibliography.
Includes index.
ISBN 978-1-74168-232-8 (PDF); 978-1-74168-233-5 (Print)

1. Gelogy, Stratigraphic — Devonian
2. Geology — Western Australia — Canning Basin
I. Geological Survey of Western Australia.
II. Bulletin (Geological Survey of Western Australia); 145.

551.74

ISSN 0508–4741

Grid references in this publication refer to the Australian Geodetic Datum (ADG84). Locations mentioned in the text are referenced using Australian Map Grid (AMG) coordinates, Zones 51 and 52, because maps accompanying the Bulletin use that datum. All locations are quoted to at least the nearest 100 m.

Copy editor: I R Nowak
Cartography: S N Dowsett and M Jones
Desktop publishing: K S Noonan
Printed by Quality Press, Perth, Western Australia

Published 2009 by Geological Survey of Western Australia

Further details of geological publications and maps produced by the Geological Survey of Western Australia are available from:
Information Centre
Department of Mines and Petroleum
100 Plain Street
EAST PERTH, WESTERN AUSTRALIA 6004
Telephone: +61 8 9222 3459 Facsimile: +61 8 9222 3444
www.dmp.wa.gov.au/GSWApublications

Book front cover: Aerial view, looking south, towards the Classic Face at Windjana Gorge.

Book back cover: Aerial view of the Napier Range reef complex, looking northwest from Windjana Gorge. The front of the range, winding on into the distance, is the Late Devonian reef front.

Book frontispiece: Polished slab of reef limestone from the Classic Face at Windjana Gorge, showing a reef framework of the stromatoporoid *Stachyodes* and the encrusting microbe *Renalcis*, with large voids between them filled with red peloidal limestone and sparry calcite. Width of field of view 24 cm.

Box front cover: Panoramic view of the Classic Face at Windjana Gorge, showing flat-bedded back-reef and reef-flat limestones on the right, passing into massive reef-margin and steeply dipping marginal-slope deposits on the left.

Box back cover: Aerial view, looking north, over the Laidlaw Range reef platform (right), Glenister Knolls patch reefs (bottom right), Lloyd Hill atoll (centre left), and Smith Knoll pinnacle reef (bottom left).

Contents

Abstract 1
Introduction and historical review 3
Localities 8
Regional geology 8
Geomorphology 9
Limestone ranges 9
Conglomerate ranges 9
Flora 12
Fauna 12
Human occupation 12
Devonian reef complexes 17
Facies 17
Lithostratigraphy 23
Platform facies 23
Cadjebut Formation 24
Pillara Limestone 26
Windjana Limestone 43
Nullara Limestone 48
Marginal-slope and basin facies 49
Sadler Limestone 49
Gogo Formation 51
Virgin Hills Formation 54
Bugle Gap Limestone 57
Piker Hills Formation 61
Napier Formation 62
Kalmanyi Member 63
Tarakalu Member 63
Barrar Member 64
Sequence stratigraphy 64
Pillara Sequence 68
Elliott Ridge Event 68
Kellys Pass Event 68
Waggon Pass Event 69
Algae Creek Event 72
Classic Face Event 72
Frasnian–Famennian Boundary Event 72
Nullara Sequence 75
Horseshoe Range Event 75
Reef-Extinction Event 80
Platform-margin and marginal-slope relationships 81
Types of platform margins 81
Marginal-slope debris deposits 81
Geopetal structures, depositional dip, and paleobathymetry 88
McWhae Ridge 97
Effects of faulting on development of the reef complexes 105
Neptunian dykes and sills 105
Biostratigraphy 115
Stromatoporoids 115
Diagenesis 115
Early marine diagenesis 115
Stylolitization 122
Geothermal history 124
Platform evolution through time 124
Conglomerates 125
Lithostratigraphy 125
Sparke Conglomerate 127
Galeru Member 129
Bobs Bore Conglomerate 134
Elma Conglomerate 134
Mueller Conglomerate 139
Barramundi Conglomerate 139
Stony Creek Conglomerate 142
Big Spring Formation 143
Behn Conglomerate 143
Van Emmerick Conglomerate 146

Paleocurrent patterns 146
Provenance 147
Conglomerate deposition 149
Cyclicity 149
Methods of study 150
Subaqueous cycles, Pillara Sequence 150
Subaqueous to subaerial cycles, Pillara Sequence 163
Subaqueous to subaerial conglomeratic cycles, Pillara Sequence 164
Cycles, Nullara Sequence 165
Megacycle stacking patterns 166
Cycle duration 167
Climatic regime and sea-level change 175
Controls on cyclicity 175
Implications for conglomerate deposition 176
Structure 176
Faulting 176
Folding 178
Mineralization 178
Epigenetic mineralization 178
Syngenetic mineralization 184
Field relationships 189
Longs Well area 189
East Pillara Range area 199
Pillara Spring area 199
Minnie Pool area 199
Stromatolite buildups 199
Gogo concretions 202
Barite mineralization 202
Gossans and iron-sulfide mineralization 204
Epigenetic mineralization in stromatolite buildups 204
Neomorphic alteration of stromatolites 205
Barite and iron-sulfide precipitation 205
Genesis of mineralization 205
Comparisons with other seep and vent systems 206
Conclusions 206
Petroleum 207
Paleokarst 207
Late Devonian paleokarst 207
Frasnian–Famennian unconformity 207
Reef-extinction unconformity 209
Early Carboniferous hydrothermal paleokarst 209
Early Permian paleokarst 212
Early Permian unconformity 212
Glacial pavement 213
Subglacial meltwater 214
Cave systems and karst corridors 214
Subglacial channels 214
Subglacial lakes 215
Tunnels 215
Tower karst 241
Collapse breccias 241
Diagenetic effects 241
Cenozoic bone deposits 242
Anthropological aspects of early Permian paleokarst 243
Late Devonian pseudokarst 245
Key localities 249
Bugle Gap area 250
Paddys Valley 250
East side of the Emanuel Range 250
Wade Knoll 250
Lloyd Hill 257
Glenister Knolls 257
McIntyre Knolls 258
McWhae Ridge 258
Kellys Pass 274
Casey Falls 274
Teichert Hills 277
Nardji Cave 277
Mimbi Caves System 277
Ngumban Cliff 283
Deeadeea Cliff 283
Lawford Spring – Junction Dam area 286
Bobs Bore area 286

Menyous Gap area....286
Mount Pierre area....288
Pillara quarry....288
Henwood Spring area....288
Rattigan Rocks area....294
Stony Creek area....297
Horse Spring Range area....297
Horseshoe Range area....297
Shady Bore block....300
Brooking Springs area....301
Geikie Gorge....303
Dingo Gap....304
Elimberrie bioherms....313
Elimberrie no. 1 bioherm....313
Elimberrie no. 2 bioherm....321
Elimberrie no. 3 bioherm....321
Elimberrie no. 4 bioherm....321
Northwest end of the Oscar Range and Morown Cliff....321
Ellendale vents....334
Tunnel Creek....334
McSherrys Gap....335
Carpenters Gap to the west entrance to Windjana Gorge....337
Windjana Gorge....337
East end of the gorge....342
East entrance to the Classic Face....350
The Classic Face....350
Central and western parts of the gorge....355
Mingun....355
Mirrngurrwalla–Manda-yarr-yarr-wungani....362
West end of the gorge....363
Baralamma Spring....367
Yammera Gap area....367
Napier Downs Homestead to Wombarella Gap....373
Narlarla....376
Anticlinal nose west of Barker Gorge....377
Rowalamban Cave area....377
Chedda Cliffs area....377
Mount Lesley....379
Van Emmerick Range area....379
Unggumi Promontory....381
Hawkstone Creek to Limestone Spring....381
Nyangalignali area....381
Wunala area....382
Limestone Spring area....382
Future research....384
Acknowledgements....384
References....385
About the authors....396
Index....397

Appendices

1. Gilbert Klapper: Upper Devonian conodonts in the Canning Basin....405
2. R Thomas Becker and Michael R House: Devonian ammonoid biostratigraphy of the Canning Basin....415
3. Geoffrey Playford: Review of Devonian palynology, Canning Basin....441

Plates

1. Napier Range area, 1:100 000 map
2. Oscar Range area,1:100 000 map
3. Fossil Downs area, 1:100 000 map
4. Pillara Range – Emanuel Range – Sparke Range area, 1:100 000 map
5. Bugle Gap area, 1:50 000 map
6. Windjana Gorge, 1:25 000 map
7. Lennard Shelf, 1:250 000 map
8. Lennard Shelf, 1:500 000 map

Figures

1. Locality map, Devonian reef complexes of the Canning Basin 4
2. Generalized geological map, Devonian reef complexes of the Canning Basin 5
3. Diagram illustrating changing concepts in interpretation of Devonian reef complexes of the Canning Basin since 1957 6
4. Map of the Kimberley district showing the possible original extent of the 'Devonian Great Barrier Reef' 10
5. Aerial view of the northwestern Napier Range reef complex, looking southeast 10
6. Aerial view of the Napier Range at Windjana Gorge, looking northwest 11
7. Aerial view looking north over the Laidlaw Range reef complex, showing its 'tail' of Glenister Knolls patch reefs 11
8. Pavement of Quaternary (?Pleistocene) calcrete conglomerate in the creek immediately north of Kellys Pass 13
9. Patterned ground in black-soil plain, looking east near Big Dam Bore 13
10. Sparke Range, looking west-northwest, showing the characteristic morphology of Devonian conglomerate ranges 14
11. *Langurrngurru* cliff and cave in Pillara Limestone near Windjana Gorge 14
12. Cycad palms in a karst corridor in Pillara Limestone, southwestern Oscar Range 15
13. Fresh-water crocodiles (*Crocodylus johnsoni*) near the west entrance to Windjana Gorge 15
14. Tall termite mound near Lawford Spring, Sparke Range 16
15. Tribal distribution map of the southern Kimberley area 17
16. Block diagram illustrating the morphology of the reef complexes 18
17. Diagrammatic cross section illustrating the morphology and facies relationships of the reef complexes 18
18. Correlation chart of Devonian and Lower Carboniferous units on the Lennard Shelf 19
19. Stylized cross section illustrating relationships between lithostratigraphic units of the Devonian reef complexes 19
20. Diagrammatic section illustrating the lithostratigraphy, sequence stratigraphy, and conodont biostratigraphy 20
21. Diagrammatic section illustrating the lithostratigraphy, sequence stratigraphy, and conodont biostratigraphy 21
22. Diagram to illustrate changes in the morphology of the Devonian limestone platforms that resulted from pressure-solution compaction 22
23. Moulds after hopper crystals of halite in dolomite of the Cadjebut Formation, Emanuel Range 24
24. Moulds after crystals of skeletal halite, in the Cadjebut Formation, Emanuel Range 25
25. Intraformational folding in dolomite of the Cadjebut Formation, Emanuel Range 25
26. Angular unconformity between Ordovician Gap Creek Formation (below) and late Givetian Cadjebut Formation (above), in the Emanuel Range near Gap Creek 26
27. Subvertical to steeply dipping sheets of stromatoporoids in late Frasnian reef-margin subfacies (Pillara Limestone) 28
28. Stromatolites in sandy limestone and calcareous sandstone of the Pillara Limestone (reef-flat subfacies) in the Classic Face 28
29. Geological map of part of the Geikie Gorge area showing the distribution of dolomite (now dedolomite) in platform facies 29
30. Fragments of *Amphipora*, forming 'spaghetti rock', in Pillara Limestone (bank subfacies) in the northern Emanuel Range 29
31. Shrub-like colony of *Amphipora* that fell over more-or-less intact, in Pillara Limestone (bank subfacies) 30
32. *Actinostroma* and *Amphipora* in back-reef subfacies of the Pillara Limestone in central Geikie Gorge 30
33. Back-reef limestone of the Pillara Limestone in Geikie Gorge showing strong stylolitization 32
34. Fore-reef limestone of the Napier Formation at Linesmans Creek, Oscar Range, showing stylolites with vertical teeth 32
35. *Actinostroma windjanicum* in reef-flat limestone of the Pillara Limestone in the Classic Face at Windjana Gorge 33
36. Bed of subspherical *Actinostroma* in back-reef subfacies, Pillara Limestone, Hull Range 33
37. Colonies of the coral *Disphyllum*, overlain by breccia composed of fragments of *Disphyllum* and *Thamnopora* 34
38. Vertical cross-section view of megalodont bivalves in their growth positions, in late Frasnian Pillara Limestone 34
39. Closer vertical cross-section view of megalodont bivalves in their growth positions in late Frasnian Pillara Limestone 35
40. Colony of *Actinostroma windjanicum* in the Classic Face, Windjana Gorge 35
41. Colony of *Renalcis* in reef subfacies (Pillara Limestone), from an allochthonous block in the Piker Hills Formation 36
42. Thin section of a former cavity in reef limestone (Pillara Limestone) showing *Renalcis* that grew into the cavity 36
43. Thin section of a former cavity in reef limestone showing *Renalcis* that grew down into the cavity 37
44. Polished slab of reef limestone (Pillara Limestone) from an allochthonous block in marginal-slope deposits at McIntyre Knolls 37
45. Polished slab of reef limestone (Pillara Limestone) from McIntyre Knolls, showing dense *Renalcis* encrusting stromatoporoids 38

46. Polished slab of reef limestone (Pillara Limestone) from an allochthonous block in marginal-slope deposits at McIntyre Knolls 38
47. Branching stromatolite columns built by *Sphaerocodium* 40
48. Thin section of narrow stromatolite columns, built by *Sphaerocodium* and non-skeletal sediment-binding microbes 40
49. The Frasnian–Famennian unconformity in platform facies at the northwest end of the Oscar Range 41
50. The Frasnian–Famennian unconformity near Limestone Spring in the northwestern Napier Range 41
51. Pillara Limestone (reef-flat subfacies) containing the ammonoid *Beloceras* 42
52. Unconformity within the Frasnian Pillara Limestone in the Limestone Billy Hills 42
53. Diagram illustrating the five major mass extinctions of the Phanerozoic 43
54. Diagram (not to scale) illustrating the increased development of deepwater stromatolites in the reef complexes 43
55. Stromatactis cavity-fillings (calcite and calcareous sandstone) in deep-water microbial reef limestone 44
56. A stromatactis cavity-filling in microbial reef limestone of the Windjana Limestone near the west entrance to Windjana Gorge 44
57. Thin section of stromatactis cavity fillings from the Virgin Hills Formation near Galeru Gorge 45
58. Polished slab of stromatactis limestone from an allochthonous block of reefal-slope limestone in fore-reef deposits 45
59. Megalodont bivalves in their growth positions in sandy limestone of the Nullara Limestone (Famennian), near Longhole Bore 46
60. Lithiotid bivalves in their growth positions, in Nullara Limestone east of Pothole Bore 47
61. Densely packed lithiotid bivalves in their growth positions in Nullara Limestone east of Pothole Bore, Fossil Downs Station 47
62. Tepee structure in Nullara Limestone near the northwest end of the Oscar Range, showing crestal breaching 48
63. The upper surface of a bed with polygonal tepee structures in the uppermost part of the Nullara Limestone 49
64. Aerial view, looking northeast, of large allochthonous blocks (as much as 120 m across) in Sadler Limestone 50
65. Silicified fossils, mainly brachiopods, in Sadler Limestone on the east side of the Emanuel Range 51
66. Aerial view, looking southeast, over Gap Creek and the Emanuel Range 52
67. *Aulopora* encrusting a bed in Sadler Limestone (fore-reef subfacies), on the east side of the Emanuel Range 52
68. Gogo nodules (limestone concretions) weathered out of the Gogo Formation near Longs Well 53
69. Core from a mineral-exploration drillhole in the Limestone Billy Hills area showing compaction around a concretion 54
70. Radiolarians etched out of a Gogo concretion, from near the northwest end of the Pillara Range 54
71. Sketch by E T Hardman of Mount Pierre (on the right), showing Hardman collecting ammonoids from the Virgin Hills Formation 55
72. Photograph, taken in 2003, of the same view of Mount Pierre and adjoining hills as shown in Figure 71 55
73. Early Famennian columnar stromatolites that grew vertically on a marginal slope in the Virgin Hills Formation, Ngumban Cliff 56
74. Early Famennian longitudinal stromatolites in the Virgin Hills Formation on the east side of the South Lawford Range 57
75. Remains of a 'head-dress sponge' (left centre) and receptaculitids in reefal-slope subfacies of the Napier Formation 58
76. A spar-filled cavity system in the Virgin Hills Formation, marginal-slope facies near Henwood Spring 58
77. A layered spar-filled cavity system in the Virgin Hills Formation, marginal-slope facies, near Henwood Spring 59
78. Spar-filled cavity system in the Virgin Hills Formation, marginal-slope facies, near Henwood Spring 59
79. Layered spar-filled cavity system 60
80. 'Cross-bedded spar' in the Virgin Hills Formation, distal marginal-slope to basin facies, north of Waggon Pass in Bugle Gap 60
81. Stromatactis structures in the Virgin Hills Formation, distal marginal-slope to basin facies, north of Waggon Pass in Bugle Gap 61
82. *Kalmanyi*, a slab of reefal-slope limestone that has peeled off the east side of the Napier Range south of Tunnel Creek 63
83. Massive receptaculitid–coral–microbial bioherm developed below the Frasnian–Famennian boundary 66
84. Diagram illustrating the rate of accumulation in platform facies 66
85. Diagrammatic section illustrating the Devonian of Alberta and Saskatchewan 67
86. Comparative cross sections through some Devonian reef complexes in the Canning Basin and Alberta 67
87. Aerial view of Elliott Ridge on the north side of the Laidlaw Range, looking southeast 69
88. Backstepped Frasnian platform of the Pillara Limestone at Kellys Pass, between Pillara Sequences 2 and 3 70
89. Angular discordance along the Kellys Pass sequence boundary (between Pillara Sequences 2 and 3) 70
90. Angular discordance at the Kellys Pass sequence boundary (between Pillara Sequences 2 and 3) 71
91. Back-reef Pillara Limestone with probable karst breccia below the Kellys Pass sequence boundary 71

92. Sadler Limestone (dipping to the left), overlying Pillara Limestone (dipping to the right), 2 km north of Waggon Pass ... 72
93. The Classic Face at Windjana Gorge, with the boundary between Pillara Sequences 5 and 6 marked by a white line ... 73
94. Closer view of part of the sequence boundary in the Classic Face, between Pillara Sequences 5 and 6 ... 73
95. Closer view of the upper part of the erosional unconformity marking the Classic Face sequence boundary ... 74
96. Immediately downstream from the Classic Face at Windjana Gorge, showing the unconformity between Pillara Sequences 5 and 6 ... 74
97. Plan view of the Frasnian–Famennian unconformity in the Napier Range near Chedda Cliffs, showing paleokarst cavities ... 76
98. The Frasnian–Famennian sequence boundary at the northwest end of the Oscar Range ... 76
99. The Frasnian–Famennian boundary, marked by a white line, in marginal-slope deposits (Napier Formation) ... 77
100. The Frasnian–Famennian boundary in the western part of Windjana Gorge ... 77
101. Virgin Hills Formation on the west side of McWhae Ridge, showing trenches cut to sample for conodonts and ammonoids ... 78
102. Columnar section illustrating part of the Virgin Hills Formation at McWhae Ridge ... 78
103. Virgin Hills Formation near Horse Spring in the Horse Spring Range ... 78
104. Part of Morown Cliff near its southeastern end ... 80
105. Sections illustrating the principal types of platform margin in the reef complexes ... 82
106. Upright scarp of massive reef-margin subfacies (Pillara Limestone) beside Nardji Cave ... 82
107. Upright-rollover platform margin in the Pillara Range, 1 km northwest of Menyous Gap ... 83
108. Upright-rollover platform margin in the Pillara Range, 0.7 km northwest of Menyous Gap ... 83
109. Collapsed platform margin opposite the Classic Face in Windjana Gorge ... 84
110. Collapsed margin near *Mirrngurrwalla* in the western part of Windjana Gorge ... 84
111. Retreating (retrograding) margin in the north Laidlaw Range ... 85
112. Retreating (retrograding) platform margin on the north side of Menyous Gap near its east entrance ... 85
113. Retreating (retrograding) platform margin, 1 km south of Menyous Gap in the Pillara Range ... 86
114. Advancing (prograding) platform margin in the Napier Range, 5.5 km northwest of Windjana Gorge ... 86
115. Aerial view of a faulted platform margin in the Emanuel Range, looking east ... 87
116. Aerial view of Wade Knoll pinnacle reef (stromatoporoid–microbial reef limestone), showing its south-directed 'tail' ... 87
117. Diagram illustrating the development of various types of pinnacle reefs in the reef complexes ... 88
118. Part of a block of reef limestone (lower central part of photo) encrusted by *Sphaerocodium* ... 89
119. Block diagram illustrating the origin of marginal-slope debris flows and allochthonous blocks ... 89
120. Block diagram illustrating the collapse of a platform margin, controlled by neptunian fissures ... 90
121. Diagrammatic cross section illustrating features of debris-flow deposits in fore-reef deposits ... 90
122. Typical debris-flow megabreccia in fore-reef subfacies (Napier Formation), Dingo Gap, Napier Range ... 91
123. Debris-flow deposit in fore-reef subfacies of the Napier Formation in Dingo Gap, showing reverse grading ... 91
124. A slide plane at the base of a debris-flow megabreccia in fore-reef Napier Formation in McSherrys Gap ... 92
125. 'Plough-furrow' folding of marginal-slope limestones below a debris-flow breccia in Napier Formation, Dingo Gap ... 92
126. A chisel-shaped block of reef limestone at the base of a debris-flow deposit in the Napier Formation, Dingo Gap ... 93
127. Megabreccia in Napier Formation, fore-reef subfacies, Dingo Gap ... 93
128. Allochthonous block of reef limestone in fore-reef subfacies (Napier Formation) south of McSherrys Gap ... 94
129. Lenses of scheck breccias in Napier Formation (fore-reef subfacies), northwest of Napier Downs Homestead ... 94
130. Scheck breccia in Napier Formation (fore-reef subfacies), north of Napier Downs Homestead ... 95
131. Thin section of a scheck breccia in Virgin Hills Formation from the South Lawford Range ... 95
132. Thin section of a scheck breccia in Virgin Hills Formation near Galeru Gorge ... 96
133. Corroded clast of reef limestone in fore-reef breccia, Napier Formation (fore-reef subfacies), Dingo Gap ... 96
134. Scheck breccia with calcite cement ... 97
135. Diagram illustrating types of geopetal structures found in the Devonian limestones. ... 98
136. Brachiopods showing 'spirit level' geopetal fillings in each closed shell, from the Sadler Limestone ... 99
137. Thin section of a brachiopod at the same locality as Figure 136, showing the nature of the geopetal infilling ... 99
138. Histogram illustrating geopetal measurements taken at the same locality as Figure 136 ... 100
139. 'Double-geopetal' filling in a block of Frasnian reef limestone in fore-reef deposits of the Napier Formation ... 100
140. Block of Famennian reefal-slope stromatactis limestone in Famennian fore-reef deposits, showing 'double-geopetal' fillings ... 101
141. Part of the west flank of McWhae Ridge showing marginal-slope deposits of the Sadler Limestone ... 101
142. Diagram illustrating geopetal structures and the amount of depositional and post-depositional dip in Sadler Limestone ... 102
143. Oncolites and capped oncolites in Sadler Limestone in the karst corridor on the west side of McWhae Ridge ... 102

144. Receptaculitid in marginal-slope Sadler Limestone in the karst corridor on the west flank of McWhae Ridge, showing a geopetal infilling 103
145. Histograms showing geopetal measurements in Sadler Limestone in the karst corridor..... 103
146. Bedding plane in Sadler Limestone on the west side of McWhae Ridge, showing straight nautiloids 104
147. Radial histograms illustrating orientations of the apertures of straight nautiloids lying on bedding plane. 104
148. Diagrammatic cross section through the west side of McWhae Ridge, illustrating water-depth estimates 105
149. Diagrammatic cross section illustrating factors responsible for fracturing and submarine landsliding in early cemented limestones 106
150. Network of small neptunian dykes 2 km north of Brooking Springs Homestead..... 107
151. Neptunian dyke 2 km north of Brooking Springs Homestead. 107
152. Spar balls of radiaxial calcite in a wide neptunian dyke beside the Cadjebut Fault on the southeast side of the Emanuel Range..... 108
153. Spectacular spar balls in a neptunian dyke in reef subfacies near Rowalamban Cave, Napier Range 108
154. Aerial view, looking east, over the northeast side of the Oscar Range 109
155. Aerial view of the southern end of the Oscar Range, looking northwest..... 109
156. Neptunian sills and dykes in distal marginal-slope facies of the Famennian Virgin Hills Formation at Ngumban Cliff..... 110
157. Neptunian sill of sparry calcite with small layers of internal sediment, in the Virgin Hills Formation on the west flank of McWhae Ridge 110
158. A major neptunian dyke at the southern end of the Oscar Range, showing its infilling of banded radiaxial calcite 111
159. Neptunian-dyke network in reef of the Pillara Limestone near the southern end of the Oscar Range 111
160. Aerial view, looking southeast along the Napier Range, with part of Dingo Gap on the right..... 112
161. Diagram illustrating development of a typical neptunian dyke..... 113
162. Part of a very wide neptunian dyke 4 km north-northeast of Brooking Springs Homestead..... 113
163. Part of the very wide neptunian dyke 114
164. Thin section of microbial stromatoporoid reef limestone (Pillara Limestone), showing a large cavity 114
165. Diagram illustrating the biotic distribution of the principal organisms in the Frasnian reef complexes..... 116
166. Diagram illustrating the biotic distribution of the principal organisms in the Famennian reef complexes..... 117
167. Diagram illustrating the water-depth distributions of various organisms that lived in or beside the Frasnian reef complexes 118
168. Diagram illustrating the ranges of various groups of organisms from the Middle Devonian to the Lower Carboniferous..... 118
169. Diagram illustrating the extent of pressure-solution and mechanical compaction, dolomitization, porosity, early marine cementation, stromatactis, and neptunian dykes 119
170. Diagram illustrating the distribution of various types of early marine cements in the reef complexes. ... 120
171. Thin section of laminated radiaxial spar cement from the lower Nullara Limestone at the northwest end of the Oscar Range 120
172. Debris-flow breccia from fore-reef Napier Formation, 0.5 km north-northeast of Carpenters Gap 121
173. Diagrammatic cross section through a Frasnian reef complex, showing porosity..... 121
174. Pillara Limestone 3 km south of Sheep Camp Yard in Geikie Gorge 122
175. Mud cracks (shrinkage cracks) in fenestral limestone of the Nullara Limestone 123
176. Frasnian conglomerate composed of blocks of stylolitized Devonian limestone, with a few blocks of Precambrian rocks..... 123
177. Locations of measured sections in the Devonian reef complexes and conglomerates..... 125
178. Estimated ages of measured sections shown on Figure 177. Platform sections shown in blue, conglomerate sections in red..... 126
179. Block diagram illustrating alluvial-fan, fan-delta, and submarine-fan facies in conglomerates..... 126
180. Block diagram showing the Oscar Range and Napier Range reef complexes and conglomerate bodies 127
181. Sparke Conglomerate, alluvial-fan facies, in the Sparke Range 128
182. Scree from Sparke Conglomerate 128
183. Aerial view of the Galeru Member of the Sparke Conglomerate, looking north, showing conspicuous cyclicity 129
184. Measured section of Galeru Member, central Sparke Range 130
185. Legend for measured sections. 132
186. Sparke Conglomerate near Lawford Spring showing alternations of sandstone and cobble conglomerate 133
187. Deep-water (distal fore-reef) Virgin Hills Formation interbedded with and grading into Bobs Bore Conglomerate near Bobs Bore 133
188. Mount Elma from the north, showing the rounded topography that is typical of most conglomerate outcrops 135
189. Large quartzite boulder in Elma Conglomerate, south of Mount Elma 135
190. Elma Conglomerate, fan-delta facies, on the east side of Painted Rocks 136
191. Elma Conglomerate on the east side of Painted Rocks showing stromatolitic encrustations 136
192. Aerial view, looking east, over the south flank of Mount Elma, showing megacycles 137
193. Part of one of the reefal bodies (Pillara Limestone) shown in Figure 192 on the south flank of Mount Elma 137

194. Interfingering between Frasnian back-reef subfacies (Pillara Limestone) and Elma Conglomerate 138
195. Aerial view of the Mueller Conglomerate, looking north-northwest 139
196. The eastern Barramundi Range, showing the characteristic rounded outlines of the conglomerate outcrops 140
197. Barramundi Conglomerate, alluvial-fan facies, in the Barramundi Range 140
198. Closer view of the Barramundi Conglomerate shown in the previous figure 141
199. Barramundi Conglomerate in the Barramundi Range, showing induration along joints and minor faults 141
200. Measured section, Barramundi Conglomerate, northeast Barramundi Range 144
201. Measured section, Nullara Limestone interfingering with Barramundi Conglomerate near Fly Bore. 145
202. Cyclic conglomerate in the Stony Creek Conglomerate adjoining the Stony Creek Fault 145
203. Scour-and-fill structures in Van Emmerick Conglomerate 147
204. Regional paleocurrent data for the Devonian conglomerates 148
205. Idealized metre-scale cycles for Givetian–Frasnian platforms, based on measured sections 150
206. Measured section of lower Pillara Limestone, Menyous Gap 151
207. Measured section of lower Pillara Limestone, Guppy Hills 154
208. Measured section of lower Pillara Limestone, Horse Spring Range 156
209. Measured section of basal Pillara Limestone, near Turnoff Dam, Brooking Springs Station 157
210. Measured section of Pillara Limestone, Shady Bore, Fossil Downs Station. 158
211. Measured section of upper Pillara Limestone, south of Lawford Spring 159
212. Measured section of upper Pillara Limestone, near McSherrys Gap. 160
213. Measured section of upper Pillara Limestone, Windjana Gorge, east end, above *Malambeea* 161
214. Measured section of upper Pillara Limestone, Surfboard Point, northwest Napier Range 162
215. Diagram illustrating cycles in the back-reef Pillara Limestone at Windjana Gorge 162
216. Diagram illustrating cycles in the Galeru Member of the Sparke Conglomerate 163
217. Aerial view of the Hull Range, looking southeast, showing well-defined subaqueous cyclicity 166
218. Aerial view of Guppy Hills, looking east, showing well-developed cyclicity 167
219. Measured section of Nullara Limestone and lowermost Fairfield Group, Horseshoe Range 168
220. Measured section of upper Nullara Limestone, southeast of Limestone Spring, in the northwest Napier Range 172
221. Measured section, lower Nullara Limestone, near Nippers Bore, Larrawa Station 173
222. The north wall of Windjana Gorge at *Mingun*, showing megacycles in the Pillara Limestone 173
223. Measured section near the east end of Windjana Gorge, showing metre-scale cycles and cycle stacking patterns 175
224. Map showing numerous north- and northeast-trending faults in the Limestone Billy Hills and northwestern Pillara Range 178
225. Aerial view, looking west, over a synclinal fold against the Mount Elma Fault on the east side of the Horseshoe Range 179
226. Oblique aerial photograph of the Bobs Bore area, looking northwest 179
227. Small left-lateral fault in reef-margin limestone (Pillara Limestone), 2 km north of Brooking Springs Homestead 180
228. Geological map and cross section of McWhae Ridge 181
229. Successive cross sections illustrating the development of McWhae Ridge 182
230. Network of neptunian dykes in Famennian limestone of the Virgin Hills Formation adjoining the Virgin Hills Fault near Bobs Bore 182
231. Famennian limestone of the Virgin Hills Formation adjoining the Virgin Hills Fault near Bobs Bore 183
232. Klippe of reefal limestone (Napier Formation) surrounded by Precambrian metamorphic rocks 183
233. Receptaculitids with geopetal infillings in the klippe shown in Figure 232, demonstrating that the limestone is steeply overturned 184
234. Zinc–lead occurrences and minesites on the Lennard Shelf 185
235. Locations of Devonian exhalative deposits and economic zinc–lead deposits in the southeastern Lennard Shelf 186
236. Diagrammatic cross section showing the development of exhalative deposits 186
237. Diagrammatic cross section through a Frasnian exhalative deposit 187
238. Diagrammatic cross section through lobes of an exhalative deposit 187
239. Geological maps showing the locations of Devonian exhalative deposits in the southeastern Lennard Shelf 188
240. Broken concretions weathered out of the Gogo Formation, showing concentric growth rings and fibrous structures 189
241. Bulbous stromatolites in an allochthonous block, east Pillara Range area, Conglomerate 1 deposit 190
242. Bands of branching, columnar, exhalative stromatolites in an allochthonous block, east Pillara Range area, Conglomerate 2 deposit. 190
243. Bulbous exhalative stromatolite forming an allochthonous block, Conglomerate 1 deposit 191
244. Finely laminated columnar exhalative stromatolites, Longs Well area 191
245. Exhalative stromatolites forming part of a bulbous growth in an allochthonous block, east Pillara Range area, Conglomerate 2 deposit 192
246. Fibrous exhalative stromatolites, Minnie Pool area 192
247. Cross section through a small spherical exhalative stromatolite body, east Pillara Range area 193
248. Branching columnar stromatolites that grew steeply downward into mud of the Gogo Formation, Longs Well area 193
249. Barite ‘shrub’ in stromatolitic limestone, Longs Well area 194
250. Barite ‘shrubs’ that grew contemporaneously with the enclosing exhalative stromatolites, Longs Well area 194

251. Plumose barite, which grew laterally, associated with exhalative stromatolites, Minnie Pool area 195
252. Gossan dyke (after iron sulfides) cutting through exhalative stromatolites, Longs Well area 195
253. Gossan dyke cutting through exhalative stromatolites that are partly altered to dark sparry calcite 196
254. Exhalative stromatolites, partly altered through low-temperature metasomatism associated with a gossan dyke 196
255. Exhalative stromatolites altered to white and dark spar 197
256. Bedding plane showing heads of exhalative stromatolites surrounded by iron oxide 197
257. Gossan dyke, originally composed of stromatolitic iron sulfides, East Pillara Range area 198
258. Spherules of laminated calcite in an exhalative deposit, Minnie Pool area 198
259. Sheared lime mudstone and concretions in steeply dipping Gogo Formation beside the Albatross Fault 200
260. Diagram illustrating the different types of stromatolites recognized in the reef complexes 200
261. Oxygen- and carbon-isotope values for stromatolites, Gogo concretions, Sadler Limestone, and Gogo Formation 201
262. The relationships between contents of iron and strontium, and manganese and magnesium, in stromatolites 201
263. Sulfur-isotope values for Cadjebut epigenetic Zn–Pb mineralization, Middle to Late Devonian seawater, and Late Devonian exhalative sulfides and barite 203
264. Paragenetic sequences of exhalative phases, calcite cements, and epigenetic phases 203
265. Geological map of the northwest part of the Devonian reef complexes showing the subsurface extent of the Famennian platform facies and the positions of oilfields 208
266. Cross section through the Goongewa hydrothermal orebodies 209
267. Diagrammatic representation of the eastern face of the Pillara quarry 210
268. Panoramic view of the eastern face of the Pillara quarry as shown in Figure 267 210
269. Closer view of the eastern face of the Pillara quarry 210
270. The southern face of the Pillara quarry 211
271. Boulder of Pillara Limestone blasted from the wall of the Pillara quarry, showing rectilinear mineralized fractures 211
272. Part of the floor of the Pillara quarry, showing a joint that was enlarged by solution in basin-derived fluids 212
273. Diagrammatic cross section illustrating features formed by the solution of Devonian limestone by subglacial meltwater 216
274. Diagrammatic south polar projection showing the Early Permian ice sheet that covered the southern part of the Gondwana supercontinent, showing the directions of ice movement 216
275. Generalized geological map of the northern Canning Basin, showing the directions of Early Permian ice movement 217
276. Directions of Early Permian ice movement as determined at various localities in Western Australia 217
277. Aerial view, looking southeast, near Deeadeea Cliff 218
278. Closer aerial view, looking southeast, towards Deeadeea Cliff, showing outliers of the Carolyn Formation resting on strongly karstified Bugle Gap Limestone 218
279. Unconformity between sandstone of the Grant Group (Lower Permian) and strongly karstified Nullara Limestone 219
280. Aerial view of Kimberley Rover solution doline in the northern Laidlaw Range 219
281. Aerial view of Kimberley Rover solution doline, looking north-northeast towards another solution doline in the right background 220
282. Kimberley Rover solution doline 220
283. Deeadeea Cliff beside the Great Northern Highway 221
284. Glaciated cobble (a dropstone) of basalt from the Ngumban Claystone Member in its type section 221
285. Striated and polished glacial pavement in the Goongewa box-cut 222
286. Striated and polished glacial pavement in the Goongewa box-cut 222
287. Part of the striated and polished glacial pavement on Pillara Limestone in the Goongewa box-cut 223
288. Striated, sculptured, and polished glacial pavement on Pillara Limestone in the Goongewa box-cut 223
289. Planar glacial unconformity in the Goongewa box-cut 224
290. Graphs of temperature in relation to depth of ice in holes drilled through the Antarctic ice cap 224
291. Geological map of the southern part of the Lawford Range 225
292. The mapped part of the Mimbi Caves System. 226
293. 'Carrot' stalactite, Mimbi Caves System 227
294. 'The crucifix', consisting of broken and regrown stalagmites and stalactites, Mimbi Caves System 227
295. 'Coral' stalagmite, Mimbi Caves System 228
296. Closer view of 'coral' stalagmite, Mimbi Caves System 228
297. Shawl speleothem, composed of crystalline spar, on a wall of Uranus Cave, near Ngumban Cliff 229
298. Spectacular flowstone speleothems on a wall of Uranus Cave, near Ngumban Cliff 229
299. Illawarra Corridor, a major karst corridor in the Mimbi Caves System 230
300. Rough karst surface, due to modern karstification, on top of the Lawford Range above the Mimbi Caves System 230
301. Menyous Gap in the Pillara Range from the air, looking north 231
302. Aerial view of Unggumi Promontory in the Napier Range 231
303. Aerial view of Unggumi Promontory, looking west-southwest 232
304. Aerial view of Unggumi Promontory , looking south-southeast 232
305. Map of the northern Emanuel Range and Sadler Ridge areas, showing the sites of subglacial lakes, part of the Kunian Gap subglacial channel, and a cave-collapse breccia 233

306. Aerial view of Windjana Gorge, looking east-southeast over the Napier Range reef complex 233
307. Geological map of the Windjana Gorge area. 234
308. Aerial view of the central part of Geikie Gorge, looking east, showing the southeast wall of the gorge 234
309. Brooking Gorge, looking northwest, near the gorge entrance 235
310. Geological map of the Boggy Creek area, South Lawford Range, showing the former extent of Early Permian subglacial lakes and channels 235
311. Aerial view of part of the Boggy Creek area 236
312. Tower karst in the Paddys Spring area, northern Laidlaw Range 236
313. Kevins Cave (left) and the entrance to Mindiwilli Tunnel (right) in the Boggy Creek area 237
314. Panorama at Lloyd Hill of a solution doline filled with poorly exposed sandstone of the Lower Permian Grant Group 237
315. Aerial view of Lloyd Hill atoll, looking north 238
316. Aerial view of two of the Glenister Knolls patch reefs 238
317. Solution doline filled with Lower Permian Grant Group (foreground and middle distance) in the largest of the Glenister Knolls 239
318. Entrance to Peara Cave in the northern Napier Range 239
319. Map of the Peara Cave area showing the known extent of the cave system and the Old Napier solution doline 240
320. Map showing the lower part of the Peara Cave system 240
321. Cave-collapse breccia in marginal-slope limestones, central Oscar Range 241
322. Cemented layer of masticated small reptile and mammal bones and gastroliths in the Dingo Gap area 242
323. Conglomerate with large crocodile and turtle bones in a small cavern about 40 m above the river bed in Windjana Gorge 243
324. Aboriginal cave painting of a *Wandjina* Dreamtime figure, known as *Rowalamban*, in the northwestern Napier Range 244
325. Stalagmite near the entrance to Peara Cave 244
326. Geological map of part of Dingo Gap showing the locations of pseudokarst 'sand-tube' allochthonous blocks 245
327. Block diagram illustrating the origin of pseudokarst sand tubes in allochthonous blocks at the base of the Barrar Member 246
328. Plan view of part of a pseudokarst block in Dingo Gap 246
329. One of the allochthonous blocks from group no. 3 in Dingo Gap 247
330. Part of a pseudokarst block from group no. 3 in Dingo Gap 247
331. Closer view of one of the stromatolite columns shown in Figure 330 248
332. Plan view of one of the pseudokarst blocks from group no. 3 in Dingo Gap 248
333. Columnar stromatolite in a pseudokarst block from group no. 2 in Dingo Gap 249
334. Geological map of the Bugle Gap area 251
335. Aerial view, looking south, over Paddys Valley towards Lloyd Hill atoll (centre background) 252
336. Aerial view, looking east, over part of the western flank of Paddys Valley 252
337. North flank of the small patch reef on the west side of Paddys Valley 253
338. Colony of the dendroid coral *Disphyllum* in fore-reef strata on the northwest flank of the small patch reef 253
339. Aerial view of Wade Knoll pinnacle reef 254
340. *Sphaerocodium* stromatolites in marginal-slope strata of Wade Knoll pinnacle reef 254
341. Aerial photograph of Wade Knoll, looking south 255
342. Sections through cycles in the Gogo Formation adjoining Wade Knoll 256
343. Aerial view, looking north, over two of the Glenister Knolls patch reefs 259
344. Closer aerial view, looking north, over two of the Glenister Knolls patch reefs 259
345. Aerial view of Lloyd Hill atoll, looking northwest 260
346. Aerial view of Lloyd Hill atoll, looking east towards the Laidlaw Range platform. 260
347. Geological map and cross section of Lloyd Hill atoll 261
348. Polished slab of zebra rock from the reef-flat subfacies of the Pillara Limestone at Lloyd Hill 262
349. Thin section of zebra rock from the reef-flat subfacies of the Pillara Limestone at Lloyd Hill 262
350. Geological map of Lloyd Hill atoll, southern Laidlaw Range platform, and Glenister Knolls patch reefs. 263
351. Cross sections A–B through Lloyd Hill atoll and southern Laidlaw Range platform, and C–D through a Glenister Knolls patch reef and Ross Hill 263
352. *Sphaerocodium* stromatolites in reefal-slope subfacies from the 'tail' of the Laidlaw Range platform 264
353. Polished slab of microbial limestone from a microbial bioherm or allochthonous block 264
354. Geological map of the McIntyre Knolls area in the Old Bohemia Valley 265
355. Aerial view of McIntyre Knolls, looking northeast towards the North Lawford Range platform 266
356. One of the McIntyre Knolls, looking east 266
357. Geological map of the southern Bugle Gap area, showing the principal localities discussed in the text 268
358. Aerial view, looking north, over the McWhae Ridge reef spine 269
359. Diagrammatic section of part of the west flank of McWhae Ridge 269
360. Part of the west flank of McWhae Ridge, looking towards the location illustrated in Figure 359 270
361. Thin-bedded distal fore-reef limestone onlapping stromatolitic limestone 270
362. Part of the east flank of McWhae Ridge, looking south 271
363. Famennian silty limestone of the Virgin Hills Formation east of McWhae Ridge 271

364. The south wall of the small karst corridor in Sadler Limestone illustrated in Figure 141 272
365. Thin section showing colonies of the iron cyanobacterium *Frutexites* 272
366. Thin section showing colonies of the iron cyanobacterium *Frutexites* in a groundmass of microbial limestone 273
367. Thin section showing colonies of *Frutexites* in a groundmass of microbial limestone 273
368. Thin section of a succession of holdfasts of crinoids and a coral 274
369. Masses of ammonoids (*Torleyoceras* and *Praemeroceras*) 275
370. The top of a fallen block of deep-water columnar stromatolites in Virgin Hills Formation at Casey Falls 275
371. Mound-shaped stromatolite in Virgin Hills Formation near Casey Falls 276
372. Famennian marginal-slope limestone of the Virgin Hills Formation southwest of Casey Falls 276
373. Geological maps illustrating two prominent Frasnian backstepping events, at Teichert Hills and Elliott Ridge 278
374. Small patch reef that developed on the northern margin of the Teichert Hills platform 278
375. Aerial view of the southwestern Teichert Hills platform (Frasnian), showing chute-and-buttress (or spur-and-groove) structures 279
376. Closer aerial view, looking east, of chute-and-buttress structures 279
377. Straight nautiloids and phosphatic microbial limestone that accumulated on the steep walls of a chute 280
378. Shawl speleothem, composed of sparkling crystalline spar, in Mimbi Caves 281
379. Rimmed terraces with cave pearls, Mimbi Caves System 282
380. Pluto's Way Cave, on the east side of the Emanuel Range opposite the Mimbi Community settlement. 282
381. Two views of statues of North American Indians sculptured by Gutha Rokylle 283
382. The tops of closely spaced stromatolite columns, viewed from above, in early Famennian Virgin Hills Formation 284
383. Reticulate stromatolites, Famennian Virgin Hills Formation, Ngumban Cliff 284
384. Thin section of small neptunian dykes and sills in early Famennian Virgin Hills Formation at Ngumban Cliff 285
385. Retreating platform margin 1 km northwest of the north entrance to Menyous Gap 287
386. Geological map of a locality 1.5 km east of Mount Pierre, adjoining Mount Pierre Creek 289
387. Aerial view of the locality shown in Figure 386 289
388. View of the surface of the Virgin Hills Formation at the locality shown in Figure 386 290
389. Tepee in sandy calcareous siltstone of the Virgin Hills Formation at the locality shown in Figure 386 290
390. Tepee in sandy calcareous siltstone of the Virgin Hills Formation at the locality shown in Figure 386 291
391. The surface of a bed of calcareous siltstone between tepees in the Virgin Hills Formation 291
392. Symmetrical ripple marks in sandy calcareous siltstone of the Virgin Hills Formation 292
393. Asymmetrical (current) ripple marks, with the flow direction towards the left, in sandy calcareous siltstone of the Virgin Hills Formation. 292
394. Underside of a tabular stromatoporoid colony from the Pillara Limestone in the Pillara quarry 293
395. Close-up view of the underside of the stromatoporoid colony shown in Figure 394 293
396. Vertical aerial view, looking east, 2.1 km west-northwest of Henwood Spring 294
397. The Frasnian–Famennian unconformity 2.1 km west-northwest of Henwood Spring 295
398. Conglomerate at the base of the Nullara Limestone 295
399. Conglomerate interfingering with basal Nullara Limestone 296
400. Aerial view of Rattigan Rocks, looking northwest 296
401. Aerial view, looking northwest, in the Stony Creek area 298
402. Aerial view, looking east, in the Stony Creek area 298
403. Aerial view, looking north-northeast, in the Stony Creek area 299
404. Cobble of granite encrusted by a stromatoporoid colony in the Stony Creek Conglomerate 299
405. Cavity filling of Virgin Hills Formation in fore-reef megabreccia of the Sadler Limestone near Horse Spring 300
406. Aerial view of the Shady Bore block, looking east 301
407. Cyclicity in steeply dipping Pillara Limestone near Shady Bore 302
408. Aerial view, looking northeast, over a faulted area beside the Black Hills Fault in the Minnie Pool area 302
409. Neptunian dyke in reef-margin limestone of the Pillara Limestone 303
410. Sketch of the south entrance to Geikie Gorge in 1883, by geologist E T Hardman 305
411. Geological map of the Geikie Gorge area 305
412. Rollover platform margin on the east wall of Geikie Gorge, 3 km northwest of Sheep Camp Yard 306
413. Geikie Gorge near the south entrance 306
414. Geikie Gorge near its south entrance 307
415. Aerial view of the southeast wall of Geikie Gorge in its central part, looking east 307
416. The southeast wall of Geikie Gorge in its central part 308
417. The wall of Geikie Gorge, showing neptunian dykes filled with orange-coloured silty limestone 308
418. Reefal-slope limestone at Geikie Gorge, 3 km northeast of Sheep Camp Yard 309
419. Dolomite (now altered to dedolomite) in near-reef back-reef in Geikie Gorge. 309
420. Block of *Renalcis* reef that was carried in a debris flow to near the base of the fore-reef slope 310
421. Pillara Limestone, showing irregular patches of microbial *Amphipora*-rich back-reef limestone that were cemented soon after deposition 310
422. Aerial view of Dingo Gap (right and centre), looking northwest 311

423. Blocks at the base of a debris-flow deposit in the Barrar Member of the Napier Formation in Dingo Gap 312
424. Bedding plane in fore-reef subfacies of the Napier Formation in Dingo Gap, with abundant invertebrate trails 312
425. Antiformal stromatolite in Napier Formation, fore-reef subfacies, near Dingo Gap 313
426. Geological map of the Elimberrie bioherms 314
427. Geological map of Elimberrie no. 1 bioherm 315
428. Aerial view looking northeast over Elimberrie no. 1 bioherm, showing its circular outline, with a 'tail' to the south 316
429. Aerial view of the eastern pinnacle reef (lower middle) and the adjoining part of Elimberrie no. 1 bioherm, looking west 316
430. Aerial view of the narrow 'tail' of Elimberrie no. 1 bioherm, looking southwest 317
431. Erosional contact in Elimberrie no. 1 bioherm 317
432. Polished slab from the eastern pinnacle reef in Elimberrie no. 1 bioherm 318
433. Thin section of the erosional contact in Elimberrie no. 1 bioherm 318
434. Reef limestone from the eastern pinnacle reef of Elimberrie no. 1 bioherm, showing gash veins filled with dolomite 319
435. Receptaculitids in dolomitic limestone, Elimberrie no. 1 bioherm 319
436. Receptaculitid in microbial limestone in Elimberrie no. 1 bioherm, showing its characteristic ' snowflake' structure 320
437. Gossan cutting through fore-reef strata adjoining the northwest flank of Elimberrie no. 1 bioherm 320
438. Geological map of Elimberrie no. 2 bioherm 322
439. Diagrammatic cross section through Elimberrie no. 2 bioherm 323
440. Aerial view, looking north, over the southwest culmination of Elimberrie no. 2 bioherm 323
441. The northern culmination of Elimberrie no. 2 bioherm, looking northeast 324
442. The central crest of Elimberrie no. 2 bioherm, looking southwest 324
443. Thin section showing stromatolite columns constructed by *Sphaerocodium* and non-skeletal microbes 325
444. Columnar stromatolites from Elimberrie no. 2 bioherm, built jointly by *Sphaerocodium* and non-skeletal microbes 325
445. Thin section of a columnar stromatolite from Elimberrie no. 2 bioherm 326
446. Scalloped stromatolites on a flank of Elimberrie no. 2 bioherm 326
447. Chains of the coral *Aulopora* encrusted on the surface of microbial limestone in the axial area of Elimberrie no. 2 bioherm 327
448. Part of Elimberrie no. 3 bioherm with abundant receptaculitids 327
449. Straight nautiloid in the steeply dipping core of Elimberrie no. 3 bioherm 328
450. Thin section of stromatolitic limestone from the core of Elimberrie no. 3 bioherm 328
451. Aerial view of the northwestern part of the Oscar Range, looking northwest 329
452. A higher altitude aerial view of the north-western part of the Oscar Range, looking northwest 330
453. Series of diagrams illustrating development of the Oscar Range reef complex through time 330
454. Wire Spring (*Bullulu*) 331
455. The Frasnian–Famennian boundary at the northwestern end of the Oscar Range 331
456. Oncolitic limestone of the back-reef Nullara Limestone at the northwestern end of the Oscar Range 332
457. Morown Cliff, forming the northern margin of the Oscar Range reef complex 332
458. Morown Cliff, showing vertical karren formed by modern karst erosion 333
459. Ellendale leucite-lamproite vent no. 38 333
460. Aerial view of Tunnel Creek, looking northeast 334
461. Antiformal stromatolite on the south wall of McSherrys Gap 335
462. Debris-flow megabreccia on the southwest side of the Napier Range 336
463. Ball-and-pillow structure in red sandy siltstone at the top of a cycle in the Pillara Limestone, north of McSherrys Gap 336
464. Contorted beds in fore-reef strata of the Napier Formation, near Carpenters Gap 338
465. *Tangalma* cave or rock shelter, near Carpenters Gap on the north side of the Napier Range 338
466. Pillara Limestone (platform facies) on the left, abutted by Napier Formation (marginal-slope facies) on the right 339
467. Debris-flow deposit beside *Munggurrma* Valley south of the east entrance to Windjana Gorge 339
468. Flame structure developed in marginal-slope limestone directly below the debris flow deposit shown in Figure 467 340
469. Aerial view, looking south, near the east entrance to Windjana Gorge 340
470. Closer aerial view of the platform facies at *Langurrngurru* (near the east entrance to Windjana Gorge) 341
471. Closer aerial view of the eastern part of Figure 470 341
472. The west entrance to Windjana Gorge ('Devil's Pass'), as sketched by E T Hardman in 1883 343
473. The east entrance to Windjana Gorge, as sketched by E T Hardman in 1883. 343
474. Aboriginal cave painting near the east entrance to Windjana Gorge, showing a *Wandjina* figure 344
475. Map of Windjana Gorge showing Aboriginal place names 344
476. Entrance to a 'chimney' through limestone talus, known to the Aborigines as *Marli* 345
477. Scenic view of Windjana Gorge taken from the north bank of the Lennard River near *Mirrngurrwalla* 345
478. The west end of Windjana Gorge taken from the top of the gorge near *Mandjalan* Pass 346
479. Geological map and cross section of the Napier Range at Windjana Gorge 347
480. Marginal-slope limestone and dolomite of the fore-reef Napier Formation on the north wall of Windjana Gorge 348

481. Breccia of reefal-slope clasts in fore-reef Napier Formation on the north wall of Windjana Gorge 348
482. Scheck breccia in fore-reef Napier Formation on the north wall of Windjana Gorge beside the east entrance 349
483. Conglomerate of subrounded to subangular boulders of igneous and metamorphic Precambrian rocks 349
484. Panorama and equivalent sketch of the south face of Windjana Gorge beside the east entrance..... 350
485. Panorama and equivalent sketch of the south face of Windjana Gorge from the southern end of the Classic Face to the east entrance..... 351
486. Panorama and equivalent sketch of the Classic Face at Windjana Gorge 351
487. Panorama and equivalent sketch of Windjana Gorge immediately downstream from the Classic Face... 352
488. Panorama and equivalent sketch of the south wall of Windjana Gorge in the *Mirrngurrwalla* area..... 352
489. Panorama and equivalent sketch of Windjana Gorge from *Mirrngurrwalla* to the west entrance..... 353
490. The Frasnian–Famennian boundary in fore-reef deposits of the Napier Formation in Windjana Gorge..... 353
491. The south face of Windjana Gorge east of the Classic Face 354
492. Aerial view of the Classic Face at Windjana Gorge, looking south 356
493. Platform-margin unconformity near the eastern wall of Windjana Gorge opposite the Classic Face..... 356
494. Aerial view, looking west towards the Napier Range at Windjana Gorge 357
495. Platform-margin unconformity in the Classic Face in Windjana Gorge 357
496. Elongate colony of the stromatoporoid *Actinostroma windjanicum* in reef-flat deposits of the Pillara Limestone..... 358
497. Colony of the dendroid stromatoporoid *Stachyodes costulata,* intergrown with *Renalcis* 358
498. Polished slab of reef limestone from a talus block at the foot of the Classic Face at Windjana Gorge.... 359
499. Closer view of part of the polished slab of reef limestone shown in Figure 498 359
500. Club-shaped columnar fenestral stromatolites in reef-flat deposits in the Classic Face at Windjana Gorge..... 360
501. A large cavity filling (dubbed 'the biggest stromatactis in the world') in reef-flat limestones in the Classic Face at Windjana Gorge..... 360
502. Polished slab of part of the right-hand side of the cavity filling shown in Figure 501 361
503. Neptunian dyke filled with red laminated peloidal limestone..... 361
504. Back-reef Pillara Limestone at *Mingun* in Windjana Gorge, showing cyclicity 362
505. Low-level aerial view, looking north, immediately north of Windjana Gorge, showing strong cyclicity in Pillara Limestone..... 363
506. *Mirrngurrwalla*, a talus block in the bed of the Lennard River at Windjana Gorge 364
507. *Manda-yarr-yarr-wungani*, stalactites on the north wall of central Windjana Gorge..... 364
508. South wall of Windjana Gorge near *Mirrngurrwalla*, showing a collapsed platform..... 365
509. Closer view of the south wall of Windjana Gorge near *Mirrngurrwalla,* showing the collapsed platform margin..... 365
510. Aerial view of the central and eastern parts of Windjana Gorge, looking southeast..... 366
511. Aerial view, looking south, immediately north of Windjana Gorge..... 366
512. Looking south, about 500 m north of Windjana Gorge..... 367
513. Deep-water reef limestone of the Windjana Limestone on the south side of Windjana Gorge..... 368
514. Windjana Limestone on the south side of Windjana Gorge near the west entrance 368
515. The north wall of Windjana Gorge near the west entrance 369
516. The west entrance to Windjana Gorge, known to the Aborigines as *Weenan* 369
517. Aerial view, looking northeast towards the west entrance to Windjana Gorge 370
518. Straight nautiloid in the lower (deep-water) part of the Famennian reef (Windjana Limestone) 370
519. Small neptunian dyke in microbial (*Renalcis*-rich) reef limestone (Windjana Limestone)..... 371
520. Limestone on the north side of Windjana Gorge near the west entrance 371
521. Closer view of parts of the microbial reef lenses shown in Figure 520 372
522. Aboriginal paintings of two defecating dingoes in a small cave beside Baralamma Spring. 372
523. Biohermal 'swellings' built by stromatoporoids and microbes in reef-flat deposits of the Pillara Limestone..... 373
524. Small antiformal stromatolites in Frasnian fore-reef deposits (Napier Formation) south of Yammera Gap..... 374
525. Antiformal stromatolite in fore-reef deposits (Napier Formation) north of Napier Downs Homestead..... 374
526. Linked antiformal stromatolites in fore-reef deposits (Napier Formation) north of Napier Downs Homestead..... 375
527. Linked antiformal stromatolites in fore-reef deposits (Napier Formation)..... 375
528. Lenses of scheck breccias in fore-reef deposits (Napier Formation) north of Napier Downs Homestead..... 376
529. Aerial view, looking north, over Barker Gorge and part of the Napier Range..... 377
530. Cyclone Rock (*Walangina*) on the left and Willy Willy Rock (*Djalawunna*) on the right 378
531. Frasnian reef limestone (Pillara Limestone, Sequence 6) directly below the Frasnian–Famennian boundary..... 379
532. Biohermal 'noses' of microbial and receptaculitid limestone in the Napier Range north of Unggumi Promontory..... 380
533. Conglomeratic, sandy, fenestral limestone of the Pillara Limestone, immediately north of Hawkstone Creek 380
534. The Frasnian–Famennian boundary in the Napier Range near Wunala Hill..... 382
535. Imbricate blocks of Pillara Limestone at the base of the Nullara Limestone near Wunala Hill. 383
536. 'Balancing rock' in Nullara Limestone south of Limestone Spring in the Napier Range..... 383

Abstract

Middle and Upper Devonian (Givetian, Frasnian, and Famennian) reef complexes are spectacularly exposed on the Lennard Shelf, along the northern margin of the Canning Basin. They form a belt of rugged limestone ranges, some 350 km long and as much as 50 km wide, that is commonly known as the 'Devonian Great Barrier Reef'. The reef complexes have been studied by geologists of the Geological Survey of Western Australia (GSWA) and other organizations over more than 50 years. The most recent GSWA study has involved re-mapping and re-interpreting the reef complexes and integrating the results of other research projects.

The reef complexes form a northwest-trending barrier-reef system, composed of fringing reefs, atolls, and banks, that grew along the mountainous mainland shore of the Kimberley block and around rugged islands of Proterozoic igneous and metamorphic rocks. One reef complex grew on a fault block of Ordovician dolomite and shale. The maximum thickness of the Devonian rocks is estimated to be at least 2500 m.

Primary fabrics are very well preserved in the reef complexes. They have remained virtually unaltered since deposition, other than where early dolomitization has occurred in an estimated 15% of the section. In some areas the reef complexes are cut by normal faults, some of which moved during the Devonian, with associated tilting and folding, but over large areas the Devonian rocks are almost undeformed. Conglomerates that interfinger with or extend through the reef complexes were derived from the scarps of active faults in adjoining Precambrian basement rocks. Movement along some faults continued during the Carboniferous, but there has been little or no tectonism in the area since then.

Three main facies are recognized in the reef complexes: platform, marginal-slope, and basin facies. The reefal platforms, which stood tens to hundreds of metres above the adjacent sea floor, were constructed by shallow-water organisms, especially stromatoporoids, corals, and microbes. Many platforms were rimmed by rigid wave-resistant reefs. The platform facies is subdivided into reef-margin, reef-flat, pinnacle-reef, and back-reef subfacies. Where no reef is developed around a platform margin, that platform is regarded as a bank and its deposits are placed in the bank subfacies.

The platform deposits were laid down essentially horizontally, in shallow subtidal to intertidal and supratidal environments. The reef-margin and reef-flat deposits developed mainly in shallow water, but in some places the reef grew in water as much as a few tens of metres deep. The back-reef areas ranged from supratidal to subtidal, with estimated water depths of as much as 10 m. Strongly developed cyclicity is evident in many back-reef deposits.

Marginal-slope deposits were laid down on slopes in front of the platforms, reaching depths of as much as several hundred metres. The marginal-slope facies in front of reefal platforms is subdivided into reefal-slope and fore-reef subfacies. Where the platform is a bank, lacking a reef rim, the slope deposits are regarded as fore-bank facies.

Reef-margin and reef-flat boundstones and back-reef biostromes were built by microbes, stromatoporoids, and corals during the late Givetian and early Frasnian, by microbes and stromatoporoids during the late Frasnian, and by microbes alone in the Famennian. The reefal-slope subfacies consists of microbial boundstone that accreted at the tops of the marginal slopes. The reefal-slope deposits show depositional dips ranging from nearly vertical to about 40°, and they pass downwards into fore-reef subfacies.

The fore-reef deposits consist largely of platform-derived debris, and include debris flows and isolated allochthonous blocks of reef, together with indigenous fossil organisms and terrigenous clastic material. Depositional dips in the fore-reef subfacies decline progressively from about 40° at the top of a slope to a few degrees at the foot, where the fore-reef subfacies interfingers with basin facies. Fore-bank deposits generally lack steep depositional dips, and interfinger directly with bank deposits at the top of the slope and basin facies at the base. The basin facies, which was laid down essentially horizontally in water depths from a few tens to several hundred metres, consists largely of calcareous shale, siltstone and sandstone, with some interbedded turbidites and debris-flow limestones. Some shaly basin deposits have undergone major post-burial mechanical compaction (as much as about 75%).

The reef complexes range in age from Middle Devonian (late Givetian) to Late Devonian (Frasnian and Famennian). Most exposed reefs are Frasnian or Famennian in age. The most precise dating of the reef complexes is based on conodonts and ammonoids in basin and marginal-slope deposits. Conodonts are absent and ammonoids are very rare in platform deposits.

Two second-order sequences are recognized in the reef complexes: the Givetian–Frasnian Pillara Sequence and the Famennian Nullara Sequence. The boundary between them is an unconformity in platform and upper marginal-slope deposits and a conformity in deeper marginal-slope and basin deposits. The fall in sea level that was associated with this unconformity is estimated to have been about 50 m.

The base of the late Givetian to Frasnian Pillara Sequence is defined by an unconformity over Precambrian and Ordovician rocks, and its top is the Frasnian–Famennian unconformity. The Famennian Nullara Sequence overlies that unconformity, and at its top is defined by the late Famennian reef-extinction unconformity, overlain by the late Famennian and Tournaisian Fairfield Group. Six third-order sequences are recognized in the Pillara Sequence, five of which are defined by backstepping episodes associated with retreating platforms. The sixth (top) sequence is marked by an advancing platform following a small backstepping event. The succeeding second-order Nullara Sequence is marked by strongly advancing platforms. Two third-order sequences in the Nullara Sequence were separated by a pronounced backstepping event.

The change from retreating (retrograding) and backstepping platforms during the Givetian through latest Frasnian to advancing (prograding) platforms during the latest Frasnian and Famennian, may have been linked to a long-term rise and fall in global sea level. According to this hypothesis, sea level rose while regional subsidence continued, so that platforms of the Pillara Sequence accreted and retreated up to the late Frasnian. Then, during the latest Frasnian, global sea level began falling and continued falling during the Famennian, while subsidence was maintained as before. The rate of sea-level fall was less than the rate of subsidence, resulting in a continuing but slower transgression during deposition of the latest Pillara Sequence and throughout the Nullara Sequence.

The Frasnian–Famennian boundary marks the culmination of a global mass extinction of metazoan organisms that began during the latest Frasnian. Whereas the late Frasnian in the northern hemisphere was marked by major anoxic events (known as the Upper and Lower Kelwasser), there is no evidence for such anoxia in the Canning Basin at that time. Among the conodonts the main extinction occurred at the end of Frasnian Zone 13b (see Klapper, Appendix 1). Manticoceratids and all other ammonoids disappeared at the end of the Frasnian, and no ammonoids have been found in the lowest Famennian *triangularis* and Lower *crepida* Zones in the Canning Basin (see Becker and House, Appendix 2). Unlike the metazoans, microbes survived the late Frasnian mass extinction virtually unscathed. *Renalcis* is prominent as a reef builder in both Frasnian and Famennian platforms, but non-skeletal microbes were even more important as reef builders in the Frasnian and Famennian platforms.

Deep-water stromatolites are conspicuous features of some marginal-slope deposits, especially above and immediately below the Frasnian–Famennian boundary. They may have thrived at that time because the latest Frasnian extinction events had removed most metazoans that would otherwise have consumed stromatolite-building microbes.

Boundstones of the reef-margin and reef-flat subfacies formed rigid frameworks that were subjected to strong early marine cementation which largely destroyed their primary porosities. On the other hand, large parts of the back-reef subfacies were not subjected to early cementation and when first buried they largely retained their high primary porosities. As a result, the tightly cemented reef and reef-flat deposits have been subjected to little or no post-depositional compaction, whereas the back-reef deposits have compacted considerably through pressure-solution (stylolitization), which destroyed most of their original porosities.

The rigid early-cemented reef-margin and reef-flat limestones were subjected to fissuring in response to earthquake shaking, slippage along underlying marginal-slope deposits, and differential compaction of underlying basin deposits over buried basement topography. The fissures were filled with sediment, calcite cement, and organic growths, forming networks of neptunian dykes. Although neptunian fissures developed mainly in reef limestones, they also formed in those parts of the back-reef and marginal-slope deposits that were subjected to early cementation.

Masses of terrigenous conglomerate interfinger with and extend through the reef complexes at various localities along the outcrop belt. They are highstand deposits that interfinger with platform, marginal-slope, and basin deposits and were laid down as alluvial-fan, fan-delta, and submarine-fan deposits in front of the scarps of active faults. Large volumes of sand and mud poured into basins adjoining the conglomerate bodies, so that the basin deposits are largely terrigenous.

The Lennard Shelf is bounded on one side by the Pinnacle Fault and its projection along a system of parallel faults, and on the other by the unconformity between Proterozoic basement and the Phanerozoic sedimentary succession. The overall structure of the area has resulted from extensional tectonics. Most of the larger faults trend northwest and show normal movements, throwing down to the southwest in the Phanerozoic, although some are thought to also have had strike-slip components during stages of their history. Between the northwest-trending normal faults there is a series of north-trending transfer faults in the Limestone Billy Hills and Horseshoe Range areas. Many of the faults were active during growth of the reef complexes in the Middle and Late Devonian, and fault activity continued strongly throughout the Carboniferous. Most of the Lennard Shelf area has been tectonically quiescent since the Early Permian, although a few faults have moved since then.

The largest fault in the area is the Pinnacle Fault, which moved as a normal fault during the Devonian, Carboniferous, and Permian, with a vertical displacement of as much as 7000 m. Its movement was reversed, to a much smaller extent, as a result of right-lateral wrenching of the Fitzroy Trough during the Mesozoic. That wrench faulting gave rise to the series of large anticlines in the Fitzroy Trough. Although the wrenching

seems to have had relatively little effect on faulting on the Lennard Shelf, the rocks there must have been subject to compression during that period, and some faults can be seen to have had small components of transcurrent movement that may have been associated with the wrench movements.

The area was subjected to glaciation by continental ice sheets, perhaps a few kilometres thick, during the Late Carboniferous and Early Permian. These glaciations had profound effects on the Devonian rocks. The tops of the limestone ranges were planed off by 'dirty' ice at the base of the ice sheets and were extensively karstified by the corrosive action of subglacial water under high pressures and subzero temperatures. Major cave systems, karst corridors, solution dolines, and subglacial channels, formed in the limestones below the ice sheets at that time.

In some areas, stromatolite–barite–sulfide exhalative deposits were formed at or immediately below the basin floor during the late Frasnian, over cool-fluid seepages driven by compaction of shales in the basin deposits. The expelled fluids carried dissolved carbonate, barium, iron, and reduced sulfur, and are thought to have nourished chemosynthetic bacteria that built stromatolites and deposited barite and iron sulfides.

Economic deposits of zinc and lead sulfides have been mined in several places along the reef belt, mainly in the southeastern part, at Pillara, Cadjebut, Goongewa, and Kapok. These deposits are thought to have been carried into the Devonian limestones by hot fluids expelled from shales deep in the Fitzroy Trough. They follow faults and hydrothermal caverns in the limestones. The age of this epigenetic mineralization is Early Carboniferous (early Tournaisian).

Several small oilfields have been located in late Famennian reef limestone and overlying deposits in the subsurface of the northwestern Lennard Shelf. The Famennian reef margin has been well defined in this area through conventional seismic surveys. Although Frasnian reef complexes are known from drilling to occur below the Famennian in this area, their detailed distribution cannot be delineated by 2-D seismic surveys. It is believed that Frasnian reef complexes have the best prospects for future oil discoveries, and it seems likely that they could be successfully delineated using 3-D seismic techniques.

KEYWORDS: Devonian, reef complexes, Canning Basin, Lennard Shelf, sequence stratigraphy, lithostratigraphy, carbonate facies, debris flows, allochthonous blocks, bioherms, conglomerates, cyclicity, mineralization, petroleum, paleokarst, Permian glaciation.

Introduction and historical review

Devonian reef complexes are spectacularly exposed in a series of rugged limestone ranges along the northern margin of the Canning Basin (Figs 1, 2). They form what is generally recognized as the world's best example of an ancient barrier-reef system. This system was named 'The Great Devonian Barrier Reef' by Teichert (1949) and has since become more widely known as the 'Devonian Great Barrier Reef' (Playford, 1970, 1980). As the Devonian carbonates are prospective for both minerals and petroleum, and are also of major academic significance, these rocks have been the subject of considerable exploration and research.

The first geologist to observe the reef complexes was E T Hardman in 1883. As the temporary Government Geologist of the colony of Western Australia he accompanied an expedition to the Kimberley District led by John Forrest, during which he examined the Devonian limestones at Windjana Gorge, Geikie Gorge, Mount Pierre, and adjoining areas (Hardman, 1884; Playford, 1972, 2005; Playford and Ruddock, 1985). Hardman suggested that the limestones were Carboniferous in age, but his fossil collection was soon identified as Devonian by Nicholson (1890), Hinde (1890), and Foord (1890). Hardman did not recognize that the limestone ranges constituted an ancient reef system.

The reefal origin of the Devonian limestones was first recognized by Wade (1924) who stated that the Pillara Range (then, with the Emanuel Range, known as 'Rough Range') appeared to be an ancient reef deposit. This was confirmed through his subsequent investigations for the Freney Kimberley Oil Company Ltd (Wade, 1936, 1938). He described the long belt of limestone ranges as being remnants of an ancient barrier reef (Wade, 1936). However, Wade was primarily interested in the petroleum prospects of the large anticlines in Permian rocks of the Fitzroy Trough, and the scope of his work did not permit more than a superficial examination of the Devonian rocks.

In 1940 and 1941, geologists of Caltex (Australia) Oil Development Pty Ltd carried out reconnaissance exploration in the northern Canning Basin, in order to assess its oil potential (Maddox, 1941; Findlay, 1942; Kraus, 1942). Curt Teichert, then at the University of Western Australia, studied paleontological material collected by the Caltex geologists, and participated in some of their field studies. He published a series of papers on the paleontology and stratigraphy of what he termed the 'Great Devonian Barrier Reef' (Teichert, 1939, 1940, 1941, 1943, 1947, 1949). Teichert was the first geologist to deduce that the platform limestones are facies equivalents

of adjoining basinal deposits, although he did not recognize the steep depositional nature of dips in strata adjoining the reefal limestones (Teichert, 1949).

The Commonwealth Bureau of Mineral Resources (BMR) undertook a regional geological mapping program in the Canning Basin from 1948 to 1952 (Guppy et al., 1958). They realized that the steep dips in strata adjoining the reefs are largely depositional, but did not recognize the equivalence of the various facies of the reef complexes. They thought that the Pillara Limestone, now regarded as the Givetian–Frasnian platform facies, was entirely Givetian in age, and considered that it was overlain unconformably by Frasnian strata that are now known to be its marginal-slope and basin equivalents (Fig. 3).

In 1956, geologists of West Australian Petroleum Pty Ltd (WAPET) undertook detailed studies of the Oscar Range reef complex (Smith et al., 1957; McWhae et al., 1958). They were the first to recognize the equivalence of reef, back-reef, and fore-reef deposits — a major breakthrough in the understanding of the reef complexes. They also recognized the importance of reef-building microbes, especially forms that they termed 'ghost algae' (now known as *Renalcis*). Further studies of the reef complexes were made at Windjana Gorge by WAPET (Playford and Johnstone, 1959a; Playford, 1961) and in association with WAPET (Wells, 1960). Playford and Johnstone were the first to describe the superb feature in the gorge that came to be known as the 'Classic Face'.

These pioneering studies formed the foundation on which subsequent research has been carried out by Geological Survey of Western Australia (GSWA) geologists and other research workers. Successive interpretations of the reef complexes, beginning with the study of Smith et al. (1957), are shown on Figure 3. The GSWA research program began with a regional study of the entire reef belt in 1962–63 (Playford and Lowry, 1966; Playford, 1967), and continued with detailed studies of the Bugle Gap and Windjana Gorge areas in 1968 and 1972. Reports on aspects of that work were published by Playford (1976a, 1980, 1981, 1984a), Cockbain and Playford (1988), and Playford and Cockbain (1989, 1992).

Logan and Semeniuk (1976) presented a radically different interpretation of the Devonian rocks, using a structural–metamorphic model rather than reef models (Fig. 3). They claimed that the Devonian rocks lie within a major shear zone; that the metamorphic grade is as high as greenschist facies; and that the boundaries between all rock units are major sinuous strike faults. According to their interpretations, steep-dipping 'homoclines', characterized by strong cataclastic metamorphism, adjoin stable blocks, termed 'idens'. Logan (1984) and Logan et al. (1994)

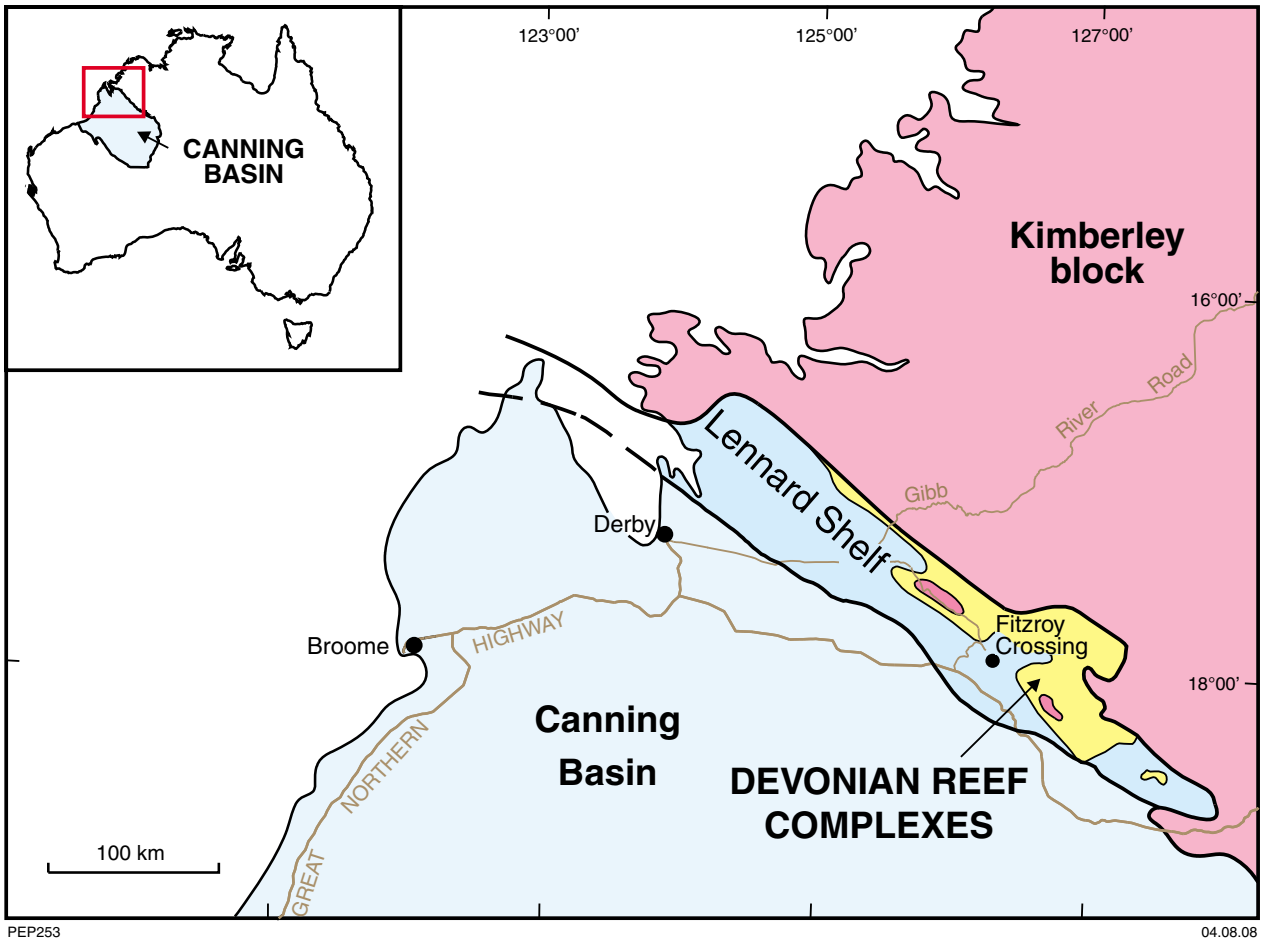

Figure 1. Locality map, Devonian reef complexes of the Canning Basin.

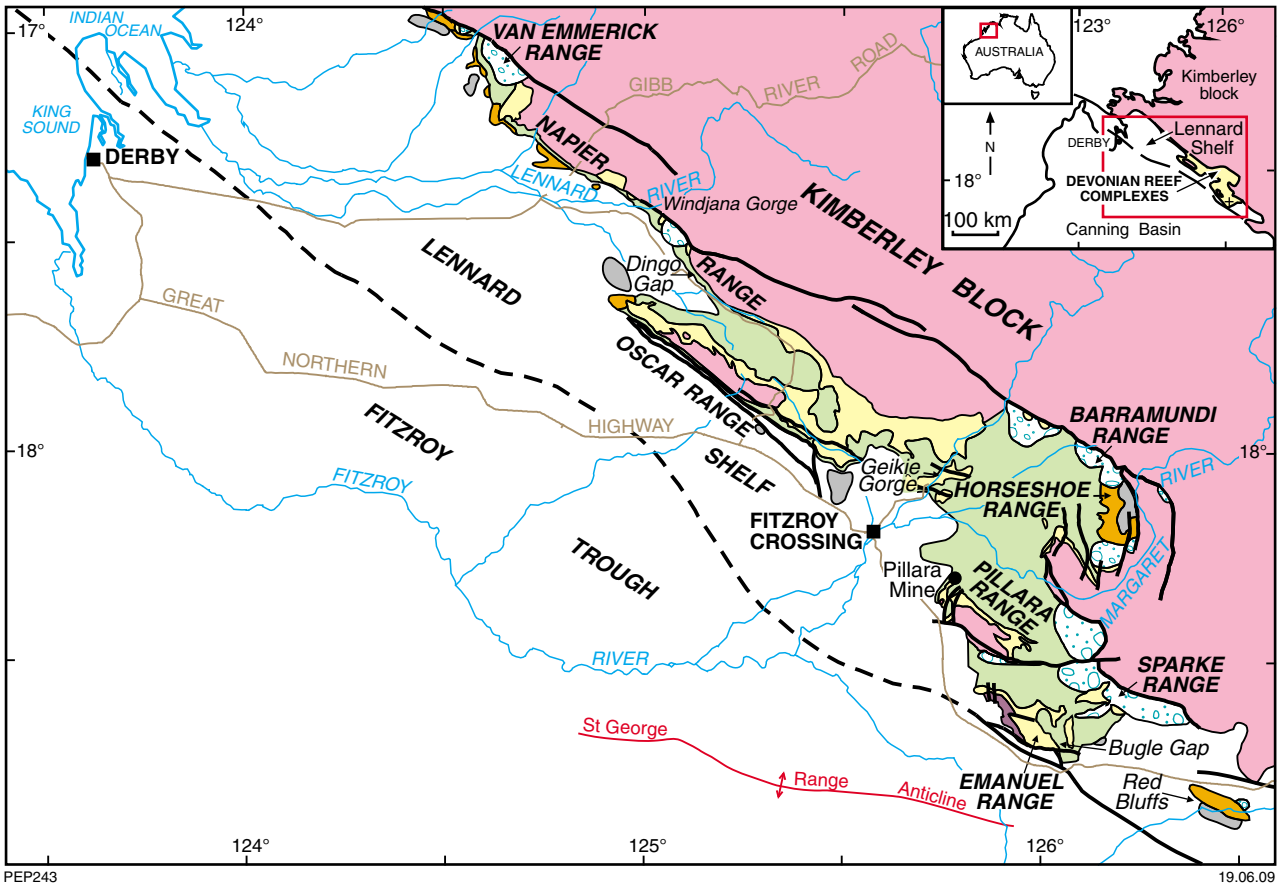

Figure 2. Generalized geological map, Devonian reef complexes of the Canning Basin.

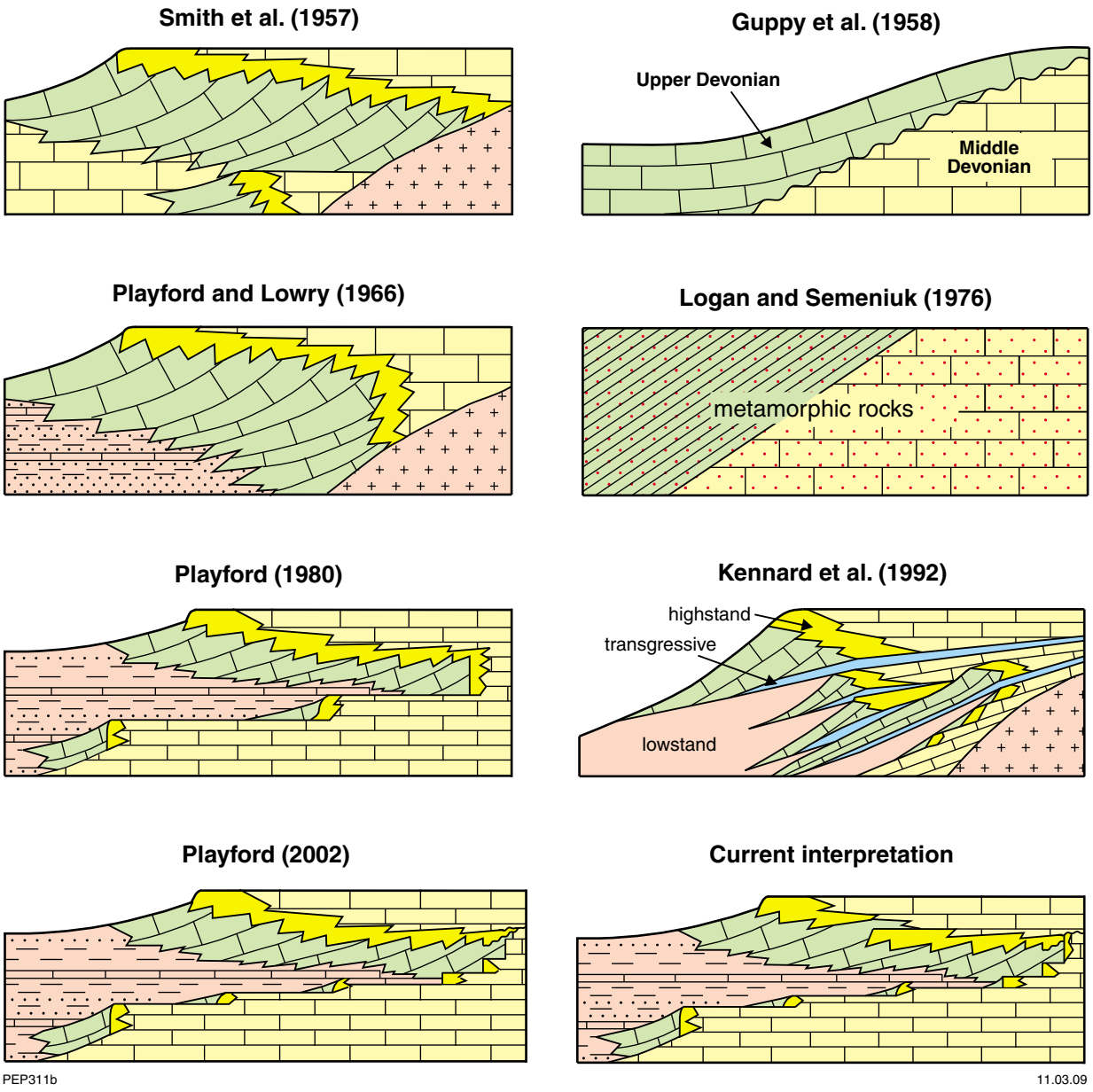

INTERPRETIVE MODELS OF THE REEF COMPLEXES 1957–2007

Figure 3. Diagram illustrating changing concepts in interpretation of Devonian reef complexes of the Canning Basin since 1957.

further extended those ideas. However, their interpretations have not been supported by other geologists who have studied the Devonian limestones (e.g. Playford, 1980; Kerans, 1985; Hurley, 1986; Wallace, 1987; Vearncombe et al., 1995a,b; Dörling et al., 1995; Ward, 1996). All of those other workers confirmed that the limestones form exceptionally well-preserved and unmetamorphosed reef complexes that have been subjected to relatively mild faulting, tilting, and folding. They showed that depositional fabrics are very well displayed, most platform margins are not faulted, and the steep dips in marginal-slope deposits are primarily depositional rather than tectonic.

Work by GSWA geologists on the reef complexes continued periodically during the 1980s and 1990s, including many collaborative projects with various universities and other organizations (including Petersen, 1975; Kerans, 1985; Hurley, 1986; Wallace, 1987; Playford et al., 1989; Pedone, 1990; Tornatora, 1992; Becker et al., 1993; Tompkins, 1994; George et al., 1994; Vearncombe et al., 1995a; Dörling, 1995; Ward, 1996; Klapper and Becker, 1999; Playford and Wallace, 2001).

In 1992, GSWA began a mapping program designed to produce a new series of more detailed geological maps and increase understanding of the reef complexes. This work was undertaken by Playford and Hocking, building on earlier detailed mapping by Playford and Cockbain in the Bugle Gap area (1968) and Playford at Windjana Gorge (1972). The principal biostratigraphic components of the program were conducted by Gilbert Klapper (conodonts) and Thomas Becker and Michael House (ammonoids), with results published by Klapper (1995, 1997b, 2000, 2007), Klapper and Becker (1999), Becker et al. (1991, 1993) and Becker and House (1997).

Summaries of knowledge of the conodont and ammonoid faunas and palynology are given in Appendices to this Bulletin by Gilbert Klapper (Appendix 1, conodonts), Thomas Becker and Michael House (Appendix 2, ammonoids), and Geoffrey Playford (Appendix 3, palynology).

Subsurface studies were undertaken by GSWA to collate and interpret data obtained through extensive company drilling for minerals (Copp, 2000) and petroleum (Crostella, 1998b). The field mapping program resulted in the production of eight geological maps of the reef belt, forming Plates 1–8 in the present Bulletin, the first seven of which were released in 1999 (Playford and Hocking, 1999a). A further map, at 1:500 000 scale, is also included in this Bulletin (Plate 8). Publications resulting from the recent research program include those by Hocking et al. (1996), Copp (2000), Playford and Wallace (2001), Hocking and Playford (1988a–d), Playford and Hocking, (1998a,b), Hocking and Playford (2001, 2002), and Playford (2002a,b).

The primary objective of the present Bulletin is to integrate the results of field research by GSWA and its co-workers. Some illustrations and parts of the text are derived from publications by Playford and Lowry (1966), Playford and Cockbain (1976), Playford (1980), Playford (1981), Playford (1984a), Kerans et al. (1986), Wallace et al. (1991), Playford and Wallace (2001), and Playford (2002a).

Successive advances in understanding of the reef complexes, outlined in various reports and publications since 1957, may be summarized as follows:

Recognition of:

- the facies equivalence of platform, marginal-slope, and basin deposits, the significance of steep depositional dips in marginal-slope deposits, and the major role of microbes in development of the reef complexes (Smith et al., 1957; Playford and Johnstone, 1959a);
- precise biostratigraphic zonations of slope and basin deposits using conodonts and ammonoids (Glenister, 1958; Glenister and Klapper, 1966);
- the interrelationships between carbonate facies of the reef complexes and contemporaneous conglomerates (Playford and Johnstone, 1959a; Playford and Lowry, 1966; Hocking and Playford, 2002);
- fracturing of early-cemented limestones resulted in networks of neptunian dykes, platform-margin collapse, and major debris-flow deposits (Playford and Lowry, 1966; Playford, 1980);
- the importance of contemporaneous tectonism and sea-level change in controlling development of the reef complexes (Playford and Lowry, 1966; Playford, 1984a, 2002a);
- the use of geopetal structures in quantifying depositional dips, deducing water depths, and recognizing allochthonous blocks (Playford and Cockbain, 1969; Playford, 1980);
- differential compaction of the various carbonates controlled by degrees of stylolitization (Playford, 1969, 1980);
- deep-water stromatolites and large microbial and receptaculitid bioherms that grew in water more than 100 m deep (Playford and Cockbain, 1969; Playford et al., 1976);
- The Frasnian–Famennian unconformity and mass extinction (Playford, 1984a, 2002a)
- well-developed cyclicity in back-reef deposits (Read, 1973a; Playford, 1976a);
- two major phases of reef building, giving rise to the Givetian–Frasnian Pillara Sequence and the Famennian Nullara Sequence (Playford and Cockbain, 1976; Playford, 2002a);
- well-defined cement stratigraphy in the reef limestones (Kerans 1985; Wallace et al., 1991);
- backstepping episodes defining the detailed sequence stratigraphy of the reef complexes (Ward, 1999; Playford, 2002a);
- major stromatolite mounds formed over cool-water seepages on or immediately below the sea floor, with associated barite and iron-sulfide mineralization (Playford and Wallace, 2001);

- the role of the Permian glaciation in planation of the reef complexes and forming subglacial karst, caverns, solution dolines, and subglacial channels (Playford, 2002a).

Localities

Grid references in this publication are referred to the Australian Geodetic Datum (AGD84). Locations mentioned in the text quote Australia Map Grid (AMG) coordinates because the maps accompanying this Bulletin are referred to that datum. Coordinates derived from recent GPS observations are noted as such, and have been converted to AMG using GDAit and Western Australia grid files. As the reef complexes span the boundary between Zones 51 and 52, the zone concerned is noted in each grid reference, to avoid ambiguity. The accuracy of each reference reflects its data source, with locations derived from maps or air photos being given to the nearest 100 m, and locations directly from recent GPS readings being given to the nearest 10 m.

Regional geology

The Devonian reef complexes form a series of rugged limestone ranges that extend along the northern margin of the Canning Basin in a belt some 350 km long and as much as 50 km wide (Figs 1, 2). The Canning Basin is the largest Phanerozoic sedimentary basin in Western Australia, covering an area of more than 500 000 km^2, and containing at least 13 000 m of Ordovician to Cretaceous sedimentary rocks (Veevers and Wells, 1961; Playford et al., 1975; Towner and Gibson, 1983; Purcell, 1984; Middleton, 1990). The reef complexes may have originally extended for more than 1000 km around the western and northern sides of the mountainous Kimberley block, linking with similar Devonian reef complexes that are exposed in the Bonaparte Basin (Fig. 4; Playford, 1980; Mory and Beere, 1985, 1988).

The reef complexes occur in a structural subdivision of the Canning Basin known as the Lennard Shelf (Playford and Johnstone, 1959b; Figs 1, 2), which is bounded to the southwest by the Fitzroy Trough, a deep fault-bounded trough of Paleozoic sedimentary rocks, and to the northeast by Proterozoic rocks of the King Leopold and Halls Creek Orogens and the Kimberley Basin, which together are here referred to as the Kimberley block**.** The boundary between the Fitzroy Trough and the southeastern part of the Lennard Shelf is defined by the Pinnacle Fault, which has a maximum vertical displacement of about 6000 m. This fault parallels major shear zones along the southwest margin of the King Leopold Orogen (Griffin and Tyler, 1995), and is assumed to be an inherited Proterozoic structure that was reactivated through extensional normal movement during the Middle and Late Devonian. Movement along this fault is thought to have been normal during the Paleozoic, and reverse during the Mesozoic, associated with right-lateral wrenching of the Fitzroy Trough (Rattigan, 1967; Smith, 1968; Kennard et al., 1994; Dörling, 1995).

The reef complexes grew in Middle and Late Devonian times (Givetian, Frasnian, and Famennian), as a series of fringing reefs, atolls, and banks along the mountainous mainland shore of the Kimberley block and around rugged islands of Proterozoic metasedimentary and igneous rocks. The Emanuel Range reef complex grew on a fault block of Ordovician rocks. Low-relief banks, lacking reef rims, developed in some areas, especially during the late Givetian, but most Late Devonian platforms had well-developed reef rims. The maximum thickness of the reef complexes is estimated to be at least 2500 m.

The Devonian platforms ranged from extensive bodies covering hundreds of square kilometres to small platform atolls and pinnacle reefs. Water depths over the platforms are thought to have generally been less than 5 m, and were intertidal in some areas. Most of the exposed platforms throughout the reef belt are Late Devonian (Frasnian and Famennian) in age, but Middle Devonian (Givetian) strata are also present at the base of platforms in the Emanuel and Pillara Ranges. The most extensive platforms grew in the Famennian, but these have now largely been removed by erosion. The principal remaining outcrops of Famennian platforms are in the northern Napier Range, the northwestern Oscar Range, and the Horseshoe Range (Plates 1–4, 6–8).

Some faults were active in the area during growth of the reef complexes in the Middle and Late Devonian, coinciding with a major phase of the Alice Springs Orogeny in central Australia. The mountainous terrain may have had several thousand metres of relief. Watercourses that drained the mountains deposited masses of conglomerate and finer terrigenous debris that interfingered with or passed through the reef complexes. The main bodies of conglomerate form conspicuous ranges, especially the Van Emmerick, Barramundi, and Sparke Ranges.

Reef growth ceased during the late Famennian, after an abrupt regression that resulted in relatively brief exposure and erosion of the reefal platforms. The extinct reef complexes were then covered by the Upper Devonian (Famennian) to Lower Carboniferous (Tournaisian) Fairfield Group (Thomas, 1959; Druce and Radke, 1979; Balme and Hassell, 1962; G Playford, 1976).

The reef complexes were further deformed through Carboniferous faulting, tilting, and mild folding, and were planed down to a near-level surface during the middle Carboniferous to Early Permian by a succession of continental ice sheets (Playford, 2002a). Throughout most of the outcrop area the Devonian rocks are overlain with angular unconformity by shale, sandstone, and glacial deposits of the Lower Permian Carolyn Formation, at the base of the Grant Group (Apak and Backhouse, 1998). The near-horizontal glaciated surface was subjected to deep karstification by subglacial water, with caves, karst corridors and karst depressions extending as much as 200 m or more below the glaciated surface (Playford, 2002a). Sedimentary rocks (largely shale, siltstone, and sandstone) of the Carolyn Formation overlying the glacial unconformity have been largely stripped away by Mesozoic and Cenozoic erosion, leaving the eroded reefal platforms as flat-topped limestone ranges, with softer basin

deposits in the intervening valleys. Most of the Devonian conglomerate ranges stand as much as 100 m above the level of the adjacent reef complexes, presumably reflecting the greater resistance of conglomerates to erosion below ice.

Small lamproite plugs of Miocene age, known as the Fitzroy Volcanics, have intruded the Paleozoic and Proterozoic rocks in the area (Prider, 1960; Jaques et al., 1986). They range from less than 100 m to 1.8 km across. Several lamproite plugs adjoining the northwest end of the Oscar Range, known as the Ellendale Vents, are diamond bearing (Jaques et al., 1986), and some are currently being mined.

Sections through the reef complexes are well exposed in gorges where rivers and streams pass through the limestone ranges, the most spectacular being Windjana, Geikie, and Brooking Gorges. Detailed studies of these gorges and other key localities are described individually in this Bulletin.

Geomorphology

The limestone ranges of the West Kimberley District extend for about 350 km, from the Napier Range in the northwest (Plate 1) to Bugle Gap and Red Bluffs in the southeast (Plates 4, 5, 7, 8). They constitute one of the major karst areas of Australia. The geomorphology of the ranges has been discussed by Jennings and Sweeting (1961, 1963), Playford and Lowry (1966), Goudie et al. (1989), Viles and Goudie (1990), and Playford (2002a), among others.

The climate of the area of Devonian outcrop is tropical semi-arid, with mild dry winters and hot wet summers. The annual rainfall ranges from about 800 mm at the northwest end of the Napier Range to less than 500 mm near Bugle Gap. Approximately 85% of the rain falls during the summer, from November to March, when the plains adjoining the ranges are subjected to periodic flooding. River and creek beds are mostly dry during the winter, apart from temporary pools and some larger bodies of permanent water, such as those in Geikie, Brooking, and Windjana Gorges. Many picturesque springs, some permanent, issue from the limestone ranges.

Conditions for field work are pleasant in winter (the 'dry season') from June to August, when the humidity is low and maximum temperatures during the day generally range from about 25º to 35ºC. However, field conditions are unpleasant during most of the spring, summer, and autumn (the 'wet season'), from September to May, when the humidity is high, maximum temperatures range from about 35º to 45ºC, and sporadic heavy rain occurs. In addition, roads and tracks over black-soil plains adjoining the ranges often become impassable because of boggy conditions.

Limestone ranges

The limestone ranges commonly rise about 30 to 80 m above the surrounding plains They are characterized by rough karst topography, with sharp ridges and karren formed by modern subaerial karstification, and deep karst corridors (grikes) formed along joints by subglacial solution under the Early Permian ice sheet and modified by modern subaerial processes (Playford, 2002a). In some places it is impracticable or dangerous to traverse the ranges on foot.

The major part of the limestone ranges consists of platform facies (reef, back-reef, and bank subfacies) and marginal-slope facies of the reef complexes, with interbedded and interfingering terrigenous clastic deposits, especially in areas adjoining conglomerate bodies and the Kimberley block. The basin facies is essentially absent from the ranges, being largely confined to the valleys, where it is rarely exposed. The present-day topography mimics that of the Devonian sea floor, so that from the air it might appear that the sea has only recently withdrawn from the area, leaving the reefs standing up in their original form (Figs 5–7).

The strongly karstified upper surface of each limestone range is nearly horizontal, ranging from about 150 to 250 m above sea level. These level surfaces mark the exhumed Early Permian unconformity, which formed by planation and karstification below the last of a series of middle Carboniferous to Early Permian ice sheets. The Early Permian glacial surface has been exhumed and modified by Cenozoic erosion, and the modern karst has incorporated many features of the ancient subglacial karst (Playford, 2002a).

A feature of the slopes of many hills in the limestone ranges and the valleys between them is the occurrence of thin discontinuous calcrete layers, generally pale yellow, that partially cover the ground surface. Fragments of adjacent limestones are frequently bound into the calcrete by concentric layers of cement. A typical example is shown in Figure 8. The calcrete may record a more pluvial climate in the area during the recent past, but no research has yet been carried out on this topic. There is also a potential for paleoclimatological research on the massive tufa deposits that are associated with present and former water seepages in the area (Viles and Goudie, 1990). Some of the tufa deposits appear to have formed during more pluvial periods in the recent past.

A common feature of the black-soil plains is the occurrence of patterned ground, resulting from repeated swelling of the clayey soils during the summer wet season and shrinking when they dry out in winter (Fig. 9).

Bush fires are important agents in erosion of the limestone. Dense spinifex, which commonly adjoins the limestone outcrops, is highly inflammable, largely because of the resin that it contains. When lit with a match a clump of growing spinifex will burst into flames, which may extend as much as five metres high and cause adjoining limestone surfaces to exfoliate. Fire is thus a major pediment-forming agent around the limestone ranges.

Conglomerate ranges

The conglomerate ranges consist of gently to moderately sloping masses of conglomerate, rising as much as 100 m above the adjacent limestone ranges, and forming a

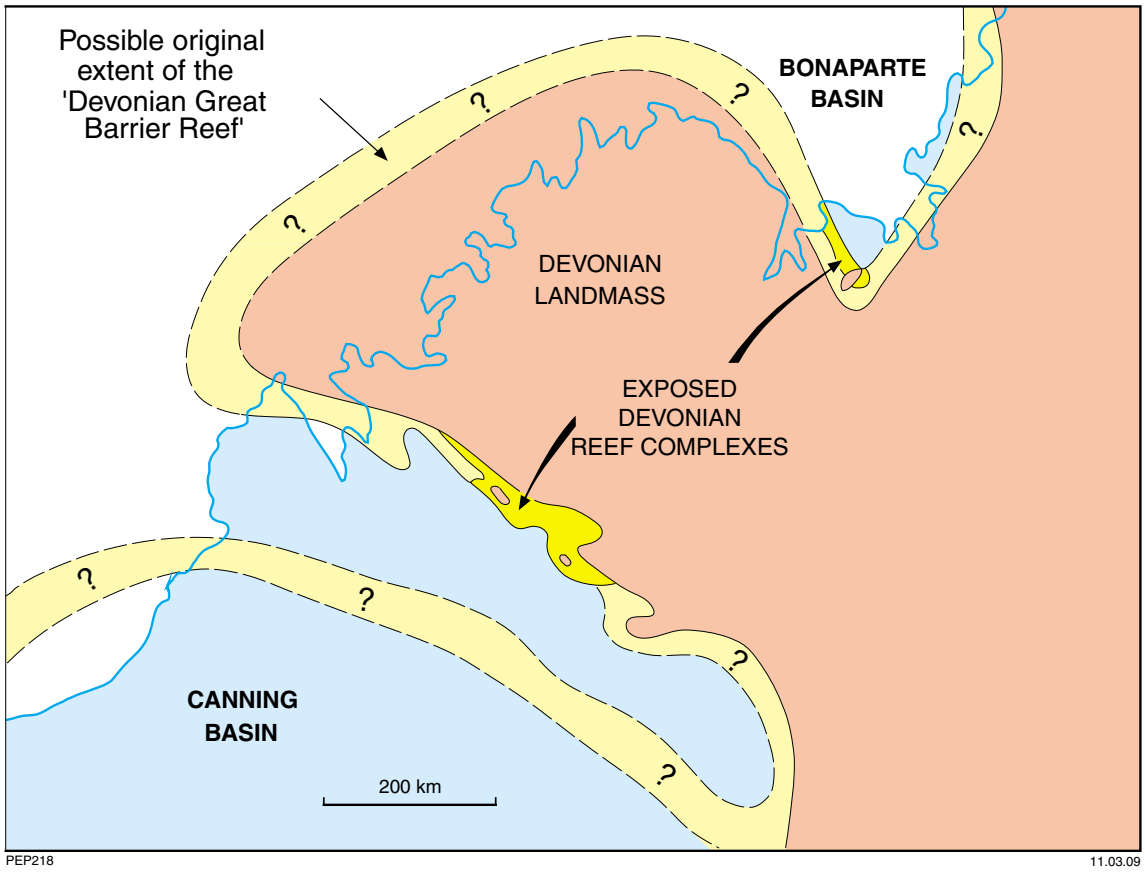

Figure 4. **Map of the Kimberley district showing the possible original extent of the 'Devonian Great Barrier Reef' in the Canning and Bonaparte Basins.**



Figure 5. **Aerial view of the northwestern Napier Range reef complex, looking southeast. The reef complex winds across the countryside, mimicking its form during the late Famennian. Hawkstone Creek is in the foreground, Unggumi Promontory is in the right middle distance, and the Van Emmerick Range is in the left middle distance.**



Figure 6. Aerial view of the Napier Range at Windjana Gorge looking northwest. The sinuous front of the range is essentially the late Famennian reef scarp.

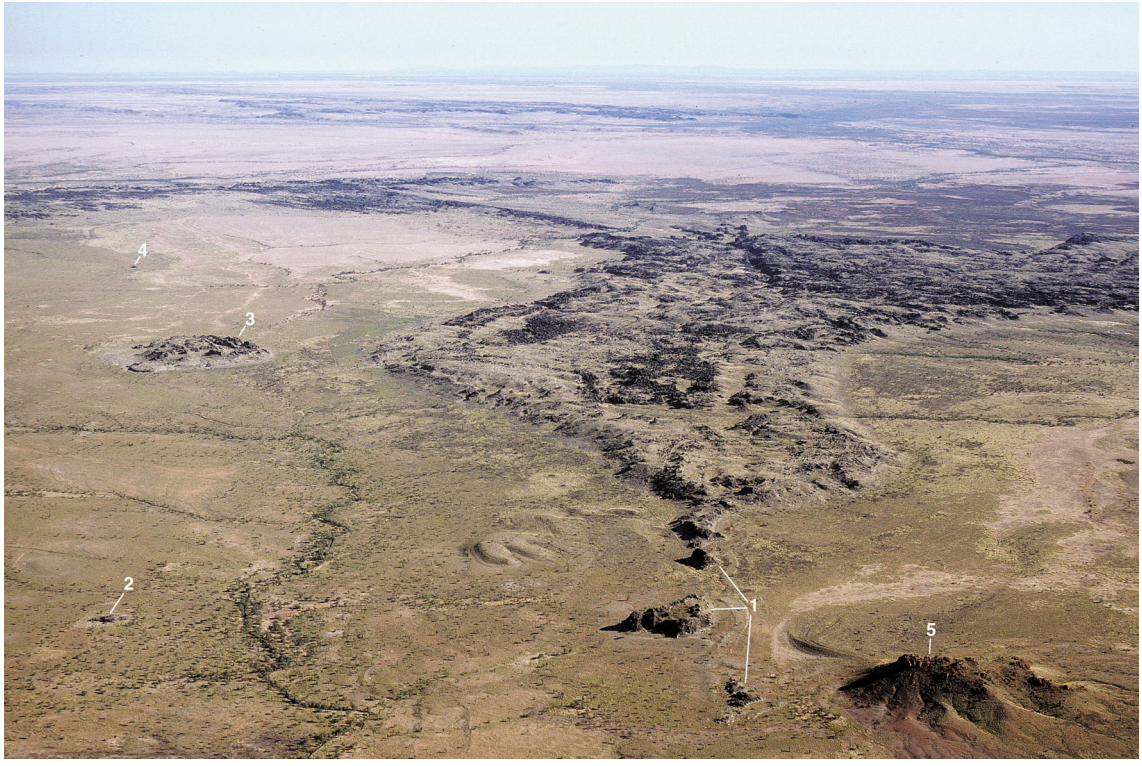

Figure 7. Aerial view looking north over the Laidlaw Range reef complex, showing its 'tail' of Glenister Knolls patch reefs (arrow 1). On the left are Smith Knoll pinnacle reef (arrow 2), Lloyd Hill atoll (arrow 3), and Wade Knoll pinnacle reef (arrow 4). Ross Hill (arrow 5), is composed of Lower Permian sandstone, which unconformably overlies the reef complex.

characteristic rolling topography (Fig. 10). The hills are generally clad by residual lags of boulders and cobbles of Precambrian rocks.

Flora

Most parts of the ranges consist of bare limestone, with vegetation restricted to patches of soil in narrow corridors and other depressions. This vegetation is dominated by spinifex (*Triodia* spp.), with a few trees, mainly eucalypts, *Bauhinia*, figs (*Ficus* spp.), grevillias, and wattles (*Acacia* spp.). Boab trees (*Adansonia gregorii*) are attractive features of the limestone ranges and adjoining plains in the western part of the area, extending from the Napier Range to Fossil Downs (Fig. 11). Cycad palms are rare elements of the flora, being restricted to Cycad Hill in the Napier Range and a few karst corridors in the southwestern Oscar Range (Fig. 12).

The limestones are for the most part covered by thin dark-grey films of epilithic and endolithic microbes, which play important roles in corrosion of the limestones. The opaque microbial films largely obscure details of the limestone on which they grow. The films are absent from paths frequented by kangaroos, whose acidic excrement is effective in killing the microbes, leaving clean exposures of limestone. From this observation it was deduced that the microbial films might be removed from outcrops with acid. This method, using concentrated hydrochloric acid, proved to be very effective, allowing details of the rock to be clearly displayed. The microbes are very slow growing, and when they have been removed by acid they do not re-colonize the limestone surfaces for many years — some surfaces subjected to acid treatment in 1968 (at McWhae Ridge) remain free from microbial cover today. The limestone also lacks microbial films in places where hot bushfires have swept over the limestone surfaces, causing them to exfoliate, as previously discussed. That observation suggested another method of removing microbial films, by using a blowtorch. However, surfaces heated in this way tend to explode, showering the operator with red-hot splinters of limestone. Consequently this method was not continued.

Conglomerate ranges in the eastern part of the area support little vegetation other than spinifex. The density of trees growing on those ranges rises progressively with increased rainfall from southeast to northwest. Thus, there are virtually no trees on the Sparke Conglomerate (in the southeast), whereas the lithologically similar Van Emmerick Conglomerate (in the northwest) has a well-developed tree cover. Alluvial plains adjoining the limestone and conglomerate ranges support a savannah-grassland vegetation, with the density of trees (mainly species of *Eucalyptus*, *Acacia*, and *Bauhinia*) increasing progressively from southeast to northwest.

Fauna

The most conspicuous fauna of the area now consists of non-indigenous species, especially cattle, horses, and cats. Feral donkeys were once very numerous (providing a primary food source for geologists), but they have now largely been eliminated as a result of an eradication program by the State Government. Kangaroos and wallabies are common in some areas, but the numbers of some species, especially the little river kangaroos, have declined significantly in recent years. Dingoes are occasionally seen and can sometimes be heard howling at night. The freshwater crocodile, *Crocodylus johnsoni*, is abundant in Windjana and Geikie Gorges (Fig. 13), and is occasionally found in isolated springs and waterholes. Other reptiles are sparse to common, including various lizards and snakes (including the highly venomous King Brown and Death Adder, and large, but harmless, pythons). Termite mounds are prominent features of the plains and conglomerate ranges, some of the tallest being in the Sparke Range (Fig. 14).

Birds of the area are abundant and diverse, especially around bodies of permanent water. Some species have apparently survived the impact of European settlement without major adverse effects, but it is noticeable that bustards (bush turkeys) have become fewer in recent years, and emus have almost disappeared.

Human occupation

The limestone ranges of the Devonian reef complexes are currently included in pastoral leases (for cattle) and conservation reserves (for national parks and conservation parks). Tenements for mineral exploration and mining cover some areas. Derby (population about 5000) and Fitzroy Crossing (population about 1500) are the only towns in the area.

The limestone ranges and associated gorges are among the principal tourist attractions of the Kimberley. Large numbers of tourists from Australia and overseas now visit Windjana Gorge, Geikie Gorge, and Tunnel Creek every year, and those numbers can be expected to increase substantially in the future. Other features of the Devonian Great Barrier Reef that may warrant increased tourism, provided appropriate conservation measures are in place, include Mimbi Caves, Brooking Gorge, Galeru Gorge, the Oscar Range, and Aboriginal rock-art sites. It will be important to ensure that if tourism is allowed in those places, practical measures are taken to safeguard the natural environment and cave art.

Prior to the arrival of British colonists during the 1880s, the area in and around the limestone ranges had been occupied by Aboriginal people for more than 40 000 years (O'Connor, 1995). Three tribes (language groups) — *Unggumi*, *Bunaba*, and *Gooniyandi* (*Kuniandi*) — were then living in the area (Playford, 1960, 2007; Fig. 15). No accurate information is available on Aboriginal population numbers when the whites first arrived, but about 2000 seems to be a reasonable estimate. Elkin (1932) suggested that the Kimberley district as a whole had a population of about 10 000 Aborigines prior to European colonization. The numbers declined rapidly after colonization, largely as a consequence of introduced diseases. The last *Unggumi*-speaking person (Billy Munro), died in 1993, but the



Figure 8. Pavement of Quaternary (?Pleistocene) calcrete conglomerate in the creek immediately north of Kellys Pass.



Figure 9. Patterned ground in black-soil plain, looking east near Big Dam Bore.

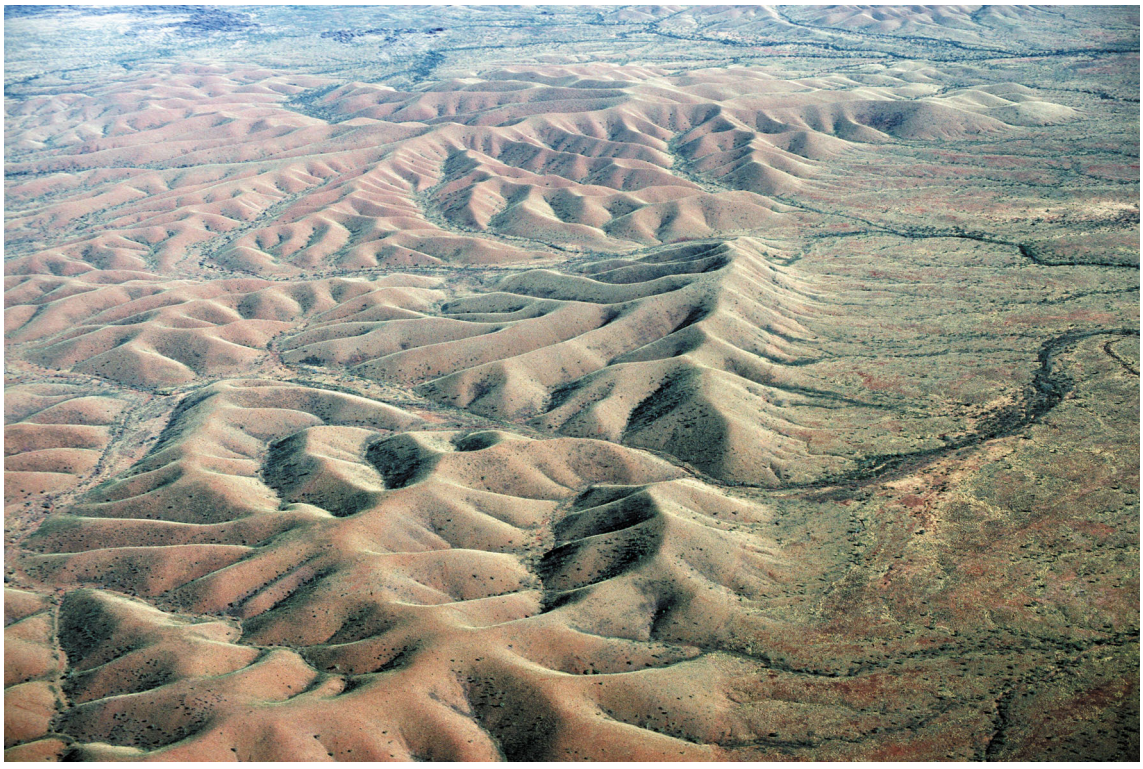

Figure 10. Sparke Range looking west-northwest, showing the characteristic morphology of Devonian conglomerate ranges in the Canning Basin. The Sparke Range Fault separates the Sparke Conglomerate, forming the rounded hills on the left, from Precambrian rocks with subdued topography on the right.

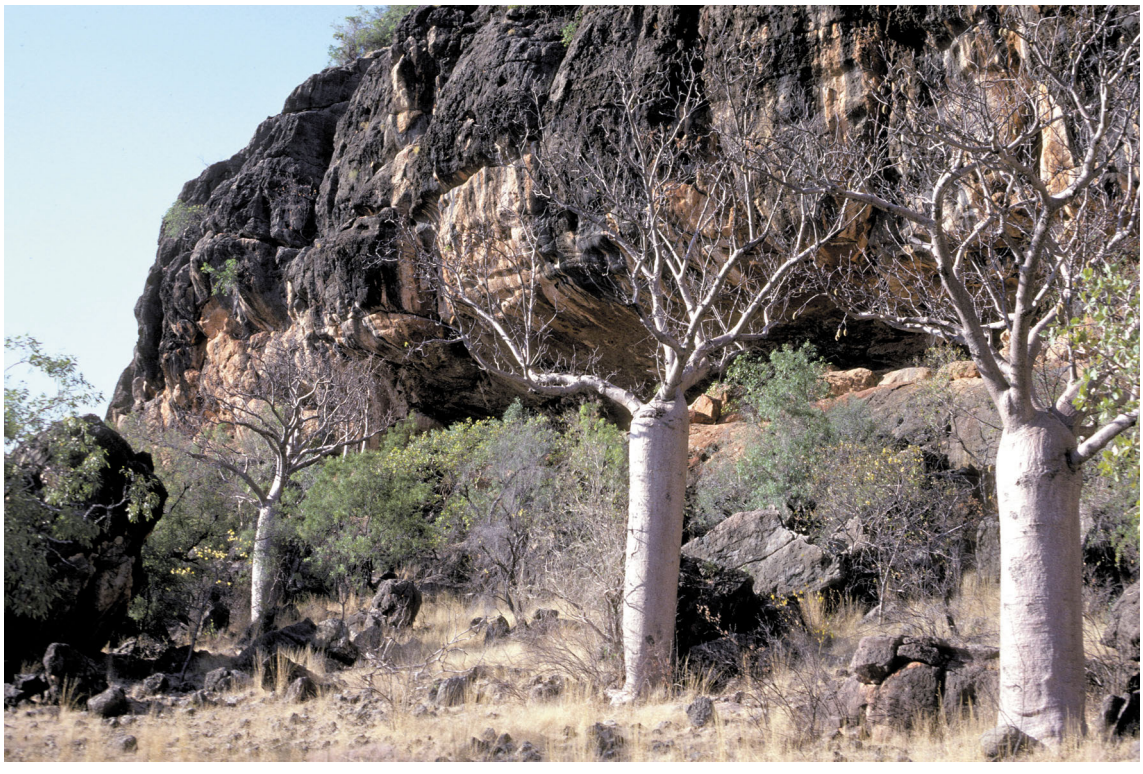

Figure 11. *Langurrngurru* cliff and cave in Pillara Limestone near Windjana Gorge, showing the large boab trees that are so typical of this area. The cave beneath the large overhang contains a large *Wandjina* painting, which is also named *Langurrngurru.*



Figure 12. Cycad palms in a karst corridor in Pillara Limestone, southwestern Oscar Range.



Figure 13. Fresh-water crocodiles (*Crocodylus johnsoni*) near the west entrance to Windjana Gorge. The largest of these reptiles is about 2 m long.



Figure 14. Tall termite mound near Lawford Spring, Sparke Range.

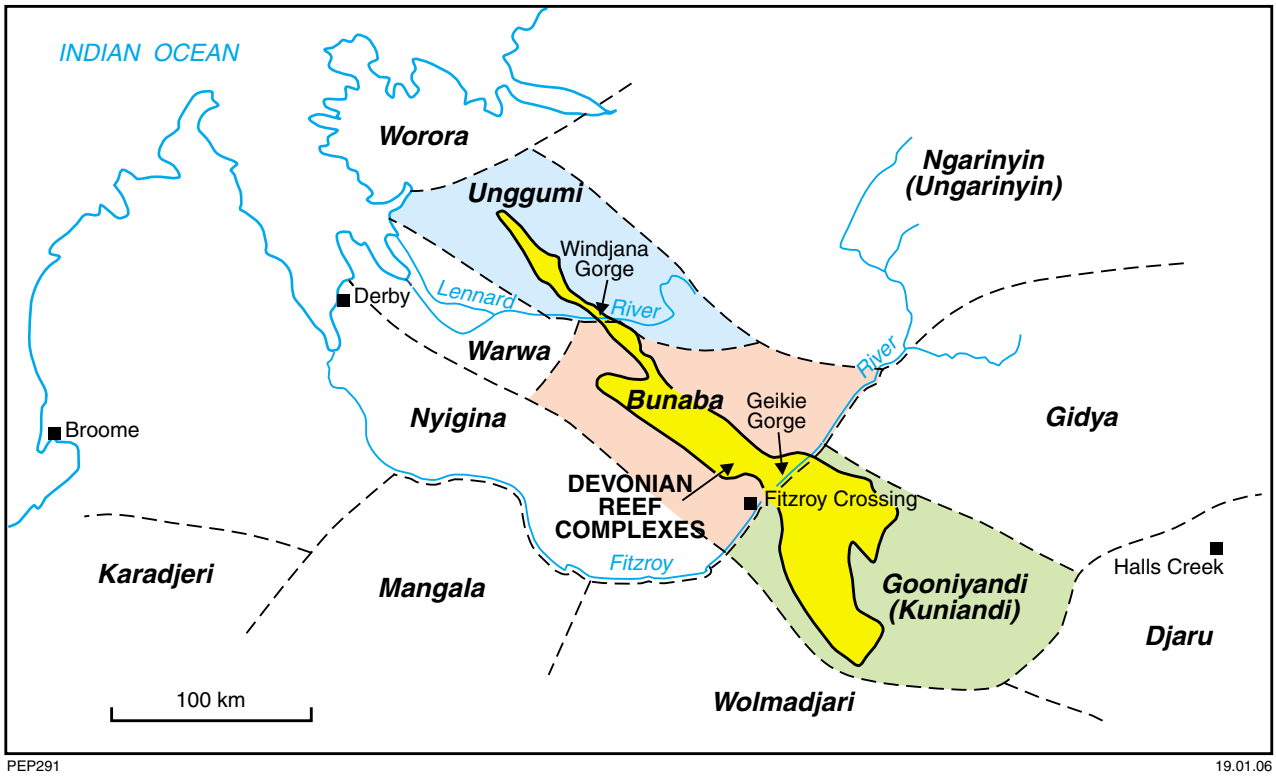

Figure 15. Tribal distribution map of the southern Kimberley area (modified after Playford, 1960) showing the areas occupied by Aboriginal tribes (language groups) prior to European settlement, highlighting the territories of the *Unggumi*, *Bunaba*, and *Gooniyandi* tribes over the Devonian limestone ranges.

Bunaba and *Gooniyandi* are now increasing in numbers, largely because of improved health conditions and high birth rates. Most Aboriginal people in the area now live in Fitzroy Crossing, Derby, outlying community settlements, and Aboriginal-owned pastoral stations; they no longer follow traditional hunter–gatherer lifestyles.

Caves in the limestone ranges were used by the Aborigines as dwellings, rock-art galleries, and tombs for the dead (Playford, 1960, 2007). Most Aboriginal names for topographic features in the area are now lost, but many were obtained by Playford from Aboriginal elders, and are shown on Plates 1–7.

Devonian reef complexes

The Devonian facies, lithostratigraphy, and sequence stratigraphy of the reef complexes are shown in Figures 16–21 (modified from Playford, 2002a). The reef complexes were formed as limestone platforms, generally fringed by reefs and flanked by steeply dipping marginal-slope deposits. A few platforms were banks, lacking reef rims or having only sporadic reef development around their margins. Marginal slopes flanking the platforms descended to the surrounding basin floors in depths estimated to have ranged from about 50 to at least 300 m. Most platforms were originally flat topped, but many are now concave because of differential compaction of the platform interiors through pressure solution (Fig. 22).

Facies

The main facies units recognized in the reef complexes are shown on Figures 16 and 17 (modified from Playford, 2002a). The three basic facies are referred to as platform, marginal-slope, and basin facies. The platform facies is subdivided into reef-margin, reef-flat, back-reef, bank, and pinnacle-reef subfacies, while the marginal-slope facies is subdivided into reefal-slope, fore-reef, and fore-bank subfacies. The basin facies is not subdivided.

The platforms range from extensive bodies covering hundreds of square kilometres to small platform atolls and pinnacle reefs. The platform-building organisms were dominated by microbes, stromatoporoids, and corals in the Givetian and early Frasnian, by microbes and stromatoporoids in the middle and late Frasnian, and almost solely by microbes in the Famennian.

The reef-margin and reef-flat subfacies form narrow zones, discontinuous in some places, around the margins of most platforms. The reef-margin subfacies is massive and ranges from a few metres to a few hundred metres wide. It is usually backed by wider reef-flat subfacies which is crudely bedded to well bedded. Contacts between reef-margin, reef-flat, and back-reef subfacies are generally interfingering or gradational.

The reefs were constructed by microbes and metazoans. They were lithified penecontemporaneously by submarine cementation to form rigid wave-resistant bodies. The well-

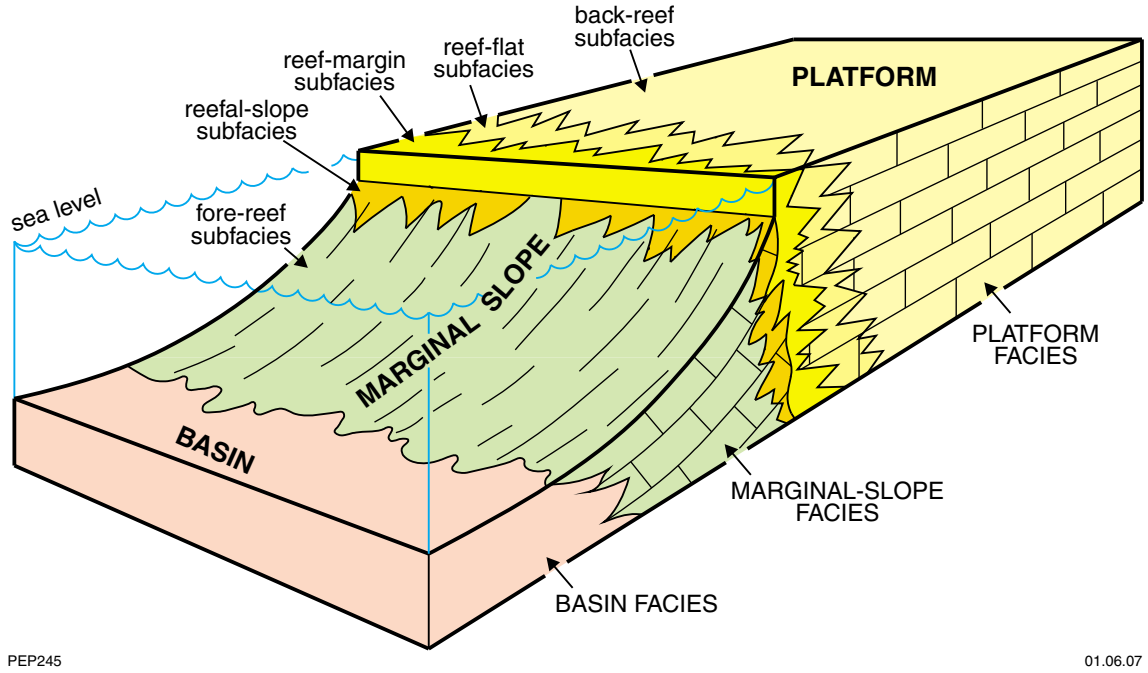

Figure 16. Block diagram illustrating the morphology of the reef complexes and relationships between platform, marginal-slope, and basin facies.

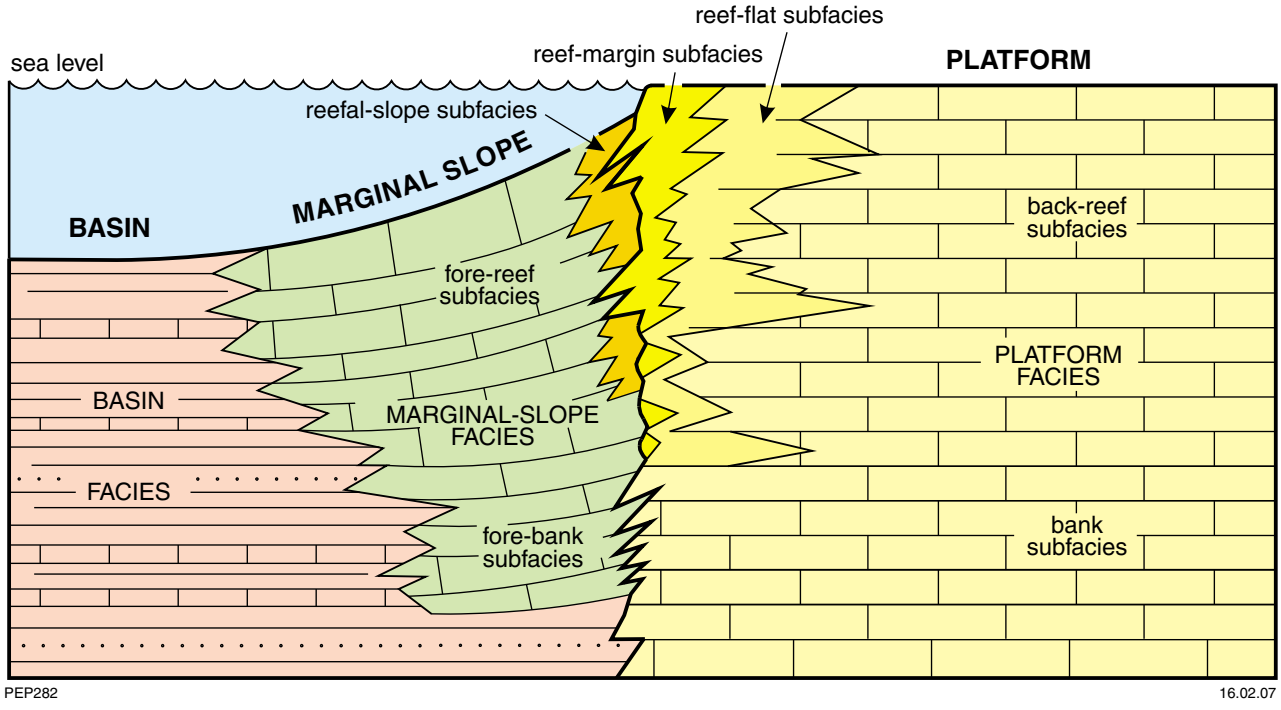

Figure 17. Diagrammatic cross section illustrating the morphology and facies relationships of the reef complexes.

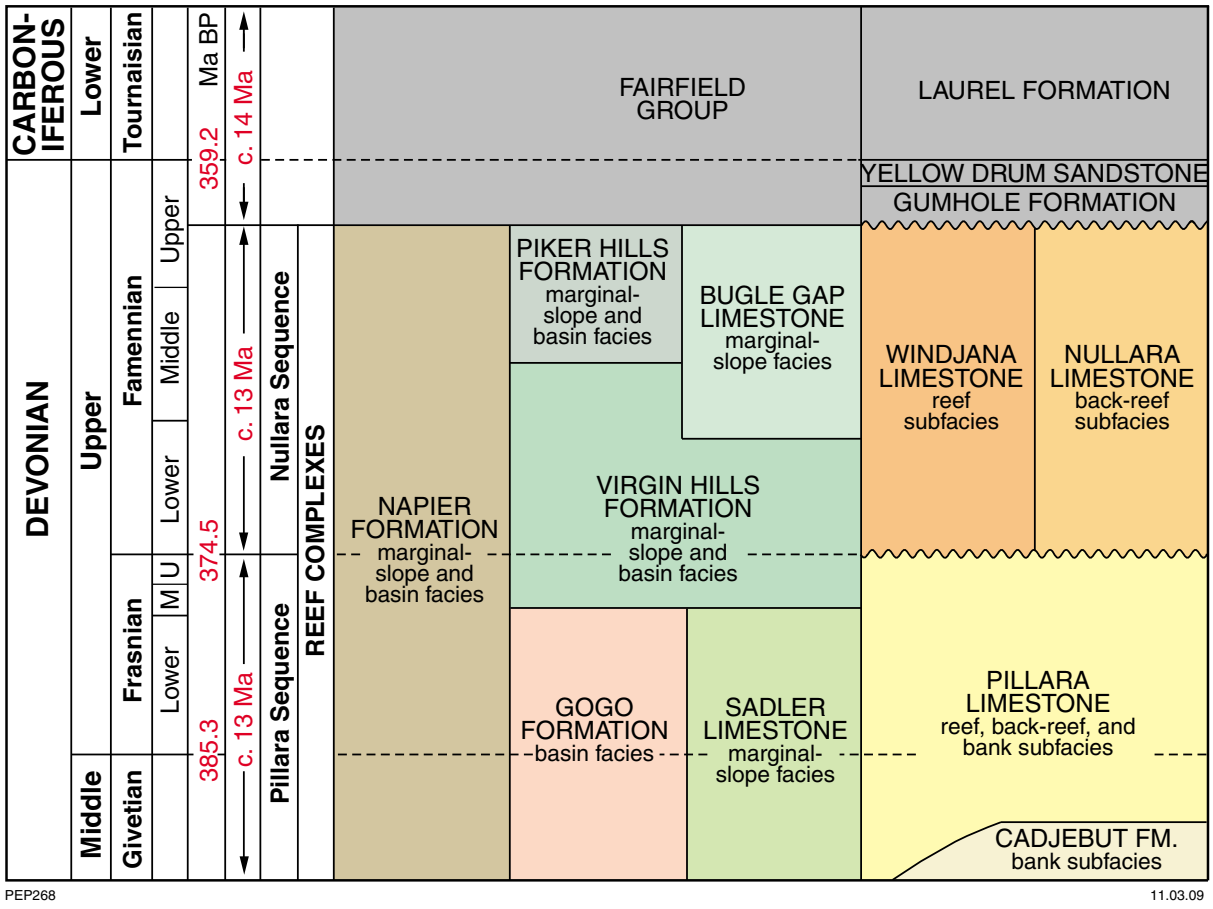

Figure 18. Correlation chart of Devonian and Lower Carboniferous units on the Lennard Shelf.

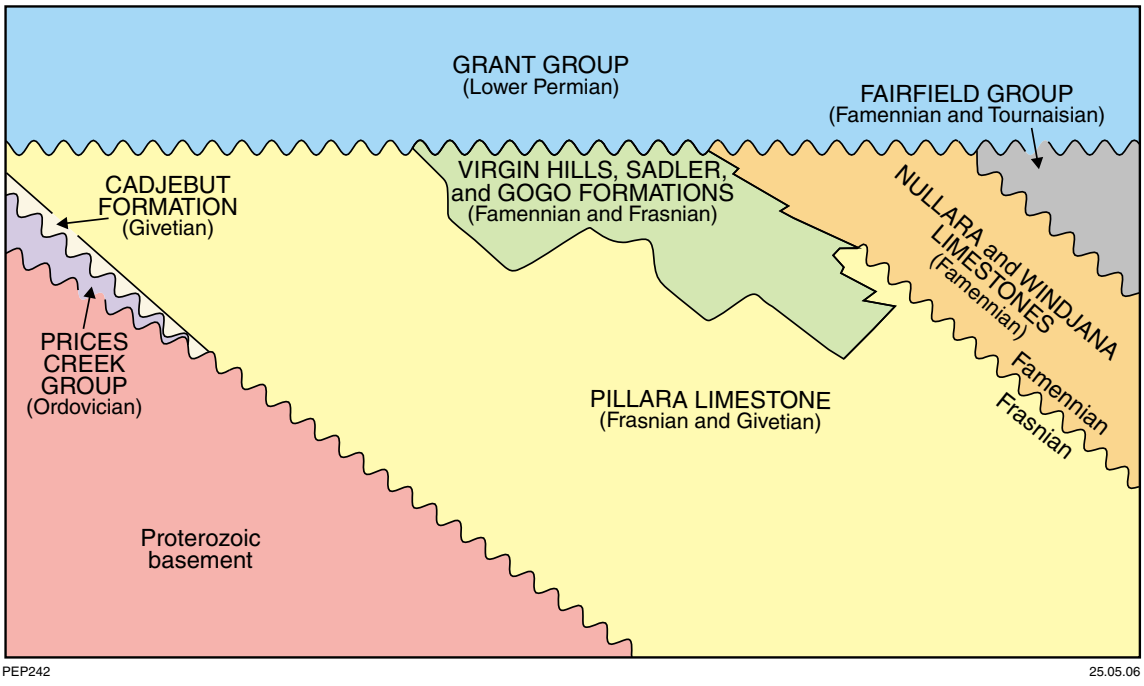

Figure 19. Stylized cross section illustrating relationships between lithostratigraphic units of the Devonian reef complexes and their relationships to Precambrian and Ordovician basement, Upper Devonian to Lower Carboniferous Fairfield Group, and Lower Permian Grant Group. Note the planar glacial unconformity beneath the Grant Group.

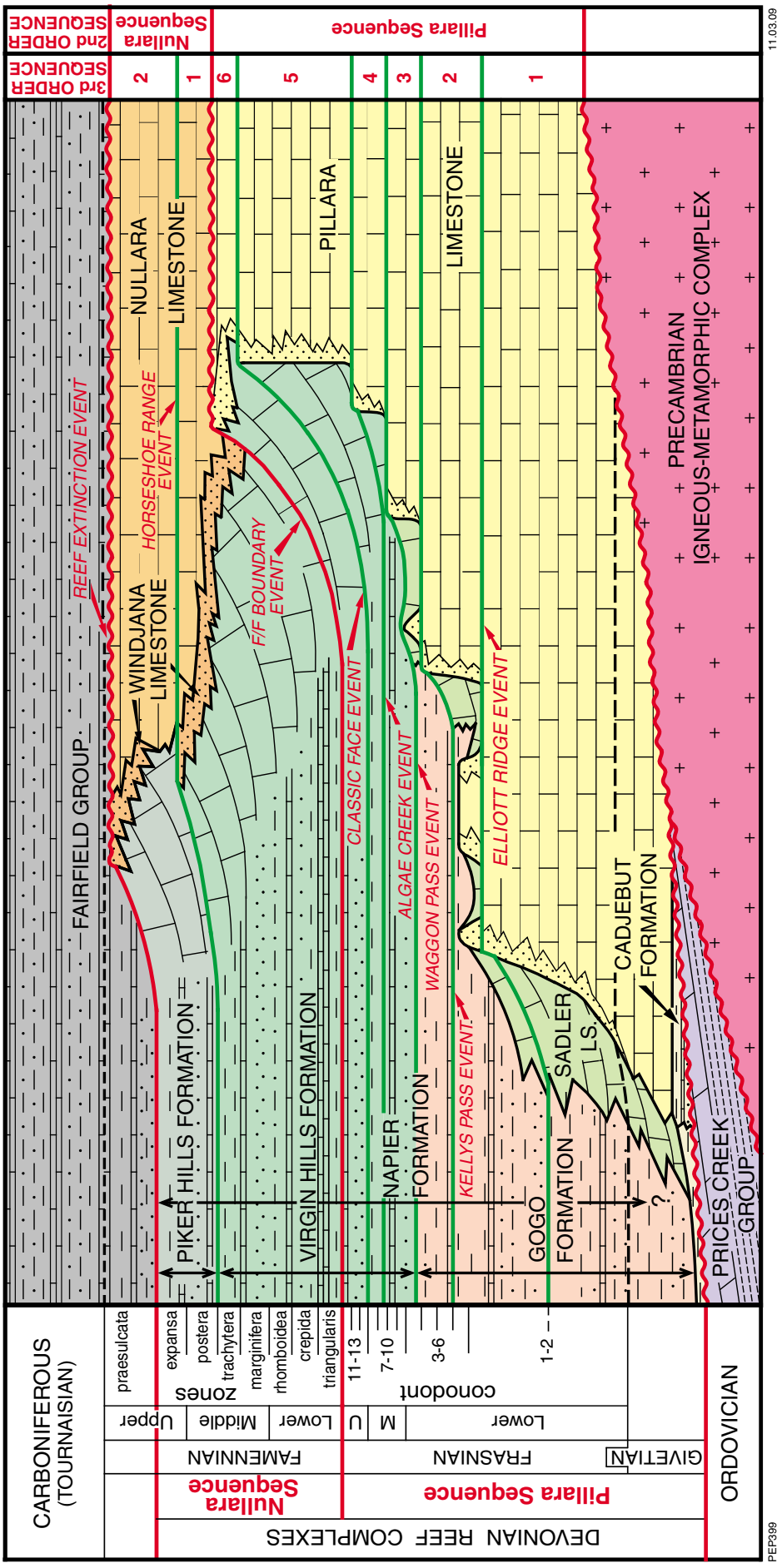

Figure 20. Diagrammatic section illustrating the lithostratigraphy, sequence stratigraphy, and conodont biostratigraphy of Devonian reef complexes on the Lennard Shelf, coloured to highlight the lithostratigraphy.

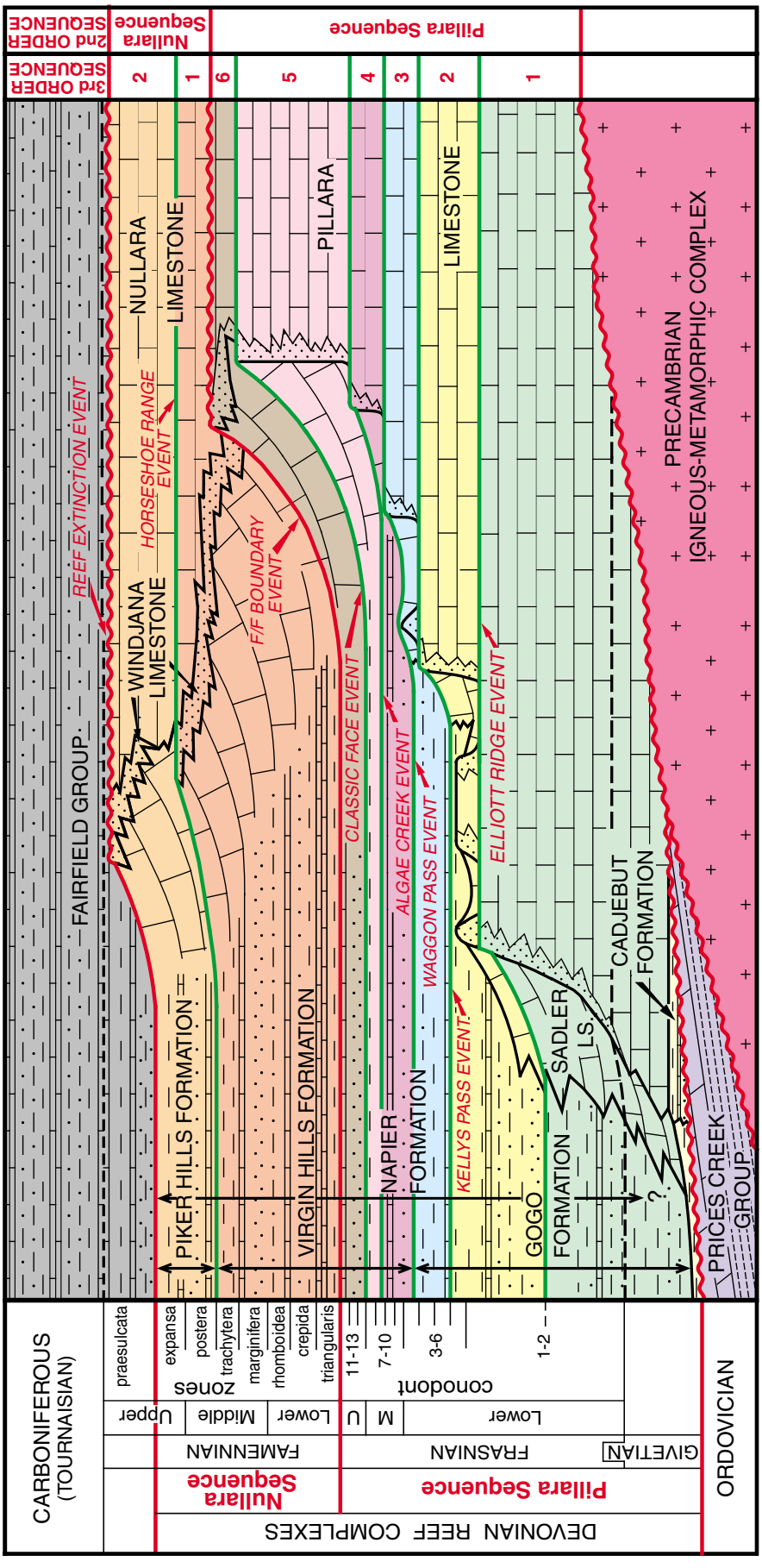

Figure 21. Diagrammatic section illustrating the lithostratigraphy, sequence stratigraphy, and conodont biostratigraphy of Devonian reef complexes on the Lennard Shelf, coloured to highlight the sequence stratigraphy.

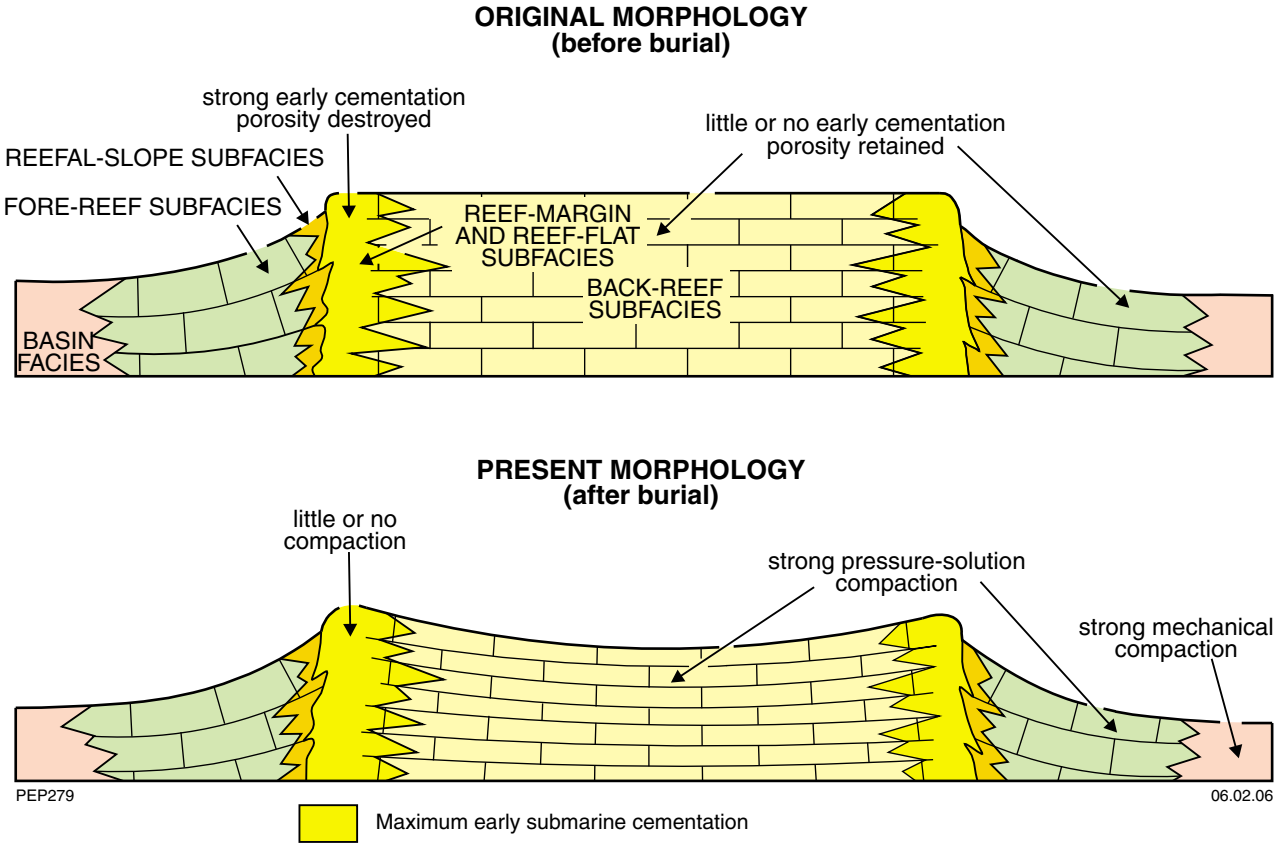

Figure 22. Diagram to illustrate changes in the morphology of the Devonian limestone platforms that resulted from pressure-solution compaction after burial.

bedded back-reef and bank subfacies commonly show regular metre-scale cyclicity, especially in the Frasnian. Most back-reef and bank deposits remained weakly cemented or uncemented at the time of burial, although some smaller parts of those facies were subjected to early cementation. The Givetian and Frasnian back-reef and bank subfacies accumulated as stromatoporoid and coral biostromes, fenestral (microbial) limestone, lime sand, and oolite. In the Famennian, those subfacies contained similar fenestral limestone, lime sand, and oolite, but without metazoan biostromes. Sandstone and conglomerate are interbedded with the Frasnian and Famennian back-reef and bank deposits in many areas that adjoin large conglomerate bodies and Precambrian basement. In some places where reef boundstone is absent around platform margins, the margin deposits consist of early-cemented calcarenites with little direct evidence of microbial binding.

The platform deposits were laid down in shallow water, generally close to sea level, and nearly horizontal. Water depths over the reef margin, reef flat, back-reef, and bank areas of each platform are estimated to have been seldom greater than 5 to 10 m, and often less than a metre. Some other parts of the back-reef and bank areas are interpreted to have been intertidal to supratidal. The presence of metre-scale cycles in the back-reef subfacies, each cycle generally ranging from about 2 to 8 m thick, is consistent with these depth estimates. The intertidal parts of the platform interiors are marked by fenestral limestones (showing mud cracks in some beds), and terrigenous deposits, some of which were probably supratidal to subaerial deposits. The reef-margin and reef-flat deposits rimming the platforms were commonly laid down at about the same level as the back-reef deposits. However, the reef was shallower than the back-reef in some places, and in others the reef was deeper than the back reef, reaching water depths estimated to have been as much as 10 m.

Microbial organisms were major reef and platform builders, and in many cases were the principal agents responsible for precipitation of reef limestones. Some microbes were skeletal forms, including especially *Renalcis* and *Sphaerocodium* (=*Rothpletzella*) (Wray, 1967; Playford et al., 1976), while others formed non-skeletal stromatolites or massive microbial limestone. In many cases a microbial origin has been inferred but not proved. Thus, limestones having fenestral fabrics or with indistinct wavy lamination are thought to be microbial, even though they lack preserved skeletal microbial material.

The back-reef and bank subfacies occupy the largest areas of most platforms. In the Givetian and Frasnian those deposits consist largely of stromatoporoid biostromes, with interbedded or interfingering coral biostromes, fenestral limestone, peloidal calcarenite, oolite, oncolitic limestone, and terrigenous clastic sediments (mainly

sandstone). Metazoans made only minor contributions to most Famennian platforms, although bivalves, including lithiotids and megalodonts, are common in some places, especially in near-reef environments. Cyclicity is evident in some Famennian back-reef deposits, but is not as prominent as it is in the Frasnian.

Marginal-slope deposits accumulated on depositional slopes in front of the platforms. They consist largely of platform-derived debris, with variable contributions from terrigenous sediments and organisms living on the slopes, especially microbes, brachiopods, and receptaculitids. Depositional dips were commonly as high as 35º to 40º in loose detritus, but were even higher (up to vertical) where microbial binding was associated with early cementation. The reefal-slope subfacies formed in the uppermost parts of many marginal slopes, adjoining reef-fringed platforms. The reefal-slope deposits are poorly bedded to unbedded, and are generally very steeply dipping to vertical. They are characterized by in-place reefal features, especially microbial and receptaculitid limestones. Because of outcrop limitations, it is difficult in some places to identify the boundary between reef-margin and reefal-slope subfacies.

Fore-reef deposits, consisting largely of reef-derived debris, were developed below reef-rimmed platforms and reefal slopes, commonly interfingering with reefal-slope deposits. Fore-reef debris deposits laid down high on the slopes have steep depositional dips (as much as a maximum of about 40º) and these flatten gradually to a few degrees where they interfinger with basin facies. Fore-reef deposits commonly include massive megabreccias and isolated allochthonous blocks of reef as much as 200 m across.

Fore-bank subfacies adjoin platforms that lack reef rims. The fore-bank deposits are generally characterized by low depositional dips (commonly less than 10º) and are usually more thinly bedded than fore-reef deposits. Fore-bank deposits were built largely of bank-derived sediments, including lime muds, sands, ooids, intraclasts, and skeletal material, especially stromatoporoids, corals, and brachiopods. Boundaries between bank and fore-bank deposits are marked by the change from flat-lying bank to dipping fore-bank deposits. Allochthonous blocks of platform-derived limestone are absent or rare in fore-bank deposits.

Sediments of the basin facies were deposited nearly horizontally on the floors of inter-reef basins, in water depths ranging from a few tens to several hundreds of metres. They consist largely of terrigenous deposits (calcareous shale, siltstone, sandstone, and conglomerate), with some interbedded pelagic limestones and detrital limestones containing debris derived from adjoining platforms. The basin facies is the most poorly exposed part of the reef complexes, present in valleys between the limestone ranges. That contrasts with the excellent exposures of platform and marginal-slope facies that occur in the ranges.

The marginal-slope and basin facies of the reef complexes have been precisely dated using conodonts and ammonoids (Appendices 1 and 2; Klapper, 1995, 1997b; Becker et al., 1993; Becker and House, 1997). Conodonts are especially valuable because they are found in most occurrences of these facies, particularly where the deposits contain shelly fossils. On the other hand, it is not yet possible to precisely date most outcrops of the platform facies, because no zonally significant conodonts have been found there and ammonoids are very rare.

Lithostratigraphy

Nine formations are recognized in the reef complexes in the southeastern area of the reef complexes, from immediately southeast of Geikie Gorge to the Red Bluffs area (Plates 3–5). These are:

- Cadjebut Formation (upper Givetian bank subfacies),
- Pillara Limestone (upper Givetian to uppermost Frasnian platform facies),
- Windjana Limestone (Famennian reef-margin and reef-flat subfacies),
- Nullara Limestone (Famennian back-reef and bank subfacies),
- Sadler Limestone (upper Givetian to lower Frasnian marginal-slope facies),
- Gogo Formation (upper Givetian to lower Frasnian basin facies),
- Virgin Hills Formation (lower Frasnian to middle Famennian basin and marginal-slope facies),
- Piker Hills Formation (middle to upper Famennian basin and marginal-slope facies), and
- Bugle Gap Limestone (middle to upper Famennian marginal-slope facies).

In the northwestern part of the reef complexes, the Pillara, Windjana, and Nullara Limestones are also recognized, extending from the northwest end of the Napier Range to just southeast of Geikie Gorge (Plates 1–3). None of the outcropping Pillara Limestone in that area is known to be Givetian, but it is expected to be partly of that age in the subsurface. The name Napier Formation is applied to all of the exposed marginal-slope and basin facies in that area. Parts of this formation are equivalent to the Virgin Hills Formation, Piker Hills Formation, Bugle Gap Limestone, Sadler Limestone, and Gogo Formation (Figs 18–21). Most of the outcropping part of the unit is middle Frasnian to late Famennian in age, equivalent to parts of the Virgin Hills Formation, Piker Hills Formation, and Bugle Gap Limestone. However, the part of the formation that is exposed in the Leopold Downs Embayment (Plate 2) is probably equivalent to part of the Sadler Limestone. The oldest Napier Formation, in the subsurface, probably extends down into the Givetian, although this has yet to be proved.

Platform facies

Four formations form parts of the platform facies in the Devonian reef complexes: the Givetian Cadjebut Formation, the Givetian and Frasnian Pillara Limestone, and the Famennian Windjana and Nullara Limestones.

Cadjebut Formation

The Cadjebut Formation is the oldest of the outcropping Devonian units. It overlies Ordovician rocks of the Prices Creek Group in the eastern part of the Emanuel Range (Plates 4, 5), and is regarded as the evaporitic base of the Emanuel Range reef complex. The Cadjebut Formation is interpreted to be a bank deposit, formed close to sea level, where supratidal sabkhas and hypersaline lagoons alternated with, or lay behind, stromatoporoid–coral biostromes and silty shoals. No parts of the Cadjebut platforms are known to have been rimmed by reefs.

Definition

The name Cadjebut Formation was introduced by Hocking et al. (1996) for a Givetian evaporitic unit at the base of the Emanuel Range reef complex. It had previously been considered to be part of the Pillara Limestone (Playford and Lowry, 1966; Pedone, 1990). The formation is named after Cadjebut Spring, and the type section is located on the southwest side of the Emanuel Range, about 300 m north of Emanuel Creek (AMG Zone 51, 807900E 7935500N). A reference section is in BHP drillhole CD 113 (AMG Zone 51, 817000E 7928000N), where it occurs between 421.8 and 458.3 m.

Lithology

The Cadjebut Formation is a unit of vuggy dolomite with interbedded siltstone, evaporites, and breccia. It commonly contains relict stromatolites and corals, with associated vugs. Stromatolitic bedding is locally well preserved. Evaporites do not occur in outcrop, but their former presence can be recognized from pseudomorphs of halite and anhydrite in dolomite (Figs 23, 24) and the presence of collapse breccias. The breccias resulted from crystallization-induced movement of evaporitic horizons or the removal of evaporite minerals by solution. Halite and anhydrite remain in the subsurface, where the anhydrite has usually been replaced by gypsum. Collapse breccias and contorted bedding commonly occur where beds of evaporite have been completely dissolved away (Fig. 25).

Epigenetic zinc–lead mineralization has been introduced into the formation in some areas by fluids flowing along faults and other pathways into hydrothermal voids.

Four shallowing-upward cycles, each about 10 m thick, have been recognized in the formation (Hocking et al., 1996). Each consists of dolomitic grainstone at the base, overlain successively by siltstone, dolomite, and former evaporites. Most dolomite in the formation is thought to have formed during very early diagenesis, although some could be a primary precipitate (Pedone, 1990).

Stratigraphic relationships

The Cadjebut Formation unconformably overlies dolomite and shale of the Lower to Middle Ordovician Prices Creek Group (Emanuel and Gap Creek Formations). The unconformity is angular, with maximum discordances of about 25° (Fig. 26). The Cadjebut Formation is overlain with apparent conformity in outcrop and the subsurface by the Pillara Limestone. Locally, the contact is transitional, so that it can be difficult to place a definitive boundary between the two formations.

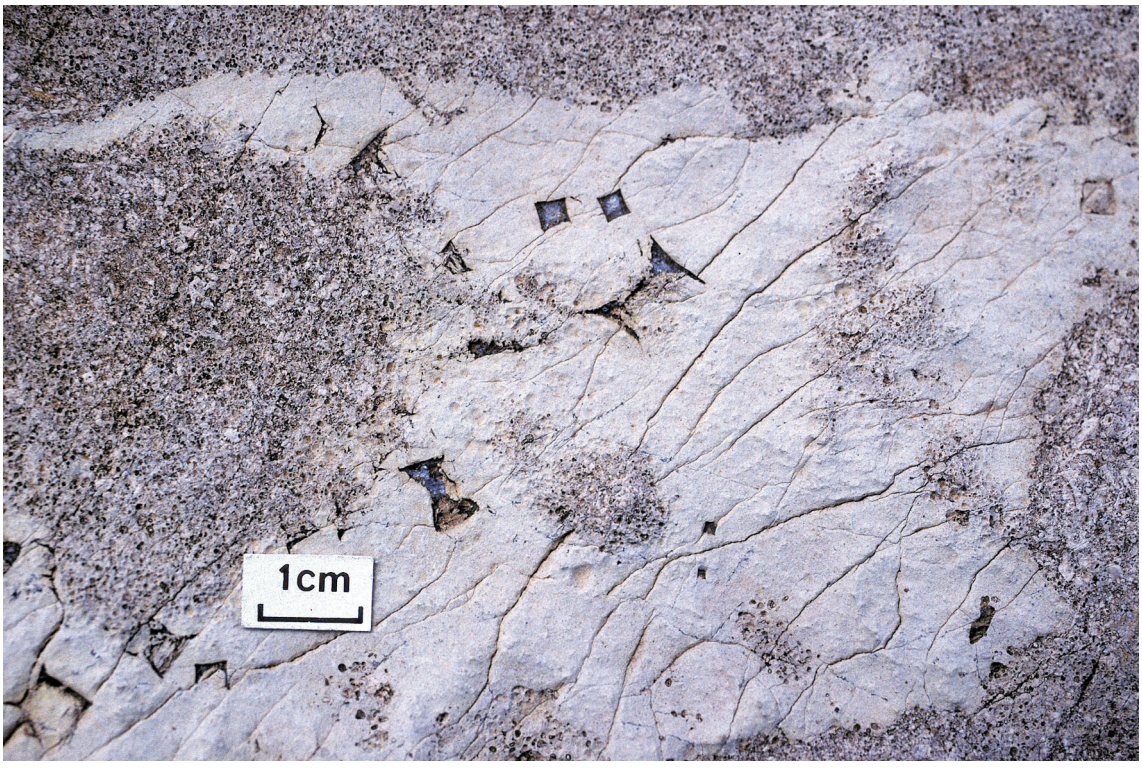

Figure 23. Moulds after hopper crystals of halite in dolomite of the Cadjebut Formation, Emanuel Range.

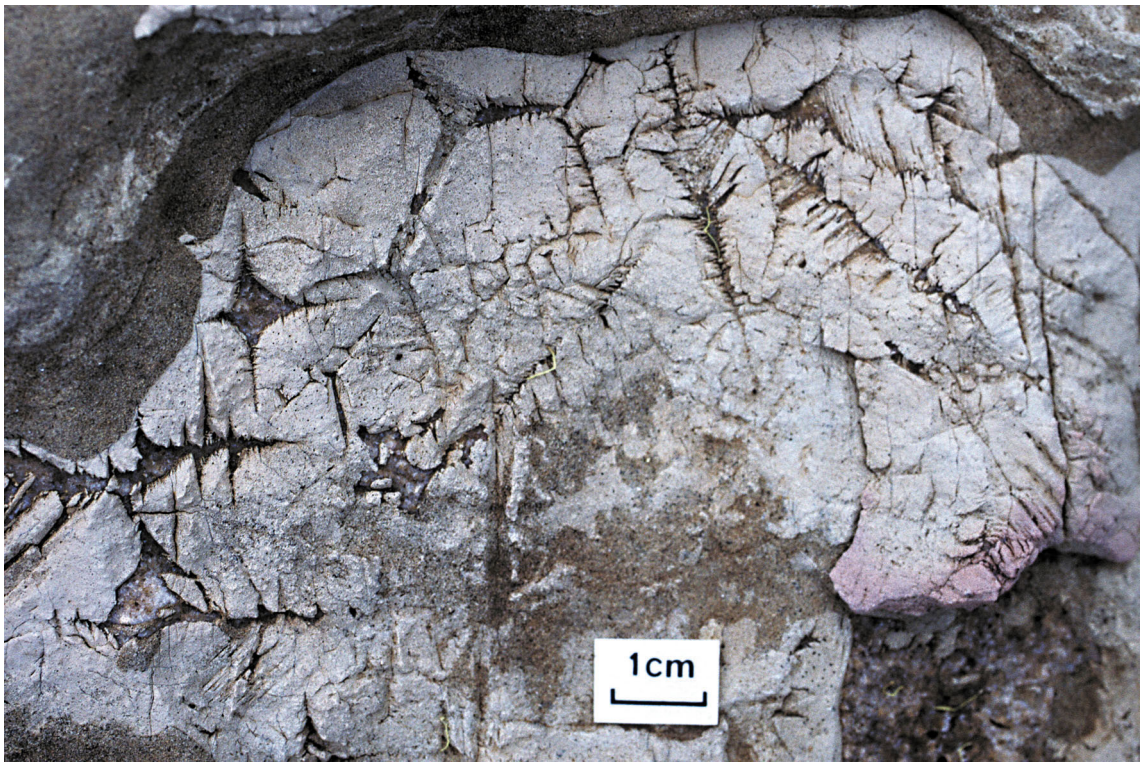

Figure 24. Moulds after crystals of skeletal halite, in the Cadjebut Formation, Emanuel Range.



Figure 25. Intraformational folding in dolomite of the Cadjebut Formation, Emanuel Range. The folding is thought to be associated with the solution of evaporites.

The Cadjebut Formation is regarded as being part of the reef complexes because of the presence within the unit, prior to dolomitization, of stromatoporoids, corals, and stromatolites. The formation is the lowermost unit of Pillara Sequence 1.

Distribution and thickness

The Cadjebut Formation in outcrop is confined to the southwestern side of the Emanuel Range (Plates 4, 5), but it is known in the subsurface below and north of that range, where it has been identified in several drillholes. The thickness of the formation is 52 m in the type section and 36.5 m in the subsurface reference section (Hocking et al., 1996).

Fossils and age

Most of the Cadjebut Formation consists of unfossiliferous dolomite, apart from the presence of relict stromatoporoids, stromatolites, and corals in some places. Stromatolite mounds, more than 3 m high and as much as 7 m across, occur 300 m east of Emanuel Creek within siltstone and former-evaporite layers, immediately south of an east-trending fault (GPS AMG Zone 52, 808380E 7935710N). Smaller domal stromatolites are present locally.

The formation is Givetian, probably late Givetian, in age, based on its spore assemblage and the presence of the Givetian brachiopod *Stringocephalus fontanus* in the directly overlying part of the Pillara Limestone (Hocking et al., 1996). *Stringocephalus* is known to be restricted worldwide to the Givetian, and the highest known range is in the upper part of the *hermanni* Zone (Johnson et al., 1980; G Klapper, 2008, written comm.).

Pillara Limestone

Definition

The name Pillara Limestone was first used by Playford and Lowry (1966), replacing the name 'Pillara Formation' of Guppy et al. (1958). This change was made because the dominant and most characteristic lithology of the formation is limestone, although sandstone, siltstone, shale, and conglomerate also occur in some areas. The unit is named after the Pillara Range (Plate 4), and the type section is in that range at Menyous Gap, from AMG Zone 51, 799800E 7964100N to 799600E 7962600N.

Playford and Lowry (1966) used the name Pillara Limestone to embrace all Givetian, Frasnian, and Famennian back-reef carbonates on the Lennard Shelf. However, the importance of the Frasnian–Famennian unconformity was not appreciated at that time. Its significance was first recognized by Playford and Cockbain (1976) and Playford (1980), who restricted the name Pillara Limestone to the Givetian and Frasnian platform deposits and gave a new name (Nullara Limestone) to the Famennian back-reef and bank deposits, and confined usage of the name Windjana Limestone to the Famennian reef-margin and reef-flat subfacies.

The boundary between Frasnian reef and back-reef is usually indistinct and transitional, and consequently no separate stratigraphic name has been applied to the reef-



Figure 26. Angular unconformity between Ordovician Gap Creek Formation (below) and late Givetian Cadjebut Formation (above), in the Emanuel Range near Gap Creek.

margin and reef-flat subfacies of the Pillara Limestone. This contrasts with the Famennian platforms, where the reef is much more distinct, and the boundary between reef (Windjana Limestone) and back-reef (Nullara Limestone) can be mapped readily.

Lithology

The Pillara Limestone consists of platform facies: reef-margin, reef-flat, back-reef, and bank subfacies. Most of the unit belongs to the back-reef subfacies. Reef-margin and reef-flat subfacies occupy only narrow zones along the platform margins and they generally have transitional boundaries with the back-reef subfacies. The formation was deposited close to sea level on flat-topped limestone platforms that were commonly, but not always, reef fringed. The maximum water depths over the platforms probably did not exceed 10 m in most areas, based on the thickness of shallowing-upward infill cycles in back-reef limestones. It is clear that in some areas the water depths over the reef margin were deeper than those in the platform interior, but in most areas there was little or no depth difference between them. In other cases it seems clear that the reef was the shallowest part of a platform. Back-reef limestones are well bedded, and commonly form shallowing-upward cycles (either Milankovitch or tectonic cycles), as described by Read (1973a,b), Playford (1981), Brownlaw et al. (1996), Brownlaw (2000), and Hocking and Playford (2001).

The reef-margin subfacies is characteristically massive or very thick bedded. It was built mainly by microbes, stromatoporoids, and corals during the Givetian and early Frasnian, and by microbes and stromatoporoids, without corals, during the middle and late Frasnian. In some areas during the late Frasnian, microbes became progressively more prevalent (at the expense of the stromatoporoids). Much of the latest Frasnian reef-margin subfacies in such areas consists of massive microcrystalline limestone of presumed microbial origin, commonly containing abundant or scattered *Renalcis.* However, in other areas the latest Frasnian reef consists of stromatoporoid and microbial limestone, in which stromatoporoid*s* formed subvertical sheets at the reef front (Fig. 27).

Reef-flat beds are usually well bedded and were built by reef-building stromatoporoids (especially *Actinostroma* and *Stachyodes*), fenestral stromatolites, and structureless microbial limestone. The bedding planes in some areas, such as the Classic Face in Windjana Gorge, are marked by thin beds of terrigenous detritus, which must have periodically flooded the reef flats, bringing reef building to a temporary halt in those areas. However, the thin sandstone beds often contain irregular columnar stromatolites (Fig. 28).

The back-reef subfacies consists predominantly of medium-bedded biostromes of stromatoporoid, coral, and algal limestone, with interbedded oolite, calcarenite, and calcilutite. Coral-bearing calcareous siltstone is present near the base of the Pillara Limestone in the lower parts of many cycles, but is absent at higher levels and in areas that are more distant from the basin margin, such as the Oscar Range. In some areas, especially in the late Frasnian of the southern Oscar Range to Geikie Gorge area, the back-reef subfacies is almost entirely composed of fenestral limestone, with or without oolite.

Terrigenous sedimentary rocks (sandstone, conglomerate, siltstone, and shale) are interbedded with carbonates in Pillara Limestone adjacent to major conglomerates or Precambrian rocks of the Kimberley block. A terrigenous lithofacies (typically siltstone and sandstone) occurs in many areas adjoining Precambrian basement, at the tops of cycles in the upper Pillara Limestone where terrigenous sediment has prograded over the back-reef areas. Locally, terrigenous channel deposits cut through and replace the lower parts of cycles, as in the area north of McSherrys Gap and Surfboard Point in the Napier Range.

Dolomitization of the formation is common in some areas, particularly in the back-reef subfacies, but overall the amount of dolomite in the unit is estimated to be only 10 to 15%. Most dolomite in outcrop has been dedolomitized (altered to limestone), perhaps through reaction with Permian subglacial meltwater. However, it still retains the visual appearance and textural characteristics of dolomite. Whereas the unaltered limestones are typically yellow, yellow-grey, or pink in colour, the dolomite and dedolomitized limestone are characteristically yellowish brown. Dolomitization destroyed, or largely destroyed, fossils that were present in the original limestones.

The most dolomitized beds are those that had high primary porosities at the time of burial. This is particularly well shown 1.2 km northeast of Sheep Camp Yard on the walls of Geikie Gorge (AMG Zone 51, 790700E 8003500N), where the intensity of dolomitization (i.e. dedolomitized limestone) in Frasnian platform and marginal-slope facies increases progressively moving from the reef-margin to the back-reef in one direction, and to the fore-reef in the other (Playford, 1981; Wallace, 1987; Wallace et al., 1991; Fig. 29). Dolomitization was controlled by the porosity remaining in the limestones after early burial, dolomitizing fluids having been derived from the adjoining basin (Wallace et al., 1991). There is relatively little dolomitization in reef-margin, reef-flat and reefal-slope limestones at this locality, because their primary porosities had usually been destroyed by marine cementation, whereas porous more-distal fore-reef deposits and those parts of the back-reef deposits that are close to the reef were strongly dolomitized. It is thought that dolomitizing fluids, derived from compacting basin deposits, entered porous parts of the fore-reef limestones and passed via neptunian fissures through non-porous well-cemented reefal-slope and reef limestone to meet porous near-reef parts of the back-reef subfacies.

Some stromatoporoids and corals in back-reef biostromes remain in their growth positions, but others have been broken up and deposited nearby. The fragmented colonies of *Amphipora* form characteristic spaghetti-like beds. It seems clear that they had a bushy form while growing and broke into fragments soon after death (Figs 30, 31).

Colonies of bulbous stromatoporoids (probably mainly *Actinostroma*) are very abundant in places, giving a conglomerate-like appearance to some beds. Bulbous stromatoporoids locally show evidence of boring activities, probably by sponges (Fig. 32).



Figure 27. Subvertical to steeply dipping sheets of stromatoporoids in late Frasnian reef-margin subfacies (Pillara Limestone) west of Henwood Spring. The stromatoporoids grew on successive reef fronts (from right to left on the photo) during Frasnian Sequence 6, while the reef was advancing strongly.

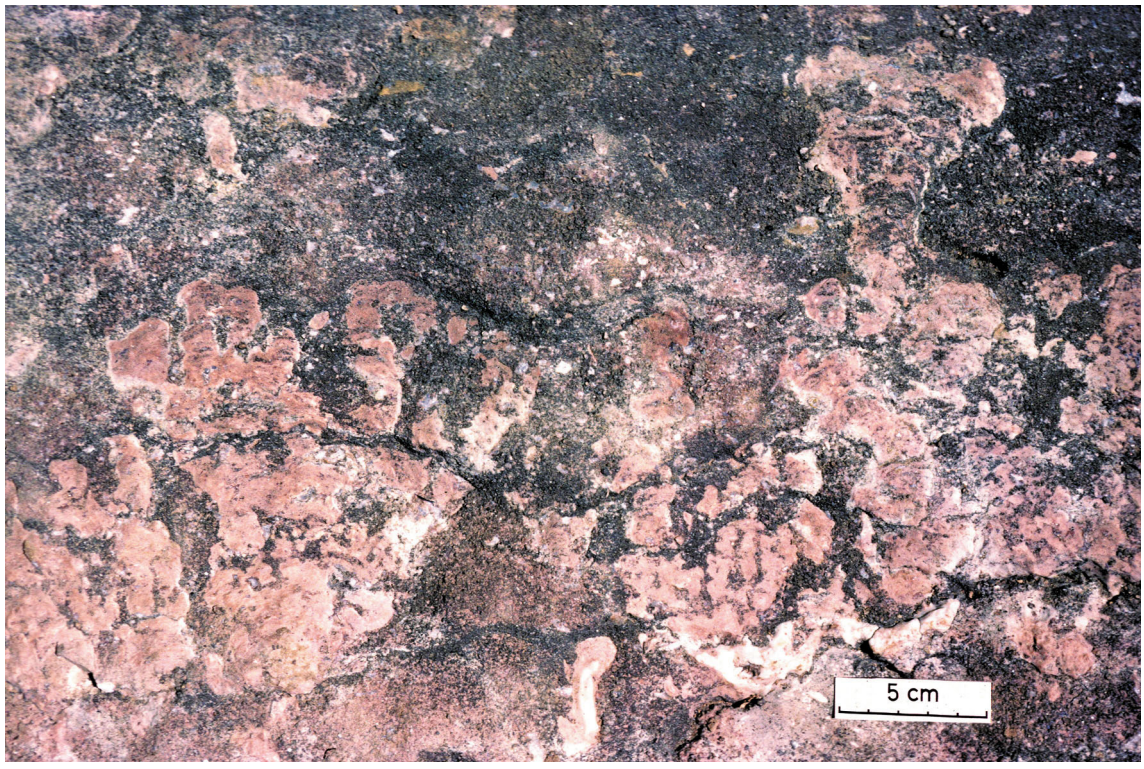

Figure 28. Stromatolites in sandy limestone and calcareous sandstone of the Pillara Limestone (reef-flat subfacies) in the Classic Face at Windjana Gorge.

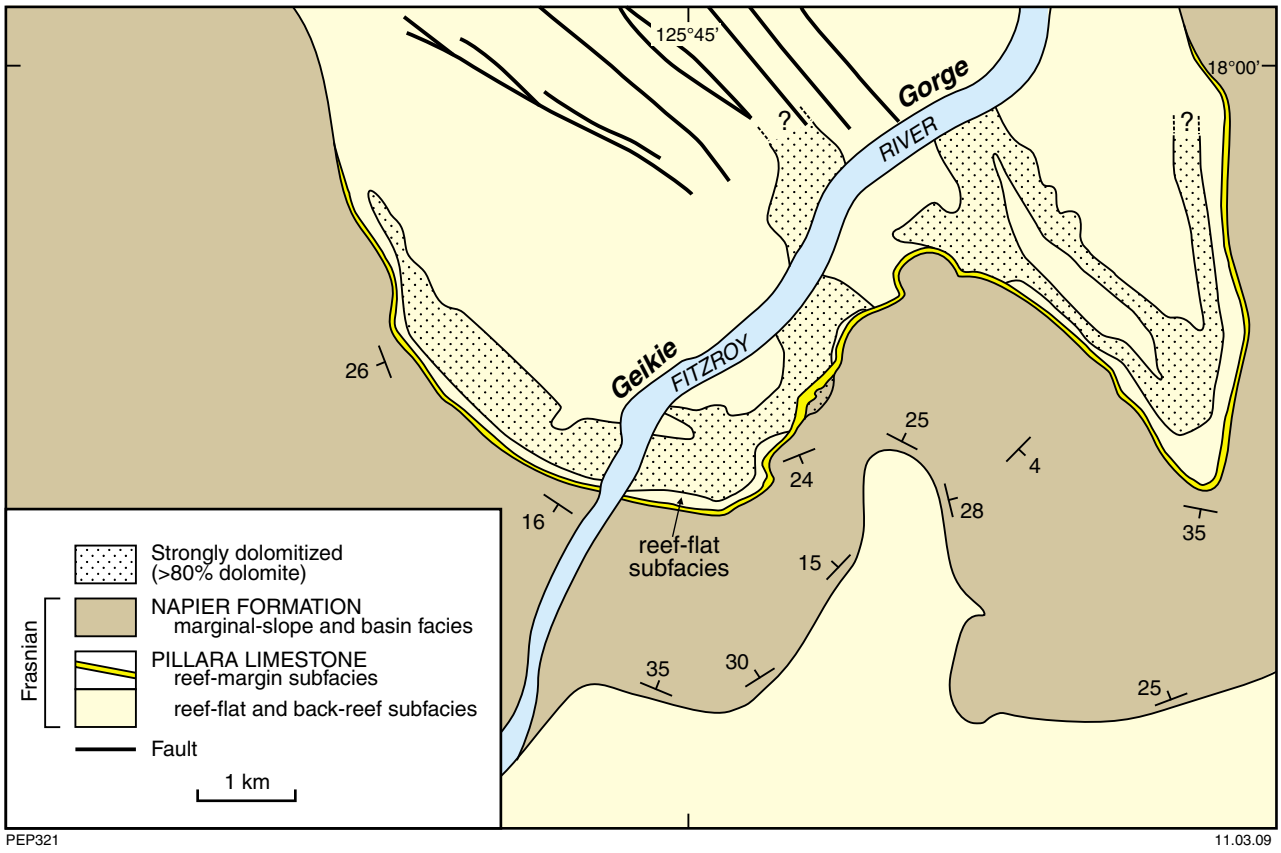

Figure 29. Geological map of part of the Geikie Gorge area showing the distribution of dolomite (now dedolomite) in platform facies (Pillara Limestone) (from Wallace et al., 1991).



Figure 30. Fragments of *Amphipora*, forming 'spaghetti rock', in Pillara Limestone (bank subfacies) in the northern Emanuel Range, south of Gap Creek.

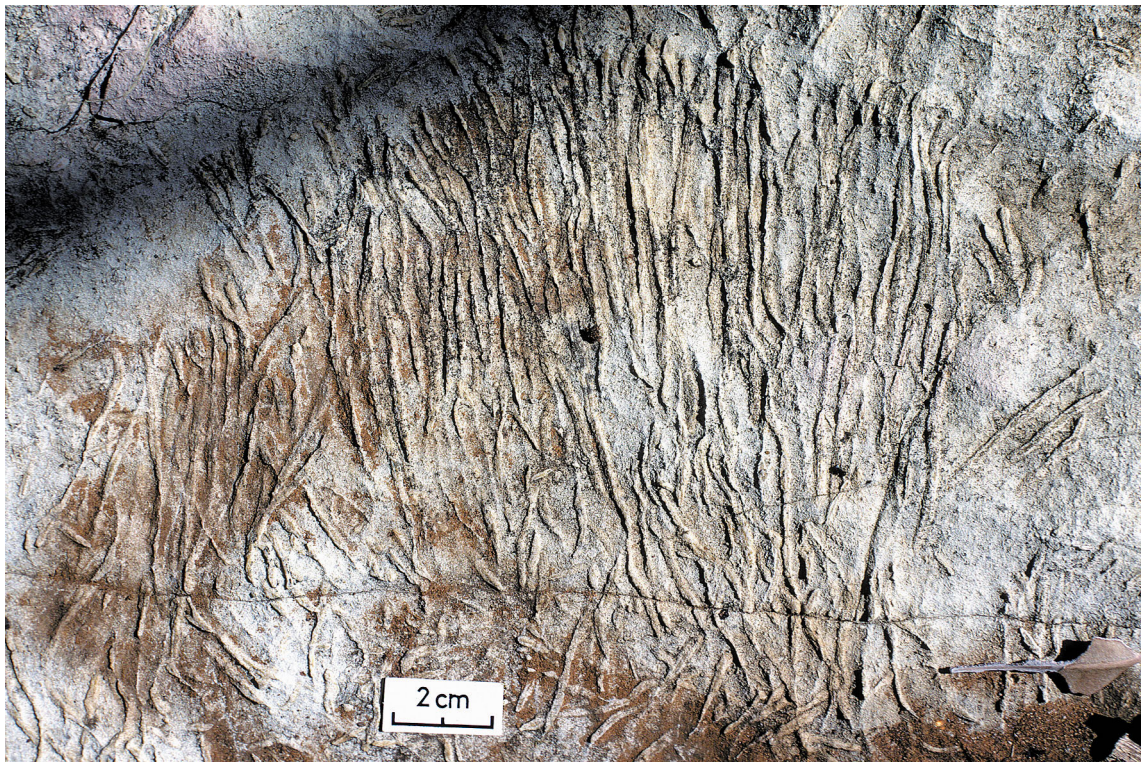

Figure 31. Shrub-like colony of *Amphipora* that fell over more-or-less intact, in Pillara Limestone (bank subfacies), northern Emanuel Range, south of Gap Creek.

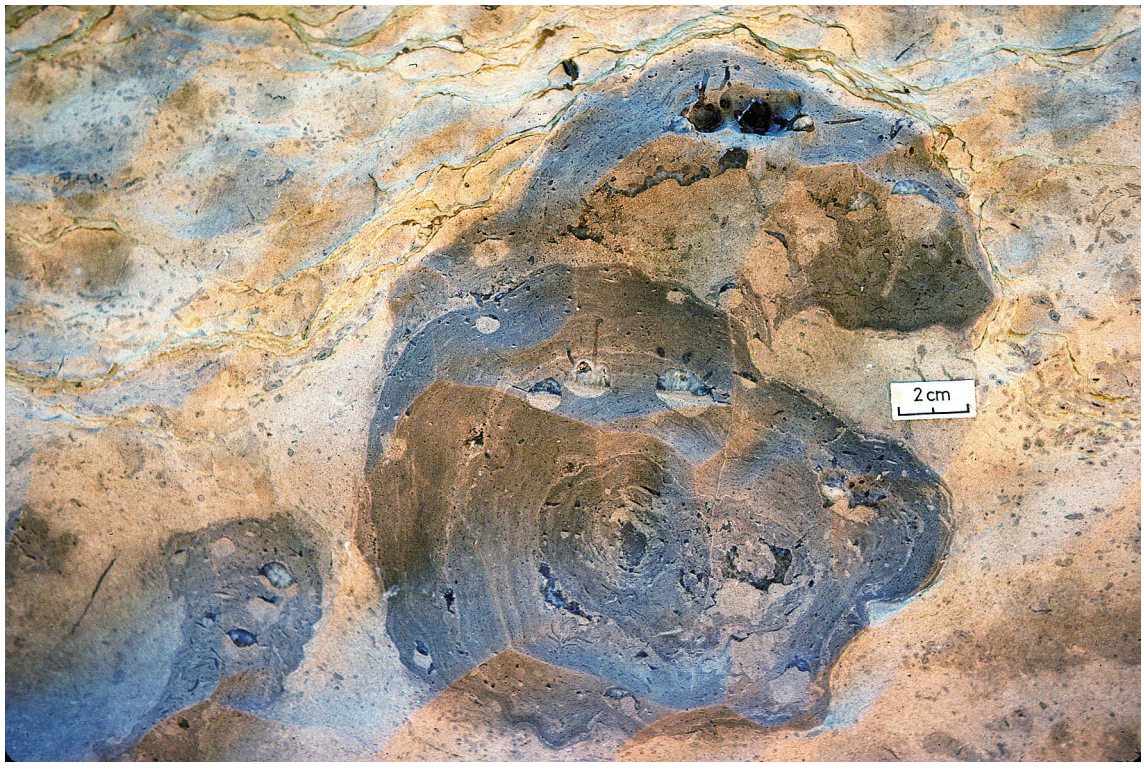

Figure 32. *Actinostroma* and *Amphipora* in back-reef subfacies of the Pillara Limestone in central Geikie Gorge on the east side. Note prominent sponge borings in the *Actinostroma* colony.

Bedding planes in the Pillara Limestone are commonly stylolitized, with thin layers of residual silt and sand remaining along the stylolites after calcium carbonate had been dissolved through pressure solution and re-precipitated in nearby pore space (Fig. 33). Although most stylolites are localized by bedding planes, and have vertical teeth in response to vertical (compactional) stress (Fig. 34), others are oblique to bedding, and may have subhorizontal teeth, apparently in response to horizontal compression. There is little or no stylolitization in the early cemented reef-margin, reef-flat, and reefal-slope subfacies, contrasting with high levels of stylolitization in back-reef deposits that were uncemented and retained high porosities at the time of burial. The resulting differential compaction by pressure solution has resulted in the typical 'dished shape' of many Pillara platforms (Fig. 22).

Stratigraphic relationships

The Pillara Limestone conformably overlies the Cadjebut Formation, and is unconformably overlain by the Famennian Nullara and Windjana Limestones. Where platform drowning has occurred, the Pillara Limestone is overlain by various marginal-slope and basin deposits (Sadler Limestone, Gogo Formation, and Virgin Hills Formation in the southeast Lennard Shelf, and Napier Formation in the northwest). The Pillara Limestone consists of six third-order sedimentary sequences (Pillara Sequences 1–6; Fig. 21), which are defined by episodes of backstepping, when the platform margin retreated abruptly into the former platform interior, preceded in some (and perhaps all) cases by a brief fall in sea level.

Distribution and thickness

The Pillara Limestone is widely distributed along the northern margin of the Lennard Shelf, in a belt extending some 300 km from near the northwest end of the Napier Range to the Emanuel Range. The thickness of the formation as preserved in outcrop ranges from less than 200 m in the Napier Range to a maximum of perhaps 2000 m in the Lawford Range (Plates 1, 4, 5). More than 1000 m of Pillara Limestone was penetrated in borehole CD48 (AMG Zone 51, 821200E 7923100N), near the entrance to Paddys Valley, and regional considerations suggest that 1000 m is close to the average depositional thickness of the formation over the Lennard Shelf as a whole (see cross sections in Plates 1–5).

The name Pillara Limestone has also been used by some geologists for Frasnian limestone and dolomite intersected in the subsurface along the southern margin of the Fitzroy Trough (Lehmann, 1984). However, few detailed facies studies have been conducted in those areas and rock unit identifications there seem questionable.

Fossils and age

The Pillara Limestone in many areas is richly fossiliferous, some of the characteristic fossils being shown in Figures 27, 30–32 and 35–46, with abundant stromatoporoids (Cockbain, 1984; Figs 30–32, 35, 36), corals (Hill and Jell, 1970; Brownlaw, 2000; Fig. 37), brachiopods (Coleman, 1951; Veevers, 1959a,b; Sartenaer, 1971, 1999), microbes and algae (Wray, 1967; Figs 41–46), stromatolites (Playford et al., 1976; Fig. 28), bivalves (Teichert, 1943; Figs 38, 39), palynomorphs (Grey, 1991, 1992; G Playford, Appendix 3), gastropods (Cook et al., 2003), nautiloids (Teichert, 1939), and fish (Long, 1988, 1995). Sponges and crinoids are generally uncommon (Rigby, 1986). Ammonoids are very rare in the Pillara Limestone, the best example known being in reef-flat subfacies 4 km north of Brooking Springs Homestead (GPS AMG Zone 51, 780910E 7999200N). No conodonts have been found in the formation.

The late Givetian and early Frasnian platforms were built by stromatoporoids, corals, and microbes (probably mainly cyanobacteria), with some contributions from bivalves and other organisms (Figs 35–46). Corals declined abruptly during the early Frasnian (Zone 1), leaving microbes and stromatoporoids to form the main platform-building consortium. They continued in that role for the rest of the Frasnian, and although stromatoporoids probably declined to some extent before the close of the Frasnian (in Zones 12 and 13), the latest Frasnian reefs still contained abundant stromatoporoids (Fig. 27). They almost disappeared at the close of the Frasnian, as a result of the global mass extinction of shallow-water metazoans at and just below the Frasnian–Famennian boundary (Copper, 1986, 1994; Stearn, 1987; McGhee, 1996; Hallam and Wignall, 1997; Racki, 1998, 2005; Stock, 2005).

Stromatoporoids are especially characteristic megafossils in the Pillara Limestone (Cockbain, 1984). The most common forms are species of *Actinostroma* and *Amphipora* (Ripper, 1937; Figs 30–32). The masses of *Amphipora* commonly form what is colloquially termed 'spaghetti rock'. *Amphipora* was once thought to be restricted to the Middle Devonian (Teichert, 1949), but is now known to occur throughout the Frasnian and Givetian parts of the Pillara Limestone (Playford, 1980; Cockbain, 1984). It was because of the incorrect belief that *Amphipora* was restricted to the Middle Devonian that caused Guppy et al. (1958) to postulate an unconformity between the Pillara Limestone and Upper Devonian units that are now known to be its facies equivalents.

Amphipora originally grew as delicate 'shrubs' that fell over after death. Usually the skeleton broke into short pieces which were distributed randomly over the adjoining sea floor, to form 'spaghetti rock'. However, in rare cases the original shrub-like form was retained after the shrub fell over (Fig. 31). Bivalves, especially megalodonts (Figs 38, 39) are very abundant in some parts of the formation, commonly preserved in their original growth positions.

The microbe *Renalcis* (Wray, 1967) is common in the Frasnian reef-margin and reef-flat limestones, but is less abundant in the oldest Frasnian and Givetian reefs (Fig. 41). *Renalcis* can be detected readily with the practised eye, as minute milk-white patches and spots in limestone. With a hand lens or microscope *Renalcis* can be seen to consist of irregularly oval or bulbous bodies less than a millimetre in diameter, rimmed by dark micrite, the centres being filled by clear sparry calcite thought to have been precipitated

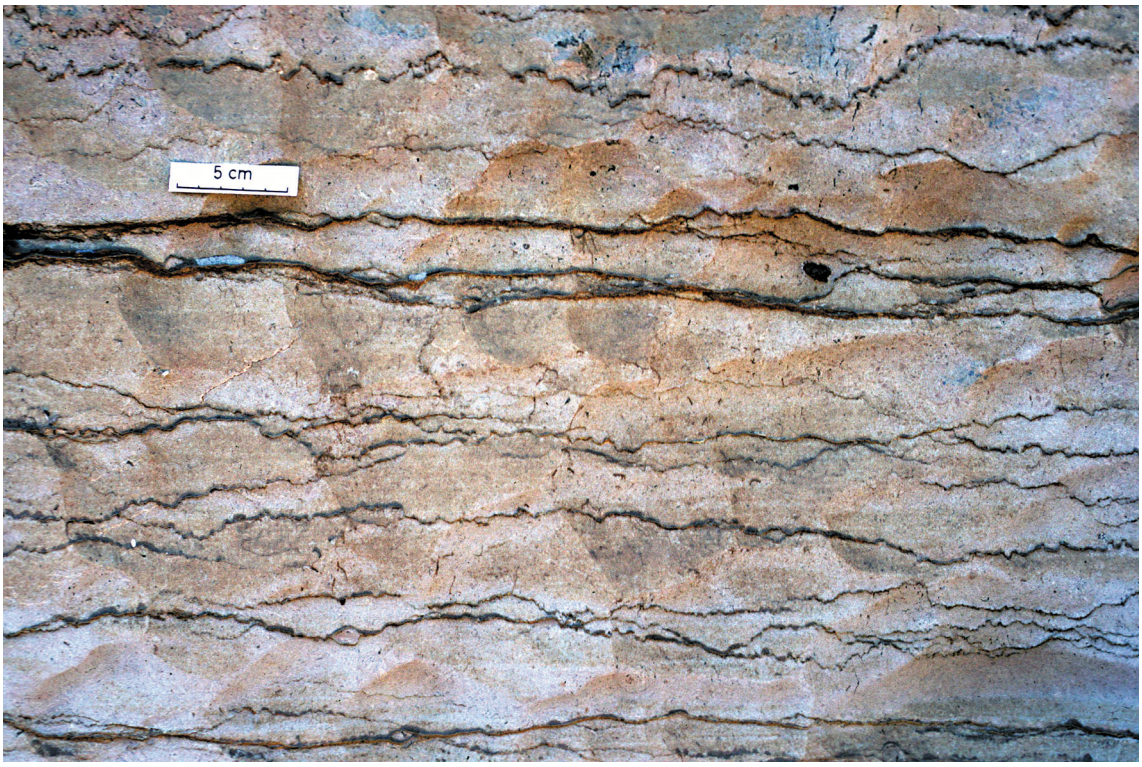

Figure 33. Back-reef limestone of the Pillara Limestone in Geikie Gorge showing strong stylolitization, linked with high primary porosity at the time of burial.

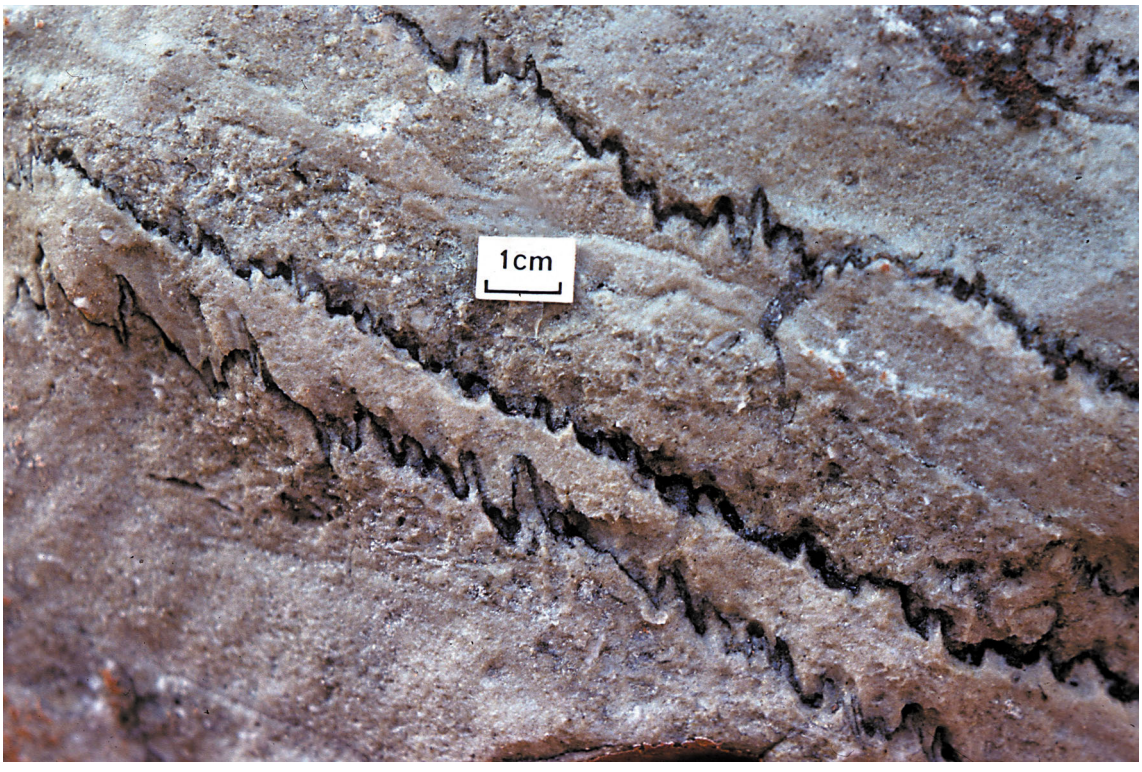

Figure 34. Fore-reef limestone of the Napier Formation at Linesmans Creek, Oscar Range, showing stylolites with vertical teeth along steeply dipping bedding planes. The steep dips are primarily depositional, and the vertical teeth show that the stylolites formed in response to vertical (compactional) stress.

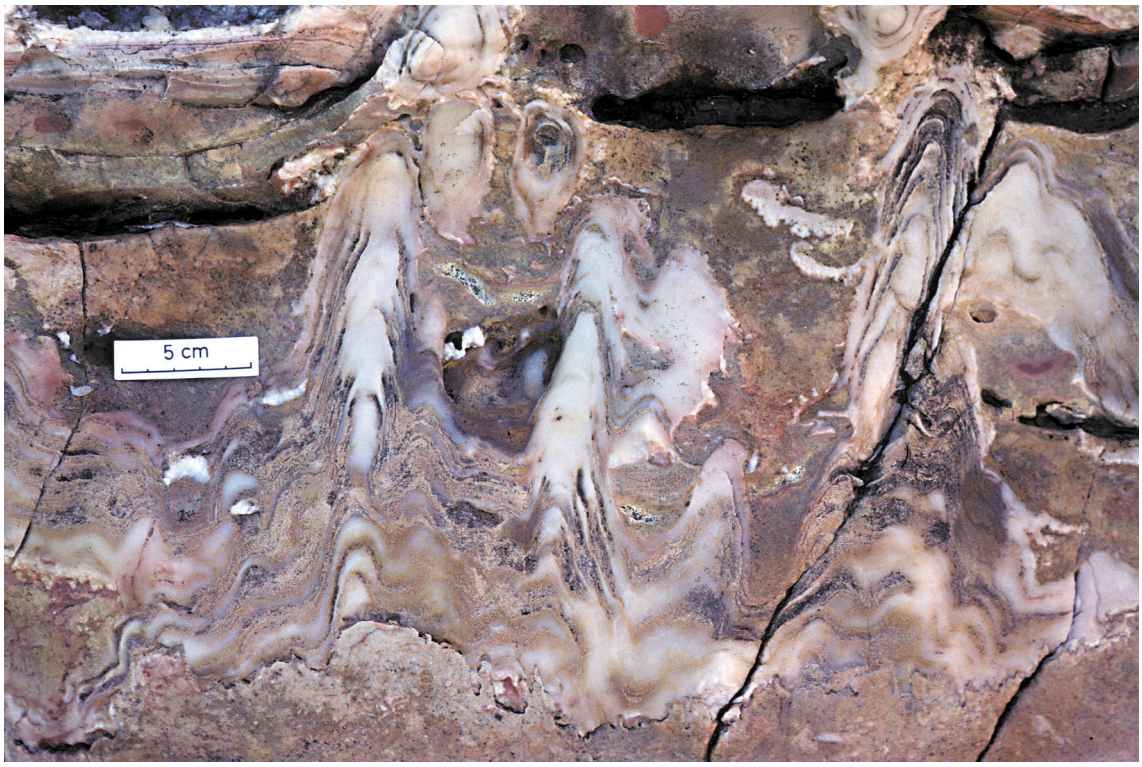

Figure 35. ***Actinostroma windjanicum*** **in reef-flat limestone of the Pillara Limestone in the Classic Face at Windjana Gorge.**



Figure 36. Bed of subspherical ***Actinostroma*** **in back-reef subfacies, Pillara Limestone, Hull Range.**



Figure 37. Colonies of the coral *Disphyllum,* overlain by breccia composed of fragments of *Disphyllum* and *Thamnopora*, from the base of a cycle in back-reef subfacies of the Pillara Limestone in central Menyous Gap.

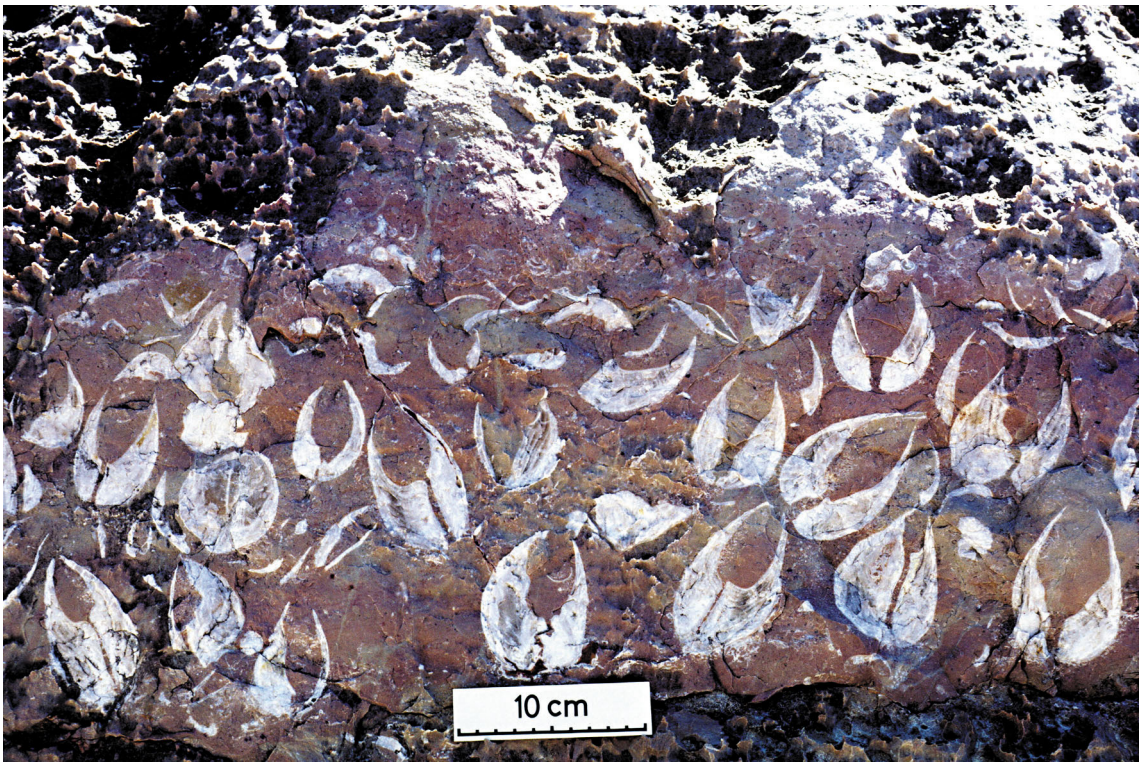

Figure 38. Vertical cross-section view of megalodont bivalves in their growth positions, in late Frasnian Pillara Limestone (reef-flat subfacies), on the east side of a patch reef in the Copley Valley Embayment area, 2 km northeast of Mad Russian's Well.

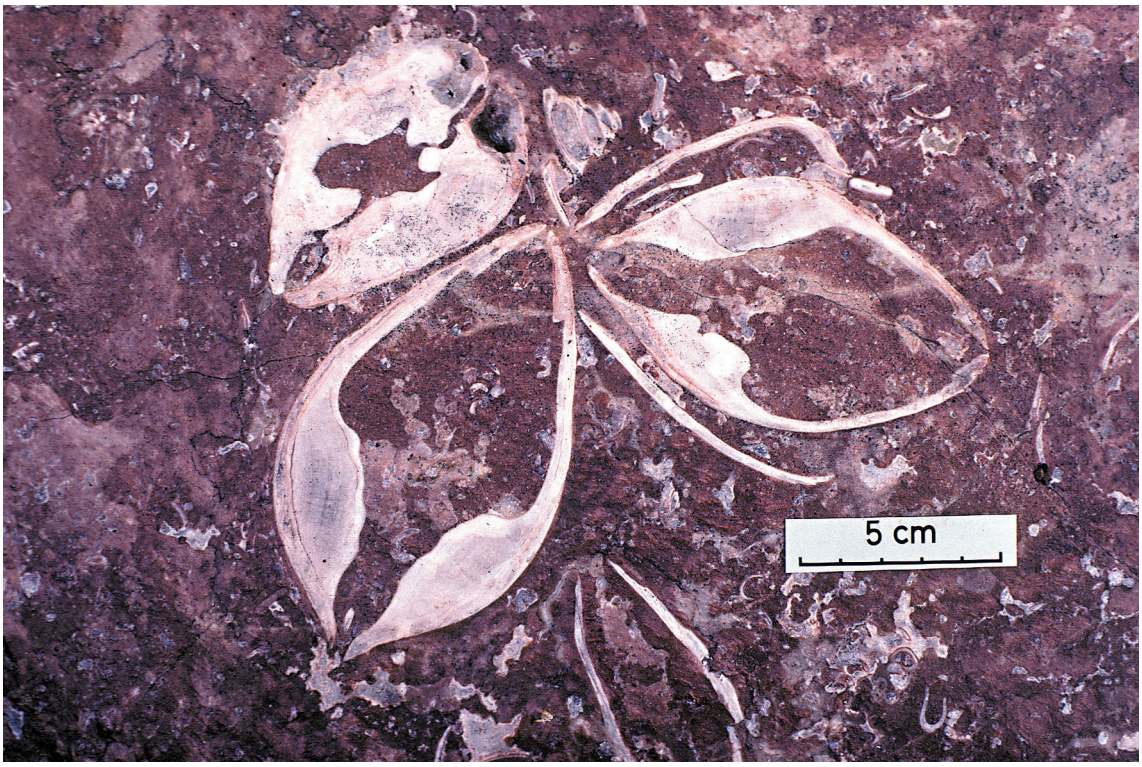

Figure 39. Closer vertical cross-section view of megalodont bivalves in their growth positions in late Frasnian Pillara Limestone (reef-flat subfacies), on the east side of a patch reef in the Copley Valley Embayment area, 2 km northeast of Mad Russian's Well.



Figure 40. Colony of *Actinostroma windjanicum* in the Classic Face, Windjana Gorge, showing *Renalcis* colonies that grew down from the roofs of former shelter cavities, the rest of the cavities having been filled with radiaxial sparry calcite and laminated red peloidal limestone.

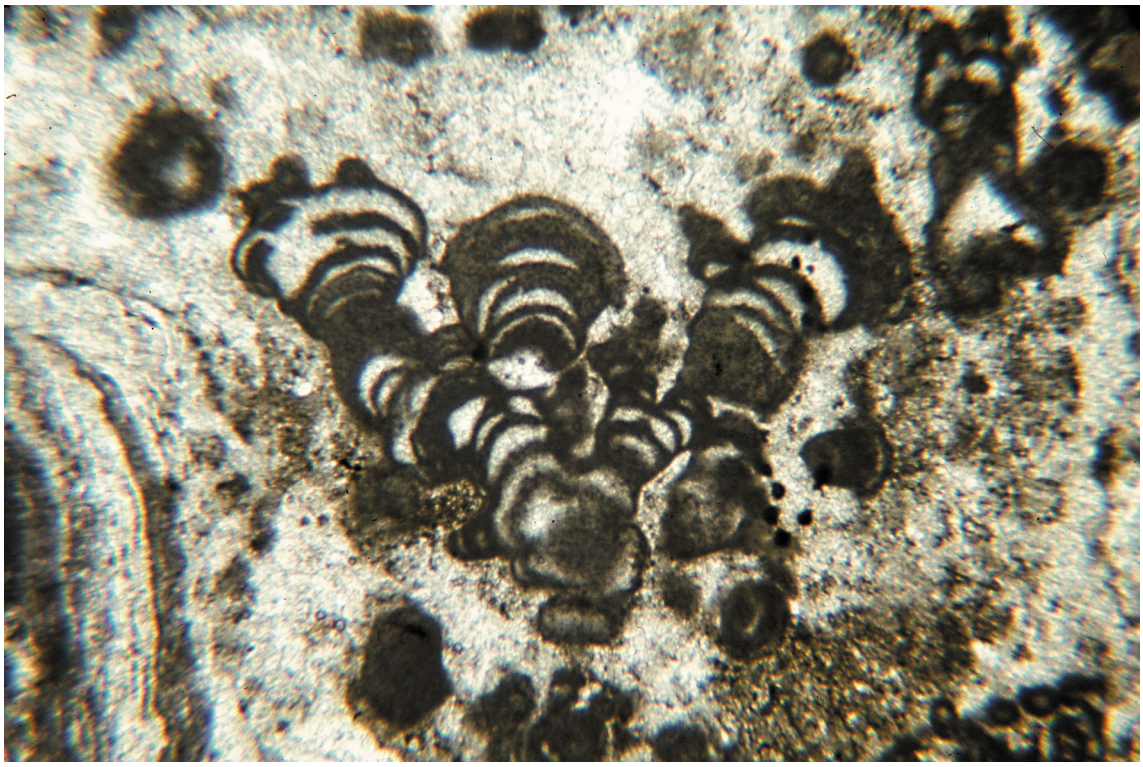

Figure 41. Colony of *Renalcis* in reef subfacies (Pillara Limestone), from an allochthonous block in the Piker Hills Formation at Mount Pierre. GSWA sample no. 3411. Width of field of view 3.6 mm.

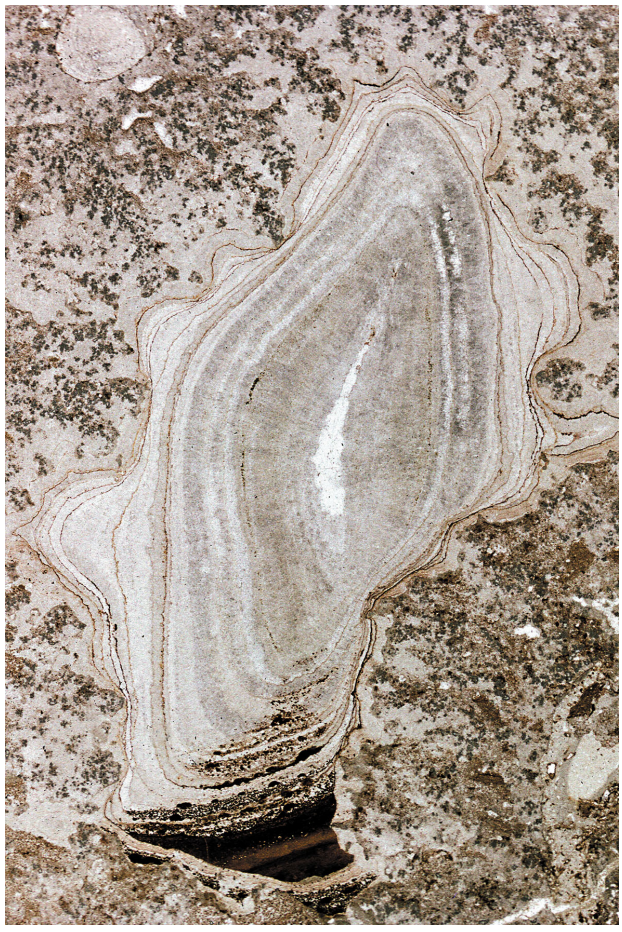

Figure 42. Thin section of a former cavity in reef limestone (Pillara Limestone) showing *Renalcis* that grew into the cavity, the rest of which was filled successively with red laminated cavity peloids, turbid radiaxial spar, and clear blocky calcite. Width of field of view 30 mm.



Figure 43. Thin section of a former cavity in reef limestone showing *Renalcis* that grew down into the cavity, the rest of which was filled firstly with laminated radiaxial calcite, interlaminated at the base with red cavity peloids, and then by clear blocky sparry calcite. From Windjana Gorge, Classic Face, GSWA sample no. 2000A. Width of field of view 42 mm.

Figure 44. (below) Polished slab of reef limestone (Pillara Limestone) from an allochthonous block in marginal-slope deposits at McIntyre Knolls, showing a colony of *Stachyodes* that fell over before being encrusted by *Renalcis.* The rest of the cavity system was then filled successively with red laminated peloidal limestone and clear sparry calcite. GSWA sample no. 3219.

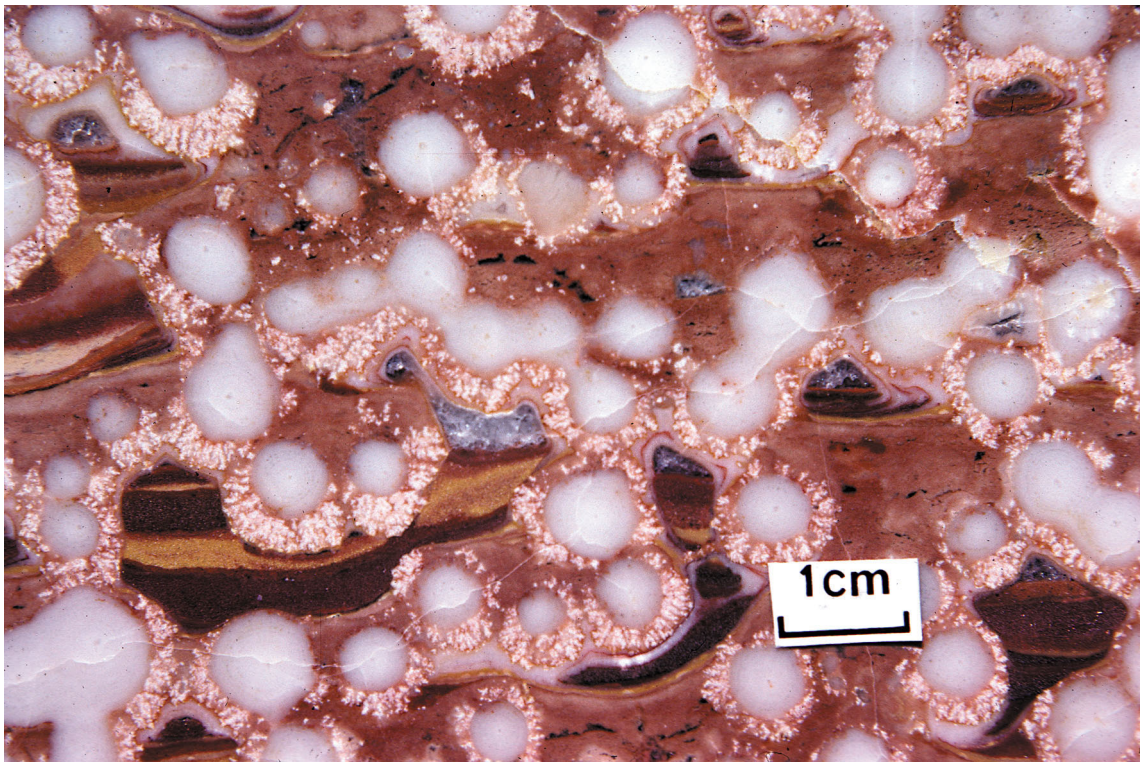



Figure 45. **(above) Polished slab of reef limestone (Pillara Limestone) from McIntyre Knolls, showing dense *Renalcis* encrusting stromatoporoids, the remaining cavities having been filled with red laminated peloidal limestone and white radiaxial calcite. GSWA sample no. 3497(5).**



Figure 46. **Polished slab of reef limestone (Pillara Limestone) from an allochthonous block in marginal-slope deposits at McIntyre Knolls. It shows *Stachyodes* encrusted with dense *Renalcis,* the remaining cavity having been filled with radiaxial sparry calcite and red peloidal limestone. Clear blocky calcite filled the last-remaining part of the cavity. GSWA sample no. 3497(4).**

as marine cement (Figs 40–46). The bodies commonly form clusters rimming stromatoporoid fragments and other fossils, or extend downward into 'umbrella' voids below platy stromatoporoids and in stromatactis cavities. In other cases *Renalcis* colonies are scattered through structureless micrite. In limestone platforms *Renalcis* is restricted to the reef-margin, reef-flat, and near-reef back-reef subfacies. It is also commonly abundant in reefal-slope subfacies, and is known to have grown to considerable depths (estimated to be more than 80 m) on marginal slopes.

Sphaerocodium (*Rothpletzella* of Riding, 2000) is another common cyanobacterium in reef-margin and reef-flat subfacies of the Pillara Limestone, but is most abundant in deeper-water deposits of the reefal-slope and fore-reef subfacies (Figs 47, 48; Wray, 1967). Non-skeletal microbes also played important roles in deposition of the Pillara Limestone (reef-margin, reef-flat, and back-reef subfacies; Wood, 2000b) and in deposition of most other parts of the Devonian reef complexes.

Most of the Pillara Limestone is Frasnian in age, based on the age of equivalent marginal-slope and basin facies. Fossils in the formation do not permit precise dating. However, the brachiopod *Stringocephalus fontanus* occurs in the oldest Pillara Limestone in the Emanuel, Home, and Pillara Ranges, and this genus is known in other parts of the world to be restricted to the Givetian (Johnson et al., 1980). The oldest known basin and marginal-slope deposits in the Limestone Billy Hills area, which are equivalent to the oldest part of the Pillara Limestone, are no older than *hermanni* Zone (G Klapper, 2004, written comm.). They contain palynological floras belonging to the mid-Givetian *lemurata–magnificus* palynomorph Zone (Grey, 1991, 1992), and consequently, Grey (1991) considered that deposition of the Pillara Limestone probably began during the middle Givetian. However, G Playford (Appendix 3) has expressed the opinion that the palynological evidence is insufficient to differentiate middle from upper Givetian in Australia. It is consequently concluded, placing main weight on the conodont evidence, that deposition of the outcropping Pillara Limestone and its oldest equivalent formations (Gogo Formation and Sadler Limestone) probably began during the late Givetian *hermanni* Zone. However, it is possible that older Givetian deposits could occur in the subsurface.

Deposition is thought to have continued, with only minor interruptions associated with backstepping events, throughout the Frasnian. The top of the Pillara Limestone at the Frasnian–Famennian boundary is an unconformity, exhibiting mild karstification in some areas, and having local relief of as much as 5 m (Fig. 49). The amount of section removed through this erosion is uncertain, but it may have been as much as 50 m in the northern Napier Range, where the unconformity cut down into the Frasnian reefal-slope subfacies (Napier Formation; Fig. 50).

The one known locality where abundant ammonoids occur in the Pillara Limestone is 4 km north of Brooking Springs Homestead (GPS AMG Zone 51, 780910E 7999200N), where *Beloceras* and rare *Manticoceras* are poorly preserved in microbial reef-flat deposits near the platform margin (Fig. 51). This horizon is late Frasnian in age, probably correlating with Zone 13 (Pillara Sequence 6), equivalent to the upper *Beloceras* bed in the Virgin Hills Formation at McWhae Ridge, although it could possibly correlate with Zone 12, equivalent to the lower *Beloceras* bed (M R House and R T Becker, 1994, written comm.; G Klapper, 2004, written comm.).

At some localities there is evidence of erosion surfaces within the Pillara Limestone that may be correlated with regional backstepping. An example of this is exposed on the northwest side of the Limestone Billy Hills (Fig. 52; AMG Zone 51, 791130E 7969520N), where reef-margin subfacies is overlain by back-reef facies, the boundary between them being an erosion surface showing planar truncation of heads of *Actinostroma.* This record of brief emergence may correlate with the Elliott Ridge Event, marking the boundary between Pillara Sequences 1 and 2.

The Frasnian–Famennian boundary marks one of the five major mass extinctions known from the stratigraphic record (Raup and Sepkoski, 1982; Fig. 53). In the Canning Basin that extinction is marked by the virtual disappearance of platform-building stromatoporoids and many of the shallow-water metazoans that previously characterized the platforms (Pillara Limestone) and upper marginal slopes (Virgin Hills and Napier Formations). However, the extinction event seems to have had little effect on the microbes, which continued their platform-building roles as before (see discussion in Wood, 1998, 2000a, and Playford et al., 2001). Deep-water receptaculitids, sponges, brachiopods, and crinoids were also able to survive the mass extinction, and some moved later in the Famennian into shallow water. Thick-shelled gastropods and bivalves that lived in shallow water were also able to survive. Deep-water stromatolites first became prominent on marginal slopes during the latest Frasnian Zone 13, and flourished in some areas during the early Famennian, possibly due to the elimination of microbe-consuming metazoans at that time (Fig. 54).

Reef-building corals that made significant contributions to the Givetian and early Famennian reefs had virtually disappeared in most areas before the middle Frasnian. However, *Disphyllum* is locally common in the younger part of the section in some areas, notably just north of McSherrys Gap (GPS AMG Zone 51, 723000E 8059900N), which is thought to be middle Frasnian in age. Stromatoporoids may have first started to decline during the latest Frasnian, before virtually disappearing at the close of that stage.

The disappearance of reef-building corals, and the possible decline of stromatoporoids in the late Frasnian, may have resulted from steadily falling water temperatures as Australia drifted away from the equator into cooler seas. Perhaps the reef-building corals were more sensitive to falling temperatures than the stromatoporoids, and were therefore eliminated earlier.



Figure 47. Branching stromatolite columns built by *Sphaerocodium*, in reefal-slope deposits adjoining the 'tail' of the Laidlaw Range platform.

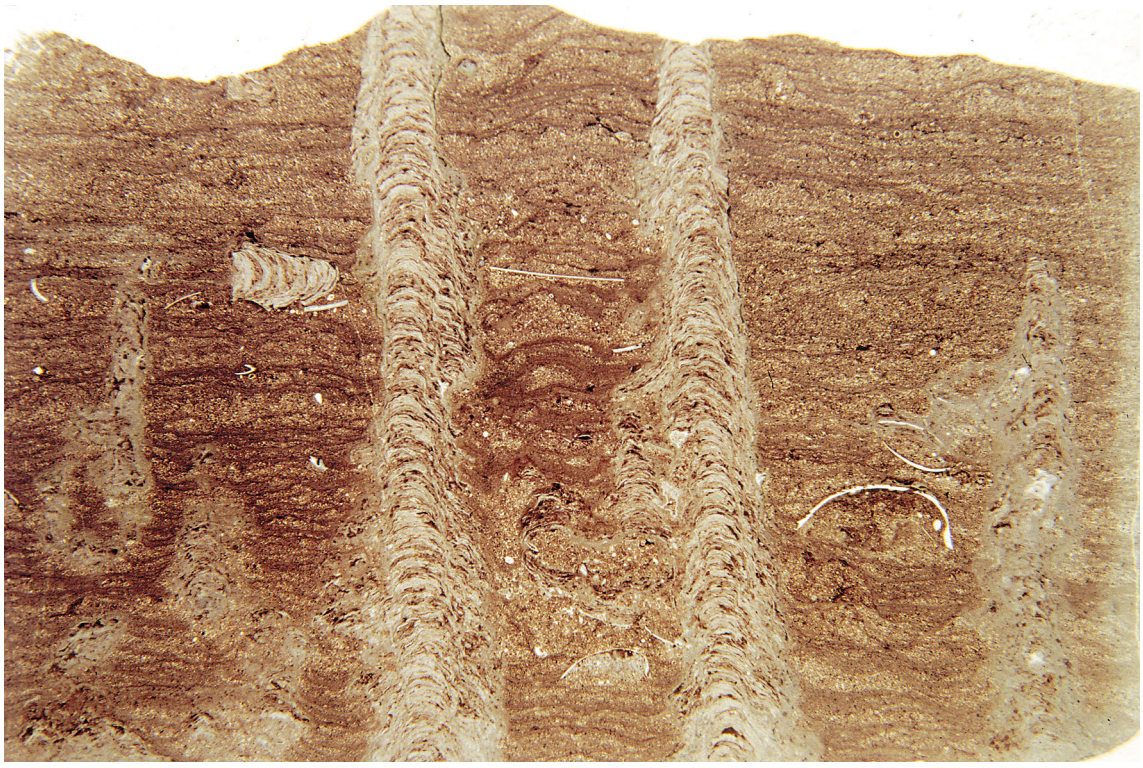

Figure 48. Thin section of narrow stromatolite columns, built by *Sphaerocodium* and non-skeletal sediment-binding microbes. The red micritic laminae between the columns are also thought to be microbially bound. Note the broken fragment of a column. GSWA sample no. 21655 (6), from Elimberrie no. 2 bioherm. Width of field of view 46 mm.



Figure 49. The Frasnian–Famennian unconformity in platform facies at the northwest end of the Oscar Range, showing well-bedded Nullara Limestone (early Famennian back-reef subfacies) overlying massive Pillara Limestone (late Frasnian, Pillara Sequence 6, reef-margin subfacies). The unconformity here has a relief of as much as 2 m.



Figure 50. The Frasnian–Famennian unconformity near Limestone Spring in the northwestern Napier Range, showing well-bedded Nullara Limestone (Famennian back-reef subfacies) overlying crudely bedded Napier Formation (late Frasnian reefal-slope subfacies). The dip in the Napier Formation is largely depositional. Photo by Roger Hocking.

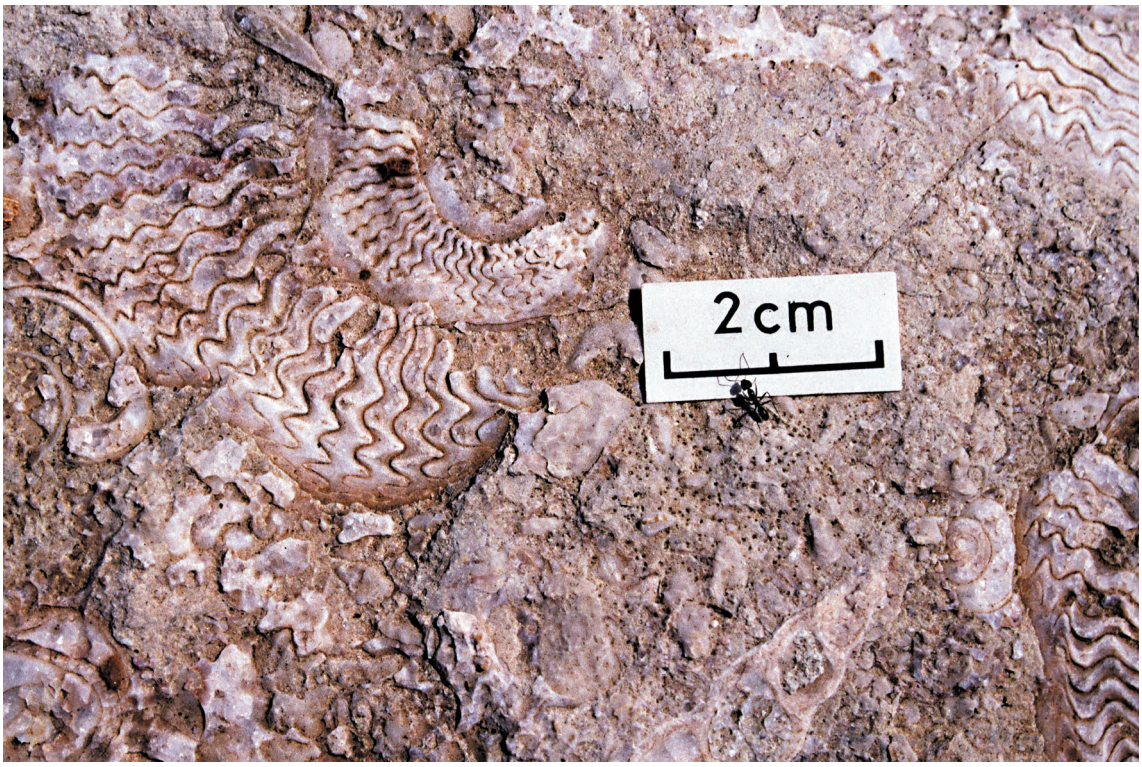

Figure 51. Pillara Limestone (reef-flat subfacies) containing the ammonoid *Beloceras*, at a locality 4 km north of Brooking Springs Homestead. The limestone here is late Frasnian in age, correlating with Pillara Sequence 6.



Figure 52. Unconformity within the Frasnian Pillara Limestone in the Limestone Billy Hills, showing well-bedded back-reef limestone overlying massive reef limestone. This boundary probably correlates with the early Frasnian Elliott Ridge Event, which marks the boundary between Pillara Sequences 1 and 2.

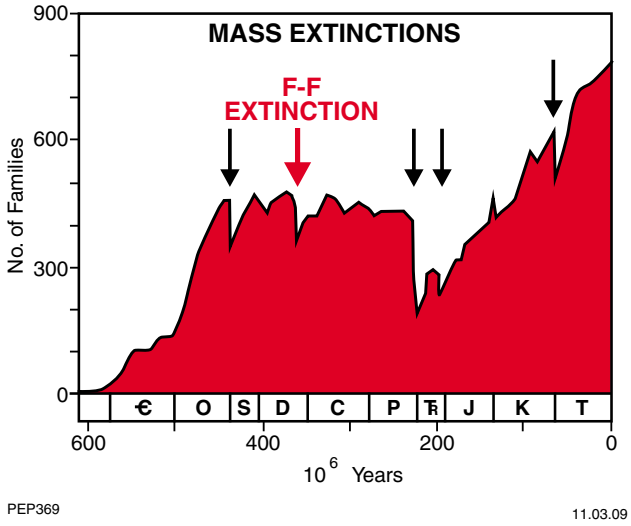

Figure 53. Diagram illustrating the five major mass extinctions of the Phanerozoic (from Raup and Sepkoski, 1982).

Windjana Limestone

Definition

The name Windjana Limestone was proposed by Playford and Lowry (1966) for the reef facies of the Devonian reef complexes. It was originally applied to both Famennian and Givetian–Frasnian reef limestones, but Playford and Cockbain (1976) and Playford (1980) restricted usage of this name to the Famennian reef-margin and reef-flat deposits.

The unit is named after Windjana Gorge (Plates 1, 6) in the Napier Range, where the type section extends along the southeastern wall of the gorge near the west entrance (AMG Zone 51, 706500E 8074000N). The limestones in this section lack microbial coatings, having been washed clean by the Lennard River during times of flood.

Lithology

The Windjana Limestone is typically a massive to very crudely bedded reef limestone, white, yellow, or pale red in colour. The reef was built primarily by microbes, with smaller contributions by receptaculitids, sponges, and stromatoporoids. The reef-margin subfacies, which makes up most of the formation, is typically massive. It interfingers with bedded back-reef limestones of the Nullara Limestone, and with crudely bedded reefal-slope deposits of the Napier Formation.

Micritic limestone, thought to have been precipitated by microbial activity, makes up most of the reef-margin and reef-flat deposits in the Windjana Limestone. The reef limestone was clearly rigid and wave resistant, as it contributed blocks of strongly cemented limestone to the fore-reef talus. Some workers would use the term ‘mud mound’ for buildups of such micritic limestone (e.g. Monty et al., 1995; Webb, 2001). However, that would not be an appropriate usage, as the limestones in these buildups never formed mounds of ‘mud’ — they were precipitated by microbes as rigid masses of rock, largely composed of micrite. It seems likely that many other so-called ‘mud mounds’ in the stratigraphic record (Monty et al., 1995; Webb, 2001) are similarly microbial bioherms.

Renalcis, which is common in many Frasnian reefs (especially those in the middle and upper Frasnian) is even more important in the Windjana Limestone, where it played a major role, together with non-skeletal microbes, in reef building.

Playford and Lowry (1966, p. 38) recognized that the turbid micritic or sparry groundmass in which *Renalcis* occurs ‘may in some cases be a primary precipitate’, but concluded that in other cases the groundmass ‘seems to be due to recrystallization or replacement’. Similarly, they regarded the banded layers of fibrous calcite in stromatactis cavities as having been formed by replacement of an earlier limestone. However, it is now clear that such micrites and banded spars are cavity-filling primary precipitates, although some may subsequently have been recrystallized to some extent (Kerans et al., 1986).

Stromatactis is a form of cavity filling in which the original cavity was formed by the decay of organic material, such as a sponge, and was filled at an early stage by sparry calcite, with or without detrital material and microbial peloids (Figs 55–58).

Stratigraphic relationships

The reef-margin and reef-flat subfacies represented by the Windjana Limestone interfinger with contemporaneous deposits of the back-reef subfacies, and with reefal-slope and fore-reef subfacies of the marginal-slope facies. The formation is thus the facies equivalent of the Nullara Limestone back-reef deposits and much of the Napier Formation marginal-slope deposits.

Throughout much of its history the Windjana Limestone advanced (prograded) over equivalent reefal-slope and fore-reef deposits of the Napier Formation. Tongues of reef commonly grew down the marginal slopes, probably

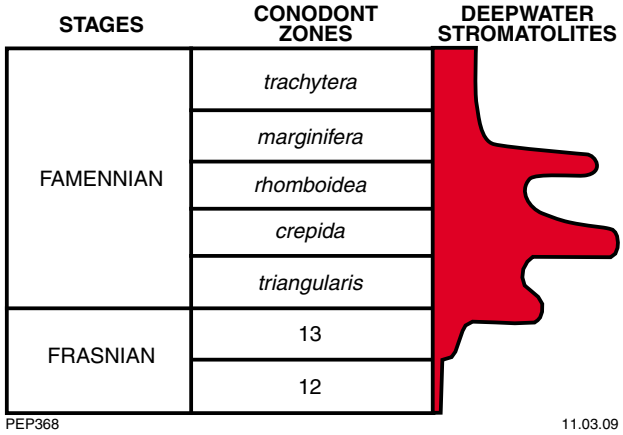

Figure 54. Diagram (not to scale) illustrating the increased development of deepwater stromatolites in the reef complexes during the latest Frasnian and early Famennian.

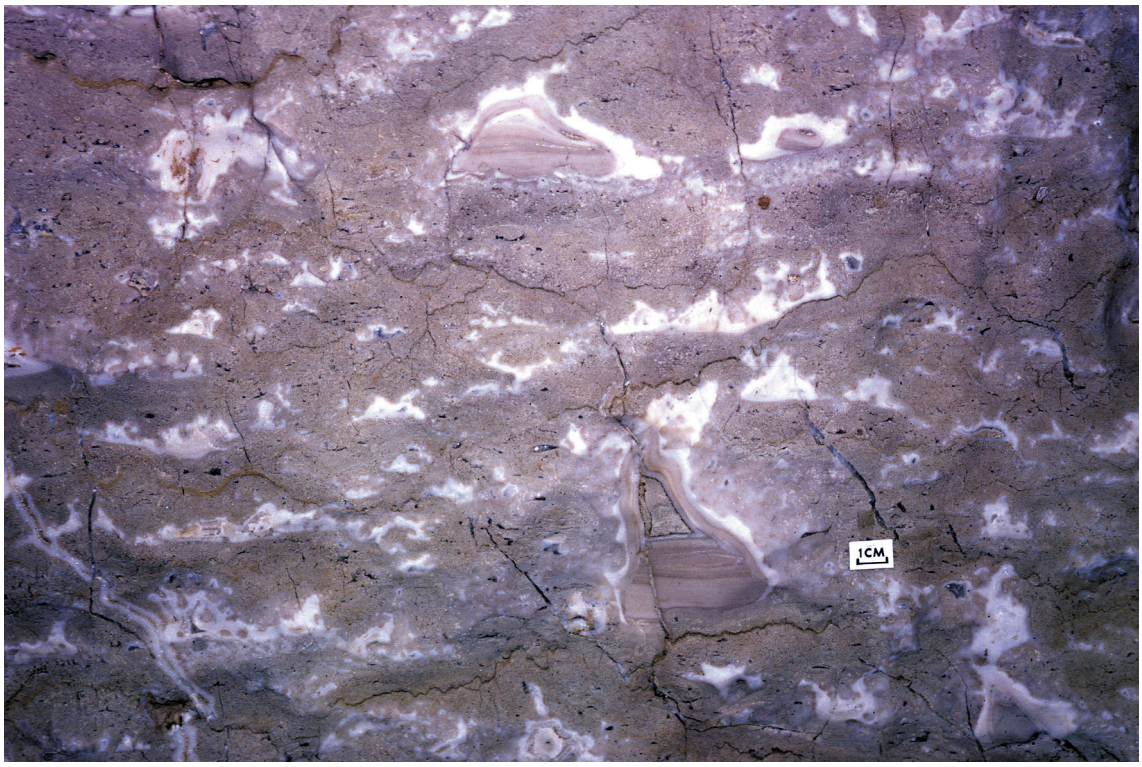

Figure 55. Stromatactis cavity-fillings (calcite and calcareous sandstone) in deep-water microbial reef limestone of the Windjana Limestone near the west entrance to Windjana Gorge.

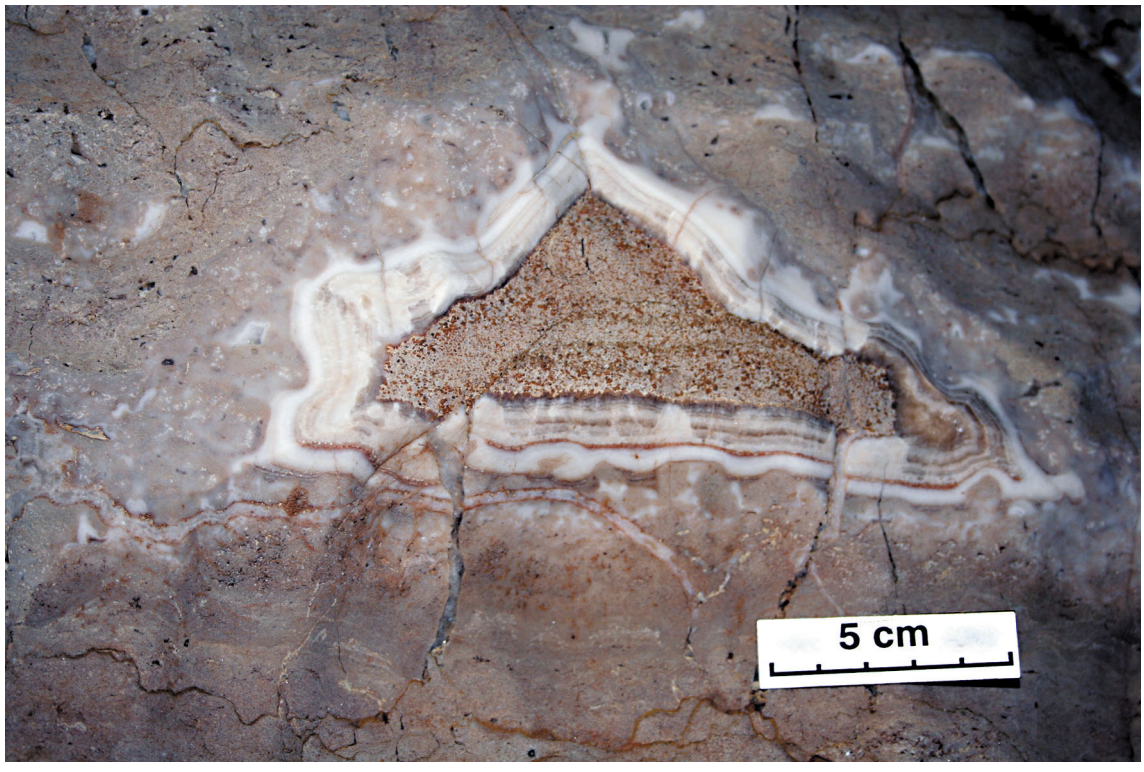

Figure 56. A stromatactis cavity-filling in microbial reef limestone of the Windjana Limestone near the west entrance to Windjana Gorge. The cavity was lined with laminated radiaxial calcite before the rest was filled with calcareous sandstone, identical with the sandstone that fills a nearby neptunian dyke.

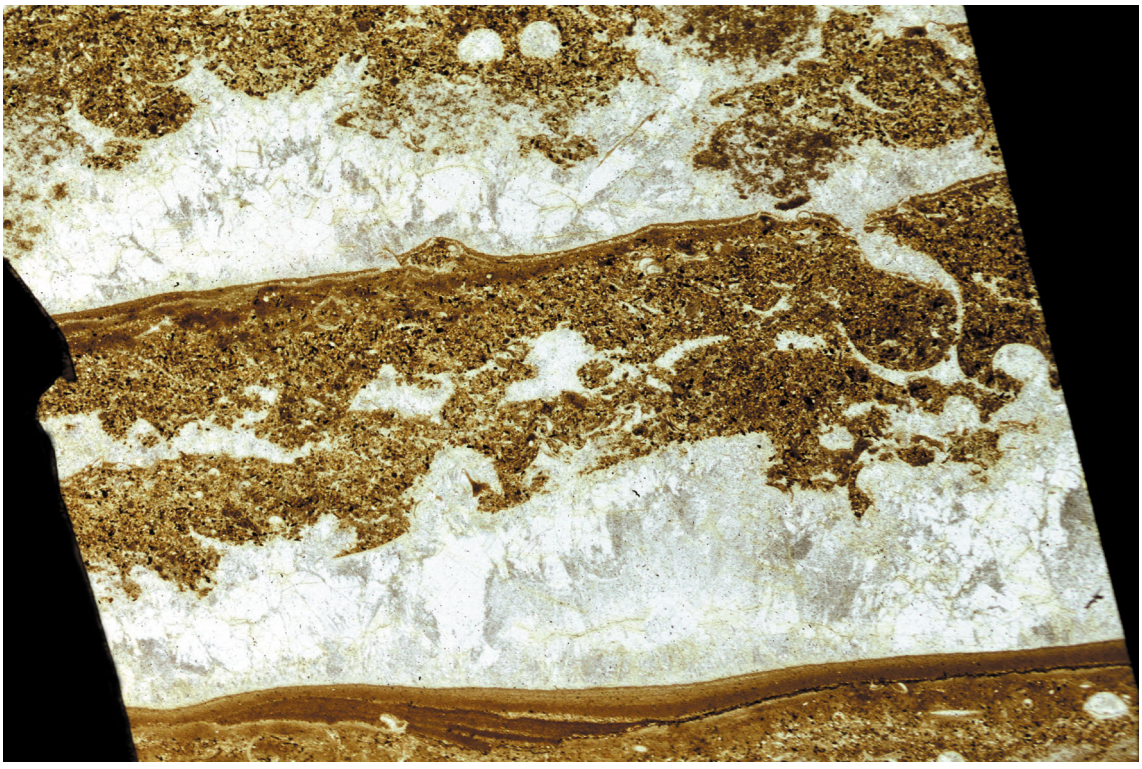

Figure 57. Thin section of stromatactis cavity fillings from the Virgin Hills Formation near Galeru Gorge. Laminae of cavity peloids were deposited on the floors of the cavities, followed by clear, equant, sparry calcite filling the rest. The cavities are thought to have resulted from the decay of organic material. GSWA sample no. 3261A. Width of field of view 33 mm.

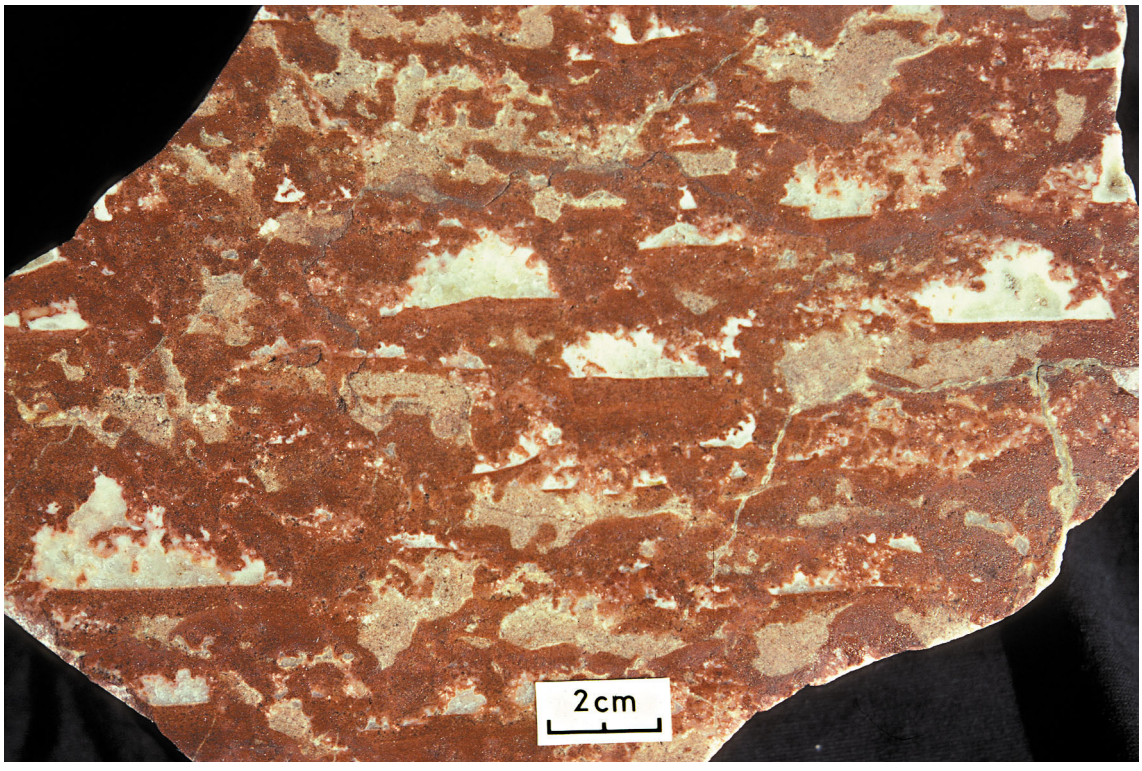

Figure 58. Polished slab of stromatactis limestone from an allochthonous block of reefal-slope limestone in fore-reef deposits of the Napier Formation beside Dingo Gap. GSWA sample no. 29499A.

extending to depths of more than 80 m. In some areas other reef tongues extended into back-reef deposits (Fig. 17).

The Windjana Limestone and its back-reef equivalent, the Nullara Limestone, are overlain unconformably by non-reefal shales and limestones of the late Famennian to Tournaisian Fairfield Group that were deposited after a regression had exposed the platforms for a relatively brief period (perhaps a few hundred thousand years), and the platforms had been subjected to subaerial erosion and mild karstification.

Distribution and thickness

The Windjana Limestone is exposed sporadically throughout much of the Devonian outcrop belt, from the Napier Range to the Horseshoe Range (Plates 1–3). The exposed width of the reef in this area ranges from less than 50 m to more than 1.5 km. However, the actual width of the living reef may not have exceeded a few hundred metres; where exposures of reef are wider than this, the increase can generally be attributed to basinward tilting since deposition.

The Windjana Limestone is not always present around the margins of Famennian limestone platforms, as in part of the area on the west side of the Horseshoe Range (Plate 3). Following the Horseshoe Range Event a large part of the platform became a bank, without a reef rim, adjoining a relatively shallow basin.

Fossils and age

Microbes were the main reef-building organisms in the Windjana Limestone, the most conspicuous of which are the microbe *Renalcis* (Wray, 1967) and stromatolite-building forms (Playford et al., 1976). Indeed, the presence of *Renalcis* is characteristic of much of the Windjana Limestone, although that fossil is also common in parts of the Frasnian Pillara Limestone reef, where it is commonly accompanied by stromatoporoids.

Although stromatoporoids are normally absent or rare in the Windjana Limestone, they are common in a few places, especially in some allochthonous blocks of middle and upper Famennian reef at the front of the Napier Range. Stromatoporoids also occur, less conspicuously, in the formation at its type locality on the southeast side of Windjana Gorge. Sponges (Rigby, 1986) and receptaculitids are common in some places, especially in the deeper parts of the reef where it interfingers with reefal-slope deposits. Megalodont and lithiotid bivalves occur in the formation and near-reef parts of the equivalent Nullara Limestone in some areas (Figs 59–61).

None of the fossils in the Windjana Limestone are known to be of value for precise dating of the formation. However, its Famennian age is shown by conodonts from interfingering parts of the Napier Formation.

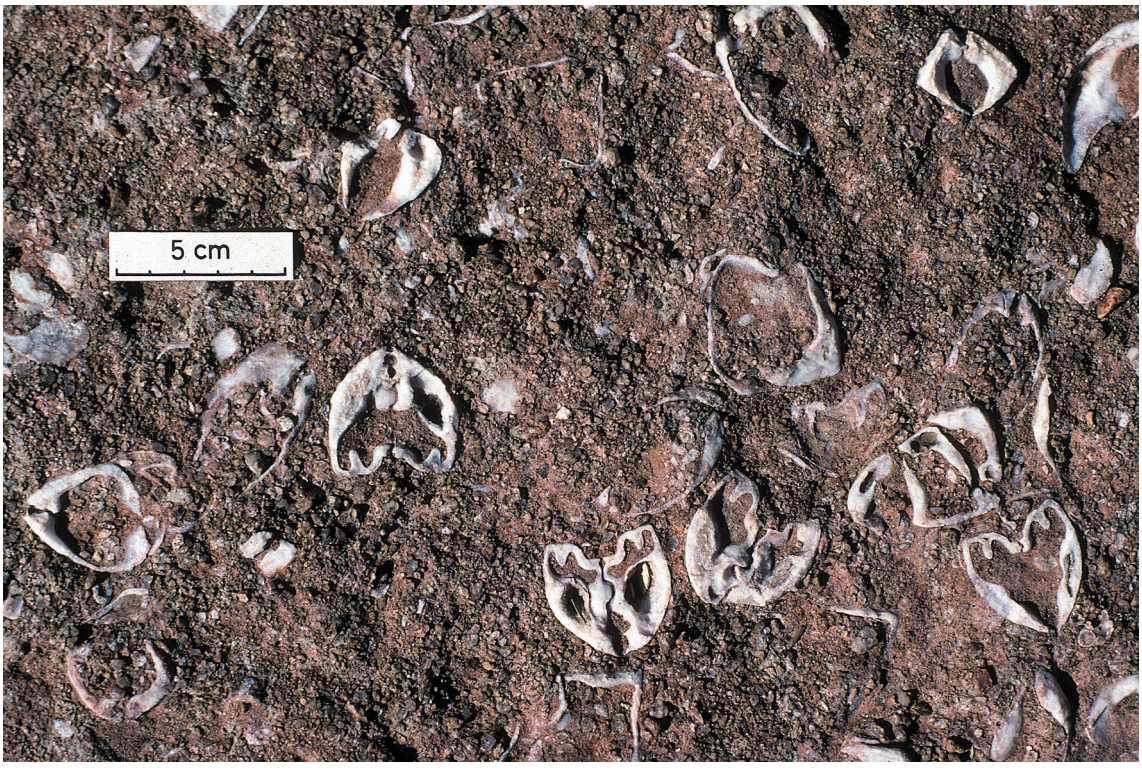

Figure 59. Megalodont bivalves in their growth positions in sandy limestone of the Nullara Limestone (Famennian), near Longhole Bore, Fossil Downs Station.



Figure 60. Lithiotid bivalves in their growth positions, in Nullara Limestone east of Pothole Bore, Fossil Downs Station.

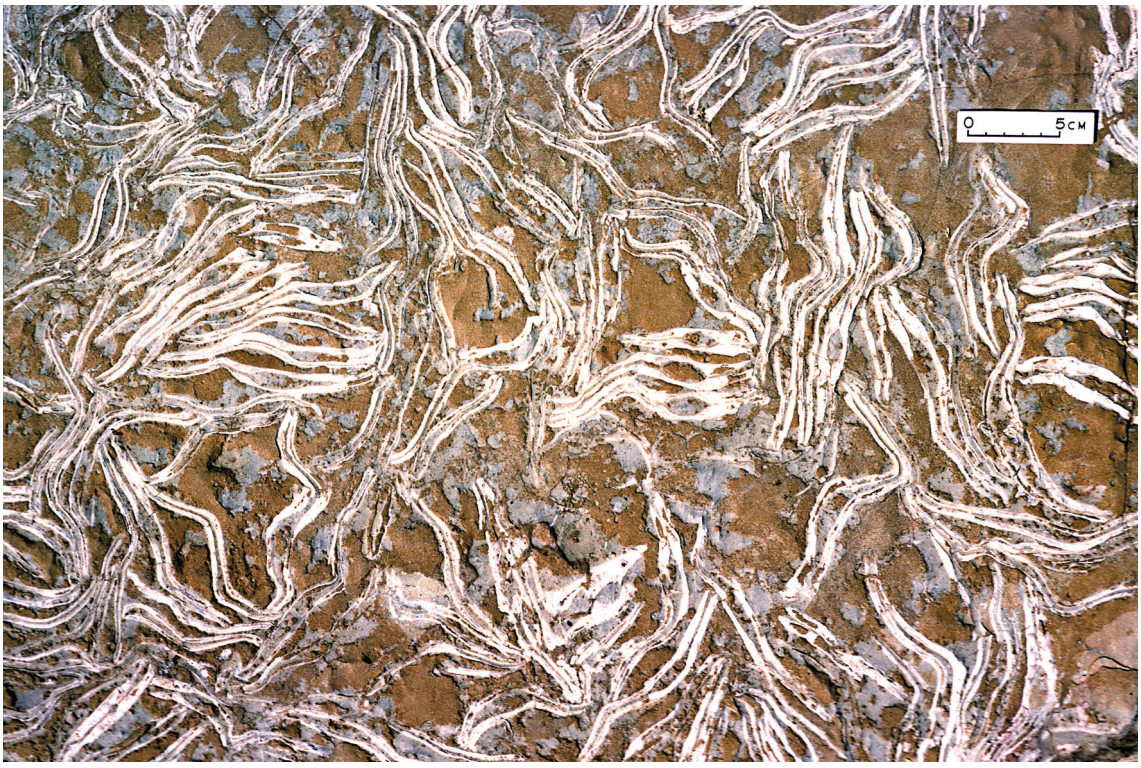

Figure 61. Densely packed lithiotid bivalves in their growth positions in Nullara Limestone east of Pothole Bore, Fossil Downs Station.

Nullara Limestone

Definition

The name 'Nullara Oolite' was first introduced for this unit by Smith et al. (1957), who mistakenly regarded it as a fore-reef deposit. The name was revised to Nullara Limestone by Playford and Cockbain (1976), who applied the name to Famennian back-reef and bank subfacies of the platform facies. The name is taken from Nullara Spring near the northeastern end of the Oscar Range (Plate 2), and the type section is situated nearby (AMG Zone 51, 705800E 8047700N).

Lithology

The Nullara Limestone consists predominantly of well-bedded fenestral (microbial) calcarenite and oolite, with some interbeds of sandstone and siltstone. Oncolite-rich beds also occur, and columnar stromatolites are common in some areas. Like other Devonian units on the Lennard Shelf, the Nullara Limestone in outcrop is overlain with angular unconformity by the Lower Permian Grant Group. Metre-scale cyclicity is present in the limestone, but the cycles are much thinner and less clearly expressed than in the Pillara Limestone.

Well-developed tepee structures have been noted in several localities, notably at the west end of the Oscar Range (Fig. 62), near Chedda Cliffs, in Billy Munro Gorge, and at the top of the Nullara Limestone in the Horseshoe Range. Linked polygonal structures on bedding surfaces, outlined in fenestral limestone (Fig. 63), are also associated with tepee structures.

Chow and George (2004) claimed that tepee structures near Chedda Cliffs are microbial structures formed by draping of strata over microbial mounds, rather than being tepees formed by early intrastratal compression. However, field examination of the examples that they describe, and others in the same area, show that the structures are true tepees, with crestal breaching and overthrusting indicative of a compressive origin. Cavities below the disrupted strata were filled with microbial deposits soon after the tepees formed. More studies are required to determine the cause of the compression, but it might be due to expansion resulting from carbonate crystallization in intertidal to supratidal environments. Although no evaporite pseudomorphs have been found in the associated strata, it is also possible that crystallization of evaporites in the back-reef environment produced the observed compression.

Stratigraphic relationships

The Nullara Limestone is a back-reef and bank unit, which, together with the Windjana Limestone, makes up the Famennian platform facies of the reef complexes. The formation unconformably overlies Pillara Limestone and interfingers with Windjana Limestone. In the Horseshoe Range area (Plate 3) the Nullara Limestone interfingers with fore-bank subfacies of the Piker Hills Formation. The Nullara Limestone is overlain unconformably by the Fairfield Group in the Horseshoe Range and Red Bluffs areas (Plates 4, 7) and subsurface well sections.



Figure 62. Tepee structure in Nullara Limestone near the northwest end of the Oscar Range, showing crestal breaching.



Figure 63. The upper surface of a bed with polygonal tepee structures in the uppermost part of the Nullara Limestone in the Horseshoe Range.

Distribution and thickness

The Nullara Limestone is exposed sporadically from the Napier Range in the north (Plate 1) to Red Bluffs in the south (Plates 4, 7). The formation is 135 m thick in the type section at the northwestern end of the Oscar Range (Hurley, 1986), and the thickest known section, 470 m, is in the Horseshoe Range. It seems clear that the formation is considerably thinner (more condensed) in the Napier and Oscar Ranges, presumably because less subsidence occurred during the Famennian in those areas than in the Horseshoe Range. The Mount Elma Fault beside the Horseshoe Range is thought to have been active during the Famennian, with normal displacement, which led to deposition of the Elma and Barramundi Conglomerates in front of the fault scarp and to a thicker development of Nullara Limestone in that area than in other parts of the Lennard Shelf.

Fossils and age

Most of the Nullara Limestone consists of unfossiliferous microbial limestone and oolite, and fossils that are known in the unit have little value for precise dating. The Famennian age of the formation has been established through conodont and ammonoid dating of equivalent marginal-slope and basin deposits (Fig. 20).

Some beds in the Nullara Limestone contain abundant thick-shelled bivalves (lithiotids and megalodonts, Figs 59–61) and a few other skeletal fossils, including thick-shelled gastropods and bulbous bryozoans. Stromatoporoids are very rare other than in some late Famennian parts of the formation.

Marginal-slope and basin facies

Six formations are recognized in the marginal-slope and basin facies of the reef complexes. In the southeastern Lennard Shelf these are the Givetian–Frasnian Sadler Limestone and Gogo Formation, the Frasnian–Famennian Virgin Hills Formation, and the Famennian Bugle Gap Limestone and Piker Hills Formation. The equivalent marginal-slope deposits in the central and northwestern parts of the shelf are placed in the Frasnian–Famennian Napier Formation.

Sadler Limestone

Definition

The name ‘Sadler Formation’ was introduced by Guppy et al. (1958) for the limestones exposed at Sadler Ridge (AMG Zone 51, 810700E 7939300N; Plates 4, 5) and along the north side of the Emanuel Range. The name was amended to Sadler Limestone by Playford and Lowry (1966) because limestone is the dominant and characteristic lithology in the formation. It is entirely a marginal-slope deposit.

Lithology

The Sadler Limestone consists of thin-bedded light-grey to yellow-grey calcarenite (packstone, grainstone, and wackestone), with lesser thicknesses of interbedded calcareous shale and siltstone that are only rarely exposed. Most of the formation belongs to the fore-reef subfacies, grading into reefal-slope subfacies where it adjoins Pillara

platforms. The formation commonly contains reef-derived detritus, including some medium- to thick-bedded breccias and massive debris-flow megabreccias. In some places the Sadler Limestone contains large allochthonous blocks of reef limestone, as much as 120 m across, that have rolled or slid down the fore-reef slopes following major platform-margin collapse (e.g. near Sadler Ridge, Fig. 64). Thin-bedded limestones in the formation are contorted in certain areas, due to down-slope sliding on interbedded shales or compaction over allochthonous blocks or buried pinnacle reefs, for example beside the Wade Knoll pinnacle reef (GPS AMG Zone 52, 183460E 7934320N).

A characteristic feature of much of the limestone in this formation is the occurrence of abundant silicified fossils on weathered surfaces (Fig. 65). Most are brachiopods, which flourished on the fore-reef slopes. Associated with them are fragmentary stromatoporoids and corals, shed from the adjoining platforms. The silica is thought to have been derived from skeletons of radiolarians that accumulated in vast numbers in the adjoining basins. Most were crushed and dissolved during compaction of the enclosing shales and siltstones, and the silica-bearing fluids expelled during compaction migrated into the adjoining limestones of the Sadler Limestone, where they selectively silicified fossils.

Stratigraphic relationships

The Sadler Limestone abuts and interfingers with the equivalent platform facies (Pillara Limestone) and basin facies (Gogo Formation). In some places where it is associated with backstepping events in the adjoining platforms, the formation downlaps onto Pillara Limestone. In most areas the boundary with the Gogo Formation is mapped only approximately, because exposures in the Gogo Formation are poor or may be absent.

Fore-reef depositional dips in the Sadler Limestone are commonly as high as 30° in fore-reef deposits, and more than that in reefal-slope deposits, where microbial precipitation and binding occurred. The depositional dip is much lower (commonly 5° or less) in fore-bank deposits that interfinger directly with bank subfacies of the Pillara Limestone, such as on the north side of the Emanuel Range near Kudata Gap (Fig 66). The depth of water in the basin was relatively shallow in such areas, and the platform environment was unsuitable for the development of reef rims.

Distribution and thickness

The Sadler Limestone is recognized in the southeastern Lennard Shelf, from Horse Spring Range to Bugle Gap and the Old Bohemia Valley, as shown on Plates 3, 4, 5, and 7. Northwest of Horse Spring Range the correlative marginal-slope deposits are assigned to the Napier Formation. The maximum thickness of the formation is estimated to be at least 700 m, based on the thickness of equivalent parts of the Pillara Limestone. Guppy et al. (1958) measured 375 m in the type section at Sadler Ridge, but this did not take depositional dip into account, and the true vertical thickness of that section is estimated to be about 250 m.

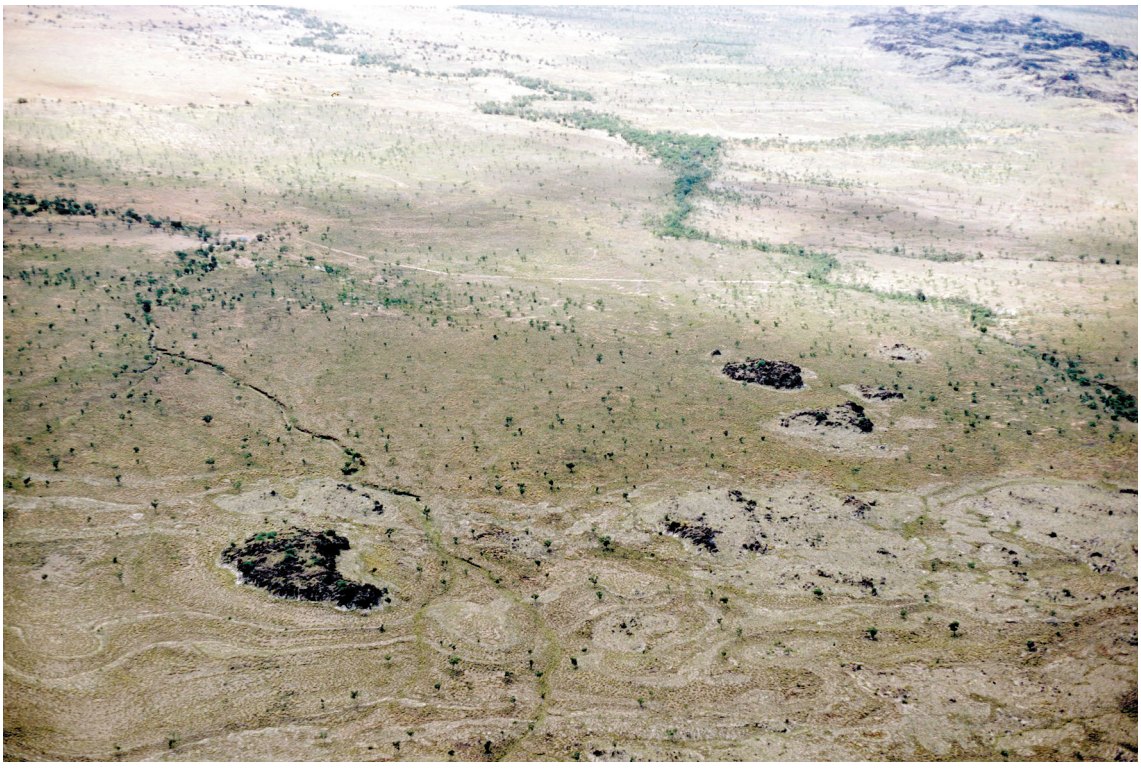

Figure 64. Aerial view, looking northeast, of large allochthonous blocks (as much as 120 m across) in Sadler Limestone (fore-reef subfacies) near Longs Well. The blocks, resulting from large-scale collapse of the platform margin, rolled and slid to near the base of the marginal slope.



Figure 65. Silicified fossils, mainly brachiopods, in Sadler Limestone on the east side of the Emanuel Range. Silicification is attributed to the expulsion and migration of silica-rich fluids derived from abundant radiolarians in adjoining basin deposits of the Gogo Formation. Field of view ~15 cm.

Fossils and age

The Sadler Limestone is one of the most richly fossiliferous formations in the reef complexes. The abundant macrofauna is characterized especially by brachiopods (Veevers, 1959a,b; Grey, 1978), which are commonly silicified and tend to weather out of the limestones in excellent states of preservation (Fig. 65). The fossil fauna also includes corals (Fig. 67; Hill and Jell, 1970; Brownlaw, 2000), stromatoporoids (Cockbain, 1984, 1989), gastropods (Cook et al., 2003), and bryozoans (Ross, 1961). Most stromatoporoids and corals in the formation are believed to have been derived from the adjoining platforms, although some grew in situ in the shallow-water part of the Sadler Limestone. The most common detrital stromatoporoids are fragments of *Amphipora*. Some tabular and laminar stromatoporoids and a few bulbous forms also occur in situ in the formation. They grew on the upper slopes, extending to maximum water depths of about 25 m.

Goniatites are abundant in some horizons, as described by R T Becker and M R House in Appendix 2 and by Glenister (1958), Becker et al. (1993), and Becker and House (1997). The assemblage correlates with the lower *Manticoceras* Zone of the German succession. Conodonts are abundant in some sections, as described by G Klapper in Appendix 1, Klapper (1995), and Klapper and Becker (1999). They indicate that the formation ranges from the late Givetian *hermanni* Zone to Frasnian Zone 5 (Klapper and Becker, 1999; G Klapper, 2004, written comm.). Note that the Frasnian conodont zones adopted here are those of Klapper (1997a, 2000, 2007).

Gogo Formation

Definition

The Gogo Formation was named after Gogo Station pastoral lease by Guppy et al. (1958), for a unit of siltstone and shale with thin beds of limestone, commonly containing distinctive limestone concretions ('Gogo nodules'). The type section is situated southeast of the northern entrance to Menyous Gap (AMG Zone 51, 799900E 7964200N; Plate 4).

The Gogo Formation underlies the Virgin Hills Formation and interfingers with the Sadler Limestone. Exposures everywhere are poor, but the unit has been cored in many mineral-exploration drillholes (Copp, 2000).

Lithology

The Gogo Formation is characterized in the subsurface by grey to black shales and siltstones with sporadic thin limestones composed of platform- and slope-derived debris (Copp, 2000). The breccias have probably been carried into the basins as debris flows, but in some cases there is evidence of deposition by turbidity currents. It is clear that most of the formation was laid down under hypoxic conditions.

Sandstone and conglomerate forming deep-water extensions of the lowermost Sparke Conglomerate interfinger with shales of the Gogo Formation in some areas, notably at the southeast end of the Pillara Range (AMG Zone 51, 814600E 7952900N)

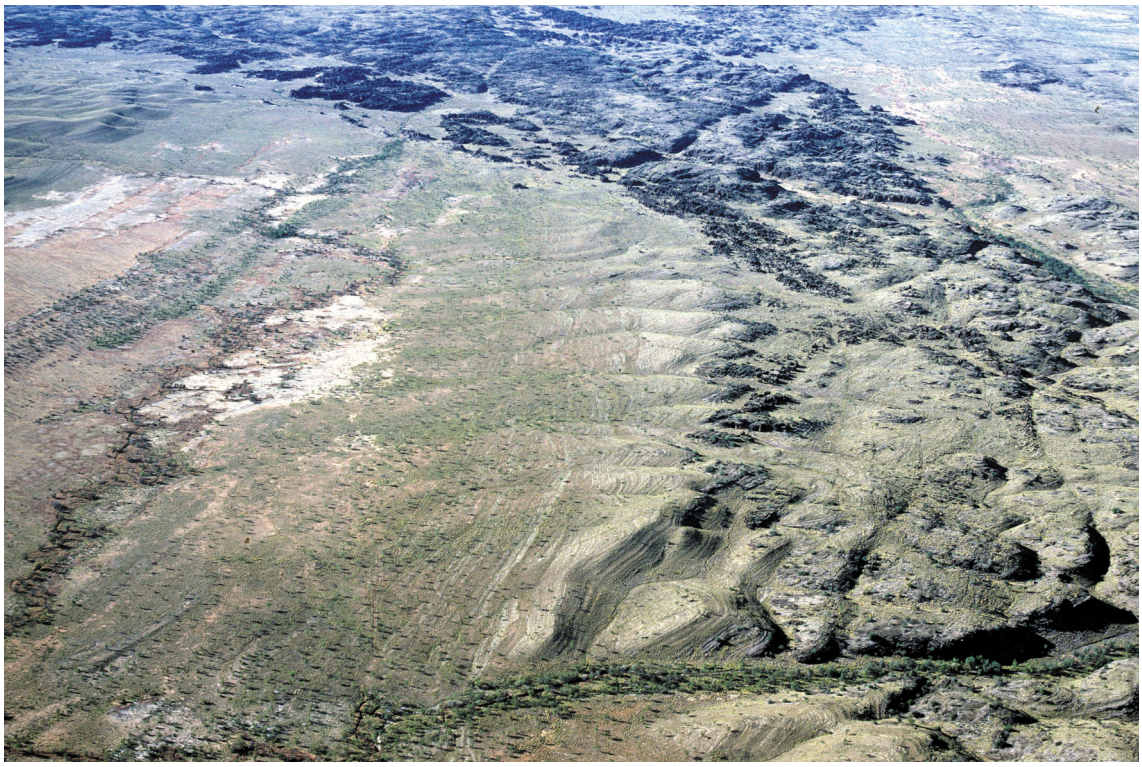

Figure 66. Aerial view looking southeast over Gap Creek and the Emanuel Range. Bank subfacies of the early Frasnian or late Givetian Pillara Limestone interfingers with fore-bank facies of the Sadler Limestone.

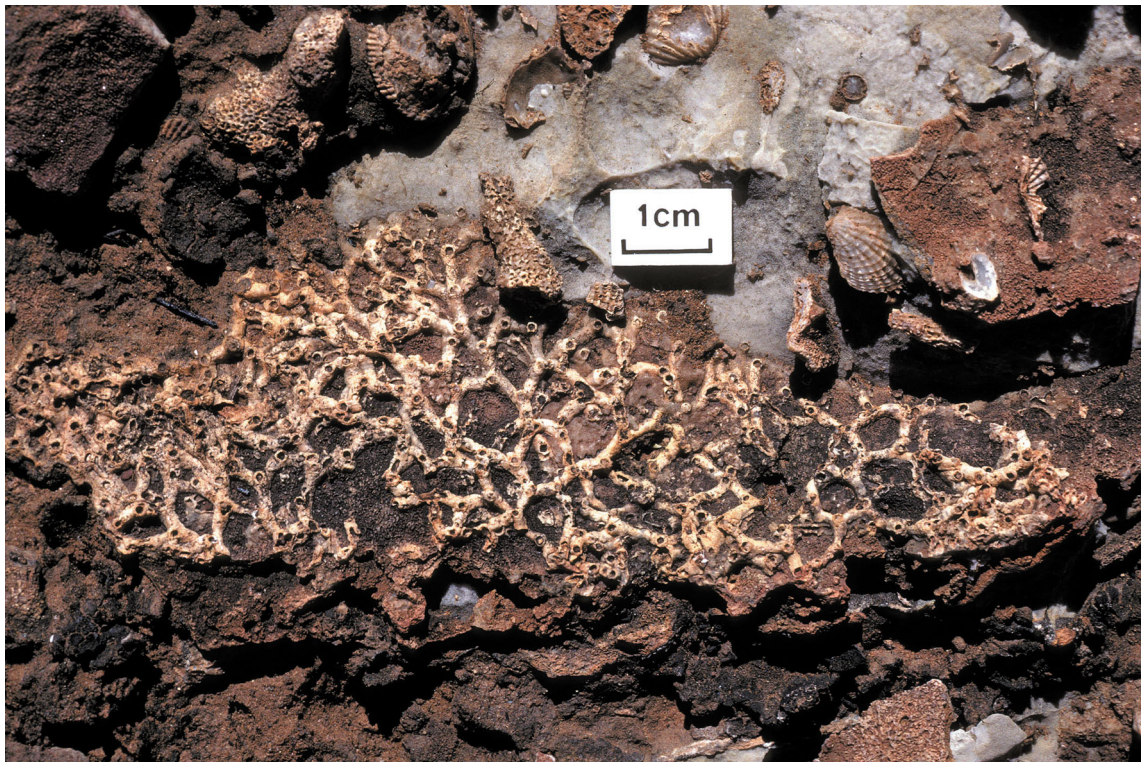

Figure 67. *Aulopora* encrusting a bed in Sadler Limestone (fore-reef subfacies), on the east side of the Emanuel Range.

Horizons with limestone concretions ('Gogo nodules') are rarely seen in coreholes that penetrate the Gogo Formation, other than in areas where that unit interfingers with or abuts the Sadler Limestone or occurs in enclosed basins such as the Paddys Valley embayment (Plates 4, 5). In some places the concretions are associated with stromatolite–sulfide buildups that developed along contacts between the Gogo Formation and Sadler Limestone, or beside active faults (Playford and Wallace 2002). The concretions (Figs 68, 69) are thought to have been precipitated by bacterial action in anoxic muds, before those muds were compacted to form shales. Some concretions were precipitated around fish and arthropods, perfectly preserving their uncrushed skeletons (Long, 1988). Where concretions were formed in radiolarian oozes, the radiolarians are similarly uncrushed and very well preserved (Fig. 70; Nazarov and Ormiston, 1983; Nazarov et al., 1982; Aitchison, 1993; Won, 1997a,b).

Stratigraphic relationships

The Gogo Formation is the basinal equivalent of the marginal-slope Sadler Limestone, with which it interfingers. The formation is overlain by the Virgin Hills Formation, conformably or unconformably in various places. The contact with that formation coincides with the Waggon Pass Event, at the boundary between Pillara Sequences 5 and 6.

In some places the Gogo Formation directly overlies pinnacle reefs of Pillara Limestone. This relationship can be inferred at a number of localities in outcrop, for example at Wade Knoll, Lloyd Hill, and Glenister Knolls (Plate 5), but is shown most clearly in drillholes (Copp, 2000). The pinnacle reefs may in some cases have emerged very briefly above sea level before being drowned and overlain by shale of the Gogo Formation.

Elsewhere in the subsurface, and in some places in outcrop, there is a conformable and gradational contact between black or dark-grey shales of the Gogo Formation and green or red shales of the Virgin Hills Formation. Gradation between the Gogo Formation and those units can extend over about one to five metres (Copp, 2000). Such a gradational change between the two units can also be seen in outcrop in the Old Bohemia area, near McPhee Knoll (AMG Zone 52, 193700E 7936800N).

Distribution and thickness

The Gogo Formation has been mapped in the Bugle Gap, Emanuel Range, and Pillara Range areas, but exposures are poor throughout. Guppy et al. (1958) recorded that the thickness of the formation in its type area beside the Pillara Range is about 425 m. The maximum thickness of the unit is expected to be at least as much as that of the Sadler Limestone (probably not less than 700 m).

Fossils and age

The fossil fauna in the Gogo Formation occurs mainly in calcareous concretions ('Gogo nodules') and thin limestone beds. Concretions and limestone weathered out of the formation commonly occur in clayey soil



Figure 68. Gogo nodules (limestone concretions) weathered out of the Gogo Formation near Longs Well.



Figure 69. Core from a mineral-exploration drillhole in the Limestone Billy Hills area showing compaction around a concretion ('Gogo nodule') in the Gogo Formation. The concretion was precipitated around a goniatite and has not compacted since deposition, whereas the shale has compacted by about 70%, as determined by correlating bedding in the concretion with equivalent bedding in the shale.

derived from soft shales that are themselves only rarely exposed. The fauna is typically pelagic, and is especially notable for its fossil fish (Long, 1988), arthropods (Young et al., 2000), radiolarians (Aitchison, 1993), and phytoplankton (Colbath, 1990). Other pelagic fossils found in the formation include conodonts (Glenister and Klapper, 1966; Klapper and Becker, 1999), goniatites (Glenister, 1958; Becker et al., 1993; Becker, 2000), tentaculitids (Cockbain, 1976b), and nautiloids (Teichert, 1939). The Gogo Formation is known to range from the *hermanni* Zone of the late Givetian to Zone 5 of the early Frasnian (G Klapper, 2004, written comm.).

Virgin Hills Formation

Definition

The Virgin Hills Formation is named after the Virgin Hills (AMG Zone 51, 801200E 7953650N) on Gogo Station, where the unit is well exposed. The type section is located east of Needle Eye Rocks (AMG Zone 51, 802000E 7977800N), where goniatites and other fossils were first collected from the formation by Hardman in 1883 (Hardman, 1884; Figs 71, 72). The type section is located in the basin facies of the unit, but the formation in other areas also includes extensive developments of marginal-slope facies.

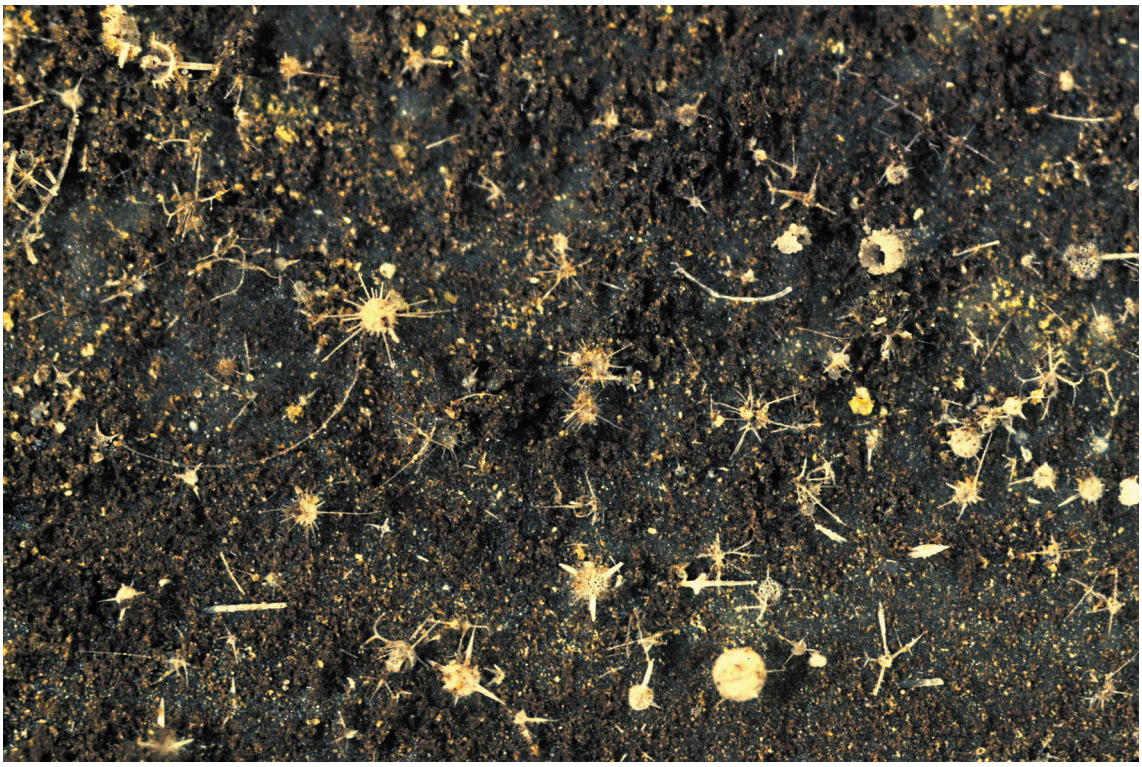

Figure 70. Radiolarians etched out of a Gogo concretion, from near the northwest end of the Pillara Range. These delicate fossils are preserved in their original forms because the concretion has remained uncompacted after being precipitated at an early stage (probably immediately below the sea floor) in mud containing abundant radiolarians. Field of view 1.5 cm.



Figure 71. Sketch by E T Hardman of Mount Pierre (on the right), showing Hardman collecting ammonoids from the Virgin Hills Formation. This is one of a series of sketches made by Hardman in 1883 during his expedition to the Kimberley District with John Forrest (Hardman, 1884).



Figure 72. Photograph, taken in 2003, of the same view of Mount Pierre and adjoining hills as shown in Figure 71. Mount Pierre is capped by Piker Hills Formation, over Virgin Hills Formation.

Lithology

The Virgin Hills Formation is characterized especially by the bright red colour of some beds, although other parts are white, yellowish grey, and green. The red colouration is especially prominent in basin facies of the formation, which consists of thin-bedded calcareous siltstone and shale, interbedded with limestone, sandstone, and minor conglomerate. Limestone breccias that occur interbedded in the basin deposits commonly contain platform- and marginal-slope-derived material, deposited by debris flows and turbidity currents (Copp, 2000). Deep-water sandstone and conglomerate in the formation are the 'tails' of submarine fans that extended down from the Sparke Conglomerate and other conglomerate formations.

The marginal-slope subfacies of the Virgin Hills Formation consists predominantly of very thick- to medium-bedded sandy breccias, megabreccias, and calcarenites, that are typically red to reddish and yellowish grey in colour. The breccias and megabreccias have mostly been deposited as debris-flow deposits, with large blocks of reef-margin, reef-flat, and reefal-slope limestones forming the major parts of many flows. McIntyre Knolls and Rattigan Rocks are prominent examples of huge allochthonous reef blocks in the Virgin Hills Formation (Plate 5), with individual blocks as much as about 200 m across.

Stratigraphic relationships

The boundary between the Virgin Hills Formation and the underlying Sadler Limestone and Gogo Formation can be conformable or unconformable, depending on the location. In some places, such as in the Shady Bore block, the Virgin Hills Formation overlies the Pillara Limestone with angular unconformity.

The Virgin Hills Formation is overlain conformably by the Piker Hills Formation. It interfingers with the lower and middle parts of the Bugle Gap Limestone and is equivalent to much of the exposed part of the Napier Formation.

Distribution and thickness

The Virgin Hills Formation has been mapped in the part of the Lennard Shelf east of Boab Creek, in the Virgin Hills, Outcamp Hill, Bugle Gap, Old Bohemia, Horse Spring Range, and Mount Elma areas. The maximum thickness of the unit is unknown, but is expected to exceed 750 m in some areas (Plates 4, 5). The type section measured near Needle Eye Rocks by Guppy et al. (1958) is 220 m thick, but this does not include the Frasnian part of the formation.

Fossils and age

The Virgin Hills Formation contains rich fossil biotas that include goniatites (Teichert, 1941; Glenister, 1958; Petersen 1975; Becker et al., 1991; Becker et al., 1993; Becker and House, 1997), conodonts (Glenister and Klapper, 1966; Druce, 1976; Seddon, 1970; Klapper, 1995; Klapper and Becker, 1999), nautiloids (Teichert, 1939), gastropods (Cook et al., 2003), brachiopods (Veevers, 1959a,b; Grey, 1978), crinoids (Jell and Jell, 1999), microbes and algae (Wray, 1967; Edgell, 2003), sponges (Rigby 1986), tentaculitids (Cockbain, 1976b), trilobites

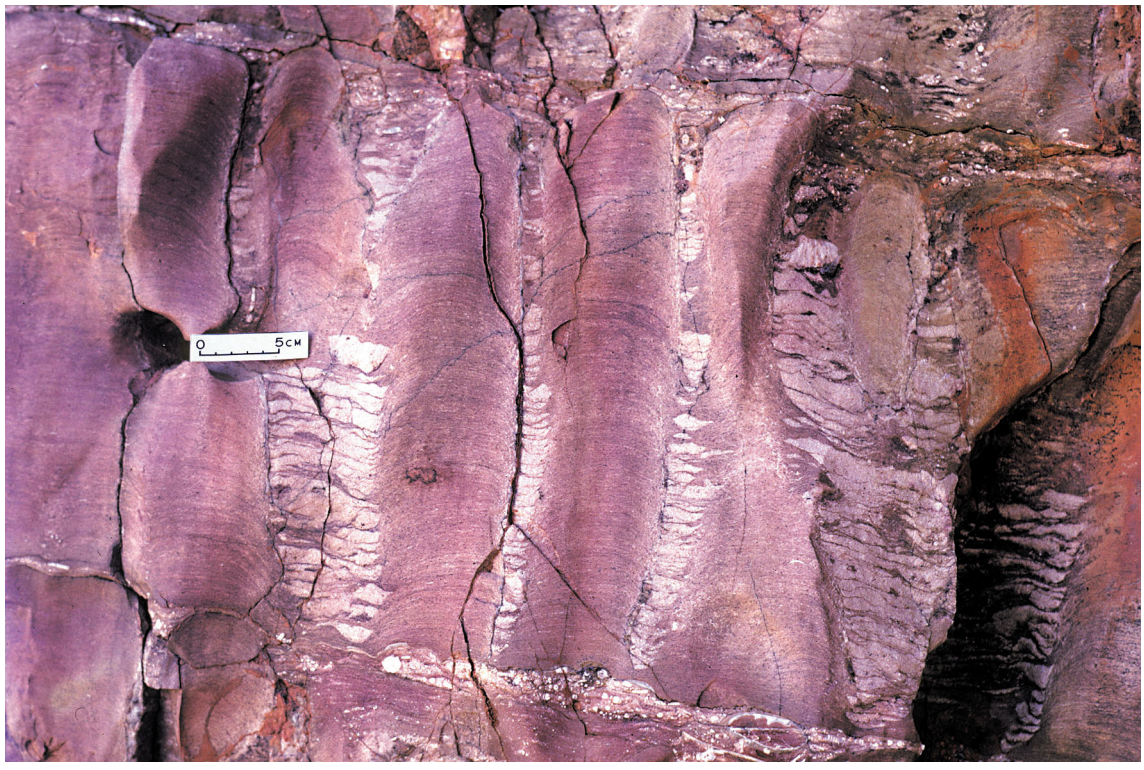

Figure 73. Early Famennian columnar stromatolites that grew vertically on a marginal slope in the Virgin Hills Formation, Ngumban Cliff.



Figure 74. Early Famennian longitudinal stromatolites in the Virgin Hills Formation on the east side of the South Lawford Range near Kellys Pass.

(Teichert, 1949; Feist and Becker, 1997; McNamara et al., 2009), stromatolites (Playford et al., 1976; Figs 73, 74), and foraminifers (Crespin, 1961; Mamet and Playford, 1968; Edgell, 2004). The Devonian ammonoid faunas are among the most diverse known in the world (Talent et al., 2000). Conodonts show that the formation ranges in age from Zone 6 (early Frasnian) through to the top of the *trachytera* Zone (middle Famennian; G Klapper, 2004, written comm.; Playford, 2002a).

The Frasnian part of the Virgin Hills Formation includes Pillara Sequences 4, 5, and 6, the base being defined by the Waggon Pass Event and the top by the Frasnian–Famennian Boundary Event. There is no discernible hiatus between the Frasnian and Famennian parts of the formation in the basin and fore-reef subfacies. On the other hand there is an erosional unconformity between the Famennian and the Frasnian in reefal-slope and platform deposits.

The Famennian part of the Virgin Hills Formation comprises the marginal-slope and basin facies of the lower Nullara Sequence, from the *triangularis* Zone to the *trachytera* Zone (Fig. 20; G Klapper, 2004, written comm.).

Some beds in the Virgin Hills Formation contain abundant sponges and receptaculitids. Few of these fossils are well preserved. Where the sponges and receptaculitids were not calcified, the cavities produced when they decayed were soon filled with sediment and fibrous-calcite marine cement. Much of the resulting rock consists of this cavity-filling spar together with lithified lime mud and sand, retaining only poorly defined evidence of sponges and receptaculitids (Fig. 75). Some cavity fillings are regarded as forms of stromatactis, but in other cases the spar content may exceed 75% of the rock, as in an area west of Henwood Spring (Figs 76–79). Cross-bedding can also be seen in some spar-rich beds (Fig. 80), in which the spar fills or partly fills stromatactis cavities (Fig. 81). The original clasts in such rocks were probably either organic material that decayed or aragonite that was replaced by calcite spar soon after burial.

Bugle Gap Limestone

Definition

The name Bugle Gap Limestone was introduced by Guppy et al. (1958) for the unit of limestone that overlies the Virgin Hills Formation in the Bugle Gap and Old Bohemia areas. The type section is near the southwestern end of Bugle Gap (AMG Zone 52, 191500E 7924700N), but the best exposures are along the creek 3.2 km east-southeast of Cave Spring, southeast of Casey Falls (AMG Zone 52, 193020E 7925840N; Plates 4, 5).

Lithology

The Bugle Gap Limestone consists of white, grey, and pink, medium- to thick-bedded calcarenite (packstone, grainstone, and wackestone), with some beds of reef-derived breccia and large allochthonous reef blocks. Crinoidal debris is abundant in some beds, with individual crinoid stems commonly oriented in the direction of the depositional dip, which can be as high as 35°.

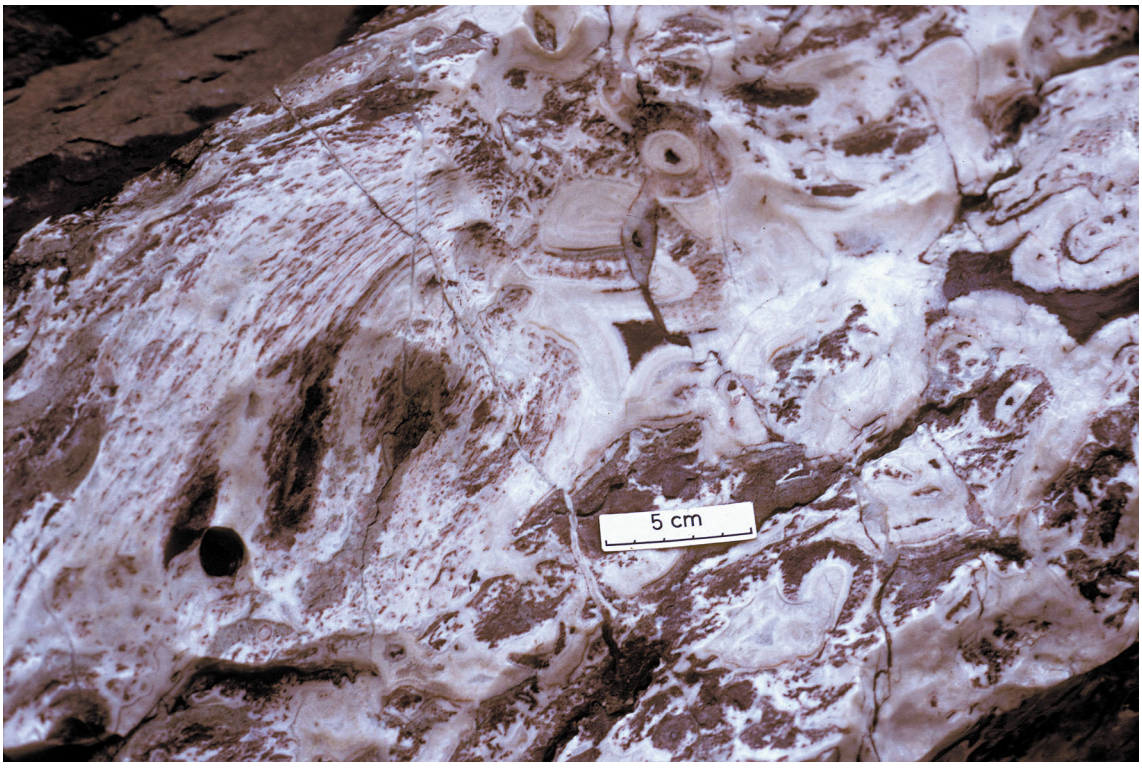

Figure 75. Remains of a 'head-dress sponge' (left centre) and receptaculitids in reefal-slope subfacies of the Napier Formation on the north wall of Windjana Gorge, near the west entrance.



Figure 76. A spar-filled cavity system in the Virgin Hills Formation, marginal-slope facies near Henwood Spring. The cavities formed by the decay of soft-bodied organisms (receptaculitids and/or sponges), and were largely filled at an early stage by sparry calcite and red lime mudstone. The inner parts of some cavities have remained open.



Figure 77. A layered spar-filled cavity system in the Virgin Hills Formation, marginal-slope facies, near Henwood Spring. Lenticular cavities were formed by the decay of soft-bodied organisms (receptaculitids and/or sponges), and were almost totally filled at an early stage by sparry calcite and red lime mudstone.



Figure 78. Spar-filled cavity system in the Virgin Hills Formation, marginal-slope facies, near Henwood Spring, in which subround cavities were formed by the decay of soft-bodied organisms (receptaculitids and/or sponges), and were filled at an early stage by sparry calcite and red lime mudstone.

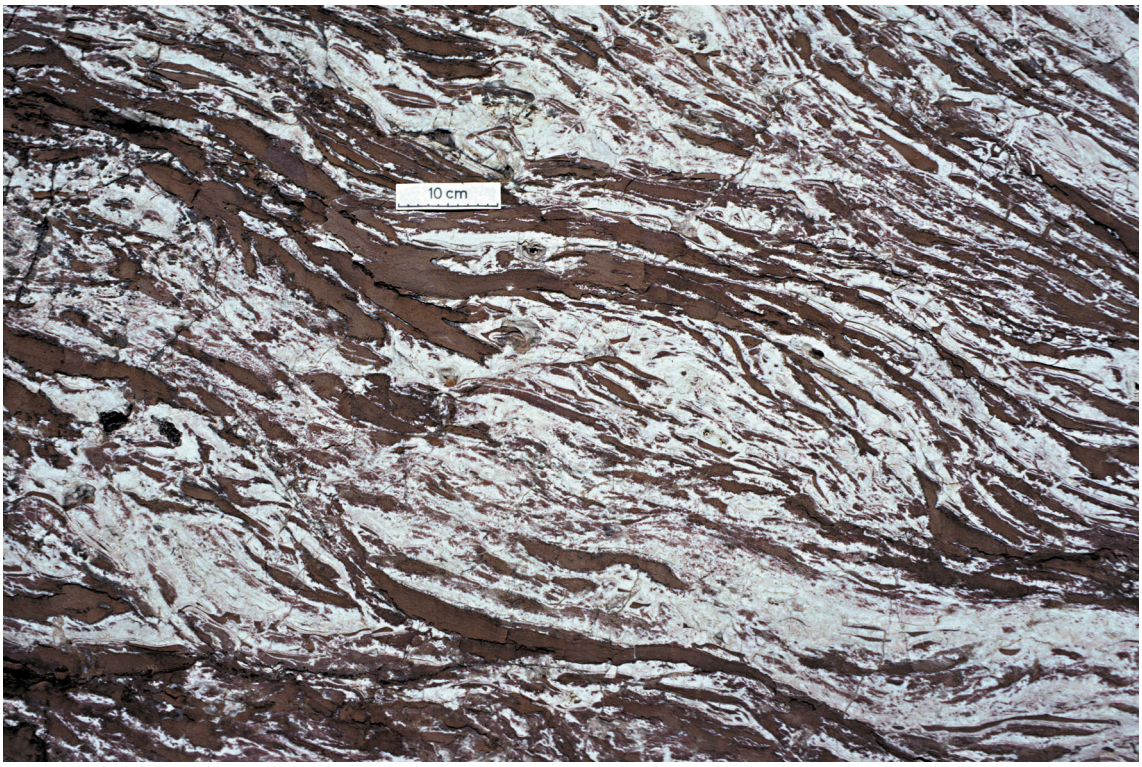

Figure 79. Layered spar-filled cavity system, in which cavities parallel to the depositional dip were formed by the decay of soft-bodied organisms (receptaculitids and/or sponges), in the Virgin Hills Formation, marginal-slope facies, near Henwood Spring. The resulting cavities were filled almost totally at an early stage by sparry calcite and red lime mudstone.



Figure 80. 'Cross-bedded spar' in the Virgin Hills Formation, distal marginal-slope to basin facies, north of Waggon Pass in Bugle Gap. This feature probably formed from fragments of soft-bodied organisms (perhaps sponges) that were distributed by currents on the sea floor and afterwards decayed, the resulting cavities being filled at an early stage by sparry calcite.

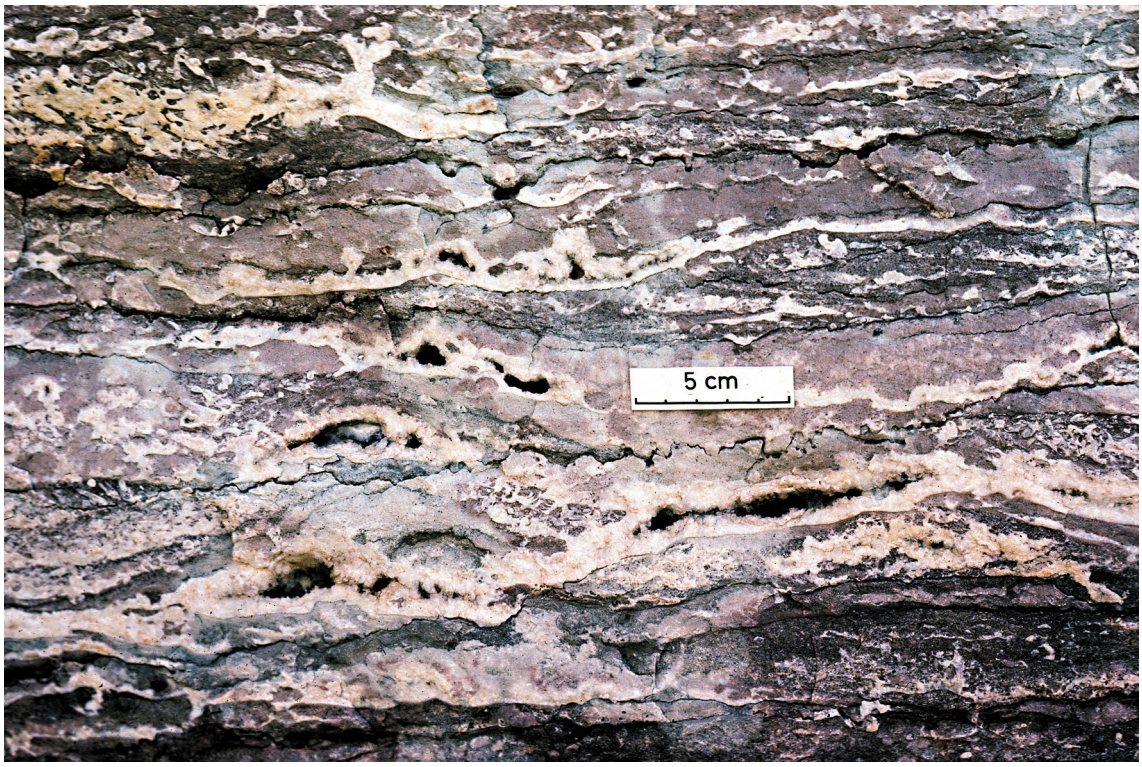

Figure 81. Stromatactis structures in the Virgin Hills Formation, distal marginal-slope to basin facies, north of Waggon Pass in Bugle Gap. The stromatactis cavities, thought to have formed by the decay of soft-bodied organisms, are largely filled with sparry calcite, but some have remained partly open.

Stratigraphic relationships

The Bugle Gap Limestone forms the uppermost part of the Famennian fore-reef subfacies in the southern exposures of the reef complexes. It overlies and interfingers with the Virgin Hills Formation and is equivalent to the younger part of the Napier Formation and (in part) the Piker Hills Formation. In the type section the contact with the Virgin Hills Formation is placed directly above the highest bed of red calcareous siltstone. The Bugle Gap Limestone is overlain abruptly in the southern Old Bohemia area, approximately 3 km north of the Great Northern Highway (AMG Zone 52, 197600E 7928500N), by very poorly exposed shale and limestone of the upper Famennian part of the Fairfield Group. The depositional dip of the Bugle Gap Limestone in that area is about 35º, whereas the Fairfield Group is flat lying, and the contact between them is thought to be unconformable. Elsewhere in this area the Bugle Gap Limestone is overlain with angular unconformity by glacigene shale, diamictite, and sandstone of the Carolyn Formation, the basal unit of the Lower Permian Grant Group (Playford, 2002a).

Distribution and thickness

The Bugle Gap Limestone is recognized only in the area around the southern end of Bugle Gap, extending east to the Old Bohemia valley and west to the Emanuel Range. The vertical thickness of the formation has not been established. Guppy et al. (1958) measured 375 m in the type section, but this did not take into account the depositional dip, and the true vertical thickness is estimated to be less than 200 m.

Fossils and age

The Bugle Gap Limestone contains a relatively sparse megafauna, consisting of brachiopods (Veevers, 1959a,b), rare corals (Hill and Jell, 1970), and crinoid columnals. Conodonts indicate that the base of the unit correlates with the uppermost *marginifera* or lowermost *trachytera* Zone. The age of the top of the unit has not been proved, but it is expected to lie within the *expansa* Zone (Fig. 20; G Klapper, 2004, written comm.).

Piker Hills Formation

Definition

The name Piker Hills Formation was proposed by Playford and Lowry (1966) for the Famennian marginal-slope and basin facies that overlies the Virgin Hills Formation on part of Fossil Downs Station (Plate 3). The formation is named after Piker Hills, the type locality (AMG Zone 52, 187800E 8002800N).

Lithology

The basin facies of the Piker Hills Formation consists of poorly exposed interbedded shale, siltstone, and limestone. The parts containing most limestone form low hills, such as the Piker Hills. The limestones are white to yellow calcarenites — medium- to very fine-grained

wackestones, packstones, and grainstones. They are commonly thin bedded and cross bedded, and outcrop as large slabs in the soil. Many limestones are sandy to conglomeratic, with grains and granules of quartz and other Precambrian rocks, and they grade locally into calcareous sandstone and granule conglomerate, as in the low hills east of Pothole Bore (at GPS AMG Zone 52, 196040E 7990850N). The shales and siltstones are rarely exposed. Some are calcareous, and in places they contain abundant brachiopods. Limonitic (originally pyritic) fossils, nodules, concretions, and cubes commonly weather out in the soil.

The marginal-slope facies of the Piker Hills Formation has depositional dips as high as 35°, which flatten as the formation passes into basin facies at the base of the depositional slopes. The marginal-slope facies consists predominantly of limestone (calcarenite and calcirudite), some of which is partly dolomitized. Allochthonous blocks of reef limestone and reef-derived debris-flow deposits occur in some areas. Reefal-slope subfacies is developed in places where the formation adjoins Windjana Limestone, but most of the exposed Piker Hills Formation consists of fore-reef and fore-bank subfacies. The fore-bank subfacies interfingers directly with the bank subfacies of the Nullara Limestone in the Horseshoe Range, 9 km east of Pothole Bore (around AMG Zone 52, 197500E 7989500N).

Stratigraphic relationships

The Piker Hills Formation comprises the youngest marginal-slope and basin facies in the southeastern part of the Lennard Shelf. It rests conformably on the Virgin Hills Formation and interfingers with or abuts the Windjana and Nullara Limestones and interfingers with the Barramundi and Stony Creek Conglomerates. Much of the formation is equivalent to the upper Bugle Gap Limestone and upper Napier Formation. The formation is overlain in the subsurface by the Fairfield Group. The arbitrary boundary between the Piker Hills Formation and the laterally equivalent part of the Napier Formation is placed along Boab Creek on Fossil Downs Station.

Distribution and thickness

The Piker Hills Formation is exposed between Mount Pierre, Piker Hills, and the Barramundi Range on Fossil Downs Station (Plate 3). Exposures are generally poor. The total thickness of the formation is unknown because of the discontinuous nature of the exposure, but it is probably less than 350 m. Only about 25 m of section is exposed at the type locality.

Fossils and age

Brachiopods are the most conspicuous elements of the megafauna in the Piker Hills Formation, and ammonoids, bryozoans, and foraminifers also occur sporadically (Playford and Lowry, 1966). The conodonts and ammonoids indicate that much of the formation correlates with the *postera* Zone (G Klapper, 2004, written comm.), and on stratigraphic grounds it seems clear that it ranges up into the *expansa* Zone.

Napier Formation

Definition

The name Napier Formation was proposed by Guppy et al. (1958) for a unit of limestone and interbedded sandstone that is exposed in the Napier and Oscar Ranges, the type section being in Barker Gorge. The present usage of the term is essentially the same as that of Playford and Lowry (1966): it is applied to the marginal-slope and basin deposits exposed between the Napier Range (Plate 1) and immediately east of Geikie Gorge on the west side of the Margaret Embayment (Plate 3).

Lithology

The dominant lithology of the Napier Formation is limestone, with dolomitic limestone and dolomite (now altered to dedolomite at the surface) in some areas, but the formation also includes substantial thicknesses of calcareous sandstone and siltstone, with some shale and conglomerate. Terrigenous sedimentary rocks are most common along the Napier Range, adjoining Precambrian rocks that supplied a great deal of terrigenous detritus during the Late Devonian. On the other hand, terrigenous sedimentary rocks form only minor parts of the formation in the Oscar Range reef complex, as the islands of Precambrian rocks around which it developed, although rugged, were too small to yield much terrigenous detritus.

Limestones in the Napier Formation range from fine-grained calcarenites to coarse megabreccias. They include submarine talus and debris-flow deposits, consisting of material derived from the collapse of reef margins and other types of platform erosion (Playford, 1984a; George et al., 1995; Ward, 1999; Playton, 2008). They also contain material sourced from the back-reef subfacies. The debris flows usually contain fragments of reef-margin, reef-flat, and reefal-slope limestones. However, some debris flows were caused by slides on the marginal slopes, without significant contributions from the platforms. Blocks of reef in the debris-flow deposits can be very large (commonly as much as 100 m across). Isolated allochthonous blocks of reef limestone also occur in fore-reef deposits. They resulted from platform collapses that did not initiate major debris flows.

Stratigraphic relationships

The Napier Formation interfingers with or abuts the Windjana Limestone and the Pillara Limestone, except in limited areas where it downlaps onto the Pillara Limestone, associated with backstepping events.

The Napier Formation is a lateral equivalent of the marginal-slope and basin facies that are recognized in the southeastern Lennard Shelf — Sadler Limestone, Gogo Formation, Virgin Hills Formation, Bugle Gap Limestone, and Piker Hills Formation. Much of the exposed Napier Formation can be correlated with the Virgin Hills Formation. Only a few exposures of the Napier Formation, in the Leopold Downs Embayment, are thought to correlate with the Sadler Limestone, and none of the outcropping parts of the formation can be correlated with the Gogo Formation.

The Napier Formation is here subdivided in the Dingo Gap area into the Kalmanyi, Tarakalu, and Barrar Members, as shown on Plate 2. The type sections for all three members essentially follow the line of section E–F shown on Plate 2 (AMG Zone 51, 732900E 8045600N to 731000E 8044500N).

Kalmanyi Member

The Kalmanyi Member is named after *Kalmanyi*, the Aboriginal (*Bunaba*) name for a pinnacle of rock in this member, situated between Tunnel Creek and Dingo Gap (Fig. 82). The pinnacle is a phallic symbol that features in the *Tchularga* song cycle of the *Worora, Unggumi, Bunaba, Gooniyandi, Wolmadjari, Kukadja, Pintubi,* and *Ngadadjara* people. The story of *Tchularga* tells of exploits on his journey from the Kimberley coast to near Giles in the Gibson Desert, a distance of some 1000 km, and then back again. Recordings of parts of this song cycle, made by Playford during 1962–63, have been donated to the Australian Institute of Aboriginal and Torres Strait Islander Studies in Canberra, with copies to the Western Australian Museum in Perth.

The Kalmanyi Member consists of upper Frasnian and lower Famennian grey and reddish-grey calcarenite (packstone and grainstone), breccia, and debris-flow megabreccia, with scattered allochthonous blocks of reef limestone. The Frasnian–Famennian boundary occurs in the lower half of the unit (Plate 2), directly above a brachiopod-rich layer. A large receptaculitid–coral–microbial bioherm is also developed nearby in the member, just below the Frasnian–Famennian boundary (Fig. 83). Large antiformal stromatolites occur in the Famennian and latest Frasnian parts of the unit, some of which were developed over allochthonous blocks of reef limestone.

The thickness of the type section of the member (disregarding the depositional nature of the dip) is 230 m in the section measured by Tornatora (1992) and 240 m in that of George et al. (1997).

Tarakalu Member

The Tarakalu Member is named after *Tarakalu*, the Aboriginal (*Bunaba*) name for Dingo Gap. The member consists predominantly of medium-grained quartz–feldspar sandstone, which is very poorly exposed or unexposed in the lower and middle parts of the member, where it localizes the valley of Dingo Gap. Sandstone in the upper part of the unit is calcareous and contains interbeds of siltstone, calcarenite, and breccia. Some large allochthonous blocks containing sand tubes that occur in the uppermost part of the unit were described as karst features by Playford (1981) and George and Powell (1997). However, detailed examination by Kerans (1985), Tornatora (1992), and Playford (2002a) has shown that the tubes and associated microbial limestone are growth features, unrelated to karst. They are referred to as 'pseudokarst' by Playford (2002a).



Figure 82. ***Kalmanyi*, a slab of reefal-slope limestone that has peeled off the east side of the Napier Range south of Tunnel Creek. This feature is identified in Aboriginal mythology as the phallus of the culture hero *Tchularga*.**

The only fossils known in the member are minor stromatolites (Tornatora, 1992) and conodonts. The conodonts (G Klapper, 2004, written comm.) show that the age of the Tarakalu Member is largely early Famennian, in the *crepida* and *rhomboidea* Zones, perhaps extending into the middle Famennian *marginifera* Zone in its upper part. The very poor nature of exposures in the lower and middle parts of the unit makes it impossible to measure the thickness of the unit accurately. It is 98 m in the section measured by Tornatora (1992), and 144 m in that measured by George et al. (1997), in both cases disregarding the mainly depositional nature of the dips.

Barrar Member

The name of the Barrar Member is taken from *Barrar*, the Aboriginal (*Bunaba*) name for the narrow incised valley at the southwestern entrance to the tunnel of Tunnel Creek. Like *Kalmanyi* this feature is included in the *Tchularga* song cycle.

The Barrar Member consists of interbedded calcarenite (grainstone, packstone, and wackestone), alternating with debris-flow megabreccias and containing some enormous allochthonous blocks of reef limestone.

The thickness of the member, disregarding the depositional dip component, is 230 m according to Tornatora (1992), and 195 m according to George et al. (1997). The unit is middle to late Famennian in age (*marginifera* Zone to *expansa* Zone, G Klapper, 2004, written comm.).

Distribution and thickness

The Napier Formation is recognized from the northwestern end of the Napier Range to the Geikie Gorge area. The eastern boundary is taken as the western flank of the Margaret Embayment (see Plate 3), so that west of Boab Creek the marginal-slope facies is mapped as Napier Formation, and its equivalent section to the east is included in the Virgin Hills Formation, Piker Hills Formation, and Bugle Gap Limestone.

Guppy et al. (1958) measured the thickness of the Napier Formation as 310 m in its type section (Barker Gorge), and 1020 m in a section east-northeast of the original Old Napier Downs Homestead (Plate 1). However, these measurements do not represent true thicknesses, because the measured dip in each case is largely depositional. The maximum vertical thickness of the formation in the Napier Range area is estimated to be about 500 m (Plate 1).

Fossils and age

The Napier Formation in outcrop is apparently entirely Frasnian and Famennian in age — no Givetian strata have been identified. Conodonts recovered from the formation range from early Frasnian to late Famennian, reaching as high as the *expansa* Zone in the youngest part of the unit (G Klapper, 2004, written comm.).

Apart from conodonts, fossils observed in the Napier Formation comprise nautiloids, rare ammonoids, crinoids, corals, bivalves (especially megalodonts and lithiotids derived from the equivalent platforms), sponges (Rigby, 1986), receptaculitids, microbes (including *Renalcis* and *Sphaerocodium*), fish (Cockbain, 1976a), brachiopods, gastropods, ostracods, bryozoans, rare stromatoporoids (Cockbain, 1984, 1989), and stromatolites (Playford et al., 1976; George, 1999).

Stromatolites in the Napier Formation are most abundant from a few metres below the Frasnian–Famennian boundary (in Zone 13) to several tens of metres above it (*triangularis* and *crepida* Zones). The Frasnian–Famennian boundary has been mapped in the Oscar Range and Geikie Gorge areas taking the base of a band of abundant stromatolites as the approximate boundary (Hurley, 1986; Wallace, 1987). The abundance of stromatolites at that horizon is thought to be linked with the Frasnian–Famennian mass extinction, which extinguished many metazoan species that would otherwise have grazed on stromatolite-building microbes. However, the actual Frasnian–Famennian boundary is higher than the first appearance of abundant stromatolites in the section. Abundant deep-water stromatolites appear in Zone 13, suggesting that the disappearance of many metazoans, associated with the Frasnian–Famennian mass extinction, first began in the latest Frasnian.

Sequence stratigraphy

Interpretations of the Devonian sequence stratigraphy on the Lennard Shelf, based on studies of seismic and drillhole data, have been presented by Middleton (1987), Jackson et al. (1992), Kennard et al. (1992, 1994), and Southgate et al. (1999). With the exception of Middleton (1987), these papers adhere to what Miall and Miall (2002) have termed the 'Exxon paradigm' of sequence stratigraphy (Vail et al., 1977; Van Wagoner et al., 1988). Proponents of that paradigm maintain that eustatic fluctuations in sea level during the Devonian gave rise to third-order sequences and 'reciprocal sedimentation', resulting in highstand carbonate platforms and lowstand terrigenous-clastic deposits. However, many of those interpretations of the subsurface sequence stratigraphy (stylized in Fig. 3) cannot be reconciled with features of the reef complexes and associated conglomerate bodies that are so well displayed in outcrop.

Other interpretations of the Devonian sequence stratigraphy, based on several outcrop localities on the Lennard Shelf, have been made by Holmes and Christie-Blick (1993), Whittam et al. (1994), and George et al. (1997, 2002). Again, those interpretations seem to be driven by the reciprocal-sedimentation 'Exxon paradigm' model and their accounts of field relationships cannot be reconciled with our observations at the same localities.

Conglomerates interfinger and are interbedded with platform, basin and, to a lesser extent, marginal-slope deposits. They are to be considered as highstand deposits — the reciprocal-sedimentation model cannot explain their deposition. George et al. (1997, 2002) agreed that the outcropping limestone platforms represent highstands, but they nevertheless claimed that large basinal conglomerate and sandstone wedges were deposited during sea-level lowstands. On the contrary, we conclude that all or most of those wedges were also deposited during sea-level highstands.

Miall (1992) and Miall and Miall (2001, 2002) pointed out that almost all proponents of the 'Exxon paradigm' emphasize the importance of relatively rapid and regular worldwide fluctuations of sea level in controlling the architecture of stratigraphic sequences. Miall and Miall (2001, 2002) suggest that those proponents have mostly failed to present good evidence to support the time correlations on which their global interpretations are said to be based, sometimes claiming commercial sensitivity as a reason for withholding data. Many of those proponents have ignored or discounted the importance of tectonism in controlling sedimentary sequences on a local to regional (as distinct from global) scale.

We maintain that contemporaneous tectonism in the Canning Basin played a significant role in shaping the reef complexes. However, eustacy is also thought to have been important in controlling at least one and perhaps both of the regressions that resulted in the second-order sequence boundaries associated with the Frasnian–Famennian Event and the late Famennian Reef Extinction Event (Fig. 20). The Frasnian–Famennian boundary in the Canning Basin was marked by a fall in sea level, and it seems clear that this was also a global event (Copper, 1986, 1994). However, detailed biostratigraphic studies will be needed elsewhere in the world to determine whether the abrupt late Famennian regression that resulted in reef extinction in the Canning Basin was also a global event.

A long-term eustatic rise and fall of sea level, combined with continuing subsidence, is thought to have controlled the second-order Pillara and Nullara Sequences. Subsidence combined with rising sea level resulted in the aggrading to retreating late Givetian to middle Frasnian platforms, while subsidence and falling sea level resulted in the latest Frasnian and Famennian advancing platforms. These long-term cycles were punctuated by tectonic episodes that resulted in third-order backstepping events.

The sequence stratigraphic interpretation of the Devonian reef complexes presented here is an outcome of the GSWA detailed investigations throughout the reef belt, supported by detailed biostratigraphic studies by G Klapper (using conodonts, Appendix 1) and R T Becker and M R House (using ammonoids, Appendix 2).

The Devonian reef complexes comprise two second-order sedimentary sequences, the Givetian–Frasnian Pillara Sequence below and the Famennian Nullara Sequence above (Figs 20, 21, 84; Playford, 2002a). These sequences were originally termed 'cycles' by Playford (1980). Estimates of rates of deposition and absolute ages for the Devonian rocks in these sequences are based on the time scale of House and Gradstein (2004), who estimated that the duration of the Famennian was 15.3 m.y., the Frasnian being 10.8 m.y. and the Givetian being 6.5 m.y.

The Pillara and Nullara Sequences accumulated during prolonged periods of subsidence and transgression on the Lennard Shelf, separated by a brief regression at the Frasnian–Famennian boundary and punctuated by brief tectonic episodes, which are thought to have been responsible for backstepping events in the Pillara Sequence (Figs 21, 84). At least some of the backstepping events were preceded by brief regressions (Playford et al., l989; Playford, 2002a).

The thickness of the Givetian–Frasnian Pillara Sequence varies considerably (based on drillhole intersections), but probably averages about 1000 m. The sequence was deposited over some 13 m.y. (nearly 11 m.y. for the Frasnian plus about 2 m.y. for the late Givetian). The Famennian Nullara Sequence, which has an estimated average thickness of about 200 m, was deposited in about 11.5 m.y. Assuming that these estimates are approximately correct, the average rate of deposition of the Pillara Sequence was nearly 4.5 times that of the Nullara Sequence. In other words, the amount of accommodation created during deposition of the Nullara Sequence (due to subsidence combined with relative rise in sea level) was less than a quarter of that of the Pillara Sequence. Because of this slower rate of vertical growth, the Famennian platforms advanced (prograded) strongly over their equivalent marginal-slope and basin deposits. This contrasted with the vertical (aggrading) to backstepping and retreating (retrograding) growth mode that characterized the Givetian and Frasnian platforms, apart from the youngest Frasnian platforms, which advanced (prograded) during Zones 11–13. Thus, slowing in the rate of accommodation was not linked with the boundary between the Pillara and Nullara Sequences; i.e. it is not directly related to the Frasnian–Famennian Boundary Event.

Combining the effects of any long-term sea-level change with a relatively constant rate of basin subsidence could explain the retreating and advancing patterns: if a long-term global rise in sea level was combined with constant subsidence, accommodation would be high, relative transgression would be rapid, and retreating to vertical platform growth would result. Sudden changes in sea level, probably associated with tectonic episodes, is thought to have been responsible for backstepping. This scenario may explain the overall pattern of platform development in the Pillara Sequence. During the subsequent Nullara Sequence, a long-term global fall in sea level would counteract continuing subsidence, so that accommodation would be less, and transgression would slow.

However, the observed growth patterns could otherwise be explained by a relatively constant sea level, with high rates of subsidence causing the vertical to retreating platform growth in all but the uppermost part of the Pillara Sequence, and relatively brief changes in subsidence (probably as a result of tectonic pulses) could be responsible for the backstepping episodes. In the subsequent Nullara Sequence a slowing in the rate of subsidence might have resulted in advancing platforms.

We are inclined to favour the first of these alternatives; i.e. that the pattern of platform development has resulted from long-term global changes in sea level superimposed on constant subsidence. This is because the same pattern of retreat during the Givetian and most of the Frasnian, followed by advance during the latest Frasnian and the Famennian, also applies to the Devonian reef complexes of Canada (Atchley et al., 2006; Fig. 85). In relation to that similarity between Devonian reef complexes of Canada and the Canning Basin, it should be noted that the topography of reefal platforms in Alberta is much more subdued than that of their Canning Basin equivalents (Playford, 1969; Fig. 86).



Figure 83. Massive receptaculitid–coral–microbial bioherm developed below the Frasnian–Famennian boundary in the fore-reef Napier Formation at Dingo Gap. That boundary is immediately over the base of the thin-bedded unit overlying the massive bioherm.

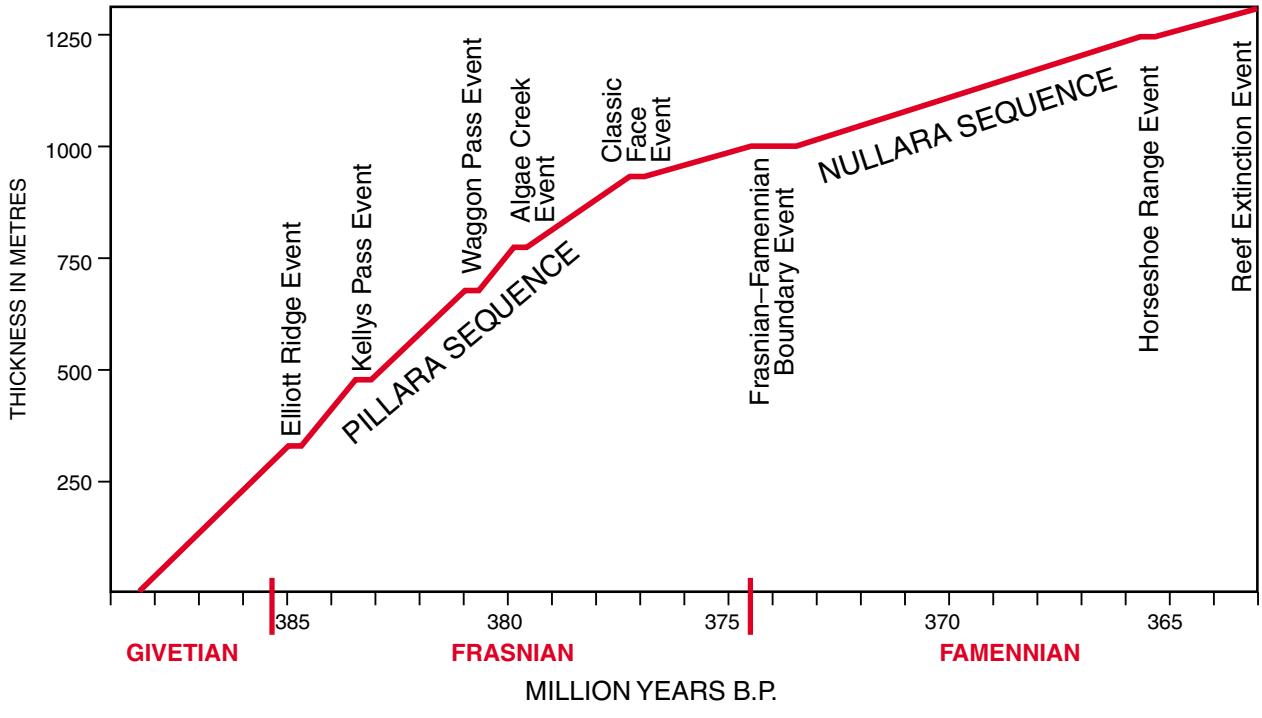

Figure 84. Diagram illustrating the rate of accumulation in platform facies during the Givetian–Frasnian Pillara Cycle and the Famennian Nullara Cycle.

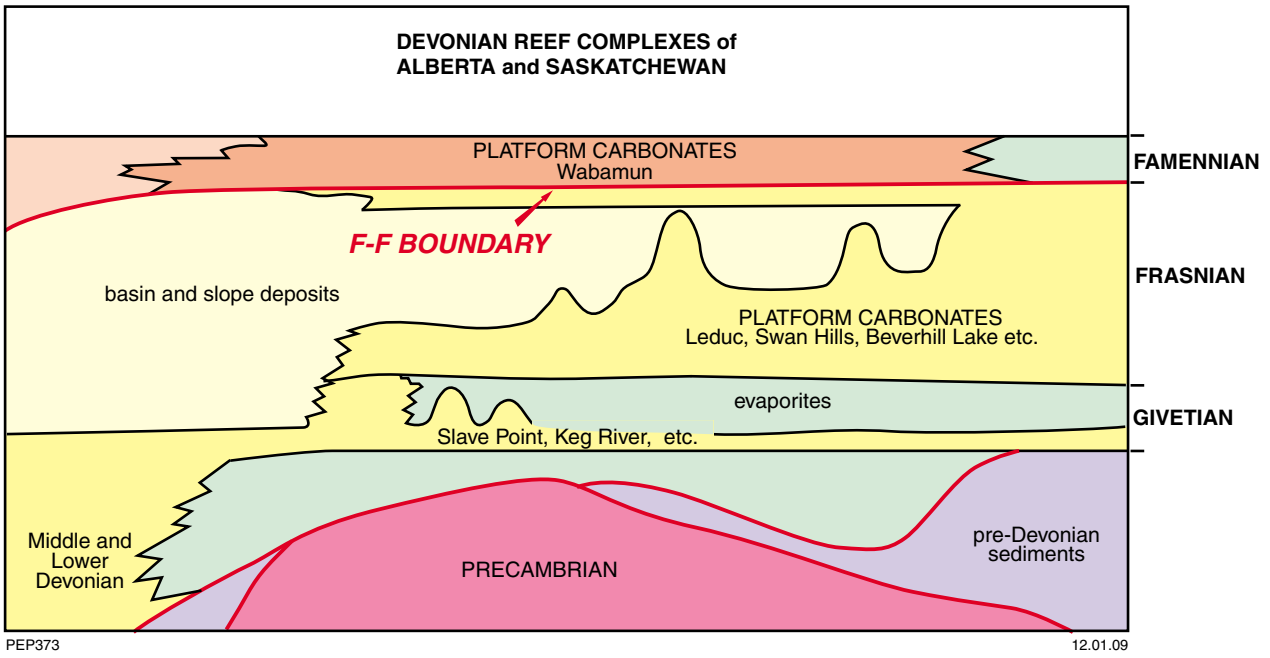

Figure 85. Diagrammatic section illustrating the Devonian of Alberta and Saskatchewan (simplified, after Atchley et al., 2006). The pattern of reef development in these Canadian reef complexes resembles that in the Canning Basin, suggesting significant global controls on their development.

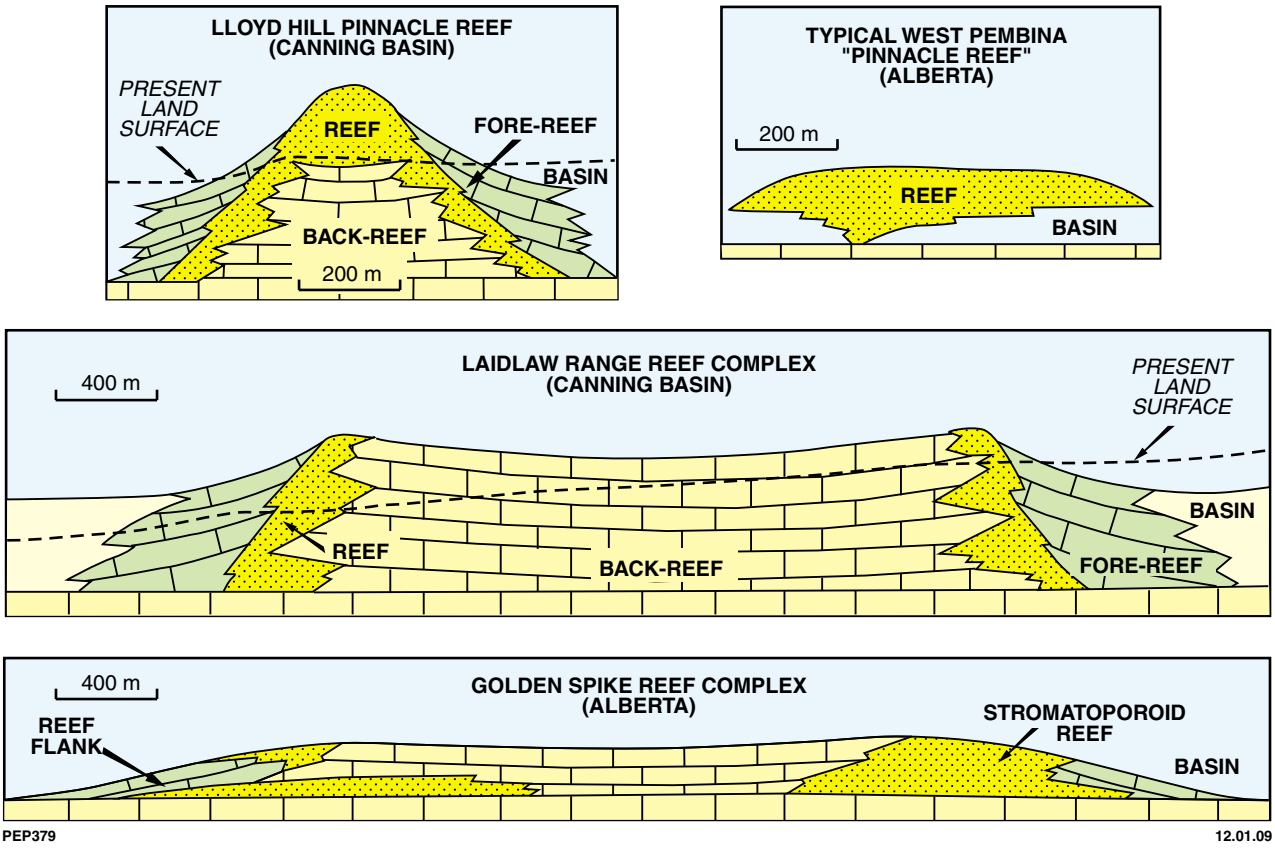

Figure 86. Comparative cross sections through some Devonian reef complexes in the Canning Basin and Alberta, illustrating that the Canning Basin platforms had much higher growth relief than their subsurface equivalents in Alberta.

Pillara Sequence

The Pillara sequence is defined at its base by an angular unconformity over Ordovician or Precambrian rocks (Fig. 20), and at the top by the Frasnian–Famennian boundary. This boundary is an unconformity in platform and uppermost reefal-slope deposits and a conformity in deeper marginal-slope and basin deposits. Small paleokarst features, in the form of sinkholes as much as 50 cm across and 1 m deep, occur in platform facies at the Frasnian–Famennian unconformity in some parts of the Napier Range (around AMG Zone 51, 732900E 8045600N), but in other areas the contact is quite smooth. Observed relief on the unconformity surface is as much as 5 m, as at the western end of the Oscar Range (Fig. 49; Playford, 1982, 2002a). The duration of the regression at the Frasnian–Famennian boundary is unknown, but it seems likely to have been relatively brief (perhaps less than a million years).

The oldest exposed platform of the Pillara Sequence is in the Emanuel Range. Platform development began in that area during the middle Givetian, with deposition of the Cadjebut Formation (Fig. 20; Hocking et al., 1996). As previously described, this unit consists primarily of stromatolitic and stromatoporoidal dolomites (which were probably dolomitized at a very early stage), interbedded with siltstone and thin evaporites, which overlie Ordovician shale and dolomite of the Prices Creek Group (Guppy and Öpik, 1950). Halite and gypsum have been recognized in the subsurface, but are not exposed at the surface. Their former presence is recognized in outcrop by distinctive moulds of those minerals, together with breccias and folding that are thought to have been associated with evaporite solution (Figs 23–25).

The evaporitic platform facies represented by the Cadjebut Formation has no known reef rim, and equivalent marginal-slope and basin facies are not recognized in outcrop. The Cadjebut Formation has a transitional contact with the overlying bank facies of the Pillara Limestone, the lower part of which is also Givetian as shown by the presence of the Givetian index fossil *Stringocephalus fontanus*. Although Givetian platform deposits of the Pillara Limestone occur in parts of the Pillara and Home Ranges, the Cadjebut Formation is not recognized there.

Reef rims that developed around the platforms during the late Givetian and earliest Frasnian grew almost vertically upward (Fig. 20), in response to rapid rates of subsidence combined with rising sea level. The subsequent Frasnian platforms exhibit rapid changes in architecture, associated with abrupt backstepping events (Playford, 1980, 2002a; Playford et al., 1989; Ward, 1999). At least some of those events were preceded by short regressions, when the outer parts of platforms were eroded and minor karstification may have occurred in some places.

The best exposed example of an erosion event preceding backstepping is seen in the Classic Face at Windjana Gorge. There, the erosion surface is smooth and unkarstified, and the amount of backstepping is small (approximately 50 m). In other places where there has been larger scale backstepping (in some cases as much as 800 m), the mechanical explanation for the backstepping process is uncertain. Perhaps the old platform was more eroded around its margins during a brief regression, and after renewed transgression the new platform was re-established over the highest, least-eroded part of the previous platform. Alternatively, tectonic tilting may have been responsible for some backstepping.

Five backstepping events and the Frasnian–Famennian Boundary Event define the tops of six third-order sequences within the second-order Pillara Sequence. These third-order sequences are referred to by Playford (2002a) as Pillara Sequences 1 to 6. The sequence boundaries have been dated by correlation with the conodont zonation of Klapper (1989, 1997a, 2000) and Klapper and Becker (1999), using data provided by G Klapper (2004, written comm.). In ascending order, the five backstepping events (amended from Playford, 2002a) are named the Elliott Ridge, Kellys Pass, Waggon Pass, Algae Creek, and Classic Face Events, after places where backstepping sequence boundaries are well displayed.

Elliott Ridge Event

The Elliott Ridge Event is named after Elliott Ridge in the northern Laidlaw Range (Fig. 87). The ridge was named by Playford after Robin Elliott, a WAPET geologist with wide experience in the Canning Basin during the 1950s. This event marks the first significant backstepping of the early Frasnian (probably within Zone 1), and marks the boundary between Pillara Sequences 1 and 2. Using House and Gradstein's (2004) Devonian scale, the age of the Elliott Ridge Event is about 385 Ma. Elliott Ridge itself is marked by a line of pinnacle reefs that continued to grow along the old reef margin while the new margin (lacking a reef rim) backstepped about 750 m to the south (Fig. 87). Marginal-slope deposits of the Sadler Limestone were then deposited over the drowned part of the old platform.

From the descriptions of Sandberg et al. (2002), the Elliott Ridge Event could be about the same age as the Amönau Event of Germany. That German event is marked by a widespread breccia layer, possibly resulting from volcanism associated with an asteroid impact and a rise in relative sea level.

Kellys Pass Event

The Kellys Pass Event is clearly displayed in Kellys Pass (AMG Zone 52, 191800E 7926800N), where a four-wheel-drive track crosses the southern end of the Lawford Range. At this locality, on the east side of the South Lawford Range, the reef margin at the top of Pillara Sequence 2 retreated abruptly for about 100 m during the early Frasnian (Zone 3). Steeply dipping fore-reef strata of the Sadler Limestone, Pillara Sequence 3, were then deposited over the older back-reef platform (Fig. 88). The age of the event is about 383.5 Ma, based on the scale of House and Gradstein (2004).

There is evidence immediately north of Kellys Pass that the contact at the top of Sequence 2 is an angular unconformity. Discordance is evident between strata above and below the contact near the platform margin, which seems to indicates a tectonic origin for the backstepping event (Figs 88–90). There also appears to be evidence of small-scale karstification below the boundary, in the form

of localized brecciation of back-reef limestones (Fig. 91). Further detailed work is required to fully understand this important boundary.

Figure 92 shows an unconformable relationship between Pillara Limestone and Sadler Limestone north of Waggon Pass (in the Bugle Gap area), which probably correlates with the Kellys Pass Event.

Waggon Pass Event

The Waggon Pass Event is named after Waggon Pass, where a track from Bugle Gap to the Old Bohemia area crosses the reef spine between the North and South Lawford Ranges. Playford (2002a) originally named this event the 'Shady Bore Event', but that name is now deemed unsuitable, as it has not been possible to confidently correlate this sequence boundary with the angular discordance between the Pillara Limestone and the Virgin Hills Formation in the Shady Bore area.

The Waggon Pass Event marks the boundary between Pillara Sequences 3 and 4 and Zones 5 and 6, and has an age of 381 Ma using House and Gradstein's (2004) timescale. The sequence boundary, between the Virgin Hills Formation (above) and the Gogo Formation (below), is unconformable in some places and conformable in others. An unconformable contact can be seen 1.5 km south-southeast of the west entrance to Waggon Pass, in a low scarp immediately west of a reef spine (AMG Zone 52, 190600E 7935600N). At this locality the Virgin Hills and Gogo Formations are separated by a thin wedge of deep-water conglomerate that is assigned to the Sparke Conglomerate. The wedge of Sparke Conglomerate, as much as about 5 m thick, occurs in the eastern part of this scarp. Its deposition was associated with brecciation in the underlying Gogo Formation. The conglomerate pinches out some 300 m to the west, where Virgin Hills Formation rests directly on Gogo Formation, with an eroded contact between them. The erosion is attributed to bottom currents associated with the outpouring of conglomerate. The conglomerate must have formed the western edge of a submarine fan of Sparke Conglomerate that spilled over the drowned reef spine, into deep water on its western side. This is the oldest known part of the Sparke Conglomerate.

The Waggon Pass Event is also well displayed below the westernmost block of Rattigan Rocks, where a thin debris flow in Virgin Hills Formation immediately below the block rests on pale-grey Sadler Limestone. The Waggon Pass Event may have been a major faulting episode that triggered extensive collapse of the reef margin in this area. The lowermost Elma Conglomerate similarly lies at, or only slightly above, the contact between the Sadler Limestone and the Virgin Hills Formation.

However, in some places in outcrop, and more commonly in the subsurface, the boundary between the Gogo Formation (Pillara Sequence 3) and the Virgin Hills Formation (Pillara

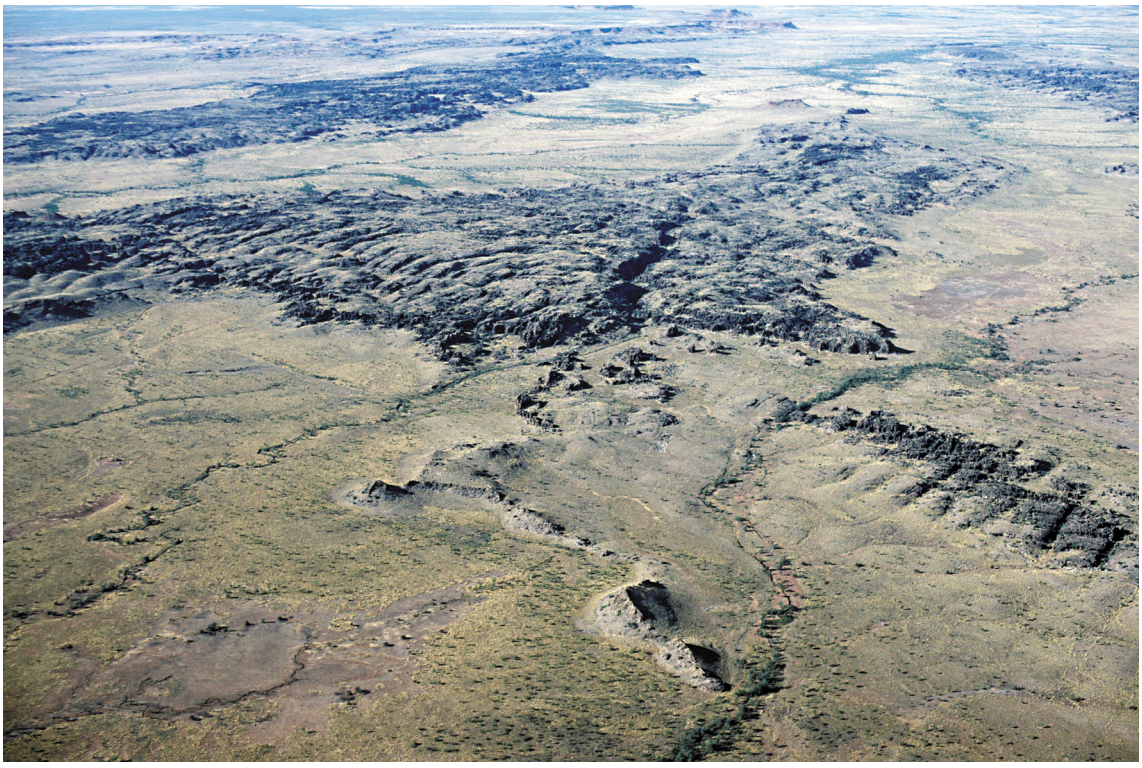

Figure 87. Aerial view of Elliott Ridge on the north side of the Laidlaw Range, looking southeast. The ridge (centre foreground) consists of a line of pinnacle reefs that grew along the margin of a drowned platform after the main platform stepped back to a new position shown on the right-hand side of the photo. The backstepping resulted from the Elliott Ridge Event, between Pillara Sequences 1 and 2.



Figure 88. Backstepped Frasnian platform of the Pillara Limestone at Kellys Pass, between Pillara Sequences 2 and 3, resulting from the Kellys Pass Event. The old platform (foreground) backstepped to a new position marked by the massive reef limestone in the right background. Dipping marginal-slope beds of the Sadler Limestone, in the centre left background, were piled onto the older platform.



Figure 89. Angular discordance along the Kellys Pass sequence boundary (between Pillara Sequences 2 and 3), immediately north of Kellys Pass. Limestone beds in the younger platform are dipping at a low angle, overlying more steeply dipping beds in the older platform. The angular discordance points to a tectonic origin for this sequence boundary.



Figure 90. Angular discordance at the Kellys Pass sequence boundary (between Pillara Sequences 2 and 3), about 70 m from the boundary shown in Figure 89. Shallow-dipping beds of the younger platform overlie more steeply dipping beds of the older platform.

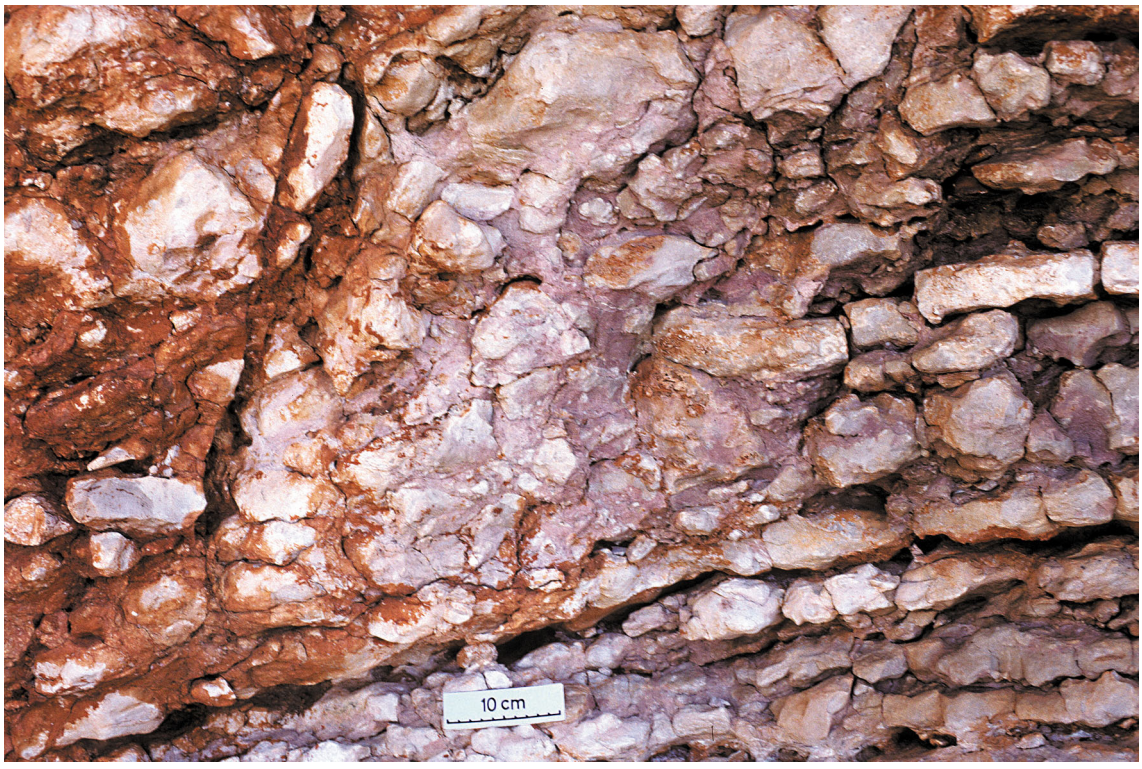

Figure 91. Back-reef Pillara Limestone with probable karst breccia below the Kellys Pass sequence boundary, immediately north of Kellys Pass.



Figure 92. Sadler Limestone (dipping to the left), overlying Pillara Limestone (dipping to the right), 2 km north of Waggon Pass in the South Lawford Range. The contact is an erosion surface that probably correlates with the Kellys Pass Event.

Sequence 4) appears to be conformable. In deep-water sections the boundary is generally gradational, extending over as much as 5 m of section (Copp, 2000).

The Waggon Pass Event could possibly correlate with the Alamo Event, a bolide impact evidenced by the Alamo Breccia, deposited along the western margin of Laurasia (presently Nevada) during the *punctata* Zone (Sandberg et al., 2002). That would place the impact in Zones 5 or 6, at about the time of the Waggon Pass Event.

Algae Creek Event

The Algae Creek Event is clearly evidenced where Algae Creek cuts through the northern Lawford Range (Plate 5; AMG Zone 52, 193500E 7940900N). The boundary separates Pillara Sequences 4 and 5, and is thought to be within Zone 8 of the middle Frasnian. Using House and Gradstein's (2004) Devonian timescale, the age of the Algae Creek Event is about 380 Ma. The event is marked by the incursion of a tongue of Virgin Hills Formation into the Pillara Limestone, with associated abrupt backstepping amounting to some 500 m. There is some evidence for tilting of the old platform immediately prior to this backstepping event, as expressed by angularity within the Pillara Limestone beside Algae Creek, but more detailed field work is needed to examine this interpretation.

Classic Face Event

The Classic Face Event, which is well displayed in the Classic Face at Windjana Gorge, is marked by an erosion surface in the Pillara Limestone that formed as a result of a very brief emergence of the platform, probably within Zone 12 (Figs 20, 93–96; 377 Ma according to House and Gradstein, 2004). The subvertical part of the boundary originated from platform-margin collapse followed by relatively minor erosion. The erosion surface defines the boundary between Pillara Sequences 5 and 6. It truncates strata for at least 250 m behind the platform margin, and has a vertical relief of about 19 m (N Frost, 2004, written comm.). Strong erosion was apparently confined largely to the platform margin in the area of the Classic Face, so that relief on the contact gradually disappears in platform deposits to the northwest, around the corner of the gorge (Fig. 96). However, even where there is the appearance of conformity, it seems likely that a significant amount of section is missing below the contact. It is also clear that the cycles evident in Figure 96 above the boundary (in Pillara Sequence 6) are significantly thinner than those below the boundary (in Sequence 5).

During Pillara Sequence 6, within Zones 11–13 (probably in Zones 12 and 13), the Pillara platform advanced (prograded) over its equivalent marginal-slope and basin facies. This pattern of advancing platform growth continued in the Famennian, during deposition of the succeeding Nullara Sequence.

Frasnian–Famennian Boundary Event

The Frasnian–Famennian Boundary Event, which occurred immediately before deposition of the Nullara Sequence, is expressed as an erosional unconformity





Figure 93. (above) The Classic Face at Windjana Gorge, with the boundary between Pillara Sequences 5 and 6 marked by a white line. This boundary is an erosional unconformity. The steep front of the platform (Pillara Limestone Sequence 5) is a collapse scarp, modified by erosion prior to deposition of the steeply dipping reefal-slope and fore-reef deposits (Napier Formation Sequence 6), shown in the centre and left of the photo.

Figure 94. Closer view of part of the sequence boundary in the Classic Face, between Pillara Sequences 5 and 6, marked by a white line. Crudely bedded, steeply dipping, reefal-slope beds (Napier Formation, Sequence 6) on the left were deposited against and over the reef margin and reef flat (Pillara Limestone) on the right. The contact is an eroded collapse scarp.



Figure 95. Closer view of the upper part of the erosional unconformity marking the Classic Face sequence boundary, above and to the right of the view in Figure 94, showing backstepping of the platform margin over a deeply incised erosion surface.



Figure 96. Immediately downstream from the Classic Face at Windjana Gorge, showing the unconformity between Pillara Sequences 5 and 6 in back-reef Pillara Limestone, marked by a white line. Relief on the unconformity surface disappears on the right (passing into the platform interior). Note the regular, relatively thin, cycles above the boundary in Sequence 6 and thicker cycles below the boundary in Sequence 5.

in platform and uppermost marginal-slope facies, and as a conformity in deeper marginal-slope and basin facies. The event was associated with a brief fall in sea level, probably amounting to no more than 50 m. It was associated with one of the five principal mass extinctions known from the stratigraphic record (Fig. 53). The duration of the fall in sea level is uncertain, although the relatively small amount of erosion that is evident on the platforms suggests that it was relatively brief, perhaps less than a million years. House and Gradstein (2004) placed the Frasnian–Famennian boundary at 374.5 Ma.

The best localities to examine the unconformity in platform and uppermost marginal-slope deposits are at the northwest end of the Oscar Range and in the Napier Range northeast of Chedda Cliffs and west of *Wunala* Hill (Playford, 2002a; Figs 49, 50, 97, 98).

As a result of the small Frasnian–Famennian fall in sea level, the Pillara platforms were eroded and slightly karstified while deposition continued uninterrupted in the basins and deeper parts of the marginal slopes. The Frasnian–Famennian boundary in deep marginal-slope deposits has been defined precisely at three localities in Windjana Gorge (in the Napier Formation), and at McWhae Ridge and in the Virgin Hills Formation near Horse Spring (Figs 99–103). At each of these localities the boundary appears conformable, and there is no evidence of any significant time break, as shown by conodont analyses (G Klapper, 2004, written comm.).

In platform facies the boundary is marked by the virtual disappearance of stromatoporoid reef builders, their place being taken over by microbes. Microbes had previously made major contributions to the Givetian and Frasnian reefs, but they became virtually the sole reef builders in the Famennian. Deep-water stromatolites became prominent on some marginal slopes during Zone 13, and thrived there during the early Famennian, perhaps as a result of the extinction of microbe-consuming organisms (Fig. 54).

The extinction of conodonts and ammonoids, culminating at the Frasnian–Famennian boundary, began at the top of Zone 13b and continued through Zone 13c (Klapper, G, Appendix 1). Because of this 'step-wise' extinction, the conodont fauna became progressively more restricted and most ammonoids disappeared during Zone 13c. Among the ammonoids, only two species of manticoceratids and one tornoceratid survived to the end of the Frasnian, when they became extinct at the top of Zone 13. Ammonoids were totally absent during the earliest Famennian in the Canning Basin, eventually reappearing during the *crepida* Zone, having perhaps migrated from the northern hemisphere (Becker, R T and House, M R, Appendix 2).

The reason for the Frasnian–Famennian global mass extinction is uncertain. Possible causes, involving bolide impacts, global anoxia, and abrubt cooling associated with glaciation, have been suggested by various authors (including Copper, 1986; Playford et al., 1984b; Nicoll and Playford, 1993; Racki, 1999, 2005; Bond et al., 2004; Over et al., 2005; McGhee, 2005).

One explanation that has been put forward is that the extinction could have coincided with a global fall in temperature, associated with the development of polar ice caps (Copper, 1986; McGhee, 1996; Joachimski et al., 2003). Indeed, glacial deposits of Famennian age are known from several parts of Gondwana (Caputo, 1985; Caputo and Crowell, 1985; McGhee, 1996), but not from Australia. Abrupt cooling might conceivably have caused the brief fall in sea level and emergence of the reefal platforms. However, if this did result from an abrupt glaciation, it must have been very brief, as cycles in the succeeding Famennian platforms are small (average about 1.5 m), whereas much higher amplitudes (tens of metres) would have been expected from glacially driven sea-level changes.

Multiple bolide impacts during the late Frasnian have also been hypothesized as a cause of the Frasnian–Famennian mass extinction (McGhee, 1996; Sandberg et al., 2002; Ellwood et al., 2003). Such impacts could also have led to cooling of oceanic water and glaciation around the South Pole. However, no good evidence to support this hypothesis has been found in the Canning Basin.

An iridium anomaly in the Virgin Hills Formation at McWhae Ridge was once thought to have coincided with the Frasnian–Famennian boundary, possibly pointing to a bolide impact as the cause of the mass extinction (McLaren, 1982; Playford et al., 1984b). However, more detailed sampling has shown that the anomaly is in the early Famennian *crepida* Zone; moreover, the iridium concentration is biogenic in origin, associated with the iron cyanobacterium *Frutexites* (Nicoll and Playford, 1993).

Anoxic periods, known as the Kelwasser Events, are evident below the Frasnian–Famennian boundary at several places in the northern hemisphere (Bond et al., 2004) and it has been suggested that they were responsible for the mass extinction. However, no evidence of anoxia is known in the latest Frasnian in the Canning Basin.

It is thought possible that detailed geochemical studies across the boundary in the Canning Basin, following up the work of Stephens and Sumner (2003b), might provide the best chance of obtaining definitive evidence of the cause of the Frasnian–Famennian mass extinction.

The conodont zonation of the condensed Frasnian section at Horse Spring is described in detail by Klapper (2007), and the Frasnian–Famennian boundary there, based on conodonts, is defined by Klapper et al. (1993).

Nullara Sequence

The Nullara Sequence is bounded by the Frasnian–Famennian boundary Event below and the Reef-Extinction Event above. The Reef-Extinction Event is marked by an unconformity separating platform limestones of the Windjana and Nullara Limestones from overlying non-reefal shales and limestones of the Fairfield Group.

Horseshoe Range Event

The second-order Nullara Sequence is divided into two third-order sequences, known as Nullara Sequences 1 and 2, and the boundary between them resulted from the

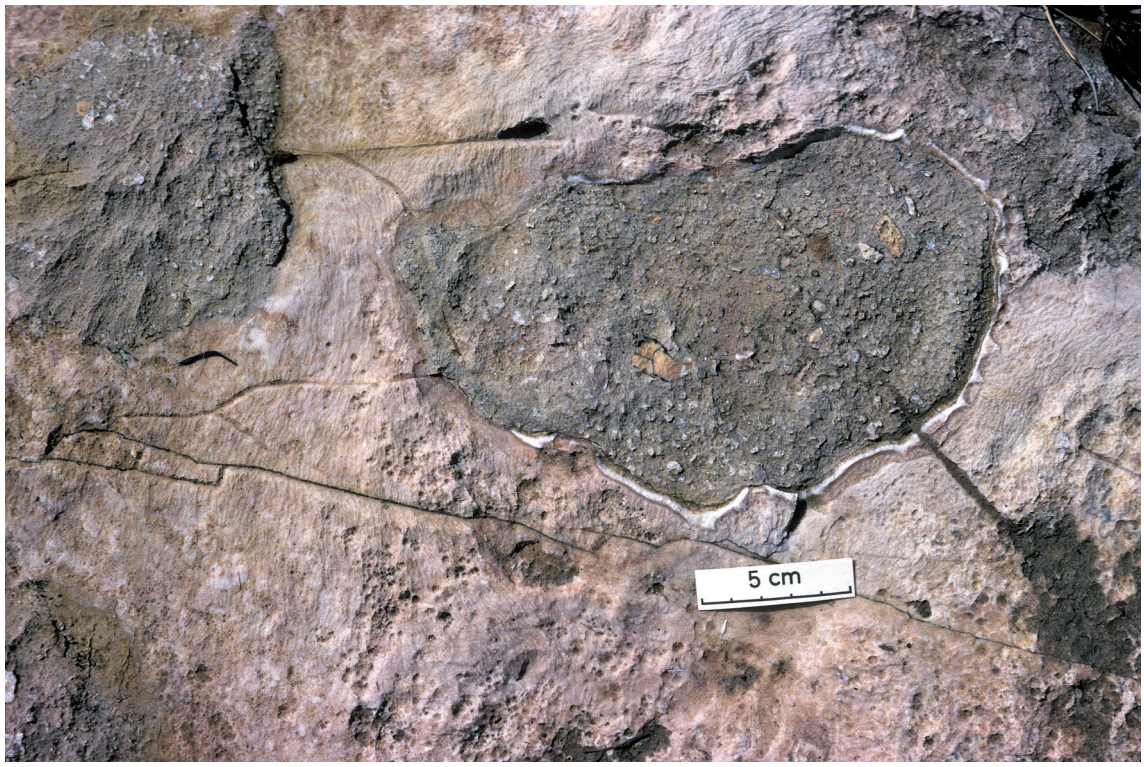

Figure 97. Plan view of the Frasnian–Famennian unconformity in the Napier Range near Chedda Cliffs, showing paleokarst cavities (potholes) in the Pillara Limestone below the unconformity, filled with dark fenestral limestone of the overlying Nullara Limestone.



Figure 98. The Frasnian–Famennian sequence boundary at the northwest end of the Oscar Range, between Frasnian Pillara Limestone (reef-margin subfacies) below, and well-bedded Famennian Nullara Limestone (back-reef subfacies) above. The contact between them is a planar unconformity.



Figure 99. The Frasnian–Famennian boundary, marked by a white line, in marginal-slope deposits (Napier Formation) in the eastern part of Windjana Gorge on its south side. The Frasnian deposits on the right are generally well bedded, whereas the Famennian deposits on the left are poorly bedded and marked by many allochthonous blocks of reef limestone. Note the undulating bedding, which is probably stromatolitic, directly above the boundary.



Figure 100. The Frasnian–Famennian boundary in the western part of Windjana Gorge, on its south side, in marginal-slope facies of the Napier Formation. The boundary is the prominent steep bedding plane in the centre of the photo.



Figure 101. Virgin Hills Formation on the west side of McWhae Ridge, showing trenches cut to sample for conodonts and ammonoids. The Frasnian–Famennian boundary is at the foot of the lower person; the red back-pack, above the upper person, is resting beside the *Frutexites* bed.

Figure 102. (facing page above right) Columnar section illustrating part of the Virgin Hills Formation at McWhae Ridge, showing the *Frutexites* bed, in the lower Famennian *crepida* Zone, associated with a prominent iridium anomaly resulting from the microbial concentration of iridium and other metals from Devonian seawater.

Figure 103. (facing page below right) Virgin Hills Formation near Horse Spring in the Horse Spring Range. The Frasnian–Famennian boundary is at the base of a massive Famennian megabreccia over bedded distal fore-reef Frasnian limestones.

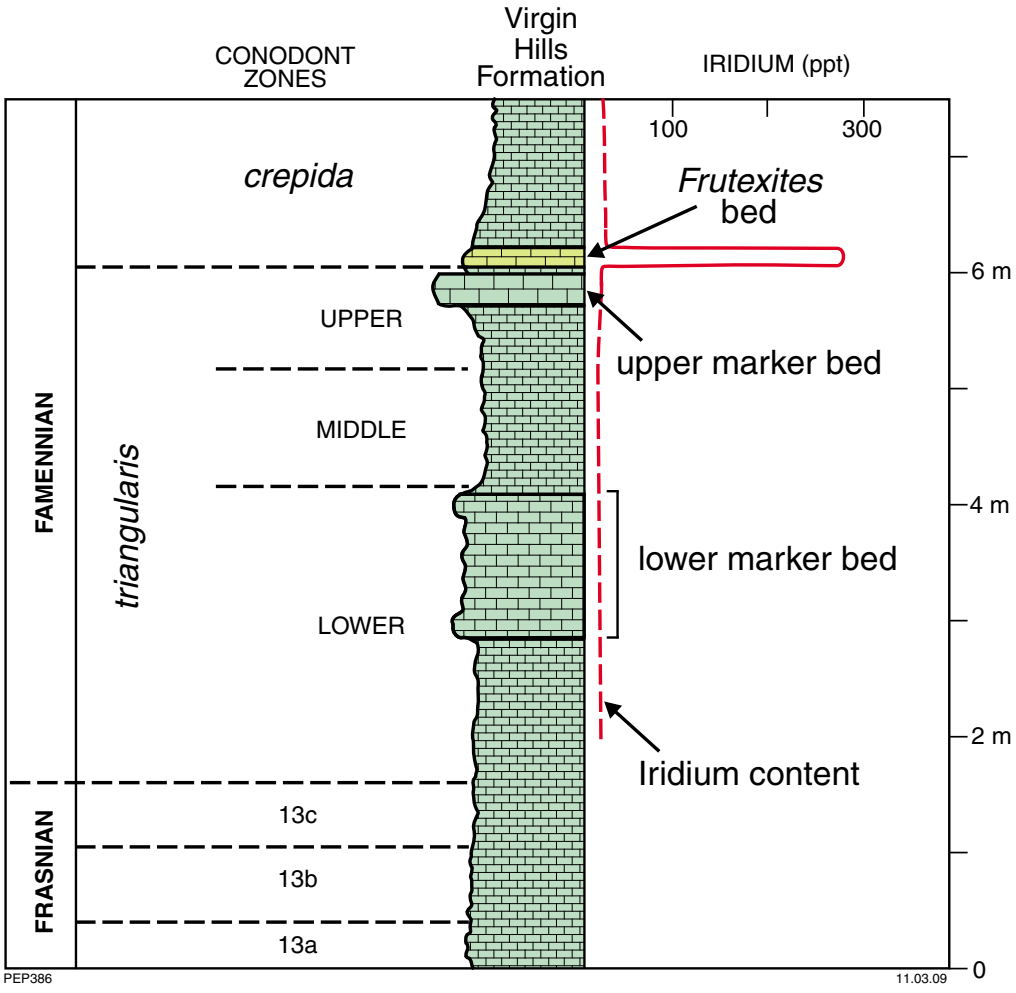
CONODONT ZONES
Virgin Hills Formation
IRIDIUM (ppt)
100
300
crepida
Frutexites bed
6 m
UPPER
upper marker bed
MIDDLE
4 m
lower marker bed
LOWER
2 m
Iridium content
FAMENNIAN
triangularis
FRASNIAN
13c
13b
13a
0
PEP386
11.03.09



Horseshoe Range Event (Fig. 21). The boundary between Nullara Sequences 1 and 2 correlates approximately with the boundary between the *trachytera* and *postera* Zones, dated as 365.5 Ma by House and Gradstein (2004). In the Horseshoe Range the sequence boundary is marked by abrupt backstepping of the Nullara platform and a change from steep-dipping marginal-slope deposits of the Virgin Hills Formation to low-dipping fore-bank deposits of the Piker Hills Formation (AMG Zone 52, 198000E 7985800N). At the beginning of Nullara Sequence 2 the Nullara platform had no reef rim, and bank deposits of the Nullara Limestone interfingered directly with flat-lying fore-bank deposits of the Piker Hills Formation. However, during the later phase of Nullara Sequence 2 the Nullara Limestone platform was again rimmed by reef of the Windjana Limestone.

It should be noted that although only two sequences have been distinguished in the outcropping Famennian platforms on the Lennard Shelf, as many as eight events have been postulated in the Famennian elsewhere in the world. Sandberg et al. (2002) attributed those events to glacial–interglacial episodes in a pattern of gradually increasing southern hemisphere glaciation, but the evidence in the Canning Basin does not support that hypothesis, as previously discussed. It is possible that additional sequence boundaries have not yet been recognized in the Nullara Limestone because of the general lack of thick well-exposed sections through the formation.

In the Horseshoe Range, recognizable cycles in the Nullara Limestone are 3 to 4 m thick, which is more than twice the cycle thickness evident in equivalent strata in Billy Munro Gorge and the northwest end of the Oscar Range (N Frost, 2007, written comm.). It seems likely that the amount of subsidence during deposition of the Nullara Sequence was greater in the Horseshoe Range than elsewhere on the Lennard Shelf because of contemporaneous movement along the Mount Elma Fault.

Reef-Extinction Event

The reef complexes became extinct during the late Famennian, at or about the boundary between the *expansa* and *praesulcata* Zones, dated as about 363 Ma, according to House and Gradstein (2004). Reef extinction was associated with an abrupt fall in sea level, estimated to have been at least 80 m, when the limestone platforms and upper marginal slopes were exposed to subaerial erosion. The exposed platforms were mildly karstified, as shown in the uppermost Nullara Limestone directly below the Fairfield Group in the Horseshoe Range, where sinkholes and tepee structures occur in Nullara Limestone immediately below the boundary. Karstification below this boundary seems more intense than that at the Frasnian–Famennian boundary.

The reef scarp skirting the late Famennian platform on the north flank of the Oscar Range was eroded by streams, forming conspicuous v-shaped valleys (Fig. 104). Caves seen in the reef front may have been formed through karstification following reef extinction. Alternatively, they may have formed below the Early Permian ice sheet. Shales of the Fairfield Group were deposited during the following transgression, filling karst features and valleys along the platform margins, as evidenced by Shell Metals

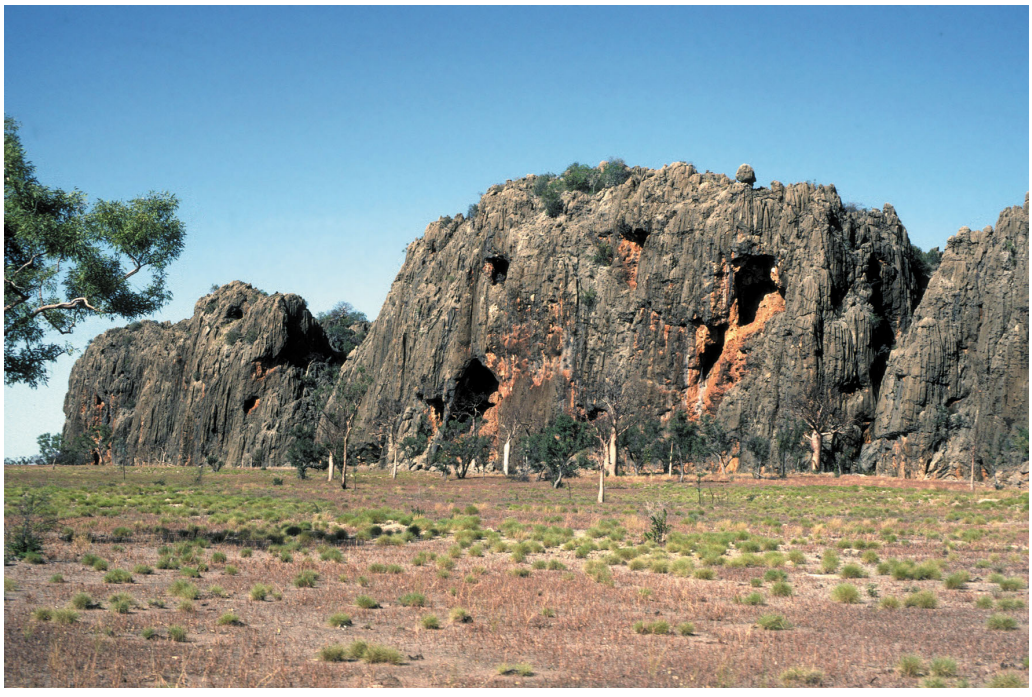

Figure 104. Part of Morown Cliff near its southeastern end, showing the abrupt cliff of late Famennian reef (Windjana Limestone) that resulted from the regression linked with the Reef Extinction Event. Note the V-shaped valleys that were eroded into the scarp following the late Famennian fall in sea level. Caves in the reef front formed as a result of karstification during either the late Famennian or the Early Permian.

drillhole NRD 99 in the Napier Range (AMG Zone 51, 653700E 8097600N) and Pickands-Mather drillhole AH2 in the Oscar Range (AMG Zone 51, 705500E 8048500N).

This abrupt regression was of major importance in the Canning Basin, as it resulted in the total extinction of the reef complexes. Whether or not this resulted from a global event must await more detailed late Famennian correlations between Western Australia and other parts of the world. The Famennian extinction event in the Canning Basin predates the latest Famennian regression recognized by Johnson et al. (1985) and Sandberg et al. (2002), which is said to have led to the Devonian–Carboniferous extinction.

It is not known how long the platforms remained exposed, but it was probably for only a relatively brief period, perhaps less than a million years, as the platforms were not strongly eroded and the lower part of the succeeding Fairfield Group is also late Famennian in age. A major change in environmental conditions must have been associated with the regression, as sediments of the succeeding late Famennian to Tournaisian Fairfield Group lack any reefs. The microbial assemblage that constructed the Famennian reefs disappeared from the area, and non-reefal shale, sandstone, and limestone, some being rich in bryozoans, were deposited over the extinct reefs (Ross, 1961; Druce and Radke, 1979). The cause of these abrupt changes in sea level and faunas could be a sudden decrease in seawater temperatures following an onset of glaciation in southern polar regions, in accord with views expressed by Caputo and Crowell (1985), McGhee (1996), and Sandberg et al. (2002). The faunas of the latest Frasnian and Tournaisian Fairfield Group, which are rich in bryozoans, would seem to be consistent with that cold-water hypothesis.

Platform-margin and marginal-slope relationships

Types of platform margins

The principal types of platform margins recognized in the reef complexes are shown on Figure 105. These types commonly grade from one to another both laterally and vertically.

The different types of margin are as follows:

- *upright-scarp margin*, where a well-developed reef grew vertically to form a reef scarp, with adjoining marginal-slope deposits progressively mounting up against it (Fig. 106);
- *upright-rollover margin*, where the sea floor abruptly 'rolled over', passing from a shallow-water flat-topped platform to a steep marginal slope without any intervening scarp (Figs 107, 108);
- *collapsed margin*, where there was submarine collapse and landsliding of a platform margin, leaving a sheer scarp (Figs 109, 110);
- *retreating margin*, where a platform was steadily shrinking in extent as it grew upward (Figs 111–113);
- *advancing margin*, where a platform advanced over its own marginal-slope deposits (Fig. 114);
- *backstepping margin*, where a platform margin retreated abruptly into the platform interior (Figs 87, 88);
- *fault-controlled margin*, where a margin coincided with an active fault (Fig. 115);
- *interfingering bank margin*, where a flat-lying bank interfingered directly with gently dipping marginal-slope deposits (Fig. 66);
- *pinnacle reef* (having breadth to height less than about 2:1), where a platform or atoll was progressively being drowned (Figs 116, 117).

The different types of platform margin are believed to have formed in response to several factors, including basement topography, water depths in the adjoining basin, degree of submarine cementation, contemporary faulting and associated earthquakes, types of reef-building organisms, and rates of subsidence. Subsidence rates may vary from one area to another, causing variations in the platform margins. Differing water depths in the adjoining basins may also have influenced the types of platform margins in particular areas.

Marginal-slope debris deposits

The marginal-slope deposits include large volumes of coarse platform-derived debris, much of which was deposited as submarine debris flows and talus. Individual reef blocks in the debris are as much as about 200 m across. Early workers in the area did not recognize these blocks as being allochthonous, regarding them instead as in-place bioherms (e.g. Smith et al., 1957; Guppy et al., 1958; Playford and Johnstone, 1959a). The allochthonous origin of such reef blocks was first recognized by Playford and Lowry (1964), and has since been documented by Playford (1980, 1984a), Tornatora (1992), and George et al. (1997), among others. Although some in-place microbial bioherms occur in marginal-slope deposits, most large reefal masses in those deposits are allochthonous blocks derived from reef-margin, reef-flat, and reefal-slope limestones. However, it should be noted that autochthonous microbial mounds have grown in some places on the tops of allochthonous reef blocks (Fig. 118).

Most debris-flow deposits in the reef complexes are believed to have originated through the collapse of sections of the platform margins, resulting in submarine rockfalls that initiated landsliding of the marginal-slope deposits (Playford, 1984a). In many cases this collapse was probably brought about by earthquake shaking, and perhaps by associated tsunamis. The mass of debris from each rockfall incorporated mud and sand from the marginal slopes below, forming debris flows that moved down-slope, generally in shallow channels, the widths of which were largely controlled by the extent of the original collapses (Figs 119, 120). Some debris flows may have been as much as a kilometre wide, but most were considerably less than this, with widths ranging from several hundreds to a few tens of metres. Debris flows commonly stopped at or near the base of the marginal slopes, but some came to rest higher on the slopes and others extended far out on the adjoining basin floors, where some initiated turbidites.

Some characteristics of debris-flow deposits in the Canning Basin are illustrated on Figures 119–127. They commonly fill channels, which were eroded deepest on relatively

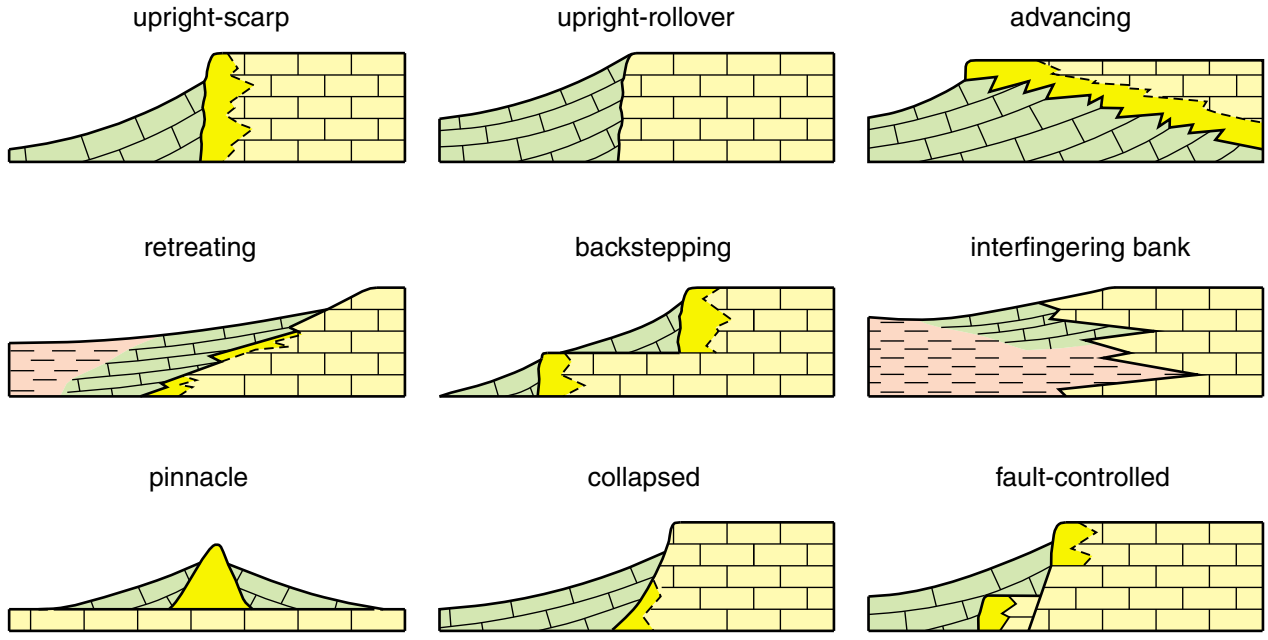

Figure 105. Sections illustrating the principal types of platform margin in the reef complexes.



Figure 106. Upright scarp of massive reef-margin subfacies (Pillara Limestone) fronted by steeply dipping fore-reef subfacies (Sadler Limestone) beside Nardji Cave, South Lawford Range.



Figure 107. Upright-rollover platform margin in the Pillara Range, 1 km northwest of Menyous Gap, showing reef-flat subfacies (Pillara Limestone) 'rolling over' into fore-reef and reefal-slope subfacies (Sadler Limestone).



Figure 108. Upright-rollover platform margin in the Pillara Range, 0.7 km northwest of Menyous Gap, showing bedding in the reef-flat subfacies (Pillara Limestone) thickening as it passes into massive reef-margin subfacies and rolls over into the marginal-slope Sadler Limestone.



Figure 109. Collapsed platform margin opposite the Classic Face in Windjana Gorge. Flat-lying reef-flat to reef-margin subfacies (Pillara Limestone, on the left), is abutted by reefal-slope subfacies of the Napier Formation (on the right). The boundary was formed as a steep, slightly eroded collapse scarp, in front of which are dipping reefal-slope and fore-reef deposits.



Figure 110. Collapsed margin near *Mirrngurrwalla* in the western part of Windjana Gorge, showing flat-lying, well-bedded to massive, back-reef and reef limestones of the Pillara Limestone (on the left), truncated by a steep slightly eroded collapse surface abutted by crudely bedded to unbedded, steeply dipping, reefal-slope deposits of the Napier Formation (on the right).



Figure 111. Retreating (retrograding) margin in the north Laidlaw Range, showing bedded fore-reef limestone of the Sadler Limestone (on the right) mounting over massive reef limestone of the Pillara Limestone (on the left).



Figure 112. Retreating (retrograding) platform margin on the north side of Menyous Gap near its east entrance, showing steeply dipping marginal-slope facies (Sadler Limestone) mounting over thick-bedded to massive platform facies (Pillara Limestone).



Figure 113. Retreating (retrograding) platform margin, 1 km south of Menyous Gap in the Pillara Range showing steeply dipping marginal-slope facies (Sadler Limestone) mounting over massive to thick-bedded reef-flat limestone (Pillara Limestone).



Figure 114. Advancing (prograding) platform margin in the Napier Range, 5.5 km northwest of Windjana Gorge, showing massive reef (Windjana Limestone) overlying and interfingering with marginal-slope limestone (Napier Formation).

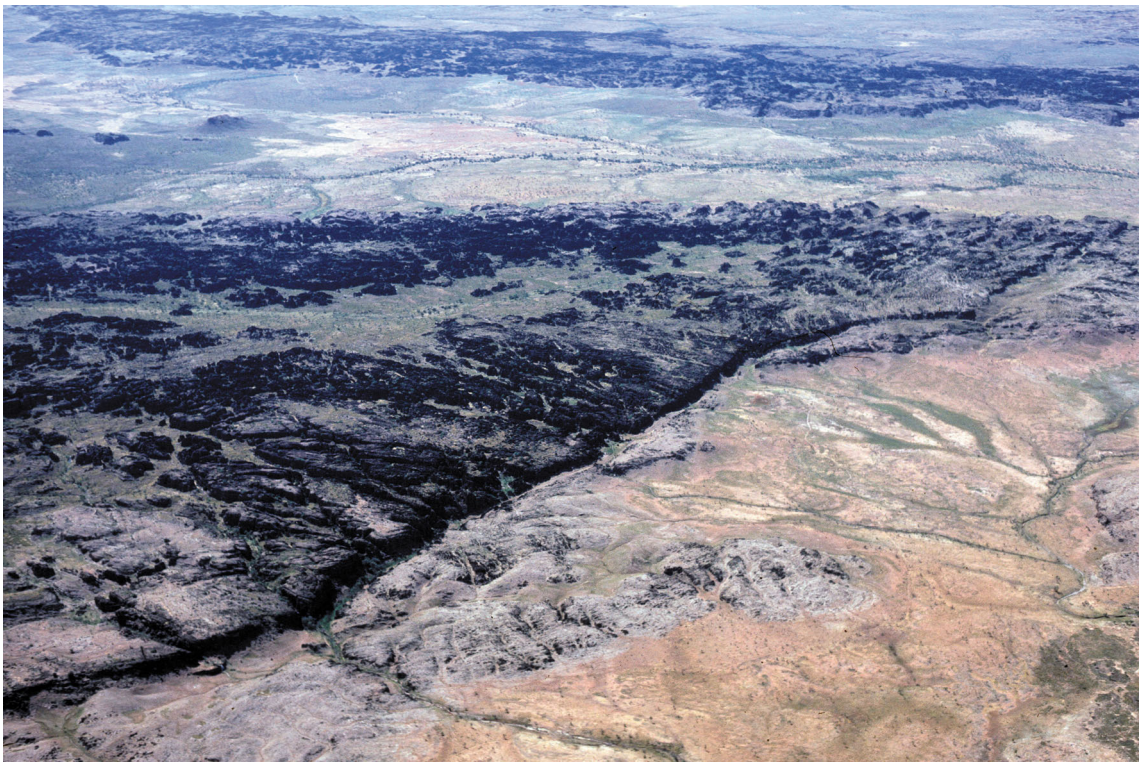

Figure 115. Aerial view of a faulted platform margin in the Emanuel Range, looking east. It shows the Cadjebut Fault, which was active during the Devonian and formed the margin of the reefal platform. The range is composed of Pillara Limestone (back-reef and reef subfacies), while the more subdued topography in the right foreground is composed of Virgin Hills Formation (fore-reef subfacies).



Figure 116. Aerial view of Wade Knoll pinnacle reef (stromatoporoid–microbial reef limestone), showing its south-directed 'tail'. The massive reef limestone (Pillara Limestone) is encircled by bedded fore-reef limestones (Sadler Limestone) and poorly exposed cyclic basin deposits (Gogo Formation). Thin white beds in the Gogo Formation are turbidites and distal debris-flow deposits, thought to be interbedded with siltstone and shale, which do not outcrop. The cyclicity is attributed to metre-scale sea-level fluctuations.

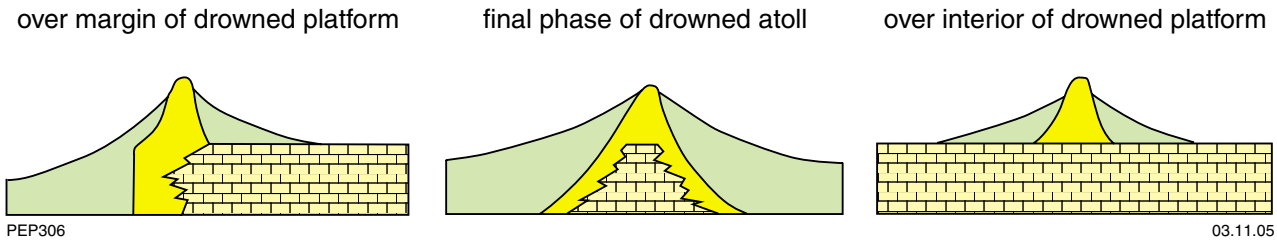

Figure 117. Diagram illustrating the development of various types of pinnacle reefs in the reef complexes.

steep slopes, and frequently show large limestone blocks 'floating' in a finer groundmass of calcarenite, sandstone, or siltstone. Reverse grading is common, and rock slabs tend to be oriented parallel to the flow margins, indicating laminar rather than turbulent flow. The upper surface of a debris-flow deposit is typically irregular, with large rafted blocks protruding into the overlying deposits (Fig. 123). Where flow occurred in a channel, the underlying sediments were eroded, and may show evidence of shearing and/or folding caused by movement of the debris (Figs 124, 125). After the flows came to rest, some of the blocks that they contained sank into soft underlying sediments, distorting them or forming flame structures through the injection of soft sediments between blocks in the debris flow (Fig. 126). Debris-flow (laminar-flow) mechanisms are thought to have prevailed in most mass flows on the marginal slopes, but some could have formed as grain flows (Lowe, 1979).

Some debris-flow breccias contain blocks of reefal-slope limestone and early-cemented fore-reef limestone, with little or no reef-derived material. These breccias were initiated by landsliding of uncemented and early-cemented deposits on the fore-reef slopes, without any associated platform-margin collapses (Fig. 119).

Most megabreccias in marginal-slope deposits were formed as debris flows. However, some form sheets or lenses consisting of closely packed reef blocks without matrix support (Fig. 127), and others are probably talus deposits that accumulated progressively, piece-by-piece, as rubble derived from the reef front. Isolated allochthonous blocks of reef in the marginal-slope deposits originated by breaking away from a reef and sliding or rolling down the slopes (Fig. 128). They can generally be distinguished from autochthonous bioherms by the use of geopetal structures that they contain. Unlike in-place bioherms, allochthonous blocks have haphazard orientations relative to their original growth orientations; for example, some are lying on their sides and others are upside down.

Adnet breccias, consisting of irregular nodular clasts (commonly red in colour) in a muddy or sparry matrix are conspicuous finer grained mass-flow deposits in some marginal-slope deposits (Garrison and Fischer, 1969; Kerans and Playford, 1984; Kerans, 1985; Böhm et al., 1995). Scheck breccias are those adnet breccias in which the matrix between clasts consists of sparry calcite. Adnet breccias typically occur as small lenses, from about one to several metres long (Fig. 129). Many adnet and scheck breccias show reverse grading, which is typical of debris-flow transport, while others show 'double' grading, having finer clasts at the base and top and coarser clasts in the middle (Fig. 130). The matrix in double-graded adnet breccias commonly consists of mud between finer clasts at the base and top of each bed, and sparry calcite between coarser clasts in the middle.

Individual clasts in some breccias show evidence of corrosion, which may have occurred either just before or soon after the clasts were deposited (see also Garrison and Fischer, 1969). Such corroded clasts are most conspicuous in scheck breccias (Figs 131, 132), but they also occur in other types of fore-reef breccias (Fig. 133). Scheck breccias, with their sparry-calcite matrixes, often pass laterally and abruptly into adnet breccias with mudstone or sandstone matrices (Fig. 134). Further study of the origin of these breccias and corroded clasts is clearly warranted.

Geopetal structures, depositional dip, and paleobathymetry

Geopetal structures are features of sedimentary rocks that show the original orientation of those rocks at the time of deposition. Many geopetal structures are recognized in the Devonian reef complexes and are valuable tools in determining depositional dips and distinguishing whether reefal masses are autochthonous or allochthonous. They are also important in understanding the diagenetic history of the carbonates (Playford and Cockbain, 1972).

Geopetal structures in the Devonian limestones are of two types — cavity fillings and organic growth forms (Fig. 135). Sediments filling or partly filling cavities in the limestones were generally introduced soon after deposition, before the rocks were subjected to tilting or other deformation, or they broke away to form allochthonous blocks. Sediment cavity fillings were commonly interlaminated with early marine fibrous cement and overlain by clear sparry calcite. The calcareous sediment may have been wholly or partly dolomitized. The original horizontal when the geopetal structures first formed is shown by laminations within their contained sediment, and by the contact between that sediment and overlying spar. Thus they form 'fossil spirit levels'. Geopetal growth forms are organic structures that commonly grew nearly vertically, towards the light or under the influence of gravity. They can be considered as 'fossil plumb lines'.

The recognition of steep depositional dips in marginal-slope deposits is of fundamental importance in understanding the structure of the reef complexes and original water depths down the marginal slopes. The depositional nature

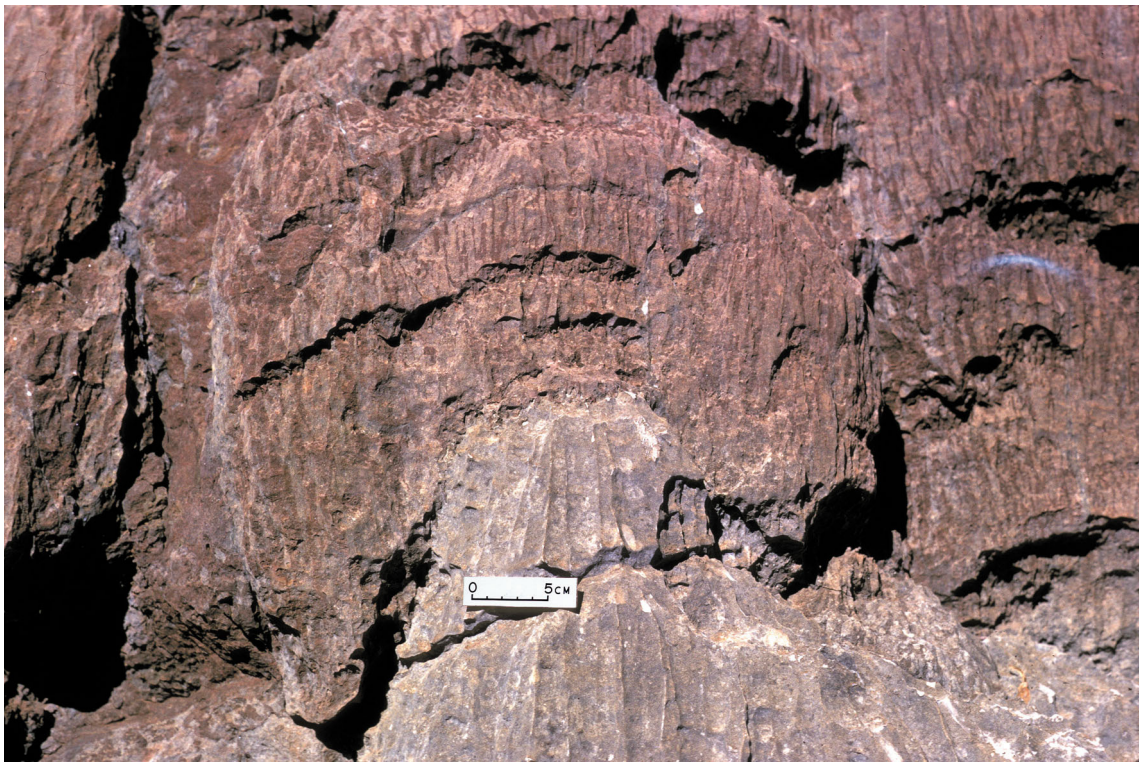

Figure 118. **Part of a block of reef limestone (lower central part of photo) encrusted by vertical densely packed 'fingers' of the cyanobacterium *Sphaerocodium*, in the eastern part of Windjana Gorge.**

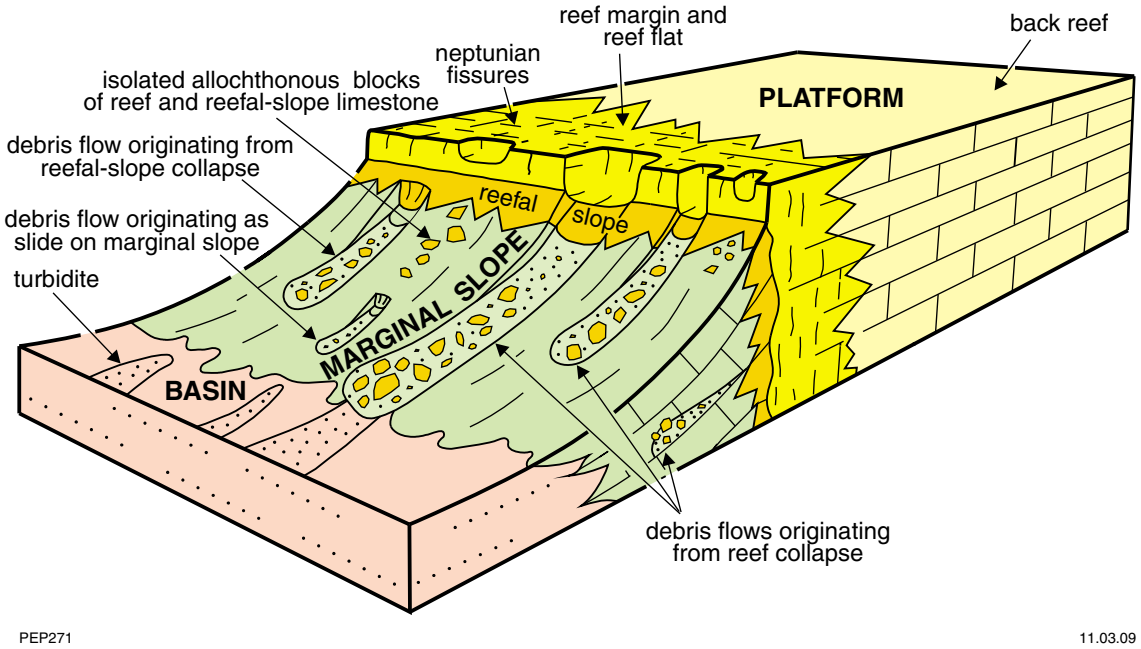

Figure 119. **Block diagram illustrating the origin of marginal-slope debris flows and allochthonous blocks by the partial collapse of platform margins and submarine sliding of marginal-slope deposits. Turbidites generated by the debris flows were spread over the adjoining basin.**

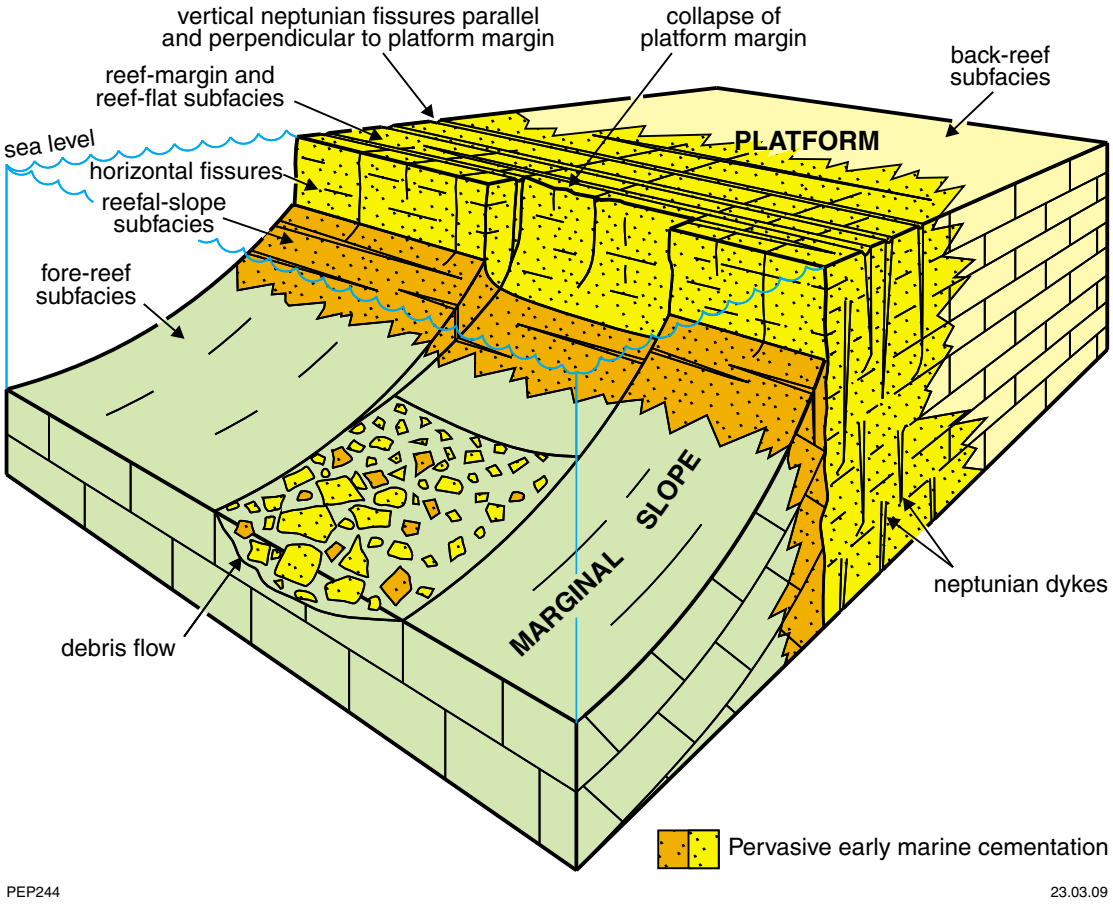

Figure 120. **Block diagram illustrating the collapse of a platform margin, controlled by neptunian fissures, leading to the development of a debris flow on the adjoining marginal slope.**

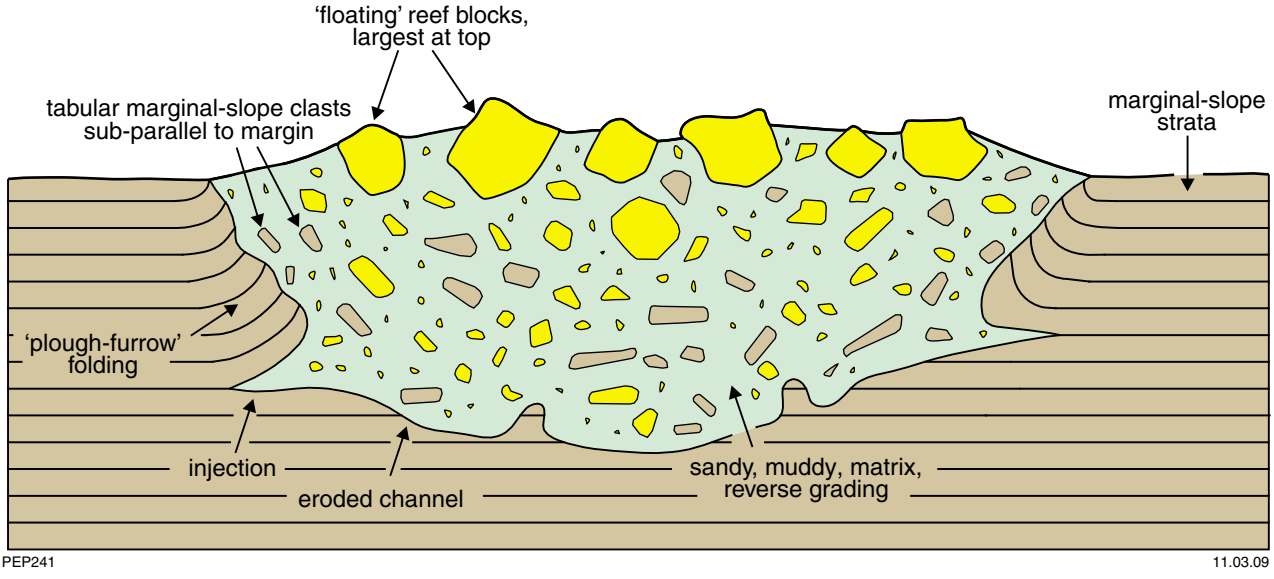

Figure 121. **Diagrammatic cross section illustrating features of debris-flow deposits in fore-reef deposits of the Devonian reef complexes.**



Figure 122. Typical debris-flow megabreccia in fore-reef subfacies (Napier Formation), Dingo Gap, Napier Range. The megabreccia is composed of blocks of reef and reefal-slope limestones in a matrix of calcareous sandstone.



Figure 123. Debris-flow deposit in fore-reef subfacies of the Napier Formation in Dingo Gap, showing reverse grading, with the largest blocks at the top of the flow.



Figure 124. **A slide plane at the base of a debris-flow megabreccia (upper part of photo) in fore-reef Napier Formation in McSherrys Gap, showing shearing, fracturing, and folding of strata under the slide plane.**



Figure 125. **'Plough-furrow' folding of marginal-slope limestones below a debris-flow breccia in Napier Formation, fore-reef subfacies, beside Dingo Gap.**



Figure 126. A chisel-shaped block of reef limestone at the base of a debris-flow deposit in the Napier Formation, Dingo Gap. The block sank into underlying strata after the debris flow had come to rest.



Figure 127. Megabreccia in Napier Formation, fore-reef subfacies, Dingo Gap. This mass-flow deposit consists of reef blocks with very little matrix.



Figure 128. Allochthonous block of reef limestone in fore-reef subfacies (Napier Formation) 0.5 km south of McSherrys Gap, Napier Range. A thin (about 15 cm thick) layer of deep-water stromatolites grew on top of the block after it came to rest. This layer can be discerned at the foot of the person in the photograph.



Figure 129. Lenses of scheck breccias in Napier Formation (fore-reef subfacies), northwest of Napier Downs Homestead.

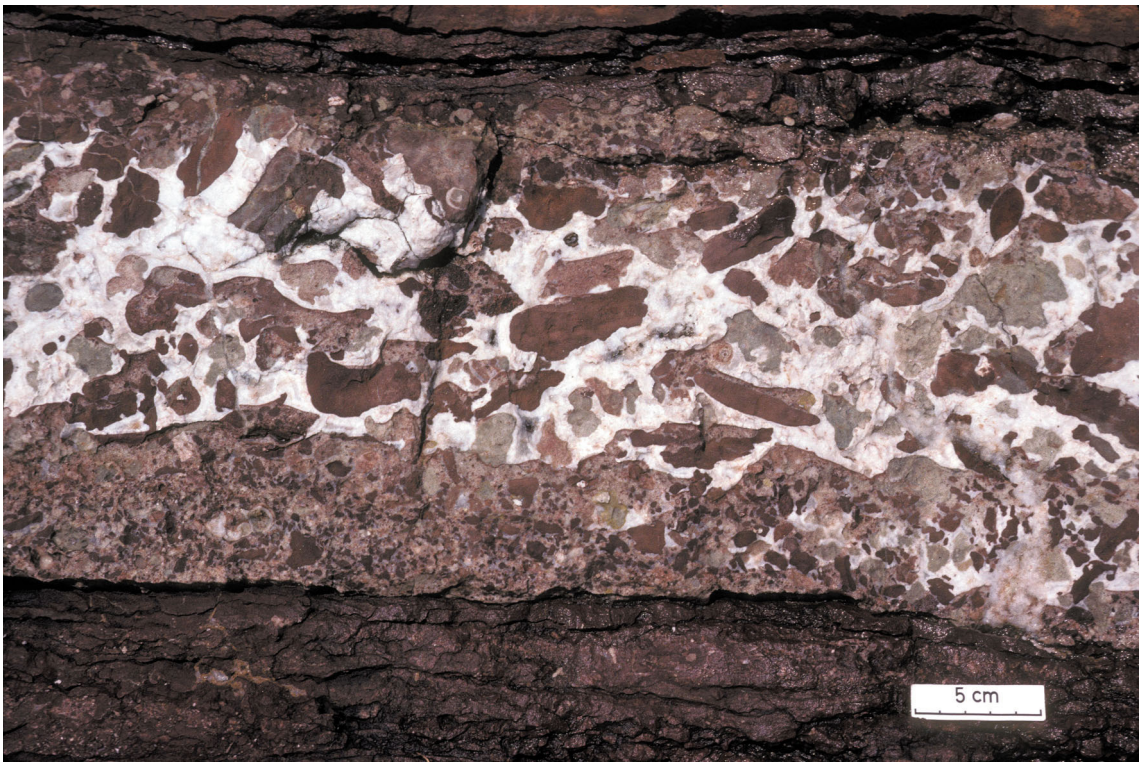

Figure 130. Scheck breccia in Napier Formation (fore-reef subfacies), north of Napier Downs Homestead. Note the double grading of the bed. The finest material at the base, the coarsest material, with sparry cement, is in the middle, and finer material with a muddy matrix, is at the top.

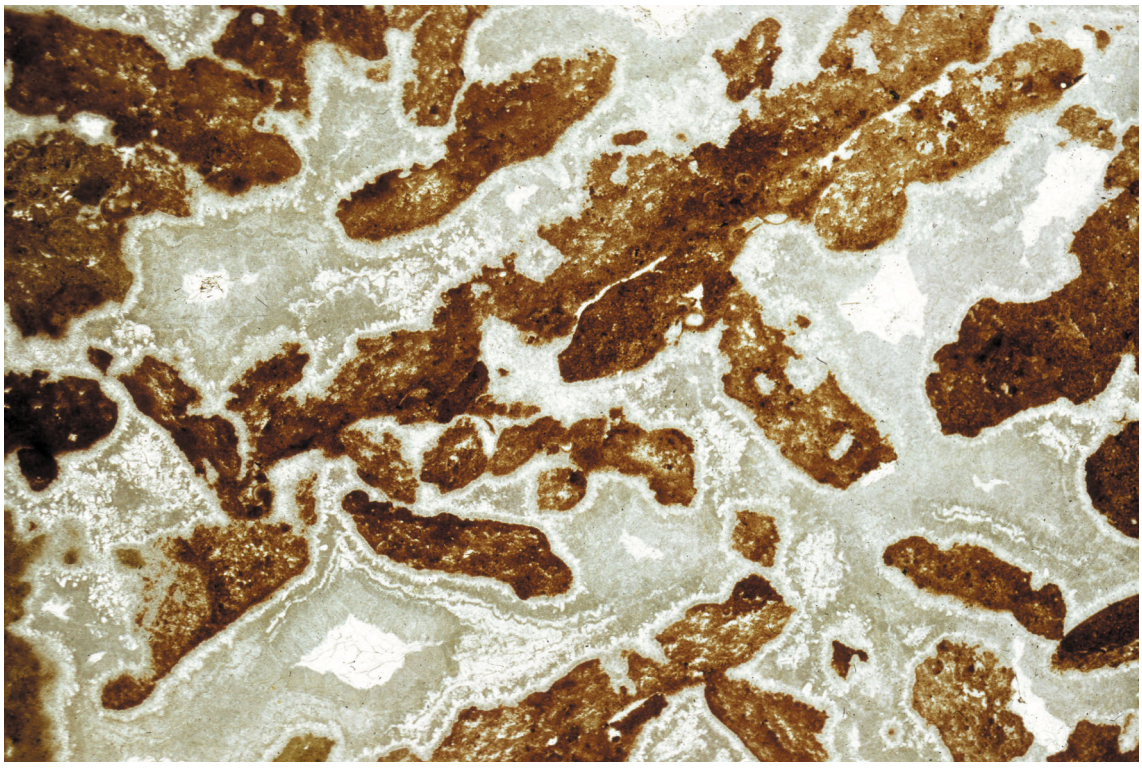

Figure 131. Thin section of a scheck breccia in Virgin Hills Formation from the South Lawford Range, showing corroded clasts of fine wackestone in a groundmass of sparry calcite. GSWA sample no. 19255. Width of field of view 65 mm.

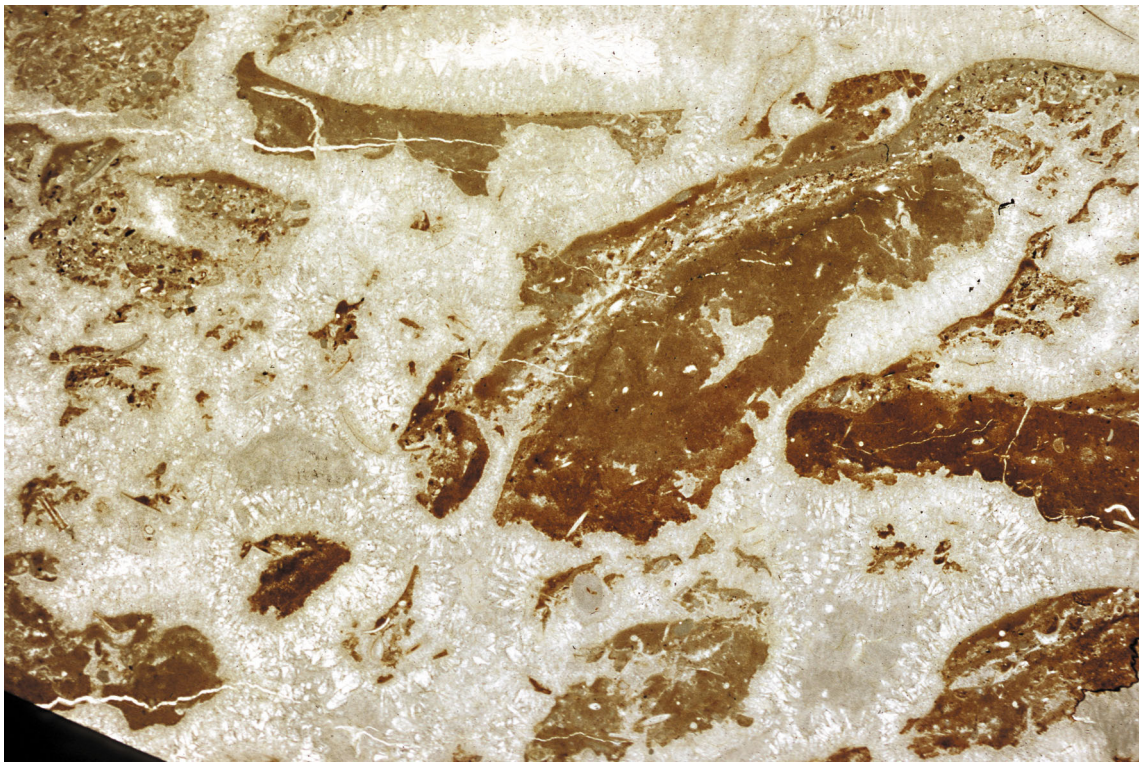

Figure 132. Thin section of a scheck breccia in Virgin Hills Formation near Galeru Gorge showing corroded clasts of fine wackestone in a groundmass of sparry calcite. GSWA sample no. 11680C. Width of field of view 43 mm.



Figure 133. Corroded clast of reef limestone in fore-reef breccia, Napier Formation (fore-reef subfacies), Dingo Gap.

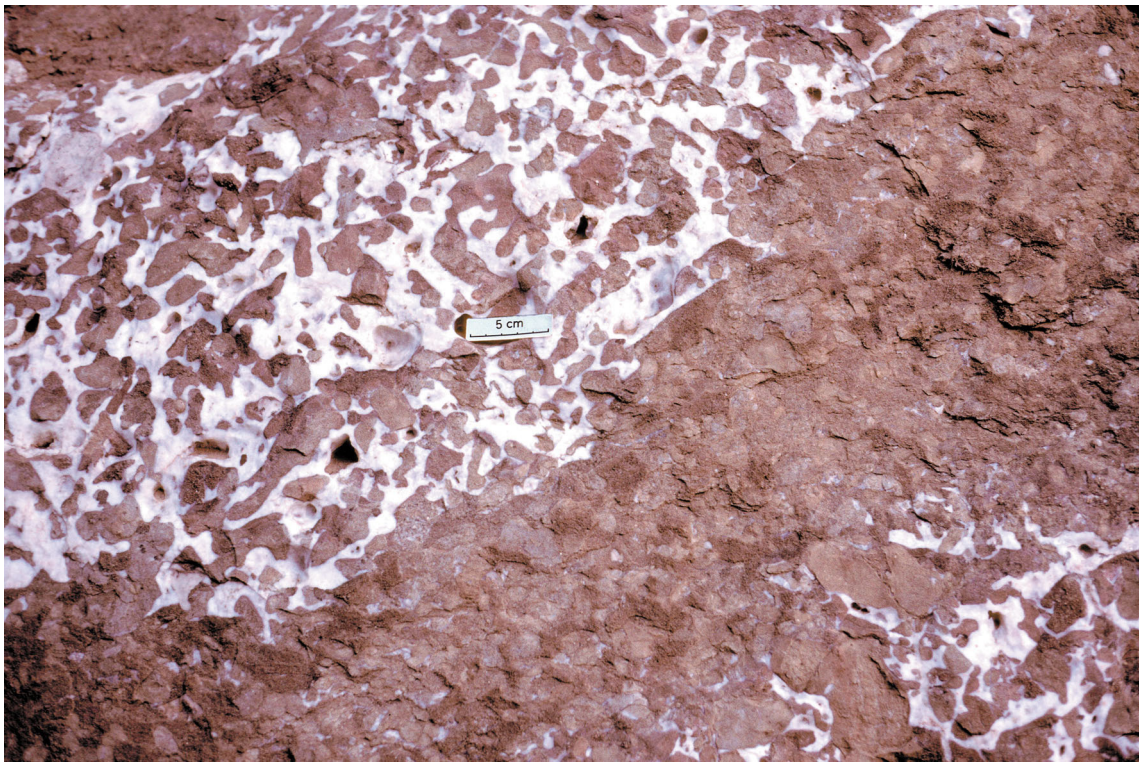

Figure 134. Scheck breccia with calcite cement (on the left), passing abruptly into adnet breccia with a muddy matrix and back again into scheck breccia (bottom right), from the north side of Windjana Gorge beside the east entrance.

of the steep dips in relevant parts of the complexes was first reported by Smith et al. (1957), Guppy et al. (1958), and Playford and Johnstone (1959a). Since then, the detailed study of geopetal structures in these rocks has allowed depositional and post-depositional components of observed dips to be quantified (e.g. Playford and Lowry, 1966; Playford and Cockbain, 1972; Playford, 1976a, 1981).

Geopetal structures are also used to differentiate in-place bioherms and pinnacle reefs from allochthonous blocks of reef that have slid, rolled, or been carried in debris flows down the marginal slopes. Geopetal cavity fillings in allochthonous blocks are also important in demonstrating the stage of diagenesis that had been attained in the reef limestones before the blocks were detached. The most useful geopetal structures for determining depositional dips are sediment and sparry-calcite fillings of fossils, especially closed brachiopod valves (Figs 136, 137). The sediment entered through pedicle openings and gaps between valves.

In cases where the sediment has poured in from one side of a cavity, that sediment may have had a depositional dip, but in most cases it came to rest nearly horizontally. In using geopetal cavity fillings to deduce the amount of depositional dip it is necessary to take measurements on many cavity fillings at a particular locality, in order to average out the effects of any depositional dips within the cavities themselves (Fig. 138).

In some cases 'double-geopetal' fillings are developed in allochthonous blocks of reef limestone. A cavity may have been partly filled with sediment and spar when the limestone was still in place in the reef (thereby indicating the original horizontal), and the rest of the cavity was filled after the block broke away and rolled or was otherwise carried down the marginal slope. The first geopetal infilling shows the original horizontal, and the last shows the horizontal after the block had come to rest on the slope (Figs 139, 140).

McWhae Ridge

A good example of the use of geopetal structures to determine depositional dip is displayed on the west side of McWhae Ridge at the southern end of the South Lawford Range (Playford, 1980, 1981). There, marginal-slope limestones of the Sadler Limestone and Virgin Hills Formation dip away on either side of a reef spine, at as much as 41° on the west side and 28° on the east side. Geopetal measurements were taken in Sadler Limestone at a locality on the west side of the ridge, where the unit is well exposed on two sides of a shallow karst corridor (Figs 141–148) at GPS AMG Zone 52, 191950E 7926120N. Several square metres of the limestone surfaces were cleaned of their pervasive cover of grey epilithic microbial films, using many litres of concentrated hydrochloric acid (a somewhat hazardous procedure). Surfaces cleaned in this way in 1968 had still not been re-colonized by microbes in 2007.

The strata dip west at 41° and contain a wide variety of geopetal structures — cavity fillings in brachiopods, receptaculitids, nautiloids, and stromatactis, and organic

growth forms consisting of *Sphaerocodium* caps on *Girvanella* oncolites. The oncolites formed originally on top of the reef spine and were periodically swept off on either side, coming to rest on steep depositional slopes. In some layers of oncolites, especially the final layer, caps of *Sphaerocodium* grew vertically on top of the spherical oncolites, to form spectacular 'capped oncolites' (Fig. 143).

Statistical measurements were made in the field on both cavity fillings in fossils (tilt from the present horizontal) and caps on oncolites (tilt from the present vertical), and the results are illustrated in Figure 142. The mean post-depositional tilt, as deduced separately from the fossil 'spirit levels' and 'plumb lines', is very similar (6.3° west for cavity fillings, 5° west for caps on oncolites). The measurements were taken on the walls of the karst corridor, which is at an angle of 20° to the dip direction, and by adjusting geopetal measurements to the dip direction it is concluded that the post-depositional dip component (probably resulting largely from differential compaction through pressure solution) is approximately 7° west, so that the original depositional dip was about 34° west (Playford, 1980, 1981).

The bedding plane marking the top of the Sadler Limestone has large numbers of subparallel straight nautiloids, most of which (93% of 269 that were measured) have their apical ends pointed up dip (Figs 146, 147). They have a mean orientation of 260°, compared with the present dip direction of 250°. The equivalent bed occurs on the other side of McWhae Ridge, and again the apical ends of the nautiloids point up dip, towards the reef crest. Clearly, the nautiloids came to rest in the stable position for conical bodies lying on a steep slope (Playford, 1980, 1981).

The quantification of depositional dips provides the basis for paleobathymetric reconstructions. Where an observed dip is entirely depositional, the difference in original water depth between any two points on a bedding plane is the same as the present elevation difference between them. Where there has been post-depositional tilting, appropriate corrections need to be applied in determining water depths. Thus, at McWhae Ridge, where the dip has been increased by about 7° since deposition, a metre of elevation on a bedding plane is equivalent to about 0.8 m of water depth in the Devonian sea. In this way it can be demonstrated that the oncolite caps grew in water at least 35 m deep (and probably much more; Playford and Cockbain, 1969). Similarly, reconstructions show that that the stromatolites in the Virgin Hills Formation at McWhae Ridge grew in water at least 45 m deep, and probably more than 60–80 m deep (Playford, 1980). Indeed, it is estimated that the shallowest stromatolites over the crest of McWhae Ridge probably grew in water more than 100 m deep (Fig. 148).

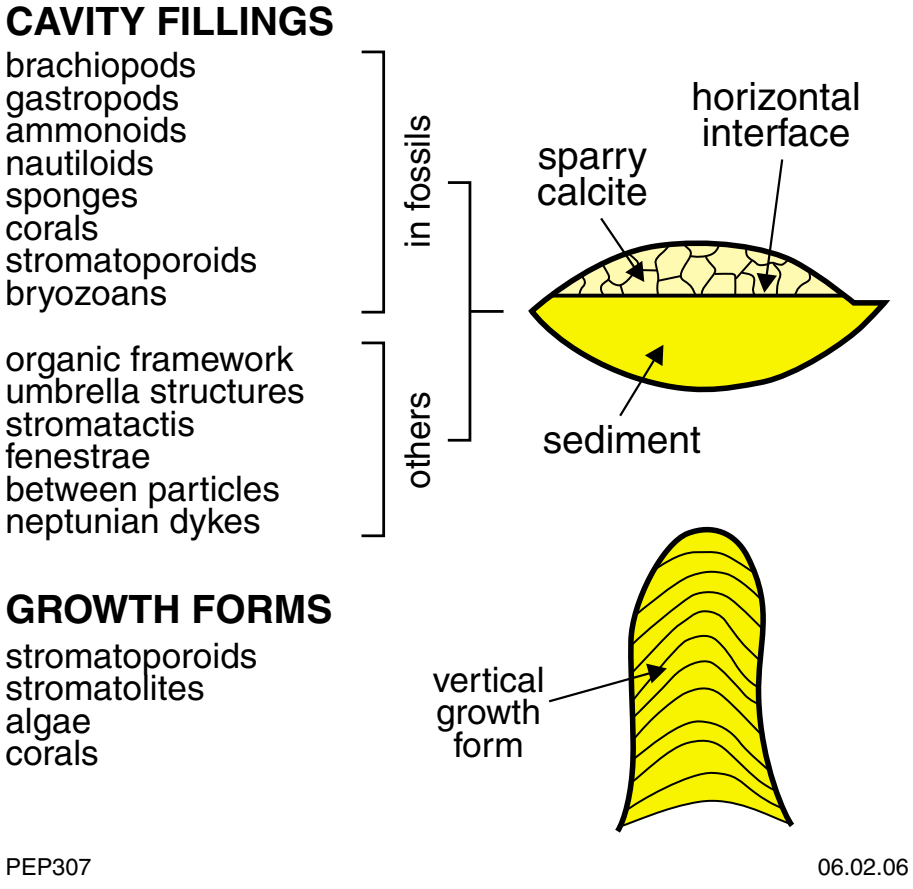

Figure 135. Diagram illustrating types of geopetal structures found in the Devonian limestones.

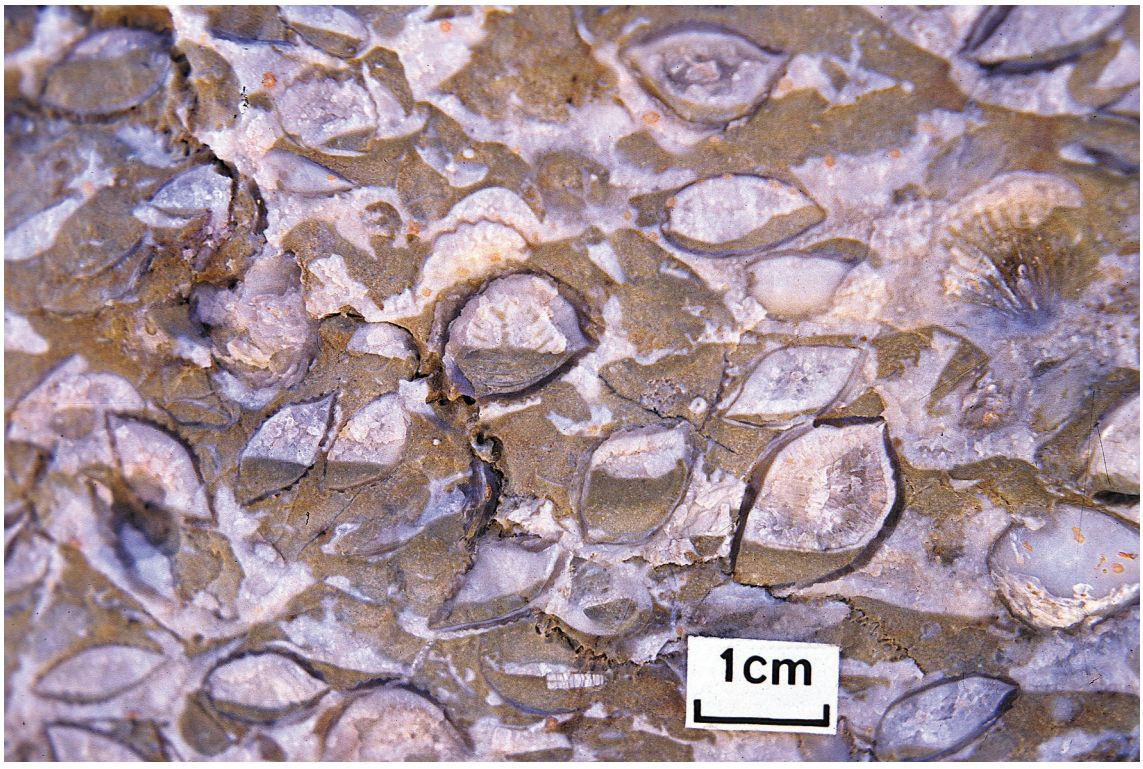

Figure 136. Brachiopods showing 'spirit level' geopetal fillings in each closed shell, from the Sadler Limestone on the eastern side of the Emanuel Range. The mud entered the valves through their pedicle openings or gaps between the valves, and the rest of the cavity was then filled by sparry calcite. The boundary between spar and mudstone approximates the original horizontal.

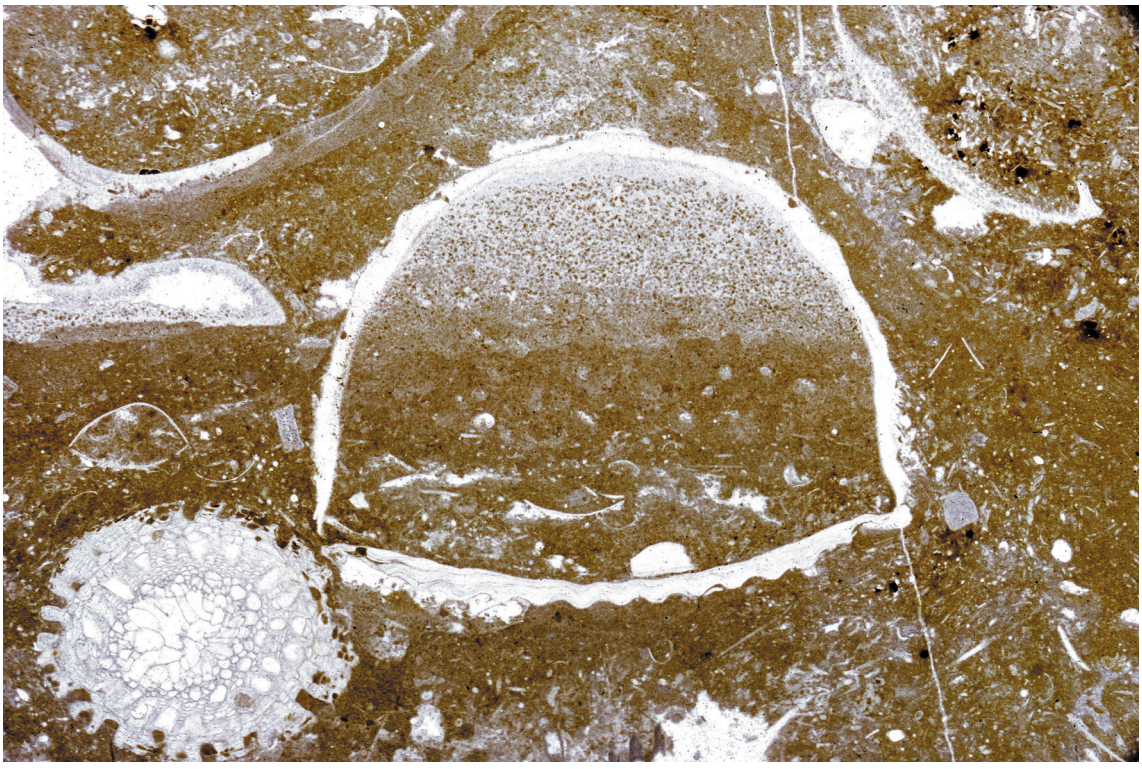

Figure 137. Thin section of a brachiopod at the same locality as Figure 136, showing the nature of the geopetal infilling. In this brachiopod the filling consists of lime mudstone and calcarenite with fossil fragments at the base, and sparry calcite with cavity peloids at the top. The contact between these two fillings is close to the original horizontal. GSWA sample no. 3488(C). Width of field of view 20 mm.

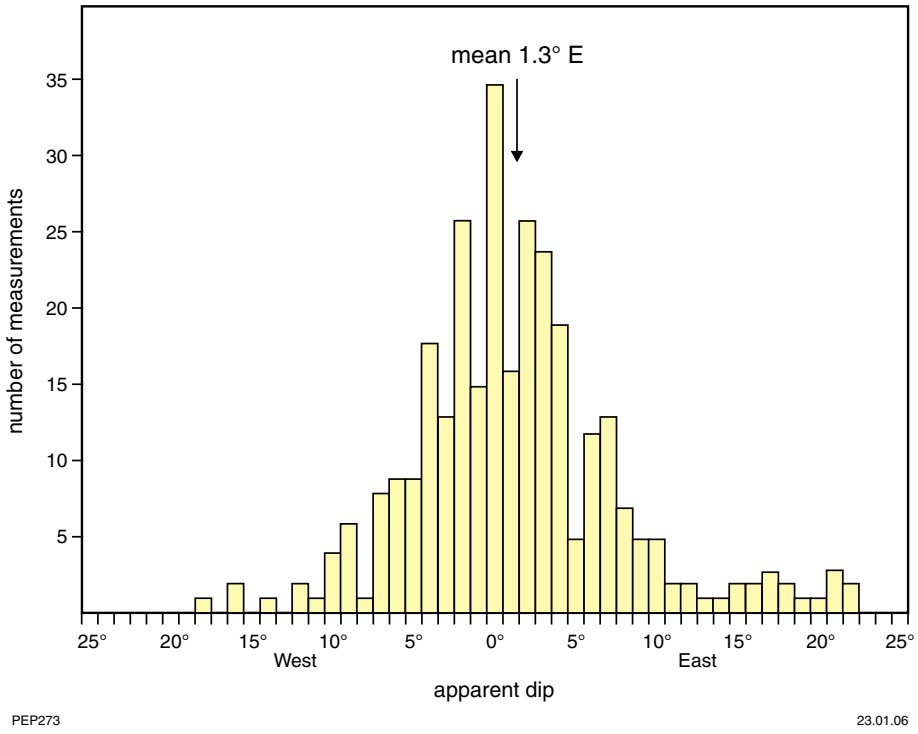

Figure 138. **Histogram illustrating geopetal measurements taken at the same locality as Figure 136, showing that strata at this locality have been tilted about 1.3° east since deposition.**



Figure 139. **'Double-geopetal' filling in a block of Frasnian reef limestone in fore-reef deposits of the Napier Formation in Geikie Gorge. The original horizontal (which formed when the block was part of the living reef) is shown by the steeply dipping laminae of lime mudstone on the left of the structure, while the fillings on the right show successive orientations of the block as it settled to its stable position on the fore-reef slope. The contact between the final filling of sparry calcite and the underlying lime mudstone is close to the present horizontal.**

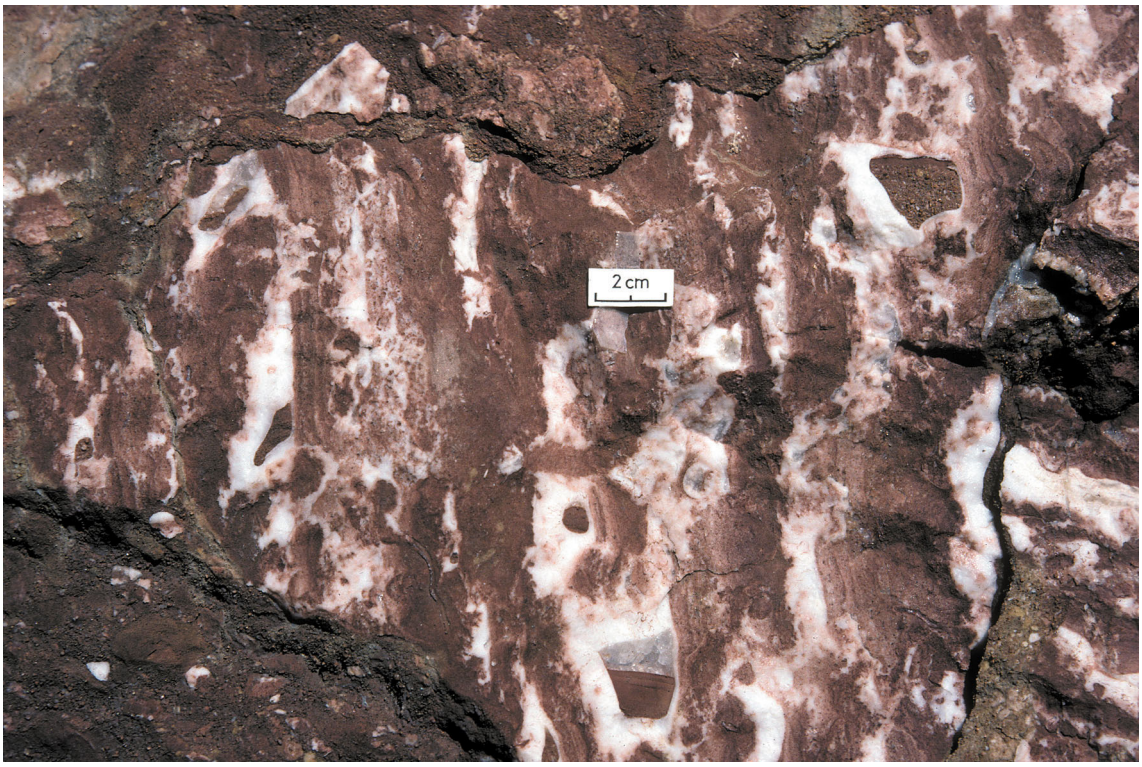

Figure 140. Block of Famennian reefal-slope stromatactis limestone in Famennian fore-reef deposits, showing 'double-geopetal' fillings. The original horizontal (when the block was in place on the reefal slope) is indicated by the vertical base of each stromatactis structure, and the final horizontal is shown by the stromatactis cavity filling in the centre lower part of the photograph.



Figure 141. Part of the west flank of McWhae Ridge showing marginal-slope deposits of the Sadler Limestone. The dip in the Sadler Limestone is largely depositional (it has been increased since deposition by about 7°). Geopetal features are exposed in the small karst corridor in the foreground.

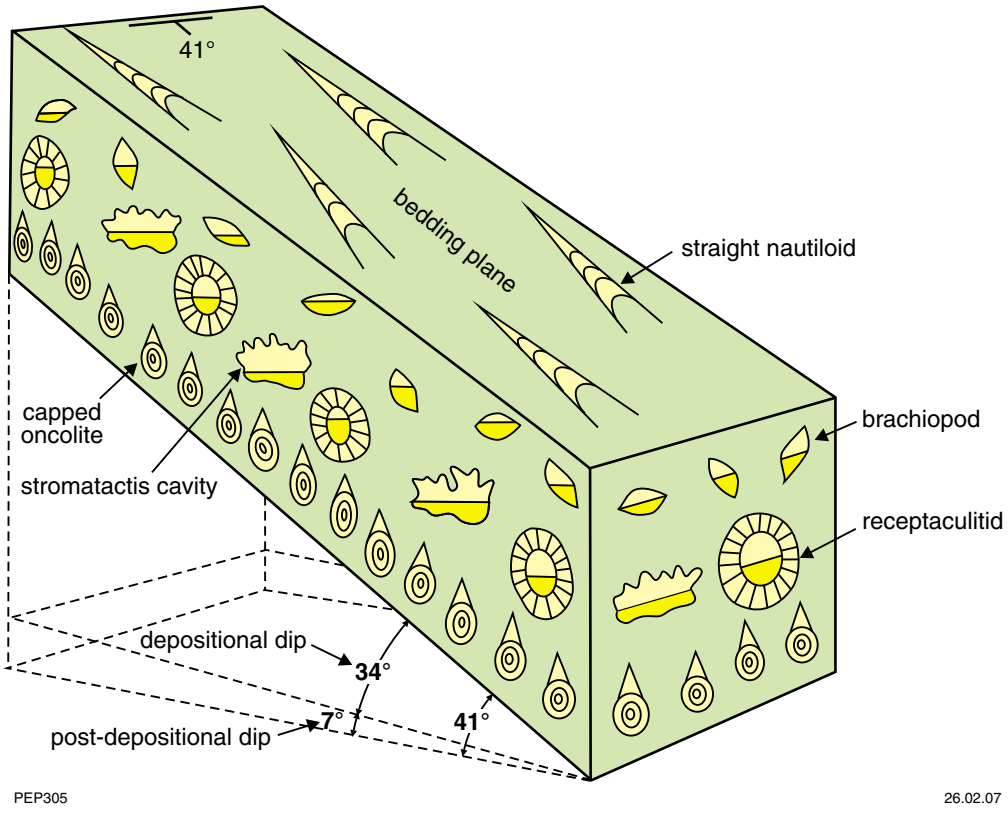

Figure 142. **Diagram illustrating geopetal structures and the amount of depositional and post-depositional dip in Sadler Limestone on the west flank of McWhae Ridge in the karst corridor shown in Figure 141.**



Figure 143. **Oncolites and capped oncolites in Sadler Limestone in the karst corridor on the west side of McWhae Ridge. The oncolites were built by *Girvanella*, and caps on the oncolites in the final layer were built by *Sphaerocodium*.**

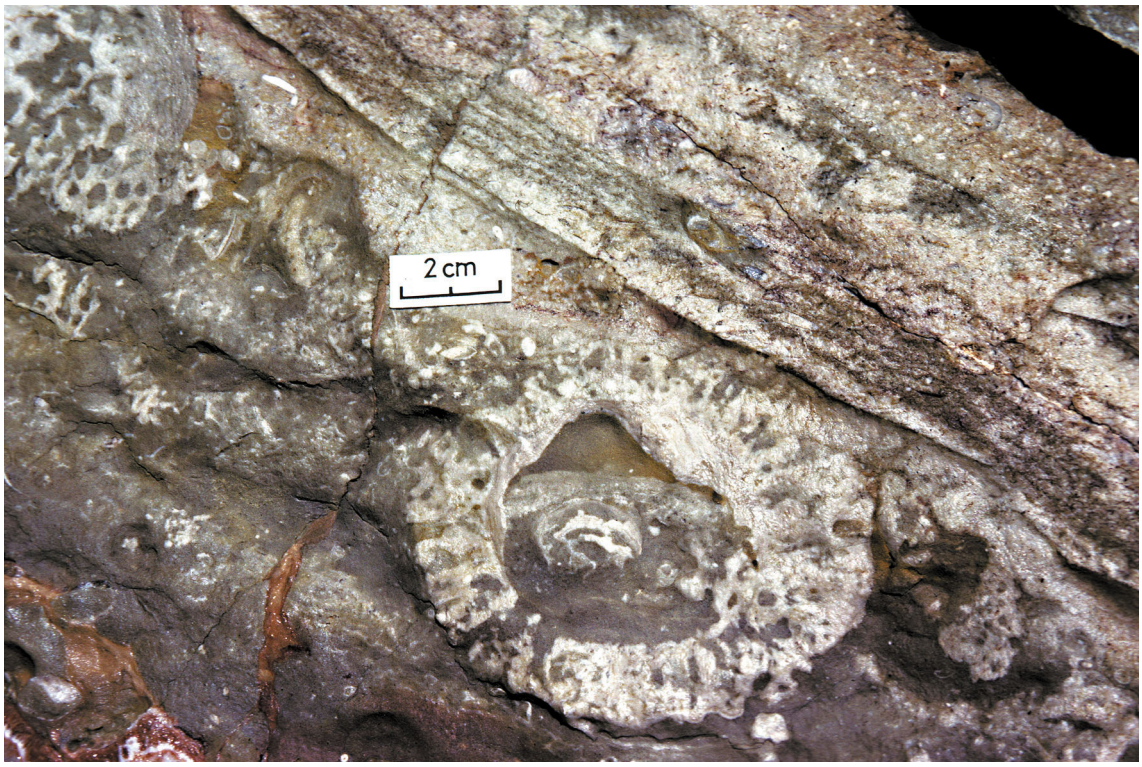

Figure 144. **Receptaculitid in marginal-slope Sadler Limestone in the karst corridor on the west flank of McWhae Ridge, showing a geopetal infilling that marks the approximate horizontal at the time of deposition, compared with the depositional dip of the marginal-slope limestones.**

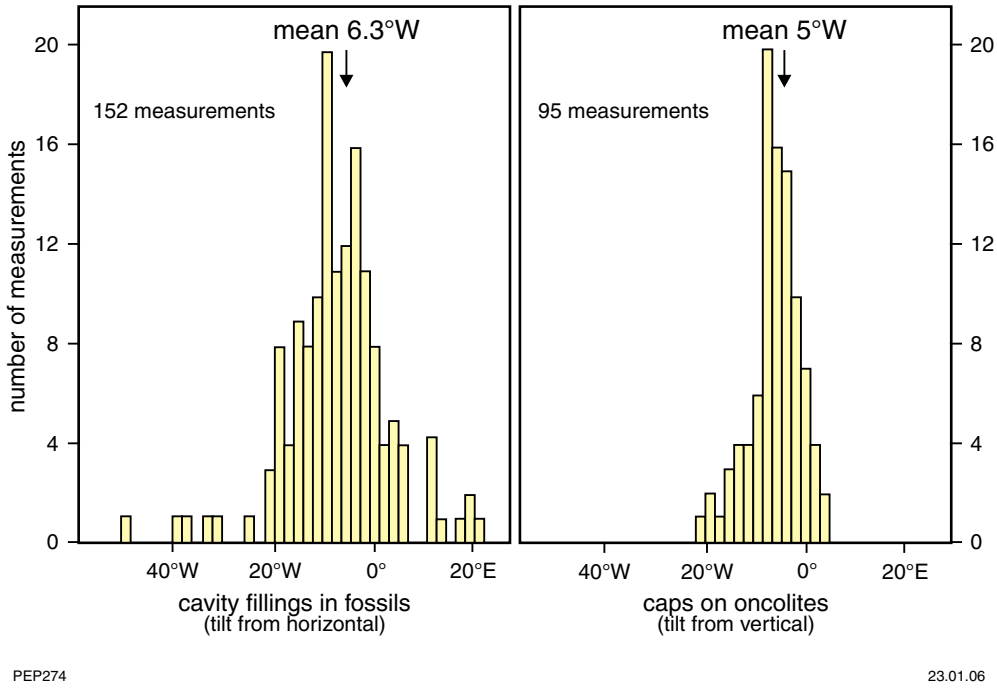

Figure 145. **Histograms showing geopetal measurements used in determining the post-depositional dip component in Sadler Limestone in the karst corridor on the west side of McWhae Ridge shown in Figure 141.**

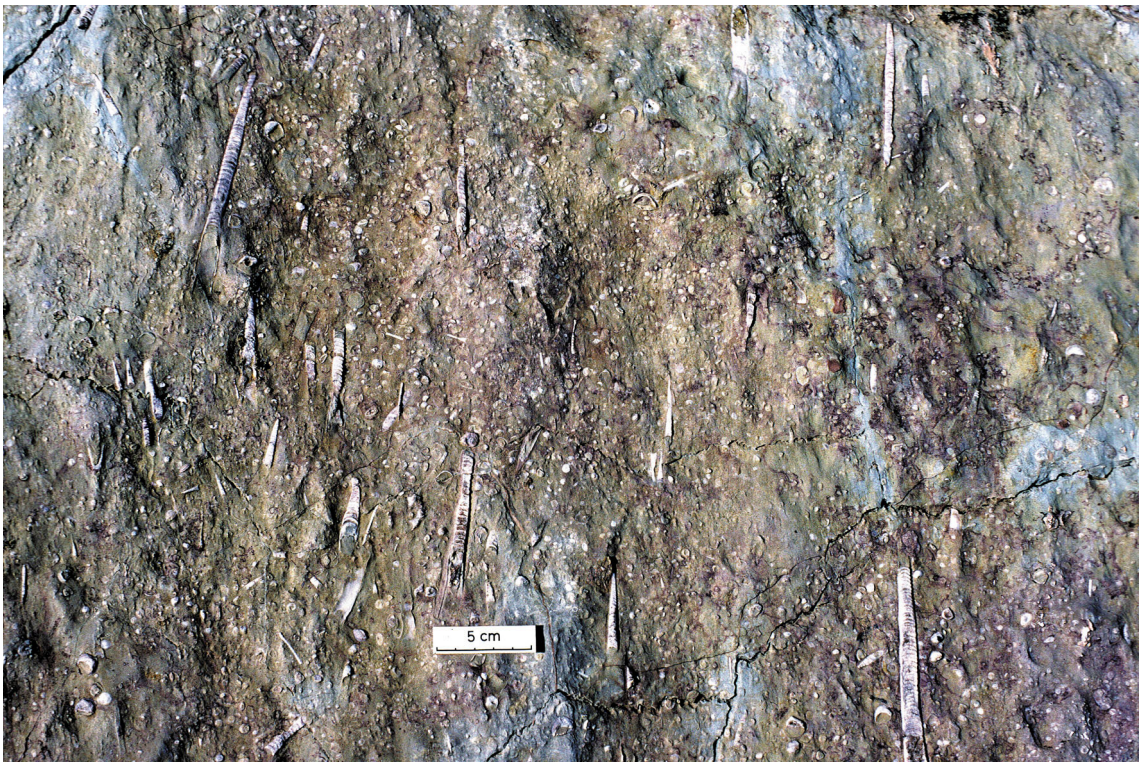

Figure 146. **Bedding plane in Sadler Limestone on the west side of McWhae Ridge, showing the orientations of straight nautiloids lying on the steeply sloping marginal-slope bed. Nearly all are lying parallel to the depositional dip, with their apices oriented up dip, towards the reef crest.**

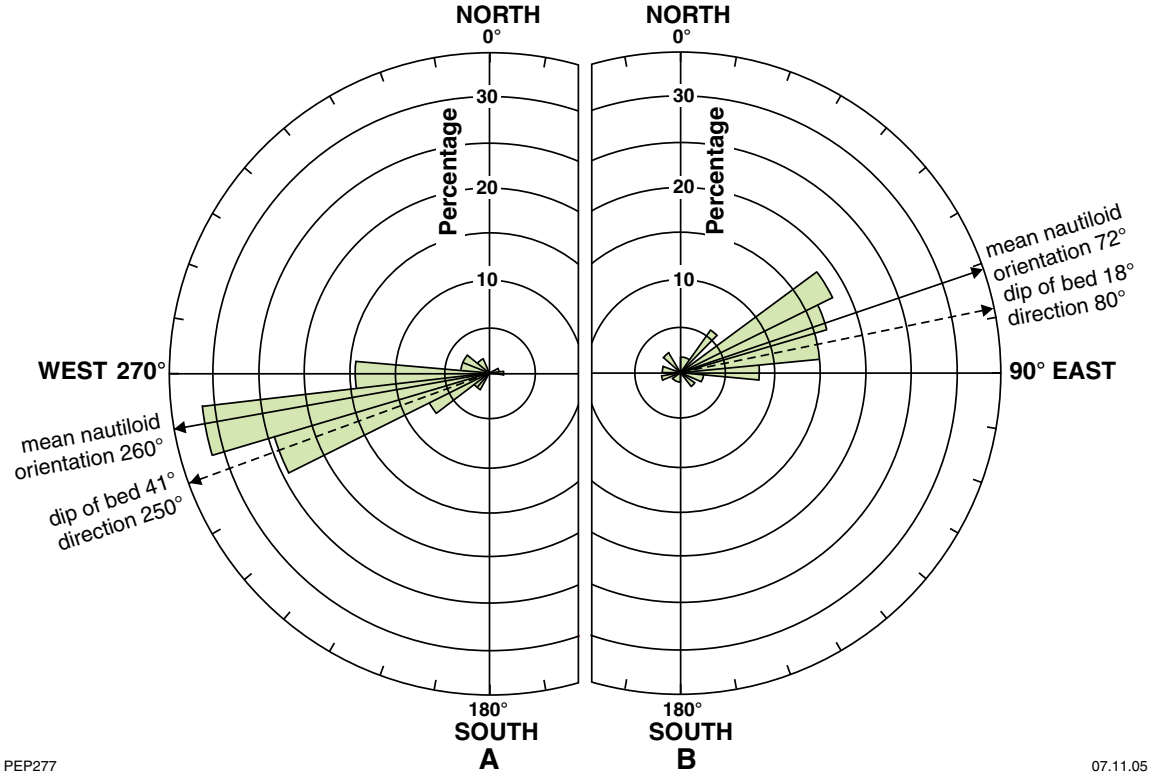

Figure 147. **Radial histograms illustrating orientations of the apertures of straight nautiloids lying on bedding planes: a) on the west side of McWhae Ridge (269 measurements); and b) on the east side of the ridge (153 measurements). In each case the mean orientation is close to the dip direction and the apices are directed up dip, towards the reef crest.**

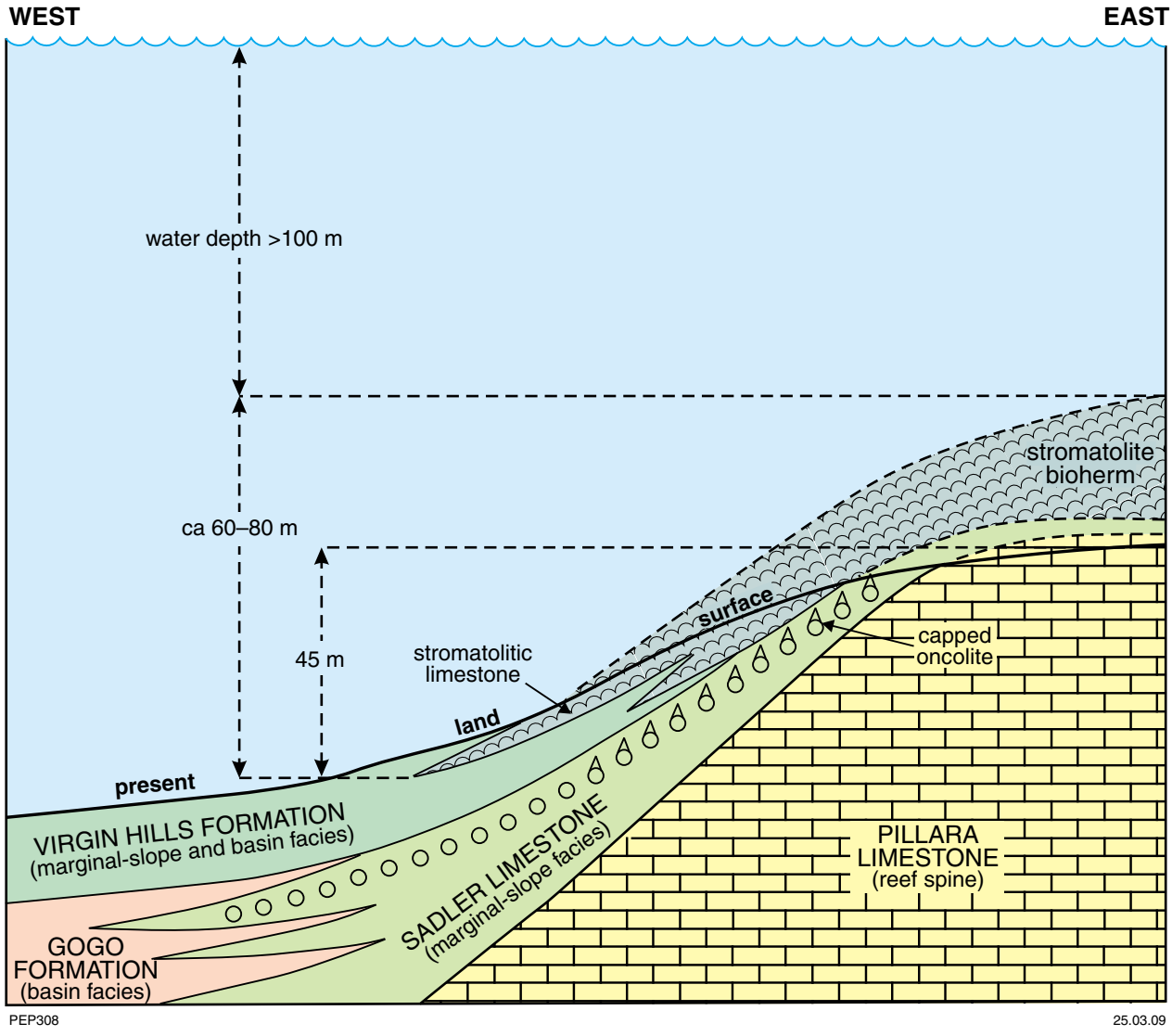

Figure 148. Diagrammatic cross section through the west side of McWhae Ridge, illustrating water-depth estimates. Measurements have been corrected for a post-depositional tilt of 7° west. Stromatolites at this locality probably grew in water more than 150 m deep.

Effects of faulting on development of the reef complexes

Faulting before and during growth of the reef complexes influenced platform development in many ways. From the beginning of reef growth it commonly controlled the original basement topography on which the platforms were developed. Contemporary faulting during growth of the complexes influenced platform-to-basin morphologies, and associated earthquake shaking resulted in fracturing of early-cemented limestones, the collapse of platform margins, and the development of neptunian fissures. Contemporary faulting was also a major control on the influx of terrigenous clastics that interfinger with the reef complexes.

Platform margins were occasionally coincident with active faults, a prominent example being the southwest margin of the Emanuel Range reef platform, on the upthrown side of the Cadjebut Fault (Fig. 115). Two small faults at McWhae Ridge at the southern end of the Lawford Range reef complex are linked with a branch of the Cadjebut Fault, and can also be shown to have moved during the Frasnian, as the measured displacements along these faults in the Sadler Limestone are about 30 m greater than in the Virgin Hills Formation (Playford 1981).

Neptunian dykes and sills

The term ‘neptunian dyke’ is applied to sedimentary and cement fillings of submarine fissures that cut the bedding of a host rock, whereas neptunian sills are similar fissure fillings that essentially follow bedding planes. Neptunian dykes, first recognized in the Canning Basin by Playford and Lowry (1966), were described further by Playford (1980, 1984a), Kerans (1985), Wallace (1987), Frost et al. (2006), and Frost (2007a,b). Much of the description of

neptunian dykes in this Bulletin is taken from the paper by Playford (1984a), adjusted in view of more recent interpretations.

Neptunian dykes formed in early-cemented limestones relatively soon after deposition. Because of their rigidity, those limestones were liable to break open as linear fissures in response to earthquake shaking associated with local tectonism. Slippage along marginal-slope bedding and compaction of basin muds were probably other important factors leading to fissuring of early-cemented limestones (Fig. 149). The open fissures were filled through combinations of sediments pouring in from above, organic growths, and sparry calcite cements that are the same as those filling primary cavities in the reef frameworks. The dykes are most common along platform margins, generally decreasing in frequency in reef-flat subfacies towards platform interiors and down marginal slopes in reefal-slope subfacies (Fig. 149). However, some also occur (abundantly in some areas) in early-cemented parts of the fore-reef and back-reef subfacies. *Renalcis*, other microbes, and stromatolites grew down the sides of some open neptunian fissures. The fissures also contain other early fillings, including fossil debris, oolite, lime sand, lime mud, terrigenous sand, radiaxial calcite, cavity peloids, breccia, and spar balls (Figs 150–153). The organic and early sedimentary infillings were commonly followed by early marine sparry calcite.

Most neptunian dykes are parallel to the platform margins in reef-margin, reef-flat, and reefal-slope subfacies, and are commonly clearly visible on air photos (Figs 154, 155). Some examples in reef-flat limestones terminate below in neptunian sills parallel to the bedding, but others simply wedge out. The dykes range from less than a millimetre to more than 100 m wide, and are as much as several hundred metres long.

In the fore-reef subfacies neptunian dykes are restricted to limestones that were penecontemporaneously well cemented. Some were repeatedly fractured (probably as a result of down-slope sliding), resulting in several generations of closely spaced neptunian dykes cutting one another. Some dykes in this subfacies are approximately perpendicular to bedding, but most are oblique and some pass into neptunian sills along steep bedding planes. Neptunian dykes in fore-reef deposits range from a few millimetres to about two metres wide, and are filled with contemporary sediment and/or banded fibrous spar (Figs 156, 157).

Neptunian dykes are especially well developed in the northwestern and southeastern parts of the Oscar Range, where they occur in reef limestone of the Windjana Limestone, early-cemented back-reef limestone of the Famennian Nullara Limestone, and reef and back-reef limestone of the Frasnian Pillara Limestone (Hurley, 1986; Figs 154, 155, 158, 159). Individual dykes in this area are as much as 6 km long, 20 m wide, and probably more than 80 m deep (Playford et al., 1984a). However, most are less than 100 m long and a metre wide. They generally pinch out at depth, but some pass into neptunian sills in the underlying marginal-slope deposits. Most fissures formed essentially parallel to the original reef front, while others are approximately at right angles to that direction. In some areas the fractures at right angles to the reef front largely remained closed, so that they did not form wide neptunian dykes. The two fracture systems often led to the collapse of sections of the platform margins and the development of debris flows down the marginal slopes. A conspicuous

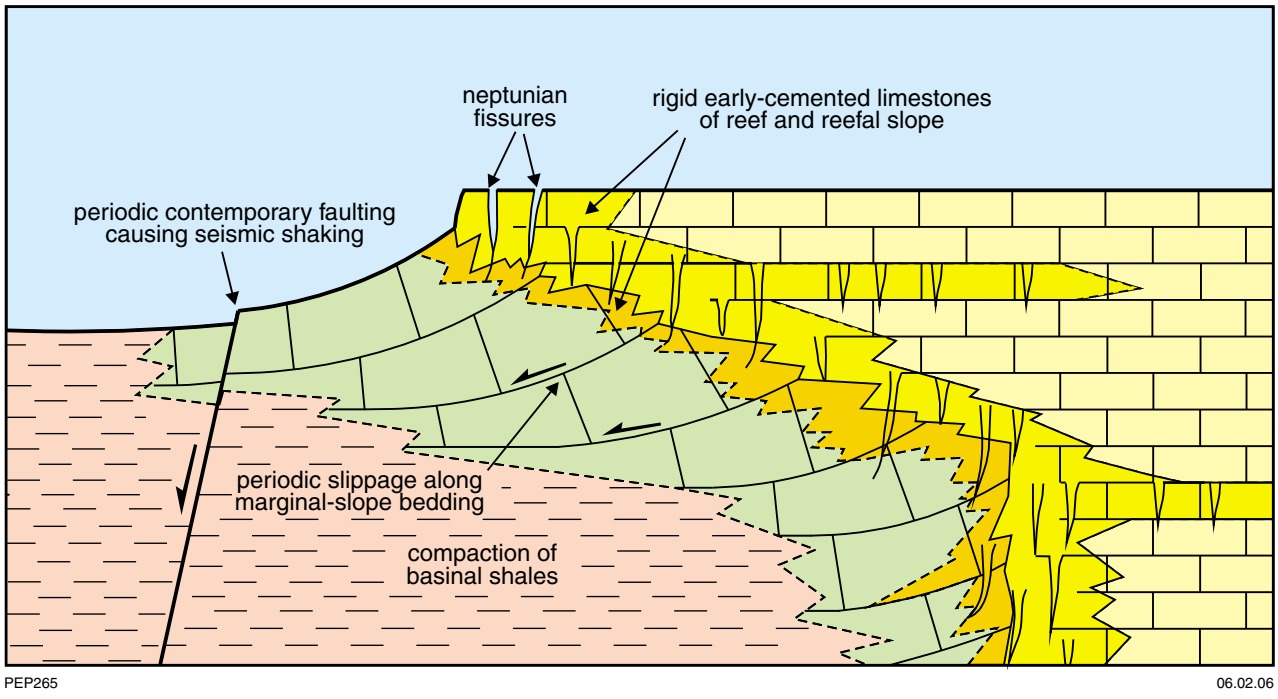

Figure 149. Diagrammatic cross section illustrating factors responsible for fracturing and submarine landsliding in early cemented limestones of the reef complexes.



Figure 150. Network of small neptunian dykes 2 km north of Brooking Springs Homestead. The fissures are approximately at right angles to one another and are lined with *Renalcis*.

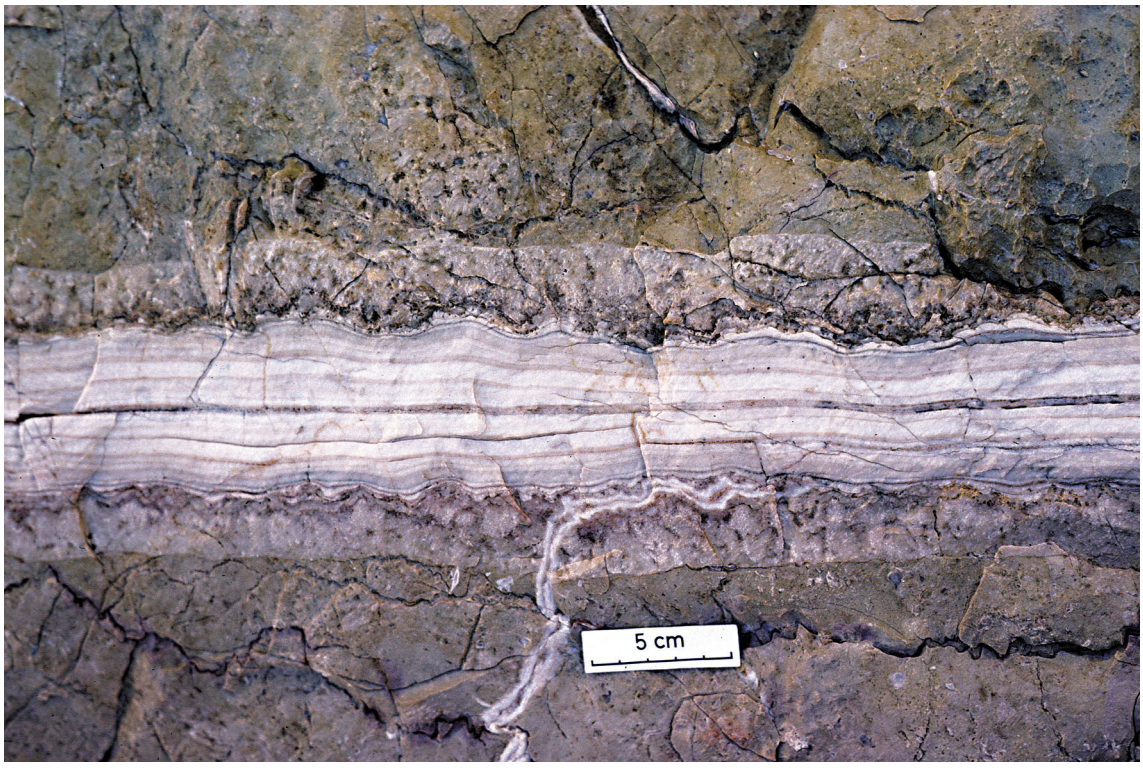

Figure 151. Neptunian dyke 2 km north of Brooking Springs Homestead. The dyke was lined with *Renalcis*, and the rest of the cavity was filled soon afterwards with radiaxial sparry calcite.

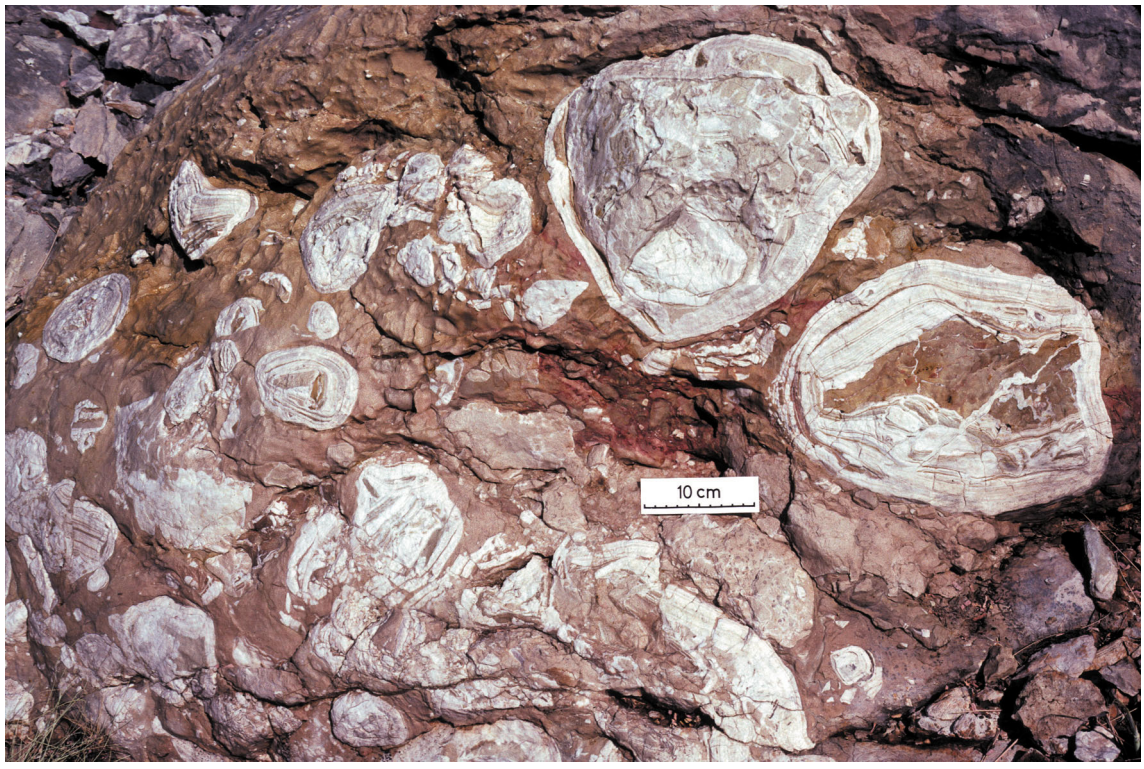

Figure 152. Spar balls of radiaxial calcite in a wide neptunian dyke beside the Cadjebut Fault on the southeast side of the Emanuel Range. The spar balls are thought to indicate strong water flows in the submarine fissure, probably induced by wave surge.

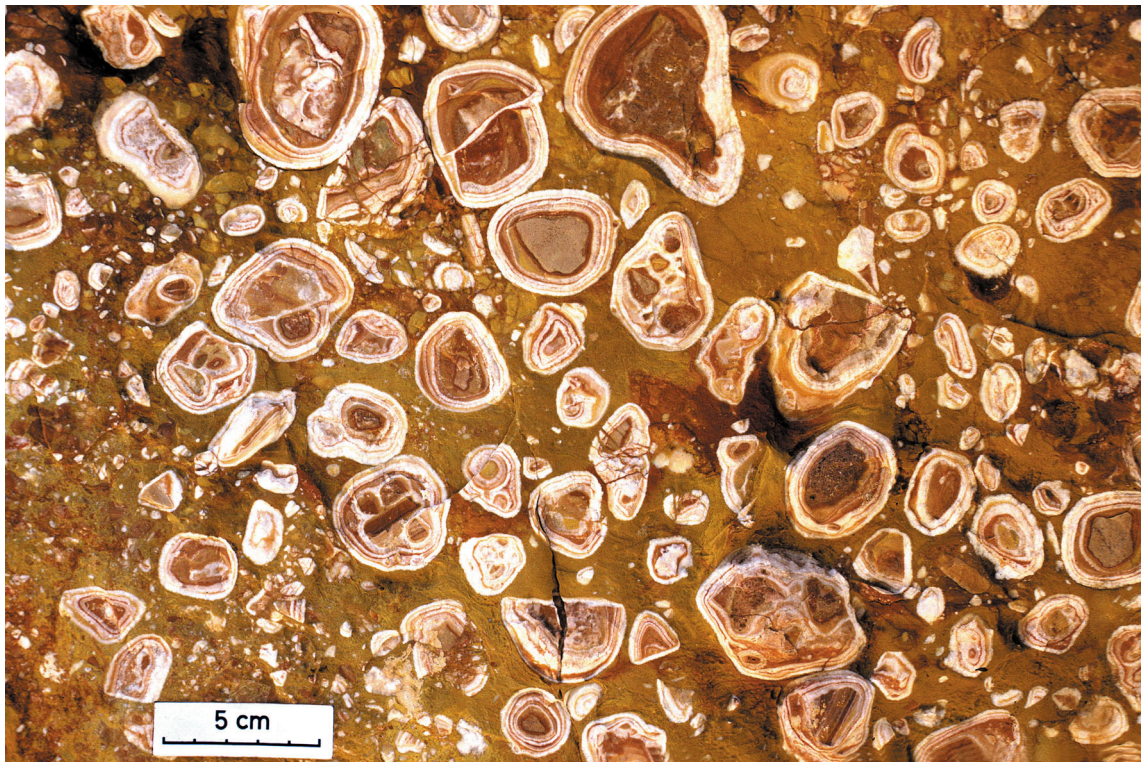

Figure 153. Spectacular spar balls in a neptunian dyke in reef subfacies near Rowalamban Cave, Napier Range. The core of each ball is a fragment of an earlier limestone infilling of the neptunian dyke, which became coated by laminae of sparry calcite.

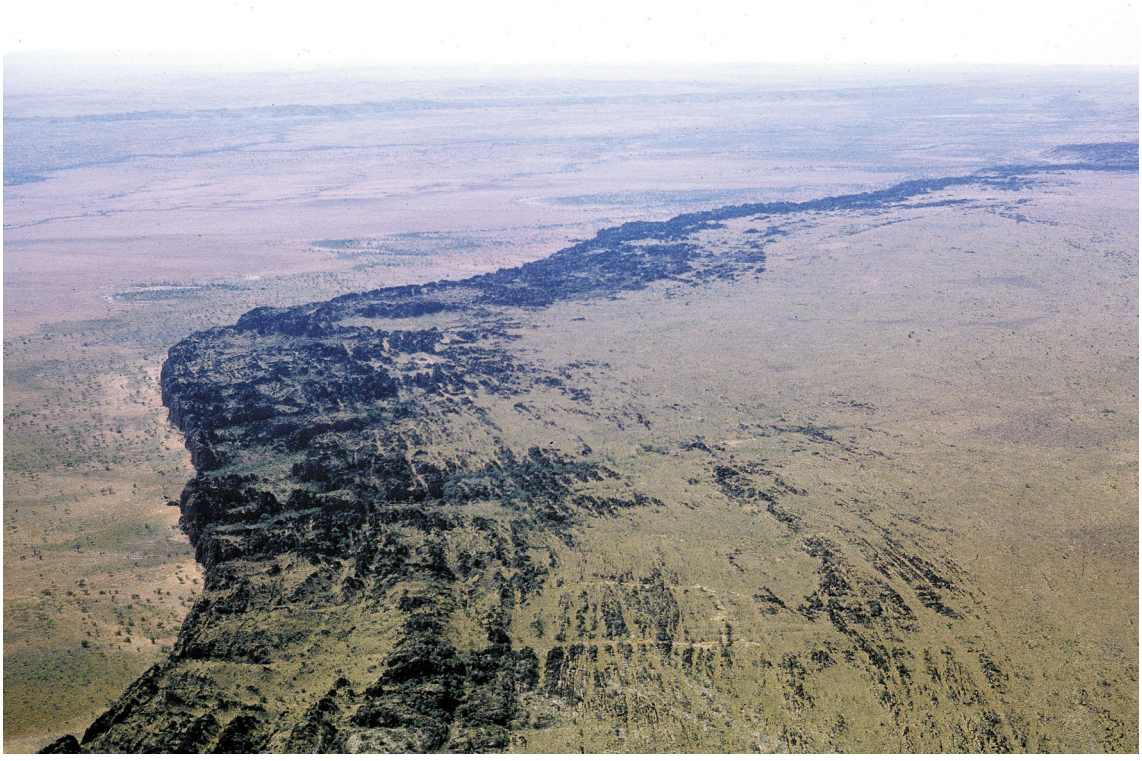

Figure 154. Aerial view, looking east, over the northeast side of the Oscar Range. Morown Cliff, at the front of the range, is essentially the exhumed late Famennian reef scarp. Note linear corridors following neptunian dykes parallel to the reef front, with a subsidiary fracture system at right angles to those dykes.

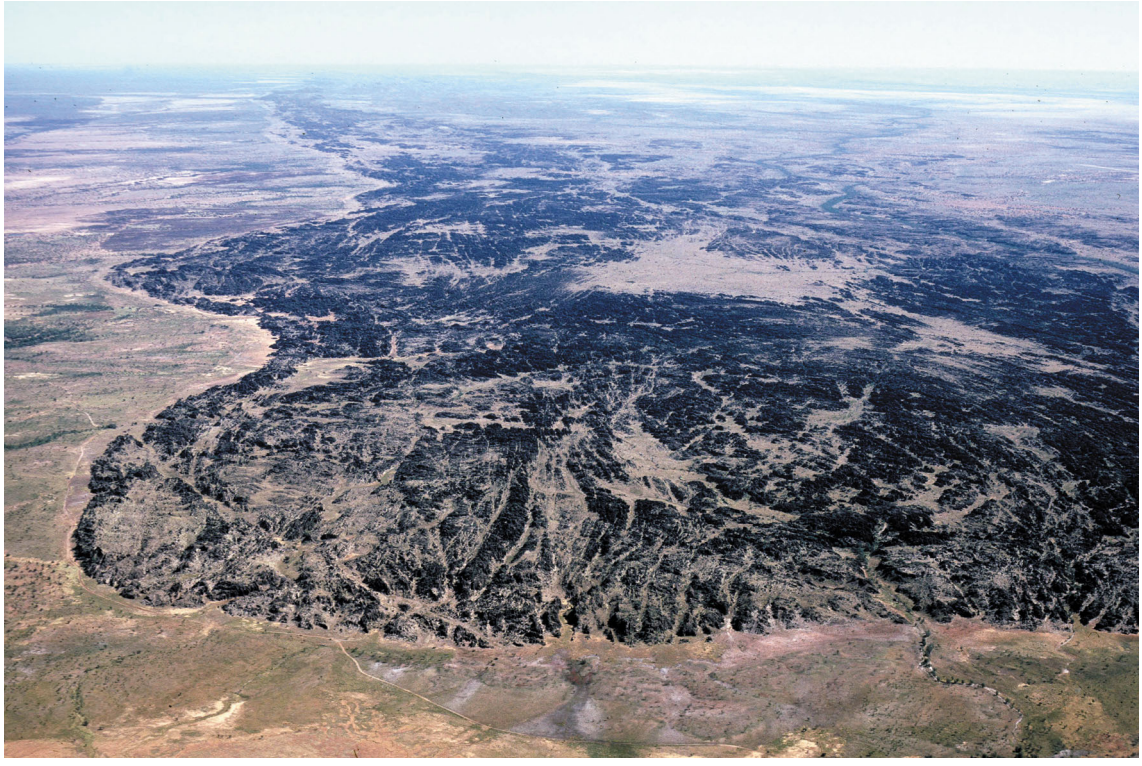

Figure 155. Aerial view of the southern end of the Oscar Range, looking northwest, showing the change in direction of the reef complex, from northwest on the left to northeast in the foreground. Major neptunian dykes are at right angles to the northeast-trending part of the reef and parallel to the northwest-trending part. This major neptunian fissuring probably resulted from differential compaction over the buried ridge of Proterozoic rocks that localized the reef complex.

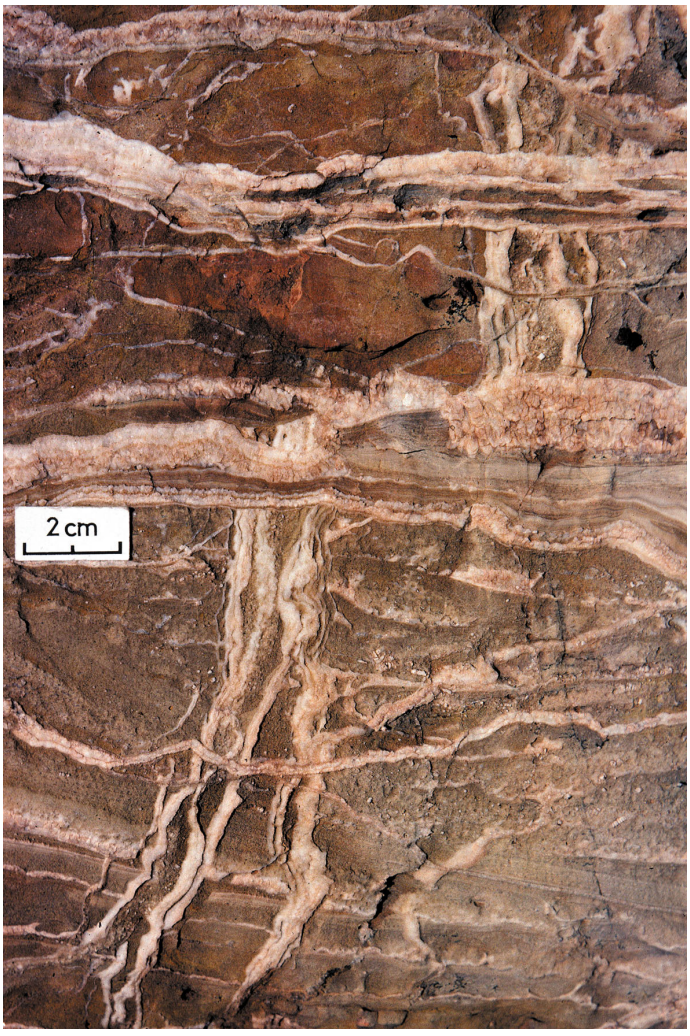

Figure 156. **Neptunian sills and dykes in distal marginal-slope facies of the Famennian Virgin Hills Formation at Ngumban Cliff.**

Figure 157. **(below) Neptunian sill of sparry calcite with small layers of internal sediment, in the Virgin Hills Formation on the west flank of McWhae Ridge, at the contact between the *Frutexites* bed above and distal fore-reef silty limestone below. Note a much thinner and buckled neptunian sill below the main sill. The buckling is probably a result of down-slope sliding.**





Figure 158. A major neptunian dyke at the southern end of the Oscar Range, showing its infilling of banded radiaxial calcite.

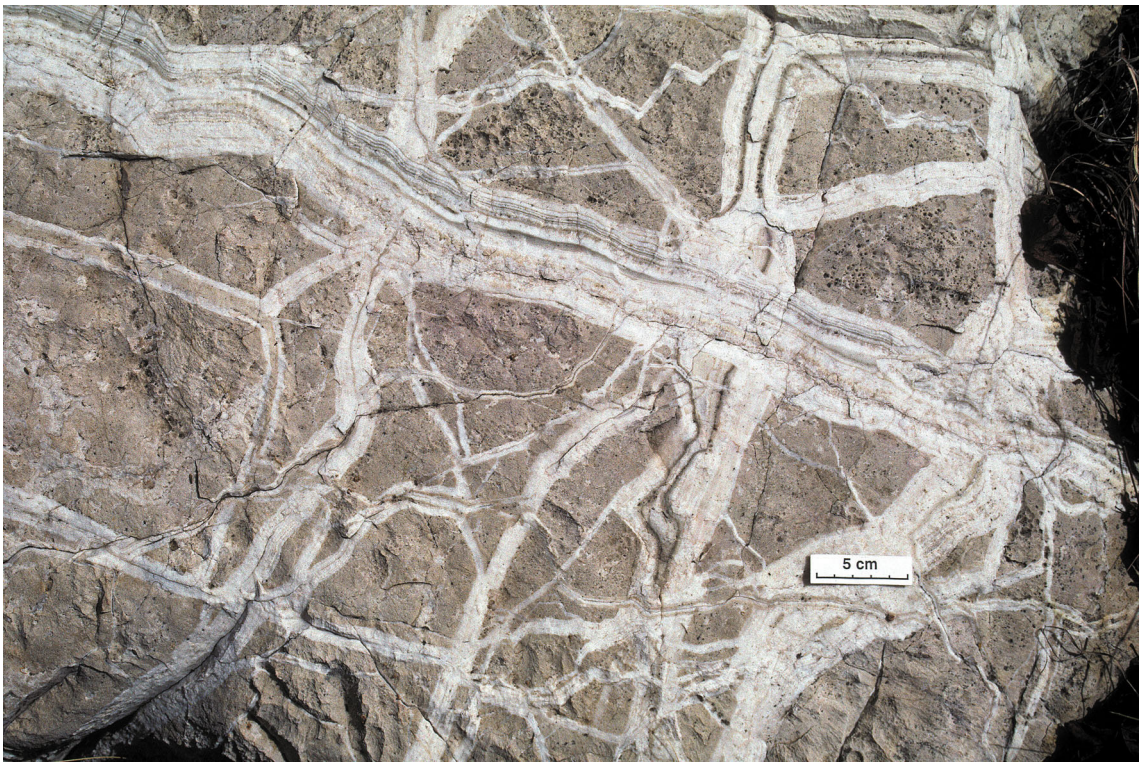

Figure 159. Neptunian-dyke network in reef of the Pillara Limestone near the southern end of the Oscar Range.



Figure 160. Aerial view, looking southeast, along the Napier Range, with part of Dingo Gap on the right. The orthogonal collapsed margin of the Frasnian platform (Pillara Limestone) can be seen in the centre. The reef-collapse scarp followed orthogonal neptunian fissuring, parallel and at right angles to the original platform margin.

example of orthogonal fracturing of a platform margin is present near Dingo Gap (Ward, 1996; Fig. 160).

Neptunian sills are most frequently developed in marginal-slope deposits, and are thought to have resulted from down-slope sliding of cemented parts of the fore-reef and reefal-slope deposits along thin interbedded layers of uncemented mud or sand. Fissures essentially parallel to bedding result where there is a flattening in the depositional dip. The fissures filled, soon after they were formed, with sediment and spar, to form neptunian sills. The thickness of individual sills is as much as 2 m, but most are less than 2 cm. Some subhorizontal sills also developed through fissuring of reef-margin and reef-flat limestones. Anastomosing sets of neptunian dykes and sills in marginal-slope deposits can similarly represent repeated episodes of fracturing associated with down-slope sliding.

Some neptunian dykes and sills are associated with extensional faults. A conspicuous example is the major neptunian dyke system along the Cadjebut Fault at the south end of the Emanuel Range (see Fig. 115 and Plates 4, 5). This fault was active during reef growth, and defined part of the western reef margin of the Emanuel Range platform. Neptunian dykes are also localized by upright reef margins in some areas, notably in central Geikie Gorge.

Dykes and sills commonly show a complex history of fissure development, filling, early cementation, and re-fracturing. A typical sequence of dyke development in reef limestone is illustrated diagrammatically in Figure 161. Such repeated episodes of fissuring were responsible for the very wide dykes found in some areas. A notable example is 5.5 km north of Brooking Springs Homestead (AMG Zone 51, 780800E 8000000N; Figs 162, 163; Wallace, 1987; Playford, 2002b). This remarkable neptunian-dyke system is more than 100 m wide and 1 km long, and has formed as a result of repeated opening and infilling of successive fissures, each as much as about 50 cm wide. The infillings consist largely of laminated white fibrous spar, thought to have been mediated by microbial activity.

The maximum measured horizontal extension resulting from neptunian fissuring is near the northwestern end of the Oscar Range, where it amounted to 6.6% over a distance of some 500 m in the Nullara and Windjana Limestones (Hurley, 1986).

Cavity peloids are distinctive silt-size spheres, red or yellow in colour, that fill neptunian dykes and other cavities, such as stromatactis cavities. They are often interlaminated with, and cemented by, radiaxial spar (Fig. 164). These distinctive peloids are known only from reef and reefal-slope cavities and neptunian dykes, and are thought to be of microbial origin. They commonly occur in association with tiny troglobitic fossils, thought to be ostracods.

Spar balls are unusual features of some neptunian dykes (Figs 152, 153). The subspherical balls, as much as about 25 cm in diameter, are composed of radiaxial spar and have

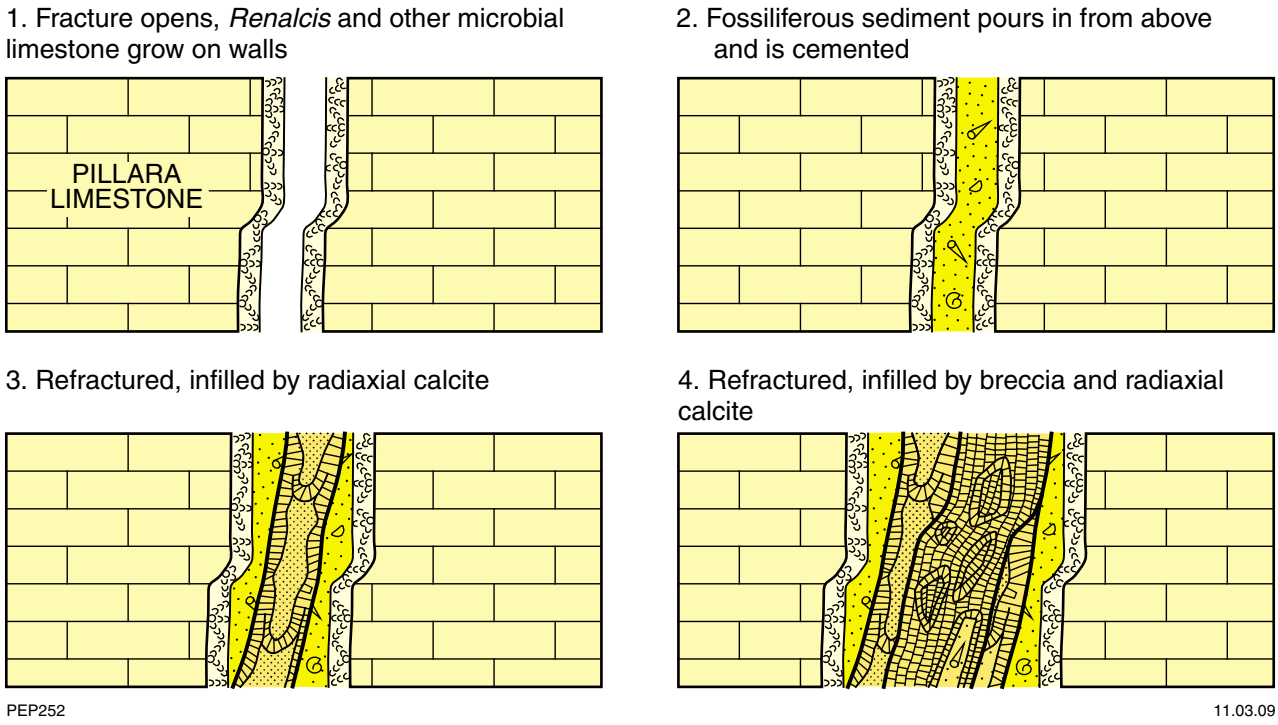

Figure 161. Diagram illustrating development of a typical neptunian dyke, by repeated opening, fracturing, and cementation.

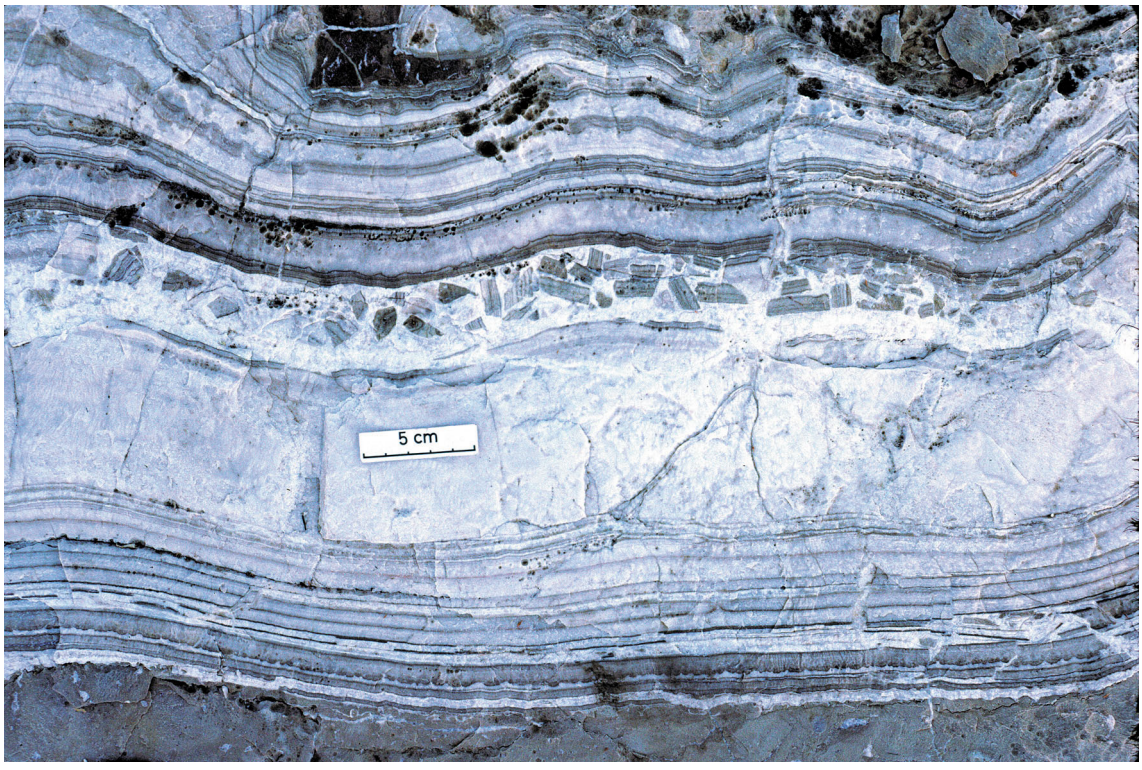

Figure 162. Part of a very wide neptunian dyke 4 km north-northeast of Brooking Springs Homestead, showing layers of sparry calcite and breccia.



Figure 163. Part of the very wide neptunian dyke 4 km north-northeast of Brooking Springs Homestead, showing breccia of calcite fragments that were broken up after being precipitated earlier in the fissure.

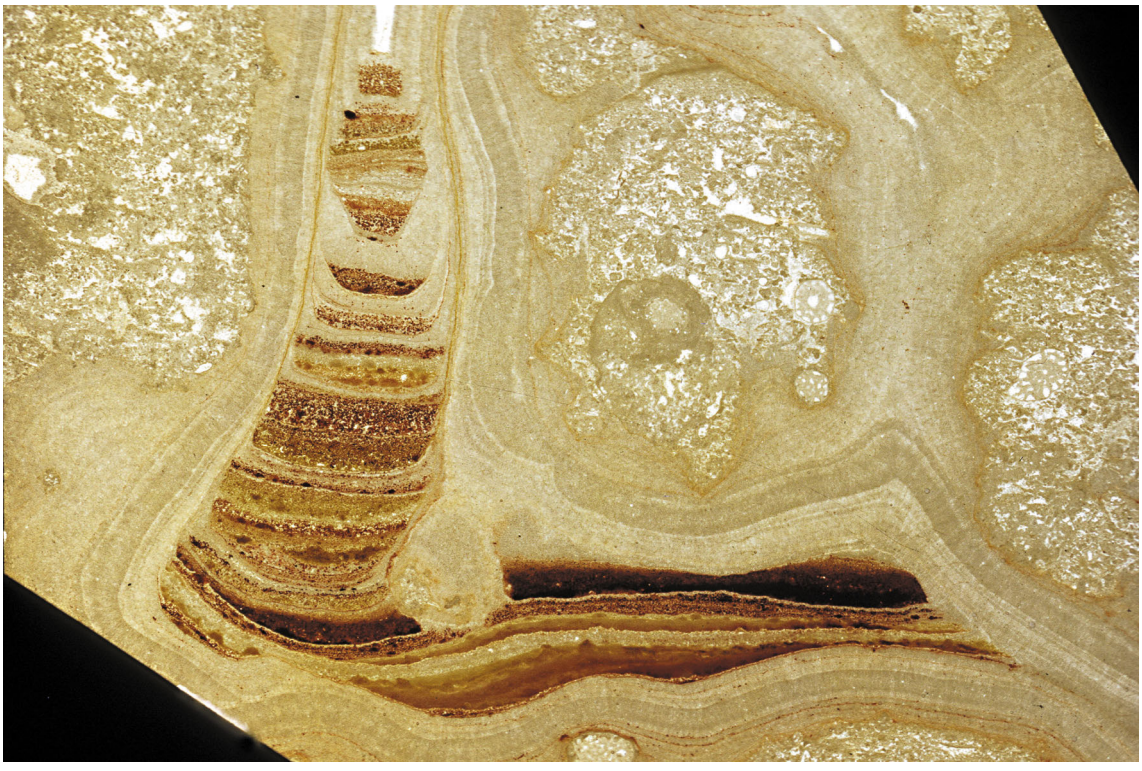

Figure 164. Thin section of microbial stromatoporoid reef limestone (Pillara Limestone) showing a large cavity filled with interlaminated fibrous sparry calcite and red cavity peloids, from an allochthonous block at McIntyre Knolls. GSWA sample no. 3497(F). Width of field of view 60 mm.

usually nucleated around fragments of earlier dyke-filling material. Very strong water movement must have been needed to rotate such balls during cement precipitation; perhaps wave surge was responsible. Access to the fissures for wave surge may have been facilitated by the collapse of sections of the platform margin (Figs 120, 149).

Neptunian fissures played important roles in the early post-burial diagenesis of the reef complexes, as they allowed ready access of seawater to carbonates as much as 100 m below the sea floor. Dolomitizing fluids could also move through the fissure systems. In addition, the neptunian dykes and sills formed planes of weakness along which later fracturing could occur, potentially allowing ingress of petroleum and fluids carrying base metals. Neptunian dykes also localized some subglacial karst features during the Early Permian.

Biostratigraphy

The prolific fossil biotas of the Devonian reef complexes have been the subject of publications by many paleontologists. The principal studies are summarized by Talent et al. (2000), and in a reference list by Skwarko (1988) that gives a compilation of all Devonian paleontological references relating to Western Australia up to 1988. A summary of knowledge on the conodonts, ammonoids, and palynomorphs is given in Appendices 1–3, by G Klapper (conodonts), R T Becker and M R House (ammonoids), and G Playford (palynomorphs). Other discussions of the various groups will essentially be confined to their distribution in time, facies, and water depths.

The distribution of the main biotic constituents in the various facies of the Pillara and Nullara Sequences is illustrated in Figures 165 and 166. These diagrams illustrate the living distributions of the organisms. However, many platform-dwelling organisms rolled or slid down the marginal slopes after they died, so that shallow-water benthic remains commonly occur in deep-water marginal-slope deposits.

Indigenous fossil biotas in the Givetian and Frasnian Pillara Sequence are generally dominated in platform facies by colonial stromatoporoids, corals, and microbes; in marginal-slope facies by benthic brachiopods, crinoids, receptaculitids, sponges, and microbes; and in basin facies by pelagic and nektonic organisms (especially conodonts, ammonoids, nautiloids, fish, crustaceans, radiolarians, and tentaculitids). The biotic distribution of most organisms in the Famennian Nullara Sequence is similar to that in the Givetian–Frasnian Pillara Sequence, but because of the Frasnian–Famennian mass extinction of shallow-water organisms, the Famennian platform faunas are much less diverse, the major platform-building role in them having been taken over almost entirely by microbes, with only minor contributions by bryozoans, stromatoporoids, and other metazoans.

Figure 167 shows depth relationships of the various organisms, as deduced from paleobathymetric observations made throughout the outcrop belt, and Figure 168 shows the ranges of some colonial organisms in the Middle and Upper Devonian and the Lower Carboniferous. In the Frasnian and Givetian reef complexes, the platform-building stromatoporoids and corals were restricted mainly to water depths of less than about 10 m. Tabular and laminar stromatoporoids extended a little deeper than bulbous and massive forms. The microbes *Renalcis* and *Sphaerocodium* are typical of the reef margin, reef-flat, reefal-slope and upper fore-reef subfacies in both Frasnian and Famennian reef complexes. They are especially important in the Famennian, but are less significant in the Givetian and earliest Frasnian. Microbes had much greater depth ranges than the other reef builders. *Renalcis* is deduced to have reached depths of at least 80 m, and *Sphaerocodium* extended even deeper, perhaps to as much as 150 m. Fenestral stromatolites, oncolites, and flat microbial mats were restricted to shallow water (less than about 10 m, with peak abundance less than 5 m), but non-fenestral stromatolites extended to considerable depths, to 150 m or more (Playford et al., 1976).

Stromatoporoids

Stromatoporoids in the Devonian reef complexes have been described by Cockbain (1984). They were important platform-building organisms in the middle Givetian to late Frasnian, and virtually disappeared at the Frasnian–Famennian boundary, along with most shallow-water metazoans (Fig. 168). They may have been in decline prior to the Frasnian–Famennian mass extinction, although they were still very prominent as reef builders in the latest Frasnian (Fig. 27).

Stromatoporoids are rare in most Famennian platforms (Cockbain, 1984). However, they experienced a mild resurgence during the late Famennian, as shown by the relative abundance of some stromatoporoids (*Clathrocoilona saginata* and *Stromatopora lennardensis*) in some late Famennian reef limestone (Windjana Limestone), for example near the west end of Windjana Gorge and in allochthonous reef blocks in fore-reef deposits in the upper Napier Formation in the Napier Range.

There are several possible reasons for the virtual disappearance of stromatoporoids at the Frasnian–Famennian boundary followed by their mild resurgence in the middle to late Famennian. These range from the brief development of a polar ice cap to the effects of one or more bolide impacts (Copper, 1986; McGhee, 1996; Sandberg et al., 2002; Joachimski et al., 2003).

Diagenesis

Early marine diagenesis

The importance of marine cementation in the early diagenesis of parts of the Devonian reef complexes has been documented in papers by Playford (1980, 1984a), Kerans et al. (1986), and Wallace et al. (1991), among others. Their studies have shown that the strongest marine cementation occurred in reef-margin, reef-flat, and reefal-slope deposits. Back-reef, bank, fore-reef, and basin deposits were less subject to early cementation (Fig. 169). The overall intensity of early marine cementation in these

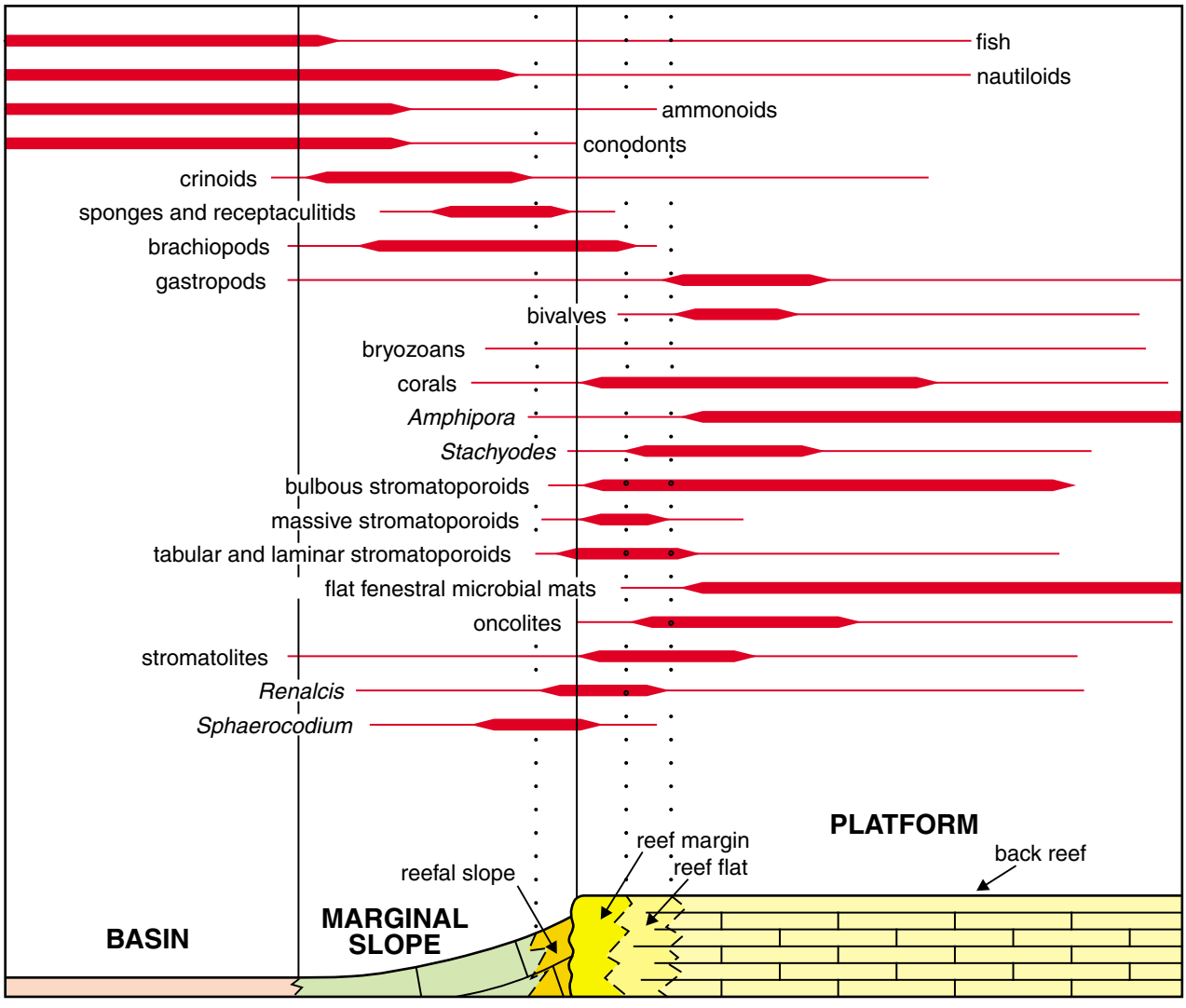

Figure 165. Diagram illustrating the biotic distribution of the principal organisms in the Frasnian reef complexes.

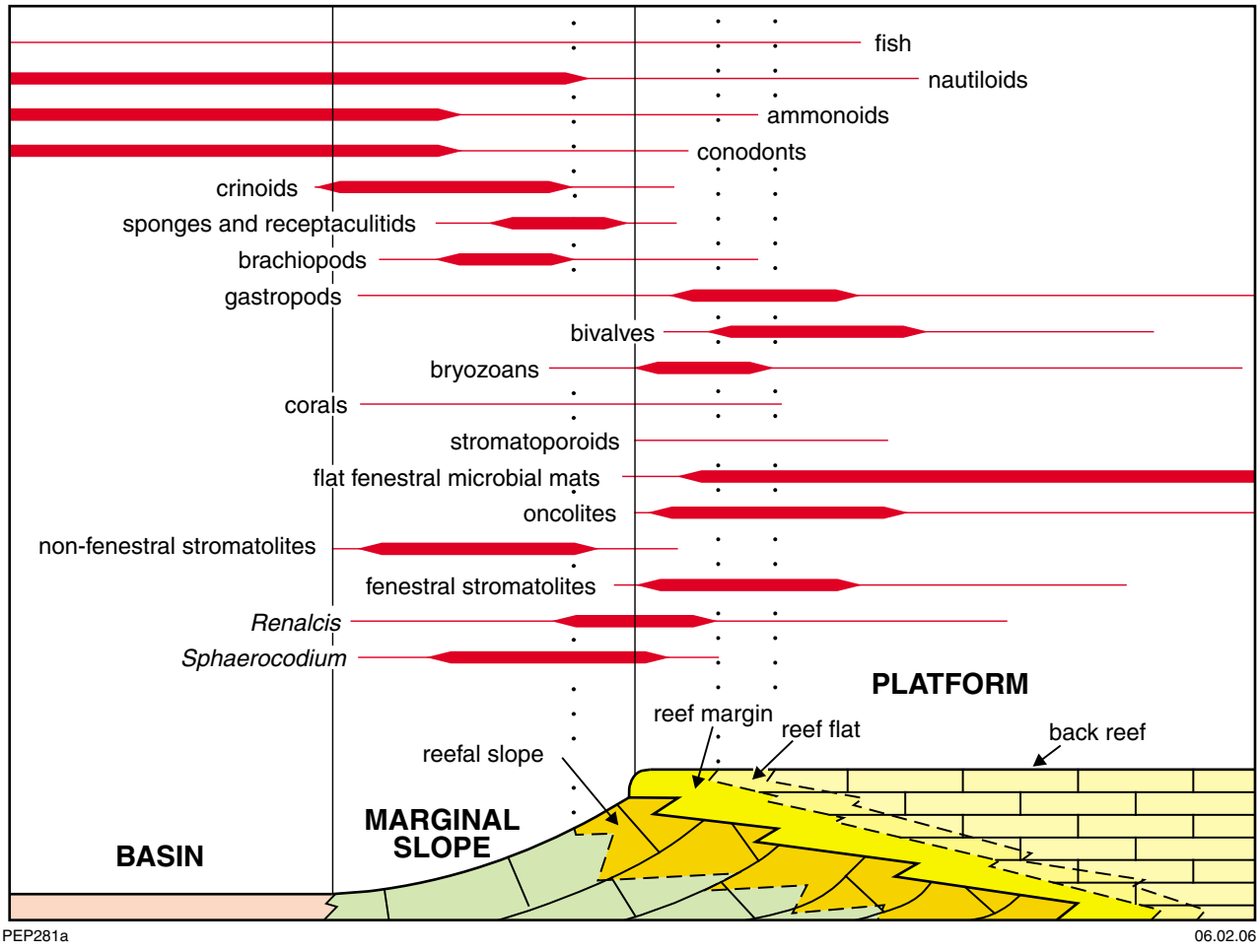

Figure 166. Diagram illustrating the biotic distribution of the principal organisms in the Famennian reef complexes.

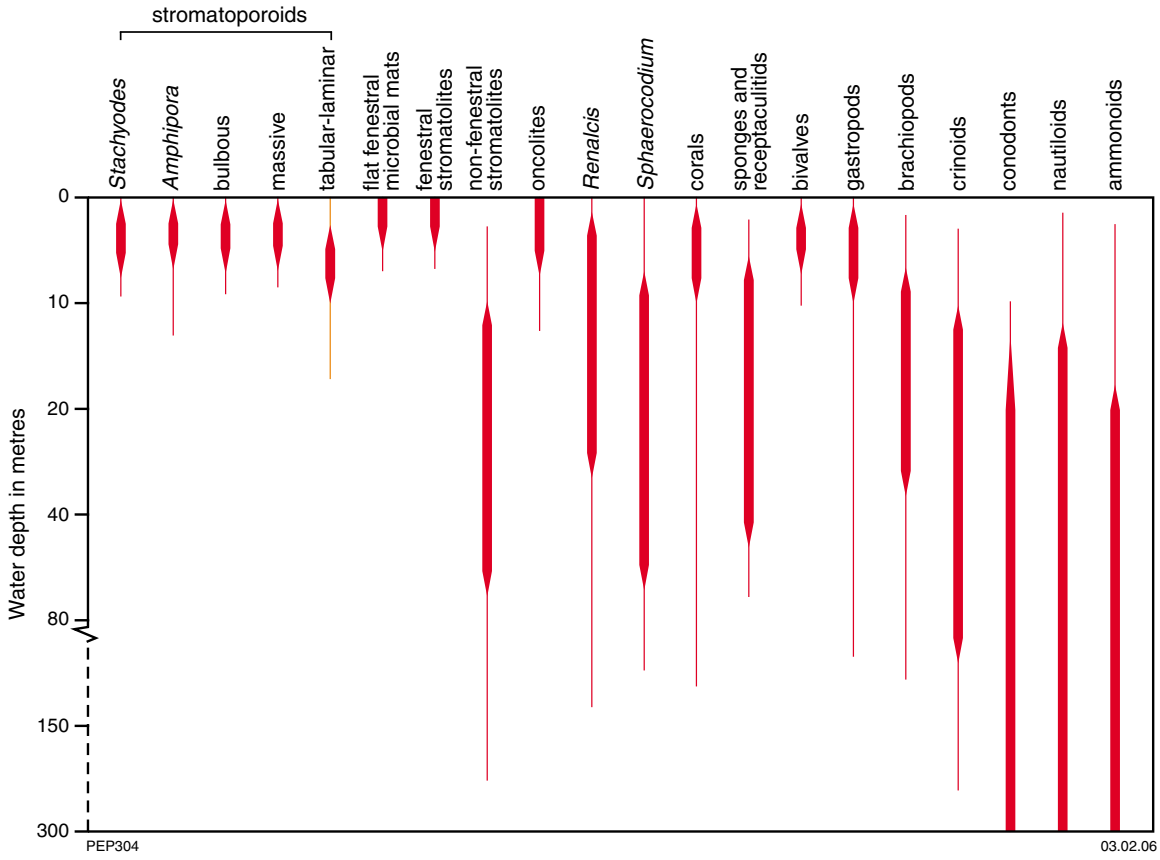

Figure 167. **Diagram illustrating the water-depth distributions of various organisms that lived in or beside the Frasnian reef complexes.**

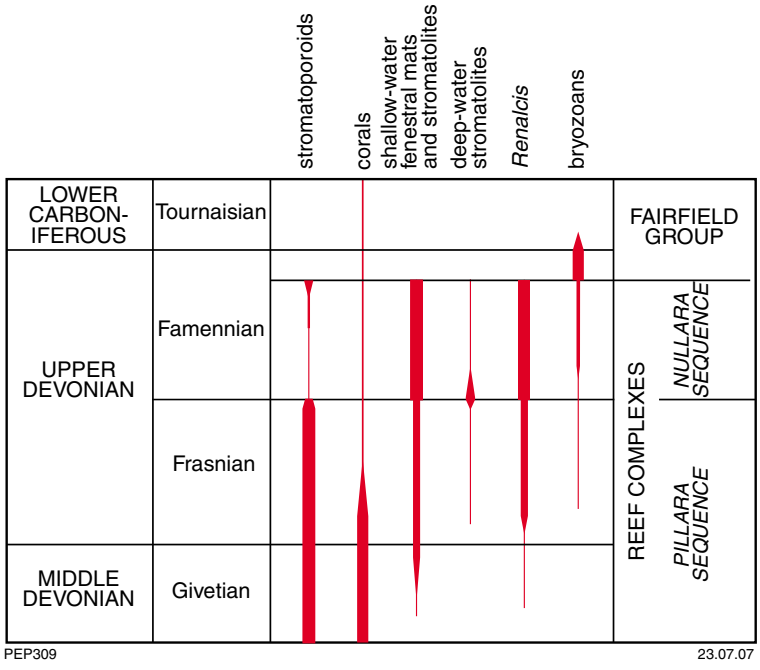

Figure 168. **Diagram illustrating the ranges of various groups of organisms from the Middle Devonian to the Lower Carboniferous in the Canning Basin. Bryozoans alone among this group flourished after the reef-extinction event in the late Famennian.**

Devonian limestones seems to have been much greater than that recorded in modern reef complexes. The distribution of the various types of marine cements (after Kerans et al., 1986) is shown in Figure 170.

Part of the evidence for early marine cementation in these rocks comes from the study of fillings of cavities and neptunian dykes. Cavity fillings, ranging from a few millimetres to more than a metre across, are widespread in organic frameworks of the reef-margin, reef-flat, and reefal-slope subfacies. Some cavities formed as a result of 'bridging' by reef-building organisms (mainly stromatoporoids and microbes), forming networks of voids in the reefal limestones (Fig. 40). Others probably resulted from the early decay of organic material in the limestones — many stromatactis cavities are thought to have formed in that way. Smaller numbers of cavities were formed by boring organisms, especially sponges (Fig. 32).

Cavities in the reef-margin, reef-flat, and reefal-slope subfacies commonly show early infillings of sediment, interlaminated with fibrous sparry calcite. In some cases the earliest infillings are dolomitized. The upper parts of cavities were often filled with equant spar, although the uppermost parts may have remained open. The infilling sediment may include bioclastic and terrigenous material, and commonly includes silt-grade peloids 'floating' in fibrous-calcite cement. Precipitation of both peloids and fibrous calcite may have been controlled by microbes, and microbial filaments occur in some fibrous-calcite laminae (Fig. 171).

The microcrystalline limestone (micrite) that makes up large parts of reef-margin, reef-flat, and reefal-slope deposits in many areas is also thought to have been microbial in origin (Playford, 1980; Kerans et al., 1986). The microbe *Renalcis* is common in many of those microcrystalline limestones, but in some it is only a minor component. The fact that micrite in reefal limestones was precipitated as solid rock, rather than lime mud, is shown by the fact that it was fractured along contemporary neptunian fissures and occurs as allochthonous blocks in associated fore-reef deposits (Fig. 172).

High primary depositional porosities were present in reef frameworks around platform margins, but that porosity was commonly destroyed or largely destroyed by penecontemporaneous marine cementation and associated void sedimentation. Consequently, the highest primary porosity remaining in the reef complexes after early marine diagenesis was in uncemented or weakly cemented biostromes, oolites, and clastic limestones of the back-reef and bank subfacies, and some clastic limestones of the fore-reef subfacies (Fig. 173).

Conodont evidence shows that fore-reef deposits that were well cemented at an early stage were also deposited very slowly, coinciding with condensed sequences (Druce, 1976). Deep-water stromatolites, commonly red in colour, are often associated with those condensed sequences in latest Frasnian and Famennian deposits (Playford et al., 1976).

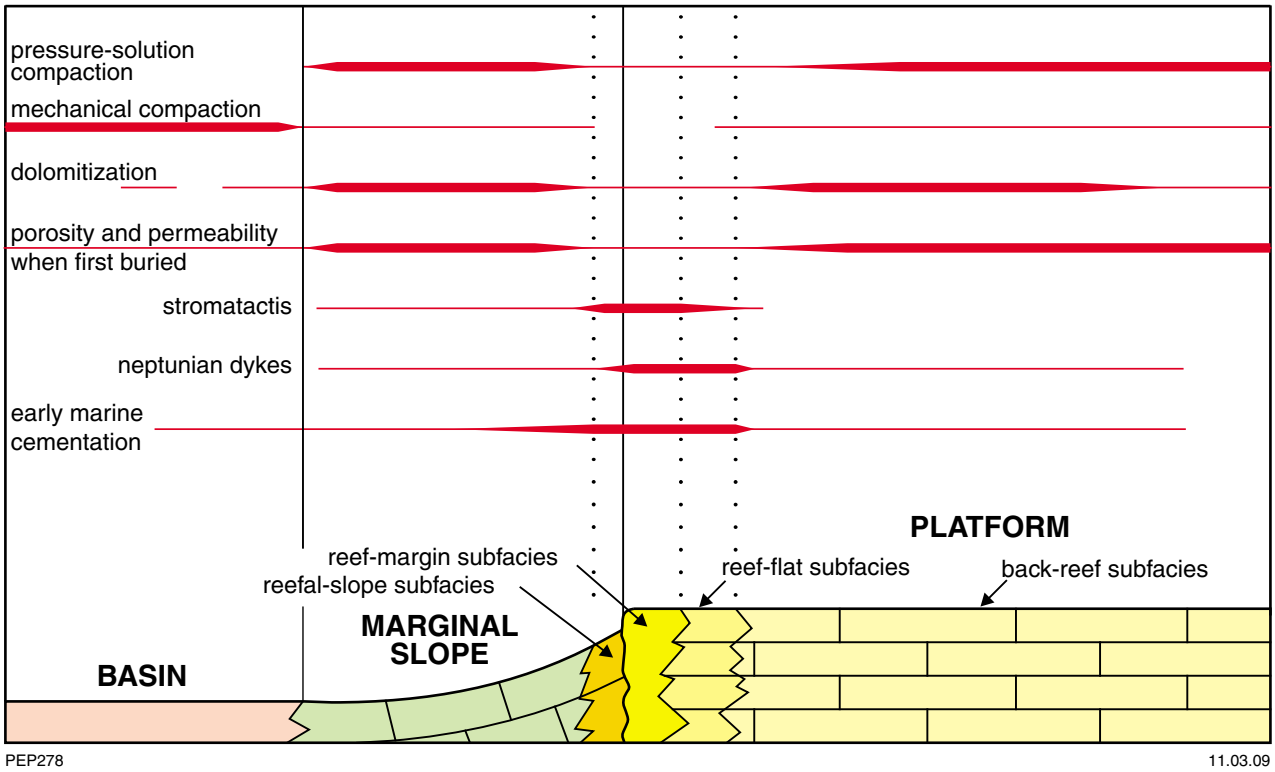

Figure 169. Diagram illustrating the extent of pressure-solution and mechanical compaction, dolomitization, porosity, early marine cementation, stromatactis, and neptunian dykes in the reef complexes.

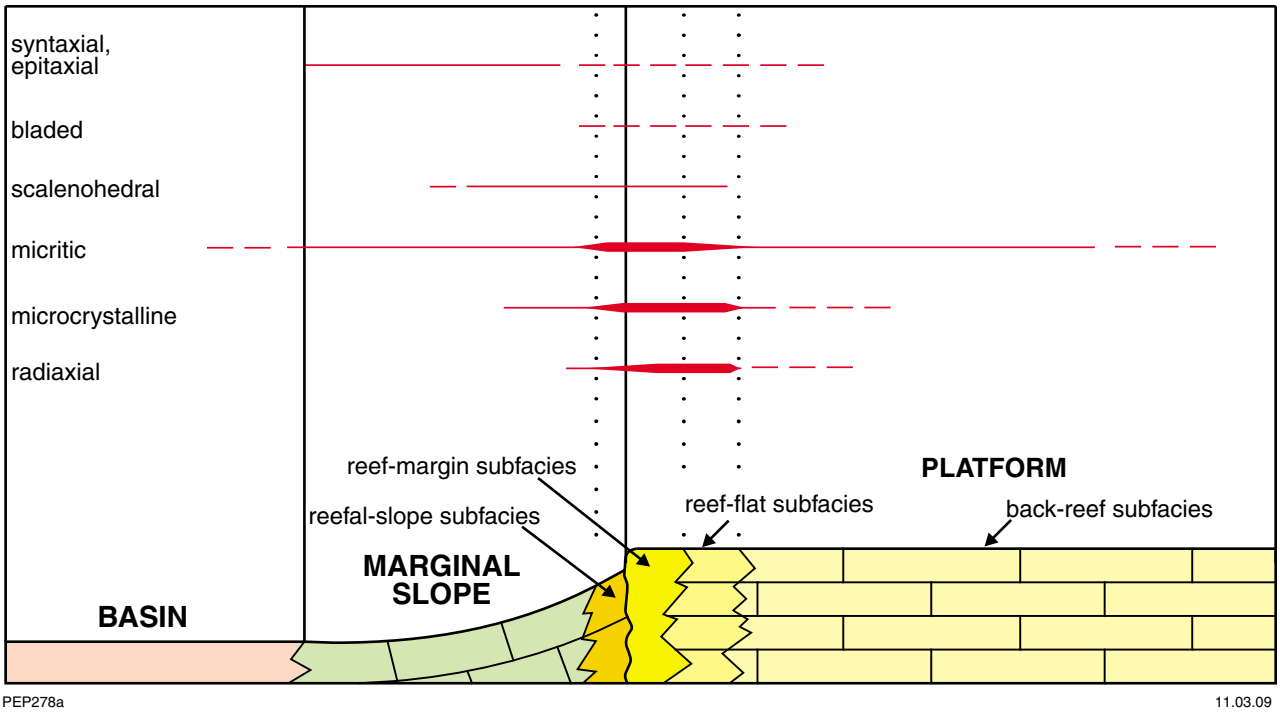

Figure 170. Diagram illustrating the distribution of various types of early marine cements in the reef complexes.

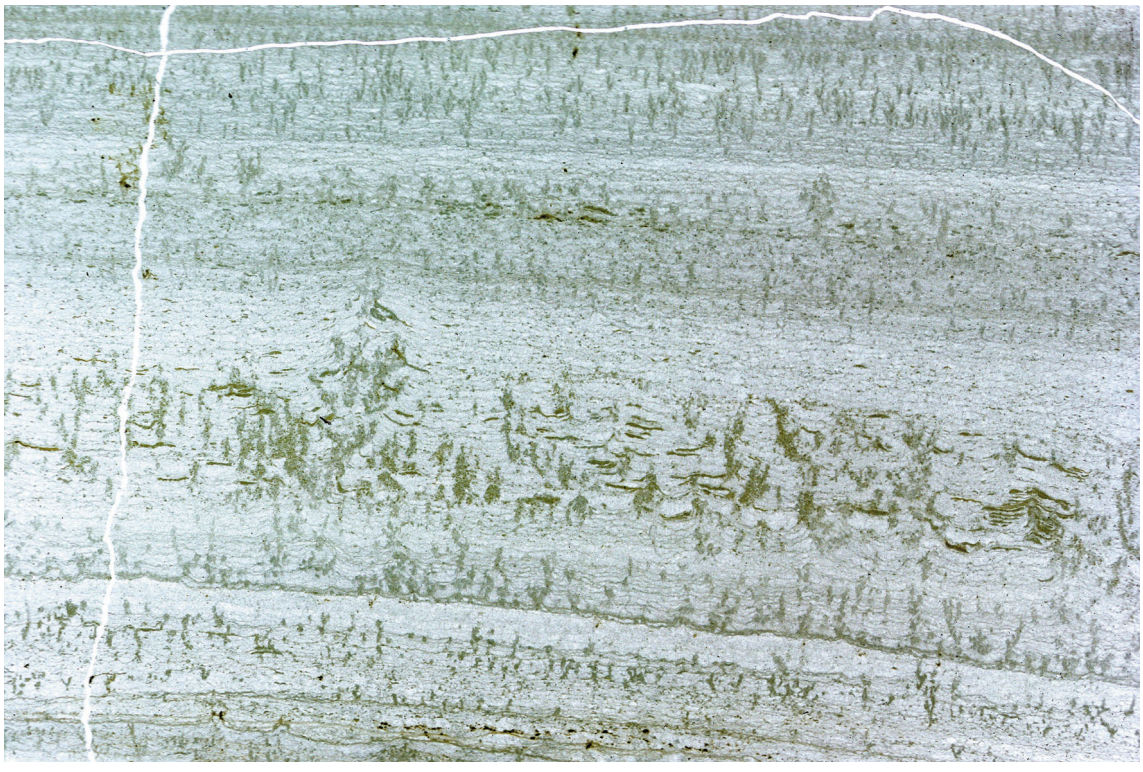

Figure 171. Thin section of laminated radiaxial spar cement from the lower Nullara Limestone at the northwest end of the Oscar Range, showing microbial filaments that were associated with fibrous-spar deposition. GSWA sample no. 21654. Width of field of view 40 mm.

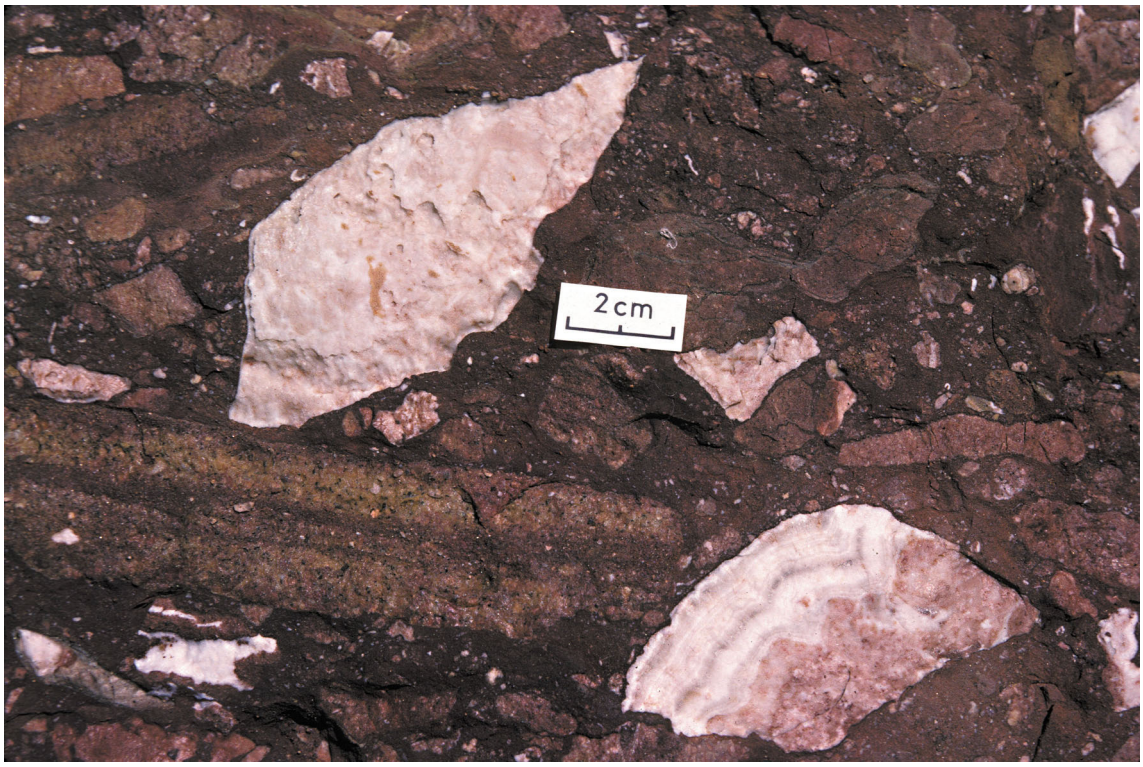

Figure 172. **Debris-flow breccia from fore-reef Napier Formation, 0.5 km north-northeast of Carpenters Gap. Note the clasts of reef limestone, one of which contains a truncated fissure filling of laminated sparry calcite. Other clasts are of marginal-slope sandy limestone.**

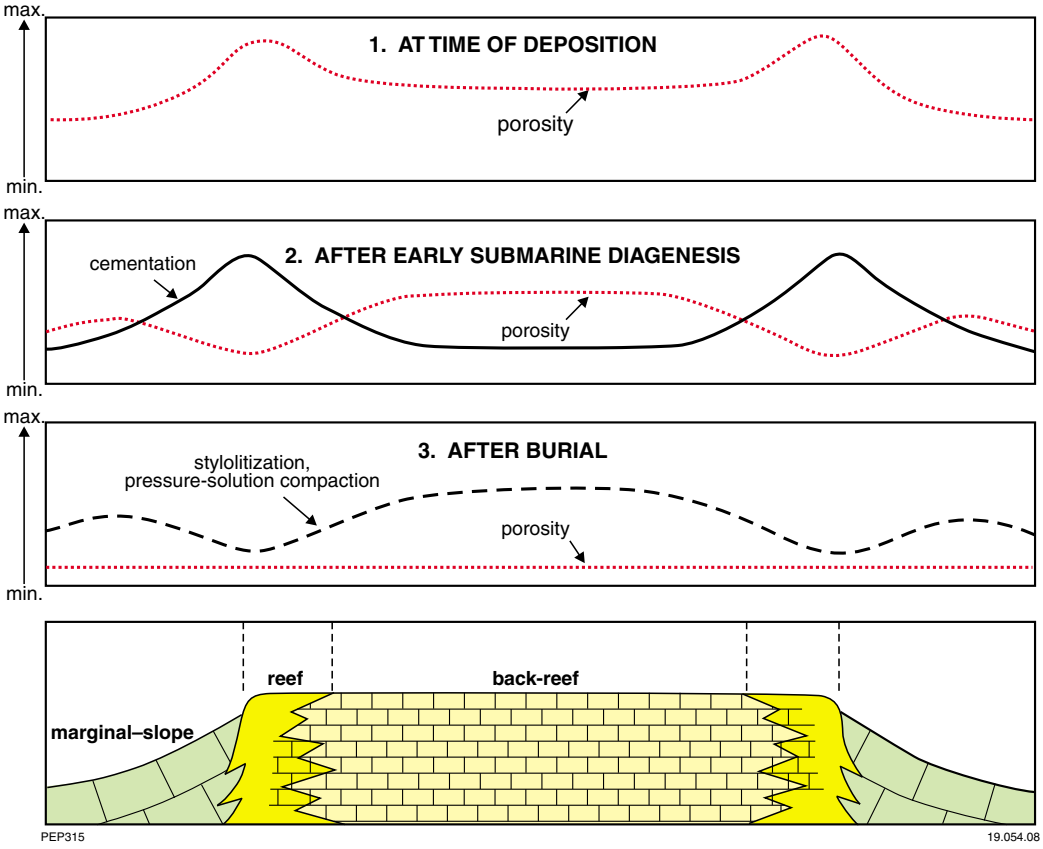

Figure 173. **Diagrammatic cross section through a Frasnian reef complex showing porosity: 1) when first deposited; 2) after cementation through early marine diagenesis; and 3) after burial and pressure-solution compaction.**

Early marine cementation was generally not extensive in back-reef and bank deposits, which normally retained most of their original porosities at the time of burial. However, some back-reef limestones include small neptunian dykes that apparently resulted from brittle fracturing following early marine cementation (Fig. 174). Some back-reef fenestral limestones show mud cracks (shrinkage cracks) that formed by desiccation following subaerial exposure (Fig. 175).

Stylolitization

Stylolites are strongly developed in some limestones in the reef complexes, commonly following bedding planes, including the inclined bedding of marginal-slope limestones. Dolomites in the reef complexes were also subject to stylolitization, but to a lesser extent than limestones. Major stylolite 'teeth' in the carbonates are usually aligned nearly vertically, indicating that pressure solution resulting in stylolitization was a consequence of vertical pressure associated with sediment loading (Figs 33, 34). However, in some areas, notably near large faults, there are stylolites with near-horizontal teeth, indicating that the limestones there were subjected to tectonic compression. In places where both types of stylolites occur together in the one bed the stylolites with horizontal teeth are usually younger than those with vertical teeth, which means that the tectonism responsible for horizontal-teeth stylolites occurred after compaction had given rise to vertical-teeth stylolites.

Pressure-solution stylolitization through sediment loading results in compaction and loss of porosity in limestone, as calcium carbonate dissolves along stylolites and is precipitated in available pore space. The thickness of overburden required to initiate stylolitization in these rocks is uncertain, but it is estimated to have been about 1000 m. During the Late Carboniferous and Early Permian the reef complexes lay below a succession of continental ice sheets, perhaps more than one or two kilometres thick, which must have played significant roles in the stylolitization and late diagenesis of the limestones.

However, some stylolitization, probably tectonically induced, was very early. Blocks of stylolitized back-reef Pillara Limestone occur in Frasnian conglomerates in the Sparke Range area. These limestone blocks show strong stylolitization that was clearly developed prior to incorporation of the blocks in the conglomerate (Fig. 176). They suggest that strong stylolitization of limestone occurred in areas where active faulting was taking place along the basin margin during growth of the reef complexes.

Pressure-solution compaction through stylolitization is normally much more intense in the back-reef subfacies than in equivalent reef-margin and reef-flat subfacies of most limestone platforms. Consequently, a platform interior has usually compacted more through pressure solution than the margins, resulting in a characteristic dished shape, contrasting with the original flat-topped form (Fig. 22).

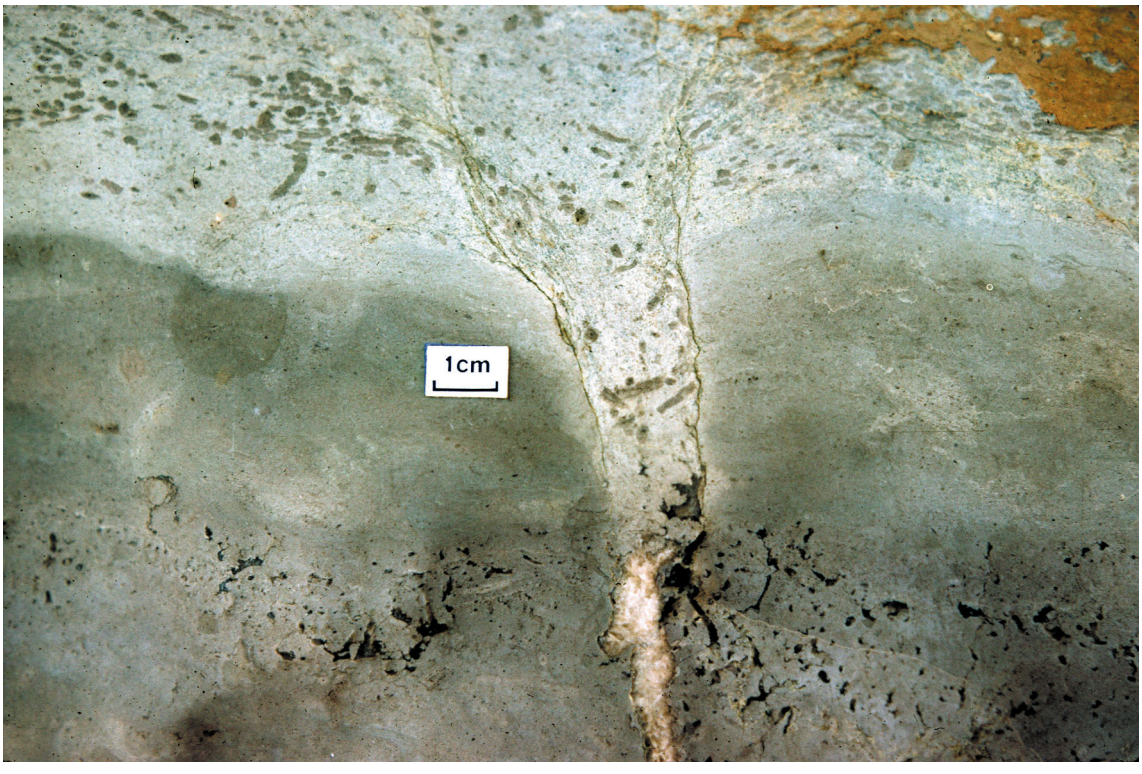

Figure 174. Pillara Limestone 3 km south of Sheep Camp Yard in Geikie Gorge, showing microbial limestone that was cemented and cracked open soon after deposition, allowing *Amphipora*-bearing lime mud to pour into the open fissure.

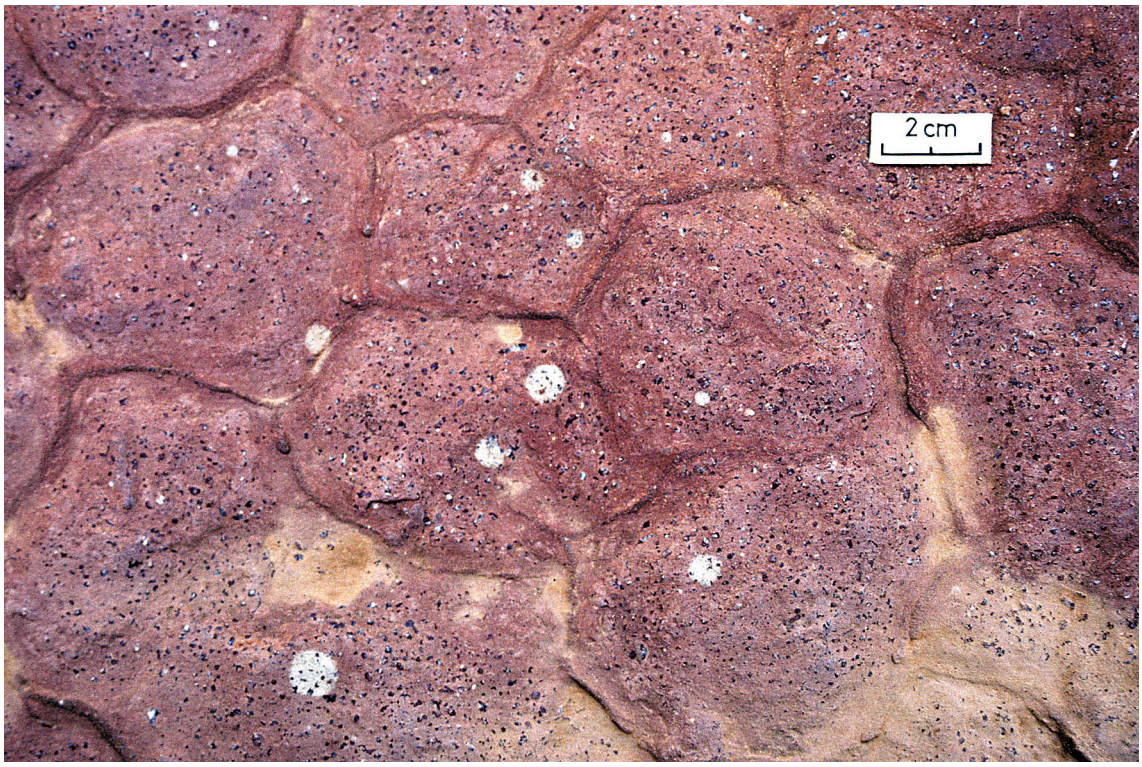

Figure 175. Mud cracks (shrinkage cracks) in fenestral limestone of the Nullara Limestone in the bed of Christmas Creek in the Red Bluffs area.



Figure 176. Frasnian conglomerate composed of blocks of stylolitized Devonian limestone, with a few blocks of Precambrian rocks, in the Galeru Member of the Sparke Conglomerate. Stylolitization must have occurred before the limestone blocks were deposited in the conglomerate.

This explanation of the dished shape of limestone platforms was first suggested by Playford (1969), and was since confirmed (Playford, 1980) by measurements of the spacing and amplitude of stylolites, using the approach of Mossop (1972). It is estimated that the average amount of compaction in back-reef and bank limestones in the reef complexes is commonly more than 25%, whereas in reef-margin and reef-flat limestones it is usually less than 5%. Measurements taken at 22 localities near Nardji Cave in the South Lawford Range show that, on average, the back-reef compaction is 3.5 times that of the reef-margin, twice that of the reef-flat, and 1.5 times that of the marginal-slope deposits (Playford, 1981).

The more intense stylolitization of back-reef limestones, compared with that of reef limestones, is linked to their differing porosities at the time of burial. The highest remaining porosity and least cementation in the platforms at the time of burial was in the back-reef limestones. Pressure solution and resulting compaction is most intense in porous limestones having interconnected pore space, which facilitated fluid movement and provided void space for the precipitation of the calcium carbonate dissolved by pressure solution along stylolites. The formerly porous and permeable limestones in back-reef deposits became strongly stylolitized and compacted after burial. However, reef limestones that were tightly cemented at the time of burial had little pore space remaining, so that they experienced minimal stylolitization and associated compaction through pressure solution. As a result of the effects of early porosity reduction through penecontemporaneous marine cementation and later porosity reduction from pressure-solution compaction, little primary porosity now remains in the outcropping reef complexes.

Although the central area of most platforms is now depressed relative to the margins, the structure of the platform interiors has been further modified by variations in the amount of compaction that has occurred in the back-reef deposits, giving rise to undulations in the dips of those deposits. The variations in compaction have resulted from differences in the original primary porosity and degree of early cementation, and from buried topography in the underlying basement rocks. Furthermore, as dolomite is less susceptible to pressure solution than calcite (Glover, 1955), variations in the degree of dolomitization have also led to differential compaction.

The degree of stylolitization in marginal-slope deposits is variable. Stylolites are relatively minor in most reefal-slope deposits because of strong early marine cementation and consequent early porosity destruction. Stylolites in fore-reef deposits that were subjected to moderate early marine cementation are widely spaced and have low amplitudes. On the other hand, where fore-reef deposits experienced little or no early cementation, and high primary porosities remained at the time of burial, stylolites are closely spaced and have high amplitudes. The result is that many marginal-slope deposits have compacted more than the adjoining platform margins, resulting in increased dips. However, the dip components due to compaction in marginal-slope deposits are much less than those due to primary depositional dips.

Thus, differential stylolitization has significantly modified the shapes of individual Devonian reef complexes, and the resulting compaction and cementation has destroyed most of the primary porosity that remained in the limestones after early marine diagenesis.

Geothermal history

The geothermal history of sedimentary rocks in the Canning Basin has been analysed by Burne and Kanstler (1971), Nicoll and Gorter (1984a,b), Arne et al. (1989), Arne (1996), and Wallace et al. (2002), using vitrinite reflectance, fission-track, conodont-colour alteration, and fluid-inclusion microthermometry methods. The highest temperatures recorded in boreholes in Devonian rocks on the Lennard Shelf are 97°C at 2486 m in Meda 1 and 116°C at 3355 m in Mount Hardman 1. Wallace et al. (2002) concluded that the maximum temperatures achieved in the exposed and near-surface rocks on the Lennard Shelf are unlikely to have been more than 60° to 70°C, which is in line with conclusions reached in paleotemperature studies by Burne and Kanstler (1971), Arne et al. (1989), and Arne (1996). An exception to these cool temperatures is recorded by Nicoll (1981), from limestones of the Napier Formation adjoining a leucite-lamproite plug 3 km south-southeast of JJ Bore on Leopold Downs Station (AMG Zone 51, 761700E 7913100N). This lamproite raised the temperature of limestones within about 1.5 m of the intrusion to more than 600°C (Nicoll, 1981; Playford, 1981; Nicoll and Gorter, 1984a,b). The immediately adjoining limestones are also blackened, and have a foetid odour when struck with a hammer, probably indicating that hydrocarbons, distilled from source rocks by the heat of the intrusion, were introduced into those limestones by the lamproite intrusion.

Platform evolution through time

Diagrammatic representations of the evolution of the reef complexes during the Givetian, Frasnian, and Famennian is illustrated in Figures 20 and 21. The Givetian platforms of the Pillara Limestone were mainly low-relief banks, commonly with retreating margins and little or no true reef development. Parts of the late Givetian and early Frasnian deposits below the weathered zone are dark grey to black, with relatively high contents of organic matter. They potentially form good source rocks for petroleum (Alexander et al., 1985). None of the younger platform carbonates are as dark in colour; indeed most are light grey to white and lack significant amounts of organic carbon.

Stronger reef growth took place along the platform margins in the latest Givetian to earliest Frasnian, so that they tended to grow steeply upward or vertically, with prominent reef scarps — the ‘keep-up’ style of James and Macintyre (1985) and Neumann and Macintyre (1985). Abrupt backstepping of the platforms occurred on four occasions during the early to late Frasnian, probably associated with pulses of tectonic activity in the area. For a short period in the latest Frasnian (Zones 11–13) the platforms advanced (prograded), and had well-developed reef margins. Then followed an abrupt and relatively brief regression at the Frasnian–Famennian boundary, when the platforms were exposed and eroded.

During the Famennian transgression after the Frasnian–Famennian regression, the reefal platforms continued to advance strongly, extending over marginal-slope and basin facies. An abrupt fall in sea level occurred in the late Famennian, at about the end of the *expansa* Zone. This regression marked the close of reef growth in the Canning Basin.

Conglomerates

Siliciclastic conglomerates and sandstones interfinger with, cut through, and are intercalated with the reef complexes in various localities through the Lennard Shelf. Deposition took place in hinterland basin, platform, marginal-slope, and basin settings during the Givetian, Frasnian, and Famennian. Nine major conglomerate and sandstone bodies are known (Fig. 177), and the approximate ages of measured sections in those bodies and associated reef complexes are shown on Figure 178. The conglomerates and sandstones were shed from active fault scarps and laid down in alluvial-fan, fan-delta, and submarine-fan environments (Figs 179, 180).

Lithostratigraphy

Nine conglomerate or conglomeratic formations have been mapped in the area. These are, from south to north, the Sparke Conglomerate, Bobs Bore Conglomerate, Elma Conglomerate, Mueller Conglomerate, Barramundi Conglomerate, Stony Creek Conglomerate, Big Spring Formation, Behn Conglomerate, and Van Emmerick Conglomerate. Only the larger conglomerate bodies have been distinguished as separate formations; smaller conglomerate deposits are included in other formations (such as the conglomerate near the east entrance to Windjana Gorge that is included in the Napier Formation).

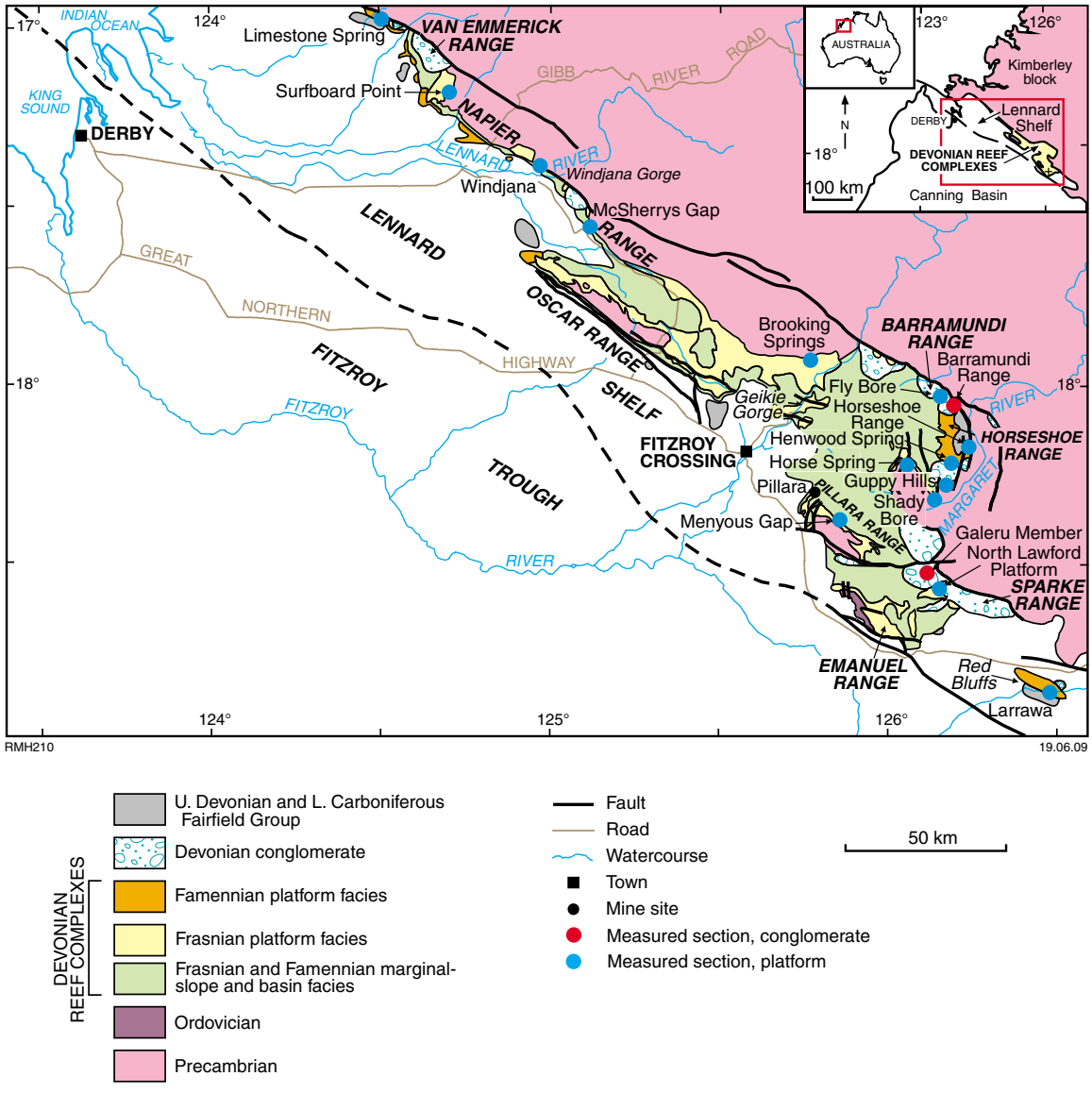

Figure 177. Locations of measured sections in the Devonian reef complexes and conglomerates.

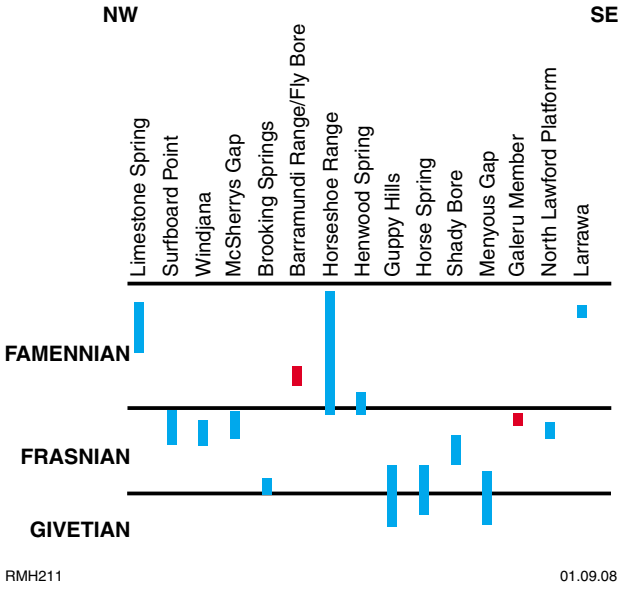

Figure 178. **Estimated ages of measured sections shown on Figure 177. Platform sections shown in blue, conglomerate sections in red.**

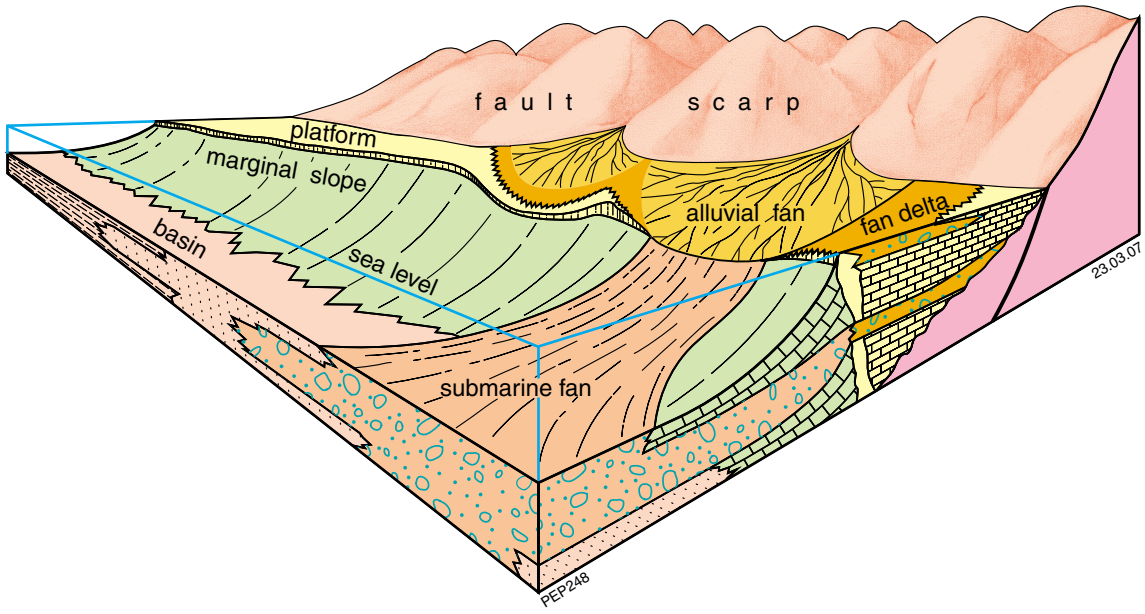

Figure 179. **Block diagram illustrating alluvial-fan, fan-delta, and submarine-fan facies in conglomerates, and contemporaneous facies of the Devonian reef complexes.**

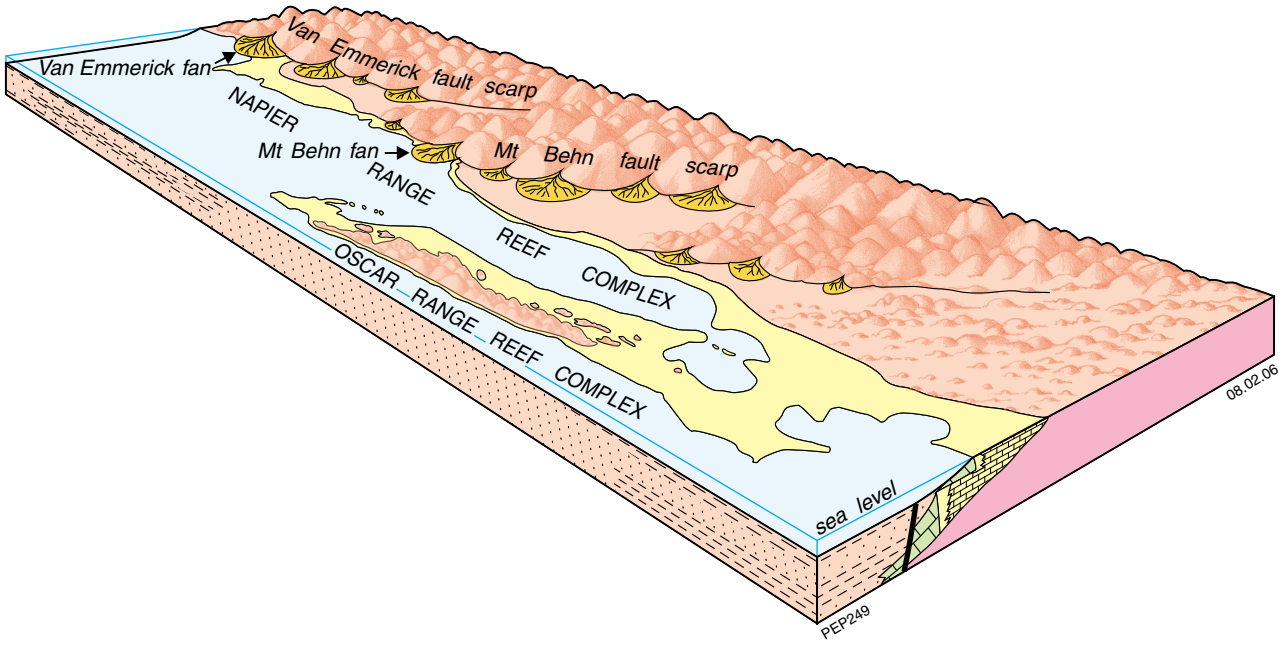

Figure 180. Block diagram showing the Oscar Range and Napier Range reef complexes and conglomerate bodies. The conglomerates were shed from the scarps of active faults during the Devonian.

Sparke Conglomerate

The Sparke Conglomerate is the most extensive of the conglomerate bodies associated with the reef complexes. It forms the Sparke Range (Fig. 10) in the eastern Lennard Shelf, and extends into Old Bohemia Valley. The conglomerate is composed mainly of Precambrian clasts, but it interfingers with, and contains clasts derived from, the Pillara Limestone and the lower Virgin Hills Formation (Figs 181–183). It includes the cyclic Galeru Member. Much of the Sparke Range rises to a higher elevation than the adjoining reef complexes, presumably because of its greater resistance to Early Permian subglacial erosion.

Definition

Guppy et al. (1958) applied the name Sparke Conglomerate to conglomerate bodies in the Sparke Range and neighbouring areas. They proposed a type area around Trig Stations J7 and J8 (north and east of Lawford Spring, from around AMG Zone 52, 190000E 7961000N to 202500E 7942800N). This area encompasses most of the northern and central outcrop areas of the Sparke Conglomerate. The conglomerate body around Virgin Hills, once included in the Sparke Conglomerate, is now placed in the Bobs Bore Conglomerate.

Lithology

The Sparke Conglomerate is dominated by boulder conglomerate with lesser pebble conglomerate, coarse- to fine-grained sandstone, and minor siltstone. Clasts of Precambrian rocks in the conglomerate are commonly more than 3 m in diameter, and isolated allochthonous blocks of Devonian limestone more than about 6 m across are also present. The dominant clast type is quartzite derived from the Kimberley Basin, with lesser igneous, gneissic and metasedimentary rocks from the King Leopold Orogen. Clast lithologies vary over the lateral extent of the Sparke Conglomerate and through its vertical section, but not in any discernible pattern.

Distribution and thickness

The Sparke Conglomerate as presently recognized forms the eastern and northern Sparke Range and a separate lobate body of conglomerate that extends from the junction of the North and South Lawford Ranges past McIntyre Knolls to near Waggon Pass in the Old Bohemia Valley (Plate 4).

At least 2 km stratigraphic thickness of conglomerate is present in the area between Lawford Spring and Junction Dam, and is thought to overlie a basal fault (glide plane) that was active during deposition of the conglomerate.

Stratigraphic relationships

The Sparke Conglomerate interfingers with platform, marginal-slope, and basin facies. The lowermost part of the formation in the Sparke Range rests on marginal-slope deposits that apparently correlate with the lower Virgin Hills Formation. West of the Sparke Range, the lowermost Sparke Conglomerate is exposed above basin facies of the Gogo Formation. A small isolated tongue of the formation is exposed west of the Lawford Range reef spine, south of Waggon Pass, where it is present between the Gogo and Virgin Hills Formations. This tongue is thought to have been linked to the deep-water conglomerate body that is exposed in Old Bohemia Valley.

These relationships suggest that deposition of the Sparke Conglomerate began about 380 m.y. ago, based on the estimated age of the base of the Virgin Hills Formation. This is at the boundary between Frasnian Zones 5 and



Figure 181. Sparke Conglomerate, alluvial-fan facies, in the Sparke Range. Boulders and smaller clasts are composed of various Precambrian rocks.



Figure 182. Scree from Sparke Conglomerate, containing light-coloured boulders of Pillara Limestone and smaller clasts of Precambrian rocks. From the central part of the Galeru Member. Photo by Roger Hocking.



Figure 183. Aerial view of the Galeru Member of the Sparke Conglomerate, looking north, showing conspicuous cyclicity. The rocks dip to the right at about 35°. A left-lateral bounding fault has produced the drag to the left that is evident in the upper part of the photo.

6, which is dated as about 381 m.y. ago by House and Gradstein (2004).

Clasts in the Sparke Conglomerate consist wholly of Precambrian rocks in most exposures, but clasts of Pillara Limestone and, less commonly, Frasnian Virgin Hills Formation, are present in some horizons (Figs 176, 181, 182). No clasts or intercalations of Famennian limestone have been found. The evidence suggests that the exposed Sparke Conglomerate is middle to late Frasnian in age, with a depositional time span of about 5 to 6 m.y., based on the scale of House and Gradstein (2004).

Galeru Member

The Galeru Member (Hocking and Playford, 1998d; Plates 4, 5) is named after Galeru Gorge. It is a distinctive cyclic unit in the middle Sparke Conglomerate, composed of subaqueous to subaerial shallowing- and coarsening-upward fan-delta cycles.

The member is known only in the Lawford Spring to Junction Dam area on Mount Pierre Station in the central Sparke Range, south of the Virgin Hills Fault (Fig. 183). The type section runs east–west along a fault compartment northwest of Lawford Spring (from AMG Zone 52, 195203E 7945500N to 198600E 7944500N). Only the lower 909 m of this section has been measured (Fig. 184, see legend for measured sections in Fig. 185), and there is an estimated 900 to 1000 m of additional section in the member above the measured interval. The member was laid down mainly in shallow fan-delta environments.

Like other conglomeratic units, exposures are generally poor. Cycles consist ideally of a lower siltstone or silty sandstone, in places bioturbated and/or containing atrypid brachiopods, coarsening upward through sandstone to pebbly sandstone and pebble to cobble and boulder conglomerate. The coarsest conglomerate is at the top of each cycle. In one area, several cycles include thin beds (1–2 m thick) of stromatoporoid limestone or fenestral limestone of the platform facies at the base of cycles, overlain by sandstone grading up into conglomerate at the top. The average thickness of these cycles is between 5 and 10 m. Exposures are commonly poor, and some cycles are discernible more from topography than actual exposure. Clasts in most beds of conglomerate consist wholly of Precambrian rocks, but some contain boulders and smaller clasts of stylolitized Pillara Limestone, demonstrating that some Givetian or earlier Frasnian platforms were exposed and being eroded at that time (Figs 176, 182).

The precise age of the Galeru Member has not been established, because of a lack of conodonts and ammonoids. However, the presence of atrypid brachiopods and typical Frasnian stromatoporoids, without corals, at the base of some cycles, indicates that the age of the unit is Frasnian, and stratigraphic relationships suggest that it is late Frasnian.

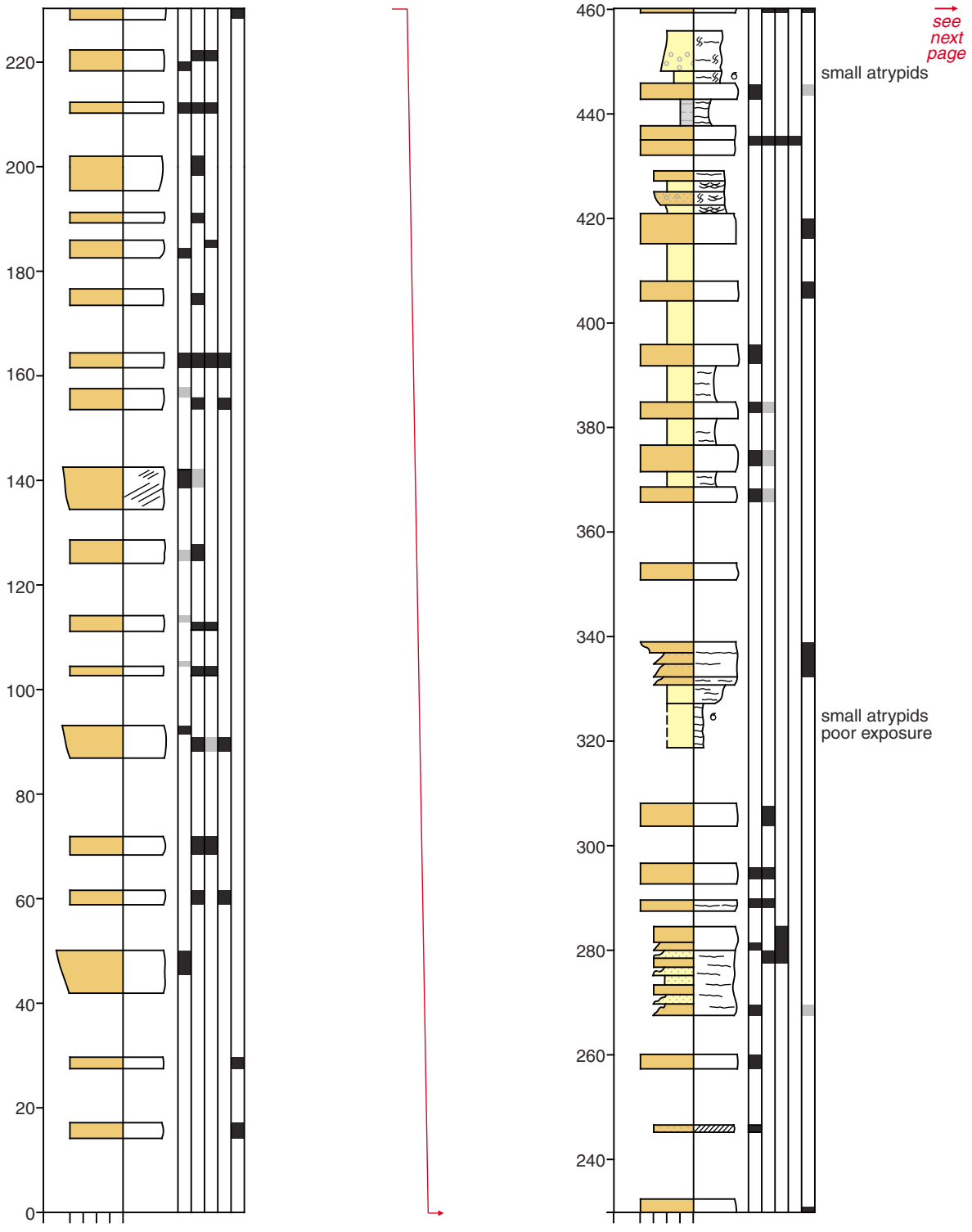

Figure 184. **Measured section of Galeru Member, central Sparke Range. This represents the lower part of the type section. Clast lithology shown on right of section. black shade = common to abundant, grey shade = present. For legend see Figure 185.**

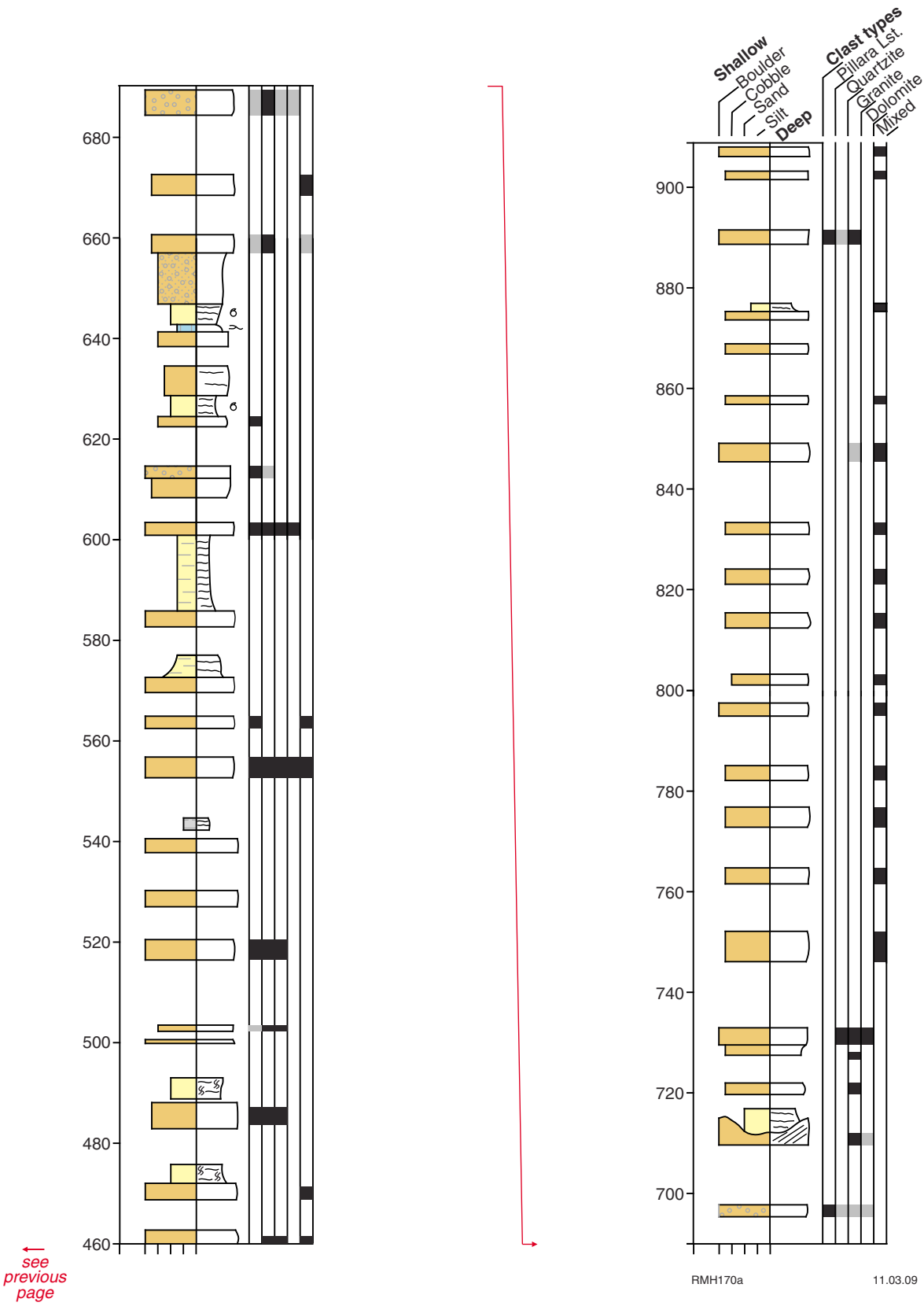
Shallow
Boulder
Cobble
Sand
Silt
Deep
Clast types
Pillara Lst.
Quartzite
Granite
Dolomite
Mixed
680
660
640
620
600
580
560
540
520
500
480
460
900
880
860
840
820
800
780
760
740
720
700
see previous page
RMH170a
11.03.09

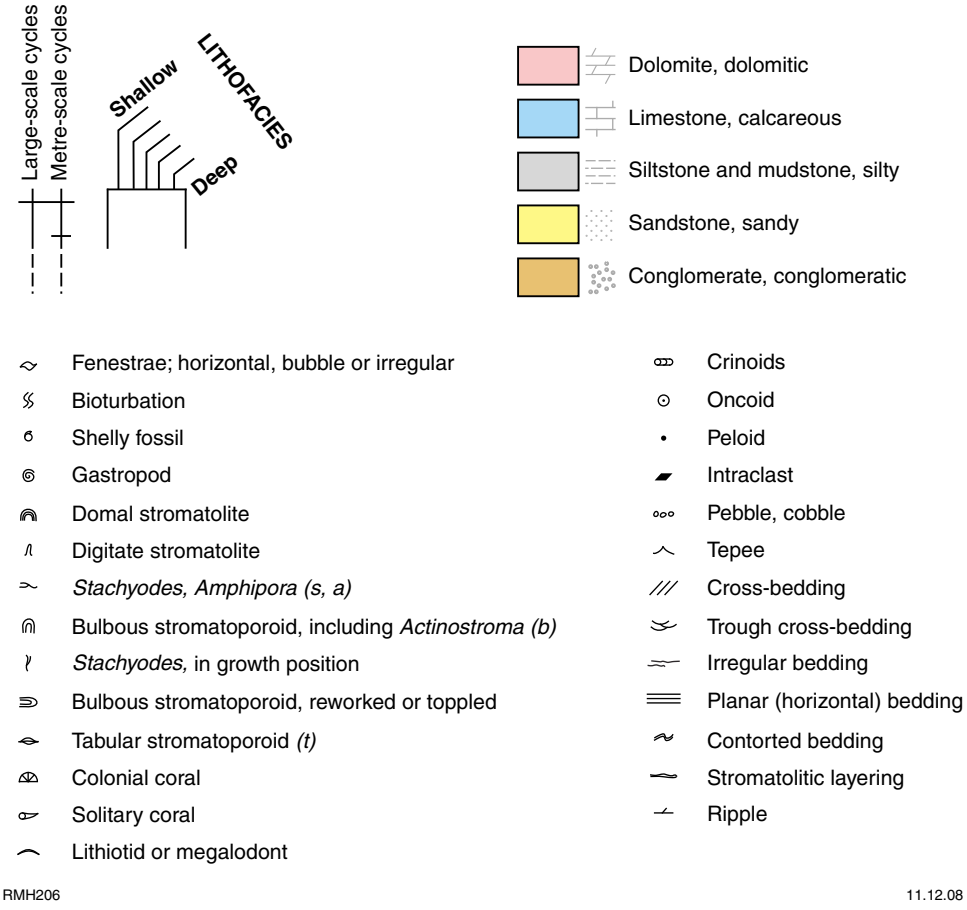

Figure 185. Legend for measured sections.



Figure 186. Sparke Conglomerate near Lawford Spring showing alternations of sandstone and cobble conglomerate, with well-rounded clasts of Precambrian rocks, thought to have been deposited in a shallow-marine fan delta or possibly a subaerial alluvial fan.



Figure 187. Deep-water (distal fore-reef) Virgin Hills Formation interbedded with and grading into Bobs Bore Conglomerate near Bobs Bore. Note the reworked angular slabs of dark silty limestone.

Bobs Bore Conglomerate

The Bobs Bore Conglomerate includes three separate bodies of cobble to boulder conglomerate, centred on Bobs Bore near the southeastern end of the Pillara Inlier (Plate 4). The unit is a deep-water submarine-fan deposit associated with basin and lower marginal-slope facies (Virgin Hills Formation) of middle Frasnian to early Famennian age (Fig. 187).

Definition

The type section for the Bobs Bore Conglomerate is in the Virgin Hills, from about 5 km west to 7 km west-northwest of Bobs Bore (from AMG Zone 51, 803500E 7950200N to 802400E 7951800N). This poorly exposed section has not been measured, but is estimated to be 200 to 300 m thick.

Lithology

The Bobs Bore Conglomerate consists of cobble and boulder conglomerate with lesser interbedded coarse-grained conglomeratic sandstone. Clasts are dominantly quartzite derived from the Kimberley Basin, with minor granitic and metamorphic rocks and, locally, clasts and blocks of reworked reefal limestone. The matrix of boulder conglomerates, where exposed, is commonly sandstone or granule to pebble quartzose conglomerate. As with other conglomerates, true exposures are rare — commonly, only a lag deposit of cobbles and boulders is present, forming low, rounded hills.

Distribution and thickness

The Bobs Bore Conglomerate extends along the south side of the Pillara Inlier, south of the Virgin Hills and west of Mount Pierre Creek. The maximum thickness can only be estimated, given the paucity of exposed strata, but is probably not more than about 400 m.

Stratigraphic relationships

The Bobs Bore Conglomerate includes three separate conglomerate bodies. Both the western body (containing the type section) and the eastern body rest on Frasnian Virgin Hills Formation and are overlain by early Famennian Virgin Hills Formation. The central body is stratigraphically lower than the other two, and may overlie the uppermost Gogo Formation. These relationships suggest that deposition of the Bobs Bore Conglomerate began in the middle or late Frasnian and continued into the early Famennian, from about 381 to 374 m.y. ago, which is a period similar to that of the Elma Conglomerate. The outcrops suggest that there may have been a hiatus in deposition early in that period, marked by the tongue of Virgin Hills Formation that separates the western and central exposures of the formation.

Elma Conglomerate

The Elma Conglomerate is an extensive middle Frasnian to early Famennian conglomerate unit that outcrops in the eastern Margaret Embayment, immediately west of the basin-bounding Mount Elma Fault. Deposition occurred in alluvial-fan, fan-delta, and submarine-fan settings. Mount Elma itself extends about 100 m above the topographic level of the surrounding platform carbonates (Fig. 188).

Definition

The Elma Conglomerate was first named the 'Mount Elma Conglomerate' by Guppy et al. (1958). Playford and Lowry (1966) did not use the name, considering that part of the conglomerate was post-Devonian. However, field examination for this Bulletin indicates that the unit is entirely coeval with the reef complexes, so the name has been revived, as Elma Conglomerate, on maps by Tyler et al. (1998) and with this Bulletin (Plates 3 and 7). Guppy et al. (1958) did not specify a type section, but implied a type locality at Mount Elma. This is accepted here, specifically on the northeast side of Mount Elma (around AMG Zone 52, 207500E 7982500N) where a deep gully cuts towards the peak of the mountain and is reasonably accessible. The area east of Rattigan Rocks (around AMG Zone 52, 197000E 7976000N) is a reference locality for the base of the formation.

Lithology

The Elma Conglomerate consists of quartzite-dominated cobble to boulder conglomerate, laid down as alluvial-fan, fan-delta, and submarine-fan deposits. Subrounded to angular quartzite boulders more than 4 m in diameter are present south of Mount Elma (at GPS AMG Zone 52, 206045E 7978910N), immediately west of the Mount Elma Fault (Fig. 189). At this locality, the nearest in-place quartzite is about 5 km east in Margaret Gorge in the Mueller Ranges. Larger blocks of reworked reefal limestone are present, but not common, in deep-water submarine-fan conglomerates in the formation.

At Painted Rocks, a sparry matrix is present between rounded clasts in some conglomerate beds in the fan-delta deposits (Fig. 190), most commonly near or at the tops of beds, suggesting early subaqueous winnowing of any former matrix between the clasts. There is also evidence of cut-and-fill structures within the conglomerate, with microbial encrustations on cut surfaces and over pebbles and cobbles (Fig. 191).

Conglomerates of the Elma Conglomerate north and west of Mount Elma grade laterally into back-reef facies of the upper Pillara Limestone and lower Nullara Limestone, with interfingering limestone and conglomeratic horizons. Reefal limestone is interbedded with fan-delta conglomerate on the northern side of Painted Rocks.

In an arc extending around the south to southwest flank of Mount Elma (from GPS AMG Zone 52, 206700E 7979800N to about 205400E 7981700N), a series of small atoll-like reefal platforms are attached to the sides of the major conglomerate fan (Figs 192–194). Each of these platforms developed progressively further west and higher stratigraphically on the fan. Several shallowing-upward cycles can be seen in each platform. The cycles are 7 to 10 m thick, and grade from cobble to boulder conglomerate at the base to fenestral sandstone and sandy reef-flat to



Figure 188. Mount Elma from the north, showing the rounded topography that is typical of most conglomerate outcrops on the Lennard Shelf. Nullara Limestone is in the foreground.



Figure 189. Large quartzite boulder in Elma Conglomerate, south of Mount Elma. Photo by Roger Hocking.



Figure 190. Elma Conglomerate, fan-delta facies, on the east side of Painted Rocks. Note the sparry calcite cement between clasts.



Figure 191. Elma Conglomerate on the east side of Painted Rocks showing stromatolitic encrustations on well-rounded clasts of Precambrian rocks deposited in a fan-delta environment.



Figure 192. Aerial view looking east over the south flank of Mount Elma, showing megacycles in Frasnian shallow-subaqueous conglomerate (Elma Conglomerate), and discrete bodies of reefal limestone (Pillara Limestone). Each limestone body grew on, and interfingered with, conglomerate, before being overwhelmed by the next pulse of conglomerate deposition.



Figure 193. Part of one of the reefal bodies (Pillara Limestone) shown in Figure 192 on the south flank of Mount Elma, illustrating cyclical interfingering between reefal limestone and conglomerate. The reefal limestones are most extensive at the tops of megacycles.



Figure 194. Interfingering between Frasnian back-reef subfacies (Pillara Limestone) and Elma Conglomerate on the south flank of Mount Elma.

back-reef *Amphipora* and *Stachyodes* limestone at the top. Tongues of back-reef carbonates at the top of each cycle extended progressively further away from the platform core, over a stratigraphic thickness of about 50 m. An influx of conglomerate overwhelmed the top of each platform, extinguishing reef growth until the next platform became established, slightly higher and further west on the fan. In the highest occurrence, southwest of Mount Elma (AMG Zone 52, 205400E 7981680N to 205750E 7981750N), both reefal-slope and platform facies are exposed.

Cycles are marked primarily by successive outcrops of reefal limestones, with interbedded conglomerates marked by cobble and boulder lag deposits. The cycles are shallowing-upward infill cycles, comparable with infill cycles seen elsewhere in the lower and middle Pillara Limestone, except that at the base of each cycle the siltstone seen elsewhere is replaced by conglomerate. This pattern of conglomerate deposition at the base of a cycle, followed by limestone at the top, suggests either a tectonic or a climatic control, with conglomerate influx controlled by regular pulses of faulting or changes in local rainfall, over tens of thousands of years.

Coarse-grained arkosic sandstone, essentially decomposed granite, is exposed west of Painted Rocks (at AMG Zone 52, 202600E 7977500N). The sandstone contains scattered pebbles and cobbles of quartzite, granite and dolerite. Laterally persistent siltstone bands are the only bedded structures visible, and clasts are not imbricated. This is interpreted as representing deposition in shallow fan-delta conditions.

Distribution and thickness

The Elma Conglomerate extends from north of Mount Elma southwest to Rattigan Rocks and south to Guppy Hills. In general, exposures are younger to the north and east, as might be expected if basin-bounding faults were active during deposition. It is estimated that the total thickness of the Elma Conglomerate may be more than 1000 m.

Stratigraphic relationships

The base of the main body of Elma Conglomerate is placed at the same level as the series of allochthonous blocks forming Rattigan Rocks, which are at the base of the Virgin Hills Formation, indicating that conglomerate deposition may have begun in that area during the middle Frasnian. The Frasnian–Famennian boundary lies near the top of the Elma Conglomerate, as shown by Famennian Nullara Limestone above and interbeds of Frasnian Pillara Limestone below. West of Henwood Spring (at AMG Zone 52 200800E 7981400N), the top of the conglomerate is almost at the Frasnian–Famennian boundary, whereas close to the bounding fault with the Precambrian northwest of Mount Elma the top is within the Famennian.

The boundary between the Virgin Hills Formation and Sadler Limestone is middle Frasnian (about 381 Ma), coinciding with the base of the Elma Conglomerate. The top of the formation generally lies immediately above the Frasnian–Famennian boundary (374.5 ± 2.5 Ma according to House and Gradstein, 2004), so that deposition of the Elma Conglomerate is estimated to have spanned about 7 m.y.

A small outcrop of conglomerate immediately south of Guppy Hills (GPS AMG Zone 52, 200910E 7973570N) is not formally included in the Elma Conglomerate, because more than 200 m of limestone separates it from the main body of that formation. This limestone is a coral-rich unit of the Pillara Limestone that is probably of Givetian age, as similar coral-rich beds in the Emanuel and Home Ranges are known to be Givetian, based on the presence there of *Stringocephalus*.

Mueller Conglomerate

The name Mueller Conglomerate was introduced by Hocking and Playford (1998c; Plate 3) for an isolated conglomerate body surrounded by Precambrian rocks east of the Margaret Embayment, immediately west of the Mount Winifred Fault (Plate 3). This conglomerate was shown previously on the Mount Ramsay 1:250 000 map as Elma Conglomerate (Tyler et al., 1998). The formation is named after the Mueller Ranges, which lie east of the conglomerate, and the type locality is arbitrarily placed near the southern end of the outcrop ridge (at AMG Zone 52, 204900E 7991400N). The unit is inaccessible by motor vehicle. A brief visit by helicopter revealed the presence of large cobble and boulder conglomerate, with clasts dominated by rocks derived from the Kimberley Basin (Fig. 195).

The age of the Mueller Conglomerate has not been established. There is no doubt that it post-dates the King Leopold Orogeny (c. 550–600 Ma) as it is not cleaved, fractured, or folded like the Neoproterozoic conglomerates that predate the orogeny, near the edge of the Kimberley plateau. The characteristic geomorphology and lithology of the formation suggest that it is coeval with one of the conglomerates associated with the reef complexes. Its estimated thickness is about 100 m, based on SRTM satellite data. The formation is probably entirely an alluvial-fan deposit.

Barramundi Conglomerate

The Barramundi Conglomerate forms the Barramundi Range, in the northeast corner of the Margaret Embayment (Figs 196–199). The range rises about 160 m above the adjoining plain level and 100 to 120 m above adjoining limestones. The Barramundi Conglomerate is the only conglomerate body that appears in outcrop to be wholly Famennian in age, although Frasnian strata are probably present in the formation in subcrop. The conglomerate is bounded to the north by the Barramundi Fault, and to the east by the northernmost part of the Mount Elma Fault. The exposed part of the formation was laid down largely as an alluvial-fan deposit, with some shallow-water fan-delta deposits intercalated in the Nullara Limestone.

Definition

The Barramundi Conglomerate was originally known as the ‘Burramundi Conglomerate’ (Guppy et al., 1958), named after the ‘Burramundi’ Range (now spelled Barramundi Range). Playford and Lowry (1966) did not



Figure 195. Aerial view of the Mueller Conglomerate, looking north-northwest. The Mount Winifred Fault runs along the eastern (right) margin of the conglomerate body. The conglomerate overlies Precambrian rocks.



Figure 196. The eastern Barramundi Range showing the characteristic rounded outlines of the conglomerate outcrops.



Figure 197. Barramundi Conglomerate, alluvial-fan facies, in the Barramundi Range.



Figure 198. Closer view of the Barramundi Conglomerate shown in the previous figure. It consists of rounded to subrounded clasts of Precambrian rocks, mainly quartzite.



Figure 199. Barramundi Conglomerate in the Barramundi Range, showing induration along joints and minor faults.

use the name and considered that part of the conglomerate in the Stony Creek area was probably Permian. However, the present study has shown that the whole of the conglomerate is Upper Devonian, and the name has been revived as Barramundi Conglomerate (Plates 3 and 7; Griffin and Tyler, 1995; Tyler et al., 1998). The type locality is here specified as a deep gully leading to a peak on the northeast side of the Barramundi Range (around AMG Zone 52, 203000E 8001400N). Figures 200 and 201 show measured sections in the type area of the formation and the area where the conglomerate interfingers with Nullara Limestone between the two main fan bodies of conglomerate.

Lithology

The Barramundi Conglomerate, like the other conglomerate bodies associated with the reef complexes, consists of cobble to boulder conglomerate with minor intercalated coarse-grained sandstone and reefal carbonates (Figs 200 and 201). Quartzite clasts are dominant, but granitic, metasedimentary, doleritic, gneissic, and reefal limestone clasts are locally common.

The Barramundi Conglomerate interfingers with cyclic Nullara Limestone 1.4 km west of Fly Bore (AMG Zone 52, 196900E 8003300N). In this area, the Nullara Limestone consists largely of microbially bound siliciclastic sandstone. The limestone contains compound stromatolitic columns as much as 30 cm high and about 1 cm wide, which probably grew in a shallow-water shoreline setting. Higher in the section, microbial to stromatolitic limestone is interbedded with sandy and conglomeratic limestone.

Distribution and thickness

The Barramundi Conglomerate forms the Barramundi Range, and grades laterally into Famennian carbonates (Piker Hills Formation) immediately south of Boab Creek. Some 300 to 400 m of conglomerate is exposed in the range, but the stratigraphic base is not seen there, so the total thickness could be much greater, especially if deposition spanned a period similar to that of the Elma Conglomerate.

Stratigraphic relationships

The Barramundi Conglomerate interfingers with Nullara Limestone in the gap in the range around Fly Bore, and west towards **Longhole Bore**. The exposed conglomerate is thus Famennian. It was laid down largely as an alluvial-fan deposit, with lesser amounts of fan-delta and submarine-fan deposits. The formation interfingers with and is overlain by the Famennian Piker Hills Formation 3 km south of Fly Bore, but elsewhere it interfingers with Nullara Limestone.

No intercalations of Frasnian platform carbonates or the Frasnian part of the Virgin Hills Formation are known, but they may be present at depth. The lower age limit is thus unconstrained. The silty marginal-slope deposits of the Virgin Hills Formation indicate an influx of silty terrigenous material into the basin, and deposition of the lower part of the Barramundi Conglomerate may coincide with that of the Virgin Hills Formation. Some of the Piker Hills Formation is very sandy, grading to granule and pebble conglomerate, and may be a distal facies of the Barramundi Conglomerate. If so, conglomerate deposition extended into the *postera* Zone (about 366 Ma, Gradstein et al., 2004) and spanned a total of more than 15 m.y.

Stony Creek Conglomerate

The Stony Creek Conglomerate is exposed west-northwest of the Barramundi Range, immediately south of the Stony Creek Fault and west of Boab Creek. It is apparently wholly Frasnian, based on intercalated platform limestones of that age. The conglomerate was laid down largely as fan-delta deposits, with some submarine-fan deposits. It is the only large conglomerate body that is not topographically higher than the adjacent reefal carbonates.

Definition

The name Stony Creek Conglomerate was given by Guppy et al. (1958) to a conglomerate unit in the Stony Creek area, west of the Barramundi Range. They briefly described the unit. Playford and Lowry (1966) provided further descriptions, but did not specify a type locality. It is here specified as the area from midway between Stony Creek Bore and 600 Bore, north to the bounding fault with the Precambrian (from about AMG Zone 51, 817500E 8009300N to 816000E 8014300N). This area shows interfingering between the conglomerate and both platform (Pillara Limestone) and basin (Virgin Hills Formation) deposits.

Lithology

The Stony Creek Conglomerate consists of subrounded to well-rounded polymictic cobble and boulder conglomerate, with lesser sandstone. North of Stony Creek, the formation contains a higher percentage of granitic clasts than other conglomerate bodies; as much as about 80% according to Playford and Lowry (1966). Many clasts include the same rock types as those exposed immediately to the north in the King Leopold Orogen.

Exposures south of Stony Creek show abundant quartzite pebbles, and Playford and Lowry (1966) doubted that this part of the conglomerate could be Devonian, based on its apparently unconformable onlap onto older conglomerate as shown from air-photo trends. However, intercalations of Pillara Limestone into this quartzite-rich conglomerate were identified during the present mapping program, near Blue Bush Bore, showing that the whole of the conglomerate body is Devonian in age. The apparent unconformity is attributed to fan avulsion, and the lithological change resulted from a local variation in provenance.

Distribution and thickness

The Stony Creek Conglomerate is recognized in the Stony Creek area in the northern Margaret Embayment, both north and south of Stony Creek. Playford and Lowry (1966) considered that the formation was probably

less than 150 m thick. However, with the inclusion of conglomerate south of Stony Creek, the thickness is here estimated to be 200 to 300 m. The southward dips seen south of Stony Creek (see Plates 3 and 7) are interpreted to be mainly depositional.

An east-trending fault compartment immediately south of Stony Creek (centred on AMG Zone 52, 185000E 8011000N) contains a cyclic succession of conglomerate with consistent eastward dips of about 18° (Fig. 202). The conglomerate there has an apparent stratigraphic thickness of 500 to 550 m. The fault compartment is similar in nature to those that bound most of the Galeru Member of the Sparke Conglomerate. A basal glide plane grading into a listric fault against basement is postulated at the eastern end of the compartment, generating the eastward dips, and with hangingwall conglomerates moving progressively further west. The convergence nearby of the Barramundi Fault and the Stony Creek Shear Zone suggests that the compartment may be a local transtensional feature.

Stratigraphic relationships

The Stony Creek Conglomerate interfingers with platform facies of the Pillara Limestone and marginal-slope facies of the Virgin Hills Formation, and is overlain by Frasnian marginal-slope and basin deposits mapped as Napier Formation (near Panorama Bore). The formation is thought to have been laid down as fan-delta and submarine-fan deposits during the middle and late Frasnian.

Big Spring Formation

The Big Spring Formation is a sandstone-dominated unit that rests on the Precambrian Hooper Complex in the Leopold Downs area and grades up into Pillara Limestone.

Definition

The Big Spring Formation was named and described as the Big Spring Member of the 'Pillara Formation' by Read (1973b) after Big Spring on Leopold Downs Station, and was amended to Big Spring Formation by Hocking and Playford (1998b; Plate 2). Read proposed a type section (shown as a representative section by Read, 1973b) along the northeast-flowing creek adjacent to Big Spring, from AMG Zone 51, 754400E 8036500N to about 754000E 8035000N. Hocking and Playford (1998b; Plate 2) mapped a substantially thinner section, north of AMG Zone 51, 754300E 8036100N. The upper part of the unit grades into the Pillara Limestone and the top is placed below it at the first stromatoporoid-limestone bed, although sandstone interbeds continue above this for a few tens of metres.

Lithology

The Big Spring Formation is dominated by sandstone rather than conglomerate. The formation consists of cyclic units as much as 20 m thick, consisting largely of coarse-grained arkosic sandstone but also containing red and green siltstone, shale, and (towards the top of the unit) dolomite and limestone (Read, 1973b). A thin basal conglomerate contains granitic, fine-grained mafic-igneous, and vein-quartz clasts. The overlying section grades upward into the Pillara Limestone by a gradual increase in interbeds of back-reef limestone and dolomite, and a corresponding decrease in the thickness and number of sandstone beds.

Distribution and thickness

The formation is more than 200 m thick near the basin margin in the southeastern Napier Range to Oscar Plateau area, although the thickness is difficult to measure due to poor exposure. Read (1973b) claimed that the unit was present but less than 15 m thick at the base of the section in the Oscar, Pillara, and Emanuel Ranges. However, the present work has shown that the formation is absent in those ranges. In the Emanuel Range the basal Devonian unit is placed in the Cadjebut Formation, while in the other two ranges the basal section forms part of the Pillara Limestone.

Stratigraphic relationships

The Big Spring Formation is Frasnian in age, based on its gradational contact with the overlying Frasnian Pillara Limestone.

Behn Conglomerate

The Behn Conglomerate adjoins the Mount Behn Fault in the central Napier Range. Intercalated platform and marginal-slope limestones show that the unit is of late Frasnian and Famennian age. As with the Sparke, Elma, Barramundi, and Van Emmerick Conglomerates, the conglomerate mass rises to a significantly higher elevation than the preserved top of the reef complexes (about 325 m compared with about 200 m, from SRTM satellite data). The conglomerate cuts through the reef platform with a relatively sharp but interfingering contact, more abruptly than is the case with most conglomerate bodies.

Definition

The Behn Conglomerate (Guppy et al., 1958) forms Mount Behn in the central Napier Range. No type section was designated by Guppy et al., but Mount Behn itself is clearly the type locality.

Lithology

The Behn Conglomerate consists of polymictic pebble, cobble, and boulder conglomerate, with lesser siltstone and coarse-grained poorly sorted sandstone. Quartzite clasts are dominant, but igneous and metamorphic rock types are also present. Locally derived garnetiferous mica-schist boulders and cobbles are locally abundant. Reefal clasts are present but rare, and the clasts are subrounded to well rounded. Slight imbrication and crude bedding are common, and large cross-bedded channel forms are locally recognizable. In one channel, a central conglomerate grades laterally into sandstone at the channel sides. Arcing trails and trackways are locally preserved on sandstone bedding planes, indicating subaqueous deposition.

There is a suggestion of two units within the Behn Conglomerate, a lower, sandier, polymictic conglomerate,

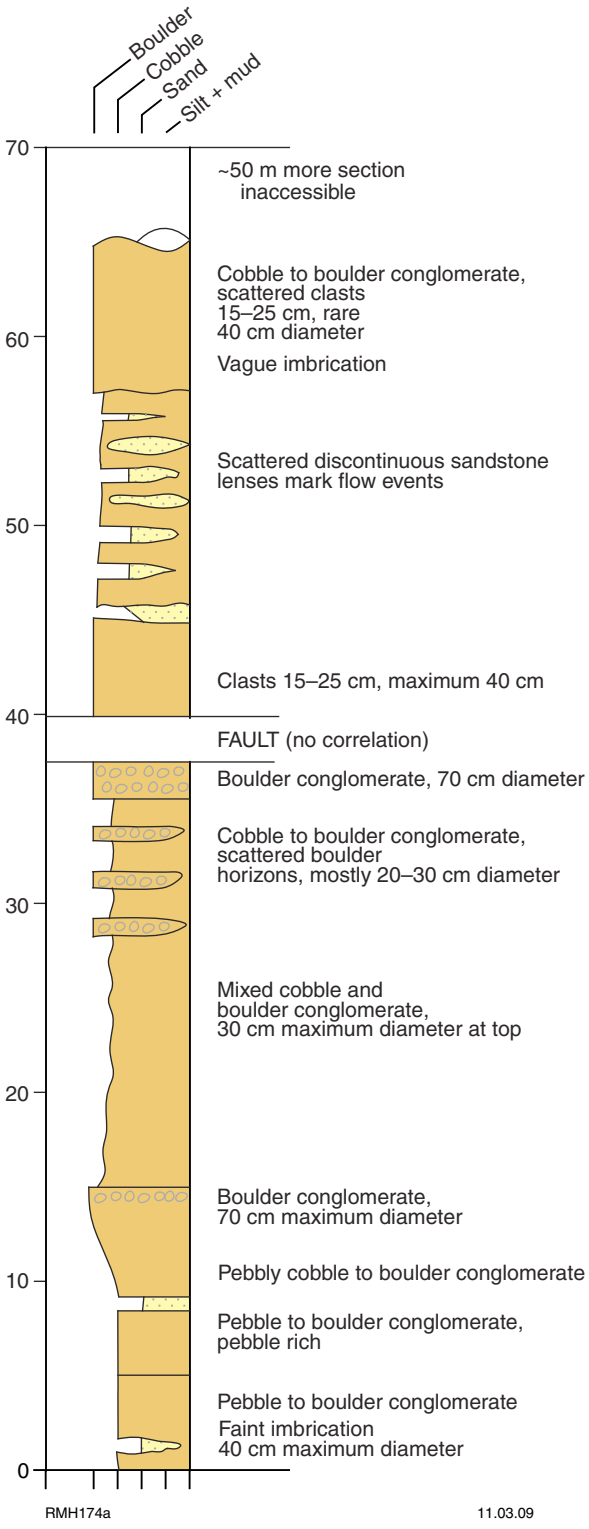

Figure 200. Measured section, Barramundi Conglomerate, northeast Barramundi Range. For legend see Figure 185.

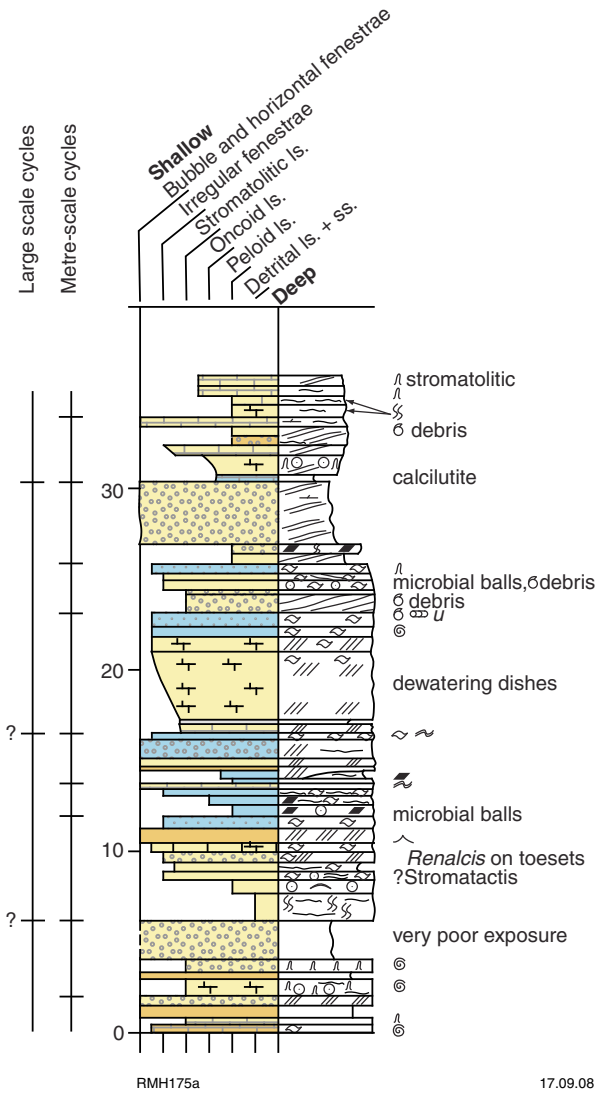

Figure 201. **Measured section, Nullara Limestone interfingering with Barramundi Conglomerate near Fly Bore. The section is located between the two main conglomerate fans that form the Barramundi Conglomerate. For legend see Figure 185.**

Figure 202. **(below) Cyclic conglomerate in the Stony Creek Conglomerate adjoining the Stony Creek Fault. Each cycle is about 5–10 m thick, with recessive-weathering granule conglomerate 1–2 m thick at the base, and pebble to boulder conglomerate forming the rest of each cycle.**



and an upper, less-sandy, conglomerate, with quartzite clasts predominating. This may reflect local variations in provenance and energy levels, rather than being a significant stratigraphic difference.

Amphipora limestone (Pillara Limestone) is present on the northwest face of Mount Behn, interbedded with cobble and boulder conglomerate dominated by quartzite and metamorphic clasts.

Distribution and thickness

The Behn Conglomerate outcrops in a well-defined area about 6.5 km wide, centred on Mount Behn. The conglomerate body is largely flat lying, and the height of Mount Behn above the plain, about 230 m, provides a minimum thickness for the unit. At least another 100 m is likely to be present in subcrop.

Stratigraphic relationships

An interfingering tongue of *Amphipora*-rich Pillara Limestone (Frasnian) is exposed on the northwest side of Mount Behn (AMG Zone 51, 718300E 8065900N), and on the southeast side of the mountain the conglomerate interfingers with and grades into Famennian marginal slope deposits. The conglomerate grades up into distal Napier Formation containing a Famennian fauna on the south side of Mount Behn (AMG Zone 51, 720300E 8061500N). These relationships indicate a late Frasnian and Famennian age for the formation, and deposition is thought to have been in lower alluvial-fan, fan-delta, and submarine-fan settings. The base of the conglomerate is not exposed, but is thought to be early to middle Frasnian.

Van Emmerick Conglomerate

The Van Emmerick Conglomerate is the most northwestern of the conglomerate bodies associated with the reef complexes, and is of Frasnian and Famennian age. It is bounded to the north by the normal Van Emmerick Fault, which in the Precambrian hinterland joins the Mondooma Thrust.

Definition

The Van Emmerick Conglomerate (Guppy et al., 1958) forms the Van Emmerick Range (near the northwest end of the Napier Range), the conglomerate that forms Wunala Hill (northwest of Hawkstone Creek), and a much smaller body of conglomerate, 5 km northwest of Wunala Hill. The type section of the formation is here specified as being along the eastern edge of the Van Emmerick Range, where conglomerate is exposed in a strike ridge and gully, from about AMG Zone 51, 676600E 8109400N to 675600E 8109800N.

Lithology

The Van Emmerick Conglomerate consists of polymictic pebble and boulder conglomerate, with lesser amounts of intercalated coarse-grained poorly sorted sandstone. The conglomerate is notably richer in granitic clasts than most other conglomerate bodies, with those clasts commonly making up more than 20% of the total clasts and increasing upwards to about 95%. Clasts are usually well rounded, most being around 15 to 20 cm and rarely more than 1 m in diameter. Sandstone interbeds commonly show large-scale cross-bedding, unlike the conglomerates, which generally appear massive but in places are steeply imbricated. Most bedded units dip southward, forming very large-scale foresets, tens of metres thick, that outline alluvial-fan to fan-delta shapes. Both the conglomerates and interbedded sandstones show complex scour-and-fill structures, indicative of rapid episodic flow and shallow-water conditions (Fig. 203). Bioturbation is locally present in sandstone bodies, in places forming burrowed laminated beds that are generally near the top of conglomerate–sandstone couplets. Superimposed conglomerate bodies can be distinguished on the basis of morphology, with the higher bodies being perched on, and prograding over, the lower bodies.

Distribution and thickness

The peak of the Van Emmerick Range is 185 m above the plain level, and the conglomerate is estimated to be at least 200 m, and probably more than 300 m, thick. Elevations above sea level are: about 275 m at the peak, about 165 m on the limestone plateau, and about 90 m on the plain (based on SRTM satellite data).

Stratigraphic relationships

The base of the Van Emmerick Conglomerate is not exposed. The formation interfingers with the Frasnian Pillara Limestone and the Frasnian and Famennian Napier Formation. It is thought to have been deposited as alluvial-fan, fan-delta, and submarine-fan deposits. The formation appears to form two distinct superimposed bodies, the older being Frasnian and perhaps early Famennian, and the younger being Famennian. The Famennian age of the upper conglomerate is based on lycopod impressions found near the peak of the range. The formation may be similar in age to the combined Elma and Barramundi Conglomerates.

Paleocurrent patterns

Paleocurrent measurements in the conglomerate bodies are based on cross-bedding in sandstone interbeds and imbrication in conglomerates (Fig. 204). In some exposures in the Van Emmerick Range, large-scale bedforms can be distinguished in places where cone-shaped bodies make up a significant part of the outcrop. Foreset shapes are several tens of metres high and hundreds of metres long. Small-scale sedimentary features such as cross-bedding, scour-and-fill, bioturbation, and clast orientation (transverse rather than down-slope elongations) indicate deposition in subaerial to shallow subaqueous environments, with transport mainly by traction currents rather than mass-flow processes.

Paleocurrent datasets are available for the Van Emmerick, Barramundi, Sparke, and Bobs Bore Conglomerates, and for a siliciclastic interval within the Nullara Limestone on Larrawa Station, at the southeastern end of the Devonian

outcrops. The paleocurrent data from these locations reflect local exposures and positions on conglomerate fans (e.g. an overall westward-facing fan may locally show northwest or southwest directions of sediment flow). The Sparke Conglomerate and Larrawa exposures share similar westward flow patterns, presumably arising from their positions at the junction of the Proterozoic King Leopold and Halls Creek Orogens, where drainage may have been influenced by the Proterozoic Glidden Fault and similar structures, that caused flow to be channelled in this direction. Slightly further west, the Bobs Bore Conglomerate, in deep-water submarine-fan sandstone and conglomerate, shows a west to northwest current pattern, parallel to the margin of the Pillara Inlier. This feature is interpreted to be a result of longshore flow.

The Barramundi and Van Emmerick Conglomerates show more diffuse fan-like patterns, normal to the basin boundary and suggestive of point sources. In detail, paleocurrents fanned out radially, with, for example, southward dominance on the south side of the Van Emmerick body. Directions facing towards the basin margin are generally derived from small cross-sets that may have formed in part by minor reworking by waves in shallow subaqueous conditions. However, they do not appear to be winnowed enough to be the result of wave reworking, and must instead have been formed in part from eddies on the faces of fan deltas.

Provenance

The conglomerate bodies are all polymictic, but to varying degrees. The dominant clast types vary between and within bodies, but quartzite, identical to that in the Proterozoic Kimberley Basin, is dominant. Granitic clasts are locally abundant, and characterize much of the Van Emmerick and Stony Creek Conglomerates. The granitic clasts were derived from the directly adjacent King Leopold Orogen. Fine-grained, dark-coloured mafic clasts are readily matched with the Hart Dolerite, which intrudes the King Leopold Orogen and the Kimberley Basin. Phyllitic clasts, derived from the King Leopold Orogen, are also present. Clasts derived from Precambrian carbonates (primarily Neoproterozoic) are rare. Both granitic and mafic-igneous clasts are commonly fresh, with only minor weathering of feldspars and mafic minerals. Clasts derived from Devonian reefal platforms are present locally, and clearly indicate syndepositional tectonism, with significant burial followed by uplift of platforms. In the Galeru Member, the dominant clast types vary from cycle to cycle and a few cycles are dominated by reefal clasts. The source area for conglomerate in the member was clearly variable, and no consistent pattern has been recognized from changes in clast dominance through the measured section.

From the rock types present as clasts, the King Leopold Orogen and Kimberley Basin clearly served as the main sources of the conglomerates. Many clasts are well

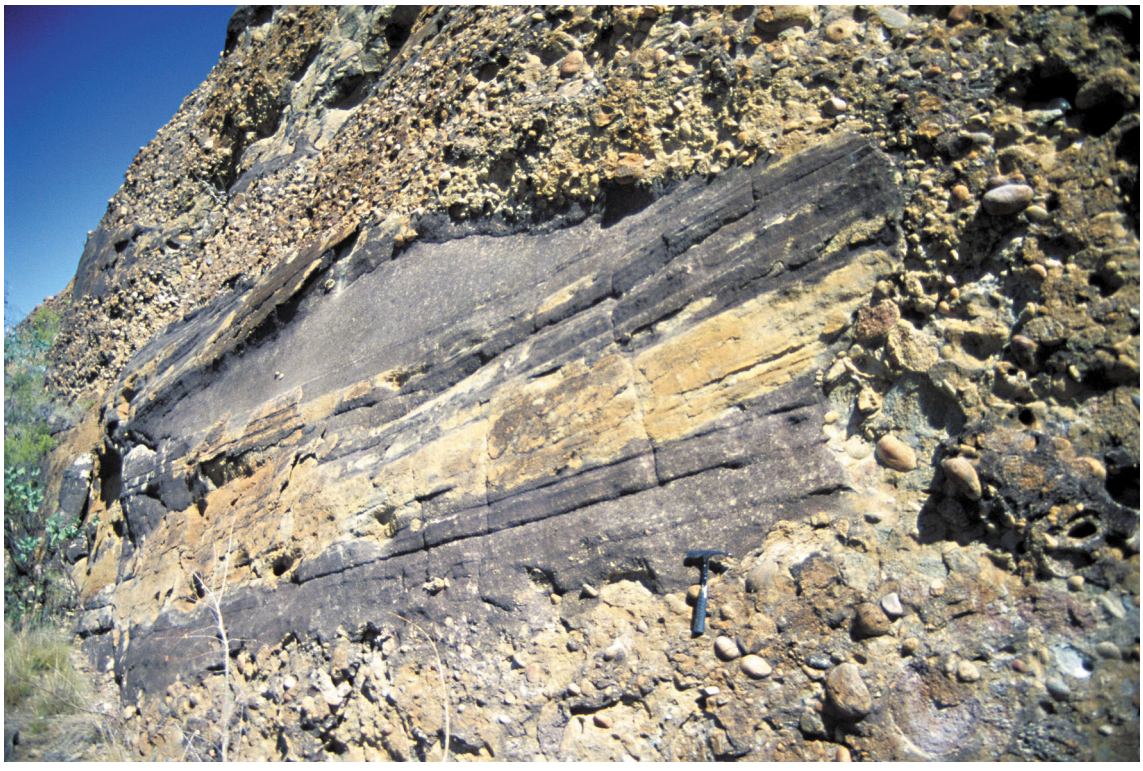

Figure 203. Scour-and-fill structures in Van Emmerick Conglomerate, showing a mass of coarse-grained cross-bedded sandstone that is underlain, overlain, and truncated by conglomerate. Photo by Roger Hocking.

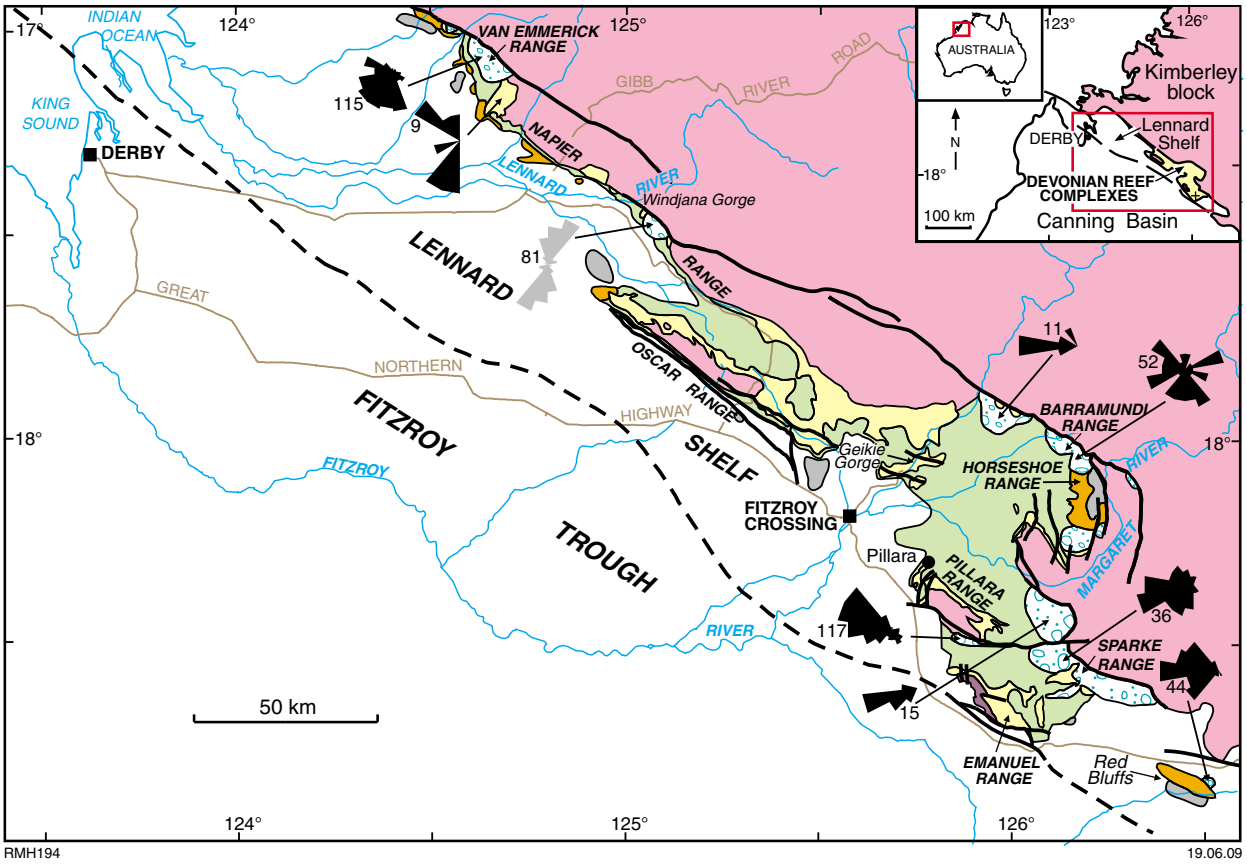

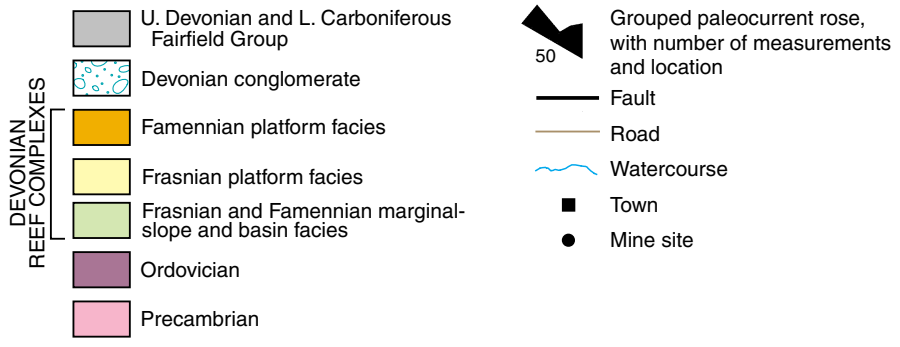

Figure 204. Regional paleocurrent data for the Devonian conglomerates. These data generally reflect local conditions in conglomerate bodies rather than regional trends, except for those in the Sparke and Bobs Bore Conglomerates.

rounded, even though the source areas are commonly only 10 km or less away. The conglomerates have bulbous fan shapes and were laid down in front of faults that were active during the Devonian. The conglomerates formed alluvial fans, passing into fan deltas and submarine fans (Figs 179, 180).

Boulders of Kimberley Basin quartzite several metres in diameter are present on the south side of Mount Elma (Fig. 189; GPS AMG Zone 52, 206045E 7978910N and 206120E 7978935N), and these are thought to have originated as talus from the scarp of the Mount Elma Fault. The large boulders must have come from a source somewhat closer than the nearest exposure of Kimberley Basin quartzite today, which is about 6 km to the east. Perhaps they came from an unrecognized fault sliver like the one situated 8 km north of Mount Elma (AMG Zone 52, 207500E 7990300N).

It is possible that some clasts in the conglomerates are derived from the Neoproterozoic diamictites that are known from the Kimberley Plateau, but there is no direct evidence to support that possibility. If a conglomerate had been sourced from a glacigene diamictite it might be expected to show a wide range of rock types in the clasts, whereas many of the conglomerate bodies are virtually monomictic. For example, granitic clasts dominate in the Van Emmerick and Stony Creek conglomerates, and most others are dominated by quartzite clasts.

Conglomerate deposition

The conglomerate bodies were built as alluvial fans, fan deltas, and submarine fans (Figs 179, 180). Depositional slopes of conglomerate fans were generally in the range of 10° to 20°. The depositional settings of the conglomerates are determined largely from their relationships to the interfingering reef complexes, and by sedimentary structures in the conglomerates and other associated siliciclastic rocks. Intercalations or lenses of platform facies (Pillara and Nullara Limestones) and marginal-slope facies (mainly Virgin Hills, Piker Hills, and Napier Formations) are commonly associated with the conglomerates. For example, transitions from platform to marginal-slope facies directly associated with conglomerate are clearly visible on the western and southern flanks of Mount Elma (around AMG Zone 52, 205750E 7981800N to 205350E 7981650N) and in the central Sparke Range area (around AMG Zone 52, 197800E 7955500N). Conglomerates are most commonly associated with platform, basin, and lower marginal-slope carbonates of the reef complexes. They occur less commonly with reefal-slope and upper fore-reef deposits, presumably because the depositional slopes were higher than the angle of repose for conglomerates.

The geometry of most conglomerate bodies is fan shaped or consists of a series of fans, indicating single or multiple point sources. The Sparke Range is a linear apron or wedge of conglomerate, but within the apron, individual fans can be distinguished as local culminations.

In the Van Emmerick Range, the fan-shaped geometry can be distinguished in major bedding planes that extend for hundreds of metres down the depositional slopes at angles of several degrees, and with complex scour-and-fill structures indicative of rapid episodic flow and shallow-water conditions (Fig. 203). Traces of bioturbation are present. These features point to subaqueous fan-delta settings, although other parts of the formation were no doubt deposited as subaerial alluvial fans.

As noted earlier, small patch reefs with associated marginal-slope deposits interfinger with the Mount Elma Conglomerate south and southwest of Mount Elma (Figs 192, 193). It is remarkable that the reefs were able to continue growing in an environment that was subject to periodic floods of fresh water carrying masses of coarse conglomerate and finer terrigenous detritus.

Each of the major outcropping conglomerate bodies was deposited during periods ranging from perhaps 5 to more than 15 m.y. They are not the products of reciprocal deposition during lowstands as claimed by Kennard et al. (1992), Whittam et al. (1994), and Southgate et al. (1999), but were laid down as alluvial-fan, fan-delta, and submarine-fan deposits during sea-level highstands, contemporaneous with the Devonian reef complexes. Conglomerate deposition was most pronounced at times when accommodation was greatest, and deposition of the conglomerates is thought to have resulted from major tectonic pulses. Most conglomerate bodies seem to be of similar ages, perhaps culminating in the late Frasnian and the early to middle Famennian. In the Van Emmerick Range, and possibly elsewhere, conglomerate deposition is thought to have continued into the late Famennian.

Frasnian terrigenous clastic deposits are known in several wells on the outer Lennard Shelf including Aquanita 1, Blina 1, Ellendale 1, Janpam 1, Janpam North 1, Terrace 1, and possibly Meda 1, Meda 2, Mellany 1, Napier 1, and Napier 5 (Crostella, 1998b). They separate the Famennian Nullara Limestone and equivalent marginal-slope deposits from the Frasnian Pillara Limestone and its equivalent marginal-slope deposits. These terrigenous deposits are thought to be equivalents of the major phase of conglomerate deposition that resulted in the Sparke, Mount Elma, and lower Van Emmerick Conglomerates. The 'Famennian redbeds' in Blina 1 and the basal Famennian sands in May River 1 may equate with the younger parts of the Behn and Van Emmerick Conglomerates. Again, these subsurface intersections are interpreted to be long-term, tectonically triggered, highstand deposits rather than reciprocal lowstand deposits.

Cyclicity

Metre-scale cyclicity in sedimentary sequences has been a subject of study for many years, and has long been viewed as a fundamental aspect of platform carbonates (Goldhammer et al., 1987; Anderson and Goodwin, 1990; Elrick and Read, 1991). Interest in sedimentary cycles has sharpened since the development of sequence stratigraphy. Metre-scale cycles are seen to be the building blocks of depositional sequences (Crevello et al., 1989; Drummond and Wilkinson, 1996). Such cyclicity is commonly, but not always, attributed to orbital forcing (Milankovich cyclicity) as discussed by Fischer and Bottjer (1991),

Franseen et al. (1991), De Boer and Smith (1994), Read et al. (1995), House and Gale (1995), Satterley (1996), and Muller and MacDonald (1997).

The expression and causes of metre-scale cyclicity in carbonate platforms has been the subject of numerous papers (e.g. Koerschner and Read, 1989; Osleger and Read, 1991; Goldhammer et al., 1987, 1990, 1993; Kominz and Bond, 1990, 1992; Yang et al., 1995; Sami and James, 1994). Three main mechanisms have been proposed: autocyclicity (Ginsburg, 1971; James, 1984; Hardie et al., 1991), tectonism (Hardie et al., 1986, 1991; Cisne, 1986), and glacially driven eustacy (Fischer, 1964; Goodwin and Anderson, 1985; Read et al., 1986; Goldhammer et al., 1987; Koerschner and Read, 1989; Osleger and Read, 1991).

Two principal types of shallowing-upward metre-scale cycles are present in the platform facies of the Devonian reef complexes: (a) subaqueous cycles, generally limestone dominated, and (b) subaqueous to subaerial cycles, generally limestone dominated in the lower part and sandstone dominated in the upper part (Fig. 205). Recognition of the first cycle type is based primarily on measured sections in the lower Pillara Limestone in the southeast Lennard Shelf (Figs 205–210; Brownlaw et al.,1996; Brownlaw, 2000). A variant of the first cycle type, subaqueous conglomerate shallowing up to platform carbonates, has been noted where the Elma Conglomerate interfingers with platform carbonates, south of Mount Elma. The second type is recognized from sections in the upper Pillara Limestone in the central and northwest Lennard Shelf (Figs 211–215). An extension of the second cycle type, subaqueous to subaerial cycles, is found as the Galeru Member in a localized tectonic setting in the Sparke Range, in the southeast Lennard Shelf (Fig. 216). Subaqueous cycles are also common in the Famennian Nullara Limestone, but have not been studied in as much detail in the present study, partly because of the relatively limited exposures of Nullara Limestone in comparison with the Frasnian Pillara Limestone. They are described separately below because of the differences in lithofacies components between the Frasnian and Famennian.

Methods of study

Sections with a resolution of about 20 cm minimum unit thickness were measured where convenient along the extent of the Lennard Shelf in Frasnian and Famennian platform facies (Figs 206–214). Cycle boundaries were noted during measuring, and the lateral extent of the units was confirmed, generally for more than 200 m. Idealized cycles were recognized at this stage, and verified or amended as sections were drawn up.

Limited statistical manipulation of data has been undertaken. Different lithofacies in the cycles have had markedly different deposition rates and degrees of compaction, ranging from slow deposition and high compaction for shale and some calcareous facies, to fast deposition and moderate compaction for some calcareous facies, and fast deposition with minimal compaction for sandstone and conglomerate. Therefore, the thickness of a lithofacies cannot be used as an analogue for time. Fisher plots and other means of statistical analysis, such as time-series analysis, are of limited use for detailed cycle analysis because the relative proportions of lithofacies in each cycle vary.

Subaqueous cycles, Pillara Sequence

Subaqueous cycles show few or no signs of emergence or subaerial terrigenous progradation. These cycles are present in the lower and middle Pillara Limestone in the southeast Lennard Shelf (Figs 205–210), such as the Hull Range and Guppy Hills (Figs 217, 218) and in the upper Pillara Limestone in the central Lennard Shelf, north of McSherrys Gap (Fig. 212). This type of cycle is commonly

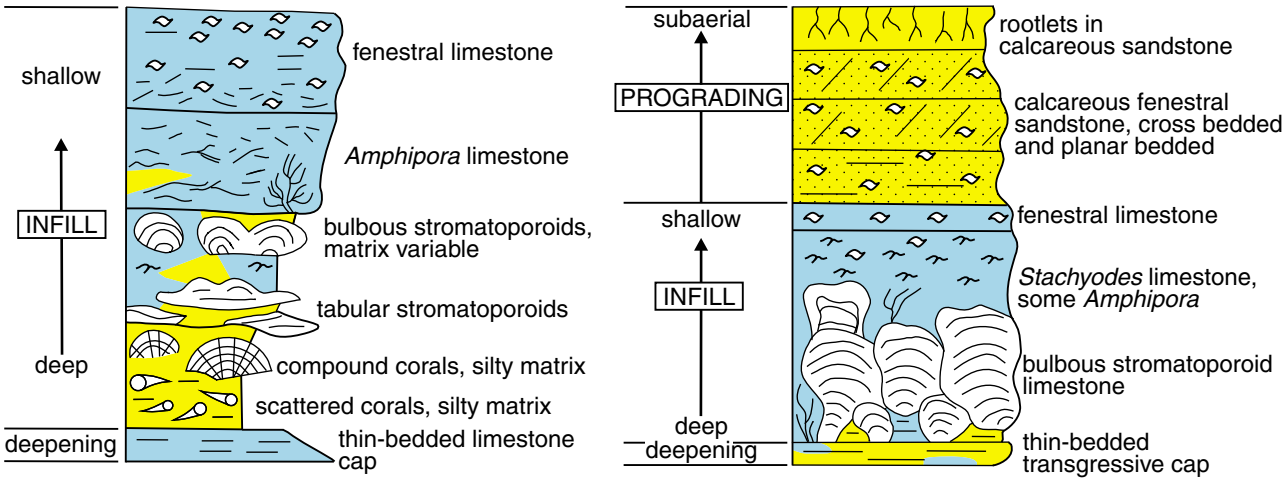

Figure 205. Idealized metre-scale cycles for Givetian–Frasnian platforms, based on measured sections: a) subaqueous cycles, Pillara Limestone, cycle thickness 2 to 6 m, average about 3.5 m; b) subaqueous to subaerial cycles, Pillara Limestone, cycle thickness 2 to 12 m, average about 4 m. For legend see Figure 185.

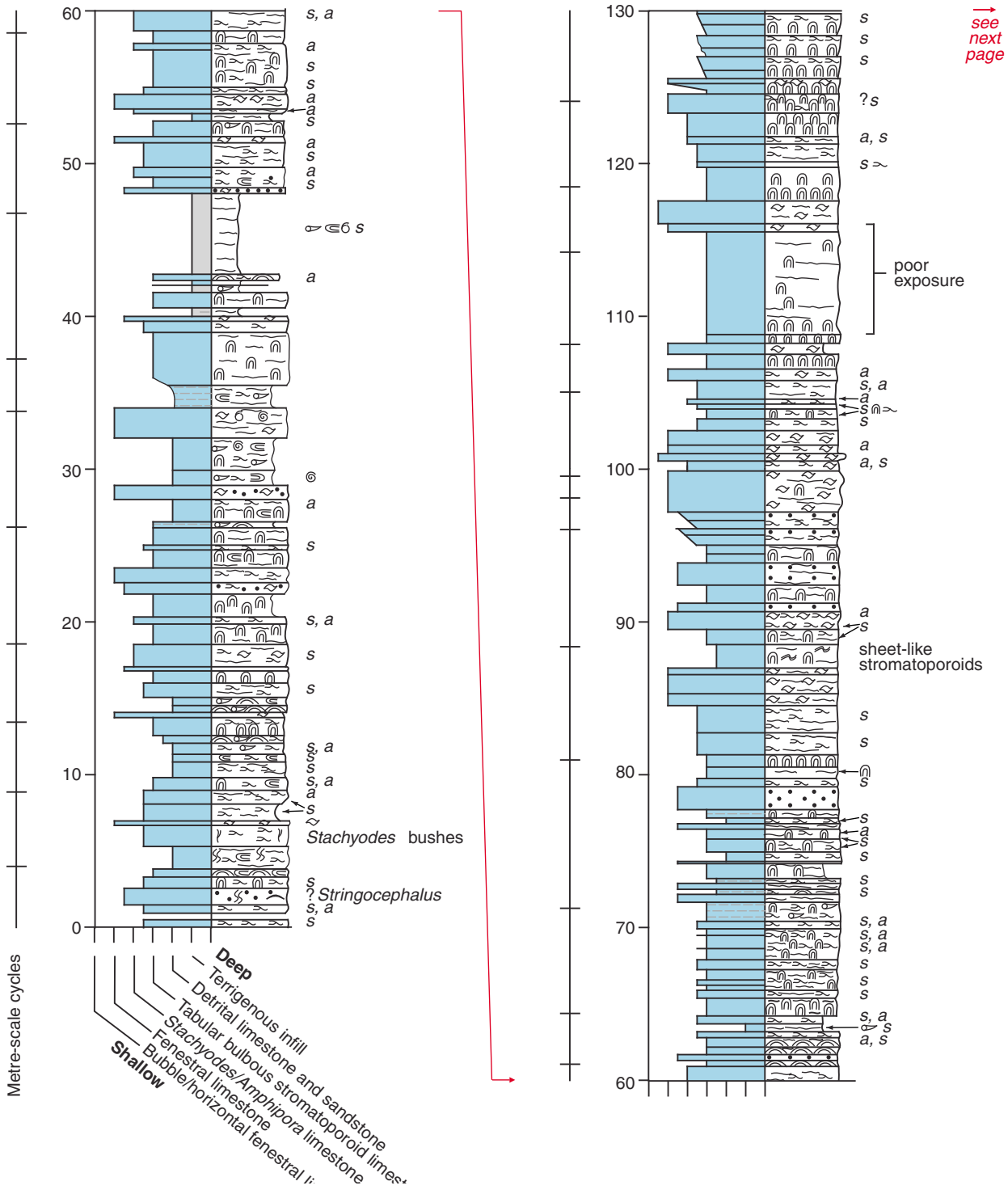

Figure 206. Measured section of lower Pillara Limestone, Menyous Gap. For legend see Figure 185.

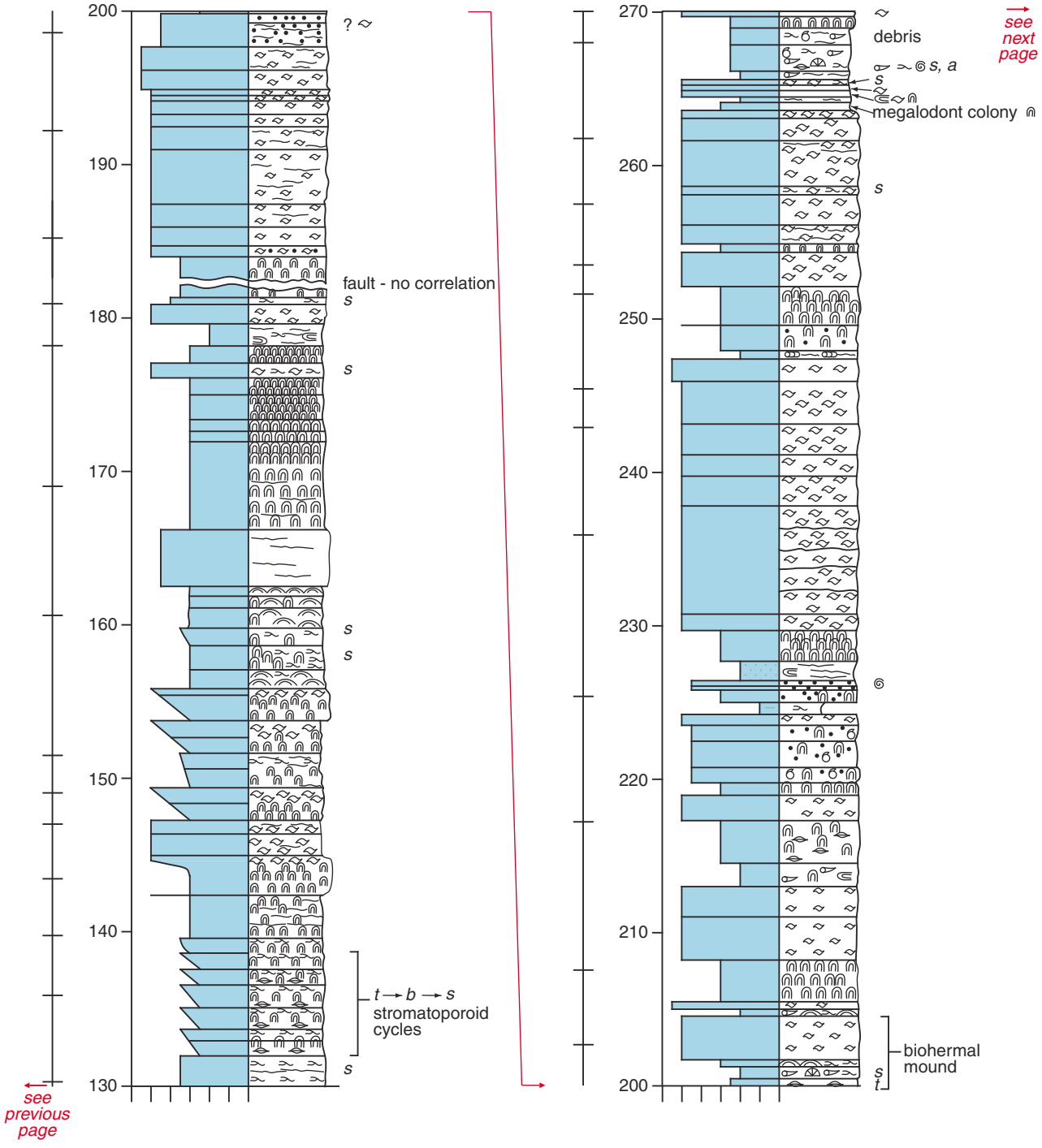
200
190
180
170
160
150
140
130
? ⌓
fault - no correlation
s
s
s
s
t → b → s
stromatoporoid
cycles
s
see
previous
page
270
260
250
240
230
220
210
200
see
next
page
debris
s, a
s
megalodont colony
s
biohermal
mound
s
t

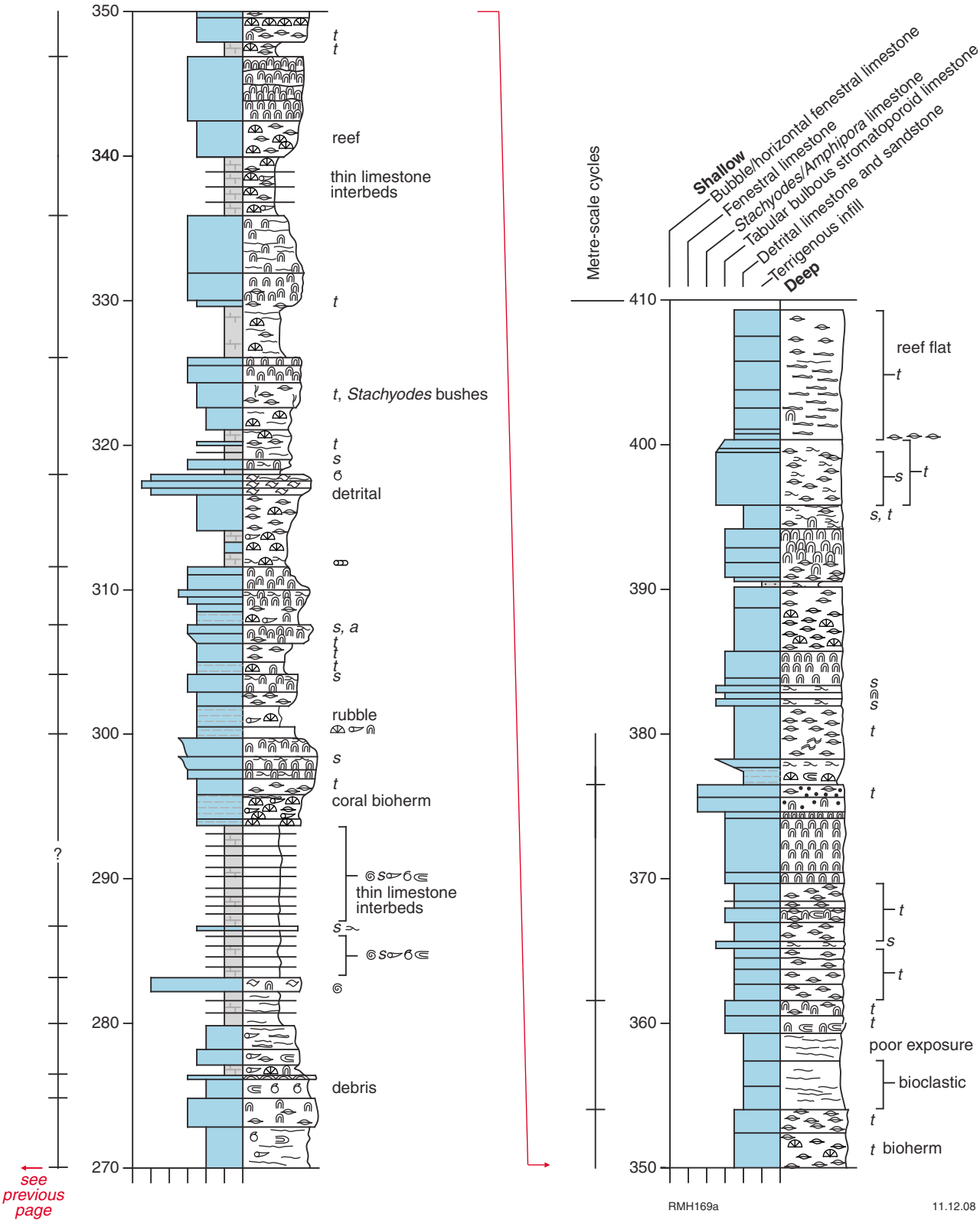
350
340
330
320
310
300
290
280
270
?
reef
thin limestone interbeds
t, Stachyodes bushes
detrital
rubble
coral bioherm
thin limestone interbeds
debris
see previous page
Metre-scale cycles
Shallow
Bubble/horizontal fenestral limestone
Fenestral limestone
Stachyodes/Amphipora limestone
Tabular bulbous stromatoporoid limestone
Detrital limestone and sandstone
Terrigenous infill
Deep
410
400
390
380
370
360
350
reef flat
poor exposure
bioclastic
t bioherm
RMH169a
11.12.08

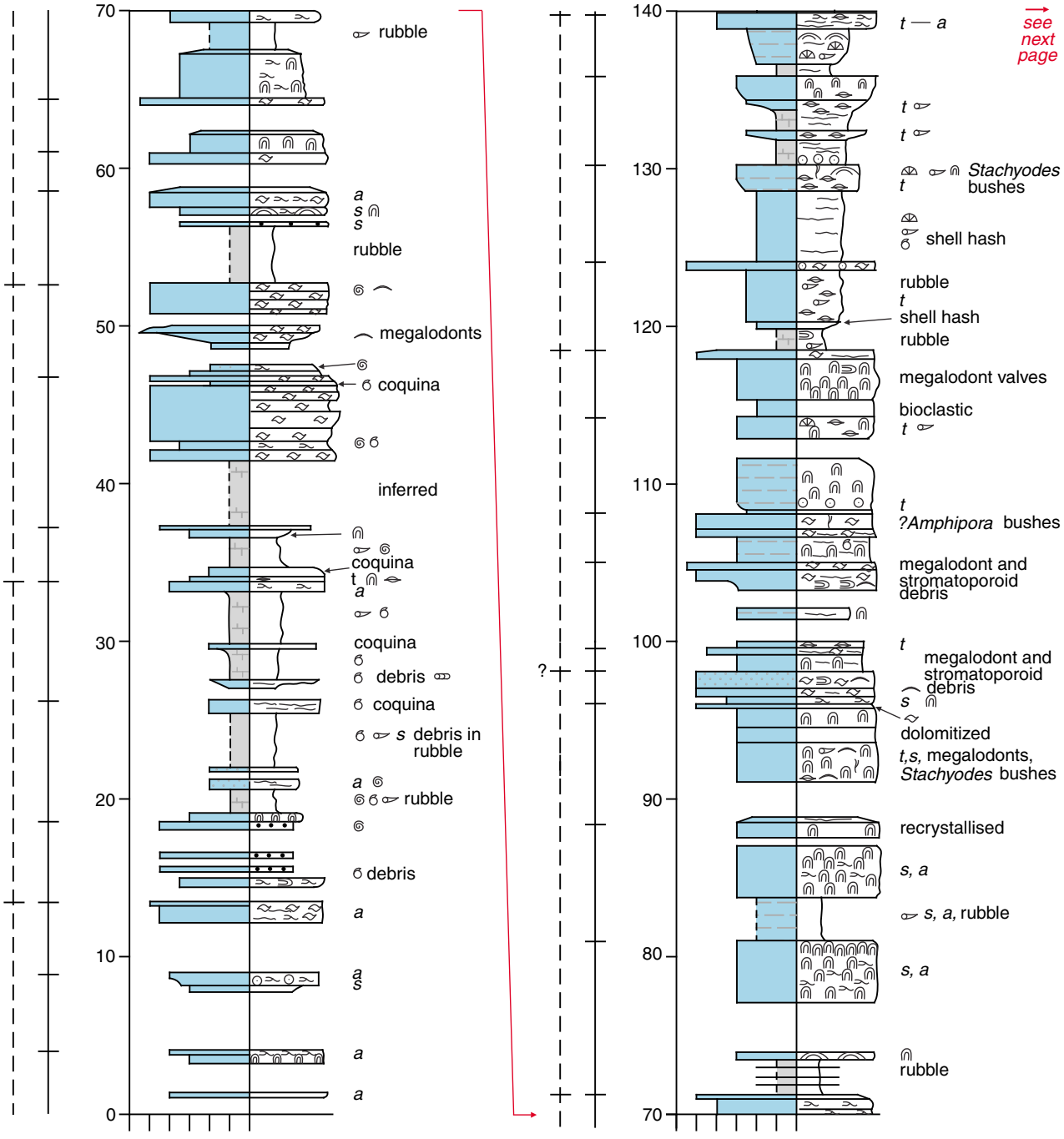

Figure 207. Measured section of lower Pillara Limestone, Guppy Hills. For legend see Figure 185.

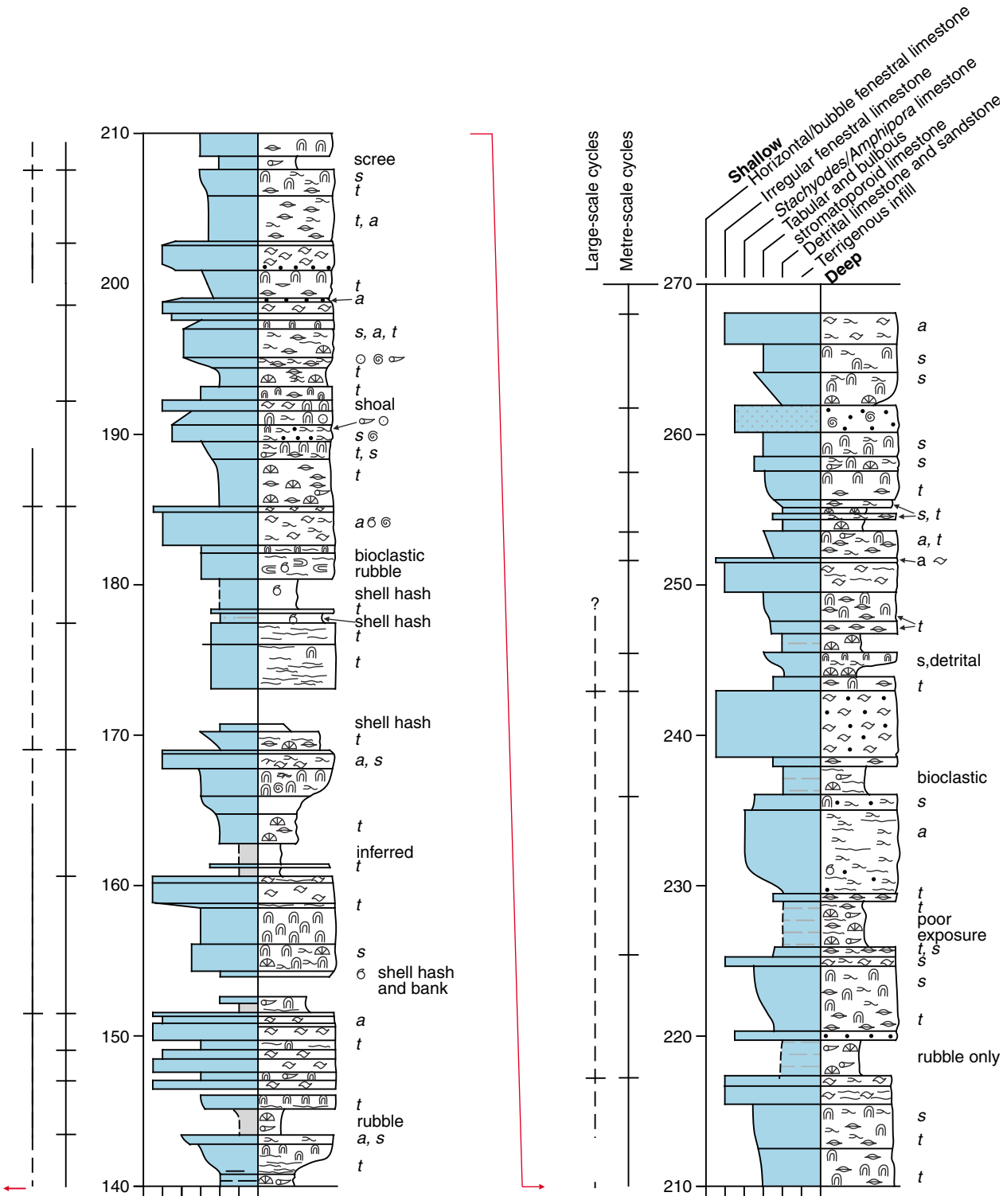
210
200
190
180
170
160
150
140
scree
s
t
t, a
t
a
s, a, t
t
t
shoal
s
t, s
t
a
bioclastic rubble
shell hash
t
shell hash
t
t
shell hash
t
a, s
t
inferred
t
t
s
shell hash and bank
a
t
t
rubble
a, s
t
Large-scale cycles
Metre-scale cycles
?
Shallow
Horizontal/bubble fenestral limestone
Irregular fenestral limestone
Stachyodes/Amphipora limestone
Tabular and bulbous stromatoporoid limestone
Detrital limestone and sandstone
Terrigenous infill
Deep
270
260
250
240
230
220
210
a
s
s
s
s
t
s, t
a, t
a
t
s,detrital
t
bioclastic
s
a
t
t
poor exposure
t, s
s
s
t
rubble only
s
t
t

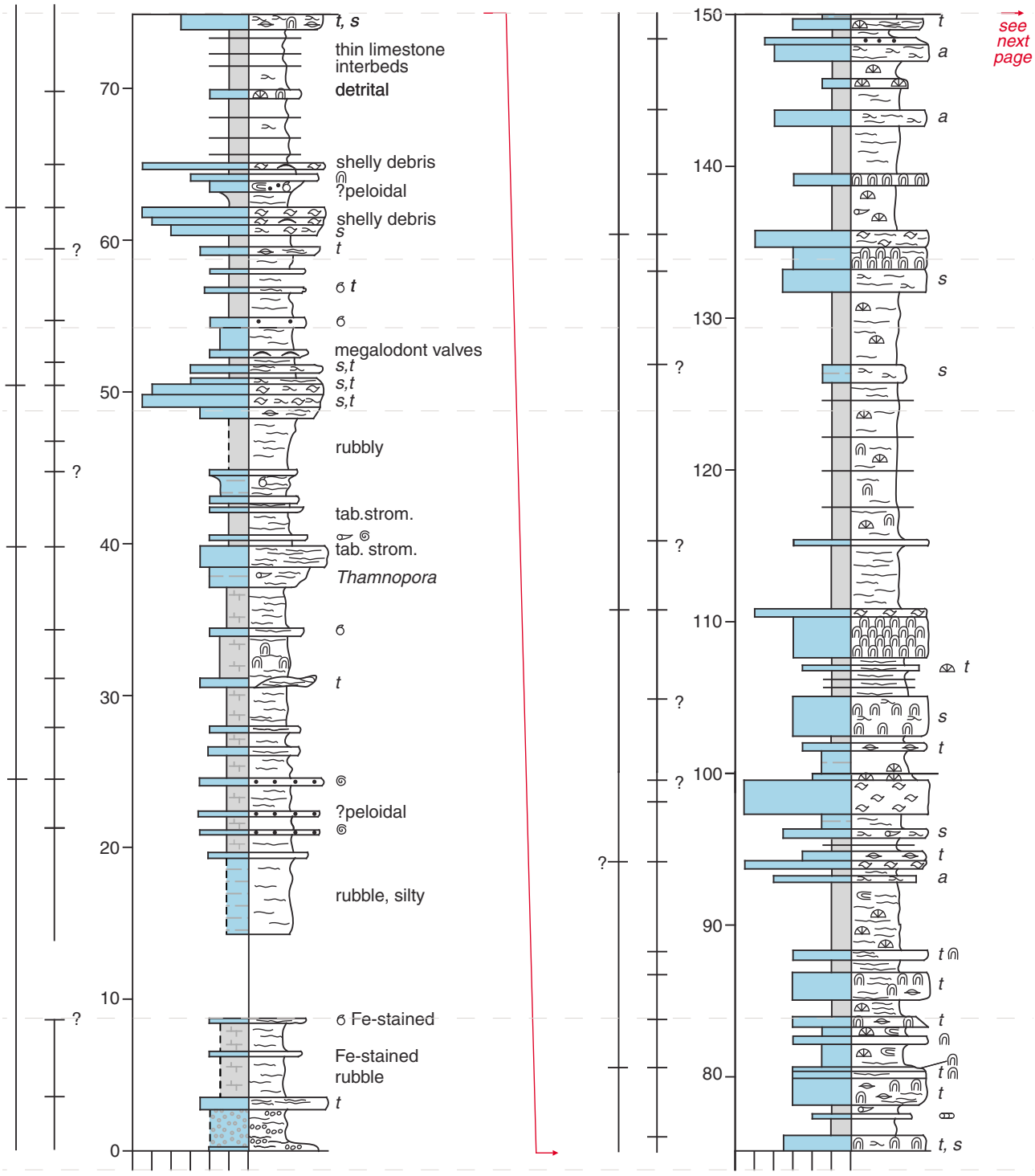

Figure 208. Measured section of lower Pillara Limestone, Horse Spring Range. For legend see Figure 185.

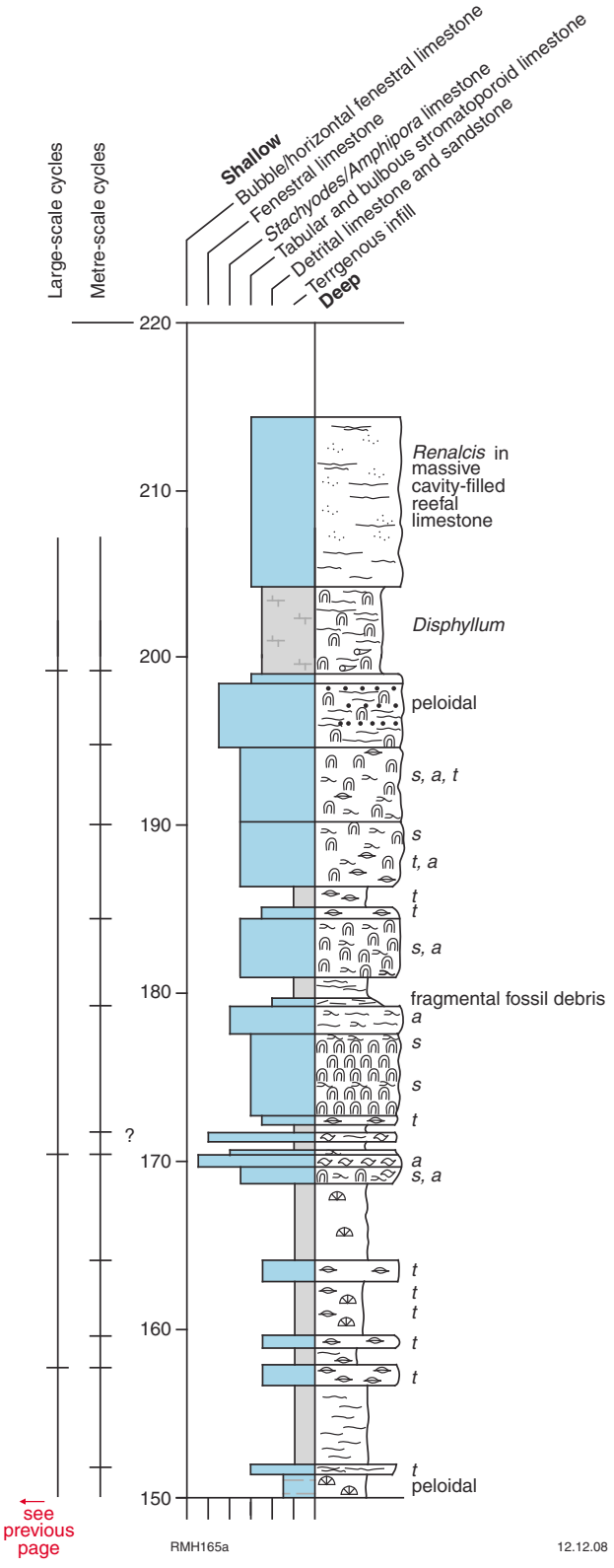

Figure 208 (continued)

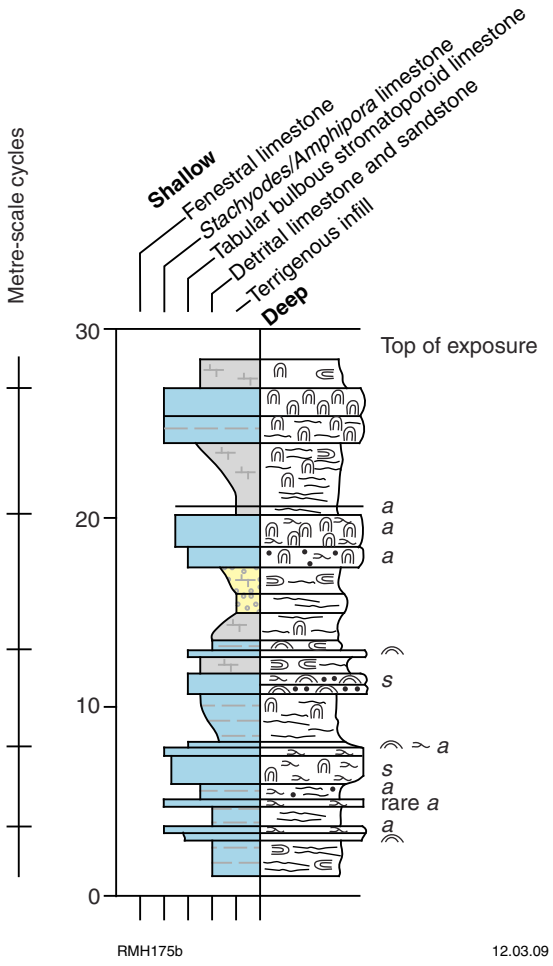

Figure 209. Measured section of basal Pillara Limestone, near Turnoff Dam, Brooking Springs Station. For legend see Figure 185.

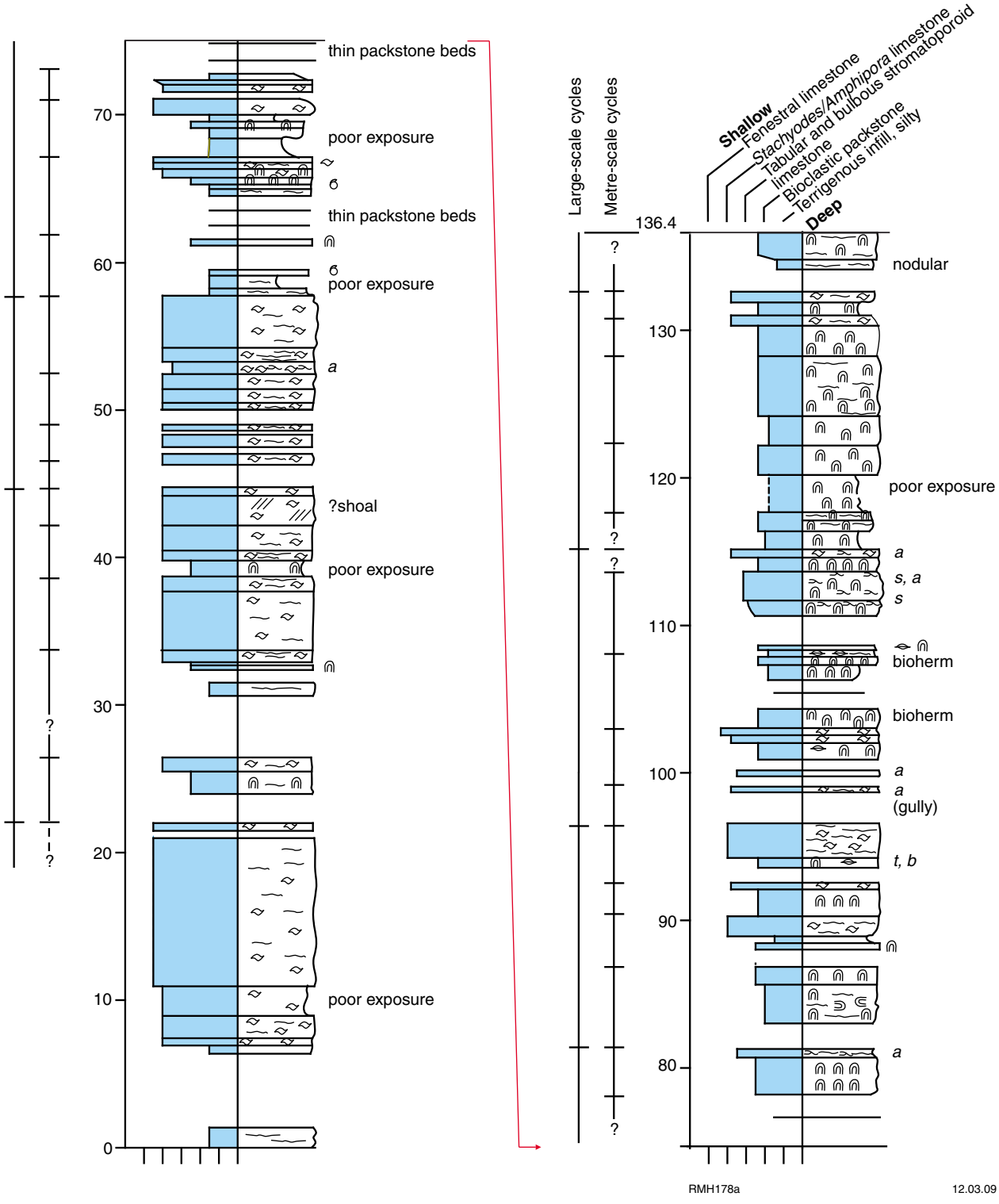

Figure 210. Measured section of Pillara Limestone, Shady Bore, Fossil Downs Station. For legend see Figure 185.

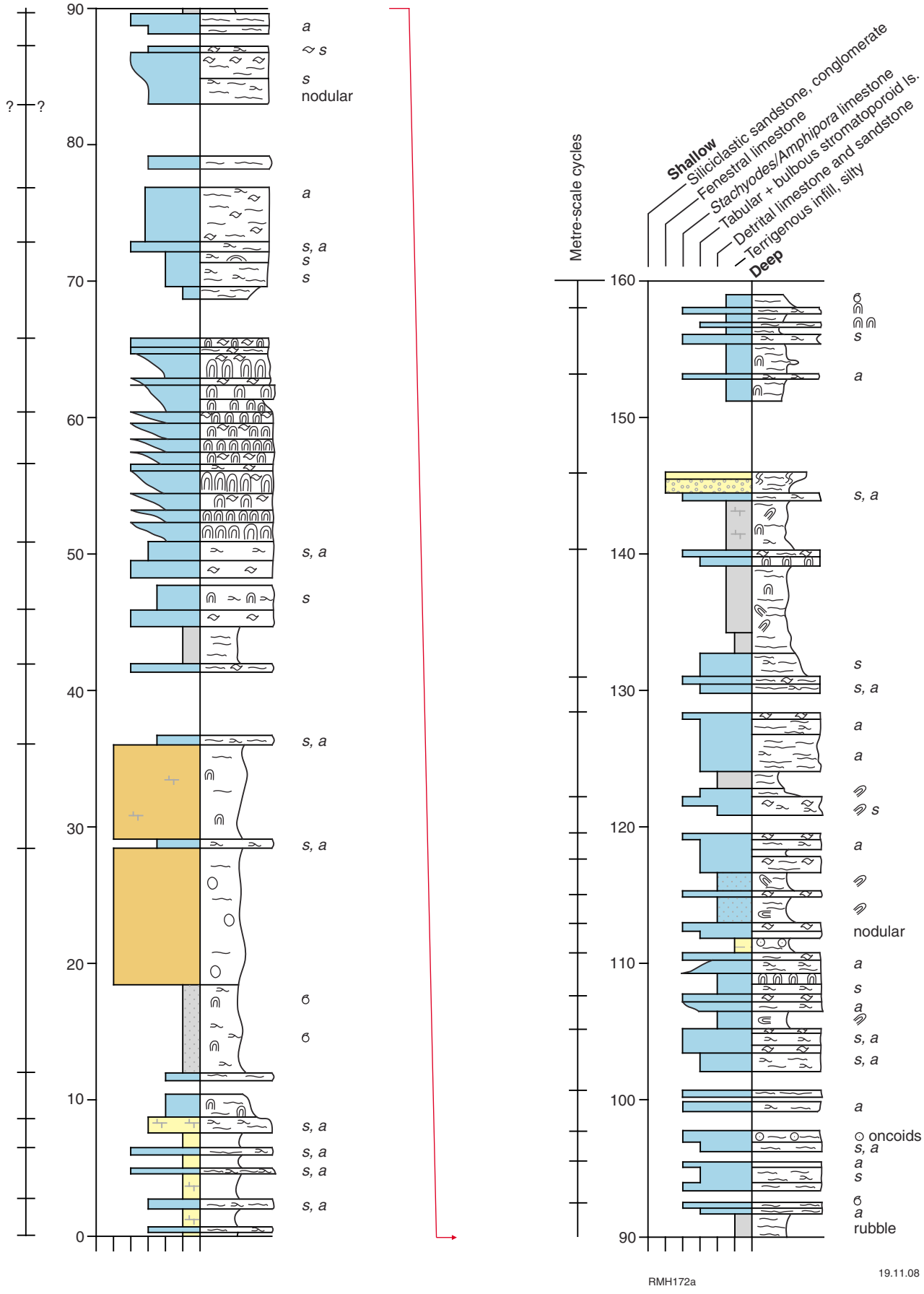

Figure 211. Measured section of upper Pillara Limestone, south of Lawford Spring. For legend see Figure 185.

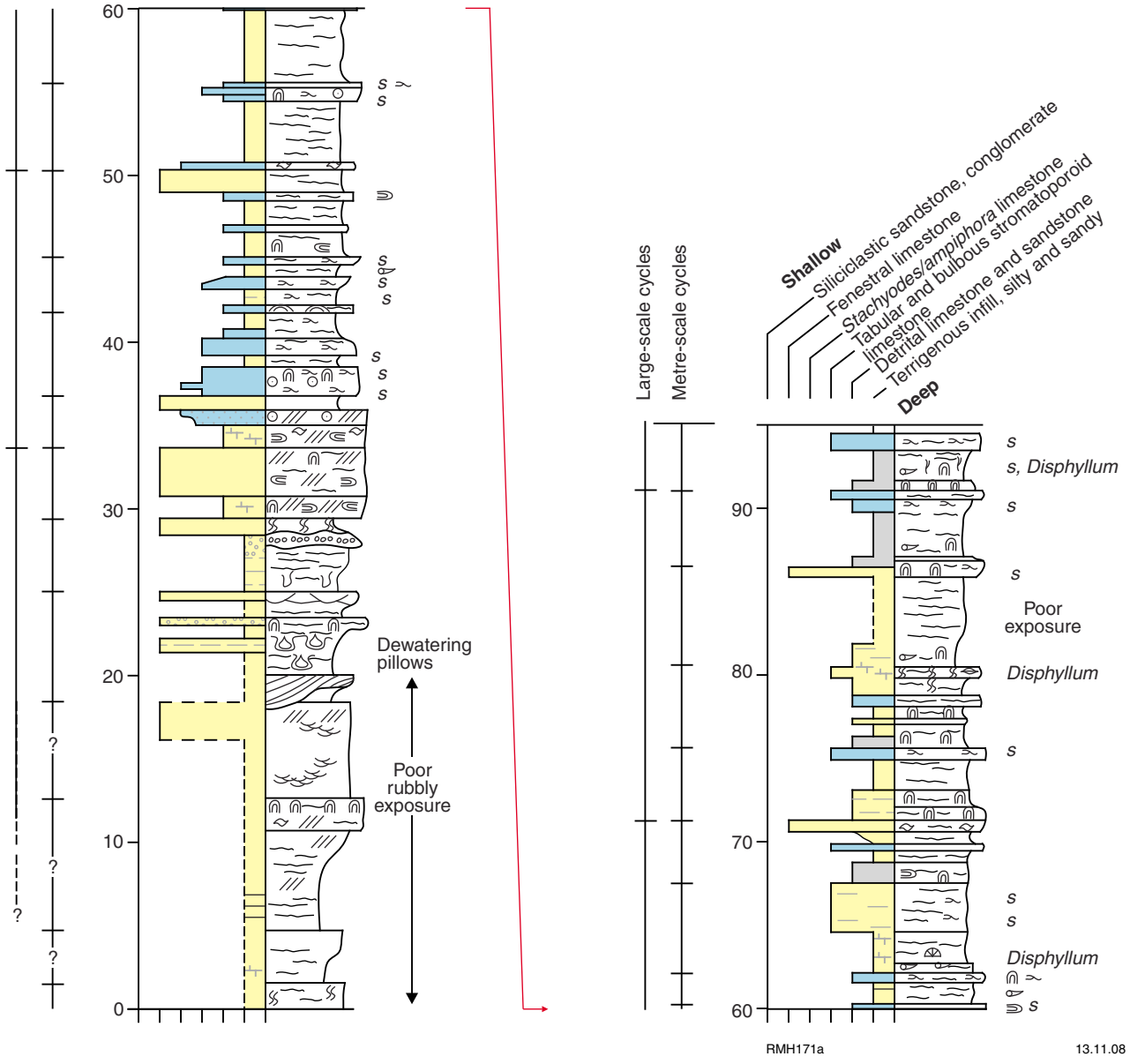

Figure 212. Measured section of upper Pillara Limestone, near McSherrys Gap. For legend see Figure 185.

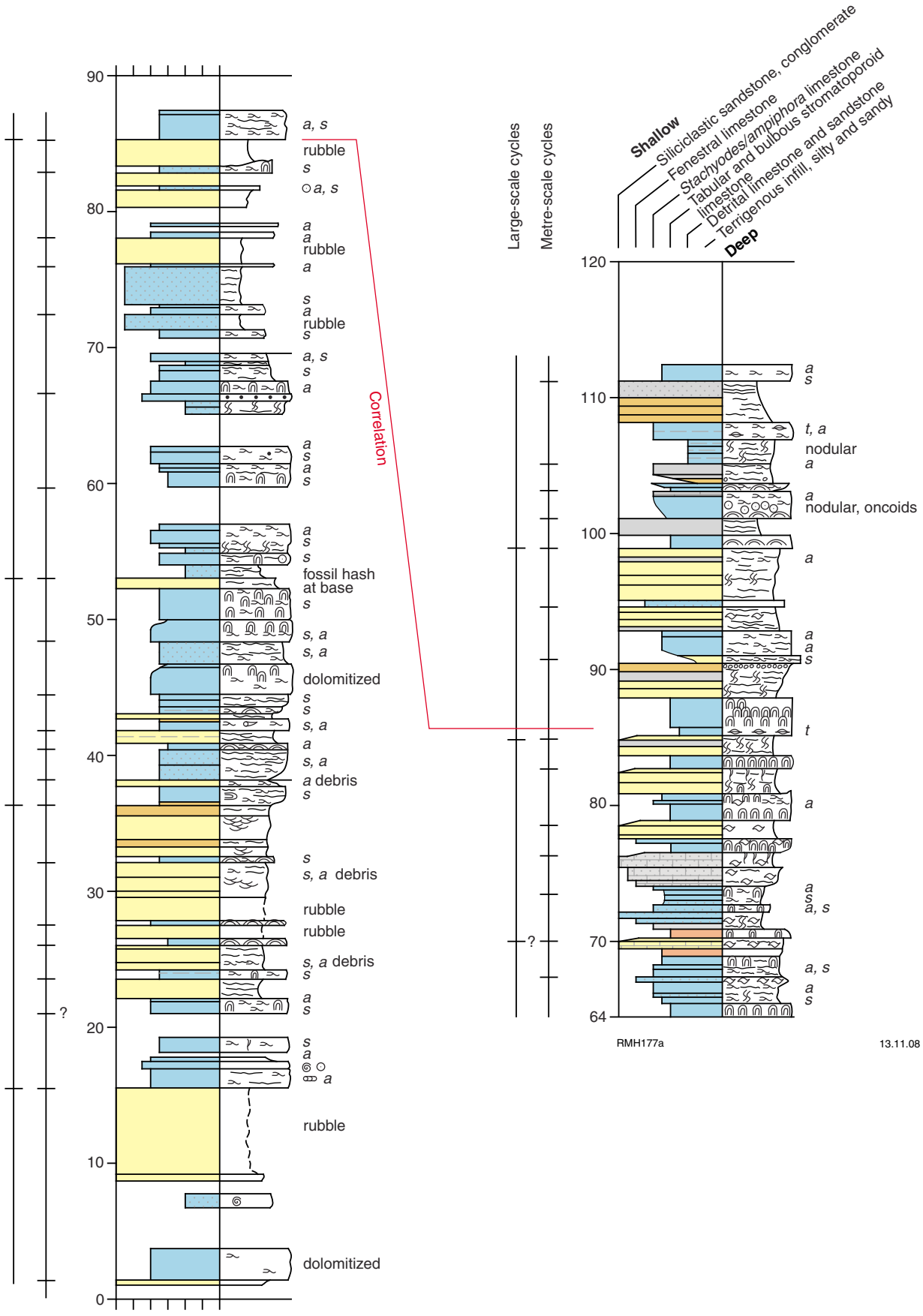

Figure 213. Measured section of upper Pillara Limestone, Windjana Gorge, east end, above *Malambeea*. Left-hand section extends north of the gorge to the *Malambeea* saddle; right-hand section is within the gorge, extending west from below the saddle. For legend see Figure 185.

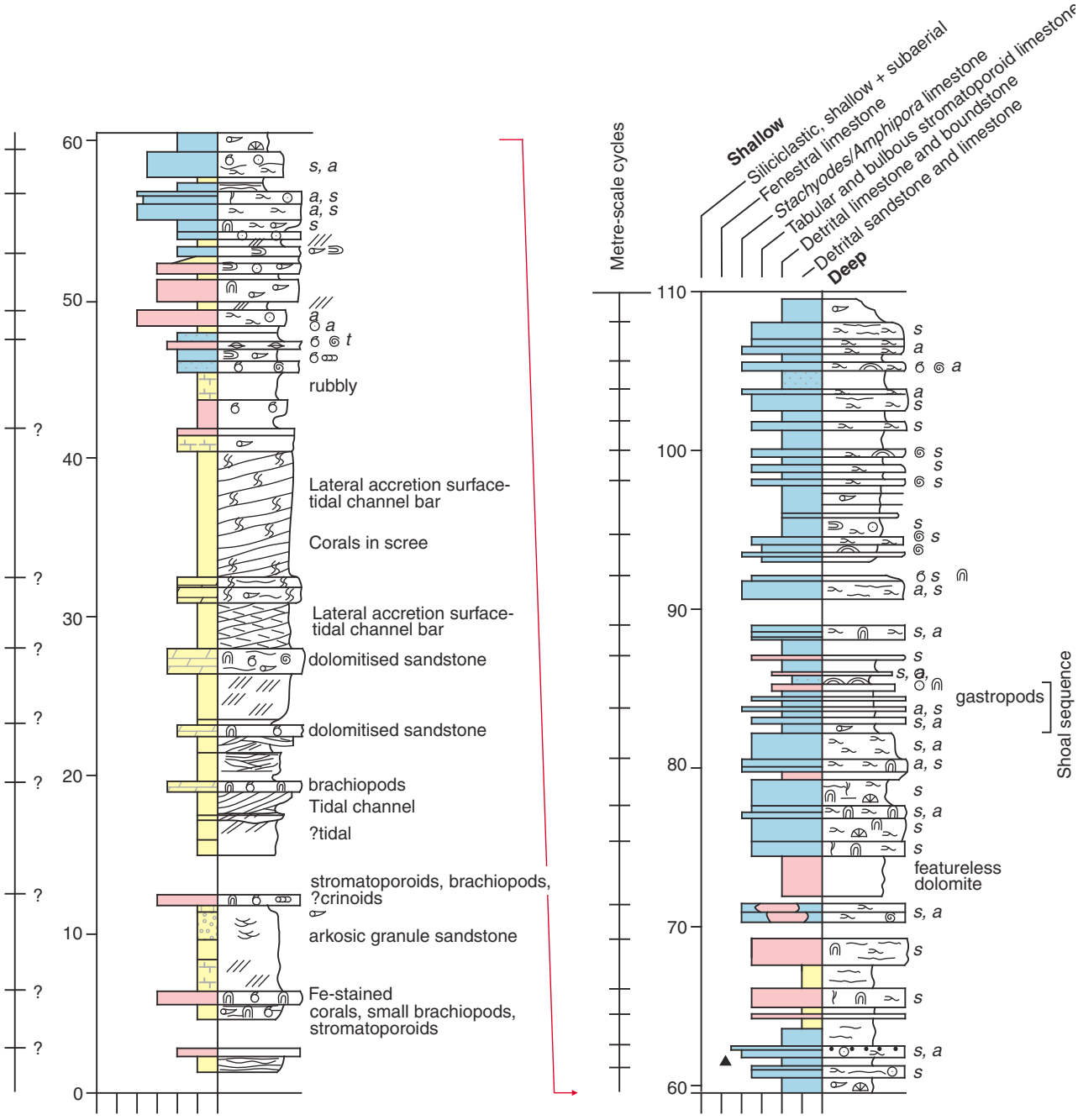

Figure 214. Measured section of upper Pillara Limestone, Surfboard Point, northwest Napier Range. For legend see Figure 185.

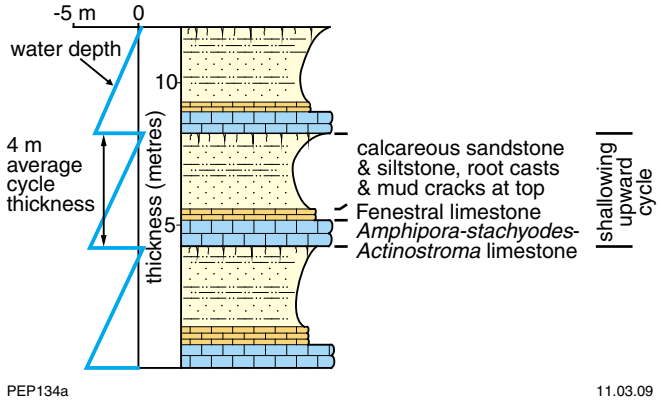

Figure 215. Diagram illustrating cycles in the back-reef Pillara Limestone at Windjana Gorge. Note the 'saw-tooth' nature of relative sea-level, which may be more suggestive of tectonic rather than eustatic control.

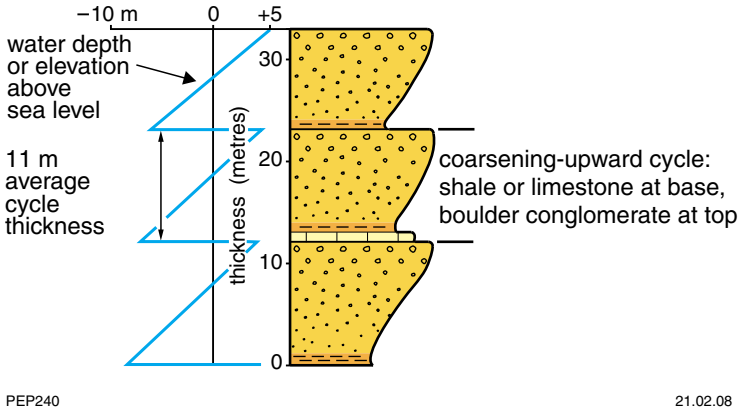

Figure 216. Diagram illustrating cycles in the Galeru Member of the Sparke Conglomerate. The cycles are marine at the base and probably subaerial in the upper part.

masked by terrigenous influx in areas near conglomerate bodies, such as the Margaret Embayment. The cycles described by Read (1973a) from Menyous Gap and by Brownlaw et al. (1996) from Guppy Hills are typical of the subaqueous type. The idealized complete cycle is as follows:

	Lithology	*Depositional setting*	*Common thickness*
Top (shallow)	Thinly laminated fenestral and detrital limestone	Drowning	<20 cm
	Thickly bedded fenestral limestone	Intertidal	30 cm to 2 m
	Peloidal limestone	Intertidal to very shallow subtidal	<50 cm
	Amphipora-rich detrital limestone	Very shallow subtidal	20 cm to 1 m
	Stachyodes-rich detrital limestone	Shallow subtidal	20 cm to 2 m
	Subspherical stromatoporoid-rich detrital limestone	Shallow subtidal	30 cm to 2 m
	Tabular-stromatoporoid-rich detrital limestone and siltstone	Shallow subtidal	30 cm to 1 m
	Detrital bioclastic limestone	Shallow to deep subtidal	20 cm to 2 m
Base (deep)	Terrigenous siltstone, commonly coral-rich and/or calcareous	Deep subtidal	30 cm to 2 m

Each cycle represents the gradual infill of a carbonate platform, from relatively quiet but oxygenated water of a few metres depth (terrigenous lithofacies), through progressively shallower, more agitated water (various stromatoporoid lithofacies), to shallow subtidal or intertidal flats on which microbial mats thrived (fenestral lithofacies). The fenestral limestones contain mud cracks in some areas, testifying to periodic subaerial exposure. The thin-bedded cap at the top of some cycles is interpreted to be the transgressive drowning phase prior to the re-establishment of deeper water conditions at the start of the next cycle.

Variations from the ideal complete cycle tend to occur as groups of cycles, indicating longer term controls over accommodation than those applicable to individual cycles. Where the basal siltstone lithofacies is present, cycles commonly do not have a fenestral cap, but shallow upward to *Stachyodes* or *Amphipora* limestones. Conversely, where well-developed, thick, fenestral limestone units are present, the basal siltstone and tabular-stromatoporoid limestone lithofacies may be absent. Thick beds composed almost wholly of subspherical stromatoporoids or fenestral limestone occur in the central part of the section in Menyous Gap, where cycle boundaries are commonly very subtle or indistinguishable.

Cycle thicknesses range from 2 to 6 m, with an average of 3.5 m. Apparent cycles less than 2 m thick are generally interpreted here as being due to local banks or mounds rather than representing externally driven cycles, because the stromatoporoid limestones that cap the apparent cycles cannot be traced laterally for more than a few tens of metres. However, Brownlaw (2000) regarded those thin intervals as discrete cycles.

Subaqueous to subaerial cycles, Pillara Sequence

Cycles that show subaqueous shallowing-upward to intertidal deposition are common in the upper Pillara Limestone in the central to northwest Napier Range.

These are the cycles described by Playford et al. (1989; Fig. 215). A model complete cycle is:

	Lithology	*Depositional setting*	*Common thickness*
Top	Thin-bedded calcareous sandstone	Drowning	<20 m
	Coarse sandstone with rootlets	Subaerial to supratidal	<2 m
	Coarse, fenestral, calcareous sandstone	Intertidal to supratidal	50 cm to 2 m
	Fenestral limestone	?Intertidal	30 cm to 3 m
	Stachyodes limestone, some *Amphipora*	Shallow subtidal	50 cm to 3 m
Base	Subspherical stromatoporoid limestone (*Actinostroma*), partly reefal; and cross-bedded sandstone with stromatoporoid fragments	Subtidal bioherms and channels	50 cm to 5 m

Each cycle represents moderate- to high-energy subtidal deposition at the base, firstly as stromatoporoid bioherms or stromatoporoid limestone and sandstone in subtidal channels, followed by very shallow subtidal deposition (*Amphipora* limestone where present, and fenestral limestone), then by intertidal to perhaps supratidal terrigenous deposits (fenestral sandstone) containing fossil rootlets (clay- or sand-filled tubes, and branching subvertical fenestrae) and diffuse mottled textures (Figs 212–215). Thin-bedded caps on some cycles mark the transgressive drowning phase, heralding the start of the next cycle. Cycles range from 2 to 12 m in thickness, with an average of about 4 m.

The character of these subaqueous to subaerial cycles is far more varied than with the simpler subaqueous cycles. Cross-bedded sandstone is commonly present at the base of each cycle instead of the stromatoporoid limestone that occurs in the simple subaqueous cycles (Figs 211, 212). Moderate sorting, double-draped foresets, wrinkly toesets (Dalrymple, 1992), and stromatoporoid and shelly debris indicate that these sandstone units are tidal-channel and bar deposits, laid down in shallow water depths. These tidal channels and bars could have a significant effect on average cycle thicknesses, since some are clearly erosion based. One large lateral accretion surface on the side of a tidal bar in the Surfboard Point section (Fig. 214) is 8 m thick. This lateral gradation is similar to that noted elsewhere by Adams and Grotzinger (1996). Parasequence (cycle) boundaries can be followed for several kilometres on the ground or on air photographs.

Poorly sorted very fine- to coarse-grained calcareous sandstone, commonly with fenestral fabrics, occurs in the upper parts of cycles, above stromatoporoid and fenestral limestone. This sandstone was apparently deposited in intertidal and perhaps supratidal environments in small fluvially dominated channels, and by sheet floods. Sporadic fossil-rootlet horizons, mud cracks, diffuse mottled textures, clay- or sand-filled tubes, and branching subvertical fenestrae, are indications of intertidal to supratidal conditions. Evaporite pseudomorphs have not been found, suggesting that the supratidal areas were not evaporitic saline flats and ponds, but were sparsely vegetated flats.

Subaqueous to subaerial conglomeratic cycles, Pillara Sequence

Conglomeratic cycles are present in the Frasnian Galeru Member of the Sparke Conglomerate in the central Sparke Range area (Figs 183, 184). They occur in east–west oriented fault compartments controlled by sinistral strike-slip bounding faults, and are thought to be floored by shallow subhorizontal glide planes. The setting seems comparable with that of the Hornelen Basin and associated basins in Norway (Steel et al., 1977; Hossack, 1984; Steel, 1988; Osmundsen et al., 2000). These conglomeratic cycles differ from other subaqueous to subaerial cycles in that the average cycle thickness, 11.3 m, is much greater than for other cycles, and at least 50%, and commonly much more, of each cycle consists of boulder to pebble conglomerate. The conglomerates contain a mixture of rock types derived from the Precambrian King Leopold Orogen and Kimberley Basin, together with rounded to subangular and stylolitized blocks of Pillara Limestone (Fig. 176). This mixture of local and exotic clasts is also seen in non-cyclic parts of the Sparke Conglomerate that are present adjacent, below, and above the cyclic section.

The cycles dip east at 30° to 40° and have a total stratigraphic thickness of more than 1000 m. The measured section (Fig. 184) is 909 m thick, and stops some distance west of the stratigraphically highest cycle. The unit is thought to have developed in part through syndepositional strike-slip movement along the basin-bounding faults, which carried the cyclic deposits progressively further west and created accommodation over a basal glide plane, resembling the coarsening-upward cycles in the Hornelen Basin (Steel et al., 1977). A glide plane or thrust, overlain by conglomerate and limestone, is exposed 1.3 km west-southwest of Junction Dam (AMG Zone 52, 198450E 7949900N), in another compartment, north of those that contain the cyclic conglomerates.

The cycles overlie a prominent north-trending tongue of Pillara Limestone that grades laterally into Sparke Conglomerate and in turn overlies Frasnian Virgin Hills Formation. Exposures of the cycles are generally poor because weathering has resulted in lag deposits of loose

boulders and cobbles. Cycles are commonly distinguished only by strike ridges or spurs underlain by boulder-rich horizons, alternating with strike valleys (over recessive sandstone and siltstone). Provenance varies through the succession. Some cycles are rich in quartzite clasts derived from the Kimberley Basin, while others have abundant clasts of Pillara Limestone (Fig. 176), and many have mixed rock types. This is taken to reflect lateral variations in drainage feeding into the basin, and lateral migration and avulsion of lobes on the fan surface. The abundance of quartzite boulders increases up section, with boulders of Pillara Limestone becoming less common. A typical cycle consists of:

	Lithology	*Depositional setting*	*Common thickness*
Top	Boulder conglomerate, commonly as two or three fining-upwards bed-sets, with boulders to about 1.5 m in diameter, grading down into:	Primarily subaerial sheetflood and braided channel	2 to 8 m
	Cobble conglomerate, commonly in several fining-upwards bed-sets, grading via finer grained conglomerate and coarse-grained sandstone down into:	Subaerial to shallow subaqueous, tidal	5 to 10 m
	Calcareous sandstone, with some thin calcarenite interbeds, locally fossiliferous and/or bioturbated, planar to poorly bedded, grading down into:	Shallow subtidal, above wave-base	5 to 10 m
Base	Fine-grained silty sandstone to sandy siltstone, weakly bedded, locally fossiliferous, commonly with abundant *Atrypa,* and/or bioturbated	Subtidal, wave-base to slightly below wave-base	1 to 5 m

In the lower parts of the cyclic successions, some cycles contain back-reef to reef-flat beds of *Stachyodes* limestone as much as 1 m thick, above conglomerate. *Renalcis* is locally abundant in the limestone, which is variably sandy. In a few cycles, the *Stachyodes* limestone is overlain by weakly laminated fenestral limestone. In places the uppermost limestone layers have sand and granule conglomerate filling eroded channels and potholes in the limestone, suggesting that some subaerial erosion occurred after the limestone was deposited. Clasts in conglomerate layers below the limestones are generally pebbles and cobbles rather than boulders. Where visible, the base of a cycle is seen to be bioturbated and indistinctly bedded sandstone. As elsewhere, this is interpreted to indicate shallow-water deposition, below wave-base.

Cycles at the base of the cyclic succession are thought to be subaqueous to intertidal and subaerial cycles that developed prior to the major progradation of conglomerate at the start of a tectonic phase. This phase was responsible for sinistral strike-slip movement and associated westward migration of successive cycles; hinterland erosion of the King Leopold Orogen and the Kimberley Basin; and uplift and erosion of some reef platforms at the basin margin.

The conglomeratic cycles are of late Frasnian age, based on exposures of late Frasnian Virgin Hills Formation below and above the cyclic levels, and the occurrence at the base of some cycles of the brachiopod *Atrypa*, and beds of Frasnian stromatoporoid limestone at the base of others. No Famennian clasts have been found within the Sparke Conglomerate, and there are no intercalations of Famennian limestone, suggesting that the conglomerate as a whole is Frasnian. Deposition of the conglomeratic cycles must have been coeval with parts of the Pillara Limestone platforms of the northern Lawford Range. Their age may be further constrained by the presence of stylolitized Pillara Limestone boulders within the cycles (Fig. 176). The limestone source for these boulders had to have been buried deep enough, or subjected to sufficiently high tectonic compression, for stylolites to have developed. The stylolitized rocks then had to be uplifted, exposed, and eroded.

The cycles themselves are regarded as being of the same duration as other metre-scale cycles in the platform succession. The greater thickness is attributed to steady tectonic extension of the strike-slip basins during deposition, which created additional accommodation.

Cycles, Nullara Sequence

Few thick sections of the Nullara Limestone have been measured. The Horseshoe Range alone records a complete section of Nullara Limestone (Fig. 219), and this thick section is thought to have been tectonically thickened because of syndepositional movement on the Mount Elma and Painted Rocks Faults. Oolitic and oncolitic limestones occur in Famennian cycles in similar positions to stromatoporoid limestones in the Frasnian cycles, and there is more cyanobacterial binding apparent in the Famennian limestones. Fenestral limestones and tepee-like deformation are abundant in the Famennian (Figs 219–221), reflecting wider and shallower platform areas. Supratidal deposits and high-energy grainstones are also more common in the Famennian (Frost et al., 2006; Frost, 2007a,b). Famennian cycles are of comparable thickness to Frasnian cycles in the Horseshoe Range section (about 3.5 m), but elsewhere they have only 1.25 m average thickness (Frost et al., 2006). An idealized full cycle, assembled from various sections in the Nullara Limestone, is as follows:

	Lithology	*Depositional setting*	*Common thickness*
Top	Thin-bedded fenestral limestone to peloidal limestone	Transgressive, present only locally	<20 cm
	Bubble fenestral limestone, sandy limestone, or calcareous sandstone	Supratidal	20 cm to 2 m
	Fenestral limestone, horizontal fenestrae, commonly peloidal	Intertidal to shallow subtidal	20 cm to 1 m
	Fenestral limestone, irregular fenestrae, commonly peloidal, in places oncoidal and/or oolitic	Intertidal to shallow subtidal	20 cm to 1.5 m
	Oncoidal and oolitic limestone to stromatolitic boundstone	Intertidal to shallow subtidal	30 cm to 2 m
Base	Terrigenous siltstone and sandstone, variably calcareous, locally with some cyanobacterial binding	Subtidal, in areas of marked terrigenous influx	50 cm to 3 m

Tepee structures are common in the Famennian fenestral limestones (Frost et al., 2006; Frost, 2007a,b). They range in height from a few centimetres to almost a metre, although most are less than 50 cm high and as much as three or four metres across (Fig. 62). Frost et al. (2006) recognized tepee complexes (consisting of several cycles) as much as 13.5 m thick in Billy Munro Gorge. Bedding-plane exposures of tepee structures in the uppermost Nullara Limestone in the Horseshoe Range show well-developed polygonal patterns, with each polygon 2 to 3 m across (Fig. 63). In the type area, ooids and small oncoids fill the hollows between adjacent tepees and the space created by uplift of the structures. Many tepees are asymmetrical, with breaching of the crests, but broad domal structures, with little or no breaching, are also common.

Megacycle stacking patterns

Some cycle boundaries define groups of metre-scale cycles that form megacycles. However, megacycles are more subjectively defined than the metre-scale cycles.

Repeated regular megacycles are most readily recognized near the east end of Windjana Gorge, in the upper Pillara Limestone (Fig. 222). There, the metre-scale cycles are arranged into sets of cycles that grade from limestone dominated at the base to sandstone dominated at the top, over five or six cycles (Fig. 223). In this way they mirror, but on a larger scale, the normal subaqueous–subaerial cycles in the Windjana Gorge area. At Windjana Gorge these megacycles are 20 to 30 m thick.



Figure 217. Aerial view of the Hull Range, looking southeast, showing well-defined subaqueous cyclicity in platform facies (back-reef and bank subfacies) of the Pillara Limestone.

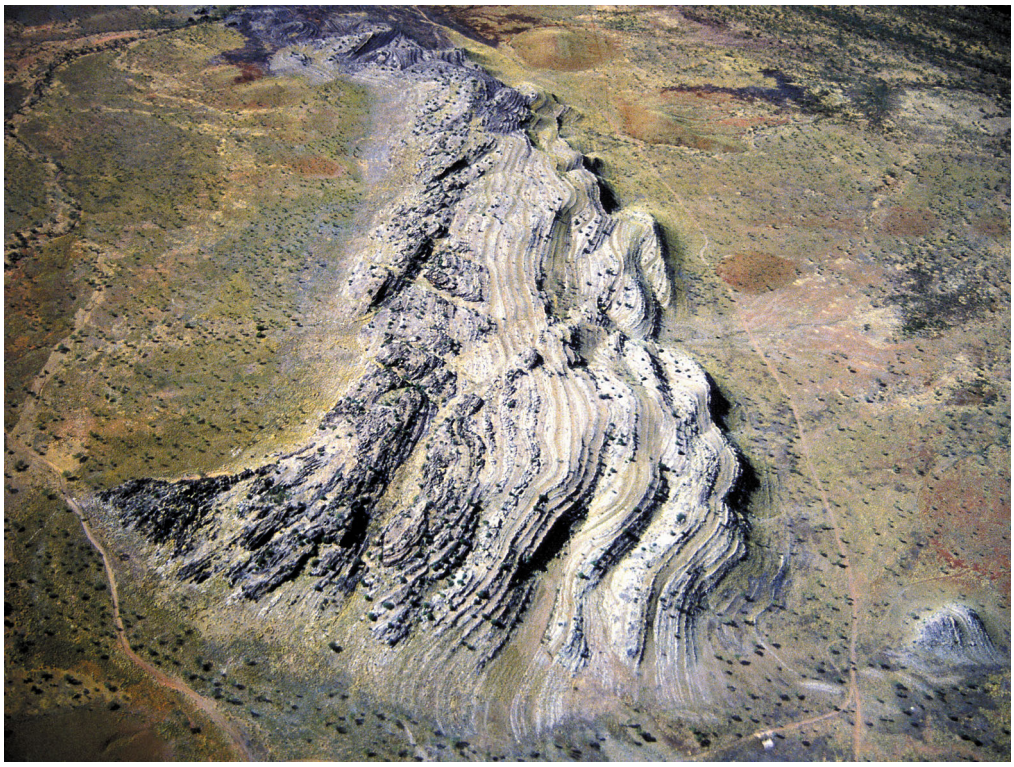

Figure 218. Aerial view of Guppy Hills, looking east, showing well-developed cyclicity in back-reef and bank subfacies of the Pillara Limestone.

In other sections of the upper Pillara Limestone (Surfboard Point, McSherrys Gap, northern Lawford Range) comparable large-scale cycle-stacking patterns (megacycles) can be recognized, but they are not as clearly developed as at Windjana Gorge.

Sections through the lower Pillara Limestone do not show megacycle stacking patterns as clearly as those in the upper Pillara Limestone. Groups of cycles can be distinguished in aerial views at the west end of Guppy Hills, but they are not obvious in a measured section through the same area, except as broad alternations of groups of deeper and shallower facies. In Menyous Gap there are broad trends in lithofacies passing through the section, but megacycles are not readily apparent.

Cycle duration

Order-of-magnitude estimates of the duration of individual cycles can be made for some measured sections. The durations of those sections have been estimated using the absolute ages of House and Gradstein (2004), by applying known paleontological zonation and apparent stratigraphic correlation to tie into the various events in the Devonian time scale. The thickness and number of cycles in each section are then used to derive an estimate of cycle duration, as outlined below. This contrasts with the method adopted by Brownlaw et al. (1996) and Brownlaw (2000), who took the thickness of each section as a fraction of a hypothetical maximum thickness of the Pillara Limestone and applied that figure in estimating the total depositional duration of the formation.

The ages of various events defining the sequence stratigraphy of the reef complexes has been discussed earlier. Measured sections have been correlated with those events as closely as possible, although the estimated time ranges of most sections are very subjective. The age of the platform succession in the North Lawford Range area is perhaps the most closely constrained, and it is used as the basis for estimations of cycle duration. The lowest back-reef limestones in that area are a little older than the Algae Creek Event. There are no Famennian limestones or clasts in the Sparke Conglomerate, but middle to late Frasnian corals (Brownlaw, 2000) are present midway between the uppermost limestone and the Sparke Range Fault, within silty intervals of the Sparke Conglomerate. Brownlaw (2000) considered that most corals in this section belong to Zones 8 to 11, but a few might range as high as Zone 13.

The age of the North Lawford platform is estimated, using House and Gradstein's (2004) figures, as being between 3 and 5 m.y., from 379.5 to 374.5 – 376.5 Ma. A measured section (Fig. 211) extends through the uppermost 160 m of the platform, of which 102 m is cyclic, with an average cycle thickness of 3.8 m. Sufficient dips and strikes are known to give a good estimate of the thickness of the whole platform and, from this, the estimated number of backreef cycles that are represented there. There are approximately 950 m of cyclic back-reef limestones in the North Lawford platform, and as the average cycle thickness

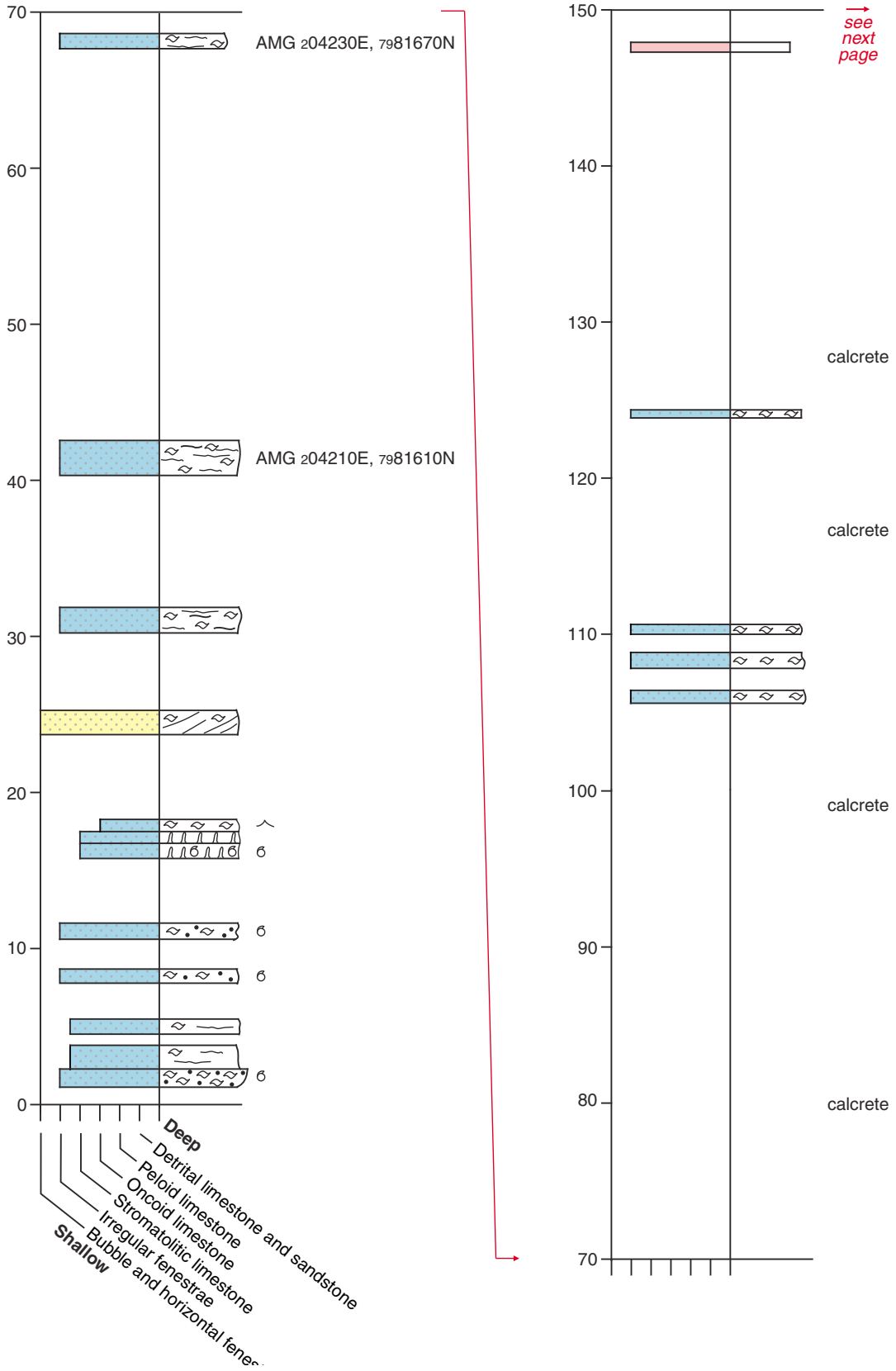

Figure 219. Measured section of Nullara Limestone and lowermost Fairfield Group, Horseshoe Range. For legend see Figure 185.

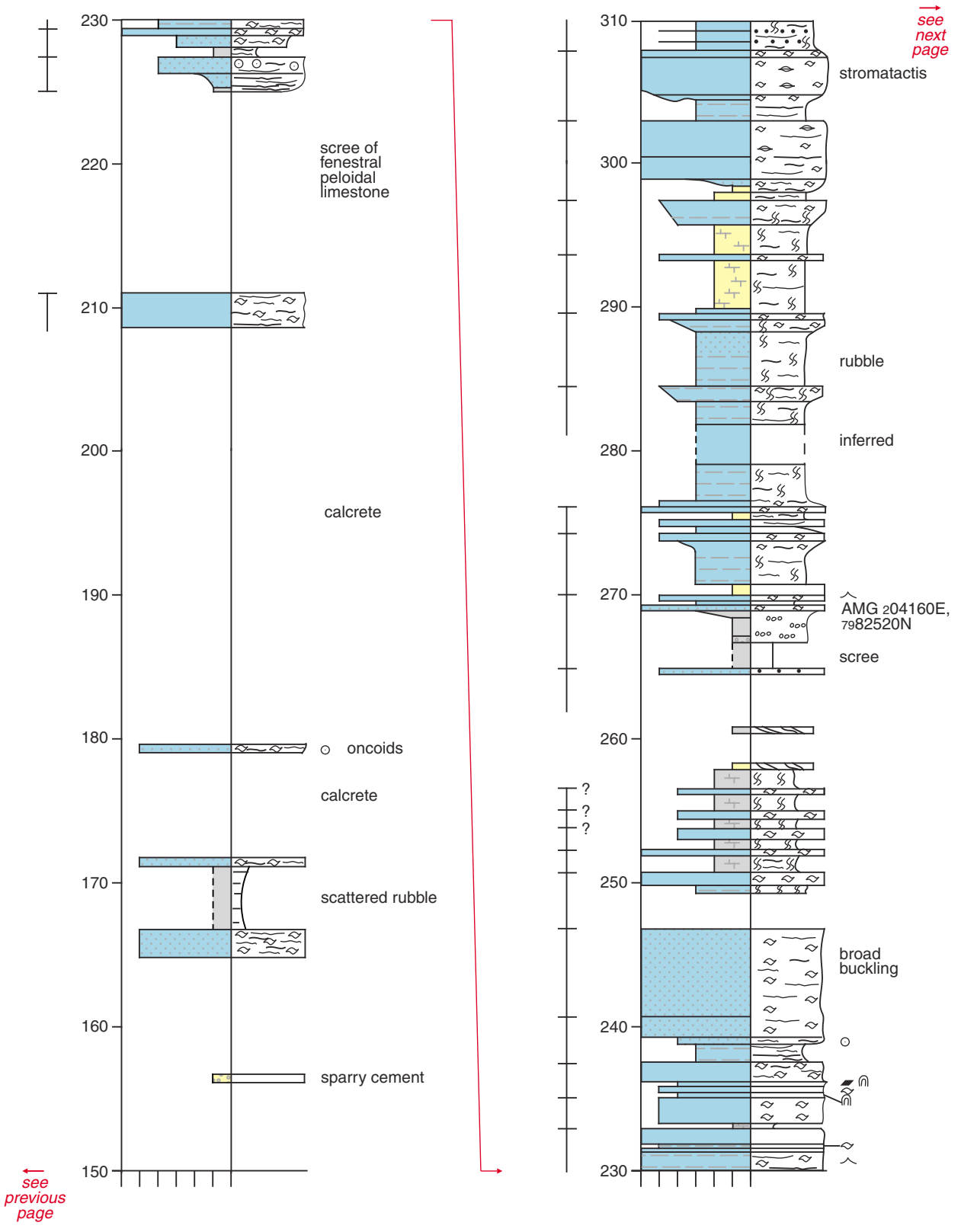
230
220
210
200
190
180
170
160
150
scree of fenestral peloidal limestone
calcrete
oncoids
calcrete
scattered rubble
sparry cement
see previous page
310
300
290
280
270
260
250
240
230
see next page
stromatactis
rubble
inferred
AMG 204160E, 7982520N
scree
broad buckling
?
?
?

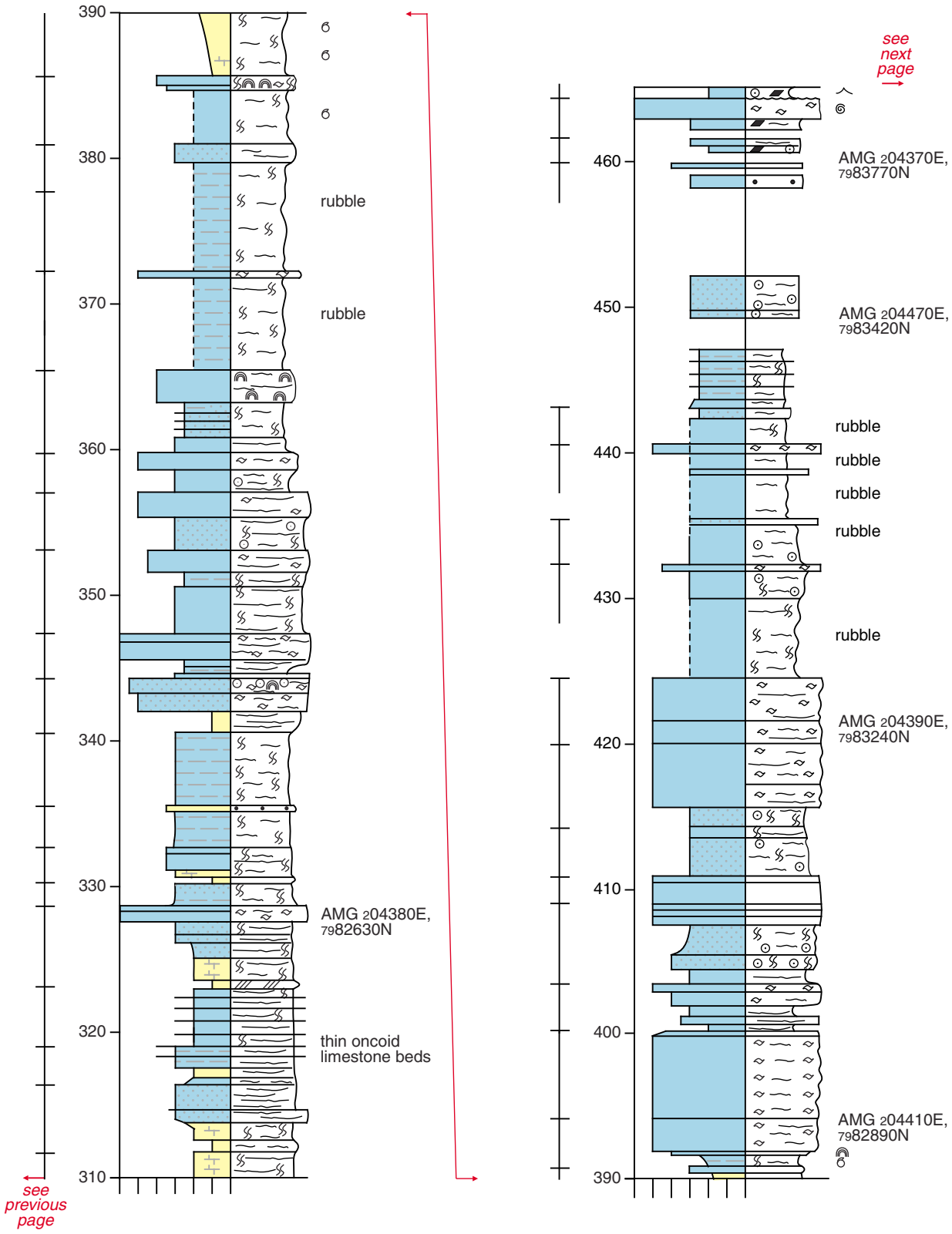
390
380
370
360
350
340
330
320
310
rubble
rubble
AMG 204380E,
7982630N
thin oncoid
limestone beds
see
previous
page
see
next
page
460
450
440
430
420
410
400
390
AMG 204370E,
7983770N
AMG 204470E,
7983420N
rubble
rubble
rubble
rubble
rubble
AMG 204390E,
7983240N
AMG 204410E,
7982890N

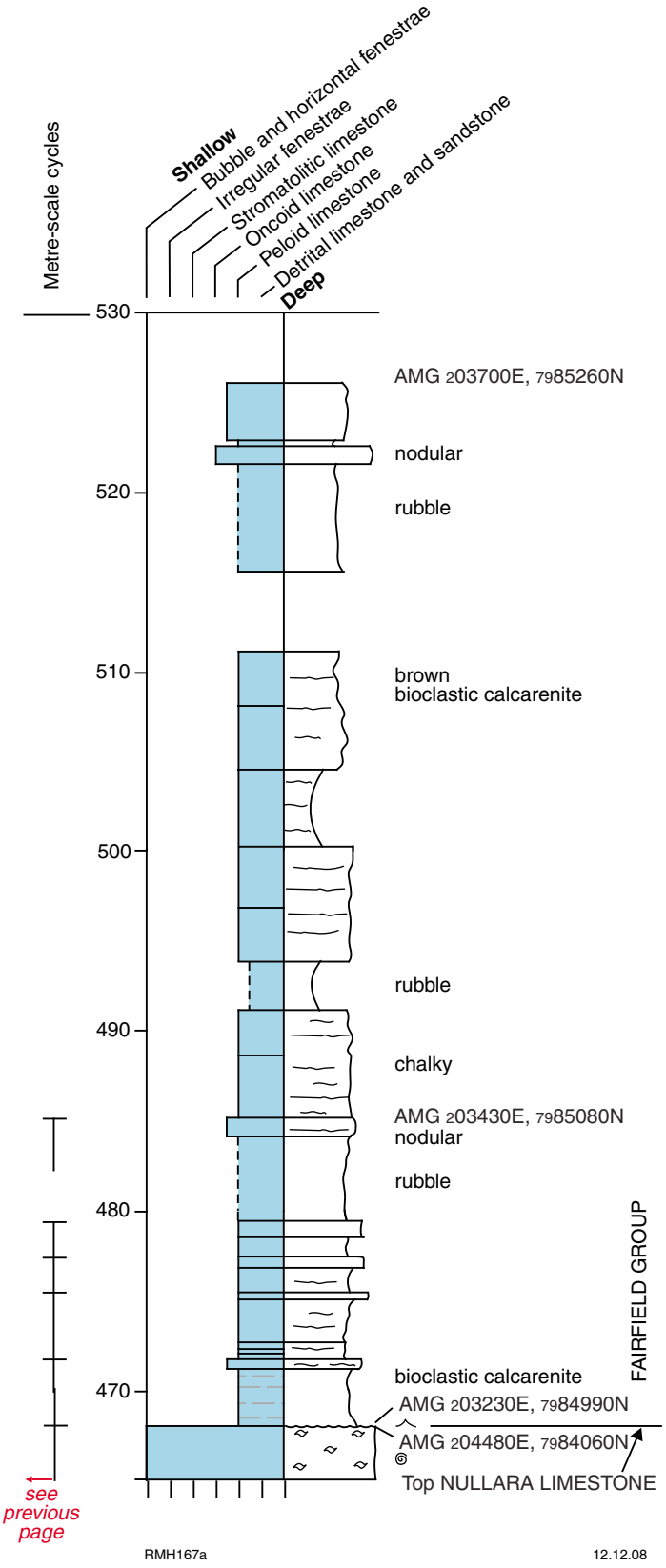
Metre-scale cycles
Shallow
Bubble and horizontal fenestrae
Irregular fenestrae
Stromatolitic limestone
Oncoid limestone
Peloid limestone
Detrital limestone and sandstone
Deep
530
520
510
500
490
480
470
AMG 203700E, 7985260N
nodular
rubble
brown
bioclastic calcarenite
rubble
chalky
AMG 203430E, 7985080N
nodular
rubble
bioclastic calcarenite
AMG 203230E, 7984990N
AMG 204480E, 7984060N
Top NULLARA LIMESTONE
FAIRFIELD GROUP
see previous page
RMH167a
12.12.08

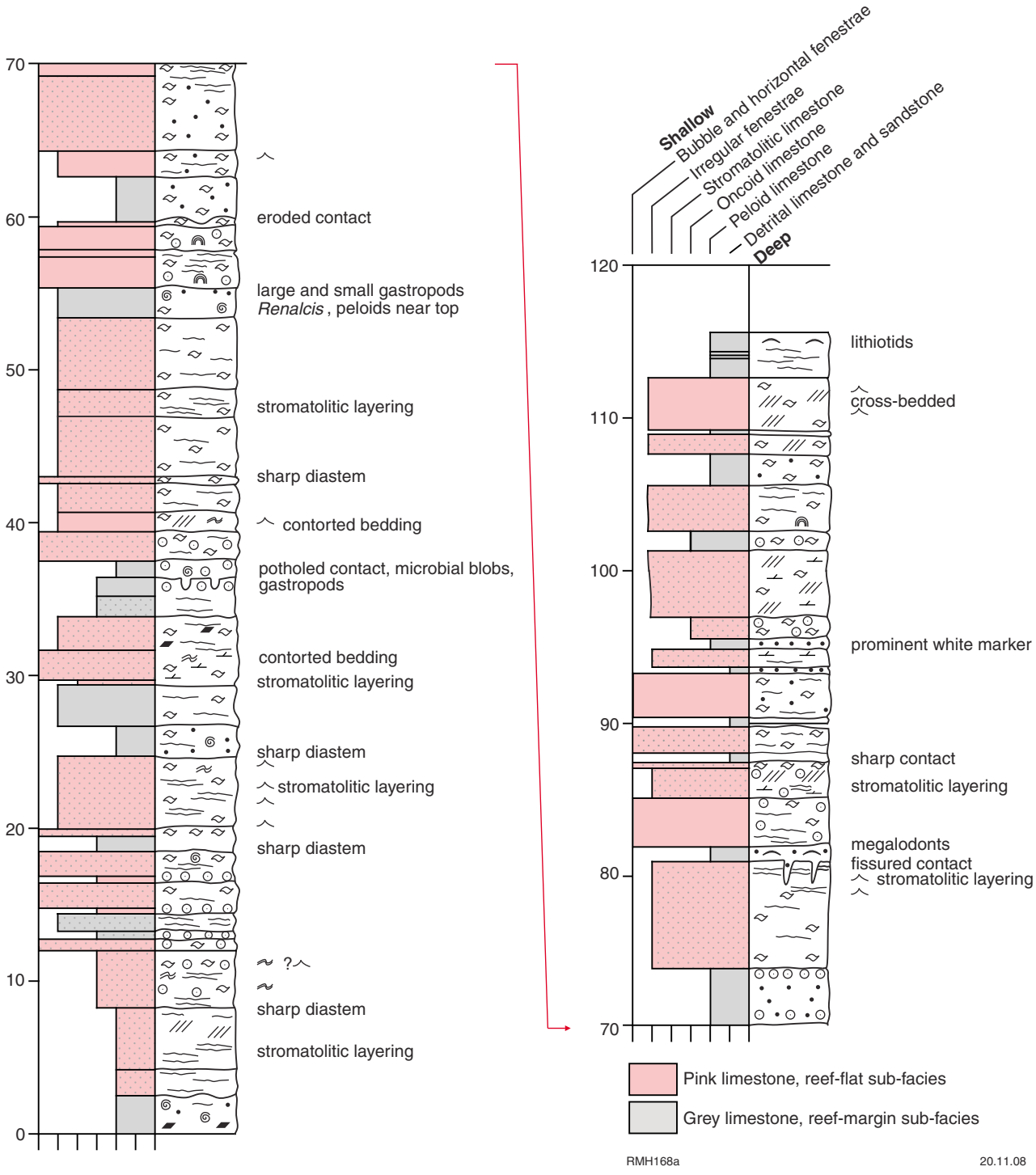

Figure 220. Measured section of upper Nullara Limestone, southeast of Limestone Spring, in the northwest Napier Range. The section is predominantly limestone, sandy in part, with shading differentiating subfacies rather than lithology. For legend see Figure 185.

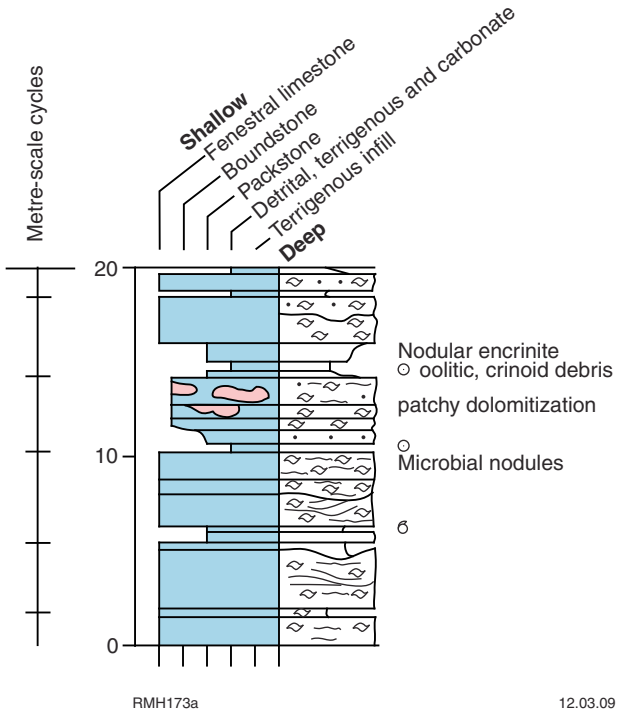

Figure 221. Measured section, lower Nullara Limestone, near Nippers Bore, Larrawa Station. For legend see Figure 185.



Figure 222. The north wall of Windjana Gorge at *Mingun* showing megacycles in the Pillara Limestone, defined by prominent limestone-dominated cycles at the base of each megacycle and regressive-weathering sandstone-dominated cycles at the top. Five or six megacycles are recorded in this cliff.

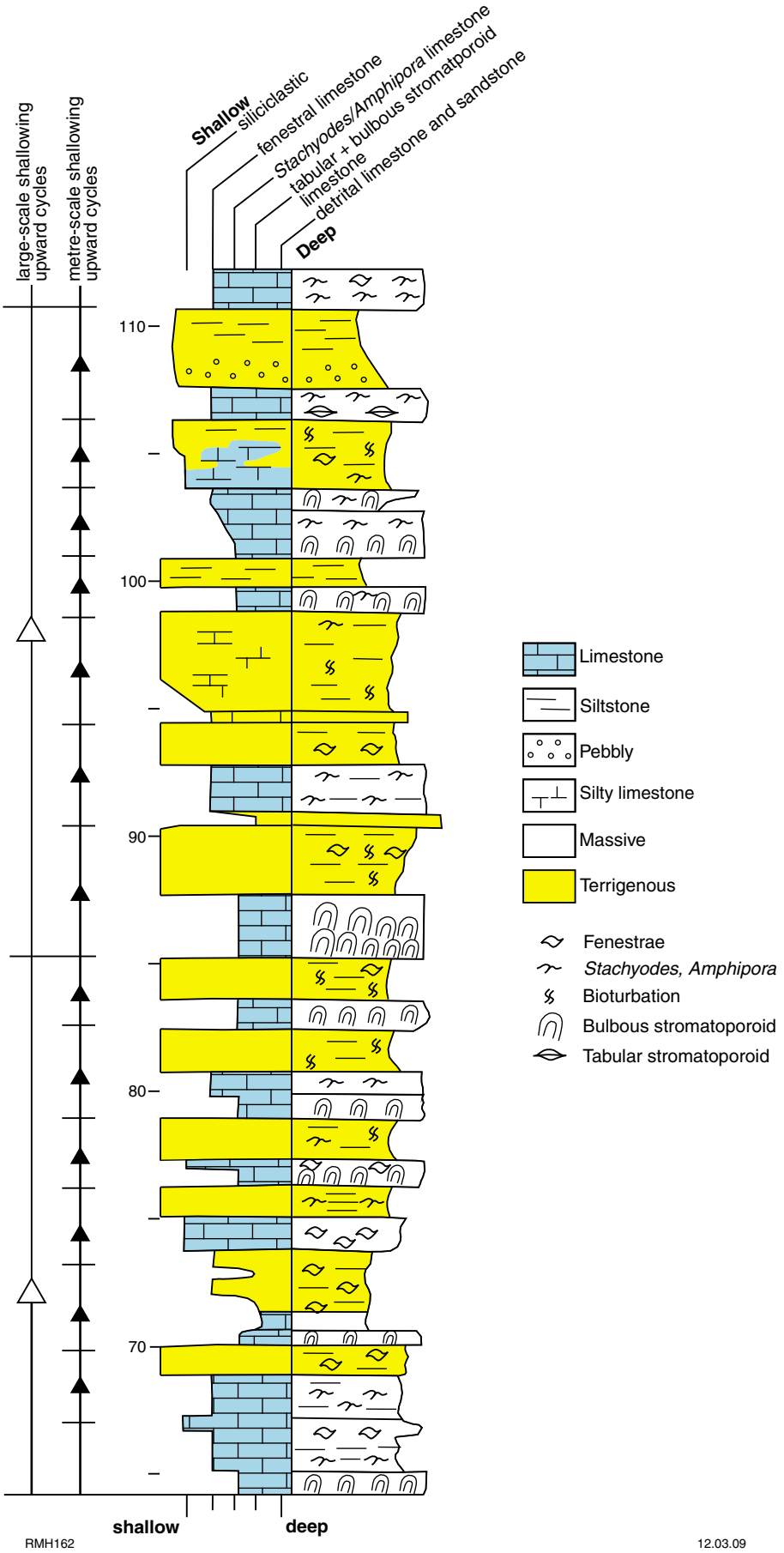
large-scale shallowing upward cycles
metre-scale shallowing upward cycles
Shallow
siliciclastic
fenestral limestone
Stachyodes/Amphipora limestone
tabular + bulbous stromatoporoid limestone
detrital limestone and sandstone
Deep
110
100
90
80
70
shallow
deep
RMH162
12.03.09
Limestone
Siltstone
Pebbly
Silty limestone
Massive
Terrigenous
Fenestrae
Stachyodes, Amphipora
Bioturbation
Bulbous stromatoporoid
Tabular stromatoporoid

in the measured section is 3.8 m, it is estimated that there are some 250 metre-scale cycles in this platform. Those cycles were deposited in about 3 to 5 m.y., and the average duration of each cycle is thus estimated to be between 12 000 and 20 000 years.

Climatic regime and sea-level change

The Late Devonian is regarded by some authors as a transitional period from greenhouse conditions in the Frasnian to early Famennian to icehouse conditions in the late Famennian and Carboniferous (Caputo and Crowell, 1985; Sandberg et al., 2002; Joachimski et al., 2003).

Under greenhouse conditions there are no polar ice caps, and no large eustatic changes in sea level as a result of glacial waxing and waning. Under those conditions eustatic sea-level changes are restricted to metre-scale oscillations caused by Milankovich temperature variations. The regular cycles in the reefal platforms of the Canning Basin show that such metre-scale oscillations prevailed throughout both the Pillara and Nullara Sequences, and indicate that greenhouse rather than icehouse conditions prevailed throughout that time. It is conceivable, but probably unlikely, that the brief regression at the Frasnian–Famennian boundary was due to an abrupt and very short-lived phase of glaciation at the close of the Frasnian, followed by a return to greenhouse conditions soon afterwards during deposition of the Famennian Nullara Sequence. On the other hand, icehouse conditions might have prevailed during deposition of the Fairfield Group in the latest Famennian and Early Carboniferous (Tournaisian), after reef growth had ceased.

The Famennian platform succession is about 500 m thick in the Horseshoe Range, but it is only about 200 m thick over the rest of the Lennard Shelf. The Nullara Limestone was deposited in about 11.5 m.y. The average total thickness of the late Givetian and Frasnian platforms was about 1000 m, and they were deposited in about 14 m.y. The average thickness of recognizable metre-scale cycles is about 3.5 m in the Frasnian but only 1.25 m in the Famennian (Frost et al., 2006). The reduced thickness of the Nullara platforms reflects lesser creation of accommodation during the Famennian, interpreted as being due to a long-term global fall in sea level during that period, counteracting continued subsidence. However, transgression was ongoing during the Famennian, because continuing subsidence counteracted falling global sea level. An alternative interpretation would be that the fall in the rate of transgression during the Famennian was due to slowing in the rate of subsidence, with little or no global change in sea level.

Figure 223. (facing page) Measured section near the east end of Windjana Gorge, showing metre-scale cycles and cycle stacking patterns. The section extends upward in the face of the gorge from *Mingun*. The thickness is from a full measured section (Fig. 213) extending over the saddle at *Malambeea*. For legend see Figure 185.

Controls on cyclicity

Both metre-scale and larger scale cycles (megacycles) are products of repeated shallowing-upward episodes, separated by abrupt deepening episodes.

The carbonate-dominated lower parts of some metre-scale platform cycles are interpreted as having resulted from abrupt deepening episodes, when accommodation was large and carbonate productivity was high, leading to strong stromatoporoid and microbial growth. Terrigenous material was either trapped along the basin margin or, if silty, was carried into deeper areas to form the siltstone lithofacies at the base of some cycles. As sedimentation continued, the platform areas shallowed and terrigenous influx occurred (forming calcareous sandstone) or microbial mats developed (forming fenestral limestone) at the tops of cycles.

Megacycles resulted where successively shallower subaqueous to subaerial cycles were followed by a sudden increase in accommodation, followed in turn by another regular succession of shallowing cycles.

The pattern of cycles involving gradual infill and progradation followed by abrupt drowning can be ascribed to a combination of eustacy and subsidence. Eustatic sea-level rise combined with steady subsidence resulted in increased accommodation, whereas eustatic sea level fall together with continued steady subsidence led to less accommodation and either intertidal–supratidal or subaerial deposition. An alternative explanation is that the cycles are the result of repeated pulses of subsidence resulting from regular tectonism.

Orbital forcing (Milankovich cyclicity) is a likely control for short-term eustatic variations. Orbital forcing comprises four principal cycles that can influence deposition (De Boer and Smith, 1994; Fischer and Bottjer, 1991): precession (20 to 25 thousand years), obliquity (40 thousand years), short-term eccentricity (100 thousand years) and long-term eccentricity (400 thousand years). The estimated durations in the Pillara Limestone of metre-scale cycles (12 to 20 thousand years) and large-scale stacking patterns (100 thousand years) may perhaps correlate with precession and short-term eccentricity respectively.

However, a tectonic control over cyclicity cannot be ruled out. The Lennard Shelf lies along the northern margin of the Canning Basin, adjacent to the King Leopold Orogen, and in the southeast it abuts the southern end of the Halls Creek Orogen. Individual faults appear to continue from the Halls Creek Orogen into the Devonian succession in the Sparke Range and Barramundi Range areas, and fault movement during the Devonian is known to have occurred on the Lennard Shelf and in the Ord Basin to the northeast (Thorne and Tyler, 1996). A tectonic control on cyclicity would have had to act regularly over the length of the Lennard Shelf, about 500 km, by repeated jerky subsidence due to faulting on a vertical scale of less than 10 m.

Such a tectonic control on cyclicity was debated by Hardie et al. (1991) and Read et al. (1991). Hardie et al. noted that the frequency of major earthquakes would need to be in a range similar to that of Milankovich cyclicity,

and be able to drop areas 100 to 200 km wide and several hundred kilometres long (i.e. similar in size to the Lennard Shelf) by 2 to 4 m. The controlling mechanism would be periodic release of tension as a threshold is reached. Read et al. noted that the modern record is geologically very brief, and that Hardie et al.'s views are largely conjectural. Moreover, Read et al. claimed that there would need to have been many smaller earthquakes in such a setting. The smaller earthquakes, if real, should leave a sedimentary record, such as liquefaction, synsedimentary slumping, contortion, and brecciation of sediment, even in limestones that lithified relatively quickly. Such features are indeed common in slope deposits of the reef complexes, and they have also been recognized in platform deposits.

Implications for conglomerate deposition

In standard sequence-stratigraphic theory, as outlined in Wilgus et al. (1988), terrigenous clastic deposition is expected to occur during lowstands of sea level, when accommodation is low, forming lowstand terrigenous fans, while the buildup of carbonates prevails during highstands. According to that reciprocal-sedimentation model for the Canning Basin, terrigenous clastic material would be stored in the hinterland during highstands, and large conglomerate bodies in the basin such as the Elma, Van Emmerick, Sparke, and Bobs Bore Conglomerates would be linked to lowstands, and the Mueller Conglomerate, perched in the hinterland east of the Margaret Embayment, would be a highstand storage area. Such a reciprocal model for the Canning Basin carbonates and terrigenous clastics was invoked by Kennard et al. (1992), Whittam et al. (1994), and Southgate et al. (1999).

However, major conglomerate bodies were deposited over periods ranging from about 5–7 m.y. (Sparke, Bobs Bore, Elma, and Stony Creek Conglomerates) to 15 m.y. or more (Barramundi, Behn, and Van Emmerick Conglomerates). That is many times longer than any cyclic pattern that would arise from orbital forcing (about 500 000 years maximum), and much longer than the third-order cycles suggested by Kennard et al. (1992), Whittam et al. (1994), and Southgate et al. (1999). Moreover, the Elma, Sparke, Behn, and Stony Creek Conglomerates can be shown to interfinger with tens of cycles in shallow-water platform carbonates, showing that conglomerates and platform carbonates were coeval over long periods of time. The outcropping conglomerate bodies are not reciprocal lowstand deposits, but are highstand deposits coeval with the platform carbonates.

Faults moving within and outside the basin are thought to have generated both conglomerate influx and increased subsidence. A tectonic cause for Devonian conglomerate influx has also been established in the Ord and Bonaparte Basins (Thorne and Tyler, 1996), and a major phase of the Alice Springs Orogeny in the central Australian basins is known to have occurred during the Devonian (Haines et al., 2001). Boulders of Frasnian reefal carbonates in the Sparke Conglomerate point to rapid burial of platforms followed by uplift and erosion.

These observations show that the conglomerate bodies exposed on the Lennard Shelf are not linked with lowstands, but were laid down as highstand deposits linked with active tectonism.

Structure

The Lennard Shelf (Playford and Johnstone, 1959b) is the northern subdivision of the Canning Basin. It extends northwest–southeast for about 400 km, is an average of 50 km wide, and is bounded to the north by Precambrian basement and to the south by the deep Fitzroy Trough (Figs 1, 2). The shelf is occupied by relatively thin sedimentary rocks overlying basement, which contrasts with the very thick sedimentary sequence in the adjoining Fitzroy Trough. The boundary between shelf and trough is marked by the Pinnacle Fault and its projection along a system of parallel faults to the northwest.

The most detailed recent discussions of the structure of the Lennard Shelf are given by Dörling (1995), Dörling et al. (1996), and Miller et al. (2007). Earlier accounts include those by Guppy et al. (1958), Playford and Johnstone (1959b), Rattigan and Veevers (1961), Playford and Lowry (1966), Playford et al. (1975), Forman and Wales (1981), Brown et al. (1984), Hall (1984), Yeates et al. (1984), Begg (1987), Drummond et al. (1988, 1991), Middleton (1990), and Shaw et al. (1994).

Faulting

The overall structure of the area has resulted from extensional tectonics (Dörling et al., 1995, 1996; Miller et al., 2007). Most of the larger faults trend northwest and show normal movement, throwing down to the southwest in the Phanerozoic, although some are thought to have had strike-slip components during some stages of their history. These large normal faults include the Pinnacle, Sparke Range, Black Hills, Virgin Hills, Home Range, Mount Elma, Barramundi, Stony Creek, Oscar, Mount Behn, and Van Emmerick Faults.

Between these northwest-trending normal faults there is a series of north-trending transfer faults in the Limestone Billy Hills, Horse Spring Range, and Horseshoe Range areas, which also show predominantly normal displacements (Dörling et al., 1995, 1996; Miller et al., 2007).

The major northwest-trending faults are generally interpreted to be listric faults, with dips in outcrop ranging from less than 50° to about 80°. Some appear to be reactivated Proterozoic structures, the sense of movement having changed in several cases. For example, the Van Emmerick Fault appears to pass laterally into the Mondooma Thrust, the Mount Behn Fault into the Granite Range Fault (thrust), and the Stony Creek Fault into the Stony Creek Shear Zone (which exhibits both thrust and strike-slip movements). Many were active during growth of the reef complexes in the Middle and Late Devonian, and fault activity continued strongly throughout the Carboniferous. Most of the Lennard Shelf area has been

tectonically quiescent since the Early Permian, although a few faults have moved to a relatively small extent since then.

Pre-Devonian movements along some northwest-trending faults are thought to have been responsible for localizing the islands now represented by the Oscar Range and Pillara Range Inliers, around which reef complexes were established.

In some parts of the southeast Lennard Shelf there are many closely spaced, steep-dipping, north–south faults, especially in the northwestern Emanuel Range, Pillara Range (Fig. 224), Limestone Billy Hills, Horse Spring Range, and Horseshoe Range. The largest are the en-echelon Guppy Hills, Painted Rocks, and Mount Elma Faults. Note that the Guppy Hills Fault is not named on Plates 3, 4, and 7, but it is shown as a fault on those maps extending from the southeast end of the Hull Range to the west end of Guppy Hills. At its northern end the Mount Elma Fault turns around to join the northwest-trending Barramundi Fault and the projected extension of the Mount Winifred Fault, which lies further east.

The large north-trending faults dip to the west and are thought to have had predominantly normal displacements, although strike-slip movement is possible in some places. The apparent left-lateral offset between the Guppy Hills and Hull Range reefal platforms along the Guppy Hills Fault, and the drag adjoining that fault that is seen at the south end of the Hull Range, could be explained by sinistral movement during the Devonian, or perhaps by large post-Devonian west-block-down normal movement of a tilted Devonian succession. Further east, both the Painted Rocks and Mount Elma Faults are thought to have moved during the Devonian, based on the deposition of conglomerates adjacent to those faults, with side-attached reefs (half atolls) stepping around and up conglomerate fans. The fault movement is thought to have been normal (Dörling et al., 1996; Miller et al., 2007).

The large syncline forming the Horseshoe Range and the smaller syncline southwest of Blood Yard Bore (Fig. 225) have apparently formed by drag against the Painted Rocks and Mount Elma Faults respectively. The small outcrop of Grant Group against the fault in the core of the syncline southwest of Blood Yard (AMG Zone 52, 207800E 7987000N), and a smaller outcrop of Grant Group northwest of Blood Yard (AMG Zone 52, 207000E 7990700N) dipping at 30° away from the fault, indicate that some fault movement has occurred since the Early Permian.

Some of the smaller north-trending faults dip to the west and the others to the east. Most are thought to have had normal displacements, but some significant left-lateral components are also evident (Dörling et al.,1996).

The largest fault in the area is the Pinnacle Fault, which moved as a normal fault during the Devonian, Carboniferous, and Permian, with a vertical displacement of as much as 7000 m. Its movement was reversed, to a much smaller extent, as a result of right-lateral wrenching of the Fitzroy Trough during the Mesozoic (Rattigan, 1967; Smith, 1968). That wrench faulting gave rise to the series of large anticlines in the Fitzroy Trough. Although it has not been shown to have had significant effects in the Lennard Shelf, the rocks there must have been subject to compression during that period, and some evidence of this is expressed in the Devonian rocks. Some faults may have had minor components of transcurrent movement, as for example the small fault in Pillara Limestone near Brooking Springs Homestead that is illustrated in Figure 227.

The Cadjebut Fault, a branch of the Pinnacle Fault that was active as a normal fault during the Frasnian and probably earlier in the Givetian, localized the southern margin of the Emanuel Range reefal platform (Fig. 115). The fault is also known to have moved to a small extent since the Early Permian, as shown by the displacement of the Early Permian glacial erosion surface that forms the tops of the limestones on either side of the fault. In the area where it curves from east to southeast the fault zone follows a narrow trench, about 20 to 40 m wide, that is filled with banded radiaxial spar. This is a marine cement that filled successive voids created by pull-apart movement along the fault. A feature of this cement in one place (AMG Zone 52, 184200E 7926500N) is the occurrence of large (as much as 25 cm in diameter) spar balls (Fig. 152). They point to very strong water movement, probably resulting from wave or tidal action, that rotated the balls while radiaxial spar was being deposited.

A branch of the Cadjebut Fault runs eastward past McWhae Ridge, where two small faults form a graben along the crest of the ridge. These small faults can be shown to have moved during deposition of the Frasnian Sadler and Virgin Hills Formations, resulting in differences in thickness of parts of the Sadler Limestone and Virgin Hills Formation on either sides of the faults (Figs 228, 229).

The Virgin Hills Fault is a major structural feature of the southeast Lennard Shelf (Fig. 226) that can be traced west-northwest from the Sparke Range area to near Outcamp Hill. It is thought to join the Pinnacle Fault below an area to the northwest where it is obscured by soil. From field relationships, the Virgin Hills Fault can be shown to have had normal movement during the Devonian and presumably also in the Carboniferous and Permian.

Movement during the Late Devonian is evidenced near Bobs Bore where strongly fractured limestone of the Virgin Hills Formation directly adjoining the fault is overlain by early Famennian stromatolitic limestone that was less fractured through subsequent fault movement (Figs 230, 231). This points to an episode of early Famennian movement along the fault. The Famennian Virgin Hills Formation in this area is folded in a conspicuous syncline against the fault (Fig. 226).

In the area where it meets the Sparke Range Fault, the Virgin Hills Fault splits into several branches. The structure of that area is marked by strong shearing of the Devonian limestones, associated with high-angle left-lateral faults and low-angle thrusts. Immediately south of the junction between the two major faults is a group of three parallel west-trending left-lateral transcurrent faults in the Galeru Member of the Sparke Conglomerate. Two small klippen of steeply overturned marginal-slope limestone of the Virgin Hills Formation are situated

1.5 km southwest of Junction Dam (Figs 232, 233). These are separated from the underlying Precambrian mica schist by a subhorizontal glide plane or thrust. There is a need for more detailed analysis of the complex structure of this area, in order to fully elucidate the relationships between normal, transcurrent, and thrust faulting. The origin of the overturned klippen is puzzling as they occur in what otherwise appears to have been an extensional rifting regime.

The large faults that mark the northeastern boundaries of the large masses of conglomerate that form the Van Emmerick, Behn, Stony Creek, Barramundi, Mount Winifred, and Sparke Conglomerates were strongly active during the Devonian, forming scarps that sourced and localized the conglomerates.

Folding

Most folds that are developed in the area are depositional structures, resulting from changing depositional dips in marginal-slope deposits and differential pressure-solution compaction in platform carbonates over irregular topography in basement rocks. However, other folds have resulted from movement along faults, the largest being the syncline of the Horseshoe Range, associated with the Mount Elma Fault, which is interpreted to have had normal movement.

Mineralization

Two types of mineralization are known in the reef complexes: syngenetic mineralization during the early Frasnian, and epigenetic (Mississippi-Valley-type) mineralization that was emplaced during the early Carboniferous (Tournaisian), soon after the late Famennian extinction of the reefs.

Epigenetic mineralization

Epigenetic mineralization, forming Mississippi-Valley-type (MVT) zinc–lead deposits, has long been known to occur in the Devonian reef complexes. Hardman (1884) reported minor traces of copper at several localities, and lead–zinc mineralization was recorded in 1901 from a gossan in the Napier Range at Narlarla (Hassan, 2004). The deposit was mined briefly in 1906, but was judged to be uneconomic (Woodward, 1907; Basedow, 1918). It was

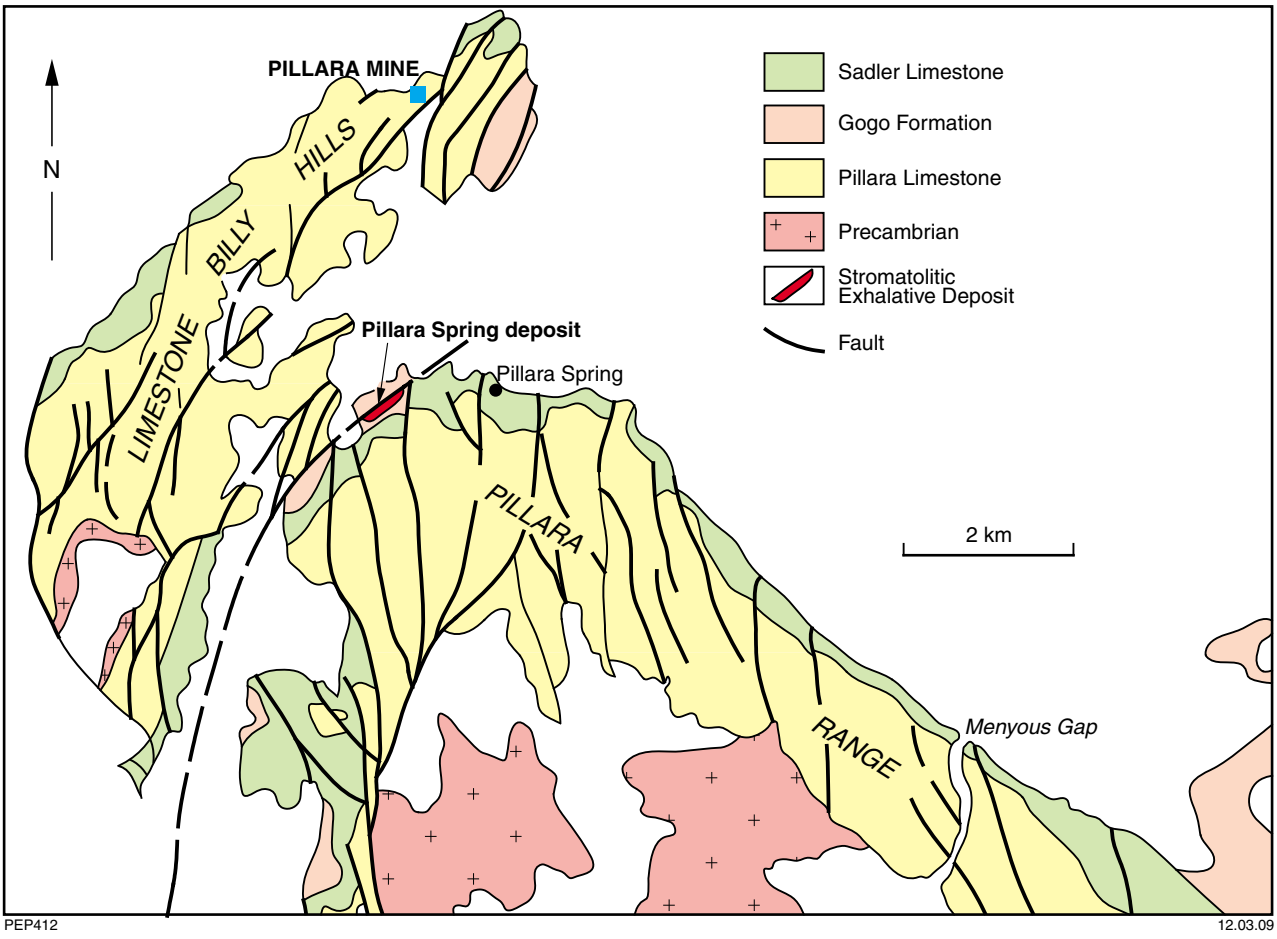

Figure 224. Map showing numerous north- and northeast-trending faults in the Limestone Billy Hills and northwestern Pillara Range showing the locations of the Pillara zinc–lead mine and the Pillara Spring exhalative deposit.



Figure 225. Aerial view looking west over a synclinal fold against the Mount Elma Fault on the east side of the Horseshoe Range. In the centre foreground, very poorly exposed Fairfield Group underlies Permian sandstone and overlies well-bedded and well-exposed uppermost Nullara Limestone.

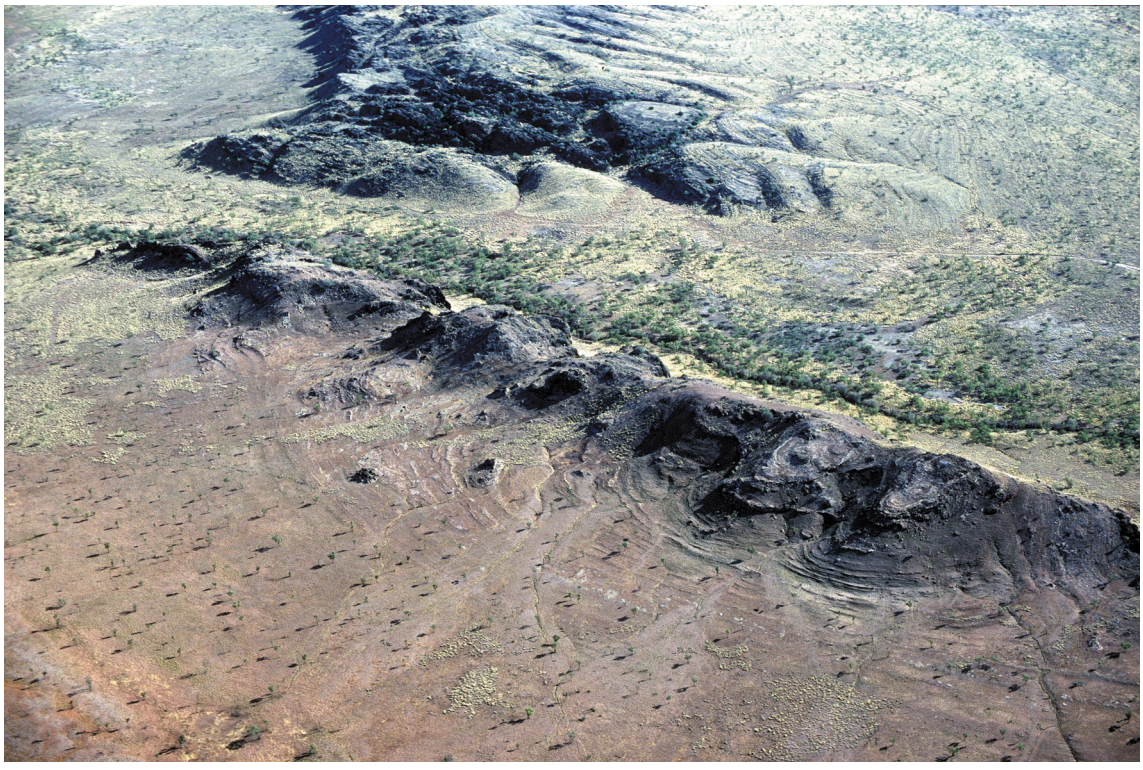

Figure 226. Oblique aerial photograph of the Bobs Bore area, looking northwest, showing Famennian marginal-slope limestones of the Virgin Hills Formation in the foreground and middle distance, folded into a syncline on the downthrown side of the Virgin Hills Fault. The Home Range reefal platform is in the background, on the upthrown side of the fault.

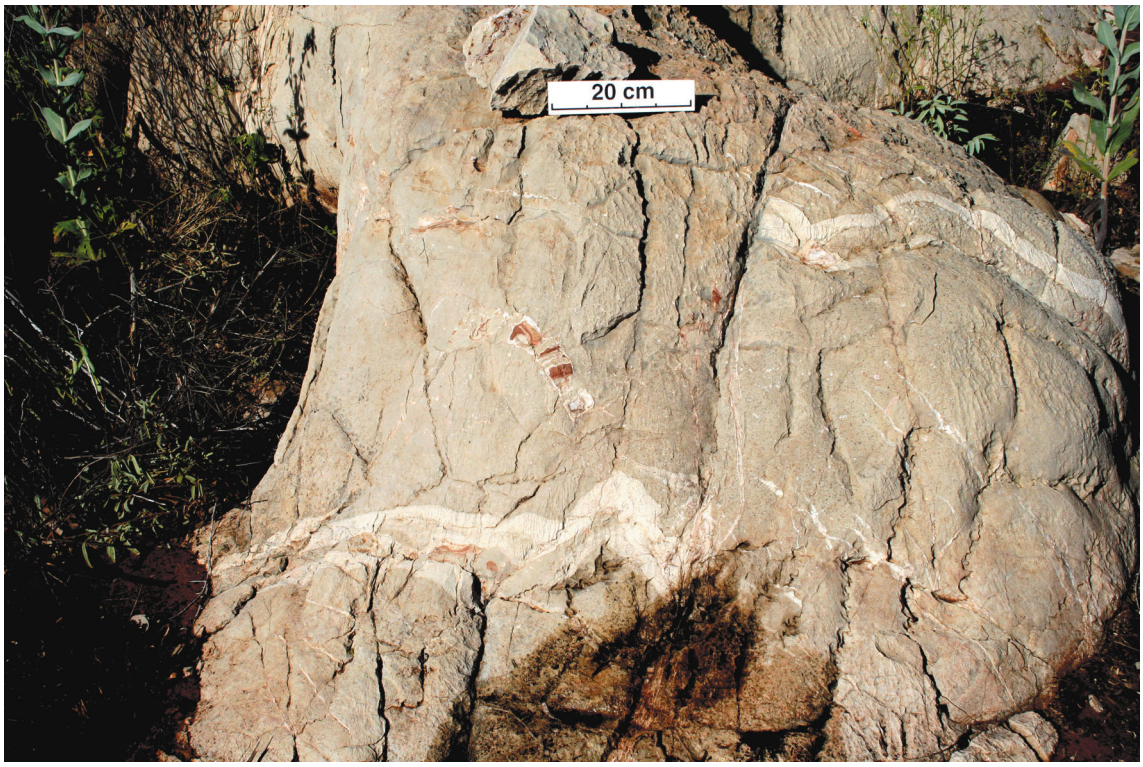

Figure 227. Small left-lateral fault in reef-margin limestone (Pillara Limestone), 2 km north of Brooking Springs Homestead. Lateral fault movement of about 50 cm is shown by displacement of a white *Renalcis*-filled neptunian dyke.

eventually developed commercially by Devonian Pty Ltd from 1948 to 1954 and again from 1964 to 1966, essentially exhausting the small, but rich orebody (Blockley, 1971; Playford, 1976b; Ringrose, 1989).

Matheson and Guppy (1949) reported small veins of galena in the Limestone Billy Hills area, not far from the present Pillara minesite. However, it was not until 1971 that intensive exploration was conducted in the area (Henderson, 1971), leading to the discovery of the Pillara orebody (formerly known as Blendevale) in 1978 (Murphy et al., 1986; Hassan, 2000, 2004). Subsequent grid drilling by a BHP–Shell partnership located further economic zinc–lead deposits at Cadjebut in 1984, Goongewa in 1985, and Kapok in 1989. All of these discoveries were developed commercially, and continuing exploration has located several other smaller prospects in the southeastern Lennard Shelf and the Napier Range. Zinc–lead minesites and the locations of other zinc–lead occurrences, at and below the surface, are shown in Figure 234.

In 1994, the BHP–Shell interests were purchased by Western Metals NL (subsequently Western Metals Ltd), and from 1997 to 2003 that company produced 744.5 kt of zinc and 272 kt of lead before its mines were closed, the company went into receivership, and its tenements were purchased by Teck Cominco Ltd. That company formed a partnership with Xstrata plc and recommenced mining at Pillara in 2007, but ceased production in August 2008 because of falling zinc and lead prices. Teck Cominco had reported in 2007 that its tenements had reserves of 3 Mt at an average grade of 7.3% zinc and 1.9% lead.

The most recent comprehensive study of controls on epigenetic mineralization in the Devonian reef complexes is that of Wallace et al. (2002). They pointed to a synchronous relationship between emplacement of MVT sulfides and hydrocarbons in the reef complexes. Several indicators of thermal maturation demonstrate that the sedimentary rocks in this area are immature, having reached peak temperatures of 60° to 70°C during the Paleozoic and 70° to 90°C during the Mesozoic. The associated hydrocarbons and mineralization in the southeastern Lennard Shelf are thought to have been derived from fluids sourced by compaction of shales deep in the Fitzroy Trough and funnelled along faults (especially the Pinnacle and Cadjebut Faults) into the adjoining reef complexes (Ferguson et al., 1992, 1993). However, the Fitzroy Trough is unlikely to have been the source of mineralization at Narlarla as the two are separated by more than 50 km (Fig. 234). The source of the mineralizing fluids there was probably shales in Devonian basin facies in front of the Napier Range reef complex.

The main epigenetic zinc–lead (Zn–Pb) deposits in the southeast Lennard Shelf are thought to have formed where mineralizing fluids passed along faults and joints and through hydrothermal-karst caverns in the Devonian carbonates (Wallace et al., 2002). McManus and Wallace (1992) deduced on petrological grounds that the epigenetic Zn–Pb mineralization was formed during the latest Devonian (late Famennian) or Early Carboniferous (Tournaisian). Their interpretation was refined by Christensen et al. (1995), who dated the mineralization as

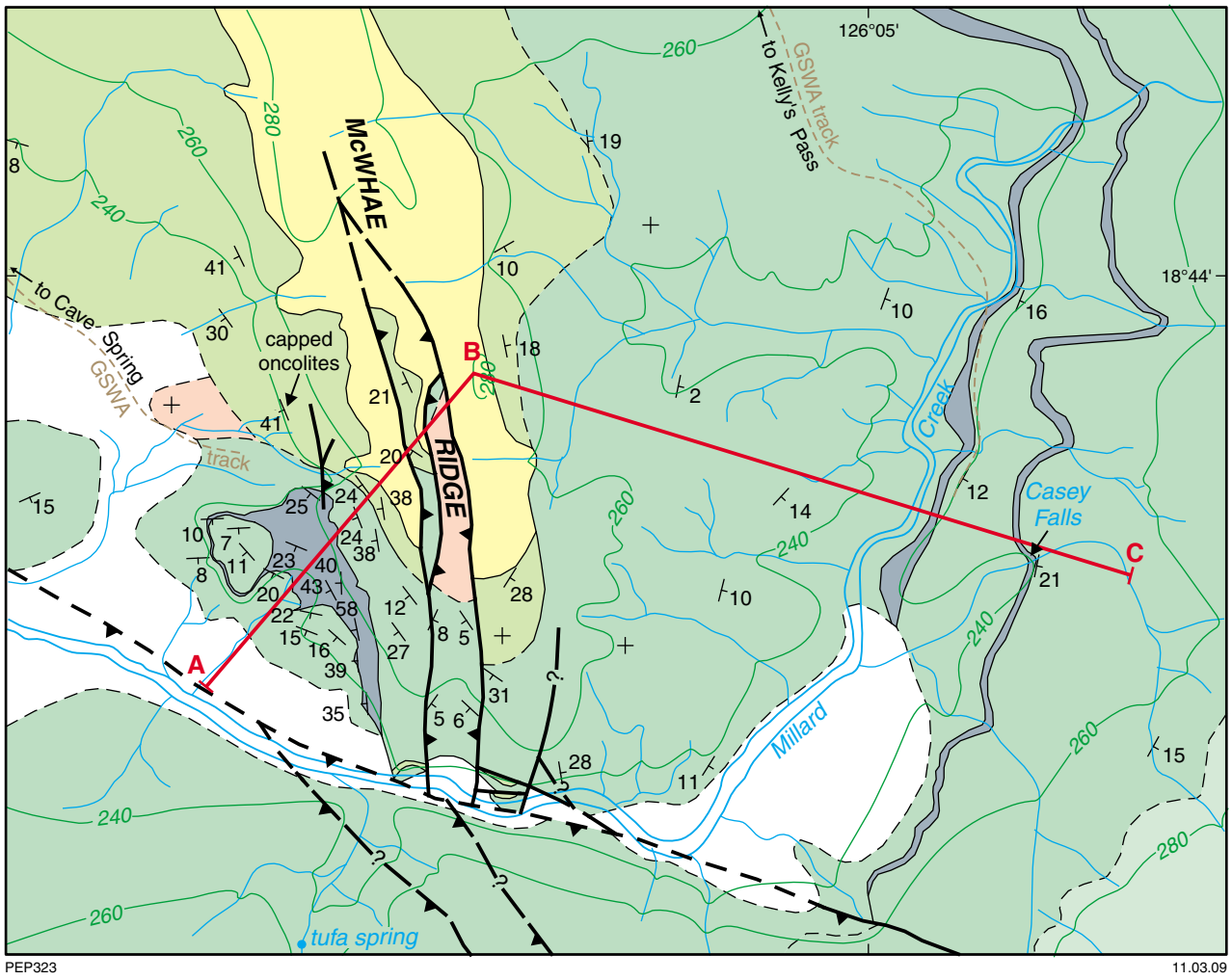

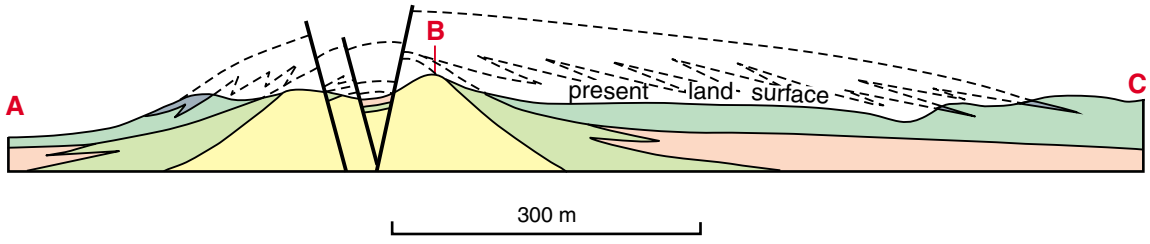

QUATERNARY — Superficial deposits

UPPER DEVONIAN

- Famennian — BUGLE GAP LIMESTONE, marginal–slope facies
- Famennian–Frasnian — VIRGIN HILLS FORMATION, marginal–slope to basin facies; stromatolite bioherm
- Frasnian — SADLER LIMESTONE, marginal–slope facies; GOGO FORMATION, basin facies; PILLARA LIMESTONE, reef–margin facies

Geological boundary — position accurate; position approximate

Fault — position accurate; position approximate; concealed; probable

240 **Contour** (metres above sea level)

Watercourse

Track

Figure 228. Geological map and cross section of McWhae Ridge. Successive cross sections A–B–C are shown in Figure 229.

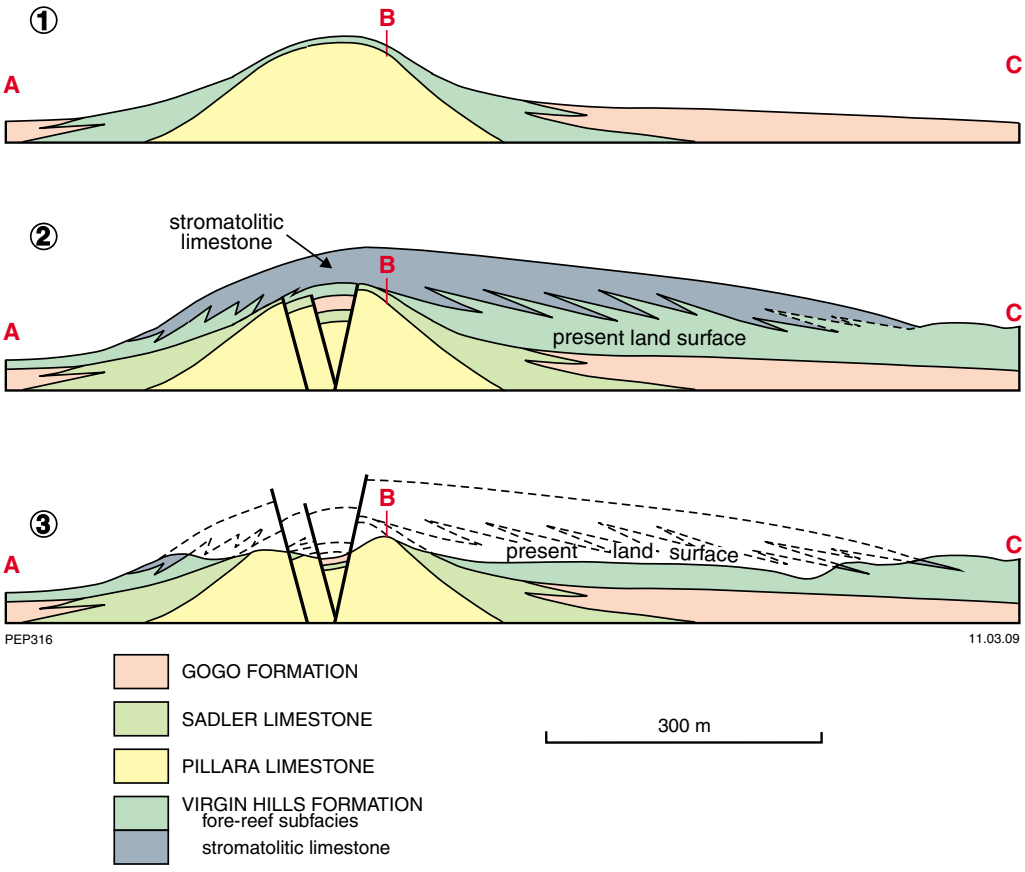

Figure 229. **Successive cross sections illustrating the development of McWhae Ridge: 1) during the late Frasnian, after drowning of the reef spine; 2) during the early Famennian, following development of a deep-water microbial bioherm over the buried reef spine; and 3) showing the present erosion surface. A–B–C marks the line of section on the map of McWhae Ridge (Fig. 228).**



Figure 230. **Network of neptunian dykes in Famennian limestone of the Virgin Hills Formation adjoining the Virgin Hills Fault near Bobs Bore.**

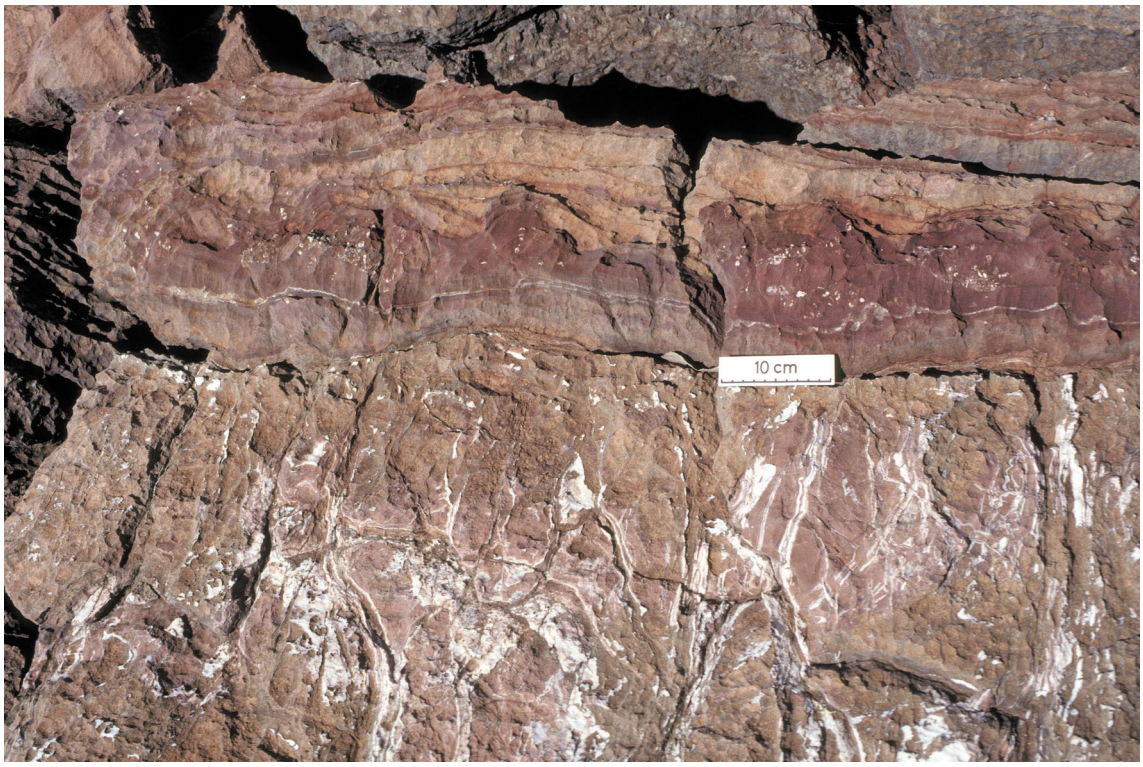

Figure 231. Famennian limestone of the Virgin Hills Formation adjoining the Virgin Hills Fault near Bobs Bore, showing abundant neptunian dykes, largely filled by spar, overlain by stromatolitic limestone without neptunian dykes. This points to an episode of faulting during the early Famennian.



Figure 232. Klippe of reefal limestone (Napier Formation) surrounded by Precambrian metamorphic rocks 1 km west southwest of Junction Dam. A horizontal thrust is present below the steeply dipping limestone.



Figure 233. Receptaculitids with geopetal infillings in the klippe shown in Figure 232, demonstrating that the limestone is steeply overturned.

357 ± 3 Ma using Rb–Sr and U–Pb isotope techniques, and Brannon et al. (1996), who dated it as 351 ± 15 Ma. Those dates would place the mineralization in the earliest Carboniferous (Tournaisian) according to the timescale of Gradstein et al. (2004). Christensen et al. (1995) further concluded that the mineralizing fluids were derived by dewatering of Devonian shales, and speculated that exhalative mineralization, equivalent in age to the epigenetic deposits, might occur in the late Famennian and Tournaisian Fairfield Group overlying the reef complexes. However, no such deposits have yet been found in that group.

Hydrothermal fluids dissolved carbonates to form cavity systems in which sulfides were precipitated. Some mineralization is also interpreted to have replaced Devonian carbonates and evaporites (Tompkins et al., 1994a,b, 1997; Vearncombe et al., 1995a,b; Wallace et al., 2002). The epigenetic Zn–Pb sulfides post-date marine cements and regional dolomitization.

MVT sulfides on the Lennard Shelf lack evidence of surrounding thermal haloes, and it is clear that mineralization must have occurred under conditions of regional burial and relatively low temperatures. The sulfides are associated with bitumen in some of the orebodies, and there is evidence that sulfides and hydrocarbons were emplaced synchronously. There are also indications of the former presence of H_2S associated with the mineralization, notably at Cadjebut, where mineralization was localized at the crest of a small anticlinal structure (Wallace et al., 2002). The H_2S probably formed as a result of bacterial sulfate reduction in association with hydrocarbons. The sulfate would have come from local evaporites and perhaps other sources. The H_2S presumably reacted with metalliferous brines derived from the Fitzroy Trough, to produce the MVT sulfides (Wallace et al., 2002).

Syngenetic mineralization

All of the Zn–Pb deposits listed above are epigenetic. However, an earlier phase of syngenetic mineralization, associated with stromatolite buildups, was discovered during the current research program in the southeast Lennard Shelf (Playford and Wallace, 1998, 2001; De Kever, 1998; Mason, 1998; Playford, 1999; Playford et al., 1999b). In this Bulletin most of the text and illustrations describing these deposits are taken directly from the paper by Playford and Wallace (2001), updated and amended where appropriate.

Mounds of distinctive stromatolitic limestone, commonly intergrown with barite and cut by gossan veins, are exposed at several localities in basin facies of the Gogo Formation in the southeastern Lennard Shelf (Figs 235, 236), mainly at or near the top of that formation. The descriptive term 'buildup' is used to describe these mounds, rather than the genetic term 'bioherm', because both organic and inorganic precipitation could have been involved in their growth. Further, in view of the different ways in which the term 'stromatolite' has been applied by various authors, it is necessary to clarify the usage adopted here. We concur with Playford and Wallace (2001) in defining stromatolites as 'columnar, digitate, and domal growth structures formed by organic or inorganic processes'. This broad usage does

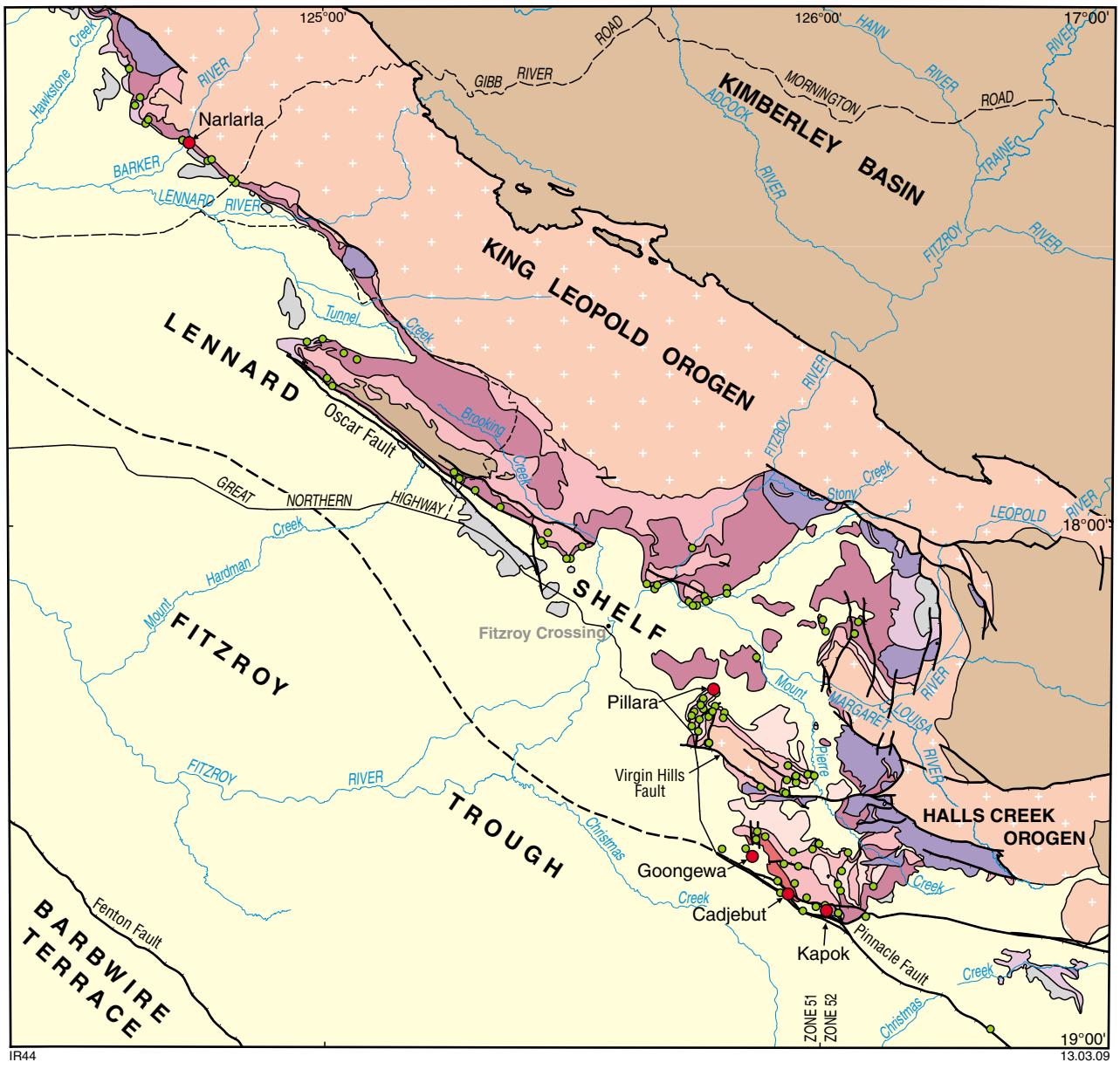

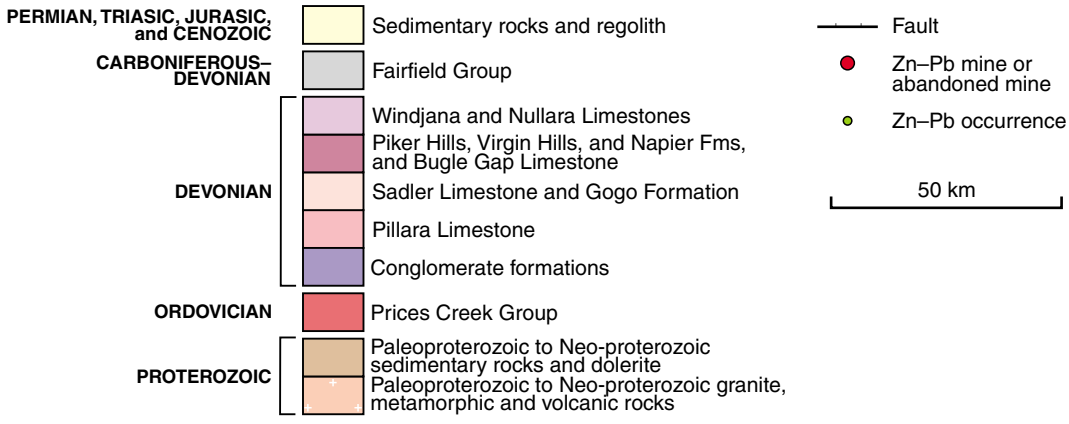

Figure 234. Zinc–lead occurrences and mine sites on the Lennard Shelf.

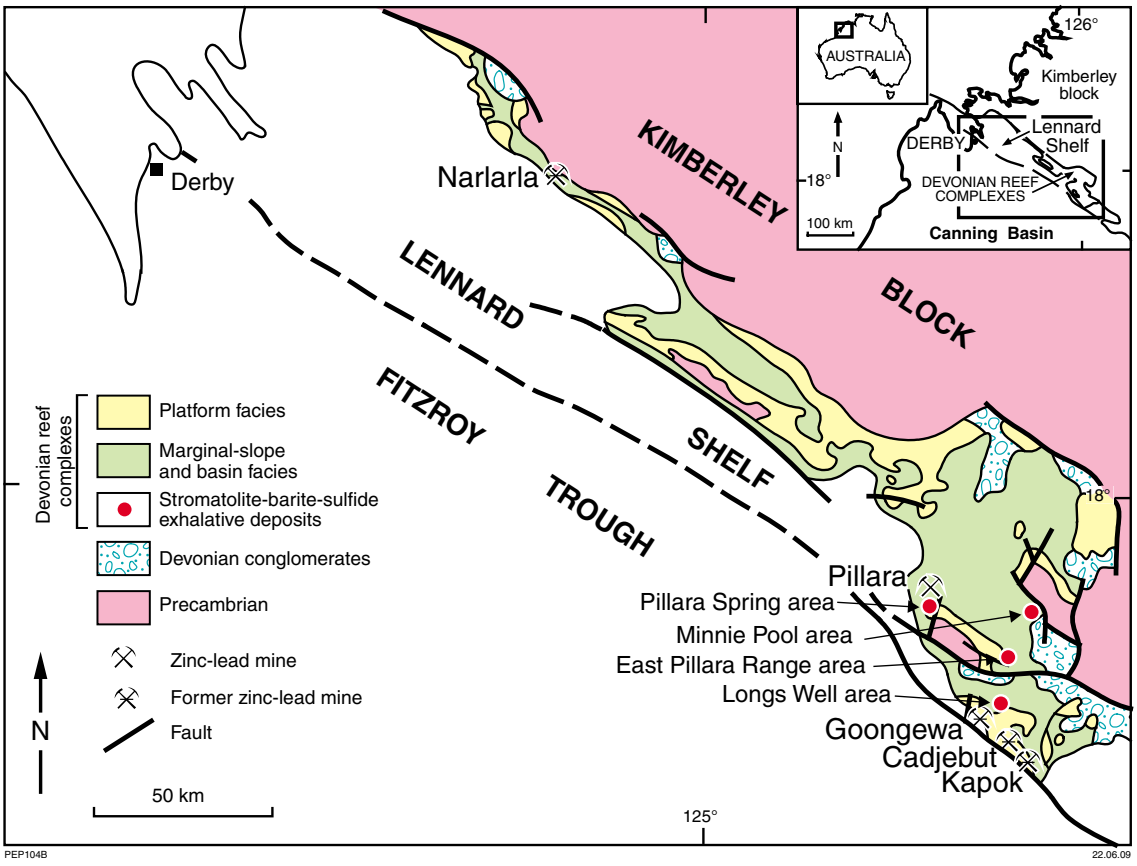

Figure 235. **Locations of Devonian exhalative deposits and economic zinc–lead deposits in the southeastern Lennard Shelf (after Playford and Wallace, 2001).**

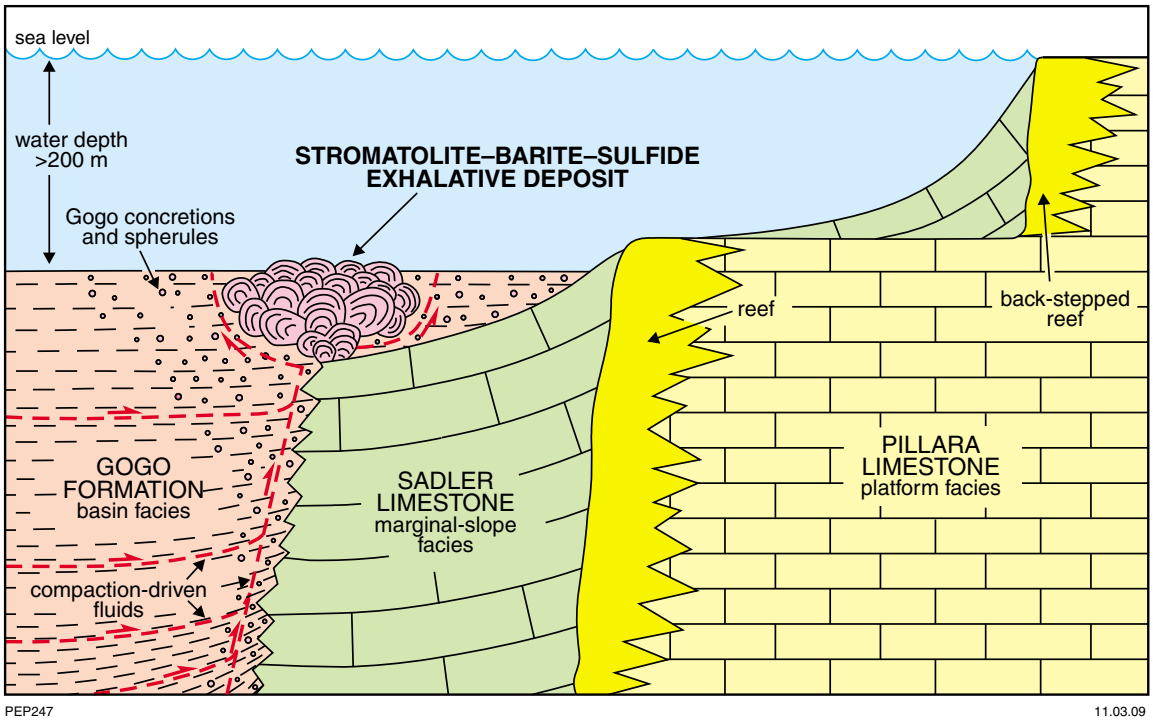

Figure 236. **Diagrammatic cross section showing the development of exhalative deposits above the contact between the Gogo Formation and the Sadler Limestone after a backstepping episode (after Playford and Wallace, 2001).**

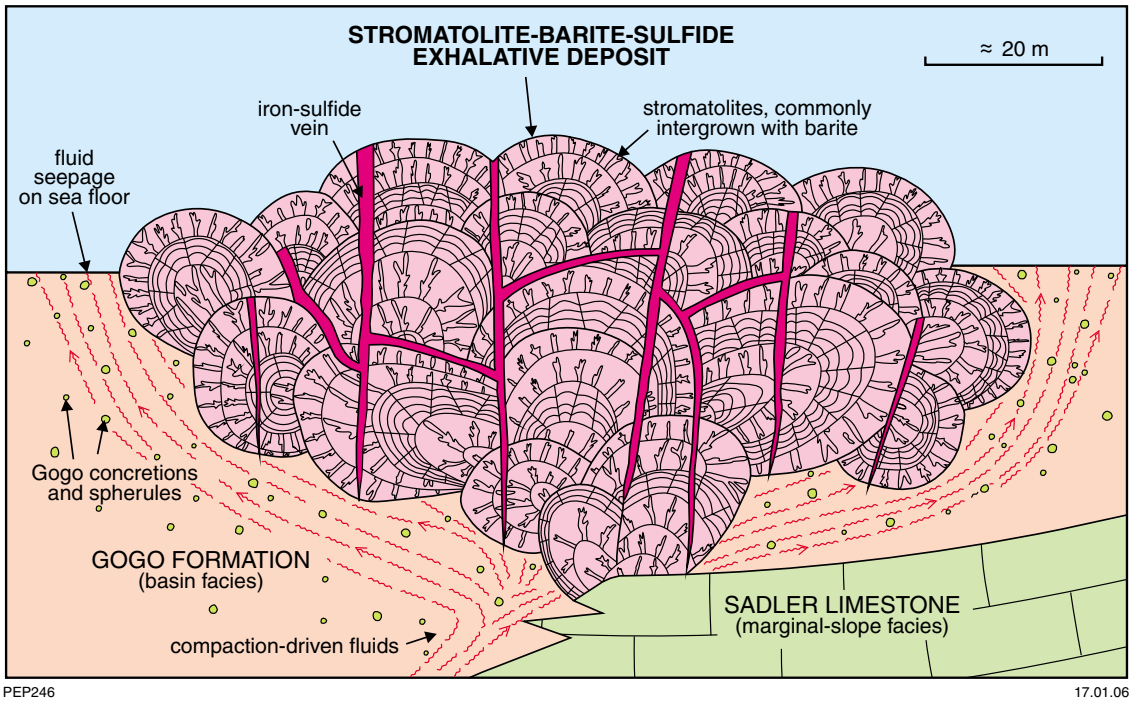

Figure 237. Diagrammatic cross section through a Frasnian exhalative deposit (after Playford and Wallace, 2001).

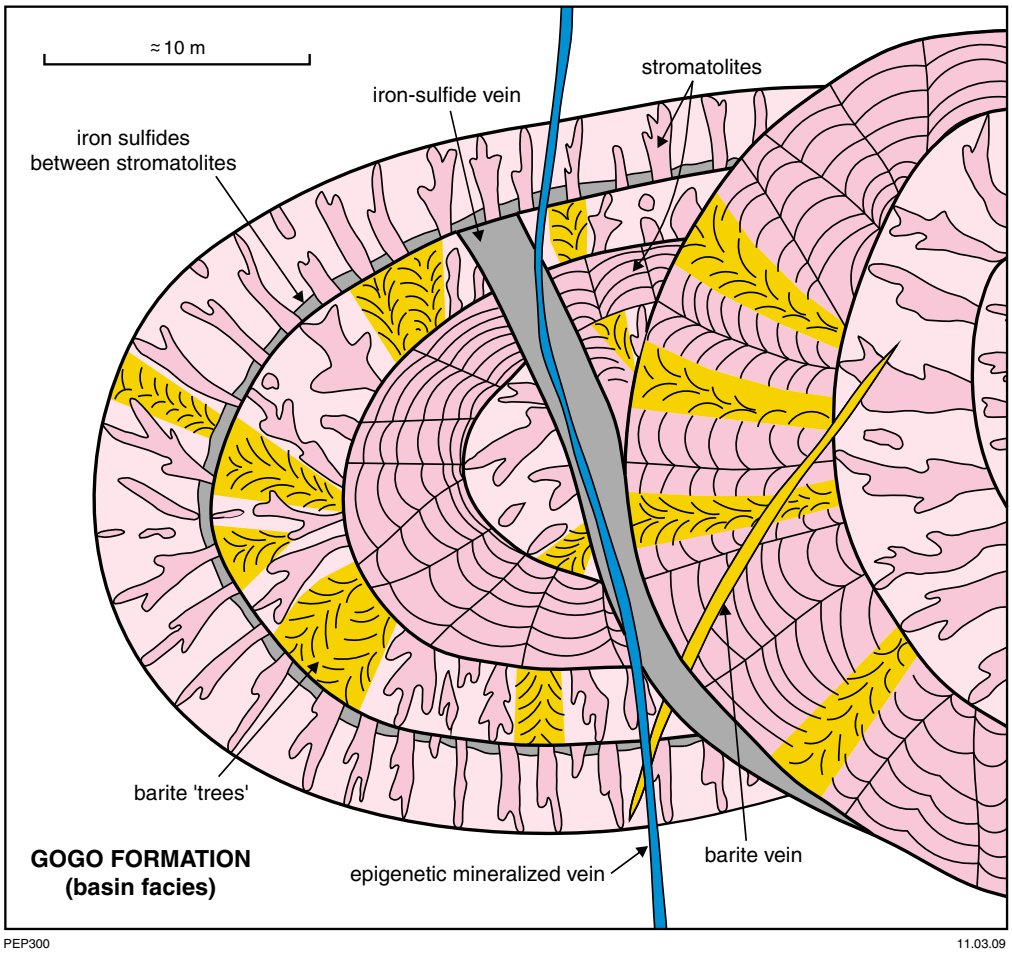

Figure 238. Diagrammatic cross section through lobes of an exhalative deposit, showing the relationships between stromatolites, barite 'trees' and veins, iron-sulfide veins, and later epigenetic mineralized veins (after Playford and Wallace, 2001).

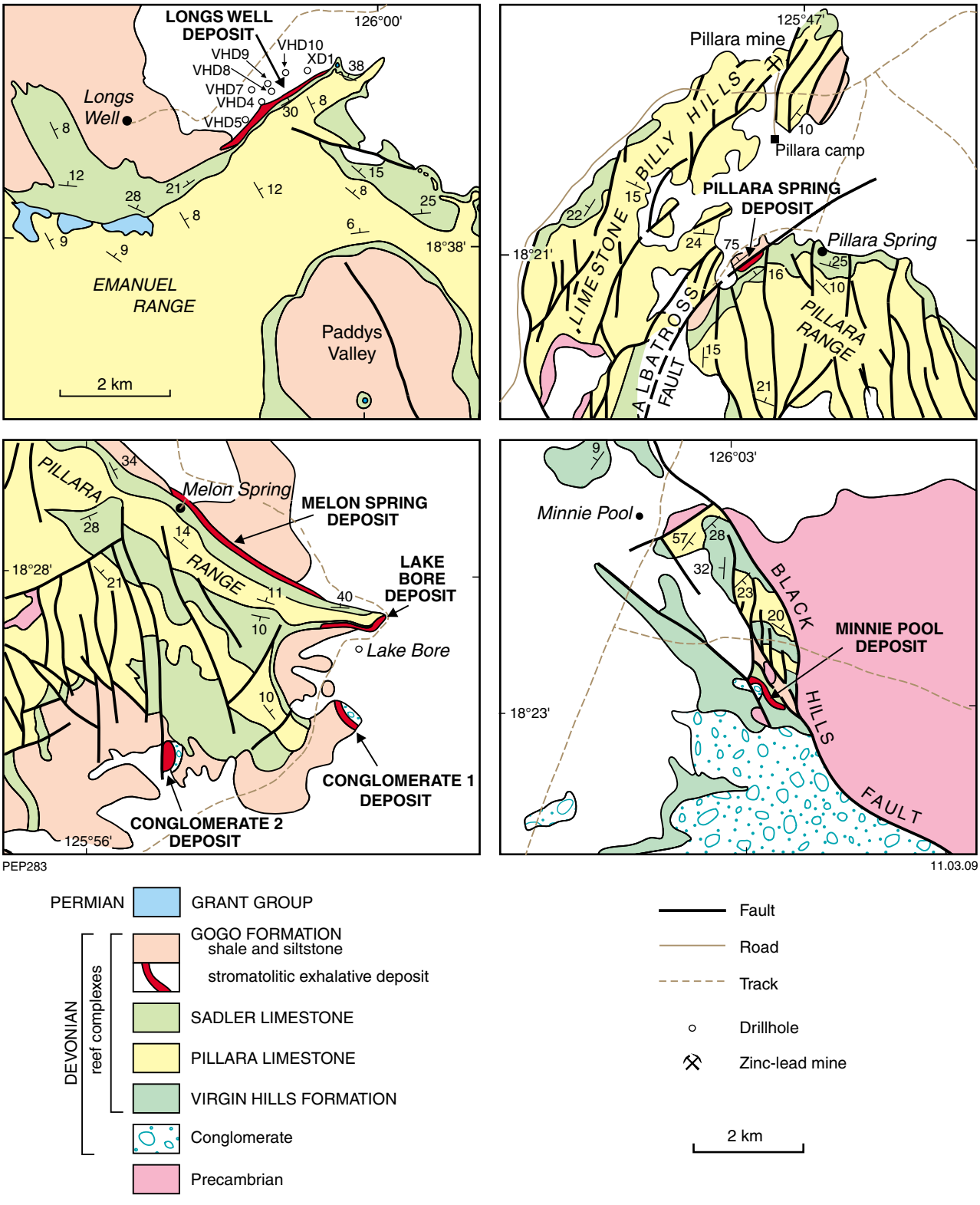

Figure 239. Geological maps showing the locations of Devonian exhalative deposits in the southeastern Lennard Shelf (after Playford and Wallace, 2001).

not comply with some more restricted definitions that require stromatolites to be organic (e.g. Walter, 1976) or laminated (e.g. Riding, 1999).

The stromatolite–barite–gossan deposits occur (a) where the basin facies represented by the Gogo Formation adjoins marginal-slope facies of the Sadler Limestone, (b) at other places where the Gogo Formation is cut by synsedimentary faults, and (c) as allochthonous blocks in penecontemporaneous debris-flow conglomerates that intertongue with the Gogo Formation.

In each of these places the stromatolitic buildups are cut by limonitic gossan veins and dykes, most of which are nearly vertical and approximately parallel or perpendicular to the trend of the buildup. Other veins developed where fissures opened along bulbous bedding. Drilling has shown that the gossans formed by weathering of iron sulfides (pyrite and marcasite). Neomorphic alteration adjacent to the gossans has resulted in recrystallization of the stromatolitic limestones, with partial or total destruction of their original stromatolitic fabrics.

The major part of the Gogo Formation in the areas of the buildups consists of shale and siltstone, containing many limestone concretions ('Gogo nodules') that occur most commonly in places where the formation adjoins Sadler Limestone and in the vicinity of stromatolitic buildups (Figs 68, 240).

The exhalative deposits known in the Gogo Formation have not been dated by radiometric methods, but equivalent strata in the youngest part of the formation are known from conodonts to be early Frasnian (about 380 Ma), within Frasnian Zone 5 (G Klapper, 2004, written comm.).

Field relationships

Photographs and diagrams relating to field occurrences of the stromatolite–barite–gossan (sulfide) syngenetic deposits are shown in Figures 235–258. The four principal areas where the deposits are exposed are referred to as the Longs Well, East Pillara Range, Pillara Spring, and Minnie Pool areas (Figs 235, 239).

Longs Well area

A belt of stromatolitic limestone, intergrown with barite and cut by prominent gossan veins, forms a linear buildup, 2.6 km long, 150 m wide, and at least 50 m thick, along the north side of the Emanuel Range near Longs Well (Figs 234, 235, 239; Fleming, 1983; Bennett, 1992, 1994; De Kever, 1998). The buildup occurs within the Gogo Formation, adjoining its contact with the Sadler Limestone.

The buildup formed as a coalesced series of bulbous stromatolitic growths (Figs 236–238, 248). Barite was deposited contemporaneously with the stromatolites, as fibrous or bladed crystals and rosettes and dendritic forms intergrown with stromatolites (Figs 249–251), but some also fills narrow fissures cutting stromatolites.

The stromatolitic buildup is cut by many black, brown, and red gossan veins, occupying fissures as much as 5 m wide and a few tens of metres long (Figs 252, 253), surrounded



Figure 240. Broken concretions weathered out of the Gogo Formation, showing concentric growth rings and fibrous structures. From the East Pillara Range area, Conglomerate 1 deposit.



Figure 241. Bulbous stromatolites in an allochthonous block, east Pillara Range area, Conglomerate 1 deposit.

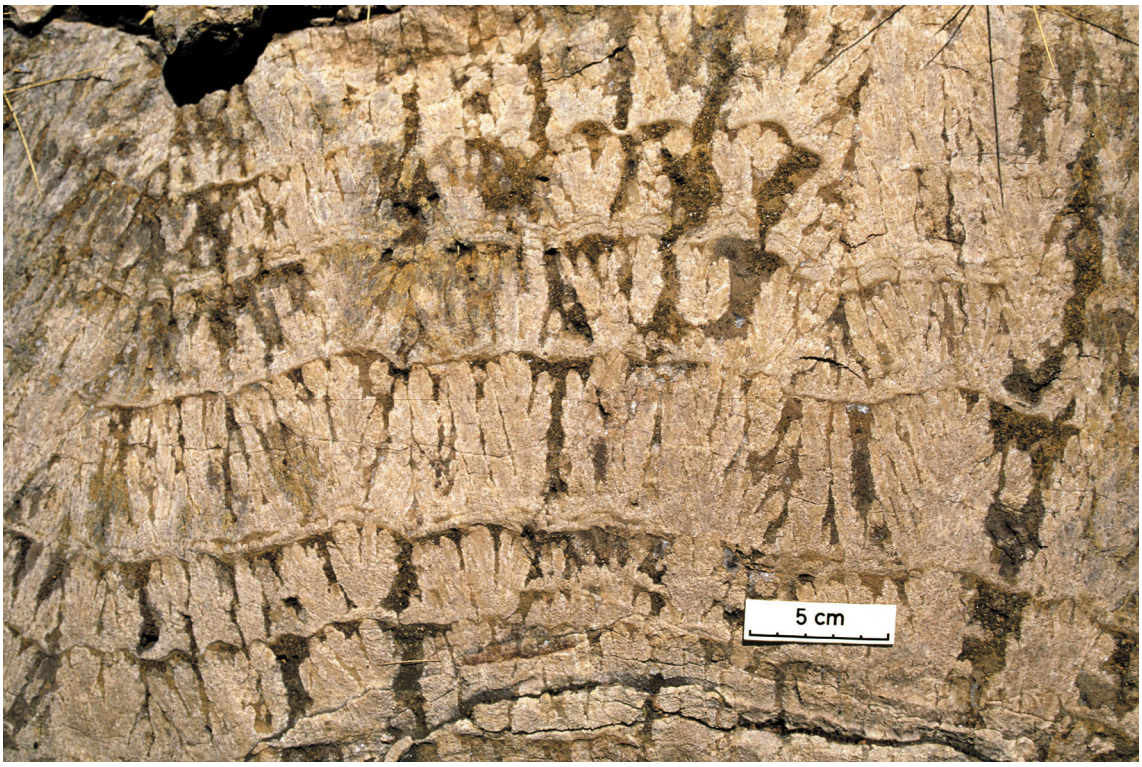

Figure 242. Bands of branching, columnar, exhalative stromatolites in an allochthonous block, east Pillara Range area, Conglomerate 2 deposit.



Figure 243. Bulbous exhalative stromatolite forming an allochthonous block, Conglomerate 1 deposit.

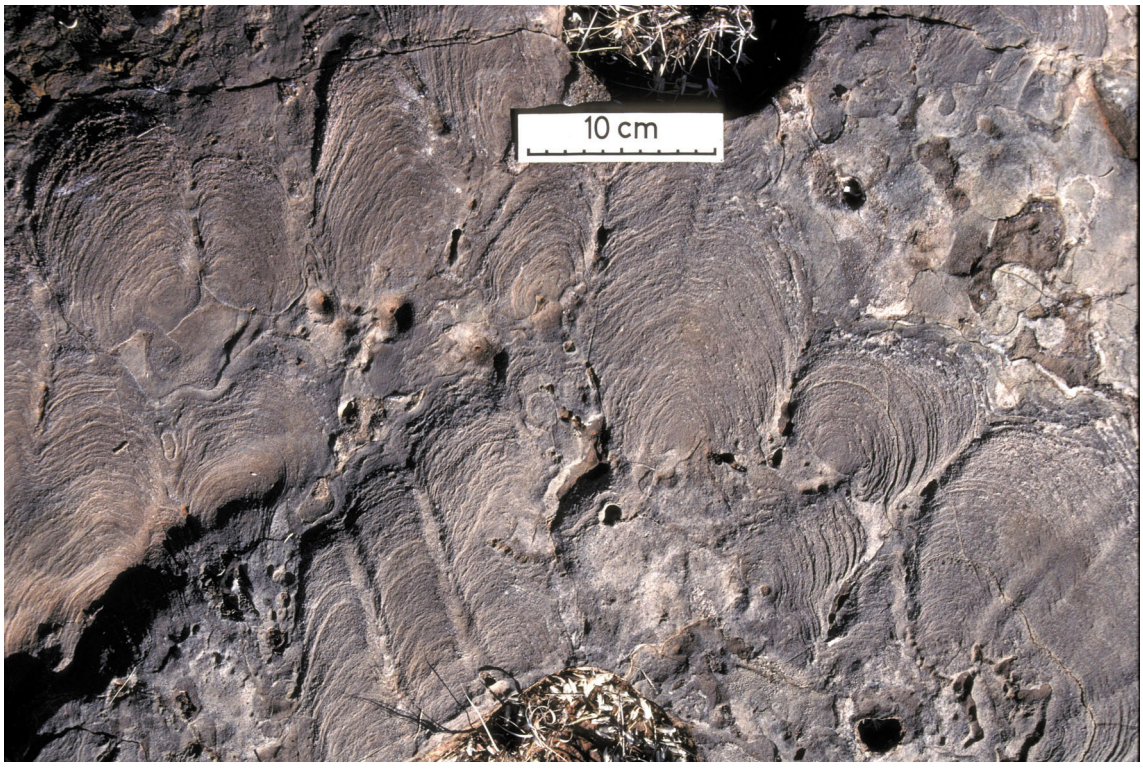

Figure 244. Finely laminated columnar exhalative stromatolites, Longs Well area.



Figure 245. **Exhalative stromatolites forming part of a bulbous growth in an allochthonous block, east Pillara Range area, Conglomerate 2 deposit.**

Figure 246. **(below) Fibrous exhalative stromatolites, Minnie Pool area.**

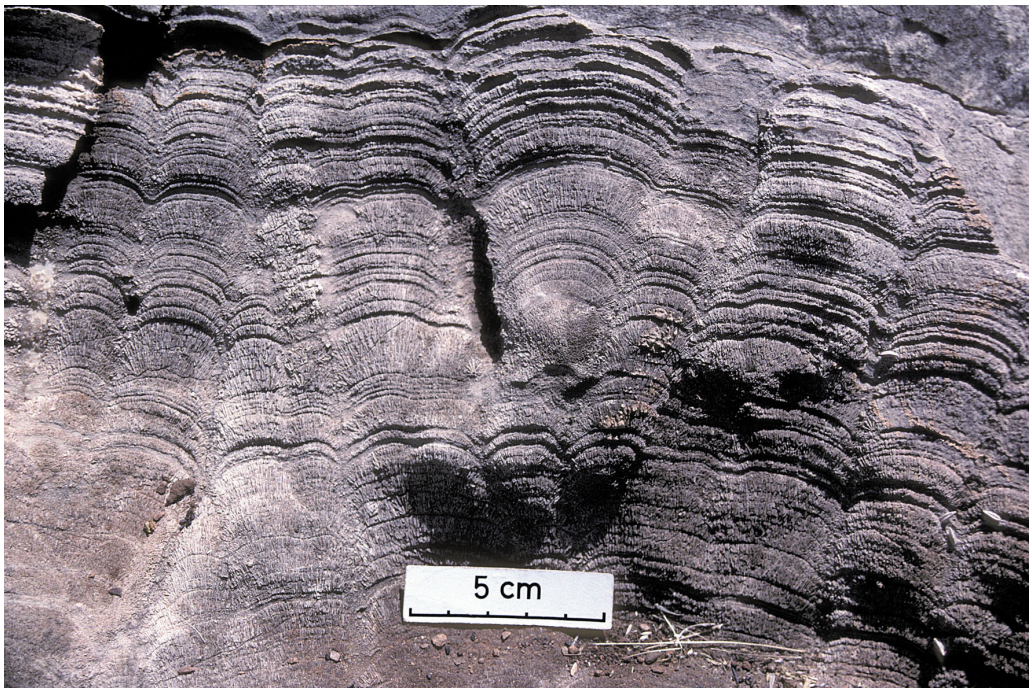



Figure 247. Cross section through a small spherical exhalative stromatolite body, east Pillara Range area, Conglomerate 1 deposit.

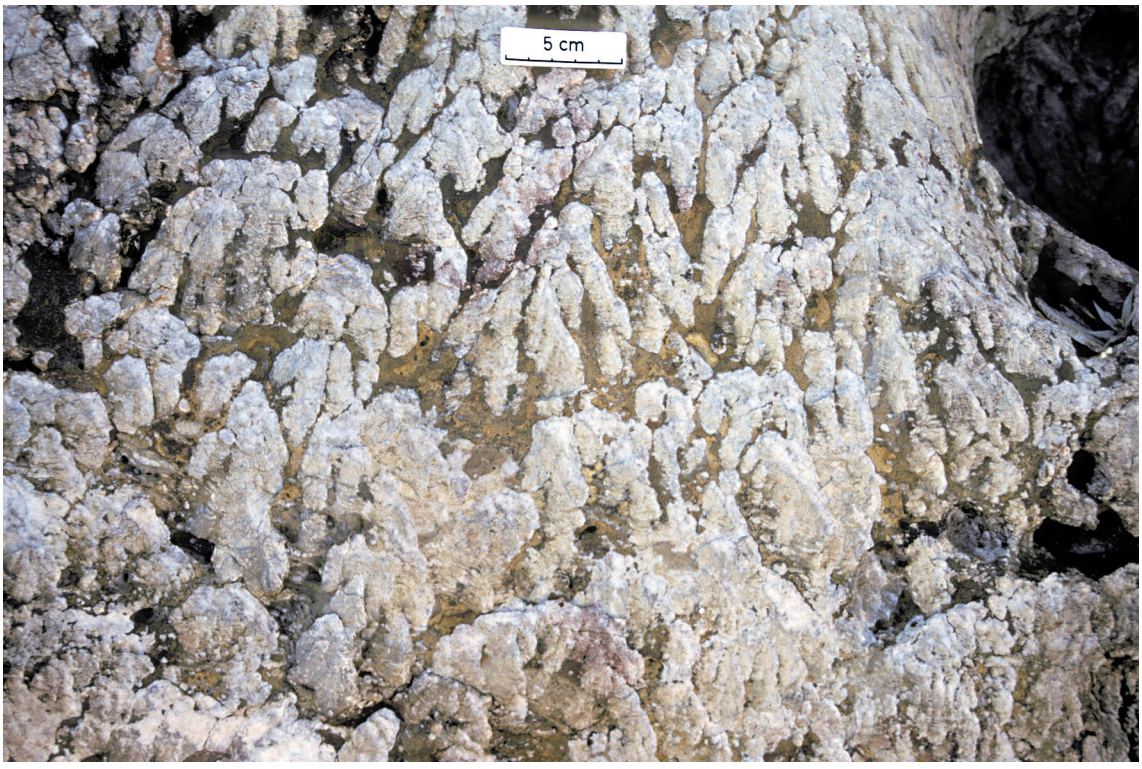

Figure 248. Branching columnar stromatolites that grew steeply downward into mud of the Gogo Formation, Longs Well area.

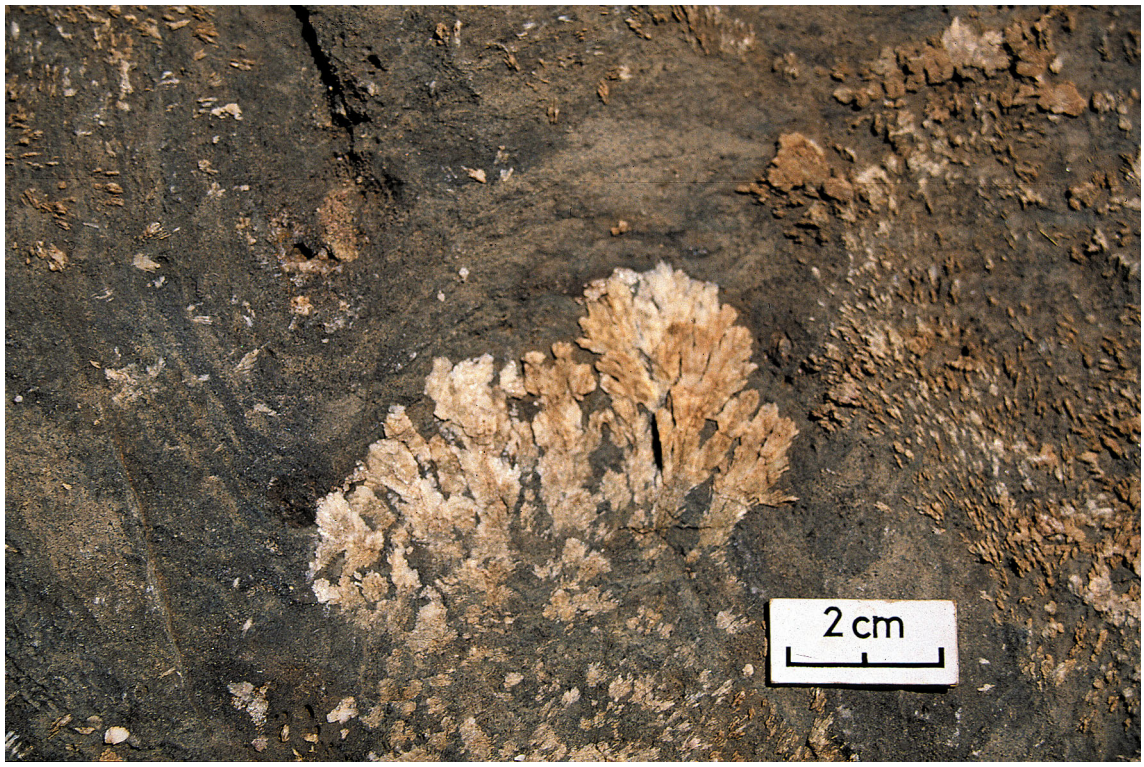

Figure 249. Barite 'shrub' in stromatolitic limestone, Longs Well area.



Figure 250. Barite 'shrubs' that grew contemporaneously with the enclosing exhalative stromatolites, Longs Well area.

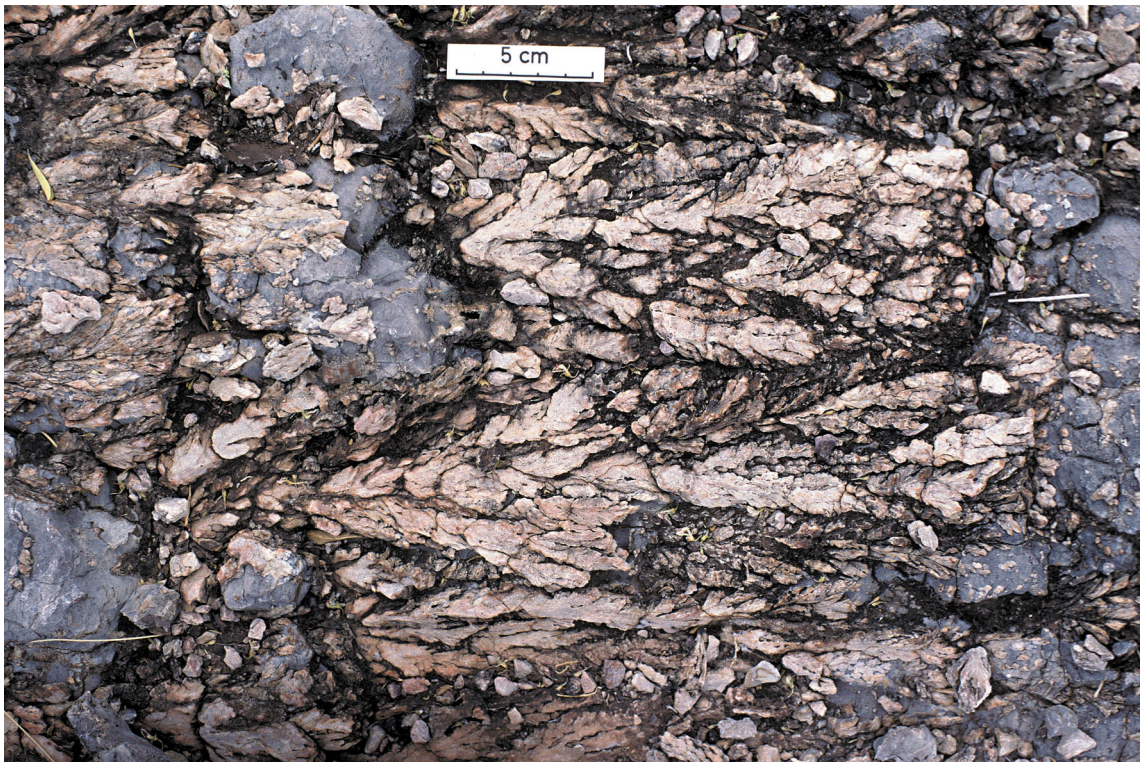

Figure 251. Plumose barite, which grew laterally, associated with exhalative stromatolites, Minnie Pool area.



Figure 252. Gossan dyke (after iron sulfides), cutting through exhalative stromatolites, Longs Well area.

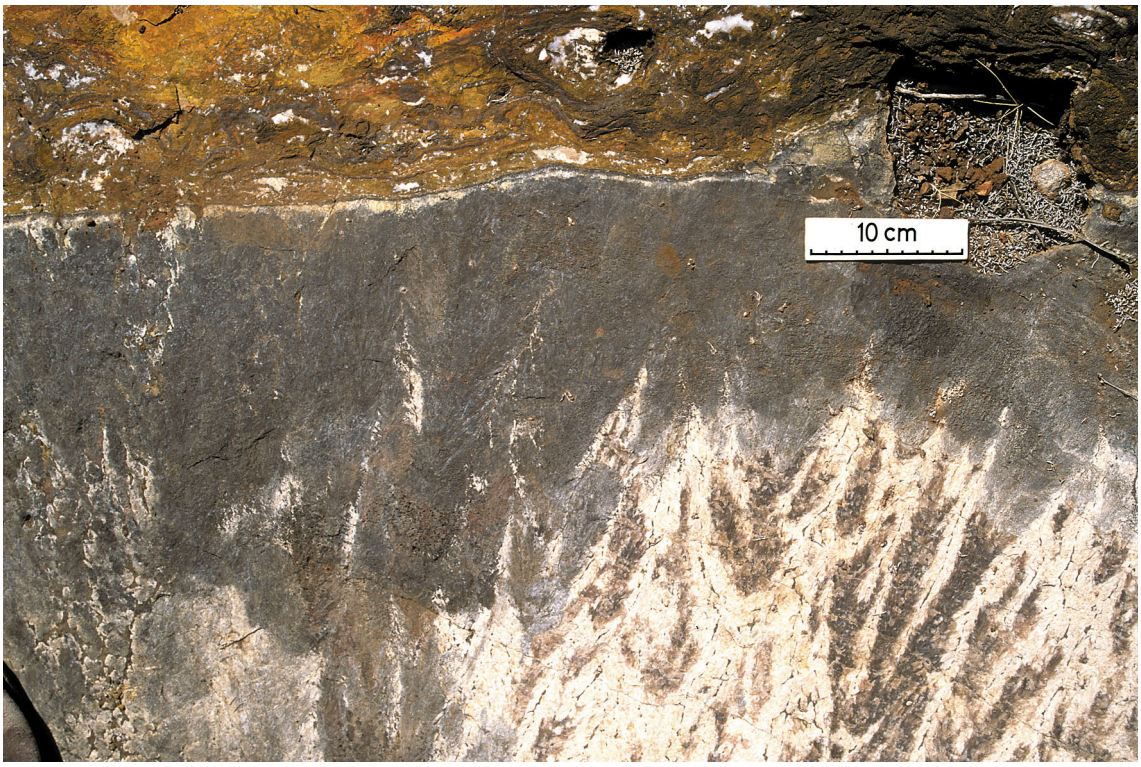

Figure 253. Gossan dyke (upper part of photo) cutting through exhalative stromatolites that are partly altered to dark sparry calcite in which stromatolitic textures have been largely destroyed, and light sparry calcite in which those textures are somewhat better preserved. Longs Well area.



Figure 254. Exhalative stromatolites, partly altered through low-temperature metasomatism associated with a gossan dyke (off the photo), Longs Well area. Stromatolitic textures are partly preserved in the light-coloured limestone, but are totally destroyed in the dark-coloured limestone.

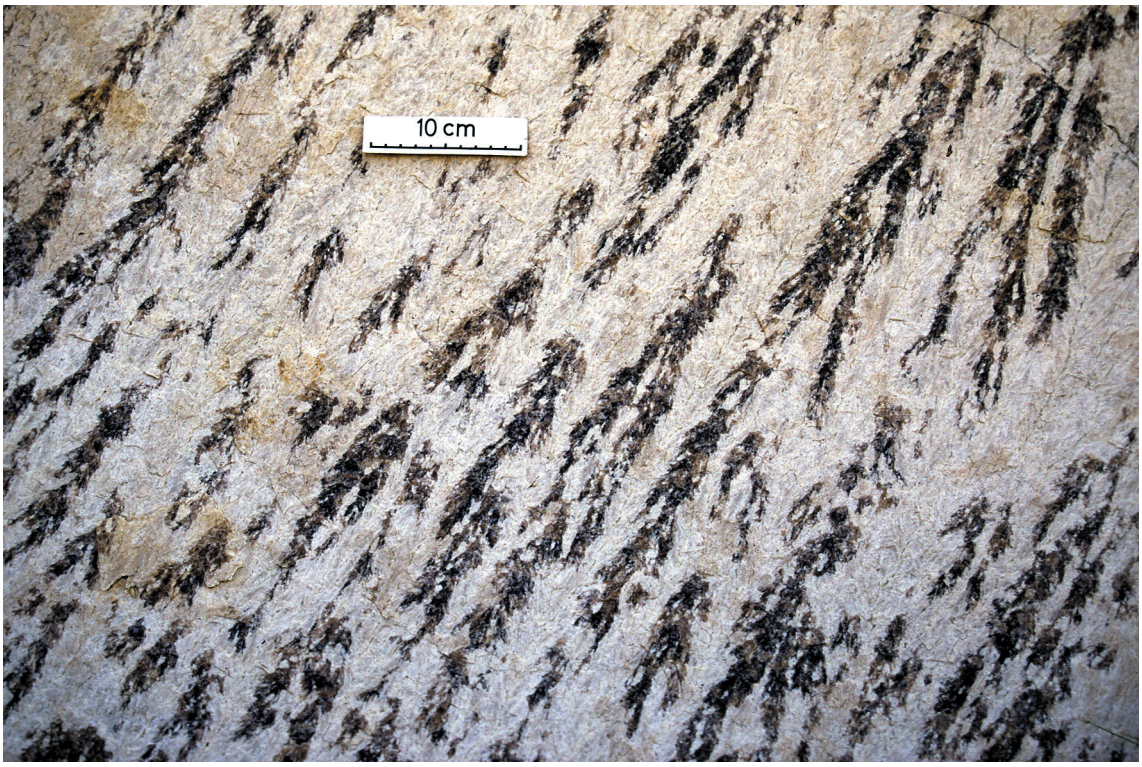

Figure 255. Exhalative stromatolites altered to white and dark spar, partly preserving their original stromatolitic forms in the white spar and completely destroying them in the dark spar, Longs Well area.



Figure 256. Bedding plane showing heads of exhalative stromatolites surrounded by iron oxide, thought to have been formed by weathering of penecontemporaneous iron sulfides, Longs Well area.

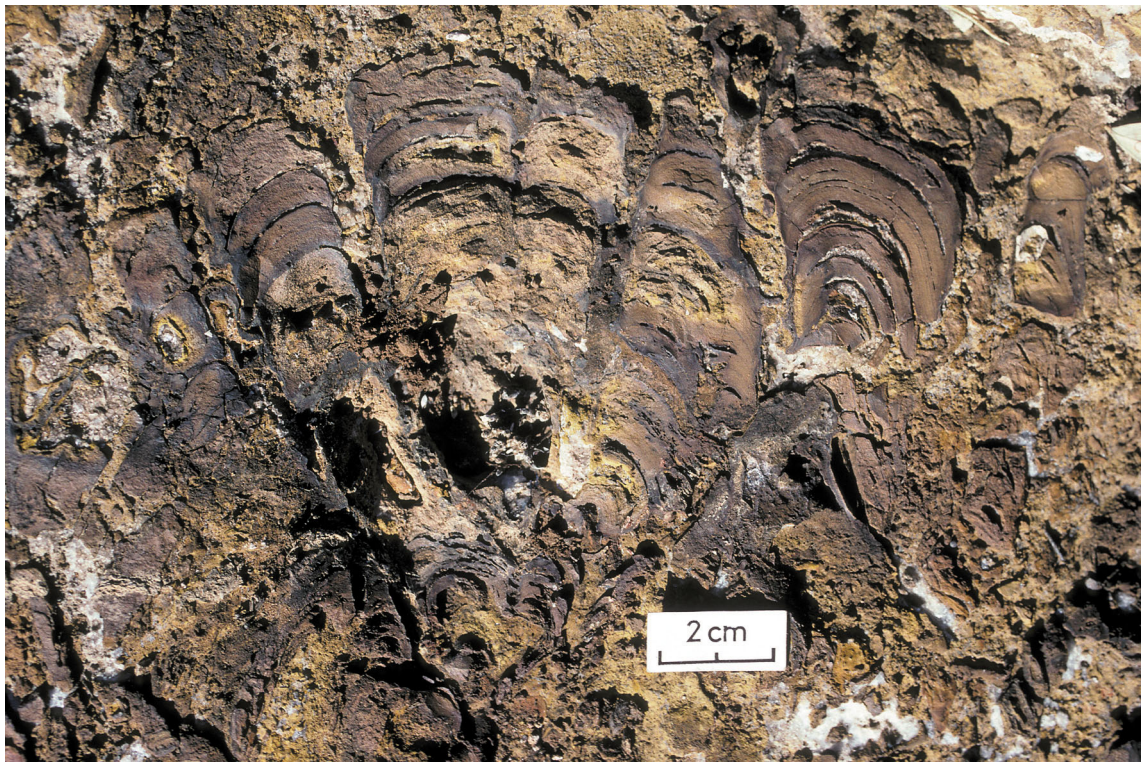

Figure 257. Gossan dyke, originally composed of stromatolitic iron sulfides, East Pillara Range area.

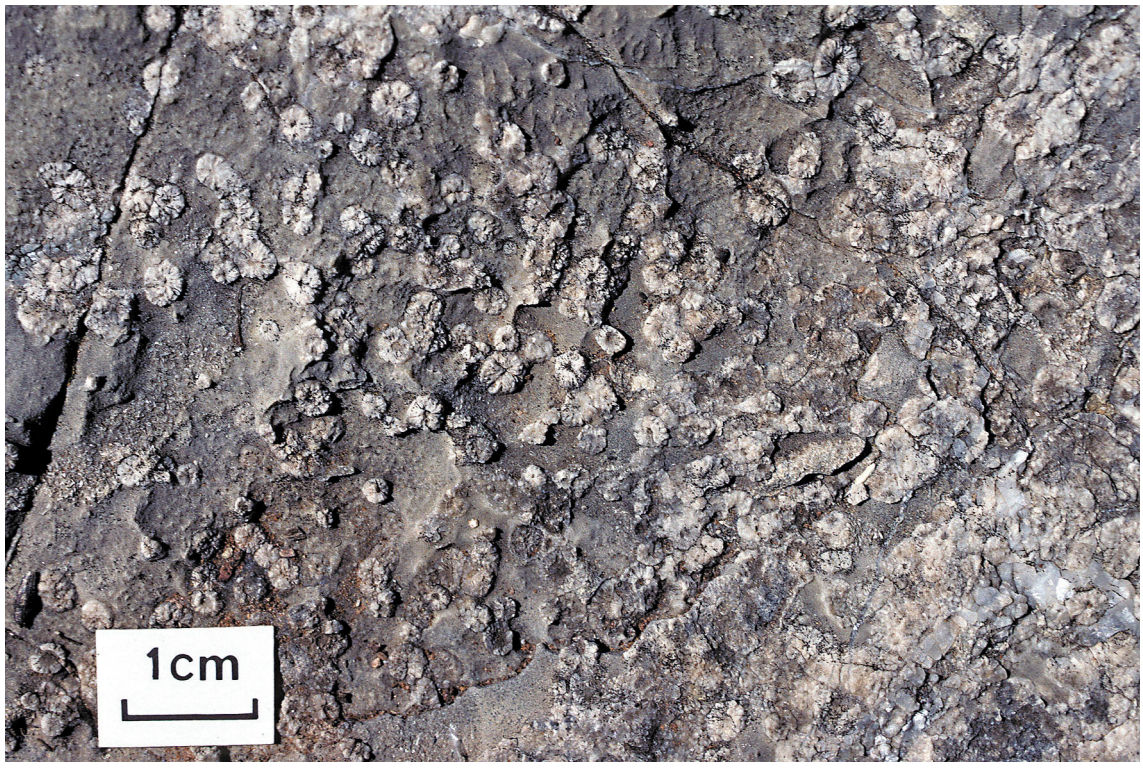

Figure 258. Spherules of laminated calcite in an exhalative deposit, Minnie Pool area.

by zones of fibrous recrystallized calcite (Figs 253–255). Drillholes show that the gossans originated through the weathering of pyrite and marcasite. In a few places, gossanous material fills spaces between stromatolite columns (Fig. 256), and some gossan dykes exhibit stromatolitic layering, testifying to the role of microbes in sulfide deposition (Fig. 257).

East Pillara Range area

Four stromatolite–barite–gossan deposits, referred to as the Melon Spring, Lake Bore, Conglomerate 1, and Conglomerate 2 deposits, occur in the vicinity of the east Pillara Range (Fig. 239). The Melon Spring and Lake Bore deposits resemble the Longs Well deposit, but are less well exposed. Some gossans in the Lake Bore deposit display well-defined stromatolitic structures (Fig. 257).

In the Conglomerate 1 and Conglomerate 2 deposits the stromatolite–barite–gossan association is represented by large allochthonous blocks in debris-flow conglomerates that interfinger with the Gogo Formation. Those conglomerates contain rounded boulders and cobbles of Precambrian quartzite, together with angular blocks of stromatolitic limestone as much as 18 m long, smaller blocks of gossan and barite, reworked Gogo concretions (Fig. 240), and some clasts of marginal-slope and platform limestones. The Conglomerate 1 deposit also displays some remarkable circular stromatolitic bodies, thought to have grown as near-spherical forms below the surface of muds in the Gogo Formation (Figs 241, 243). In some ways they resemble very large Gogo concretions, but unlike most of those concretions they exhibit well-developed spherical layering.

Many blocks of stromatolitic limestones in the conglomerates are wholly or partly recrystallized, although their stromatolitic layering has commonly been maintained (Figs 241–245). Recrystallization is thought to have occurred very early, pre-dating the incorporation of the stromatolitic blocks in the conglomerate. Debris flows sweeping into the basin must have broken up stromatolite–barite–sulfide buildups that were then growing on the basin floor and being altered by exhalative fluids, before carrying them down slope with other debris.

Pillara Spring area

The Pillara Spring deposit (Fig. 239) is a discontinuous belt of stromatolitic limestone situated in the valley between the Pillara Range and Limestone Billy Hills reef complexes. The deposit adjoins the Albatross Fault, a northeast-trending synsedimentary normal fault with a left-lateral component of movement (Dörling et al., 1995). The limestone in the deposit consists of contiguous columns of fibrous stromatolites, largely recrystallized, and cut by a few prominent gossans, but no barite has been observed. Gogo concretions and spherules are abundant in steeply dipping Gogo Formation on the northwest side of the fault (Fig. 259).

Minnie Pool area

The Minnie Pool deposit (Figs 239, 246, 251, 258) consists of stromatolites intergrown with barite and cut by veins of gossan and barite. The deposit adjoins Sadler Limestone and underlies Virgin Hills Formation, forming low outcrops within a strongly faulted zone (Plate 3). Stromatolites are well preserved in some exposures (Fig. 246), but in others the stromatolitic fabrics have largely been destroyed through recrystallization, especially where the limestone adjoins gossans. There is clear evidence, in the form of penecontemporaneous neptunian dykes containing fragments of barite and Devonian limestones, that the faulting was synsedimentary.

Stromatolite buildups

A variety of shallow- and deep-water stromatolites has been recorded from the Devonian reef complexes of the Canning Basin (Fig. 260), but the exhalative forms described in this section differ from those previously recorded by Playford et al. (1976). Whereas the previously known stromatolites formed on shallow reefal platforms and down fore-reef slopes, and were associated with open-marine benthic faunas, the stromatolites discussed here grew on or just below the floors of deep inter-reef basins without associated benthic faunas, and surrounded or enveloped by anoxic muds (Figs 236, 237). Most of the present forms, unlike those previously described, are composed of radiating fans of fibrous calcite, commonly interspersed with micritic laminae. Continuous gradations are found between columns composed entirely of calcite fibres and those consisting largely of laminated micrite. The fibrous calcite forms radiating fans that generally have fan lengths of around 10 to 20 mm (Fig. 246).

Stromatolitic fabrics have largely been destroyed through recrystallization in some outcrops, and the recrystallized calcite may be either dark or light coloured. Inclusions are very abundant in calcite of the unrecrystallized stromatolites but are rare in recrystallized calcite. Most inclusions in the unrecrystallized calcite are subspherical and opaque to translucent, and may be composed of organic material. Fluid inclusions are less common and are mostly small (less than 10 μm) and single phase, indicating that the calcite was precipitated at relatively low temperatures, probably less than 60ºC (Goldstein and Reynolds, 1994).

The recrystallized calcite is clearly an alteration product, as it cuts across primary stromatolitic fabrics (Figs 253–255). Patches of recrystallized calcite are commonly dispersed through the unaltered stromatolites, and vice versa, usually with sharp boundaries between them. Sparse pyrite inclusions, less than 10 μm in diameter, are present in subsurface samples of the recrystallized calcite, but are absent in the unaltered stromatolites. The pyrite inclusions weather to iron oxide at the surface.

The recrystallized limestone occurs in zones, ranging from less than a metre to several metres wide, mostly adjoining gossan veins. Recrystallized calcite has uniform stable-isotope compositions, with $\delta^{18}O$ and $\delta^{13}C$ values ranging from –7 to –5‰ PDB and –22 to –19‰ PDB respectively. Calcite in unaltered stromatolites is much more variable, with $\delta^{18}O$ and $\delta^{13}C$ values ranging from –12 to –6‰ PDB and –20 to –7‰ PDB respectively (De Kever, 1998; Mason, 1998). Relative to marine carbonates, both types of calcite have very negative carbon-isotope signatures, with recrystallized calcite having lower $\delta^{13}C$ and higher $\delta^{18}O$ values than calcite in unrecrystallized stromatolites (Fig. 261).

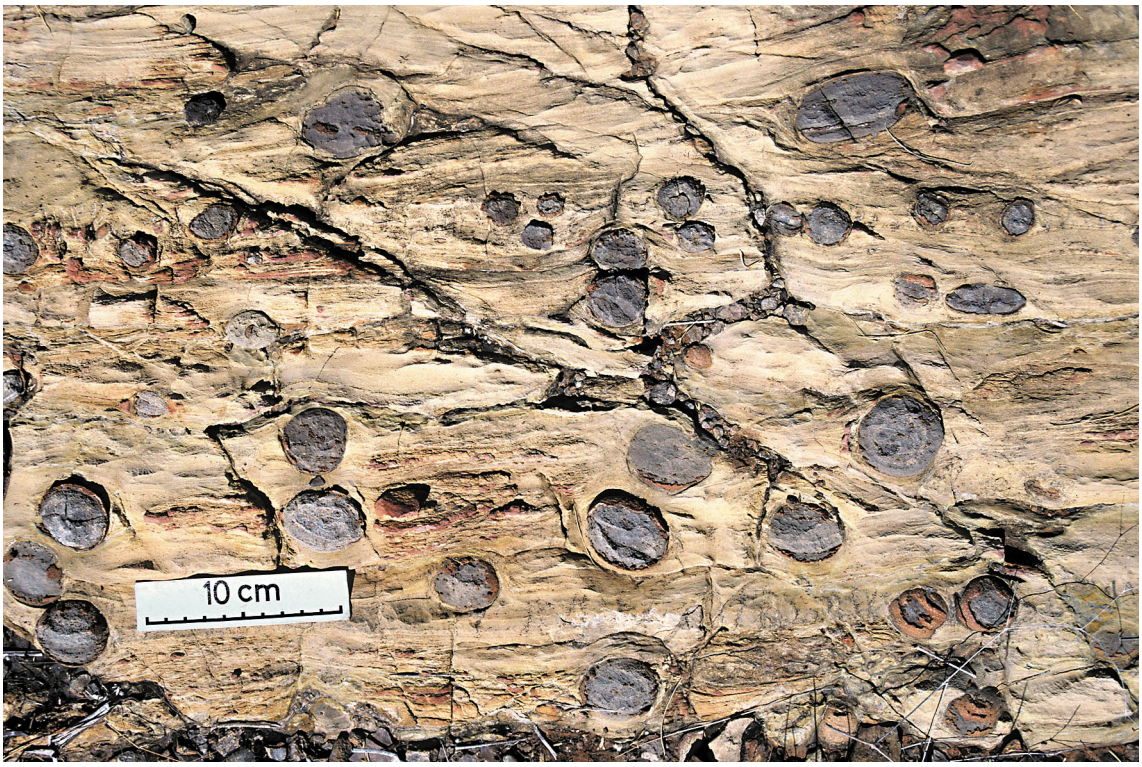

Figure 259. Sheared lime mudstone and concretions in steeply dipping Gogo Formation beside the Albatross Fault, Pillara Spring area.

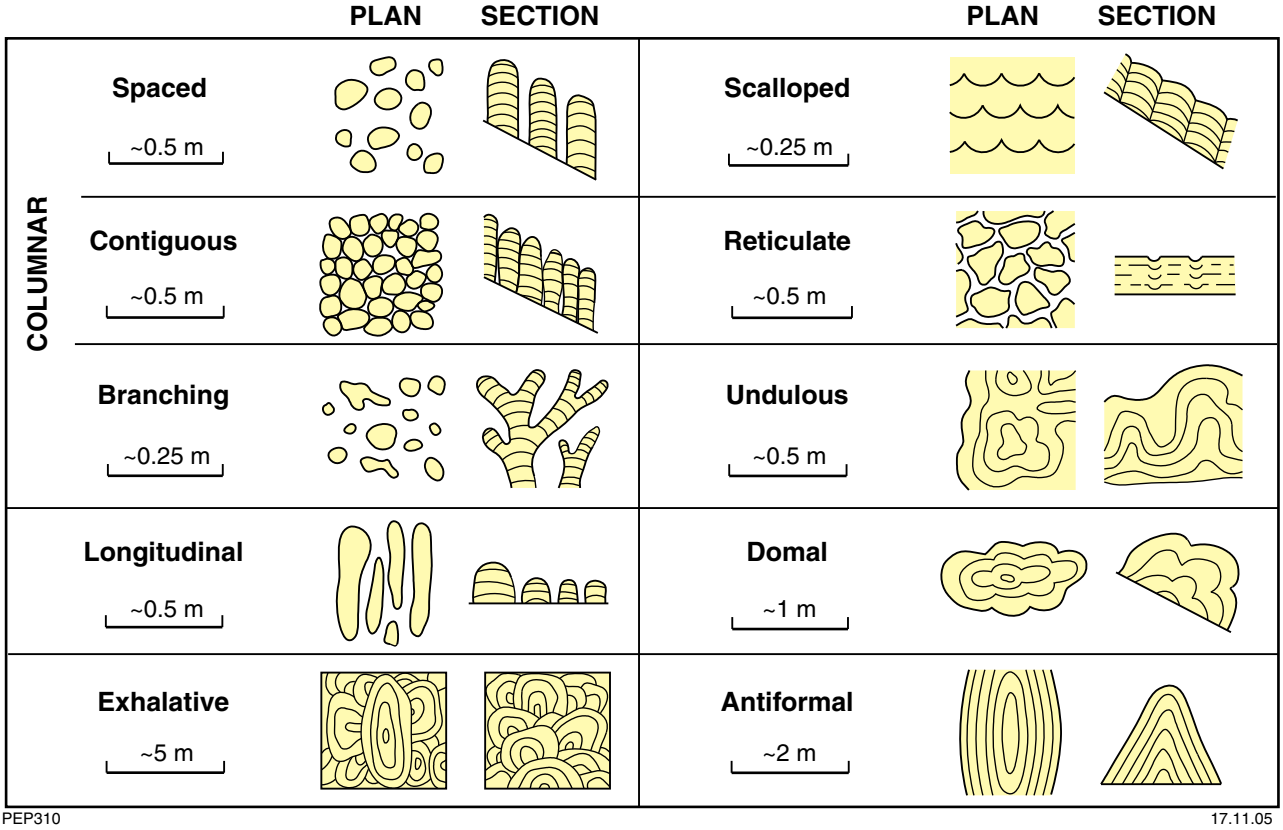

Figure 260. Diagram illustrating the different types of stromatolites recognized in the reef complexes.

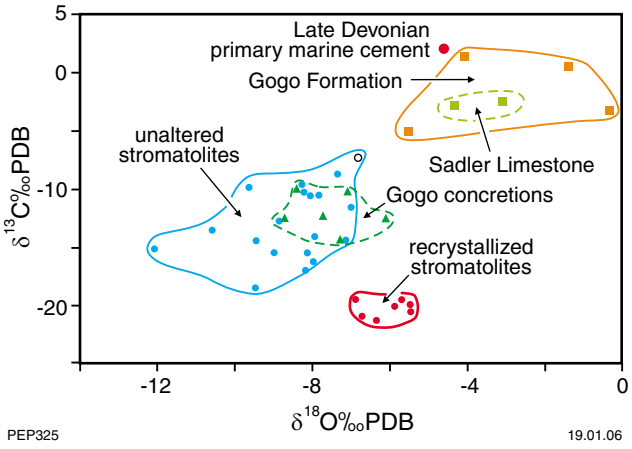

Figure 261. Oxygen- and carbon-isotope values for stromatolites, Gogo concretions, Sadler Limestone, Gogo Formation, and Late Devonian primary marine cements (after Playford and Wallace, 2001).

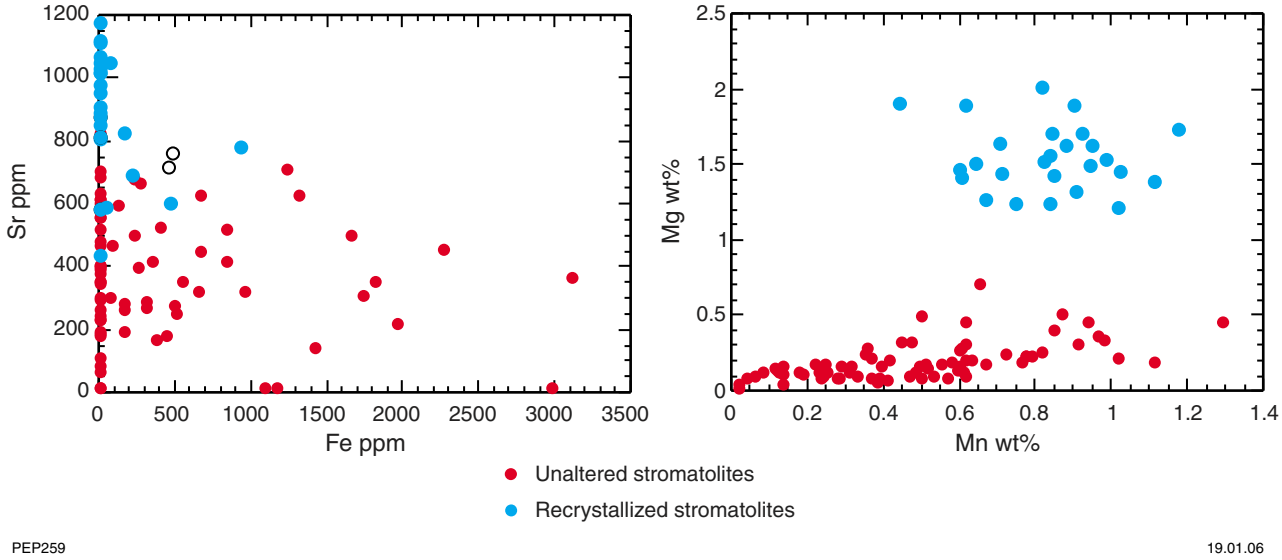

Figure 262. The relationships between contents of iron and strontium, and manganese and magnesium, in unaltered and recrystallized stromatolites (after Playford and Wallace 2001).

Trace element compositions of unrecrystallized calcite in stromatolites are quite distinct from those of recrystallized calcite (De Kever, 1998; Mason, 1998). Recrystallized calcite has higher concentrations of magnesium, strontium, and manganese (magnesium values from 1.2 to 2.1 wt%, strontium from 400 to 1200 ppm, and manganese from 0.4 to 1.2 wt%) than unrecrystallized calcite (magnesium from 0 to 0.8 wt%, strontium from 0 to 800 ppm, and manganese from 0 to 1.1 wt%). Recrystallized calcite generally has lower concentrations of iron (0 to 1000 ppm) than unaltered calcite (0 to 3000 ppm; Fig. 262).

The stromatolitic buildups formed where the upper Gogo Formation overlapped Sadler Limestone, associated with abrupt backstepping of the platforms in the early Frasnian (Fig. 236). Deposition in the basin was very slow at those times, as little reef-derived debris was able to reach the basins. The buildups generally began growth directly on Sadler Limestone, developing as bulbous outgrowths, about 5 to 40 m across, which coalesced to form lenticular buildups as much as 3.5 km long, 150 m wide, and 50 m thick. Each bulbous outgrowth consists of successive layers of spaced, contiguous, and branching columnar stromatolites (Figs 241–246).

Unlike the stromatolites described by Playford et al. (1976), which commonly grew vertically, towards light or under the influence of gravity, individual stromatolites in these buildups grew radially outward, at right angles to the bulbous layering. Thus, a bulbous outgrowth can include stromatolites that grew downward at the base, horizontally on the sides, and upward on top. Chemosynthetic bacteria are thought to have played significant roles in carbonate precipitation and associated barite and sulfide mineralization, although this has not been proved, as no cellular or filamentous structures have been identified.

Field evidence, in the form of sediment draped over the tops of buildups, might suggest that they grew as low mounds on the sea floor. However, it is clear that stromatolites at the base of some bulbous bodies grew downward (Fig. 248), almost certainly into mud rather than water. Moreover, it is clear that the fibrous rims on Gogo concretions (described below, see Fig. 240) grew totally enclosed in mud, and the fibres in those concretions have the same characteristics as those in stromatolites. Consequently it is apparent that much, if not all, of the major buildups grew in mud, immediately below the basin floor.

Gogo concretions

A characteristic feature of the Gogo Formation in the vicinity of the stromatolitic buildups is the presence of abundant spherical to ovoid limestone concretions, commonly known as 'Gogo nodules'. They are generally 5 to 20 cm in diameter (Figs 68, 69, 240, 259), and commonly weather out at the surface in large numbers. In some cases, the outer layers of the concretions consist of radial fibrous calcite (Fig. 240) that must have grown by displacement of surrounding mud, but in others the concretions have formed wholly by precipitation of calcium carbonate in mud, retaining the original pre-compaction bedding of that mud (Fig. 69).

Masses of small spherules, about 2 to 15 mm in diameter, are associated with concretions and stromatolitic buildups in some areas (Fig. 258). They consist of radial calcite fibres, of the same type as those that surround some Gogo concretions, and are similarly thought to have grown in mud, immediately below the sea floor.

The concretionary calcite has $\delta^{18}O$ and $\delta^{13}C$ values ranging from –8.4 to –6.0‰ PDB and –14.5 to –10‰ PDB respectively, values that are similar to those for calcite in fibrous stromatolites (Playford and Wallace, 2001; Fig. 261). The trace element content of concretionary fibrous calcite is also similar, with magnesium ranging from 0.04 to 0.25 wt%; strontium from 0 to 700 ppm, manganese from 0 to 0.6 wt%, and iron from 0 to 600 ppm (De Kever, 1998; Mason, 1998).

Relatively thick lamination that is preserved in some concretions can be traced into very fine lamination in the adjoining compacted shales (Fig. 69). Measurements of bedding thicknesses in concretions and equivalent laminae in shales show that post-depositional compaction was commonly as much as 75%. That major compaction must have resulted in the expulsion of large volumes of intrastratal water and gas.

Barite mineralization

Barite is widespread in many stromatolitic buildups, mainly in the form of dendritic growths and 'shrubs' of fibrous barite, which form layers as much as 2 m thick, intergrown with stromatolites (Figs 249–251). The dendritic barite resembles 'plumose barite' as described by Kaiser et al. (1987), and its inter-relationships with calcite indicate that the two minerals were co-precipitated. Barite also occurs as veins generally less than a metre wide, cutting through slightly older barite and stromatolites, and as small rosettes and randomly oriented blades replacing calcite. Analyses show barium contents ranging from 32% in dendritic barite to 54% in a barite vein. The total barite content of buildups is estimated to range from 5% to 10% in the Minnie Pool and Longs Well deposits. No barite has been recognized in the Pillara Spring deposit.

Barite has $\delta^{34}S$ values ranging from +38 to +50‰ CDT (Fig. 263). These are consistent with derivation of the mineralizing fluids from residual sulfur remaining after extensive sulfate reduction in a closed system. The sulfur-isotope composition in the barite is not consistent with marine fluids, as marine sulfates are characterized by lower $\delta^{34}S$ values (Claypool et al., 1980). The isotopic composition of the barite also suggests that evaporites in the Cadjebut Formation, which have $\delta^{34}S$ values of about +20‰ CDT (Tompkins et al., 1994b), did not constitute a source of sulfate for the deposits.

Sulfur isotopes enriched in $\delta^{34}S$ have been recorded where bacterial sulfate reduction is taking place in pore waters of modern sediments (Masuzawa et al., 1992). Moreover, barium is commonly present in relatively high concentrations (250 to 800 ppm) in shales, either as barite or combined with organic matter (Paytan et al., 1993). In either case, barium can be mobilized readily in the zone of sulfate reduction (Goldberg and Arrhenius, 1958; Church,

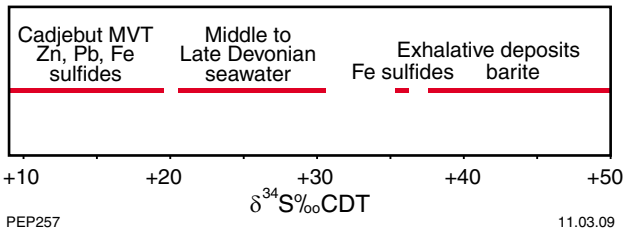

Figure 263. Sulfur-isotope values for Cadjebut epigenetic Zn–Pb mineralization, Middle to Late Devonian seawater, and Late Devonian exhalative sulfides and barite (after Playford and Wallace 2001).

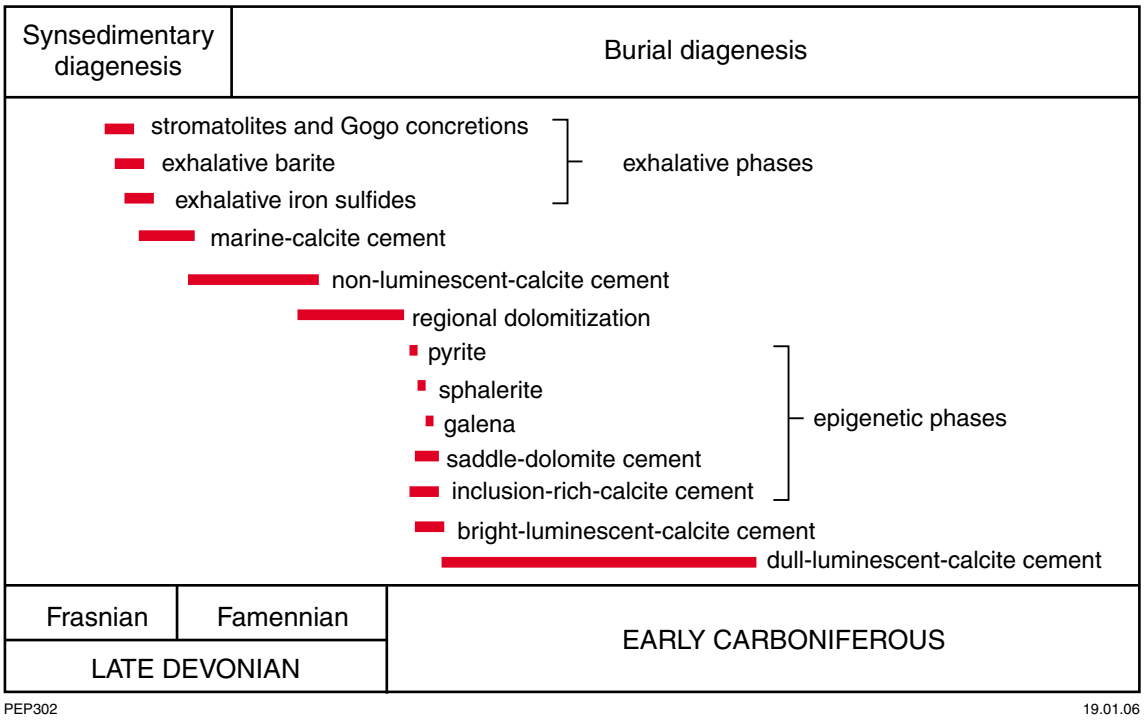

Figure 264. Paragenetic sequences of exhalative phases, calcite cements, and epigenetic phases (after Playford and Wallace 2001).

1979; Torres et al., 1996). It thus seems apparent that the barium was derived from shales in the Gogo Formation and transported by fluids generated during early diagenesis.

Gossans and iron-sulfide mineralization

One of the most conspicuous features of the outcropping exhalative stromatolitic buildups is the presence of black, brown, and red gossan veins, commonly as much as several metres wide and tens of metres long, cutting through the buildups (Figs 252, 253, 257). Drillholes show that these limonitic gossans are weathering products of pyrite and marcasite.

The gossan veins fill fissures that opened up periodically during growth of the stromatolitic buildups, probably as a result of seismic activity and the early compaction of muds adjoining and underlying the buildups. Most fissures are subvertical or follow the bulbous bedding of major stromatolitic outgrowths (Fig. 238). The gossans are generally massive, but some display evidence of microbial involvement in growth of the precursor iron sulfides, in the form of well-preserved columnar stromatolites (Fig. 257). Others have wavy lamination that is also suggestive of microbial activity. At a few localities, small amounts of gossanous material fill the inter-areas between stromatolite columns, suggesting that iron sulfides were periodically precipitated over stromatolite growth surfaces (Fig. 256). This points to a syngenetic origin of the sulfides, as does the occurrence of gossan clasts in penecontemporaneous debris-flow deposits in the Conglomerate 1 and 2 deposits in the East Pillara area.

Sulfur isotopes in synsedimentary pyrite and marcasite have very positive $\delta^{34}S$ values, ranging from +33 to +37.5‰ CDT, although these values are less than the extremely high values for synsedimentary barite (+38 to +50‰ CDT; Fig. 263). Electron-microprobe analyses indicate that the iron sulfides in drillcores contain measurable concentrations of zinc, ranging from 730 ppm to 2080 ppm, and this metal is thought to be bound into the crystal lattice of the pyrite and marcasite. No sphalerite has been detected, other than in epigenetic Zn–Pb veins. Anomalously high zinc values (as much as 7410 ppm) have also been recorded from some gossan outcrops, perhaps derived from zinc bound into the crystal lattice of the original iron sulfides. Lead values are generally very low in the iron sulfides, although one sample contained 2040 ppm of lead.

Epigenetic mineralization in stromatolite buildups

Minor epigenetic mineralization, in the form of galena, sphalerite, and iron sulfides, occurs in drillhole cores from the stromatolitic buildups, filling fissures as much as a few centimetres wide, and as replacements of exhalative iron sulfides. Those epigenetic Zn–Pb sulfides are more coarsely crystalline than the exhalative sulfides.

Where the epigenetic Zn–Pb sulfides fill or partly fill primary porosity, they post-date early non-luminescent calcite and regional dolomite, but are older than dull-luminescent calcite cements. They are also coeval with saddle dolomite, inclusion-rich calcite, and bright-luminescent calcite cements (Fig. 264). These paragenetic relationships are consistent with those reported by McManus and Wallace (1992) in their study of the regional timing of epigenetic Zn–Pb mineralization on the Lennard Shelf.

Based on radiometric dating of sphalerite from the Pillara mine and ore-stage calcite from the Goongewa mine, Christensen et al. (1995) and Brannon et al. (1996) have shown that the Zn–Pb epigenetic mineralization occurred about 351 to 357 m.y. ago, during the Early Carboniferous (according to the timescale of Gradstein et al., 2004). That dating shows that the epigenetic mineralization is about 20 to 30 m.y. younger than growth of the stromatolitic buildups and their associated synsedimentary (exhalative) mineralization. It is estimated that during the later episode of epigenetic mineralization the exhalative deposits would have been buried below more than 1000 m of Upper Devonian sedimentary rocks.

The Zn–Pb sulfides previously documented from the Cadjebut deposit have $\delta^{34}S$ values ranging from +15 to +20‰ CDT (Tompkins et al., 1994b), which are somewhat lower than those for evaporites in the Middle Devonian Cadjebut Formation (about +20‰ CDT), and much lower than those for the exhalative iron sulfides and barite (+33 to +37.5‰ CDT and +38 to +50‰ CDT respectively).

Genesis of syngenetic deposits

The stromatolite–barite–sulfide deposits are interpreted to have formed on or immediately below the sea floor by precipitation over seepages of cool fluids. Those fluids were exhaled as a result of compaction of basinal shales in the Gogo Formation.

The major chemical processes involved in forming the mineralizing fluids are thought to have been organic-matter oxidation and sulfate reduction during early diagenesis of shales in the Gogo Formation. Such reactions in organic-rich sediments are relatively well understood, and include (from earliest to latest): bacterial oxidation of organic matter, bacterial sulfate reduction, and bacterial fermentation (methanogenesis) (Curtis et al., 1972; Irwin et al., 1977). Such reactions liberate bicarbonate to the pore waters and produce $\delta^{13}C$-depleted fluids, together with reduced sulfur.

The calcite in stromatolites of the exhalative buildups is characterized by very negative carbon isotopes, with $\delta^{13}C$ values ranging from –7 to –22‰ PDB, which suggests that organic carbon made significant contributions to the mineralizing fluids (Hoefs, 1973). The Gogo Formation is more organic rich than other units on the Lennard Shelf (Alexander et al., 1985), and there can be little doubt that the anoxic muds which compacted to form black shales in that formation were the source of the carbon involved. The lack of extremely negative carbon isotopes (i.e. $\delta^{13}C$ values below –25‰ PDB) in the deposits indicates that methane oxidation (Irwin et al., 1977; Schoell, 1988) did not have a dominant role in their development, as the $\delta^{13}C$ values of stromatolites in the buildups are never below

–22‰ PDB and are commonly significantly above that value (as high as –7‰ PDB). However, it is nevertheless possible that the lowest values represent some mixing of marine and methane-derived carbon.

Iron and barium in the mineralizing fluids are thought to have been sourced from muds in the Gogo Formation. Compaction-driven fluids derived from those horizons can be expected to have carried varying amounts of iron and barium in solution, depending on the concentrations of those elements in the source horizons and the prevailing chemical conditions.

Neomorphic alteration of stromatolites

Petrologic and field observations of the recrystallized fibrous calcite indicate that it is a neomorphic alteration product of calcite in unaltered stromatolites. Two observations indicate that the sulfide-precipitating fluids were responsible for this recrystallization because of

- the outcrop association between gossan veins and recrystallized calcite (Figs 253, 254);
- the presence of micro-inclusions of pyrite in recrystallized calcite, but not in unaltered calcite of stromatolites.

Recrystallized calcite has uniform stable-isotope values, with very negative carbon isotopes and oxygen isotopes similar to those of primary marine cements (Fig. 261). This is in accord with the interpretation that fluids responsible for recrystallization were early-diagenetic marine waters that had been involved in bacterial sulfate reduction and organic-matter oxidation.

The trace element concentrations also reveal much about the nature of fluids involved in forming the different calcites in the buildups. The matrix of the recrystallized calcite generally has lower iron values and higher manganese, strontium, and magnesium values than calcite in unaltered stromatolites (Fig. 261). The low iron values and high ratios of manganese to iron are to be expected if the fluids that precipitated sulfides were also responsible for recrystallization. That is because a fluid remaining after iron-sulfide precipitation would be depleted in iron, but not in manganese. The high strontium and magnesium concentrations point to a marine-like fluid as being responsible for recrystallization (Veizer, 1983).

The occurrence, petrology, and geochemistry of the recrystallized calcites indicate that recrystallization occurred during very early diagenesis, by the same fluids that precipitated the iron sulfides. This recrystallization resulted in the destruction of many original fabrics. The unaltered calcites in stromatolites, on the other hand, have retained their primary fabrics, and their mineralogy was probably stabilized later, during deeper burial diagenesis, as indicated by their lower magnesium, strontium, and oxygen-isotope values (Choquette and James, 1987). The higher $\delta^{13}C$ values in the unaltered calcites indicate that their carbon was derived from both marine and organic sources, and their fabric-retaining form suggests that the precursor mineral was high-magnesium calcite, which was altered after burial to low-magnesium calcite (James and Choquette, 1984).

Barite and iron-sulfide precipitation

After precipitating iron sulfides in fissures and recrystallizing adjoining parts of the stromatolitic limestones, the fluids reached the upper surfaces of the buildups, where they nourished microbial communities and mixed with oxygenated seawater. Barium dissolved in the fluids was oxidized, precipitating barite, intergrown with stromatolites and filling fissures. Sulfur in the barite is extremely heavy ($\delta^{34}S$ values ranging from +38 to +50‰ CDT), which is consistent with a residual sulfur source after extensive bacterial sulfate reduction in a closed system. This barite contrasts with marine barite described by previous authors (e.g. Cortecci and Longinelli, 1972), which has lighter values, similar to that of seawater (about +20‰ CDT).

The precipitation of barite in the upper parts of the buildups indicates that water conditions on or near the sea floor were more oxidized than at the sulfate–sulfide boundary. However, the lack of any marine benthic faunas, and the periodic precipitation of iron sulfide over stromatolites, indicates that oxygen levels were low. Most iron-sulfide precipitation occurred in subsurface fissures under anoxic conditions.

Iron sulfides within the buildups occur mainly as fissure fillings, and to a lesser extent as other cavity fillings and replacements of micrite matrix. As is the case with barite, the high sulfur-isotope values of the iron sulfides ($\delta^{34}S$ values ranging from +33 to +37.5‰ CDT) are consistent with a source of residual sulfur after sulfate reduction in the Gogo Formation. The iron is also probably derived from that formation, where it was present either as iron oxides or combined in clay minerals. It is possible that some of the early reduced sulfur was consumed in iron-bearing horizons within the Gogo Formation, through the precipitation of iron sulfides, and that the remaining sulfur was expelled in iron-free compaction fluids. The reduced sulfur in those fluids would then be transported until it encountered a new source of iron, probably contained in compaction fluids derived from other horizons in the Gogo Formation. Iron-sulfide precipitation would then occur where reduced-sulfur- and iron-bearing fluids were mixed in suitable environments, such as fissures within the buildups. Any remaining reduced sulfur would be oxidized in seawater at or near the tops of the buildups, resulting in barite precipitation, as previously described.

Genesis of mineralization

The only epigenetic sulfide mineralization that has been found within the stromatolite–barite–sulfide buildups are thin veins of zinc, lead, and iron sulfides, not more than a few centimetres wide, that crosscut and replace the earlier exhalative iron sulfides (Fig. 238). They have been identified in drillhole cores, not in outcrop.

The main reasons for the lack of Zn and Pb sulfides contemporaneous with the exhalative buildups are probably that the fluids involved were too cool and not saline enough to carry significant amounts of zinc and lead. High concentrations of chloride (>100 000 mg/L) seem to be necessary before substantial quantities of those

metals can be transported in solution, and their solubility rises steeply with increasing temperature (Hanor, 1996). The epigenetic deposits are believed to have formed from relatively high-temperature brines derived from the Fitzroy Trough (Arne, 1996), whereas the exhalative fluids responsible for the Devonian buildups apparently had temperatures lower than 60ºC, and probably less than 40ºC. Iron and barium can be carried readily in such cool fluids, but not lead and zinc (Barnaby and Rimstidt, 1989; Garels and Christ, 1990).

Both the epigenetic and syngenetic (exhalative) types of mineralization on the Lennard Shelf were probably sourced from basinal shales, the mineralizing fluids being driven by compaction. Such compaction must have commenced immediately after deposition of muds in the Gogo Formation, and continued for millions of years during the remainder of the Late Devonian and Early Carboniferous. The total amount of compaction in these muds and the resulting shales was as much as 75%.

In the case of the epigenetic Zn–Pb deposits on the Lennard Shelf (principally the Pillara, Cadjebut, and Goongewa deposits; Figs 234, 235) the mineralizing system was on a much larger scale, and the fluids are thought to have originated during the Early Carboniferous (Tournaisian) through the deep-burial diagenesis of shales (probably Devonian or Ordovician). This occurred at a time when the adjoining Fitzroy Trough was subjected to strong subsidence and extension. Hot (as much as about 90ºC) zinc-, lead-, and iron-bearing brines were probably derived from thick Devonian shales in the Fitzroy Trough. The expelled fluids were channelled along faults into carbonates of the Devonian reef complexes on the adjoining Lennard Shelf, where Zn–Pb sulfides were precipitated in fractured carbonates, hydrothermal-karst cavities, and evaporitic beds (Vearncombe et al., 1995a,b).

One of the principal questions remaining is whether significant sea-floor exhalation of fluids continued during the prolonged interval between deposition of the stromatolite–barite–sulfide deposits and that of the epigenetic sulfides. Perhaps fluid expulsion was a steady process linked with the progressive compaction of shales throughout the Late Devonian and Early Carboniferous. Alternatively, major expulsion of fluids may have been episodic, associated with rapid compaction during periods of strong tectonism.

Comparisons with other seep and vent systems

The stromatolite–barite–sulfide deposits described here have some characteristics different from those of other buildups known to have formed over cold-seep and hot-vent systems in modern and ancient environments. Numerous examples have been documented of modern and ancient carbonate buildups related to hydrocarbon seeps (e.g. Beauchamp and Savard, 1992; Carney, 1994; Aharon et al., 1997; Hovland, 1992). However, there is no clear evidence that hydrocarbons were associated with the Devonian exhalative buildups of the Lennard Shelf. Moreover, whereas well-developed benthic faunas (forming 'oases' surrounded by 'deserts') are known to be intimately associated with modern exhalative buildups, no such faunas are preserved in the Devonian buildups. This could perhaps be explained if those buildups developed in muds immediately below the surface of the sea floor rather that standing up as mounds above that surface.

In most modern and ancient exhalative systems, extremely negative carbon isotopic values occur in the associated carbonates and pore fluids (having $\delta^{13}C$ values less than –25 ‰ PDB), pointing to the influence of biogenic or abiogenic methane (e.g. Cavagna et al., 1999; Stakes et al., 1999; von Rad et al., 1996). High methane concentrations have also been measured from bottom waters sampled around modern sea-floor seeps (e.g. Kulm et al., 1986; Boulegue et al., 1987). Although methane can be expected to have been one of the gases exhaled during early compaction of shales in the Gogo Formation, there is no isotopic evidence to show that it was a major source of the associated carbonates. Instead, the evidence points to bacterial oxidation of organic matter rather than methanogenesis as the principal source of those carbonates.

Texturally, the Lennard Shelf buildups are unusual, in having been constructed mainly by fibrous-calcite stromatolites. Other known cool-seep carbonates, both modern and ancient, consist predominantly of micrite (e.g. Belka, 1998; Stakes et al., 1999; von Rad et al., 1996), although fibrous stromatolitic calcites are known from non-marine deposits, including tufa (Freytet and Verrecchia, 1999) and hot travertine (Chafetz and Guidry, 1999).

Conclusions

- Stromatolite–barite–sulfide deposits in Devonian reef complexes of the Canning Basin are interpreted to be exhalative deposits, formed above cool-water seepages, either as low mounds on the surface of the sea floor, or immediately below that surface.
- The exhalative interpretation is based on the following observations and interpretations: a) major compaction of basinal shales in the Gogo Formation, beginning soon after deposition, must have resulted in the expulsion of large volumes of interstitial fluids; b) the in-situ deposits are lenticular stromatolitic buildups localized over features that could be expected to have acted as pathways for compaction-driven fluids, especially synsedimentary faults and contacts between shales of the Gogo Formation and marginal-slope limestones of the Sadler Limestone; c) isotopic and petrographic evidence suggest that early diagenetic reactions in shales of the Gogo Formation, involving bacterial sulfate reduction and bacterial oxidation of organic matter, were important in forming the mineralizing fluids; and d) the syngenetic origin of the mineralization is shown by the occurrence in penecontemporaneous debris-flow deposits partly composed of blocks derived from stromatolite–barite–sulfide buildups, and by some sulfide deposition that occurred over stromatolite columns on or immediately below the sea floor.

- Chemosynthetic bacteria, nourished by cool-water seepages, are likely to have played significant roles in precipitating stromatolites, barite, iron sulfides, and concretions, although inorganic precipitation could also have been involved.
- Sedimentary dykes and veins of iron sulfide (pyrite and marcasite), now weathered to limonitic gossans, filled early fissures in the stromatolite buildups, and may have been precipitated by the mixing of sulfur- and iron-bearing compaction-driven fluids.
- The mineralizing fluids permeated and recrystallized adjoining parts of the stromatolite buildups, and were oxidized by seawater at the upper surfaces of those buildups, resulting in the precipitation of barite intergrown with stromatolites and filling small veins.
- Syngenetic mineralization in the exhalative buildups is of no economic value, but at least one buildup is cut by minor veins of epigenetic Zn–Pb mineralization, and important epigenetic Zn–Pb deposits, formed 20 to 30 m.y. after growth of the buildups, have been mined in the same general area of the basin.
- The epigenetic phase of mineralization, like the earlier exhalative phase, is interpreted to have resulted from dewatering of basinal shales, but it is unsure whether those two phases represent end-members of a continuing process, involving steady rates of shale compaction, fluid expulsion, and sulfide precipitation, or were episodic, resulting from major pulses of tectonism.

Petroleum

The Devonian reef complexes of the Canning Basin have long been regarded as prime targets for petroleum exploration, as large oilfields have been found in closely similar rocks in various parts of the world, notably in Canada (Playford, 1969; Crostella 1998a,b; Atchley et al., 2006; Figs 85, 86).

The first oil discovery in the Canning Basin was in the Blina no. 1 well in 1981 (Playford, 1982, 1984b; Moors et al., 1984; Jonasson and Reiser, 2002). That discovery was made in fractured reefal limestones of the Nullara Limestone. GSWA has not made a detailed study of seismic surveys and wells in the area, but Crostella (1998a,b) produced up-to-date summaries of data on Blina and other fields on the Lennard Shelf. Blina is the only field that produces from the Devonian; the others occur in younger rocks, although they occur above the Famennian platform margin (Fig. 265). Blina has produced 294 000 kL of oil to date, and is producing (August 2008) at a rate of 65 kL per month. Other wells have produced oil as follows: Sundown, 65 000 kL, now producing 23 kL per month; West Terrace, 37 500 kL, now producing 40 kL per month; Lloyd, 30 000 kL, now shut down; Boundary, 20 000 kL, now shut down; West Kora, 3700 kL, now shut down.

Seismic surveys have clearly delineated the Famennian platform margin in the subsurface of the Lennard Shelf, and, given the amount of drilling that has already occurred, it seems unlikely that large reserves remain undiscovered in the Famennian section. The best chance for future commercial discoveries is likely to be in the Frasnian reef complexes, which are poorly defined on existing 2-D seismic lines. Prime targets for the future may be atolls or pinnacle reefs comparable with the outcropping Lloyd Hill pinnacle reef, that were drowned and covered by shale of the Gogo Formation. These prospects could best be defined using modern 3-D seismic surveys.

Paleokarst

Karst (now forming paleokarst) was developed in limestones of the Devonian reef complexes during the Late Devonian, Early Carboniferous, and Early Permian. The Early Permian paleokarst is the most extensive and has had a major influence on development of the modern karst topography. It is marked by a major unconformity between the Early Permian Grant Group and the Devonian limestones (Fig. 19).

Most of the text and illustrations in this section are based on Playford (2002a), updated and amended where appropriate.

Late Devonian paleokarst

The principal features of Late Devonian paleokarst were formed in platform facies after regressions at the Frasnian–Famennian unconformity and after reef growth had ceased in the late Famennian,. These two intervals of paleokarst development define second-order sequence boundaries within the Devonian succession (Figs 20, 21).

Frasnian–Famennian unconformity

Small paleokarst features, forming sinkholes as much as 50 cm across and 1 m deep, occur in platform facies at the Frasnian–Famennian unconformity in parts of the Napier Range, near Chedda Cliffs (AMG Zone 51, 673300E 8096500N; Playford et al., 1989; Fig. 97) and west of Hawkstone Creek near Wunala Hill (AMG Zone 51, 664000E 8118600N). However, the Frasnian–Famennian unconformity surface in other areas is quite smooth, with local relief of as much as 5 m, and it lacks any obvious karst features (e.g. in parts of the area west of Hawkstone Creek and at the northwest end of the Oscar Range; AMG Zone 51, 705950E 8046500N; Playford, 1982; Figs 49, 98).

The fall in sea level that resulted in this unconformity was probably not more than 50 m. Conodont analyses by G Klapper (2004, written comm.) show that there was no hiatus at the Frasnian–Famennian boundary in deeper water parts of the marginal-slope facies, for example, at three localities where that boundary has been defined in the Napier Formation in Windjana Gorge (Plate 6). However, the shallowest part of the reefal-slope subfacies is truncated at a locality in the Napier Range west of Hawkstone Creek (GPS AMG Zone 51, 663660E

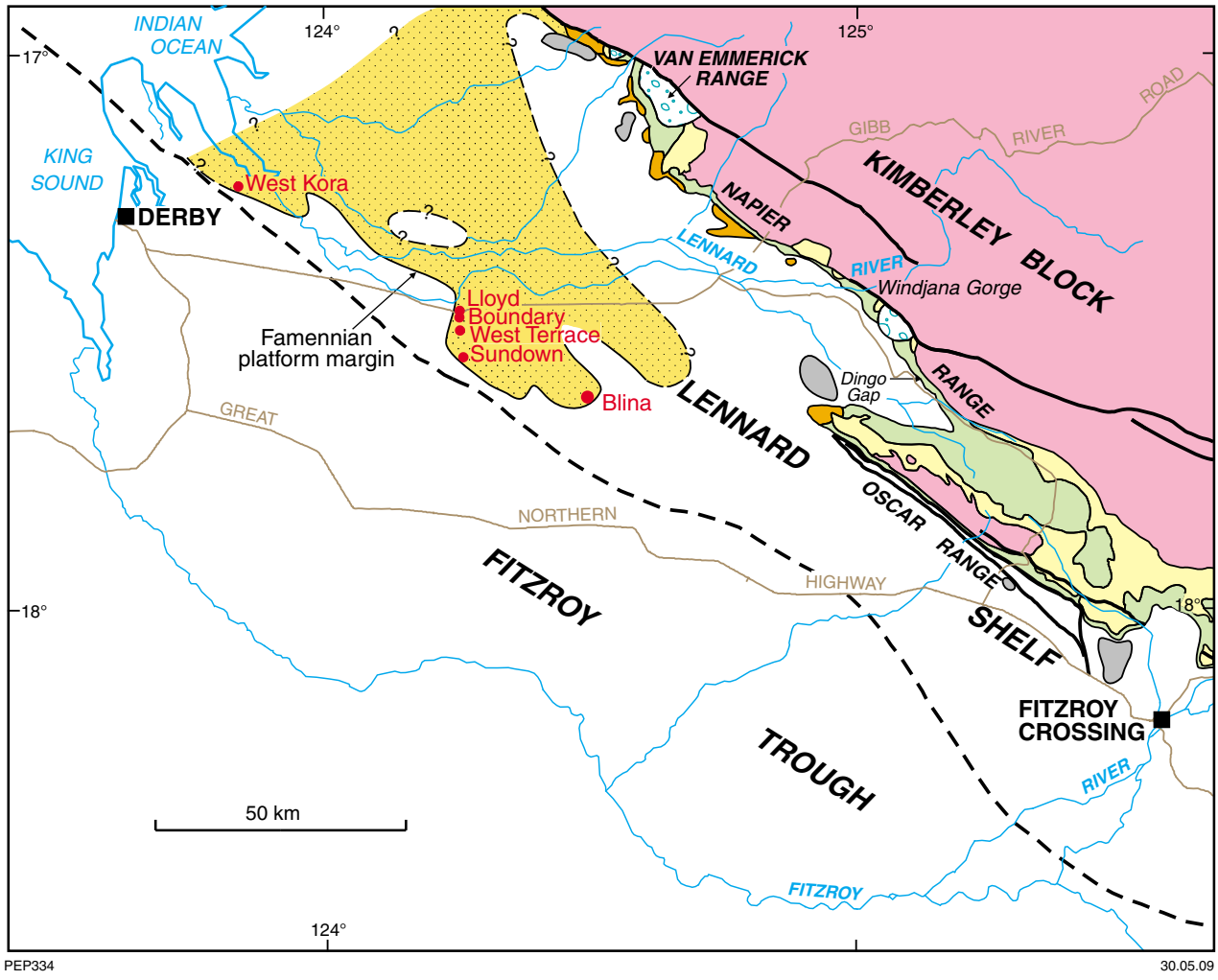

Figure 265. **Geological map of the northwest part of the Devonian reef complexes showing the subsurface extent of the Famennian platform facies and the positions of oilfields discovered in the area.**

8118460N), suggesting that significant erosion of the Frasnian reef complex had taken place in that area before Famennian deposition began (Fig. 50).

Reef-extinction unconformity

Another important fall in sea level occurred during the late Famennian, at the top of the Nullara Sequence. This marked the end of reef growth in the Canning Basin, resulting in the sudden emergence of the platforms, bounded by steep reef scarps. The emergent limestones were subjected to mild karstification, and the scarps were incised by streams to form small v-shaped valleys (Fig. 104). Shales of the Fairfield Group were deposited during the following transgression, filling valleys and filling or partly filling caves along platform margins, as evidenced by drill core from Shell Metals drillhole NRD 99 in the Napier Range (AMG Zone 51, 653730E 8097580N), and Pickands-Mather drillhole AH2 in the Oscar Range (AMG Zone 51, 705500E 8048490N).

Early Carboniferous hydrothermal paleokarst

The hydrothermal fluids that introduced epigenetic zinc–lead mineralization into the Devonian rocks dissolved carbonates, forming cavernous systems in which sulfides were precipitated (Wallace et al., 2002). One of the largest hydrothermal karst features known on the Lennard Shelf is in the former Goongewa mine, adjoining the Cadjebut Fault (Fig. 266). The main cavern at Goongewa was originally some 600 m long and 70 m across, and is thought to have formed above the hangingwall of the Cadjebut Fault, by solution of limestone in hydrothermal fluids at depths of about 2 km below the surface. Most of the cavernous system was filled, when or soon after it was formed, by zinc, lead, and iron sulfides, sparry calcite, and solution-related breccias and sediments. The mine was abandoned in 2000, after the ore reserves had been exhausted.

The hydrothermal fluids that formed the caverns and induced mineralization at Goongewa also dolomitized some of the surrounding limestone and introduced minor amounts of hydrocarbons (Wallace et al., 2002). The fluids are thought to have been derived from compaction of Devonian or Ordovician shales deep in the Fitzroy Trough and channelled along the Cadjebut Fault, which was active at that time.

On a smaller scale, hydrothermal paleokarst in some areas follows minor joints, which formed especially in homogeneous limestones. Good examples are seen in the Pillara quarry (GPS AMG Zone 51, 789060E 7968000N; Figs 267–272), where hydrothermal paleokarst and mineralization formed along joints in brittle microbial and stromatoporoid reef limestone (Pillara Limestone) but did not extend into the more flexible interbedded limestone and shale of the adjoining and overlying marginal-slope deposits (Sadler Limestone). The hydrothermal fluids dissolved reef limestone along the joints, and the resulting cavities were filled penecontemporaneously with iron, zinc, and lead sulfides and sparry calcite.

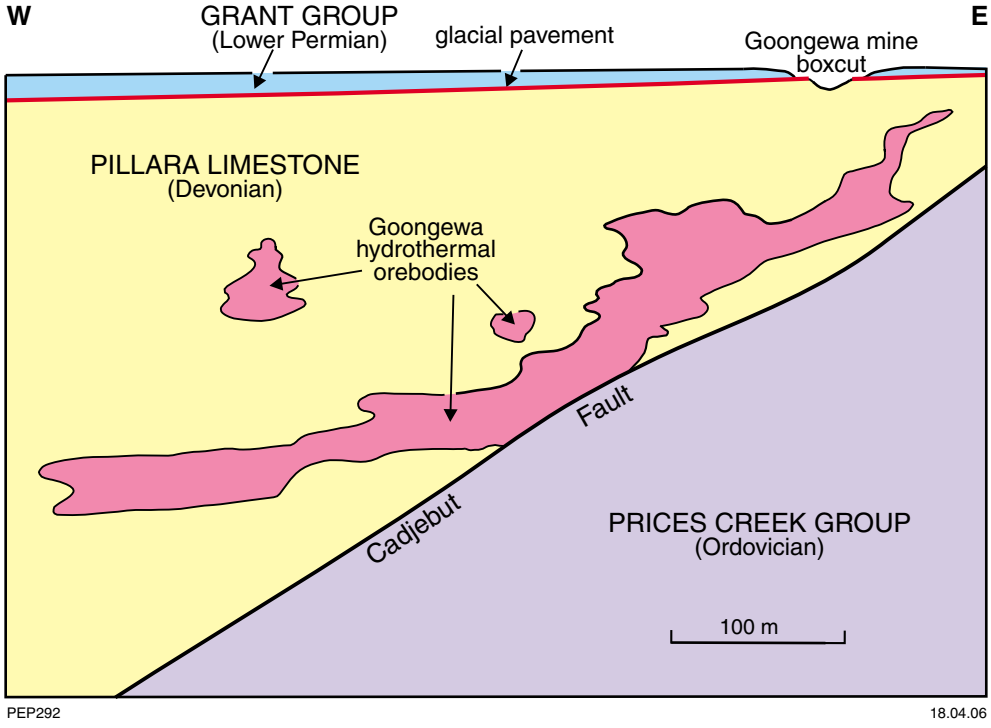

Figure 266. Cross section through the Goongewa hydrothermal orebodies which filled caverns in Pillara Limestone on the downthrown side of the Cadjebut Fault. Also showing the glacial unconformity at the base of the Lower Permian Grant Group.

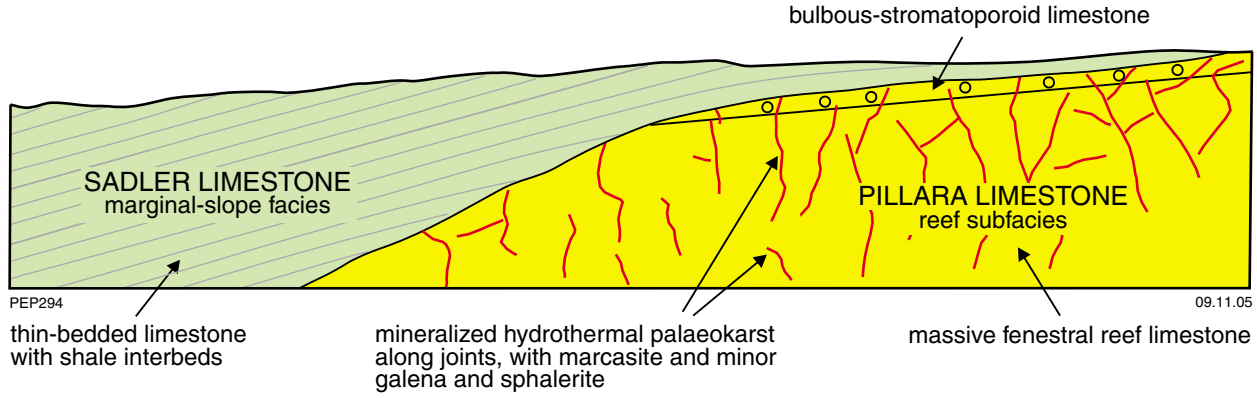

Figure 267. **Diagrammatic representation of the eastern face of the Pillara quarry (not to scale) showing reef subfacies of the Pillara Limestone (probably late Givetian) onlapped by marginal-slope deposits of the Sadler Limestone. The Pillara Limestone contains numerous mineralized hydrothermal-karst veins, following joints in the limestone.**



Figure 268. Panoramic view of the eastern face of the Pillara quarry as shown in Figure 267.



Figure 269. **Closer view of the eastern face of the Pillara quarry showing bedded Sadler Limestone (fore-reef subfacies) abutting and mounting over Pillara Limestone (platform facies). Brown streaks on the exposure of Pillara Limestone mark iron oxide resulting from weathering of marcasite in mineralized joints.**

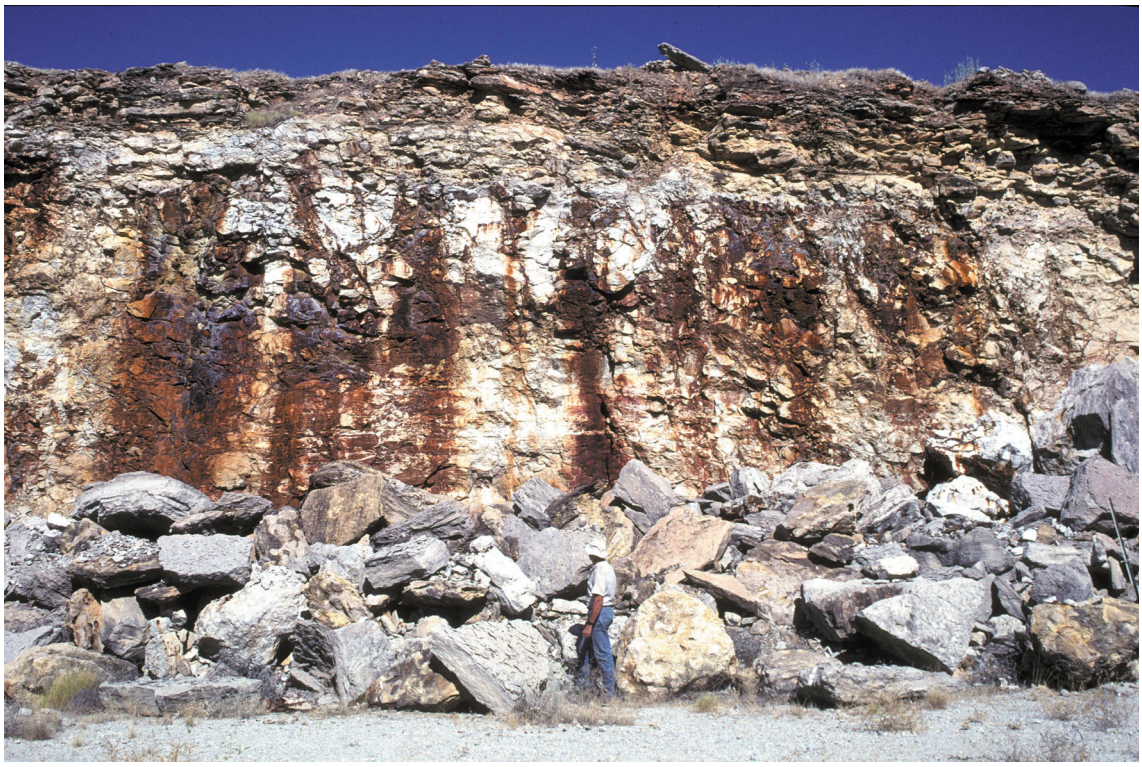

Figure 270. The southern face of the Pillara quarry. Sadler Limestone is at the top of the face, overlying massive Pillara Limestone, with brown streaks on the face marking weathering of marcasite in mineralized joints.

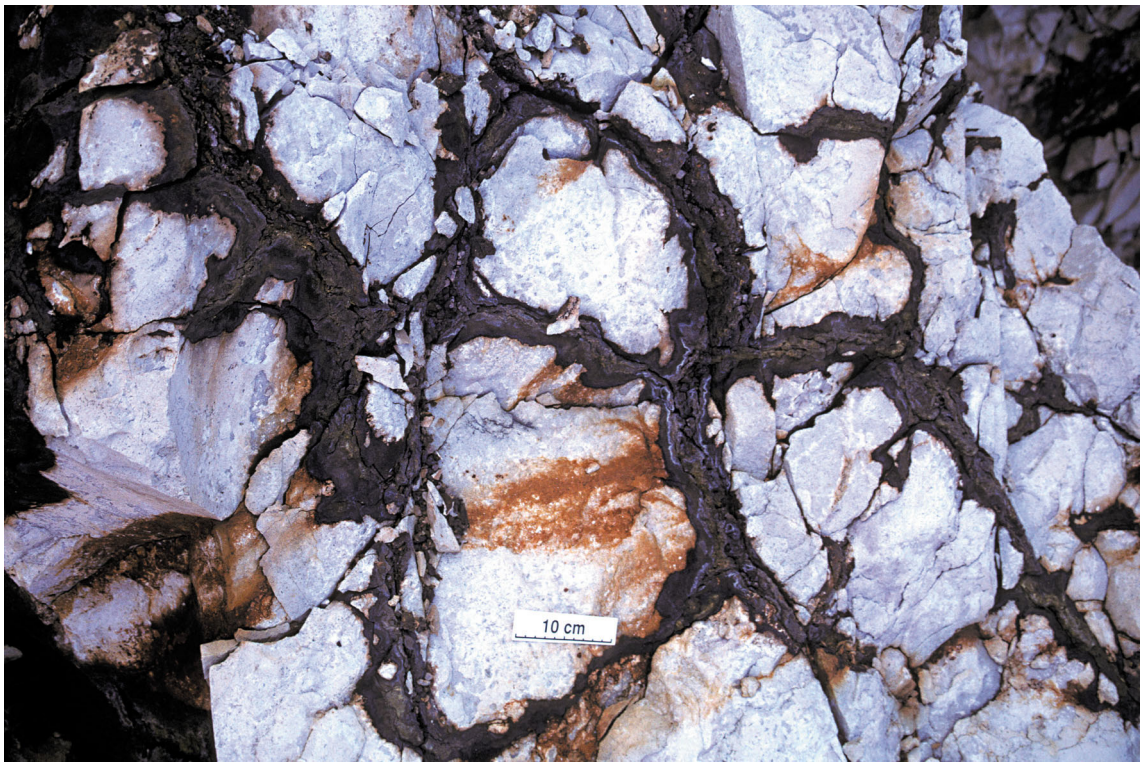

Figure 271. Boulder of Pillara Limestone blasted from the wall of the Pillara quarry, showing rectilinear mineralized fractures originally filled with marcasite (recently weathered to iron oxide) and minor zinc and lead sulfides.



Figure 272. Part of the floor of the Pillara quarry, showing a joint that was enlarged by solution in basin-derived fluids, followed by precipitation of marcasite (recently oxidized to iron oxide) and sparry calcite.

Early Permian paleokarst

The most extensive paleokarst in the Devonian limestones is associated with the Early Permian unconformity. This paleokarst is thought to have formed by solution of limestone in subglacial meltwater, below the final Early Permian continental ice sheet (Playford, 2002a; Fig. 273). It includes cave systems, karst corridors (grikes), solution dolines and pipes, subhorizontal tunnels, tower karst, subglacial channels, and collapse breccias (Figs 273–321).

Early Permian unconformity

The Devonian reef complexes and overlying Fairfield Group were tilted, faulted, and mildly folded in the Early and middle Carboniferous, during a widespread tectonic phase that may correlate with the final pulse of the Alice Springs Orogeny (Haines et al., 2001), although that name is not considered appropriate for use in the Canning Basin. Tectonism continued for about the next 20 m.y. while the region was being eroded below a succession of Late Carboniferous to Early Permian continental ice sheets. By Early Permian times the reef complexes had been planed down to a nearly level surface (Fig. 19). Continental ice sheets, flowing towards the north and north-northwest (Figs 274–276), are thought to have been the agents responsible for this planation. 'Dirty' ice at the base of the ice sheet, containing rock clasts ranging from boulders to silt and clay ('rock flour'), scoured and polished the underlying bedrock. This planation, combined with subglacial karstification of the limestones, wore down the reef complexes to a relatively flat surface, However, compared with its level over the limestones, the glacial unconformity was as much as 120 m higher over the more resistant Devonian conglomerates and 35 m lower over soft shales of the basin facies and Fairfield Group. Since the Early Permian there has been relatively little tectonism on the Lennard Shelf, and in most areas the nearly horizontal tops of the ranges are still close to the level of the Early Permian unconformity (Playford and Lowry, 1966; Playford, 2002a).

The final continental ice sheet of the Permo-Carboniferous glaciation melted and retreated during the Early Permian, causing sea level to rise and sediments of the Asselian to Sakmarian Grant Group (Apak and Backhouse, 1998) to be deposited over the glaciated and karstified unconformity. At various places on the Lennard Shelf the Carolyn Formation at the base of the Grant Group overlies Proterozoic basement, Early to Middle Ordovician Prices Creek Group, Middle and Upper Devonian reef complexes, and post-reef sediments of the Famennian to Lower Carboniferous (Tournaisian) Fairfield Group. The near-horizontal glacial unconformity at the base of the group truncates more than 2000 m of faulted, tilted, and mildly folded Ordovician, Devonian, and Lower Carboniferous sedimentary rocks (Fig. 19).

Some of the best examples of exhumed Early Permian paleokarst are seen in the southernmost outcrops of the reef complexes, around Bugle Gap (Figs 277, 278) and in an isolated inlier around Red Bluffs (AMG Zone 52,

229000E 7914000N; Fig. 279). The Early Permian surface was exhumed in those areas in late Tertiary to Holocene times by the removal of most of the Grant Group, leaving only remnants of that group overlying the glaciated surface, filling dolines (Figs 280, 281) and other paleokarst features. The Carolyn Formation at the base of the Grant Group still covers the reef complexes in the part of the Lennard Shelf southeast of Bugle Gap (Figs 277–279) and in the subsurface of the northwestern Lennard Shelf.

Lower Permian rocks exposed in the vicinity of the Devonian limestone ranges are shown as undifferentiated Grant Group on Plates 1–8, because there was uncertainty regarding correlations of some outcrops with the formations of the Grant Group as defined by Crowe and Towner (1976) in the Fitzroy Trough and elsewhere in the Canning Basin. However, from Crowe and Towner's descriptions and regional considerations, it now seems clear that exposures of sandstone and shale in the southeastern Lennard Shelf do form part of the Carolyn Formation, at the base of the Grant Group. The formation in that area consists of two members, named the Ngumban Claystone Member (at the base) and the Deeadeea Sandstone Member (above) by Playford (2002a). The type sections extend from the road cut on the Great Northern Highway (GPS AMG Zone 52, 192140E 7924100N; Fig. 283) to the top of Deeadeea Cliff, with thicknesses of 50 m for the Ngumban Claystone Member and 19 m for the Deeadeea Sandstone Member. The respective members are named after Deeadeea Cliff and the nearby Ngumban Cliff (Plate 5).

The Ngumban Claystone Member contains dropstones, ranging in size from pebbles to boulders, of Precambrian granite and basalt, together with some Devonian limestone and other rocks. Some clasts are faceted and striated (Fig. 284). The dropstones must have been shed from melting icebergs, and were probably derived from mountain glaciers established on the Kimberley block during the waning phase of the Early Permian glaciation. Sea level rose when the main continental ice sheet melted, probably leaving mountain glaciers or small ice caps on elevated areas of the Kimberley, Pilbara, Yilgarn, and Musgrave blocks.

The upper unit of the Carolyn Formation in the Bugle Gap area, the Deeadeea Sandstone Member, is a poorly bedded, partly cross-bedded, moderately sorted, reddish-brown sandstone, with well-rounded sand grains, which is thought to have been deposited under marine conditions. The sandstone is silicified in some areas, especially where it fills paleokarst depressions (Figs 280, 281). The sand grains may have been rounded as a result of eolian action, possibly associated with the waning phase of glaciation.

Glacial pavement

The best example of a glacial pavement in this area, first recognized by geologists of Western Metals Ltd, was exposed from 1994 to 2007 in the box-cut entrance to the Goongewa Mine (GPS AMG Zone 51, 801370E 7937810N; Figs 285–289). Unfortunately, this exposure was lost after the box-cut was filled and rehabilitated in 2007, following closure of the mine in 2000. However, a large piece of the glacial pavement was removed by the company before the box-cut was filled, and it is now stored at the GSWA store in Carlisle, near Perth.

The basal unit of the Grant Group at the Goongewa mine, the Ngumban Claystone Member of the Carolyn Formation, overlies a horizontal unconformity on reef subfacies of the Pillara Limestone (Fig. 289). The unconformity surface, as it was exposed in the box-cut, is a glacial pavement, parts of which are highly polished and show striations, grooves, and small-scale crag-and-tail ('rat-tail') structures (Figs 285–288). These features indicate that the ice sheet moved towards the north to north-northwest (average 350º). Some parts of the pavement in the box-cut had lost their small-scale glacial features before being buried by the Ngumban Claystone Member, presumably as a result of submarine weathering before burial. The places that remained with well-preserved striations and other glacial features were more deeply scoured parts of the pavement that must have been buried under marine clay before significant weathering could occur.

A similar, but very small and poorly preserved, glacial pavement could at one time be seen on Famennian fore-reef limestone (Bugle Gap Limestone) in an excavation beside the road cut on the Great Northern Highway near Deeadeea Cliff (GPS AMG Zone 52, 192210E 7924000N). This exposure has since been covered with soil and rubble. It similarly shows that the ice sheet was moving towards the north to north-northwest. The same direction is evidenced by many Early Permian glacial pavements and striated and grooved unlithified sedimentary rocks over widely separated areas of Western Australia (Fig. 276; Playford, 2001). This direction is also confirmed by glacial grooves in sandstone of the Grant Group in Grant Range and elsewhere in the Fitzroy Trough (Fig. 276; O'Brien and Christie-Blick, 1992; Mory et al., 2008). The consistency of this ice-flow direction indicates that major continental ice sheets covered Western Australia, and probably the whole of Australia, during the Early Permian and Late Carboniferous, when the Australian continent formed part of the Gondwana supercontinent. The ice flowed in a northward direction, i.e. away from the South Pole (Fig. 274).

Glacial pavements have not been observed on Devonian limestones elsewhere on the Lennard Shelf because Cenozoic erosion must have destroyed the original pavements while gradually lowering the surfaces of the ranges. Only ten years of weathering (from 1994 to 2004) were sufficient to destroy parts of the polish and some other minor features on the pavement in the Goongewa box-cut, and it seems unlikely that original glacial features on limestone pavements could survive subaerial exposure for more than several tens of years.

The glacial pavement at Goongewa is less than 25 m above the top of the zinc–lead orebody (Fig. 266). If that orebody had been breached by glacial erosion, it would have been directly exposed to subglacial meltwater, and the sulfide mineralization might well have been destroyed or replaced by gossan. Gossanous dolines having anomalous values of zinc and lead, exposed at other localities on the Lennard Shelf, might have developed in that way.

It is conservatively estimated that the thickness of the Early Permian ice sheet was as much as 2 km over the Lennard Shelf and probably more than 4 km over other parts of Western Australia, as deduced by comparison with the modern Antarctic ice cap, which reaches a maximum thickness of 4.8 km (Paterson, 1994). Indeed, it seems clear that parts of the Permo-Carboniferous ice caps covering Australia and other parts of Gondwana must have been even thicker than this, as they covered much larger areas than present-day Antarctica (Fig. 274).

Subglacial meltwater

Knowledge of subglacial meltwater under continental ice caps is derived largely from drilling and radio echo-sounding in Antarctica, together with field studies of recently deglaciated areas in the northern hemisphere (Benn and Evans, 1998). Drilling through the Antarctic ice cap has shown that the temperature of the ice steadily increases with depth (Paterson, 1994; Fig. 290), no doubt mainly as a consequence of geothermal heat flow, although friction between ice and bedrock, as the ice moves away from the centre of maximum ice accumulation, must also have generated some heat.

The temperature at the contact with bedrock below the present Antarctic ice cap generally reaches the melting point of ice. That melting temperature decreases with depth because of increasing pressure, so that ice at the base of the ice sheet melts at several degrees below 0ºC. Extensive meltwater lakes have developed beneath parts of the Antarctic ice cap, some covering areas of as much as 8000 km^2, but in other places the meltwater forms only thin films at ice–bedrock contacts (Benn and Evans, 1998). Where continental ice overlies mountains or hills, the temperature and pressure at the base of the ice may not have been high enough to achieve melting, thereby minimizing ice movement in those areas. In intermontane areas, where the ice sheet is wet based, it moves much more rapidly, commonly forming ice streams (Paterson, 1994; Benn and Evans, 1998).

In this manner, very large volumes of subglacial meltwater can be expected to have been generated below the Late Carboniferous – Early Permian ice sheets on the Lennard Shelf. This meltwater would have been fresh and have contained dissolved CO_2. The solubility of calcium carbonate in water rises significantly with decreasing temperature and increasing pressure (Linke, 1958) so that the Devonian limestones would have been highly soluble in subglacial meltwater. As a result, extensive subglacial karst developed at the Permian–Devonian unconformity over wide areas of the Lennard Shelf.

Cave systems and karst corridors

Numerous cave systems and associated karst corridors are developed in the Devonian outcrop belt (Jennings and Sweeting, 1963; Lowry, 1967; Jolly and Lance, 1980; Davey, 1980; Dicker, 1987; Dicker and Robinson, 1993; Playford, 1997, 2002a; Ford and Williams, 2007). These major karst features were interpreted by Playford (1997, 2002a) to have formed below a thick Early Permian ice sheet and been filled or partly filled with claystone and sandstone during the following transgression. The caves, corridors, and other karst features were exhumed during the Cenozoic by the removal through erosion of the weakly lithified Lower Permian sedimentary rocks that once lay above or within them.

The best examples of subglacial karst on the Lennard Shelf are in the Lawford and Emanuel Ranges, particularly in the Bugle Gap area, where the cover of Ngumban Claystone Member has only recently been removed. The largest, best known, and most spectacular cave and karst-corridor networks in this area form the Mimbi Caves System, situated in the southern Lawford Range (Figs 291–296; Lowry, 1967; Dicker, 1987; Playford, 1997, 2002a). Other cave systems in the Bugle Gap area are also impressive and contain attractive speleothems (Dicker and Robinson, 1993; Figs 297, 298).

The Mimbi Caves are interpreted to have formed originally through Early Permian subglacial solution along a series of rectilinear joints, forming a maze of narrow cave passages and karst corridors, several kilometres long and as much as 50 m deep. These caves, and others in the area, are attractively decorated with modern speleothems (Figs 293–296). During the wet season Mimbi Creek flows underground and in open karst corridors through the cave system, following a circuitous path when the water level is low (Fig. 292), but inundating most of the system during times of flood (Playford,1997). Probably not more than 50% of the system has been mapped to date, by members of the Illawarra Speleological Society (Dicker, 1987).

The width of the caves and associated karst corridors in the Mimbi Caves System is usually between two and five metres, and the walls are generally quite smooth and parallel (Fig. 299). These distinctive characteristics are thought to have resulted from the uniform solution of limestone in subglacial meltwater. The smooth and regular surfaces of the subglacial karst contrast with the rough irregular surfaces and sharp karren that are products of modern subaerial karstification (Fig. 300).

Subglacial channels

Much of the subglacial meltwater below the Early Permian ice sheet is thought to have drained away along networks of channels cut in bedrock (here termed subglacial channels), which eventually discharged into the sea. Such channels are well known from recently deglaciated areas in the northern hemisphere (Benn and Evans, 1998). Many of the winding channels incised into the Devonian carbonates at the Early Permian unconformity on the Lennard Shelf are thought to have formed by subglacial erosion.

Subglacial channels formed in the Devonian carbonates by a combination of mechanical erosion, by flowing meltwater carrying rock debris, and subglacial solution. Some still contain Permian sedimentary rocks, but others have been deepened below the Permian level by recent erosion. Many are dry throughout most of the year, but others are occupied by modern rivers and creeks containing permanent or intermittent water. The larger

subglacial channels would be termed 'tunnel valleys' by Benn and Evans (1998) and some other glaciologists, and all such channels on the Lennard Shelf were referred to by Playford (2002a) as 'Nye channels'. However, 'tunnel valleys' were roofed by ice, whereas in this Bulletin the term 'tunnel' is applied to features that are roofed by rock., and it seems inappropriate to use the term 'Nye channel' for these features as many are considerably larger than the channels known by that name in the Quaternary.

Menyous Gap in the Pillara Range (Fig. 301; AMG Zone 51, 799900E 7964200N), Billy Munro Gorge (*Tchangalagnarri*) in the northwest Napier Range (Figs 302–304; Plate 1; AMG Zone 51, 664600E 7999300N), and Kunian Gap in the Emanuel Range (Fig. 305; AMG Zone 51, 808300E 7938000N) are interpreted to be examples of large dry subglacial channels, exhumed through the removal by Cenozoic erosion of the Lower Permian sedimentary rocks that once filled them. Several major gorges along existing rivers and creeks, including Windjana Gorge (Figs 306, 307), Geikie Gorge (Fig. 308; AMG Zone 51, 787000E 7998000N), Brooking Gorge (Fig. 309; AMG Zone 51, 766000E 7907000N), and Galeru Gorge (AMG Zone 52, 192500E 7939200N) are similarly thought to have originated as large subglacial channels.

Subglacial lakes

Flat depressions that are floored by sandstone and claystone of the Grant Group and surrounded by Devonian limestone interspersed with tower karst, are interpreted to be the sites of Early Permian subglacial lakes (Figs 310–312). Some of the lakes occupied solution dolines as much as several hundred metres across and more than 200 m deep. Others formed over small solution pipes, less than 100 m wide and at least a few tens of metres deep, such as those in the Lloyd Hill atoll and the largest patch reef of Glenister Knolls (Figs 314–317). In those examples the Grant Group filling the dolines is poorly exposed, but some contain conspicuous outcrops of siliceous sandstone and claystone of the Grant Group, a good example being Kimberley Rover Doline in the northern Laidlaw Range (Figs 280, 281; AMG Zone 52, 187980E 7936510N). Drilling has shown that some dolines are more than 200 m deep (Copp, 2000), although in most cases depths are estimated to be from 50 to 100 m. Some dolines can be shown to have been linked with subglacial channels, tunnels, karst corridors and cave systems (Figs 305, 310, 311, 313).

The Early Permian subglacial lakes and channels were localized in some places along stratigraphic boundaries and faults in the Devonian limestones. For example, the subglacial paleolake near Sadler Ridge (Fig. 305; AMG Zone 51, 810300E 7937600N) was formed along a platform margin in Pillara Limestone, and the course of the Kunian Gap subglacial channel, which drained the lake, is partly controlled by a pre-existing fault.

The limestone walls of Early Permian dolines, where they have been subjected to little recent erosion, are notably smooth (Fig. 317). As with karst corridors, this is thought to have been because they formed through the steady solution of limestone in subglacial meltwater below a thick ice sheet. In some places in outcrop the smooth surfaces are coated with thin siliceous films that protect them from solution by rainwater.

Where the Grant Group has been mapped in solution dolines and other paleokarst features (Plates 1–7), sandstones in the group have been silicified, resulting in prominent outcrops (Figs 280–282). However, closer examination of some flat-floored depressions in the ranges, made since Plates 1 to 7 were released in 1999, has shown that many of those depressions are underlain by soft unsilicified sandstone and claystone of the Grant Group that were not recognized during the previous mapping programs, for example in the Boggy Creek area of the Lawford Range (Figs 310, 311).

Flat-floored depressions on top of the Napier Range beside Windjana Gorge are other examples (Figs 306, 307). Dense spinifex covers the floors of the depressions, obscuring any low Permian outcrops that may occur there, so that they were not differentiated on earlier maps (e.g. Plate 7). However, after the dense spinifex in Bristow Amphitheatre had been burnt, small outcrops of soft sandstone of the Grant Group were revealed on the flat floor of the depression, confirming that it occupies an Early Permian solution doline. Similar depressions in this area, delineated on air photos, are thought to have had the same origin.

Tunnels

Subhorizontal rock tunnels are known in several places in the Devonian limestones. They range from a few metres to about 50 m across and as much as several hundred metres long. Some join former subglacial lakes (e.g. Mindiwilli Tunnel in the southern Lawford Range; Fig. 313), whereas others are linked with solution dolines (e.g. Peara Tunnel below Old Napier Doline in the Napier Range; Figs 318–320), or they pass through a limestone barrier, such as Tunnel Creek (AMG Zone 51, 727300E 8051500N), which passes under the Napier Range. Many contain permanent bodies of water (e.g. Peara Tunnel and Tunnel Creek) but others are dry for most of the year (e.g. Mindiwilli Tunnel).

Kevins Cave (AMG Zone 52, 189900E 7931100N; Fig. 313) is probably the entrance to an Early Permian tunnel, but it is now blocked about 20 m from its entrance. The higher Mindiwilli Tunnel, 25 m to the south-southeast, is more than 100 m long, 20 m high, and an average of 5 to 10 m wide. It joins parts of the paleolake system and is open throughout its length.

Such tunnels were probably formed in response to anomalously high pressures generated in meltwater below the Early Permian ice sheet. Water pressures would have risen in places where subglacial water movement in channels and between lakes was impeded by freezing of parts of the drainage system. Water may then have forced its way through joints or faults in adjoining limestones, dissolving out tunnels and allowing meltwater to escape freely to unfrozen parts of the subglacial drainage system.

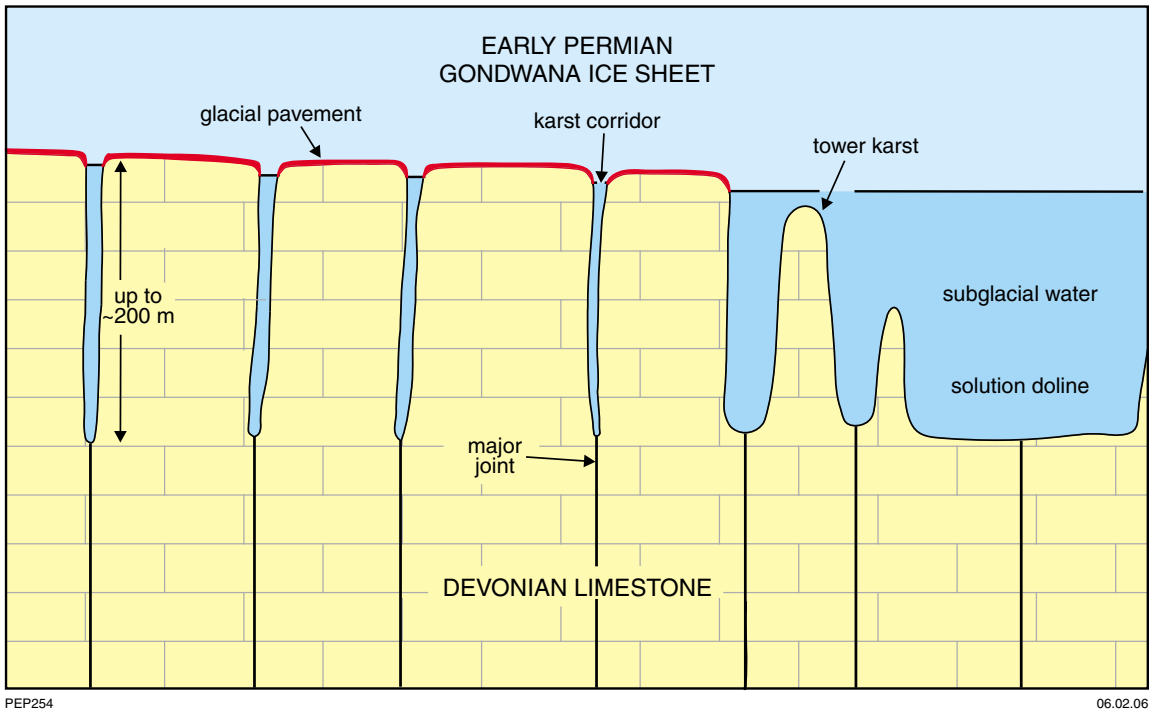

Figure 273. **Diagrammatic cross section illustrating features formed by the solution of Devonian limestone by subglacial water below the Early Permian continental ice sheet.**

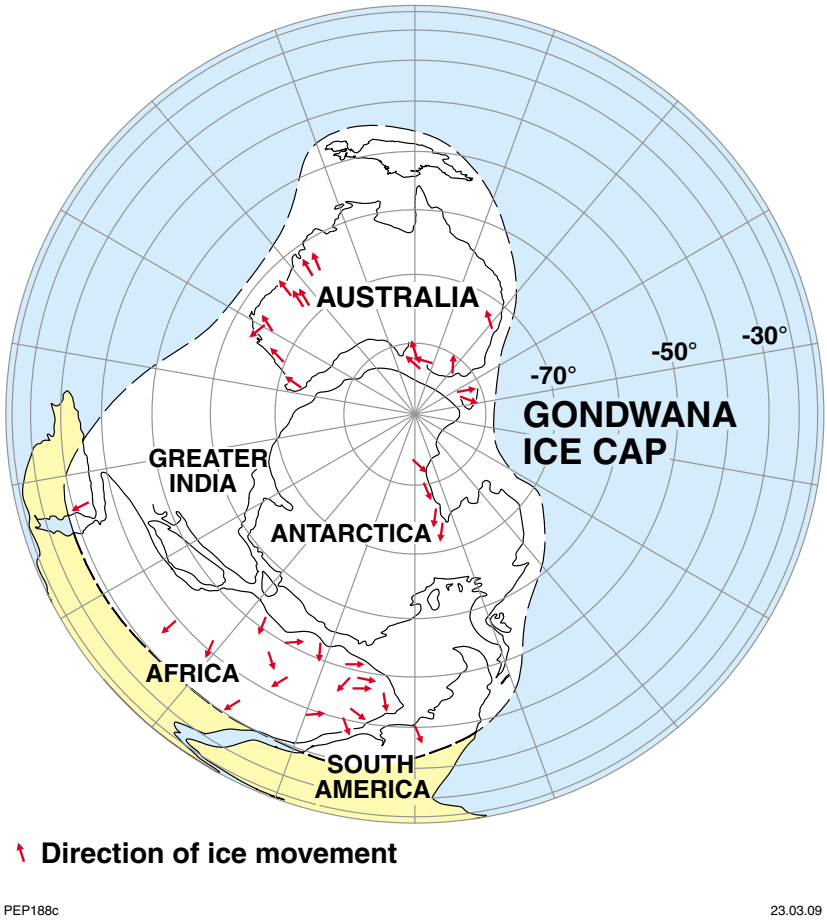

Figure 274. **Diagrammatic south polar projection showing the Early Permian ice sheet that covered the southern part of the Gondwana supercontinent, showing the directions of ice movement as deduced from striated glacial pavements and other features.**

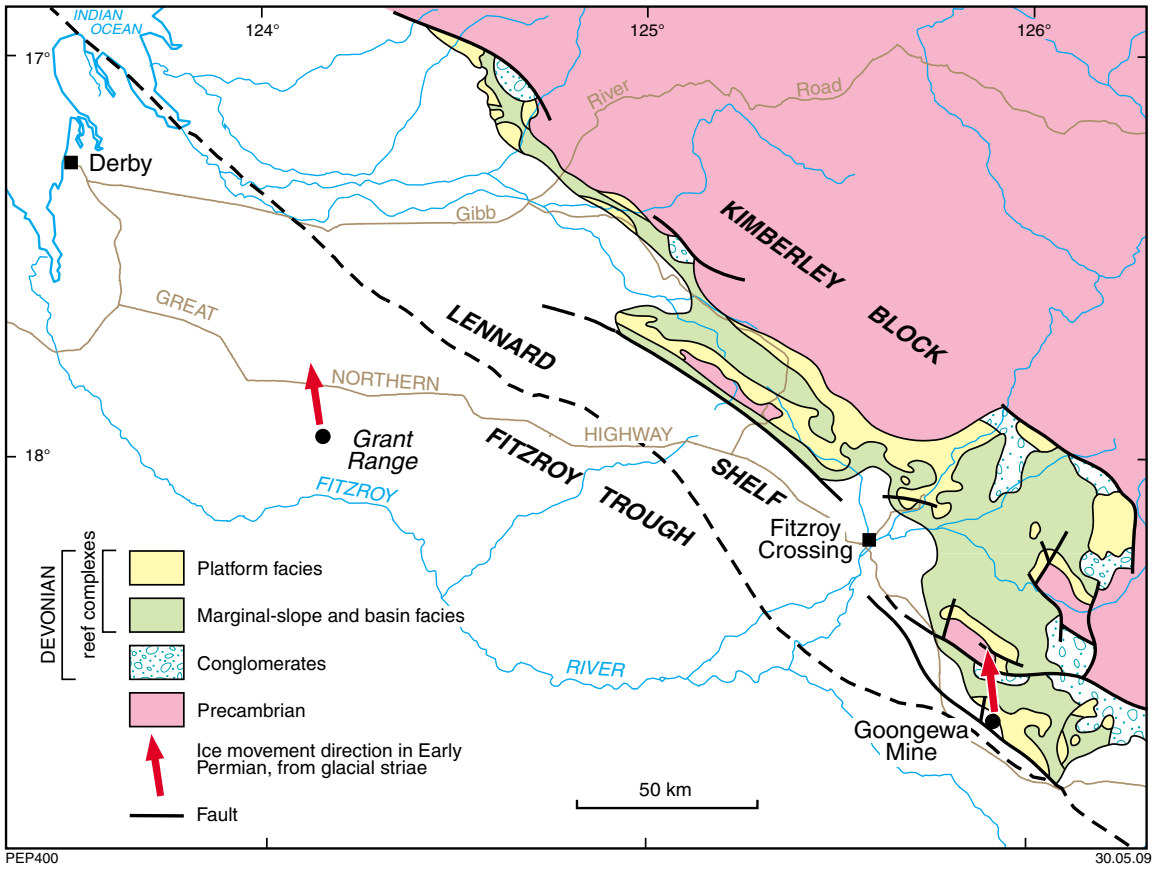

Figure 275. Generalized geological map of the northern Canning Basin, showing the directions of Early Permian ice movement as deduced at the Goongewa box-cut and Grant Range.

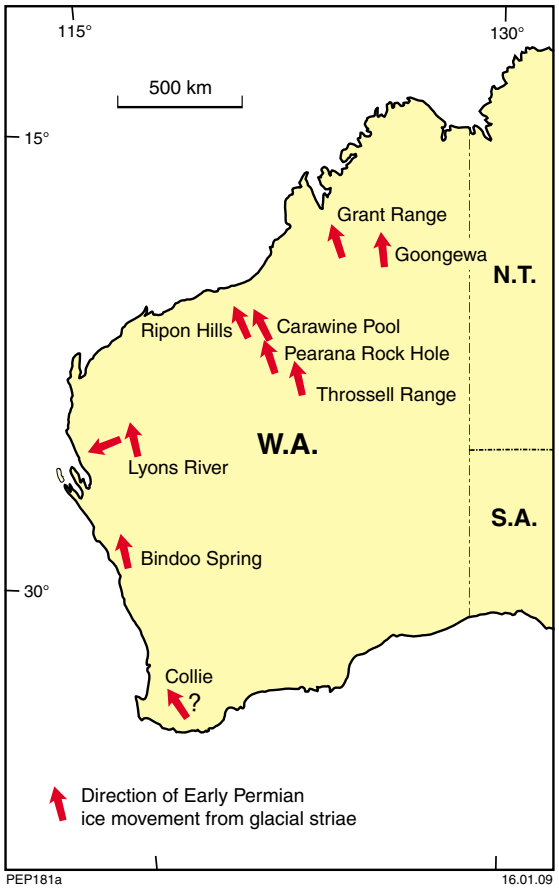

Figure 276. Directions of Early Permian ice movement as determined at various localities in Western Australia.

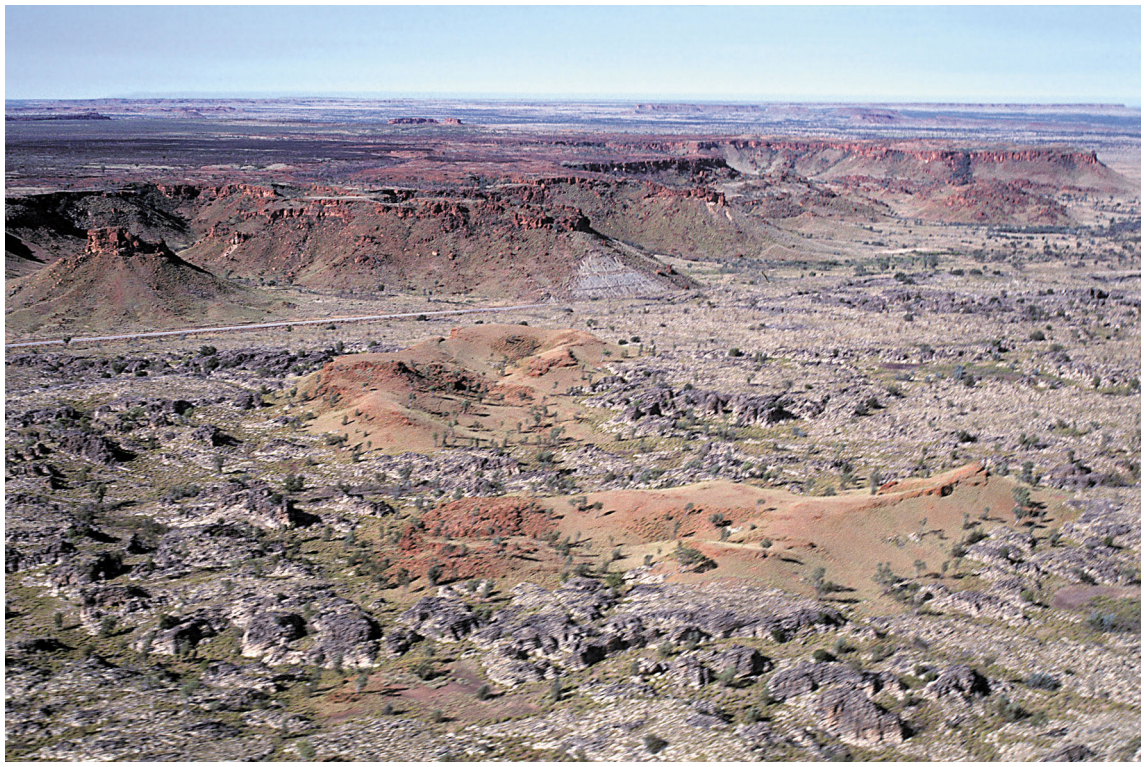

Figure 277. **Aerial view, looking southeast near Deeadeea Cliff, showing the cliff-forming Deeadeea Sandstone Member and underlying Ngumban Claystone Member of the Carolyn Formation (Grant Group), and outliers of those members overlying karstified limestone of the Devonian reef complex.**



Figure 278. **Closer aerial view, looking southeast towards Deeadeea Cliff, showing outliers of the Carolyn Formation resting on strongly karstified Bugle Gap Limestone.**



Figure 279. Unconformity between sandstone of the Grant Group (Lower Permian) and strongly karstified Nullara Limestone at Red Bluffs, the southernmost exposure of the Devonian reef complexes.



Figure 280. Aerial view of Kimberley Rover solution doline in the northern Laidlaw Range, looking northwest, showing outcrops of Lower Permian silicified sandstone within the doline, surrounded by karstified Pillara Limestone. Karst corridors follow joints in the limestone, and a significant cave system (Kimberley Rover Cave) underlies the dark rugged limestone on the upper right.



Figure 281. Aerial view of Kimberley Rover solution doline looking north-northeast towards another solution doline in the right background. Karst corridors follow joints in the limestone, and a cave system (Kimberley Rover Cave) extends from the upper part of the doline below the dark band of rugged limestone in the upper central part of the image.



Figure 282. Kimberley Rover solution doline, looking southwest, showing orange-coloured hills of silicified sandstone of the Lower Permian Grant Group within the doline, surrounded by karstified Upper Devonian limestone. Also note well-developed karren, resulting from modern karstification, in the foreground.



Figure 283. Deeadeea Cliff beside the Great Northern Highway, showing the type sections of members of the Carolyn Formation: Deeadeea Sandstone Member above (the scarp forming the cliff top) and Ngumban Claystone Member below. Photo by Arthur Mory.

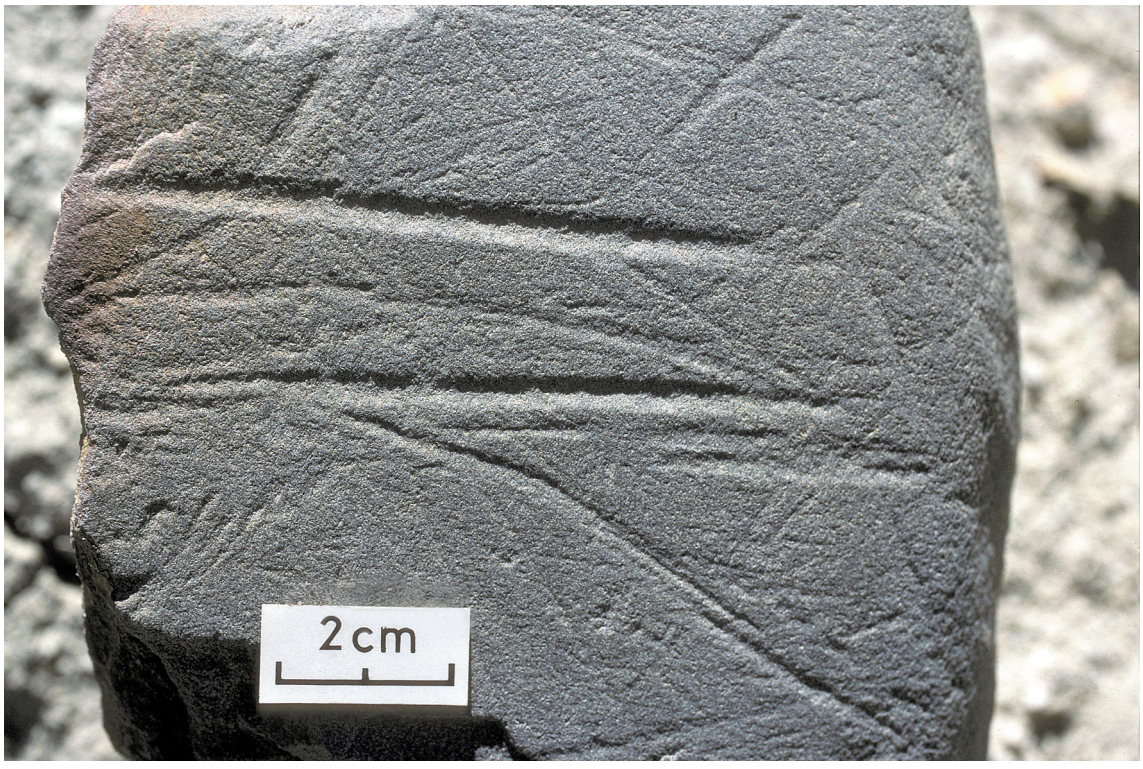

Figure 284. Glaciated cobble (a dropstone) of basalt from the Ngumban Claystone Member in its type section, showing well-developed striations and faceting.



Figure 285. **Striated and polished glacial pavement in the Goongewa box-cut, showing a striated and polished glacial pavement on reef limestone of the Pillara Limestone.**

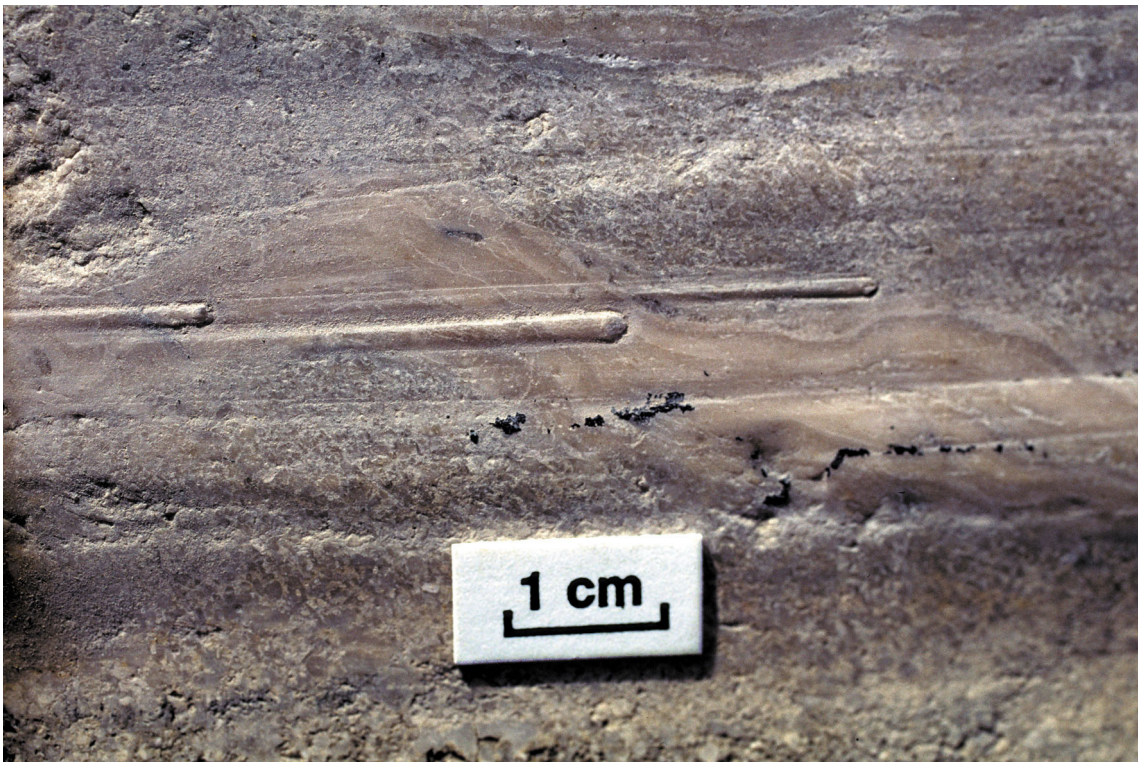

Figure 286. **Striated and polished glacial pavement in the Goongewa box-cut, showing small-scale crag-and-tail structures. Ice movement was from south to north, right to left on the photo.**



Figure 287. Part of the striated and polished glacial pavement on Pillara Limestone in the Goongewa box-cut. Ice movement was from south to north, right to left on the photo.

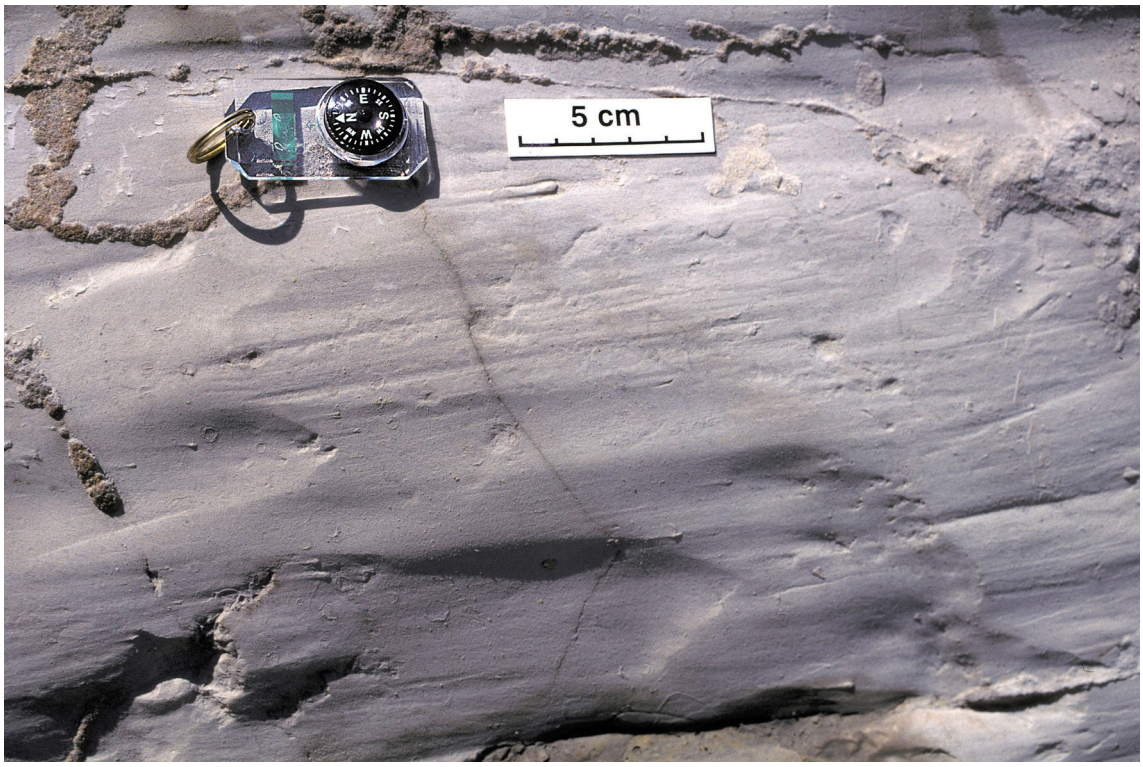

Figure 288. Striated, sculptured, and polished glacial pavement on Pillara Limestone in the Goongewa box-cut. Ice movement was from south to north, right to left on the photo, as indicated by the compass.



Figure 289. Planar glacial unconformity in the Goongewa box-cut, between Pillara Limestone (reef-margin to reef-flat subfacies) below and Ngumban Claystone Member above.

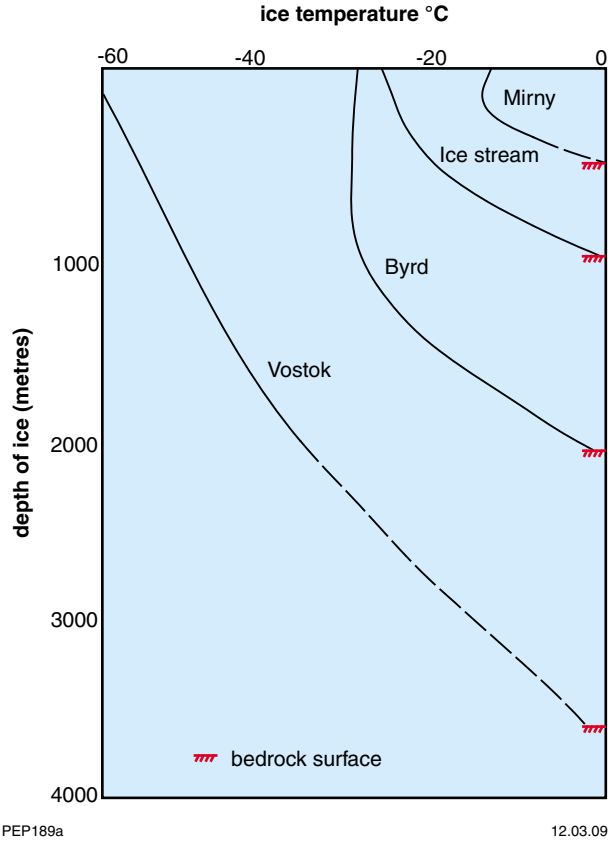

Figure 290. Graphs of temperature in relation to depth of ice in holes drilled through the Antarctic ice cap. The dashed parts of the graph are estimates (modified from Paterson, 1994, and Benn and Evans, 1998).

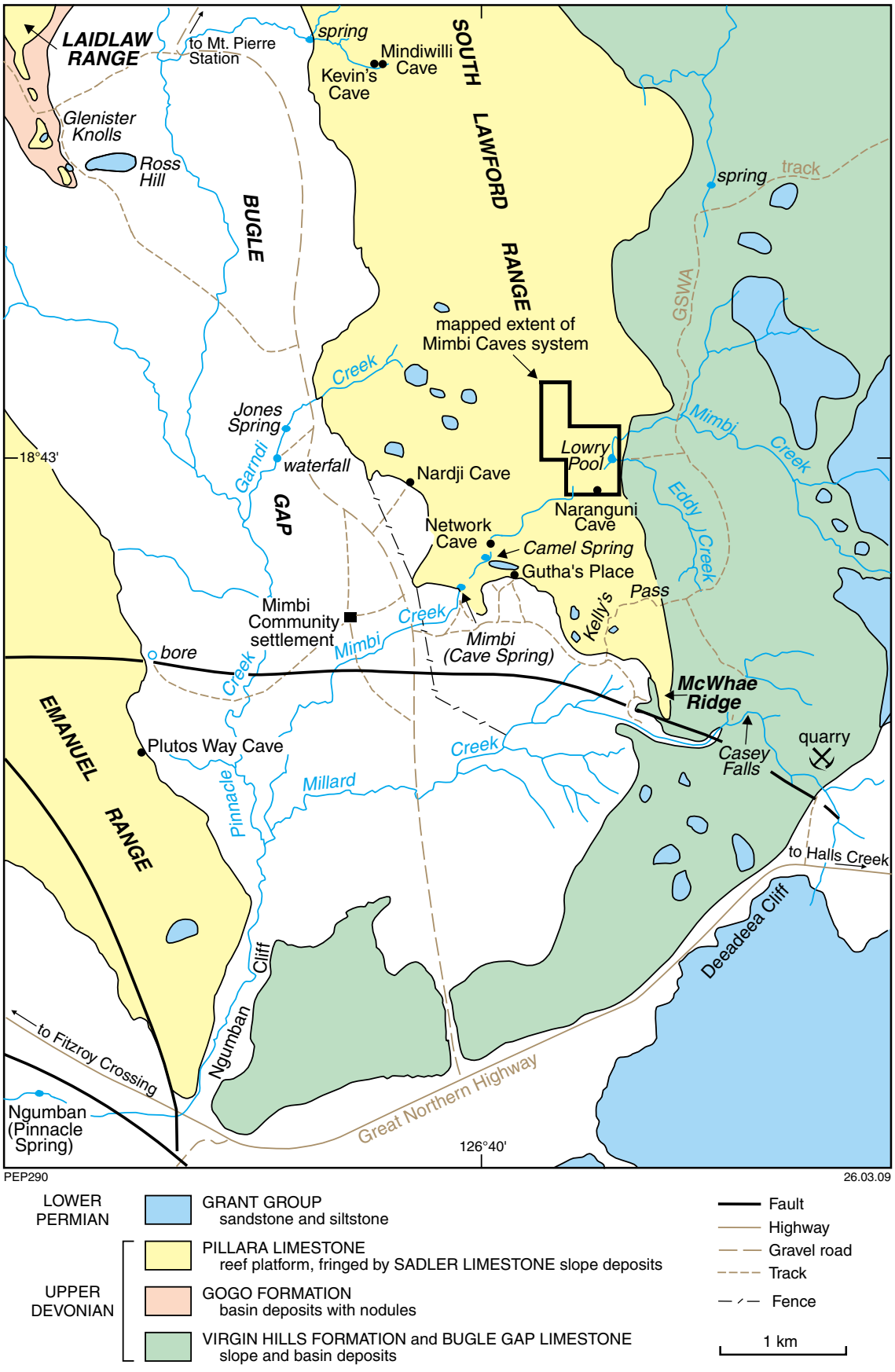

Figure 291. Geological map of the southern part of the Lawford Range, showing the locations of the Mimbi Caves System, Cave Spring (Mimbi), McWhae Ridge, Deeadeea Cliff, and Gutha's Place.

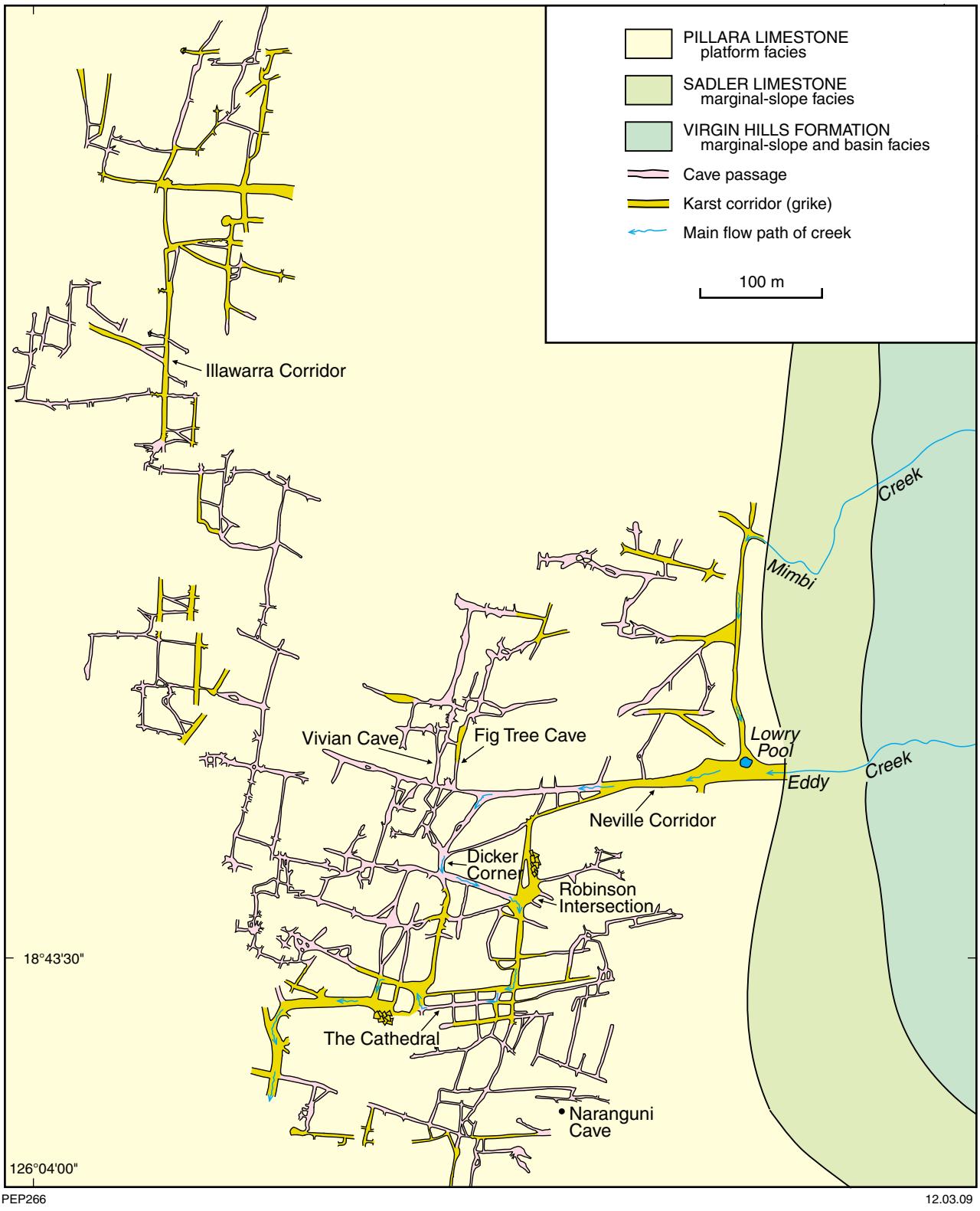

Figure 292. The mapped part of the Mimbi Caves System, after Playford (2002a), modified from Dicker, 1987.



Figure 293. 'Carrot' stalactite, Mimbi Caves System.



Figure 294. 'The crucifix', consisting of broken and regrown stalagmites and stalactites, Mimbi Caves System.

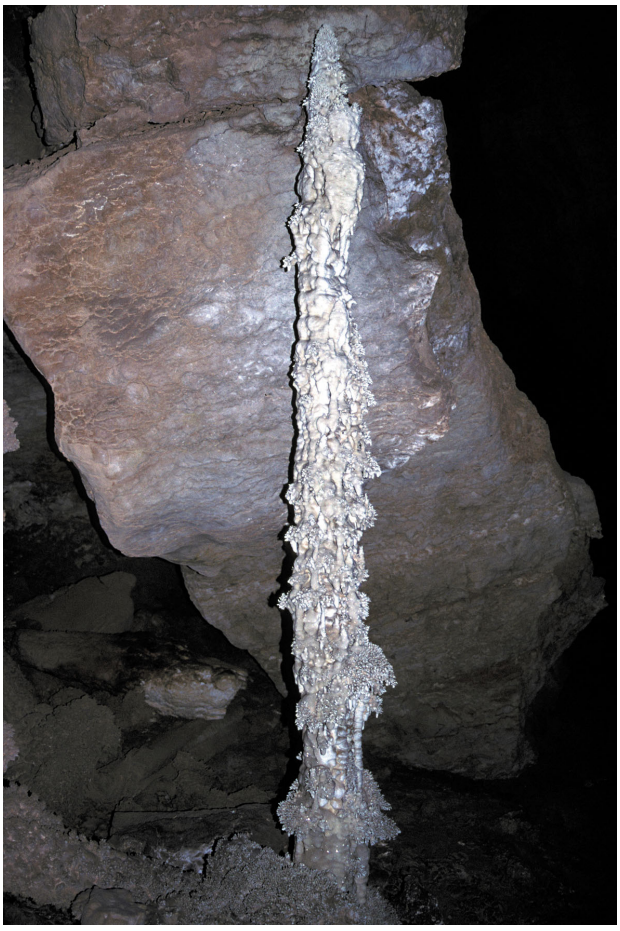

Figure 295. 'Coral' stalagmite, Mimbi Caves System.



Figure 296. Closer view of 'coral' stalagmite, Mimbi Caves System.



Figure 297. Shawl speleothem, composed of crystalline spar, on a wall of Uranus Cave, near Ngumban Cliff.



Figure 298. Spectacular flowstone speleothems on a wall of Uranus Cave, near Ngumban Cliff.

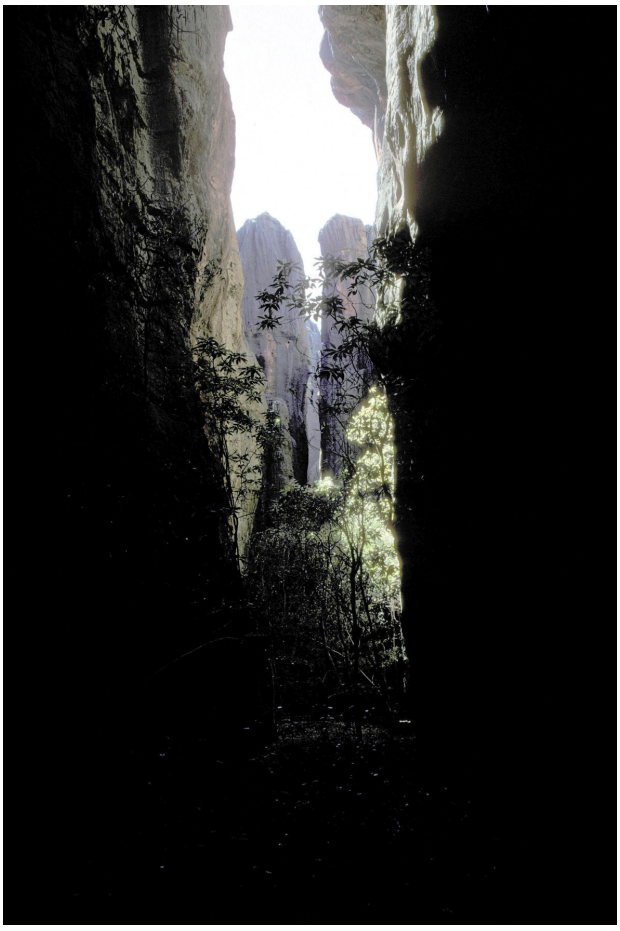

Figure 299. **Illawarra Corridor, a major karst corridor in the Mimbi Caves System formed by solution of limestone in subglacial meltwater along a major joint. Note the smooth parallel walls of the corridor, which is about 4 m wide and 30 m high.**



Figure 300. **Rough karst surface, due to modern karstification, on top of the Lawford Range above the Mimbi Caves System.**



Figure 301. Menyous Gap in the Pillara Range from the air, looking north. The gap, 2 km long, is interpreted to be a large subglacial channel, exhumed through the removal of Lower Permian deposits by Cenozoic erosion.

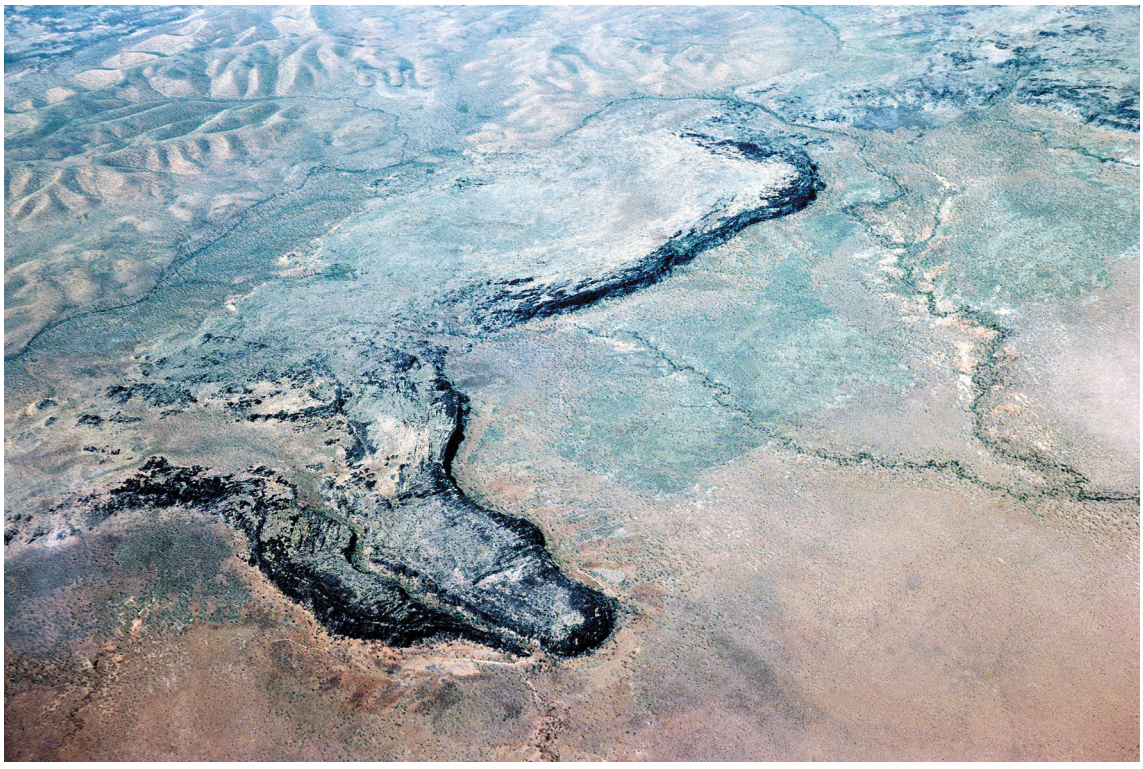

Figure 302. Aerial view of Unggumi Promontory in the Napier Range, looking southeast. Billy Munro Gorge can be seen extending along the core of the promontory. A small area of Van Emmerick Conglomerate is in the left background, behind the Napier Range reef complex. The gorge is dry throughout much of the year and is thought to have originated as a subglacial channel, cut and dissolved into the limestone during the Early Permian.

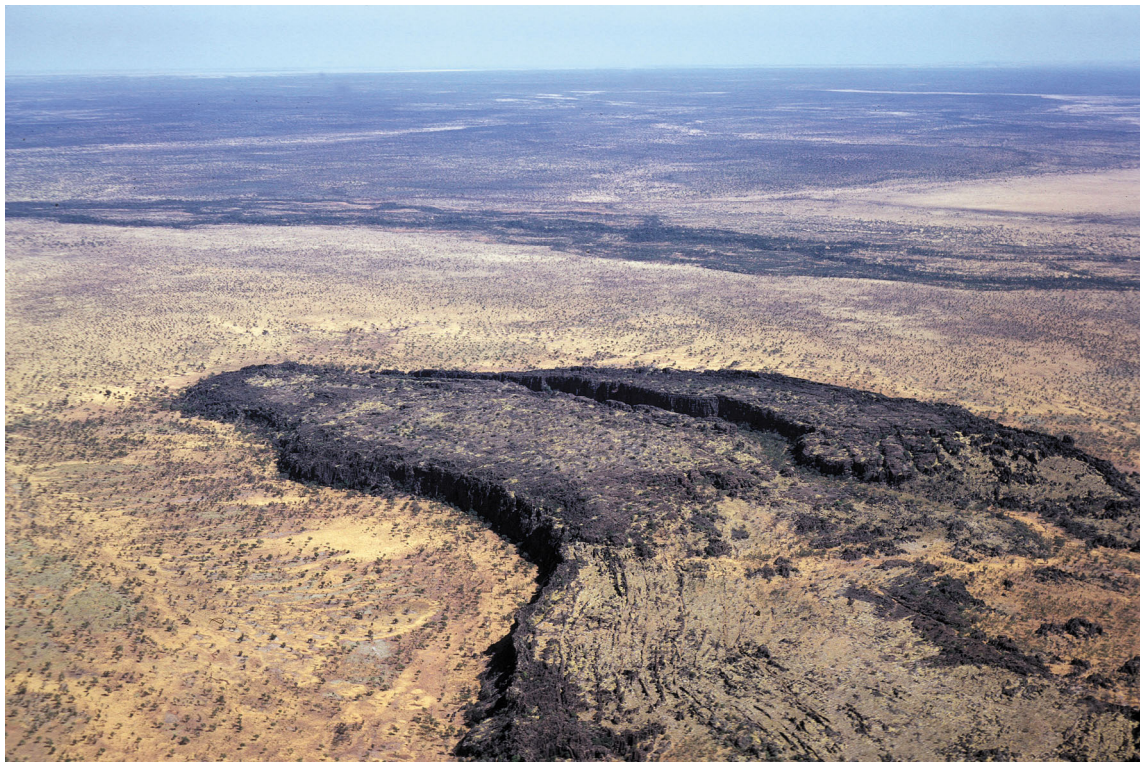

Figure 303. Aerial view of Unggumi Promontory, looking west-southwest. Billy Munro Gorge can be seen on the centre right. Note neptunian fissures in Nullara Limestone, parallel to the platform margin in the centre foreground.

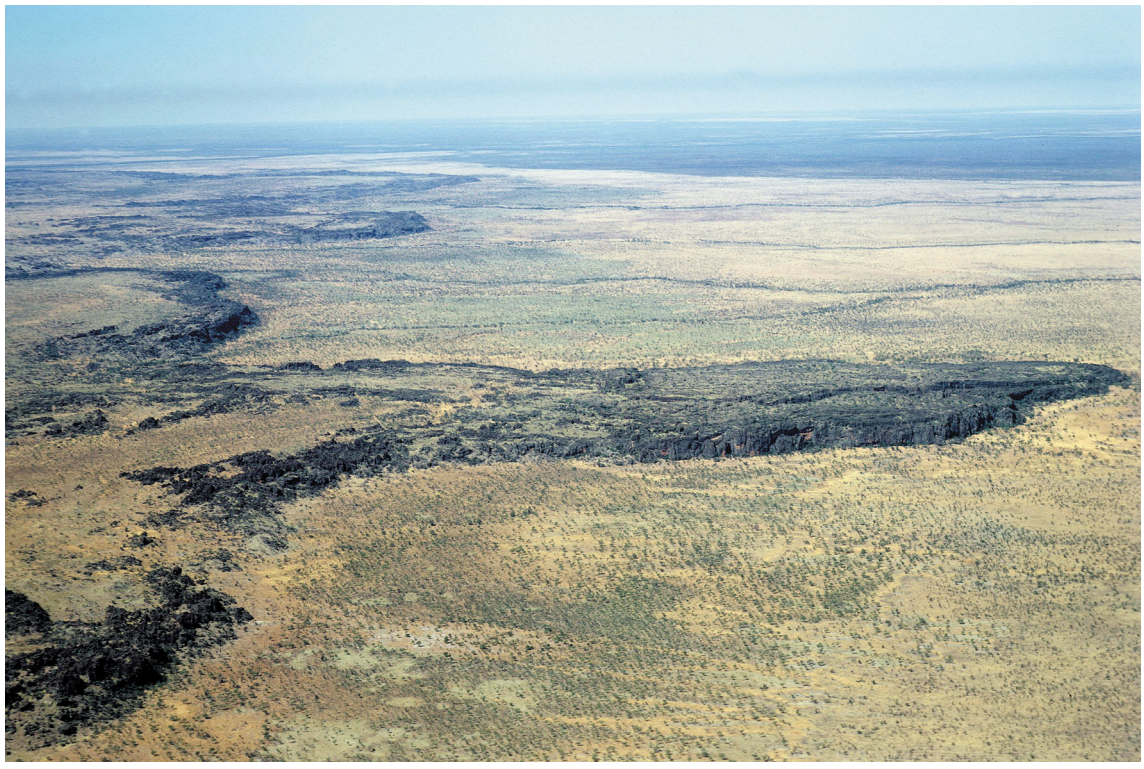

Figure 304. Aerial view of Unggumi Promontory, looking south-southeast along the front of the Napier Range. Billy Munro Gorge can be seen extending along the core of the promontory.

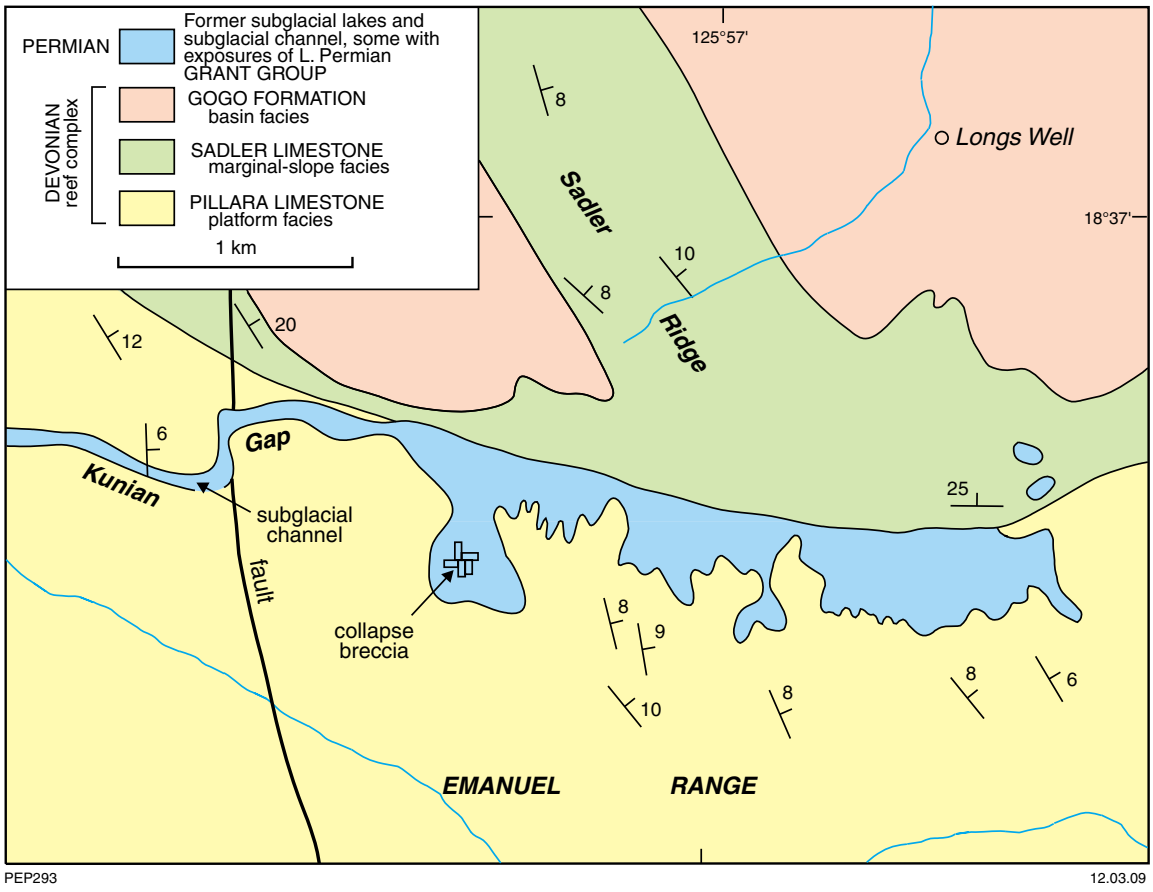

Figure 305. Map of the northern Emanuel Range and Sadler Ridge areas, showing the sites of subglacial lakes, part of the Kunian Gap subglacial channel, and a cave-collapse breccia.



Figure 306. Aerial view of Windjana Gorge looking east-southeast over the Napier Range reef complex. The subhorizontal top of the range is the Early Permian glaciated surface modified by Cenozoic erosion. Flat-floored depressions on top of the range are thought to mark Early Permian solution dolines. The gorge is interpreted to be an exhumed Early Permian subglacial channel.

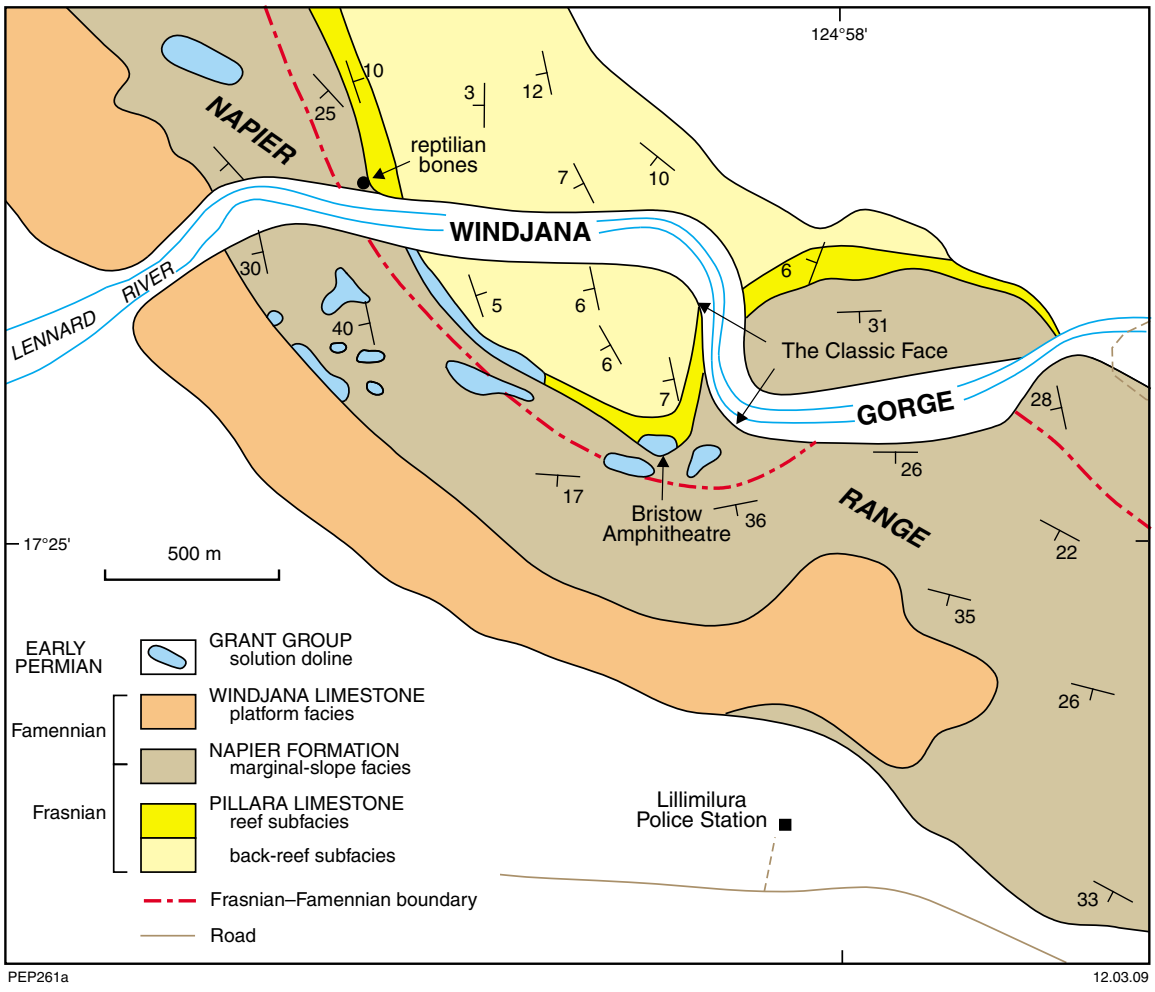

Figure 307. **Geological map of the Windjana Gorge area. Note the trace of the Frasnian–Famennian boundary and the interpreted occurrences of Lower Permian Grant Group filling solution dolines on top of the range.**



Figure 308. **Aerial view of the central part of Geikie Gorge, looking east, showing the southeast wall of the gorge. Flat-lying platform limestones of the Pillara Limestone on the right are fronted by steeply dipping marginal-slope limestones of the Napier Formation on the left. The gorge is thought to be an exhumed Early Permian subglacial channel.**



Figure 309. Brooking Gorge, looking northwest, near the gorge entrance. The gorge is thought to be an exhumed Early Permian subglacial channel.

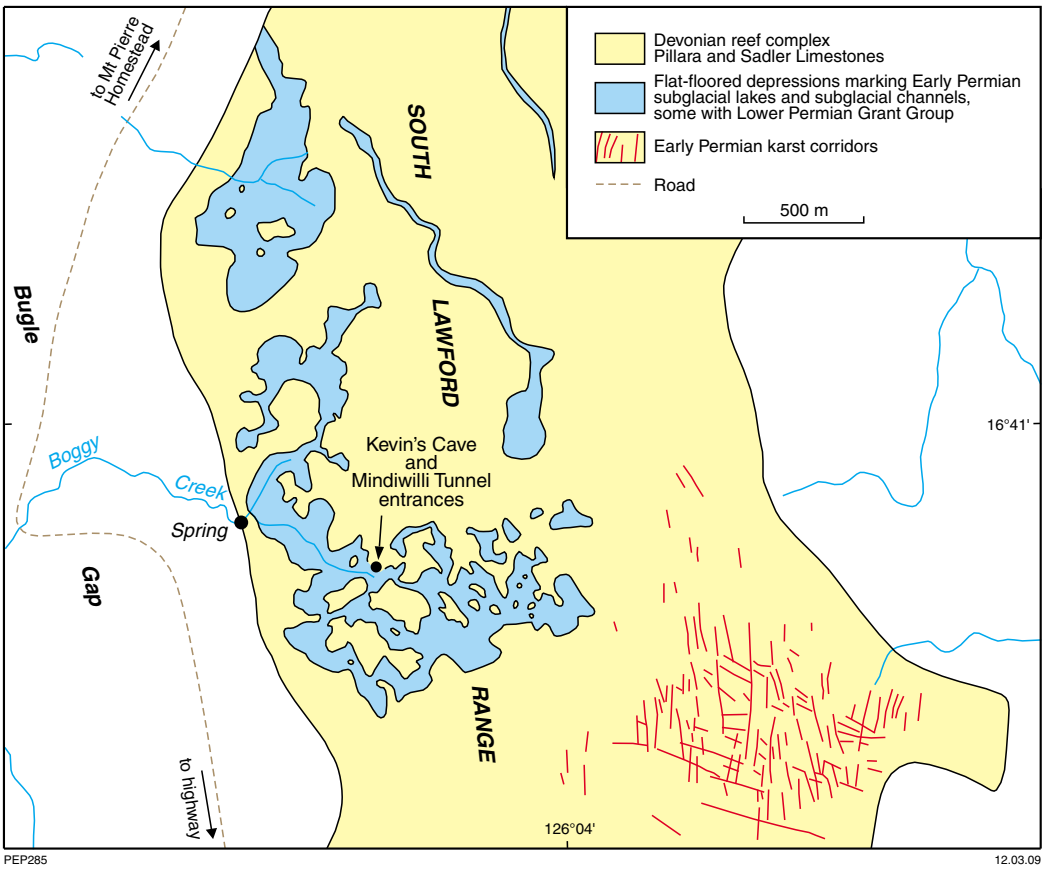

Figure 310. Geological map of the Boggy Creek area, South Lawford Range, showing the former extent of Early Permian subglacial lakes and channels.

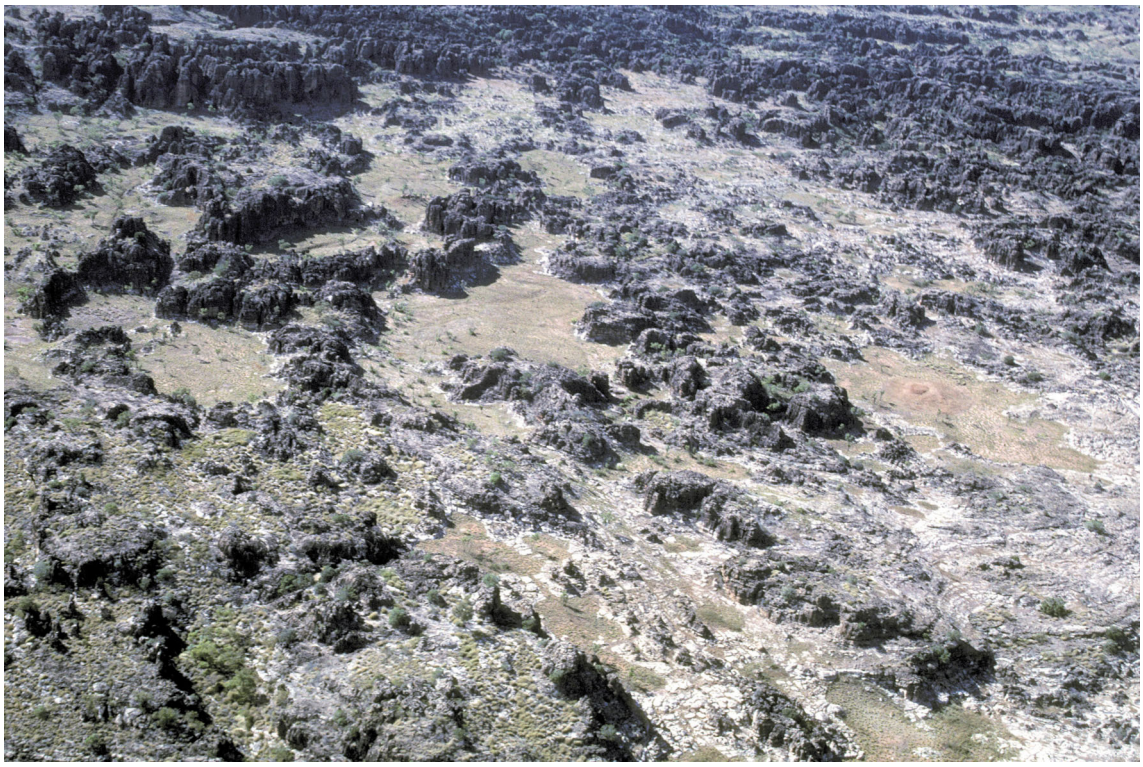

Figure 311. Aerial view of part of the Boggy Creek area, showing flat areas occupied by poorly exposed sandstone of the Grant Group.



Figure 312. Tower karst in the Paddys Spring area, northern Laidlaw Range. The level ground between the towers is underlain by poorly exposed soft sandstone of the Grant Group.



Figure 313. Kevins Cave (left) and the entrance to Mindiwilli Tunnel (right) in the Boggy Creek area. The flat ground in the foreground is underlain by poorly exposed soft sandstone of the Early Permian Grant Group.



Figure 314. Panorama at Lloyd Hill of a solution doline filled with poorly exposed sandstone of the Lower Permian Grant Group, looking southwest towards flat-lying reef-flat limestone overlain by massive reef-margin limestone.



Figure 315. Aerial view of Lloyd Hill atoll, looking north. The solution doline shown in Figure 314 is situated below the round green patch in the upper right part of the atoll.

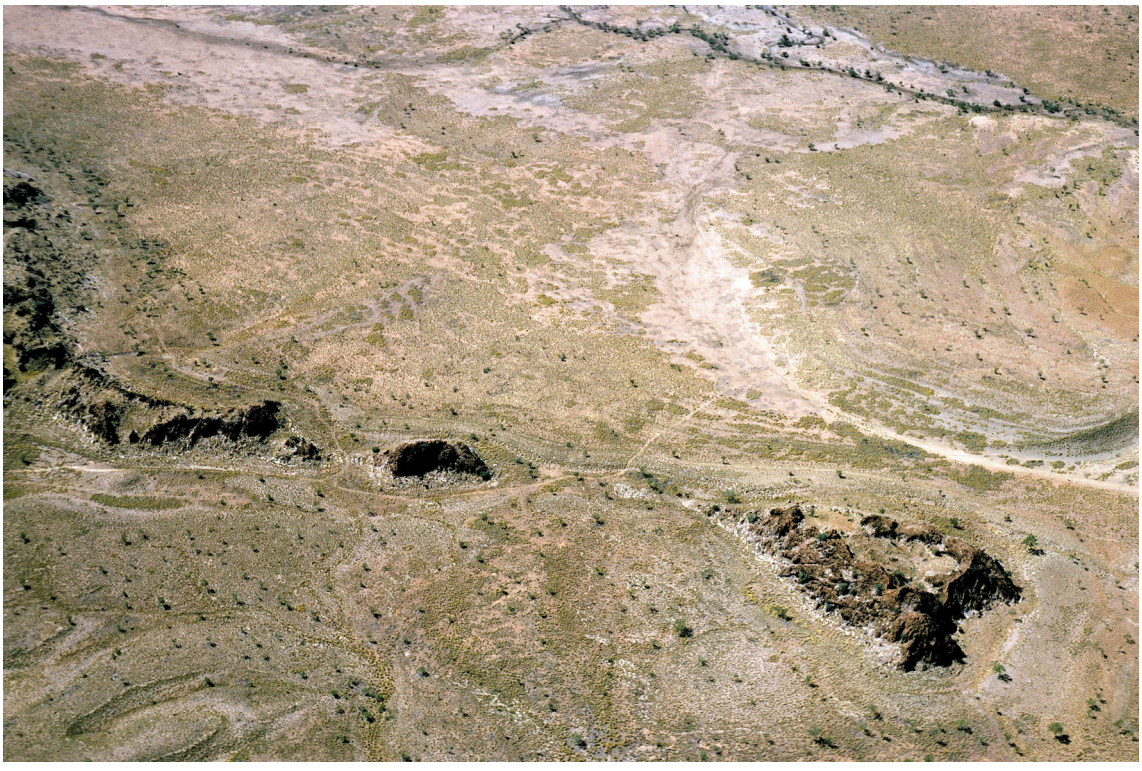

Figure 316. Aerial view of two of the Glenister Knolls patch reefs (middle and right), with the 'tail' of the Laidlaw Range platform on the left. A solution doline filled with glacigene Lower Permian Grant Group can be seen in the core of the larger knoll on the right.



Figure 317. Solution doline filled with Lower Permian Grant Group (foreground and middle distance) in the largest of the Glenister Knolls, looking south. Note the relatively smooth wall of the doline.



Figure 318. Entrance to Peara Cave in the northern Napier Range.

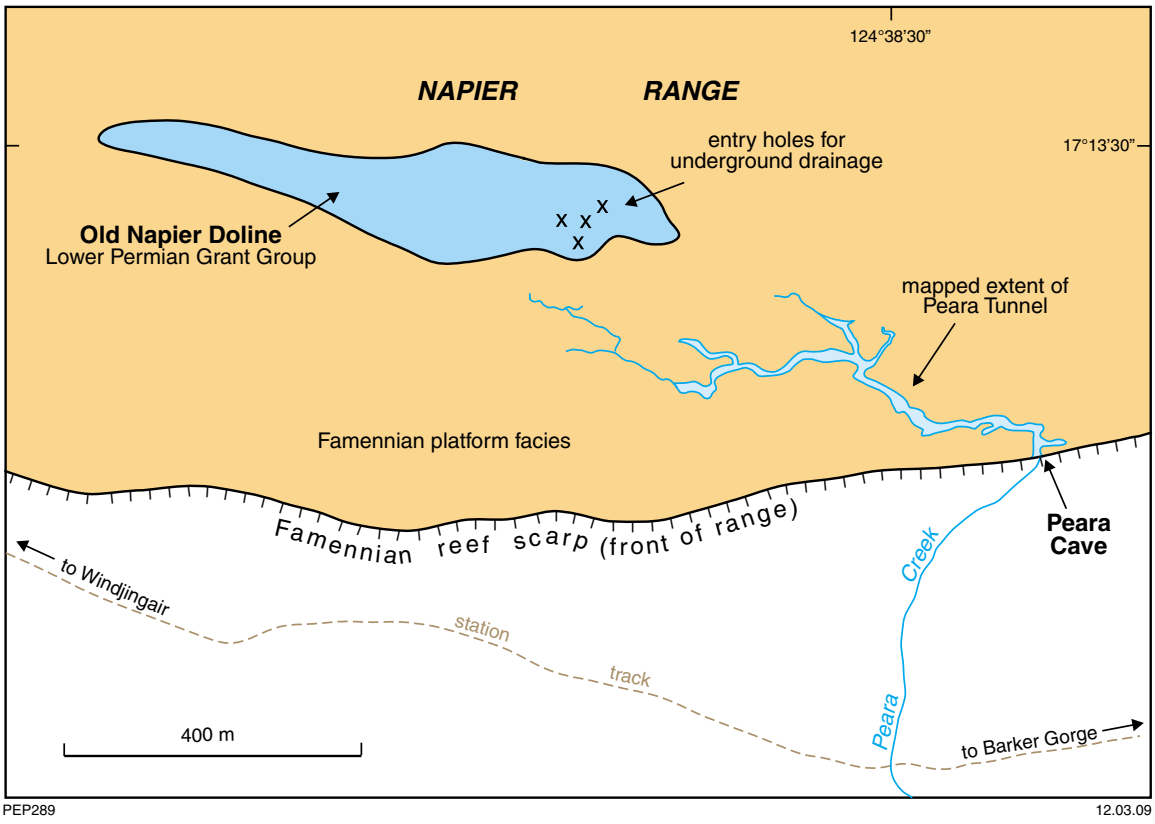

Figure 319. **Map of the Peara Cave area showing the known extent of the cave system and the Old Napier solution doline. After Playford (2002a), modified from Colette et al. (2000).**

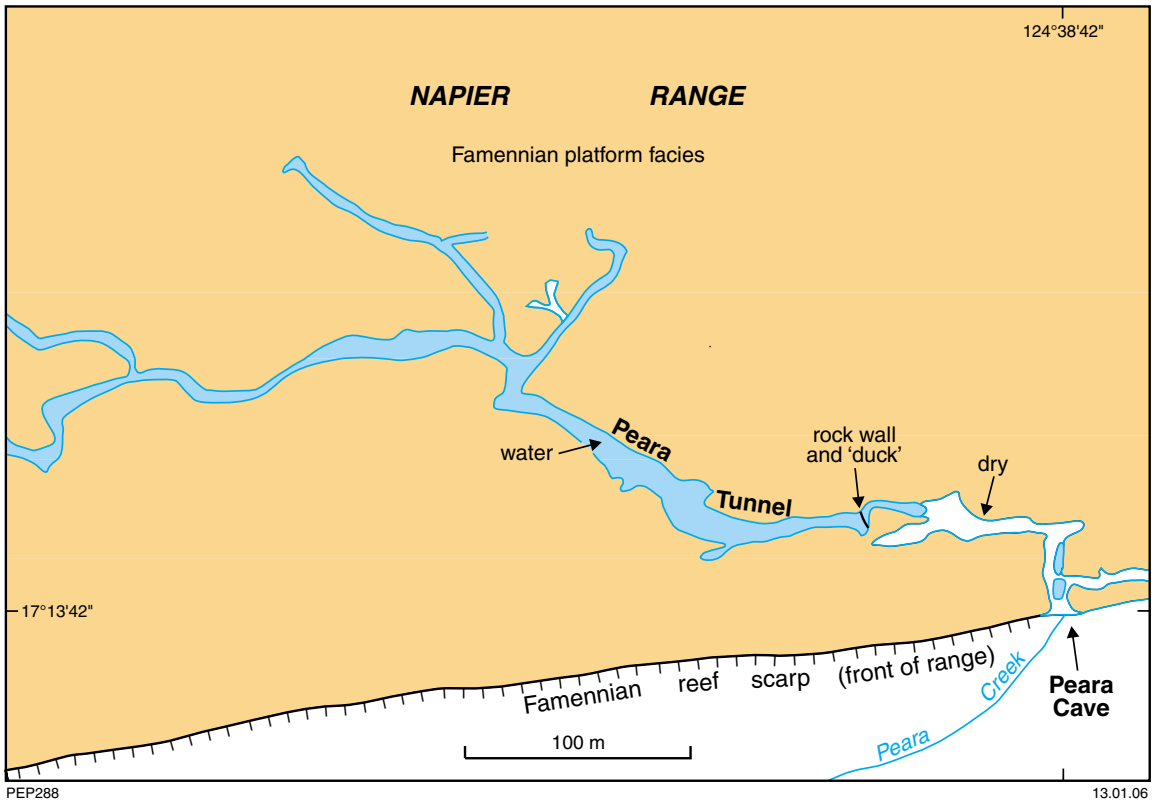

Figure 320. **Map showing the lower part of the Peara Cave system. After Playford (2002a), modified from Colette et al. (2000).**



Figure 321. Cave-collapse breccia in marginal-slope limestones, central Oscar Range, thought to have formed by the collapse of a cave formed by subglacial solution during the Early Permian.

In some cases, networks of small tunnels join to form much larger features, such as the remarkable Peara Tunnel system ('Lake Cave' on Plate 1) in the Napier Range (entrance at GPS AMG Zone 51, 674900E 8094440N), which is more than 750 m long and emerges about 10 m up the face of the range (Figs 318–320; Colette et al., 2000). The full extent of this tunnel system has yet to be determined, but its source is clearly in the Old Napier Doline. Rainwater drains through the floor of the doline in a number of small irregular holes that are expected to lead to branches of the tunnel. The doline contains sandstones of the Grant Group, showing that it is Early Permian in age.

Most of Peara Tunnel is flooded with water throughout the year. Only the western end, extending for 120 m behind the tunnel entrance, is readily accessible. This section, containing permanent pools of water, ends in a wall of rock. However, speleologists discovered that this section is linked underwater with the rest of the tunnel via a 'duck' 4 m long below the rock wall (Fig. 320; Collette et al., 2000).

Tower karst

Columns of limestone, as much as 30 m high and 10 m wide, are referred to as tower karst (Fig. 312). They commonly formed on the floors of subglacial lakes, by the prolonged solution of limestone along intersecting karst corridors. Like other types of subglacial karst, the walls of the towers are still smooth in places where the soft Lower Permian sedimentary rocks that once enclosed them have only recently been eroded away.

Collapse breccias

Breccias, apparently formed by the collapse of Early Permian caves, are exposed at many places in the reef complexes, especially in the Oscar and Napier Ranges (Playford and Lowry, 1966; Ward, 1996; Tornatora, 1992; see Plate 2); a large example is shown on Plate 2 behind *Mandaway* Spring in the central Oscar Range (AMG Zone 52, 733600E 8023800N). The breccias are composed of angular blocks of limestone, of the same types as those in the adjacent Devonian reef complexes (Fig. 321).

Other collapse breccias are largely or wholly surrounded by sandstone and claystone of the Grant Group; for example the breccia that occurs in the paleolake doline near Sadler Ridge (Fig. 305; AMG Zone 51, 810300E 7937600N).

Diagenetic effects

Kerans (1985), Hurley and Lohmann (1989), and Wallace et al. (1991) each recognized that the middle Carboniferous to Early Permian period of erosion must have had important diagenetic effects on the limestones, but they were not aware of the roles of subglacial meltwater and ice loading in diagenesis. No detailed re-examination of

the cement stratigraphy to take account of these factors has been undertaken during the present study. However, it seems possible that the late-stage banded-luminescent calcite cement of Wallace et al. (1991) was generated by diagenesis below the Permo-Carboniferous ice sheets. It is also likely that some pressure-solution compaction of the limestones resulted from ice loading.

Subglacial cementation processes may have resulted in the destruction of much of any remaining porosity in the Devonian limestones after early burial diagenesis and pressure-solution compaction.

Cenozoic bone deposits

The Early Permian paleokarst was modified to varying degrees as it was incorporated into the modern karst geomorphology. Most of the dolines, caves, and karst corridors that feature so prominently in the modern karst were formed originally as subglacial karst below the Early Permian ice sheet, and were exhumed and modified during the Cenozoic.

The gradual lowering of the upper surfaces of the Devonian limestone ranges during the Cenozoic, with partial destruction of Early Permian paleokarst, is illustrated at a locality found by Tornatora (1992) near Dingo Gap (GPS AMG Zone 51, 733250E 8045030N). At that locality, dense masses of very small masticated bones and small gastroliths are cemented into crevices and over surfaces in the fore-reef limestone (Fig. 322). These bones are thought to be late Tertiary or early Pleistocene in age, pre-dating the arrival of *Rattus* in Australia, and were derived from the faeces of ghost bats that roosted in caves during the day and preyed on small rodents, lizards, and marsupials at night (Aplin, K and Baynes, A, 2000, 2002, written comms). The masticated bone deposits must have accumulated on the floor of an Early Permian cave that has now disappeared as a result of late Cenozoic erosion.

Windjana Gorge (Figs 306, 307; Plate 6) is thought to be localized by a major subglacial channel that was exhumed during the Cenozoic by the progressive removal of its infilling of Lower Permian sandstone and claystone of the Grant Group.

At one locality in the west-central part of Windjana Gorge, about 40 m above the present river bed, river gravels containing reptilian bones were deposited in what is interpreted to be a truncated Early Permian cave, now largely eroded away (GPS AMG Zone 51, 707100E 8074130N; Fig. 323). The cave directly adjoined the river when it was flowing at that level. The conglomerate in the eroded cave includes pebbles and cobbles of various Precambrian rocks, Grant Group sandstones, and laterite, together with bones of extinct turtles and a large crocodile, estimated to have been about 7 m long (Gorter and Nicoll, 1978). The precise age of this reptilian deposit has not been determined, but it may be middle Tertiary. It was laid down when the river had exhumed only the upper



Figure 322. Cemented layer of masticated small reptile and mammal bones and gastroliths in the Dingo Gap area. This is thought to be a Tertiary or early Pleistocene cave deposit formed from the faeces of ghost bats. The field of view is about 15 cm wide.



Figure 323. Conglomerate with large crocodile and turtle bones in a small cavern about 40 m above the river bed in Windjana Gorge. The cavern is thought to be a Late Permian karst feature, and the conglomerate must have been deposited when the river was flowing at this level, perhaps during the middle Tertiary.

part of the existing gorge, to about a half of its present depth.

Bones of *Diprotodon*, a giant Pleistocene marsupial, were discovered in 1883 in river gravels in the bed of Windjana Gorge (Hardman, 1887), but none have been found since then. It seems probable that those bones came from a riverine deposit that is younger than the known reptilian-bone deposit. Clearly, there are good prospects for the further discoveries of Tertiary and Pleistocene vertebrate fossils in the many caves and other karst features in the Lennard Shelf area.

Anthropological aspects of early Permian paleokarst

Some of the exhumed Early Permian caves were used as dwelling places, tombs, and rock-art galleries by Aborigines of the *Unggumi*, *Bunaba*, and *Gooniyandi* (*Kuniandi*) Tribes, whose territories include the exposed Devonian reef complexes (Fig. 15; Playford, 1960, 2007). Many of the more prominent caves are decorated with rock art of the *Wandjina* style (Fig. 324), and there are a few possible examples of the older Bradshaw style. Some caves were used to inter the remains of deceased Aborigines, the bones of each having been placed in a paper-bark coffin, bound together with human-hair or boab-fibre string. There is considerable potential for further archaeological research in many of the caves, designed to expand knowledge of the early history of human occupation in the Kimberley District.

Peara Tunnel was referred to as 'Old Napier Downs Cave' and 'Lake Cave' in earlier publications (Jennings and Sweeting, 1963; Colette et al., 2000). However, the *Unggumi* Aborigines knew it as '*Peara*', and that name is adopted in this Bulletin. According to *Unggumi* legend, *Peara* was a woman of the Dreamtime who used her digging stick to excavate the tunnel. On hearing the sound of men singing a sacred song that was never supposed to be heard by women, she crouched with her hands over her ears and her arms by her sides, endeavouring to block out the sound. However, it was too late, and she was turned to stone, in the form of a large stalagmite (Fig. 325). *Peara* was the wife of *Tchularga*, the most important culture hero of this area, who travelled during the Dreamtime for more than 1000 km along the limestone ranges and through the Great Sandy and Gibson Deserts. His story is recounted in a major song cycle, parts of which were recorded by Playford in 1962–63. The original audio tapes have been donated to the Aboriginal and Torres Strait Islander Institute, Canberra, with copies to the Western Australian Museum, Perth.



Figure 324. **Aboriginal cave painting of a *Wandjina* Dreamtime figure known as *Rowalamban*, in the northwestern Napier Range.**



Figure 325. **Stalagmite near the entrance to Peara Cave. The stalagmite is said to be the figure of a woman known as *Peara* who dug out this cave with her digging stick during the primeval Dreamtime. She was turned to stone, crouching with her hands over her ears and her arms by her sides, while trying to block out the sound of men singing part of a sacred song cycle that was never to be heard by women.**

Late Devonian pseudokarst

The term 'pseudokarst' is applied to tubular structures, circular to lobate in cross section, that have been regarded as karst features by some authors, but are interpreted by others as growth structures formed during development of the enclosing microbial reef limestones (Playford, 1981, 2002a; Kerans, 1985; George and Powell, 1997; Stephens and Sumner, 2002).

Playford (1981) discussed an allochthonous block of reef limestone in Famennian marginal-slope deposits at Dingo Gap in the Napier Range (no. 1 on Fig. 326). The block consists of sandy, fenestral, microbial reef limestone, containing tubes of calcareous sandstone that are roughly circular to lobate in cross section and average about 10 cm in diameter. The tubes are 20 cm apart and as much as 4 m long. They commonly have a thin outer lining of microbial micrite, and are filled with very coarse calcareous sandstone, commonly containing large fragments of mollusc shells (Figs 326–333). Other allochthonous blocks with similar tubes occur at several places along the same horizon in Dingo Gap and at many other localities on the Lennard Shelf.

The tubes in individual allochthonous blocks are subparallel. Some were nearly vertical when they formed in the reef, whereas others were oblique or curved. Playford (1981) interpreted the pipes as karst features, formed on an exposed reef after a brief regression.

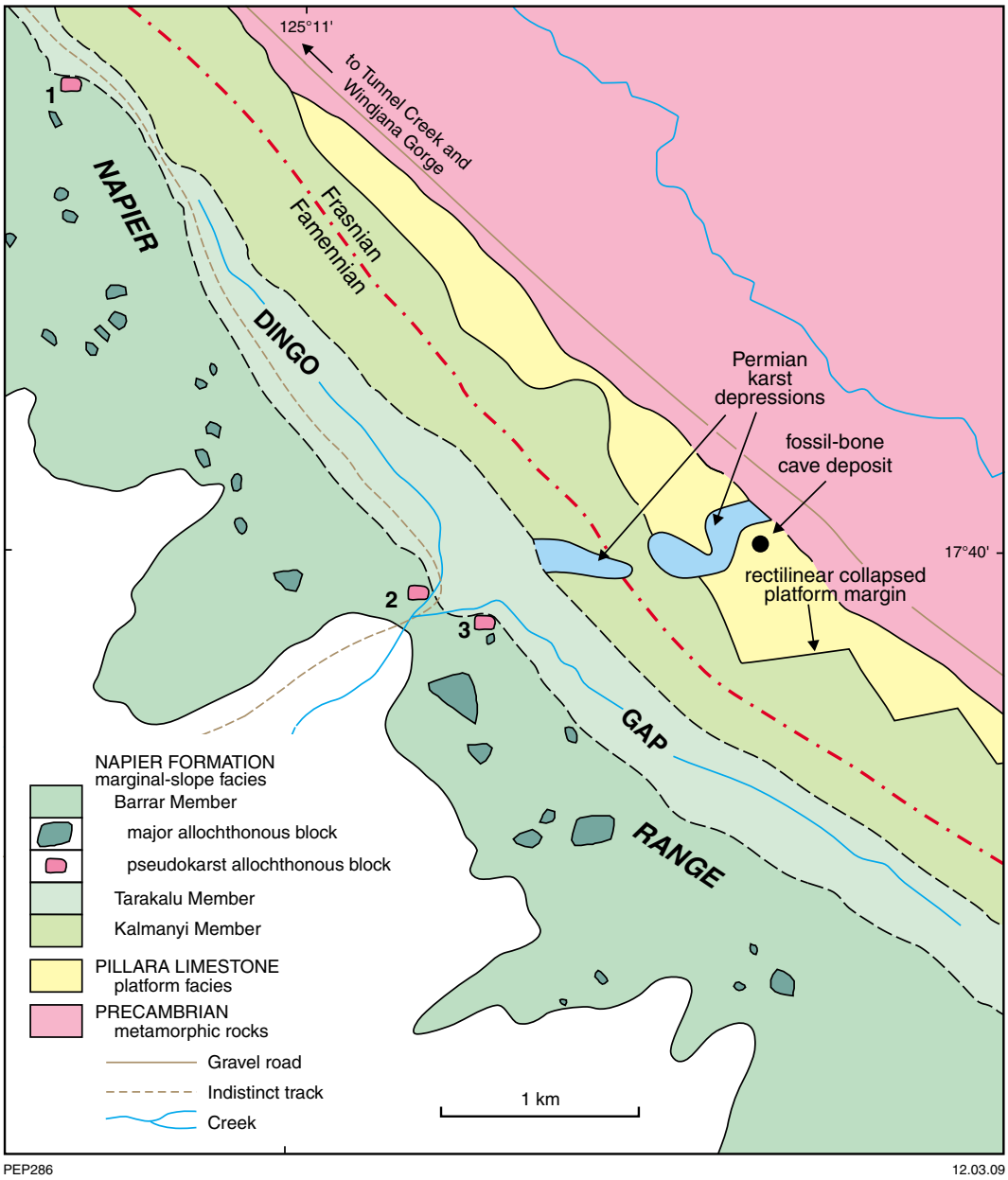

Figure 326. Geological map of part of Dingo Gap showing the locations of pseudokarst 'sand-tube' allochthonous blocks and the deposit of small fossil masticated bones that is shown in Figure 322.

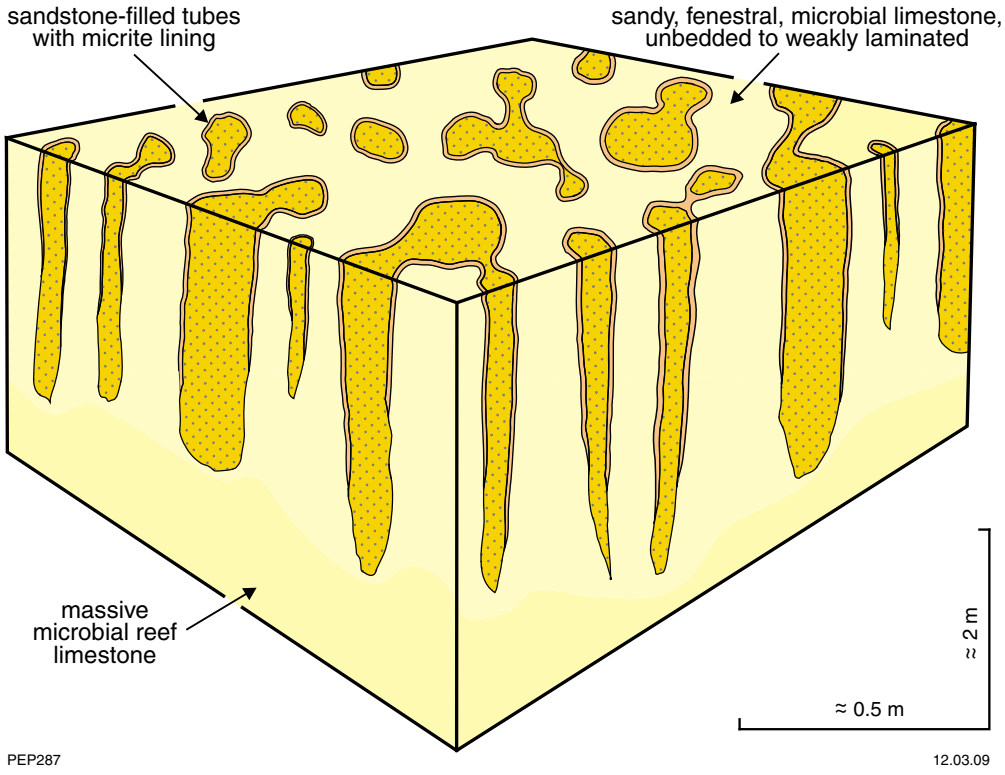

Figure 327. **Block diagram illustrating the origin of pseudokarst sand tubes in allochthonous blocks at the base of the Barrar Member of the Napier Formation in Dingo Gap.**

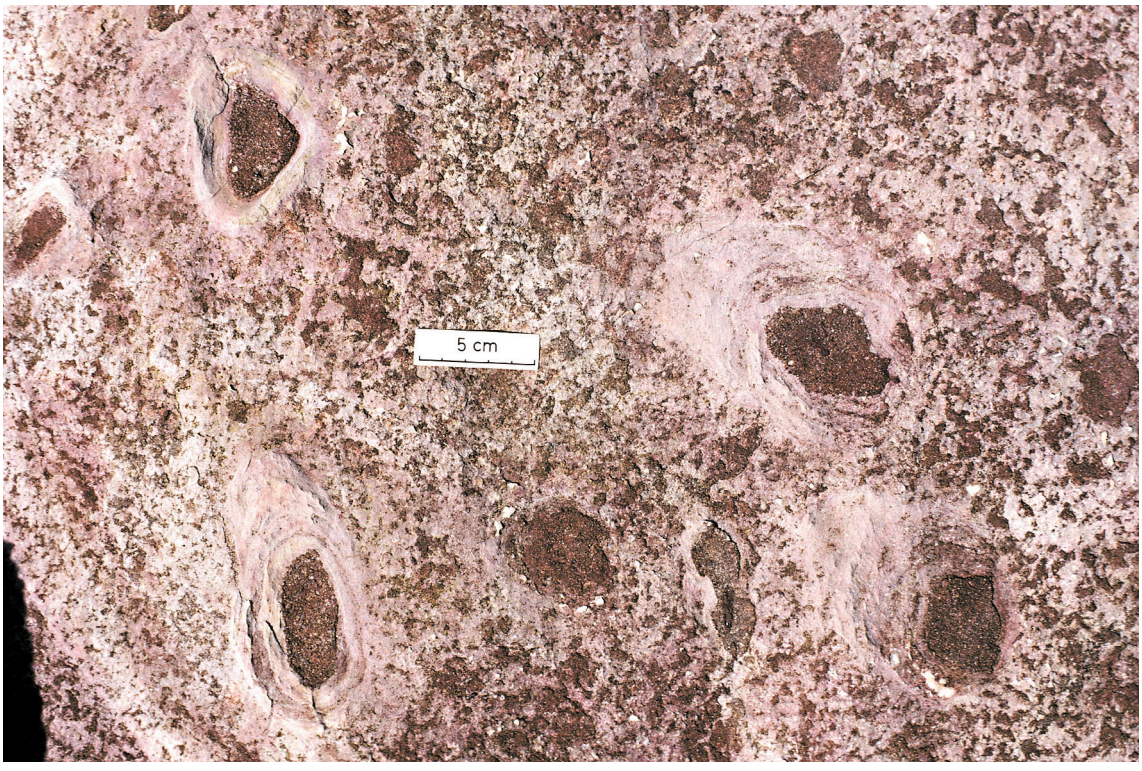

Figure 328. **Plan view of part of a pseudokarst block (in group no. 3, Fig. 326) in Dingo Gap, showing layers of *Renalcis* micrite that lined the tubes before they were filled with calcareous sandstone.**



Figure 329. **(left) One of the allochthonous blocks from group no. 3 (see Fig. 326) in Dingo Gap. The block is upside down. Note the curvature of dark-coloured sand tubes in the upper part of the block.**

Figure 330. **(below) Part of a pseudokarst block from group no. 3 (see Fig. 326) in Dingo Gap, showing columns of red microbial limestone separating tubes of dark-coloured calcareous sandstone.**

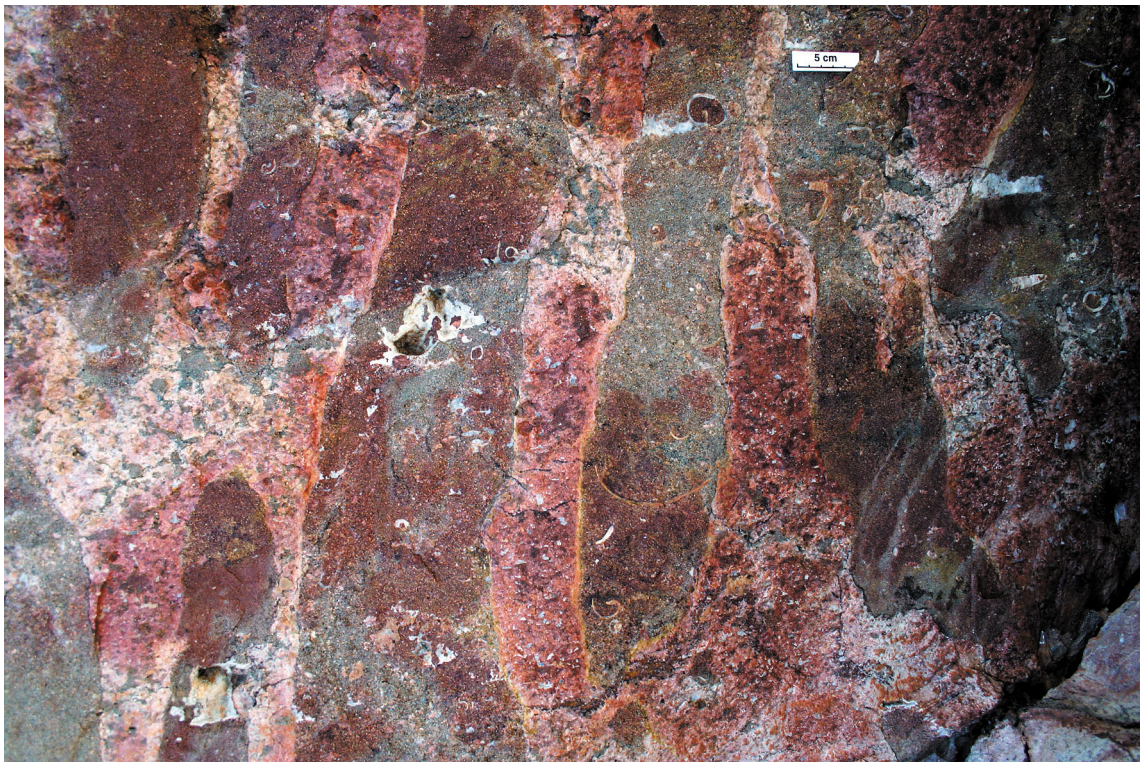



Figure 331. Closer view of one of the stromatolite columns shown in Figure 330. Note the thrombolitic texture and fenestral cavities with geopetal infillings in the column and fragments of molluscs in the dark-coloured sand tubes. Width of field of view 100 mm.

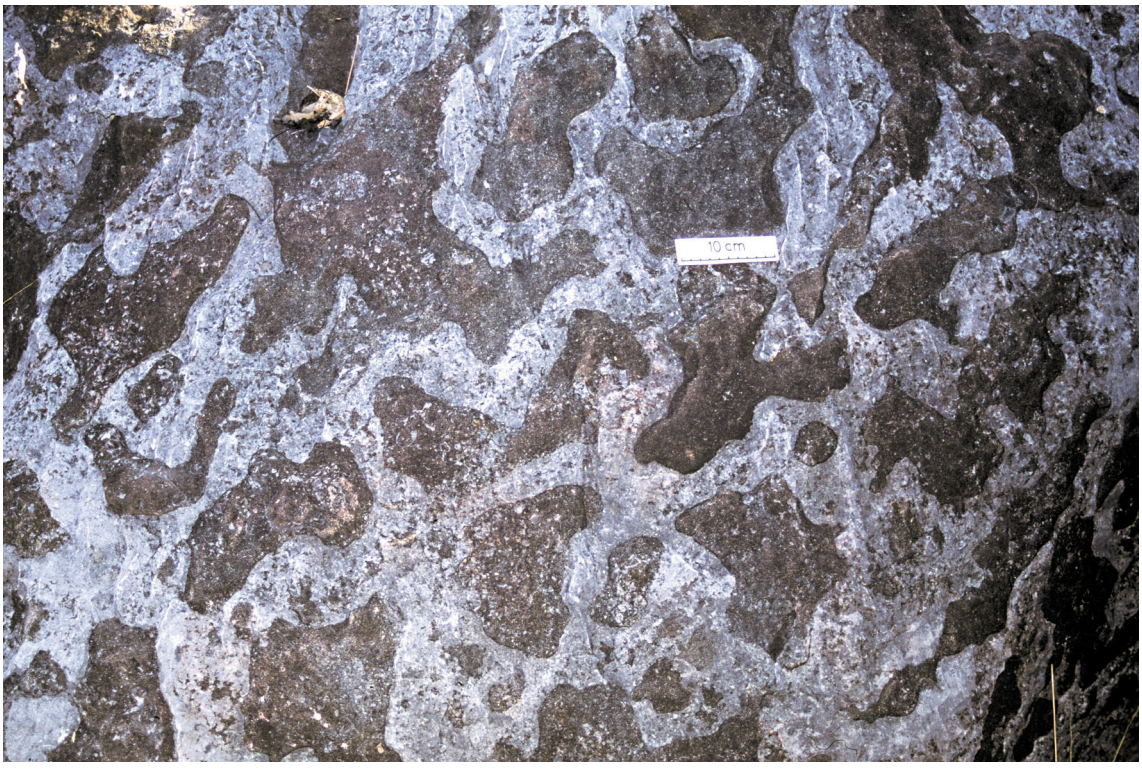

Figure 332. Plan view of one of the pseudokarst blocks from group no. 3 (see Fig. 326) in Dingo Gap, showing lobate dark-coloured sand tubes between a framework of microbial limestone.



Figure 333. Columnar stromatolite in a pseudokarst block from group no. 2 (see Fig. 326) in Dingo Gap. It is a club-shaped stromatolite of microbial limestone intergrown with calcareous sandstone.

Contrary to that interpretation, Kerans (1985) presented evidence that the tubes formed as growth structures, by the coalescence of microbial columns, and that they were probably kept open by wave surge. That interpretation was supported by Tornatora (1992). However, Whittam et al. (1994) and George and Powell (1997) agreed with Playford's earlier karst interpretation, and interpreted the tubes as karst features below a Famennian sequence boundary.

More detailed studies (Playford, 2002a; Stephens and Sumner, 2002, 2003a) have since supported the interpretations of Kerans (1985) and Tornatora (1992). These studies have been conducted principally on allochthonous blocks of reef limestone in Dingo Gap (nos 1–3 in Fig. 326). Blocks 1 and 2 are large isolated blocks, whereas block 3 has two large and several smaller blocks lying closely together. Similar allochthonous blocks have been examined at other localities over wide areas in the Devonian reef belt. The same types of tubular structures also occur in situ in Famennian reef-margin subfacies (Windjana Limestone) at the west end of the Oscar Range (GPS AMG Zone 51, 704980E 8045860N) and in Famennian reef-flat subfacies (Nullara Limestone) in the Napier Range near Waggon Pass (GPS AMG Zone 51, 672140E 8097735N). The tubular features, which commonly branch downward, were formed between coalesced columns of fenestral microbial limestone, and were probably kept open by wave or tidal surge. The regularity of the tubes, the lack of solution features, and the fact that they are commonly curved and subparallel are not in accord with a karst interpretation.

George and Powell (1997) stated that field examination of the blocks did not reveal evidence for columnar or other growth forms. That is not so; stromatolitic columns are clearly evident beside many of the sand tubes (e.g. Figs 330, 331, 333). As pointed out by Kerans (1985), the margins of some stromatolitic columns show evidence of erosion before 'rinds' of microbial micrite grew over them. This is to be expected if there was strong water movement, driven by wave surge, between the columns while they were growing.

The stromatolitic columns are massive (thrombolitic) or have weak convex-up lamination (Figs 330, 331, 333). They are thought to have lithified while the fenestrae and tubes remained open, so that the reef formed a porous and highly permeable mass, through which seawater, driven by wave or tidal surge, could pass freely. Growth of the reef ceased temporarily after it was overwhelmed by terrigenous sand, which filled the open tubes.

Key localities

The geology of key localities, where particular features of the reef complexes are well exposed and which have not been fully described in other parts of this Bulletin, is outlined below.

Many of these localities have been stops for national and international field excursions led by Playford, beginning with the International Geological Congress of 1976 (Playford, 1976a). Since then there have been numerous

excursions, including most recently, the International Paleontological Congress excursion of 2002 (Playford, 2002b) and those organized for Chevron Australia Pty Ltd in 2005, 2006, and 2007. Another excursion will be run in 2009 for the 7th International Conference on Geomorphology.

Bugle Gap area

Bugle Gap, at the southern end of the reef belt (Plates 4, 5, 7, 8; Fig. 334), is one of the most important areas for the study of the Devonian reef complexes, as many facies and their relationships to one another can be examined there in a relatively small area.

Paddys Valley

Paddys Valley occupies an inter-reef embayment, opening to the south, between the Laidlaw Range on the east and the Emanuel Range on the west (Plate 5; Figs 334, 335).

East side of the Emanuel Range

The bedded marginal-slope deposits of the Sadler Limestone at this locality in Paddys Valley (GPS AMG Zone 51, 815345E 7933715N) dip east at 33°, and consist of calcarenite (wackestone and packstone) containing abundant atrypid brachiopods with well-developed geopetal fillings (Figs 136, 137). The average of 204 measurements taken on these fillings indicates that the observed dip is almost entirely depositional, having been increased by only about 1.3º since deposition (Fig. 138).

The adjoining reef-flat subfacies (Pillara Limestone) is nearly horizontal. It contains abundant heads of the coral *Argutastrea* and the stromatoporoid *Actinostroma*, many of which are in growth positions, while others are overturned. Some beds in the reef-flat deposits contain many tabular and laminar stromatoporoids in their growth positions, together with abundant atrypid brachiopods.

A well-exposed patch reef or bioherm, situated some 300 m south-southeast of this locality (GPS AMG Zone 51, 815545E 7933310N), is elliptical in plan and about 140 m long by 80 m wide (Fig. 336).

The reef was built mainly by microbes and sheets of tabular stromatoporoids (*Actinostroma*), individual sheets being as much as 1 m long and 15 cm thick (Fig. 337). Some conspicuous zebra limestones (microbial-mat deposits) also occur. The spar-filled bands in the zebra limestones are thought to have filled cavities left by the decomposition of sheets of organic material that originally filled them. On the flanks of the patch reef there are a few heads of the dendroid coral *Disphyllum*, as much as 1 m across, that must have grown in water at least 20 m deep (Fig. 338).

The tabular stromatoporoids show quaquaversal depositional dips, reaching as high as 25°, around the core of the patch reef. It is estimated that the crest of this reef probably grew in relatively deep water (probably at least 10 m), while depths on the flanks must have been as much as several tens of metres. The patch reef is surrounded by fore-reef strata of the Sadler Limestone, dipping away from it at angles from 8° to 20°.

A small allochthonous block of reef limestone, about 10 m across, is situated about 200 m south-southeast of the patch reef, in fore-reef strata of the Sadler Limestone (GPS AMG Zone 51, 815730E 7933190N; Fig. 336). It consists of stromatoporoid limestone with abundant brachiopods. Geopetal fillings in the brachiopods show that the block in its present position dips nearly vertically, strikes in the direction 040°, and has its original top to the southeast.

The Sadler Limestone in this area contains a rich fauna of silicified brachiopods (especially *Atrypa*) and fragmentary stromatoporoids (Fig. 65). Masses of silicified *Amphipora*, derived from the adjoining platform, occur at one place in the fore-reef limestone.

Wade Knoll

Wade Knoll is the top of a pinnacle reef that was apparently drowned as a result of rapid subsidence and was overwhelmed by basinal deposits of the Gogo Formation (Figs 116, 339–342; GPS AMG Zone 52, 183445E 7934300N). The knoll was named (by Playford) after Arthur Wade of the Freney Kimberley Oil Company, the first geologist to recognize the reefal origin of the Devonian limestone ranges. The pinnacle reef (Pillara Limestone) consists of massive stromatoporoid and microbial limestone constructed largely by stromatoporoids, with clastic and microbial limestone filling interstices between the stromatoporoid colonies. Unlike the patch reef previously described in the eastern Emanuel Range, this reef must have grown in shallow water (probably less than about 5 m deep).

The reef core is rimmed by marginal-slope facies (Sadler Limestone), which in turn is surrounded by basin facies (Gogo Formation). Zoning in the marginal-slope facies outwards from the reef shows a band 1 to 2 m wide of reefal-slope subfacies, consisting of brachiopod-rich limestone with an outer horizon of branching columnar *Sphaerocodium* stromatolites 0.1 to 0.7 m wide (Fig. 340), followed by fore-reef subfacies consisting of detrital stromatoporoid breccia, as much as 2 m wide. The pinnacle reef has an elongate ‘tail’ to the south (Figs 116, 339), but is otherwise subcircular in outline. Fore-reef deposits are absent on the south side, probably indicating that the prevailing wind and wave directions were from the north.

Exposures of the Gogo Formation adjoining the marginal-slope deposits consist of thin beds of limestone alternating with unexposed units, thought to be beds of siltstone and/or shale (Figs 116, 339, 341, 342).

The Gogo Formation was apparently laid down over and around the pinnacle reef after extinction of the pinnacle at the close of Pillara Sequence 1, following abrupt drowning associated with the Elliott Ridge Event. Contortion in thin limestones in the Gogo Formation adjoining Wade Knoll is probably a result of early differential compaction over the drowned pinnacle reef of basin muds interbedded with the limestones. The limestones consist of breccia,

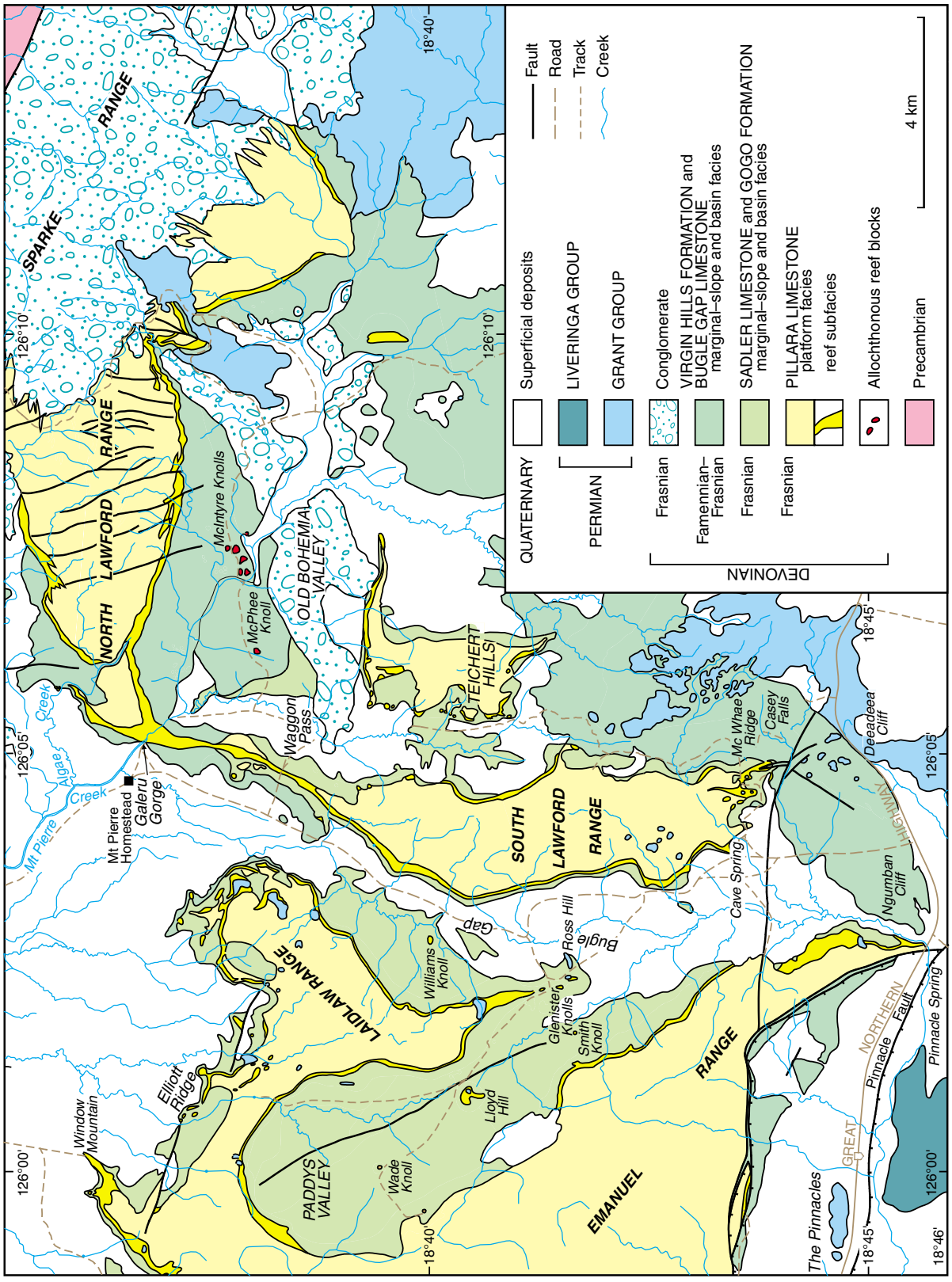

Figure 334. Geological map of the Bugle Gap area.

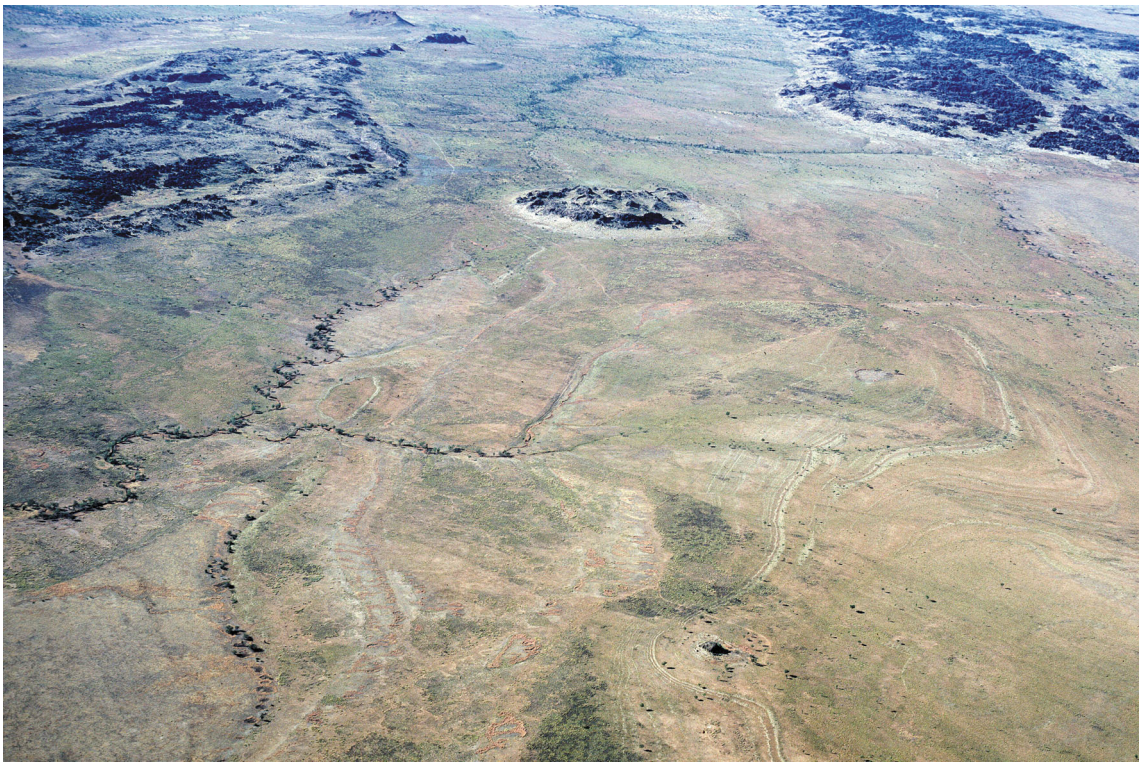

Figure 335. Aerial view looking south over Paddys Valley towards Lloyd Hill atoll (centre background). The Laidlaw Range reefal platform is to the left of Lloyd Hill, and the Emanuel Range platform is to its right. Note the small black outcrop in the centre foreground which is Wade Knoll pinnacle reef. Thin beds of limestone in the Gogo Formation (basin facies) form the wavy lines on the photo.

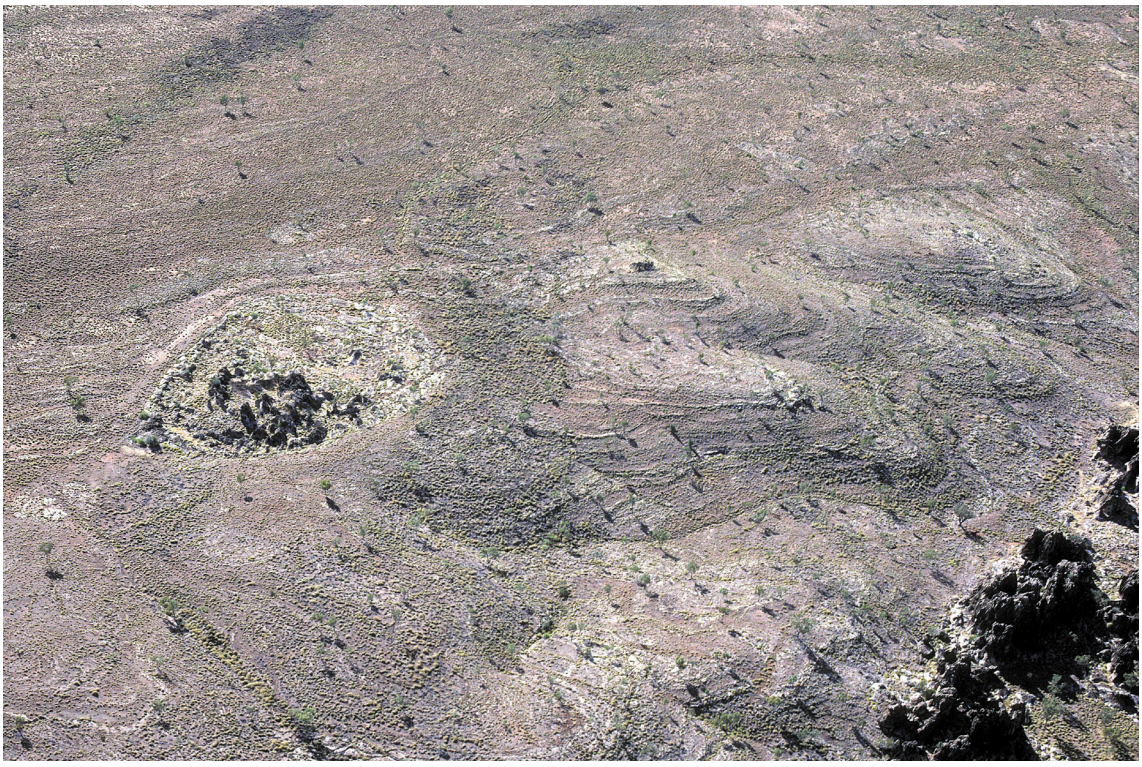

Figure 336. Aerial view looking east over part of the western flank of Paddys Valley, showing a small patch reef in the centre left of the photo, surrounded by well-bedded fore-reef deposits of the Sadler Limestone. A small allochthonous block can be seen in the centre right. Massive reef limestones of the Pillara Limestone are in the lower right.



Figure 337. North flank of the small patch reef on the west side of Paddys Valley shown in Figure 336, showing sloping sheets of stromatoporoids in microbial limestone. The slopes are almost entirely depositional.



Figure 338. Colony of the dendroid coral *Disphyllum* in fore-reef strata on the northwest flank of the small patch reef shown in Figure 336.



Figure 339. Aerial view of Wade Knoll pinnacle reef (built by stromatoporoids and microbes), looking south, showing concentric marginal-slope deposits and cyclic basin strata around the reef. Note also the 'tail' of the reef, directed towards the south.



Figure 340. *Sphaerocodium* stromatolites in marginal-slope strata of Wade Knoll pinnacle reef.

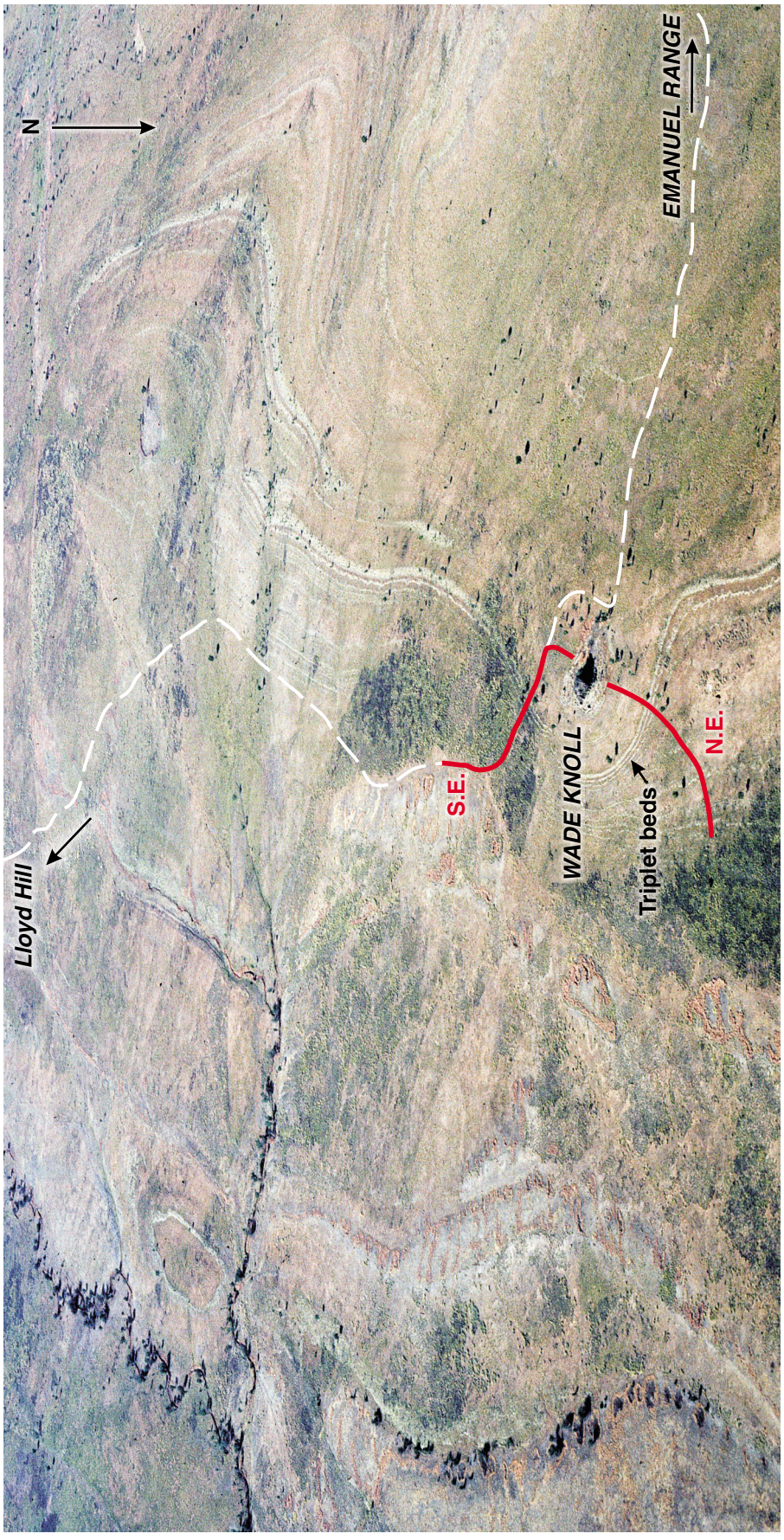

Figure 341. Aerial photograph of Wade Knoll, looking south, showing the locations of the two sections represented in Figure 342.

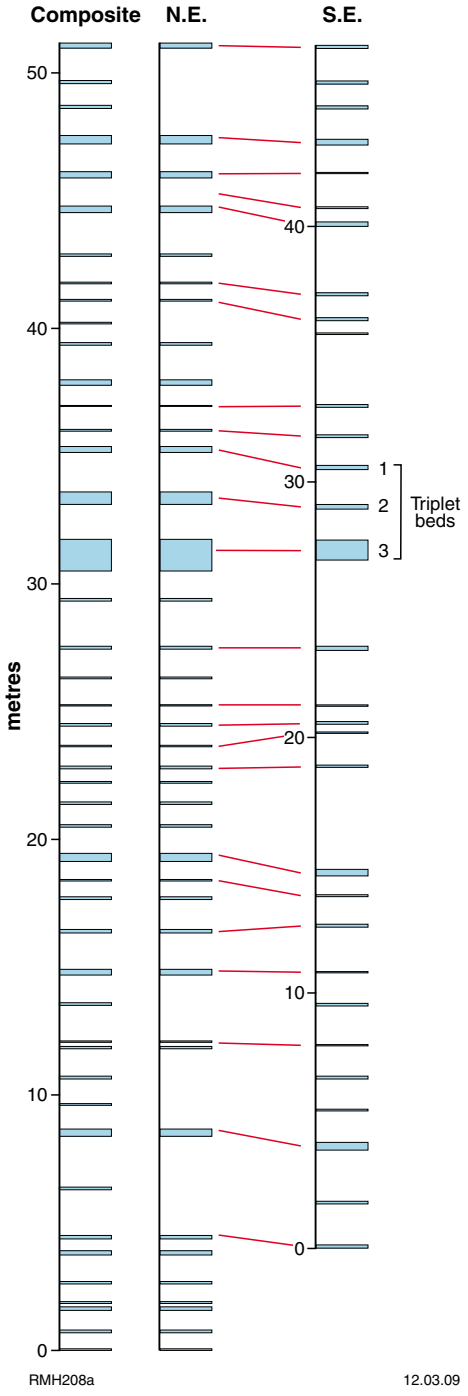

Figure 342. **Sections through cycles in the Gogo Formation adjoining Wade Knoll, northeast and southeast of the knoll, as shown on Figure 341. The covered sections (uncoloured) between the thin limestone beds (coloured blue) are thought to consist of shale and siltstone. Correlations of limestone beds between the two sections are indicated, together with a composite section bringing them together.**

calcarenite, calcisiltite and calcilutite. Reef-derived debris in the breccias was apparently transported by mass-flow mechanisms from the Laidlaw Range and/or Emanuel Range platforms, primarily as debris flows. Paleocurrent directions deduced from the orientation of nautiloids and other fossil fragments are generally towards the east-southeast, with slight deflections around the knoll.

The thin limestone beds form parallel concentric rings, at relatively regular intervals around the central core of Wade Knoll and its marginal-slope deposits. Pebble- and granule-size breccias in those beds generally form discontinuous lenses as much as 20 cm thick. Most beds in the limestones consist of calcisiltite, in places graded, and commonly massive. Some beds have brown upper crusts that may be phosphatic, suggestive of prolonged hiatuses. There is no exposure in the intervals between limestone beds, but those intervals are thought to be occupied by shales or siltstones. This cyclical alternation of limestones and shales (or siltstones) probably correlates with cycles in the back-reef facies of the Pillara Limestone. Cycles in the Gogo Formation are much thinner (approximate average thickness 0.9 m) than those in equivalent parts of the Pillara Limestone (approximate average thickness 3.5 to 4 m). This difference is no doubt primarily because of the much greater compaction that has occurred in shales and siltstones of the Gogo Formation compared with limestones in the Pillara Limestone.

Two sections were measured out from the knoll, on its northeast and southeast sides, and were correlated using a distinctive triplet of debris-flow beds present in both sections (Figs 341, 342). Comparing the two sections, and closely examining aerial photos, many thin limestone beds are seen to be discontinuous. Walking out the beds indicates that some persist for only a few hundred metres, except for thicker beds, like the triplet of debris flows shown on Figures 341 and 342, that are known to continue for more than 500 m. Each section has a number of missing correlations, but placed together they are seen to record fairly regular cycles (Fig. 342). The thin limestone beds in the Gogo Formation may correspond to the upper parts of cycles in equivalent platform deposits.

A stratigraphic bore (Noonkanbah no. 5) was drilled 245 m north of Wade Knoll to a depth of 160 m by the Bureau of Mineral Resources in 1972. It penetrated Gogo Formation throughout.

Lloyd Hill

The Lloyd Hill pinnacle reef and platform atoll (Figs 343–351; GPS AMG Zone 52, 185155E 9732560N) is thought to have developed on a broad limestone platform that elsewhere was drowned by rapid subsidence associated with the Elliott Ridge Event, leading to development of the Paddys Valley Embayment. The atoll is thought to have had a conical shape, culminating as a pinnacle reef comparable with Wade Knoll. Eventually it was presumably drowned and completely covered by Gogo Formation.

The platform facies (Pillara Limestone) in Lloyd Hill consists of massive reef-margin and bedded reef-flat limestones. The reef margin is composed of microbial and stromatoporoid limestones, with abundant *Renalcis* and tabular stromatoporoids in some parts. It is notably elongate to the south (Figs 315, 345), comparable with the southerly elongation of Wade Knoll and Smith Knoll, and the 'tail' of the Laidlaw Range (Fig. 343). In the lower part of the exposure at Lloyd Hill the reef rim surrounds crudely bedded reef-flat deposits that consist of stromatoporoid, coral (*Disphyllum*), oncolite, and microbial-mat (zebra) limestones (Figs 348, 349). In the upper part of the exposure the massive reef extends right across the bedded reef-flat deposits, so that it eventually formed a pinnacle reef comparable with Wade Knoll (Fig. 347).

The fore-reef and reefal-slope subfacies (Sadler Limestone) show quaquaversal dips around the atoll. The dips have been steepened by about 10° on the northeast side because of post-depositional tilting in that direction. Geopetal brachiopod fillings show that after removing that amount of tectonic tilt the marginal-slope depositional dips ranged from about 18° to 40°. The fore-reef beds are irregularly well bedded, whereas the reefal-slope limestones, some of which contain abundant brachiopods, are crudely bedded to massive. The basin facies (Gogo Formation) is very rarely exposed in front of the marginal-slope facies.

A solution pipe (small solution doline) in the eastern part of Lloyd Hill occupies a flat-floored depression that contains poor outcrops of weakly lithified sandstone of the Grant Group (GPS AMG Zone 52, 185115E 7932490N; Figs 315, 350, 351). A much smaller pipe (less than 10 m across), containing similar sandstone, occurs in reef limestone in the central part of the atoll. The two pipes are thought to have formed by solution in subglacial meltwater below the final Early Permian ice sheet.

Glenister Knolls

Glenister Knolls form a line of three patch reefs extending from the tail of the Laidlaw Range platform atoll (Figs 343, 344, 350, 351). The knolls were named (by Playford) after Brian Glenister, formerly of The University of Western Australia and the University of Iowa. One of the patch reefs has recently been described in detail by Hasler et al. (in press).

Like Wade Knoll, Smith Knoll, and Lloyd Hill, these patch reefs are thought to mark the end phase of Pillara Sequence 1, and their drowning resulted from the Elliott Ridge Event (Fig. 21). The patch reefs were constructed mainly by massive and tabular stromatoporoids. Very steeply dipping reefal-slope limestones and dolomites were encrusted on the steep slopes that form the margins of the reefs. The reefal-slope carbonates contain abundant *Sphaerocodium*, especially on their southern, leeward margins (Fig. 352), together with crinoids, brachiopods, receptaculitids (and/or sponges), and brachiopods (mainly atrypids).

Steeply dipping grey shale and siltstone with concretions (Gogo Formation) are poorly exposed in some places adjoining the patch reefs. A band of coarse breccia occurs

within the Gogo Formation adjoining Glenister Knolls. It is thought to represent one or more debris-flow deposits, originally deposited subhorizontally in basin muds laid down over the drowned patch reefs. It owes its present position and steep dips to the very large compaction that occurred when the porous muds were compacted into shales and siltstones. Playford and Wallace (2001) have shown that such compaction can amount to as much as 75% (Fig. 69). Narrow solution pipes (or dolines) filled with Grant Group penetrate two of the patch reefs and adjoining marginal-slope limestones. The pipes formed by solution in subglacial meltwater below the last of the Early Permian ice sheets (Playford, 2002a). One of the solution pipes is situated at the crest of the largest patch reef (GPS AMG Zone 52, 187285E 7930520N), and is noticeable for the smoothness of the wall where siltstone and sandstone of the Grant Group has only recently been eroded away (Figs 316, 317).

A mound of microbial limestone beside the track 1 km northwest of the tail of the Laidlaw Range has been mapped as an allochthonous block (Fig. 353; Plate 5). However, there is no definitive evidence to show that it is allochthonous, and it is now regarded as an in-place microbial bioherm.

McIntyre Knolls

McIntyre Knolls form a group of huge allochthonous reef blocks, situated in the Old Bohemia Valley (Figs 354–356; Plate 5; AMG Zone 52, 196000E 7937500N). They are named after James McIntyre, a former geologist of WAPET, who recommended in 1955 that the company should undertake research on the Devonian reef complexes. That recommendation led to the study of the Oscar Range by Smith et al. (1957).

The allochthonous blocks forming McIntyre Knolls are of reef-margin and reef-flat subfacies of the Pillara Limestone, and are each as much as 200 m across. They occur within submarine debris-flow deposits in the Frasnian part of the Virgin Hills Formation (fore-reef subfacies). Geopetal fabrics indicate that the blocks are lying haphazardly on their sides, mostly right-way up, but some are upside down (Plate 5). The debris flows must have originated through the mass collapse of a large part of the reef margin of the North Lawford Range platform, 2 km to the northeast.

The blocks are composed predominantly of *Renalcis* and stromatoporoid reef limestone, and many have the red colouration that characterizes middle Frasnian reef complexes in the Canning Basin.

McWhae Ridge

McWhae Ridge is a key locality for the understanding of the reef complexes. It is a faulted reef spine, flanked by marginal-slope and basin deposits, at the southern end of the Lawford Range reef complex (Figs 101, 102, 141–148, 157, 228, 229, 291, 357–363). The ridge was named (by Playford) after J R H (Ross) McWhae, formerly Staff Stratigrapher of WAPET.

The marginal-slope deposits at McWhae Ridge, represented by the Frasnian Sadler Limestone and the Frasnian to Famennian Virgin Hills Formation, were laid down with steep depositional dips over a drowned Frasnian reef spine (Pillara Limestone). The reef was built by microbes and stromatoporoids, especially *Stachyodes* and *Actinostroma*. Among the reef-building microbes, *Renalcis* and *Sphaerocodium* are readily recognizable, but most of the others are non-skeletal forms. The Gogo Formation (basin facies) abuts, and is thought to interfinger with, the Sadler Limestone. It also occurs, very poorly exposed, in a graben on top of the reef spine (Fig. 228).

The geology of the area around McWhae Ridge and some phases in its development are illustrated on Figure 229. The reef spine was abruptly drowned during the early Frasnian, probably associated with the Elliott Ridge Event. *Girvanella* oncolites developed on top of the drowned reef, rotating during growth as a result of wave and current action. Some oncolites were fixed on the crest by *Sphaerocodium* growths, but most were swept off, perhaps during major storms or tsunamis. They came to rest in beds on steep marginal slopes on each side of the reef spine, forming part of the Sadler Limestone (Figs 142, 143). The oncolites, ranging from about 0.5 to 3 cm in diameter, are of the same size in individual beds. Each bed probably represents a ‘generation’ of oncolites that reached a particular size before being swept off the reef. Many more oncolites were deposited on the west than on the east side of the spine, suggesting that major waves or storm surges came most often from the east.

Oncolite growth ceased during the early Frasnian (probably Zone 3), and with continued subsidence and faulting along the crest of the reef spine, shale of the basin facies (Gogo Formation) was deposited over the Sadler Limestone and in the graben on the crest of the ridge (Fig. 358). A stromatolite bioherm is interpreted to have grown over the ridge during the latest Frasnian and Early Famennian. Tongues of stromatolitic limestone interfingered with marginal-slope deposits of the Virgin Hills Formation on the flanks of the bioherm. During deposition of the Virgin Hills Formation, less sedimentation occurred on the west than on the east side of the ridge, and consequently maximum lateral growth of the bioherm was towards the east. Most of the bioherm has since been stripped away by erosion, but tongues of stromatolitic limestone that originally formed part of the bioherm now outcrop on the west flank of McWhae Ridge and to the east around Casey Falls.

Faulting continued later in the Famennian and may have persisted to a small extent during the Carboniferous. The present topography of McWhae Ridge is shown superimposed on the hypothetical section through the ridge in Figure 229. Intraformational slump folding, probably indicative of a tectonic event, is present in distal marginal-slope deposits of the Virgin Hills Formation east of McWhae Ridge (Figs 362, 363).

Capped oncolites are well displayed in a small karst corridor (Figs 141–143) on the west side of McWhae Ridge (GPS AMG Zone 52, 191950E 7926120N). This corridor is thought to have formed along a joint in the limestone by subglacial solution below the final Early

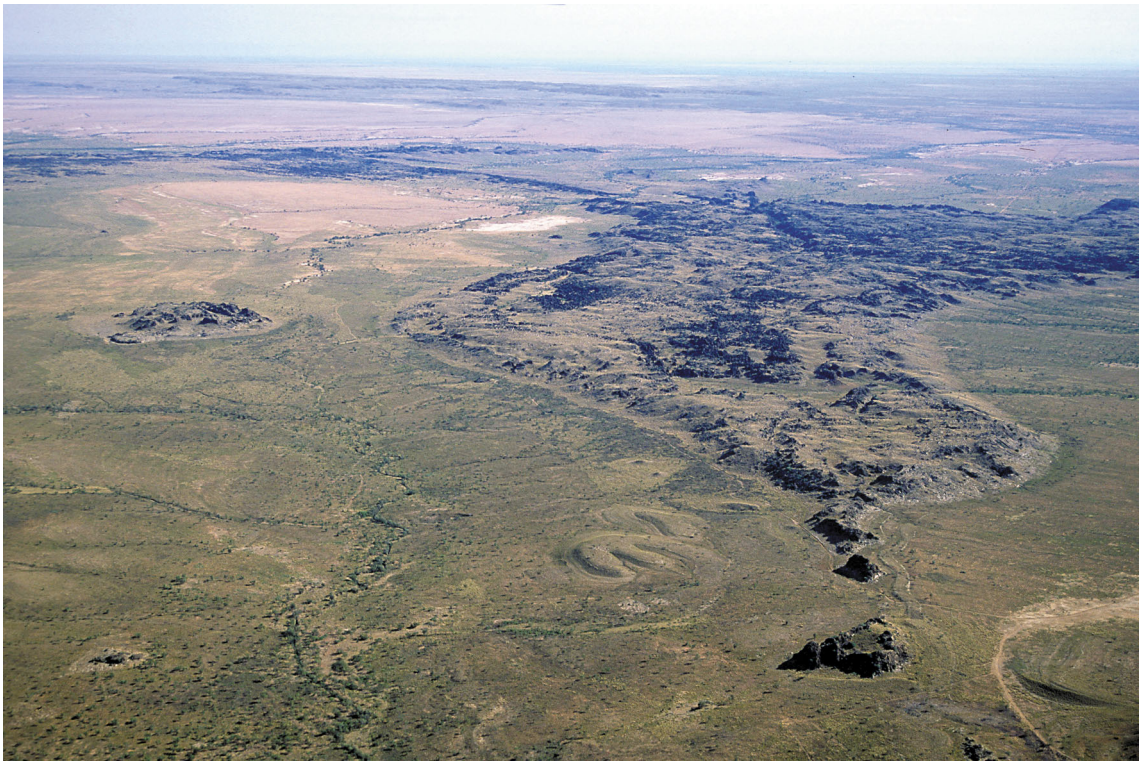

Figure 343. Aerial view looking north over two of the Glenister Knolls patch reefs (right of centre, foreground), the Laidlaw Range platform (right centre), Lloyd Hill atoll (left centre), and Smith Knoll pinnacle reef (left foreground).



Figure 344. Closer aerial view looking north over two of the Glenister Knolls patch reefs (left foreground), the Laidlaw Range platform (centre), and the Lloyd Hill atoll (left centre).



Figure 345. Aerial view of Lloyd Hill atoll, looking northwest. Note the tail of the atoll on the left. See also Figure 315.

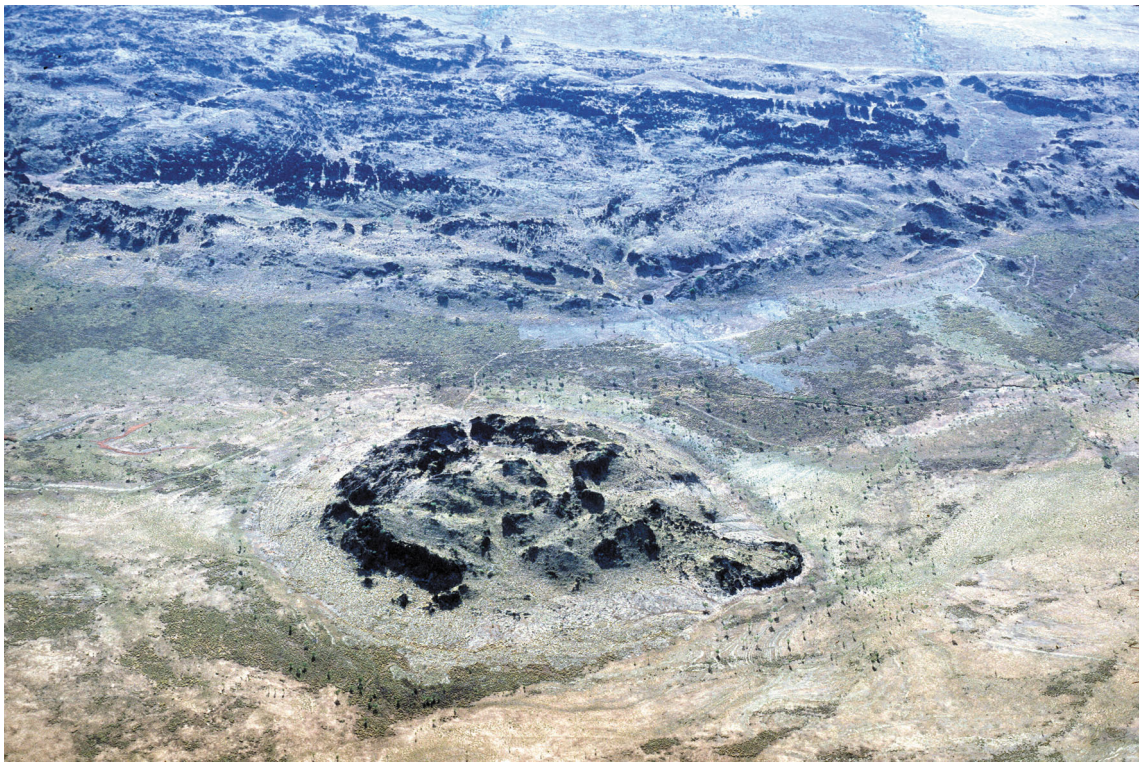

Figure 346. Aerial view of Lloyd Hill atoll, looking east towards the Laidlaw Range platform.

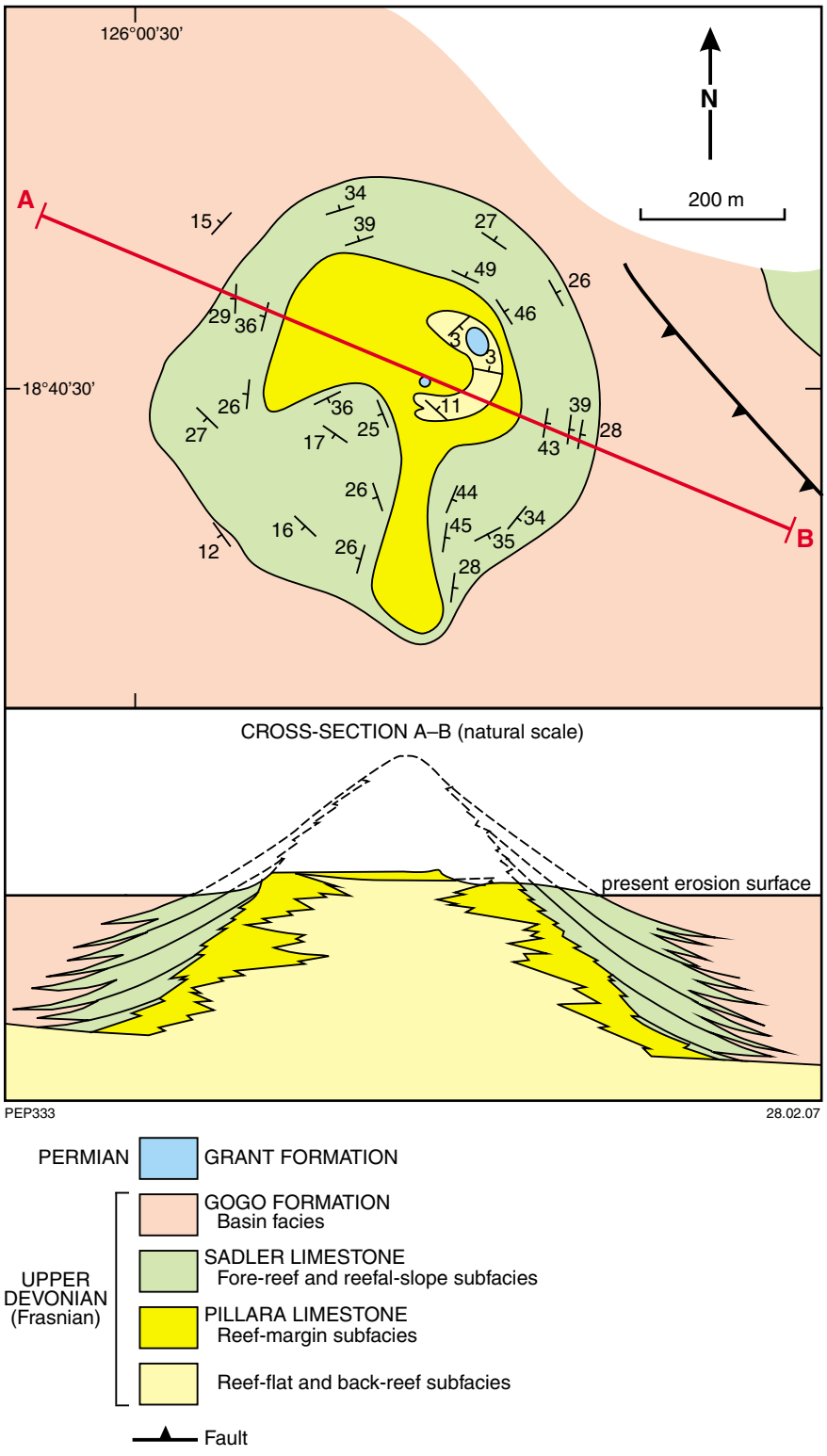

Figure 347. Geological map and cross section of Lloyd Hill atoll.

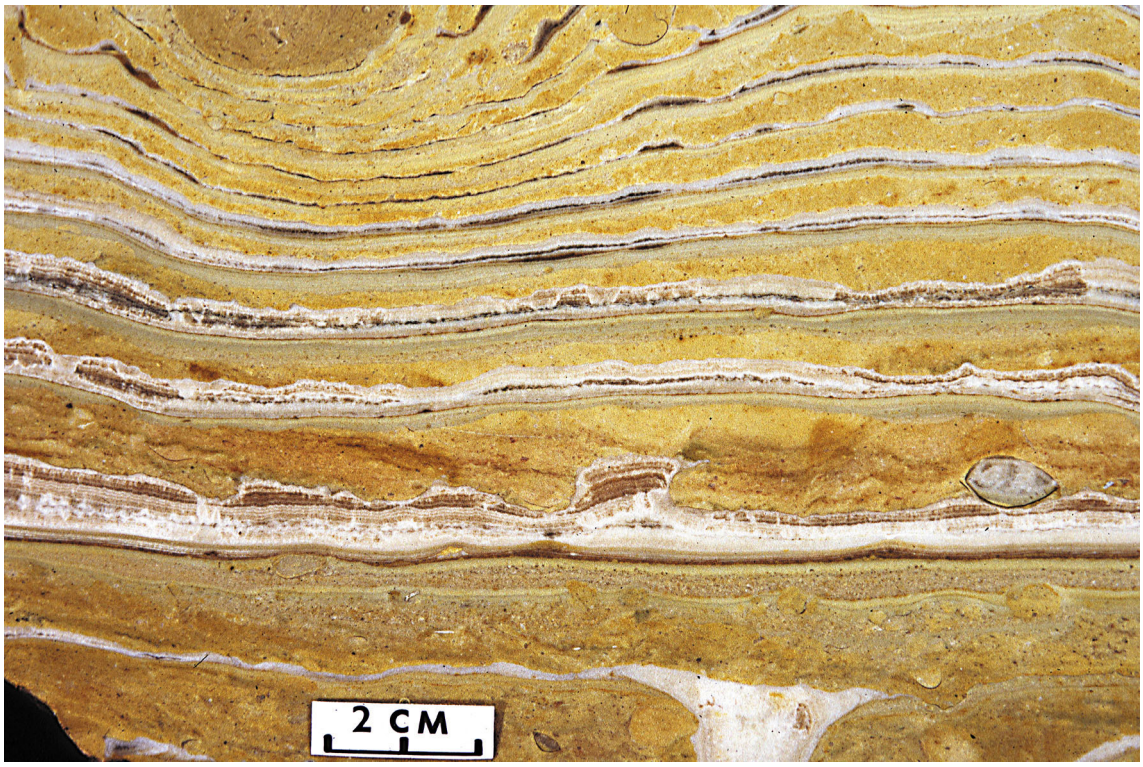

Figure 348. Polished slab of zebra rock from the reef-flat subfacies of the Pillara Limestone at Lloyd Hill, showing an oncolite that sank into unlithified wackestone interlaminated with organic layers that afterwards rotted away. The resulting cavities were then filled by laminated lime mudstone and sparry calcite. GSWA sample no. 19329(A).

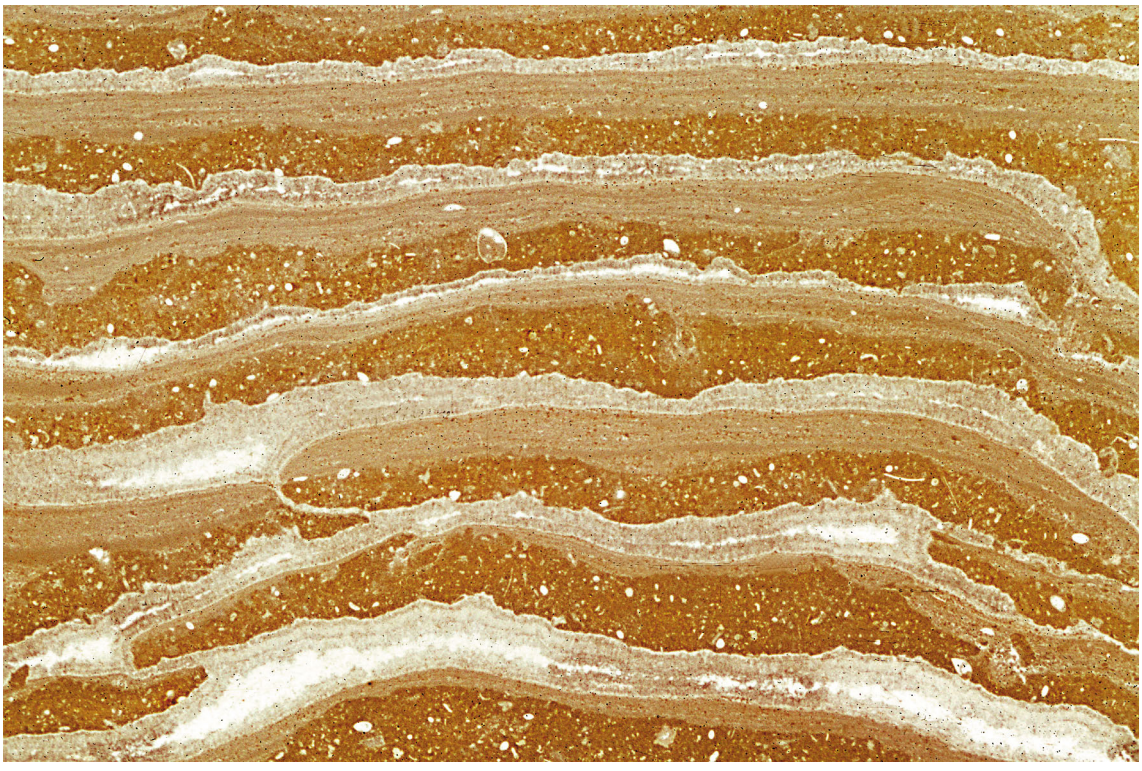

Figure 349. Thin section of zebra rock from the reef-flat subfacies of the Pillara Limestone at Lloyd Hill, showing alternating layers of wackestone and cavity-filling laminated lime mudstone and sparry calcite. GSWA sample no. 21518. Width of field of view 62 mm.

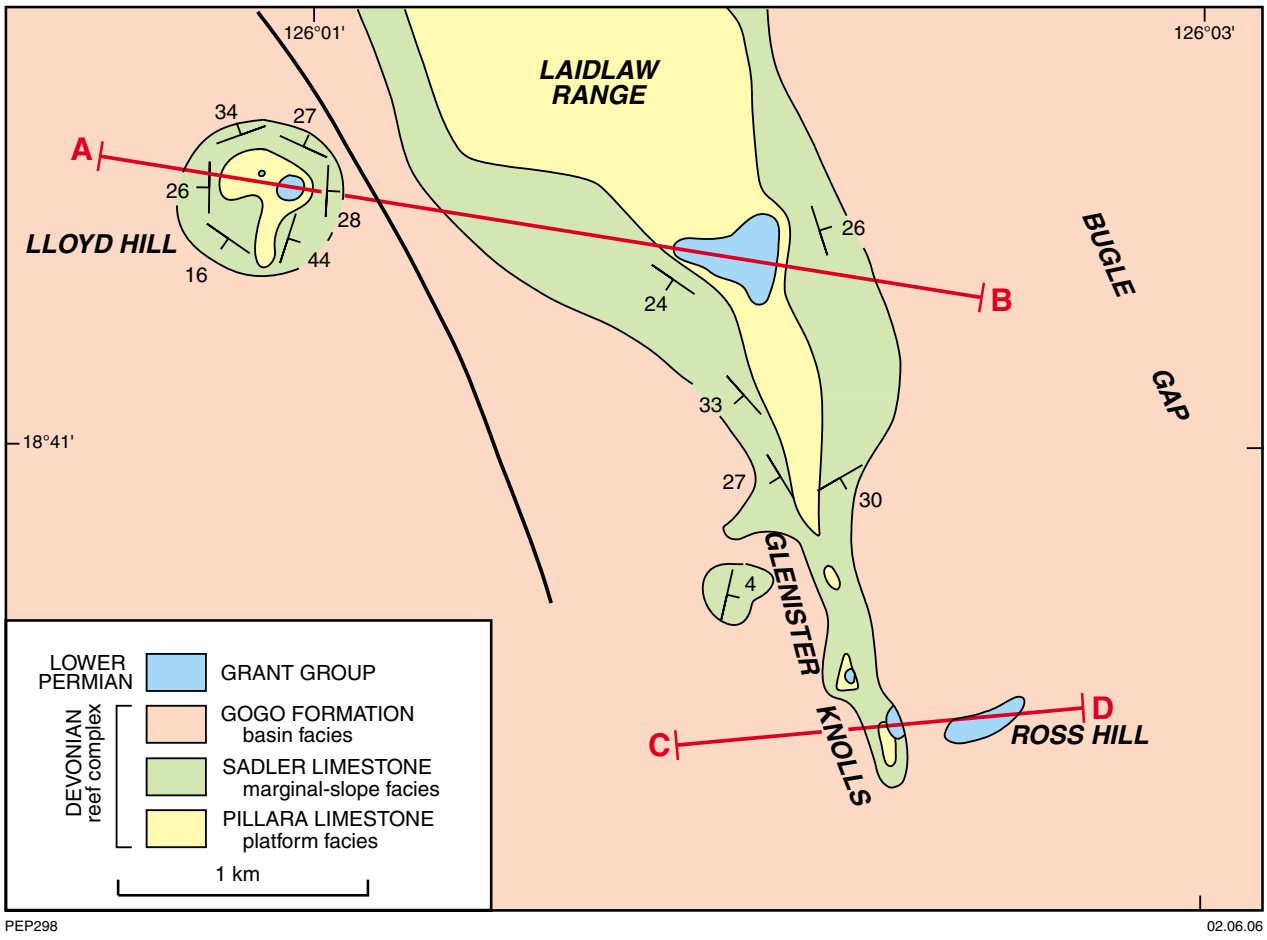

Figure 350. **Geological map of Lloyd Hill atoll, southern Laidlaw Range platform, and Glenister Knolls patch reefs, showing the lines of cross sections in Figure 351.**

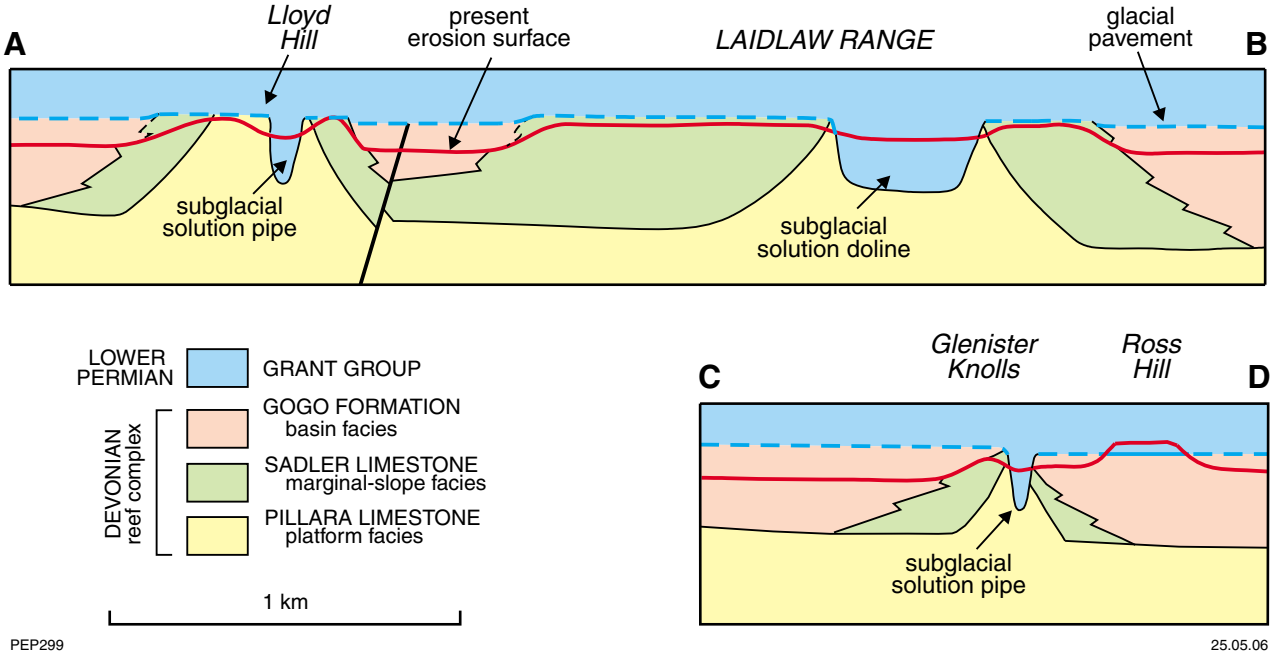

Figure 351. **Cross sections A–B through Lloyd Hill atoll and southern Laidlaw Range platform, and C–D through a Glenister Knolls patch reef and Ross Hill, an outlier of Lower Permian Grant Group. The section lines are plotted on the geological map shown as Figure 350.**



Figure 352. ***Sphaerocodium*** **stromatolites in reefal-slope subfacies from the 'tail' of the Laidlaw Range platform.**

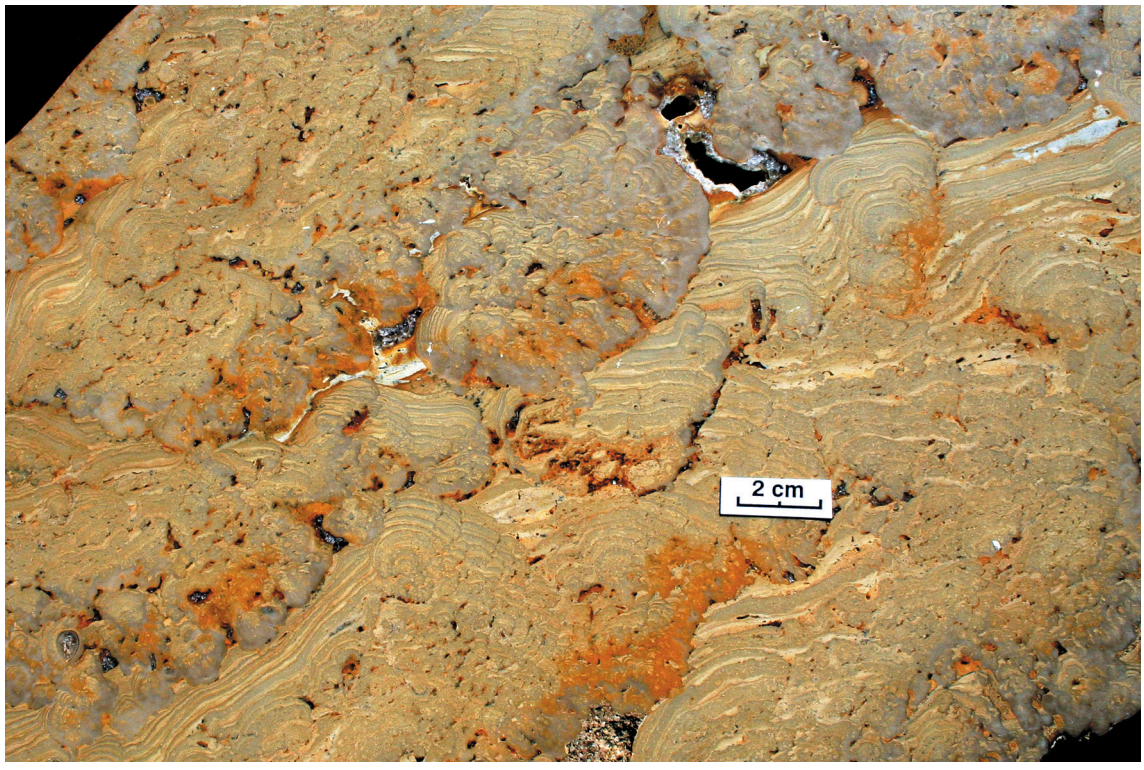

Figure 353. Polished slab of microbial limestone from a microbial bioherm or allochthonous block, 1 km northwest of the 'tail' of the Laidlaw Range.

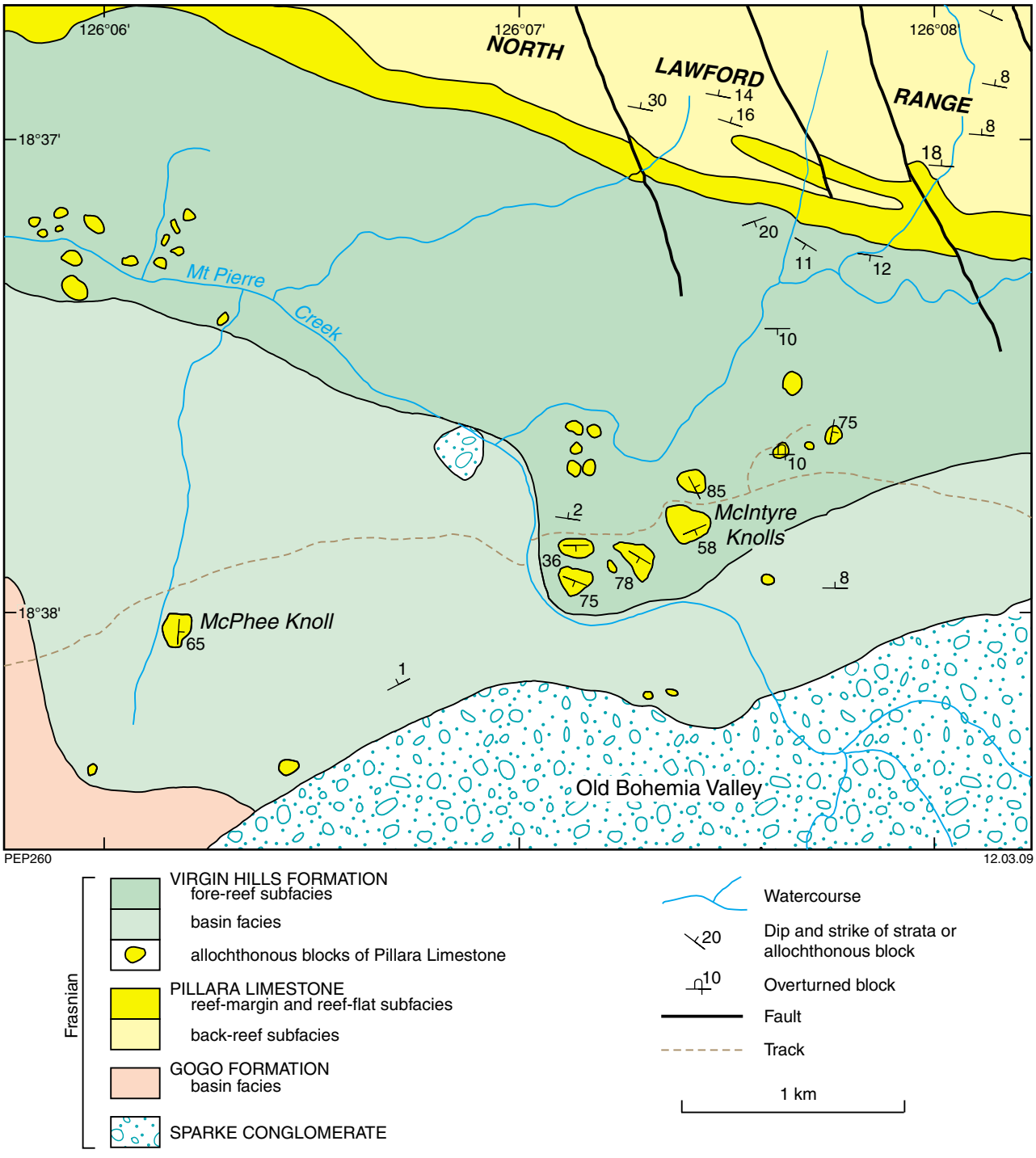

Figure 354. Geological map of the McIntyre Knolls area in the Old Bohemia Valley, showing large allochthonous reef blocks and the orientations of some as determined from geopetal structures.



Figure 355. Aerial view of McIntyre Knolls looking northeast towards the North Lawford Range platform from which the blocks were derived.

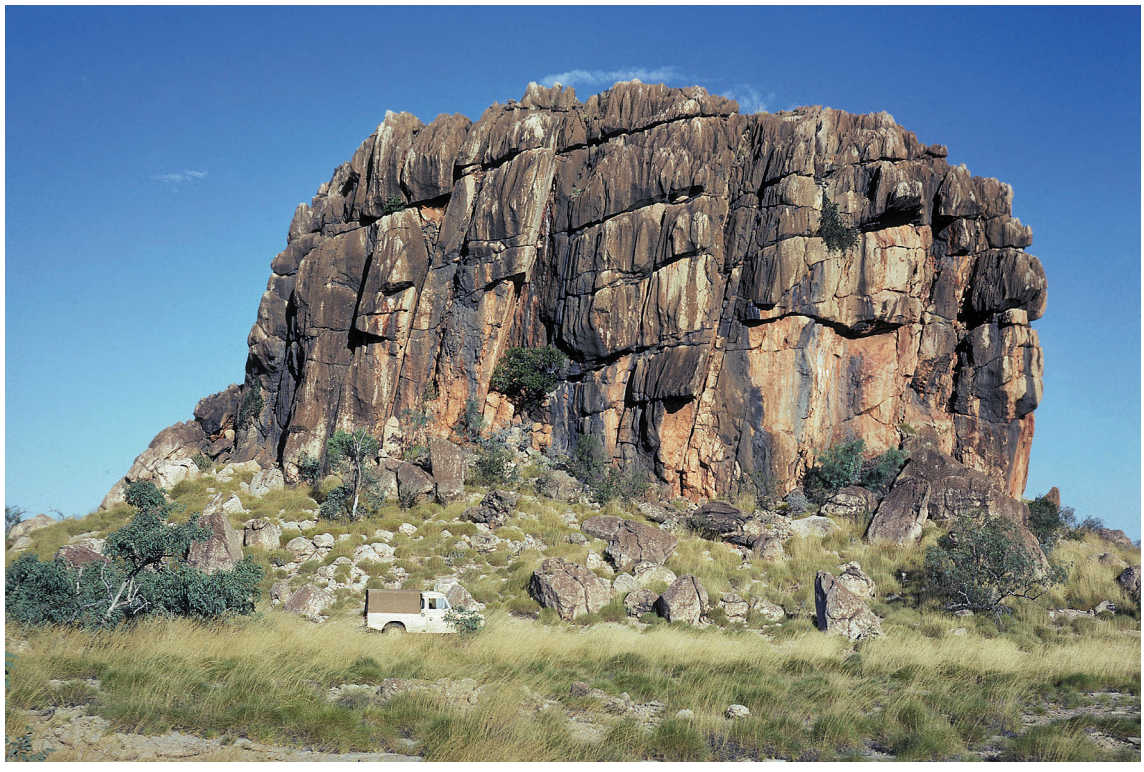

Figure 356. One of the McIntyre Knolls, looking east. This reef block is lying on its side with thick bedding sloping very steeply to the left. Jointing in the limestone dips to the left at a lower angle.

Permian ice cap. A wide range of geopetal structures can be seen on the walls of the corridor. Measurements have been made of the geopetal fillings of 105 brachiopods, 39 receptaculitids, and 8 other fossils. These geopetal measurements indicate that the observed dip of 41° consists of two components, a depositional dip of about 34° and a post-depositional dip of about 7° (due to tectonism and/or compaction; Fig. 142).

The capped oncolites consist of subspherical *Girvanella* oncolites capped by conical growths of *Sphaerocodium*. The caps grew approximately vertically. As shown in Figure 145, the average tilt from the vertical of 95 caps is virtually the same (within about 1.3°) as the tilt from the horizontal of the associated geopetal infillings. The oncolite bed is exposed nearly continuously up the side of McWhae Ridge. Towards the top of the ridge the *Sphaerocodium* caps become considerably larger, and in some cases they fuse to form microbial reefal layers. Elevation data show that the lowest exposed *Sphaerocodium* caps must have grown in water more than 35 m deep, and it seems likely that the actual water depth was much more than this, perhaps as much as 100 m (Fig. 148).

Small neptunian dykes cut some marginal-slope strata of the Sadler Limestone at this locality (Fig. 364). They are filled with crinoidal material from the overlying bed, showing that the strata had lithified rapidly and were then fractured (possibly in response to earthquake shocks). The fractures were filled with loose sediment from the succeeding crinoidal layer.

Numerous conical straight nautiloids occur on a prominent bedding plane above the crinoidal layer, immediately below the top of the Sadler Limestone. The nautiloids are subparallel, with most of their apices oriented up dip (Figs 146, 147). Measurements of 269 nautiloids at this locality show that their mean orientation direction is 260°, compared with the dip direction of 250°. More than 90% of individuals have their apices pointed up dip, which is the most stable position for conical bodies lying on a steep slope.

The equivalent bedding plane occurs on the east side of McWhae Ridge, where it dips in the opposite direction. The nautiloids on this bedding plane are again oriented with their apices pointed up dip, towards the reef spine. The mean direction of 153 nautiloids on the east side of the ridge is 72°, compared with the dip direction of 80°, and 82% have their apices oriented up dip (Figs 146, 147). Therefore, the nautiloid orientation is, as might be expected, controlled by the depositional dip on either side of the reef spine. The average orientation on each side is skewed towards the north, as shown on Figure 147, and this is probably due to small post-depositional tilting of the area towards the south.

The Virgin Hills Formation adjoining McWhae Ridge is richly fossiliferous in several layers. Especially notable is the abundance of *Manticoceras* and *Beloceras* in two beds on either side of the ridge. A prominent dark reddish-brown stromatolitic bed known as 'the *Frutexites* bed', as much as 30 cm thick, occurs at the top of a slope on the west side (GPS AMG Zone 51, 191908E 7926030N). It was constructed by the iron cyanobacterium *Frutexites*, which also concentrated iridium and other metals in the horizon (Figs 101, 102; Playford et al., 1984b). Playford et al. concluded that the iridium concentration in this bed was due to either a bolide impact or biogenic concentration by the *Frutexites* microbe of iridium and associated metals. Careful analyses of *Frutexites* filaments showed that iridium and other metals were indeed concentrated within those filaments (Playford et al., 1989), and Nicoll and Playford (1993) showed that the bed was not at the Frasnian–Famennian boundary, as had previously been believed, but was in the *crepida* Zone of the lower Famennian. The Frasnian–Famennian boundary is 4.5 m below the *Frutexites* bed (GPS AMG Zone 51, 191906E 7926040N; Figs 101, 102). The rate of deposition of the *Frutexites* bed must have been especially slow, as Hurley and Van der Voo (1987, 1990) found that 14.5 cm of section in this bed exhibited three normal and two reverse magnetic polarities. Their paleomagnetic studies also indicated that the Late Devonian paleopole for Gondwana lay in central Africa, a conclusion subsequently confirmed by Chen et al. (1995).

The *Frutexites* bed, like other stromatolitic horizons in the Bugle Gap area, shows clear evidence of early lithification, in the form of crinoid and coral holdfasts that could only have grown on hard rock substrates. A closely similar horizon containing *Frutexites* occurs nearby at Ngumban Cliff (Figs 365–368).

The Virgin Hills Formation was laid down over the Sadler Limestone, with less-steep depositional dips. Conspicuous stromatolite beds are present in the Virgin Hills Formation, interfingering with the other distal marginal-slope deposits, primarily red sandy calcarenites and sandy calcareous siltstones. The stromatolitic limestones pinch out down the flanks of the ridge, where the depositional dips flatten and the facies becomes more basinal (Figs 148, 359). This loss of stromatolites may have been the result of reduced light penetration associated with increased water depths, or it could have resulted from higher rates of sedimentation on the flanks of the ridge. The difference in elevation between the lowest stromatolites and the eroded crest of the reef spine is about 55 m, and if post-depositional tilting is removed, that is equivalent to an original difference in water depth of about 45 m (Fig. 148). However, reconstructions suggest that the water depth was much greater than this, and that the lowest stromatolite tongue grew in water more than 160 m deep (Fig. 148).

The stromatolite bioherm that capped the McWhae Ridge spine became extinct in early Famennian times, probably because increased rates of subsidence took it to excessive water depths, where it was enveloped in red and grey silty and sandy limestone. These limestones mounted successively up the steeply dipping west flank of the bioherm, forming an angular depositional unconformity, which grades into a conformity over a distance of about 150 m (Figs 148, 359–361).

The crest of McWhae Ridge (GPS AMG Zone 52, 192150E 7925920N) is marked by a small graben parallel to the reef crest (Fig. 358), with poorly exposed siltstone of the Gogo

Formation at one location (GPS AMG Zone 52, 192110E 7926030N). The faults bounding this graben moved after deposition of the oncolite bed and prior to deposition of the Virgin Hills Formation, and continued during deposition of that formation. Displacements along these faults are as much as 30 m greater in the Sadler Limestone than in the Virgin Hills Formation. The oldest Virgin Hills Formation adjoining the western fault is brecciated, and the breccia is overlapped by limestone without breccia, indicating that periodic faulting continued during deposition of that formation. The small faults forming the graben trend north–south, whereas the main fault that they meet south of the ridge trends west-northwest, and it in turn joins the Cadjebut Fault, which is part of the Pinnacle Fault system. These faults were clearly active during the Devonian, and some are thought to have continued moving during the Carboniferous and Permian.

The coincidence between the McWhae Ridge graben and the reef spine is clear, but puzzling, as it would seem more likely for a reef to grow above a horst rather than a graben. Perhaps the footwall sides of the bounding faults rose into shallow water, and that is why the reef spine came to be located there. The graben trends in the same direction as the Lawford Range reef complex, but the faults at the surface die out at the north end of McWhae Ridge. Earlier faulting may have controlled the early development of platforms in the Bugle Gap area, but if so, none of the faults have been active since then, apart from the small faults at McWhae Ridge.

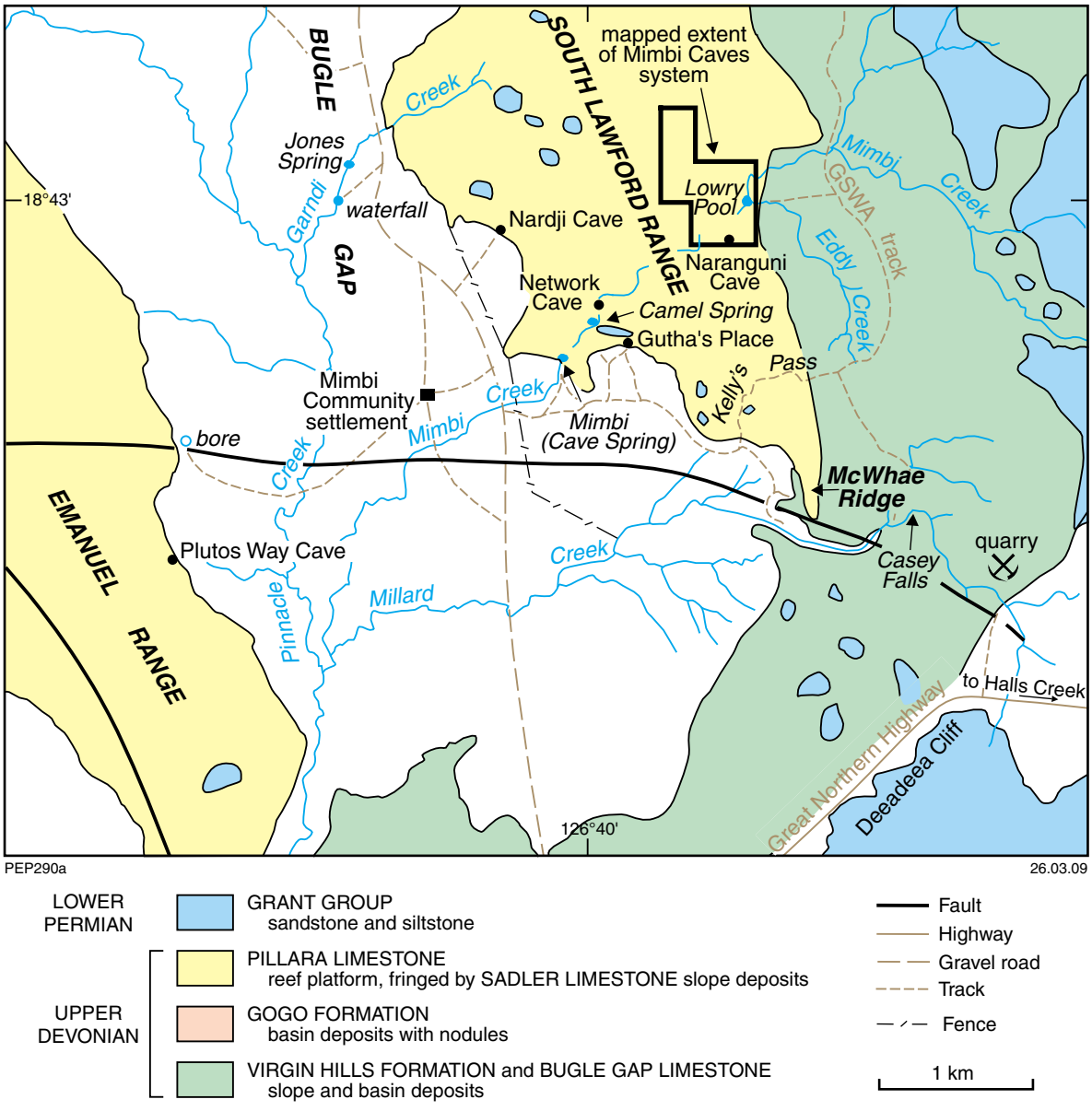

Figure 357. Geological map of the southern Bugle Gap area, showing the principal localities discussed in the text.



Figure 358. Aerial view looking north over the McWhae Ridge reef spine, showing the graben developed in reef of the Pillara Limestone, with fore-reef Sadler Limestone and Virgin Hills Formation on each side of the ridge.

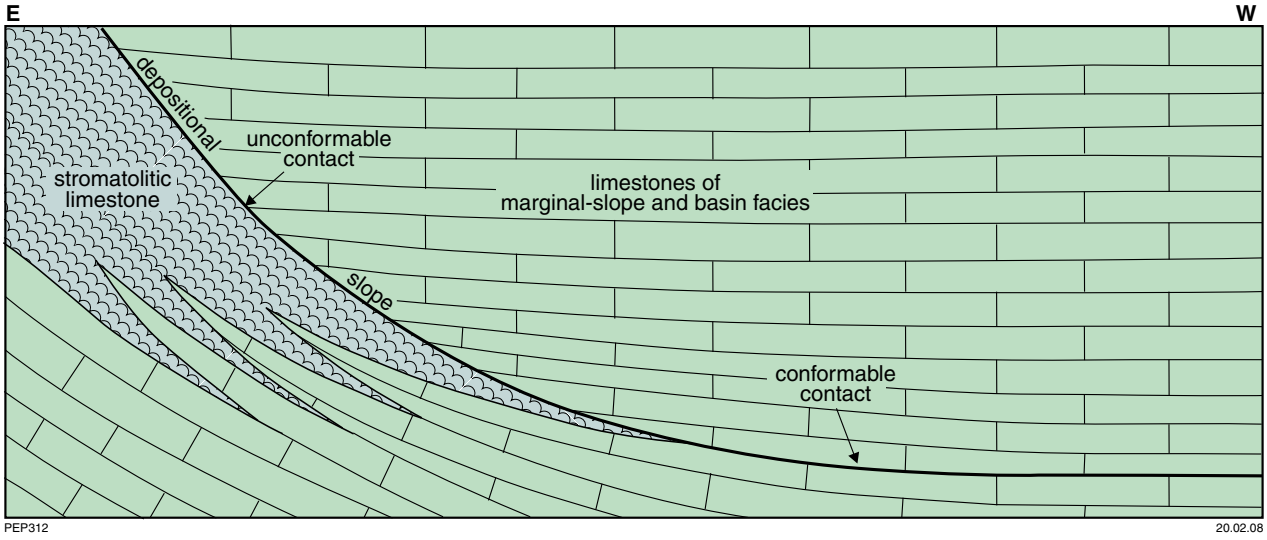

Figure 359. Diagrammatic section of part of the west flank of McWhae Ridge, illustrating the development of a depositional unconformity on stromatolitic limestone in the Famennian Virgin Hills Formation.



Figure 360. Part of the west flank of McWhae Ridge looking towards the location illustrated in Figure 359, where Virgin Hills Formation onlaps older stromatolitic limestone of the same formation, giving rise to a depositional angular unconformity.



Figure 361. Thin-bedded distal fore-reef limestone onlapping stromatolitic limestone, giving rise to a depositional angular unconformity within the Virgin Hills Formation, as illustrated in Figures 359 and 360.



Figure 362. Part of the east flank of McWhae Ridge looking south, showing strata of the Virgin Hills Formation dipping east, away from the ridge crest. Note the slump folding in Frasnian beds, truncated by overlying beds. The slumping was probably a result of late Frasnian earthquake activity.



Figure 363. Famennian silty limestone of the Virgin Hills Formation east of McWhae Ridge, showing intraformational slump folding, probably indicative of a tectonic event.

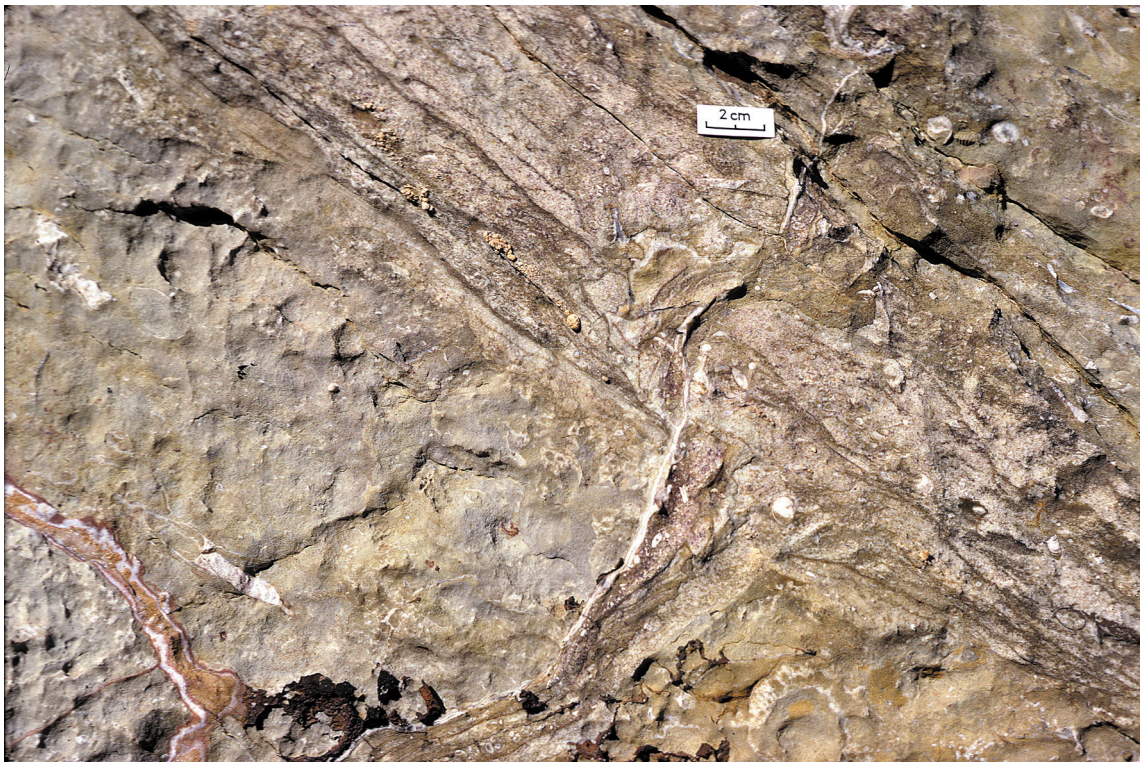

Figure 364. **The south wall of the small karst corridor in Sadler Limestone illustrated in Figure 141, showing that sediment poured into a neptunian dyke from the overlying bed. This indicates slow sedimentation and early lithification of the lower limestone. Earthquake activity may have been responsible for the fissuring.**

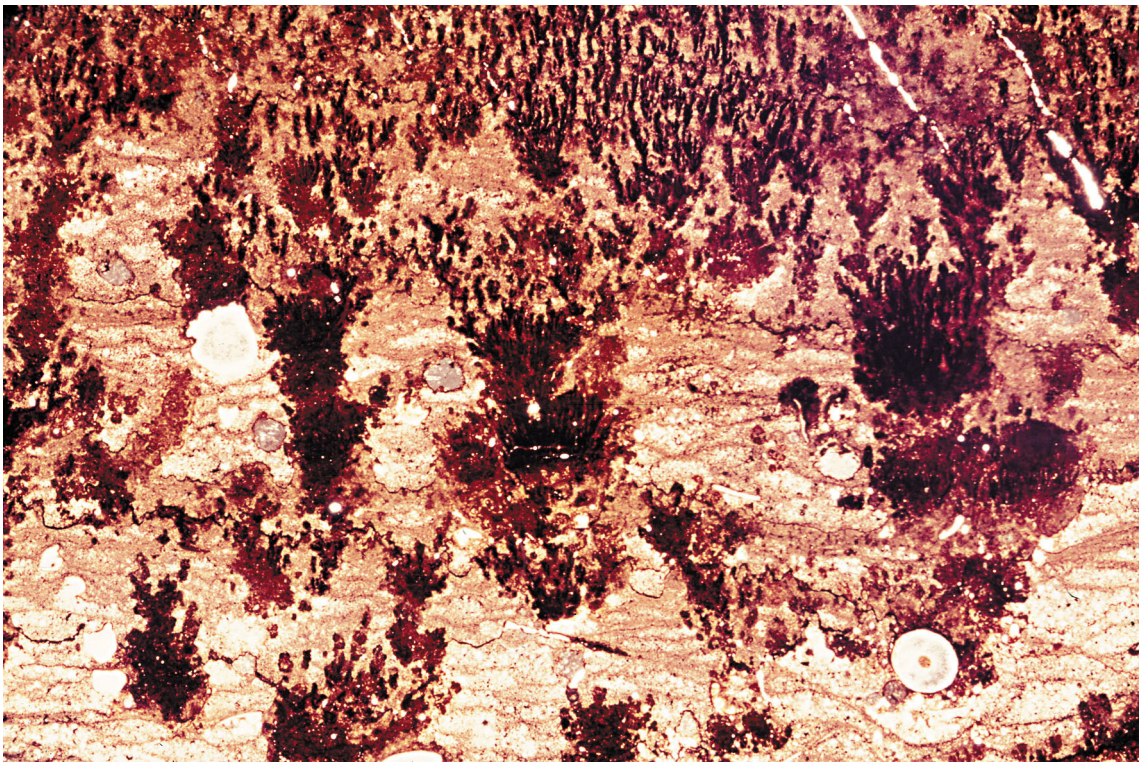

Figure 365. **Thin section showing colonies of the iron cyanobacterium *Frutexites*, with small fragments of crinoids and corals in a groundmass of laminated microbial limestone. From the Virgin Hills Formation at Ngumban Cliff, GSWA sample no. 19292A. Width of field of view 20 mm.**

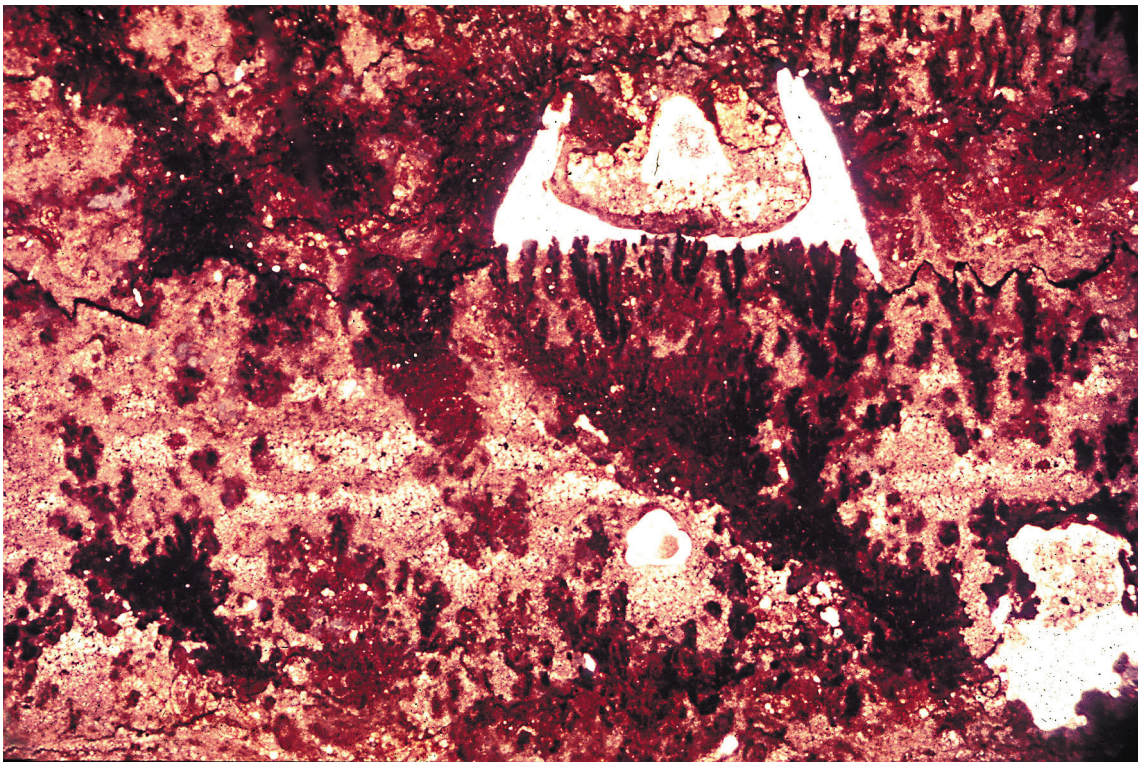

Figure 366. Thin section showing colonies of the iron cyanobacterium *Frutexites* in a groundmass of microbial limestone. The holdfast of a small solitary coral has grown on top of one colony, which indicates early lithification of the microbial limestone. From the Virgin Hills Formation at Ngumban Cliff, GSWA sample no. 19292B. Width of field of view 8 mm.

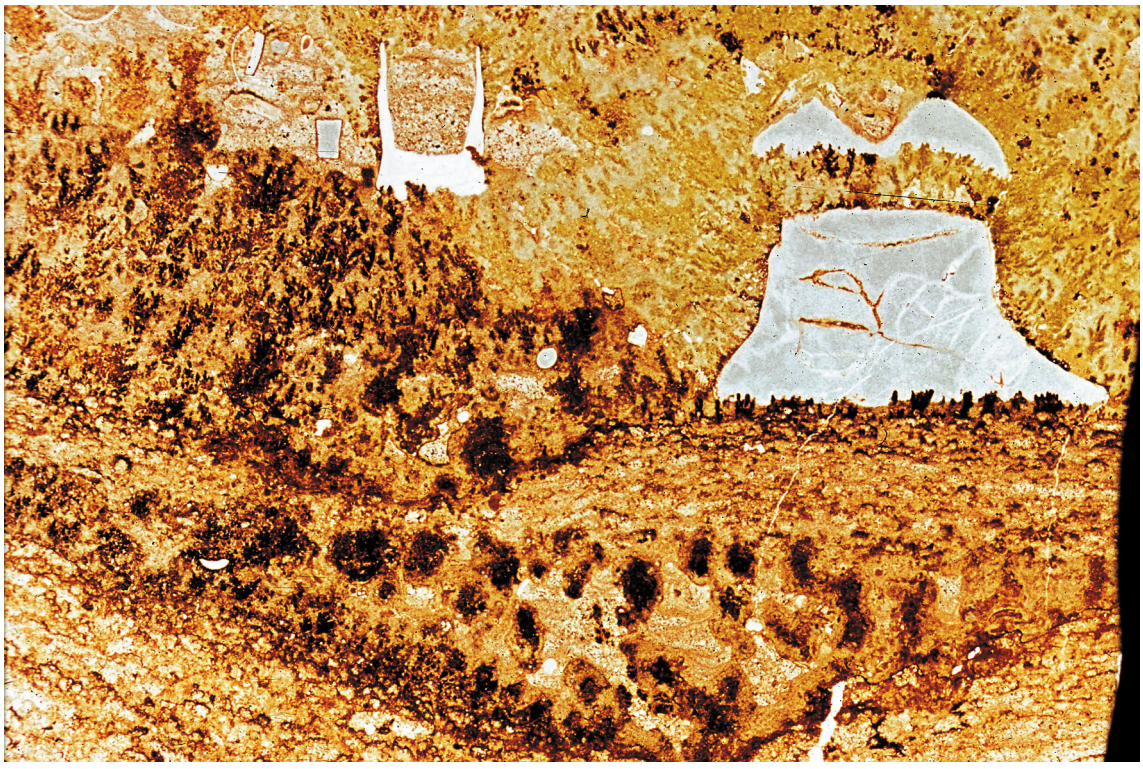

Figure 367. Thin section showing colonies of *Frutexites* in a groundmass of microbial limestone, with holdfasts of a solitary coral and two crinoids that grew on parts of the colonies, indicating early lithification of the microbial limestone. From the Virgin Hills Formation at Ngumban Cliff, GSWA sample no. 19292C. Width of field of view 30 mm.

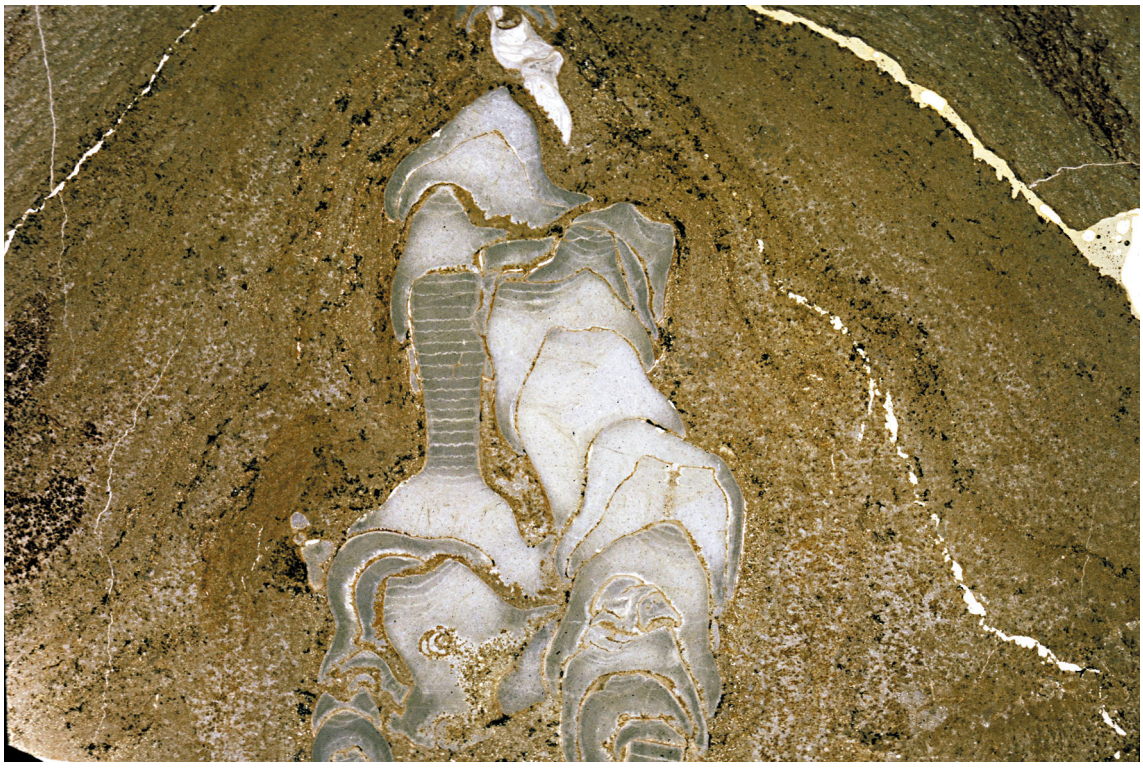

Figure 368. Thin section of a succession of holdfasts of crinoids and a coral in microbial limestone from the Virgin Hills Formation at Ngumban Cliff, GSWA sample no. 19292D. Width of field of view 50 mm.

Kellys Pass

Kellys Pass is a rough track through the South Lawford Range, first established in 1968 by GSWA field assistant Kelly O'Neill (after whom it is named). The most significant geological feature displayed in the pass is the backstepping of the platform margin that resulted from the Kellys Pass Event (Figs 88–90). This backstepping is seen best near the northern end of the pass (at GPS AMG Zone 52, 191800E 7926830N). The reef margin at this locality has stepped back for a distance of about 150 m, with dipping fore-reef strata of the Sadler Limestone downlapping onto flat-lying Pillara Limestone. Truncation that is evident in the Pillara Limestone on the backstepped surface in this area amounts to more than 20 m of section. Minor tilting and localized deformation of strata beneath the unconformity suggest that backstepping was associated with a tectonic event. Deformation is most pronounced near the platform margin. Some evidence of minor solution in the Pillara Limestone immediately below the unconformity surface can be observed approximately 150 m north of the pass (Fig. 91; AMG Zone 52, 191800E 7926900N). These features indicate that the platform was briefly uplifted, tilted, and eroded prior to backstepping of the platform margin.

Parts of the Virgin Hills Formation east of Kellys Pass are very richly fossiliferous, containing vast numbers of goniatites and nautiloids. A notable example is shown in Figure 369.

Casey Falls

The waterfall of Casey Falls has formed where Millard Creek flows over a resistant layer of limestone built by columnar stromatolites, in the early Famennian part of the Virgin Hills Formation (Fig. 370). The falls have been named after John Casey, formerly a geologist of the Bureau of Mineral Resources and a co-author of the publication by Guppy et al. (1958).

An older (early Famennian) bed of limestone with prominent domal stromatolites is exposed nearby (Fig. 371). These two prominent stromatolite horizons are separated by 35 m of red laminar calcareous siltstone in which reticulate stromatolites are common. Crinoid columnals are prominent on bedding planes and have average orientations parallel to the depositional dips.

The lower stromatolite horizon (GPS AMG Zone 52, 192635E 7926085N), which correlates with the *crepida* Zone, is marked by domal stromatolites as much as 2 m long and 1.5 m high (Fig. 371; Playford et al., 1976). It also contains some undulous, columnar, and reticulate forms. The domal stromatolites show elongation in the direction of the depositional strike of the Virgin Hills Formation, and have abundant fossil material (mainly crinoid columnals, nautiloids, and ammonoids) that were concentrated on the up-dip sides of the domes. In addition, thickets of the coral *Aulopora* are preserved on the up-dip sides, together with the holdfasts of crinoids and small solitary corals.

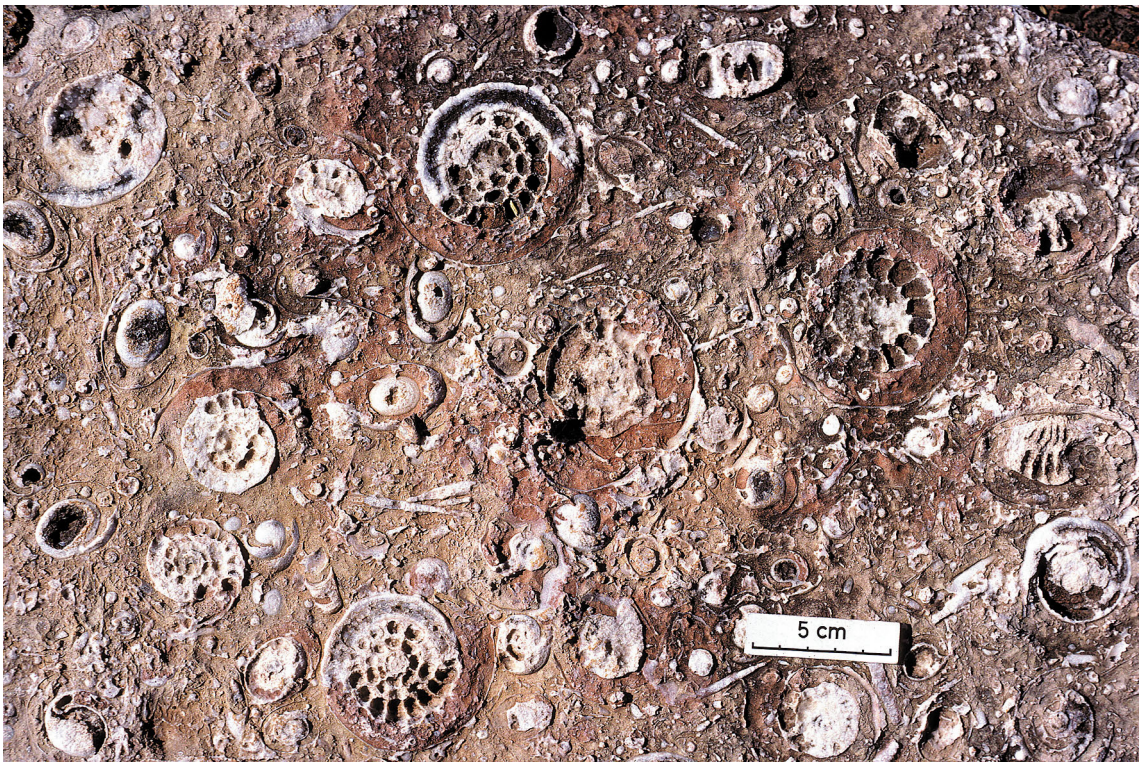

Figure 369. Masses of ammonoids (*Torleyoceras* and *Praemeroceras*) and other fossils in early Famennian Virgin Hills Formation east of Kellys Pass. Chambers in the ammonoids are mostly filled with sparry calcite, but some voids have remained open.



Figure 370. The top of a fallen block of deep-water columnar stromatolites in Virgin Hills Formation at Casey Falls, showing the rounded tops and close spacing of stromatolite columns at this locality.

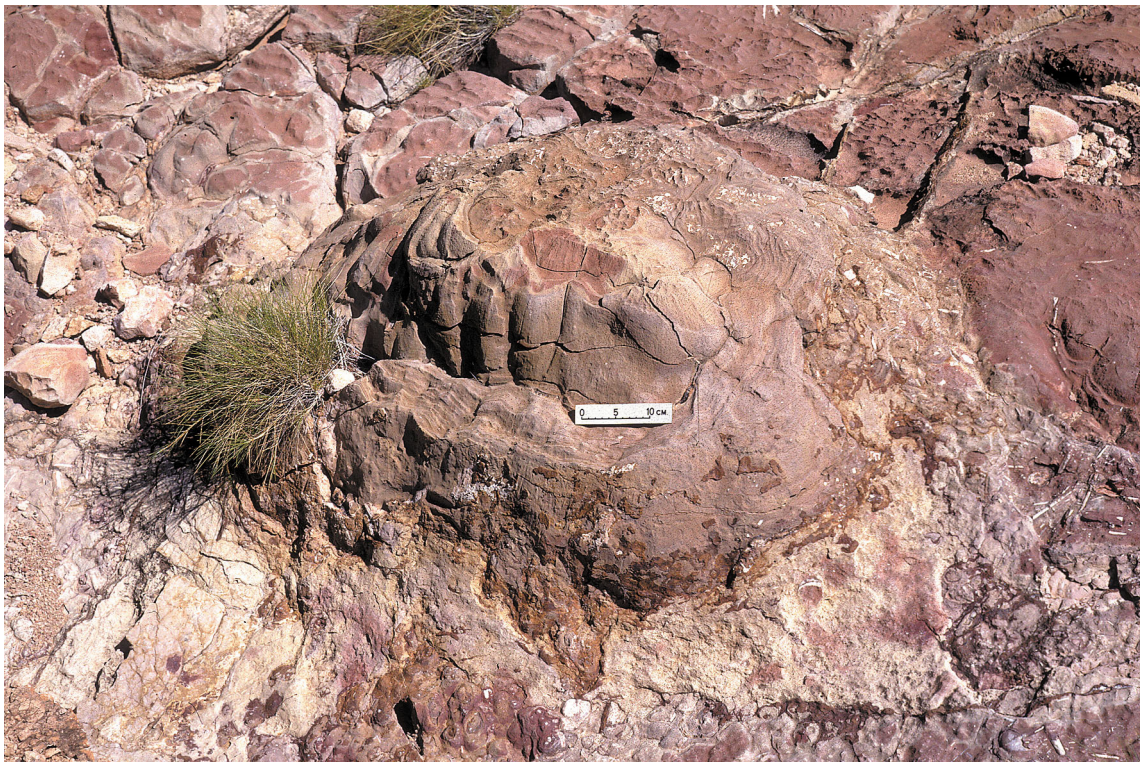

Figure 371. Mound-shaped stromatolite in Virgin Hills Formation near Casey Falls showing cuspate layering and many holdfasts of small corals and crinoids attached on the up-dip side. Sediment that slid down the depositional slope also tended to accumulate on that side.



Figure 372. Famennian marginal-slope limestone of the Virgin Hills Formation southwest of Casey Falls, showing cyclicity in marginal-slope limestones (wackestones) of the Virgin Hills Formation. This cyclicity is mainly due to variations in the degree of cementation, rather than any distinct compositional changes. These cycles, which average about 1.8 m thick, may correlate with cycles in platforms of the Nullara Sequence.

The upper stromatolite layer, 10 m thick, is characterized by spaced to contiguous columnar stromatolites that form spectacular cliff exposures in the falls and talus blocks below (Fig. 370). Individual columns are as much as 0.5 m high, with the interstices between columns filled largely by crinoidal debris and peloidal grainstones. The down-dip sides of the columns are coated with white microbial micrite. This stromatolite-bearing bed pinches out about 250 m southwest of Casey Falls, in an area where clear cyclicity is displayed in the Virgin Hills Formation (Fig. 372).

Teichert Hills

Teichert Hills form a small platform atoll which, at the time represented by the present exposed section, was shrinking in extent and probably drowned soon afterwards. Small patch reefs were developed in places along the reef margin while it was being drowned (Figs 373, 374). The hills forming this platform atoll were named (by Playford) after Curt Teichert, a pioneer of stratigraphic and paleontological work in the Devonian of this area.

A series of well-preserved chute-and-buttress (or spur-and-groove) structures occur in the reef rim of a Pillara Limestone platform along its southwest margin (Figs 375–377; Playford, 1981; Wood and Oppenheimer, 2000). The chutes are from 10 to 30 m wide, and originally plunged away from the platform at about 25° to 30° (now reduced to 15° to 20° as a result of 10° of post-depositional eastward tilting). They range from about 5 to 20 m wide, and because of their smooth forms are thought to be growth rather than erosional features. Reef forming the adjoining buttresses is composed of microbial–stromatoporoid–coral (*Alveolites*) limestone, with some prominent stromatactis cavities. *Renalcis* also occurs in the reef, but is rarely prominent.

The chutes apparently acted as channels for sediment derived from the platform to flow down into the basin. Similar chute-and-buttress structures could have been temporary features of other reef margins, but are no longer recognizable because of continued reef growth. In the present case the features were probably preserved as a result of abrupt subsidence, which drowned the platform margin and allowed the reef topography to be covered with soft basin and slope deposits, thus preserving the chute-and-buttress morphology.

Plastered on the walls of several chutes is a thin bed (5–20 cm thick) of micritic limestone, commonly containing abundant straight nautiloids and having fine, wavy, brown to orange-coloured, phosphatic laminations (Fig. 377). The phosphate (first identified by Peter Southgate) is suggestive of very slow deposition or a prolonged submarine hiatus. The nautiloids are oriented in the slope directions of the chutes, with their apices directed up dip. This bed is thought to have been laid down in relatively deep water (probably more than 50 m deep), soon after drowning of the platform margin. It is of the same age as the straight-nautiloid horizon in the Sadler Limestone on the flanks of McWhae Ridge (Zone 4 of the Frasnian conodont zonation), which is at the boundary between Pillara Sequences 2 and 3, formed by the Kellys Pass Event. A seemingly identical horizon has also been found in the Limestone Billy Hills area on the flanks of a drowned pinnacle reef (GPS AMG Zone 51, 794830E 7971860N).

In the back-reef to reef-flat area, a short distance behind the chute-and-buttress structures of the reef margin, there are blocks of massive stromatoporoid limestone (as much as 10 m across) that are clearly allochthonous. They may have been torn from the reef margin by a tsunami or strong wave action.

Nardji Cave

Nardji Cave (KL-6 of Jolly and Lance, 1980) is situated 1 km north-northwest of Mimbi (Cave Spring). The cave is about 150 m long and contains some well-developed speleothems. Of passing interest, it is worth recording that in the late 1950s Playford was told by the Manager of Christmas Creek Station (Vic Jones) that food and other necessities had been stored in this cave in 1942, for possible use as a hideout in the event of a Japanese invasion.

The platform margin beside Nardji Cave is a good example of an upright-scarp margin, showing reef-margin subfacies (Pillara Limestone) abutted by fore-reef subfacies (Sadler Limestone; Fig. 106). The fore-reef deposits have depositional dips of about 25°, and they abut a near-vertical face of reef-margin subfacies, with some interfingering between the two subfacies. The reef consists of stromatoporoid–microbial reef limestone, containing a little *Renalcis*. Reef-flat and back-reef deposits of the Pillara Limestone dip away from the reef margin at about 10°. The back-reef deposits notably include strongly stylolitized *Amphipora* limestones.

Measurements were made of the amplitude and spacing of 143 sets of stylolites in reef-margin, reef-flat, back-reef, and fore-reef limestones at this locality, in accordance with the methods of Mossop (1972). These show that the ratio of stylolite amplitude to stylolite spacing (as an index of the degree of stylolitization and pressure-solution compaction) ranges from 0.018 in the reef margin to 0.032 in the reef flat, 0.041 in the fore reef, and 0.063 in the back reef. From this it seems that the amount of compaction through stylolitization at this locality is least in the reef-margin subfacies and most in the back-reef subfacies, with compaction in the back-reef subfacies being approximately 3.5 times that in the reef-margin subfacies, twice that in the reef-flat subfacies, and 1.5 times that in the fore-reef subfacies (Playford, 1981). This differential compaction has resulted in the back-reef and reef-flat limestones dipping away from the reef-margin limestone at about 10°, and in an increase (estimated to be about 5° to 7°) in the dip of the fore-reef deposits.

Mimbi Caves System

The Mimbi Caves System is situated in the southern Lawford Range, some 100 km southeast of Fitzroy Crossing and 4 km north of the Great Northern Highway (Fig. 357). The origin of the cave system, through subglacial solution in meltwater below the Early Permian ice sheet, has previously been discussed.

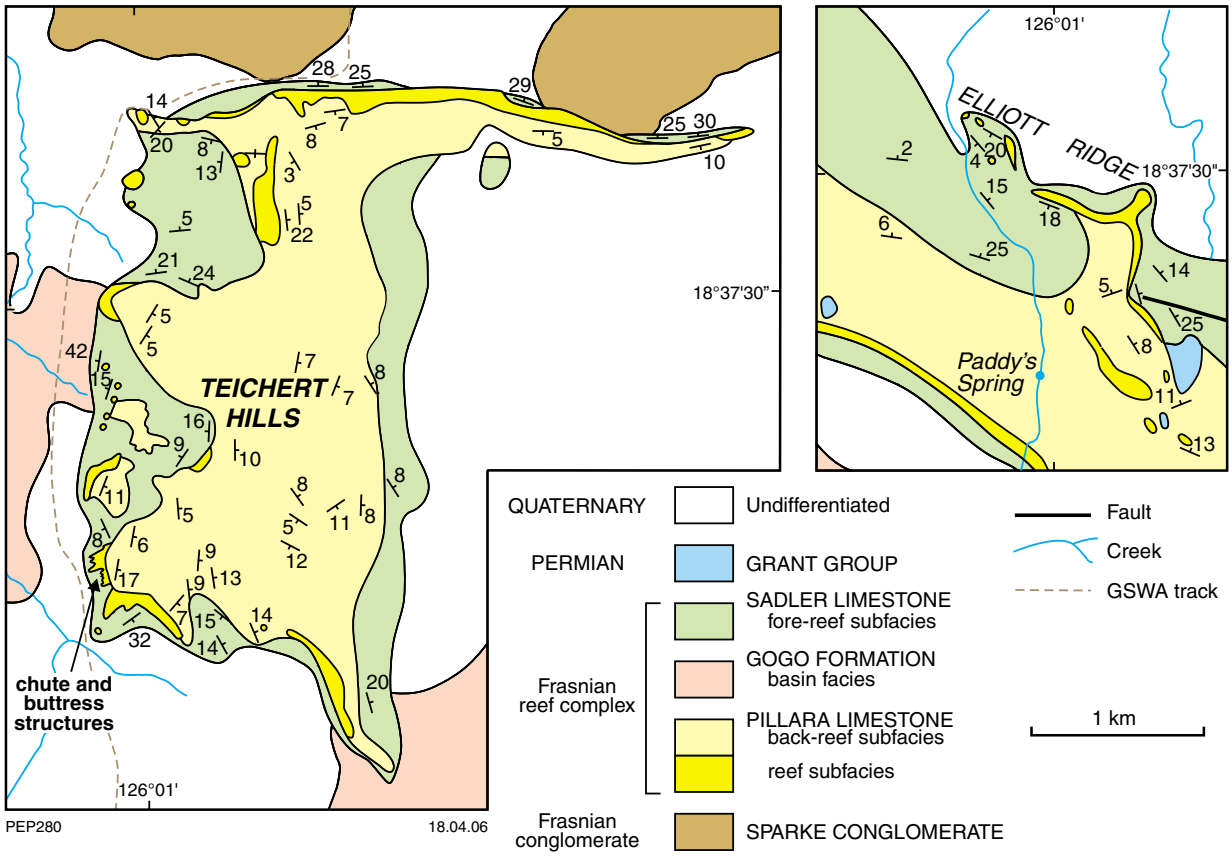

Figure 373. Geological maps illustrating two prominent Frasnian backstepping events, at Teichert Hills and Elliott Ridge. These two events were associated with the Kellys Pass and Elliott Ridge Events respectively.



Figure 374. Small patch reef that developed on the northern margin of the Teichert Hills platform (Pillara Limestone) during a drowning (backstepping) phase thought to correlate with the Kellys Pass Event.



Figure 375. Aerial view of the southwestern Teichert Hills platform (Frasnian), showing chute-and-buttress (or spur-and-groove) structures in the reef margin, with bedded back-reef deposits behind.

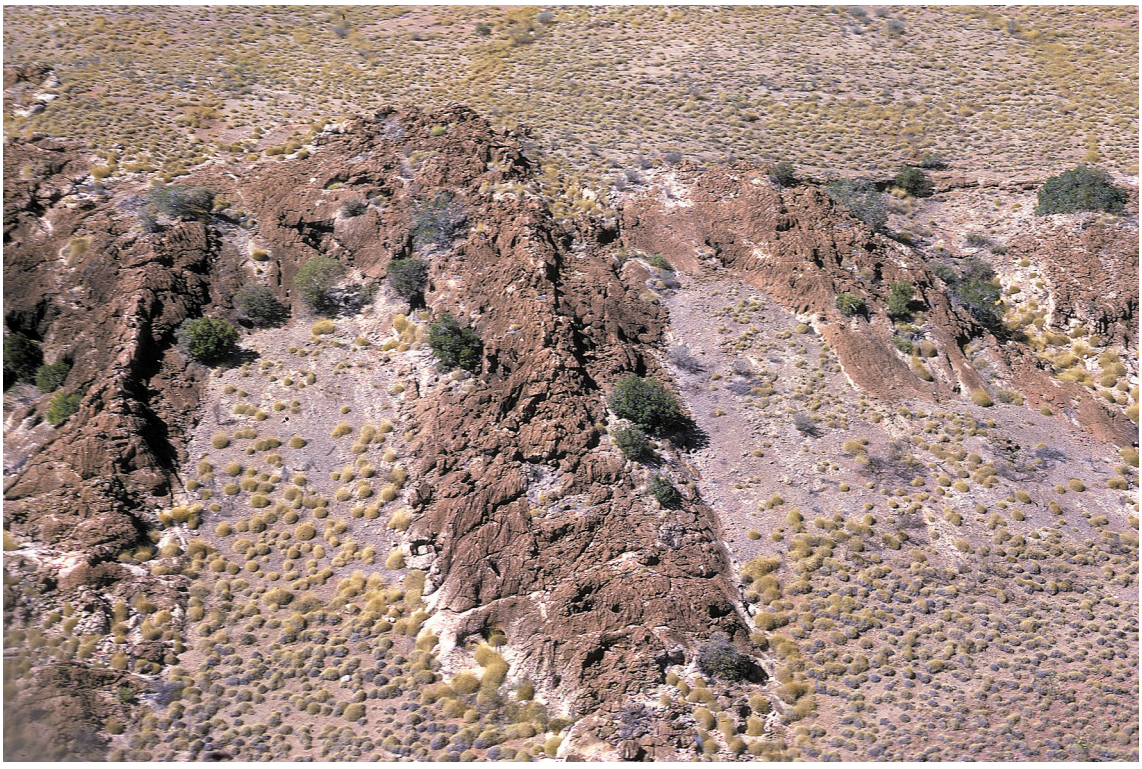

Figure 376. Closer aerial view, looking east, of chute-and-buttress structures along the southwestern reef margin of the Teichert Hills platform. They are thought to be growth rather than erosional features.

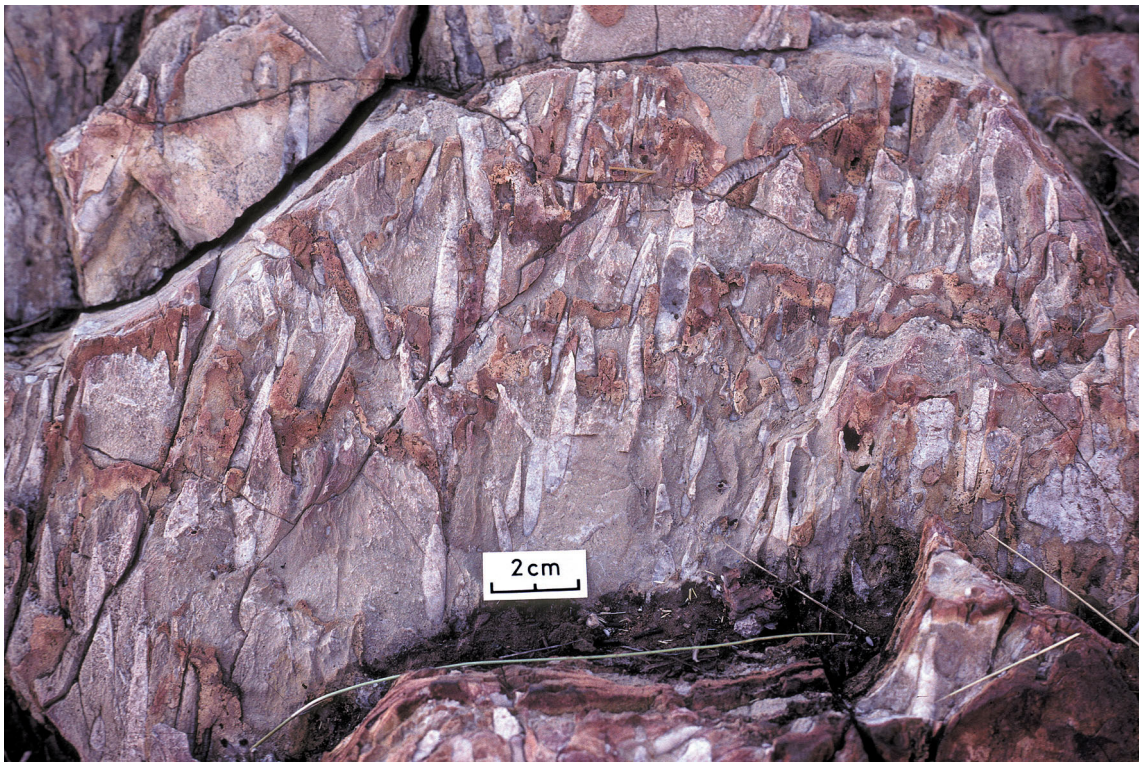

Figure 377. Straight nautiloids and phosphatic microbial limestone that accumulated on the steep walls of a chute on the west side of the Teichert Hills platform. The apices of nautiloids are directed up dip. This bed is thought to represent very slow deposition after drowning of the platform.

The caves and karst corridors forming the cave system have developed through the solution enlargement of a series of near-vertical rectilinear joints, forming an interlocking maze of narrow passages and corridors (Fig. 292). Most cave passages and karst corridors are one to three metres wide and the caves are three to five metres high, but some caves form impressive larger chambers (more than eight metres high), such as 'The Cathedral' (Fig. 292). Some open karst corridors (grikes), are hundreds of metres long and extend upward several tens of metres to the top of the range (Fig. 299). The mapped length of passages and corridors in the system is at least 5 km, but the total length could be more than twice that figure.

The Mimbi Caves System is known to have first been explored in 1963, by David Lowry (Lowry, 1967), and since then extensive speleological mapping has been conducted there by members of the Illawarra Speleological Society (Dicker, 1987). An examination of air photographs of the area suggests that less than 50% of the system has been mapped to date. When fully mapped it may prove to be one of the longest and most complex cave systems known in Australia.

The mapped part of the main cave system (termed 'Mimbi Cave', KL-5, by Jolly and Lance, 1980; 'Mimbi Cave [Upper]', KL-5, by Matthews, 1985) extends west of Lowry Pool. Other less-extensive caves occur north of Camel Spring (Network Cave of Jennings and Sweeting, 1963; KL-4 of Jolly and Lance, 1980) and at Mimbi Spring on the west side of the South Lawford Range (KL-1 of Jolly and Lance, 1980). The Mimbi Caves system is the longest in a series of spectacular caves in this area (Dicker and Robinson, 1993).

The Mimbi caves contain spectacular active speleothems, including tall slender stalagmites with well-developed 'coral' on their sides, and long conical 'carrot' stalactites, together with beautiful shawls, flowstones, and terraces with cave pearls (Figs 293–296, 378, 379). At several localities it seems that some vandalism or unauthorised collecting of stalactites, stalagmites, and shawls has occurred, notably in a remote part of the cave system where recently broken speleothems are scattered over the cave floor.

Mimbi Creek flows underground and in open corridors through part of the cave system. At low flow levels it follows a well-defined circuitous path through the caves and corridors (Fig. 292). However, in most wet seasons the creek reaches much higher flood levels, and cave passages and corridors throughout the system are inundated. Impacts by floating wood during high floods have probably been responsible for the breakage of many speleothems. However, others could have been fractured by earthquakes. Many of the broken speleothems have partially regrown from their fractured ends.

Aboriginal people of the *Gooniyandi* Tribe believed that the Mimbi Caves System was formed during the Dreamtime by *Galeru*, the rainbow snake, who was also responsible for creating Galeru Gorge (where Mount Pierre Creek flows through the Lawford Range, 12 km

north of the Mimbi Caves System). During the Dreamtime, *Galeru* pursued people in the caves and they repelled him by throwing stones. As a result, traditional Aborigines, when entering the caves, pick up flat pieces of limestone and hit them together, resulting in a distinctive clacking sound, which is intended to warn the snake spirit to get out of their way.

Apart from the Mimbi Caves System many other cave networks are known in the southeastern part of the Devonian outcrop belt, including Pluto's Way (Fig. 385), Nardji, Uranus (Figs 297, 298), Kimberley Rover, Titan's, Rookie's, Monday, Victory, Whalemouth, and Illawarra Caves (Dicker and Robinson, 1993). None of these other cave systems are known to be nearly as extensive as the Mimbi Caves System, but they show similar characteristics, with narrow parallel-sided walls controlled by joint systems in the limestones. They have been partially explored and mapped by members of the Illawarra Speleological Society. Several were shown to Playford by Lloyd Robinson, one of the society's leading members, on the condition that their exact locations would not be made public at that time (in order to minimize the possibility of human damage). Exceptions were made for Mimbi, Pluto's Way (Fig. 380), and Kimberley Rover doline (Fig. 280) and the associated caves and karst corridors (Plate 5). All of the cave systems are thought to have originated by subglacial solution in meltwater below the Early Permian ice sheet. The reason for their abundance in this part of the Devonian outcrop belt, rather than elsewhere, is that the Lower Permian shale and sandstone that once covered the reef complexes in this area has been eroded away relatively recently (probably in late Tertiary and Quaternary times). Consequently, the directly underlying subglacial features have remained relatively well preserved.

Gutha's Place, near Mimbi Caves, was the campsite of Gutha Rokylle and her partner, Esko Routasuo, who resided there continuously for three years in 1987–90. They lived in a caravan parked in a concealed karst corridor, disguising the route to the site so that very few people were aware of their presence. In the corridor they built a little shelter (still standing) from local rocks and cement, using it as a library for their many books. Gutha Rokylle is an accomplished sculptor, and during her sojourn there she crafted three large statues of North American Indians, placing them on a cement platform in the karst valley between their campsite and Camel Spring (Fig. 381). After she and her partner had left the area, the statues were removed and the platform was destroyed at the request of local Aborigines. The statues were placed at a location near the Pillara minesite, where they remain today.



Figure 378. Shawl speleothem, composed of sparkling crystalline spar, in Mimbi Caves. Width of field of view about 90 cm.

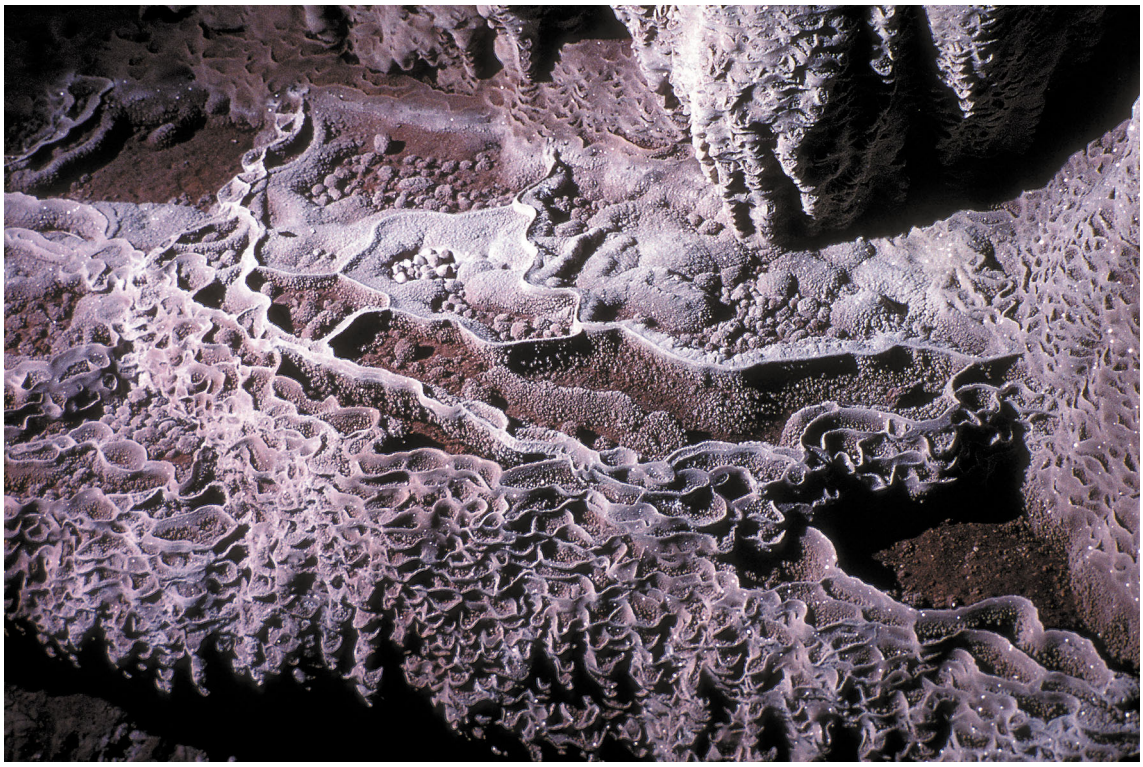

Figure 379. Rimmed terraces with cave pearls, Mimbi Caves System. Width of field of view about 40 cm.



Figure 380. Pluto's Way Cave, on the east side of the Emanuel Range opposite the Mimbi Community settlement.

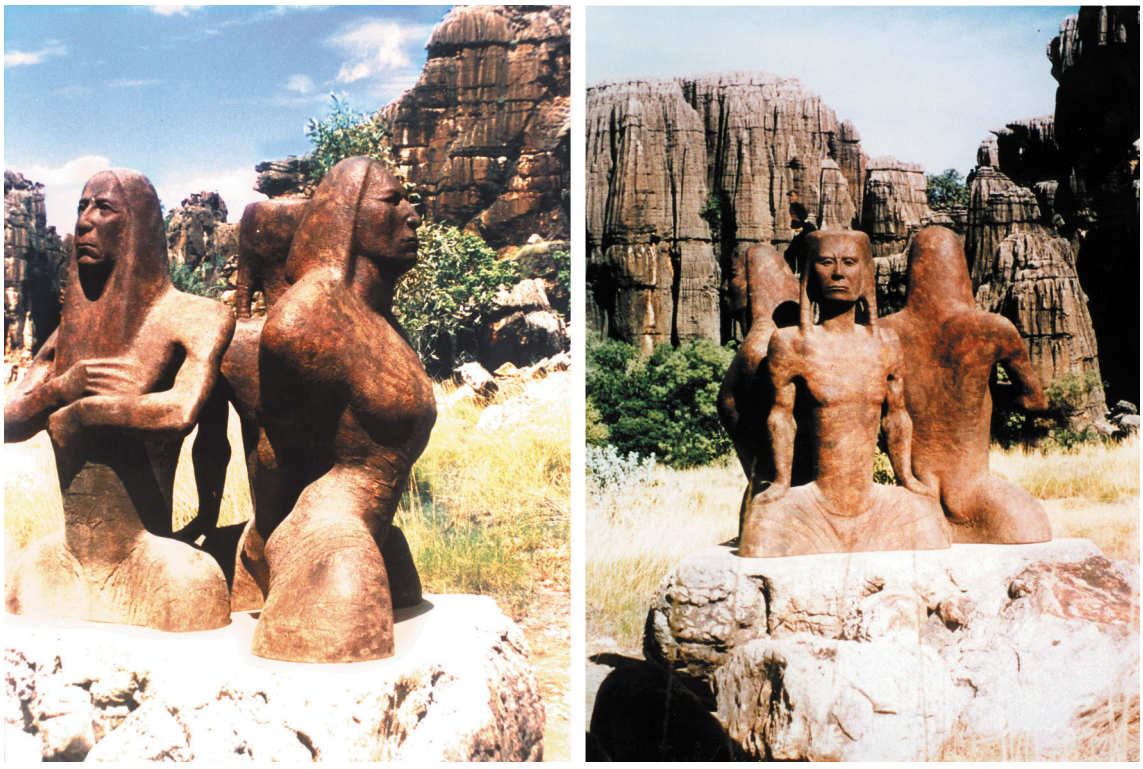

Figure 381. Two views of statues of North American Indians sculptured by Gutha Rokylle, while she and her partner lived nearby during the period 1987–90 at a locality in the South Lawford Range now known as Gutha's Place (Fig. 291). The individuals represented are based on portraits of Red Cloud (a Sioux chief), Chief Joseph (a Nez Perce chief), and Set-Tainte, (a Kiowa chief). Photos courtesy of Gutha Rokylle.

Ngumban Cliff

Ngumban Cliff (AMG Zone 52, 189000E 7923700N) is situated at the southern end of Bugle Gap. It exposes fore-reef subfacies of the Virgin Hills Formation and includes stromatolite horizons with excellent examples of spaced to contiguous columnar forms, as much as 1 m high (Figs 73, 382). The relief of these columnar stromatolites during growth was not more than about 5 cm, as shown by linkages between individual columns. The columns grew vertically on marginal slopes that had depositional dips of about 12°. Carbonate detritus rich in crinoidal material is present between the columns. Reticulate stromatolites are also well developed in the Virgin Hills Formation at this locality (Fig. 383).

The marginal-slope deposits at Ngumban Cliff were subjected to early cementation and neptunian fissuring, resulting in many small dykes and sills filled with fibrous calcite and sediments that poured in from above (Figs 156, 384).

Deeadeea Cliff

Deeadeea Cliff is the type locality for the Ngumban Claystone and Deeadee Sandstone Members of the Carolyn Formation, at the base of the Grant Group in the southeastern Lennard Shelf. '*Deeadeea*' means 'mudlark' in the *Gooniyandi* language, and the cliff features in an important Dreamtime story of the tribe, which involves *Deeadeea* and a blue-tongue lizard named *Looma*, whose activities included travelling during a flood past Deeadeea Cliff, Mimbi Caves, and Galeru Gorge, and from there to a locality east of Derby now named Looma, near Mount Anderson. The Gooniyandi people also knew Galeru Gorge as *Looma*, but as that name could be confused with Looma near Mount Anderson (where a large Aboriginal community is based), Playford chose to formally name the gorge Galeru Gorge, with the approval of local Aboriginal people, after the rainbow serpent, *Galeru,* who is said to have formed the gorge. The Aboriginal community that now lives nearby is known as the Galeru Community.

The Ngumban Claystone Member is well exposed in a road cut at the foot of Deeadeea Cliff (Fig. 283). This section, 50 m thick, consists of sandy claystone with sporadic pebble- to boulder-size clasts of granite, basalt, dolerite, quartzite, and limestone, most of which are less than 20 cm across. Some are distinctly faceted and striated (Fig. 284). Along the cliff face extending to the south-southwest, the member contains many large clasts of granite, some as much as 2 m across. These erratics apparently fell as dropstones from melting icebergs during the waning phase of the Early Permian glaciation. Lithologies represented in the erratics suggest that some came from the King Leopold Orogen and others from the Kimberley Basin, which would be the logical source of mountain glaciers at that time. However, some glaciers



Figure 382. The tops of closely spaced stromatolite columns, viewed from above, in early Famennian Virgin Hills Formation at Ngumban Cliff.



Figure 383. Reticulate stromatolites, Famennian Virgin Hills Formation, Ngumban Cliff.



Figure 384. Thin section of small neptunian dykes and sills in early Famennian Virgin Hills Formation at Ngumban Cliff. The fissures were filled with locally derived sediment and sparry calcite. GSWA sample no. 11677B. Width of field of view 40 mm.

were also eroding Devonian reef complexes, so that a few faceted and striated cobbles of Devonian limestone occur in the member.

The Deeadeea Sandstone Member, above the Ngumban Claystone Member, is a section 19 m thick of medium- to very coarse-grained, crudely bedded, orange- to brown-coloured sandstone. Sand grains in this unit are well rounded, pointing to strong wind action during the waning phase of glaciation.

At this locality some small remnants of glacial striae on Bugle Gap Limestone were exposed beside the road cut, and they indicated movement of the ice cap towards the north to north-northwest. That glaciated surface has since been covered. The outermost marginal slope of the Bugle Gap Limestone at this locality is thought to be directly below the Fairfield Group. That group is not exposed here, but forms poor outcrops 6 km to the northeast, immediately above the Bugle Gap Limestone (Plate 5).

Lawford Spring–Junction Dam area

The Lawford Spring–Junction Dam area is a zone of left-lateral faulting situated north of the North Lawford Range (Plate 4). It lies immediately southwest of the intersection between the Sparke Range and Virgin Hills Faults, both of which are major normal faults that were active during deposition of the Sparke Conglomerate and the Pillara Limestone. The Virgin Hills Fault branches where it meets the Precambrian rocks; one spur joins the Sparke Range Fault, and another apparently links with the Glidden Fault, a major Precambrian structure that forms the boundary between rocks of the Kimberley Basin and those of the southernmost Halls Creek Orogen.

The relatively small occurrences of Pillara Limestone in this area interfinger with the older part of the Sparke Conglomerate, and are overlain by, and transitional into, the Galeru Member of the Sparke Conglomerate (Plate 4; Fig. 183). The type section of the member is northwest of Lawford Spring, in a fault compartment between two left-lateral faults that is thought to be floored by a basal detachment fault (AMG Zone 52, 195200E 7945500N to 198600E 7944500N). The member consists of coarsening-upward cyclic sequences (Figs 184, 216). At the base of many cycles are thin marine units of platform limestone, or fossiliferous siltstone, or fine- to medium-grained sandstone. These basal units grade successively upward into beds of coarse sandstone and granule, pebble, cobble, and boulder conglomerate. The tops of the cycles are at least partly subaerial. In some places recognition of the cycles is subjective, because of outcrop limitations. There are about 75 cycles in the section, totalling 910 m in thickness, with individual cycles ranging from 5 to 21 m and averaging 12.5 m in thickness. It is estimated that the member as a whole consists of approximately 150 cycles, about 1800 m thick.

The Galeru Member is Frasnian in age, based on the presence of abundant *Atrypa* at the base of several cycles and of Frasnian stromatoporoids, corals, and bivalves at the base of others. It seems clear that the member is upper Frasnian, probably within Pillara Sequence 4 or Sequence 5. If that is so, the member may have been deposited in an estimated 3 to 5 m.y., the duration of each cycle being about 12 000 to 20 000 years.

This area is very important for the understanding of cyclicity in the Devonian rocks and aspects of the relationships between conglomerates and the Devonian reef complexes. However, the structure of the area is not fully understood, and more detailed investigation of this aspect of the geology is warranted.

Bobs Bore area

Rocks exposed in the Bobs Bore area, between the Virgin Hills and Big Dam Bore, consist of Bobs Bore Conglomerate and the Famennian part of the Virgin Hills Formation (Plate 4). These rocks are downthrown along the Virgin Hills Fault, which is interpreted to be a normal fault with about 1000 m of vertical displacement. Rocks on the upthrown side consist of Pillara Limestone, Sadler Limestone, and Gogo Formation, and are of early Frasnian and late Givetian age. Famennian Virgin Hills Formation is exposed on the downthrown (south) side of the fault (Fig. 226).

The Bobs Bore Conglomerate interfingers with red silty limestones of the basin facies of the Virgin Hills Formation (Fig. 187). Limestones of the Virgin Hills Formation adjoining the fault are strongly fractured, the fissures being filled with banded fibrous calcite (marine cement). At one locality (AMG Zone 51, 809800E 7950200N) it can be seen that limestones with many calcite-filled fissures were overgrown by early Famennian stromatolites (Fig. 231) before being subjected to further fissuring associated with renewed movement along the fault. In addition, some large blocks of Virgin Hills Formation in the area were broken up and displaced as a result of the faulting, before being overgrown by stromatolites. On a broader scale, the Virgin Hills Formation adjoining the fault is folded into conspicuous synclines (Fig. 226). These observations constitute evidence of normal movement along the Virgin Hills Fault during deposition of the Upper Devonian rocks.

The Bobs Bore area is also important because the boulder and cobble conglomerates there were clearly deposited in deep water, probably deeper than 100 m. They interfinger with and overlie silty limestones of the basin facies of the Virgin Hills Formation, and exposures are of massive unbedded conglomerate, probably deposited as debris flows.

Menyous Gap area

Menyous Gap is thought to have originated as a large subglacial channel below the Early Permian ice sheet. Soon after the ice withdrew, the channel was filled with shale and sandstone of the Grant Group, which has since been removed through Cenozoic erosion (Fig. 301). Menyous Gap exposes the type section of the Pillara Limestone, consisting of a succession of shallowing-upward limestone cycles, as discussed elsewhere in this Bulletin (see also Read, 1973a,b; Hocking and Playford, 2001).

The section exposed in Menyous Gap belongs mainly to the back-reef and bank subfacies of the Pillara Range reef complex. The platform was generally bordered by a retreating margin, with only minor reef development, as exposed at and near the north entrance to the gap and at other localities along the margin to the northwest and southeast (Figs 107, 108, 112, 113). A prominent coral layer, dominated by *Disphyllum*, is exposed about 600 m south of the north entrance to the gap, on its western side (Fig. 37; AMG Zone 51, 799830E 7963570N).

Most details of the rocks on each side of the platform margin at the north entrance were obscured by dark microbial coatings. These have now been removed in places on the walls of the gap using hydrochloric acid, in order to allow more detailed observations. The reefal platform margin exposed at the north entrance to the gap (AMG Zone 51, 799890E 7964050N) is narrow — less than 50 m wide — and contains abundant massive and laminar stromatoporoids and large stromatactis cavities. The adjoining reefal-slope subfacies is massive, pinches out up the slope, and contains steeply sloping laminar sheets, each about 10 mm thick and as much as 0.5 m long, of the coral *Alveolities*, with some *Thamnopora* and other corals. Stromatactis shelter cavities occur below some of the coral sheets. Some 'zebra limestone', comparable with that at Lloyd Hill and the bioherm on the east side of the Emanuel Range, is also present in the reefal-slope deposits. The stromatactis cavities are filled with dark-red, yellow, and grey laminated micrite (lime mudstone), overlain by banded sparry calcite. Abundant brachiopods are present in some places.

Geopetal measurements in brachiopods and stromatactis cavities indicate that post-depositional tilting in the marginal-slope Sadler Limestone amounts to about 17°, which is the same as the tectonic dip evident in the adjoining platform deposits. The depositional dip was about 25° in the reefal-slope deposits and 15° to 20° in the fore-reef deposits, and the observed dip has been increased to 30° to 40° as a result of tectonic tilting.

One kilometre northwest of the northern entrance to Menyous Gap (at GPS AMG Zone 51, 799100E 7964500N) is a very well exposed upright-rollover platform margin (Fig. 107). In the platform on the southeast side of the gully, a narrow reefal rim is exposed in the lower part of the face, but thin-bedded bank deposits extend up to the margin in the upper part, before 'bending over' into the slope deposits. One of these beds in the bank deposits contains many corals, including large in-situ heads of *Argutastrea*. Fragmentary corals occur on the slope, where they are commonly overgrown by stromatoporoids. Above the coral horizon in the platform is a bed of laminar stromatoporoids, which 'bends over' passing down the slope, where stromatoporoids are partly in situ and partly detrital. Some of the matrix in the slope deposits is dolomitized.

On the northwest side of this gully (GPS AMG Zone 51, 799150E 7964735N) the contact between platform and slope is abrupt, forming a retreating margin (Fig. 385). The stromatoporoid bed on the slope consists of broken fragments of stromatoporoids, lacking the in-place forms that occur on the southeast side of the gully. A similar retreating margin is also exposed 1 km southeast of the northern entrance to Menyous Gap (Fig. 113).



Figure 385. Retreating platform margin 1 km northwest of the north entrance to Menyous Gap. Pillara Limestone forms the platform deposits and Sadler Limestone the marginal-slope deposits.

Mount Pierre area

Virgin Hills Formation, consisting of red and light-grey silty shale and sandy calcarenite grading to very fine-grained sandstone, is exposed 1.5 km east of Mount Pierre. It forms a north-northwesterly trending strip about 100 m wide and 750 m long beside Mount Pierre Creek (AMG Zone 51, 805500E 7975000N; Figs 386, 387). The rocks are subhorizontal and very thin bedded to laminated. They contain a deep-water fauna of conodonts (early Famennian *rhomboidea* Zone), ammonoids, crinoid columnals, occasional brachiopods, and a small solitary coral. The exposure resulted from the removal of a layer of grey-brown clayey soil, about 1 to 2 m thick, that formerly covered the Virgin Hills Formation beside the creek. The sheet erosion that removed this soil was apparently initiated by the grading of an airstrip during the 1970s, removing spinifex that had previously bound the soil together.

The layers of Virgin Hills Formation directly below the soil show very well-developed tepee structures (Figs 388–390). The structures are generally linear, having on average two crest directions, 060° and 160°. Some straight or curved lines of tepees are more than 100 m long. They outline approximate parallelograms, the larger ones averaging about 30 by 30 m, enclosing smaller examples averaging about 8 by 8 m (Figs 386–388). They may be localized by joints in the Virgin Hills Formation.

The origin of the tepees is thought to be linked with shrinking and swelling of the near-surface strata of the Virgin Hills Formation, caused by desiccation (with shrinkage) during the dry season and water saturation (with expansion) during the wet season. The shrinkage resulted in polygonal cracking of the weathered shales and clayey limestones (Fig. 391). The open cracks then filled with soil, so that when expansion of the strata occurred during the wet season the strata tended to slide along bedding planes, folding and fracturing the strata to form tepees, which were localized by former joints.

The tepees were very well exposed in 1992, when they were first photographed and mapped. At that time they may have been uncovered for only five to ten years, but since then continuing erosion has resulted in many being partly eroded away.

Similar, but less well-developed, structures are known in other localities in the south-eastern Lennard Shelf, where weathered Virgin Hills Formation is exposed below soil. Unlike tepees that have been described elsewhere in the world (and those in the Nullara Limestone), these structures have resulted solely from near-surface fresh-water weathering; they are unrelated to evaporitic conditions.

Well-developed symmetrical ripple marks are present in calcareous siltstone in the Virgin Hills Formation at this locality, trending 050° to 060°, with wave lengths of between 15 and 21 cm and amplitudes of 1 to 2 cm (Fig. 392). Horizons of asymmetrical ripple marks, with wave lengths of 10 to 15 cm, and amplitudes of as much as 1 cm, overlie the symmetrical ripple surfaces (Fig. 393). The asymmetrical ripples trend 160° and indicate water flow from the east-northeast. The Virgin Hills Formation at this locality was deposited in a basin setting, midway between the Pillara Range reef complex and the Hull Range to Horse Spring Range reef complexes, where water depths were at least 100 m and probably more than 200 m. Both symmetrical and asymmetrical ripples have been recorded from other deep-water settings below wave base (Allen, 1982; Higgs et al., 1998), but their origins remain equivocal. The symmetrical forms may have formed where mass flows set up local orbital vortices in deep water, while the asymmetrical forms must have resulted from linear currents flowing above the sea floor.

Pillara quarry

The Pillara quarry, situated in the southwestern part of the Limestone Billy Hills (AMG Zone 51, 789060E 7967750N), is approximately 85 m long, 35 m wide, and as much as 11 m deep. It was excavated for road-building purposes in reefal Pillara Limestone (platform facies) and fore-reef Sadler Limestone (marginal-slope facies).

The Pillara Limestone in the quarry is composed of massive microbial (fenestral) limestone, capped by a unit of bulbous-stromatoporoid limestone (Figs 267–272). The Sadler Limestone, which abuts and overlies the Pillara Limestone, consists of interbedded reef-derived breccia, thin dark-grey to black shale, and in-situ layers of tabular and bulbous *Actinostroma*. The breccia consists largely of masses of broken corals (*Alveolites* and *Thamnopora*) and stromatoporoids. The Sadler Limestone dips at as much as 37°, of which at least 30° is depositional.

The platform margin exposed in the quarry is mainly retreating, with fore-reef Sadler Limestone extending progressively back over the platform (Figs 267–269). The reef limestones are mineralized, especially in the uppermost four to six metres. Joints in the Pillara Limestone were enlarged by deep subsurface solution, providing space for the precipitation of iron, zinc, and lead sulfides and sparry calcite (Figs 267–272). Jointing does not extend into the overlying Sadler Limestone, apparently because shales in that formation allowed the interbedded limestone beds to adjust to stress without fracturing. The sulfides consist primarily of marcasite (now oxidized to dark-brown iron oxide), with minor sphalerite and galena.

Some slabs of tabular stromatoporoids from the Sadler Limestone show concentric growth lines on their undersides (Fig. 394), and parts of those surfaces are encrusted with solitary tube worms and bryozoans (Fig. 395). Similar features have been observed on the undersides of tabular stromatoporoids in some deeper-water (coralline) parts of platform cycles in central Menyous Gap.

Henwood Spring area

The Frasnian–Famennian boundary is well exposed in platform facies 2.1 km west of Henwood Spring (AMG Zone 52, 200900E 7981500N; Fig. 396). An isolated mass

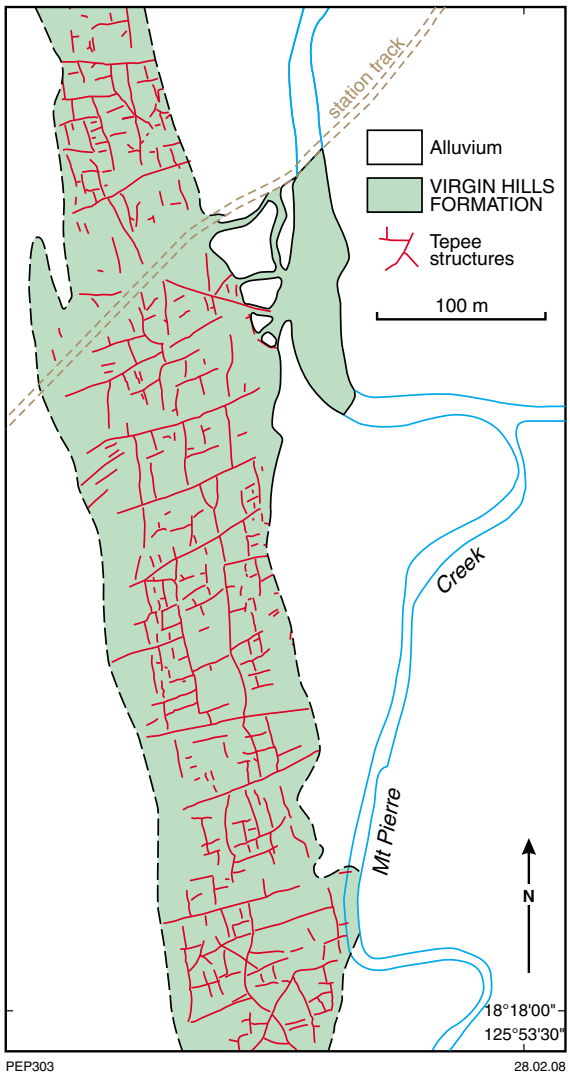

Figure 386. **Geological map of a locality 1.5 km east of Mount Pierre, adjoining Mount Pierre Creek, where orthogonal networks of recent tepee structures are developed in Famennian Virgin Hills Formation.**

Figure 387. **(below) Aerial view of the locality shown in Figure 386, looking northwest, showing the orthogonal networks of tepee structures.**





Figure 388. View of the surface of the Virgin Hills Formation at the locality shown in Figure 386, taken when the soil cover had only recently been eroded away, exposing the crests of tepee structures. The tepees formed in siltstones by shrinkage during the dry season followed by expansion during the wet season.



Figure 389. Tepee in sandy calcareous siltstone of the Virgin Hills Formation at the locality shown in Figure 386.



Figure 390. Tepee in sandy calcareous siltstone of the Virgin Hills Formation at the locality shown in Figure 386.

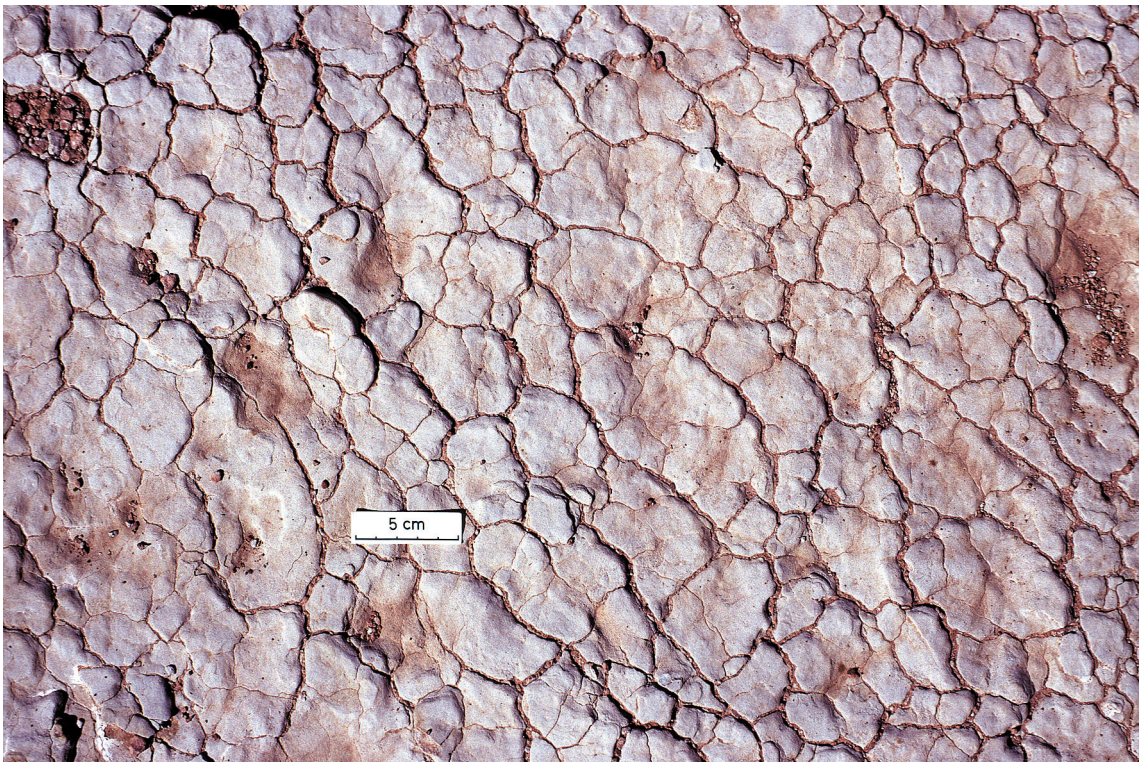

Figure 391. The surface of a bed of calcareous siltstone between tepees in the Virgin Hills Formation, at the locality shown in Figure 386, showing polygonal joints filled with sandy clay. The siltstone, which is water saturated during the wet season, becomes desiccated during the dry season, causing it to shrink and crack open. The cracks then become filled with sediment, so that when the bed again becomes water saturated and expands, it results in compression and folding into tepee structures.

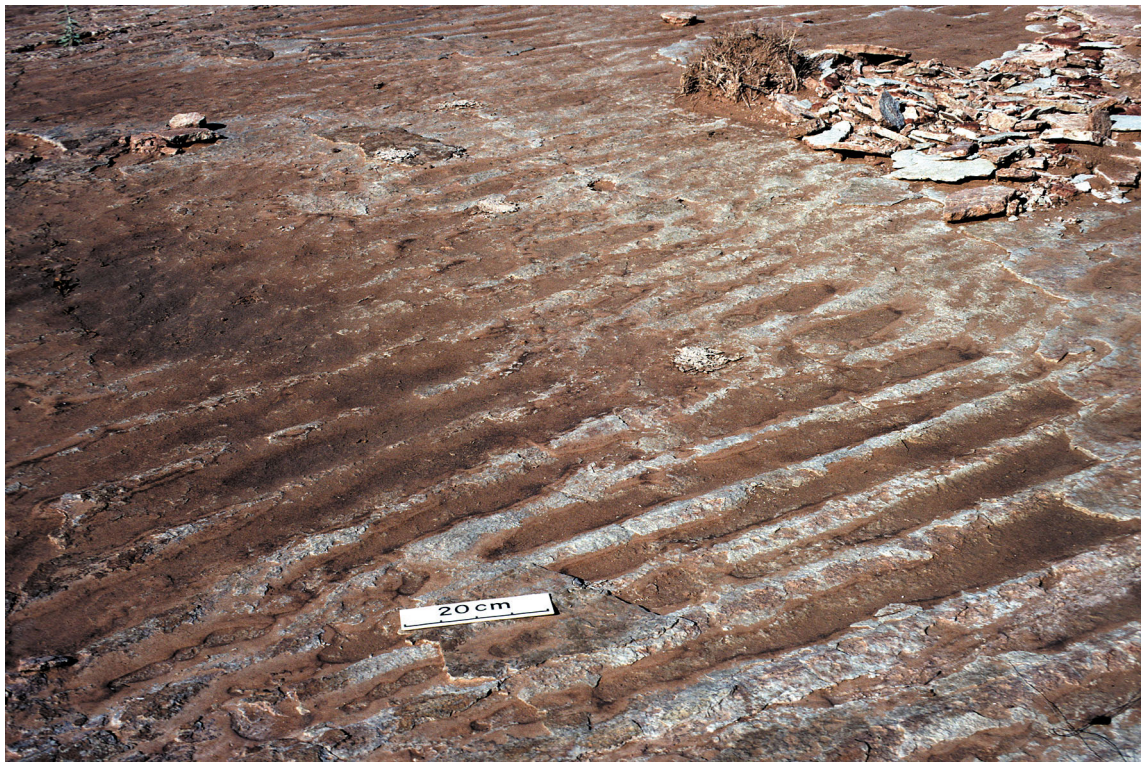

Figure 392. Symmetrical ripple marks in sandy calcareous siltstone of the Virgin Hills Formation at the locality shown in Figure 386.



Figure 393. Asymmetrical (current) ripple marks, with the flow direction towards the left, in sandy calcareous siltstone of the Virgin Hills Formation at the locality shown in Figure 386.

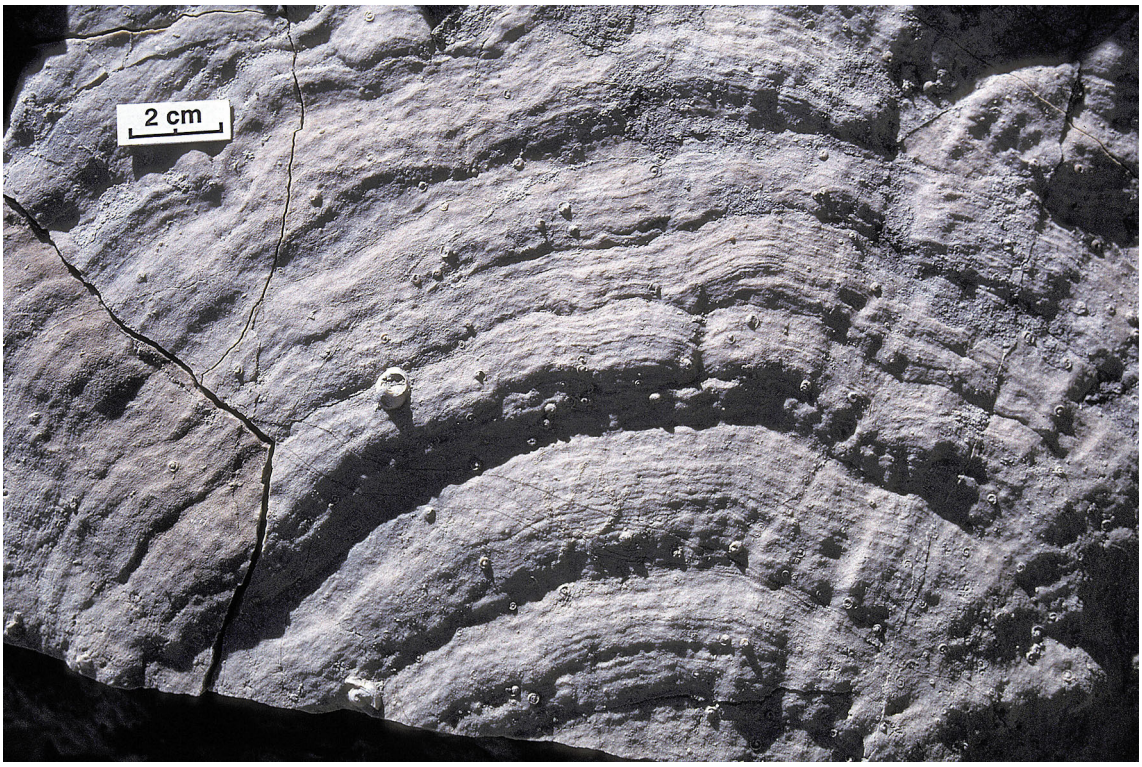

Figure 394. Underside of a tabular-stromatoporoid colony from the Pillara Limestone in the Pillara quarry. The photo shows growth bands in the stromatoporoid, and small tube worms that were attached to the underside of the colony.

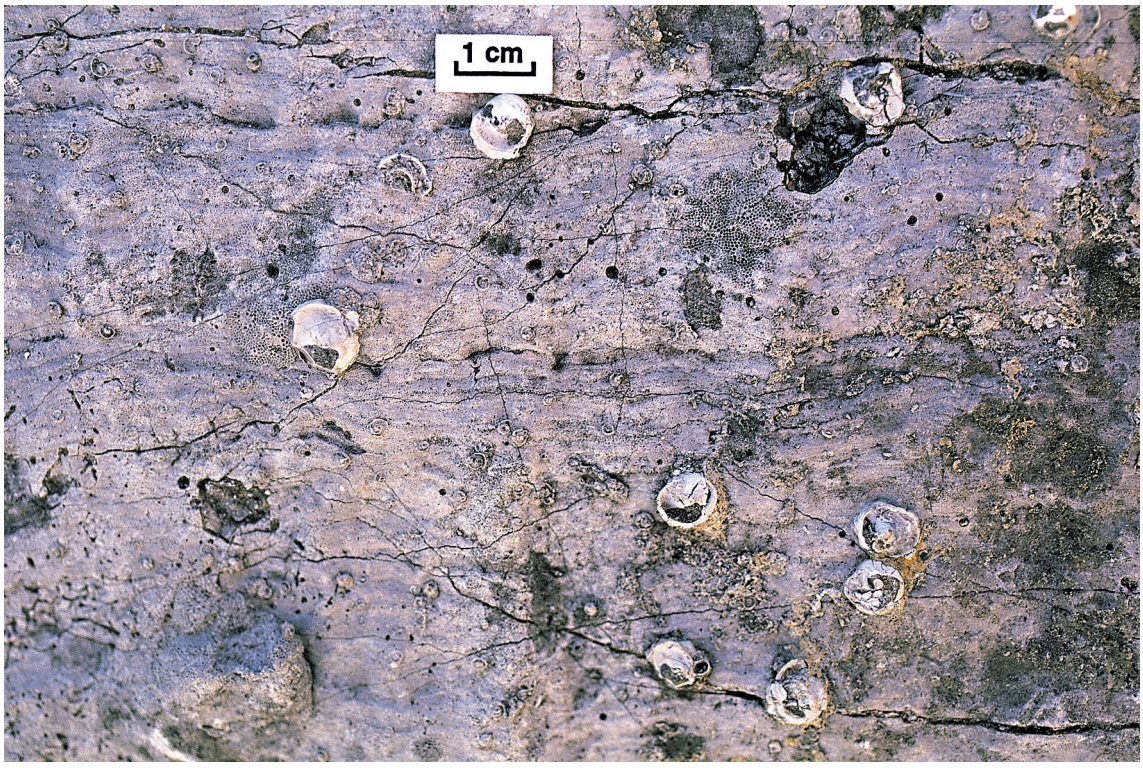

Figure 395. Close-up view of the stromatoporoid colony shown in Figure 394: underside of a tabular-stromatoporoid colony from the Pillara Limestone in the Pillara quarry. The photo shows growth bands in the stromatoporoid, and small tube worms that were attached to the underside of the colony, showing numerous tube worms and fenestellid bryozoans that were attached below the colony.

of latest Frasnian Pillara Limestone (Pillara Sequence 6), mainly reef-margin subfacies but with minor back-reef subfacies, is overlain unconformably by conglomerate at the base of the Nullara Limestone, which is in turn overlain by cyclic back-reef subfacies in that formation.

At this locality the Pillara Limestone, which contains abundant stromatoporoids (*Actinostroma*), is interpreted to have grown almost horizontally, advancing (prograding) over marginal-slope facies. Successive positions of the reef front are marked by near-vertical to overhanging layers of stromatoporoids (GPS AMG Zone 52, 200700E 7981350N; Figs 27, 397). The reef can be seen to have advanced by at least 30 m in this outcrop. Red dolomite forms the matrix between stromatoporoids. Some cavities, thought to have been left after the decay of sponges or other organisms, were lined with *Renalcis* before being filled with lime mud and sparry calcite. Measurements were made of 23 geopetal cavity fillings, showing that the average tilt to the north is 8.7°, which approximates the dip of the overlying Nullara Limestone

A strong paleokarst surface truncates the Frasnian stromatoporoid reef, above which is siliciclastic pebble and cobble conglomerate at the base of the Famennian Nullara Limestone (Figs 397, 398). The conglomerate, which fills karst depressions and caves as much as 1.5 m deep that formed in the Frasnian reef, is overlain by fenestral limestone with lesser interbeds of pebble conglomerate and sandy to conglomeratic limestone of the back-reef Nullara Limestone (Figs 396–399). The Frasnian–Famennian boundary is placed at the base of the conglomerate, although there are no age-definitive fossils in the conglomerate.

Rattigan Rocks area

Rattigan Rocks is the largest group of allochthonous blocks known on the Lennard Shelf. At least 15 enormous blocks, the largest being more than 200 m across, are present at this locality in the lowermost Virgin Hills Formation, immediately above Sadler Limestone (Fig. 400). The blocks extend northerly for about 3.8 km and southeast–northwest for about 2.6 km, over an area of some 10 km². The largest blocks (e.g. north of Shady Spring, at AMG Zone 52, 194700E 7977300N) are the furthest west, and thus most distant from the presumed source of the blocks to the northeast. Most of the large blocks are of Frasnian reefal limestone, but one consists of *Amphipora* back-reef limestone, which suggests that the platform from which it was derived had been subjected to subaerial exposure and cementation prior to its collapse, because extensive early marine cementation did not occur in such back-reef limestones. The flat-lying Virgin Hills Formation containing the allochthonous blocks grades eastward into Elma Conglomerate. Some blocks are encrusted by thin layers of red stromatolitic limestone, dated as Frasnian Zone 10 to lower Zone 11 (G Klapper, 2004, written comm.).



Figure 396. Vertical aerial view looking east, 2.1 km west-northwest of Henwood Spring, showing the unconformable contact between massive Frasnian reef limestone (Pillara Limestone) on the right and well-bedded Famennian back-reef limestone (Nullara Limestone), interbedded with Elma Conglomerate, on the left.

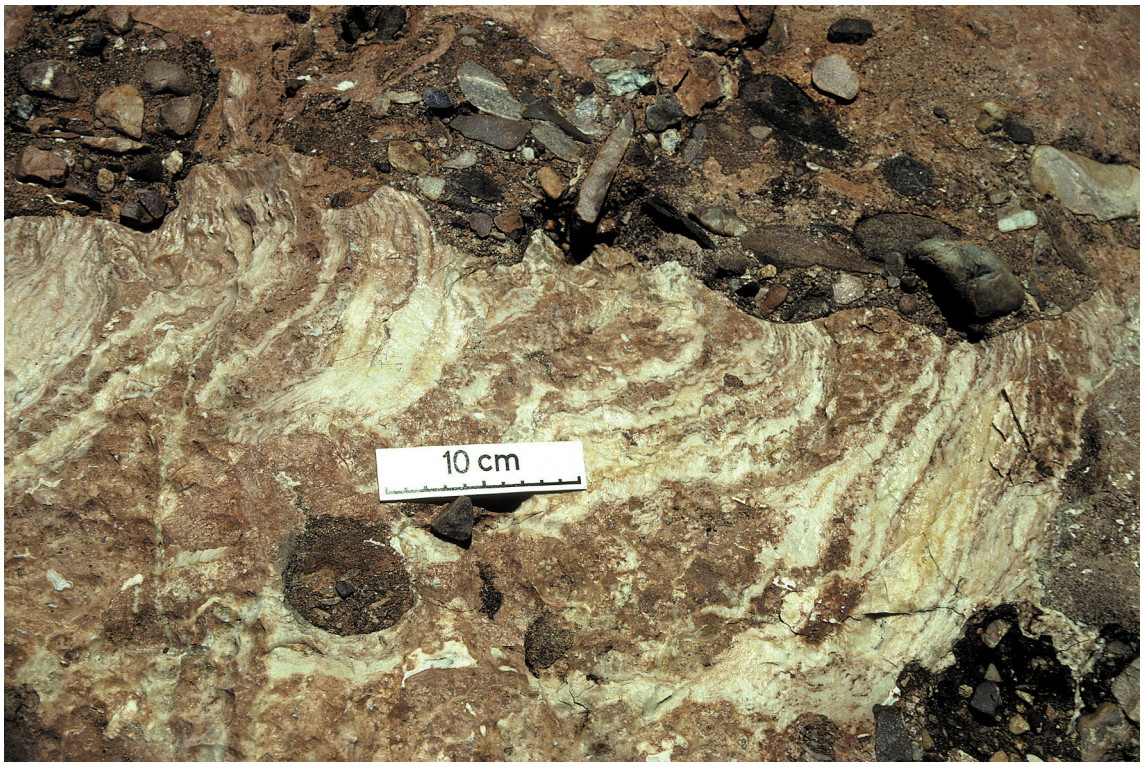

Figure 397. The Frasnian–Famennian unconformity 2.1 km west-northwest of Henwood Spring. Frasnian reef (Pillara Limestone), with steeply inclined sheets of a stromatoporoid, is overlain by fan-delta conglomerate at the base of the Famennian Nullara Limestone. The conglomerate fills a karst cavity in Pillara Limestone.



Figure 398. Conglomerate at the base of the Nullara Limestone (Famennian), filling karst cavities in reef-margin subfacies of the Pillara Limestone (Frasnian) in the area shown in Figure 396.



Figure 399. Conglomerate interfingering with basal Nullara Limestone, near the centre of the view shown in Figure 396.



Figure 400. Aerial view of Rattigan Rocks looking northwest, showing huge allochthonous blocks of Frasnian Pillara Limestone at the base of the Frasnian part of the Virgin Hills Formation. Elma Conglomerate is present below the rounded hills in the top right part of the photo.

The blocks must have resulted from the large-scale collapse of a nearby platform margin, apparently associated with the Waggon Pass Event at the base of Pillara Sequence 4 (Frasnian Zone 6). That event clearly coincided with the beginning of deposition of the Virgin Hills Formation. The huge blocks slid, rolled or were carried in debris flows, to the base of the marginal slope. The blocks probably stood above the sea floor long enough for some to become encrusted by deep-water stromatolites, before being buried by conglomerate or distal marginal-slope deposits of the Virgin Hills Formation. The eastern part of the group of blocks was overwhelmed by deep-water cobble and boulder conglomerates of the Elma Conglomerate, but the conglomerate may not have extended over the westernmost blocks near Shady Spring.

Stony Creek area

The Stony Creek area is an important locality for studying relationships between Devonian conglomerates and associated reef complexes. The small horseshoe-shaped reef complexes (half atolls) in this area grew around alluvial-fan and fan-delta conglomerate bodies that developed along the faulted basin margin (Figs 401, 402). Reef-margin, reef-flat, and back-reef limestones interfinger directly with the conglomerates and clearly wrap around the fan-shaped bodies, so that the reef platforms have characteristic horseshoe shapes, bounded on their northeast sides by the Stony Creek Fault (Figs 402, 403). Some of the deep-water conglomerates laid down as submarine fans interfinger with fore-reef and basin deposits of the Virgin Hills Formation. Granitic clasts dominate in the conglomerates (Fig. 404).

The Stony Creek Fault evidently moved as a normal fault during the Devonian, resulting in a fault scarp that sourced the Stony Creek Conglomerate as a series of alluvial fans, fan deltas, and submarine fans. Fault movement continued after the reef complexes were deposited. The fan-delta parts of the conglomerate bodies consist of a succession of cycles (Fig. 202). The conglomerates form coarsening-upwards cycles, with recessive-weathering granule conglomerate 1–2 m thick at the base and pebble or boulder conglomerate at the top of each cycle. The cycles are each about 10–15 m thick.

The Virgin Hills Formation associated with the coeval reef complexes and conglomerates in this area has been dated using conodonts as Zones 5–7 of the early to middle Frasnian (G Klapper, 2004, written comm.). The succession is regarded as being part of Pillara Sequence 4. The platform limestones are rich in stromatoporoids, including species of *Actinostroma, Stachyodes,* and *Amphipora*.

Stromatoporoid and microbial limestones commonly encrust clasts in the Stony Creek Conglomerate in the zone of interfingering between reef-flat limestones and fan-delta conglomerates (Fig. 404). The interfingering conglomerates and limestones are cyclical, with platform limestone at the base of each cycle overlain by conglomerate. Those cycles range from about 5 to 10 m in thickness. Somewhat thicker cycles, 10 to 15 m thick, are commonly evident in conglomerates that lack interfingering limestones. Each conglomerate cycle has poorly exposed granule conglomerate at the base, coarsening upward into boulder conglomerate with granitic boulders as much as 1.5 m in diameter at the top (Fig. 202).

Holmes and Christie-Blick (1993) claimed that the platform and marginal-slope facies of the Stony Creek reef complex are truncated by a major sequence boundary (see their fig. 12), but they did not give any valid evidence to support this hypothesis, and their model cannot be reconciled with the geology known from our field observations. In Holmes and Christie-Blick's (1993) key area (north of Stony Creek Bore, around AMG Zone 51, 816100E 8013500N) we have mapped east-dipping conglomerate extending from the Stony Creek Fault to the northeast and interfingering with platform carbonates (Plate 3). The eastward dip of the conglomerates is attributed to syndepositional faulting along the Stony Creek Fault. Further to the southeast, north of 600 Bore (around AMG Zone 52, 184500E 8011300N), east-dipping conglomerate cycles fill a west-trending fault compartment. The consistent eastward dip and cyclic nature may suggest syndepositional westward movement above a basal glide plane, as with the Galeru Member of the Sparke Conglomerate**.**

Horse Spring Range area

The Horse Spring Range consists of a tilted platform of Pillara Limestone overlying Precambrian schist, and fringed by Frasnian and Famennian fore-reef deposits of the Sadler Limestone and Virgin Hills Formation. The block of Pillara Limestone dips to the northeast at 10° to 25° and is extensively faulted, most faults trending north and branching off larger faults that trend north-northeast (Plate 3). All faulting is thought to be normal.

The Sadler Limestone in the area near Horse Spring consists of massive breccia, containing large cavities filled with red limestone similar to that in the deep-water Virgin Hills Formation that overlies the formation (Fig. 405). Blocks of reefal limestone at the top of the breccia are coated in places by stromatolites and *Frutexites*. The Frasnian–Famennian boundary in this area, as determined by conodonts (G Klapper, 2004, written comm.), is in the Virgin Hills Formation at the base of a Famennian fore-reef breccia over Frasnian laminated red distal fore-reef limestones (Fig. 103; GPS AMG Zone 52, 185900E 7985490N).

Horseshoe Range area

Most of the Horseshoe Range is occupied by a thick (468 m) section of Nullara Limestone, with thin very poorly exposed Fairfield Group lying above that formation. These units are folded into a large syncline against the Painted Rocks Fault (hence 'Horseshoe Range') and a smaller syncline against the Mount Elma Fault (Plate 3; Fig. 225). Both faults are thought to have had normal displacements, and have moved during the Devonian and since the Early Permian. Sandstones of the Grant Group are cut by the Mount Elma Fault, with fault drag suggestive of normal movement at the exposure 5 km northwest of Blood Yard (AMG Zone 52, 207000E 7990700N). Both of these

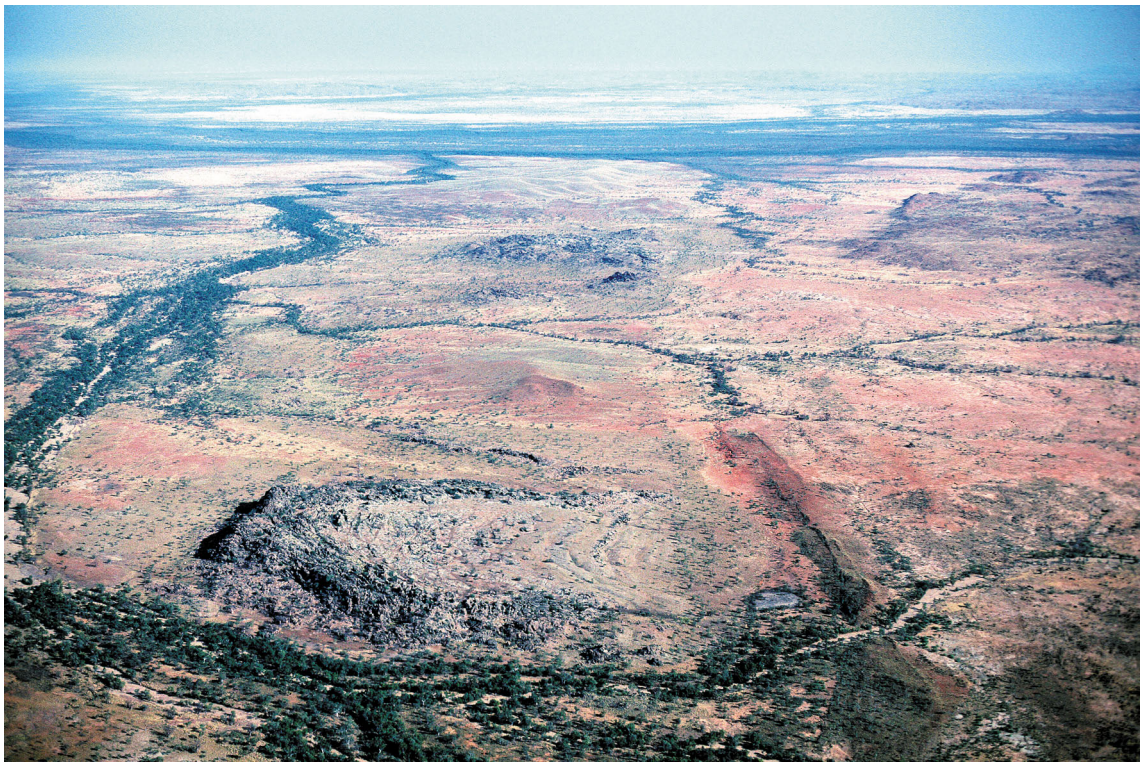

Figure 401. Aerial view looking northwest in the Stony Creek area, showing u-shaped reefal platforms of Pillara Limestone that grew beside the Stony Creek Fault. One of the platforms (in the middle distance) grew around an alluvial fan of Stony Creek Conglomerate.



Figure 402. Aerial view looking east in the Stony Creek area, showing reddish-coloured Stony Creek Conglomerate (lower left), interfingering with reef-margin, reef-flat, and back-reef Pillara Limestone (left foreground to middle distance), and the u-shaped reefal platform shown in Figure 403 (middle background). These deposits were laid down against an active fault, the Stony Creek Fault (middle left to top).



Figure 403. Aerial view looking north-northeast in the Stony Creek area, over the u-shaped reefal platform shown in Figure 402. The dark limestone in the foreground and around the sides of the platform consists of reef-margin and reefal-slope limestone, while the dish-shaped bedded limestone in the central part consists of back-reef limestone.

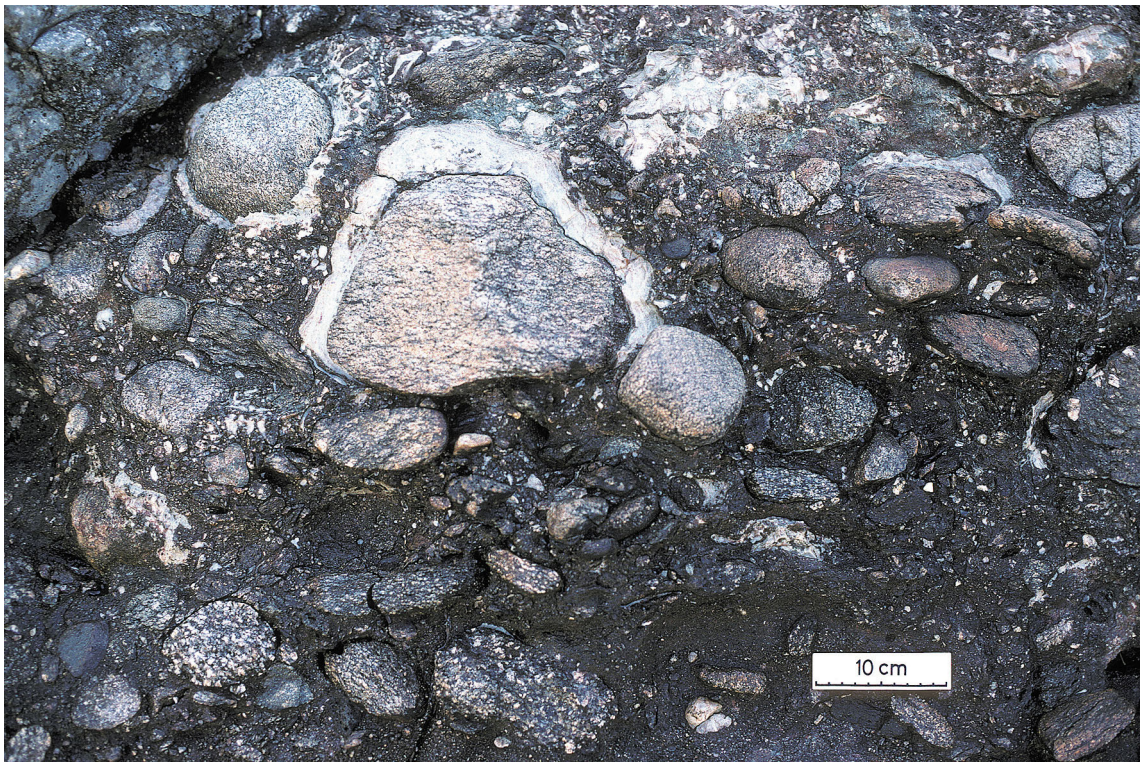

Figure 404. Cobble of granite encrusted by a stromatoporoid colony in the Stony Creek Conglomerate, shown in Figures 401 and 402, that interfingers with reef of the Pillara Limestone.



Figure 405. Cavity filling of Virgin Hills Formation in fore-reef megabreccia of the Sadler Limestone near Horse Spring.

large faults trend northerly and dip west. Movement on the faults increased to the north, on two relay ramps linking the Mount Elma Fault to the Painted Rocks Fault, and the fault at the west end of Guppy Hills. Fault shattering of Devonian and Proterozoic rocks associated with the Mount Elma Fault is exposed 4 km west-northwest of Blood Yard Bore (AMG Zone 52, 207300E 7990200N), where there are also indications of submarine fissuring and infilling by Devonian limestone along the fault plane.

The uppermost Nullara Limestone exhibits well-developed polygonal shallow tepees, one to two metres wide, in the core of the syncline about 2.5 km west-northwest of Mount Elma (Fig. 63; AMG Zone 52, 203760E 7984530N). Tepees are also present, but not so well expressed, lower in the Nullara Limestone along the main southern face of the Horseshoe Range (AMG Zone 52, 204300E 7982600N). Metre-scale cyclicity is well developed at some levels in the Nullara Limestone but others show no obvious signs of cyclicity. The cyclic nature of the lower Nullara Limestone is seen along the southeast side of the range (e.g. AMG Zone 52, 206200E 7983600N), where the formation interfingers with conglomerate of the Elma Conglomerate. Desiccation cracks can be seen in fenestral limestone at cycle tops, over conglomerate that forms the deepest parts of the cycles.

Shady Bore block

The Shady Bore block is an elongate mass of Pillara Limestone, about one kilometre long and one kilometre wide (Fig. 406), that dips steeply north (35° to 60°) and is overlain with angular unconformity by deep-water facies of the Virgin Hills Formation. The block is thought to be bounded on either side by northerly trending faults (Plate 3). The Pillara Limestone consists largely of stromatoporoid–microbial limestone, forming prominent cycles, each with an average thickness of 3.5 m (Fig. 407). These are similar to cycles known elsewhere in the lower Pillara Limestone, for example at Guppy Hills and Horse Spring Range, although the silty lower parts of cycles in those areas are commonly absent in the Shady Bore cycles. In those cycles, thin discontinuous silty limestone at the base is followed by massive bulbous stromatoporoid limestone overlain by medium-bedded *Stachyodes* and *Amphipora* limestones, with recessive, thin-bedded, strongly stylolitized, fenestral limestones at the top. No clear trends can be discerned in cycle thicknesses.

At least half of the observed tilting of the block of Pillara Limestone, which amounts to as much as 60°N, must have taken place in middle to late Frasnian times, prior to deposition of the overlying Virgin Hills Formation, as demonstrated by observed geopetal structures in both formations. Neptunian dykes of red micrite, derived from the Virgin Hills Formation, extend deep into the Pillara Limestone. No precise date has been obtained for the Pillara Limestone at this locality, but the age of the overlying Virgin Hills Formation is late Frasnian (Zones 11–13, G Klapper, 2004, written comm.). The Pillara Limestone here must be significantly older (probably early to middle Frasnian).

The block of Pillara Limestone is fault bounded against basement on the east, along a continuation of the Black Hills Fault, and on the west by an un-named fault (Plate 3). The block may have been faulted and rotated in late Frasnian times, before being overlapped by the Virgin Hills Formation. Tectonic rotation of the Pillara Limestone in this block, amounting to at least 30°, must have occurred during the Frasnian, prior to deposition of the Virgin Hills Formation. A similar amount of rotation has taken place since then, involving both formations. An alternative interpretation is that the Pillara Limestone at Shady Bore forms a gigantic allochthonous block. If so, the block must have slid or rolled from near sea level to considerable water depths (possibly several hundred metres), prior to deposition of the Virgin Hills Formation.

Faulting and steep tilting of the Pillara Limestone, prior to deposition of the Virgin Hills Formation, can possibly be shown to have occurred elsewhere along the Black Hills Fault and associated faults in the Minnie Pool area (AMG Zone 52, 187300E 7967900N). We are unsure about interpretation of the structure in this area. The area is strongly faulted, but it is debatable whether observed features of the geology can be explained by faulting and folding alone. A possible interpretation is that the Pillara Limestone in the eastern part of the exposure shown in Figure 408 (AMG Zone 52, 188400E 7967000N) rests with strong unconformity on older Pillara Limestone. It seems clear that faulting and steep tilting of the Pillara Limestone in this area preceded deposition of the Virgin Hills Formation. Unfortunately, high spinifex obscured details of critical outcrops on the two occasions when this locality was examined. If further work is carried out there to clarify the geology, it needs to take place after the area has been burnt.

Strong Frasnian tectonism is also evidenced by the presence in conglomeratic units (e.g. Sparke Conglomerate) of clasts of Pillara Limestone containing well-developed stylolites (Fig. 176). These occurrences suggest that prior to its exhumation and erosion, a Pillara Limestone platform could have been buried to depths sufficient to generate stylolites. Alternatively the stylolites may have resulted from tectonic stress in a platform of Pillara Limestone that was later eroded to supply blocks to the conglomerate.

It is uncertain where the early tectonic episode evidenced in the Shady Bore and Minnie Pool areas can be placed within the sequence-stratigraphic framework (Fig. 20). The episode may correlate with the Waggon Pass Event, or alternatively with either the Kellys Pass Event or the Algae Creek Event.

Brooking Springs area

A network of small neptunian dykes in reef-margin and reef-flat limestones is exposed 2.3 km north of Brooking Springs Homestead (GPS AMG Zone 51, 779620E 7997990N; Figs 150, 151), close to a prominent fault that is thought to have been active in Devonian times. Most

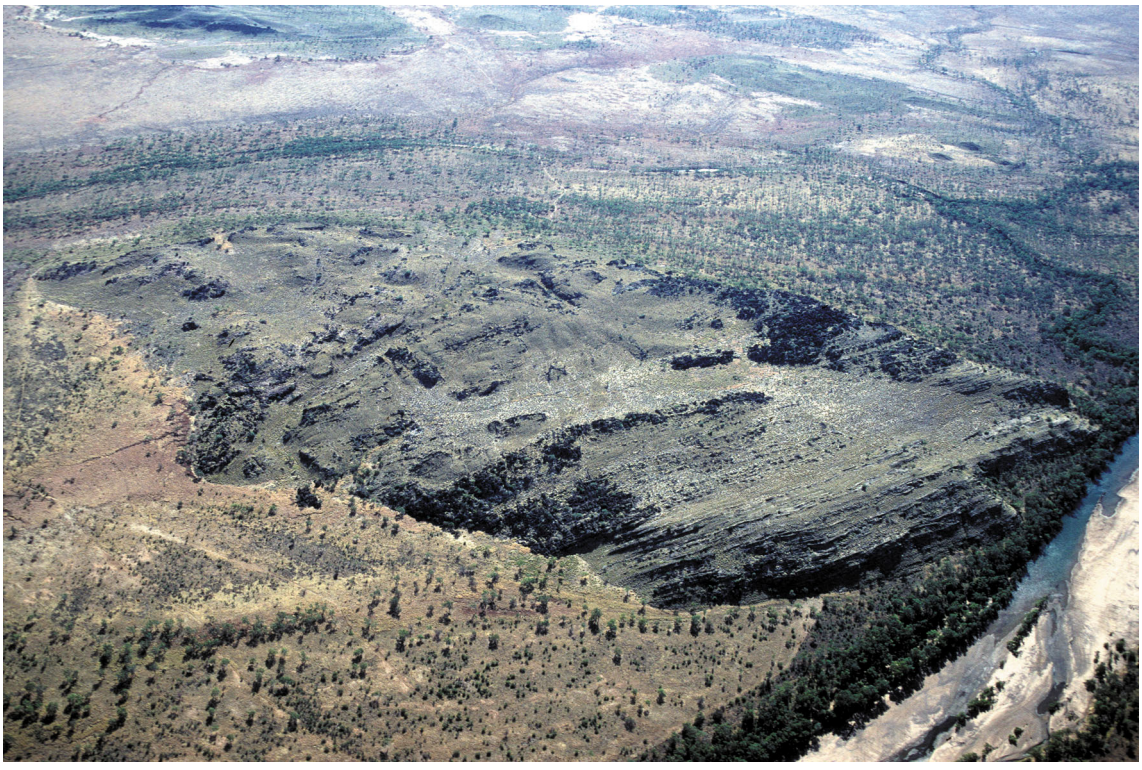

Figure 406. Aerial view of the Shady Bore block, looking east. Steeply dipping Pillara Limestone (right to centre) is overlain with angular unconformity by more gently dipping Virgin Hills Formation (centre to left).



Figure 407. Cyclicity in steeply dipping Pillara Limestone near Shady Bore. The cycles have an average thickness of 3.5 m, beginning with a recessive silty limestone (discontinuous and rarely exposed), followed successively by massive to thick-bedded bulbous stromatoporoid limestone, medium-bedded *Amphipora–Stachyodes* limestone and (at the top) massive to thin-bedded, strongly stylolitized, fenestral limestone. Note the person (lower right) for scale.



Figure 408. Aerial view looking northeast over a faulted area beside the Black Hills Fault in the Minnie Pool area, showing steeply dipping cyclic-bedded Pillara Limestone (middle and foreground), that appears to be overlain unconformably by younger Pillara Limestone (the massive limestone in the middle). The Pillara Limestone is in turn overlain unconformably by Virgin Hills Formation.

of the dykes were filled or partly filled with *Renalcis* limestone, which lined the walls of the dykes and was commonly followed by precipitation of banded fibrous sparry calcite. Gastropods partly fill some of the fissures (Fig. 409). Repeated fissuring occurred, successive fissures being filled by the same types of limestone. Clearly there was rapid submarine cementation of both reef limestones and neptunian dykes.

A wide north-trending zone of neptunian fissuring, with sparry fillings, outcrops about 1 km east of Mad Russian's Well (around GPS AMG Zone 51, 780700E 8000100N to 780700E 8000200N). Fissures locally have brecciated fillings, and there is some stromatolitic growth into the fissures, with intricate patterns of growth, brecciation, and regrowth (Figs 162, 163).

Two types of stylolites occur in limestones of this area — horizontal stylolites with vertical teeth, and later steeply dipping stylolites with subhorizontal teeth. The steeply dipping stylolites strike at 020° and the teeth are directed towards 135° (as seen on horizontal outcrops). Some steeply dipping stylolites are also associated with neptunian dykes that were subsequently sheared, with faults having left-lateral displacements (Fig. 227).

The reef-margin and reef-flat deposits at this locality consist mainly of massive to poorly bedded fenestral (microbial) limestones, with scattered to abundant megalodont bivalves, many of which are essentially in their growth positions.

Geikie Gorge

Geikie Gorge was named (as 'Geikie Cañon') by Hardman (1884) after Sir Archibald Geikie, then the Director of the Geological Survey of Great Britain. Hardman's sketch of the south entrance to the gorge is shown as Figure 410. The gorge is occupied by the Fitzroy River, which cuts through the Geikie Range reef complex, and exposes an excellent section, as described by Playford (1981) and Wallace (1987; Figs 29, 32, 139, 174, 308, 411–421). The gorge, about 13 km long, may have originated as a subglacial channel below the early Permian ice sheet. It is divided into two sections, of approximately equal length, by the eastern extension of Copley Valley Embayment. Most of the gorge is included in Geikie Gorge National Park.

The limestone walls of the gorge are generally about 30 m high. They have been cleaned and smoothed by floods to a height of about 10 m above the normal dry-season (winter) river level, and the structure and composition of the limestone are clearly displayed on the smooth surfaces. Above the flood level the limestone has its usual coating of dark-grey epilithic microbes, which obscure details of the lithology (Figs 413, 414, 417).

The modern fauna of Geikie Gorge includes sawfish and stingrays. Such fish are normally marine but here they are fully adapted to the freshwater environment. Their ancestors must have moved progressively up the Fitzroy River during times of flood, until they reached this gorge, some 300 km from the sea.

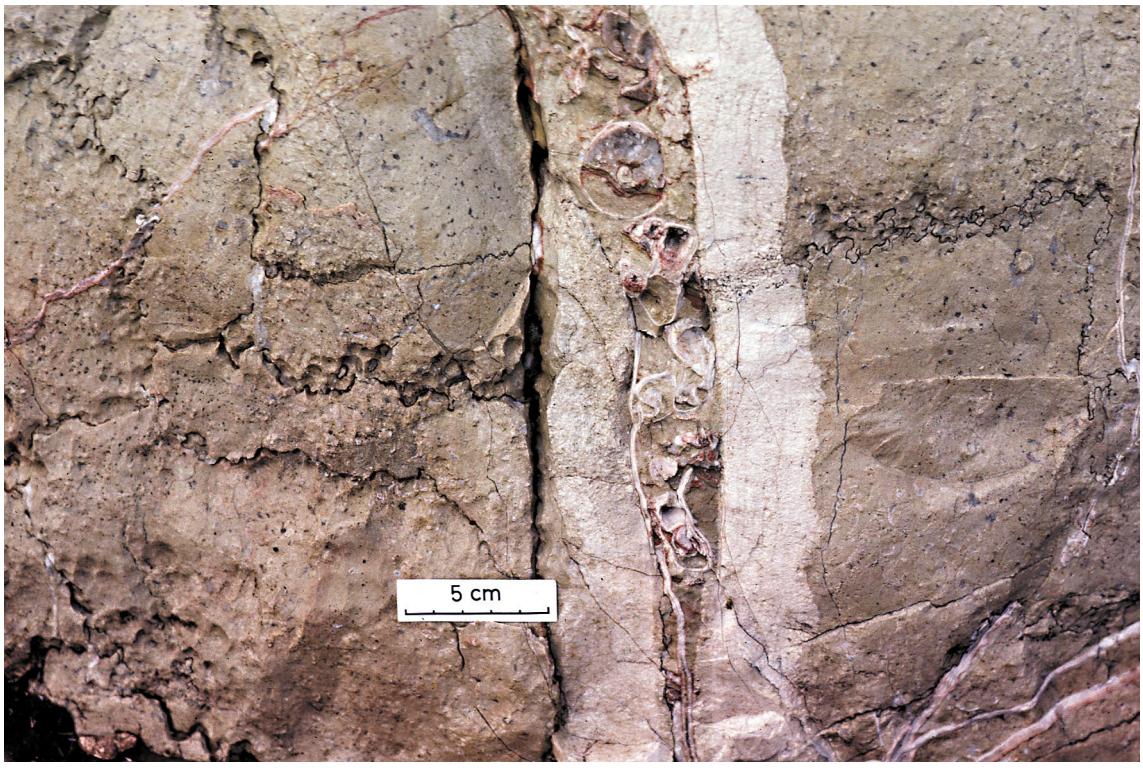

Figure 409. Neptunian dyke in reef-margin limestone of the Pillara Limestone, 4 km north-northeast of Brooking Springs Homestead, showing dense *Renalcis* lining the fissure walls, and gastropod-bearing sediment filling the rest of the fissure.

Most of Geikie Gorge is cut through middle to late Frasnian platform facies (Pillara Limestone), with narrow reef-margin and/or reef-flat subfacies rimming back-reef subfacies (Figs 29, 411, 415, 416). The back-reef deposits in the lower (southwestern) part of the gorge are largely fenestral limestones, with few stromatoporoids, whereas those in the upper (northeastern) part are dominated by stromatoporoid limestones. The Copley Valley Embayment is occupied by marginal-slope and basin facies of the Virgin Hills Formation, and is almost entirely enclosed by platforms, with small gaps to the east and west.

A classic section through fore-reef, reefal-slope, reef-margin, reef-flat, and back-reef subfacies of the Pillara Limestone is exposed 1.1 km north-northeast of Sheep Camp Yard (AMG Zone 51, 790200E 8003000N; Fig. 411). There, the fore-reef limestones were partly dolomitized soon after deposition, but the dolomite has since been transformed into dedolomite. The fore-reef deposits contain prominent blocks of reef limestone, as much as several metres across. One allochthonous block shows a 'double geopetal' filling of a large stromatactis cavity (Fig. 139). The first generation of infilling, consisting of laminated micrite, was introduced when the block was in place in the reef margin, and the subsequent sediment was emplaced after the block broke away from the platform and gradually settled into its present position on the marginal slope. The present horizontal is indicated by the horizontal contact at the base of the final filling of light-coloured sparry calcite.

Moving up the marginal slope towards the platform, the intensity of dolomitization declines as the amount of marine cementation increases. The reefal-slope deposits, with *Renalcis*, *Sphaerocodium*, in-situ stromatoporoids, corals, sponges, microbial layers, and stromatactis (Fig. 418), were subject to early marine cementation, and consequently they remained largely undolomitized. Several neptunian dykes cut the early cemented reefal-slope and reef-margin limestones, one prominent example being situated in reefal-slope deposits close to the platform margin.

The platform margin at this locality is an upright-rollover margin, with lenses of *Renalcis* limestone 'rolling over', from horizontal in the reef margin to dipping in the reefal slope (Fig. 412). *Renalcis* is abundant in the outer part of the reef, and accompanies *Sphaerocodium* in the reefal slope. The reef margin itself, which is massive and essentially undolomitized, is about 50 m wide. The reef-flat subfacies, of similar width, is bedded and largely undolomitized, containing the stromatoporoid *Stachyodes* together with *Renalcis*. Behind it are well-bedded dolomitized back-reef deposits with high mouldic porosities, the moulds having formed by solution of *Amphipora* and *Actinostroma* (Fig. 419). Dolomite, which increases passing from the reef flat into the back reef, is now converted to dedolomite, perhaps resulting from a reaction with high-pressure, very low-temperature, subglacial meltwater below the Early Permian ice sheet. Moving further upstream in the back-reef deposits, away from the platform margin, the intensity of dolomitization steadily decreases, eventually passing into typical limestones of the back-reef subfacies.

A large cavern, partly filled by equant transparent sparry calcite, is present about 80 m north of the platform margin (AMG Zone 51, 790500E 8003300N). This cavern was probably developed by subglacial solution below the Early Permian ice sheet, and the equant spar may be of similar age. It seems possible, although surprising, that much of this cavern has remained open since the Early Permian.

About 2.5 km south-southwest of Sheep Camp Yard at *Bulyurngari* (Plate 3), there is a well-exposed upright-scarp platform margin, which apparently coincides with a neptunian dyke filled with oolite (Figs 308, 415, 416). Most of the original reef margin apparently broke away to form blocks in the marginal-slope facies. The massive reef margin remaining behind the scarp is only about 2 m wide, consisting of *Renalcis*–*Sphaerocodium*–microbial limestone. It passes into crudely bedded reef-flat subfacies, approximately 150 m wide, which consists of bedded fenestral stromatolitic limestone with a few stromatoporoids, and in turn grades into well-bedded back-reef fenestral limestone. The reef-flat limestones are cut by several neptunian dykes and a neptunian sill that was partly lined with *Renalcis*. Some prominent neptunian dykes cut the back-reef fenestral limestones further downstream in the gorge, testifying to relatively early cementation.

The back-reef limestones are commonly strongly stylolitized where high porosity remained in lime muds at the time of burial (Fig. 33). However, in some cases, strong early cementation occurred in lenticular beds of back-reef lime muds (Fig. 421), and small-scale neptunian fissuring developed in such limestones after compaction of surrounding muds (Fig. 174).

The reefal-slope deposits in front of the platform at *Bulyurngari* dip northwest at 35°. They contain sponges, fragmentary stromatoporoids, and *Renalcis*, and are thought to have been bound by non-skeletal microbes. In one place they are cut by closely spaced neptunian dykes filled with fibrous spar. The fore-reef deposits include megabreccias, some of which flowed into thin-bedded calcareous muds of the basin facies, squeezing those muds between reef blocks in the megabreccias (Fig. 420).

Red micritic sandstone fills many small neptunian dykes in the east wall of the gorge near the south entrance, pinching out near the base of the wall (Fig. 417). These dykes may be paleokarst features associated with the Early Permian glaciation, although they could conceivably be Pleistocene. Their actual age might be determined by future paleomagnetic work.

Dingo Gap

Dingo Gap (*Tarakalu*) is a prominent gap extending through the core of the Napier Range south of Tunnel Creek (Fig. 422). The gap is localized by the Tarakalu Member of the Napier Formation, which consists largely of soft sandstone that is only poorly exposed or unexposed. The gap is flanked by resistant marginal-slope limestones of the Kalmanyi and Barrar Members of the Napier Formation and platform limestones of the Pillara Limestone.

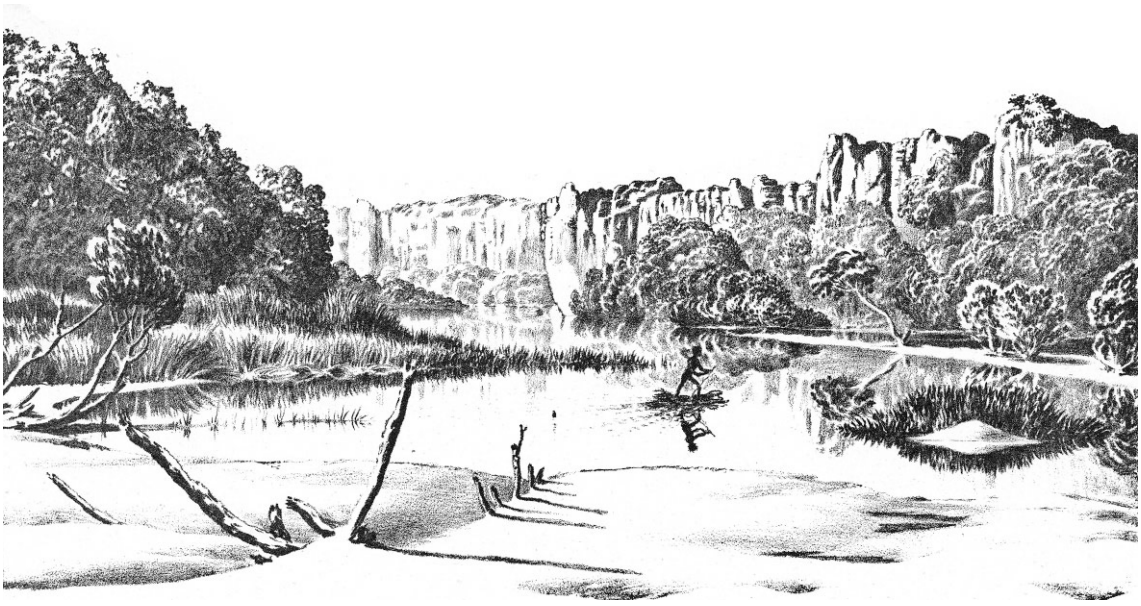

Figure 410. Sketch of the south entrance to Geikie Gorge in 1883, by geologist E T Hardman.

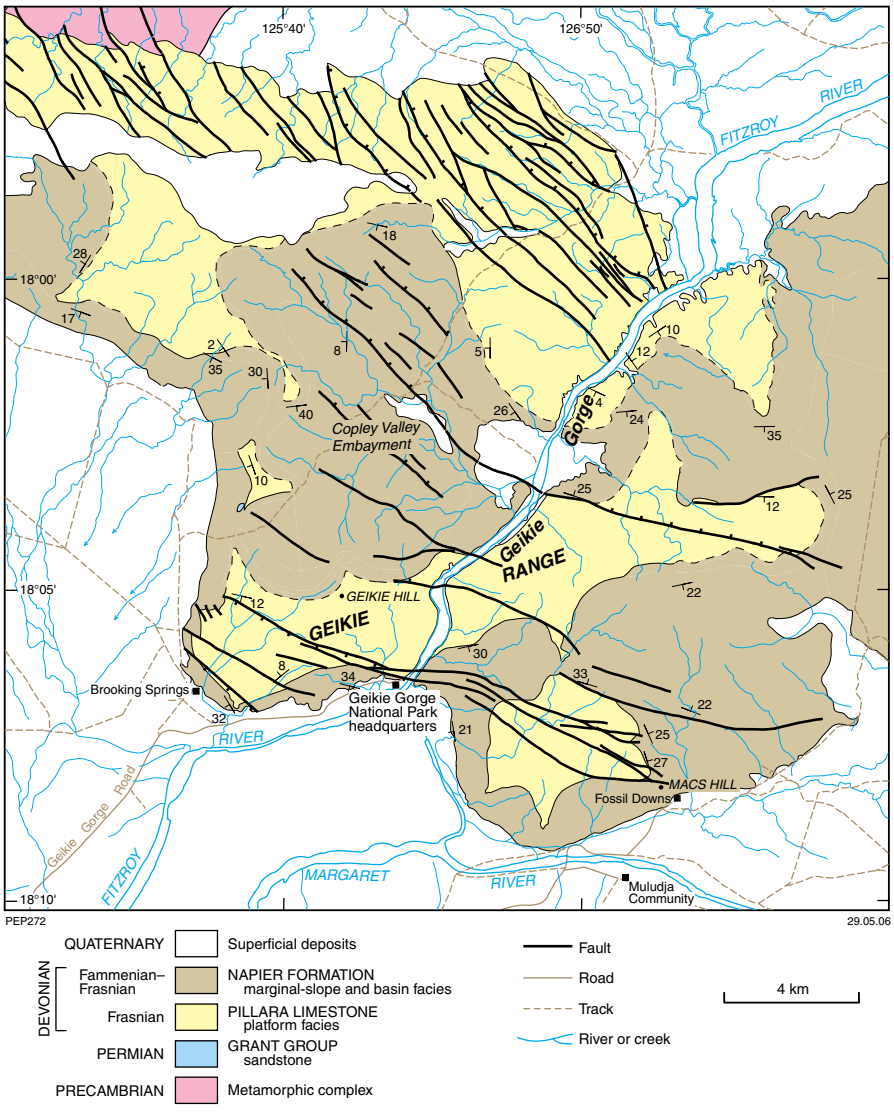

Figure 411. Geological map of the Geikie Gorge area.



Figure 412. Rollover platform margin on the east wall of Geikie Gorge, 3 km northwest of Sheep Camp Yard. Reef limestone on the left can be seen to 'roll over' into reefal slope limestone, above and immediately to the left of the person. The white lenses that 'roll over' consist of *Renalcis* limestone.



Figure 413. Geikie Gorge near the south entrance, showing reef-margin limestone on the right and reef-flat to back-reef limestone on the left. The white lower part of the gorge wall is kept clean by flood waters each year. The flood level is marked by the horizontal contact of this white limestone with the upper dark limestone, that is covered by pervasive films of epilithic microbes.



Figure 414. Geikie Gorge near its south entrance, showing massive microbial reef limestone in the centre, passing into back-reef limestone on the left. Again, the top of the white band marks the flood level.



Figure 415. Aerial view of the southeast wall of Geikie Gorge in its central part, looking east. Flat-lying platform limestones of the Pillara Limestone on the right are fronted by steeply dipping marginal-slope limestones of the Napier Formation on the left, meeting at a near-vertical platform margin.



Figure 416. The southeast wall of Geikie Gorge in its central part, showing steeply dipping marginal-slope limestones of the Napier Formation abutting flat-lying limestones of the Pillara Limestone.



Figure 417. The wall of Geikie Gorge near the centres of Figures 413 and 414, showing neptunian dykes filled with orange-coloured silty limestone. These dykes are karst cavities, probably following joints, and are thought to be either Early Permian or Cenozoic in age. The lower (white) part of the wall has been cleaned and polished by river flow up to the normal flood level. Above that level the wall is covered by pervasive films of dark-grey epilithic microbes.

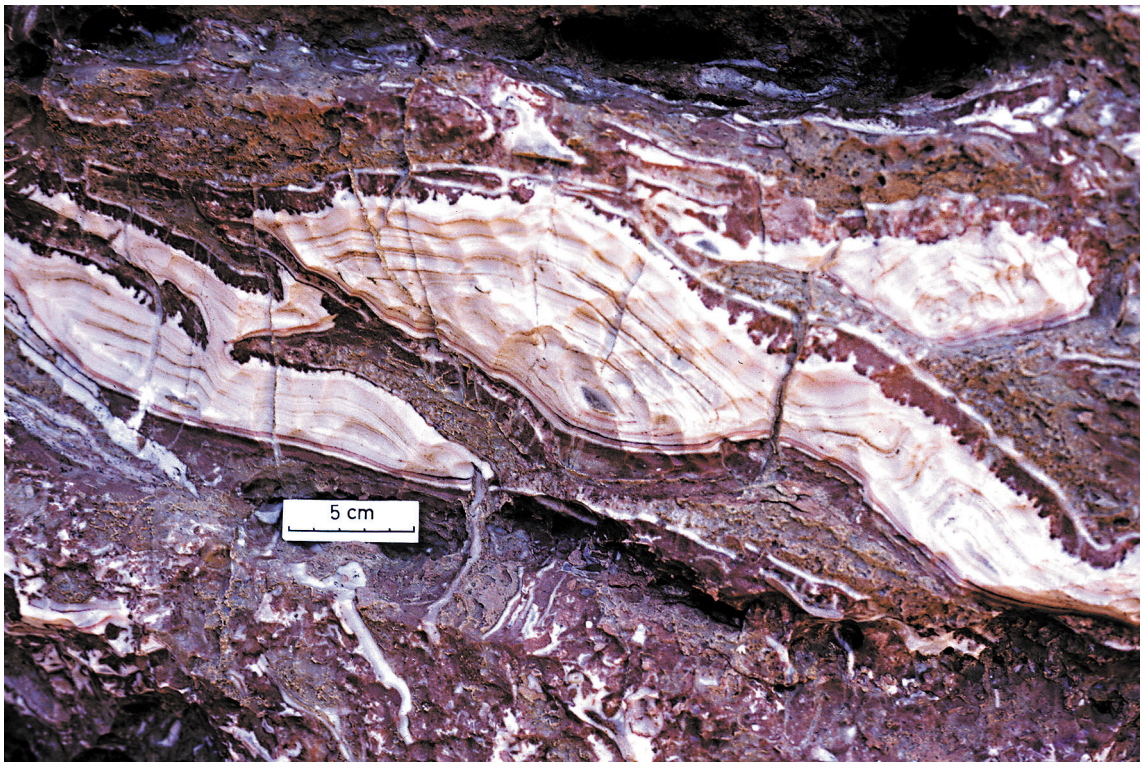

Figure 418. Reefal-slope limestone at Geikie Gorge, 3 km northeast of Sheep Camp Yard. Thin sheets of a coral (probably *Aulopora*) held up shelter cavities. The upper sides of each cavity were lined with *Renalcis*, which grew down from the coral before the rest of the cavity was filled with radiaxial calcite.



Figure 419. Dolomite (now altered to dedolomite) in near-reef back-reef in Geikie Gorge, 3 km northeast of Sheep Camp Yard. The rock has porosity resulting from the solution of fragments of *Amphipora* that had not been dolomitized.

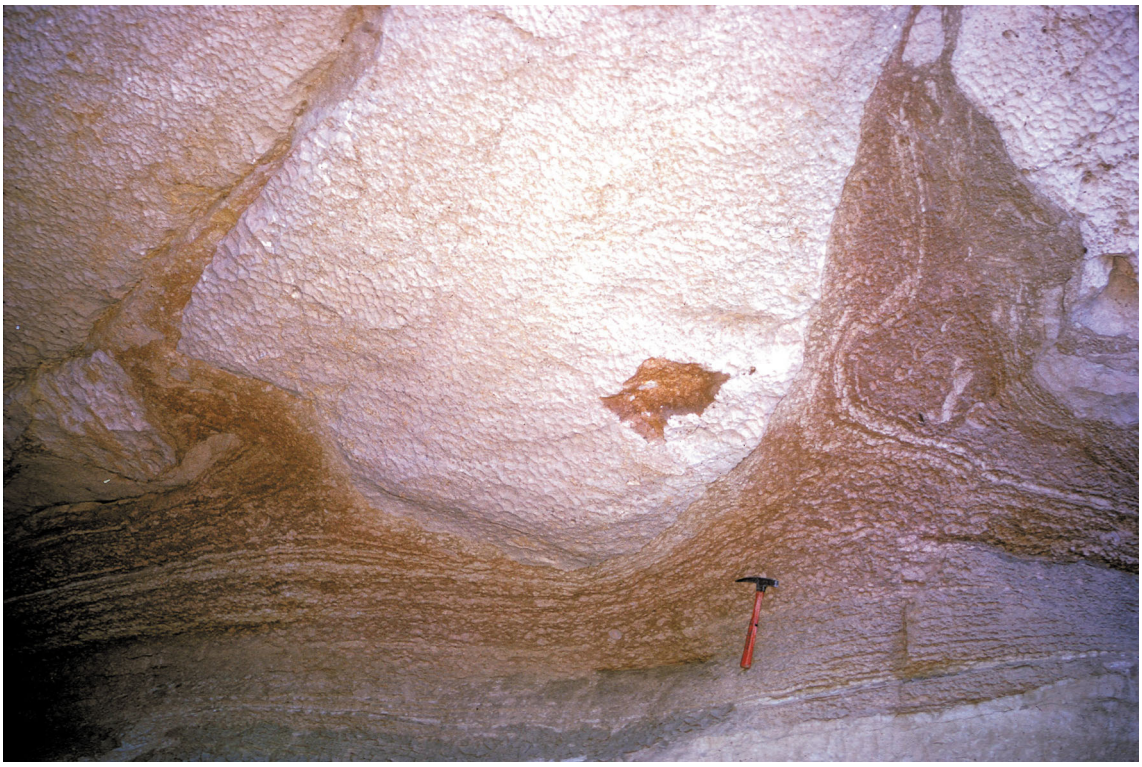

Figure 420. Block of *Renalcis* reef that was carried in a debris flow to near the base of the fore-reef slope in the Napier Formation in central Geikie Gorge, 2.3 km south of Sheep Camp Yard. The block sank into basinal mud, which was squeezed up between blocks at the base of the debris flow.

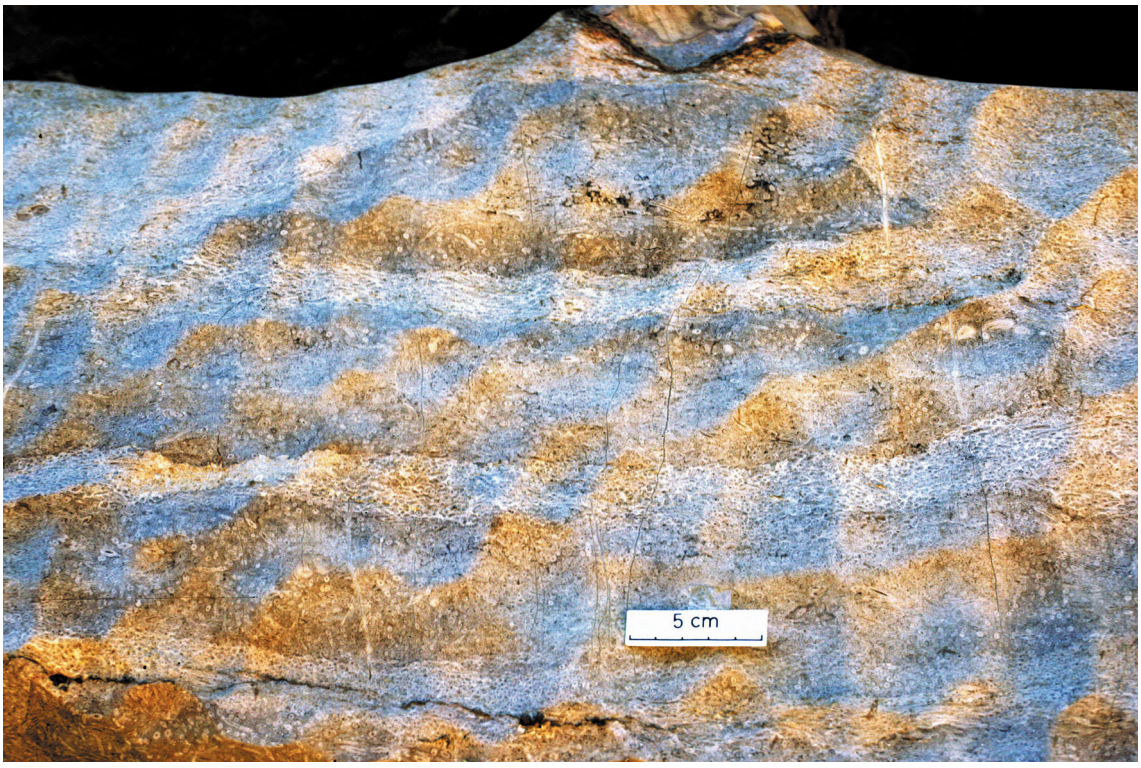

Figure 421. Pillara Limestone, showing irregular patches of microbial *Amphipora*-rich back-reef limestone that were cemented soon after deposition and remained uncompacted since then, whereas the rest of the bed has undergone pressure-solution compaction. Geikie Gorge, 1.5 km north of the south entrance.

Large allochthonous reef blocks and debris-flow deposits, derived from reef-margin limestone and marginal-slope deposits, are prominent features of the marginal-slope deposits, especially in the Barrar Member (Fig. 423). Features of debris-flow deposits and allochthonous reef blocks, including several examples from Dingo Gap, have been described earlier in this Bulletin and by Tornatora (1992) and George et al. (1994). Some of the allochthonous reef blocks in Dingo Gap near the top of the Tarakalu Member contain pseudokarst sand-tube features (Figs 326–333).

At a locality on the south side of Dingo Gap (AMG Zone 51, 732100E 8045400N) a debris-flow breccia carved a 'plough-furrow' channel into the underlying fore-reef deposits of the Barrar Member, folding and rupturing the strata at the margins (Fig. 125). The effect can be compared with that of a mouldboard plough carving a furrow through coherent soil. The fore-reef beds are folded into a recumbent syncline, the upper limb of which has been truncated by the debris flow. These rocks had a degree of cohesion when the flow occurred, probably as a result of partial marine cementation. They are stylolitized, and the stylolites are subhorizontal and subparallel to the bedding along the lower limb of the fold (which is itself parallel to the other fore-reef strata in this area), but they cut across the bedding in the axial area. The lower limb of one conspicuous bed, measured across the stylolites, is some 20% to 30% less than its thickness in the axial area of the fold, measured between stylolites. This is thought to be an approximate measure of the amount of compaction that has occurred in this bed through stylolitization.

Several other notable features of marginal-slope deposits can be observed close to this locality: A chisel-shaped allochthonous reef block has depressed the underlying strata where it sank below the base of the debris flow (Fig. 126), and a deep groove on a nearby bedding plane is thought to have been made by a block that slid or was carried down the marginal slope at the base of a debris flow. Some bedding planes in the marginal-slope deposits are strongly bioturbated, with intertwined markings of invertebrates that lived near the surface of the marginal-slope deposits (Fig. 424).

A conspicuous microbial–receptaculitid–coral bioherm is exposed near the southwest entrance to Dingo Gap, on the north side of an Early Permian subglacial karst depression (Fig. 83). This bioherm is latest Frasnian in age. It is overlain by a thin (~20 cm) brachiopod coquinite, also dated as latest Frasnian by conodonts, and this is in turn overlain by an earliest Famennian (Lower *triangularis* Zone) stromatolitic layer (G Klapper, 2004, written comm.). On the south side of the karst depression the Frasnian–Famennian boundary is 6 m above a latest Frasnian brachiopod coquinite some 4 m thick. It is notable that in this area the fore-reef bedding is generally better developed in the Famennian than in the Frasnian.

A conspicuous feature of the Frasnian fore-reef deposits of the Kalmanyi Member on the south side of the depression is a large antiformal stromatolite (Fig. 425; AMG Zone 51, 723200E 8056700N).

Part of the margin of the Pillara platform (Frasnian) in this area has an orthogonal shape, apparently as a result of

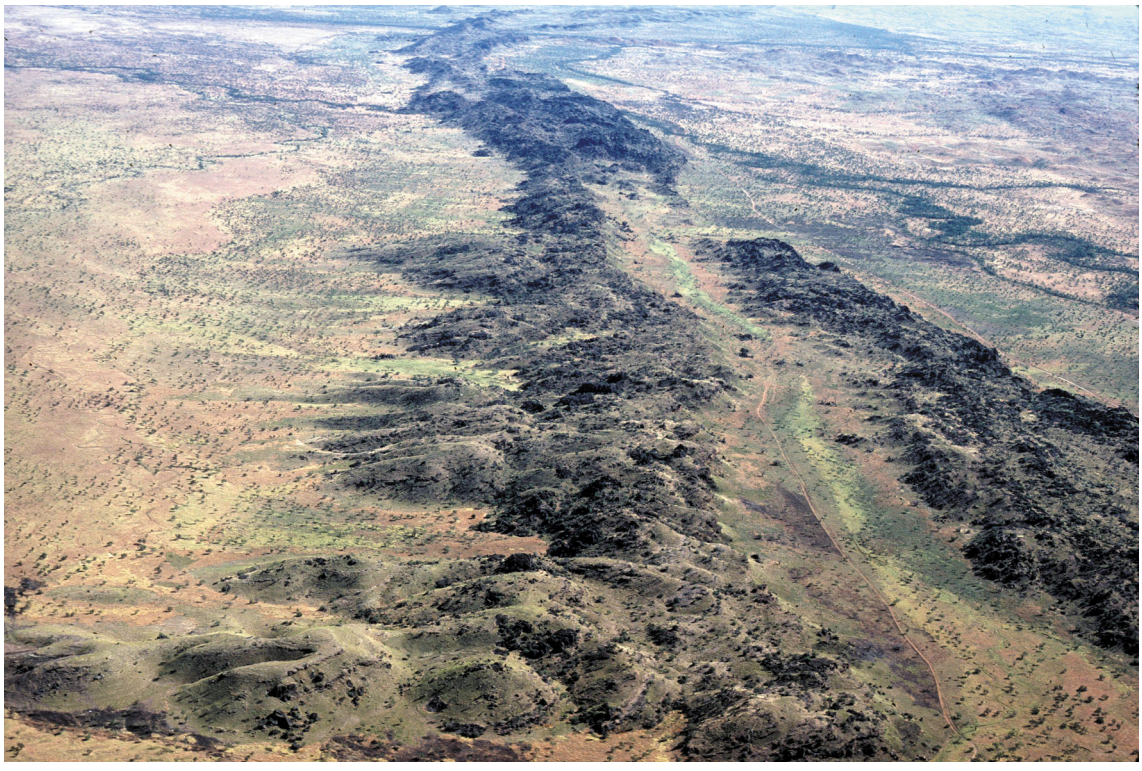

Figure 422. Aerial view of Dingo Gap (right and centre), looking northwest. The Famennian part of the Napier Formation in the foreground contains many large allochthonous blocks of reef limestone.

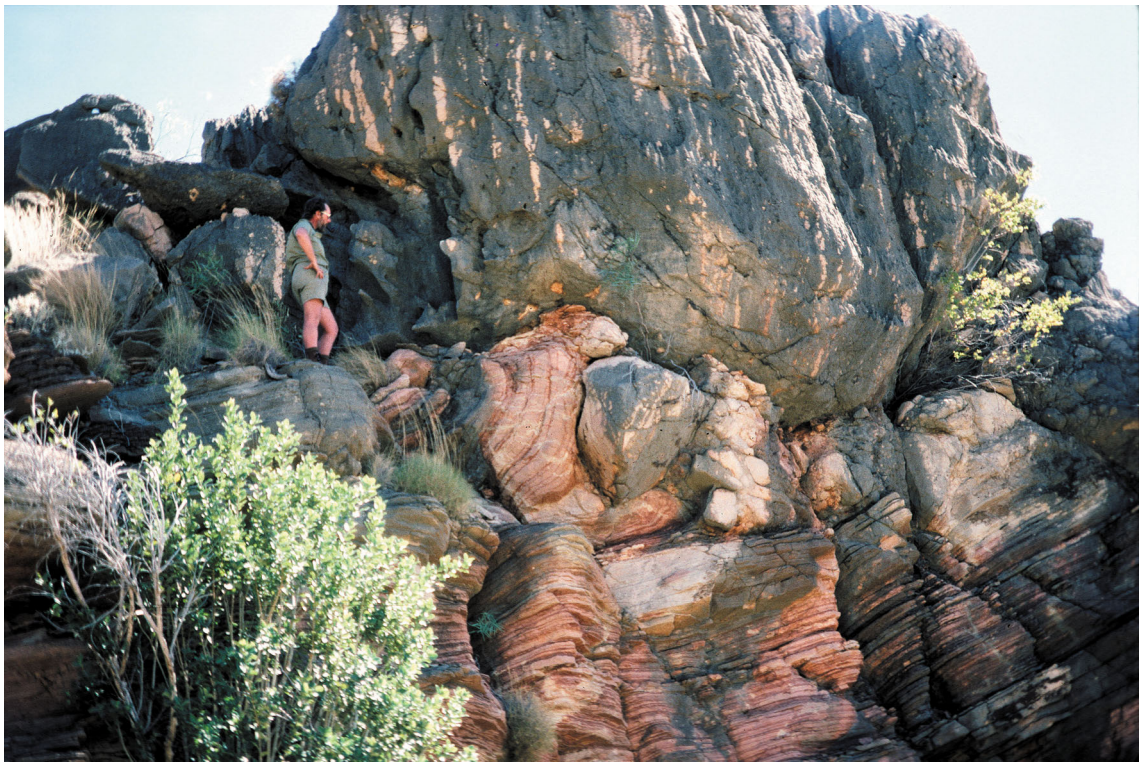

Figure 423. Blocks at the base of a debris-flow deposit in the Barrar Member of the Napier Formation in Dingo Gap. The blocks wedged up and folded thin-bedded fore-reef limestones beneath the base of the flow.

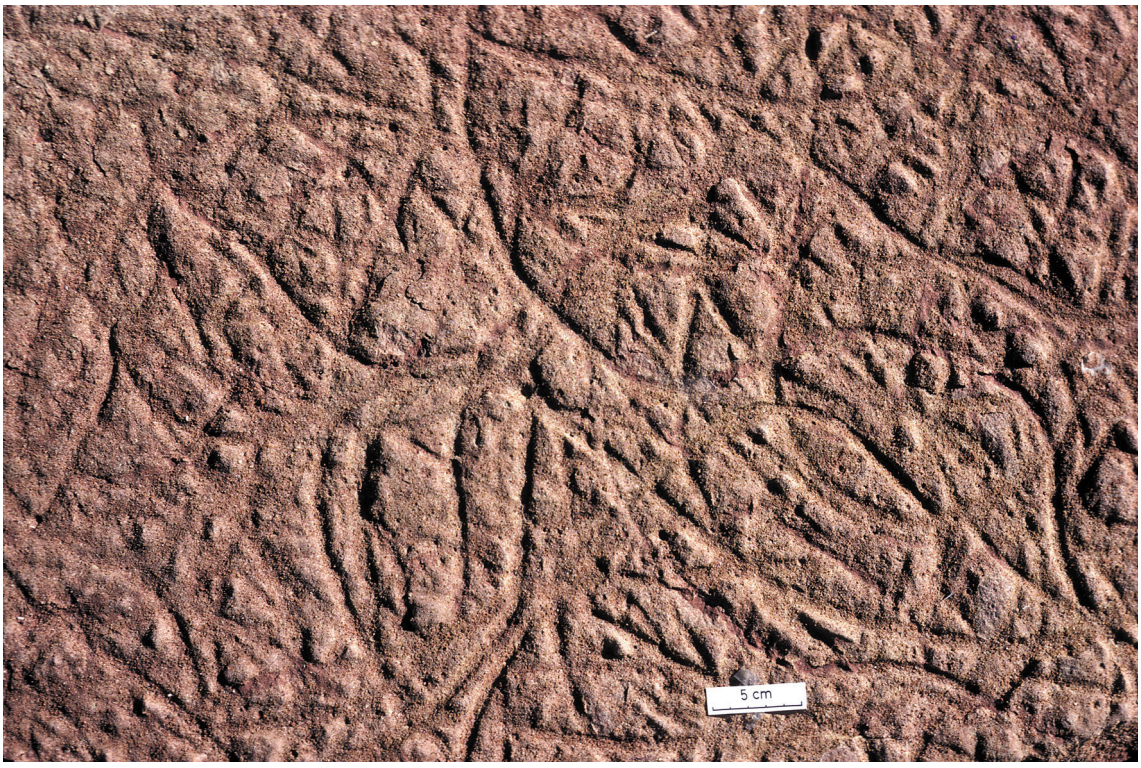

Figure 424. Bedding plane in fore-reef subfacies of the Napier Formation in Dingo Gap, with abundant invertebrate trails that indicate extensive biological reworking of the fore-reef sediments.



Figure 425. Antiformal stromatolite in Napier Formation, fore-reef subfacies, near Dingo Gap. The axis of the depositional fold is oriented down dip.

collapse of the margin along neptunian fissures that formed approximately at right angles to one another (Ward, 1996; Plate 2; Fig. 160; AMG Zone 51, 733700E 8044800N).

Elimberrie bioherms

A series of four large stromatolite and receptaculitid–sponge–stromatolite–microbial bioherms is exposed on the north side of the Oscar Range near Elimberrie Spring (Figs 426–450). These features were first mapped by Smith et al. (1957), who referred to them as 'anomalous fore-reef "tear drop" structures'. Their origin as stromatolitic bioherms was first recognized by Playford et al. (1976). Conodont analysis shows that these bioherms represent late Frasnian to early Famennian condensed sequences. They are thought to have grown in deep water over a line of drowned stromatoporoid–microbial pinnacle reefs.

Elimberrie no. 1 bioherm

Elimberrie no. 1 bioherm is a receptaculitid–sponge–stromatolite–microbial bioherm that grew over two Frasnian stromatoporoid–microbial pinnacle reefs (Figs 426–436). The contact between the eastern pinnacle reef and the bioherm is a steeply dipping eroded reef margin. The base of the bioherm was constructed by layers of *Sphaerocodium* stromatolites (Figs 431–433)

Most of the bioherm was built by non-skeletal microbes, together with receptaculitids (Figs 435, 436) and sponges, with lesser contributions from the skeletal microbe *Sphaerocodium* (especially at the base). The bioherm is generally crudely bedded, with very steep depositional dips (as much as 60°). Some beds are dolomitized, and this has resulted in the destruction of their original fabrics. The reef limestone is cut by many fissures filled with dolomite (Fig. 434), and the relatively small amount of stylolitization that is evident in the reef formed after dolomitization had occurred.

Microbes can be shown to have constructed a variety of columnar and scalloped stromatolites and wavy stromatolitic layers, but much of the limestone that is thought to be of microbial origin has little lamination and lacks direct evidence of microbial growth. Receptaculitids are conspicuous and contributed significantly to growth of this bioherm (Fig. 435). Earlier work had concluded that the receptaculitids that are so prominent here were sponges rather than receptaculitids (Rigby, 1986). However, the later discovery of 'snowflake' structures, typical of receptaculitids, in one of the spherical fossils at Elimberrie no. 1 bioherm has shown that most of those fossils are indeed receptaculitids (Fig. 436; K Rigby, 1993, written comm.). Nevertheless, there are other fossils in the bioherms that are interpreted to be siliceous sponges, now calcified.

A line of sampling through Elimberrie no. 1 has shown that the oldest part of the bioherm, 34 m thick, is of Frasnian age, ranging from within Zones 3–6 up to the Frasnian–Famennian boundary (G Klapper, 2004, written comm.). There is a hiatus between Zones 7–8 and 11–13. This hiatus marks a strong diminution in the content of shelly fossils, but receptaculitids continue, and the lithologies on either side of the hiatus are very similar.

Similarly, across the Frasnian–Famennian boundary (as defined by conodonts by G Klapper, 2004, written comm.), there is no obvious change in either lithologies or biotas — abundant receptaculitids are present in both the latest Frasnian and the earliest Famennian parts of the bioherm. This is in accord with the observation that the Frasnian–Famennian mass extinction was marked by the loss of shallow-water organisms, whereas deep-water forms (including receptaculitids) were not affected.

The bioherm continues for another 46 m above the Frasnian–Famennian boundary, to the Upper *crepida* or Lower *rhomboidea* Zone of the early Famennian, giving a total thickness of the exposed bioherm of 80 m. Thus, the bioherm extends from within Zones 3–6 of the early Frasnian to the Upper *crepida* or Lower *rhomboidea* Zone of the early Famennian, covering an interval of approximately 8 m.y. This gives an average growth rate over that period (which includes a hiatus of about 1 to 2 m.y. in the middle Frasnian) of some 10 µm per year. It is estimated that at least 250 m of subsidence occurred during that 8 m.y., based on the approximate thickness of equivalent parts of the Frasnian and Famennian platform facies. If the water depth was about 20 m when the oldest part of the bioherm began growing, and it grew about 80 m upwards, the youngest part can be expected to have grown in water at least 190 m deep.

It is remarkable that only minor changes occurred in the bioherm biota over such a long period of time. The suggested maximum water depth of at least 190 m suggests that at least some of the stromatolite-building microbes were chemosynthetic rather than photosynthetic. It should be noted that the exhalative stromatolite buildups described by Playford and Wallace (2001) and in this Bulletin are also thought to have been built by chemosynthetic microbes, although their genesis, over cool-water seepages on the sea floor, differs from that of the Elimberrie bioherms.

Elimberrie no. 1 bioherm has a ‘tail’ that is straight, long (450 m), and narrow (3 m), directed southwest and composed of microbial–receptaculitid–stromatactis limestone (Figs 427, 428, 430). The explanation for this remarkable ‘tail’ is uncertain, but its growth direction may have been controlled by sea-floor currents flowing from northeast to southwest. It should be noted that pinnacle reefs in the Bugle Gap area also display ‘tails’, which there are directed to the south.

The bioherm is bounded by steeply dipping fore-reef strata of the Napier Formation, forming a near-circular structure in plan view, but broken to the southwest by the line of the ‘tail’. This structure is one of the most striking geomorphic features of the reef complexes. The Famennian fore-reef beds that fringe the bioherm have resulted from progradation of the Famennian platform over this area. That progradation is thought to have eventually led to the development, later in the Famennian, of a small atoll or patch reef, which was eventually tied to the main platform.

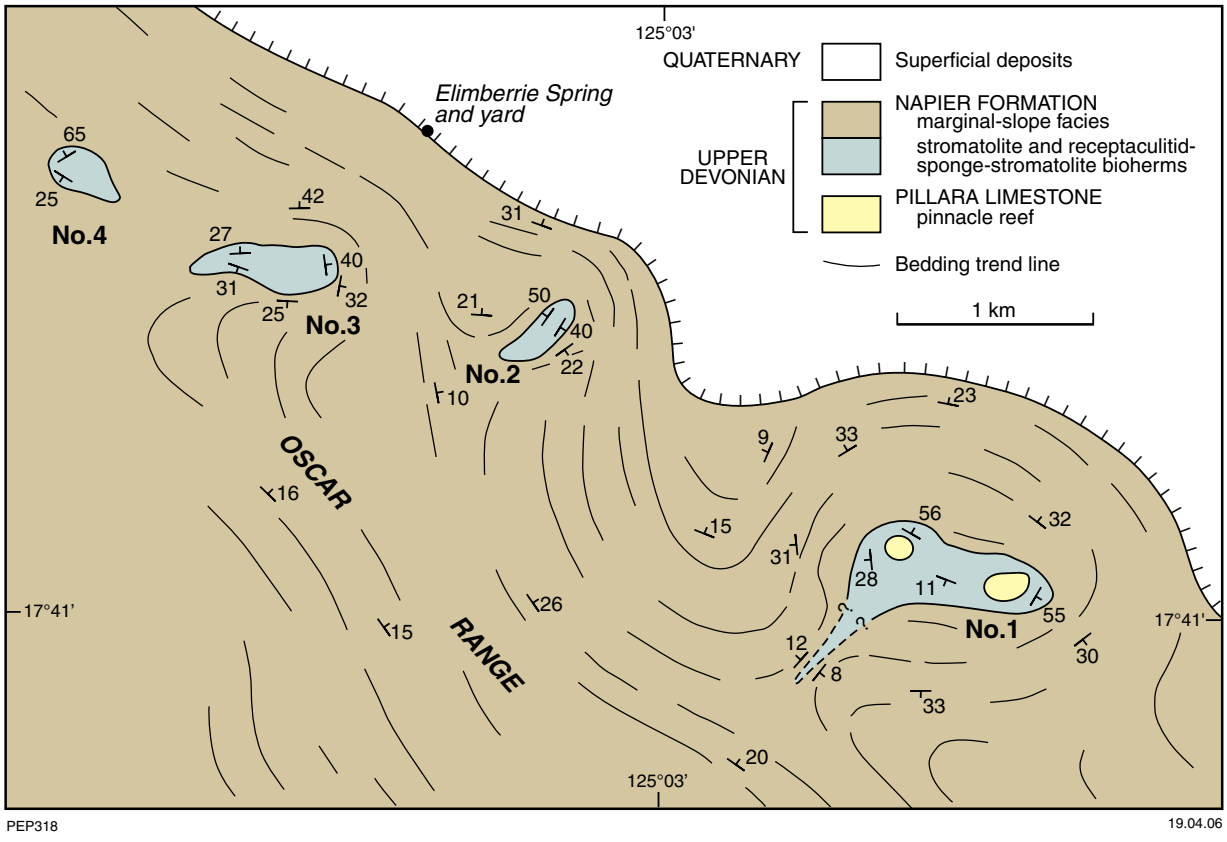

Figure 426. Geological map of the Elimberrie bioherms.

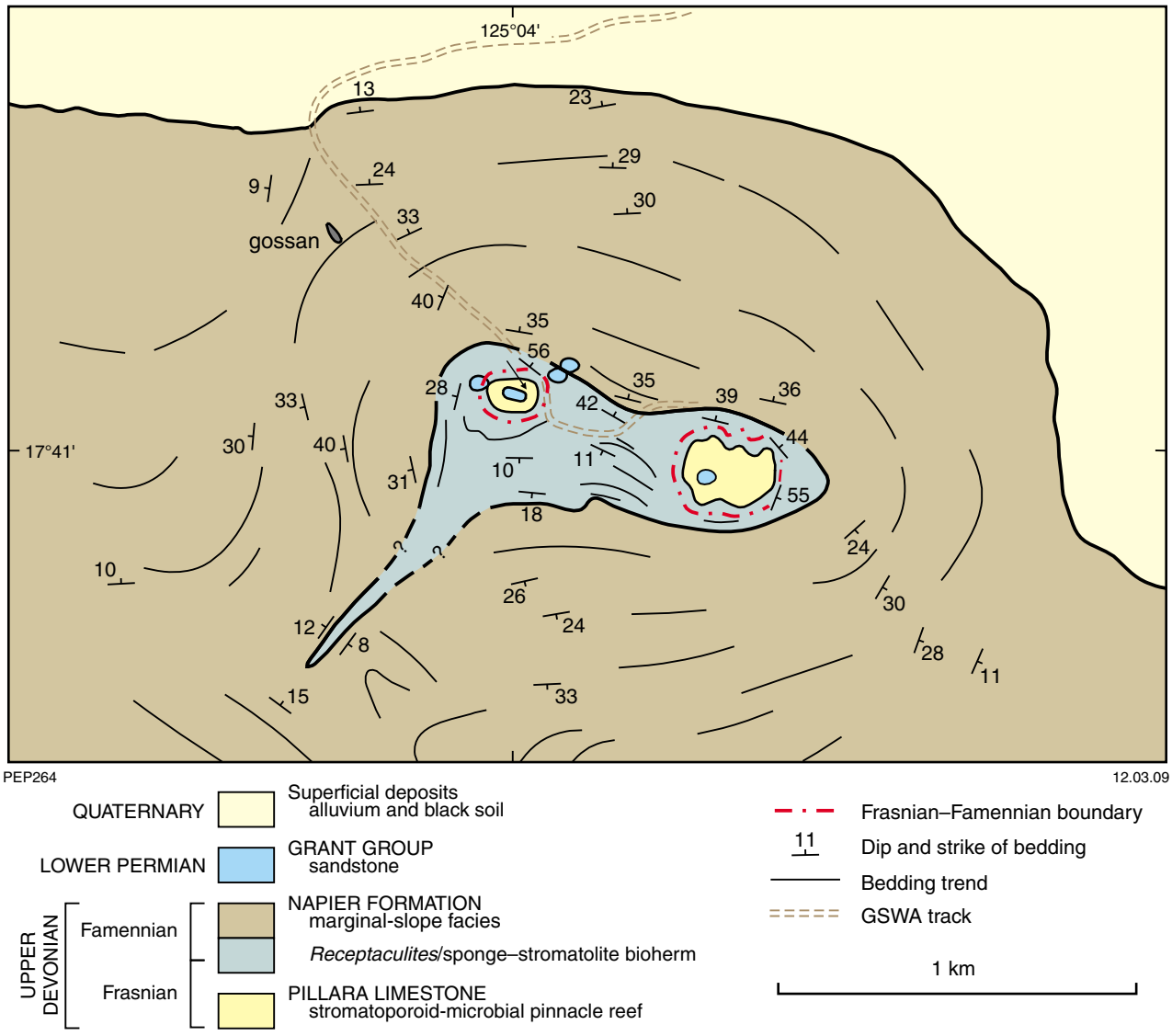

Figure 427. Geological map of Elimberrie no. 1 bioherm.

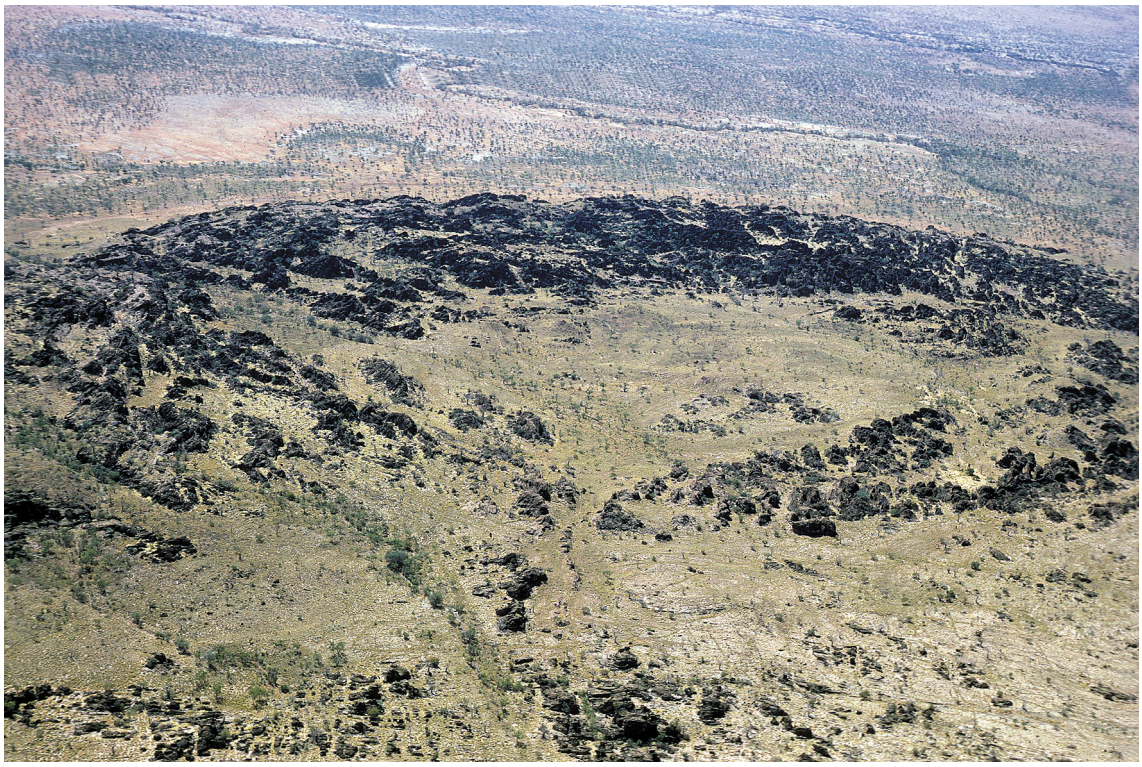

Figure 428. Aerial view looking northeast over Elimberrie no. 1 bioherm, showing its circular outline, with a 'tail' to the south.

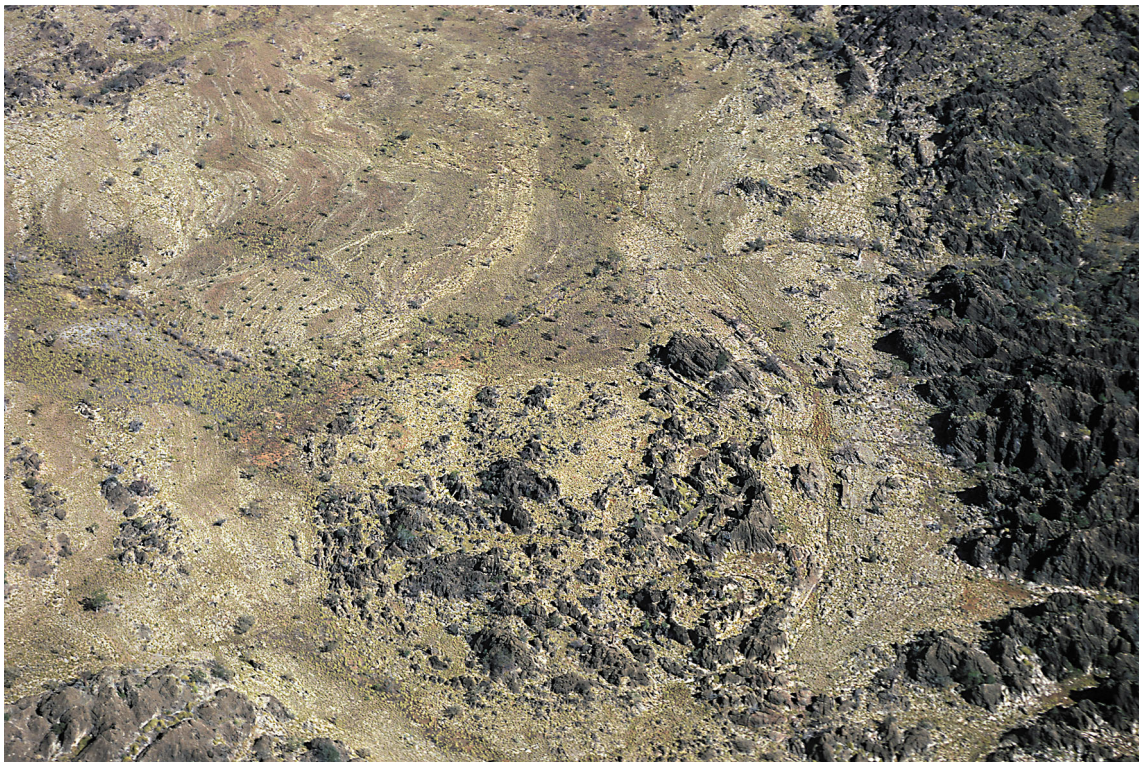

Figure 429. Aerial view of the eastern pinnacle reef (lower middle) and the adjoining part of Elimberrie no. 1 bioherm, looking west.



Figure 430. Aerial view of the narrow 'tail' of Elimberrie no. 1 bioherm, looking southwest. The 'tail' consists of red microbial limestone.

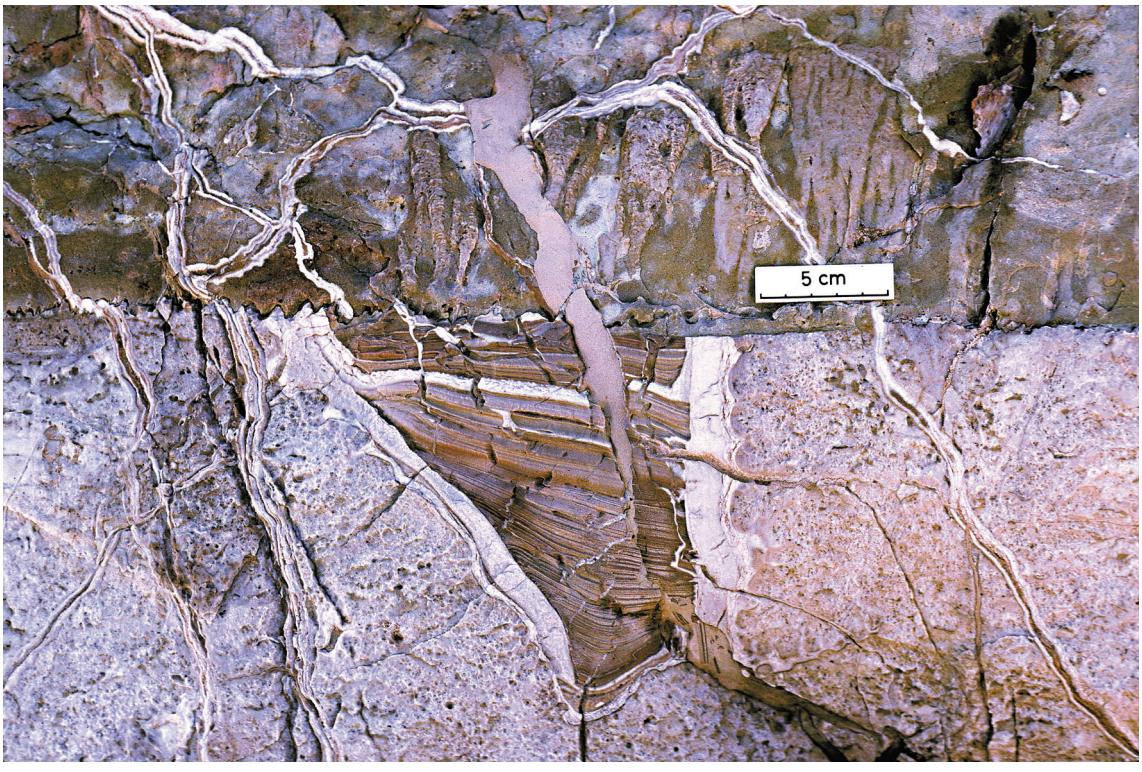

Figure 431. Erosional contact in Elimberrie no. 1 bioherm, between massive microbial reef (lower part of photo) and encrusting stromatolitic limestone, with 'fingers' of *Sphaerocodium*, above the contact. A dolomite-filled reef cavity, eroded at the contact, is in the centre. Note the many small neptunian fissures filled with calcite and sediment, and one neptunian dyke (in the centre) filled with dolomite. The contact between reef and bioherm is stylolitized, except for the part directly under the scale on the photograph.



Figure 432. Polished slab from the eastern pinnacle reef in Elimberrie no. 1 bioherm, showing *Renalcis* reef limestone (on the right) and *Sphaerocodium* stromatolitic limestone of the bioherm (on the left). The boundary between them is an erosion surface, showing truncation of a cavity system filled with laminated lime mud capped by sparry calcite.

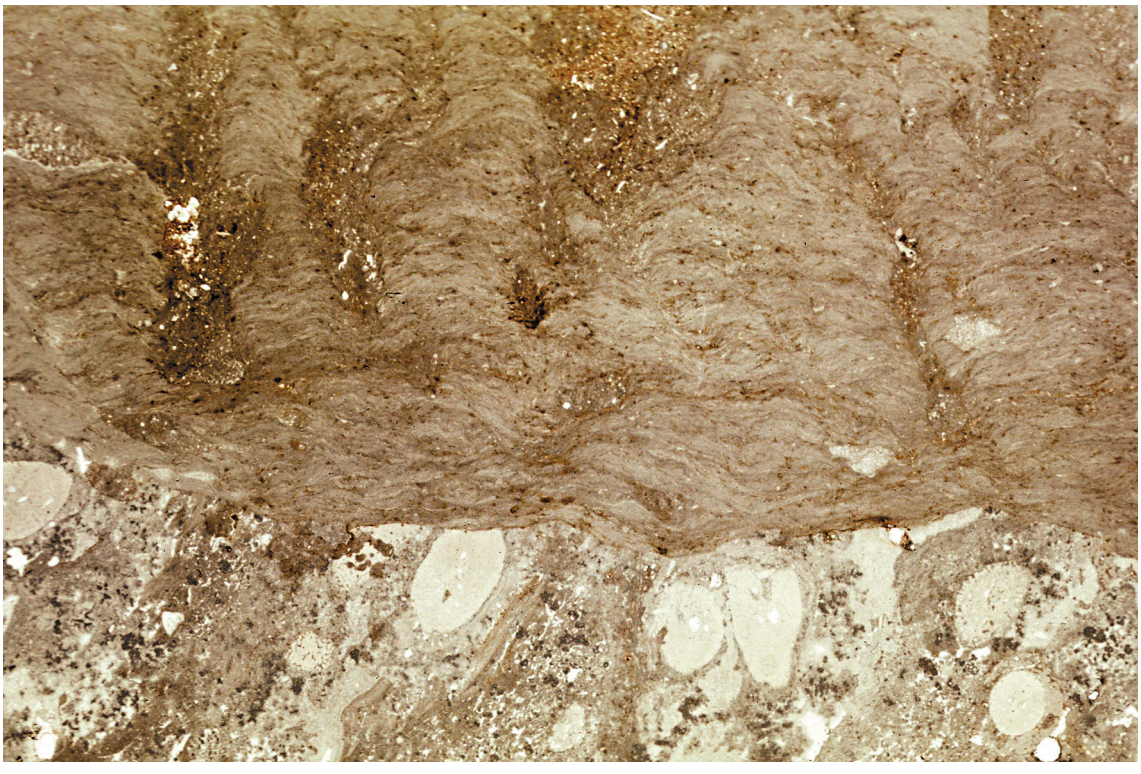

Figure 433. Thin section of the erosional contact in Elimberrie no. 1 bioherm between stromatoporoid reef (lower part of photo) and *Sphaerocodium* stromatolite above. GSWA sample no. 37285. Width of field of view 60 mm.

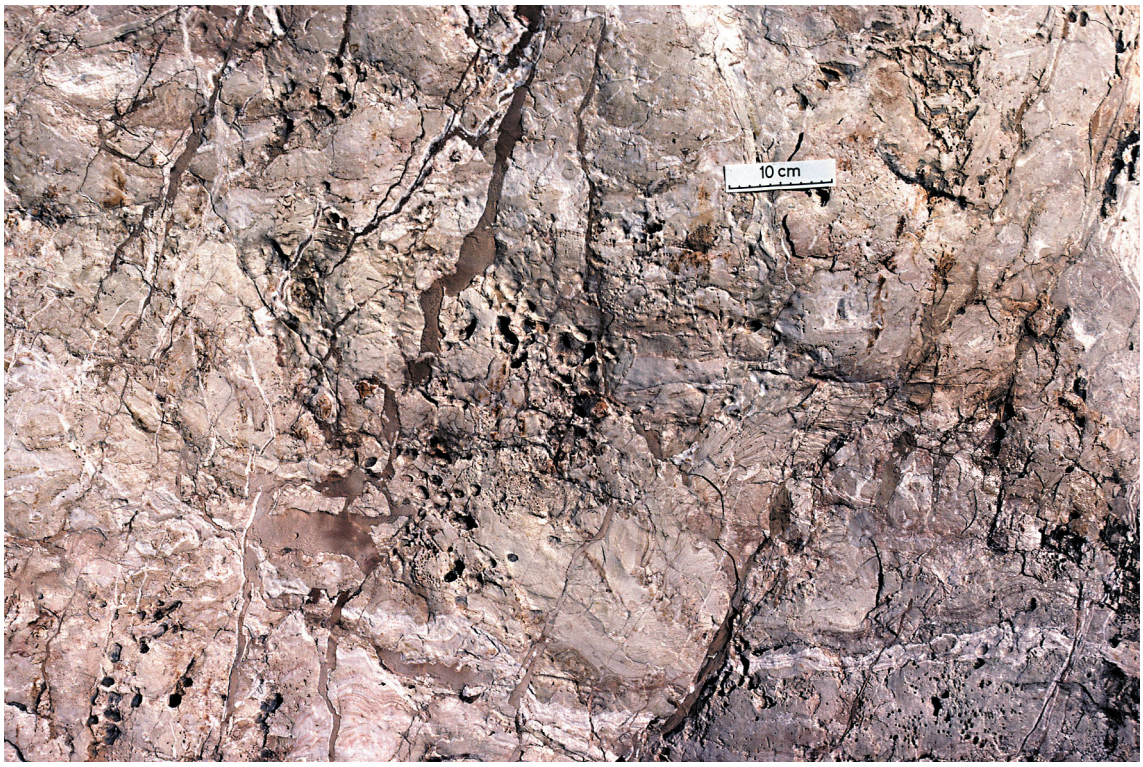

Figure 434. Reef limestone from the eastern pinnacle reef of Elimberrie no. 1 bioherm showing gash veins filled with dolomite.



Figure 435. Receptaculitids in dolomitic limestone, Elimberrie no. 1 bioherm.

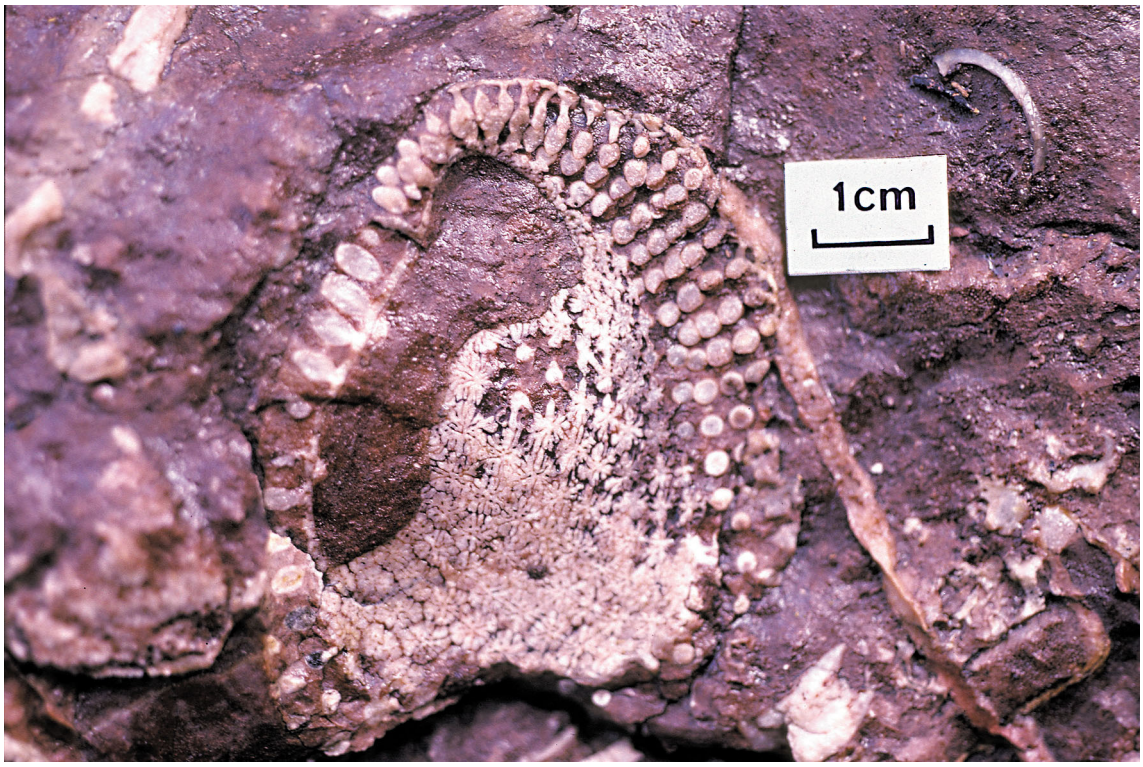

Figure 436. Receptaculitid in microbial limestone in Elimberrie no. 1 bioherm, showing its characteristic 'snowflake' structure.



Figure 437. Gossan cutting through fore-reef strata adjoining the northwest flank of Elimberrie no. 1 bioherm, showing pseudomorphs after pyrite.

A significant occurrence of gossan, apparently after pyrite, is situated near the access track 0.5 km northwest of the bioherm (Figs 427, 437), filling a fissure in the marginal-slope limestones about 20 m wide and 100 m long. The gossan exhibits cubic iron-oxide pseudomorphs after pyrite. It is not of direct economic interest as it lacks significant contents of lead or zinc.

Elimberrie no. 2 bioherm

Elimberrie no. 2 is the best exposed of the four bioherms (Figs 438–447). However, the amount of exposure that is visible at any time is controlled by the extent of spinifex (*Triodia*) growth. Exposures are excellent for a year or two after a fire, but subsequently much of the outcrop becomes obscured by large clumps of spinifex. The photos shown as Figures 440 and 441 were both taken after a recent fire.

Elimberrie no. 2 bioherm is about 500 m long and has a similar shape, on a greatly increased scale, to the mound-shaped stromatolites in the Casey Falls area of Bugle Gap (Fig. 371). Superficially, it resembles a tectonic fold, but geopetal structures (both cavity fillings and vertical-growth forms) prove that the fold is a growth feature, and is not tectonic. The core of the exposed bioherm is dated by conodonts as Middle *triangularis* Zone (early Famennian) and the outermost part belongs to the Lower *marginifera* Zone (middle Famennian; G Klapper, 2004, written comm.). The oldest part of the bioherm lies below the present erosion surface and has therefore not been dated. The outer margin is somewhat younger (perhaps by about a million years) than the outer margin of Elimberrie no. 1.

Reconstructions suggest that the relief of Elimberrie no. 2 during growth was at least 25 m, and probably more than 50 m. Large convex outgrowths on the flanks of the bioherm meet at v-junctions, and depositional slopes on the flanks are commonly more than 40°, reaching as high as 65°. The bioherm was built largely by non-skeletal stromatolites, many having spaced-columnar, contiguous-columnar, and scalloped forms (Figs 443–446). Other microbial layers are massive. *Sphaerocodium* is common, contributing from less than 5% to as much as 100% of individual stromatolite columns, and frequently forming closely spaced elongate fingers as much as about 20 cm long (Figs 443–445). *Renalcis* occurs rarely and the coral *Aulopora* forms distinctive chains that grew on the stromatolites (Fig. 447). No receptaculitids have been observed in this bioherm, unlike all of the others.

Several neptunian dykes cut across the bioherm, filled with banded sparry calcite (early marine cement) and in some cases by contemporary sediment (Fig. 438). The dykes probably formed during or very soon after growth of the bioherm. They may have resulted from compaction over the pinnacle reef on which the bioherm is thought to have been established.

A few cobbles of Precambrian granitic rocks have been noted on the south side of the bioherm, embedded in stromatolitic limestone. They are haphazardly distributed and are thought to have been dropped from the entangled roots of floating vegetation. Crinoid stems and straight nautiloids can be seen on some bedding planes, oriented directly down the depositional slopes and, in the case of nautiloids, having their apices oriented up dip.

The reason for the lack of receptaculitids in Elimberrie no. 2, contrasting with their abundance in nos 1, 3, and 4, is unsure. It is notable that the coral *Aulopora* is relatively abundant in bioherm no. 2, but is rare or absent in nos 1, 3, and 4. If *Aulopora* indicates shallower water, then water depths were probably less over Elimberrie no. 2 than the others.

Elimberrie no. 3 bioherm

Unlike nos 1 and 2, Elimberrie no. 3 is oriented east–west. This bioherm is poorly exposed, but it appears to have two culminations, the best outcrops being in the core of the western culmination. A conodont sample taken at that culmination shows that the oldest exposed part of the bioherm is late Frasnian in age (Upper Zone 11 to Zone 12; G Klapper, 2004, written comm.). However, it seems clear that most of the bioherm is Famennian.

Bioherm no. 3 was constructed by microbes (mainly non-skeletal forms) and receptaculitids (Fig. 448). *Sphaerocodium* is common, forming 'fingers' that grew vertically on the slopes, some being encrusted with crinoid and coral holdfasts (Figs 449, 450). Ammonoids and nautiloids are present in some places, and *Renalcis* is rare. Limestones making up the bioherm are usually red or grey in colour, and parts have been dolomitized.

Elimberrie no. 4 bioherm

Elimberrie no. 4 is the least known of the bioherms, being smaller, less well exposed and more difficult to access than the others (Fig. 426). As a result it was not differentiated as a separate bioherm on Plate 2. Parts of the bioherm are well bedded, forming a domal structure cut by a small fault (or perhaps a large joint) along its axis. The bioherm was constructed mainly by microbes, including *Sphaerocodium*, which formed columnar stromatolites and wavy laminae. Crinoid and coral holdfasts grew on some layers, testifying to their early lithification.

Receptaculitids occur in the outer parts of the bioherm, together with a few sponges and corals. No conodont dating has been obtained, but it seems likely that the bioherm is largely Frasnian in age. It is in line with a prong of Frasnian reef (Pillara Limestone).

Northwest end of the Oscar Range and Morown Cliff

The Oscar Range reef complex developed around a rugged island of Proterozoic metasedimentary rocks (Figs 451, 452; Plate 2). The island remained, progressively shrinking in extent, throughout development of the Frasnian Pillara Sequence, but was probably almost entirely covered by the close of the Famennian Nullara Sequence (Fig. 453).

The Oscar Range is covered by a conservation reserve. Few people currently visit the range, but it must have considerable potential as a future tourist destination. There are many attractive springs in the area (Fig. 454) and several outstanding rock-art sites (Playford, 2007).

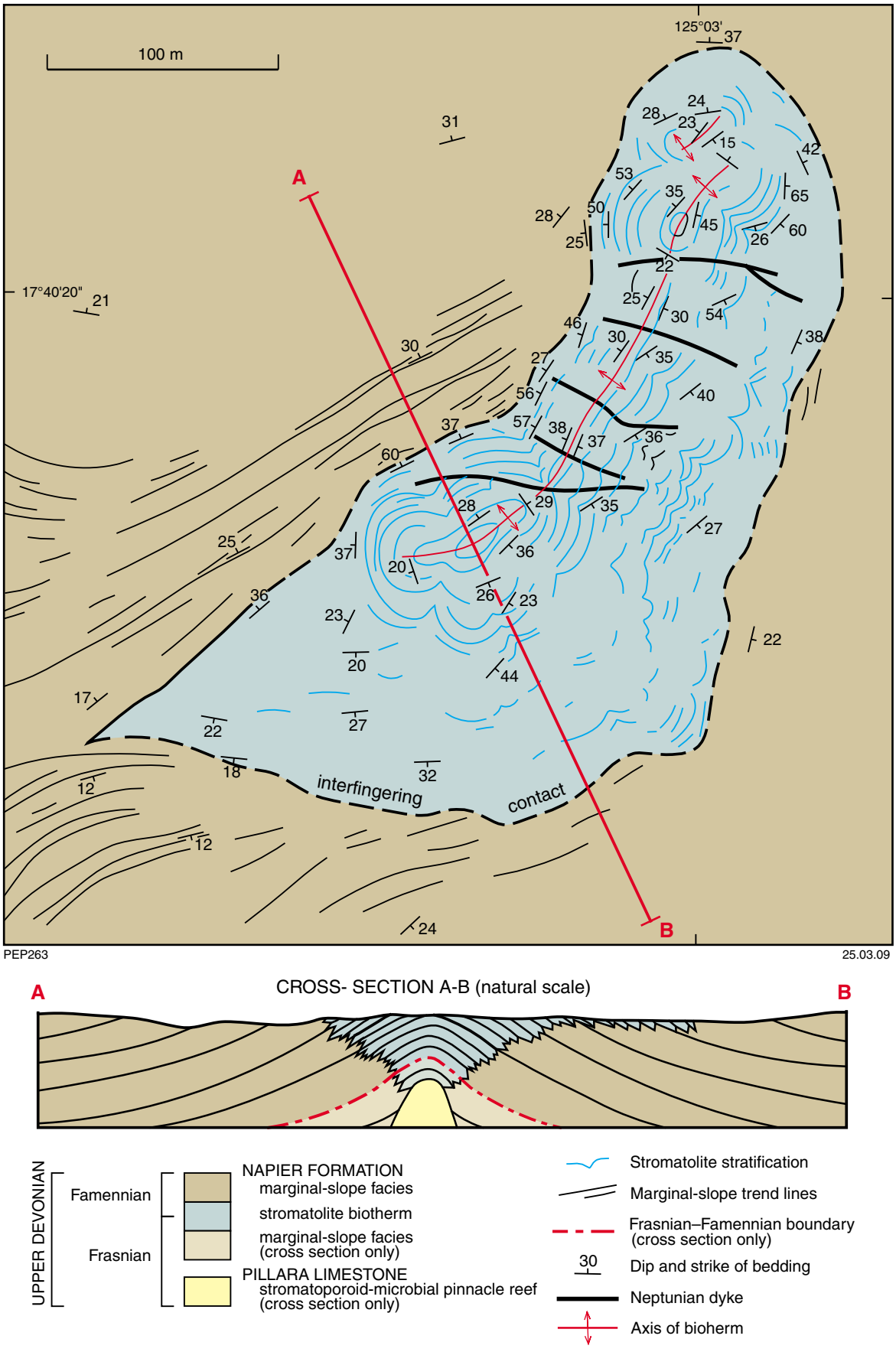

Figure 438. Geological map of Elimberrie no. 2 bioherm.

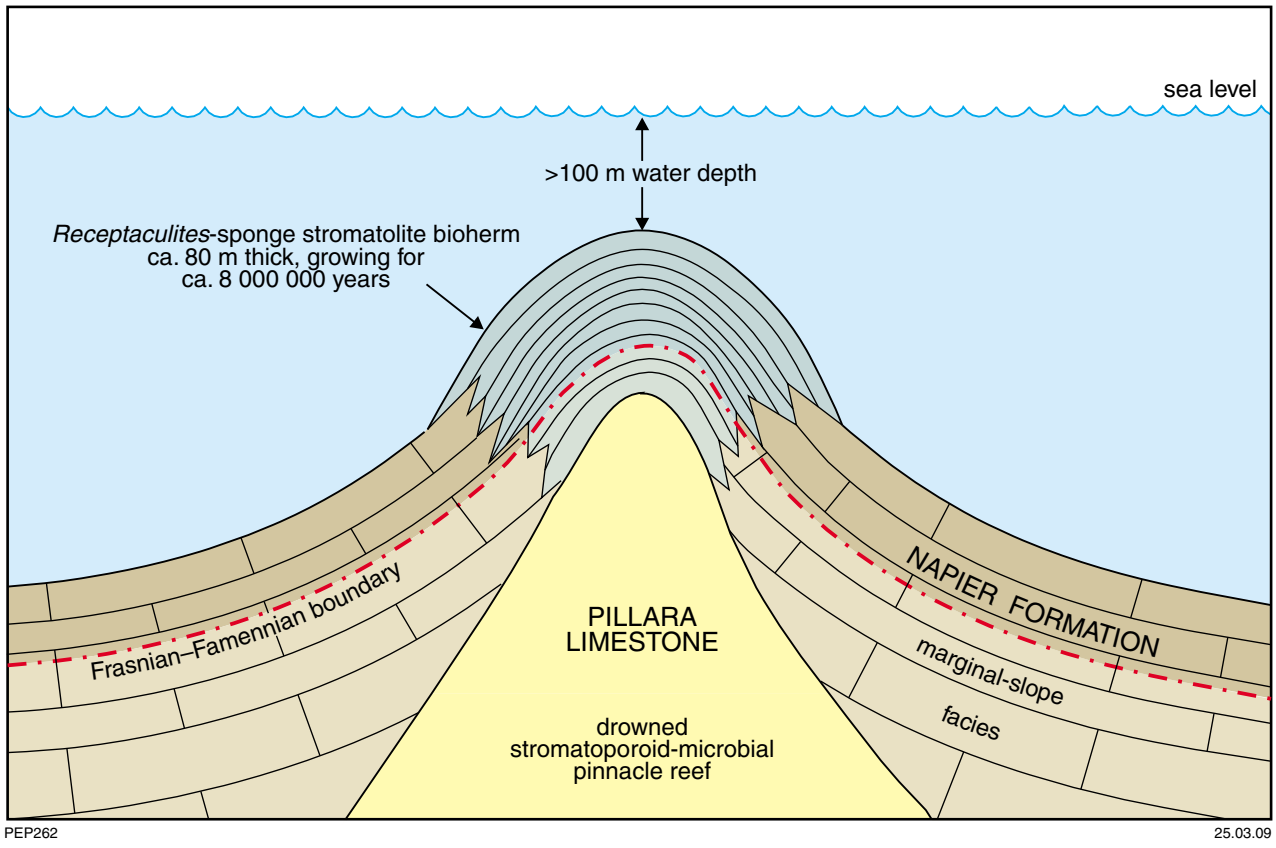

Figure 439. Diagrammatic cross section through Elimberrie no. 2 bioherm.



Figure 440. Aerial view looking north over the southwest culmination of Elimberrie no. 2 bioherm.

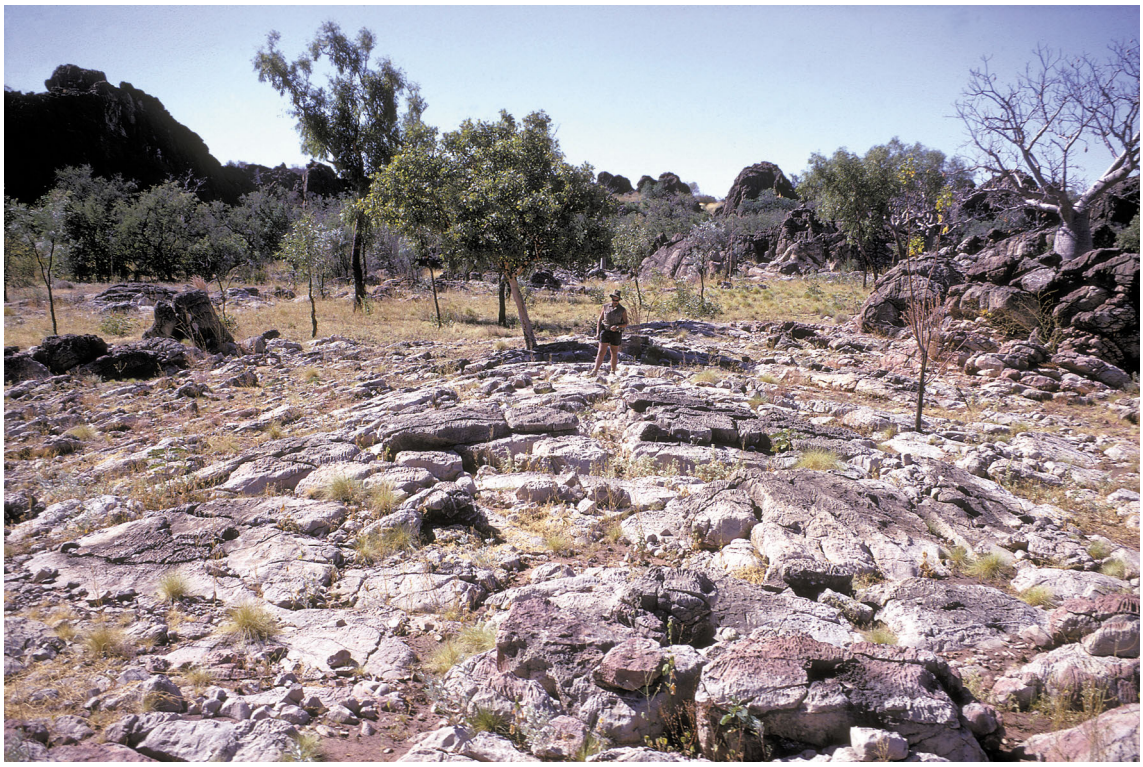

Figure 441. The northern culmination of Elimberrie no. 2 bioherm, looking northeast.



Figure 442. The central crest of Elimberrie no. 2 bioherm, looking southwest.

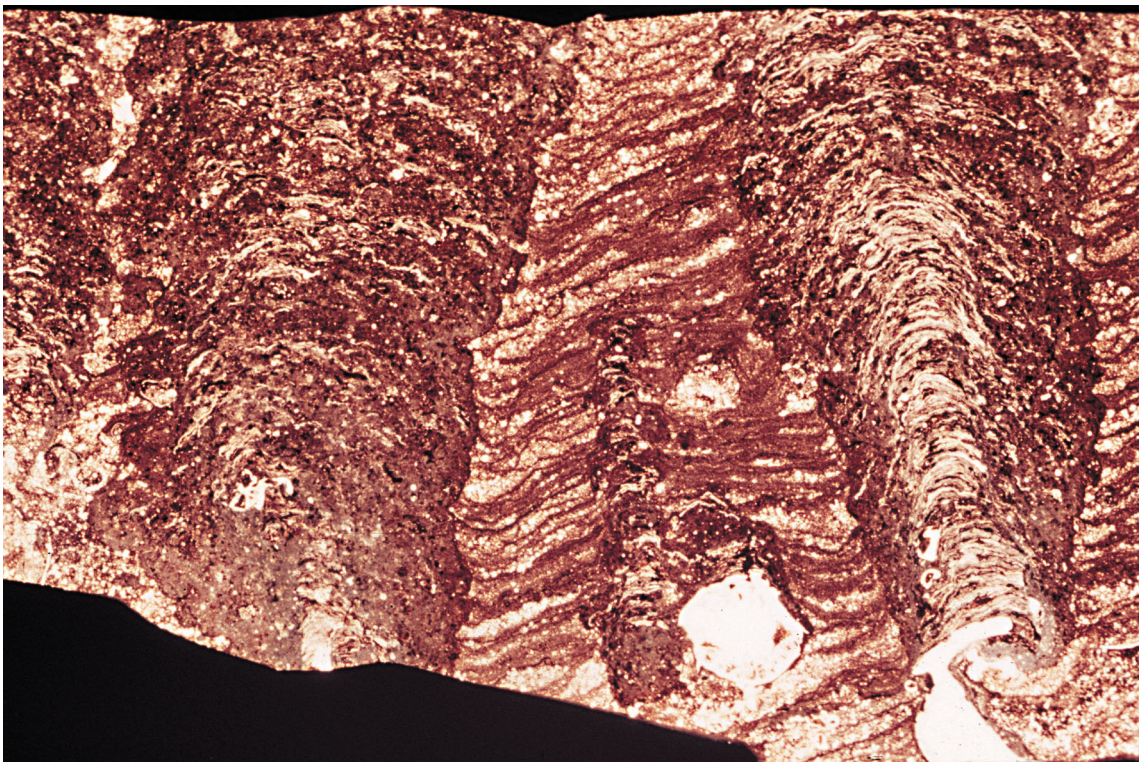

Figure 443. Thin section showing stromatolite columns constructed by *Sphaerocodium* and non-skeletal microbes, from Elimberrie no. 2 bioherm. GSWA sample no. 21655. Width of field of view 45 mm.

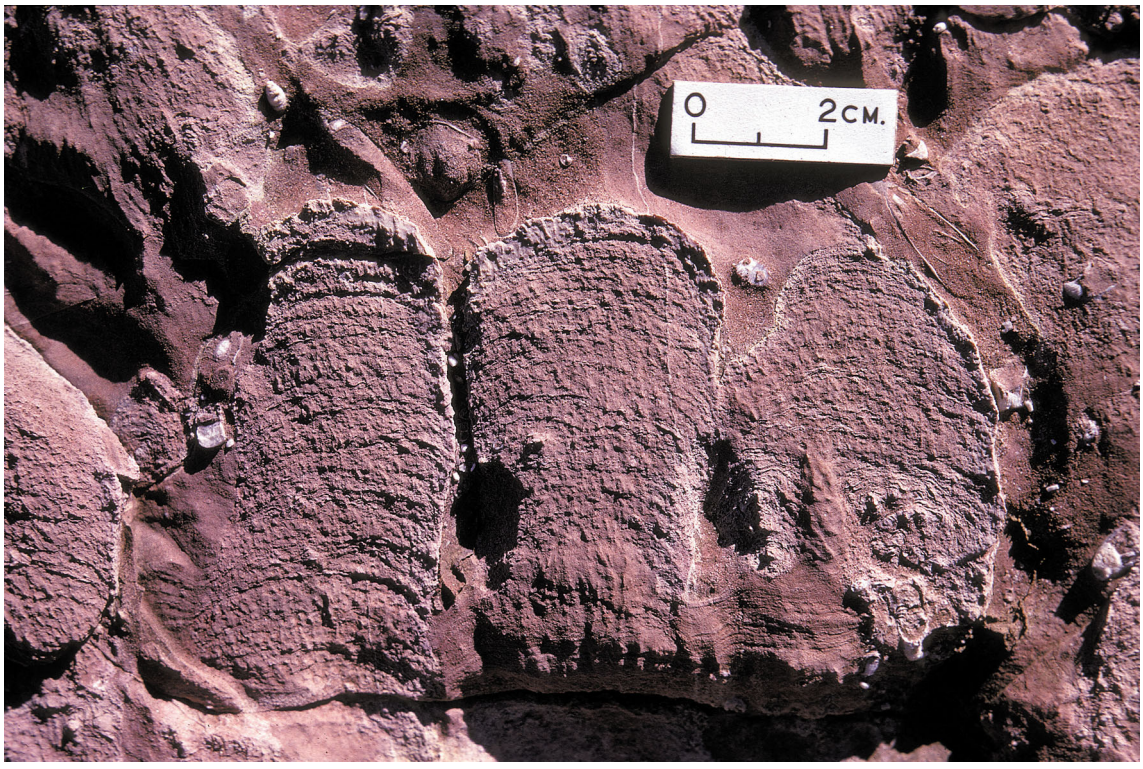

Figure 444. Columnar stromatolites from Elimberrie no. 2 bioherm, built jointly by *Sphaerocodium* and non-skeletal microbes.

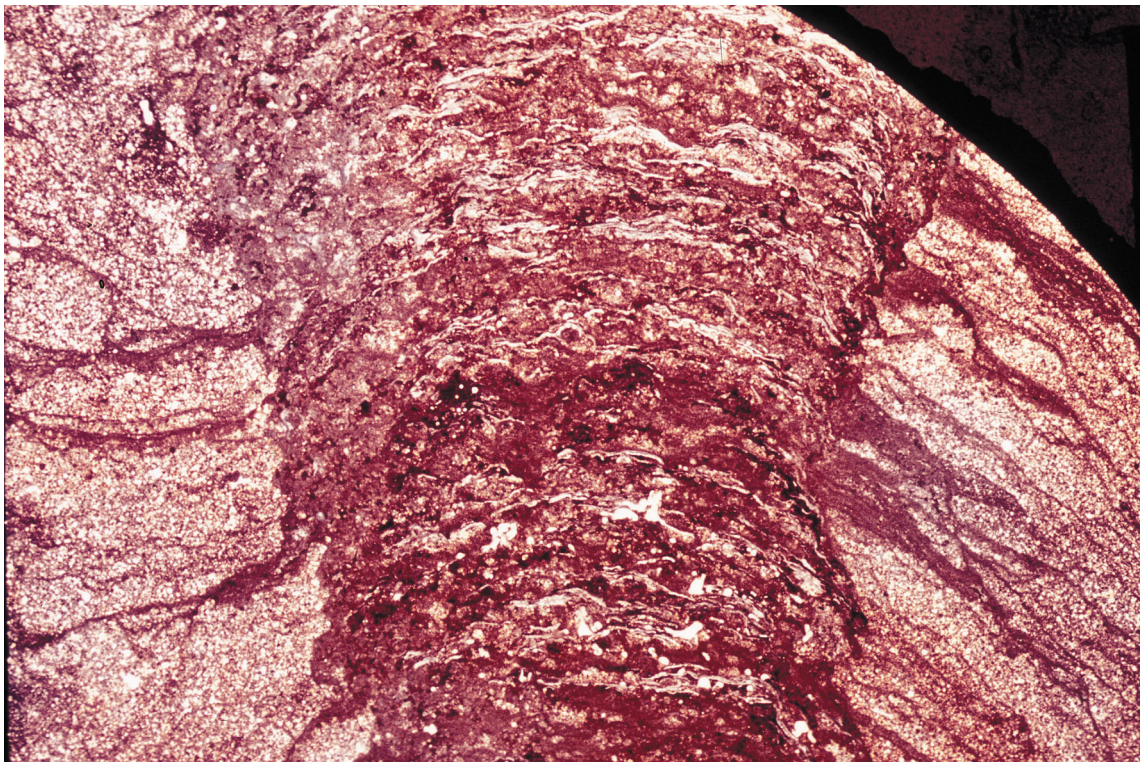

Figure 445. Thin section of a columnar stromatolite from Elimberrie no. 2 bioherm, built by a consortium of *Sphaerocodium* and non-skeletal microbes, with 'tongues' of the stromatolite extending into the microbially laminated sediment on the sides, showing that the stromatolite had only low growth relief. GSWA sample no. 21588. Width of field of view 35 mm.

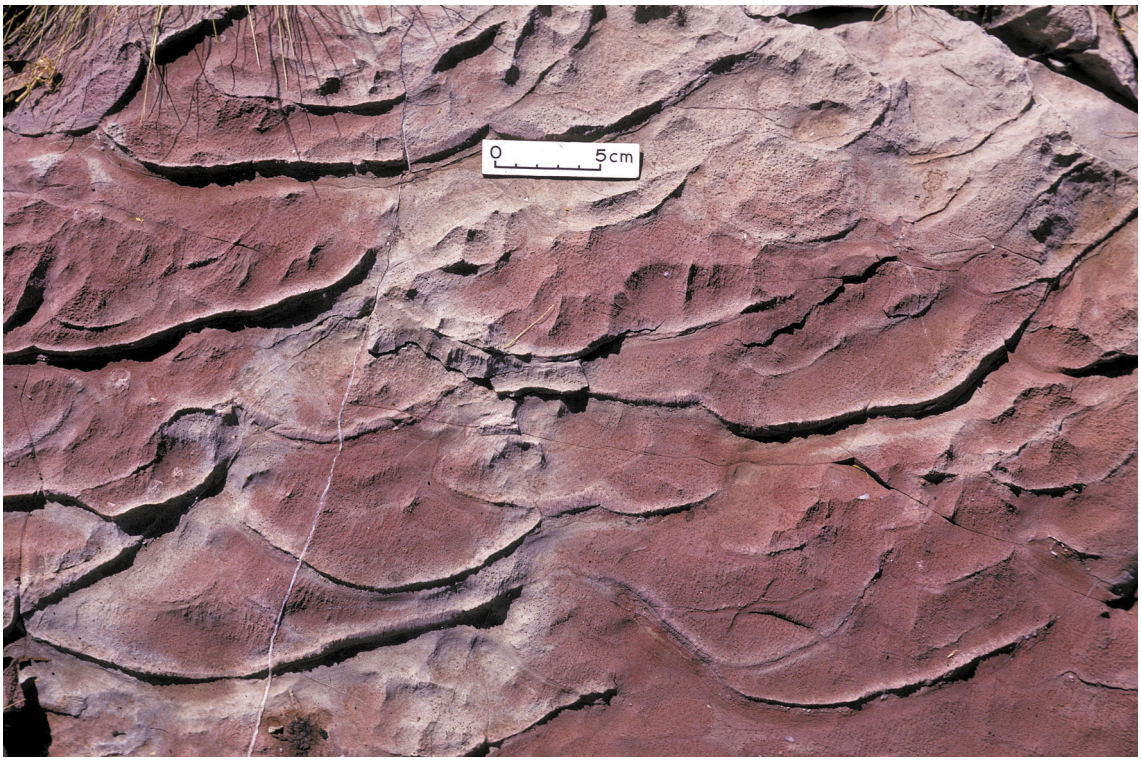

Figure 446. Scalloped stromatolites on a flank of Elimberrie no. 2 bioherm. The convex side is directed down dip.

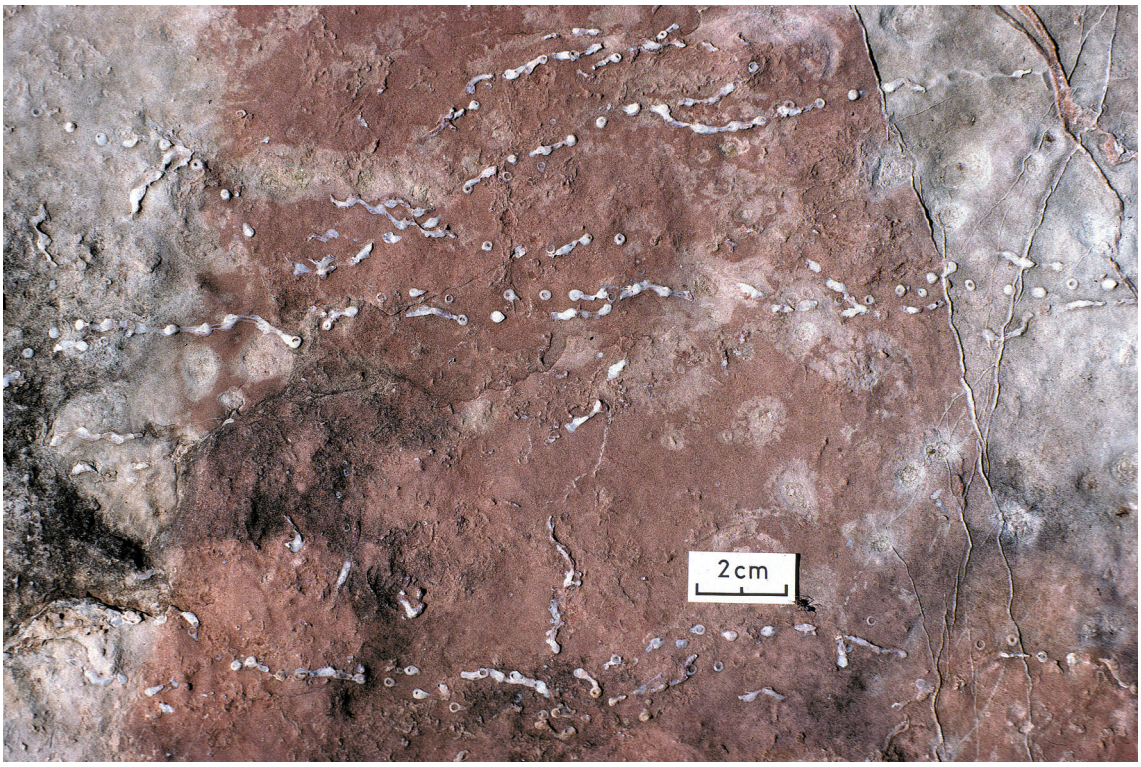

Figure 447. Chains of the coral *Aulopora* encrusted on the surface of microbial limestone in the axial area of Elimberrie no. 2 bioherm.



Figure 448. Part of Elimberrie no. 3 bioherm with abundant receptaculitids. Note the many spar- and sediment-filled cavities left by the decay of soft-bodied organisms, including receptaculitids.



Figure 449. Straight nautiloid in the steeply dipping core of Elimberrie no. 3 bioherm, showing geopetal infillings that testify to the steep depositional dip. Note stromatolitic bedding on the right, also ammonoids and crinoid holdfasts. Width of field of view about 12 cm.



Figure 450. Thin section of stromatolitic limestone from the core of Elimberrie no. 3 bioherm, showing the steep depositional dip and stromatolite columns that grew vertically on the slope. Note crinoid and coral holdfasts that grew on the stromatolites. GSWA sample no. 19969. Width of field of view 85 mm.

The Frasnian–Famennian unconformity is well displayed at the northwestern end of the Oscar Range, where Nullara Limestone overlies reef-margin subfacies of the Pillara Limestone (GPS AMG Zone 51, 705850E 8046430N and 705970E 8046200N). The contact between them is an erosional unconformity (Figs 49, 455). The massive Pillara reef was constructed by stromatoporoids (especially *Actinostroma* and *Stachyodes*) and microbes (including *Renalcis*). It grew almost horizontally, so that the Pillara reef subfacies exposed below the Frasnian–Famennian unconformity is very wide (about 700 m; Plate 2). The unconformity is generally a smooth eroded surface, without obvious karst features, and in places it has relief of as much as 2.5 m (Figs 49, 455). The overlying Nullara Limestone consists of thin-bedded fenestral limestones (ooid grainstones with some oncolite rudstones; Fig. 456). Tepee structures, commonly showing well-developed crestal breaching, are present in certain beds (Fig. 62). The tepees are at the tops of shallowing-upward metre-scale cycles, although the cyclicity is not very obvious in this area.

Some fenestral limestone beds of Nullara Limestone in this vicinity (GPS AMG Zone 51, 705250E 8048180N) contain pebbles and small cobbles of subangular to subrounded Precambrian rocks, which are thought to have been dropped from floating vegetation after it decayed.

Morown Cliff, forming the north face of part of the Oscar Range, is one of the most prominent features of the Devonian reef complexes (Figs 457, 458). It essentially represents the exhumed late Famennian reef scarp, as it was at the time of the abrupt reef-extinction regression associated with the close of the Nullara Sequence in the late Famennian. The cliff of Windjana Limestone rises abruptly for some 70 m above the adjoining flat plain. The limestone forming the cliff has been subjected to modern karstification, resulting in prominent karren that run straight down the cliff face (Fig. 458). The plain is underlain by Fairfield Group, which forms rare small exposures of shale and siltstone in front of the cliff. Those shales and siltstones are steeply dipping near the cliff because of post-depositional compaction against the Famennian reef front. The Fairfield Group has also been intersected in drillholes near Morown Cliff.

The base of the cliff is undercut in some areas (probably largely as a result of fire-induced exfoliation), and some caves are present at or near the cliff base. These undercuts and caves are commonly decorated with Aboriginal rock art (Playford, 1960, 2007).

The scarp is cut by many small v-shaped valleys (Fig. 104), thought to have been incised into the scarp during the late Famennian regression, as discussed earlier. Drilling has shown that one of the incised valleys near the west end of the range (AMG Zone 51, 706000E 8048500N) was filled by shale of the Fairfield Group. Small streams flow in some of the incised valleys during the wet season, but others are quite dry. The caves in the cliff face (Fig. 104) are thought to have resulted from either late Famennian or Early Permian karstification.



Figure 451. Aerial view of the northwestern part of the Oscar Range, looking northwest. Rugged hills of Precambrian rocks in the foreground are onlapped by limestone of the reef complex. Reef and fore-reef limestones at the edge form dark outcrops that wind off into the distance and turn around at the end of the range.



Figure 452. **(above) A higher altitude aerial view of the north-western part of the Oscar Range looking northwest, showing the reef complex filling valleys incised into the Precambrian basement rocks and wrapping around the end of the range.**

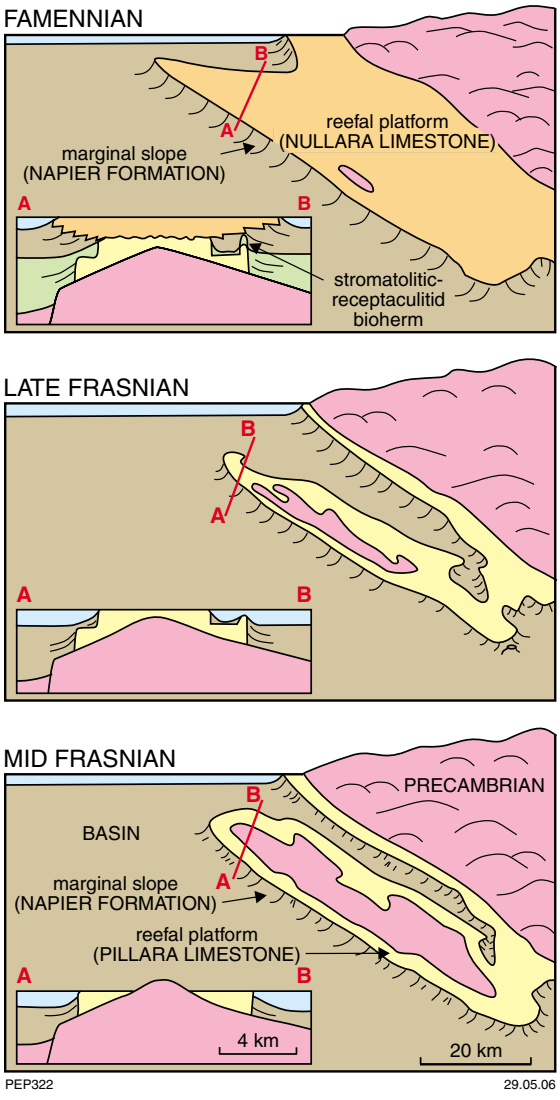

Figure 453. **Series of diagrams illustrating development of the Oscar Range reef complex through time (after Hurley, 1986).**



Figure 454. Wire Spring (*Bullulu*), an attractive permanent spring on the northeast side of the Oscar Range. A crocodile, about 1.5 m long, was seen in this pool in 2006.



Figure 455. The Frasnian–Famennian boundary at the northwestern end of the Oscar Range, looking west, showing massive reef limestone of the Pillara Limestone below and well-bedded back-reef limestone of the Nullara Limestone above. The hills on the horizon are of indurated sandstone of the Grant Group, surrounding lamproite volcanic plugs.

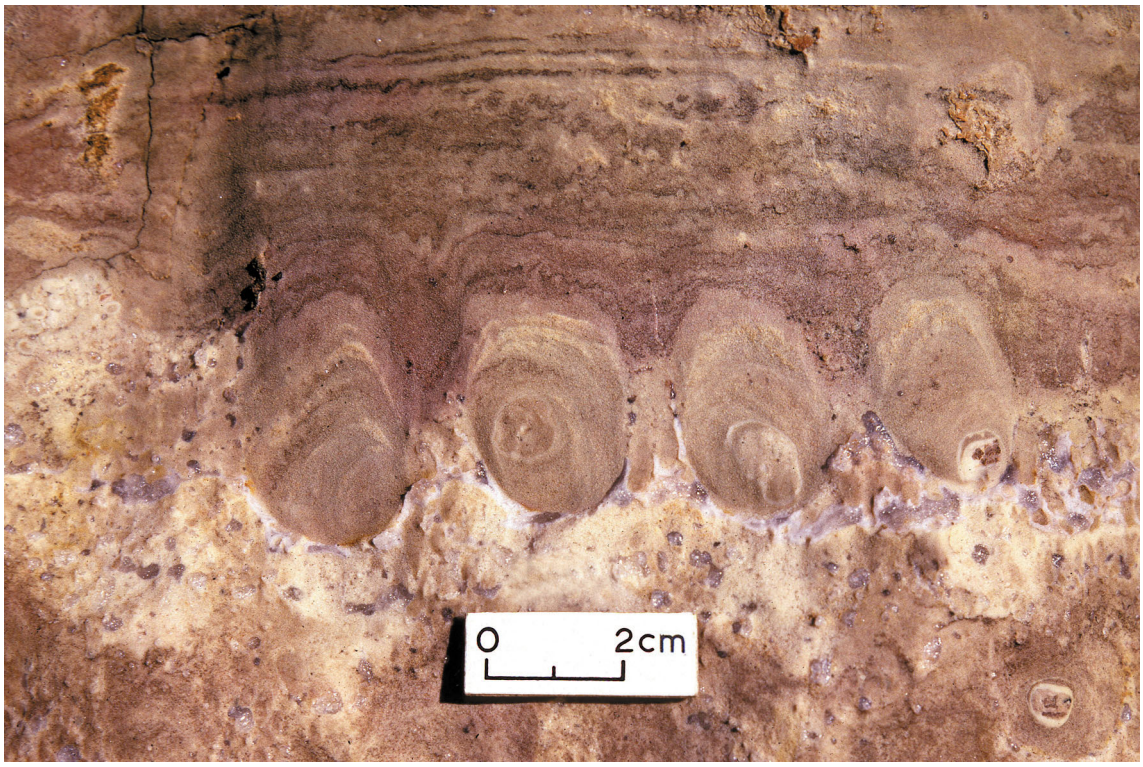

Figure 456. Oncolitic limestone of the back-reef Nullara Limestone at the northwestern end of the Oscar Range. The oncolites seen here became stabilized and capped by columnar microbial growths before passing up into laminar microbial limestone.



Figure 457. Morown Cliff, consisting of late Famennian Windjana Limestone, forming the northern margin of the Oscar Range reef complex. The scarp is essentially the original reef front, modified to some extent by modern erosion, dating from the time when the reef became extinct after the late Famennian fall in sea level.



Figure 458. Morown Cliff, showing vertical karren formed by modern karst erosion. The overhang at the base of the cliff on the right is decorated with Aboriginal rock paintings.



Figure 459. Ellendale leucite-lamproite vent no. 38. The low mound of lamproite (left of centre) intrudes marginal-slope limestone (Napier Formation).

Ellendale vents

The Ellendale vents are part of a series of lamproite diatremes that intrude Devonian to Permian sedimentary rocks of the Lennard Shelf (Plate 2) and nearby Precambrian rocks. In total, there are 45 vents in the area, extending northwest from the northwest end of the Oscar Range. A few are diamondiferous and are currently being mined. Radiometric dating indicates that the vents are of Miocene age (20–22 Ma; Jaques et al., 1986).

Lamproites are rarely exposed in the vents. A notable exception in the Oscar Range area is Ellendale 38 vent (GPS AMG Zone 51, 708400E 8043070N), which intrudes the Napier Formation on the southeast flank of the Oscar Range near Bathtub Spring (Fig. 459; Plate 2). This leucite-lamproite vent is subcircular and about 70 m across. The plug forms a low hill of sparkling lamproite, surrounded by a dark-coloured metamorphic aureole as much as about 2 m wide in fore-reef limestone of the Napier Formation. The limestone, which elsewhere is pale yellow to white, is dark grey to black in the aureole, and gives off a foetid odour when struck, apparently due to the presence of minor amounts of hydrocarbons. Nicoll (1981) showed that the colour-alteration index of conodonts in limestone adjoining a similar plug in the Old Leopold Downs area ranges from 8+ directly adjoining the plug to 1 at a distance of only 80 cm from it. Nicoll deduced from this that the temperature of the lava was in excess of 600°C.

Because the diatremes were products of short-lived explosive volcanism, the metamorphic influence on limestone was confined to a narrow aureole, leaving most of the rocks unaffected. On the other hand, where diatremes intrude sandstones of the Grant Group, the metamorphic effects extended further, resulting in induration of the adjoining sandstones, which now form conspicuous hills, such as Mount Percy near the Oscar Range (AMG Zone 51, 704300E 8051200N).

Tunnel Creek

Tunnel Creek (AMG Zone 51, 727600E 8051700N; Plate 2) flows below the Napier Range in a remarkable natural tunnel, 0.7 km long. It was localized by a small fault that may have been active during the Devonian, as evidenced by brecciation at the north entrance to the tunnel. An irregular depression is present in limestones over the tunnel, possibly indicating that the creek once flowed across the range at that level. The creek is ephemeral, but pools of water remain throughout the year, and many tourists walk the length of the tunnel during the dry season. The only light inside the tunnel comes from the entrances and in the middle where the roof has collapsed. Immediately south of the southern entrance the creek flows in a straight steep-walled valley, known by the Aboriginal name *Barrar* (Fig. 460), which features in the *Tchularga* song cycle.

It is probable that this tunnel, like others on the Lennard Shelf, originated through solution in subglacial meltwater during the Early Permian glaciation, although no proof of this hypothesis has been found, and modern erosion has substantially modified the tunnel. A poorly exposed cross-bedded granule and pebble conglomerate, first brought to my attention by Maurice Tucker, is exposed on the floor of the tunnel near the south entrance. The conglomerate might be a remnant of Permian deposits that once filled, or partly filled, the tunnel. On the other hand the conglomerate may be a Quaternary deposit.



Figure 460. Aerial view of Tunnel Creek, looking northeast. The creek flows underground upstream from the narrow valley in the foreground. This locality is known to the Bunaba Aborigines as *Barrar*.

McSherrys Gap

McSherrys Gap (*Wulambu*; AMG Zone 51, 723000E 8056900N; Plate 2) is located where McSherrys Creek cuts through the Napier Range, the sides of the gap having formed in fore-reef deposits of the Napier Formation. Like many other gaps through the limestone ranges, McSherrys Gap may have been localized by subglacial erosion during the Early Permian.

The Napier Formation is dolomitized on the south side of McSherrys Gap near its eastern entrance, but the formation contains little dolomite near the other entrance, and its primary depositional fabrics are well preserved.

A notable feature in the Napier Formation in the central south side of the gap is an antiformal stromatolite (Fig. 461). Applying the term 'antiformal' to such structures is not meant to suggest that they are tectonic folds, on the contrary they are undeformed growth structures. This particular structure has a relief of more than 2 m and is about 10 m wide. The upper layer was built by columnar stromatolites, but other parts consist of red microbial limestones without columns. The stromatolitic layers pinch out on the lower outer sides of the antiformal structure, which is overlain by a bed of yellow, sandy, bedded dolomite. The overlying bed thins over the structure, proving that it had its antiformal shape at the time of deposition.

The Napier Formation near the western end of the gap on the south face contains numerous debris-flow deposits and large allochthonous reef blocks. A bed of debris-flow megabreccia rests on a sheared layer, with associated folding and brecciation of the underlying strata and injection of breccia between beds below the main shear surface (Fig. 124). One block of Famennian reefal limestone at this locality contains abundant allochthonous lithiotid bivalves, that must be derived from the equivalent platform.

A prominent isolated allochthonous block of *Renalcis*-rich microbial reef limestone is embedded in thin-bedded fore-reef limestones about 0.5 km south of McSherrys Gap (AMG Zone 51, 723500E 8056200N; Fig. 128).

After coming to rest on the slope the block stood above the adjoining fore-reef strata long enough (probably several thousand years) to allow a layer of stromatolites about 15 cm thick to encrust its upper surface. If those stromatolites grew at a rate similar to that of the stromatolites forming Elimberrie no. 1 bioherm, then this 15 cm layer would have taken about 15 000 years to grow.

A conspicuous mass of allochthonous blocks, composed largely of distal-marginal-slope crinoidal limestone, is present in front of the Napier Range about 2 km southeast of McSherrys Gap (centred on AMG Zone 51, 723500E 8055000N; Fig. 462). This unique debris-flow deposit seems to have originated on the marginal slope during the late Famennian, shortly prior to the demise of the reefs, but its full significance has yet to be determined.

An unusual example of early deformation of distal marginal-slope deposits, giving rise to ball-and-pillow structures, is exposed on the north side of the Napier Range, about 1 km north of McSherrys Gap (Fig. 463; AMG Zone 51, 723500E 8057800N.). This structure has resulted from mud liquefaction, probably induced by seismic activity, resulting in pieces of the overlying weakly lithified sandstone sinking into the mud.



Figure 461. Antiformal stromatolite on the south wall of McSherrys Gap.



Figure 462. Debris-flow megabreccia on the southwest side of the Napier Range 2 km south-southeast of McSherrys Gap, showing a jumbled mass of marginal-slope limestone (largely encrinite, with some reef limestone), in front of the range.

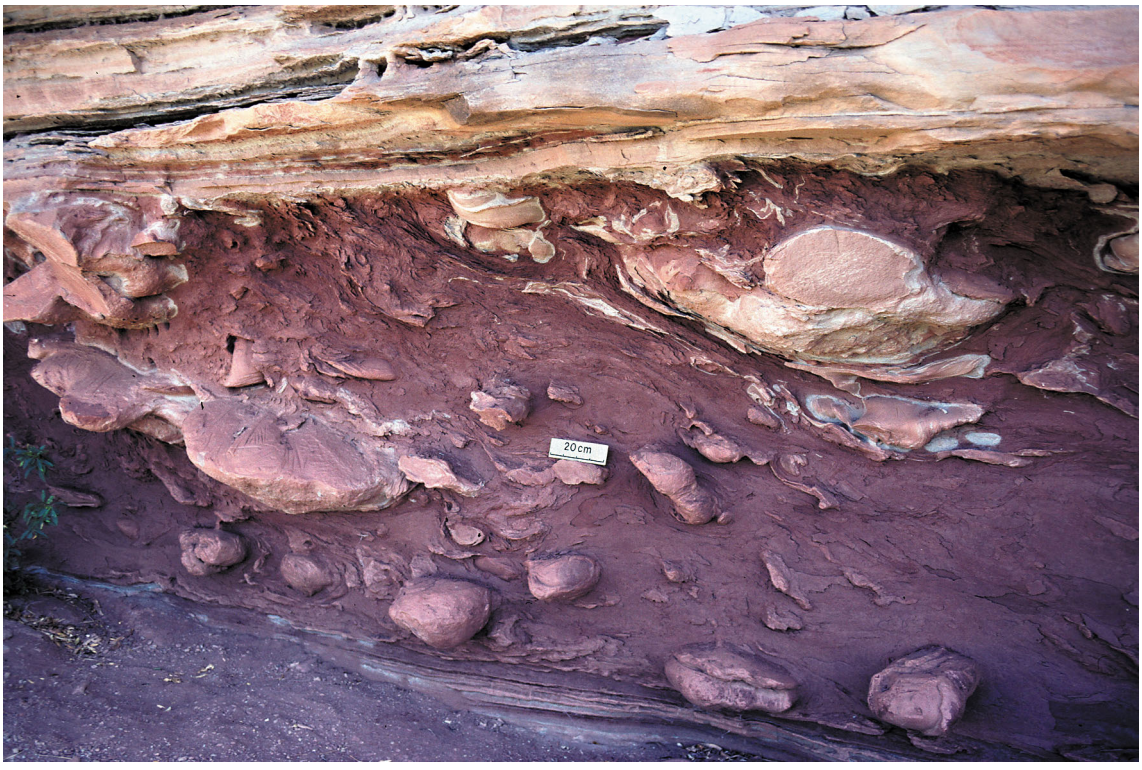

Figure 463. Ball-and-pillow structure in red sandy siltstone at the top of a cycle in the Pillara Limestone, north of McSherrys Gap. The light-coloured clasts are composed of fine-grained calcareous sandstone. This structure formed through mud liquefaction causing pieces of overlying weakly lithified sandstone to sink into the mud. The grooves in the large sandstone 'pillow' to the left of the scale were used by Aborigines to sharpen and polish their stone axes.

Carpenters Gap to the west entrance to Windjana Gorge

Carpenters Gap is a dry gap through the Napier Range, 8 km southeast of Windjana Gorge (AMG Zone 51, 713100E 8070300N; Plate 1), that may originally have formed below the Early Permian ice sheet, as part of a large subglacial channel. Fore-reef deposits of the Napier Formation containing many allochthonous blocks of reef are exposed in and adjoining the gap. Several features of particular interest are exposed in fore-reef and platform deposits from the gap to the west entrance to Windjana Gorge

A good example of a debris-flow breccia and associated intraformational distortion is exposed on the northeast side of the Napier Range, 0.3 km northwest of Carpenters Gap (AMG Zone 51, 713000E 8071200N). The debris-flow deposit includes tabular clasts of marginal-slope limestone oriented parallel to the base of the flow, indicating a laminar-flow mechanism. A large allochthonous block of reef limestone that was carried with the flow has gouged and pushed the underlying thin-bedded yellowish limestone and red shale, causing it to become strongly contorted (Fig. 464). Evidently the limestones were weakly lithified when they were folded, so that they held together, unlike the interbedded incompetent shales.

Many limestone blocks in the debris-flow breccia at this locality show evidence of strong early marine cementation that had occurred in reef-margin and marginal-slope limestones prior to their collapse into the debris flow. Former cavities in the reef limestones, filled with banded early marine fibrous-calcite cement, are now truncated at the margins of blocks (Fig. 172).

Siliciclastic conglomerates deposited in marginal slope environments are exposed in the face of the first prominent bluff southeast of Carpenters Gap (AMG Zone 51, 713900E 8070300N). They cut through, and grade into, Napier Formation, and are included in the Behn Conglomerate.

A small outlier of Pillara Limestone (platform facies) is situated 1.5 km northwest of Carpenters Gap and 3 km southeast of the east entrance to Windjana Gorge. It consists of reef-flat to back-reef limestones that are truncated by fore-reef limestones of the Napier Formation (Figs 465, 466). A large cave in this outlier, known to the *Unggumi* people as *Tangalma*, is decorated with Aboriginal paintings and carvings (Playford, 1960, 2007). The soil profile below the floor of the cave contains evidence that human usage of this cave dates back more than 40 000 years (O'Connor, 1995). O'Connor refers to this site as 'Carpenters Gap', but as it is more than a kilometre northwest of that gap it seems more appropriate to use the Aboriginal (*Unggumi*) name for the site, *Tangalma* (Playford, 2007).

Between *Tangalma* and *Langurrngurru* is *Mungurrma* Valley, at the west end of which is an excellent example of a small debris-flow deposit, which has cut into the underlying distal fore-reef deposits of the Napier Formation (Fig. 467). It must have stood as a low mound on the sea floor after coming to rest near the base of the slope, and subsequent fore-reef deposits were draped over it, although the draping effect has since been accentuated by differential compaction. A flame structure, developed at the base of the debris flow deposit as a result of loading on underlying sediments as the flow came to rest, is shown as Figure 468.

Another small outlier of Pillara Limestone (platform facies), fringed by Napier Formation (marginal-slope facies), is exposed 400–700 m east-southeast of the east entrance to the gorge. This outlier consists of massive reef and bedded reef-flat and back-reef subfacies. Bedding in these deposits is largely defined by recessive sandy and conglomeratic layers, giving rise to overhangs and caves, one of which contains many cave paintings (Fig. 11). Passing from back-reef to reef-flat and reef-margin, the beds become progressively thicker and more massive (Figs 469–471).

Windjana Gorge

Windjana Gorge is the most important locality on the Lennard Shelf for the study of the Devonian reef complexes (Figs 479–521). It exposes a classic section through the Napier Range reef complex. The gorge is included in a National Park and is regarded as an important part of Australia's natural heritage (Playford, 1984c).

Windjana Gorge has been known to geologists for more than 120 years, since it was first visited by the Government Geologist Edward T Hardman in 1883, as a member of the expedition to the West Kimberley led by John Forrest (Hardman, 1884; Playford and Ruddock, 1985; Playford, 2005; Figs 472, 473). Hardman named the gorge 'Devil's Pass', probably because of the devil-like Aboriginal rock paintings ('lightning men') that are displayed in a prominent cave, known as, *Langurrngurru*, near the east entrance (Fig. 11). The largest and most dominant painting in this cave is a large *Wandjina*, a culture hero who is also known as *Langurrngurru*, shown with his children at his feet and flanked by two 'lightning men' (*Nara Nara*) standing on either side of a yam (Fig. 474; Playford, 1960, 2007).

The early pastoralists knew this remarkable cañon as 'Windjana Gorge', the name 'Windjana' presumably being a corruption of *Wandjina*, after the prominent cave painting to be seen near the east entrance. The Aborigines had no name for the gorge as a whole, but they had many names for localities within the gorge and surrounding areas. Some of those names are shown on Plate 6 and Figure 475. Each of the named features had spiritual significance to the *Unggumi* and *Bunaba* people, associated with their ancestral legends of the Dreamtime.

The first geological description of Windjana Gorge was by Playford and Johnstone (1959a), and it was subsequently discussed in more detail by Playford and Lowry (1966). The gorge is some 4 km long, has an average width of about 180 m and a depth of about 70 m. The limestone walls are near vertical in most places, and can be ascended, with difficulty, at only a few localities. Among the main access routes to the top of the range used by the Aborigines were *Mandjalan*, *Marli*, and *Malambeea*. *Mandjalan* is a gap in the north wall of the gorge (AMG Zone 51, 706700E

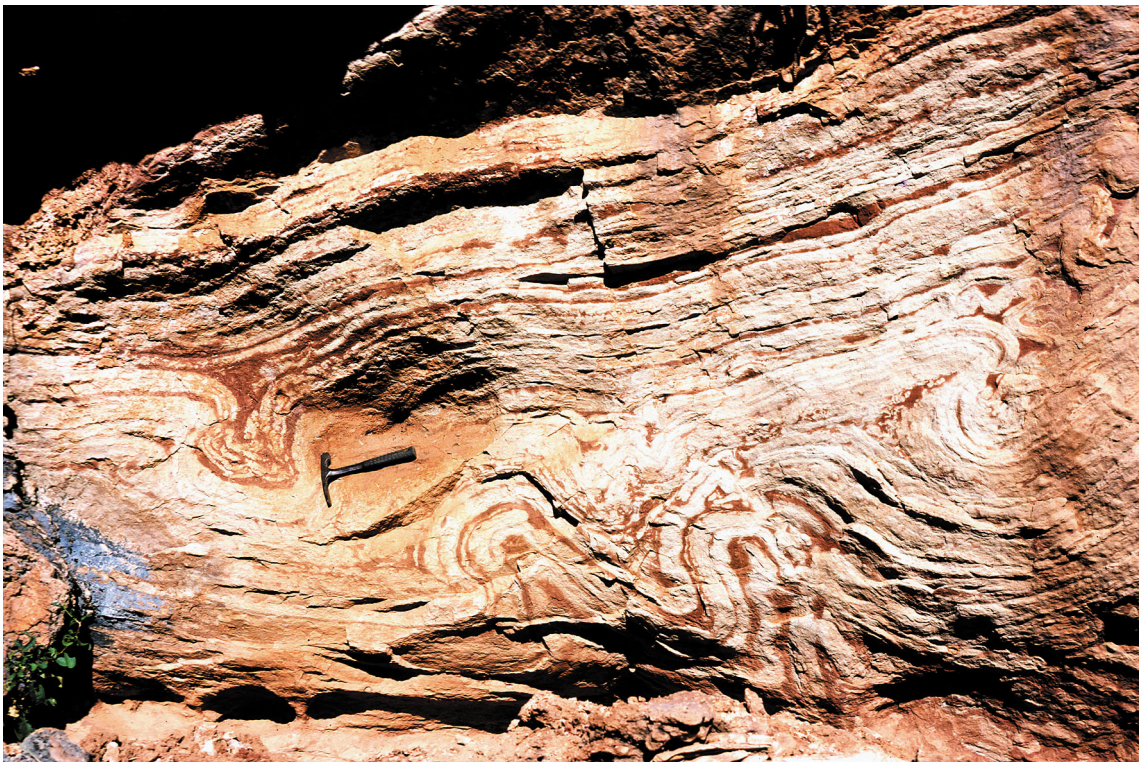

Figure 464. Contorted beds in fore-reef strata of the Napier Formation, near Carpenters Gap. The contortion was caused by a large allochthonous block of reef limestone which gouged and pushed the underlying thin-bedded limestone and shale.



Figure 465. *Tangalma* cave or rock shelter, near Carpenters Gap on the north side of the Napier Range. Aboriginal art in the cave includes a large *Wandjina* figure. Radiocarbon dating indicates that Aboriginal occupation of this cave began at least 40 000 years ago. Note the truncation of the Pillara Limestone, abutted by fore-reef deposits (Napier Formation), on the extreme left (south) side.



Figure 466. Pillara Limestone (platform facies) on the left, abutted by Napier Formation (marginal-slope facies) on the right, at the north end of the small platform at *Tangalma*.



Figure 467. Debris-flow deposit beside *Munggurrma* Valley south of the east entrance to Windjana Gorge. The deposit, containing clasts of reef and fore-reef limestone, is in fore-reef deposits of the Napier Formation. It formed a low mound on the sea floor, near the base of the marginal slope.

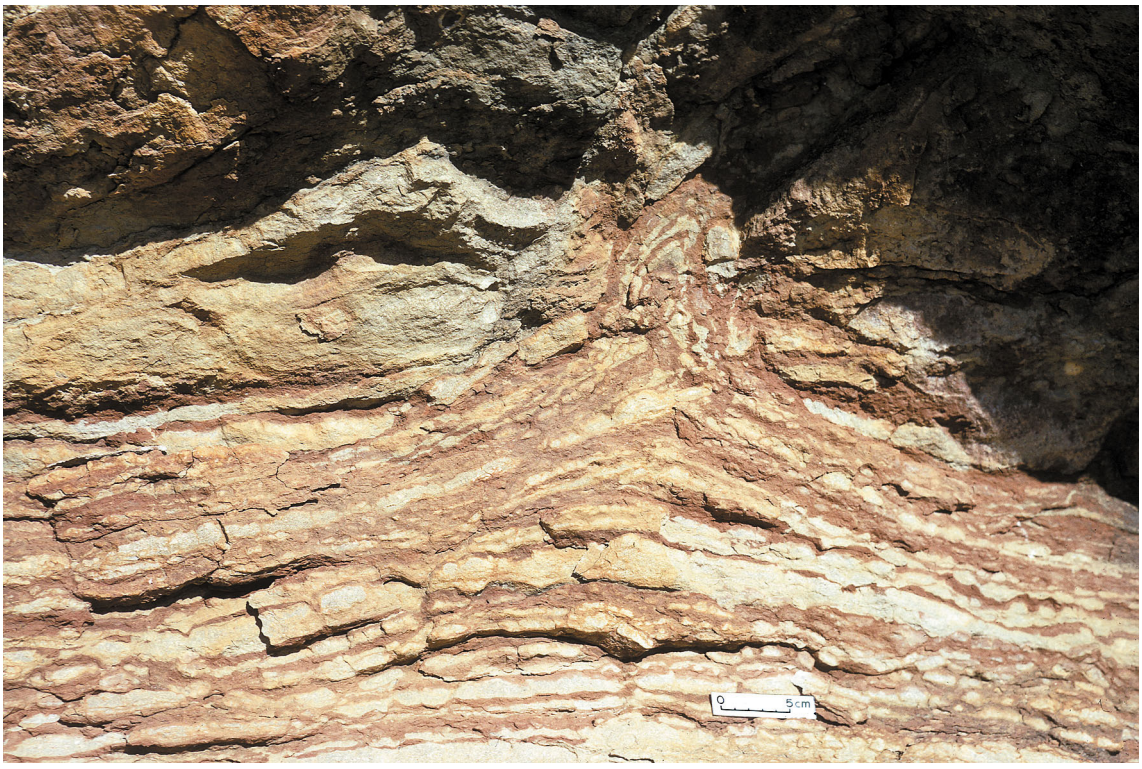

Figure 468. **Flame structure developed in marginal-slope limestone directly below the debris flow deposit shown in Figure 467.**

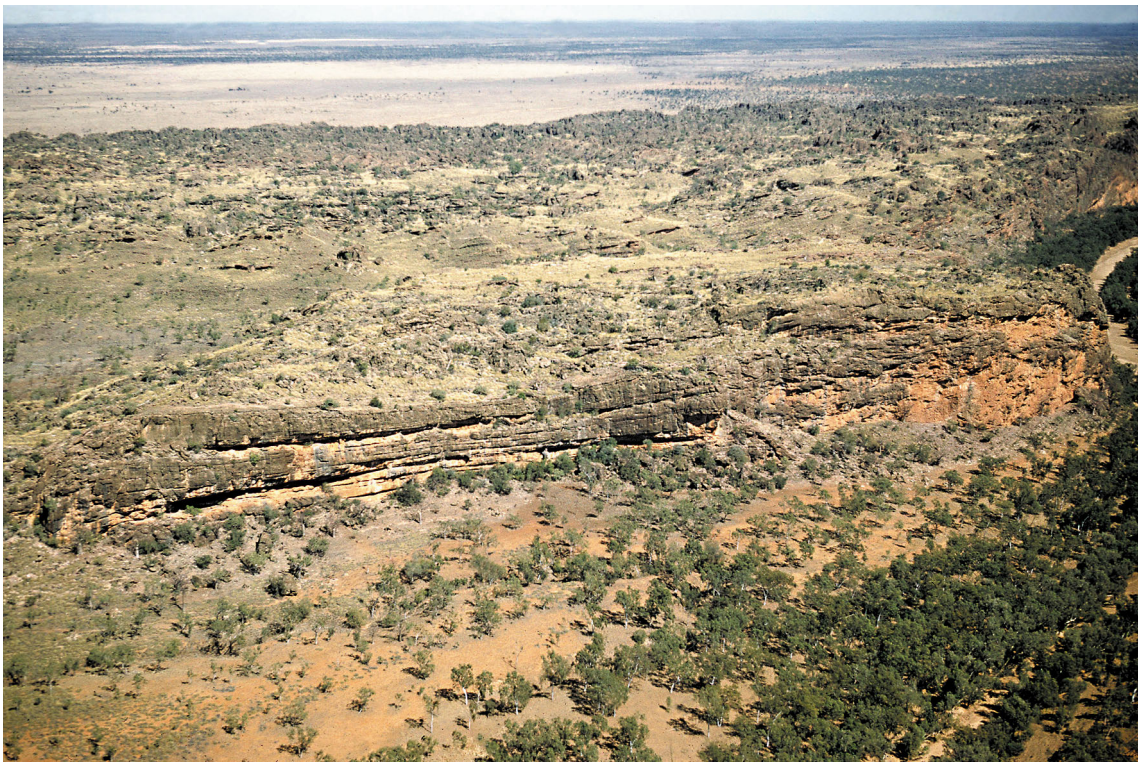

Figure 469. **Aerial view looking south near the east entrance to Windjana Gorge, showing platform carbonates of the Pillara Limestone (middle to left), interfingering with, and abutted by, fore-reef carbonates and terrigenous conglomerate of the Napier Formation (on the right).**



Figure 470. Closer aerial view of the platform facies at *Langurrngurru* (near the east entrance to Windjana Gorge), looking south, showing back-reef subfacies in the middle, and reef-flat and reef-margin subfacies on either side. The 'dished' shape of the platform resulted from increased pressure-solution compaction in the back-reef. Note that bedding progressively thickens and disappears as the platform passes from back-reef into reef limestone.

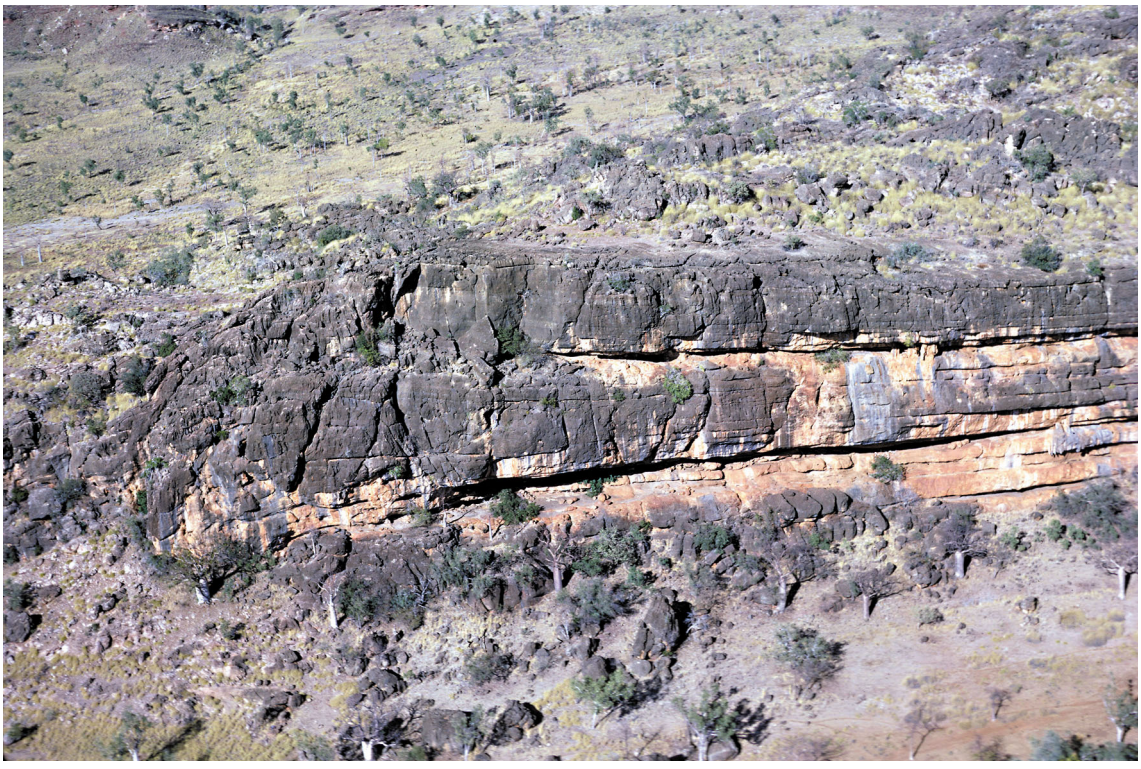

Figure 471. Closer aerial view of the eastern part of Figure 470. The *Langurrngurru* cave with a *Wandjina* painting is situated below the lower overhang, on the left-hand side. Note that bedding gradually disappears passing from back-reef into reef.

8074300N) following a major neptunian dyke. From this gap an Aboriginal path once led to the *Mangalamma* valley and on to *Baralamma* Spring. At *Marli* (AMG Zone 51, 706900E 8074200N) a remarkable 'chimney' in recent talus of limestone blocks (Figs 475, 476) allows access to the top of the range, and from there an Aboriginal path once led on to *Limalwurru* (Lillimilura Spring). This route was used by the Aboriginal outlaw *Jandamarra*, otherwise known as Pigeon, when he escaped, seriously wounded, after a battle with police in 1894 (Idriess, 1952; Pederson and Woorunmurra, 1995). *Malambeea* (meaning 'wait a while' in the *Unggumi* language), is a place on the range (AMG Zone 51, 708200E 8074200N) where Aborigines, having climbed up from the plain northeast of the gorge, would take a spell before descending to their favoured fishing spot, on rocks at *Mingun.*

The Lennard River flows strongly through the gorge during and shortly after the wet season (December to May), but in most years water is confined to pools in the main channel (Figs 477, 478). The largest and most permanent of these is located near the west entrance, around a large fallen block of Famennian reef limestone, known to the *Unggumi* and *Bunaba* Aborigines as *Bandangnan*, the Rainbow Serpent (Fig. 478). This person is said to have made the gorge during the Dreamtime, bringing the spirits of children to the waterhole and from there to their mothers' wombs. After death, a person's spirit returned to the same waterhole.

The water in the gorge is fresh but turbid, containing a rich fauna of fish and fresh-water crocodiles (Fig. 13). Many birds frequent the area, especially corellas, whose screeching cry is a characteristic sound of the gorge.

Windjana Gorge was evidently a watering place for animals during the Pleistocene, for the remains of the giant marsupial *Diprotodon* were discovered in river gravels near the west entrance in 1883 (Hardman, 1884, 1887). Nowadays the river gravels hold numerous ancient bones, but all of those that were retrieved during our work there proved to be remains of cattle. Other Cenozoic vertebrate fossils that have been found in the gorge are bones of giant crocodiles and turtles, probably mid-Tertiary in age, as discussed earlier (Gorter and Nicoll, 1978; Fig. 323).

The course of the gorge through the Napier Range is not influenced by the structure of the reef complex; it is clearly superimposed on the range. As discussed previously, the channel now forming the gorge is thought to have originally formed as a large channel cut by subglacial meltwater during the Early Permian. According to this hypothesis it was subsequently filled with Early Permian sediments and has since been exhumed as a result of Cenozoic erosion (Playford, 2002a). Some low sandstone outcrops on the floor of the gorge, first brought to my attention by Maurice Tucker, could be part of that Early Permian infill, but as the sandstone contains probable rhizoliths, it seems more likely to be a Quaternary riverine deposit.

As first suggested by Playford and Lowry (1966), the surface on top of the Napier Range beside Windjana Gorge represents the exhumed Early Permian unconformity, modified by Cenozoic karstification. Overall, the range surface is almost flat, but in places the modern karst is so rugged that it is virtually impossible to travel there on foot. Playford (2002a) concluded that many flat-floored depressions on top of the range are solution dolines filled with soft Lower Permian sandstone and shale. This was proved to be the case in Bristow Amphitheatre (Fig. 479; AMG Zone 51, 708200E 8073500N), where brown sandstone and siltstone were exposed after the dense spinifex cover had been burnt. Other flat areas interpreted as being Permian in Figures 307 and 479 have been mapped by air-photo interpretation. Many of the cave systems exposed in Windjana Gorge, including Pigeon's Cave, are probably also inherited from the Early Permian.

The outcrop geology of the Windjana Gorge area and a cross section through it are shown on Figure 479 and Plate 6, and significant features of the geology are illustrated on Figures 484–521. The Devonian rocks exposed in the gorge belong to both the Pillara and Nullara Sequences, and are correlated with the Pillara Limestone, Napier Formation, and Windjana Limestone. The following descriptions of the section exposed in the gorge progress from east to west, as shown in adjoining panoramas of the gorge in Figures 484–489.

East end of the gorge

Fore-reef limestones exposed in the northern cliff face beside the east entrance to Windjana Gorge include blocks of reef and fore-reef limestones, some as much as 10 m across. Large quantities of sparry calcite are conspicuous features of the exposure (Figs 480, 481). Many parts of the fore-reef deposits are wholly or partly dolomitized, and some contain lenses of adnet breccias. Some clasts in the breccias show evidence of corrosion before being cemented by fibrous calcite (Fig. 481) and many are partly dolomitized (Fig. 482). The corrosion probably occurred after the clasts were deposited in the breccias, or, perhaps less likely, they were corroded before being shed from the reef front during the regression associated with the Classic Face Event.

The east entrance to the gorge was known to the Aborigines as *Djamburrwurru*, meaning 'roaring water', after the roaring sound of water passing through the entrance in time of flood. On each side of the gorge at the entrance is a narrow reef margin of Pillara Limestone, abutted by fore-reef strata of the Napier Limestone, the contact being a near-vertical scarp (Fig. 484). Steeply dipping to massive terrigenous conglomerate interfingers with reef and fore-reef deposits and is well exposed in a cliff about 60 m high, 100 m east-southeast of the gorge entrance (Figs 469, 483). Lenses of conglomerate in this area interfinger with stromatoporoid–*Renalcis*–microbial limestone of the reef and reefal-slope subfacies. Clasts in the conglomerate consist of subangular to rounded pebbles, cobbles, and boulders as much as 1.5 m across. They include granitoid, gneiss, dolerite, garnetiferous mica schist, gabbro, and reworked Devonian limestone. Many of the Precambrian clasts were probably derived from only a few kilometres east to northeast of the gorge. The Mount Behn Fault, which is thought to have been active during the Devonian, probably extends across the area immediately north of the gorge, and its scarp may have been the main source of the conglomerate.



Figure 472. The west entrance to Windjana Gorge ('Devil's Pass') as sketched by Government Geologist E T Hardman in 1883 (from Hardman, 1884).

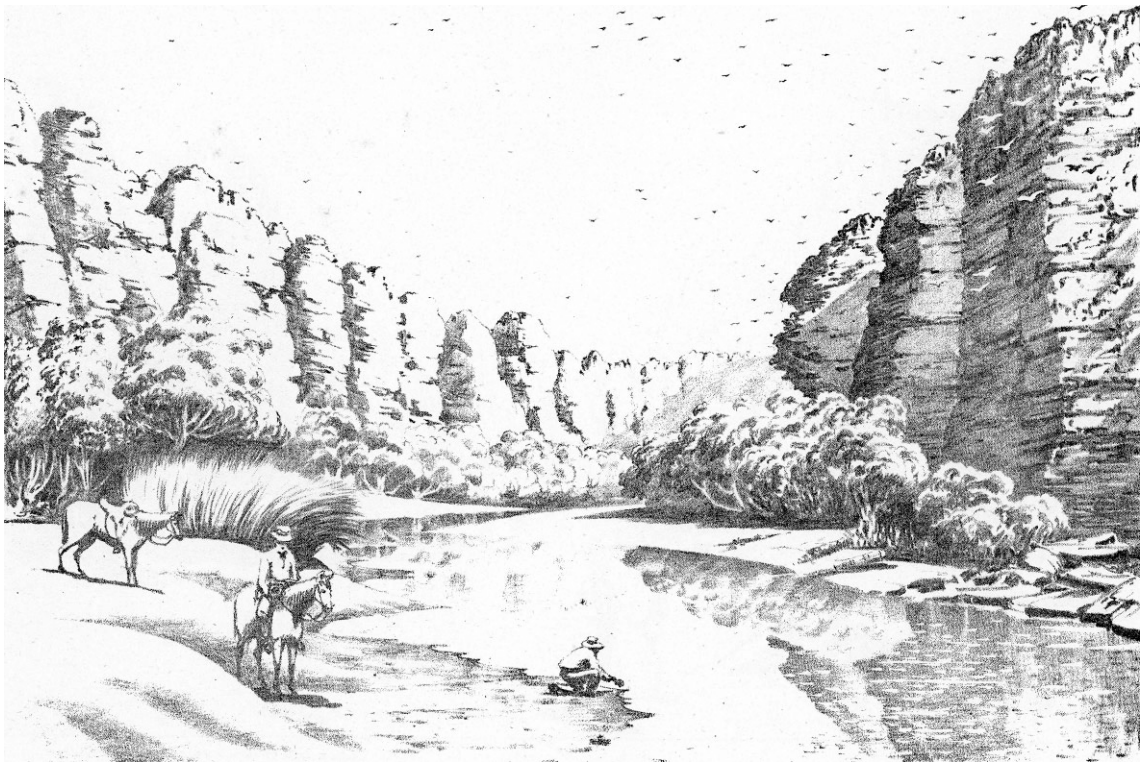

Figure 473. The east entrance to Windjana Gorge as sketched by E T Hardman in 1883 (from Hardman, 1884).

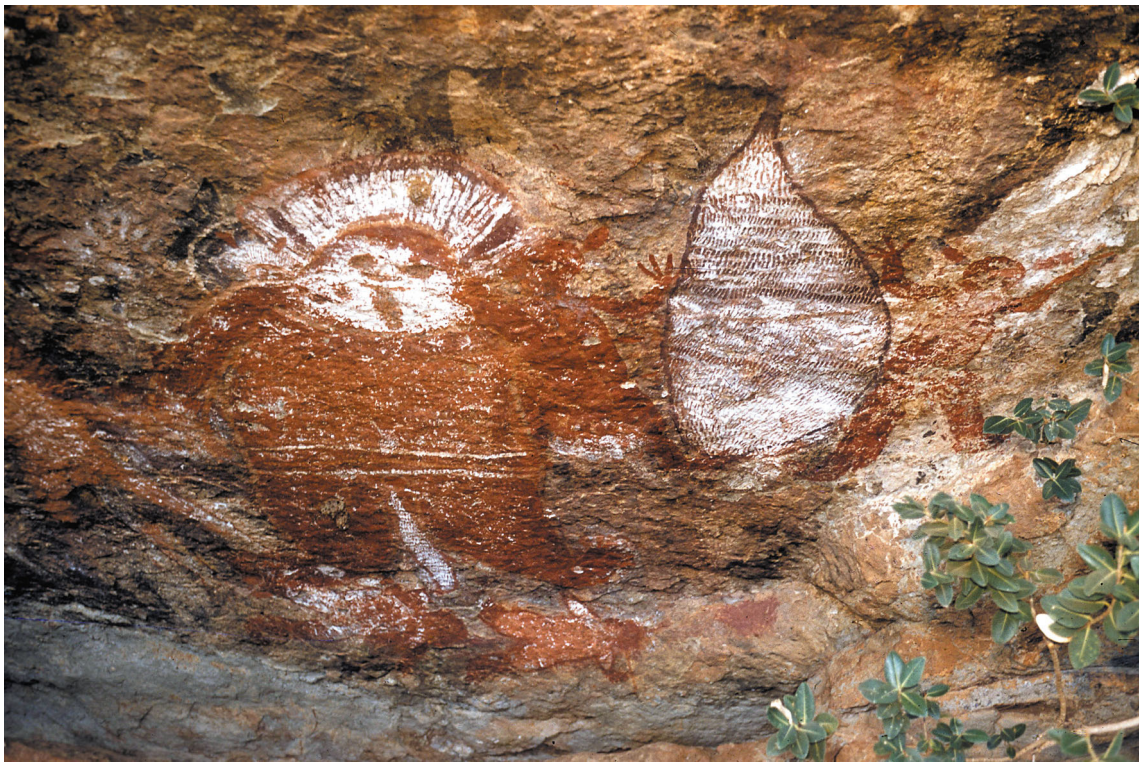

Figure 474. **Aboriginal cave painting near the east entrance to Windjana Gorge, showing a *Wandjina* figure known as *Langurrngurru*, on the left, and two 'lightning men' (*Nara Nara*) standing on either side of a yam, on the right.**

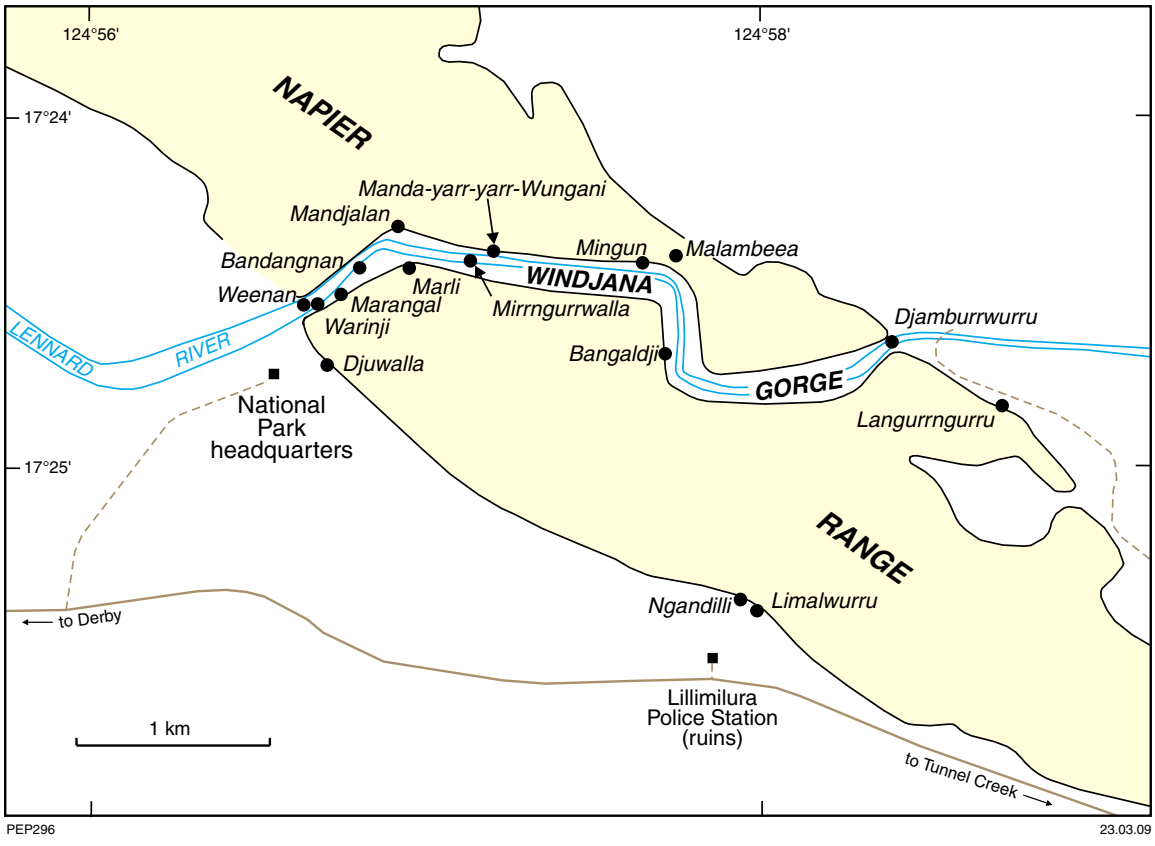

Figure 475. Map of Windjana Gorge showing Aboriginal place names.



Figure 476. **Entrance to a 'chimney' through limestone talus, known to the Aborigines as *Marli,* on the south side of Windjana Gorge near the west entrance. This 'chimney" allows access to the top of the range. It is thought to have been the route followed by the Aboriginal man *Jandamara* (otherwise known as Pigeon) when he escaped from police, while severely wounded, in 1894.**

Figure 477. **(below) Scenic view of Windjana Gorge, taken from the north bank of the Lennard River near *Mirrngurrwalla*.**





Figure 478. **The west end of Windjana Gorge taken from the top of the gorge near *Mandjalan* Pass. Note the parallelism of vertical walls of the gorge. The large block of reef limestone, in the right middle distance, resulted from a recent (but prehistoric) landslide. It is known to the Aborigines as *Bandangnan*, the rainbow serpent, which is said to have made the gorge during the primeval Dreamtime.**

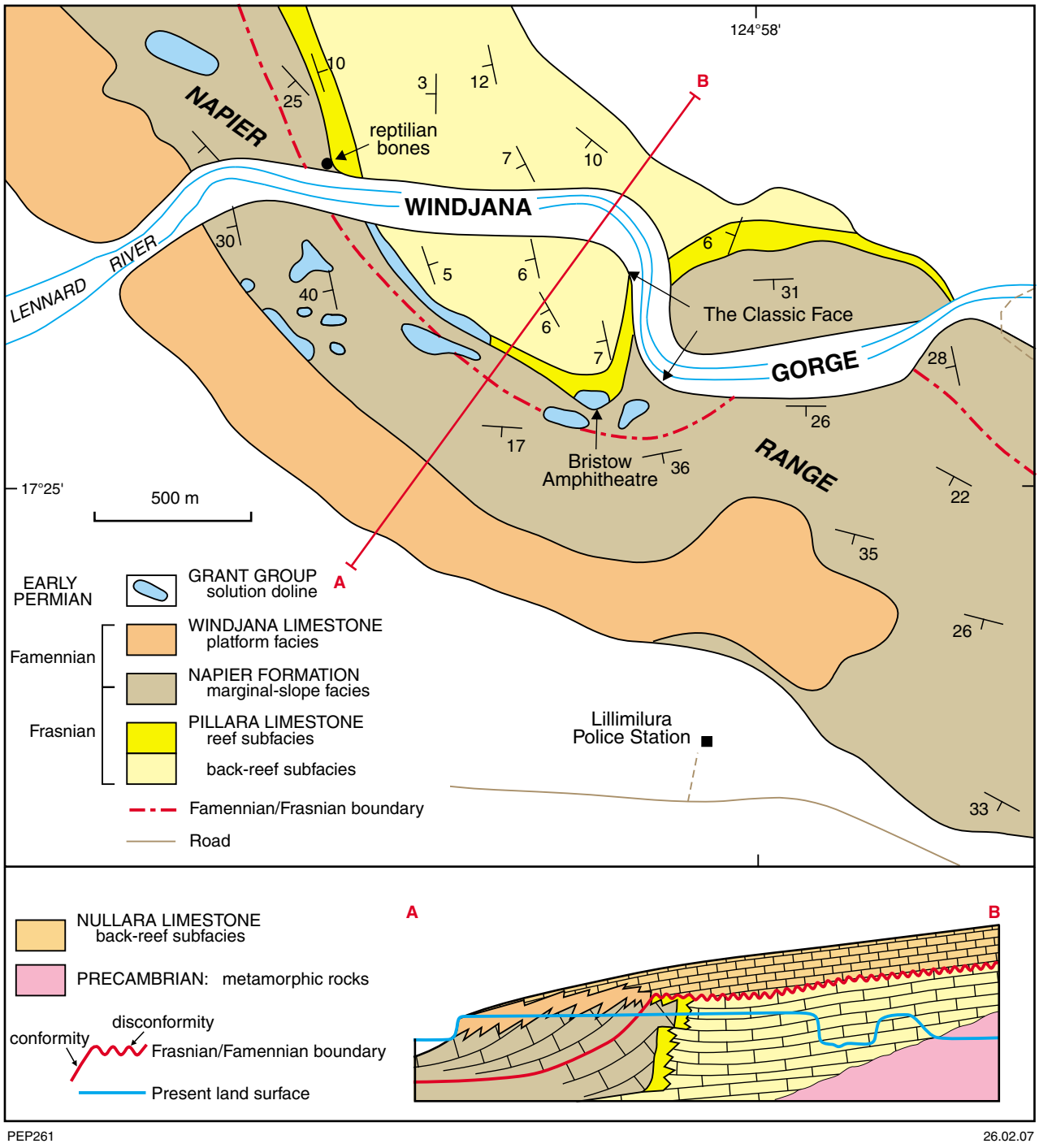

Figure 479. Geological map and cross section of the Napier Range at Windjana Gorge.



Figure 480. Marginal-slope limestone and dolomite of the fore-reef Napier Formation on the north wall of Windjana Gorge beside the east entrance. Note the large volume of white sparry calcite in these deposits.

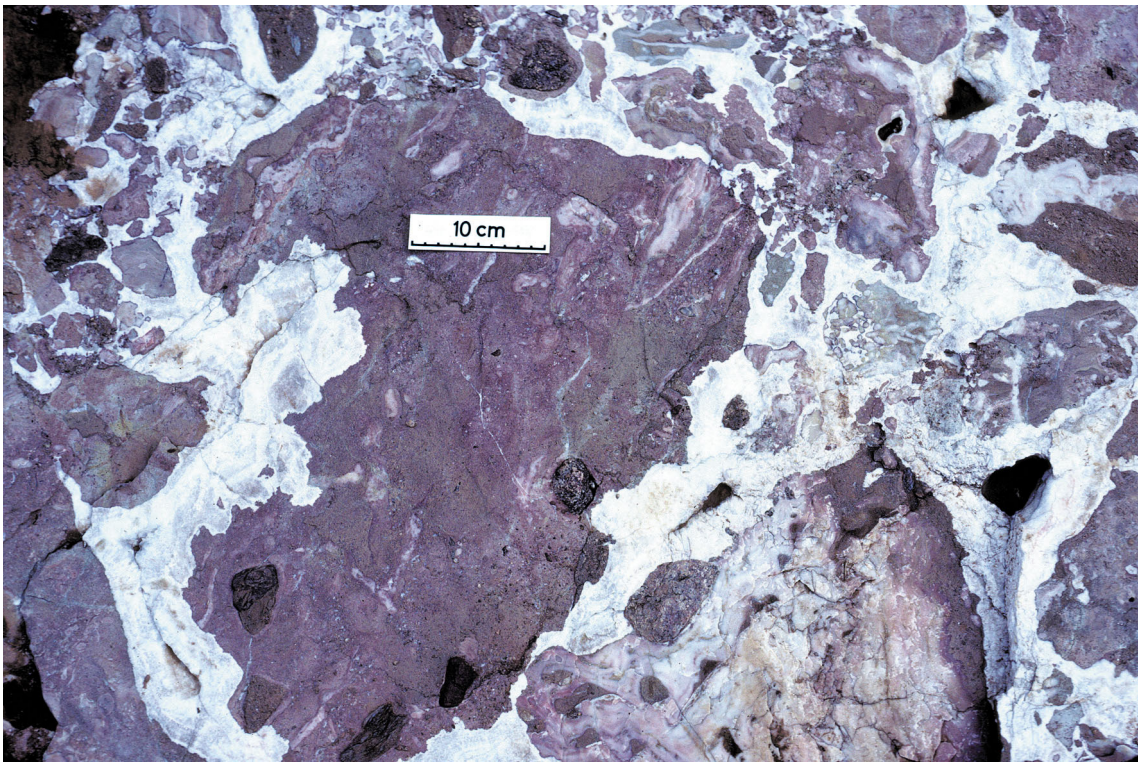

Figure 481. Breccia of reefal-slope clasts in fore-reef Napier Formation on the north wall of Windjana Gorge, beside the east entrance. The large clast shows corroded margins filled with white sparry calcite.

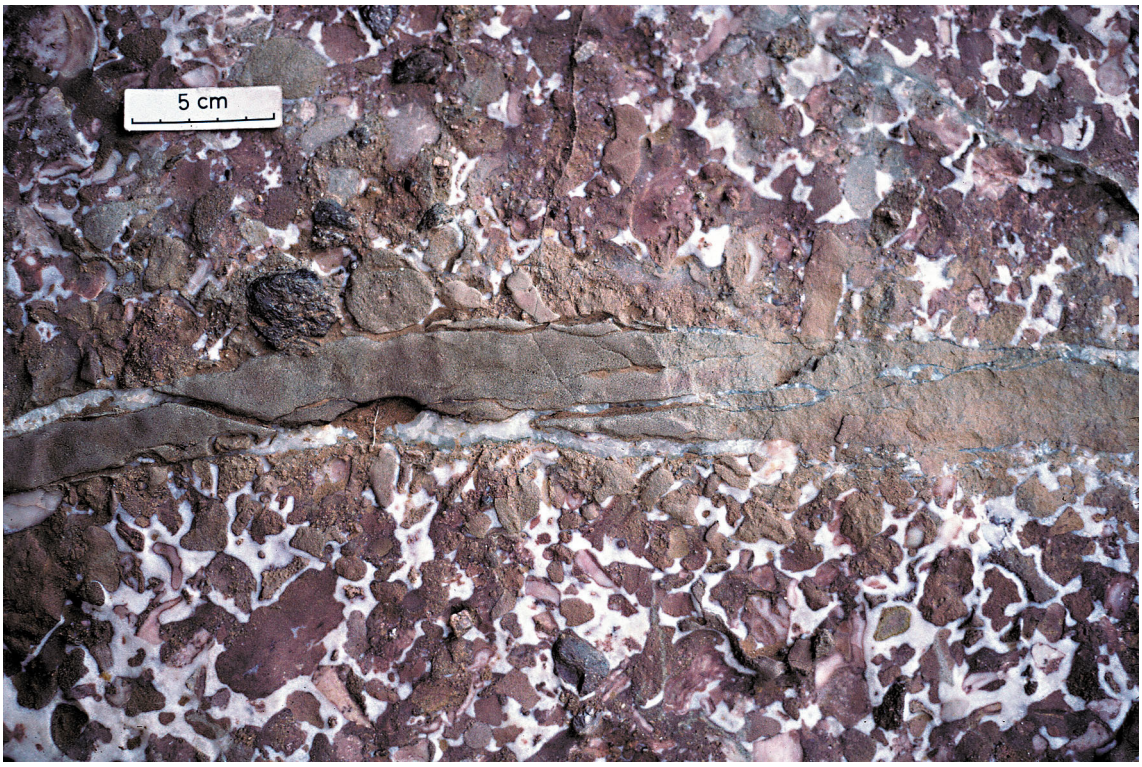

Figure 482. Scheck breccia in fore-reef Napier Formation on the north wall of Windjana Gorge beside the east entrance. The breccia is cut by a small neptunian dyke filled at an early stage by yellow dolomite, with some dolomitization extending beyond the walls of the dyke.



Figure 483. Conglomerate of subrounded to subangular boulders of igneous and metamorphic Precambrian rocks exposed immediately south of the east entrance to Windjana Gorge. The conglomerate interfingers with reef-margin and fore-reef limestones.

East entrance to the Classic Face

The section from the east entrance of the gorge to the Classic Face is illustrated in Figures 484–486. The Frasnian–Famennian boundary close to the entrance is exposed in a small overhang (Fig. 484; GPS AMG Zone 51, 708520E 8073250N), where the latest Frasnian consists of a brachiopod-rich bed containing *Atrypa*, spiriferids, rhynchonelids, nautiloids, *Manticoceras*, and fragmentary *Actinostroma*. It is largely dolomitized, and is overlain by a thin recessive bed (about 40 cm thick) of red silty limestone, deduced to be of earliest Famennian age. The red silty bed is overlain by yellow dolomitic limestone and dolomite containing early Famennian conodonts (Lower *triangularis* Zone; G Klapper, 2004, written comm.) and some unidentified brachiopods.

The Famennian fore-reef deposits exposed in this part of the gorge contain many large allochthonous blocks of *Renalcis*-rich microbial reef limestone (Playton and Kerans, 2006; Playton et al., 2007; Playton, 2008; Figs 485, 491). Some are capped by red 'fingers' and layers of *Sphaerocodium* (Fig. 118) accompanied in some cases by growths of *Renalcis*-rich microbial limestone. Much of this section consists of breccia and megabreccia, interbedded with sandy calcarenite, and having steep (up to 35°) depositional dips. Parts of this section show large-scale cross-bedding resulting from changes that occurred in the positions of the marginal slopes.

The Frasnian–Famennian boundary is exposed again on the south wall of the gorge, 850 m west-southwest of the east entrance (AMG Zone 51, 708600E 8073400N; Fig. 490). As at the previous locality near the east entrance, a thin recessive bed (45 cm thick) of red silty limestone directly overlies a Frasnian unit of limestone, partly dolomitized, containing *Atrypa*, other brachiopods, *Manticoceras*, and fragments of *Actinostroma.* The silty limestone is overlain by a thick Famennian unit of massive red, yellow, and white limestone and dolomite, which is thought to be microbially bound, at least in part. The role played by microbes in forming this unit is suggested by large domal structures immediately above the Frasnian–Famennian boundary (Fig. 99). The base of the unit is in the earliest Famennian Lower *triangularis* Zone (G Klapper, 2004, written comm.). It seems likely that the thin red recessive unit is also of that age, although that has not been proved because of a lack of conodonts in the bed.

The Classic Face

The name 'Classic Face' was first introduced by WAPET geologists for the cliff face in central Windjana Gorge where features of the platform and marginal-slope facies of the reef complex are exceptionally well displayed. This cliff face, which is surely the world's most remarkable Paleozoic reef exposure, was first described by Playford and Johnstone (1959a) and Playford (1961). It was long known to the *Unggumi* Aborigines as *Bangaldji*, a legendary place of bats during the primeval Dreamtime. The best vantage point to view the face is on the north side of the gorge at a locality (GPS AMG Zone 51, 708460E 8073740N) that can best be accessed by climbing and

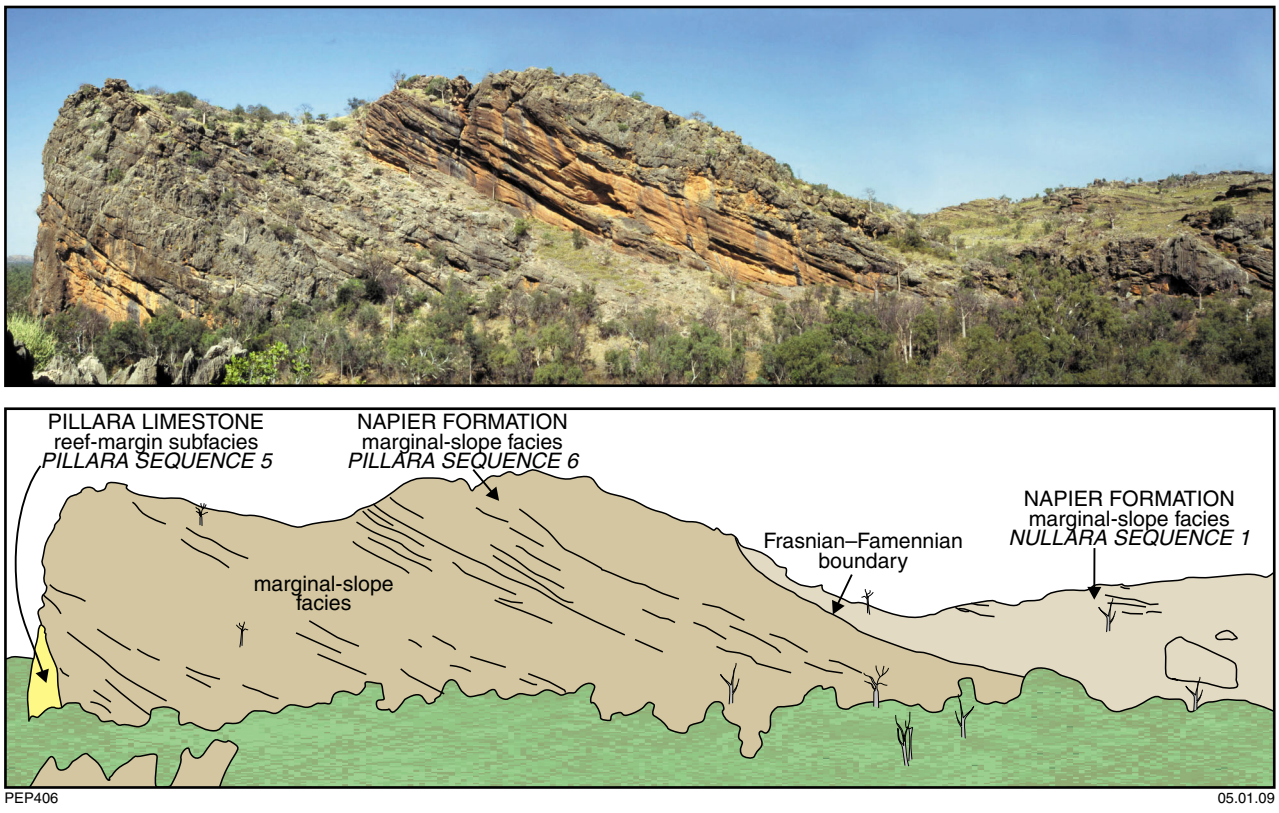

Figure 484. Panorama and equivalent sketch of the south face of Windjana Gorge beside the east entrance.

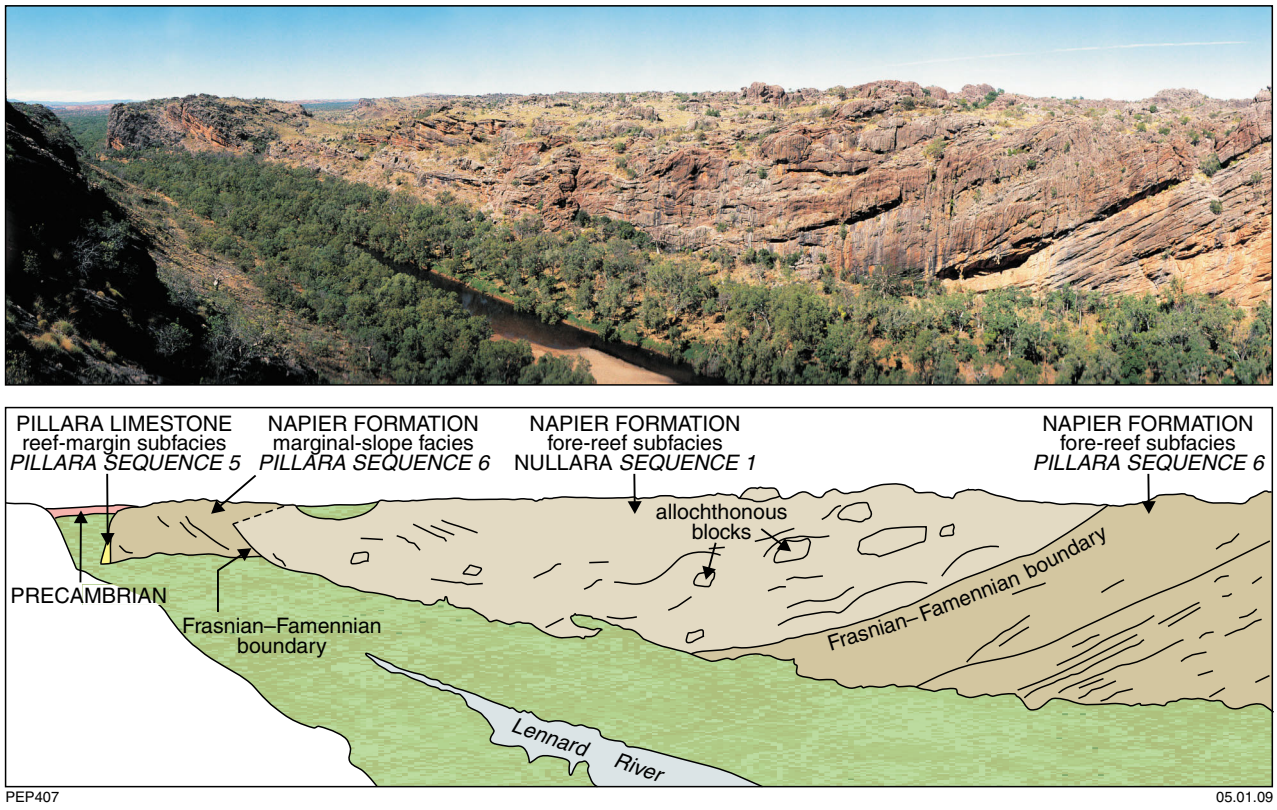

Figure 485. Panorama and equivalent sketch of the south face of Windjana Gorge from the southern end of the Classic Face to the east entrance.

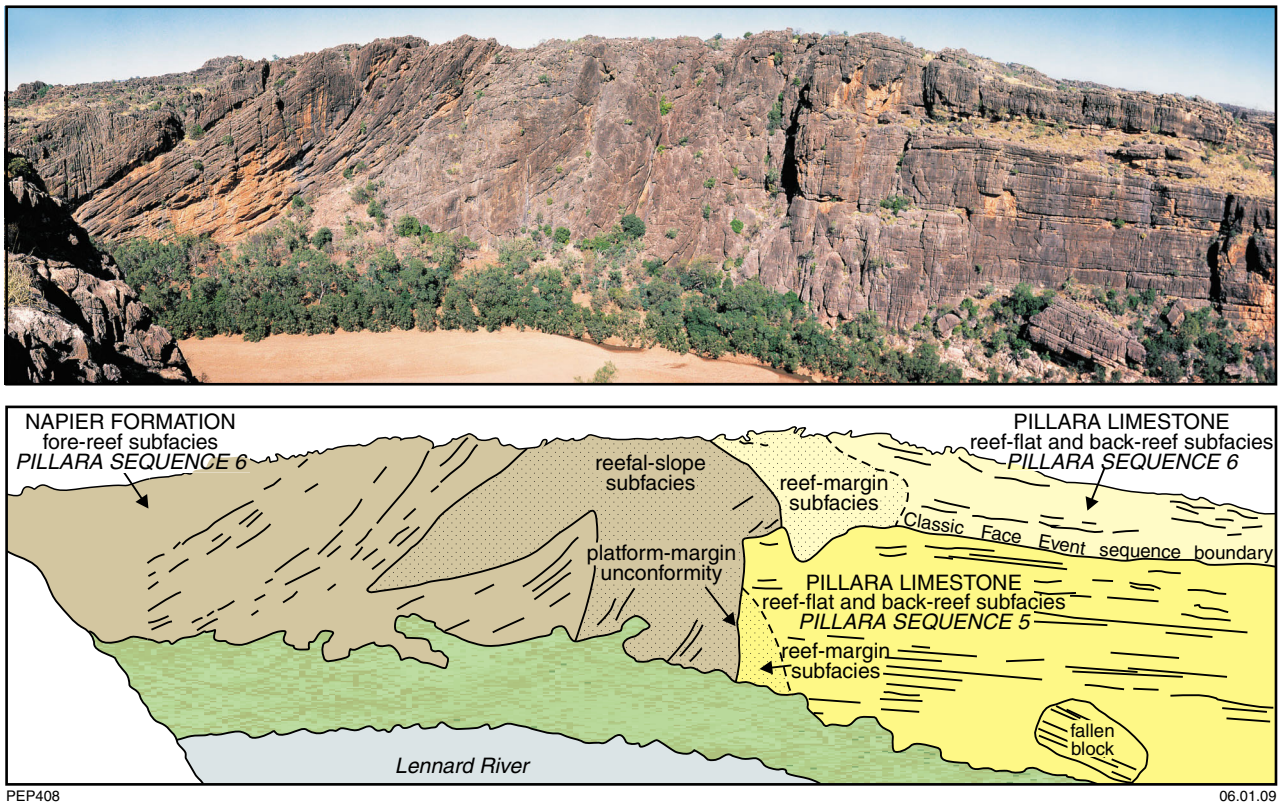

Figure 486. Panorama and equivalent sketch of the Classic Face at Windjana Gorge, showing reef-margin, reef-flat, and back-reef subfacies of the Pillara Limestone on the right, and reefal-slope and fore-reef subfacies of the Napier Formation on the left. The cliff face is about 60 m high.

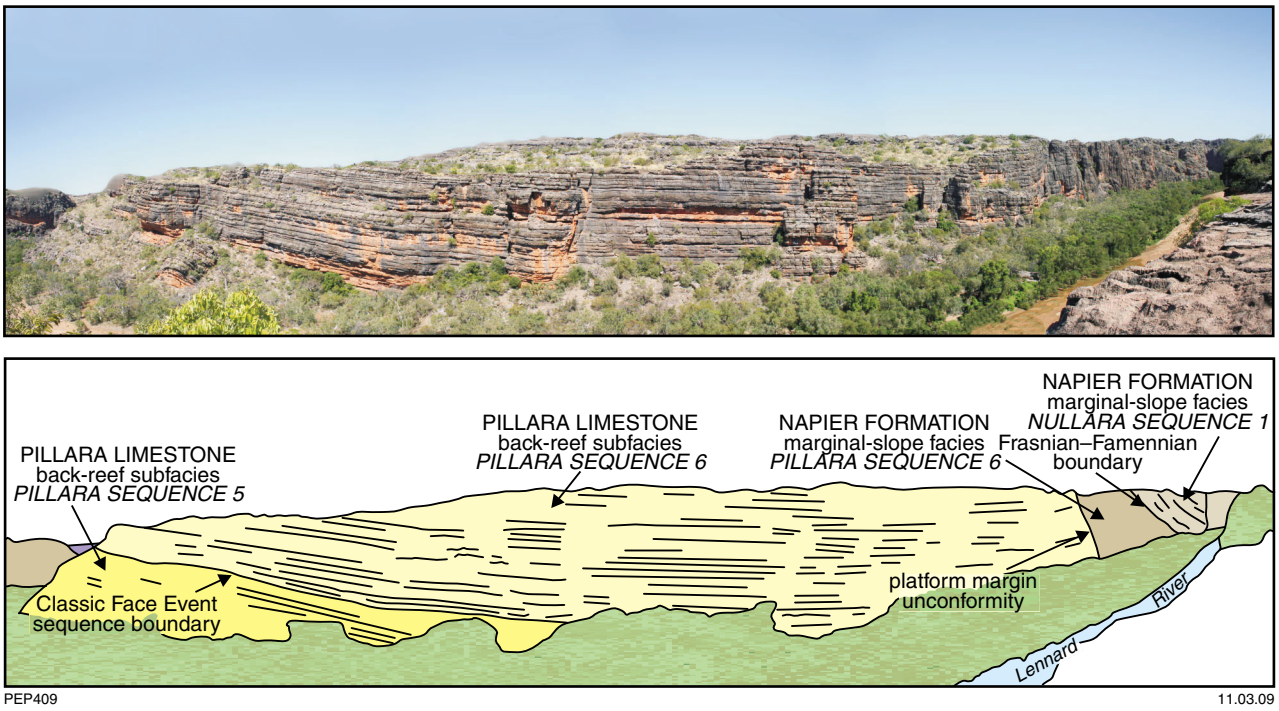

Figure 487. **Panorama and equivalent sketch of Windjana Gorge immediately downstream from the Classic Face, showing back-reef subfacies of the Pillara Limestone, Sequences 5 and 6.**

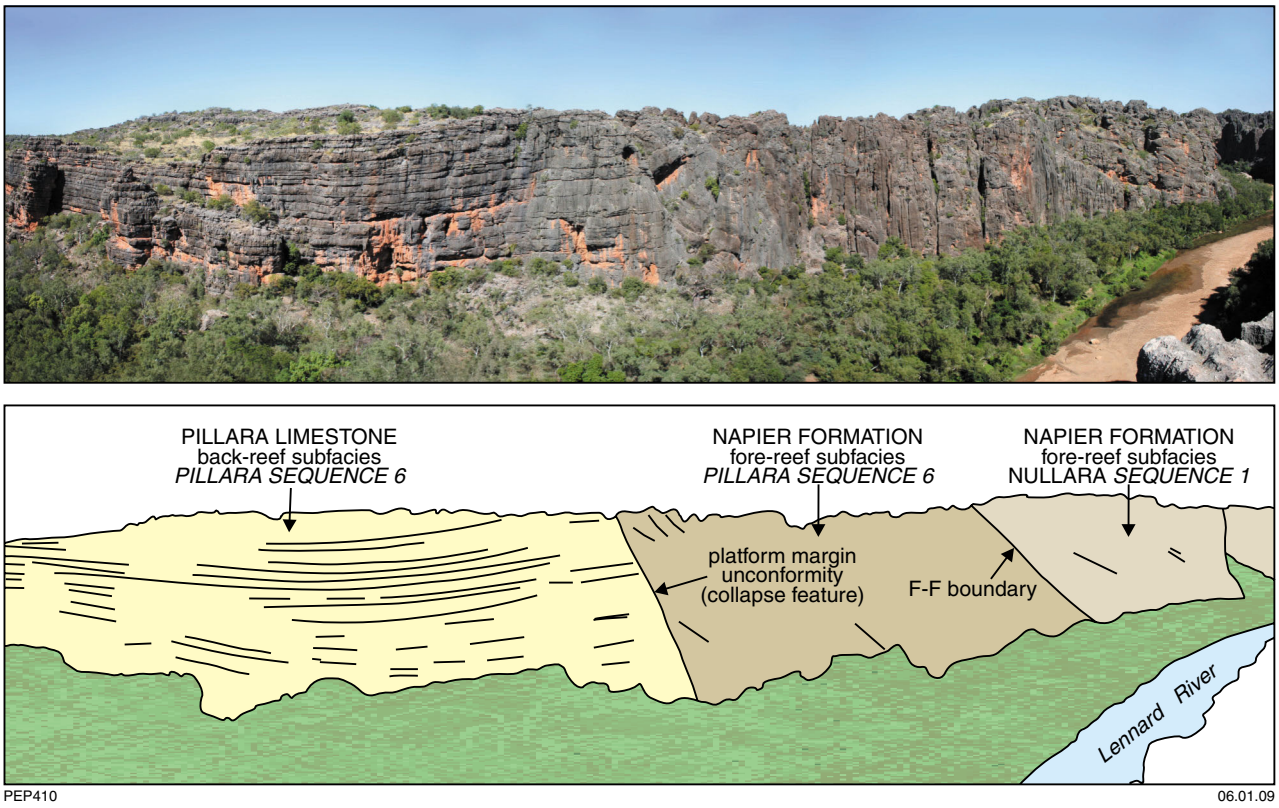

Figure 488. **Panorama and equivalent sketch of the south wall of Windjana Gorge in the *Mirrngurrwalla* area, downstream from Figure 487, showing Pillara Limestone Sequence 6 on the left, truncated by a scarp that formed as a result of collapse of the platform margin. The scarp is abutted by massive Frasnian reefal-slope limestone of the Napier Formation, Pillara Sequence 6, passing on the right into Famennian fore-reef limestone, Nullara Sequence 1, with many allochthonous reef blocks.**

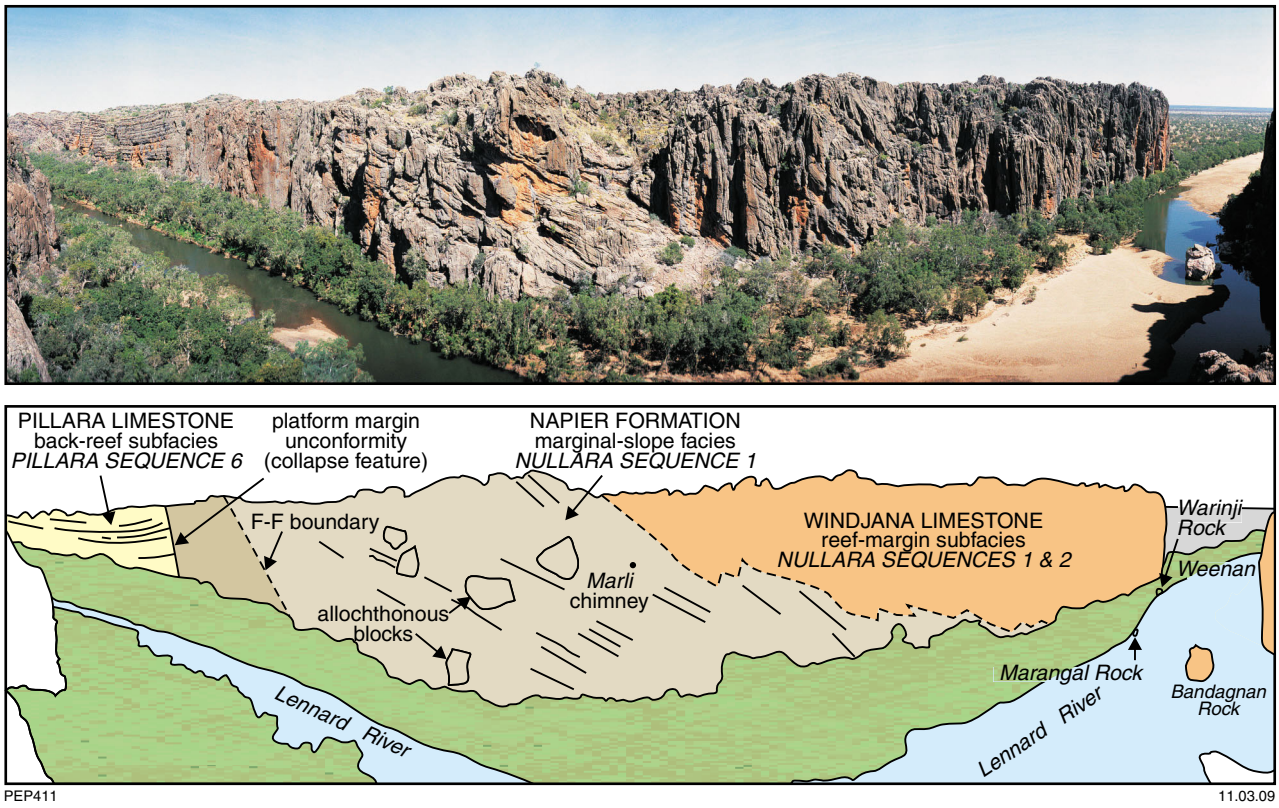

Figure 489. **Panorama and equivalent sketch of Windjana Gorge from *Mirrngurrwalla* to the west entrance, viewed from near *Mandjalan* Pass. On the extreme left are well-bedded platform strata of the Pillara Limestone, abutted by massive Frasnian and Famennian reefal-slope limestones. They are followed by crudely bedded Famennian fore-reef limestones containing allochthonous reef blocks, and massive reef limestone of the Windjana Limestone.**



Figure 490. **The Frasnian–Famennian boundary in fore-reef deposits of the Napier Formation in Windjana Gorge, east of the Classic Face. The boundary is at the base of the regressive dark-red bed of silty limestone, about 30 m thick, which is underlain by massive late Frasnian limestone and overlain by massive early Famennian limestone.**



Figure 491. The south face of Windjana Gorge east of the Classic Face, showing crudely bedded Famennian fore-reef deposits of the Napier Formation with abundant allochthonous blocks of reef limestone, many of which are capped by red *Sphaerocodium* bioherms. The Frasnian–Famennian boundary is the prominent bedding plane visible to the right of the boab tree.

walking on top of the range from near the east entrance. The view from this locality is shown in Figure 486 and an aerial view is shown as Figure 492.

The Classic Face exposes platform facies (reef-margin, reef-flat, and back-reef subfacies) and marginal-slope facies (reefal-slope and fore-reef subfacies). Details of interpretations of these rocks have changed as they have been examined increasingly more closely and the epilithic microbial films obscuring details of the rocks at some key locations have been removed using hydrochloric acid. For progressive changes in interpretation see relevant illustrations in Playford and Johnstone (1959a), Playford and Lowry (1966), and Playford (1980, 1981, 2002a).

The rocks exposed in the Classic Face are entirely Frasnian in age, and are correlated with Pillara Sequences 5 and 6 (Fig. 486). Those two sequences are separated in the platform by an erosion surface (Figs 93–95), formed during a mild regression associated with the Classic Face Event, at or near the base of Zone 11. The erosion surface has a maximum relief of about 11 m near the platform margin, where a conspicuous channel is cut into reef-flat deposits (Fig. 95). The total relief on the unconformity is at least 20 m.

Irregularity and apparent truncation on the surface decrease progressively away from the margin, so that at the river bend just past the north end of the Classic Face the unconformity is expressed by only minor undulations, with amplitudes of about 30 cm, in strata of the back-reef subfacies (Fig. 96). Little or no relief can be seen on the unconformity surface west of the river bend (Fig. 487). Overall, the lithologies in back-reef subfacies above and below the unconformity are similar, consisting of dolomitic stromatoporoid and microbial limestones.

A thin, largely covered zone at the base of Sequence 6 in the upper part of the platform facies in the Classic Face extends for about 150 m behind the reef, as far as the bend in the river (Figs 96, 486, 487). This may be regarded as a transgressive systems tract. The transgressive interval includes some unusual mounds of *Renalcis* limestone. The back-reef section above the unconformity shows more closely spaced cyclicity than that below, no doubt reflecting the change from vertical accretion in Pillara Sequence 5 to progradation in Pillara Sequence 6. There is no evidence of karstification below the unconformity, which probably represents a relatively brief episode of emergence, when sea level fell by perhaps 20–30 m, resulting in subaerial channelling of the area around the platform margin. This was followed by renewed transgression, when the margin backstepped by a little more than 15 m, much less than the backstepping that occurred at other sequence boundaries on the Lennard Shelf.

The platform-margin unconformity is a subvertical erosion surface. It is not clear how much of the erosion that occurred there was due to the fall in sea level associated with the Classic Face Event and how much resulted from normal submarine erosion, following platform-margin collapse. That collapse could have been associated with

a catastrophic event such as an earthquake and associated tsunami. The margin on the other (east) side of the gorge is a very steep, seemingly planar, surface, that must similarly have resulted from collapse of the platform margin (Figs 109, 493, 494). The margin shown in Figure 493 has been cleaned using hydrochloric acid, and it is seen to be an irregular eroded surface. This indicates that the planar surface resulting from the collapse had been subjected to mild submarine erosion as it was progressively onlapped by reefal-slope deposits.

The platform-margin erosion surface near the base of the cliff face in the Classic Face is coated with a thin layer (as much as 2 cm thick) of *Sphaerocodium–Renalcis* limestone that encrusted a reef margin consisting of microbial, tabular-stromatoporoid, and *Renalcis* limestone (Fig. 495). The adjoining microbial reefal-slope deposits include layers of *Sphaerocodium* with some *Renalcis*, brachiopods, receptaculitids, stromatactis structures, and pieces of stromatoporoid limestone derived from the reef. These deposits dip at angles in excess of 50°, and are regarded as accretionary layers built by microbes The reefal-slope deposits are sandy and some beds are strongly dolomitized. It is noticeable that reef fragments in these deposits are not dolomitized, even where they are completely surrounded by dolomite. This must be because the reef limestones had no porosity remaining after early marine cementation, and consequently did not provide access for dolomitizing fluids, whereas the reefal-slope deposits remained sufficiently porous and permeable to allow dolomitization.

Fore-reef deposits, which abut and interfinger with the reefal-slope deposits, dip at angles of as much as 40° and are largely characterized by abundant receptaculitids. A large tongue of microbial reefal-slope limestone extends down into the fore-reef deposits in the south part of the Classic Face (Fig. 486).

The transgression following the Classic Face Event marked an important change in the nature of platform growth. After that event, during Sequence 6 (Zones 11–13), the platforms throughout the Lennard Shelf advanced (prograded) over their equivalent marginal-slope deposits, whereas they grew almost vertically or backstepped abruptly in earlier Pillara Sequences, except in Pillara Sequence 1, when the platforms commonly retreated (retrograded). The whole of the reefal-slope and fore-reef deposits represented in the Classic Face belong to Pillara Sequence 6.

The reef-margin subfacies in the Classic Face is narrow (less than 50 m) and discontinuous, consisting of massive red and white microbial limestone, with abundant *Renalcis* and scattered stromatoporoids. The narrowness of the reef margin is thought to have resulted from the collapse of the reef front. The reef-margin subfacies grades into reef-flat subfacies and bedding becomes more distinct moving away from the margin. Bedding is largely defined in the reef-flat deposits by thin (20–40 cm) layers of terrigenous sandstone and sandy limestone. Those sandy layers typically contain fenestral stromatolites, built by cyanobacteria that were able to survive in the sandy environment, whereas stromatoporoids could not (Fig. 28). Limestones with little or no terrigenous sand contain abundant stromatoporoids, including species of *Actinostroma* (Figs 35 and 40) and *Stachyodes*, associated with *Renalcis* (Figs 497–499). Some of the stromatoporoids are laminar and up to several metres long (Fig. 496), whereas others are columnar (Fig. 35). Some laminar *Actinostroma* colonies were able to hold up large cavities below them, which were partly filled with *Renalcis* colonies that grew down from the roofs of the cavities, followed by red laminated lime mudstone filling the rest (Fig. 40). Some of the reef cavities were very large (Figs 501, 502).

Stromatolitic limestone makes up a significant part of the reef-flat deposits, although columnar structures (Fig. 500) are not always apparent, and the limestones are cut by a number of relatively narrow neptunian dykes (Fig. 503).

The best exposures of reef-flat deposits are to be seen in a very large fallen block and several smaller blocks at the base of the cliff, where they have been kept clean by river floodwater. However, since the 1960s, some parts of these blocks have been covered with riverine mud, laid down between and stabilized by *Melaleuca* trees, thereby obscuring some important exposures. No doubt a major flood will eventually uncover the concealed outcrop by removing the mud and trees that have grown up over the past 45 years.

Reef-flat deposits grade into back-reef deposits at the north end of the Classic Face and in the section above the unconformity that marks the Classic Face event. These back-reef deposits consist largely of well-bedded stromatoporoid (mainly *Amphipora*) limestone and microbial (fenestral) limestone, with thin interbedded sandy limestone grading into calcareous sandstone.

Central and western parts of the gorge

The central and western parts of the gorge extend from *Mingun*, at the bend in the gorge north of the Classic Face, to the west entrance, *Weenan* (Figs 487–489).

Mingun

In the cliff above *Mingun* (Plate 6), the back-reef subfacies shows well-developed cyclicity, as illustrated in Figures 504 and 505. Typical cycles in this cliff are 1.5 to 3 m thick, although their average thickness in this part of the range is about 4 m. They show clearly on a section that was measured from northeast of *Malambeea* to the cliffs above *Mingun* (Fig. 223). Each cycle typically begins at the base with a unit of stromatoporoid limestone, dolomitic limestone, or dolomite containing abundant *Amphipora*, with large heads of *Actinostroma* and patches of *Stachyodes* in some cycles (Figs 404, 504). Above this stromatoporoid limestone there are commonly thin-bedded units of *Amphipora* limestone, which are in turn typically overlain by thin fenestral (microbial) limestones containing large gastropods. The fenestral limestones become progressively more sandy upward and pass into laminated sandstones at the tops of the cycles. Some of those calcareous sandstones have fenestral fabrics, and may contain thin beds of micaceous shale. Root casts and mud cracks are present in some of the sandy units at the tops of cycles.





Figure 492. (above) Aerial view of the Classic Face at Windjana Gorge looking south, showing well-bedded, low-dipping, platform limestones of the Pillara Limestone on the right, massive reef-margin and reefal-slope limestones in the centre, and steeply dipping fore-reef limestones of the Napier Formation on the left.

Figure 493. Platform-margin unconformity near the eastern wall of Windjana Gorge opposite the Classic Face, looking east-northeast. It shows thick-bedded reef limestone of the Pillara Limestone on the left and crudely bedded reefal-slope deposits of the Napier Formation on the right. The contact (marked by chalk on the outcrop) is a collapse scarp, eroded to a small extent prior to onlap by reefal-slope deposits. The limestone surface was cleaned along the contact using concentrated hydrochloric acid to remove the epilithic bacterial coating. See also Figures 109 and 494.



Figure 494. Aerial view looking west towards the Napier Range at Windjana Gorge, showing a prominent linear ridge marking the reef-margin subfacies, adjoining reef-flat and back-reef subfacies (Pillara Limestone) on the right, and recessive, poorly bedded, marginal-slope limestones (Napier Formation) on the left. Figure 493 was taken near the end of this ridge, close to the gorge, looking in the opposite direction. Photo courtesy of West Australian Petroleum Pty Ltd.

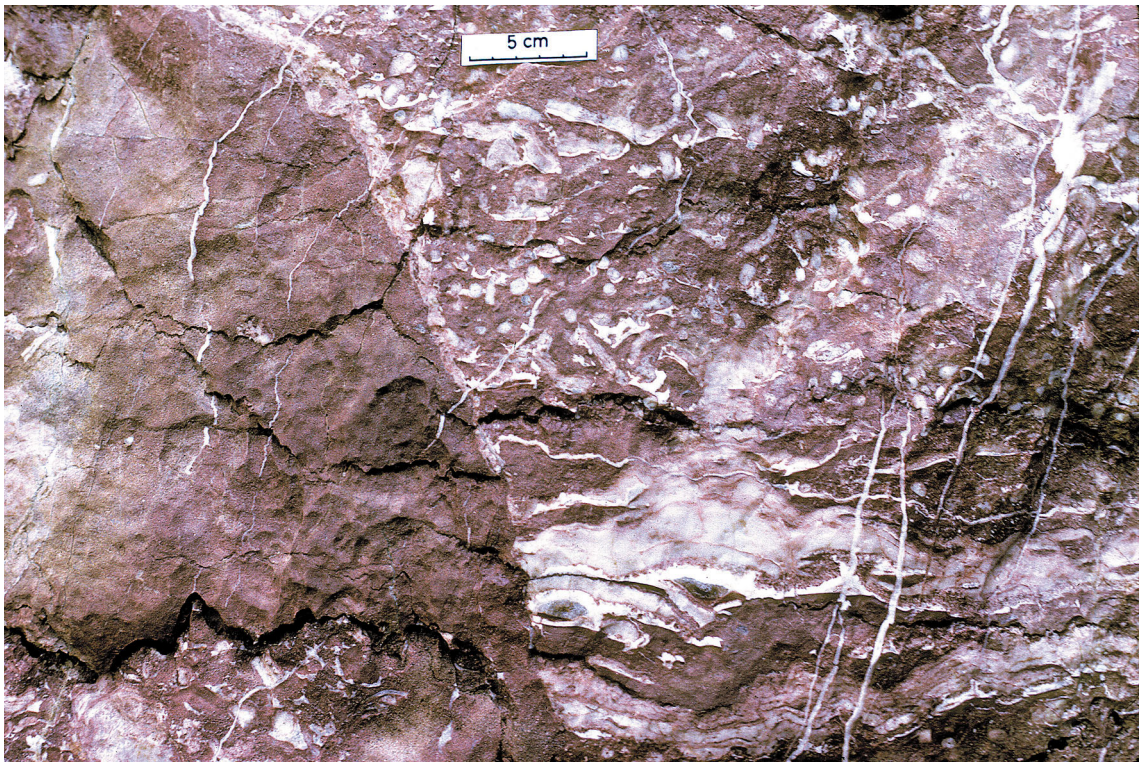

Figure 495. Platform-margin unconformity in the Classic Face in Windjana Gorge, showing massive reef-margin subfacies (microbial and stromatoporoid boundstone) on the right and massive reefal-slope subfacies on the left. Note the truncation of *Actinostroma* colonies at the contact and the thin layer of *Sphaerocodium* that grew on the unconformity surface.

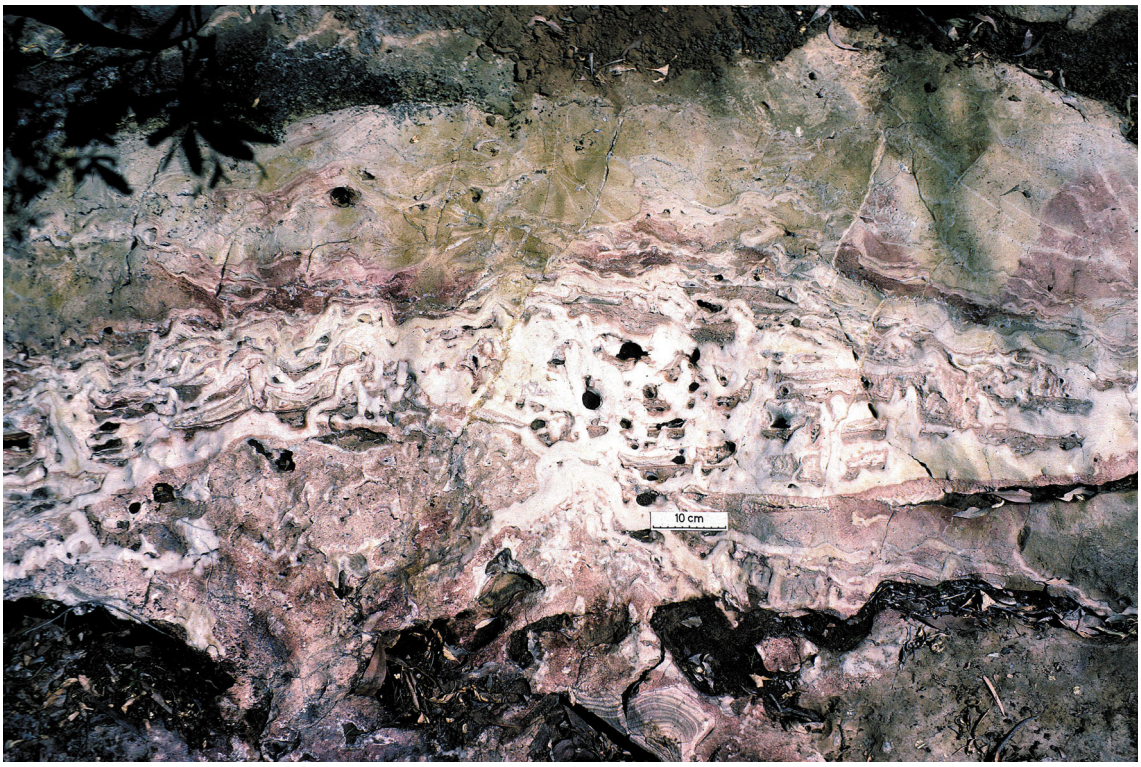

Figure 496. Elongate colony of the stromatoporoid *Actinostroma windjanicum* in reef-flat deposits of the Pillara Limestone, Sequence 5, at the Classic Face in Windjana Gorge, showing shelter cavities below the stromatoporoid. The cavities were partly filled with colonies of *Renalcis* that grew downward into the cavities, and were later filled with laminated peloidal limestone and sparry calcite.

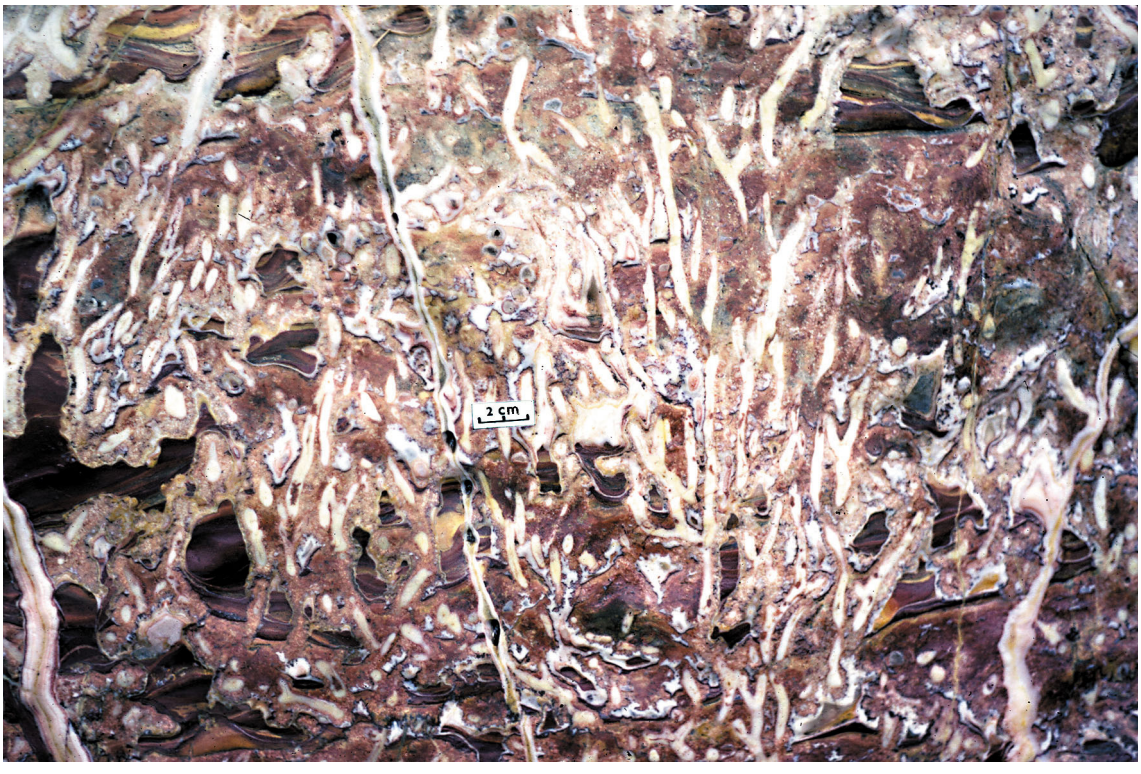

Figure 497. Colony of the dendroid stromatoporoid *Stachyodes costulata,* intergrown with *Renalcis* in reef-flat subfacies of the Pillara Limestone in the Classic Face at Windjana Gorge. Cavities in the reef were filled with laminated red peloidal limestone and calcite spar.

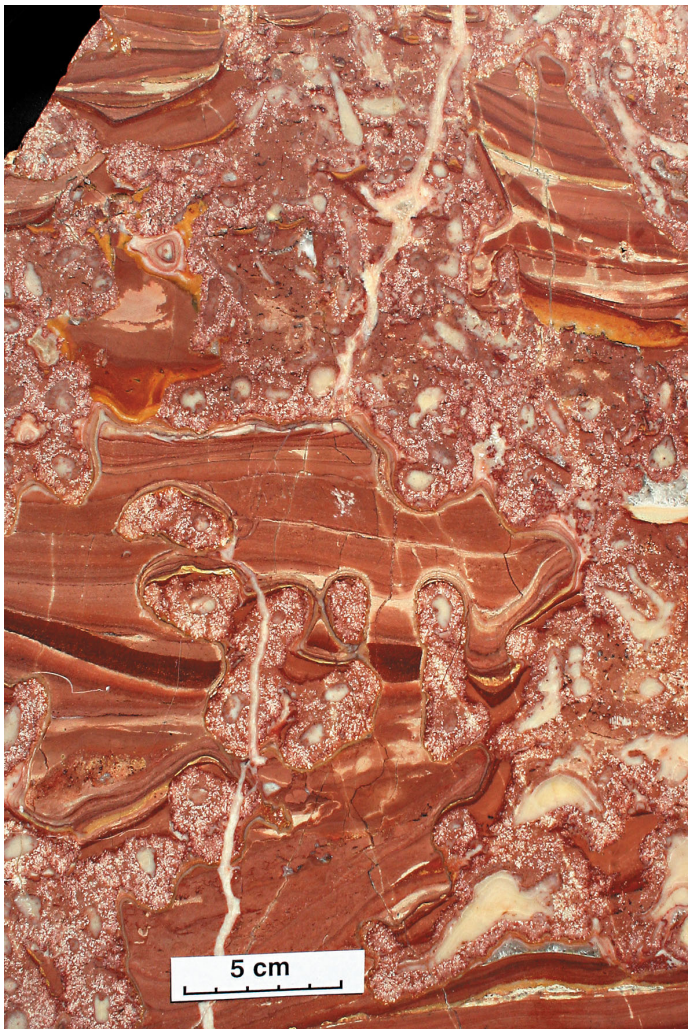

Figure 498. Polished slab of reef limestone from a talus block at the foot of the Classic Face at Windjana Gorge, showing a framework of the stromatoporoid *Stachyodes* encrusted by dense *Renalcis,* the remaining interstices being filled with red, laminated, peloidal limestone. GSWA sample no. 37054.

Figure 499. (below) Closer view of part of the polished slab of reef limestone shown in Figure 498, showing dense *Renalcis* encrusting *Stachyodes*, with laminated red peloidal limestone filling the remaining interstices in the reef. GSWA sample no. 37504.

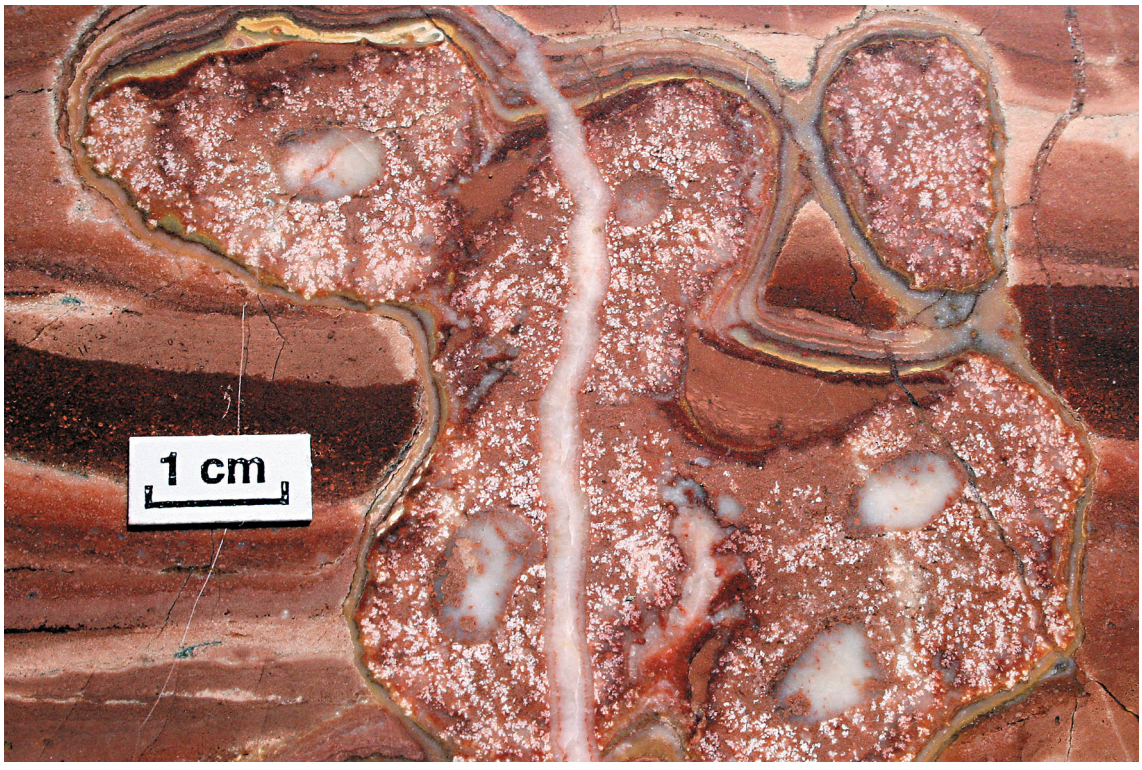

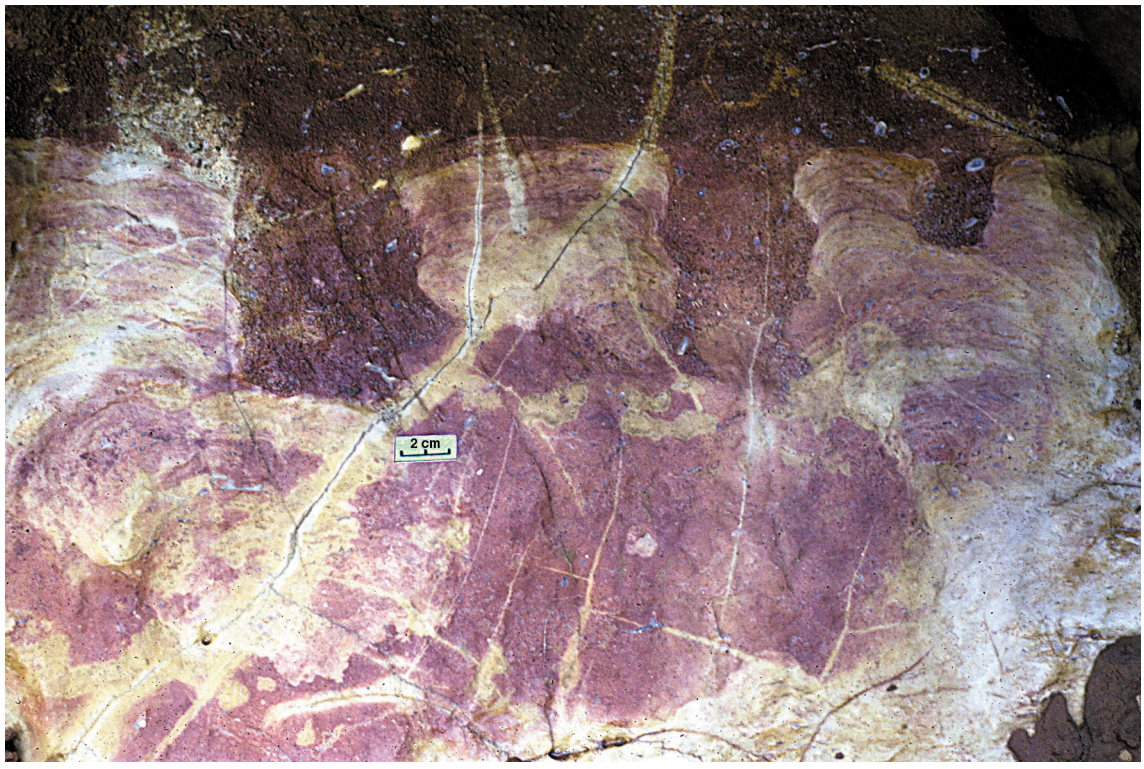

Figure 500. Club-shaped columnar fenestral stromatolites in reef-flat deposits in the Classic Face at Windjana Gorge. The stromatolites are overlain by sandstone. This outcrop, photographed in 1992, is now covered by riverine mud.

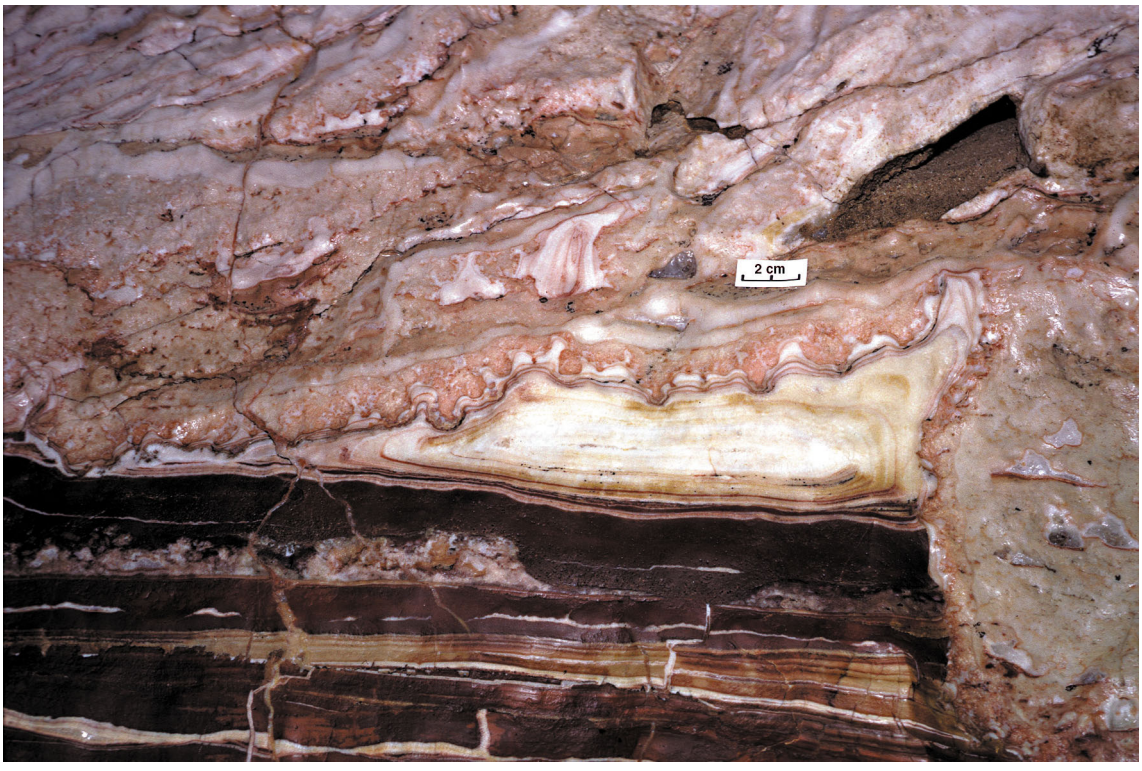

Figure 501. A large cavity filling (dubbed 'the biggest stromatactis in the world') in reef-flat limestones in the Classic Face at Windjana Gorge. The roof and parts of the sides of the cavity were first lined with *Renalcis*, which grew down and outward from the laminar stromatoporoid. The major part of the cavity was then filled with red, laminated, peloidal limestone and sparry calcite.

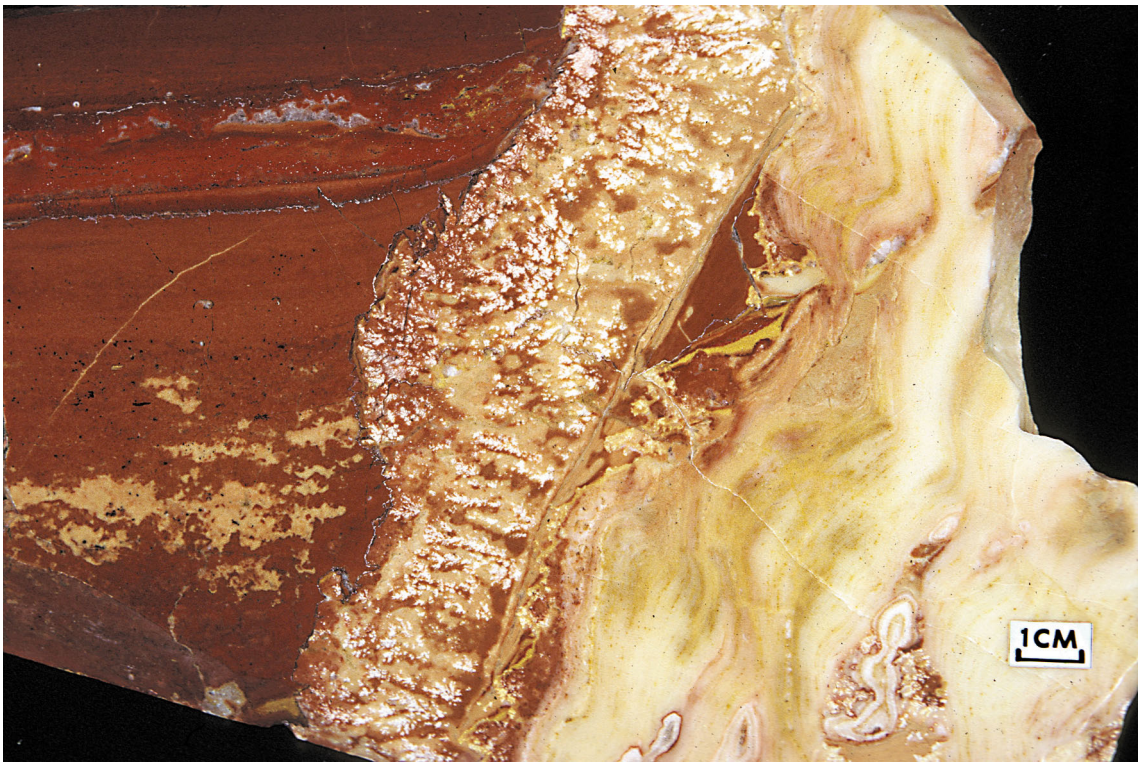

Figure 502. Polished slab of part of the right-hand side of the cavity filling shown in Figure 501, showing stromatoporoid reef on the right and cavity-filling lime mudstone on the left. The cavity was initially lined with *Renalcis*, growing outward from the margin, and was then filled with red laminated peloidal lime mud.

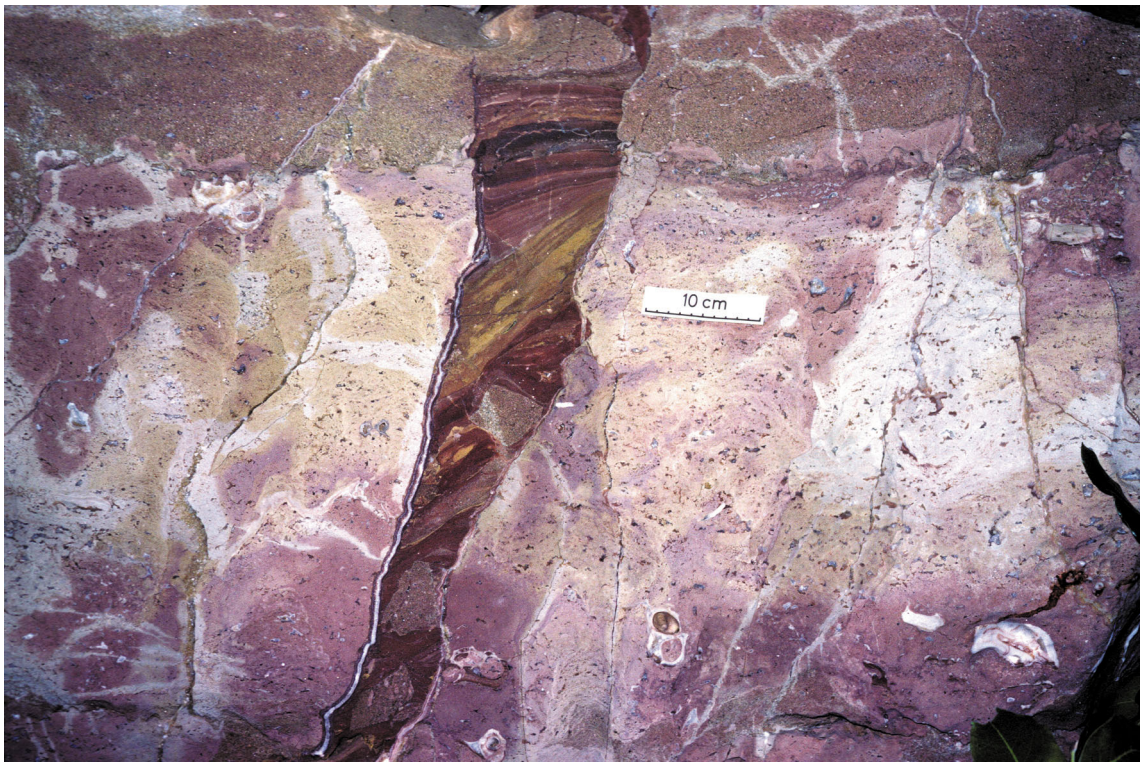

Figure 503. Neptunian dyke filled with red laminated peloidal limestone, cutting through light-coloured fenestral stromatolitic limestone and dark coarse calcareous sandstone, in reef-flat deposits of the Pillara Limestone in the Classic Face at Windjana Gorge.

Above the base of each cycle, limestone deposition in deeper water was followed by an increasing influx of terrigenous detritus, and its deposition caused water depths to become steadily shallower, eventually reaching intertidal or supratidal levels prior to initiation of the next cycle (Fig. 215; Playford, 1981; Hocking and Playford, 2001). The sandstones in the upper parts of cycles are regressive weathering, and generally do not outcrop on the range, whereas the limestones are resistant and well exposed (Fig. 505). Thinly bedded transgressive units of detrital calcarenite rarely overlie the sandstones. Sets of megacycles can also be recognized, each consisting of five to seven ordinary cycles (Fig. 222).

As discussed previously, these cycles may have resulted from repetitive eustatic sea-level changes combined with subsidence. An alternative explanation is that they have resulted from abrupt tectonism causing 'jerky subsidence', as discussed by Hardie et al. (1991) and Read et al. (1991). The Lennard Shelf was a tectonically active area in the Devonian, resulting in periodic earthquake activity, so a tectonic origin of the platform cyclicity seems possible. The 'saw-tooth' nature of the sea-level curve shown in Figure 215 may be more suggestive of a tectonic than a eustatic origin.

Mirrngurrwalla– Manda-yarr-yarr-wungani

Mirrngurrwalla, a fallen block in the middle of the gorge, is said by Aboriginal people to be the figure of an ancestral woman from the Dreamtime (Fig. 506; AMG Zone 51, 707200E 8074200N). *Manda-yarr-yarr-wungani* (meaning 'gum hanging down' in the *Unggumi* language) is a prominent group of stalactites on the north wall of the gorge (AMG Zone 51, 707300E 8074200N), said to represent edible gum exuded from a Coolamon tree during the Dreamtime (Fig. 506).

The margin of the Pillara platform in this area is a steeply sloping surface that resulted from collapse of the reef margin and reef flat (Figs 508–512). Parts of this surface can be closely examined on the north side of the gorge (AMG Zone 51, 707200E 8074300N) beside the reptilian-bones-bearing cavern described earlier (Fig. 323). The surface is irregular on a small scale, and the platform facies (Pillara Limestone) was eroded into small 'steps', against which red, silty, sandy, microbial limestone of the reefal-slope subfacies (Napier Formation) was deposited. Erosion of the collapse surface resulted from either submarine processes or a brief period of emergence. North of the gorge, successive beds of southwest-dipping reef-flat beds of the Pillara Limestone are truncated along the collapse surface, with steeply dipping reefal-slope limestone and dolomite of the Napier Formation abutting against that surface (Figs 510–512). The original relief of the collapse scarp is estimated to have exceeded 200 m.

The reefal-slope subfacies of the Napier Formation is crudely bedded to massive, and is thought to be microbial in origin. It contains some detrital *Actinostroma* and *Stachyodes*. Several neptunian dykes cut through reefal-



Figure 504. Back-reef Pillara Limestone at *Mingun* in Windjana Gorge, showing cyclicity. Massive stromatoporoid limestone at the base of each cycle is overlain by thin-bedded fenestral limestone and calcareous sandstone.



Figure 505. Low-level aerial view looking north immediately north of Windjana Gorge, showing strong cyclicity in Pillara Limestone, back-reef subfacies. Prominent white limestone at the base of each cycle is overlain by recessive-weathering calcareous sandstone. Two thicker limestone beds (bottom right and upper centre) each mark the base of a megacycle, which is here composed of six metre-scale cycles. Photo courtesy of West Australian Petroleum Pty Ltd.

slope limestone and dolomite, including one, about 2 m wide, near the Frasnian–Famennian boundary, that contains some remarkable structures (thought to be relict microbial features) in fibrous calcite cement that fills most of the dyke (AMG Zone 51, 707200E 8074100N).

The Frasnian–Famennian boundary near *Mirrngurrwalla* is exposed on the south side of the gorge as a steep bedding plane, dipping southwest at an angle of 48°, of which 37° can be shown to be depositional, as deduced from geopetal structures (AMG Zone 51, 707200E 8074100N; Figs 100, 488, 489). Atrypid brachiopods are abundant in Frasnian red and white dolomitic limestone below the boundary. Above the boundary is 15–30 cm of limestone that is devoid of megafossils (but dated as earliest Famennian using conodonts, by G Klapper, 2004, written comm.). This is overlain by red and white limestone with abundant thin-shelled brachiopods (probably productids) and some ammonoids. It has not been practicable to see exactly where this boundary continues above the lower part of the cliff face.

West end of the gorge

The Famennian reefal-slope deposits west of *Mirrngurrwalla* are succeeded by fore-reef deposits that consist of sandy calcarenites and breccias containing many allochthonous reef blocks and debris flows. Near the pass at *Mandjalan*, massive reef can be seen to overlie and interfinger with the marginal-slope limestones. The upper reefal-slope deposits underlying the reef contain abundant receptaculitids and sponges (Figs 75, 513).

From near *Bandangnan* rock (Fig. 478) to the west entrance (*Weenan*; Figs 516, 517) reef limestone of the Windjana Limestone extends over the reefal-slope deposits of the Napier Formation, with interfingering contacts between them (Fig. 515). Geopetal structures indicate that the rocks in this part of the gorge have been tilted basinward (i.e. towards the southwest) at average angles of 10–15°. The reef deposits are microbial limestones containing *Renalcis* and abundant stromatactis, with receptaculitids, a few stromatoporoids, and nautiloids. The nautiloids must have originally sunk to the bottom with their apical ends pointing vertically upward (no doubt due to gas remaining in the nautiloid chambers; Fig. 518), but they are now tilted about 10° southwest because of the tectonic and/or compactional tilt that has occurred in this part of the gorge. The same tilt is evident in abundant stromatactis cavities in the reef and reefal-slope limestones (Figs 55, 56).

The reef limestones are cut by many neptunian dykes, most of which are filled with calcareous sandstone and fibrous spar, while others contain calcarenite and oolite (Fig. 519). They are as much as 60 cm wide, and measurements of 13 dykes exposed along the south side of the gorge show that the total expansion resulting from neptunian fissuring amounted to about 3.5%. Several dykes widen upward in the cliff face, some pinch out downward, and at least one



Figure 506. ***Mirrngurrwalla*, a talus block in the bed of the Lennard River at Windjana Gorge, said to represent a woman featuring in an Aboriginal legend from the Dreamtime.**



Figure 507. ***Manda-yarr-yarr-wungani*, stalactites on the north wall of central Windjana Gorge, said to represent edible gum (tree sap) from the primeval Dreamtime.**



Figure 508. South wall of Windjana Gorge near *Mirrngurrwalla*, showing a collapsed platform margin between reef-flat to back-reef Pillara Limestone, Sequence 6, on the left and massive reefal-slope Napier Formation, Sequence 6, on the right. This slightly eroded collapse scarp is estimated to have had a total relief of at least 200 m when it formed during the late Frasnian.

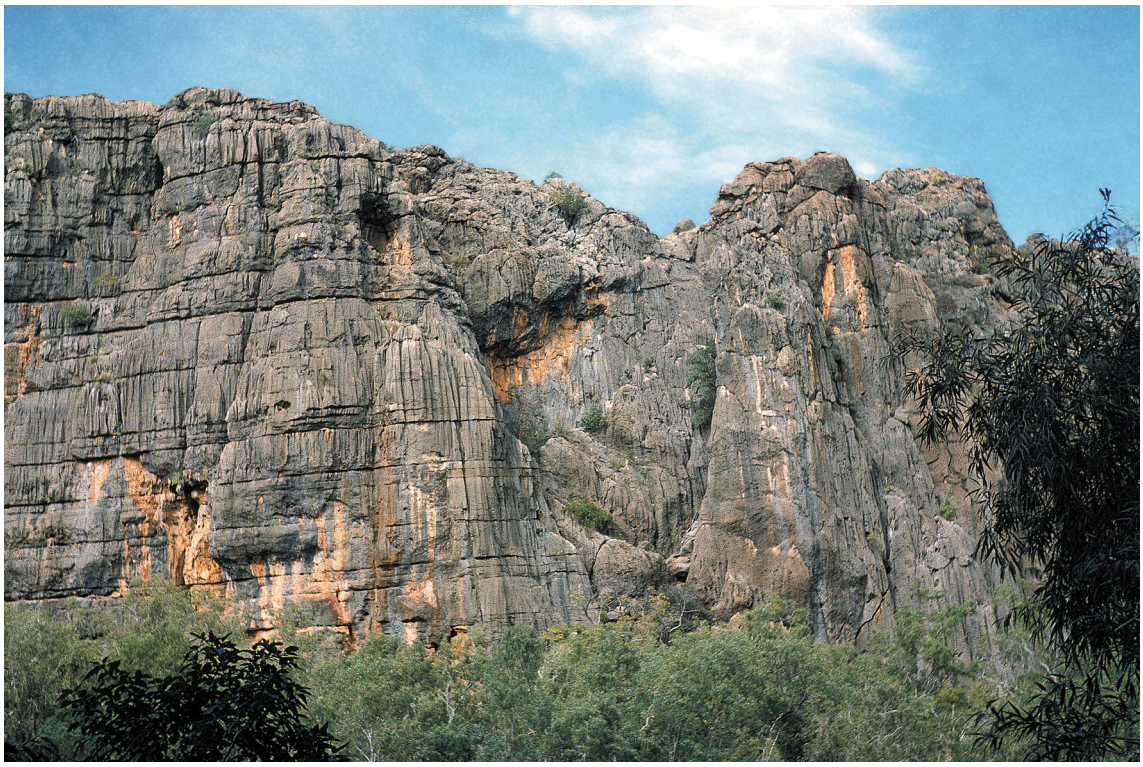

Figure 509. Closer view of the south wall of Windjana Gorge near *Mirrngurrwalla,* showing the collapsed platform margin, which was slightly eroded before being onlapped by reefal-slope deposits.



Figure 510. Aerial view of the central and eastern parts of Windjana Gorge looking southeast. Bedding in platform limestone of the Pillara Limestone is truncated by dark-coloured reefal-slope limestone and dolomite of the Napier Formation in the central lower part of the view.



Figure 511. Aerial view looking south immediately north of Windjana Gorge, showing well-bedded platform limestone of the Pillara Limestone on the left truncated by massive reefal-slope limestone and dolomite of the Napier Formation. The approximate Frasnian–Famennian boundary is indicated by a dashed white line.



Figure 512. Looking south about 500 m north of Windjana Gorge, showing steeply dipping reefal-slope dolomite of the Napier Formation (Frasnian) on the right abutting well-bedded reef-margin limestone of the Pillara Limestone on the left. The contact is a steep eroded collapse surface (within Pillara Sequence 6), estimated to have had an original relief of at least 200 m.

seems to pass into a neptunian sill in bedded reefal-slope deposits near the base of the cliff.

A noticeable feature of the reef subfacies exposed beside the gorge is the presence of lenses and tongues of calcareous sandstone interfingering with *Renalcis*–receptaculitid–microbial limestone (Figs 514, 520, 521). The limestone lacks stylolites, whereas they are very abundant in the calcareous sandstone. This is because the microbial limestone was deposited as strongly cemented limestone without any porosity, whereas the calcareous sand had high porosities and was consequently subjected to strong stylolitization after burial. The early-cemented microbial limestone is also subject to more early neptunian fissuring than the calcareous sandstone (Fig. 521).

A prominent cave exposed on the north face of the gorge near the west entrance is thought to be an Early Permian karst feature (Fig. 515). It is commonly known as 'Pigeon's Cave', although it had no role in the history of the Aboriginal 'outlaw' or 'freedom fighter' named Pigeon (*Jandamarra*).

Baralamma Spring

Baralamma is the Aboriginal name for a permanent spring situated in the Napier Range about 7 km northwest of Windjana Gorge (AMG Zone 51, 707200E 8074100N). It was an important mythological place for the *Unggumi* people, and a small cave beside the spring is decorated with Dreamtime paintings of two defecating dingoes, known as *Baralamma* (Fig. 522; Playford 1959, 2007).

The platform facies in this area has a well-defined reef rim of microbial and stromatoporoid limestone containing pockets of sandstone. The reef-flat and back-reef subfacies interfinger, with large (~10 m across) biohermal mounds and swellings of microbial–stromatoporoid limestone intercalated in the near-reef part of the back-reef deposits (Fig. 523).

Yammera Gap area

Many antiformal stromatolites occur in marginal-slope deposits of the Napier Formation on the northern side of the range, 4 km east-southeast of Yammera Gap (AMG Zone 51, 697400E 8081200N). These distinctive stromatolites (Fig. 524) overlie a massive unit of upper Frasnian breccia and conglomerate, composed of small angular to rounded clasts of stromatoporoid, microbial, fenestral, and reefal limestones, and rounded clasts of Precambrian rocks (mainly quartz, dolerite, and mica schist), cemented by sparry calcite. Some of the limestone clasts appear to have been corroded, either before or soon after deposition. This unit in turn overlies a conglomerate unit containing rounded Precambrian cobbles and small boulders. All of this section is included in the Napier Formation.

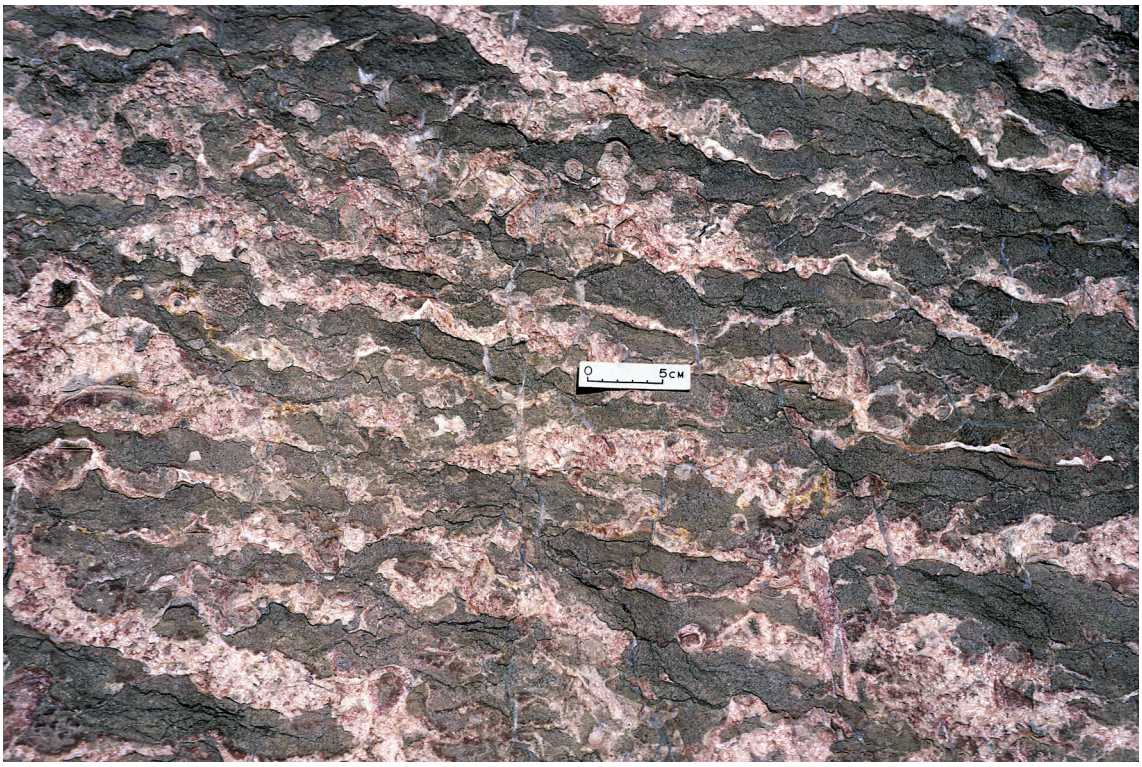

Figure 513. Deep-water reef limestone of the Windjana Limestone on the south side of Windjana Gorge, about 400 m upstream from the west entrance, showing dark-coloured sandy limestone with lenses of light-coloured microbial–receptaculitid limestone.



Figure 514. Windjana Limestone on the south side of Windjana Gorge near the west entrance, showing white microbial reef limestone interfingering with dark-coloured sandy marginal-slope limestone. The sandy limestone is strongly stylolitized as a result of post-depositional compaction, whereas the microbial reef limestone, which was strongly cemented at a very early stage, has no stylolites.



Figure 515. The north wall of Windjana Gorge near the west entrance. Massive Famennian microbial reef limestone (Windjana Limestone) in the upper part of the cliff overlies and interfingers with dipping fore-reef limestones (Napier Formation) in the lower part. The steep linear fissures in the cliff face mark neptunian dykes, which were originally nearly vertical, but are now tilted west as a result of post-depositional tilting of the reef complex. Pigeon's Cave, thought to be an Early Permian karst feature, is in the upper left of the photo.



Figure 516. The west entrance to Windjana Gorge, known to the Aborigines as *Weenan*. See also Figure 472.



Figure 517. Aerial view looking northeast towards the west entrance to Windjana Gorge, showing the exhumed late Famennian reef scarp at the front of the Napier Range. Precambrian rocks of the King Leopold Orogen outcrop behind the range.



Figure 518. Straight nautiloid in the lower (deep-water) part of the Famennian reef (Windjana Limestone) on the south side of Windjana Gorge near the west entrance. The nautiloid is oriented with its apex upwards, probably as a consequence of gas in chambers that were afterwards filled with calcareous sediment and sparry calcite.

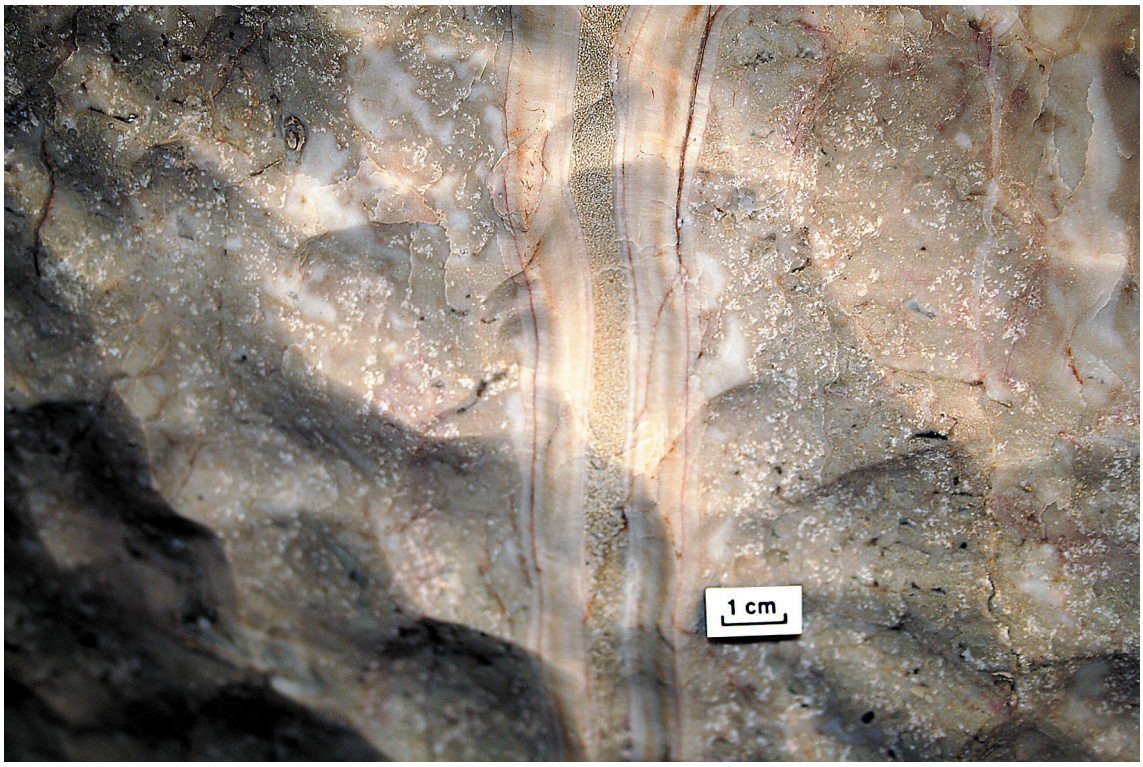

Figure 519. Small neptunian dyke in microbial (*Renalcis*-rich) reef limestone (Windjana Limestone) on the south wall of Windjana Gorge near the west entrance. The dyke was lined first with banded radiaxial calcite and then by oolite derived from overlying back-reef Nullara Limestone.



Figure 520. Limestone on the north side of Windjana Gorge near the west entrance, showing lenses of white microbial reef interfingering with steeply dipping dark-coloured marginal-slope sandy limestone. This is in the zone of interfingering between reef (Windjana Limestone) and marginal-slope (Napier Formation).

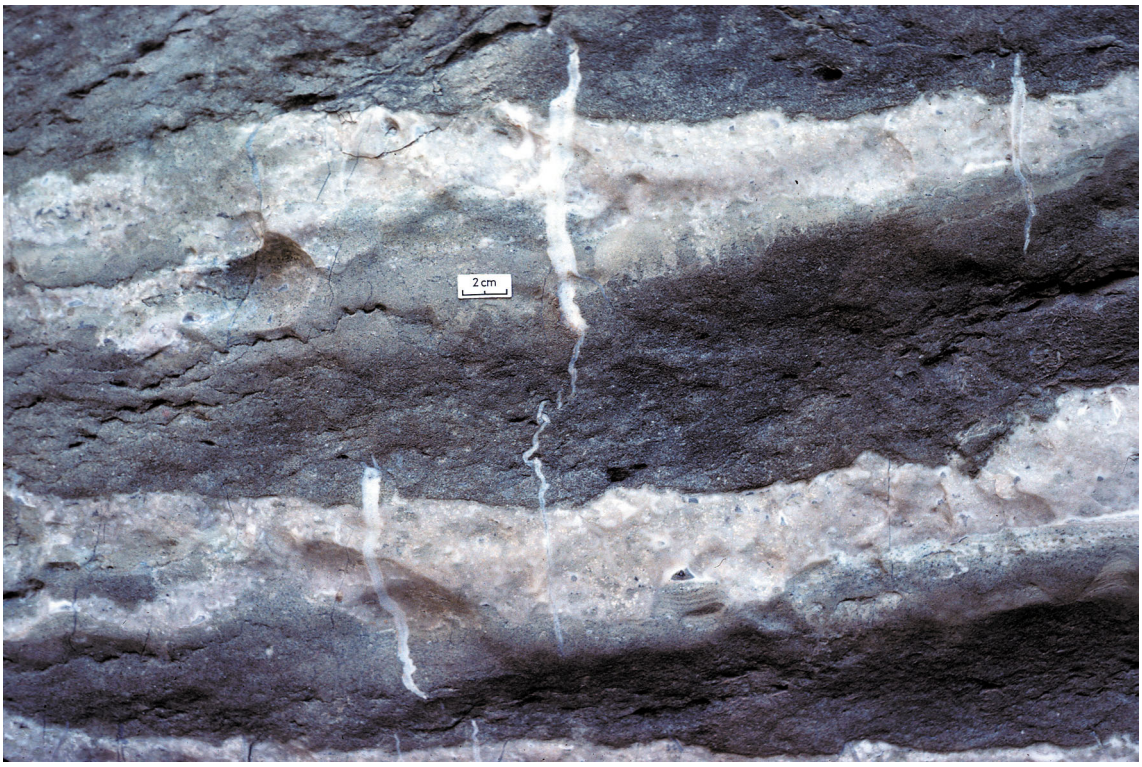

Figure 521. **Closer view of parts of the microbial reef lenses shown in Figure 520. The lenses were strongly cemented at the time of deposition and fractured soon afterwards, the fissures being filled with white sparry calcite.**



Figure 522. Aboriginal paintings of two defecating dingoes in a small cave beside Baralamma Spring.



Figure 523. Biohermal 'swellings' built by stromatoporoids and microbes in reef-flat deposits of the Pillara Limestone near Baralamma Spring, Napier Range.

The antiformal stromatolites range in age from Zone 13 (uppermost Frasnian) at the base, immediately above the conglomerate, to at least as high as the Upper *crepida* Zone or *rhomboidea* Zone (Lower Famennian), 22 m above the base (G Klapper, 2004, written comm.). Other antiformal stromatolites occur even higher, extending over a total of about 80 m of section. Rare stromatoporoid fragments are present in the basal limestones, extending as much as 2 m above the conglomerate, and these must also be Frasnian in age. One bed contains large clasts of antiformal stromatolites that were incorporated into a debris flow.

Napier Downs Homestead to Wombarella Gap

Marginal-slope deposits of the Napier Formation are well exposed on the northern side of the Napier Range, between Napier Downs Homestead and Wombarella Gap. Two important localities for antiformal stromatolites and adnet breccias are situated 4 km and 6 km northwest of Napier Downs Homestead (Figs 525–528).

At the first locality, 4 km northwest of the homestead (GPS AMG Zone 51, 689970E 8085480N), well-developed red antiformal stromatolites (Figs 525, 526) occur within marginal-slope deposits that overlie terrigenous conglomerate, in turn resting on Precambrian basement. The axes of the depositional folds trend directly down the depositional slopes of the marginal-slope deposits. In one place near this locality an allochthonous block of reef limestone apparently came to rest on the side of an antiformal stromatolite, and was then overgrown by another. Stromatolitic features are best displayed at the tops of these depositional folds.

At the second locality, 6 km northwest of the homestead (GPS AMG Zone 51, 689830E 8085580N), four prominent antiformal stromatolites have their axes parallel to the depositional slope (Fig. 527). Fragmentary stromatoporoids are present in breccias associated with some of the antiformal structures, but are absent above them, pointing to a latest Frasnian age for these stromatolites. The antiform stromatolites are associated with lenticular beds of adnet breccias, which are particularly well exposed 100 m northwest of the series of stromatolites (Fig. 528). Some adnet breccia beds are 'double graded', showing fine breccia with a clayey to sparry matrix at the base and top, and coarse breccia with a spar matrix (scheck breccia) in the middle (Fig. 130). The double grading suggests emplacement of these beds by a combination of debris flows (in the lower and middle parts of a bed) and turbidity currents (in the upper part). Some nodular clasts in the adnet breccias have formed around gastropods, but most lack any obvious core. The nodular clasts probably formed as microbial concretions before being carried down the slopes. Some show evidence of the curious corrosion noted earlier at the east entrance to Windjana Gorge (Figs 131, 132). Pieces of *Renalcis* limestone and Precambrian rocks also occur in some breccias.



Figure 524. Small antiformal stromatolites in Frasnian fore-reef deposits (Napier Formation) south of Yammera Gap in the Napier Range. Dark sandy limestone is present between the red antiformal columns of microbial limestone.



Figure 525. Antiformal stromatolite in fore-reef deposits (Napier Formation) north of Napier Downs Homestead. Each layer of the structure is built of small columnar stromatolites.



Figure 526. Linked antiformal stromatolites in fore-reef deposits (Napier Formation) north of Napier Downs Homestead.



Figure 527. Linked antiformal stromatolites in fore-reef deposits (Napier Formation) north of Napier Downs Homestead.



Figure 528. Lenses of scheck breccias in fore-reef deposits (Napier Formation) north of Napier Downs Homestead.

Narlarla

Narlarla (*Kalyarr*) is the site of the first zinc–lead–silver mining operation on the Lennard Shelf. Mining began soon after the orebodies were first discovered and pegged in 1906, and continued periodically on a small scale until 1966, when most of the ore had been removed (GPS AMG Zone 51, 683580E 8090630N; Ringrose, 1984, 1986, 1989). The largest of the two orebodies (no. 2) yielded almost all of the zinc–lead–silver production. It is now marked by a water-filled open pit (Fig. 529; Plate 1). The smallest (orebody no. 1) is marked by a very minor excavation (see fig. 1 of Ringrose, 1984).

The no. 2 orebody is almost in line with the axis of a stromatolite bioherm (Plate 1; Ringrose, 1984, 1989; George, 1999), with the no. 1 orebody situated northeast of the bioherm. This bioherm forms a depositional anticlinal nose following the axis of a much larger depositional fold in marginal-slope deposits of the Napier Formation (Plate 1). The anticlinal form of the marginal-slope deposits at this locality must have resulted from a change in direction of the reef front, probably controlled by basement topography. The bioherm itself was largely constructed by microbes that formed columnar and scalloped stromatolites and wavy laminae, interfingering with sandy marginal-slope deposits.

The bioherm has been dated from three samples. It is Frasnian Zones 11–13 in its lower part, Zone 13 in its middle to upper part, and Famennian *triangularis* Zone in its uppermost part (G Klapper, 2004, written comm.). The bioherm is approximately 50 m thick.

George (1999) suggested that the rate of growth of this bioherm was about 50–100 µm per year over a total duration of 0.5 to 1 m.y., and that the Narlarla bioherm developed entirely within Zone 13 of the Frasnian and the *triangularis* Zone of the Famennian. Such a growth rate is much faster than the estimate of 10 µm per year for growth of the Elimberrie no. 1 stromatolite–receptaculitid bioherm, which extends from within Zones 3–6 of the early Frasnian to the upper *crepida* or lower *rhomboidea* Zone of the early Famennian, an interval of approximately 8 m.y. The estimated growth rate for Elimberrie no. 1 is based on 26 dated samples, compared with only three at Narlarla. The lower part of the Narlarla bioherm (not the base) contains conodonts from within Frasnian Zones 11–13 (as determined by G Klapper, 2004, written comm.), not Zone 13 as stated by George (1999). Moreover, the oldest of these three samples at Narlarla was collected higher than the base of the bioherm, and consequently the lowest part could be older than Zone 11. This suggests that rather than having grown during a period of 0.5 to 1 m.y., the bioherm may have grown for as many as 4 m.y., at about 12 µm per year, compared with 50–100 µm per year estimated by George (1999). The estimated rate of 12 µm per year is a little faster than 10 µm per year deduced for Elimberrie no. 1 bioherm, and this may be accounted for by the greater influx of terrigenous material at Narlarla compared with Elimberrie. In any case, it is clear that both bioherms represent periods of extremely slow deposition.



Figure 529. Aerial view looking north over Barker Gorge and part of the Napier Range. The abandoned water-filled Narlarla opencut mine can be seen at the end of the track on top of the range.

Barker River to Hawkstone Creek

The part of the Napier Range between Barker Gorge (*Kowlera*) and the gap of Hawkstone Creek (*Nyangalignali*) includes many significant Frasnian and Famennian reefal features and demonstrates some key aspects of the relationships between conglomerates and the reef complexes, as summarized below.

Anticlinal nose west of Barker Gorge

A microbial bioherm forms a depositional anticlinal nose 3 km east-northeast of Barker Gorge (Plate 1; AMG Zone 51, 680200E 8092400N). The bioherm was constructed by microbes, forming *Sphaerocodium* fingers and wavy laminae, with masses of receptaculitids. This bioherm is considerable larger than the Narlarla bioherm, but unlike that bioherm it is not localized by any significant change in depositional-slope directions in underlying marginal-slope limestones of the Napier Formation. Any controls that determined the location of this bioherm are not readily apparent. However, the bioherm itself controls depositional dip directions in equivalent and overlying strata of the Napier Formation.

Rowalamban Cave area

Rowalamban is a large overhanging cave in reef-margin subfacies of the Pillara Limestone. It contains an extensive Aboriginal art gallery featuring a large *Wandjina* painting (named *Rowalamban*) and various other paintings, including those of the rainbow serpent (Plate 1; Fig. 324; Playford, 2007; AMG Zone 51, 678100E 8095400N). A neptunian dyke filled with spectacular spar balls occurs in reefal-slope subfacies of the Napier Formation 200 m southwest of the cave (Fig. 153; GPS AMG Zone 51, 678000E 8095320N). Two nearby karst pinnacles in reef limestone, named *Walanginna* (Cyclone Rock) and *Djalawunna* (Willy Willy Rock), also feature in *Unggumi* mythology (Fig. 530).

The cave and pinnacles are thought to have formed by subglacial karstification during the Early Permian, and both have since been modified by Cenozoic erosion.

Chedda Cliffs area

Chedda Cliffs form a line of sheer cliffs, as much as about 50 m high, that essentially mark the reef scarp that remained after the late Famennian Reef Extinction Event. They resemble Morown Cliff in the Oscar Range. Marginal-slope deposits of the Napier Formation can be seen in some places along the cliff, underlying and abutting reef limestone of the Windjana Limestone. Peara Cave (Lake Cave) in the south-central face of Chedda Cliffs is a spectacular tunnel (Figs 318–320, 325), thought to have formed by solution in subglacial meltwater during the Early Permian glaciation, as described earlier and in Playford (2002a).

Well-developed tepee structures occur in fenestral limestones of the Nullara Limestone east of Chedda Cliffs,



Figure 530. Cyclone Rock (*Walangina*) on the left and Willy Willy Rock (*Djalawunna*) on the right, in reef-margin subfacies (Pillara Limestone) near *Rowalamban* Cave, Napier Range.

closely resembling those found at the northwestern end of the Oscar Range and Billy Munro Gorge. They show clear evidence of disruption of the microbial limestones by syndepositional compression, leading to crestal breaching (e.g. GPS AMG Zone 51, 672130E 8096845N) and overthrusting (e.g. GPS AMG Zone 51, 672025E 8096805N). They cannot be ascribed to deposition over 'agglutinated microbialite mounds' as claimed by Chow and George (2004). Although the material beneath the breached crest is microbial limestone, it developed by infilling of the cavity beneath the developing tepee. The tepees range in height from tens of centimetres to more than a metre, and have lateral extents of a few metres.

The Frasnian–Famennian boundary, between Frasnian reef-margin subfacies (Pillara Limestone) and Famennian back-reef subfacies (Nullara Limestone), is exposed at several localities behind Chedda Cliffs (AMG Zone 51, 673400E 8096400N; Playford et al., 1989; Playford 2002a; Playford and Hocking, 2006). It is clear at those localities that the latest Frasnian Pillara reef must have grown nearly horizontally for considerable distances. At one locality (AMG Zone 51, 673400E 8097100N) a thin belt of reefal-slope subfacies of the Napier Formation (too narrow to be mapped on Plate 1) is intercalated in the wide Frasnian reef. The Pillara Limestone consists of dolomitized stromatoporoid–microbial reef, while the Nullara Limestone consists of fenestral oolite, calcarenite, and pisolite, with blocks of Pillara Limestone, as much as 1 m across, at the base of the formation in some places. The Frasnian–Famennian contact is an erosional unconformity, with relief of as much as 5 m. Subcircular karst depressions in the Nullara Limestone are as much as 30 cm across, and most are filled with oolite (Fig. 97). Some karst holes contain megalodonts, gastropods and poorly preserved ammonoids. Large oncolites and thick-shelled megalodonts occur in several beds in the basal part of the Nullara Limestone.

At another locality near Chedda Cliffs (GPS AMG Zone 51, 673150E 8096870N), the Frasnian–Famennian boundary was described by George et al. (2002, 2006), and Chow et al. (2004) as an angular unconformity between Famennian back-reef limestone (Nullara Limestone) above and tectonically tilted Frasnian fore-reef limestone (Napier Formation) below. However, careful examination of the site failed to validate their description of the geology (Playford and Hocking, 2006). The Famennian back-reef Nullara Limestone at this locality typically consists of grey and pink fenestral limestone, and this overlies latest Frasnian reef of the Pillara Limestone. The stromatoporoid–microbial reef includes steeply dipping sheets of a stromatoporoid, marking successive reef fronts (Fig. 531). The reef grew almost horizontally, just as it did elsewhere on the Lennard Shelf in the latest Frasnian. There is no evidence to support the claim by Chow et al. (2004) that fore-reef strata with dips of about 25° to 30° are present below the Frasnian–Famennian boundary. No Frasnian fore-reef deposits can be seen at this locality, nor is there any sign of angular discordance between the Frasnian and Famennian limestones. The Frasnian–Famennian unconformity shows evidence of minor karstification of the Frasnian reef, similar to the type previously recorded by Playford et al. (1989), and this is compatible with a eustatic regression at the close of the Frasnian.

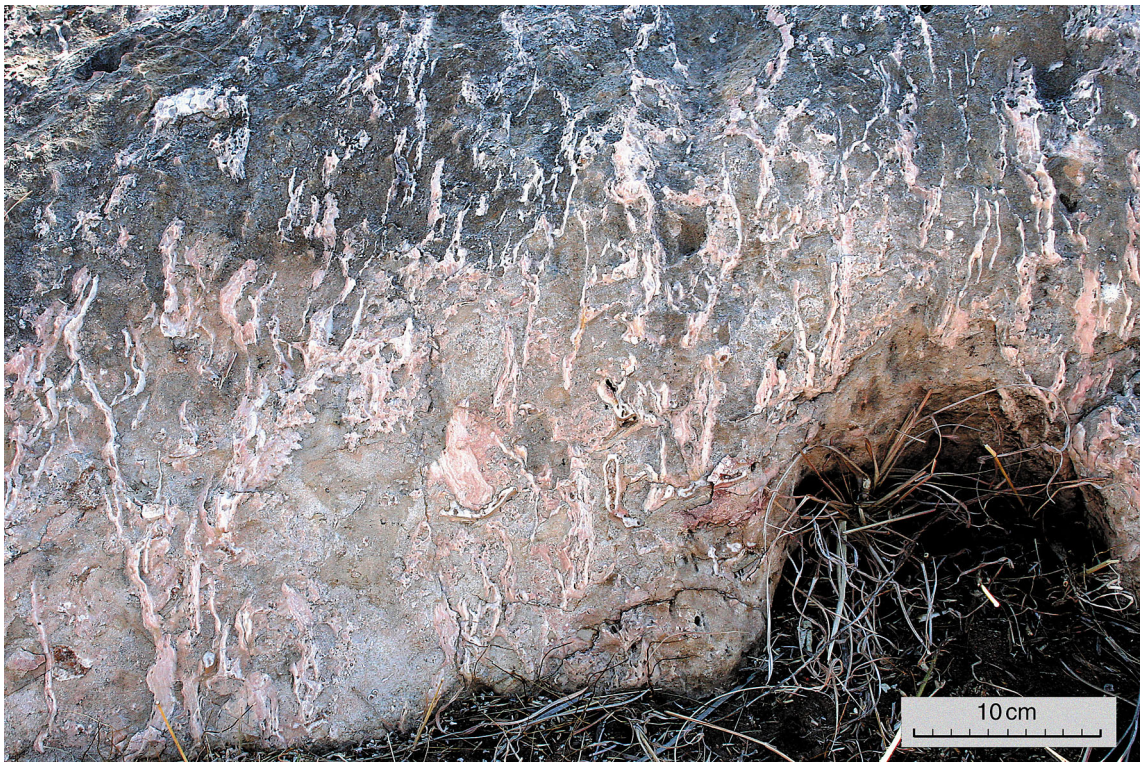

Figure 531. Frasnian reef limestone (Pillara Limestone, Sequence 6) directly below the Frasnian–Famennian boundary in the Napier Range near Chedda Cliffs. Steeply dipping sheets of stromatoporoids mark successive reef fronts (compare with Figure 27).

Mount Lesley

At Mount Lesley, north of the original Old Napier Downs Homestead, there is a small outcrop of Nullara Limestone on top of the Napier Range. It is approximately 100 m thick, and overlies and interfingers with Windjana Limestone. The Nullara Limestone is well exposed, consisting of medium- to thin-bedded oolite, fenestral limestone, oncolitic limestone, and coquinites of thick-shelled megalodonts. No cyclicity is apparent.

A contact between bedded back-reef Nullara Limestone and relatively massive Windjana Limestone is exposed along the western side of the belt of Nullara Limestone (AMG Zone 51, 670000E 8103370N). The contact undulates and truncates bedding below, suggesting that it resulted from a brief emergence. Such an emergence could be associated with a brief regression in the Middle Famennian, possibly associated with the Horseshoe Range Event.

About 70 m to the northeast (AMG Zone 51, 670050E 8103400N), a finely fenestral, sandy, red limestone contains abundant detrital megalodonts and rip-up clasts as much as 40 cm across. The clasts include lime mudstone, *Renalcis* limestone, and microbial Nullara Limestone. Desiccation polygons outlined by fenestrae cap the unit, which rests with a sharp, probably erosive, contact on a limestone containing irregular fenestrae and a few gastropods and quartz pebbles. The rip-up clasts suggest that it may be a transgressive lag deposit.

Van Emmerick Range area

The Van Emmerick Range is a mass of terrigenous conglomerate, consisting mainly of rounded to subrounded boulders, cobbles, and pebbles of quartzite and granitic rocks, with lesser amounts of other Precambrian rocks. Two superimposed conglomerate bodies can be seen on aerial images, pointing to a possible hiatus between them, perhaps at the time when the deep-water Preema Bioherms (see below) were deposited. As with most other conglomerate bodies, the range is significantly higher than the reef complex around it. The formation interfingers with both Frasnian and Famennian marginal-slope deposits of the Napier Formation.

The fault plane forming the basin margin is well exposed at two places, juxtaposing conglomerate with granitic rocks (up slope from AMG Zone 51, 676900E 8112500N) and sheared quartzite and chert (AMG Zone 51, 677900E 8111000N). Wunala Hill and a smaller conglomerate body northwest of Hawkstone Creek are included in the Van Emmerick Conglomerate (AMG Zone 51, 664500E 8119900N, and 659700E 8122900N). Both of these bodies are thought to have been shed from the eroded scarp of the Van Emmerick Fault.

The proportion of granitic clasts increases from about 20% in the lowest exposures to more than 90% near the crest of the range. Sorting also increases upwards. The geometry of the conglomerate is clearly that of a large fan. Giant ‘foresets’, several tens of metres high, can be discerned within the conglomerate, and paleocurrent directions suggest a point source for the main conglomerate body.

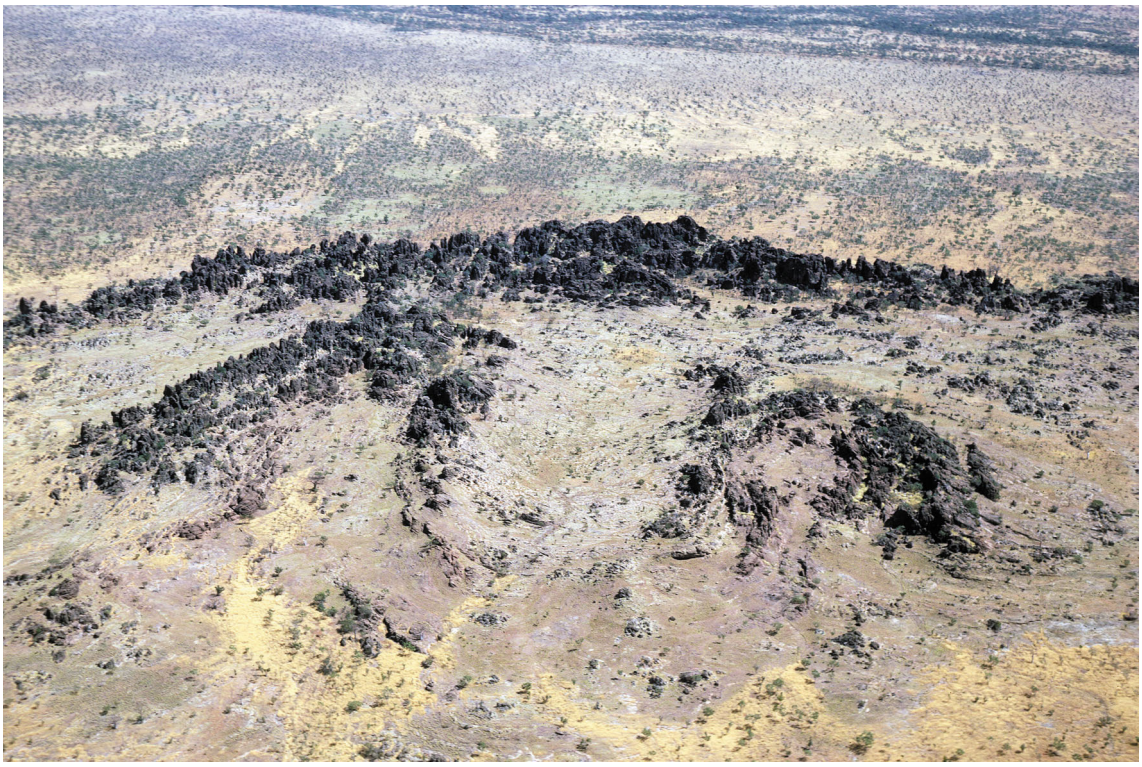

Figure 532. Biohermal 'noses' of microbial and receptaculitid limestone in the Napier Range north of Unggumi Promontory. They are two of a group of five such bioherms, named the Preema Bioherms.

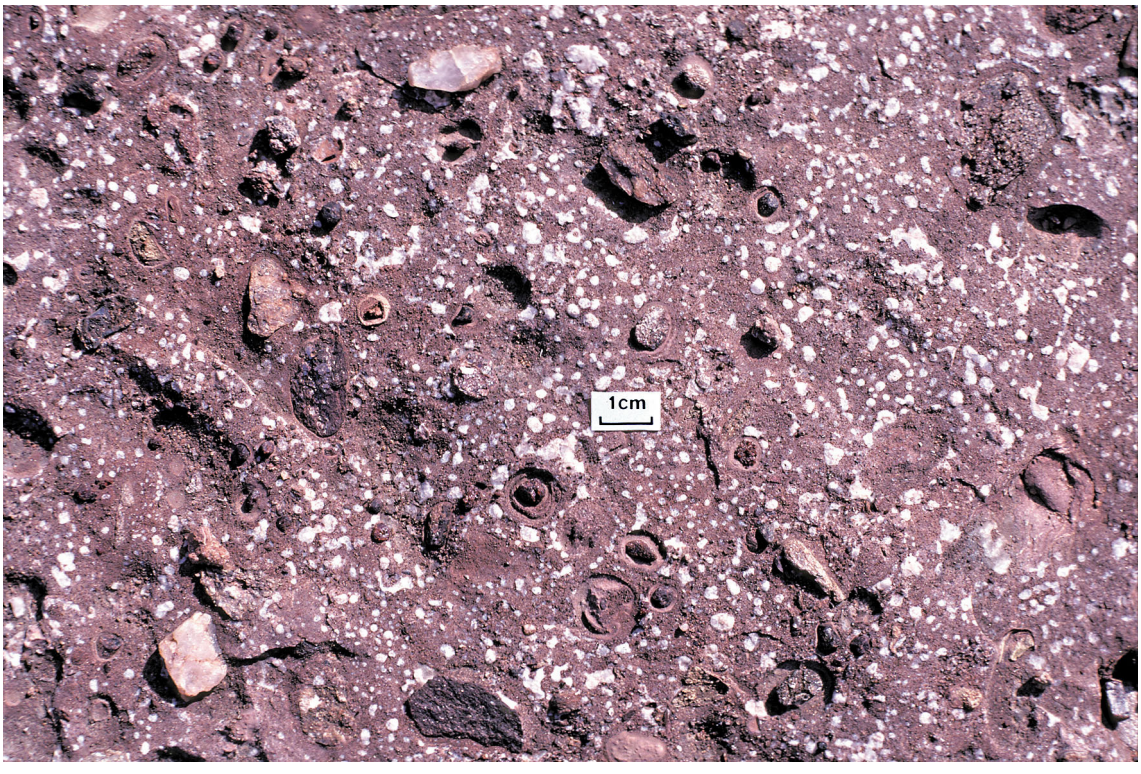

Figure 533. Conglomeratic, sandy, fenestral limestone of the Pillara Limestone, immediately north of Hawkstone Creek in the Napier Range. Microbial oncolites have formed around clasts of Precambrian rocks and garnet crystals.

There are abundant cut-and-fill structures as well as interfingering between conglomerate and cross-bedded sandstone (e.g. GPS AMG Zone 51, 676300E 8109900N), indicating that deposition occurred in rapidly avulsing channels on the surface of a fan. Siltstone drapes between clasts suggest occasional breaks in deposition. Bioturbation can be seen in some sandstone interbeds, which together with down-slope long-axis imbrication of clasts and interfingering with marginal-slope deposits, indicates that this part of the conglomerate is a fan-delta deposit. However, most of the formation is thought to represent subaerial alluvial-fan deposition.

Small lycopod impressions preserved in bioturbated siltstone near the crest of the range are thought to be of Famennian age (GPS AMG Zone 51, 675400E 8109750N).

Holmes and Christie-Blick (1993) made a detailed sequence-stratigraphic interpretation of a small area of the Van Emmerick Conglomerate, 1.3 km south-southeast of Preema Pass (GPS AMG Zone 51, 669600E 8116100N). They indicated that an incised valley at least 10 m deep was cut into limestone (which they termed 'foreslope floatstone'), stating that conglomerate and sandstone are preserved locally as a veneer against a vertical contact with the limestone (Holmes and Christie-Blick, 1993, p. 193). This locality is at the northwest edge of the main mass of Van Emmerick Conglomerate, and our detailed examination of the area failed to support their interpretation. Imbrication indicates a current direction from the east, and the conglomerate can be seen to grade up into dolomitic marginal-slope deposits of the Napier Formation. The limestones contain allochthonous blocks of reefal limestone (Pillara Limestone) greater than 10 m in size. The interpreted lower transgressive systems tract sequence boundary shown in Holmes and Christie-Blick's figure 19 is apparently based on a large, flat-based rectangular block of Pillara Limestone resting on marginal-slope conglomeratic limestone. The block is oriented nearly parallel to bedding, as might be expected from its shape. The regional strike of bedding in the Napier Formation is 190° and the dip is 20°W, while the block dips north at about 10°. The supposed upper transgressive systems tract shown on their figures 17 and 19 is marked by another large allochthonous block. Neither Holmes and Christie-Blick's incised valley nor their 'veneer of siliciclastic rocks against the valley wall' are valid interpretations, and there is no sound basis for their sequence-stratigraphic interpretation.

A prominent feature of the western part of the Napier Range south of Preema Pass is the presence in the Napier Formation of many receptaculitid–stromatolite bioherms, here termed the Preema Bioherms. These form depositional anticlinal noses, resembling giant antiformal stromatolites, each having its long axis oriented in the dip direction of the marginal slope (Plates 1, 7, 8; Fig. 532). The bioherms are late Frasnian to early Famennian in age. Most are characterized by abundant receptaculitids, together with stromatolitic limestone containing *Sphaerocodium* fingers, columnar and scalloped stromatolites, and wavy microbial laminae. Some of the bioherms are thought to have been localized by underlying lobes of Van Emmerick Conglomerate.

Unggumi Promontory

A conspicuous reef promontory in the Barnett Spring area (*Tchangalagnarri*, AMG Zone 51, 666000E 8110500N) has been formally named Unggumi Promontory (by Playford), to commemorate the *Unggumi* Tribe that once inhabited this area. The promontory is formed of Famennian platform facies (Windjana and Nullara Limestones). These platform limestones were truncated horizontally by the Early Permian ice sheet, and covered by Permian and younger sediments that have since been removed by erosion. The exhumed promontory has an outline that is essentially the same as it had when the reefs became extinct in the Late Famennian (Figs 5, 302–304). The reef forming the promontory was localized by a stromatolite–receptaculitid depositional anticlinal nose, comparable with those forming the Preema Bioherms (AMG Zone 51, 667900E 8113700N).

Billy Munro Gorge, a deep and precipitous channel that is dry for most of the year, cuts through the length of Unggumi Promontory (Figs 302–304). It has been named (by Playford) after Billy Munro, the last *Unggumi*-speaking man (who died in 1993). Unggumi Promontory and Billy Munro Gorge together form one of the most striking geomorphic features in the Devonian reef belt.

The gorge is 120–150 m wide and 2.2 km long. It is defined by parallel precipitous walls as much as about 40 m high. Barnett Spring, near the entrance to the gorge, is small and ephemeral. A little creek, which carries water during the wet season only, runs along the length of the gorge and disappears on the adjoining plain a short distance from the gorge mouth. It is clear that such a small stream could not have been responsible for carving out this gorge. Indeed, it would be difficult to imagine how any usual processes of fluvial erosion could have formed such a gorge, with its parallel and precipitous sides. Instead, it is thought to have developed as a subglacial channel that carried torrents of meltwater during the Early Permian. This channel would afterwards have been filled with Permian sediments that have been removed through Cenozoic erosion.

The gorge exposes transitions from poorly bedded reef-flat to massive reef margin near the entrance, through to bedded reef-flat and back-reef limestones in the heart of the gorge (Plate 1). Tepees as much as 70 cm high and 2 to 3 m across occur on the walls of the gorge (Frost et al., 2006; Frost, 2007a,b). Brecciation and breached cores can be seen, and overthrusting of beds is apparent in some places (e.g. GPS AMG Zone 51, 666370E 8110625N).

Hawkstone Creek to Limestone Spring

Nyangalignali area

Nyangalignali is the *Unggumi* name of the gap where Hawkstone Creek flows through the Napier Range. The Pillara Limestone on the northwest side of the gap interfingers with and overlies Van Emmerick Conglomerate of the *Wunala* fan. The Pillara Limestone at this locality

consists of red conglomeratic fenestral limestone, with clasts up to pebble size of quartz and mica schist. Oncolites have developed around some clasts and around garnet crystals up to granule size that are locally derived from garnetiferous mica schist (Fig. 533). Alluvial garnet that has weathered out of such schist was once mined in this area at the Russell mine (Plate 1).

Wunala area

Wunala is a low hill of conglomerate, thought to be Frasnian in age, exposed as a close-packed lag deposit of cobbles and boulders. About 70% of the clasts are granitic near the base of the hill, rising to 90 or 95% at the top. The maximum clast size is about 1.2 m near the hill top, and clasts are smaller near the base. Deposition of the outcropping conglomerate is thought to have been mainly as an alluvial fan, and perhaps partly as a fan delta.

The Frasnian–Famennian boundary unconformity is well exposed at several localities about 1.3 km southwest of *Wunala*, where the Famennian Nullara Limestone (back-reef subfacies) overlies either Pillara Limestone (reef subfacies) or Napier Formation (reefal-slope subfacies; Figs 50, 534).

The unconformity surface is generally smooth, with local relief of as much as 2 m, but in places it shows minor evidence of karstification. The Pillara Limestone consists of massive, red to grey, sandy, fenestral limestone and dolomite. Well-developed stromatoporoid-rich sandy reef limestone and dolomite occur in some places. The adjoining reefal-slope deposits of the Napier Formation contain some *Renalcis* and *Stachyodes* that appear to be in situ. They must have grown high on the reefal slopes that fronted the Pillara reef. The oldest exposed Nullara Limestone in the area consists of well-bedded reddish fenestral limestone, containing some blocks of Pillara Limestone and early-cemented Nullara Limestone (Fig. 535).

At one spectacular locality (Fig. 50; AMG Zone 51, 663800E 8118600N) and nearby, it can be shown that the Frasnian–Famennian erosion surface was cut down into latest Frasnian reefal-slope deposits. Famennian back-reef subfacies (Nullara Limestone) overlies Frasnian reefal-slope subfacies (Napier Formation) along the Frasnian–Famennian unconformity. It is unsure how much vertical section was eroded away along this unconformity, but it could have amounted to a few tens of metres. The initial dip of the reefal-slope deposits was about 24°S, and the observed dip has been increased to 30° as a result of post-depositional tilting. That tilting is confirmed by geopetal structures within the reefal-slope deposits, and is the same as in the overlying Nullara Limestone.

Limestone Spring area

Limestone Spring (*Tilingair*) is situated near the northwest end of the outcropping Napier Range Reef Complex. Geophysics and drilling show that the reef complexes continued to the northwest, where they are covered by post-reef shale, limestone, and sandstone of the latest Famennian to Early Carboniferous Fairfield Group,



Figure 534. The Frasnian–Famennian boundary in the Napier Range near *Wunala* Hill, showing sandy limestone of the back-reef Nullara Limestone overlying reef of the Pillara Limestone.



Figure 535. Imbricate blocks of Pillara Limestone at the base of the Nullara Limestone near *Wunala* Hill.



Figure 536. 'Balancing rock' in Nullara Limestone south of Limestone Spring in the Napier Range. Photo by Steve Wallace.

or shale, diamictite, and sandstone of the middle Carboniferous to Early Permian Grant Group.

Exposures in the Limestone Spring area consist mainly of fenestral back-reef limestones of the Nullara Limestone, in some places containing coquinites of lithiotid and megalodont bivalves, interfingering with reef-flat limestones of the Windjana Limestone. A remarkable 'balancing rock' of Nullara Limestone is located in this area (Fig. 536).

The Fairfield Group is poorly exposed in creeks close to the spring. Conglomerate and sandstone overlying that group have been mapped as Grant Group, but they could conceivably be equivalent to the Lillybooroora Conglomerate, 70 km to the northwest, which Botten (1984) correlated with the Fairfield Group (latest Devonian to Early Carboniferous).

Future research

A great deal of research has now been carried out in the Devonian Great Barrier Reef, but there remains ample scope for further work. Among topics that warrant future research are the following:

- Achieve reliable correlation between platform, marginal-slope, and basin facies using magneto-stratigraphy and isotope stratigraphy;
- Investigate whether the palynology of subsurface shales and siltstones (using core samples) can be used to obtain reliable correlations between platform, marginal-slope, and basin facies;.
- Reprocess and re-interpret existing seismic and well data on the Lennard Shelf, to improve correlation between the outcropping reef complexes and their subsurface equivalents;
- Conduct 3-D seismic surveys to interpret the subsurface Devonian reef complexes, with particular attention to the Frasnian–Givetian Pillara Sequence;
- Undertake detailed field studies of known sequence boundaries as defined by backstepping events;
- Undertake petrographic and field studies of beds that show dissolution of clasts in marginal-slope deposits, especially in adnet/scheck breccias;
- Undertake detailed studies of the Nullara Limestone, concentrating on cyclicity, patterns of thickness variation, and evidence of sequence boundaries;
- Make more detailed comparisons with Devonian platform carbonates elsewhere in the world, especially Canada;
- Undertake detailed paleontological, geochemical, and paleomagnetic studies across the Frasnian–Famennian boundary, seeking to determine the cause of the Frasnian–Famennian mass extinction;
- Undertake detailed structural studies in key areas, especially in the vicinity of the confluence between the Virgin Hills and Sparke Range Faults and along the Black Hills Fault;
- Undertake detailed studies of the relationships between faulting, platform development, and platform-margin collapse;
- Revise the paleontology of the brachiopod faunas; and
- Undertake detailed studies of renalcids and other microbial reef builders.

Acknowledgements

Over the past 50 years many people have contributed to the data and interpretations that are covered in this Bulletin.

Firstly we express appreciation to geologists of WAPET who participated in the early studies: Doug Smith and Frank Williams who worked with Playford at the Oscar Range in 1956, and Murray Johnstone, who joined him at Windjana Gorge in 1958. The early work by GSWA in 1962–1963, 1968, 1972 was strongly supported by Joe Lord, then Director of the organization, and that support was maintained by his successors, Alec Trendall and Phil Playford. David Lowry made important contributions to field work in 1962–63 that resulted in the first major publication on the reef complexes (Bulletin 118). Ed Druce and Bob Nicoll, geologists of the Bureau of Mineral Resources (now Geoscience Australia), contributed their conodont expertise in detailed studies at Bugle Gap in 1968 and Windjana Gorge in 1972. Iain Copp of GSWA gave valuable assistance in the field during 1993–1995 and made a detailed study of cores derived from company zinc–lead exploration.

In 1984–85, Charles Kerans conducted a two-year study on the petrography of the Devonian carbonates, in association with GSWA, under a grant from the Western Australian Mining and Petroleum Research Institute. The resulting report made an important contribution to knowledge of the reef complexes.

Malcolm Wallace has advanced knowledge of the reef complexes, especially in relation to mineralization, since earning a PhD for his study of the Geikie Gorge area in 1985–87. His contributions to our project are very much appreciated.

Many other geologists from universities in Australia and overseas have undertaken post-graduate studies in the reef complexes, beginning with Neil Hurley at the Oscar Range in 1983–86. Among others who participated in those studies we would especially like to acknowledge Scott Brownlaw, Nicole De Kever, Simon Dörling, Ned Frost, Annette George, Andrew McManus, Rebecca Mason, Vicki Pedone, Ted Playton, Nat Stephens, Dawn Sumner, Linda Tompkins, Phil Tornatora, and Bruce Ward.

The most recent phase of mapping and research in the reef complexes by GSWA began in 1992. Since then the project has had strong support from successive Directors — Pietro Guj, David Blight, and Tim Griffin — for which we are very grateful. Thanks are also due to Gilbert Klapper, Thomas Becker, and the late Michael House for their important roles in the research through detailed conodont

and ammonoid studies. Geoffrey Playford is also thanked for his contribution to knowledge of the palynology.

GSWA has sponsored some fifteen field excursions to the reef complexes since 1974, mostly in association with various geological conferences. Thanks are due to the many participants on those excursions who contributed observations and suggestions that have served to advance our understanding of the reef complexes.

We are indebted to Lloyd Robinson for showing us through Mimbi, Uranus, and Kimberley Rover Caves in the Bugle Gap area.

Useful advice was given by Peter Haines, who reviewed and gave comments on the draft manuscript, and Ian Ruddock and Lee Hassan, who provided material for the section on epigenetic mineralization. Thanks are also due to Ian Nowak for his skilled role as editor, to Murray Jones for designing the covers, and to Kath Noonan for preparing the text for publication. Cartographers of GSWA have skilfully drafted the diagrams and maps, and special thanks for this are due to Suzanne Dowsett, Michael Prause, Shaun Coldicutt, and David Ladbrook. Photographs included in this Bulletin were taken by Playford, unless otherwise acknowledged in the captions.

Special thanks are due to many Aboriginal elders, especially Billy Munro (*Unggumi*), Billy Oscar, George Brooking, and Banjo Woorunmurra (*Bunaba*), and Bohemia Jack and Neville Sharp (*Gooniyandi*) for providing Aboriginal names for many features in the area and explaining their Dreamtime significance. Hugh Edwards is also thanked for his role in helping to identify sites associated with the *Bunaba* outlaw, Jandamarra (Pigeon).

Finally, we wish to record appreciation to our wives, Cynthia Playford, Margaret Hocking, and Sheila Cockbain, for their support and encouragement, and for their understanding during our many long absences from home while engaged in field work in the Canning Basin.

References

Adams, R D and Grotzinger, J P 1996, Lateral continuity of facies and parasequences in Middle Cambrian platform carbonates, Carrara Formation, southeastern California, USA: Journal Sedimentary Research, v. 66, p. 1079–1090.

Aharon, P, Schwarcz, H P and Roberts, H H 1997, Radiometric dating of submarine hydrocarbon seeps in the Gulf of Mexico: Geological Society of America Bulletin, v. 109, p. 568–579.

Aitchison, J C 1993, Late Devonian (Frasnian) Radiolaria of the Canning Basin, Western Australia: Paleontographica Abteilung A 228, p. 105–128.

Allen, J R L 1982, Sedimentary structures — their character and physical basis: Developments in Sedimentology, v. 30A, Elsevier, Amsterdam.

Alexander, R, Cumbers, K M, Hartung, B and Kagi, R I 1985, Petroleum geochemistry of the Canning Basin: Western Australian Mining and Petroleum Research Institute, Report 20, 119p.

Anderson, E J and Goodwin, P W 1990, The significance of metre-scale allocycles in the quest for a fundamental stratigraphic unit: Journal Geological Society of London, v. 147, p. 507–518.

Apak, S N and Backhouse, J 1998, Re-interpretation of the Permo-Carboniferous succession, Canning Basin, Western Australia, *in* The sedimentary basins of Western Australia 2 *edited by* P G Purcell and R R Purcell: Proceedings of Petroleum Exploration Association of Australia Symposium, Perth, Western Australia, 1998, p. 683–694.

Arne, D 1996, Thermal setting of the Cadjebut Zn–Pb deposit, Western Australia: Journal of Geophysical Exploration, v. 57, p. 45–56.

Arne, D C, Green, P F, Duddy, I R, Gleadow, A J W, Lambert, I B and Lovering, J F 1989, Regional thermal history of the Lennard Shelf, Canning Basin, from apatite fission track analysis: implications for the formation of Pb–Zn ore deposits: Australian Journal of Earth Sciences, v. 36, p. 495–513.

Atchley, S C, West, W and Sluggett, J R 2006, Reserves growth in a mature oil field: the Devonian Leduc Formation at Innisfail field, south-central Alberta, Canada: AAPG Bulletin, v. 90, p. 1153–1169.

Balme, B E and Hassell, C W 1962, Upper Devonian spores from the Canning Basin, Western Australia: Micropaleontology, v. 8, p. 1–28.

Barnaby, R J and Rimstidt, J D 1989, Redox conditions of calcite cementation interpreted from Mn and Fe contents of authigenic calcites: Geological Society of America, Bulletin 101, p. 795–804.

Basedow, H 1918, Narrative of an expedition of exploration in northwestern Australia: Royal Geographical Society of Australia, South Australian Branch, Transactions, v. 18, p. 105–295.

Beauchamp, B and Savard, M 1992, Cretaceous chemosynthetic carbonate mounds in the Canadian Arctic: Palaios, v. 7, p. 434–450.

Becker, R T 2000, Ammonoidea, *in* Paleobiogeography of Australasian faunas and floras *edited by* A J Wright, G C Young, J A Talent, and J R Laurie: Association of Australasian Paleontologists, Memoir 23, p. 177–180.

Becker, R T and House, M R 1997, Sea level changes in the Upper Devonian of the Canning Basin, Western Australia: Courier Forschungsinstitut Senckenberg, v. 199, p. 129–146.

Becker, R T, House, M R and Kirchgasser, W T 1993, Devonian goniatite biostratigraphy and timing of facies movements in the Frasnian of the Canning Basin, *in* High resolution stratigraphy *edited by* E A Hailwood and R B Kid: Geological Society of London, Special Publication v. 70, p. 293–321.

Becker, R T, House, M R, Kirchgasser, W T and Playford, P E 1991, Sedimentary and faunal changes across the Frasnian/Famennian boundary in the Canning Basin of Western Australia: Historical Biology, v. 5, p. 183–196.

Begg, J 1987, Structuring and controls on Devonian reef development on the north-west Barbwire and adjacent terraces, Canning Basin: APEA Journal, v. 27, p. 137–151.

Belka, Z 1998, Early Devonian Kess-Kess carbonate mud mounds of the eastern Anti-Atlas (Morocco), and their relation to submarine hydrothermal venting: Journal of Sedimentary Research, Section A: Sedimentary Petrology and Processes, v. 68, p. 368–377.

Benn, D I and Evans, D J A 1998, Glaciers and glaciation: Arnold, Hodder Headline, London, 734p.

Bennett, M R C 1992, Reports on drilling programme, Virgin Hills (EL 04/610), April 1991 – June 1992: Geopeko unpublished reports WA92/22S, WA93/610: Geological Survey of Western Australia, Statutory petroleum exploration report, A35758, A57568.

Bennett, M R C 1994, Final report for Virgin Hills E 04/610 for the period May 1992 to July 1993: Geopeko unpublished report WA 94/46S: Geological Survey of Western Australia, Statutory petroleum exploration report, A39973.

Blockley, J G 1971, The lead, zinc, and silver deposits of Western Australia: Geological Survey of Western Australia, Mineral Resources Bulletin 9, 234p.

Böhm, F, Dommergues, J L and Meister, C 1995, Breccias of the Adnet Formation: indicators of a mid-Liassic tectonic event in the Northern Calcareous Alps (Salzburg/Austria): Geologische Rundschau, v. 84, p. 272–286.

Bond, D, Wignall, P B and Racki, G 2004, Extent and duration of marine anoxia during the Frasnian–Famennian (Late Devonian) mass extinction in Poland, Germany, Austria, and France: Geological Magazine, v. 141, p. 1–29.

Botten, P 1984, Uranium exploration in the Canning Basin — a case study, *in* The Canning Basin, WA *edited by* P G Purcell: Geological Society of Australia and Australian Petroleum Exploration Society Canning Basin Symposium, Perth, WA, 1984, Proceedings, p. 485–501.

Boulegue, J, Iiyama, J T, Charlou, J and Jedwab, J 1987, Nankai Trough, Japan Trench and Kuril Trench; geochemistry of fluids sampled by submersible 'Nautile': Earth and Planetary Science Letters, v. 83, p. 363–375.

Brannon, J C, Cole, S C, Podosek, F A, Ragan, V M, Coveney, R M Jr, Wallace, M W and Bradley, A J 1996, Th–Pb and U–Pb dating of ore-stage calcite and Paleozoic fluid flow: Science, v. 271, p. 491–493.

Brown, S A, Boserio, I M, Jackson, K S and Spence, K W 1984, The geological evolution of the Canning Basin — implications for petroleum exploration, *in* The Canning Basin, WA *edited by* P G Purcell: Proceedings of the Canning Basin Symposium, Geological Society of Australia and Petroleum Exploration Association of Australia, p. 85–96.

Brownlaw, R L S 2000, Rugose coral biostratigraphy and cyclostratigraphy of the Middle and Upper Devonian carbonate complexes, Canning Basin, Western Australia: The University of Queensland, PhD thesis (unpublished).

Brownlaw, R L S, Hocking, R M and Jell, J S 1996, High frequency sealevel fluctuations in the Pillara Limestone, Guppy Hills, Lennard Shelf, northwestern Australia: Historical Biology, v. 11, p. 187–212.

Burne, R V and Kanstler, A J 1971, Geothermal constraints on the hydrocarbon potential of the Canning Basin, Western Australia: Australia, Bureau of Mineral Resources Journal of Geology and Geophysics, v. 2, p. 271–281.

Caputo, M V 1985, Late Devonian Glaciation in South America: Paleogeography, Paleoclimatology, Paleoecology, v. 51, p. 291–317.

Caputo, M V and Crowell, J C 1985, Migration of glacial centers across Gondwana during Paleozoic era: Geological Society of America Bulletin, v. 96, no. 8, p. 1020–1036.

Carney, R S 1994, Consideration of the oasis analogy for chemosynthetic communities at Gulf of Mexico hydrocarbon vents: Geo-Marine Letters, v. 14, p. 149–159.

Cavagna, S, Clari, P and Martire, L 1999, The role of bacteria in the formation of cold seep carbonates; geological evidence from Monferrato (Tertiary, NW Italy): Sedimentary Geology, v. 126, p. 253–270.

Chafetz, H S and Guidry, S A 1999, Bacterial shrubs, crystal shrubs, and ray-crystal shrubs: bacterial vs abiotic precipitation: Sedimentary Geology, v. 126, p. 57–74.

Chen, Z, Li, X and Powell, C M 1995, Paleomagnetism of the Upper Devonian reef complexes, Canning Basin, Western Australia: Tectonics, v. 14, p. 154–167.

Choquette, P W and James, N P 1987, Diagenesis in limestones 3; the deep burial environment: Geoscience Canada, v. 14, p. 3–35.

Chow, N and George, A 2004, Tepee-shaped agglutinated microbialites: an example from a Famennian carbonate platform on the Lennard Shelf, northern Canning Basin, Western Australia: Sedimentology, v. 51, p. 253–265.

Chow, N, George, A D and Trinajstic, K M 2004, Tectonic control on development of a Frasnian–Famennian (Late Devonian) paleokarst surface, Canning Basin reef complexes, northwestern Australia: Australian Journal of Earth Sciences, v. 51, p. 911–917.

Christensen, J N, Halliday, A N, Vearncombe, J R and Kesler, S E 1995, Testing models of large-scale crustal fluid flow using direct dating of sulfides; Rb–Sr evidence for early dewatering and formation of Mississippi Valley-type deposits, Canning Basin, Australia: Economic Geology, v. 90, p. 877–884.

Church, T M 1979, Marine barite, origin and occurrence, *in* Marine minerals *edited by* RG Burns: Mineralogical Society of America Reviews in Mineralogy, v. 6, p. 175–209.

Cisne, J L 1986, Earthquakes recorded stratigraphically on carbonate platforms: Nature, v. 323, p. 320–322.

Claypool, G E, Holster, W T, Kaplan, I R, Sakai, H and Zak, I 1980, The age curves of sulfur and oxygen isotopes in marine sulfate and their mutual interpretation: Chemical Geology, v. 28, p. 199–260.

Cockbain, A E 1976a, *Stromatoporella kimberleyensis* Etheridge Jr. 1918 is a piece of bone: Geological Survey of Western Australia, Annual Report 1975, p. 133–135.

Cockbain, A E 1976b, Devonian tentaculitids from the Canning Basin reef complexes: Geological Survey of Western Australia, Annual Report 1975, p. 135–136.

Cockbain, A E 1984, Stromatoporoids from the Devonian reef complexes, Canning Basin, Western Australia: Geological Survey of Western Australia, Bulletin 129, 108p.

Cockbain, A E 1989, Distribution of Frasnian and Famennian stromatoporoids: Association of Australasian Palaeontologists, Memoirs no. 8, p. 339–345.

Cockbain, A E and Playford, P E 1988, The Devonian of Western Australia, a review, *in* Devonian of the world *edited by* N J McMillan, A F Embry, and D J Glass: Proceedings of the second international symposium on the Devonian System, v. 1, Regional Syntheses, Canadian Society of Petroleum Geologists Memoir, v. 14, pt 1, p. 743–754.

Colbath, G K 1990, Devonian (Givetian–Frasnian) organic-walled phytoplankton from the Limestone Billy Hills reef complexes, Canning Basin, Western Australia: Paleontographica Abteilung B, v. 217, p. 87–145.

Coleman, P J 1951, Atrypa in Western Australia: Journal of Paleontology, v. 25, p. 677–690.

Colette, I, Zollinger, R, Woods, D, Cavlovic, D, Vine, B, Sander, M, Kirkwood, E, Webb, R, Cugley, J, Eberhard, S and Fitzgerald, D 2000, KN1 Old Napier Downs Cave, The Western Caver, v. 40, p. 96–98.

Cook, A G, Blodgett, R B and Becker, R T 2003, Late Devonian gastropods from the Canning Basin, Western Australia: Alcheringa, v. 27, p. 181–207.

Copp, I A 2000, Subsurface facies analysis of Devonian reef complexes, Lennard Shelf, Canning Basin, Western Australia: Geological Survey of Western Australia, Report 58, 127p.

Copper, P 1986, Frasnian/Famennian mass extinction and cold-water oceans: Geology, v. 14, p. 835–839.

Copper, P 1994, Ancient reef ecosystem expansion and collapse: Coral Reefs, v. 13, p. 3–11.

Cortecci, G and Longinelli, A 1972, Oxygen isotope variations in a barite slab from the sea bottom off California: Chemical Geology, v. 9, p. 113–117.

Crespin, I 1961, Upper Devonian Foraminifera from Western Australia: Paleontology, v. 3, p. 397–409.

Crevello, P D, Wilson, J L, Sarg, J F and Read, J F (editors) 1989, Controls on carbonate platforms and basin development: SEPM Special Publication 44.

Crostella, A 1998a, The Lennard Shelf revisited, *in* The sedimentary basins of Western Australia 2 *edited by* P G Purcell and R R Purcell: Petroleum Exploration Society of Australia, West Australian Basins Symposium, Perth, Western Australia, Proceedings, p. 667–682.

Crostella, A 1998b, Oil occurrences within the Lennard Shelf, Canning Basin, Western Australia: Geological Survey of Western Australia, Report 56.

Crowe, R W A and Towner, R R 1976, Definitions of some new and revised rock units in the Canning Basin: Geological Survey of Western Australia, Record 1976/24.

Curtis, C D, Oertel, G and Petrowski, C 1972, Stable carbon isotope ratios within carbonate concretions: a clue to place and time of formation: Nature, v. 235, p. 98–100.

Dalrymple, R W 1992, Tidal depositional systems, *in* Facies models — response to sea level change *edited by* R G Walker and N P James: Geological Association of Canada, p. 195–218.

Davey, A 1980, Conservation of the West Kimberley karst: The Western Caver, v. 20, no. 2, p. 35–46.

De Boer, P L and Smith, D G 1994, Orbital forcing and cyclic sequences, *in* Orbital forcing and cyclic sequences *edited by* P L De Boer and D G Smith: International Association of Sedimentologists, Special Publication 19, p. 1–14.

De Kever, N 1998, Devonian stromatolites and exhalative mineralization, Canning Basin, Western Australia: University of Melbourne, School of Earth Sciences, BSc Hons thesis (unpublished).

Dicker, D 1987, The 1985 Kimberley trip (Kimberley 6 Expedition): Illawarra Speleological Society, v. 2, no. 5, p. 1–3.

Dicker, D and Robinson, L N 1993, Unofficial newsletter: Illawarra Speleological Society, v. 2, no. 5A, 46p.

Dörling S L, 1995, Structural evolution of the southeastern Fitzroy Trough and Lennard Shelf, Western Australia, during the Devonian–Early Carboniferous Pillara tectonic episode: implications for facies distribution and Mississippi Valley-type Pb–Zn mineralisation: The University of Western Australia, PhD thesis (unpublished).

Dörling, S L, Dentith, M C, Groves, D I, Playford, P E, Vearncombe, J R, Muhling, P and Windrim, D 1996, Heterogeneous brittle deformation in the Devonian carbonate rocks of the Pillara Range, Canning Basin: implications for the structural evolution of the Lennard Shelf: Australian Journal of Earth Sciences, v. 43, p. 15–29.

Dörling, S L, Dentith, M C and Playford, P E 1995, Deformation in the carbonate rocks of the Lennard Shelf: Society of Economic Geologists, Guidebook Series, v. 23, p. 51–80.

Druce, E C 1976, Conodont biostratigraphy of the Upper Devonian reef complexes of the Canning Basin, Western Australia: Australia, Bureau of Mineral Resources, Bulletin 158, 303p.

Druce, E C and Radke, B M 1979, The geology of the Fairfield Group, Canning Basin, Western Australia: Australia BMR, Bulletin 200, 62p.

Drummond, B J, Etheridge, M A, Davies, P J and Middleton, M F 1988, Half-graben model for the structural evolution of the Fitzroy Trough, Canning Basin, and its implications for resource exploration: Australian Petroleum Exploration Association Journal, v. 28, p. 76–86.

Drummond, B J, Sexton, M J, Barton, T J and Shaw, R D 1991, The nature of faulting along the margins of the Fitzroy Trough, Canning Basin, and its implications for the tectonic development of the trough: Exploration Geophysics, v. 22, p. 111–116.

Drummond, C N and Wilkinson, B H, 1996, Stratal thickness frequencies and the prevalence of orderedness in stratigraphic sequences: Journal Geology, v. 104, p. 1–18.

Edgell, H S 2003, Upper Devonian Charophyta from Western Australia: Micropaleontology, v. 49, p. 359–374.

Edgell, H S 2004, Upper Devonian and Lower Carboniferous Foraminifera from the Canning Basin, Western Australia: Micropaleontology, v. 50, p. 1–26.

Elkin, A P 1932, Social organization in the Kimberley region: Oceania, v. 2, p. 296–333.

Ellwood, B B, Benoist, S L, El Hassini, A and Crick, R E 2003, Possible multiple bolide impacts at the Frasnian–Famennian boundary: evidence from two sections, Bou Tchrafine and Jebel Amelane, located in the Anti-Atlas of Morocco: Geological Society of America Abstracts with Programs, v. 35, no. 6, September 2003, p. 209.

Elrick, M and Read, J F 1991, Cyclic ramp-to-basin carbonate deposits, Lower Mississippian, Wyoming and Montana, a combined field and computer modelling study: Journal of Sedimentary Petrology, v. 61, p. 1194–1224.

Feist, R and Becker, R T 1997, Discovery of Famennian trilobites in Australia (Late Devonian, Canning Basin, NW Australia: Geobios, v. 20, p. 231–242.

Ferguson, J, Etminan, H and Ghassemi F, 1992, Salinity of deep formation water in the Canning Basin, Western Australia: Australia, BMR Journal of Australian Geology and Geophysics, v. 13, p. 93–105.

Ferguson, J, Etminan, H and Ghassemi, F 1993, Geochemistry of deep formation waters in the Canning Basin, Western Australia, and their relationship to Zn–Pb mineralization: Australian Journal of Earth Sciences, v. 40, p. 471–483.

Findlay, W A 1942, Geologic report, North-western Fitzroy Basin, Kimberley Division, Western Australia: Caltex (Australia) Oil Development Pty Ltd, unpublished report.

Fischer, A G 1964, The Lofer Cyclothems of the Alpine Triassic: Bulletin of the Kansas Geological Survey, no. 169, p. 107–149.

Fischer, A G and Bottjer, D J 1991, Orbital forcing and sedimentary sequences: Journal of Sedimentary Petrology, v. 61, no. 7, p. 1063–1069.

Fleming, B S 1983, Lennard Shelf regional Pb–Zn exploration, Lawford Range EL 80/116 (formerly Emanuel Range Prospect), West Kimberley and Kimberley mineral fields, Western Australia: BHP Minerals Limited unpublished report, Geological Survey of Western Australia, Statutory petroleum exploration report, A14063.

Foord, A H 1890, Description of fossils from the Kimberley District, Western Australia: Geological Magazine, Decade III, v. 7, p. 98–106, 145–155.

Ford, D C and Williams, P W 2007, Karst hydrology and geomorphology: Wiley and Sons, Chichester, 562p.

Forman, D J and Wales, D W 1981, Geological evolution of the Canning Basin, Western Australia: Australia, Bureau of Mineral Resources, Bulletin 210, 91p.

Franseen, E K, Watney, W L, Kendall, C G StC and Ross, W (editors) 1991, Sedimentary modelling: Computer simulations and methods for improved parameter definition: Kansas Geological Survey, Bulletin 233, 524p.

Freytet, P and Verrecchia, E P 1999, Calcitic radial palisade fabric in freshwater stromatolites: diagenetic and recrystallized feature or physicochemical sinter crust: Sedimentary Geology, v. 126, p. 97–102.

Frost, E L 2007a, Geological modelling of Frasnian and Famennian carbonate platforms, Canning Basin, Western Australia: AAPG International Conference and Exhibition, Perth, Australia, Abstracts Volume, p. 49.

Frost, E L 2007b, Facies heterogeneity, platform architecture and fracture patterns of the Devonian reef complexes, Canning Basin, Western Australia: University of Texas at Austin, Texas, PhD thesis (unpublished).

Frost, E L, Playford, P E and Kerans, C 2006, Platform evolution, facies patterns, and cyclicity across the Late Devonian Frasnian/Famennian boundary — Barnett Spring platform, Canning Basin, Western Australia: AAPG International Conference and Exhibition, Perth, Australia, Abstracts Volume, p. 40.

Garrels, R M and Christ, C L 1990, Solutions, minerals and equilibria: Jones and Bartlett Publishers, Boston, 450p.

Garrison, R E and Fischer, A G 1969, Adnet Beds, in Deep-water limestones and radiolarites of the Alpine Jurassic: Society of Economic Paleontologists and Mineralogists, Special Publication 14. p. 24–29.

George, A D 1999, Deep-water stromatolites, Canning Basin, northwestern Australia: Palaios, v. 14, p. 493–505.

George, A D and Chow, N 1999, Paleokarst development in a lower Frasnian (Devonian) platform succession, Canning Basin, northwestern Australia: Australian Journal of Earth Sciences, v. 46, p. 905–913.

George, A D and Chow, N 2002, The depositional record of the Frasnian–Famennian boundary interval in a fore-reef succession (Napier Formation), Canning Basin, northwestern Australia: Paleogeography, Paleoclimatology, Paleoecology, v. 181, p. 347–374.

George, A D, Chow, N and Trinajstic, K M 2002, Integrated approach to platform-basin correlation and deciphering the evolution of Devonian reefs, northern Canning Basin, Western Australia, *in* The sedimentary basins of Western Australia 3 *edited by* M Keep and S J Moss: Proceedings of the Petroleum Exploration Society of Australia Symposium, Perth, Western Australia, p. 817–835.

George, A D, Chow, N and Trinajstic, K M 2006, Reply; Tectonic control on development of a Frasnian–Famennian (Late Devonian) paleokarst surface, Canning Basin reef complexes, northwestern Australia: Australian Journal of Earth Sciences, v. 53, p. 666–669.

George, A D, Playford, P E and Powell, C M 1994, Carbonate breccias and quartzo-feldspathic sandstones of the marginal-slope, Devonian reef complexes, Canning Basin, Western Australia, *in* The sedimentary basins of Western Australia *edited by* P G Purcell and R R Purcell: Petroleum Exploration Society of Australia, West Australian Basins Symposium, Perth, WA, 1994, Proceedings, p. 727–738.

George, A D, Playford, P E and Powell, C M 1995, Platform-margin collapse during Famennian reef evolution, Canning Basin, Western Australia: Geology, v. 23, no. 8, p. 691–694.

George, A D, Playford, P E, Powell, C M and Tornatora, P M 1997, Lithofacies and sequence development on an Upper Devonian mixed carbonate-siliciclastic fore-reef slope, Canning Basin, Western Australia: Sedimentology, v. 44, p. 843–867.

George, A D and Powell, C M 1997. Paleokarst in an Upper Devonian reef complex of the Canning Basin, Western Australia: Journal of Sedimentary Research, v. 67, p. 935–944.

Ginsburg, R N 1971, Landward movement of carbonate mud; new model for regressive cycles in carbonates: Bulletin of the American Association of Petroleum Geologists, v. 55, p. 340.

Glenister, B F 1958, Upper Devonian ammonoids from the Manticoceras Zone, Fitzroy Basin, Western Australia: Journal of Paleontology, v. 32, p. 58–96.

Glenister, B F and Klapper, G 1966, Upper Devonian conodonts from the Canning Basin, Western Australia: Journal of Paleontology, v. 40, p. 777–842.

Glover, J E 1955, Petrology and petrography of limestones from the Fitzroy Basin, Western Australia: Australia, Bureau of Mineral Resources, Report 18.

Goldberg, E D and Arrhenius, G O S 1958, Chemistry of Pacific pelagic sediments: Geochimica et Cosmochimica Acta, v. 13, p. 153–212.

Goldhammer, R K, Dunn, P A and Hardie, L A 1987, High-frequency, glacioeustatic sealevel oscillations with Milankovich characteristics recorded in Middle Triassic platform carbonates in northern Italy: American Journal of Science, v. 287, p. 853–892.

Goldhammer, R K, Dunn, P A and Hardie, L A 1990, Depositional cycles, composite sealevel changes, cycle stacking patterns, and the heirarchy of stratigraphic forcing — examples from platform carbonates of the Alpine Triassic: Geological Society of America Bulletin, v. 102, p. 535–562.

Goldhammer, R K, Lehmann, P J and Dunn, P A 1993, The origin of high-frequency platform carbonate cycles and third order sequences (Lower Ordovician El Paso Group, West Texas): constraints from outcrop data and stratigraphic modelling: Journal Sedimentary Petrology, v. 63, p. 318–359.

Goldstein, R H and Reynolds, T J 1994, Systematics of fluid inclusions in diagenetic minerals: SEPM Short Course 31, Tulsa, Oklahoma, USA, 199p.

Goodwin, P W and Anderson, E J 1985, Punctuated aggradational cycles — a general hypothesis of episodic stratigraphic accumulation: Journal of Geology, v. 93, p. 515–533.

Gorter, J D and Nicoll, R S 1978, Reptilian fossils from Windjana Gorge, Western Australia: Journal of the Royal Society of Western Australia, v. 60, p. 97–104.

Goudie, A S, Bull, P A and Magee, A W 1989, Lithological control of rillenkarren development in the Napier Range, Western Australia: Zeitschrift für Geomorphologie, v. 75, p. 95–114.

Gradstein, F M, Ogg, K G and Smith, A G 2004, A geologic time scale 2004: Cambridge University Press, Cambridge.

Grey, K 1978, Devonian atrypid brachiopods from the reef complexes of the Canning Basin: Geological Survey of Western Australia, Report 5, 70p.

Grey, K 1991, A mid-Givetian miospore age for the onset of reef development on the Lennard Shelf, Canning Basin, Western Australia: Review of Paleobotany and Palynology, v. 68, p. 37–48.

Grey, K 1992, Miospore assemblages from the Devonian reef complexes, Canning Basin, Western Australia: Geological Survey of Western Australia, Bulletin 140, 139p.

Griffin, T G and Tyler, I M 1995, Geological map of the King Leopold Orogen, West Kimberley Region: Geological Survey of Western Australia, Bulletin 143, Plate 1.

Guppy, D J, Lindner, A W, Rattigan, J H and Casey, J N 1958, The geology of the Fitzroy Basin, Western Australia: Australia, Bureau of Mineral Resources, Bulletin 36, 116p.

Guppy, D J and Öpik, A A 1950, Discovery of Ordovician rocks, Kimberley Division, WA: Australian Journal of Science, v. 12, p. 205–206.

Haines, P W, Hand, M and Sandiford, M 2001, Paleozoic synorogenic sedimentation in central and north Australia: a review of distribution and timing with implications for the evolution of intracontinental orogens: Australian Journal of Earth Sciences, v. 48, p. 911–928.

Hall, W D M 1984, The stratigraphic and structural development of the Givetian–Frasnian reef complex, Limestone Billy Hills, western Pillara Range, WA, *in* The Canning Basin, WA *edited by* P G Purcell: Geological Society Australia and Petroleum Exploration Society of Australia Symposium, Perth, p. 215–222.

Hallam, A and Wignall, P B 1997, Mass extinctions and their aftermath: Oxford University Press, Oxford, 330p.

Halligan, R 1965, The Narlarla lead–zinc deposits, Barker River area, West Kimberley goldfield: Geological Survey of Western Australia, Annual Report 1964, p. 43–45.

Hanor, J S 1996, Controls on the solubilization of lead and zinc in basinal brines, *in* Carbonate hosted lead–zinc deposits *edited by* D F Sangster: Society of Economic Geologists, Special Publication, no. 4, p. 483–500.

Hardie, L A, Bossellini, A and Goldhammer, R K 1986, Repeated subaerial exposure of subtidal carbonate platforms, Triassic, northern Italy: evidence for high frequency sealevel oscillations on a 10^4 year scale: Paleoceanography, v. 1, p. 447–457.

Hardie, L A, Dunn, P A and Goldhammer, R K 1991, Field and modelling studies of Cambrian carbonate cycles, Virginia Appalachians, discussion: Journal of Sedimentary Petrology, v. 61, p. 636–646.

Hardman, E T 1884, Report on the geology of the Kimberley District, Western Australia: Perth, Government Printer, Western Australian Parliamentary Papers, no. 31 of 1884.

Hardman, E T 1887, On the discovery of Diprotodon australis in tropical Western Australia (Kimberley District): British Association for the Advancement of Science, Birmingham Meeting, 1886, v. 56, p. 671–672.

Hasler, C A, Adams, E W, Wood, R A and Dickson, J A D in press, Fine-scale forward modelling of a Devonian patch reef, Canning Basin, Western Australia, *in* Analogue and numerical forward modelling of sedimentary systems; from understanding to prediction *edited by* P L De Boer, P Burgess, and F Van Buchem: IAS Special Publication.

Hassan, L Y 2000, Mineral occurrences and exploration potential of the east Kimberley: Geological Survey of Western Australia, Report 74, 83p

Hassan, L Y 2004, Mineral occurrences and exploration potential of the west Kimberley: Geological Survey of Western Australia, Report 88, 88p.

Henderson, D K 1971, Oscar Range zinc–lead project, Western Australia: Trend Exploration Pty Ltd (unpublished report).

Higgs, R, Reading, H G and Burne, R V 1998, Discussion and reply: Return of 'the fan that never was': Westphalian turbidite systems in the Variscan Culm Basin, Bude Formation (south-west England): Sedimentology, v. 45, p. 961–975.

Hill, D and Jell, J S 1970, Devonian corals from the Canning Basin, Western Australia: Geological Survey of Western Australia, Bulletin 121, 158p.

Hinde, G J 1890, Notes on the palaeontology of Western Australia, corals and Polyzoa: Geological Magazine, Decade 3, v. 7, p. 194–204.

Hitzman, M W and Beaty, D W 1997, The Irish Zn–Pb–(Ba) orefield, *in* Carbonate-hosted lead–zinc deposits *edited by* D F Sangster: Society of Economic Geologists, Special Publication 4, p. 112–143.

Hocking, R M, Copp, I A, Playford, P E and Kempton, R H 1996, The Cadjebut Formation: a Givetian evaporitic precursor to Devonian reef complexes of the Lennard Shelf, Canning Basin, Western Australia: Geological Survey of Western Australia, Annual Review 1995–96, p. 48–55.

Hocking, R M and Playford, P E 1998a, Devonian reef complexes of the Canning Basin: Plate 1 — Napier Range area: Geological Survey of Western Australia, Bulletin 145, Plate 1, 1:100 000 scale map.

Hocking, R M and Playford, P E 1998b, Devonian reef complexes of the Canning Basin: Plate 2 — Oscar Range area: Geological Survey of Western Australia, Bulletin 145, Plate 2, 1:100 000 scale map.

Hocking, R M and Playford, P E 1998c, Devonian reef complexes of the Canning Basin: Plate 3 — Fossil Downs area: Geological Survey of Western Australia, Bulletin 145, Plate 3, 1:100 000 scale map.

Hocking, R M and Playford, P E 1998d, Devonian reef complexes of the Canning Basin: Plate 4 — Pillara Range – Emanuel Range – Sparke Range area: Geological Survey of Western Australia, Bulletin 145, Plate 4, 1:100 000 scale map.

Hocking, R M and Playford, P E 2001, Cycle types in carbonate platform facies, Devonian reef complexes, Canning Basin, Western Australia: Geological Survey of Western Australia, Annual Review 2000–01, p. 74–80.

Hocking, R M and Playford, P E 2002, Siliciclastic conglomerates associated with Devonian reef complexes, Canning Basin, Western Australia: Geological Society of Australia, 16th Australian Geological Convention, Abstracts, p. 361.

Hoefs, J 1973, Stable Isotope Geochemistry: New York, Springer-Verlag, 140p.

Holmes, A E and Christie-Blick, N 1993, Origin of sedimentary cycles in mixed carbonate-siliciclastic systems: an example from the Canning Basin, Western Australia, *in* Carbonate sequence stratigraphy: recent developments and applications *edited by* R G Loucks and J F Sarg: American Association of Petroleum Geologists, Memoir, no. 57, p. 181–212.

Hosking, L C V 1933, Distribution of Devonian rocks in the Kimberley Division and description of a recent collection of Devonian fossils from the Kimberley Division: Royal Society of Western Australia Journal, v. 19, p. 67–77.

Hossack, J R 1984, The geometry of listric growth faults in the Devonian basins of Sunnfjord, W Norway: Journal of the Geological Society, v. 141, no. 4, p. 628–637.

House, M R and Gale, A S (editors) 1995, Orbital forcing timescales and cyclostratigraphy: Geological Society Special Publication 85.

House, M R and Gradstein, F M 2004, The Devonian Period, *in* A geologic time scale 2004 *edited by* F M Gradstein, J G Ogg, and A G Smith: Cambridge, Cambridge University Press, p. 202–221.

Hovland, M 1992, Hydrocarbon seeps in northern marine waters — their occurrence and effects: Palaios, v. 7, p. 376–382.

Hurley, N F 1986, Geology of the Oscar Range Devonian reef complexes, Canning Basin, Western Australia: University of Michigan, PhD thesis (unpublished).

Hurley, N F and Lohmann, K C 1989, Diagenesis of Devonian reefal carbonates in the Oscar Range, Canning Basin, Western Australia: Journal of Sedimentary Petrology, v. 59, p. 127–146.

Hurley, N F and Van Der Voo, R 1987, Paleomagnetism of Upper Devonian reefal limestones, Canning Basin, Western Australia: Geological Society of America Bulletin, v. 98, p. 138–146.

Hurley, N F and Van Der Voo, R 1990, Magnetostratigraphy, Late Devonian iridium anomaly, iridium anomaly, and impact hypotheses: Geology, v. 18, p. 291–294.

Idriess, I L 1952, Outlaws of the Leopolds: Angus and Robertson, Sydney.

Irwin, H, Curtis, C and Coleman, M 1977, Isotopic evidence for source of diagenetic carbonates formed during burial of organic-rich sediments: Nature, v. 269, p. 209–213.

Jackson, M J, Diekman, L J, Kennard, J M, Southgate, P N, O'Brien, P E and Sexton, M J 1992, Sequence stratigraphy, basin-floor fans, and petroleum plays in the Devonian–Carboniferous of the northern Canning Basin: Australian Petroleum Exploration Association Journal, v. 32, p. 214–230.

James, N P 1984, Shallowing-upwards sequences in carbonates, *in* Facies Models *edited by* R G Walker: Geoscience Canada, Reprint Series, no. 1, p. 213–228.

James, N P and Choquette, P W 1984, Diagenesis 6: limestones, the sea floor diagnetic environment: Geoscience Canada, v. 10, p. 162–179.

James, N P and Macintyre, I G 1985, Carbonate depositional environments, part 1: reefs: Colorado School of Mines Quarterly, v. 80, 3, 70p.

Jaques, A L, Lewis, J D and Smith, C B 1986, The kimberlites and lamproites of Western Australia: Geological Survey of Western Australia, Bulletin 132.

Jell, P A and Jell, J S 1999, Crinoids, a blastoid, and a cyclocystoid from the Upper Devonian reef complex of the Canning Basin, Western Australia: Memoirs of the Queensland Museum, v. 43, p. 201–236.

Jennings, J N and Sweeting, M M 1961, Caliche pseudoanticlines in the Fitzroy Basin, Western Australia: American Journal of Science, v. 259, p. 635–639.

Jennings, J N and Sweeting, M M 1963, The limestone ranges of the Fitzroy Basin, Western Australia: a tropical semi-arid karst, Bonner Geographische Abhandlungen, v. 32, p. 60.

Joachimski, M M, Breisig, S and Buggisch, W 2003, Climate changes in the late Frasnian: trigger of the Frasnian–Famennian crisis:

Geological Society of America, Abstracts with programs, v. 35, no. 6, September, p. 207.

Johnson, J G, Klapper, G and Sandberg, C A 1985, Devonian eustatic fluctuations in Euromerica: Geological Society of America, Bulletin, v. 96, p. 567–587.

Johnson, J G, Klapper, G and Trojan, W R 1980, Upper range of Stringocephalus (Devonian Brachiopoda): Newsletters on Stratigraphy, vol. 8, no. 3, p. 232–235.

Jolly, S and Lance, K 1980, An index of limestone caves and other karst features of the West Kimberley: The Western Caver, v. 20, no. 2, p. 29–34.

Jonnason, K E and Reiser, R F 2002, Blina Oil Field, Canning Basin, *in* The sedimentary basins of Western Australia 3 *edited by* M Keep and S J Moss: Proceedings of the Petroleum Exploration Society of Australia Symposium, Perth, Western Australia, p. 837–849.

Kaiser, C J, Kelly, W C, Wagner, R J and Shanks, W C III 1987, Geologic and geochemical controls of mineralization in the Southeast Missouri barite district: Economic Geology, v. 82, p. 719–734.

Kennard, J M, Jackson, M J, Romine, K K, Shaw, R D and Southgate, P N 1994, Depositional sequences and associated petroleum systems of the Canning Basin, WA, *in* The sedimentary basins of Western Australia *edited by* P G Purcell and R R Purcell: Petroleum Exploration Society of Australia: West Australian Basins Symposium, Perth, Western Australia, 1994, Proceedings, p. 657–676.

Kennard, J M, Southgate, P N, Jackson, M J, O'Brien, P E, Christie-Blick, N, Holmes, A E and Sarg, J F 1992, New sequence perspective on the Devonian reef complex and the Frasnian–Famennian boundary, Canning Basin, Australia: Geology, v. 20, p. 1135–1138.

Kerans, C 1985, Petrology of Devonian and Carboniferous carbonates of the Canning and Bonaparte Basins, Western Australia: Western Australian Petroleum Research Institute, Report 12, 203p.

Kerans, C, Hurley, N F and Playford, P E 1986, Marine diagenesis in Devonian reef complexes of the Canning Basin, Western Australia, *in* Reef diagenesis *edited by* J H Schroeder and B H Purser: Berlin, Springer Verlag, p. 357–380.

Kerans, C and Playford, P E 1984, Scheck breccias from Devonian reef complexes of the Canning basin, Western Australia: American Association of Petroleum Geologists, Bulletin, v. 68, p. 495.

Klapper, G 1989, The Montagne Noire Frasnian (Upper Devonian) conodont succession, *in* Devonian of the World *edited by* N J McMillan, A F Embry, and D J Glass: Canadian Society of Petroleum Geology, Memoir 14, p. 449–468.

Klapper, G 1995, Preliminary analysis of Frasnian, Late Devonian, conodont biogeography: Historical Biology v. 10, p. 103–117.

Klapper, G 1997a, Graphic correlation of Frasnian (Upper Devonian) sequences in Montagne Noire, France, and western Canada, *in* Paleozoic sequence stratigraphy, biostratigraphy, and biogeography: Studies in honor of J Granville ('Jess') Johnson *edited by* G Klapper, M A Murphy, and J A Talent: Geological Society of America, Special Paper 321, p. 113–129.

Klapper, G 1997b, Appendix: Conodont biostratigraphy, *in* A D George, P E Playford, C M Powell, and P M Tornatora, Lithofacies and sequence development on an Upper Devonian mixed carbonate-siliciclastic fore-reef slope, Canning Basin, Western Australia: Sedimentology, v. 44, p. 866–867.

Klapper, G 2000, Species of Spathiognathodontidae and Polygnathidae (Conodonta) in the recognition of Upper Devonian stage boundaries: Courier Forschungsinstitut Senckenberg, v. 220, p. 153–159.

Klapper, G 2007, Frasnian (Upper Devonian) conodont succession at Horse Spring and correlative sections, Canning Basin, Western Australia: Journal of Paleontology, v. 81, p. 513–537.

Klapper, G and Becker, R T 1999, Comparison of Frasnian (Upper Devonian) conodont zonations, *in* Studies on conodonts *edited by* E Serpagli and C Corradini: Proceedings of the Seventh European Conodont Symposium Bolletino della Societá Paleontologica Italiana, v. 37, p. 339–347.

Klapper, G, Feist, R, Becker, R T and House, M R 1993, Definition of the Frasnian/Famennian Stage boundary: Episodes, v. 16, p. 433–441.

Koershner, W F and Read, J F 1989, Field and modelling studies of Cambrian carbonate cycles, Virginia Appalachians: Journal Sedimentary Petrology, v. 59, p. 654–687.

Kominz, M A and Bond, G C 1990, A new method of testing periodicity in cyclic sediments: application to the Newark Supergroup: Earth and Planetary Science Letters, v. 98, p. 233–244.

Kominz, M A and Bond, G C 1992, Documenting the reliability and utility of the γ method as applied to cyclic sections using forward modelling: Earth and Planetary Science Letters, v. 113, p. 449–457.

Kraus, P S 1942, Geologic report, north-central part Fitzroy Basin, Kimberley Division, Western Australia: Caltex (Australia) Oil Development Pty Ltd, unpublished report.

Kulm, L-V D, Suess, E, Moore, J C, Carson, B, Lewis, B T, Ritger, S D, Kadko, D C, Thornburg, T M, Embley, R W, Rugh, W D, Massoth, G J, Langseth, M G, Cochrane, G R and Scamman, R L 1986, Oregon subduction zone; venting, fauna, and carbonates: Science, v. 231, p. 561–566.

Lehmann, P H 1984, The stratigraphy, paleogeography and petroleum potential of the lower to upper Devonian sequence in the Canning Basin, *in* The Canning Basin, WA *edited by* P G Purcell: Geological Society of Australia and Petroleum Exploration Society of Australia Symposium, Perth, Western Australia, 1984, Proceedings, p. 253–275.

Linke, W F 1958, Solubilities, inorganic and metal-organic compounds, 4th edition: American Chemical Society, Washington DC.

Logan, B W 1984, Pressure responses (deformation) in carbonate sediments and rocks analysis and application, Canning Basin, *in* The Canning Basin, Western Australia *edited by* P G Purcell: Geological Society of Australia and Petroleum Exploration Society of Australia, Canning Basin Symposium, Perth, p. 235–251.

Logan, B W, Frances, D J and Economo, M 1994, A carbonate dilaform, Brooking Springs, Canning Basin, WA, *in* The sedimentary basins of Western Australia *edited by* P G Purcell and R R Purcell: Geological Society of Australia and Petroleum Exploration Society of Australia, West Australian Basins Symposium, Perth, 1994, p. 703–726.

Logan, B W and Semeniuk, V 1976, Dynamic metamorphism, processes and products in Devonian carbonate rocks, Canning Basin, Western Australia: Geological Society of Australia, Special Publication 6, 138p.

Long, J A 1988, Late Devonian fishes from Gogo, Western Australia: National Geographic Research, v. 4, p. 436–450.

Long, J A 1995, A new plourdosteid arthrodire from the Upper Devonian Gogo Formation of Western Australia: Paleontology, v. 38, p. 39–62.

Lowe, D R 1979, Sediment gravity flows: their classification and some problems of application to natural flows and deposits, *in* Geology of continental slopes *edited by* L J Doyle and O H Pilkley: Society of Economic Paleontologists and Mineralogists, Special Publication 27, p. 75–84.

Lowry, D C 1967, The Cave Spring cave systems, Kimberley Division of Western Australia, Helictite, 5, no. 3, p. 62–68.

McGhee, G R 1996, The Late Devonian mass extinction: the Frasnian/Famennian crisis: Columbia University Press, New York, 303p.

McGhee, G R 2005, Modelling Late Devonian extinction hypotheses, *in* Understanding Late Devonian and Permian–Triassic biotic and climatic events — towards an integrated approach *edited by* D J Over, J R Morrow, and P B Wignall: Developments in paleontology and stratigraphy, no. 20, Elsevier, Amsterdam, p. 37–50.

McLaren, D J 1982, Frasnian–Famennian extinctions: Geological Society of America, special paper 190, p. 477–484.

McManus, A and Wallace, M W 1992, Age of Mississippi Valley-type sulfides determined using cathodoluminescence cement stratigraphy, Lennard Shelf, Canning Basin, Western Australia: Economic Geology, v. 87, p. 189–193.

McNamara, K J, Feist, R and Ebach, M 2009, Patterns of evolution and extinction in the last harpetid trilobites during the Late Devonian (Frasnian): Palaeontology, v. 52, p. 11–33.

McWhae, J R H, Playford, P E, Lindner, A W, Glenister, B F and Balme, B E 1958, The stratigraphy of Western Australia: Geological Society of Australia, Journal, v. 4, part 2, 161p.

Maddox W H, 1941, A geologic reconnaissance of the north-west part of the Fitzroy Basin, Western Australia: Caltex (Australia) Oil Development Pty Ltd, unpublished report.

Mamet, B and Playford, P E 1968, Sur la presence de Quasiendothyrinae (Foraminifères) en Australie occidentale (Canning Basin): Compte Rendu Sommaire des Séances de la Société Géologique de France, v. 7, séance du 28 Octobre 1968, p. 229–230.

Mason, R 1998, Exhalative carbonate mineralization of the East Pillara Range, Lennard Shelf, Western Australia: School of Earth Sciences, University of Melbourne, BSc Hons thesis (unpublished).

Masuzawa, T, Handa, N, Kitagawa, H and Kusakabe, M 1992, Sulfate reduction using methane in sediments beneath a bathyal 'cold seep' giant clam community off Hatsushima Island, Sagami Bay, Japan: Earth and Planetary Science Letters, v. 110, p. 39–50.

Matheson, R S and Guppy, D J 1949, Geological reconnaissance in the Mount Ramsay area, Western Australia: Australia, Bureau of Mineral Resources, Report 1949/48.

Matthews, P G 1985, Australian karst index 1985: Australian Speleological Federation Inc., Melbourne.

Miall, A D 1992, Exxon global cycle chart: an event for every occasion?: Geology, v. 20, p. 787–790.

Miall, A D and Miall, C E 2001, Sequence stratigraphy as a scientific enterprise: the evolution and persistence of conflicting paradigms: Earth Science Reviews, v. 54, p. 321–348.

Miall, C E and Miall, A D 2002, The Exxon factor: the roles of academic and corporate science in the emergence and legitimation of a new global model of sequence stratigraphy: Sociological Quarterly, v. 43, p. 307–334.

Middleton, M F 1987, Seismic stratigraphy of Devonian reef complexes, northern Canning Basin, Western Australia: American Association of Petroleum Geologists Bulletin, v. 71, p. 1488–1498.

Middleton, M F 1990, Canning Basin, in Geology and mineral resources of Western Australia: Geological Survey of Western Australia, Memoir 3, p. 425–457.

Miller, J M, Nelson, E P, Hitzman, M and Hall, W D M 2007, Orthorhombic fault fracture patterns and non-plane strain in a synthetic transfer zone during rifting: Lennard Shelf, Canning Basin, Western Australia: Journal of Structural Geology, v. 29, p. 1002–1023.

Monty, C L, Bosence, D W J, Bridges P H and Pratt, B R 1995, Carbonate mud-mounds, their origins and evolution: International Association of Sedimentologists, Special Publication 23, Blackwell, 544p.

Moors, H T, Gardner, W E and Davis, J 1984, Geology of the Blina oilfield, *in* The Canning Basin, WA *edited by* P G Purcell: Geological Society, Australia and Petroleum Exploration Society of Australia Symposium, Perth, p. 277–283.

Mory, A J and Beere, G M 1985, Paleozoic stratigraphy of the Ord Basin, Western Australia and Northern Territory: Geological Survey of Western Australia, Report 14, p. 36–45.

Mory, A J and Beere, G M 1988, Geology of the onshore Bonaparte and Ord Basins in Western Australia: Geological Survey of Western Australia, Bulletin 134.

Mory, A J, Redfern, J and Martin, J R 2008, A review of Permian–Carboniferous glacial deposits in Western Australia, *in* Resolving the late Paleozoic ice age, in time and space *edited by* C R Fielding, T D Frank, and J L Isbel: Geological Society of America, Special Paper 441, p. 29–40.

Mossop, G D 1972, Origin of the peripheral rim, Redwater reef, Alberta: Canadian Petroleum Geology Bulletin, v. 20, p. 238–280.

Muller, R A and MacDonald, G J 1997, Glacial cycles and orbital forcing: Science, v. 277, p. 215–218.

Murphy, G C, Bailey, A and Parrington, P J 1986, The Blendevale carbonate-hosted zinc–lead deposit, Pillara, Kimberley region, Western Australia, *in* 13th Congress of the Council of Mining and Metallurgical Institutions, Singapore *edited by* D A Berkman: Geology and Geophysics v. 2, p. 153–162.

Nazarov, B B, Cockbain, A E and Playford, P E 1982, Late Devonian Radiolaria from the Gogo Formation, Canning Basin, Western Australia: Alcheringa, v. 6, p. 161–173.

Nazarov, B B and Ormiston, A R 1983, Upper Devonian (Frasnian) radiolarian fauna from the Gogo Formation, Western Australia: Micropaleontology, v. 29, p. 454–466.

Neumann, A C and MacIntyre, I 1985, Reef response to sealevel rise: keep-up, catch-up or give-up, *in* Proceedings of the Fifth International Coral Reef Congress, Tahiti, 27 May – 1 June, Moorea, French Polynesia: Antenne Museum-EPHE, p. 105–110.

Nicholson, H A 1890, Notes on the palaeontology of Western Australia, Stromatoporoidea: Geological Magazine, Decade III, v. 7, p. 193.

Nicoll, R S 1981, Conodont colour alteration adjacent to a volcanic plug, Canning Basin, Western Australia: Australia, BMR Journal of Australian Geology and Geophysics, v. 6, p. 265–267.

Nicoll, R S and Gorter, J D 1984a, Conodont colour alteration, thermal maturation and the geothermal history of the Canning Basin, Western Australia: APEA Journal, v. 24, part l, p. 243–258.

Nicoll, R S and Gorter, J D 1984b, Interpretation of additional conodont alteration data and the thermal maturation and geothermal history of the Canning Basin, Western Australia, *in* The Canning Basin, Western Australia *edited by* P G Purcell: Geological Society of Australia and Petroleum Exploration Society of Australia, Canning Basin Symposium, Perth, p. 411–425.

Nicoll, R S and Playford, P E 1993, Upper Devonian iridium anomalies, conodont zonation, and the Frasnian–Famennian boundary in the Canning Basin, Western Australia: Paleogeography, Paleoclimatology, Paleoecology, v. 104, p. 105–113.

O'Brien, P E and Christie-Blick, N 1992, Glacially grooved surfaces in the Grant Group, Canning Basin, and the extent of Late Paleozoic Pilbara ice sheets, BMR Journal of Australian Geology and Geophysics, 13, 87–92.

O'Connor, S 1995. Carpenter's Gap rock-shelter 1: 40,000 years of Aboriginal occupation in the Napier Ranges, Kimberley, WA: Australian Archaeology no. 40, p. 58–59.

Osleger, D and Read, J F 1991, Relation of eustacy to stacking patterns of meter-scale carbonate cycles, Late Cambrian, USA: Journal Sedimentary Petrology, v. 61, p. 1225–1252.

Osmundsen, P T, Bakke, B, Svendby, A K and Andersen, T B 2000, Architecture of the Middle Devonian Kvamshesten Group, western Norway: sedimentary response to deformation above a ramp-flat extensional fault: Geological Society, Special Publications, v. 180, p. 505–535.

Over, D J, Morrow, J R and Wignall, P B (editors) 2005, Understanding Late Devonian and Permian–Triassic biotic and climatic events — towards an integrated approach: Developments in paleontology and stratigraphy, no. 20: Elsevier, Amsterdam, 337p.

Paterson, W S B 1994, The physics of glaciers, third edition: Butterworth Heinemann, Oxford, 480p.

Paytan, A, Kastner, M and Martin, E E 1993, Marine barite as a monitor of sea water strontium isotope composition: Nature, v. 366, p. 445–449.

Pederson, H and Woorunmurra, B 1995, Jandamurra and the Bunaba resistance: Magabala Books Aboriginal Corporation, Broome, Western Australia, 218p.

Pedone, V A 1990, Geology and diagenesis of Middle Devonian (Givetian) bank deposits, Emanuel Range, Canning Basin, Western Australia: State University of New York, Stony Brook, PhD thesis (unpublished).

Petersen, M S 1975, Upper Devonian (Famennian) ammonoids from the Canning Basin, Western Australia: Paleontological Society, Memoir 8, 55p.

Playford, G 1976, Plant microfossils from the Upper Devonian and Lower Carboniferous of the Canning Basin, Western Australia: Paleontographica Abteilung B, v. 158, p. 1–71.

Playford, P E 1960, Aboriginal rock paintings of the West Kimberley region, Western Australia: Royal Society of Western Australia, Journal, v. 43, 111–122.

Playford, P E 1961, Upper Devonian reef complex at Windjana Gorge, Canning Basin, Western Australia: Geological Society of America, Special Papers 68, p. 247–248.

Playford, P E 1967, Devonian reef complexes in the northern Canning Basin, Western Australia: International Symposium on the Devonian System: Alberta Society of Petroleum Geologists, v. 2, p. 351–364.

Playford, P E 1969, Devonian carbonate complexes of Alberta and Western Australia: a comparative study: Geological Survey of Western Australia, Report 1, 43 p.

Playford, P E 1970, The Devonian 'Great Barrier Reef' of Western Australia: Australian Natural History, v. 16, p. 339–343.

Playford, P E 1972, Hardman, in Australian Dictionary of Biography, v. 4, p. 342.

Playford, P E 1976a, Devonian reef complexes of the Canning Basin: 25th International Geological Congress, excursion guide no. 38A, 39p.

Playford, P E 1976b, Narlarla lead–zinc deposits, Kimberley District, *in* Economic Geology of Australia and Papua New Guinea, 1, Metals: Australian Institute of Mining and Metallurgy, p. 535–536.

Playford, P E 1980, Devonian 'Great Barrier Reef' of Canning Basin, Western Australia: American Association of Petroleum Geologists Bulletin, v. 64, p. 814–840.

Playford, P E 1981, Field excursion guidebook, Devonian reef complexes of the Canning Basin, Western Australia: Geological Society of Australia, 5th Australian Geological Convention, 64p.

Playford, P E 1982, Devonian reef prospects in the Canning Basin: implications of the Blina oil discovery: Australian Petroleum Exploration Association Journal, v. 22, p. 258–271.

Playford, P E 1984a, Platform-margin and marginal-slope relationships in Devonian reef complexes of the Canning Basin, *in* The Canning Basin, Western Australia *edited by* P G Purcell: Geological Society of Australia and Petroleum Exploration Society of Australia, Canning Basin Symposium, Perth, p. 189–234.

Playford, P E 1984b, Devonian reef prospects, Canning and Bonaparte Gulf Basins, Western Australia: Transactions third Circum-Pacific Energy and Mineral Resources Conference, Honolulu, p. 221–225.

Playford, P E 1984c, Windjana Gorge: Heritage Australia, summer 1984, p. 59–60.

Playford, P E 1997, The Mimbi Caves System, Kimberley District, Western Australia: Report to the Western Australian Department of Conservation and Land Management (unpublished).

Playford, P E 1999, Devonian stromatolites and exhalative mineralization, Canning Basin, Western Australia: Geological Survey of Western Australia, Record 1999/6, p. 14–15.

Playford, P E 2001, The Permo-Carboniferous glaciation of Gondwana: its legacy in Western Australia: Geological Survey of Western Australia, Record 201/5, p. 15–16.

Playford, P E 2002a, Paleokarst, pseudokarst, and sequence stratigraphy in Devonian reef complexes of the Canning Basin, Western Australia, *in* The sedimentary basins of Western Australia 3, *edited by* M Keep and S J Moss: Proceedings of the Petroleum Exploration Society of Australia Symposium, Perth, Western Australia, p. 763–793.

Playford, P E 2002b, Devonian reef complexes of the Canning Basin, Western Australia, Post-6 field excursion guidebook, First International Paleontological Congress, IPC2002 — Australasia.

Playford, P E 2005, The Kimberley gold rush of 1885–1886: Geological Survey of Western Australia, Annual Review for 2004–2005, p. 33–37.

Playford, P E 2007, Rock art of the limestone ranges of west Kimberley, *in* Rock art of the Kimberley *edited by* M J Donaldson and K F Kennealy:, Kimberley Society, Perth, p. 127–152.

Playford, P E and Cockbain, A E 1969, Algal stromatolites: deepwater forms in the Devonian of Western Australia: Science, v. 165, p. 1008–1010.

Playford, P E and Cockbain, A E 1972, Geopetal fabrics: important aids for interpretation of ancient reef complexes: American Association of Petroleum Geologists, Bulletin, v. 56, p. 645.

Playford, P E and Cockbain, A E 1976, Revised stratigraphic and facies nomenclature in Devonian reef complexes of the Canning Basin: Geological Survey of Western Australia, Annual Report for 1975, p. 52–56.

Playford, P E and Cockbain, A E 1989, Devonian reef complexes, Canning Basin, Western Australia, a review: Association of Australasian Palaeontologists, Memoirs, 8, 401–412.

Playford, P E and Cockbain, A E 1992, Devonian reef complexes of the Canning Basin, Western Australia: Petroleum Exploration Association of Australia and American Association of Petroleum Geologists, field trip guidebook 1, 161p.

Playford, P E, Cockbain, A E, Druce, E C and Wray, J L 1976, Devonian stromatolites from the Canning Basin, Western Australia, *in* Stromatolites *edited by* MR Walter: Amsterdam, Elsevier, p. 543–564.

Playford, P E, Cockbain, A E, Hocking, R M and Wallace, M W 2001, Novel paleoecology of a postextinction reef; Famennian (Late Devonian) of the Canning Basin, northwestern Australia: comment and reply (by R Wood): Geology, v. 29, p. 1155–1156.

Playford, P E, Cope, R N, Low, G H, Cockbain, A E and Lowry, D C 1975, Canning Basin, *in* Geology of Western Australia: Geological Survey of Western Australia, Memoir 2, p. 319–371.

Playford, P E and Hocking, R M 1998a, Devonian reef complexes of the Canning Basin: Plate 5 — Bugle Gap area: Geological Survey of Western Australia, Bulletin 145, Plate 5, 1:25 000 scale map.

Playford, P E and Hocking, R M 1998b, Devonian reef complexes of the Canning Basin: Plate 6 — Windjana Gorge: Geological Survey of Western Australia, Bulletin 145, Plate 6, 1:10 000 scale map.

Playford, P E and Hocking, R M 1999a, Devonian reef complexes of the Canning Basin, Geological Survey of Western Australia, geological maps of the Lennard Shelf (pre-prints of Plates 1–7 to accompany Bulletin 145).

Playford, P E and Hocking, R M 1999b, Devonian reef complexes of the Canning Basin: Plate 5 — Lennard Shelf: Geological Survey of Western Australia, Bulletin 145, Plate 7, 1:250 000 scale map.

Playford, P E and Hocking, R M 2006, Discussion; Tectonic control on development of a Frasnian–Famennian (Late Devonian) paleokarst surface, Canning Basin reef complexes, northwestern Australia: Australian Journal of Earth Sciences, v. 53, p. 665–666.

Playford, P E, Hocking, R M and Copp, I 1999a, New insights into Devonian reef complexes of the Canning Basin, Western Australia:

American Association of Petroleum Geologists, Annual Meeting, Abstracts, San Antonio, p. A 110–A 111

Playford, P E, Hurley, N F, Kerans, C and Middleton, M F 1989, Reefal platform development, Devonian of the Canning Basin, Western Australia, *in* Controls on carbonate platform and basin development *edited by* P D Crevello, J L Wilson, J F Sarg, and J F Read: Society of Economic Paleontologists and Mineralogists, Special Publication 44, p. 187–202.

Playford, P E and Johnstone, M H 1959a, Upper Devonian reef complex at Windjana Gorge, Kimberley District: West Australian Petroleum Pty Ltd, unpublished report, 29p.

Playford, P E and Johnstone, M H 1959b, Oil exploration in Australia: American Association of Petroleum Geologists, Bulletin, v. 43, p. 397–433.

Playford, P E, Kerans, C and Hurley, N F 1984a, Neptunian dikes and sills in Devonian reef complexes of the Canning basin, Western Australia: American Association of Petroleum Geologists, Bulletin, v. 68, p. 517.

Playford, P E and Lowry, D C 1966, Devonian reef complexes of the Canning Basin, Western Australia: Geological Survey of Western Australia, Bulletin 118, 150p.

Playford, P E, McLaren, D J, Orth, J, Gilmore, J S and Goodfellow, W D 1984b, Iridium anomaly in the Upper Devonian of the Canning Basin, Western Australia: Science, v. 226, p. 437–439.

Playford, P E and Ruddock, I 1985, Discovery of the Kimberley goldfield: Royal Western Australian Historical Society Journal and Proceedings, v. 9, part 3, p. 76–106.

Playford, P E and Wallace, M W 1998, Stromatolites and sedimentary-exhalative mineralization in the Devonian of the Canning Basin, Western Australia: Geological Society of Australia, Abstracts no. 49, 14th Australian Geological Convention, p. 357.

Playford, P E and Wallace, M W 2001, Exhalative mineralization in Devonian reef complexes of the Canning Basin, Western Australia: Economic Geology, v. 96, p. 1595–1610.

Playford, P E, Wallace M W, De Kever, N and Mason, R 1999b, Devonian stromatolites and exhalative mineralization, Canning Basin, Western Australia: AAPG, Annual Meeting, Abstracts p. A 110.

Playton, T E 2008, Characterization, variations, and controls of reef-rimmed carbonate foreslopes: University of Texas, Austin, Texas, PhD thesis (unpublished).

Playton, T E and Kerans, C 2006, Strike variability and cyclicity of Upper Devonian (Famennian) foreslopes, Canning Basin, northwest Australia: AAPG International Conference and Exhibition, Perth, p. 109.

Playton, T E, Kerans, C and Playford, P E 2007, Contrasting Upper Devonian foreslopes of the Canning Basin: examples from retrograding Frasnian and prograding Famennian platform flanks: AAPG Annual Conference and Exhibition, Long Beach, p. 111.

Prider, R T 1960, The leucite lamproites of the Fitzroy Basin: Geological Society of Australia Journal, v. 6, p. 71–118.

Purcell, P G 1984, The Canning Basin, WA — An introduction, *in* The Canning Basin, WA *edited by* P G Purcell: Geological Society of Australia and Petroleum Exploration Society of Australia; Canning Basin Symposium, Perth, WA, 1984, Proceedings, p. 3–19.

Racki, G 1998, Frasnian–Famennian biotic crisis: undervalued tectonic control: Paleogeography, Paleoclimatology, Paleoecology, v. 141, p. 177–198.

Racki, G 1999, The Frasnian–Famennian biotic crisis: how many (if any) bolide impacts: International journal of earth sciences, v. 87, p. 617–632.

Racki, G 2005, Toward understanding Late Devonian global events: few answers, many questions, *in* Understanding Late Devonian and Permian–Triassic biotic and climatic events — towards an integrated approach *edited by* D J Over, J R Morrow, and P B Wignall: Developments in paleontology and stratigraphy, no. 20, Elsevier, Amsterdam, p. 5–36.

Rattigan, J H 1967, Fold and fracture patterns resulting from basement wrenching in the Fitzroy depression, Western Australia: Australasian Institute of Mining and Metallurgy, Proceedings, v. 223, p. 17–22.

Rattigan, J H and Veevers, J J 1961, Devonian, *in* The geology of the Canning Basin, Western Australia: Australia, Bureau of Mineral Resources, Bulletin, v. 60, p. 22–61.

Raup, D M and Sepkoski, J J 1982, Mass extinctions in the marine fossil record: Science, v. 215, p. 1501–1503.

Read, J F 1973a, Carbonate cycles, Pillara Formation (Devonian), Canning Basin, Western Australia: Canadian Petroleum Geology, Bulletin, v. 21, p. 38–51.

Read, J F 1973b, Paleo-environments and paleogeography, Pillara Formation (Devonian), Western Australia: Canadian Petroleum Geology, Bulletin, v. 21, p. 344–394.

Read, J F, Grotzinger, J P, Bova, J A and Koerschner, W F 1986, Models for generation of carbonate cycles: Geology, v. 14, p. 107–110.

Read, J F, Kerans, C, Webber, L J, Sarg, J F and Wright, F M (editors) 1995, Milankovich sea-level changes, cycles, and reservoirs on carbonate platforms in greenhouse and icehouse worlds: SEPM Short Course Notes 35, 212p.

Read, J F, Koerschner, W F, Osleger, D A, Bollinger, G A and Coruh, C 1991, Field and modelling studies of Cambrian carbonate cycles, Virginia Appalachians, reply: Journal of Sedimentary Petrology, v. 61, p. 647–652.

Riding, R 1999, The term stromatolite: towards and essential definition: Lethaia, v. 32, p. 321–330.

Riding, R 2000, Microbial carbonates: the geological record of calcified bacterial-algal mats and biofilms: Sedimentology, v. 47, p. 179–214.

Rigby, J K 1986, Late Devonian sponges of Western Australia: Geological Survey of Western Australia, Report 18, 59p.

Ringrose, C R 1984, The geology and genesis of the Narlarla lead–zinc deposit, Napier Range, WA, *in* The Canning Basin, Western Australia *edited by* P G Purcell: Geological Society of Australia and Petroleum Exploration Society of Australia, Canning Basin Symposium, Perth, p. 455–463.

Ringrose, C R 1986, Occurrence, distribution and origin of smithsonite in the no. 2 lead–zinc deposit at Narlarla, Western Australia: Geological Survey of Western Australia, Professional Papers for 1984, Report 19, p. 62–69.

Ringrose, C R 1989, Studies of selected carbonate-hosted lead–zinc deposits in the Kimberley region: Geological Survey of Western Australia, Report 24, 103p.

Ripper, E A 1937, A note on the occurrence of *Amphipora ramosa* (Phillips) in Western Australia: Royal Society of Western Australia, Journal, v. 23, p. 37–41.

Ross, J P 1961, Ordovician, Silurian, and Devonian Bryozoa of Australia: Australia, Bureau of Mineral Resources, Bulletin 50, 172p.

Sami, T T and James, N P 1994, Peritidal carbonate platform growth and cyclicity in an Early Proterozoic foreland basin, upper Pethei Group, northwest Canada: Journal Sedimentary Research, v. B64, p. 111–131.

Sandberg, C, Morrow, J and Ziegler, W 2002, Late Devonian sea-level changes, catastrophic events, and mass extinctions: Geological Society of America, Special Paper 356, p. 473–487.

Sartenaer, P 1971, Genres rhynchonellides (brachiopodes) nouveaux: Institut Royal des Sciences Naturelles de Belgique, Bulletin 47, p. 1–7.

Sartenaer, P 1999, A new mid-Famennian rhynchonellid (brachiopod) genus from the Canning Basin, Western Australia: Annales de la Société géologique du Nord, v. 7, p. 79–64.

Satterley, A K 1996, The interpretation of cyclic successions of the Middle and Upper Triassic of the Northern and Southern Alps: Earth-Science Reviews, v. 40, p. 181–207.

Schoell, M 1988, Multiple origins of methane in the earth: Chemical Geology, v. 71, p. 1–10.

Seddon, G 1970, Frasnian conodonts from the Sadler Ridge – Bugle Gap area, Canning Basin, Western Australia: Geological Society of Australia, Journal, v. 16, p. 723–742.

Shaw, R D, Sexton, M J and Zeilinger, I 1994, The tectonic framework of the Canning Basin, W.A., including the 1:2 000 000 structural elements map of the Canning Basin, Australian Geological Survey Organisation, Record 1994/48.

Skwarko, S K 1988, Devonian fossils of Western Australia: Geological Survey of Western Australia, Paleontological Report 1988/8, p. 1–643.

Smith, D N, Playford, P E and Williams, F B 1957, Oscar Range reef complex, Fitzroy Basin, Western Australia: West Australian Petroleum Pty Ltd, unpublished report.

Smith, J G 1968, Tectonics of the Fitzroy wrench trough, Western Australia: American Journal of Science, v. 266, p. 766–776.

Southgate, P N, Kennard, J M, Jackson, M J, O'Brien, P E and Sexton, M J 1999, Reciprocal lowstand clastic and highstand carbonate sedimentation, subsurface Devonian reef complex, Canning Basin, Western Australia, *in* Carbonate sequence stratigraphy *edited by* R G Louks and J F Sarg: American Association of Petroleum Geologists, Memoir 57, p. 157–179.

Stakes, D S, Orange, D L, Paduan, J B, Salamy, K A and Maher, N 1999, Cold-seeps and authigenic carbonate formation in Monterey Bay, California: Marine Geology, v. 159, p. 93–109.

Stearn, C W 1987, Effect of the Frasnian–Famennian extinction event on the stromatoporoids: Geology, v. 15, p. 677–679.

Steel, R J 1988, Coarsening-upward and skewed fan bodies: symptoms of strike-slip and transfer fault movement in sedimentary basins, *in* Fan deltas: sedimentology and tectonic settings *edited by* W Nemec and RJ Steel: London, Blackie and Son.

Steel, R J, Maehle, S, Nilsen, H, Roee, S L and Spinnangr, A 1977, Coarsening-upward cycles in the alluvium of Hornelen Basin (Devonian) Norway: sedimentary response to tectonic events: Geological Society America, Bulletin, v. 88, p. 1124–1134.

Stephens, N P and Sumner, D Y 2002, Renalcids as fossilized biofilm clusters: Paleoios, v. 17, p. 225–236.

Stephens, N P and Sumner, D Y 2003a, Famennian microbial reef facies, Napier and Oscar Ranges, Canning Basin, Western Australia: Sedimentology, v. 50, p. 1283–1302.

Stephens, N P and Sumner, D Y 2003b, Late Devonian carbon isotope stratigraphy and sealevel fluctuations, Canning Basin, Western Australia: Paleogeography, Paleoclimatology, Paleoecology, v. 191, p. 203–219.

Stock, C W 2005, Devonian stromatoporoid originations, extinctions, and paleobiogeography: how they relate to the Frasnian–Famennian extinction, *in* Understanding Late Devonian and Permian–Triassic biotic and climatic events — towards an integrated approach *edited by* D J Over, J R Morrow, and P B Wignall: Developments in paleontology and stratigraphy, no. 20, Elsevier, Amsterdam, p. 71–92.

Talent, J A, Mawson, R, Aitchison, J C, Becker, R T, Bell, K N, Bradshaw, M A, Burrow, C J, Cook, A G, Dargan, G M, Douglas, J G, Edgecombe, G D, Feist, M, Jones, P J, Long, J A, Phillips-Ross, J R, Pickett, J W, Playford, G, Rickards, R B, Webby, B D, Winchester-Seeto, T, Wright, A J, Young, G C and Zhen, Y-Y 2000, Devonian paleobiogeography of Australia and adjoining regions, *in* Paleobiogeography of Australasian faunas and floras *edited by* A J Wright, G C Young, J A Talent, and J R Laurie: Association of Australasian Paleontologists, Memoir 23, p. 167–286.

Teichert, C 1939, Nautiloid cephalopods from the Devonian of Western Australia: Royal Society of Western Australia, Journal, v. 25, p. 103–121.

Teichert, C 1940, Actinosiphonate cephalopods (Cyrtoceroidea) from the Devonian of Australia: Royal Society of Western Australia, Journal, v. 26, p. 59–75.

Teichert, C 1941, Upper Devonian goniatite succession of Western Australia: American Journal of Science, v. 239, p. 148–153.

Teichert, C 1943, The Devonian of Western Australia, a preliminary review: American Journal of Science, v. 241, p. 69–94 (part 1), p. 167–184 (part 2).

Teichert, C 1947, Stratigraphy of Western Australia: American Association of Petroleum Geologists, Bulletin, v. 31, p. 1–70.

Teichert, C 1949, Stratigraphy and palaeontology of Devonian portion of Kimberley Division, Western Australia: Australia, Bureau of Mineral Resources, Report 2, 50p.

Thomas, G A 1959, The Lower Carboniferous Laurel Formation of the Fitzroy Basin: Australia, Bureau of Mineral Resources, Report 38, p. 21–36.

Thorne, A M and Tyler, I M 1996, Mesoproterozoic and Phanerozoic sedimentary basins in the northern Halls Creek Orogen: constraints on the timing of strike-slip movement on the Halls Creek Fault system: Geological Survey of Western Australia, Annual Review 1995, p. 156–168.

Tompkins, L A 1994, An integrated model for the genesis of Mississippi Valley-type Zn–Pb mineralization at the Cadjebut Mine, Lennard Shelf, Canning Basin, Western Australia: The University of Western Australia, Department of Geology and Geophysics, PhD thesis (unpublished).

Tompkins, L A, Eisenlohr, B, Groves, D I and Raetz, M 1997, Temporal changes in mineralization style at the Cadjebut Mississippi Valley-type deposit, Lennard Shelf, WA, Economic Geology, v. 92, p. 843–862.

Tompkins, L A, Pedone, V A, Roche, M T and Groves, D I 1994a, The Cadjebut deposit as an example of Mississippi Valley-type mineralization on the Lennard Shelf, Western Australia — single episode or multiple events?: Economic Geology, v. 89, p. 450–466.

Tompkins, L A, Rayner, M J, Groves, D I and Roche, M T 1994b, Evaporites; in situ sulfur source for rhythmically banded ore in the Cadjebut Mississippi Valley-type Zn–Pb deposit, Western Australia: Economic Geology, v. 89, p. 467–492.

Tornatora, P M 1992, Stratigraphy and sedimentology of the Upper Devonian Napier Formation, Dingo Gap area, Canning Basin, Western Australia: The University of Western Australia, BSc Hons thesis (unpublished).

Torres, M E, Bohrmann, G and Suess, E 1996, Authigenic barites and fluxes of barium associated with fluid seeps in the Peru subduction zone: Earth and Planetary Science Letters, v. 144, p. 469–481.

Towner, R R and Gibson, D L 1983, Geology of the onshore Canning Basin, Western Australia: Australia, Bureau of Mineral Resources, Bulletin 215, 51p.

Tyler, I M, Griffin, T G, Playford, P E and Hocking, R M 1998, Mount Ramsay, WA, Sheet SE 52-09 (Second edition): Geological Survey of Western Australia, 1:250 000 Geological Series map.

Vail, P R, Mitchum, R M, Todd, R G, Widmier, J M, Thompson, S, Sangree, J B, Budd, J N and Hatfield, W G 1977, Seismic stratigraphy and global changes of sealevel, *in* Seismic stratigraphy — applications to hydrocarbon exploration *edited by* E Payton: American Association of Petroleum Geologists, Memoir 26, p. 49–212.

Van Wagoner, J C, Posamentier, H W, Vail, P R, Sarg, J T, Loutit, T S and Hardenbol, J 1988, An overview of the fundamentals of sequence stratigraphy and key definitions: SEPM, Special Publication 42, p. 39–45.

Vearncombe, J R, Dörling, S L, Dentith, M C, Chisnall, A W, Christensen, J N, McNaughton, N J, Playford, P E, Rayner, M J and Reed, A R 1995a, Tectonic, structural and depositional controls on zinc–lead mineralization on the Lennard Shelf: Minerals and Energy Research Institute of Western Australia, Report 145, 177p.

Vearncombe, J R, Dörling, S L, Dentith, M C, Chisnall, A W, Christensen, J N, McNaughton, N J, Playford, P E, Rayner, M J and Reed, A R 1995b, Zinc–lead mineralization on the southeastern Lennard Shelf, Canning Basin, Western Australia: Society of Economic Geologists, Guidebook Series, v. 23, 218p.

Veevers, J J 1959a, Devonian brachiopods from the Fitzroy Basin: Australia, Bureau of Mineral Resources, Bulletin 45.

Veevers, J J 1959b, Devonian and Carboniferous brachiopods from north-western Australia: Australia, Bureau of Mineral Resources, Bulletin 55.

Veevers, J J and Wells, A T 1961, The geology of the Canning Basin, Western Australia: Australia, Bureau of Mineral Resources, Bulletin 60.

Veizer, J 1983, Chemical diagenesis of carbonates: theory and application of trace element technique, *in* Stable isotopes in sedimentary geology *edited by* M A Arthur: SEPM Short Course no. 10, p. 3–1 to 3–100.

Viles, H A and Goudie, A S 1990, Reconnaissance studies of the tufa deposits of the Napier Range, N.W. Australia: Earth Surface Processes and Landforms, v. 15, p. 425–443.

Von Rad, U, Roesch, H, Berner, U, Geyh, M, Marchig, V and Schulz, H 1996, Authigenic carbonates derived from oxidized methane vented from the Makran accretionary prism off Pakistan: Marine Geology, v. 136, p. 55–77.

Wade, A 1924, Petroleum prospects, Kimberley District of Western Australia and Northern Territory: Commonwealth of Australia, Parliamentary Paper, Melbourne.

Wade, A 1936, The geology of the West Kimberley District of Western Australia: Freney Kimberley Oil Company, unpublished report.

Wade, A 1938, The geological succession in the West Kimberley district of Western Australia: Australian and New Zealand Association for the Advancement of Science, Auckland meeting, 1937, Report, v. 23, p. 93–96.

Wallace, M W 1987, Sedimentology and diagenesis of Upper Devonian carbonates, Canning Basin, Western Australia: University of Tasmania, PhD thesis (unpublished).

Wallace, M W, Kerans, C, Playford, P E and McManus, A 1991, Burial diagenesis in the Upper Devonian reef complexes of the Geikie Gorge region, Canning Basin, Western Australia: American Association of Petroleum Geologists, Bulletin, v. 75, p. 1018–1038.

Wallace, M W, Moxham, H, Johns, B and Marshallsea, S 2002, Hydrocarbons and Mississippi Valley-type sulfides in the Devonian reef complexes of the Eastern Lennard Shelf, Canning Basin, Western Australia, *in* The sedimentary basins of Western Australia 3 *edited by* M Keep and S J Moss: Proceedings of the Petroleum Exploration Society of Australia Symposium, Perth, Western Australia, p. 795–815.

Walter, M R 1976, Stromatolites: Developments in Sedimentology no. 20: Amsterdam, Elsevier, 790p.

Ward, W B 1996, Platform evolution and diagenesis of Frasnian carbonate platforms, Devonian reef complexes, Napier Range, Canning Basin, Western Australia: State University of New York, Stony Brook, PhD thesis (unpublished).

Ward, W B 1999, Tectonic control on backstepping sequences revealed by mapping of Frasnian backstepped platforms, Devonian reef complexes, Napier Range, Canning Basin, Western Australia, *in* Advances in carbonate sequence stratigraphy; application to reservoirs, outcrops, and models *edited by* P M Harris and J A Saller: Society for Sedimentary Geology, Special Publication 63, p. 47–74.

Webb, G E 1996, Was Phanerozoic reef history controlled by the distribution of non-enzymatically secreted reef carbonates (microbial carbonate and biologically induced cement)?: Sedimentology, v. 43, p. 947–971.

Webb, G E 2001, Famennian mud-mounds in the proximal fore-reef slope, Canning Basin, Western Australia: Sedimentary Geology, v. 145, p. 295–315.

Wells, A J 1960, Upper Devonian reef complexes of the Lennard Shelf, northeastern Canning Basin, Western Australia: Koninklijke/Shell Exploratie en Produketie Laboratorium, Research Report R 1042.

Whittam, D B, Kennard, J M, Kirk, R B, Sarg, J F and Southgate, P N 1994, A proposed third-order sequence framework for the Upper Devonian outcrops of the northern Canning Basin, *in* The sedimentary basins of Western Australia *edited by* P G Purcell and R R Purcell: Proceedings of Petroleum Exploration Association of Australia Symposium, Perth, Western Australia, 1994, p. 697–702.

Wilgus, C K, Hastings, B S, Kendall, C G StC, Posamentier, H W, Ross, C A and Van Wagoner, J C (editors) 1988, Sea-level changes — an integrated approach: SEPM, Special Publication 42, 407p.

Won, M-Z 1997a, Review of the family Entactiniidae (Radiolaria) and taxonomy and morphology of Entactiniidae in the Late Devonian (Frasnian) Gogo Formation, Australia: Micropaleontology, v. 43, p. 333–369.

Won, M-Z 1997b, The proposed new radiolarian subfamily Retentactiniinae (Entactiniidae) from the Late Devonian (Frasnian) Gogo Formation, Australia: Micropaleontology, v. 43, p. 371–418.

Wood, R 1998, Novel fabrics from the Devonian Canning Basin, Western Australia: Sedimentary Geology, v. 121, p. 149–156.

Wood, R, 2000a, Novel paleoecology of a postextinction reef, Famennian (Late Devonian) of the Canning Basin, northwestern Australia: Geology, v. 28, p. 987–990.

Wood, R 2000b, Paleoecology of a Late Devonian back reef, Canning Basin, Western Australia: Paleontology, v. 43, p. 671–703.

Wood, R and Oppenheimer, C 2000, Spur and groove morphology from a Late Devonian reef: Sedimentary Geology, v. 133, p. 185–193.

Woodward, H P 1907, Mineral discoveries at Narlarla in the West Kimberley district: Geological Survey of Western Australia, Annual Report 1906, p. 11–13.

Wray, J L 1967, Upper Devonian calcareous algae from the Canning Basin, Western Australia: Professional Contributions to the Colorado School of Mines, v. 3, 76p.

Yang, W, Harmsen, F and Kominz, M A 1995, Quantitative analysis of a cyclic peritidal carbonate sequence, the Middle and Upper Lost Burro Formation, Death Valley, California — a possible record of Milankovich climatic cycles: Journal Sedimentary Research, v. B65, p. 306–322.

Yeates, A N, Gibson, D L, Towner, R R and Crowe, R W A 1984, Regional geology of the onshore Canning Basin, WA, *in* The Canning Basin, WA *edited by* P G Purcell: Geological Society of Australia and Petroleum Exploration Society of Australia; Canning Basin Symposium, Perth, WA, 1984, Proceedings, p. 23–55.

Young, G C 1996, Devonian (Chart 4), *in* An Australian Phanerozoic time scale *edited by* G C Young and J R Laurie: Melbourne, Oxford University Press, p. 96–109.

Young, G C and Laurie, J R (editors) 1996, An Australian Phanerozoic timescale, Melbourne, Oxford University Press, 279p.

Young, G C, Long, J and Burrow, C 2000, Vertebrata, *in* Paleobiogeography of Australasian faunas and floras *edited by* A J Wright, G C Young, J A Talent, and J R Laurie: Association of Australasian Palaeontologists, Memoir 23, p. 209–219.

About the authors



Phillip Playford was born in Western Australia, obtaining BSc (Hons) and honorary DSc degrees from the University of Western Australia and a PhD from Stanford University. He has worked for both government and industry, and is a former Director of the Geological Survey of Western Australia. His geological research has included the Devonian reef complexes of the Canning Basin, Shark Bay, the Perth Basin, and the Permian glaciation of Western Australia. Honours received include: Lewis G Weeks Gold Medal of APPEA, Medal of the Royal Society of Western Australia, Gibb Maitland Medal of the Geological Society of Australia, Special Commendation Award of the AAPG, Distinguished Member of PESA, and Member of the Order of Australia. He is currently an Honorary Associate of the Geological Survey of Western Australia and the Western Australian Museum.



Roger Hocking completed BSc (Hons) and MSc degrees at the University of New England, Armidale, New South Wales. He joined the Geological Survey of Western Australia in late 1974, rising to his present position of Chief Geoscientist. He has worked as a stratigrapher and sedimentologist on siliciclastic and carbonate rocks ranging from Holocene to Archean in age, in undeformed to moderately deformed basins and orogens across Western Australia, with a focus of assembling broad geological frameworks that give context for later workers. In the present study he has mapped throughout the reef belt, concentrating on the sedimentology and stratigraphy of the conglomerates and other terrigenous deposits that interfinger with the reef complexes, and on cyclicity in both carbonates and siliciclastics.



Tony Cockbain was born in Warrington, England, and educated at the Sir Thomas Boteler Grammar School and the University of Nottingham where he obtained BSc (Hons) and PhD degrees. He has worked in universities (Institute of Oceanography, University of British Columbia; University of Canterbury, New Zealand); geological surveys (Cyprus; Western Australia); and (briefly) in industry. Through this work he met a host of colleagues, many of whom became friends. In the study of the Devonian reef complexes his role has been mainly in mapping and biostratigraphy, including a detailed study of the stromatoporoid faunas. He became Editor of the Australian Journal of Earth Sciences after retiring as Assistant Director of the Geological Survey of Western Australia in 1993.

Index

All page numbers in **bold** indicate references occurring in figure captions

Aboriginal paintings 12, 17, 243, **244**, 321, 329, **333**, 337, **338**, **344**, **372**, 377
Aboriginal tribe
Bunaba 12, 17, **17**, 63, 64, 243, **334**, 337, 342
Gooniyandi 12, 17, **17**, 63, 243, 280, 283
Kukadja 63
Ngadadjara 63
Pintubi 63
Unggumi **10**, 12, **17**, 63, **231**, **232**, 243, 337, 342, 350, 362, 367, 377, **380**, 381
Wolmadjari 63
Aborigines 12, 17, **17**, 63, **63**, 64, 243, 280, 281, 283, 334, **334**, **336**, 337, **338**, 342, **344**–**346**, 350, 362, **364**, 367, **369**, **372**, 377
Actinostroma 27, **30**, 31, **33**, **35**, 39, 164, 250, 258, 288, 294, 297, 304, 329, 350, 355, **357**, **358**, 362
adnet breccia 88, **97**, 342, 373, 384
advancing platform 2, 65, 72, 81, **86**, 294
algae 4, 27, 31, 56
Algae Creek 68, 72, 167, 301
alluvial fan 2, 125, **126**, **128**, **133**, 134, **140**, 146, 149, 297, **298**, 381, 382
alluvial-fan deposit 2, 134, 139, 142, 146, 149, 297, 381
Alveolites, 277, 287, 288
ammonoid 1, 2, 7, 23, 31, 39, **42**, 49, **55**, 57, 62, 64, 65, 75, **78**, 115, 129, 274, **275**, 288, 321, **328**, 363, 378
Amphipora 27, **29**, **30**, 31, 51, **122**, 138, 146, 163, 164, 250, 277, 294, 297, 300, **302**, 304, **309**, **310**, 355
anhydrite 24
anoxia 2, 75, 205
anoxic mud 53, 199, 204
antiformal stromatolite 63, 311, **313**, 335, **335**, 367, 373, **374**, **375**, 381
Atrypa 165, 250, 286, 350
Aulopora **52**, 274, **309**, 321, **327**
autocyclicity 150

back reef 1, 2, 4, 7, 9, 17, 22, 23, 26, 27, **30**, 31, **32**, **33**, **34**, 39, **41**, **42**, 43, 46, 48, 62, 68, 69, **71**, **74**, **76**, **84**, **87**, 106, 115, 119, 122, 124, 134, 138, **138**, 143, **162**, 165, **166**, 167, **167**, 257, 277, **279**, 287, 294, **294**, 297, **298**, **299**, 304, **306**, **307**, **309**, **310**, **331**, **332**, 337, **341**, **351**, **352**, 354, 355, **357**, **362**, **363**, **365**, 367, **371**, 378, 379, 381, 382, 384
backstepping 2, 7, 31, 39, 50, 62, 65, 68, **69**, **70**, 72, **73**, 80, 81, 124, **186**, 202, 274, **278**, 354, 355, 384
Algae Creek Event 68, 72, 167, 301
Classic Face Event 68, 72, 342, 354, 355
Elliott Ridge Event 39, **42**, 68, **69**, 250, 257, 258, **278**
Horseshoe Range Event 46, 68, 75–80, 379
Kellys Pass Event 68, 69, **70**, **72**, 274, 277, 278, 301
Waggon Pass Event 53, 57, 68, 69, 72, 297, 301
backstepping event 2, 7, 31, 39, 50, 62, 65, 68, 72, 124, **186**, **278**, 384
bacteria 3, 31, 53, 165, 166, 184, 202, 204, 205, 206, 207, 355
chemosynthetic bacteria, 3, 202, 207
ball-and-pillow structure 335, **336**
Bandangnan 342, **346**, 363
rainbow serpent 342, **346**
Bangaldji 350
banks 1, 8, 9, 17, 22, 24, 26, 27, **29**, **30**, 46, 48, 50, **51**, 62, 68, 80, 81, 115, 119, 122, 124, 163, **166**, **167**, 287
bar deposits 164
Baralamma Spring 342, 367, **372**, **373**
barite 3, 7, 184, **187**, 189, 194, **194**, 199, 202–207, **203**
Barker Gorge 62, 64, 377, **377**
Barnett Spring 381
Barramundi Range 8, 62, 139, **140**, **141**, 142, **144**, 175
Barrar Member 63, 64, **246**, 304, 311, **312**
basin 1, 2, 3, 4, **4**–**6**, 7, 8, 9, **10**, **14**, 17, **18**, 23, 27, 31, 39, 46, 49, 50, 51, **51**, 53, 54, 56, 57, **60**, **61**, 61, 62, 64, 65, **67**, 68, 72, 75, 80, 81, **87**, **89**, 105, 106, 115, **118**, 122, 124, 125, 127, 134, 138, 139, 142, 143, 147, 149, 164, 165, 175, 176, 180, 184, 189, 199, 202, 204, 206, 207, 209, 212, **212**, 213, **217**, 250, **252**, **254**, 257, 258, 267, 277, 283, 286, 288, 297, 304, **310**, 379, 384
Bathtub Spring 334
Beloceras 39, **42**, 267
BHP–Shell 24, 180
Billy Munro Gorge 48, 80, 166, 215, **231**, **232**, 378, 381
bioherm, 7, **40**, 43, 63, **66**, 81, 88, 97, 164, **182**, 184, 250, 258, **264**, 267, 287, 311, 313–321, **314**– **320**, **322**–**328**, 335, **354**, 367, **373**, 376, 377, 379, **380**, 381
bioturbation 129, 146, 149, 165, 311, 381
bivalves 23, 31, **34**, **35**, 39, 46, **46**, **47**, 64, 286, 303, 335, 384
black-soil plains 9, **13**
Blendevale 180
Blina 149, 207
Blood Yard 177, 297, 300
Boab Creek 56, 62, 64, 142
Bonaparte Basin 8, **10**, 176
brachiopods 23, 26, 31, 39, 50, 51, **51**, 56, 61, 62, 63, 64, 97, **99**, 115, 129, 165, 250, 257, 267, 287, 288, 311, 350, 355, 363, 384
Brooking Gorge 9, 12, 215, **235**
Brooking Springs 31, 39, **42**, **107**, 112, **113**, **114**, **157**, 177, 180, 301–303, **303**
bryozoans 49, 51, 62, 64, 81, 115, **118**, 288, **293**
Bugle Gap 4, 7, 9, 50, 53, 56, 57, **60**, 61, **61**, 69, 212, 213, 214, 250–286, **251**, **268**, 314, 321, 384
Bugle Gap Limestone 23, 49, 57–61, 62, 64, 213, **218**, 286
Bulyurngari 304
Bureau of Mineral Resources 4, 257, 274

Cadjebut 3, 24, 180, 184, **203**, 204, 206
Cadjebut Fault **87**, 105, **108**, 112, 177, 180, 209, **209**, 268
Cadjebut Formation 23, 24–26, **24**, **25**, **26**, 31, 68, 143, 202, 204
calcrete 9, **13**
Caltex 3
Camel Spring 280, 281

Canada 65, 207, 384
Canning Basin 1, 2, 3, 4, **4–6**, 8, 9, **10**, **14**, 39, 65, **67**, 68, 75, 80, 81, 105, **118**, 124, 125, 175, 176, 199, 206, 207, 209, 212, 213, 217, 258
Carboniferous 1, 2, 3, 8, 9, **19**, 81, 115, 118, 122, 175, 176, 177, 178, 180, 184, 204, 206, 207, 209, 212, 213, 214, 241, 242, 258, 268, 382, 384
Carolyn Formation 8, 61, 212, 213, **218**, **221**, 283
Carpenters Gap **121**, 337, **338**
Casey Falls 57, 258, 274–277, **275**, **276**, 321
cave
  Illawarra 281
  Kimberley Rover 215, **219**, **220**, 281
  Mimbi 12, 214, **225–228**, **230**, 277–281, **281**, 283
  Monday 281
  Nardji **82**, 124, 277, 281
  Uranus **229**, 281
  Victory 281
  Whalemouth 281
cave system 3, 212, 214, 215, **219**, **220**, **240**, 277, 280, 281, 342
cavity filling **36–38**, 43, **44**, **45**, 57, **58–60**, 88, 97, 98, **99**, **101**, **107**, **114**, 119, 205, **262**, 294, **295**, **300**, 304, **309**, **317**, **318**, 321, **360**, **361**, 378
cavity peloids **35– 38**, 43, **45**, **99**, 106, 112, **114**, 119, **358–361**
cementation 2, 7, 9, 17, 22, 23, 27, 31, 39, 43, 57, 81, 88, **95**, **97**, 105, 106, **106**, 112, **113**, 115, 119, **120**, **121**, 122, **122**, 124, **136**, 177, 184, **201**, **203**, 204, 205, 242, **276**, 281, 283, 286, 294, 303, 304, **310**, 311, 321, 337, 342, 355, 363, 367, **368**, **372**, 382
Chedda Cliffs 48, 75, **76**, 207, 377, 378, **379**
chemosynthetic bacteria 3, 202, 207
Classic Face 4, 27, **28**, **33**, **35**, **37**, 68, 72, **73**, **74**, **84**, 350–355, **351**, **352–354**, **356**, **357**, **358**, **359**, **360**, **361**
climate
  greenhouse 175
  icehouse 175
collapse breccia 24, 212, **233**, 241, **241**
concretion 51, 53, **53**, **54**, 62, 189, **189**, 199, **200**, **201**, 202, 207, 257, 373
condensed sequence 49, 75, 119, 313
conglomerate 1, 2, 7, 8, 9, 12, **13**, 22, 23, 26, 27, 51, 56, 62, 64, 69, 122, 125–149, **125–127**, **148**, 150, 163, 164, 165, 176, 177, 189, 199, 212, 242, **243**, 294, **295**, **296**, 297, 300, 301, 334, 337, **340**, 342, **349**, 367, 373, 377, 379, 381, 382, 384
    provenance 142, 146, 147–149, 165
conglomerate units
  Barramundi Conglomerate 49, 62, 125, 139–142, **140**, **141**, 143, **144**, **145**, 146, 147, 176, 178
  Behn Conglomerate 125, 143–146, 149, 176, 178, 337
  Big Spring Formation 125, 143
  Bobs Bore Conglomerate 125, 127, **133**, 134, 146, 147, **148**, 176, 286
  Elma Conglomerate 49, 69, 125, 134–139, **135–138**, 142, 143, 146, 149, 150, 176, 294, **294**, **296**, 297, 300
  Mueller Conglomerate 125, 139, **139**, 176
  Sparke Conglomerate 12, **14**, 51, 56, 69, **123**, 125, 127–129, **128**, **129**, **133**, 143, 146, 147, **148**, 149, **163**, 164, 165, 167, 176, 178, 286, 297, 301
  Stony Creek Conglomerate 62, 125, 142, 143, **145**, 147, 149, 176, 178, 297, **298**, **299**
    Van Emmerick Conglomerate 12, 125, 143, 146, 147, **147**, 149, 176, 178, **231**, 379, 380, 381
  highstand 64, 149, 176
  reciprocal lowstand 64, 149, 176
conglomerate ranges 9–12, **14**
conodonts 1, 2, 7, **20**, **21**, 23, 31, 39, 46, 49, 51, 54, 56, 57, 61, 62, 64, 65, 68, 75, **78**, 115, 119, 124, 129, 189, 207, 277, 288, 297, 311, 313, 314, 321, 334, 350, 363, 376
coordinates
  Australian Map Grid (AMG) 8
Copley Valley Embayment **34**, **35**, 303, 304
corals 1, 17, 22, 23, 24, 26, 27, 31, **34**, 39, 50, 51, 61, 63, 64, **66**, 115, 129, 139, 150, 163, 167, 250, **253**, 257, 267, **272**, **273**, 274, **274**, **276**, 277, 286, 287, 288, 304, **309**, 311, 321, **327**, **328**
crepida Zone 2, 64, 75, **78**, 267, 274, 314, 373, 376
crinoids 31, 39, 56, 57, 61, 64, 115, 257, 267, **272**, **273**, 274, **274**, **276**, 277, 283, 288, 321, **328**, 335
crocodiles 12, **15**, 242, **243**, **331**, 342
cut-and-fill structures 134, 381
cyanobacteria 31, 39, 75, **89**, 165, 166, 267, **272**, **273**, 355
cycle 22, 24, 27, **34**, 48, 65, **66**, 72, **74**, 75, 80, 129, 134, 138, **145**, 147, 149–176, **150**, **162**, **163**, **173**, **256**, 257, **276**, 286, 288, 297, 300, **302**, 329, **336**, 355, 362, **363**
cycles
  cycle duration 165, 167–175, 286
  infill cycles 27, 138
  megacycle stacking 166, 167
  Milankovich 27, 149, 175
  Nullara Sequence 48, 65, **66**, 80, 150, 165, 166,
  Pillara Sequence 27, **34**, 65, **66**, 72, **74**, 138, 150–165, **150**, **162**, **173**, 257, 286, 300, **336**, **362**, **363**
  shallowing-upward cycles 24, 27, 129, 134, 138, 150, 163, 175, 286, 329
  subaqueous cycles 150–163, **150**, **166**
  subaqueous to subaerial cycles 129, 150, **150**, 163–165, 166, 175
  tectonic control 27, 65, 138, **162**, 165, 175, 362
cyclicity 1, 7, 22, 23, 48, **87**, **129**, 149–176, **166**, **167**, **276**, 277, 286, 300, **302**, 329, 354, 355, 362, **362**, **363**, 379, 384
Cyclone Rock 377, **378**

debris flow 1, 51, 56, 62, 69, 81, 88, **89**, **90**, 97, 106, 199, 257, 258, 286, 297, **310**, 311, 337, 363, 373
debris-flow deposit 1, 7, 50, 56, 62, 63, 64, 81, **87**, 88, **90–93**, **121**, 189, 199, 204, 206, 257, 258, 311, **312**, 335, **336**, 337, **339**, **340**
dedolomite **29**, 62, 304, **309**
Deeadeea Cliff, 213, **218**, **221**, **225**, 283–286
Deeadeea Sandstone Member 213, **218**, **221**, 283, 286
depositional dip 1, 4, 7, 23, **32**, **41**, 50, 57, **60**, 61, 62, 63, 64, 88–98, **101–104**, 112, 124, 143, 178, 250, 257, 258, 267, 274, 277, 283, 287, 288, 313, **328**, 350, 363, 377
depositional slope 23, 62, 98, 149, **253**, **276**, 321, 373, 377
Devonian Great Barrier Reef 1, 3, **10**, 12, 384
diamond 9, 334
Dingo Gap **45**, 63, **66**, **91**, **92**, **93**, **96**, 112, **112**, 242, **242**, 245, **245–248**, 249, **249**, 304–313, **311**, **312**, **313**
Disphyllum **34**, 39, 250, **253**, 257, 287
dissolution 3, 24, 31, 50, 122, 124, 184, 205, 209, 214, 215, **231**, 384
Djamburrwurru 342
dolomite 1, 24, **24**, **25**, 26, 27, **29**, 31, 62, 68, 122, 124, 143, 204, 257, 294, 304, **309**, 313, **317**, **319**, 335, **348**, **349**, 350, 355, 362, 363, **366**, **367**, 382
  dolomitic 24, 62, **319**, 350, 354, 355, 363, 381
double geopetal 97, **100**, **101**, 304
Dreamtime 243, **244**, 280, 281, 283, 337, 342, 346, 350, 362, **364**, 367

earthquake 2, 81, 105, 106, 175, 176, 267, **271**, **272**, 280, 355, 362
East Pillara Range 189, **189**, **190**, **192**, **193**, **198**, 199
Elimberrie bioherms
  Elimberrie no. 1 313–321, **315–320**, 335, 376
  Elimberrie no. 2 **40**, 321, **322–327**
  Elimberrie no. 3 321, **327**, **328**
  Elimberrie no. 4 321
Elimberrie Spring 313
Ellendale Vents 9, **333**, 334
Elliott Ridge 68, **69**, **278**
Emanuel Range 3, 8, 24, **24**, **25**, 26, **26**, **29**, **30**, 31, 39, 49, 50, **51**, **52**, 53, 61, 68, **87**, **99**, 105, **108**, 112, 139, 143, 177, 189, 214, 215, **233**, 250, **252**, 257, **282**, 287
endolithic 12

epilithic 12, 97, 303, **306**, **308**, 354, **356**
erratics 283
eustacy 65, 150, 175
  eustatic 64, 65, **162**, 175, 362, 378
evaporite 24, **25**, 26, 48, 68, 164, 184, 202, 204
  evaporitic 24, 68, 164, 206, 288
  pseudomorphs 24, 48, 164
exhalative deposit 3, **178**, 184, **186**–**188**, 189, **195**, **196**, **198**, 204, 205, 206, 207, 314
expansa Zone 61, 62, 64, 80, 125
extensional tectonics 2, 8, 112, 165, 176, 178, 206
extinction 2,7, 31, 39, **43**, 64, 65, 75, 80, **80**, 81, 115, **118**, 178, 250, 267, 314, 329, **332**, 381, 384

facies
  basin facies 1, 9, 17, 18, 23, 39, 49–64, **60**, **61**, 72, 75, 115, 125, 127, 180, 184, 189, 212, 250, **252**, 257, 258, 286, 304, 384
  marginal-slope facies 1, 17, 23, 27, 43, 49–64, **58**–**60**, 75, **77**, **85**, **86**, **110**, 115, 134, 143, 149, 189, 207, 250, 257, 288, 294, 297, 304, 337, **339**, 350, 354
    fore-reef subfacies 1, 17, 23, 43, 49, **50**, **52**, 57, 61, 62, **83**, **87**, **91**, **94**–**96**, 106, 115, 119, **210**, 250, 257, 258, 277, 304, **312**, **313**, **351**, 354
    reefal-slope subfacies 1, 17, 23, 31, 39, **41**, 43, 49, **58**, 62, **83**, 106, 115, 119, 138, 207, 250, 257, **264**, 287, 304, 342, **351**, 354, **357**, 362, 377, 378, 382
  platform facies 1, 4, 9, 17, 23, 27, **29**, **41**, 48, 50, **66**, 68, 75, **85**, 115, 129, 138, 143, 149, 150, **166**, 207, **208**, **210**, 257, 288, 304, 314, 337, **339**, **341**, 354, 362, 367, 381
    back-reef subfacies 1, 2, 9, 17, 22, 23, 27, **30**, **33**, **34**, 39, **41**, 43, 48, 62, **76**, **87**, 106, 119, 122, 134, **138**, **166**, **167**, 257, 277, 287, 294, 304, 337, **341**, **351**, **352**, 354, 355, **357**, **363**, 367, 378, 382
    reef-margin subfacies 1, 2, 17, 23, 26, 27, **28**, 31, 39, **41**, 43, **76**, **82**, **83**, 106, 115, 119, 122, **224**, 249, 258, 277, 294, **295**, 304, 329, **341**, **351**, 354, 355, **357**, 377, 378, **378**
    reef-flat subfacies 257, 277, 304, 362, 384
    pinnacle-reef subfacies 1, 17
Fairfield Group 382
Famennian 1, 2, 3, 7, 8, **10**, **11**, 17, 22, 23, 26, 27, 31, 39, **41**, 43, **43**, 46, **46**, 48, 49, **56**, 57, **57**, 61, 63, 64, 65, **66**, 68, 72, 75, **76**–**78**, 80, **80**, 81, **101**, 106, **109**, **110**, 115, **117**, **118**, 119, 124, 125, 129, 134, 138, 139, 142, 143, 146, 149, 150, 165, 166, 167, 175, 177, 178, **179**, 180, **182**, **183**, 184, 207, **208**, 209, 212, 213, **234**, 245, 249, 258, 267, **269**, **271**, 274, **275**, **276**, **284**, **285**, 286, 288, **289**, 294, **294**, **295**, 297, 311, **311**, 313, 314, 321, 329, **331**, **332**, 335, 342, 350, **352**–**354**, 363, **366**, **369**, **370**, 373, 376, 377, 378, 379, **379**, 381, 382, **382**, 384
fan-delta 2, 125, **126**, 129, **133**, 134, **136**, 138, 142, 143, 146, 147, 149, **295**, 297, 381, 382
fault 1, 2, 3, 8, 24, 26, 49, 53, 81, **87**, 105, 112, 122, 125, 127, **127**, 129, **129**, 138, **141**, 142, 143, 149, 164, 175, 176–178, **178**, 180, **180**, 189, 199, 206, 215, 268, 286, 297, **298**, 300, 301, 303, 321, 334, 379, 384
  Barramundi Fault 139, 143, 176, 177
  Black Hills Fault 176, 301, **302**, 384
  Cadjebut Fault **87**, 105, **108**, 112, 177, 180, 209, **209**, 268
  Glidden Fault 147, 286
  Granite Range Fault 176
  Mount Behn Fault 143, 176, 342
  Mount Elma Fault 49, 80, 134, 139, 149, 165, 176, 177, 178, **179**, 297, 300
  Painted Rocks Fault 165, 177, 297, 300
  Pinnacle Fault 2, 8, 176, 177, 180, 268
  Sparke Range Fault **14**, 167, 176, 177, 286, 384
  Stony Creek Fault 142, 143, **145**, 176, 297, **298**
  Van Emmerick Fault 146, 176, 379
  Virgin Hills Fault 129, 176, 177, **179**, **182**, **183**, 286, 384
  Mount Winifred Fault 139, **139**, 177, 178
  listric fault 143, 176
  normal fault 1, 2, 8, 49, 146, 176, 177, 178, 199, 286, 297
  thrust fault 146, 164, 176, 177, 178, **183**
  transcurrent fault 3, 177, 178
  transfer fault 2, 176
  wrench fault 2, 3, 8, 177
faulting 2, 3, 7, 8, 69, 81, 105, 106, 122, 138, 175, 176–178, **183**, 199, 212, 258, 268, 286, 297, 301, **302**, 384
fault scarp 1, 2, 49, 125, **127**, 149, 178, 297, 379
fauna 7, 12, 51, 53, 54, 57, 61, 62, 75, 81, 115, 146, 199, 205, 206, 250, 288, 303, 342, 384
fenestral limestone 22, 27, 48, **76**, 122, **123**, 129, 163, 164, 165, 166, 175, 245, 249, 288, 294, 300, **302**, 303, 304, 329, 355, **362**, 367, 377, 378, 379, **380**, 382, 384
fish 303
fissure 112, 205, 303
fissuring 112, 303
Fitzroy Trough 2, 3, 8, 31, 176, 177, 180, 184, 206, 209, 213
Fitzroy Volcanics 9
flora 12
folding 1, 7, 8, **25**, 68, 88, **92**, 139, 177, 178, **179**, 212, 258, **271**, 286, 288, **291**, 297, 301, 311, **312**, **313**, 321, 335, 337, 373, 376
fore-bank 1, 23, 48, 50, **52**, 62, 80
fore reef 1, 4, 17, 23, 27, **32**, 43, 48, 49, 50, **52**, 57, 61, 62, **66**, 68, **73**, **78**, **83**–**85**, **87**, 88, **90**–**96**, **100**, **101**, 106, **110**, 115, 119, **121**, 124, **133**, 199, **210**, 242, 250, **252**, **253**, 257, 258, **269**, **270**, 274, 277, 287, 288, 297, **300**, 304, **310**, 311, **312**, **313**, 314, **320**, 334, 335, 337, **338**–**340**, 342, **348**, **349**, 350, **351**–**353**, 354, **354**, 355, 363, **369**, **374**–**376**, 378
Fossil Downs 12, **46**, **47**, 61, 62, **158**
fossil-rootlet horizons 164, 355
Frasnian 1, 2, 3, 4, 7, 8, 17, 22, 23, 26, 27, **28**, 31, **34**, **35**, 39, **41**, **42**, 43, **43**, 46, 49, 51, **52**, 54, 56, 57, 63, 64, 65, **66**, 68, **70**, 72, 75, **76**–**78**, 80, 81, **100**, 105, 106, **112**, 115, **116**, **118**, 119, **121**, 122, **123**, 124, 125, 127, 129, 134, **137**, 138, **138**, 139, 142, 143, 146, 149, 150, **150**, 164, 165, 167, 175, 176, 177, 178, **182**, **187**, 189, 202, 207, 209, 234, 258, 267, **271**, 277, **278**, **279**, 286, 288, 294, **294**–**296**, 297, 300, 301, 304, 311, 313, 314, 321, 329, **331**, 350, **352**, **353**, 354, **354**, 363, **365**, **366**, 367, **367**, 373, **374**, 376, 377, 378, 379, **379**, 381, 382, **382**, 384
Frasnian–Famennian 2, 7, 26, 31, 39, 49, 57, 63, 64, 65, **66**, 68, 75, **76**–**78**, 80, 115, 124, 138, 175, 207, **234**, 267, 288, 294, 297, 311, 313, 314, **331**, 350, **353**, **354**, 363, **366**, 378, **379**, 382, 384
  Frasnian–Famennian Boundary Event 57, 65, 68, 72–75
  Frasnian–Famennian regression 125
  Frasnian–Famennian unconformity 2, 7, 26, **41**, 68, **76**, 207–209, **295**, 329, 378, 382
  Frasnian–Famennian mass extinction 39, 64, 65, 75, 115, 314, 384
Frutexites 75, **78**, **110**, 267, **272**, **273**, 297

Galeru Gorge 12, **45**, **96**, 129, 215, 280, 283
Galeru Member **123**, 127, **128**, 129, **129**, **130**, 143, 147, 150, **163**, 164, 177, 286, 297
Gap Creek Formation 24, **26**
gastropod 31, 39, 49, 51, 56, 64, 303, **303**, 355, 373, 378, 379
Geikie Gorge 3, 9, 12, 23, 27, **29**, **30**, **32**, 62, 64, **100**, 112, **122**, 215, **234**, 303, 304, **305**–**310**
Geikie Range 303
geomorphology 9–12, 139, 242
geopetal 7, 88–98, **98**–**103**, **184**, **248**, 250, 257, 258, **265**, 267, 287, 294, 300, 304, 321, **328**, 363, 382
geothermal history 124, 214
Givetian 1, 2, 4, 7, 8, 17, 22, 23, 24, 26, **26**, 27, 31, 39, 43, 49, 51, **52**, 54, 64, 65, **66**, 68, 75, 115, 124, 125, 129, 139, **150**, 175, 177, **210**, 286, 384
glaciation 3, 8, 75, 80, 81, 175, 212, 213, 214, **221**, **233**, 283, 286, 304, 334, 377
Glenister Knolls **11**, 53, 215, **238**, **239**, 257, 258, **259**, **263**
glide plane 127, 143, 164, 178, 297

global sea level 2, 65, 175
Gogo concretion 51, 53, **53**, **54**, 189, **189**, 199, **200**, **201**, 202, 257
Gogo Formation 23, 31, 39, 49, 50, 51–54, **51**, **53**, **54**, 56, 62, 69, **87**, 127, 134, 184, **186**, 189, **189**, **193**, 199, **200**, **201**, 202, 204, 205, 206, 207, 250, **252**, **256**, 257, 258, 267, 286
Gogo nodule 51, 53, **53**, **54**, 189, 202
Gogo Station 51, 54
Goongewa 3, 180, 204, 206, 209, **209**, 213, **217**, **222**–**224**
gossan 178, 184, 189, **195**, **196**, **198**, 199, 204, 205, 207, 213, **320**, 321
Grant Group 8, **19**, 48, 61, 177, 207, **209**, 212, 213, 215, **218**, **219**, **220**, **234**, **236**–**239**, 241, 242, 257, 258, **263**, 283, 286, 297, **331**, 334, 384
GSWA 1, 4, 7, 65, 207, 213, 274
Guppy Hills 138, 139, 150, **154**, 163, **167**, 177, 300
Gutha's Place **225**, 281, **283**

half atoll 177, 297
halite 24, **25**, 68
Halls Creek Orogen 8, 147, 175, 286
Hardman, E T 3, 54, **55**, 178, 303, **305**, 337, **343**
Hawkstone Creek **10**, 146, 207, 377, 379, **380**, 381–384
Henwood Spring **28**, 57, **58**–**60**, 138, 288–294, **294**, **295**
hermanni Zone 26, 39, 51, 54
highstand 2, 64, 149, 176
Hooper Complex 143
Horse Spring 75, **78**, 297, **300**
Horse Spring Range 50, 56, **78**, **156**, 176, 177, 288, 297, 300
Horseshoe Range 2, 8, 46, 48, 49, **49**, 62, 80, 165, 166, **168**, 175, 176, 177, 178, **179**, 297–300
Hull Range **33**, 150, **166**, 177, 288
hydrochloric acid 12, 97, 287, 354, 355, **356**
hydrothermal 3, 24, 180, 184, 206, 209, **209**, **210**

ice cap 75, 115, 175, 213, 214, **224**, 267, 286
ice sheet 3, 8, 9, 80, 122, 212, 213, 214, 215, **216**, 242, 257, 258, 277, 281, 286, 303, 304, 337, 381
Illawarra Speleological Society 214, 280, 281
inclusions 124, 143, 199, 204, 205
intertidal 1, 8, 22, 48, 163, 164, 165, 166, 175, 362
iridium anomaly 75, **78**, 267
iron sulfides 3, 7, **187**, 189, **195**, **197**, **198**, 204, 205, 207, 209, 288
islands 1, 8, 62, 177, 321
isotope 184, 199, **201**, 202, **203**, 204, 205, 384
isotope techniques, 184

Jandamarra 342, 367
jerky subsidence 175, 362
Junction Dam 127, 129, 164, 178, **183**, 286

Kalmanyi Member 63, 304, 311
Kalyarr 376
Kapok 3, 180
karst 8, 9, 63, **71**, 80, 115, 180, 206, 207, 209, **210**, 212, 214, 215, **230**, **236**, 241, 242, 243, **243**, 245, 249, 281, 294, **295**, **308**, 311, 329, **333**, 342, 367, **369**, 377, 378
karst corridor 3, 8, 9, 12, **15**, 97, 98, **101**–**103**, 212, 214, 215, **219**, **220**, **230**, 241, 242, 258, **272**, 280, 281
karstification 3, 8, 9, 39, 46, 68, 75, 80, **80**, 209, 212, 214, **218**–**220**, **230**, 329, 342, 354, 377, 378, 382
Kellys Pass **13**, **57**, 68, **70**, **71**, 274, **275**
Kellys Pass Event 68, 69, **70**, **72**, 274, 277, **278**, 301
Kelwasser Events 2, 75
Kimberley Basin 8, 127, 134, 139, 147, 149, 164, 165, 283, 286
Kimberley block 1, 8, 9, 27, 213
Kimberley Plateau 139, 149
King Leopold Orogen 8, 127, 139, 142, 147, 164, 165, 175, 283, **370**
klippen 177, 178
Kunian Gap 215, **233**

Laidlaw Range **11**, **40**, 68, 69, **85**, 215, **219**, **236**, **238**, 250, **252**, 257, 258, **259**, **260**, **263**, **264**
lamproite 9, 124, **331**, **333**, 334
Langurrngurru **14**, 337, **341**, **344**
Larrawa Station 146, **173**
Lawford Range 31, **57**, 68, 69, **72**, **82**, **95**, 97, 105, 124, 127, 165, 167, 214, 215, **225**, **230**, **235**, 258, **266**, 268, 274, 277, 280, **283**, 286
Lawford Spring **16**, 127, 129, **133**, **159**, 286
lemurata–magnificus palynomorph Zone 39
Lennard Shelf 1, 2, 3, 8, **19**–**21**, 26, 31, 48, 49, 50, 56, 62, 64, 65, 80, 124, 125, 127, **135**, 149, 150, 175, 176, 177, 180, 184, **185**, **186**, **188**, 204, 206, 207, 209, 212, 213, 214, 215, 243, 245, 283, 288, 294, 334, 337, 354, 355, 362, 376, 378, 384
Leopold Downs 124, 143, 334
Leopold Downs Embayment 23, 62
Lillybooroora Conglomerate 384
Limestone Billy Hills 2, 39, **42**, **54**, 176, 177, **178**, 180, 199, 277, 288
limestone ranges 1, 3, 8, 9, 12, **17**, 23, 213, 242, 243, 250, 335
Limestone Spring 41, **172**, 381–384
Linesmans Creek 32
lithiotid 23, 46, **47**, 49, 64, 335, 384
Lloyd Hill **11**, 53, 207, 215, **237**, **238**, **252**, 257, **259**–**263**, 287
Longs Well **50**, **53**, 189–199, **191**, **193**, **194**, **195**, **196**, **197**, 202
Looma 283
Lowry Pool 280
lowstand 64, 149, 176
lycopod 146, 381

magnetostratigraphy 384
Malambeea **161**, **175**, 337, 342, 355
Manda-yarr-yarr-wungani 362, 363, **364**
Mangalamma 342
Manticoceras 39, 267, 350
Manticoceras Zone 51
Margaret Embayment 62, 64, 134, 139, 142, 163, 176
marginal slope 1, 2, 4, 7, 17, 23, 31, **37**, **38**, 39, 43, 49, 50, 53, 56, **56**, 62, 64, 65, 68, 70, 75, 77, 80, 81–88, **83**, **86**, **89**, **90**, **92**, 97, **101**, **103**, **104**, 106, 112, 115, **121**, 122, 124, 125, 127, 142, 143, 146, 149, 177, 178, **179**, 199, 206, 209, **210**, **234**, **241**, 245, 250, **254**, 257, 258, 267, 276, 283, 286, 287, 288, 297, 304, **307**, **308**, 311, 321, **333**, 335, **336**, 337, **339**, **340**, **348**, 350, 355, **357**, 363, 367, **368**, **371**, 373, 376, 377, 379, 381, 384
marginifera Zone 61, 64, 321
marine cementation 2, 17, 27, 39, 57, 81, 88, 106, 115, 119, **120**, 122, 124, 177, 184, **201**, 205, 286, 294, 303, 304, 311, 321, 337, 355
Marli 337, 342, **345**
mass extinction 2, 7, 31, 39, **43**, 64, 75, 115, 314, 384
McIntyre Knolls **37**, **38**, 56, **114**, 127, 258, **265**, **266**
McSherrys Gap 27, 39, **92**, **94**, 150, **160**, 167, 335, **335**, **336**
McWhae Ridge 12, 39, 75, **78**, 97, 98, **101**–**105**, **110**, 177, **181**, **182**, **225**, 258–268, **269**–**271**, 277
megabreccia 23, 50, 56, 62, 63, 64, **78**, 88, **91**–**93**, **300**, **304**, 335, **336**, 350
megacycle **137**, 166, 167, **173**, 175, 362, **363**
Menyous Gap 26, **34**, 51, **83**, **85**, **86**, **151**, 163, 167, 215, **231**, 286, 287, 288
metamorphism 4, 7, 134, 143, 146, **183**, 334, **349**
metazoan 2, 17, 22, 23, 31, 39, 64, 115
microbes 1, 2, 4, 7, 12, 17, 22, 23, 27, 31, 39, **40**, 43, 46, 56, 64, 75, 97, 106, 115, 119, 199, 250, **254**, 258, 267, 303, 304, **306**, **308**, 313, 314, 321, **325**, **326**, 329, 350, 355, 373, 376, 377
microbial 1, 7, 12, 22, 23, 27, 39, **40**, 43, **44**, 48, 49, 50, 63, **66**, **78**, 81, **87**, 97, 112, **114**, 115, 119, **120**, **122**, 134, 142, 163, 175, **182**, 204, 205, 209, 245, **247**, **248**, 249, **249**, 250, **253**, 257, 258, **264**, 267, **272**–**274**, 277, **280**, 287, 288, 297, 300, 303, 304, **307**, **310**, 311, 313, 314, **317**, **320**, **321**, **326**, **327**, **332**, 335, 342, 350, 354, 355, **357**, 362, 363, 367, **368**, **369**, **371**, **372**, 373, **374**, 377, 378, 379, **380**, 381, 384
microbial peloids 43, 112, 119

micro-inclusions 205
Milankovitch 27, 149, 175
mineralization
  epigenetic 3, 24, 178–184, **187**, **203**, 204, 205, 206, 207, 209
  syngenetic 178, 184–207
  genesis 204–206
Mingun **173**, **175**, 342, 355–362, **362**
Minnie Pool 189, **192**, **195**, **198**, 199, 202, 301, **302**
Mirrngurrwalla **84**, **345**, **352**, **353**, 362, 363, **364**, **365**
Mondooma Thrust 146, 176
Morown Cliff **80**, **109**, 321–329, **332**, **333**, 377
Mount Anderson 283
Mount Behn 143, 146
Mount Elma 56, 134, **135**, **137**, 138, **138**, 149, 150, 300
Mount Lesley 379
Mount Pierre 3, **36**, **55**, 62, 288, **289**
Mount Pierre Station 129
mud cracks 22, 122, **123**, 163, 164, 355
mud mounds 43
Mueller Ranges 134, 139
Mungurrma 337
MVT sulfides 178, 180, 184

Napier Formation 23, 31, **32**, 39, **41**, 43, **45**, 46, 49, 50, 56, **58**, 61, 62, 63, 64, **66**, **73**, 75, **77**, **84**, **86**, **91**–**96**, **100**, 115, **121**, 124, 125, 143, 146, 149, **183**, 207, **234**, **246**, 304, **307**, **308**, **310**–**313**, 314, **333**, 334, 335, 337, **338**–**340**, 342, **348**, **349**, 351, **352**–**354**, **356**, **357**, 362, 363, **365**, **366**, 367, **367**, **369**, **371**, 373, **374**, **375**, 376, **376**, 377, 378, 379, 381, 382
Napier Range 8, 9, **10**, **11**, 12, 23, 27, 31, 39, **41**, 43, 46, 49, 62, **63**, 64, 68, 75, **76**, 81, **86**, **91**, **94**, **108**, **112**, 115, **127**, 143, 146, **162**, 163, **172**, 178, 180, 207, 209, 215, **231**, **232**, **233**, **239**, 241, **244**, 245, 249, 304, 334, 335, **336**, 337, **338**, 342, **347**, **357**, 367, **370**, 373, **373**, **374**, 377, **377**, **378**, 379, **379**, **380**, 381, 382, **382**, **383**
Nara Nara 337, **344**
Narlarla 178, 180, 376, 377, **377**
nautiloid 31, 54, 56, 64, 97, 98, **104**, 115, 257, 267, 274, 277, **280**, 321, **328**, 350, 363, **370**
Needle Eye Rocks 54, 56
neomorphic alteration 189, 205
Neoproterozoic 139, 147, 149
neptunian dyke 2, 7, **44**, 105–115, **107**–**111**, **113**, **114**, 119, **119**, 122, **180**, **182**, **183**, **199**, 267, **272**, **285**, 300, 301, 303, **303**, 304, **308**, **317**, 321, 342, **349**, 355, **361**, 362, 363, 367, **369**, **371**, 377
neptunian fissure 2, 27, **90**, 105, 106, **109**, 112, **112**, 115, 119, **232**, 283, 303, 313, **317**, 363, 367
Ngumban Claystone Member 213, 214, **218**, **221**, **224**, 283, 286
Ngumban Cliff **56**, **110**, 213, **229**, 267, **272**–**274**, 283, **284**, **285**
Nippers Bore 173
North Lawford Range 72, 165, 167, 258, **266**, 286
Nullara Limestone 23, 26, 27, 31, **41**, 43, 46, **46**, **47**, 48, **48**, 49, **49**, 62, 75, **76**, 80, 106, 112, **120**, **123**, 134, **135**, 138, 139, 142, **145**, 146, 149, 150, 165, 166, **168**, **172**, **173**, 175, **179**, 207, **219**, **232**, 249, 288, 294, **294**–**296**, 297, 300, 329, **331**, **332**, **371**, 377, 378, 379, 381, 382, **382**, **383**, 384
Nullara Sequence 1, 2, 7, 57, 65, 72, 75–81, 115, 165, 166, 175, 209, **276**, 321, 329, 342, 352
  Nullara Sequence 1 75, 80, 352
  Nullara Sequence 2 75, 80
Nullara Spring 48

Old Bohemia 50, 53, 56, 57, 61, 69, 127, 258, **265**
Old Napier Downs 64, 243, 379
oncolite 22, 48, 98, **102**, 115, 165, 257, 258, **262**, 267, 268, 329, **332**, 378, 379, **380**, 382
oolite 22, 27, 48, 49, 106, 119, 165, 166, 304, 363, **371**, 378, 379
orbital forcing 149, 175, 176
orebody 180, 184, **209**, 213, 376

Oscar Range 4, 8, 9, 12, **15**, 27, **32**, **41**, 48, **48**, 49, 62, 64, 68, 75, **76**, 80, 81, 106, **109**, **111**, 112, **120**, **127**, 143, 177, 207, 209, 241, **241**, 249, 258, 313, 321–329, **329**–**332**, 334, 377, 378
Outcamp Hill 56, 177

Paddys Valley 31, 53, **236**, 250–257, **252**, **253**
Painted Rocks 134, **136**, 138
paleocurrent 146, 147, **148**, 257, 258, 288, 314, 379, 381
paleokarst 68, **76**, 207–215, 242, 243, 294, 304
paleotemperature 3, 39, 75, 81, 124, 175
palynology 7, 39, 384
palynomorphs 31, 39, 115
patch reef **11**, **34**, **35**, 149, 215, **238**, 250, **252**, **253**, 257, 258, **259**, **263**, 277, **278**, 314
patterned ground 9, **13**
pediment 9
pelagic 23, 54, 115
Permian 2, 3, 8, 9, **11**, **19**, 27, 48, 61, 80, **80**, 115, 122, 127, 142, 177, **179**, 207, **209**, 212, 213, 214, 215, **216**, **217**, **219**, **220**, **231**, **233**, **234**, **235**, **237**–**239**, 241, **241**, 242, 243, **243**, 257, 258, **263**, 267, 268, 277, 281, 283, 286, 297, 303, 304, **308**, 311, 329, 334, 335, 337, 342, 367, **369**, 377, 381, 384
petroleum 3, 7, 115, 124, 207
petroleum exploration wells
  Aquanita 1 149
  Ellendale 1 149
  Janpam 1 149
  Meda 1 bore 124, 149
  May River 1 149
  Mellany 1 149
  Napier 1 149
  Terrace 1 149
phytoplankton 54
Pigeon 342, **345**, 367
Piker Hills 61, 62
Piker Hills Formation 23, **36**, 48, 49, **55**, 56, 61, 62, 64, 80, 142, 149
Pillara 3, 31, **178**, 180, 204, 206, 209, **210**–**212**, 281, 288, **293**
Pillara Inlier 1 34, 147, 177
Pillara Limestone 4, **14**, **15**, 23, 24, 26–39, **28**–**30**, **32**–**38**, **41**, **42**, 46, 48, 50, **52**, 53, 56, 62, 68, 69, **70**, **71**, 72, **72**–**74**, **76**, **82**–**87**, 106, **111**, **112**, **114**, 122, **122**, 124, 127, **128**, 129, 134, **137**, 138, **138**, 139, 142, 143, 146, 149, 150, **150**, **151**, **154**, **156**–**162**, 163, 164, 165, 166, **166**, 167, **167**, **173**, 175, 177, **180**, 209, **209**–**211**, 213, 215, **219**, **222**–**224**, **234**, 250, **252**, 257, 258, **262**, **269**, 274, 277, **278**, 286, **287**, 288, **293**, 294, **294**–**296**, 297, **298**, **299**, 300, 301, **302**, **303**, 304, **307**, **308**, **310**, 321, 329, **331**, **336**, 337, **338**–**340**, 342, **351**–**353**, **356**–**358**, **361**, 362, **362**, **363**, **365**–**367**, **373**, 377, 378, **378**–**380**, 381, 382, **382**, **383**
Pillara Range 3, 8, 26, 39, 51, 53, **54**, 68, **83**, **86**, 143, 177, **178**, 189, **189**, **190**, **192**, **193**, **198**, 199, 215, **231**, 287, 288
Pillara Sequence 1, 2, 7, 31, 65, 68–75, 115, 150–165, 175, 321, 342, 355, 384
  Pillara Sequence 1 26, 31, **42**, 68, **69**, 250, 257, 355
  Pillara Sequence 2 31, 39, **42**, 68, **69**–**71**, 277
  Pillara Sequence 3 31, 39, 68, 69, **70**, **71**, 277
  Pillara Sequence 4 31, 57, 68, 69, 72, 286, 297
  Pillara Sequence 5 31, 53, 57, 68, 72, **73**, **74**, 286, **352**, 354, **358**
  Pillara Sequence 6 31, 39, **41**, **42**, 53, 57, 68, 72, **73**, **74**, 294, **352**, 354, 355, **365**, **367**, **379**
Pillara Spring **178**, 189, 199, **200**, 202
Pinnacle Fault 2, 8, 176, 177, 180, 268
pinnacle reef 1, 8, **11**, 17, 50, 53, 68, **69**, 81, **87**, **88**, 97, 207, 250, **252**, **254**, 257, **259**, 277, 313, 314, **316**, **318**, **319**, 321
platform atoll 8, 17, 134, 257, 277
platform margin
  advancing 2, 65, 72, 81, **86**
  retreating 2, 65, 81, **85**, **86**, 124, 287, **287**, 288
  collapsed **50**, 81, **84**, **90**, **112**, **365**
  fault-controlled 81, **87**, 105

interfingering bank 81
upright-rollover 81, **83**, 287, 304, **306**
upright-scarp 81, 277, 304
pinnacle reef 81
platform-building organisms 17, 31, 39, 115
platform-derived debris 1, 23, 51, 62, 81, 106, 257, 297
platform-margin collapse 7, 50, **50**, 62, 72, 81, 88, **89**, **90**, 105, 106, 115, 258, 294, 297, 313, **352**, 354, 355, 362, 384
platform-margin unconformity 68, 354, 355, **356**, **357**
plough-furrow fold **92**, 311
porosity 2, 27, 31, **32**, 119, **119**, **121**, 122, 124, 204, 242, 304, **309**, 355, 367
postera Zone 62, 80, 142
Precambrian 1, 2, 12, **14**, **19**, 22, 27, 62, 68, 123, 127, **128**, 129, **133**, **136**, 138, 139, **139**, **141**, 142, 143, 146, 147, 164, 176, 178, 183, 199, 213, 242, 286, 297, 321, 329, **329**, **330**, 334, 342, **349**, 367, **370**, 373, 379, **380**
Preema Bioherms 379, **380**, 381
Preema Pass 381
pressure solution 2, 17, **22**, 31, 98, **119**, **121**, 122, 124, 178, 242, 277, **310**, **341**
Prices Creek Group 24, 68, 212
Proterozoic 1, 2, 8, 9, **109**, 139, 147, 149, 176, 212, 300, 321
provenance 142, 146, 147–149, 165
pyrite 189, 199, 204, 205, 207, **320**, 321

radiaxial spar **35**, **36**, **37**, **38**, **44**, 106, **107**, **108**, **111**, 112, **120**, 177, **309**, **371**
rainfall 9, 12, 138, 215
rate of deposition 65, 150, 267
Rattigan Rocks 56, 69, 134, 138, 294–297, **296**
receptaculitid 7, 23, 39, 43, 46, 57, **58**–**60**, 63, 64, **66**, 97, **103**, 115, **184**, 257, 267, 311, 313, 314, **319**, **320**, 321, **327**, 355, 363, 367, **368**, 376, 377, **380**, 381
reciprocal sedimentation 64, 149, 176
recrystallized calcite 43, 189, 199, 202, 205, 207
Red Bluffs 9, 23, 48, 49, **123**, 212, **219**
reef complexes
atoll 1, 8, 11, 17, 81, 134, 177, 207, 215, **238**, **252**, 257, **259**–**261**, **263**, 277, 297, 314
basin facies 1, 9, 17, **18**, 23, 39, 49, 50, 54, 56, 57, **60**, 61, **61**, 62, 68, 72, 75, 115, 125, 127, 180, 184, 189, 212, 250, **252**, 257, 258, 286, 304, 384
fringing reefs 1, 8, 17, 23, 27, 297
marginal-slope facies 1, 17, 23, 27, 43, **58**–**60**, 62, 64, 75, **77**, **85**, **86**, **110**, 115, 134, 143, 149, 189, 207, 250, 257, 288, 294, 297, 304, 337, **339**, 350, 354
fore-reef subfacies 1, 17, 43, 49, **50**, **52**, 57, 61, 62, **83**, 87, **91**, **92**–**96**, 106, 115, 119, 210, 250, 257, 258, 277, 304, **312**, **313**, **351**, **352**, 354
reefal-slope subfacies 1, 17, 23, 31, 39, **41**, 43, 49, **58**, 62, **83**, **84**, 106, 115, 119, 138, 207, 250, 257, **264**, 287, 304, 342, **351**, 354, **357**, 362, 377, 378, 382
platform facies 1, 4, 9, 17, 23, 27, **29**, **41**, 48, 50, **66**, 68, 75, **85**, 115, 129, 138, 143, 149, 150, **166**, 207, **208**, **210**, 257, 288, 304, 314, 337, **339**, **341**, 354, 362, 367, 381
back-reef subfacies 1, 2, 9, 17, 22, 23, 27, **30**, **33**, **34**, 39, **41**, 43, 48, 62, **76**, **87**, 106, 119, 122, 134, **138**, **166**, **167**, 257, 277, 287, 294, 304, 337, **341**, **351**, **352**, 354, 355, **357**, **363**, 367, 378, 382
reef-flat subfacies 257, 277, 304, 362, 384
reef-margin subfacies 1, 2, 17, 23, 26, 27, **28**, 31, 39, **41**, 43, **76**, **82**, **83**, 106, 115, 119, 122, **224**, 249, 258, 277, 294, **295**, 304, 329, **341**, **351**, 354, 355, **357**, 377, 378, **378**
pinnacle-reef subfacies 1, 17
reef flat 257, 277, 304, 362, 384
reefal slope 1, 17, 23, 27, 31, 39, **40**, **41**, 43, **45**, 49, 50, 56, 57, **58**, 62, **63**, 68, **73**, 81, **83**, **84**, 88, **91**, **101**, 106, 112, 115, 119, 138, 149, 207, 250, 257, **264**, 287, **299**, 304, **306**, **309**, 342, **348**, **351**–**353**, 354, 355, **356**, **357**, 362, 363, **365**, **366**, 367, **367**, 377, 378, 382
Reef-Extinction Event 65, 75, 80, **80**, 81, **118**, 377
reef-extinction unconformity 2, 75, 209
Renalcis 2, 4, 22, 27, 31, **35**–**38**, 39, 43, 46, 64, 106, **107**, 115, 119, 165, **180**, **246**, 257, 258, 277, 294, 303, **303**, 304, **306**, **309**, **310**, **318**, 321, 329, 335, 342, 350, 354, 355, **358**–**361**, 363, 367, **371**, 373, 379, 382
retreating platform 2, 65, 81, **85**, **86**, 124, 287, **287**, 288
rhomboidea Zone 64, 288, 314, 373, 376
ripple marks
asymmetrical 288, **292**
symmetrical 288, **292**
rock art 12, 17, 243, **244**, 321, 329, **333**, 337, **338**, **344**, **372**, 377
Ross Hill **11**, **263**

Sadler Limestone 23, 31, 39, 49–51, **50**–**52**, 53, 56, 62, 68, 69, **70**, **72**, **82**, **83**, **85**–**87**, 97, 98, **99**, **101**–**104**, 105, 138, 177, **186**, 189, 199, **201**, 202, 206, 209, **210**, **211**, 250, **252**, 257, 258, 267, 268, **269**, **272**, 274, 277, 286, 287, **287**, 288, 294, 297, **300**
Sadler Ridge 49, 50, 215, **233**, 241
saw-tooth **162**, 362
scheck breccia 88, **94**–**97**, **349**, 373, **376**, 384
scour-and-fill structures 146, **147**, 149
seismic surveys 3, 64, 207, 384
sequence
Nullara Sequence 1, 2, 7, 57, 65, 72, 75–81, 115, 165, 166, 175, 209, **276**, 321, 329, 342, 352
Nullara Sequence 1 75, 80, 352
Nullara Sequence 2 75, 80
Pillara Sequence 1, 2, 7, 31, 65, 68–75, 115, 150–165, 175, 321, 342, 355, 384
Pillara Sequence 1 26, 31, **42**, 68, **69**, 250, 257, 355
Pillara Sequence 2 31, 39, **42**, 68, **69**–**71**, 277
Pillara Sequence 3 31, 39, 68, 69, **70**, **71**, 277
Pillara Sequence 4 31, 57, 68, 69, 72, 286, 297
Pillara Sequence 5 31, 53, 57, 68, 72, **73**, **74**, 286, **352**, 354, **358**
Pillara Sequence 6 31, 39, **41**, **42**, 53, 57, 68, 72, **73**, **74**, 294, **352**, 354, 355, **365**, **367**, **379**
sequence stratigraphy 7, 17, **20**, **21**, 64, 65, 149, 167, 176, 301, 381
Shady Bore 69, **158**, 300, 301, **302**
Shady Bore block 56, 300, 301, **301**
shallowing-upward cycle 24, 27, 129, 134, 138, 150, 163, 175, 286, 329, 362
silicified fossils 50, 51, **51**, 250
Smith Knoll **11**, 257, **259**
solution doline 3, 8, 212, 215, **219**, **220**, **233**, **234**, **237**–**240**, 257, 258, 342
South Lawford Range **57**, 68, 69, **72**, **82**, **95**, 97, 105, 124, 127, 214, 215, **225**, **235**, 258, 274, 277, 280, **283**
Sparke Conglomerate 12, **14**, 51, 56, 69, **123**, 125, 127–129, **128**, **129**, **133**, 143, 146, 147, **148**, 149, **163**, 164, 165, 167, 176–178, 286, 297, 301
Sparke Range 8, 12, **14**, **16**, 122, 127, **128**, 129, **130**, 149, 150, 164, 175, 176, 177
sparry calcite 31, **35**, **37**, **38**, 43, **45**, 57, **58**–**61**, 88, **95**–**97**, **99**, **100**, 106, **107**, **108**, **110**, 112, **113**, **114**, 119, **120**, **121**, 134, **136**, 177, **183**, **196**, **197**, 209, **212**, **229**, 250, **262**, **275**, **281**, **285**, **287**, 288, 294, 303, 304, **318**, 321, **327**, 342, **348**, **358**, **360**, 363, 367, **370**, **372**, 373, 377
Sphaerocodium 22, 39, **40**, 64, **89**, 98, **102**, 115, 250, **254**, 257, 258, **264**, 267, 304, 313, **317**, **318**, 321, **325**, **326**, 350, **354**, 355, **357**, 377, 381
sponge 27, **30**, 31, 39, 43, 46, 56, 57, **58**–**60**, 64, 115, 119, 257, 294, 304, 313, 321, 363
Stachyodes 27, **37**, **38**, 138, 163, 164, 165, 258, 297, 300, **302**, 304, 329, 355, **358**, **359**, **362**, 382
statues 281, **283**
Stony Creek 142, 143, 297, **298**, **299**
Stony Creek Conglomerate 62, 125, 142, 143, **145**, 147, 149, 176, 178, 297, **298**, **299**
Stony Creek Shear Zone 143, 176
strike-slip movement 2, 164, 165, 176, 177

Stringocephalus 26, 39, 68, 139
stromatactis 39, 43, **44**, **45**, 57, **61**, 97, **101**, 112, 119, **119**, 277, 287, 304, 314, 355, **360**, 363
stromatolite 2, 3, 7, 22, 24, 26, 27, **28**, 31, 39, **40**, 46, 48, 53, **56**, 57, **57**, 63, 64, 98, **105**, 106, 115, 184, **187**, 189, **190**–**197**, 199, **200**, **201**, 202, 204, 205, 206, 207, **248**, **249**, 250, **254**, 258, **264**, 267, 274, **275**, **276**, 277, 283, **284**, 286, 297, 311, 313, **313**, 314, **318**, 321, **325**, **326**, **328**, 335, **335**, 355, **360**, 367, 373, **374**, **375**, 376, 381
stromatolite–barite–gossan deposit 3, **187**, 189, 199, 202, 204, 205, 206, 207
  deep-water stromatolite 2, 7, 39, **43**, 64, 75, **94**, 119, 199, **275**, 297
  stromatolitic 24, 68, **77**, **136**, 142, 166, 177, **183**, 184, 189, **194**, **196**–**198**, 199, 202, 204, 205, 206, 249, 258, 267, **269**, **270**, 294, 303, 304, 311, 313, **317**, **318**, 321, **328**, 335, 355, **361**, 373, 381
stromatoporoid 1, 17, 22, 23, 24, 26, 27, **28**, 31, **38**, 39, 43, 46, 49, 50, 51, 64, 68, 75, **87**, **114**, 115, 119, 129, 143, 163, 164, 165, 175, 209, 250, **253**, **254**, 257, 258, 277, 286, 287, 288, **293**, 294, **295**, 297, **299**, 300, **302**, 304, 313, **318**, 329, 342, 354, 355, **357**–**362**, 363, 367, **373**, 378, **379**, 382
structure
  faulting 2, 3, 7, 8, 69, 81, 105, 122, 138, 175, 176–178, **183**, 199, 258, 268, 286, 297, 301, 384
  folding 1, 7, 8, **25**, 68, 88, **92**, 178, 258, **271**, 288, **291**, 301, 311, 335
stylolite 31, **32**, 122, 124, 165, 277, 301, 303, 311, 367, **368**
stylolitization 2, 7, 31, **32**, 122–124, **123**, 129, 164, 165, 277, 300, **302**, 304, 311, 313, **317**, 367, **368**
subaerial cycles 1 29, 150, **150**, 163–165, 166, 175
subaqueous cycles 150–163, **150**, **166**
subglacial channel 3, 212, 214, 215, **231**, **233**–**235**, 242, 286, 303, 337, 381
subglacial karst 8, 9, 115, 212, 214, 241, 242, 311, 377
subglacial meltwater 3, 8, 27, 212, 213, 214, 215, **216**, **230**, 241, 257, 258, 277, 281, 304, 334, 342, 377
submarine cementation 2, 17, 27, 39, 57, 81, 88, 106, 115, 119, **120**, 122, 124, 177, 184, **201**, 205, 286, 294, 303, 304, 311, 321, 337, 355
submarine fan 2, 56, 69, 125, **126**, 134, 142, 143, 146, 147, 149, 297
subsidence 2, 49, 65, 68, 80, 81, 175, 176, 206, 250, 257, 258, 267, 277, 314, 362
sulfate reduction 184, 202, 204, 205, 206
supratidal 1, 22, 24, 48, 164, 165, 166, 175, 362
Surfboard Point, 27, **162**, 164, 167
syncline 177, 178, **179**, **286**, 297, 300, 311

Tangalma 337, **338**, **339**
Tarakalu Member 63, 64, 304, 311
Tchularga 63, 64, 243, 334
Teck Cominco 180
tectonic 2, 7, 27, 65, 68, **70**, 122, 124, 138, 149, 150, **162**, 165, 175, 176, 177, 212, 257, 258, **271**, 274, 287, 301, 321, 335, 362, 363, 378
  compression 122, 165, 177, 378
  cycles 27, 65, 138, **162**, 165, 175, 362
tectonism 1, 7, 65, 106, 122, 147, 150, 175, 176, 206, 207, 212, 267, 301, 362
Teichert Hills 277, **278**–**280**
temperature 3, 9, 39, 75, 81, 124, 175, 180, 184, **196**, 199, 206, 214, **224**, 304, 334
tepee 48, **48**, **49**, 80, 165, 166, 288, **289**–**291**, 300, 329, 377, 378, 381
terrigenous 1, 2, 8, 9, 22, 23, 27, 62, 64, 105, 106, 119, 142, 149, 150, 163, 164, 166, 175, 176, 249, **340**, 342, 355, 362, 373, 376, 379
Thamnopora 34, 287, 288
thermal maturation 180
third-order cycle 176
third-order sequence 2, 31, 64, 65, 68, 75
tidal channel 164
topography 2, 9, 12, **14**, 17, 65, 81, **87**, 105, 124, 129, **135**, 142, 178, 207, 258, 277, 376
Tournaisian 2, 3, 8, 46, 81, 175, 178, 180, 184, 206, 212
trace element 202, 205
trachytera Zone 57, 61, 80
triangularis Zone 2, 57, 64, 311, 321, 350, 376
tube worm 288, **293**
tufa 9, 206
Tunnel Creek 12, 63, **63**, 64, 215, 304, 334, **334**
turbidity currents 51, 56, 373
Turnoff Dam **157**

unconformity 1, 2, 7, 8, 9, **19**, 24, 26, **26**, 31, 39, **41**, **42**, 48, 56, 57, 61, 68, 72, **73**, **74**, 75, **76**, 142, 207, 209, **209**, 212, 213, 214, **219**, **224**, 267, **269**, **270**, 274, **295**, 300, 301, **301**, 329, 342, 354, 355, **356**, **357**, 378, 382
Unggumi Promontory **10**, **231**, **232**, **380**, 381

Van Emmerick Range 8, **10**, 146, 149, 379–381
vegetation 12, 164, 321, 329
Virgin Hills 54, 56, 127, 134, 286
Virgin Hills Formation 23, 31, 39, **45**, 49, 51, 53, 54–57, **55**–**60**, 61, **61**, 62, 64, 69, 72, 75, **78**, 80, **87**, **95**, **96**, 97, 98, 105, **110**, 127, 129, **133**, 134, 138, 142, 143, 149, 164, 165, 177, **179**, **182**, **183**, 199, 258, 267, 268, **269**–**273**, 274, **274**–**276**, 277, 283, **284**, **285**, 286, 288, **289**–**292**, 294, **296**, 297, 300, **300**, 301, **302**, 304
v-shaped valleys 80, **80**, 209, 329

Wade Knoll **11**, 50, 53, **87**, 250–257, **252**, **254**–**257**
Waggon Pass **60**, **61**, 69, **72**, 127, 249
Waggon Pass Event 53, 57, 68, 69–72, 297, 301
Wandjina **14**, 243, **244**, 337, **338**, **341**, **344**, 377
water bore
  600 Bore 142, 297
  Blue Bush Bore 142
  Bobs Bore **133**, 134, 177, **179**, **182**, **183**, 286
  Fly Bore, 142, **145**
  Longhole Bore **46**, 142
  Panorama Bore 143
  Pothole Bore **47**, 62
  Stony Creek Bore 142, 297
water depth 1, 7, 8, 22, 23, 27, 51, 81, 88, 98, **105**, 115, **118**, 164, 267, 288, 301, 314, 321, 362
Weenan 355, 363, **369**
West Australian Petroleum
  WAPET 4, 68, 258, 350
Western Metals 180, 213
Willy Willy Rock 377, **378**
Windjana Gorge 3, 4, 7, 9, **11**, 12, **14**, **15**, 27, **28**, **33**, **35**, **37**, 43, **44**, 46, **58**, 68, 72, **73**, **74**, 75, **77**, **84**, **86**, **89**, **97**, 115, 125, **161**, **162**, 166, 167, **173**, **175**, 207, 215, **233**, **234**, 242, 243, **243**, 337–342, **339**–**341**, **343**–**349**, 350, **350**–**354**, 355, **356**–**366**, 367, **367**–**371**, 372, 373
Windjana Limestone 23, 26, 27, 31, 43–46, **44**, 48, 62, 75, 80, **80**, **86**, 106, 112, 115, 249, 329, **332**, 342, **353**, 363, **368**–**371**, 377, 379, 381, 384
Wombarella Gap 373
Wunala 75, 146, 207, 379, 381, 382, **382**, **383**

Xstrata 180

Yammera Gap 367–373, **374**

zebra limestone 250, 257, **262**, 287
zinc 3, 24, 178, 180, **185**, **186**, 204, 205, 206, 209, **211**, 213, 288, 321, 376
Zn–Pb mineralization 3, 24, 178, **178**, 180, **185**, **186**, 205, 206, 209, **211**, 213, 288, 321, 376
zonation 7, 68, 75, 167, 277

Appendix 1

Upper Devonian conodonts in the Canning Basin

by

Gilbert Klapper[1]

Conodont biostratigraphy

Frasnian

A thirteen-fold Frasnian zonation was proposed for the conodont sequence in the Montagne Noire, southern France (Klapper, 1989). Originally it was thought of as a local zonation applicable to about 15 Frasnian sections in the southeastern part of the Montagne Noire. However, the Montagne Noire zonation has since been widely replicated in other Devonian tropical areas, including for example, western New York State (Kirchgasser, 1994; Kralick, 1994), Sweetland Creek in Iowa (Johnson and Klapper, 1992), the Alberta Rockies and central Alberta subsurface in Canada (McLean and Klapper, 1998), the Timan–Pechora region of the Russian Platform (Klapper et al., 1996), and in the Canning Basin (Klapper, 2007). All numbered zones refer to this zonation.

The Montagne Noire zonation is widely recognizable because it was based originally on successions characterized by the *Palmatolepis* biofacies, a biofacies that occurs in interpreted outer-shelf and basinal sequences throughout most Devonian tropical areas. Species other than those of the nominal genus, such as *Ozarkodina nonaginta* and *Ancyrognathus primus,* however, were used as integral parts of the zonation (Fig. 1.1). These species have been shown to be consistently present in the *Palmatolepis* biofacies.

A number of sections in the Canning Basin replicate substantial parts of the Montagne Noire sequence. A key section in the Virgin Hills Formation at Horse Spring in the Horse Spring Range displays all the Frasnian zones from Zone 6 through Zone 13 and ranges into the Famennian Lower *triangularis* Zone (Klapper, 2007). Horse Spring and sections in the Montagne Noire, as well as sections in the other geographic areas cited above, were used as a basis for the development of a Frasnian composite standard through the technique of graphic correlation (Shaw, 1964; Klapper et al., 1995, 1996; Klapper, 1997). Summary range charts (Figs 1.1, 1.2) show key species in terms of their Canning Basin ranges, rather than the maximum ranges derived from all the sections compiled by graphic correlation.

[1] Department of Earth and Planetary Sciences, Northwestern University; mailing address: 1010 Eastwood Road, Glencoe, Illinois 60022–1125.

The correlation of the Montagne Noire zonation with the widely used Frasnian standard zonation of Ziegler and Sandberg (1990) has been demonstrated through restudy of the Martenberg reference section in the Rhenish Slate Mountains, Germany (Klapper and Becker, 1999), a section which extends from Zone 4 through Zone 13. The Frasnian standard zonation is also based on sections in the *Palmatolepis* biofacies.

In terms of zonally diagnostic species in the Frasnian of the Canning Basin, only a few can be mentioned in this brief summary and only a selection of the most significant species is shown in Figures 1.1 and 1.2. The Sadler Limestone extends from Zone 1 near Outcamp Hill, with the early form of *Ancyrodella rotundiloba* (Fig. 1.1), through Zone 2 at Sadler Ridge with the late form of the same species, through a higher collection from the same locality that is in the range of Zones 2–3 with *A. recta.* The capped-oncolite locality at McWhae Ridge is in Zone 4, with *Palmatolepis transitans, A. rugosa,* and *A. africana.* Comparable but more diverse and abundant faunas of Zone 4 occur in the Gogo Formation at 'Timanites Hill' in Bugle Gap.

The Gogo Formation a short distance west-southwest of McPhee Knoll is in Zone 5 in collections with *Palmatolepis punctata, P. transitans, Polygnathus timanicus* (Fig. 1.3, no. 2), and *Mesotaxis johnsoni* (Fig. 1.3, no. 1). The higher part of this section in the Virgin Hills Formation is in Zone 6, with *Palmatolepis punctata, P. bohemica, Ancyrodella gigas* form 2, and *Ancyrognathus primus.* The Virgin Hills Formation east-southeast of McPhee Knoll is in Zone 6 in the lower part of the section and in Zone 7 with *Ozarkodina nonaginta* stratigraphically higher.

The aforementioned Horse Spring section in the Virgin Hills Formation spans all zones from 6 through 13, with the following biostratigraphically key species listed: Zone 6 with *Palmatolepis punctata* (Fig. 1.3, no. 12)*, P. transitans* (Fig. 1.3, no. 18)*, P. bohemica, Ancyrodella gigas* form 2, *Ancyrognathus primus, Ozarkodina trepta,* and *O. bidentatiformis;* Zone 7 with *O. nonaginta;* Zone 8 with *P. housei* (Fig. 1.3, no. 17), *P. mucronata, Ancyrognathus barba,* and *A. coeni* (Fig. 1.3, no. 7), upper part of Zone 8–Zone 9 with *P. ljaschenkoae;* Zone 10 with *P. plana;* Zone 11 with *P. semichatovae* (Fig. 1.3, no. 9)*, P. anzhelae, P. feisti* (Fig. 1.3, no. 15), and *P. playfordi*

(Fig. 1.3, no. 13); and Zone 12 with *Polygnathus samueli* (Fig. 1.3, no. 6) and *Ancyrodella ioides* (Fig. 1.3, no. 3).

The highest Frasnian zone is Zone 13 and it is well developed at Horse Spring. In the Canning Basin three subdivisions can be recognized, which Girard et al. (2006) have designated as Zones 13a, 13b, and 13c (Fig. 1.2). Zone 13a has *Palmatolepis bogartensis* (Fig. 1.3, no. 10), *P. boogaardi, P. rhenana, P. eureka, P. juntianensis,* and *P. nicolli* (Fig. 1.3, no. 14). Zone 13b at Horse Spring is characterized especially by *Palmatolepis linguiformis* (Fig. 1.3, no. 8), as well as by the highest occurrences of *P. boogaardi, P. rhenana, P. juntianensis, and P. nicolli* (Fig. 1.2). The extinction of all these species at the top of Zone 13b is matched at uppermost Frasnian sections elsewhere in the Devonian tropics.

Zone 13b is succeeded by the uppermost part of Zone 13 (13c), characterized by a low-diversity fauna consisting of *P. bogartensis* to the exclusion of almost all other species of *Palmatolepis* including *P. linguiformis,* and the presence of a few long-ranging Frasnian species of *Ancyrodella* and *Polygnathus.* These all became extinct within Zone 13c, so that the end-Frasnian conodont extinction is stepped in the Canning Basin as it is elsewhere. Species of *Icriodus* are rare in Zones 13b and 13c in the Canning Basin conodont succession, unlike many sections elsewhere.

The same three-fold subdivision of Zone 13 is also recognized at McWhae Ridge, Casey Falls, and Elimberrie No. 1 bioherm in the Canning Basin, and in the Onakawana B core in northern Ontario, Canada (Klapper et al., 2004). The lower boundary of Zone 13b is defined on the lowest occurrence of *Palmatolepis linguiformis*, as is the lower boundary of the *linguiformis* Zone in the Frasnian standard zonation of Ziegler and Sandberg (1990, p. 21). The succession of Zone 13b with *P. linguiformis,* overlain by the relatively impoverished fauna of Zone 13c without *P. linguiformis,* is represented at Kowala in the Holy Cross Mountains, Poland (Racki et al., 2002, appendix A), at Schmidt Quarry in the Rhenish Slate Mountains and Devils Gate in Nevada (Sandberg et al., 1988, tables 1, 3), and at the Upper Coumiac Quarry in the Montagne Noire (Girard et al., 2006). Sandberg et al. (2002, p. 474, fig. 1) recognized two subdivisions of the *linguiformis* Zone that correlate with Zones 13b and 13c.

Frasnian–Famennian boundary

The lowest occurrence of *Palmatolepis subperlobata* (Fig. 1.3, no. 4) at McWhae Ridge, Casey Falls, Elimberrie no. 1 bioherm, two of the sections in Windjana Gorge (the east and west-central sections), and Horse Spring, identifies the Lower *triangularis* Zone (Fig. 1.2). The lower boundary of this zone coincides with the base of the Famennian Stage at the boundary-stratotype section, Upper Coumiac Quarry in the Montagne Noire (House et al., 2000). At McWhae Ridge and Casey Falls, the interval between the uppermost part of Frasnian Zone 13 and the Lower *triangularis* Zone is less than 10 cm, at the east Windjana Gorge section it is no more than 40 cm. *Palmatolepis subperlobata* is unknown below the base of the Lower *triangularis* Zone in Frasnian–Famennian boundary sections elsewhere (Over, 2002), but *P. ultima* (= *P. praetriangularis*, Fig. 1.3, no. 5) crosses this boundary (taxonomy and biostratigraphy reviewed in Klapper et al., 2004). Rare specimens of *P. ultima* occur, for example, in highest Frasnian beds at the Schmidt Quarry (Sandberg et al., 1988, p. 279, table 1) and at the Upper Coumiac Quarry (Klapper et al., 1994, p. 436; also at the nearby Causses et Veyran section, Schülke, 1999, fig. 4, table 2, but the species is identified in both Montagne Noire papers as *P. triangularis* — see synonymy in Klapper et al., 2004). A similar situation occurs at Elimberrie no. 1 bioherm, where two specimens of *P. ultima* are in a fauna of Zone 13c, 2 m below the lowest occurrence of *P. subperlobata.* At the Windjana Gorge east-central section, *P. triangularis* s.s. (a concept that excludes *P. ultima* = *P. praetriangularis*) provides the lowest evidence for identification of the Lower–Middle *triangularis* Zone.

Famennian

Various parts of the Famennian conodont sequence in the Canning Basin have been described by Glenister and Klapper (1966), Druce (1976), Nicoll and Druce (1979), and Metzger (1994). The widely used standard zonation of the Famennian (Ziegler, 1962; Ziegler and Sandberg, 1984, 1990) is applicable to the Canning Basin Famennian succession, from the *triangularis* Zone up through the *marginifera* Zone, because all the faunas are in the *Palmatolepis* biofacies. Above the level of the *marginifera* Zone, however, it is not possible to apply the standard zonation because the Canning Basin succession lacks species of *Palmatolepis* at these higher levels and is instead largely in the *Polygnathus* biofacies. It is well known that the Famennian standard zonation is based entirely on the *Palmatolepis* biofacies up through the upper Famennian *expansa* Zone (Ziegler and Sandberg, 1984), whereas the *Polygnathus* biofacies, which is interpreted as positioned closer to shore, has not been zoned in the Famennian. This is principally due to three factors: inadequate study of the *Polygnathus* biofacies, lack of agreement on the taxonomy of that genus, and marked endemism of some species of *Polygnathus.*

Metzger (1994, fig. 3) revised conodont biostratigraphy of the Famennian part of the Virgin Hills Formation at McWhae Ridge, the WAPET B section of Glenister and Klapper (1966), based on the more detailed sampling by R S Nicoll and G Klapper in 1988. Metzger's (1994, fig. 12) sample 1 is from the *Frutexites* bed, which Nicoll and Playford (1993, table 4) have identified as within the *crepida* Zone (Lower–Middle *crepida* Zone). It should be noted that the *Frutexites* bed at McWhae Ridge, which has an iridium anomaly, is not at the position of the Frasnian–Famennian boundary but is three conodont zones higher as emphasized by Nicoll and Playford (1993). The immediately overlying sample 2 is in the Upper *crepida* Zone and the B section extends as high as the Lower *rhomboidea* Zone (Metzger, 1994, p. 622). The WAPET C section was sampled in 1990 at the levels with ammonoid faunas; Metzger's (1994, p. 622) revision demonstrates that the range of the section is from within the *rhomboidea* Zone to the Lower *marginifera* Zone.

The Famennian part of the Virgin Hills Formation at Casey Falls extends from the Lower *triangularis* Zone

up into the Upper *marginifera* Zone, with the defining subspecies *Palmatolepis marginifera utahensis*. The base of the overlying Bugle Gap Limestone in the nearby Old Bohemia area (Gl/B section of Glenister and Klapper, 1966, p. 837, table 5, Gl/B0) is within the Upper *marginifera* Zone, again on evidence of the defining subspecies. Higher collections of the Bugle Gap Limestone at this section are of low diversity but have *Scaphignathus velifer.* The lowest occurrence of this species defines the base of the Uppermost *marginifera* Zone (Ziegler and Sandberg, 1984, p. 183, fig. 2) but the species ranges as high as the Upper *trachytera* Zone. The defining and characterizing species (Murphy, 1977, p. 214–216) of the Lower and Upper *trachytera* zones (Ziegler and Sandberg, 1984, p. 183) are absent at all sampled Famennian sections in the Canning Basin.

The partial section of the Virgin Hills Formation at WAPET H near Needle Eye Rocks extends from the Upper *marginifera* Zone through collections which have the overlap of *Scaphignathus velifer* and *Palmatolepis marginifera utahensis,* indicating the Uppermost *marginifera* Zone. Highest collections at this section with *S. velifer* and *Polygnathus perplexus* might be taken to indicate the Upper *trachytera* Zone (following range charts in Ziegler and Sandberg, 1984), but *P. perplexus* has a lower range into the Upper *marginifera* Zone according to Johnston and Chatterton (2001, p. 40).

The Famennian part of the Napier Formation at Dingo Gap extends from the Lower *triangularis* Zone as high as the Upper *marginifera* Zone in beds with the defining subspecies, *Palmatolepis marginifera utahensis.* Above this level correlations are highly uncertain in terms of conodont biostratigraphy, because the collections are largely in the *Polygnathus* biofacies, as mentioned above. The highest collections at Dingo Gap with *Polygnathus perplexus,* which has an upper range into the Upper *expansa* Zone (Ziegler and Sandberg, 1984, fig. 3) and *P. collinsoni*, may be as high as the *expansa* Zone. This is uncertain, however, because *P. collinsoni* has not been reported from sections where the standard zonation is recognized. The species has been used as the nominal form for the lower zone of the two local zones in the Gumhole Formation of the Fairfield Group (Nicoll and Druce, 1979), but the *collinsoni* Zone lacks any species diagnostic of the Famennian standard zonation.

A collection with *P. collinsoni* and *P. perplexus* in the Piker Hills Formation faces the same uncertain correlation problem as the highest part of the Dingo Gap section. The Piker Hills samples have not yielded species of *Palmatolepis* nor any short-ranging species of *Bispathodus,* the species used in the standard zonation. Consequently, the abundant ammonoid faunas of the Piker Hills B section must be relied upon for correlation.

Frasnian conodont biofacies

Frasnian conodonts in the basinal parts of the Canning Basin reef complexes represent the *Palmatolepis* biofacies. Prominent examples include all collections from the basinal Virgin Hills Formation at Horse Spring and McWhae Ridge, as well as all other Bugle Gap localities in this lithofacies. This Frasnian biofacies was first recognized by Seddon (1970) and Seddon and Sweet (1971) and is characterized by diverse species of *Palmatolepis,* and only a few species of *Ancyrognathus, Ancyrodella,* and *Polygnathus.*

The *Palmatolepis* biofacies is also represented in some of the collections from the marginal-slope facies in the Napier Formation at Windjana Gorge (Playford, 1980, 1984) and in the Elimberrie no. 1 bioherm, a receptaculitid/sponge–stromatolite bioherm (Playford, 2002, p. 53, 56). The latter occurrence is remarkable in that Frasnian bioherms elsewhere rarely, if ever, contain species of the *Palmatolepis* biofacies. At Windjana Gorge, the *Polygnathus* biofacies (in the sense of Klapper and Lane, 1985) is also present in other collections from the marginal-slope facies.

This second conodont biofacies of the Frasnian was first recognized by Seddon (1970, p. 727) although he termed it the '*Icriodus* sequence' (later *Icriodus* biofacies, Seddon and Sweet, 1971). In his more abundant collections from the marginal-slope facies represented by the Sadler Limestone (e.g. Seddon, 1970, BC40-3,p. 745; BC85-10, p. 749; also Nicoll, 1984, table 2), specimens of *Polygnathus* are comparable in number to those of *Icriodus.* In our collections representing this biofacies in the marginal-slope facies of both the Sadler Limestone and the Napier Formation, however, species of *Polygnathus* predominate and *Icriodus* is rare to absent. Hence I use the term *Polygnathus* biofacies as in the carbonate shelf sequences of the Hay River – Trout River areas in the Northwest Territories, Canada (Klapper and Lane, 1985, figs 9, 10), where *Icriodus* is similarly rare to absent in many collections. This is also the case in many of the collections representing the *Polygnathus* biofacies in the central Russian Platform (Aristov, 1988, tables 3, 4; Ovnatanova and Kononova, 2001, p. 24).

Polygnathus samueli, first described from the *Polygnathus* biofacies in the Trout River area, Canada (Klapper and Lane, 1985) and also widely developed in the same biofacies in the central Russian Platform (collections of Aristov, 1988), occurs in the *Palmatolepis* biofacies in Zone 12 in the Canning Basin. This exceptional occurrence of a biostratigraphically short-ranging species in both biofacies is especially significant for correlation.

The *Polygnathus* biofacies is interpreted as positioned closer to shore than the *Palmatolepis* biofacies, although there may be some overlap as noted above in the case of Windjana Gorge. Whether there is a difference in depth represented by the two biofacies is an open question. In the depth-stratification model of Seddon and Sweet (1971), conodonts of the *Palmatolepis* biofacies were thought to have occupied a deeper position in the water column than the *Polygnathus* (or *Icriodus*) biofacies. However, one of the principal conclusions of the study by Nicoll (1984, p. 140) was that 'water depth, at least water-depth ranges of a few tens of metres, is probably not a factor in and of itself in conodont distribution.' An alternative hypothesis to the depth-stratification model is that conodont species of both biofacies occupied upper surface layers but were laterally segregated, with the *Polygnathus* biofacies further inshore in most instances. Evidence for this view

is given by the oxygen-isotope studies of Joachimski and Buggisch (2002, p. 712), in which they hypothesize 'that *Palmatolepis* was thriving in surface waters of the open ocean.'

In the marginal-slope facies represented by the Sadler Limestone at McWhae Ridge, the capped-oncolite bed (Nicoll, 1984, p. 131, table 2, WCB 811) is in the *Polygnathus* biofacies. The immediately overlying straight-nautiloid bed is still part of the Sadler Limestone (Playford, 2002, p. 38; P E Playford, 1990, written comm.), although Seddon (1970, p. 733, 746, BC75-5) referred to this bed as possibly the base of the Virgin Hills Formation and Nicoll (1984, p. 131) treated it as the basal Virgin Hills. Our collections from the nautiloid bed, as well as the next overlying bed of the Sadler Limestone, are in the *Palmatolepis* biofacies (Zone 4 with *P. transitans*; the collections of Nicoll, 1984, table 1, WCB 810, are also in the latter biofacies, again with *P. transitans*). A Zone 4 fauna occurs in the basinal Gogo Formation at 'Timanites Hill' in Bugle Gap (Glenister and Klapper, 1966, p. 836, WAPET D section), as mentioned above. Newer collections from 'Timanites Hill', taken together with R S Nicoll in 1988 and W T Kirchgasser in 1990, recovered *P. transitans* in a more diverse and abundant fauna of the *Palmatolepis* biofacies than is represented by the Sadler Limestone at McWhae Ridge.

As noted in all previous conodont studies of the Canning Basin reef complexes (Glenister and Klapper, 1966; Seddon, 1970; Druce, 1973, 1976), Frasnian conodonts are virtually absent from the Windjana Limestone (reef margin and reef flat) and the back-reef platform of the Pillara Limestone. Thus, both the *Palmatolepis* and *Polygnathus* biofacies were developed more offshore than the Frasnian reef margin, with the former present in both the marginal-slope and basin facies and the latter confined to the marginal-slope facies.

Famennian conodont biofacies have been briefly discussed in the Conodont Biostratigraphy section where they relate to problems in correlation with the standard zonation, but the main focus here is on the Frasnian.

Acknowledgements

Thanks are extended to P E Playford, former director of the Geological Survey of Western Australia, for supporting much of my field work, giving invaluable advice on the stratigraphy, collecting with me in 1992, and providing a number of critical samples especially from Windjana Gorge. R S Nicoll, formerly of the Australian Geological Survey Organisation and now with the Australian National University, was instrumental in setting up the initial field work in 1988 and he, together with R W Brown, helped immensely in the measuring and collecting of most of the sections, especially the critical one at Horse Spring. The late M R House of Hull and Southampton Universities gave inestimable advice in the field in 1990, 1993, and 1995, collected several critical conodont samples in 1989, and provided large-scale geological maps of the McWhae Ridge and McIntyre Knolls areas and elegant columnar diagrams of many of the sections. R T Becker of Münster University also helped greatly in the same three field seasons as M R House and provided important information on the correlation of the ammonoid and conodont zonations. Much of the collecting in the later seasons was focused on determining the conodont zone precisely of those beds with ammonoids discovered in the extensive field research of House, Becker, and W T Kirchgasser, SUNY College at Potsdam, begun in 1989. Kirchgasser was also an essential contributor to the 1990 field work.

C R Klug processed almost all the limestone samples. R A Metzger and J A Kralick picked a substantial number of samples — all three completed graduate degrees at the University of Iowa. Along with C R Klug, J Ormiston, then of Tulsa, Oklahoma, did a remarkable job in picking and arranging a majority of the slides, work supported by the Amoco Research Center. My field work in 1988 and 1990 was partially funded by NSF grants EAR87-06567 and EAR89-03475.

B F Glenister of the University of Iowa kindled my initial interest in Canning Basin conodonts in the early 1960s — I am deeply indebted to him. The late G Seddon, then a visiting professor at the University of Oregon, gave an important lecture at Iowa in 1970 on conodont biofacies in the McWhae Ridge area, prior to his groundbreaking paper of the same year. Thanks are extended to A E Cockbain for reviewing several versions of the manuscript.

References

Aristov, V A 1988, Devonskie konodonty tsentral'nogo Devonskogo Polya (Russkaya Platforma): Akademiya Nauk SSSR, Geologicheskiy Institut, Trudy, v. 432, 119p.

Branson, E B and Mehl, M G 1934, Conodonts from the Grassy Creek Shale of Missouri: University of Missouri Studies, v. 8, p. 171–259. [imprint 1933]

Druce, E C 1973, Upper Paleozoic and Triassic conodont distribution and the recognition of biofacies, *in* Conodont Paleozoology *edited by* F H T Rhodes: Geological Society of America, Special Paper 141, p. 191–237.

Druce, E C 1976, Conodont biostratigraphy of the Upper Devonian Reef Complexes of the Canning Basin, Western Australia: Australia, BMR, Bulletin 158, 303p.

Girard, C, Klapper, G and Feist, R 2006, Subdivision of the terminal Frasnian *linguiformis* conodont Zone, revision of the correlative interval of Montagne Noire Zone 13, and discussion of stratigraphically significant associated trilobites, *in* Understanding Late Devonian and Permian–Triassic biotic and climatic events: towards an integrated approach *edited by* D J Over, J R Morrow, and P B Wignall: Elsevier, Amsterdam, Developments in Palaeontology and Stratigraphy, v. 20, p. 181–198.

Glenister, B F and Klapper, G 1966, Upper Devonian conodonts from the Canning Basin, Western Australia: Journal of Paleontology, v. 40, p. 777–842.

Hinde, G J 1879, On conodonts from the Chazy and Cincinnati Group of the Cambro–Silurian, and from the Hamilton and Genesee–Shale divisions of the Devonian, in Canada and the United States: Quarterly Journal of the Geological Society of London, v. 35, p. 351–369.

House, M R, Becker, R T, Feist, R, Flajs, G, Girard, C and Klapper, G 2000, The Frasnian/Famennian boundary GSSP at Coumiac, southern France: Courier Forschungsinstitut Senckenberg, v. 225, p. 59–75.

Joachimski, M J and Buggisch, W 2002, Conodont apatite $\delta^{18}O$ signatures indicate climatic cooling as a trigger of the Late Devonian mass extinction: Geology, v. 30, p. 711–714.

Johnson, J G and Klapper, G, 1992, North American Midcontinent Devonian T–R cycles, *in* Special papers in paleontology and stratigraphy: a tribute to Thomas W Amsden *edited by* J R Chaplin and J E Barrick: Oklahoma Geological Survey, Bulletin 145, p. 127–135.

Johnston, D I and Chatterton, B D E 2001, Upper Devonian (Famennian) conodonts of the Palliser Formation and Wabamun Group, Alberta and British Columbia, Canada: Palaeontographica Canadiana, no. 19, 154p.

Kirchgasser, W T 1994, Early morphotypes of *Ancyrodella rotundiloba* at the Middle–Upper Devonian boundary, Genesee Formation, west-central New York, *in* Studies in stratigraphy and paleontology in honor of Donald W Fisher *edited by* E Landing: New York State Museum, Bulletin 481, p. 117–134.

Klapper, G 1989, The Montagne Noire Frasnian (Upper Devonian) conodont succession, *in* Devonian of the world *edited by* N J McMillan, A F Embry, and D J Glass: Calgary, Canadian Society of Petroleum Geologists Memoir 14, v. III, p. 449–468. [imprint 1988]

Klapper, G 1990, Frasnian species of the Late Devonian conodont genus *Ancyrognathus*: Journal of Paleontology, v. 64, p. 998–1025.

Klapper, G 1997, Graphic correlation of Frasnian (Upper Devonian) sequences in Montagne Noire, France, and western Canada, *in* Paleozoic sequence stratigraphy, biostratigraphy, and biogeography: Studies in Honor of J Granville ('Jess') Johnson *edited by* G Klapper, M A Murphy, and J A Talent: Geological Society of America, Special Paper 321, p. 113–129.

Klapper, G 2007, Frasnian (Upper Devonian) conodont succession at Horse Spring and correlative sections, Canning Basin, Western Australia: Journal of Paleontology, v. 81, p. 513–537.

Klapper, G and Becker, R T 1999, Comparison of Frasnian (Upper Devonian) conodont zonations, *in* Studies on conodonts: Proceedings of the Seventh European Conodont Symposium, Bologna-Modena 23–25 June, 1998 *edited by* E Serpagli and C Corradini: Bolletino della Società Paleontologica Italiana, v. 37(2–3), p. 339–348.

Klapper, G, Feist, R, Becker, R T and House, M R 1994, Definition of the Frasnian/Famennian Stage boundary: Episodes, v. 16(4), p. 433–441. [Imprint 1993]

Klapper, G, Kirchgasser, W T and Baesemann, J F 1995, Graphic correlation of a Frasnian (Upper Devonian) composite standard, *in* Graphic correlation *edited by* K O Mann and H R Lane: SEPM Society for Sedimentary Geology, Special Publication 53, p. 177–184.

Klapper, G, Kuz'min, A V and Ovnatanova, N S 1996, Upper Devonian conodonts from the Timan–Pechora region, Russia, and correlation with a Frasnian composite standard: Journal of Paleontology, v. 70, p. 131–152.

Klapper, G and Lane, H R 1985, Upper Devonian (Frasnian) conodonts of the *Polygnathus* biofacies, N.W.T., Canada: Journal of Paleontology, v. 59, p. 904–951.

Klapper, G, Uyeno, T T, Armstrong, D K and Telford, P G 2004, Conodonts of the Williams Island and Long Rapids formations (Upper Devonian, Frasnian–Famennian) of the Onakawana B Drillhole, Moose River Basin, northern Ontario, with a revision of Lower Famennian species: Journal of Paleontology, v. 78, p. 371–387.

Kralick, J A 1994, The conodont genus *Ancyrodella* in the middle Genesee Formation (lower Upper Devonian, Frasnian), western New York: Journal of Paleontology, v. 68, p. 1384–1395.

McLean, R A and Klapper, G 1998, Biostratigraphy of Frasnian (Upper Devonian) strata in western Canada, based on conodonts and rugose corals: Bulletin of Canadian Petroleum Geology, v. 46, p. 515–563.

Metzger, R A 1994, Multielement reconstructions of *Palmatolepis* and *Polygnathus* (Upper Devonian, Famennian) from the Canning Basin, Australia, and Bactrian Mountain, Nevada: Journal of Paleontology, v. 68, p. 617–647.

Müller, K J, 1956, Zur Kenntnis der Conodonten–Fauna des europäischen Devons, 1. Die Gattung *Palmatolepis*: Abhandlungen der Senckenbergischen Naturforschenden Gesellschaft, v. 494, 70p.

Murphy, M A 1977, On time-stratigraphic units: Journal of Paleontology, v. 51, p. 213–219.

Nicoll, R S 1984, Conodont distribution in the marginal-slope facies of the Upper Devonian reef complex, Canning Basin, Western Australia, *in* Conodont biofacies and provincialism *edited by* D L Clark: Geological Society of America, Special Paper 196, p. 127–141.

Nicoll, R S and Druce, E C 1979, Conodonts from the Fairfield Group, Canning Basin, Western Australia: Australia, BMR, Bulletin 190, 134p.

Nicoll, R S and Playford, P E 1993, Upper Devonian iridium anomalies, conodont zonation and the Frasnian–Famennian boundary in the Canning Basin, Western Australia: Palaeogeography, Palaeoclimatology, Palaeoecology, v. 104, p. 105–113.

Ovnatanova, N S 1969, Novye verkhnedevonskie konodonty tsentral'nykh rayonov Russkoy Platformy i Timana: Vsesoyuznyy Nauchno-Issledovatel'skiy Geologorazvedochnyy Neftyanoy Institut, Trudy, v. 93, p. 139–141.

Ovnatanova, N S 1976, Novye pozdnedevonskie konodonty Russkoy Platformy: Paleontologicheskiy Zhurnal, v. 1976, pt. 2, p. 106–115.

Ovnatanova, N S and Kononova, L I 2001, Conodonts and Upper Devonian (Frasnian) biostratigraphy of central regions of Russian Platform: Courier Forschungsinstitut Senckenberg, v. 233, 115p.

Over, D J 2002, The Frasnian/Famennian boundary in central and eastern United States: Palaeogeography, Palaeoclimatology, Palaeoecology, v. 181, p. 153–169

Playford, P E 1980, Devonian 'Great Barrier Reef' of Canning Basin, Western Australia: American Association of Petroleum Geologists, Bulletin, v. 64, p. 814–880.

Playford, P E 1984, Platform-margin and marginal-slope relationships in Devonian reef complexes of the Canning Basin: Proceedings of Geological Society of Australia and Petroleum Exploration Association of Australia Symposium on the Canning Basin, p. 189–214.

Playford, P E 2002, Devonian reef complexes of the Canning Basin, Western Australia: First International Palaeontological Congress, Post-6 Field Excursion Guidebook, 20–27 July 2002.

Racki, G, Racka, M, Matyja, H and Devleeschouwer, X 2002, The Frasnian/Famennian boundary interval in the south Polish–Moravian shelf basins: integrated event-stratigraphical approach: Palaeogeography, Palaeoclimatology, Palaeoecology, v. 181, p. 251–297.

Sandberg, C A, Morrow, J R and Ziegler, W 2002, Late Devonian sea-level changes, catastrophic events, and mass extinctions: Geological Society of America, Special Paper 356, p. 473–487.

Sandberg, C A, Ziegler, W, Dreesen, R and Butler, J L 1988, Late Frasnian mass extinction: Conodont event stratigraphy, global changes, and possible causes: Courier Forschungsinstitut Senckenberg, v. 102(3), p. 263–307.

Schülke, I 1999, Conodont multielement reconstructions from the early Famennian (Late Devonian) of the Montagne Noire (southern France). Geologica et Palaeontologica, Sonderband 3, 123p.

Seddon, G 1970, Frasnian conodonts from the Sadler Ridge–Bugle Gap area, Canning Basin, Western Australia: Journal of the Geological Society of Australia, v. 16, p. 723–753.

Seddon, G and Sweet, W C 1971, An ecologic model for conodonts: Journal of Paleontology, v. 45, p. 869–880.

Shaw, A B 1964, Time in stratigraphy: New York, McGraw-Hill Book Company, 365p.

Stauffer, C R 1938, Conodonts of the Olentangy Shale: Journal of Paleontology, v. 12, p. 411–433.

Youngquist, W 1947, A new Upper Devonian conodont fauna from Iowa: Journal of Paleontology, v. 21, p. 95–112.

Ziegler, W 1958, Conodontenfeinstratigraphische Untersuchungen an der Grenze Mitteldevon/Oberdevon und in der Adorfstufe: Notizblatt des Hessischen Landesamtes für Bodenforschung, v. 87, p. 7–77.

Ziegler, W 1962, Taxionomie und Phylogenie Oberdevonischer Conodonten und ihre stratigraphische Bedeutung: Abhandlungen des Hessischen Landesamtes für Bodenforschung, no. 38, 166p.

Ziegler, W and Sandberg, C A 1984, *Palmatolepis*-based revision of upper part of standard Late Devonian conodont zonation, *in* Conodont biofacies and provincialism *edited by* D L Clark: Geological Society of America, Special Paper 196, p. 179–194.

Ziegler, W and Sandberg, C A 1990, The Late Devonian standard conodont zonation: Courier Forschungsinstitut Senckenberg, v. 121, 115p.

Locality register

Casey Falls section, about 0.6 km E of McWhae Ridge, base of section is at GPS AMG Zone 52, 192718E 7926249N.

Dingo Gap section, Napier Range, base of section is at AMG Zone 51, 732900E 8045600N, Loc. 12.

Gl/B section of Glenister and Klapper, 1966, p. 837, figure 1, table 5, Gl/B0.

Elimberrie no. 1 bioherm, NE end of Oscar Range, grid reference 198–434; base of section is at GPS AMG Zone 51, 720000E 8043715N.

Horse Spring, northern Horse Spring Range, base of section about 200 m SSE of Horse Spring, base of section is at GPS AMG Zone 52, 186077E 7985602N; the F/F boundary in this section is at GPS AMG Zone 52, 186034E 7985650N.

McPhee Knoll, about 1.2 km WSW of the knoll, Old Bohemia Valley, base of the first section is at AMG Zone 52, 193800E 7936500N. Second section is about 0.5 km ESE of the knoll (base of section is at Loc 55 AMG Zone 52, 194600E 7936900N).

McWhae Ridge, 371B section crossing Frasnian/Famennian boundary and extending up through *Frutexites* bed [= WAPET B section of Glenister and Klapper (1966, p. 836, fig. 1, table 2) and Metzger (1994, fig. 1)], AMG Zone 52, 192045E 7926205N. A second section is that on the west flank of McWhae Ridge, which includes the capped-oncolite bed of the Sadler Limestone (Nicoll, 1984, p. 131, table 2, WCB 811; Playford, 2002, p. 34–37, fig. 35) at GPS AMG Zone 52, 192088E 7926291N.

Piker Hills B section, southern hill, AMG Zone 52, 190800E 7998600N.

Outcamp Hill, about 1.3 km NE of hill, Limestone Billy Hills area GPS AMG Zone 51, 792686E 7962748N.

Sadler Ridge, 300–400 m W of Longs Well, AMG Zone 51, 810700E 7939300N.

'Timanites Hill', NE of Glenister Knolls, central Bugle Gap area (=WAPET D of Glenister and Klapper, 1966, p. 836, fig. 1, table 9), AMG Zone 52, 188200E 7932400N.

WAPET C section of Glenister and Klapper (1966, p. 836, fig. 1, tables 2, 3) and Metzger (1994, fig. 1), hill separated from McWhae Ridge by Millard Creek, AMG Zone 52, 191600E 7925900N.

WAPET H section of Glenister and Klapper (1966, 836, fig. 1, table 6), section in creek about 1 km NE of Needle Eye Rocks, AMG Zone 51, 802800E 7978200N.

Windjana Gorge, three sections: 1) East Windjana Gorge, on south side slightly downstream of east entrance to gorge (Playford, 2002, fig. 54), AMG Zone 51, 708300E 8073500N. 2) East–central Windjana Gorge, upstream of the Classic Face on south side (Playford, 2002, fig. 54), GPS AMG Zone 51, 708780E 8073570N. 3). West–central Windjana Gorge, section on south side (Playford, 2002, fig. 54), GPS AMG Zone 51, 707223E 8074313N.

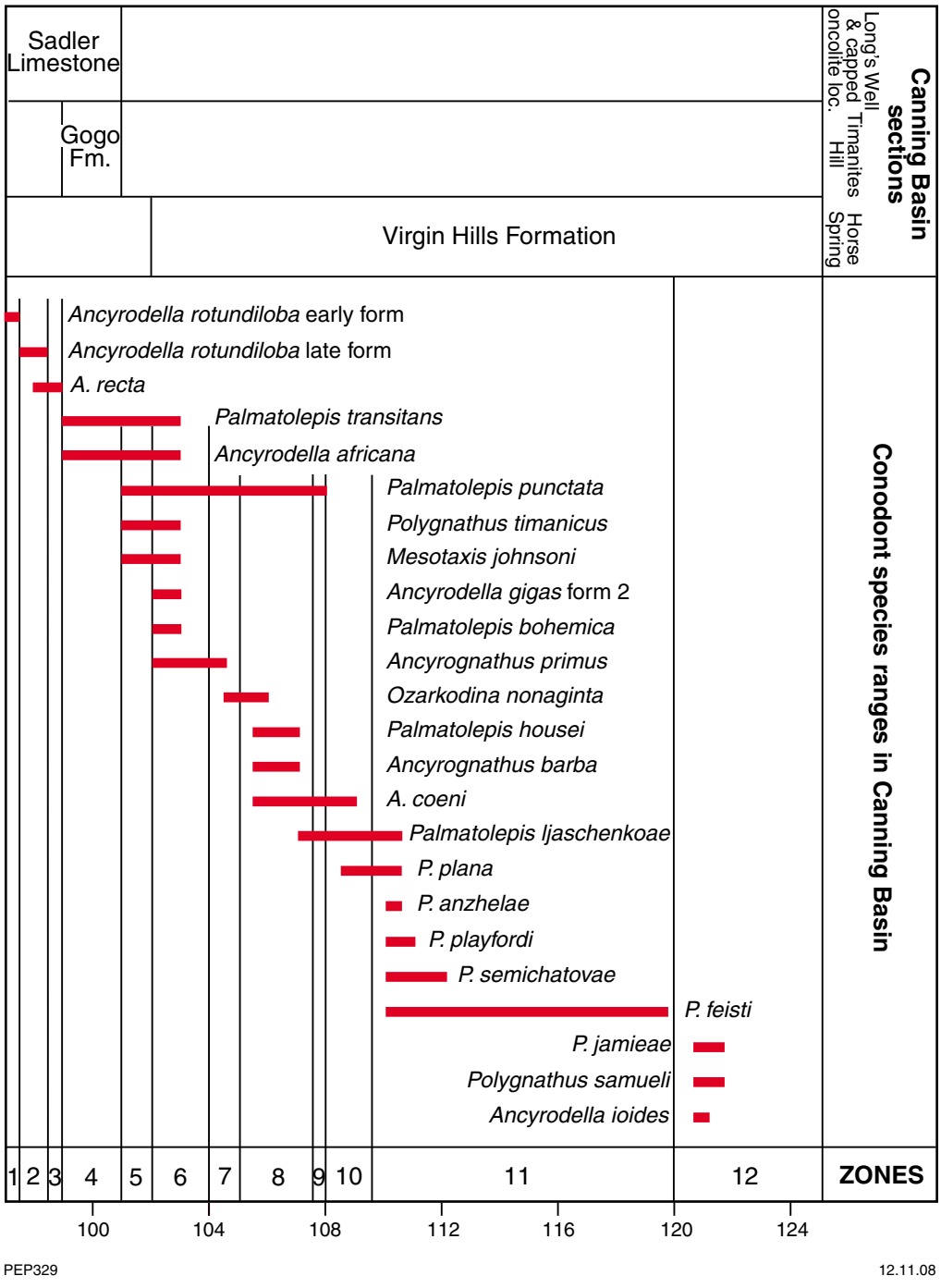

Figure 1.1. Ranges of biostratigraphically key conodont species in Frasnian Zones 1–12 of the Canning Basin. The numbered zones are those of the Montagne Noire zonation, scaled in units of the Frasnian Composite Standard (base of figure; Klapper et al., 1995, 1996; Klapper, 1997). The highest Frasnian zone, Zone 13, is shown on Figure 1.2. Bases of zones are aligned with the lowest ranges in the Composite Standard of defining species of the zonation, and not the ranges in the Canning Basin, except where they coincide as in the case of Zones 2 and 4.

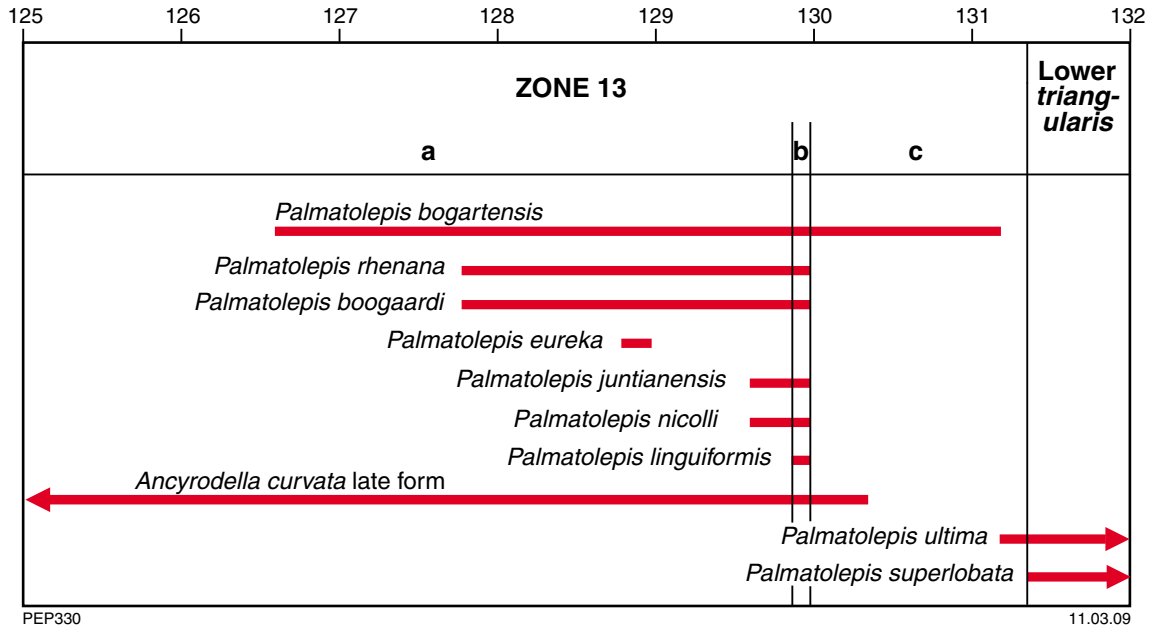

Figure 1.2. Ranges of biostratigraphically key conodont species of the highest Frasnian zone, Zone 13, and the Lower *triangularis* Zone at the base of the Famennian in the Canning Basin. Scaling is in units of the Composite Standard (top of figure); the base of Frasnian Zone 13 is aligned with the lowest range of the defining species, *Palmatolepis bogartensis*, in the Composite Standard and not its range in the Canning Basin. Zone 13 is subdivided into three units as explained in the text. Arrows indicate range extensions both below and above Zone 13. Ranges are based on graphic correlation of the Virgin Hills Formation at Horse Spring with the Composite Standard, except that the base of *Palmatolepis ultima* is taken from the Napier Formation at the Elimberrie no. 1 bioherm.

Figure 1.3. (facing page) Biostratigraphically significant conodont species in the Frasnian of the Canning Basin. All specimens are from the Virgin Hills Formation except no. 5, and all are from the Horse Spring section (HS, stratigraphic position given in Klapper, 2007, tables 1–3), except those in nos 1, 2, 4, 5, 8. Specimen nos 4–6, 8–10, 12–18, were previously illustrated in Klapper (2007). All museum numbers starting with F are GSWA numbers, SUI stands for the University of Iowa repository. All are upper views and magnifications are approximately x40. Numbered specimens are as follows:

1. ***Mesotaxis johnsoni* Klapper, Kuz'min, and Ovnatanova, 1996, F51420, McPhee Knoll, sample 10, 45.37–45.40 m, Zone 5**
2. ***Polygnathus timanicus* Ovnatanova, 1969, F51421, same locality, sample, and zone as no. 1**
3. ***Ancyrodella ioides* Ziegler, 1958, F51422, HS-34, Zone 12**
4. ***Palmatolepis subperlobata* Branson and Mehl, 1934, F51317, SW–McW–1 (Klapper, 2007, p. 536), spot sample (GSWA loc. 115326) that is no lower than Lower *triangularis* Zone**
5. ***Palmatolepis ultima* Ziegler, 1958, SUI 101633, Causses-et-Veyran South, CVS-30, Montagne Noire, Lower *triangularis* Zone**
6. ***Polygnathus samueli* Klapper and Lane, 1985, F51397, HS-43, Zone 12**
7. ***Ancyrognathus coeni* Klapper, 1990, F51423, HS-5, Zone 8**
8. ***Palmatolepis linguiformis* Müller, 1956, F51326, McW-D-B (Klapper, 2007, p. 536), Zone 13b**
9. ***Palmatolepis semichatovae* Ovnatanova, 1976, F51329, HS-16, Zone 11**
10. ***Palmatolepis bogartensis* (Stauffer, 1938), F51313, HS-65, Zone 13a**
11. ***Ancyrodella gigas* Youngquist, 1947, cf. form 2 of Klapper, 1989, F51424, HS-4a, Zone 7**
12. ***Palmatolepis punctata* (Hinde, 1879), F51419, HS-2, Zone 6**
13. ***Palmatolepis playfordi* Klapper, 2007, F51389, HS-14, Zone 11**
14. ***Palmatolepis nicolli* Klapper, 2007, F51384, HS-70, Zone 13a**
15. ***Palmatolepis feisti* Klapper, 2007, F51343, HS-25, Zone 11**
16. ***Palmatolepis jamieae* Ziegler and Sandberg, 1990, F51352, HS-45, Zone 12**
17. ***Palmatolepis housei* Klapper, 2007, F51333, HS-5, Zone 8**
18. ***Palmatolepis transitans* Müller, 1956, F51414, HS-2, Zone 6**

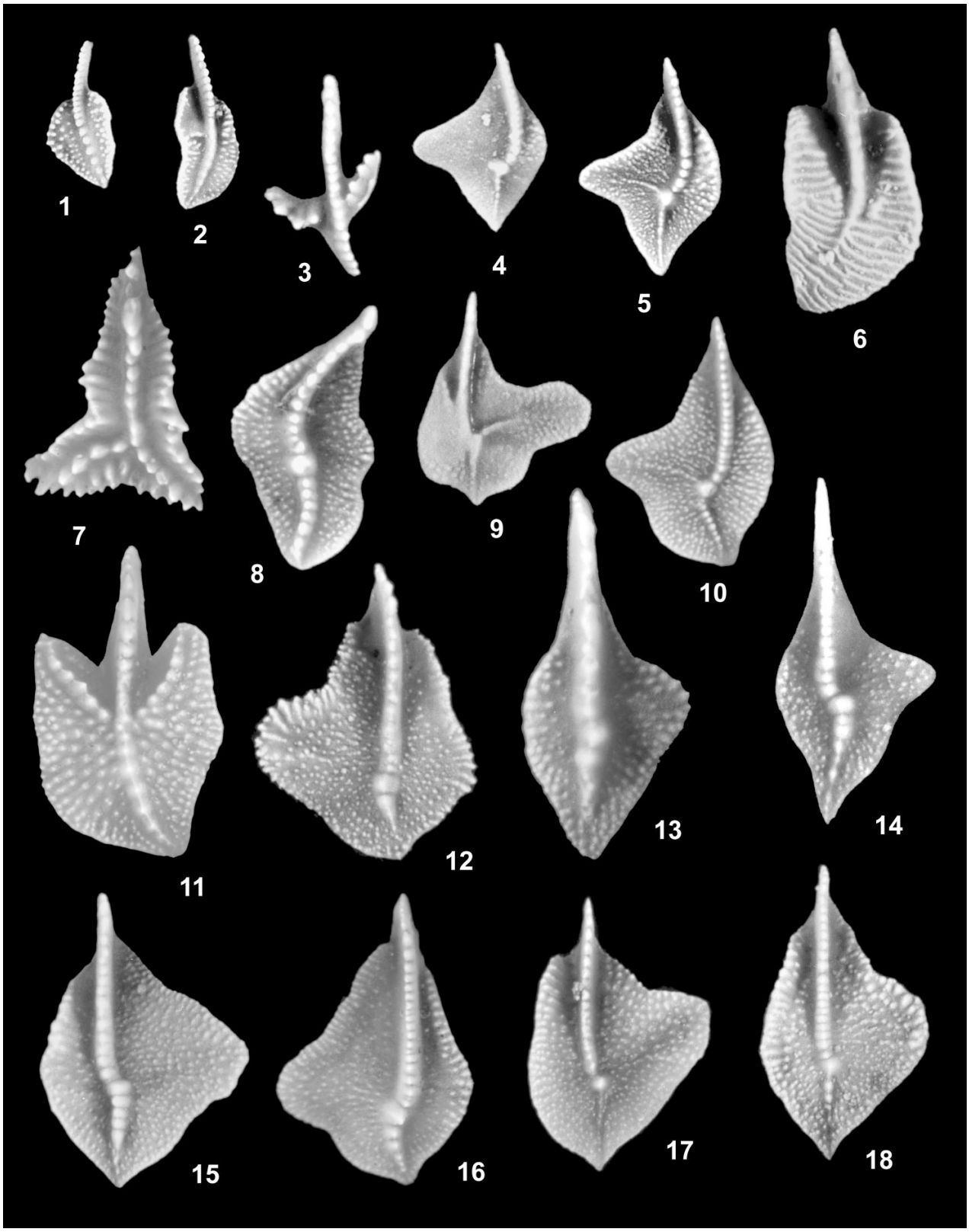
1
2
3
4
5
6
7
8
9
10
11
12
13
14
15
16
17
18

Appendix 2

Devonian ammonoid biostratigraphy of the Canning Basin

by

R Thomas Becker[1] and Michael R House[2]

Introduction

The Canning Basin is known as one of the best regions in the world for abundant and diverse Upper Devonian ammonoid faunas. They occur in numerous sections belonging to different facies of the extensive reef complexes, spanning the Lower Frasnian to early Upper Famennian, using the Upper Devonian substage definitions of the International Subcommission on Devonian Stratigraphy (Becker, 2003, 2007; Over, 2004). Many faunas show strong regional characteristics and some zones are currently known from single outcrops. However, there are close paleobiogeographic ties with distant regions of the Prototethys (Becker, 2000a; Becker *in* Talent et al., 2000), enabling ready correlation. The biofacies also makes the area one of the best known for precise ammonoid–conodont correlation.

The first Devonian ammonoids were collected by E T Hardman in 1883–84 and given to the British Museum of Natural History, where they were identified and published by Foord (1890). Later collections from the Mount Pierre area were described by Wade (1924, 1938) and Delépine (1933, 1935), who proved the presence of Frasnian and Famennian marker taxa, including several new species. Intensive stratigraphical studies commenced with the pioneer work of Curt Teichert, whose faunal lists (Teichert, 1941, 1943, 1949) indicated the presence of very rich assemblages in a succession of faunas. These and subsequent collections were later described in monographs on the Frasnian (Glenister, 1958) and Famennian (Petersen, 1975) faunas. The available collections were used to correlate the Western Australian faunas with the well-established European zones and successions (Glenister and Klapper, 1966), but the establishment of a finer and independent regional succession was not attempted. Both initial monographs suffered from the lack of designated types and adequate descriptions of most European taxa. Consequently, it is no surprise that recent revisions proved that many Canning Basin forms need to be re-assigned to other or new species. Our intensive fieldwork, mostly in the period from 1989 to 1995, and in collaboration with P E Playford (Perth), W T Kirchgasser (Potsdam, New York), G Klapper (Iowa), R S Nicoll (Canberra), R W Brown (Canberra), and others, led to the discovery of many completely new faunas, more than doubling the number of known taxa, and to the establishment of a new regional ammonoid zonation for the Frasnian (Becker et al., 1993). The new Famennian zones have so far been mentioned only briefly in studies on sea-level changes (Becker and House, 1997) and regional ammonoid paleobiogeography and diversity (Becker, 2000a). The review presented here includes all recognized zones and subzones, and briefly mentions recent taxonomic changes in order to allow an understanding of former literature. Currently, almost 170 species and subspecies are recognized, but some 45% of these still need to be named in new monographic studies. Therefore, even some important zonal markers have to be quoted in open nomenclature. The preliminary segregation of *Manticoceras* into several taxa with independent and parallel evolution, announced by Becker (2004), still requires full documentation.

[1] Geologisch-Paläontologisches Institut, Westfälische Wilhelms-Universität, Corrensstr. 24, D-48149 Münster, Germany, rbecker@uni-muenster.de

[2] Formerly of the University of Southampton, U.K., deceased 6 August 2002

Ammonoid localities

For each zone, biostratigraphic reference sections are given (Figs 2.1, 2.2). Locality names in inverted commas refer to informal field names for outcrops. If available, localities are accompanied by regional (WCB) locality numbers as used by Becker et al. (1993). The individual bed-by-bed ammonoid records of all sections are too voluminous to be presented here and, together with updated taxonomy, will be published elsewhere. For previous ammonoid locality data see Glenister (1958), Glenister and Klapper (1966), and Petersen (1975). Figured specimens and reference material for all occurrences, if not part of other collections (e.g. in Canberra and the University of Western Australia), will be deposited in the Geological Survey of Western Australia. The following sections and spot localities, roughly from northwest to southeast, have yielded important new collections:

Fore-reef subfacies of the Napier Formation at the eastern end of Windjana Gorge, southern side (AMG Zone 51, 709300E 8073600N; Playford, 1981, fig. 54; Playford, 2002, figs 17, 31).

Fore-reef subfacies, Pillara Sequence 6, of the Napier Formation in the Classic Face of Windjana Gorge,

(AMG Zone 51, 708300E 8073500N; Playford, 1981, fig. 54; Playford, 2002, figs 17, 31).

Dingo Gap, youngest parts of the Napier Formation, (AMG Zone 51, 731400E 8044700N; George et al., 1997, figs 2 and 5); 1.3 km northeast of Outcamp Hill; collections of P E Playford, GPS AMG Zone 51, 792686E 7962748N (Fig. 2.1).

WAPET H, section in creek ~1 km northeast of Needle Eye Rocks (AMG Zone 51, 802800E 7978200N), Loc. 58 (Glenister and Klapper, 1966; Petersen, 1975, fig. 1).

'Syncline Gully', shallow gully exposing a gentle syncline, ~1.5 km south of Needle Eye Rocks (AMG Zone 51, 801700E 7976400N).

'Cattle Creek', creek running in northeast direction towards Mount Pierre Creek, a tributary to the Margaret River, between 0.8 and 1.5 km east to northeast of Mount Pierre (AMG Zone 51, 804400E 7975400N).

Mount Pierre Creek, section across old airstrip, ~1.7 km east of Mount Pierre (AMG Zone 51, 805400E 7974800N).

'Straight Gully', small creek running almost straight in a northwest direction between 2.5 km southeast and 700 m east of Needle Eye Rocks, base of section at AMG Zone 51, 803700E 7976500N.

Flats beneath track, ~2 km southwest of Donalds Yard, southeast margin of Home Range (AMG Zone 51, 803700E 7976500N; Feist and Becker, 1997, fig. 2).

Sadler Ridge, 300–400 m west of Longs Well, northern Emanuel Range (AMG Zone 51, 810700E 7939300N; Becker et al., 1993, p. 303).

'Kite Hill', small hill ~5.5 km east of Bobs Bore, eastern Virgin Hills (AMG Zone 51, 803000E 7949200N; Feist and Becker, 1997, fig. 2).

'Ant Hill', northern part of a northwest-trending sequence of hills, ~3.5 km southeast of Bobs Bore, (AMG Zone 51, 806000E 7948100N; Feist and Becker, 1997, figs 2 and 3).

'Sprite Ridge', two sections (east and middle) at a prominent ridge ~700 m north of Bobs Bore (AMG Zone 51, 808900E 7950200N; Feist and Becker, 1997, figs 2, 4). Further rich goniatite collections were made by P E Playford at a cave at the eastern end of the ridge.

'King Brown Hill', small hill ~1.5 km northeast of Virgin Creek Bore, western Virgin Hills (AMG Zone 51, 800400E 7948900N; Feist and Becker, 1997, fig. 2; near DP4 *in* Petersen, 1975, fig. 1).

'Ayers Rocklet', isolated small sandstone hill ~2.3 km northwest of Bobs Bore, Virgin Hills (AMG Zone 51, 807300E 7950400N), Loc. 71. (Feist and Becker, 1997, fig. 2).

Piker Hills, various collecting spots and sections (A–G) around the southern hill of Piker Hills (AMG Zone 52, 190800E 7998600N; for section B; see Becker et al., 1993, fig. 3).

Various collection spots between 2.7 and 4.5 km south of Siphon Spring, Horse Spring Range (AMG Zone 52, 185200E 7983400N), Loc. 73 (Becker et al., 1993, p. 304).

Horse Spring, WCB 362, 364 (main section) and lateral section (southwest section) to WCB 364, northern Horse Spring Range (AMG Zone 52, 185200E 7983400N; for WCB 364; Becker et al., 1991, p. 186–189, figs 1c, 2–3, Becker et al., 1993, p. 305, and Becker and House, 1997, fig. 6).

'Timanites Hill', WCB 370, northeast Glenister Knolls, central Bugle Gap area (AMG Zone 52, 188200E 7932400N; Playford, 1980, fig. 11; Becker et al., 1993, p. 303; aerial view in Playford, 2002, fig. 21; ~WAPET D of Glenister and Klapper, 1966, Petersen, 1975, fig. 1).

Section ~1 km west of McPhee Knoll, WCB 365, northern Bugle Gap area, Old Bohemia Valley (AMG Zone 52, 193700E 7936800N), Loc. 10 (Becker et al., 1993, p. 304).

Sections ~400 m west of McIntyre Knolls, WCB 367, northern Bugle Gap area, Old Bohemia Valley (AMG Zone 52, 193900E 7936900N), Loc. 75 (Playford, 1981, fig. 32; Becker et al., 1993, p. 304–305).

Section between McPhee and McIntyre Knolls, WCB 366, northern Bugle Gap area, Old Bohemia Valley (AMG Zone 52, 194600E 7936900N), Loc. 55 (Becker et al., 1993, p. 305).

'Windy Knolls', WCB 369, 1.5 km southwest of Waggon Pass, northern Bugle Gap area (AMG Zone 52, 190600E 7935600N), Loc. 16 (Playford, 1981, fig. 11; Becker and House, 1997, fig. 2).

'Flare Hill', 1 km north of Waggon Pass, hill with top bed characterized by flare-bearing atrypids, northern Bugle Gap area (AMG Zone 52, 191700E 7937400N; see map *in* Playford, 1981, fig. 11).

Flats and trench (now filled) ~350 m west of McWhae Ridge, WCB 372, southern Bugle Gap area, southern extension of the Lawford Range (AMG Zone 52, 191700E 7926200N; Becker et al., 1993, p. 306; Becker and House, 1997, figs 4, 7).

Southwestern slope of McWhae Ridge, lateral sections WCB 371A–D around the '*Frutexites* Hill', ~WAPET B of Petersen (1975), southern Bugle Gap area (AMG Zone 52, 191900E 7926100N; Becker et al., 1991, p. 189–191, fig. 1b; Becker and House, 1997, figs 4 and 7).

McWhae Ridge, 'Graben Section', floor of graben and succession at southern end of graben in the centre of McWhae Ridge, southern Bugle Gap area (AMG Zone 52, 192000E 7926300N). Loc. 79 (Becker and House, 1997, figs 4 and 7).

'Orthoceras Hill', southwestern slope of McWhae Ridge, hill southeast of '*Frutexites* Hill' with peculiar orthoceratid marker limestone near its top, southern Bugle Gap area (AMG Zone 52, 191900E 7926000N; Fig. 2.2)

Steep slope near the southern end of McWhae Ridge, *Mesobeloceras* Section (shown to us by A Holmes), southern Bugle Gap area (Mb in Fig. 2.2; AMG Zone 52, 192000E 7926000N).

WAPET C, hill separated from McWhae Ridge by Millard Creek, southern Bugle Gap area (AMG Zone 52, 192000E 7925700N; Glenister and Klapper, 1966; Petersen, 1975, fig. 1; Becker and House, 1997, figs 4, 7).

'Red Rubble Island Section', isolated steep hill consisting of reddish limestones just east of WAPET C, southern Bugle Gap area (AMG Zone 52, 192100E 7925700N), Loc. 83 (Fig. 2.2).

'Phacopid Gully', four sections (A–D) on the southeastern slope of McWhae Ridge, southern Bugle Gap area (AMG Zone 52, 192400E 7926200N; Becker and House, 1997, figs 4, 7).

Casey Falls, east of McWhae Ridge, WCB 357, southern Bugle Gap area (AMG Zone 52, 192700E 7925900N; Playford, 1981, fig. 29; Becker et al., 1991, p. 191–193, figs 1a, 4–5; Nicoll and Playford, 1993, fig. 3; Becker and House, 1997, figs 2, 4, 5, 7).

'Calyx Corner', crinoid–ammonoid locality at the corner where the track from Kellys Pass to Casey Falls crosses the Millard Creek, ~250 m north of Casey Falls (AMG Zone 52, 192700E 7926200N; Playford, 1981, fig. 33; Fig. 2.2).

'Calyx Creek', creek leading from 'Calyx Corner' ~400 m upslope to the east (AMG Zone 52, 192800E 7926200N; Playford, 1981, fig. 33; Fig. 2.2).

'Berigora Gully', eastern slope of McWhae Ridge, ~250 m north of 'Phacopid Gully' (AMG Zone 52, 192400E 7926400N), Loc. 89 (Fig. 2.2).

'Esko Gully', named in the field after the late Esko Routasuo who showed us the collecting site, eastern slope of McWhae Ridge, ~450 m northwest of Casey Falls (AMG Zone 52, 192500E 7926200N; Fig. 2.2).

Ammonoid zones and subzones

All zones and subzones are named after the characteristic and defining taxon, which (as is normal in ammonoid biostratigraphy) is not necessarily restricted to the zone bearing its name, but may also range higher. Most distinguished intervals are defined by the entry of its marker taxon but mostly can also be positively identified with the help of other species. In some sections, the marker species may even be lacking and correlation is based on alternative index forms. Subdivisions that are less important than zones are referred to as subzones. Zonal abbreviations follow the international genozone terminology that was summarized by Becker and House (2000a). UD stands for Upper Devonian, UD I for Frasnian (Adorfian of the German terminology or *Manticoceras* Stufe), UD II for Nehdenian (*Cheiloceras* Stufe); UD III and IV for the Lower and Upper Hembergian (*Prolobites–Platyclymenia* Stufe) of the German terminology. As was shown earlier (Becker, 2000a), there are strong regional fluctuations in total diversity and the relative level of endemism from interval to interval. The Frasnian–Famennian boundary mass extinction led to a regionally complete extermination of ammonoids. After a long delay of recovery (four to five conodont zones), ammonoid faunas reappeared in the Canning Basin. There are no similarities with the sparse Famennian ammonoid faunas of southeastern Australia. In Australia, Frasnian ammonoids are so far restricted to the Canning Basin. There is no reliable regional record of any Givetian specimens, although the sedimentary record of the reef complexes extends down into the Givetian. Teichert (1949, p. 13) listed *Maenioceras*? sp. from his '*Atrypa* zone' but subsequently the presence of this Middle Givetian index genus has not been substantiated. The regional correlation given with the conodont scale (Fig. 2.2) is based either on data supplied by G Klapper (using the Montagne Noire zonation, numbered 1–13, for the Frasnian), published information (Glenister and Klapper, 1966; Nicoll and Playford, 1993; Metzger, 1994; Klapper 2007) or on known ammonoid–conodont correlation in other regions. Figure 2.3 gives an overview of the main sampled ammonoid localities, with their locations and time ranges. Figure 2.4 summarizes the overlapping stratigraphical ranges of all important marker species.

Koenenites n. sp. B Zone (UD I-B_1)

Definition: Entry of *Koenenites* n. sp. B which is related to the oldest *Koenenites, K. styliophilus*, known in North America, but differs from it in the even weaker outer umbilical lobes, oblique umbilical shoulders and suboxyconic mature stages.

Other markers: Oldest *Tornoceras contractum*.

Remarks: The oldest Canning Basin ammonoids occur as hematitic moulds (in the Gogo Formation) together with neritic faunas, such as brachiopods, in areas south of Siphon Spring and near Horse Spring. The taxonomic status, and hence the correct age assignment, was originally hampered by rather poor preservation of available material. Specimens identified as *Manticoceras* cf. *evolutum* (Becker et al., 1993), and later as *Chutoceras* n. sp. (Becker, 2000a), are now regarded as early morphotypes of the oldest known *Koenenites*, in which the outer umbilical lobes do not develop until rather late in the ontogeny. There is complete intergradation with more advanced morphotypes that show the diagnostic sutures with very weak U_2 lobe at earlier stages. Rare specimens with rounded lateral lobes and asymmetric lateral saddles of comparable size indicate the presence of intermediates between *Acanthoclymenia* and *Koenenites*. The true *Chutoceras* (Becker et al., 2000) is a descendant of *Ponticeras* and has very different, extended, semicircular flank saddles.

Reference section: Faunas are known only from isolated outcrops but the best collections come from between 3 and 4.5 km south of Siphon Spring.

Conodont correlation: The very primitive sutures of the zonal marker clearly indicate a stratigraphic position at the base of the international *Koenenites* Zone, which in New York (House and Kirchgasser, 1993) is known to start at about the base of Zone 2.

'*Hoeninghausia*' *pons* Zone (UD I-B2)

Definition: Entry of various subspecies of '*Hoeninghausia*' *pons*, characterized by strong shell compression and an incipient third umbilical lobe on the umbilical seam at maturity (Fig. 2.5, nos 1–2, GSWA F5247w).

Remarks: Becker et al. (2000) confirmed that the Russian *Protimanites* lacks a third U-lobe and that it is a subjective junior synonym of *Hoeninghausia*. Therefore, *H. pons* cannot be assigned to *Protimanites* as was advocated in Becker et al. (1993). Based on the German type species, true *Hoeninghausia* species are rather large in size and possess a single acute outer umbilical lobe, which is not the case in *H. pons*. The relatively small Canning Basin species should be placed in a new genus of the Timanitinae.

A second low-diversity and hematitic fauna was collected by P E Playford and D C Lowry 5 km southeast of Virgin Bore and contains a different and new species of *'Hoeninghausia'*, which is related to the German *'H.' galeata* and to *'H.' nalivkini* from northern Russia. All these forms retain a single rounded outer umbilical lobe and, in terms of morphology, are simpler than true *Hoeninghausia*. The new Canning Basin species may belong in a time interval between Zones I-B_1 and I-B_2. Becker et al. (1993) tentatively placed this fauna in UD I-D, but new investigations of the Timan ammonoid succession (Becker et al., 2000) proved that there are no simple-lobed Timanitinae younger than UD I-B.

Reference section: Sadler Ridge, 400 m west of Longs Well.

Conodont correlation: Zone 2 at the reference locality.

Koenenites n. sp. A Zone (UD I-B3)

Definition: Entry of various morphotypes of *Koenenites* n. sp. A that are characterized by distinctive, narrow flank saddles.

Reference section: This zone (or subzone) is only known from Sadler Ridge, 400 m west of Longs Well.

Conodont correlation: Upper part of Zone 2 to Zone 3 (level with *Ancyrodella recta*) at the reference locality.

Timanites angustus Zone and Subzone (UD I-C1)

Definition: Defined by the entry of *Timanites angustus* (Fig. 2.5, nos 3–4, GSWA F48530) which is closely related to *T. keyserlingi*, the type species of the genus from Russia, but differs in having a more highly arched ventrolateral saddle, a more asymmetric lateral lobe and, perhaps, in stronger shell compression.

Reference section: 'Timanites Hill' (WCB 370). Other records (British Museum of Natural History) are from around Longs Well, and Teichert Hills (collection of P E Playford).

Conodont correlation: Zone 4 at the reference locality. In the Timan (House et al., 2000a), the marker genus ranges from the upper part of Zone 3 to Zone 4.

Manticoceras sp. Subzone (UD I-C2)

Definition: Entry of regionally oldest *Manticoceras* sp.

Remarks: In North America (New York) oldest manticoceratids occur earlier, in UD I-B (Genundewa Limestone), but the rich collections from Sadler Ridge prove that this is not the case in northwestern Australia. The entry of the genus in the upper part of the *Timanites* faunas correlates with its entry in the upper part of division I-C in the Timan (Becker et al., 2000). Therefore, Becker et al. (1993) used it to distinguish a regional faunal level that, however, is best regarded as a subzone only. Poorly preserved manticoceratids have been found at other localities in the Gogo Formation (e.g. around Longs Well) and may fall in this subzone.

Reference section: 'Timanites Hill' (WCB 370).

Conodont correlation: By superposition, only the higher part of Zone 4 occurs at the reference locality. The oldest manticoceratids from the Timan (House et al., 2002) and Morocco (Becker and House, 2000b) also fall in Zone 4.

Topmost Lower Frasnian (UD I-D)

Remarks: Currently no Canning Basin ammonoid faunas are correlated with the level of the Middlesex Shale of New York, which contains the oldest *Sandbergeroceras*. The multilobed Triainoceratidae are completely lacking in Australia. There is also no evidence for the *Komioceras* faunas known from several regions of Russia (e.g. Becker et al., 2000).

Probeloceras lutheri lutheri Zone (UD I-E1)

Definition: Defined by the entry of *Probeloceras lutheri lutheri*, characterized by thin, flat shells and angular flank lobes and saddles, which make the form very characteristic and easily identifiable.

Other markers: The endemic *Mixomanticoceras exploratum*, oldest *Ponticeras* n. sp. (with strong ventrolateral furrows, first illustrated by Glenister, 1958, plate 5, fig. 1), *Acanthoclymenia* n. sp. A, and *A.* aff. *neapolitana* enter in this zone. Regionally this level also has the first *Manticoceras lamed* (very compressed) and *M. cordatum* (somewhat thicker). Early Australian manticoceratids lack the juvenile ribs and flares of North American species (for which the generic name *Gephuroceras* is available; Miller and Furnish, 1960). Forms previously assigned to *Aulatornoceras* n. sp. belong to a new genus that lacks the characteristic ventral band of typical members of the genus. It closes the umbilicus during ontogeny and includes the widespread *'Truyolsoceras' keyserlingi* Group.

Reference section: With certainty known only from the area west of McPhee Knoll, Old Bohemia Valley (WCB 365). Poorly preserved probeloceratids have also been observed in the Gogo Formation at Glenister Knolls and, together with *M. cordatum*, in the flats southwest of Donalds Yard (southeast end of Home Range).

Conodont correlation: Not dated at the reference section. The index species is first known from the lower Cashaqua Shale of New York, which falls in Zone 5 (House and Kirchgasser, 1993).

Ponticeras discoidale Zone (UD I-E2)

Definition: Entry of *Ponticeras discoidale* (Fig. 2.5, nos 5–6, GSWA F48531).

Remarks: The index species has also been reported from the Frasnian of Belgium and may allow international correlation.

Reference section: WCB 365, west of McPhee Knoll. Probably also present in the flat below the trench (WCB 372) at McWhae Ridge.

Conodont correlation: A level well above the base of Zone 5, with *Polygnathus timanicus* and *Ancyrognathus ancyrognathoideus* (see range of these taxa in the Timan *in* House et al., 2000a, and in the Frasnian composite of Klapper, 1997), is indicated at the reference locality in the upper part of the zone.

Manticoceras n. sp. 1 Zone (UD I-E3)

Definition: Entry of *Manticoceras* n. sp. 1 (= sp. nov. *in* Becker et al., 1993), which is characterized by very compressed and suboxyconic whorls.

Other markers: *Probeloceras lutheri* n. ssp. with rather narrow and strongly triangular flank saddle. Rare but distinctive is the regionally oldest species of *Gogoceras* (sp. A) with ribbed early whorls and convex growth lines at maturity.

Reference section: WCB 365, west of McPhee Knoll. Other good faunas occur in the lower part of WCB 367; also present in the flats below the trench (section 372, with a single but oldest *Aulatornoceras*) and in the graben at McWhae Ridge.

Conodont correlation: Higher part of Zone 5 (by superposition) at the reference locality and in the lower part of WCB 367.

Prochorites alveolatus Zone (UD I-F1)

Definition: First occurrence of *Prochorites alveolatus* which is probably an older (and valid) synonym of *P. strix* from New York.

Other markers: Oldest *Acanthoclymenia neapolitana*, *Probeloceras* aff. *lutheri* (with fastigate venter), oldest *Linguatornoceras* (still intermediate to *Tornoceras*), and a second, still unnamed, new and rare *Gogoceras* (sp. B).

Remarks: Silicified and radiolarian-rich nodules from the Gogo Formation near Outcamp Hill yielded a fauna dominated by *Probeloceras lutheri holzapfeli* (with well-rounded inner flank lobe), tornoceratids, two new species of *Acanthoclymenia*, and a new serpenticonic homeomorph of *Maternoceras*. The probeloceratid suggests a rather low level in UD I-E, but rare *Prochorites* fragments prove that at least some part of the fauna falls in I-F_1.

Reference section: WCB 367 near McIntyre Knolls, Old Bohemia Valley.

Conodont correlation: Higher part of Zone 5 (by superposition) in the reference section. Conodont correlations indicate that equivalents of the *alveolatus* Zone are present in the non-ammonoid-bearing upper part of WCB 365. In New York (House and Kirchgasser, 1993), *Prochorites* enters very high in Zone 5 and ranges into Zone 6.

Gogoceras nicolli Zone (UD I-F2)

Definition: Entry of *Gogoceras nicolli* (Fig. 2.5, nos 7–8, GSWA F48532).

Other markers: *Acanthoclymenia* aff. n. sp. A, *Manticoceras* n. sp. 2 (with evolute early whorls, previously recorded as *M.* aff. *lamed*), *Manticoceras* n. sp. 3 (relatively rare, with angular ventrolateral shoulders). Especially characteristic is a new beloceratid with an incipient third ventral lobe and pointed internal umbilical lobe, which falls in a new genus intermediate between *Probeloceras* and *Naplesites*. Becker et al. (1993) recorded it as *P. lutheri* n. ssp. Possibly it has a slightly older range than the zonal index species.

Reference section: WCB 367 near McIntyre Knolls. Also present in the graben on top of McWhae Ridge.

Conodont correlation: By superposition, highest part of Zone 5 in the reference section, laterally projecting into non-ammonoid-bearing strata in the upper part of WCB 365.

Sphaeromanticoceras affine Zone (UD I-F3)

Definition: Entry of faunas with *Sphaeromanticoceras affine* and with the related *S.* cf. *orbiculum*.

Other markers: Oldest *Aulatornoceras eifliense eifliense* and *Maternoceras* n. sp. 1, which lacks the ventral groove of the type species, *M. calculiforme*.

Remarks: In the lowermost, condensed, part of the Virgin Hills Formation near Horse Spring (WCB 362, 364), there are limestone faunas with poorly preserved oldest *Sphaeromanticoceras, Carinoceras* sp. indet., and still with *Probeloceras*. These are thought to represent the *affine* Zone in a different limestone facies.

Reference section: WCB 366 near McIntyre Knolls.

Conodont correlation: Zone 6, based on definite records of the zone in the underlying top part of WCB 365 and also based on the basal part of WCB 364.

Naplesites naplesense Zone (UD I-G1)

Definition: Entry of oldest *Naplesites* with three ventral lobes and additional outer umbilical lobe(s).

Remarks: This level was previously (Becker and House, 1997; Becker, 2000a) not separated from the next following faunal interval. There are forms with one outer umbilical lobe, resembling *N. naplesense,* and forms with two outer umbilical lobes as in *N. angustisellatus* (type species of *Chaoceras* Yatskov, 1990), and an evolute new species with three outer umbilical lobes that also occurs in Morocco.

Reference section: WCB 364 (Horse Spring), which is rather condensed in the lower part.

Conodont correlation: Zone 6 in the reference section. The same conodont correlation is indicated for the museum material of New York *Naplesites* (House and Kirchgasser, 1993). Moroccan *Naplesites* occur together with *Sandbergeroceras* in Zone 6 (Becker and House, 2000b; conodont data supplied by G Klapper).

Mesobeloceras housei Zone (UD I-G2a)

Definition: Entry of *Mesobeloceras housei* with fourth incipient ventral lobe and four outer umbilical lobes (Fig. 2.5, nos 9–10).

Remarks: The index species possesses a fourth incipient ventral lobe and in this respect is transitional between *Naplesites* and *Mesobeloceras*. Therefore, it has been variably assigned to either genera in the past. Here (Becker et al., 2004b, p. 38), more emphasis is placed on the origination of a new morphological feature that restricts *Naplesites* to species with three ventral and one to three outer umbilical lobes. The Moroccan *Merzougites* Korn and Klug (2002) is a subjective junior synonym of *Naplesites*.

Reference section: WCB 366 near McIntyre Knolls. At Horse Spring (WCB 364), the zone falls in a very condensed interval, which is difficult to separate from the next level.

Conodont correlation: Upper part of Zone 6 and Zone 7 in the reference section and at Horse Spring (within Bed 4). *M. housei* also occurs in Morocco, around styliolinites of the Rhinestreet Event and near the base of Zone 7. This suggests correlation of the main hypoxic interval (Beds 5–7) within the Virgin Hills Formation at WCB 366 with pulses of the eustatic Basal Rhinestreet Transgression (Becker and House, 1997).

Mesobeloceras thomasi Zone (UD I-G2b)

Definition: Entry of convolute *Mesobeloceras thomasi* with fully developed fourth and incipient fifth ventral lobe at maturity.

Other markers: Oldest new species of *Costamanticoceras* (related to *C. tuberculatum*) and *Playfordites* (with two pairs of spiral internal grooves), *Carinoceras vagans* (rare, first record for Australia), *Manticoceras buchii*, compressed, parallel-sided morphotype or subspecies of *Mant. lamed*. Slightly more advanced mesobeloceratids with five fully developed ventral lobes, as in *Sinobeloceras* Yatskov (1990), occur only rarely in the Canning Basin.

Reference section: Discontinuous and condensed slope section at the southern end of McWhae Ridge (*Mesobeloceras* Section). Also present in a very condensed interval at Horse Spring (WCB 364).

Conodont correlation: Zone 8 in the reference locality and at WCB 364. The closely related *Mesobeloceras kayseri* of Morocco also enters in Zone 8 (Becker and House, 2000b).

Beloceras tenuistriatum Zone (UD I-H)

Definition: Entry of the moderately involute *Beloceras* n. sp. (with six ventral lobes, some specimens with incipient seventh ventral lobes and seven umbilical lobes), or of the involute *Beloceras tenuistriatum* (early form with seven ventral lobes at maturity, as in forms assigned in other regions to *B. bogoslovskyi*, *B. shidianense*, and *B. gallicum*; Yang, 1984; Yatskov, 1990).

Other markers: The relative rare, open umbilicate *Manticoceras evolutum* with characteristic wide flank saddle. *M. ammon* with compressed but very rotund whorls is also very rarely present.

Reference section: Horse Spring (WCB 364 and locality of P E Playford in the northern part of the range); also present in the *Mesobeloceras* Section and the lower part of the now-filled trench at McWhae Ridge (WCB 372).

Conodont correlation: Upper part of Zone 8 to Zone 9 at Horse Spring and probably also in trench WCB 372. In Morocco, *Beloceras* faunas of UD I-H continue into Zone 10 (Becker and House, 2000b). The highest range of *M. ammon* in its Timan type region is Zone 9 (Becker et al., 2000).

Costamanticoceras koeneni Zone (UD I-I1)

Definition: Entry of various subspecies of the suboxyconic and only very weakly ribbed *Costamanticoceras koeneni* (Fig. 2.5, nos 11–12, GSWA F48533).

Other markers: True *Serramanticoceras serratum* with flattened venter, the parallel-sided *Manticoceras intumescens* and *M. latisellatum* Groups, *Aulatornoceras auris*, and *Linguatornoceras clausum*. *Beloceras* still displays seven ventral lobes.

Remarks: Since the trench near McWhae Ridge has been filled, without further excavation it is not possible to re-sample the oldest Canning Basin occurrence of *S. serratum*, which was originally used to define the base of I-I in the region. Consequently, a different species is now used as the index for the first Upper Frasnian ammonoid zone, which is well represented in outcrop in

the basal Virgin Hills Formation in more northern parts of the Bugle Gap area.

Reference section: 'Windy Knolls', 1 km south of Waggon Pass (WCB 369).

Conodont correlation: Zone 11 with *Palmatolepis semichatovae* in the reference section; contemporaneous with the entry of *S. serratum*, close relatives of *M. latisellatum*, and *P. semichatovae* in trench WCB 372. In the Timan (Becker et al., 2000), *M. latisellatum* and *L. clausum* also enter together with *P. semichatovae*.

Playfordites tripartitus Zone (UD I-I2)

Definition: Entry of *Playfordites tripartitus* characterized by one pair of internal spiral shell thickenings (Fig. 2.5, nos 13–14, GSWA F48534).

Other markers: *Trimanticoceras* aff. *cinctum* (more compressed and involute than *cinctum*), *Serramanticoceras* n. sp. 1 (= *serratum* ssp. A of Clausen, 1969 with rounded venter), and oldest relatives of *Manticoceras drevermanni*, a species which is normally more characteristic of the latest Frasnian of Germany (Wedekind, 1913, p. 31). Advanced *Beloceras tenuistriatum* with deep and narrow E_7 lobe and incipient E_8 lobe, for which the subspecies name *glenisteri* is available (Becker et al., 2004b), appear within I-I_2.

Remarks: In the northern Bugle Gap area, the faunal composition of contemporaneous beds (controlled by conodont correlation) is different. Here relatives of '*Maternoceras*' *prumiense*, which represent an unnamed genus with constrictions, are more characteristic. They are associated with serramanticoceratids.

Reference section: Horse Spring (WCB 364). The zone is also recognizable in the McWhae Ridge area (lower slope of WCB 371B).

Conodont correlation: By superposition, higher part of Zone 11 in the reference section and at WCB 369 ('Windy Knolls'), but *P. tripartitus* faunas extend into Zone 12 at WCB 372. At Martenberg, Germany, faunas with *P. tripartitus* (Lower *cordatum* fauna of House and Ziegler, 1977) correlate with Zone 11 (Klapper and Becker, 1999). This is also true for *P. cf. tripartitus* from the top of the Rhinestreet Shale of New York (House and Kirchgasser, 1993).

Maternoceras retorquatum Zone and Subzone (UD I-J1)

Definition: Abundant occurrence of *Maternoceras retorquatum*.

Other markers: Trimanticoceras bullatum (new generic assignment based on furrowed early stages of German specimens); *Beloceras tenuistriatum* shows eight ventral lobes at maturity.

Remarks: Contemporaneous beds at Horse Spring are poor in ammonoids. *Maternoceras* has a lower total range but earlier Canning Basin representatives are very rare forms. A single specimen from the *koeneni* Zone (Harpid Bed) of 'Windy Knolls' is already very close to *M. retorquatum*.

Reference section: McWhae Ridge, section 371A, 30 m northeast of main section. The index species is not yet recorded from the northern Bugle Gap area ('Windy Knolls', WCB 369).

Conodont correlation: Not constrained in the transition from Zone 11 to 12. *Trimanticoceras* cf. *bullatum* occurs at 'Windy Knolls' (WCB 369) in the highest part of Zone 11. This suggests that the Zone 12 *Playfordites* faunas from the McWhae Ridge trench (WCB 372) correlate with Zone I-J. A similarly high range of *Playfordites* is indicated in New York by specimens from the Angola Shale (House and Kirchgasser, 1993), which falls in Zone 12.

Virginoceras erraticum Subzone (UD I-J2)

Definition: Entry of *Virginoceras erraticum* whose lanceolate venter allows easy recognition.

Other markers: *Clauseniceras scheldense*, *C.* cf. *expectatum*, *Trimanticoceras cinctum*, *T.* n. sp. B (more compressed than *cinctum*, spiral furrow weakens early), a rather involute *Costamanticoceras*, *Manticoceras* cf. *solnzevi*, *M.* aff. *cordatum* (more evolute and thicker), and *Serramanticoceras obliquesulcatum*.

Reference section: The Lower *Beloceras* Bed at McWhae Ridge, Section 371B. There are many rich collection spots on the eastern slope of McWhae Ridge ('Berigora Gully' and 'Esko Gully') but collecting was rather poor at this level in the trench at McWhae Ridge (WCB 372) and at 'Windy Knolls' (WCB 369). Other faunas are known from Horse Spring (lateral section to WCB 364).

Conodont correlation: The reference section did not provide a diagnostic conodont fauna. Zone 12 was found at Horse Spring and WCB 372. The German Upper *cordatum* Zone of House and Ziegler (1977), which contains *C. expectatum*, also correlates with Zone 12 (Klapper and Becker, 1999). *Virginoceras ljaschenkoae* from the Timan is older (UD I-I, Zone 11) than the Canning Basin index species (House et al., 2000a) of the same genus.

Clauseniceras n. sp. Subzone (UD I-J3)

Definition: Entry of a new, slowly expanding and rather involute species of *Clauseniceras.*

Other markers: *'Maternoceras' sandbergeri* may appear in flood occurrences and is probably regionally restricted to this level. There are also very advanced *Beloceras tenuistriatum* with fully developed eight ventral and nine umbilical lobes (resembling the lectotype of *Goniatites sagittarius* Sandberger and Sandberger, 1851, pl. IV, figs 3, 3a, 3b, housed in the Museum für Naturkunde, Berlin, MB.C.4501) and intermediates between *Manticoceras lamed* and *M. lyaiolense*. Several common evolute manticoceratids of underlying beds (*Costamanticoceras, Maternoceras* s. str.) seem to be lacking, but *Serramanticoceras* n. sp. 1 is common.

Reference section: McWhae Ridge (WCB 371B: faunas at or right above a white to yellowish-grey scutelluid marker bed, here named as Esko Bed); other rich faunas are from 'Berigora Gully' east of McWhae Ridge, just above the widely exposed minor cliff of the Lower *Beloceras* Bed. Further on, at 'Esko Gully', there are only sparse faunas with *Beloceras*.

Conodont correlation: Zone 12 in the reference section and in 'Berigora Gully'. *M. lyaiolense* is characteristic for Zone 12 ammonoid faunas of the Timan (House et al., 2000a) but has a longer total range. According to new collections, '*Maternoceras*' *sandbergeri* occurs at Martenberg (Germany) also in Zone 12.

Manticoceras n. sp. 5 Zone (UD I-K)

Definition: Entry of a very compressed, involute, suboxyconic and moderately large new *Manticoceras* (n. sp. 5), which somewhat resembles the much older *Manticoceras* n. sp. 1.

Other markers: The rare (only one fragment found) *Aulatornoceras* n. sp. (with angular flank lobe) that resembles an undescribed species from the lower Hanover Shale of New York.

Remarks: Early relatives of *'M'. guppyi* (n. sp. 4, with rather angular flank saddle) occur within a condensed interval topped by an algal bed at 'Flare Hill', 1 km north of Waggon Pass, which seems to correlate in time with the Lower Kellwasser level of Europe and North Africa. The Lower Kellwasser Event, however, is not marked in the Canning Basin successions. The diverse late Frasnian faunas of UD I-J are always terminated by a regressive interval lacking ammonoids.

Reference section: 'Phacopid Gully', Section A. At Horse Spring (WCB 364) there are only a few long-ranging species. The 'Windy Knolls' section (WCB 369) contains relatives of '*M.*' *guppyi*, followed by a peculiar, spar-rich receptaculitid limestone, which perhaps correlates with the stromatolitic bed of 'Flare Hill'.

Conodont correlation: Zone 13a is recorded in the upper part of the zone in the reference section (the lower part has not been sampled for conodonts). The first *Manticoceras* n. sp. 4 of 'Windy Knolls' start rather high in Zone 12. At 'Flare Hill', Zone 13a starts within the condensed and solid ammonoid and stromatolitic limestones.

Crickites lindneri Zone (UD I-L1a)

Definition: Entry of the large and inflated *Crickites lindneri* (Fig. 2.5, nos 15–16, GSWA F48535).

Other markers: *Trimanticoceras* n. sp. A (rather large), *Idiobeloceras* n. sp. (with at least ten outer umbilical but only seven ventral lobes).

Remarks: Re-sampling proved that widespread upper units with *Beloceras* (including the Upper *Beloceras* Bed of Becker et al., 1993) are the main level of *C. lindneri*, which, therefore, resulted in a re-assignment to the *Crickites* Genozone (Becker, 2000a). Advanced *Beloceras* continue in parallel with *Idiobeloceras*.

Reference section: 'Phacopid Gully A'. Other rich occurrences are at McWhae Ridge (lateral sections WCB 371A-D, just above WCB 372, upper part of 'Graben Section'), at the base of Casey Falls, at 'Calyx Corner', and at the top of 'Windy Knolls' (WCB 369). Small faunas are known from the eastern end of Windjana Gorge and 'Flare Hill', 1 km north of Waggon Pass (Bugle Gap area).

Conodont correlation: Starting somewhat above the base of Zone 13a in the reference section and at western McWhae Ridge (WCB 371B), probably also at Windjana Gorge East. At 'Windy Knolls' (WCB 369), the level of oldest *C. lindneri* has not been sampled, but Zone 13a is recorded from the next bed above. The last, condensed limestones with beloceratids may already fall in Zone 13b at 'Flare Hill', McWhae Ridge (WCB 371D), and Horse Spring (WCB 364). Oldest *Crickites* faunas of the Montagne Noire, Belgium, and of New York also start within Zone 13a (House and Kirchgasser, 1993; House et al., 2000b).

'Manticoceras' guppyi Zone (UD I-Lb)

Definition: Flood occurrence of *'Manticoceras' guppyi* with narrow and very high flank saddle, asymmetric outer flank lobe, involute adult stages and characteristic ornament that allow generic distinction from *Manticoceras*.

Other markers: The zone includes a new and more evolute species (n. sp. L) of '*Manticoceras*' with widely spaced lirae as in aulatornoceratids, relatives of *'M.' guppyi* with thicker whorls or with more evolute and faster expanding adult stages, *Archoceras varicosum*, *A.* aff. *schlosseri* (lacking ventrolateral furrows), and *Trimanticoceras* n. sp. C (with shallow furrows and peculiar ventral edges).

Remarks: The zone can be recognized by a change from beds rich in beloceratids to mass occurrences of *'M.' guppyi* and of close relatives or subspecies. Similar shell form and ventral lobes occur earlier in the related *M.* n. sp. 4 but the other associated marker species, which are rarer but also widespread, aid the recognition of the zone. *Beloceras* continues as minor faunal element in shallow facies settings. *Crickites lindneri* is much rarer than *'M.' guppyi* at this level. *'M.'* n. sp. L occurs in equivalents of the Upper Kellwasser Limestone of Germany (only one specimen known) and of Southwest Morocco (Becker et al., 2004b) and allows correlation of the regional *'M' guppyi* marker bed of Becker et al. (1991) with the early, transgressive part of the Upper Kellwasser Event.

Reference section: 'Phacopid Gully A'. Other rich occurrences are in the creek at the base of Casey Falls, at 'Calyx Corner' (with *Trimanticoceras* and *Archoceras*), on the western side of McWhae Ridge (top of hill above trench WCB 372, lateral sections WCB 371A–D, top of 'Graben Section'), and just above the 'Gastropod Bed' (Becker and House, 1977; Cook et al., 2003) at Horse Spring.

Conodont correlation: Zone 13b (with *Palmatolepis linguiformis*) at 'Phacopid Gully A', McWhae Ridge (WCB 371B and 371D), Casey Falls, and Horse Spring. The conodont evidence supports correlation with the lower part of the Upper Kellwasser level, which in the Canning Basin, however, is not developed as an interval of low-oxygen facies. *Archoceras*, which has a longer total range, is also typical for Upper Kellwasser beds.

Manticoceras cordatum (upper range) Zone (UD I-L2)

Definition: Regional extinction of all ammonoid genera apart from *Manticoceras* and *Tornoceras*.

Remarks: The youngest Canning Basin manticoceratids mostly belong to the long-ranging *M. cordatum* but '*M.*' *guppyi* may also still be present. As with the associated conodonts, they represent a very low-diversity terminal Frasnian pelagic faunal interval and support evidence for a stepwise regional extinction pattern associated with the global Upper Kellwasser Event. Manticoceratids and *Tornoceras* seem to have survived longer in the region than all species of *Beloceras*, *Crickites*, *Trimanticoceras*, *Linguatornoceras*, and *Aulatornoceras*. It is strange that *Tornoceras* reappears as an opportunistic genus in the final phase of the extinction interval since the genus is currently unknown from older parts of the Upper Frasnian in the basin.

Reference section: 'Phacopid Gully A'; other terminal Frasnian ammonoids occur on the western side of McWhae Ridge (WCB 371C), at Horse Spring (WCB 364), and in Windjana Gorge.

Conodont correlation: Zone 13c at the reference locality and Horse Spring, probably also at Windjana Gorge East ('Red Cave') and East-Central (just upstream from the Classic Face) sections.

Basal Famennian (UD II-A/?B)

Remarks: There is no evidence for any ammonoids in the lowest part of the Famennian, which is also characterized by strong condensation in many successions, e.g. in the Bugle Gap area. This does not imply that the ammonoid-free period was of short duration. It seems that the Canning Basin needed to be repopulated by ammonoids from Europe (Becker, 2000a), after a total extinction of all manticoceratid species during the final phase of the global Frasnian–Famennian (Upper Kellwasser) mass extinction. Neither did any tornoceratid survive, unlike the western Prototethys, where *Phoenixites frechi* was an event opportunist that blossomed in the Upper Kellwasser beds through to the basal Famennian (Becker, 1993). *Linguatornoceras* is the only genus that has been found, represented by different species, in both the Upper Frasnian and the Lower Famennian of the Canning Basin. However, the Famennian record is based only on a single specimen.

Conodont correlation: Lower *triangularis* Zone (see its revision in Klapper et al., 2004) to Middle *crepida* Zone at McWhae Ridge (Nicoll and Playford 1993; Metzger, 1994) and Casey Falls.

'*Falcitornoceras*' n. sp. 1 Zone (UD II-B/C)

Definition: Entry of a new species (n. sp. 1, Fig. 2.6, nos 1–2, GSWA 48536) related to *'Falcitornoceras' korni,* included in *Tornoceras simplex* by Glenister and Klapper (1966) and Petersen (1975); both species fall in a new genus lacking the juvenile falcate ribbing of true *Falcitornoceras.*

Other markers: Several forms currently included in or close to *Cheiloceras (Puncticeras) pompeckji* (= *C. (Staffites) ovatum* in Petersen, 1975, a taxon regarded by Becker, 1993 as a *nomen dubium*; probably also including corroded specimens previously assigned to *C. (Cheiloceras) circumflexum*) and a second new species (n. sp. 2) of *'Falcitornoceras'*.

Reference section: Lateral section WCB 371B at McWhae Ridge, just above the *Frutexites* marker bed. Other occurrences are at 'King Brown Hill' and 'Kite Hill' in the Virgin Hills (see previous records from that region in Glenister and Klapper, 1966) and from 'Cattle Creek' and Mount Pierre Creek (tepee section) east of Mount Pierre.

Conodont correlation: Upper *crepida* Zone in the reference section. Previous records of cheiloceratids from the Lower *crepida* Zone (Glenister and Klapper, 1966; Petersen, 1975) probably represent faunas from the same interval in which index conodont species (e.g. *Palmatolepis termini*) are missing for biofacies reasons (see discussion in Becker, 1993). Similar problems with dating oldest cheiloceratid faunas have been encountered in Morocco. Currently there are no reliable records of cheiloceratids from beds older than the Middle *crepida* Zone on a global scale. In Morocco, *C. (P.) pompeckji* does not seem to enter earlier than UD II-D (Becker et al., 2002).

Oxytornoceras n. sp. Zone (UD II-D)

Definition: Entry of *Oxytornoceras* n. sp., assigned by Petersen (1975) to the homeomorphic latest Givetian to basal Frasnian *Epitornoceras peracutum*.

Other markers: *Armatites planidorsatus*, *Cheiloceras* (*Staffites*) *curvispina*, *C.* (*Puncticeras*) *lagowiense*, *C.* (*P.*) *schmidti*, *C.* (*P.*) *semiinversum* (and new related forms), *C.* (*P.*) *postinversum* (including compressed forms assigned by Petersen, 1975, to *C.* (*C.*) *sacculum*), *C.* (*P.*) n. sp. (with star-shaped constrictions), *Torleyoceras oxyacantha*, *Linguatornoceras* n. sp. (more compressed than the German *L. guestphalicum*), and a third (n. sp. 3) new '*Falcitornoceras*'.

Remarks: This zone contains the most abundant and diverse Famennian ammonoid assemblage of the Canning Basin.

Reference section: 'Ant Hill' southeast of Bobs Bore (Virgin Hills). Other rich occurrences are from 'King Brown Hill', 'Sprite Ridge I' (eastern end of ridge),

'Cattle Creek', Mount Pierre Creek, and McWhae Ridge (WCB 371B, extending to 371B´ and 'Orthoceras Hill'). Small faunas come from the base of WAPET C and Casey Falls. Other records are in Petersen (1975).

Conodont correlation: The upper half falls in the Lower *rhomboidea* Zone at the reference section (no data available for the lower half); Uppermost *crepida* to Lower *rhomboidea* Zone at McWhae Ridge (WCB 371B, Metzger, 1994), Lower *rhomboidea* Zone at WCB 371B (nodular faunas from upper argillaceous interval, laterally continuous with faunas from 'Orthoceras Hill'), base of WAPET C (Metzger, 1994), Casey Falls, and 'Sprite Ridge I'. The same conodont correlation has been established for UD II-D by Becker (1993) for Europe and North Africa.

Praemeroceras petterae Zone and Subzone (UD II-E_1)

Definition: Entry of *Praemeroceras petterae* in a gradual lineage coming from *Cheiloceras* (*Staffites*) *curvispina.*

Other markers: Close relatives of *Praemeroceras globosoides*, illustrated by Petersen (1975, Fig. 18D, pl. 4, figs 1–2) as *Dimeroceras* aff. *D. mamilliferum*.

Reference section: 'Cattle Creek' east of Mount Pierre. Other faunas are known from Casey Falls and WAPET C (McWhae Ridge area), 'Ant Hill' (Virgin Hills, compare section DP 4 in Petersen, 1975), and Mount Pierre Creek (Old Airstrip Section, see also sample Ta from nearby in Petersen, 1975).

*Conodont correlation***:** By superposition, higher part of Lower *rhomboidea* Zone at the reference section, WAPET C, Casey Falls, and 'Sprite Ridge I'; probably also at Mount Pierre Creek (compare sample UWA 26946c in Glenister and Klapper, 1966). The level of *P. petterae* is not yet well constrained within the *rhomboidea* Zone in Germany and Morocco (discussion in Becker, 1993).

Praemeroceras primaevum Subzone (UD II-E2)

Definition: Entry of the distinctive *Praemeroceras primaevum* (Fig. 2.6, nos 3–4, GSWA F48537) with globose, widely umbilicate early stages (= *Dimeroceras padbergense* of Petersen, 1975).

Other markers: Two new *Praemeroceras* species, identified by Petersen (1975) as *Dimeroceras* cf. *D. bredelarense*.

Reference section: 'Cattle Creek' east of Mount Pierre (compare Petersen, 1975, sample Tb). Other occurrences are in microbial coquinas of WAPET C. Contemporaneous beds at Casey Falls and in the Virgin Hills are rather poor in ammonoids.

Conodont correlation: Probably Upper *rhomboidea* Zone, which is generally difficult to recognize, at WAPET C where Metzger (1994) noted *Palmatolepis rhomboidea* without the Lower *rhomboidea* Zone index species *P. poolei* in a *primaevum* coquina bed (Bed 5). The same age was given by Price (1982) for specimens from the Beul section (Germany, identified as Gen. nov. aff. *Dimeroceras* sp. nov.; Becker, 1993, p. 293).

Paratornoceras polonicum Zone and Subzone (UD II-F1)

Definition: Entry of oldest morphotypes of *Paratornoceras polonicum* with a very late sharpening of the venter during ontogeny (possibly only a subspecies of *P. lentiforme*).

Remarks: *P. lentiforme* in the sense of its neotype (Ebbighausen et al., 2002), with early sharpening of the venter whilst the umbilicus is still widely open, enters at a higher level within the subzone. The succession of Paratornoceratinae allows a fine time discrimination within UD II-F and seems to represent a regional chronomorphocline.

Reference section: WAPET C south of McWhae Ridge (compare GSWA 1029 samples in Glenister and Klapper, 1966). Other rich faunas (collected by P E Playford) occur at 'Cave Hill' around Bobs Bore and at 'Cattle Creek'. Contemporaneous beds at Casey Falls and 'Sprite Ridge I' are poor in ammonoids. Faunas with *P. lentiforme* in Petersen (1975) may fall either in this or the next subzone.

Conodont correlation: Uppermost part of *rhomboidea* Zone with *Palmatolepis stoppeli* at the reference section (Glenister and Klapper, 1966; Metzger, 1994); also dated as *rhomboidea* Zone at Beul (Germany) by Price (1982).

Acrimeroceras clarkei Subzone (UD II-F2)

Definition: Entry of strongly compressed, oxyconic *Acrimeroceras* without constrictions (Fig. 2.6, nos 5–6, GSWA F48538 and F48539), here provisionally identified as *A. clarkei* (see original species diagnosis of Delépine, 1935, mentioning strong compression and sharp venter); included as a morphotype within *Paratornoceras lentiforme* by Glenister and Klapper (1966) and Petersen (1975). It does not overlap stratigraphically with the somewhat homeomorphic *Oxytornoceras* n. sp.

Reference section: WAPET C. Another rich fauna occurs at 'King Brown Hill' near Virgin Creek Bore (Virgin Hills) but faults have cut out contemporaneous beds in parts the Mount Pierre area (e.g. at 'Cattle Creek') where the species was first found by Delépine (1935).

Conodont correlation: Starting at the base of the Lower *marginifera* Zone in the reference section (Metzger, 1994; compare older data in Glenister and Klapper, 1966, table 5). This correlation fits the entry of the genus in a marker bed near the base of the Lower *marginifera* Zone of Germany, southern France, northern Spain, and northern Morocco (Becker, 1993).

Maeneceras meridionale Zone and Subzone (UD II-G1)

Definition: Entry of *Maeneceras meridionale*, a senior synonym of *M. subvaricatum* (Korn and Ziegler, 2002). The index form was assigned by Petersen (1975) to *Sporadoceras biferum*; revision of the *biferum* type (Bockwinkel et al., 2002), however, showed that it is not a *Maeneceras* but a junior synonym *Erfoudites ungeri*, a much younger (UD IV/V) sporadoceratid.

Other markers: Subglobular sporadoceratids previously (Petersen, 1975) assigned to *Maeneceras rotundum*; the German type of *rotundum*, however (Becker, 1993; Bockwinkel et al., 2002), may in fact belong to the younger (UD III) sporadoceratid genus *Xenosporadoceras*. The Canning Basin form seems to represent a new species of *Maeneceras* or *Lagowites*.

Reference section: WAPET C (compare Petersen, 1975). Other rich faunas come from the 'Red Rubble Island Section' (continuation of WAPET C to the east), 'King Brown Hill', 'Sprite Ridge I and II', from near Bobs Bore (collections of P E Playford, Virgin Hills Formation), and from the base of 'Syncline Gully' between Mount Pierre and Needle Eye Rocks. Contemporaneous beds at Casey Falls lack ammonoids. Small faunas occur in sandstones at 'Ayers Rocklet' (Virgin Hills) and west-northwest of Outcamp Hill (Petersen, 1975, sample T37/D17).

Conodont correlation: By superposition, starting at a middle level in the Lower *marginifera* Zone in the reference section (Metzger, 1994) and at 'Sprite Ridge I'; for identical correlation in Europe and North Africa see Becker (1993).

Maeneceras latilobatum Subzone (UD II-G2)

Definition: Entry of early morphotypes of *Maeneceras latilobatum* (outer flank A_2 lobe reaches only 35–45% of mid-flank A_1 lobe, identified as new subspecies of *M. biferum* in Becker and House, 1997; see taxonomic discussion in Bockwinkel et al., 2002).

Remarks: There is probably a morphological continuum between advanced *M. meridionale* and early *M. latilobatum*. Typical morphotypes of *M. meridionale* with much smaller A_2 lobe continue in some sections without intermediates. This indicates true speciation, not just an intraspecific chronomorphocline in early sporadoceratids. Advanced *M. latilobatum* with deeper A_2 lobes are not common in the Canning Basin.

Other markers: A new, rare species of *Maeneceras* with raised ventral saddle.

Reference section: 'Syncline Gully' (Mount Pierre area). Also recognized nearby at 'Straight Gully', WAPET H1-2 and other sections of Petersen (1975), 'Red Rubble Island Section' south of McWhae Ridge (in continuation with WAPET C and section GSWA 1029; see Glenister and Klapper, 1966), west northwest of Outcamp Hill (Petersen, 1975, sample T37/D18), and 'Ayers Rocklet' (Virgin Hills).

Conodont correlation: By superposition, higher part of Lower *marginifera* Zone, based on samples GSWA 1029-C11, WAPET H/1 and WAPET C/C66-88 in Glenister and Klapper (1966).

Sporadoceras teicherti Zone (UD II-H)

Definition: Entry of the oldest true *Sporadoceras* (species with two pointed flank lobes), *S. teicherti*.

Other markers: The large *Maeneceras milleri* (Becker, 2000a, figs 3D–E) and *Posttornoceras glenisteri*.

Reference section: 'Syncline Gully' north of Mount Pierre. Also recognized at neighbouring 'Straight Gully', WAPET H3 (Petersen, 1975), Casey Falls, above 'Red Rubble Island' just south of McWhae Ridge (compare highest part of WAPET C and top of section DP 2 in Petersen, 1975), and questionably west-northwest of Outcamp Hill (Petersen, 1975, sample T37/D19).

Conodont correlation: Starting near the base of the Upper *marginifera* Zone at Casey Falls, based on the entry of *Palmatolepis marginifera utahensis* that is well within the upper range of *P. quadrantinodosa inflexoidea*. Regionally, the Upper *marginifera* Zone is not recognized by the extinction of the latter species, as originally suggested by Sandberg and Ziegler (1973); both taxa are normally thought not to overlap (Ziegler and Sandberg, 1984; Korn and Ziegler, 2002). The same correlation applies to the reference section, to the lower part of WAPET H (Glenister and Klapper, 1966), and to samples from south of McWhae Ridge (Glenister and Klapper, 1966, WAPET C/176-198´). *Posttornoceras* enters in Germany (Becker, 1993) also near the base of the Upper *marginifera* Zone.

Dimeroceras n. sp. Zone and Subzone (UD II-I1)

Definition: Entry of a large compressed new species of *Dimeroceras* (Fig. 2.6, nos 11–12, GSWA F48542), somewhat resembling the German *D. padbergense* Wedekind (1908).

Other markers: Compressed relatives of *Sporadoceras inflexum* (Petersen, 1975, pl. 5, fig. 10).

Reference section: Casey Falls. Also known in lateral continuation at 'Calyx Creek'. Currently, evidence is lacking from contemporaneous beds around Mount Pierre.

Conodont correlation: By superposition, still lower part of Upper *marginifera* Zone in the reference section; probably also in Germany (Enkeberg).

Cycloclymenia n. sp. Subzone (UD II-I2)

Definition: Entry of a new, constricted species of the normally rare ammonoid genus *Cycloclymenia* (Fig. 2.6, nos 7–8, GSWA F48540).

Remarks: The marker species is associated with globally youngest *Armatites planidorsatus* in a narrow faunal band,

which allows a local subdivision of UD II-I. The marker genus has a strange recurrence in much younger, Upper Famennian, beds of Germany.

Reference section: Only known from Casey Falls.

Conodont correlation: By superposition, middle part of Upper *marginifera* Zone (overlapping with the highest range of *Palmatolepis quadrantinodosa inflexoidea*). Matrix from two German *Cycloclymenia* specimens also yielded conodonts of the Upper *marginifera* Zone (Price, 1982).

Sporadoceras equale Zone and Subzone (UD III-A1)

Definition: Entry of *Sporadoceras equale* introduced by R T Becker *in* Becker et al. (2002) for forms assigned by Petersen (1975) to *S. muensteri* (Fig. 2.6, nos 9–10, GSWA F48541). The latter species is a younger and widely misunderstood German species (taxonomic revision in Becker et al., 2002; Becker, 2002).

Other markers: Other sporadoceratids with equally deep adventitious lobes. Slightly higher, *Protornoceras* cf. *simplicius* (previously used as a zonal marker but most species of the genus need revision), and a new species of *Tornia* that is more involute than described Polish species. The large *Maeneceras milleri* disappears at the base of the zone. The strongly plicate rhynchonellid *Hypseloterorhynchus pennatus* Sartenaer (1971) is also typical for the subzone.

Reference section: Casey Falls. Also present in the Mount Pierre area (Petersen, 1975, sample To); first recognized in southern Morocco (Becker et al., 2002).

Conodont correlation: By superposition, middle part of Upper *marginifera* Zone above the last *Palmatolepis quadrantinodosa inflexoidea* in the reference section; compare correlation of oldest 'Sp. *muensteri*' with the Upper *marginifera* Zone in Germany (also above last *P. quadrantinosa inflexoidea*; Ziegler, 1962; Korn and Ziegler, 2002).

Pernoceras delepinei Subzone (UD III-A_2)

Definition: Entry of *Pernoceras delepinei* or of slightly more evolute related forms (aff. *delepinei*); also characterized by the regional extinction of *Dimeroceras*.

Other markers: Perhaps the relatively rare *Maeneceras descendens*.

Reference section: Casey Falls, where it is also characterized by the large marker rhynchonellid *Polyptychorhynchus cavernosus* Sartenaer (1999). Also recognized laterally at 'Calyx Creek', in the Mount Pierre area at WAPET H4-7, other sections (Petersen, 1975), and above the fault zone at 'Cattle Creek'; perhaps at 'Sprite Ridge II' (Virgin Hills) and in 'Straight Gully'.

Conodont correlation: By superposition, higher part of Upper *marginifera* Zone in the reference section (compare age of WAPET H4-7 in Glenister and Klapper, 1966), but perhaps ranging into the Uppermost *marginifera* Zone (= Lower *velifer* Zone) at 'Sprite Ridge II' and 'Straight Gully'. The corresponding *Pernoceras dorsatum* Zone of Germany also falls in the upper half of the Upper *marginifera* Zone (Becker, 1993; Korn and Ziegler, 2002; Korn, 2004).

Sporadoceras angustisellatum Subzone (UD III-B1)

Definition: Entry of *Sporadoceras angustisellatum*, identified in Delépine (1935) as *S. contiguum*, identified in David (1950, fig. 65, fig. a) and Petersen (1975) as *S. posthumum* (Becker, 2002, p. 65). Neither of these species, however, is a sporadoceratid but they belong to the somewhat homoemorphic genus *Posttornoceras*.

Reference section: 'Straight Gully'; also known at other sections in the Mount Pierre area (Glenister and Klapper, 1966; Petersen, 1975), and perhaps at the northwest end of the Virgin Hills (Petersen, 1975, section T40).

Conodont correlation: Uppermost *marginifera* Zone in the reference section (compare spot sample K495 in Glenister and Klapper, 1966); Upper *marginifera* Zone to Uppermost *marginifera* Zone in WAPET H8-11 (Glenister and Klapper, 1966). At the famous Enkeberg locality in Germany (Korn and Ziegler, 2002) and in Trench II at Seßacker (Ziegler, 1962), the oldest pseudoclymenids enter earlier than *Scaphignathus velifer* in the highest part of the Upper *marginifera* Zone. This suggests that the base of the *Pseudoclymenia* Genozone (UD III-B) correlates with a lower level in the Canning Basin than was thought previously (Becker and House, 1997). Consequently, the *angustisellatum* Subzone is re-assigned to UD III-B_1 which fits the correlation in Morocco (Becker et al., 2002).

Pseudoclymenia australis Zone and Subzone (UD III-B2)

Definition: Entry of *Pseudoclymenia australis*, a more evolute (see original diagnosis of Delépine, 1935) close relative of the German *P. dillensis*, which both have slightly more advanced sutures and conches than the German marker species of UD III-B, *P. pseudogoniatites*.

Other markers: Relatives of *Pernoceras delepinei* with lingulate flank lobe (Fig. 2.6, nos 13–14, GSWA F48543), the regionally rare but widespread (Germany, Morocco; Becker et al., 2002) index form *Planitornoceras euryomphalum*, and a compressed new *Falcitornoceras* related to *F. bilobatum*, which was first recognized by Delépine (1935) as *Tornoceras* sp. nov. *Sporadoceras angustisellatum* has its regional acme in this subzone.

Reference section: 'Straight Gully'; very fossiliferous at WAPET H and around Needle Eye Rocks (compare Petersen, 1975); perhaps (questionable specimens) recognizable at 'Sprite Ridge II' (Virgin Hills).

Conodont correlation: Uppermost *marginifera* Zone in the reference section and in WAPET H (Glenister and Klapper,

1966). German *Pseudoclymenia* faunas range from highest parts of the Upper *marginifera* Zone to the Uppermost *marginifera* Zone (Price, 1982; Korn and Ziegler, 2002). The correlation with Spanish pseudoclymeniids is unknown (Sanz-López et al., 1999).

Falcitornoceras n. sp. M (upper range) Subzone (UD III-B3)

Definition: Sudden extinction of the very distinctive, evolute pseudoclymenids, well below the entry of oldest clymenids.

Remarks: The extinction of the Pseudoclymeniidae before the appearance of the first clymenids was a widespread phenomenon in the paleotropics, affecting roughly simultaneously Germany, Russia, and Australia. This unexplained small-scale global extinction event can be used to distinguish a final subzone of UD III-B which has abundant *F.* n. sp. M (a relative of *F. bilobatum*), other longer ranging ammonoids, and a still un-named (Sartenaer, 2004) marker rhynchonellid homeomorphic to *Rozmanaria*.

Reference section: So far only recognized in WAPET H.

Conodont correlation: By superposition, higher part of Uppermost *marginifera* Zone to Lower *trachytera* Zone; the latter zones cannot be discriminated in the reference section since *Palmatolepis rugosa trachytera* is lacking in the Canning Basin. In Germany, beds at the top of the Uppermost *marginifera* Zone and of the Lower *trachytera* Zone (Kronberg et al., 1960; Ziegler, 1962; Korn and Ziegler, 2002; Schülke et al., 2003; new unpublished data of M. Piecha) contain the oldest faunas of UD III-C (= former do IIIß).

Protactoclymenia euryomphala Zone (UD III-C)

Definition: Regional first entry of clymenids, especially of compressed close relatives of *Protactoclymenia euryomphala* (Fig. 2.6, nos 15–16, GSWA F48544), which type, however, is younger (UD IV-A; Wedekind, 1914).

Other markers: A new prolobitid genus without constrictions and rare involute clymenids which resemble the poorly known *P. krasnopolski* from Russia.

Reference section: Only recognized at WAPET H. A *Cyrtoclymenia* sp. indet. reported by Glenister and Klapper (1966) from the Bugle Gap area was not described subsequently and its unusually old conodont age (older than *velifer* Zone) places doubt on the identification; confusion of convolute tornoceratids with a cyrtoclymenid is possible.

Conodont correlation: Lower to Upper *trachytera* Zone, but there are no distinctive conodont faunas from the reference section. At the Enkeberg in Germany (Korn and Ziegler, 2002), *Protactoclymenia* enters at a level in the middle part of UD III-C (upper part of *Prolobites delphinus* Subzone). It may range into the Lower *trachytera* Zone at Beringhauser Tunnel (Schülke et al., 2003).

Protactoclymenia eurylobica Zone (UD IV-A)

Definition: Entry of *Protactoclymenia eurylobica* that was originally described by Petersen (1975) as a *Platyclymenia* (*Pleuroclymenia*); see generic revision by Becker (2000b).

Other markers: *Raymondiceras inceptum* and poorly preserved *Platyclymenia* s. str.

Remarks: The sudden incursion of hypoxic and mixed neritic–pelagic faunas with many cyrtospiriferids and true *Platyclymenia* in the lower Piker Hills Formation suggests correlation with the global and transgressive *Annulata* Event (Becker and House, 1997; Becker et al., 2004a). A similar faunal assemblage with true *Raymondiceras* is typical for the far distant Trident Member of the Three Forks Formation of Montana.

Reference section: Piker Hills, section B.

Conodont correlation: Probably Upper *trachytera* Zone (= level of Annulata Event and of oldest true *Platyclymenia* in Germany, Korn and Luppold, 1987) to Lower *postera* Zone (upper part of *annulata* Zone of Germany; Korn and Ziegler, 2002; Schülke et al., 2003). Conodont faunas from the reference section are zonally undiagnostic but lack index forms of younger zones. *Polygnathus collinsoni* is first recorded somewhat above the base of the reference section and may indicate the *postera* (Z Belka *in* Ginter et al., 2002) or Lower to Middle *styriacus* Zone (Druce, 1976, p. 184). However, the range of the species is not really correlated with the deeper water conodont succession. The Trident Member of Montana falls in the Upper *trachytera* Zone (Klapper, 1966; Sandberg and Klapper, 1967).

Protoxyclymenia sp. Zone (UD IV-B/C)

Definition: Entry of *Protoxyclymenia*, probably including *Laevigites*? sp. indet. mentioned from the '*Productella* Zone' by Teichert (1949), which included the Piker Hills Formation.

Reference section: Only known from Piker Hills (Petersen, 1975). Re-sampling did not provide new material of this important marker genus. However, higher beds of Section B have large calcareous cyrtoclymenids, assigned by Petersen (1975) to *Cyrto*. cf. *stenomphala*, which need closer study and which may fall in higher parts of the *Platyclymenia* Stufe. There is also a rather large *Platyclymenia* fragment; similar giants occur in Morocco (Korn, 1999; Becker et al., 2002) just above the *Annulata* Event.

Conodont correlation: In Thuringia (section Alte Heerstrasse, ammonoids in Müller, 1956; conodonts in Brügge, 1973), *Protoxyclymenia* occurs first in limestone nodules that range, by superposition, from a high part of

the Lower *postera* Zone to the Upper *postera* Zone. The genus is also known from the Lower (new data) and Upper *postera* (Schülke et al., 2003) zones of the Rhenish Massif and the Lower *expansa* Zone of Franconia (Wäschholz, conodonts *in* Korn and Luppold, 1987).

Endosiphonites n. sp. Zone (UD V-A1)

Definition: Entry of a new species of *Endosiphonites*, with very shallow lobes on inner flanks, that is closely related to *E. muensteri* from Southwest England and Morocco and to *E. bowsheri* from New Mexico.

Remarks: *Endosiphonites* (including *Costaclymenia* as a subjective junior synonym, Becker et al., 2002) is the international marker genus of UD V-A_1 and enters in the Dasberg Event beds of Morocco (see also Korn et al., 2000; Ginter et al., 2002), the Montagne Noire, and Germany. The first record of the genus in the Canning Basin suggests that the youngest influx of ammonoids in marginal-slope deposits of the reef complex was caused by the global Dasberg Transgression. Close relationships of *Falciclymenia bowsheri* Miller and Collinson (1951) from the Box Member of the Percha Shale of New Mexico with the type species, *E. muensteri*, were first recognized by Price (1982). True *Falciclymenia* (see revision in Becker et al., 2002) are more involute and have a lobe centred on the umbilical seam.

The single clymenid described by Glenister (1962) and Petersen (1975) from the subsurface Clanmeyer Siltstone could belong to either the Rodeckiinae (protoxyclymenids and relatives) or Clymeniidae, which gives an age range from UD IV-B to UD V-B. It is not possible to refer this important specimen to one of the two youngest Canning Basin ammonoid levels.

Reference section: Dingo Gap, Section A (youngest marginal-slope facies of the Napier Formation).

Conodont correlation: The Dasberg Event beds of Morocco start at the boundary between the Lower and Middle *expansa* Zone (Ginter et al., 2002; Hartenfels and Becker, 2006). Correlation of the basal part of the Dasbergian with the Middle *expansa* Zone is now also indicated for the Rhenish Massif (transgressive Upper Knoppenbissen Formation, Piecha, 2004). The Box Member of the Percha Shale has been dated as Lower *expansa* Zone (Sandberg et al., 1989) but the conodonts recorded by Sandberg (1976, sample 8, lacking *Polygnathus styriacus*) are not in conflict with an age at the top of zone.

Facies distribution of Canning Basin ammonoids

Ammonoids occur in a wide range of microfacies and biofacies in the Canning Basin reef complexes but are normally lacking in true reefal-slope and platform limestones. A bedding-plane assemblage of *Beloceras* in platform facies near Brooking Springs Homestead is a rare exception that was probably swept in during a storm. Dead Devonian ammonoids normally became quickly water-logged, which prevented long post-mortem floating. Since most shells were rather thin, reworking normally led to crushing, resulting in poor preservation in high-energy depositional settings. However, there are some faunas from basin-floor sandstone fans and rather coarse detrital and crinoidal limestones in the Virgin Hills area. The calculated maximum implosion depths (Hewitt, 1996) of most ammonoids were less than 300 m with the lowest value for *Beloceras* (108 m), and the highest for *Tornoceras* (~300 m). This suggests that exposed parts of the inter-reef basins in the Virgin Hills area may not have exceeded more than 300 m of water depth. Most ammonoids probably lived in outer-shelf slope environments, which is supported by their wide distribution in marginal-slope facies in the Canning Basin.

The basinal Lower to Middle Frasnian Gogo Formation is characterized by low-diversity ammonoid assemblages preserved in limestone or limestone concretions, which are rich in styliolinids and radiolarians. Single concretions may contain monospecific mass occurrences or associations of two or three species. The youngest ammonoids of the Gogo Formation at Outcamp Hill fall in the *Prochorites alveolatus* Zone (UD I-F_1) and are characterized by joint occurrences with orthoconic cephalopods and various pelagic bivalve genera, such as *Buchiola* and *Ontaria*.

Hypoxic Lower to Middle Frasnian tongues within the Sadler Limestone and Virgin Hills Formation contain originally pyritic, secondarily hematitic or goethitic, low to moderately diverse ammonoid faunas. The youngest faunas fall in the *Mesobeloceras housei* Zone (UD I-G_{2a}) at WCB 366. The regionally oldest ammonoids (basal UD I-B) from near Siphon Spring are monospecific and part of a mixed neritic–pelagic association dominated by brachiopods. This composition suggests that the topographic relief of the reef complexes was still relatively low in the basal Upper Devonian, increasing, however, rapidly during the Lower Frasnian. Middle Frasnian faunas from around McIntyre Knolls have only restricted and accessory benthic faunal elements, including *Buchiola*, and some gastropods. A brachiopod-dominated, mixed neritic–pelagic and low–oxygen biofacies, but rich in plant remains, reappeared in the Late Famennian (UD IV-A/C) Piker Hills Formation at a time when the basin had become too shallow for fully pelagic faunas. This is also evidenced by the lack of the deeper shelf *Palmatolepis* biofacies at that time.

The best preserved and richest ammonoid assemblages are from reddish, condensed, and micritic cephalopod limestones of the Virgin Hills Formation, which represents a rather oligotrophic biofacies. Examples are the Middle and Upper Frasnian beloceratid beds, which transgressed reef slopes. The typical assemblage also contains small bivalves, such as *Buchiola*, weakly ornamented ostracods, trilobites, small gastropods, crinoids, solitary deeper water corals, subordinate fish remains, nautiloids, and rare rhynchonellids. As in the Montagne Noire (House et al., 2000b, p. 68) and Morocco (e.g. Becker and House, 2000b), the lack of *Beloceras* in Upper Frasnian faunas, for example in the local equivalent of the Upper Kellwasser Beds (‘*Manticoceras’ guppyi* Bed), suggests changes in trophic conditions. Other moderately diverse

faunas occur in argillaceous or bioclastic limestones of the Upper Frasnian and Famennian. A somewhat shallower setting is indicated by associations with diverse sponges, receptaculitids, large gastropods and bivalves, and large rhynchonellids. During transgressions and times of sediment starvation, low-diversity or monospecific ammonoid associations can be found in stromatolites (e.g. at Casey Falls and in the Virgin Hills) or other microbial limestones (e.g. at WAPET C). Even shallower water is indicated by the incoming of typical neritic brachiopod groups, such as atrypids (only in the Frasnian, e.g. at 'Flare Hill') or spiriferids (e.g. in the Middle Famennian at 'Sprite Ridge'). Successions of more proximal reef talus, consisting of breccias, slump beds, debris flows and proximal turbidites, which are often dolomitized, contain few or no ammonoids. This applies, for example, to the massive limestones in the top part of the Virgin Hills Formation in the Bugle Gap area, to most parts of the Frasnian Sadler Limestone, and to the Famennian Napier Formation. The youngest clymenids from the Napier Formation at Dingo Gap suggest a very brief re-immigration of ammonoids into a more proximal slope succession with a transgressive pulse.

Acknowledgements

This revision of Canning Basin ammonoid biostratigraphy would have been impossible without the encouragement, enthusiastic support, and field knowledge of P E Playford, including technical and logistic support by the Geological Survey of Western Australia. We are also indebted to the former Bureau of Mineral Resources (now Geoscience Australia), Canberra, especially to R S Nicoll. The field company of W T Kirchgasser, R W Brown, R Feist, R Crick, R M Hocking, I Copp, A D George, and others was greatly appreciated and stimulated our work. G Klapper not only accompanied us during several field seasons but also supplied us with a wealth of conodont data and reviewed the manuscript. Funding was provided by NERC (Great Britain) and the DFG (Germany).

References

Becker, R T 1993, Stratigraphische Gliederung und Ammonoideen–Faunen im Nehdenium (Oberdevon II) von Europa und Nord-Afrika: Courier Forschungsinstitut Senckenberg, v. 155, p. 1–405.

Becker, R T 2000a, Palaeobiogeographic relationships and diversity of Upper Devonian ammonoids from Western Australia: Records of the Western Australian Museum, Supplement, v. 58, p. 385–401.

Becker, R T 2000b, Taxonomy, evolutionary history, and distribution of the middle to late Famennian Wocklumeriina (Ammonoidea, Clymeniida): Mitteilungen aus dem Museum für Naturkunde Berlin, Geowissenschaftliche Reihe, v. 3, p. 27–75.

Becker, R T 2002, *Alpinites* and other Posttornoceratidae (Goniatitida, Famennian): Mitteilungen aus dem Museum für Naturkunde Berlin, Geowissenschaftliche Reihe, v. 5, p. 51–73.

Becker, R T 2003, Famennian Ammonoid Zones of the Eastern Anti-Atlas — Implications for Substage Subdivision: SDS Newsletter, v. 19, p. 20–24.

Becker, R T 2004, Ammonoid extinctions near the Frasnian–Famennian boundary: Sixth International Symposium, Cephalopods — Present and Past, September 16–19, 2004, Abstracts, p. 25–26.

Becker, R T 2007, Results of the voting on Givetian and Frasnian substages: SDS Newsletter, v. 22, p. 2.

Becker, R T, Aboussalam, Z S, Bockwinkel, J, Ebbighausen, V, El Hassani, A and Nübel, H 2004b, The Givetian and Frasnian at Oued Mzerreb (Tata region, eastern Dra Valley): Documents de l´Institut Scientifique, v. 19, p. 29–43.

Becker, R T, Ashouri, A R and Yazdi, M 2004a, The Upper Devonian *Annulata* Event in the Shotori Range (eastern Iran): Neues Jahrbuch für Geologie und Paläontologie, Abhandlungen, v. 231(1), p. 119–143.

Becker, R T and House, M R 1997, Sea-level changes in the Upper Devonian of the Canning Basin, Western Australia: Courier Forschungsinstitut Senckenberg, v. 199, p. 129–146.

Becker, R T and House, M R 2000a, Devonian ammonoid zones and their correlation with established series and stage boundaries: Courier Forschungsinstitut Senckenberg, v. 220, p. 113–151.

Becker, R T and House, M R 2000b, Late Givetian and Frasnian ammonoid succession at Bou Tchrafine (Anti-Atlas, Southern Morocco): Notes et Mémoires du Service Géologique, v. 399, p. 27–36.

Becker, R T, House, M R, Kirchgasser, W T and Playford P E 1991, Sedimentary and faunal changes across the Frasnian/Famennian boundary in the Canning Basin of Western Australia: Historical Biology, v. 5, p. 183–196.

Becker, R T, House, M R and Kirchgasser, W T 1993, Devonian goniatite biostratigraphy and timing of facies movements in the Frasnian of the Canning Basin, Western Australia, *in* High resolution stratigraphy *edited by* E Hailwood and R B Kidd: Geological Society, Special Publication 70, p. 293–321.

Becker, R T, House, M R, Menner, V V and Ovnatanova, N S 2000, Revision of ammonoid biostratigraphy in the Frasnian (Upper Devonian) of the Southern Timan (Northeast Russian Platform): Acta Geologica Polonica, v. 50, p. 67–97.

Becker, R T, House, M R, Bockwinkel, J, Ebbighausen, V and Aboussalam, Z S 2002, Famennian ammonoid zones of the eastern Anti-Atlas (southern Morocco): Münster´sche Forschungen zur Geologie und Paläontologie, v. 93, p. 159–205.

Bockwinkel, J, Becker, R T and Ebbighausen, V 2002, Morphometry and Taxonomy of Lower Famennian Sporadoceratidae (Goniatitida) from Southern Morocco: Abhandlungen der Geologischen Bundesanstalt, v. 57, p. 279–297.

Brügge, N 1973, Zur stratigraphischen Einstufung des Oberdevon-Profils 'Alte Heerstraße' bei Schleiz, Bezirk Gera: Zeitschrift für geologische Wissenschaften, v. 1(3), p. 319–327.

Clausen, C D 1969, Oberdevonische Cephalopoden aus dem Rheinischen Schiefergebirge. II. Gephuroceratidae, Beloceratidae: Palaeontographica, Abteilung A, v. 132, p. 95–178.

Cook, A G, Blodgett, R B and Becker, R T 2003, Late Devonian gastropods from the Canning Basin, Western Australia: Alcheringa, v. 27, p. 181–207.

David, T W E 1950, The geology of the Commonwealth of Australia: v. 1, 747p.

Delépine, G 1933, Upper Devonian goniatites from Mount Pierre, Kimberley District, Western Australia: Geological Society of London, Abstract and Program of Session 1932–1933, v. 1267, p. 118.

Delépine, G 1935, Upper Devonian goniatites from Mount Pierre, Kimberley District, Western Australia: Geological Society of London, Quarterly Journal, v. 91, p. 208–215.

Druce, E C 1976, Conodont biostratigraphy of the Upper Devonian reef complexes of the Canning Basin, Western Australia: Australia, Bureau of Mineral Resources, Geology and Geophysics, Bulletin 158(1), p. 1–303.

Ebbighausen, V, Becker, R T and Bockwinkel, J 2002, Morphometric analyses and taxonomy of oxyconic goniatites (Paratornoceratinae n. subfam.) from the Early Famennian of the Tafilalt (Anti-Atlas, Morocco): Abhandlungen der Geologischen Bundesanstalt, v. 57, p. 167–180.

Feist, R and Becker, R T 1997, Discovery of Famennian trilobites in Australia (Late Devonian, Canning Basin, NW Australia): Geobios, M.S., v. 20, p. 231–242.

Foord, A H 1890, Description of fossils from the Kimberley District, Western Australia: Geological Magazine, new series, v. 7, p. 98–106.

George, A D, Playford, P E, Powell, C M and Tornatora, P M 1997, Lithofacies and sequence development on an Upper Devonian mixed carbonate–siliciclastic forereef slope, Canning Basin, Western Australia: Sedimentology, p. 843–867.

Ginter, M, Hairapetian, V and Klug, C, 2002, Famennian chondrichthyans from the shelves of North Gondwana: Acta Geologica Polonica, v. 52(2), p. 169–215.

Glenister, B F 1958, Upper Devonian ammonoids from the *Manticoceras* Zone, Fitzroy Basin, Western Australia: Journal of Paleontology, v. 32(1), p. 58–96.

Glenister, B F 1962, *Clymenia* and conodonts from Frome Rocks No. 2 Well: Australia, Bureau of Mineral Resources, Geology and Geophysics, Petroleum Search Subsidy Acts Publication, v. 8, p. 32–34.

Glenister, B F and Klapper, G 1966, Upper Devonian conodonts from the Canning Basin, Western Australia: Journal of Paleontology, v. 40, p. 777–842.

Hartenfels, S and Becker, R T 2006, The *Annulata* and Dasberg Events (Famennian) in the Tafilalt and Maider (eastern Anti-Atlas, SE Morocco), *in* Ancient life and modern approaches *edited by* Q Yang, Y Wang, and E Weldon: University of Science and Technology of China Press, Abstracts of the Second International Palaeontological Congress, p. 358.

Hewitt, R A 1996, Architecture and strength of the ammonoid shell, *in* Ammonoid paleobiology *edited by* N H Landman, K Tanabe, and Y Shigeta: Topics in Geobiology, v. 13, p. 297–339.

Holzapfel, E 1882, Die Goniatiten-Kalke von Adorf in Waldeck.: Palaeontographica, neue Folge, v. 8(6), p. 225–261 and 6 plates.

House, M R, Becker, R T, Feist, R, Flajs, G, Girard, C and Klapper, G 2000b, The Frasnian/Famennian boundary GSSP at Coumiac, Southern France: Courier Forschungsinstitut Senckenberg, v. 225, p. 59–75.

House, M R and Kirchgasser, W T 1993, Devonian goniatite biostratigraphy and timing of facies movements in the Frasnian of eastern North America: Geological Society, Special Publication 70, p. 267–292.

House, M R, Menner, V V, Becker, R T, Klapper, G, Ovnatanova, N S and Kuz´min, V 2000a, Reef episodes, anoxia and sea-level changes in the Frasnian of the southern Timan (NE Russian platform): Geological Society, Special Publication 178, p. 147–176.

House, M R and Ziegler, W 1977, The Goniatite and Conodont sequence in the early Upper Devonian at Adorf, Germany: Geologica et Palaeontologica, v. 11, p. 69–108.

Klapper, G 1966, Upper Devonian and Lower Mississippian conodont zones in Montana, Wyoming, and South Dakota: The University of Kansas, Paleontological Contributions, v. 3, p. 1–43.

Klapper, G 1997, Graphic correlation of Frasnian (Upper Devonian) sequences in Montagne Noire, France, and western Canada: Geological Society of America, Special Paper 321, p. 113–129.

Klapper, G 2007, Frasnian (Upper Devonian) conodont succession at Horse Spring and correlative sections, Canning Basin, Western Australia: Journal of Paleontology, v. 81(3), p. 513–537.

Klapper, G and Becker, R T 1999, Comparison of Frasnian (Upper Devonian) conodont zonations: Bolletino della Società Paleontologica Italiana, v. 37(2–3), p. 339–348.

Klapper, G, Uyeno, T T, Armstrong, D K and Telford, P G 2004, Conodonts of the Williams Island and Long Rapids formations (Upper Devonian, Frasnian–Famennian) of the Onakawana B Drillhole, Moose River Basin, northern Ontario, with a revision of Lower Famennian species: Journal of Paleontology, v. 78, p. 371–387.

Korn, D 1999, Famennian ammonoid stratigraphy of the Ma´der and Tafilalt (eastern Anti-Atlas, Morocco): Abhandlungen der Geologischen Bundesanstalt, v. 54, p. 147–179.

Korn, D 2004, The mid-Famennian ammonoid succession in the Rhenish Mountains: the '*annulata* Event' reconsidered: Geological Quarterly, v. 48(3), p. 245–252.

Korn, D, Klug, C and Reisdorf, A 2000, Middle Famennian ammonoid stratigraphy in the Amessoui Syncline (Late Devonian, eastern Anti-Atlas, Morocco): Travaux de l´Institut Scientifique, Rabat, Série Géologie & Géographie Physique, v. 20, p. 69–77.

Korn, D and Klug, C 2002, Ammoneae Devonicae: Fossilium Catalogus I: Animalia, v. 138, 375p.

Korn, D and Luppold, F W, 1987, Nach Clymenien und Conodonten gegliederte Profile des oberen Famennium im Rheinischen Schiefergebirge: Courier Forschungsinstitut Senckenberg, v. 92, p. 199–223.

Korn, D and Ziegler, W 2002, The ammonoid and conodont zonation at Enkenberg (Famennian, Late Devonian; Rhenish Mountains): Senckenbergiana lethaea, v. 82(2), p. 453–462.

Kronberg, P, Pilger, A, Scherp, A and Ziegler, W 1960, Spuren altvariskischer Bewegungen im nordöstlichen Teil des Rheinischen Schiefergebirges: Fortschritte in der Geologie von Rheinland und Westfalen, v. 3(1), p. 1–46.

Metzger, R A 1994, Multielement reconstructions of *Palmatolepis* and *Polygnathus* (Upper Devonian, Famennian) from the Canning Basin, Western Australia and Bactrian Mountain, Nevada: Journal of Paleontology, v. 68 (3), p. 617–647.

Miller, A K and Collinson, C, 1951, A clymenoid ammonoid from New Mexico: American Journal of Science, v. 249, p. 600–603.

Miller, A K and Furnish, W M 1960, Gephyroceratidae Frech 1897: proposed acceptance of the emendation to Gephuroceratidae (Class Cephalopoda, Order Ammonoidea), Z. N.(S.) 982: Bulletin of zoological Nomenclature, v. 18(1), p. 73–74.

Montesinos, J R and Henn, A H 1986, La Fauna de *Pharciceras* (Ammonoidea) de la Formacion Cardaño (Dominio Palentino, Cordillera Cantabrica, NO de España: Trabajos de Geologia, v. 16, p. 61–76.

Müller, K J 1956, Cephalopodenfauna und Stratigraphie des Oberdevons von Schleiz und Zeulenroda in Thüringen: Beihefte zum Geologischen Jahrbuch, v. 20, p. 1–93.

Nicoll, R S and Playford, P E 1993, Upper Devonian iridium anomalies, conodont zonation and the Frasnian–Famennian boundary in the Canning Basin, Western Australia: Palaeogeography, Palaeoclimatology, Palaeoecology, v. 104, p. 105–113.

Over, J 2004, SDS — Frasnian subdivisions: SDS Newsletter, v. 20, p. 4.

Petersen, M S 1975, Upper Devonian (Famennian) Ammonoids From the Canning Basin, Western Australia: Journal of Paleontology, Memoir, v. 8, p. 1–55.

Piecha, M 2004, Late Famennian conodonts from the Refrath 1 Borehole (Bergisch Gladbach-Paffrath Syncline; Ardennes-Rhenish Massif, Germany): Courier Forschungsinstitut Senckenberg, v. 251, p. 253–265.

Playford, P E 1980, Devonian 'Great Barrier Reef' of Canning Basin, Western Australia: American Association of Petroleum Geologists, Bulletin 64 (6), p. 814–840.

Playford, P E 1981, Devonian reef complexes of the Canning Basin, Western Australia: Fifth Australian Geological Convention, Field Excursion Guidebook, 64p.

Playford, P E 2002, Palaeokarst, pseudokarst, and sequence stratigraphy in Devonian reef complexes of the Canning Basin, Western Australia, *in* The sedimentary basins of Western Australia 3 *edited by* M Keep and S J Moss: Proceedings of the Petroleum Exploration Society of Australia Symposium, Perth, Western Australia, p. 763–793.

Playford, P E and Hocking, R M 1999, Devonian reef complexes of the Canning Basin: Geological Survey of Western Australia, 7 maps.

Price, J D 1982, Some Famennian (Upper Devonian) ammonoids from north-western Europe: United Kingdom, University of Hull, PhD thesis (unpublished).

Sandberg, C A 1976, Conodont biofacies of Late Devonian *Polygnathus styriacus* Zone in Western United States: The Geological Association of Canada, Special Paper 15, p. 171–186.

Sandberg, C A and Klapper, G 1967, Stratigraphy, age, and paleotectonic significance of the Cottonwood Canyon Member of the Madison Limestone in Wyoming and Montana: Geological Survey, Bulletin 1251-B, p. 1–70.

Sandberg, C A, Poole, F G and Johnson, J G 1989, Upper Devonian of Western United States: Canadian Society of Petroleum Geologists, Memoir 14 (I), p. 183–220.

Sandberg, C A and Ziegler, W 1973, Refinement of standard Upper Devonian conodont zonation based on sections in Nevada and West Germany: Geologica et Palaeontologica, v. 7, p. 97–122.

Sandberger, G and Sandberger, F 1851, Die Versteinerungen des rheinischen Schichtensystems in Nassau, p. 73–104, pl. 9–13.

Sanz-López, J, García-López, S, Montesinos, J R and Arbizu, M 1999, Biostratigraphy and sedimentation of the Vidrieros Formation (middle Famennian–lower Tournaisian) in the Gildar-Montó unit (northwest Spain): Bolletino della Società Paleontologico Italiana, v. 37(2–3), p. 393–406.

Sartenaer, P 1971, Genres Rhynchonellides (Brachiopodes) nouveaux : Bulletin de l´Institut royal des Sciences naturelles de Belgique, v. 47(4), p. 1–7.

Sartenaer, P 1999, A new mid-Famennian rhynchonellid (brachiopod) genus from the Canning Basin, Western Australia: Annales de la Societe Géologique du Nord, v. 7 p. 79–84.

Sartenaer, P 2004, Rozmanariidae, a family with problems: Devonian neritic–pelagic correlation and events, International Meeting on Stratigraphy, Rabat, Morocco, March 1–10, 2004, Abstracts, p. 38.

Schindewolf, O H 1923, Beiträge zur Kenntnis des Paläozoikums in Oberfranken, Ostthüringen und dem Sächsischen Vogtlande. 1. Stratigraphie und Ammoneenfauna des Oberdevons von Hof a. S.: Neues Jahrbuch für Mineralogie, Geologie und Paläontologie, Beilage-Band, v. 49, p. 250–357 and p. 393–509.

Schülke, I, Korn, D, Popp, A and Ziegler, W, 2003, Potential reference section for the Early/Middle Famennian boundary at the Beringhauser Tunnel (Rheinisches Schiefergebirge, NW Germany): SDS Newsletter, v. 19, p. 36–46.

Talent, J A, Mawson, R, Aitchinson, J C, Becker, R T, Bell, K N, Bradshaw, M A, Burrow, C J, Cook, A G, Dargan, G M, Douglas, J G, Edgecombe, G D, Feist, M, Jones, P J, Long, J A, Philips-Ross, J R, Picket, J W, Playford, G, Rickards, R B, Webby, B D, Winchester-Seto, T, Wright, A J, Young, G C and Zhen, Y-Y 2000, Devonian palaeobiogeography of Australia and adjoining regions: Memoir of the Association of Australasian Palaeontologists, v. 23, p. 167–257.

Teichert, C 1941, Upper Devonian goniatite succession of Western Australia: American Journal of Science, v. 239, p. 148–153.

Teichert, C 1943, The Devonian of Western Australia, a preliminary review: American Journal of Science, v. 241, p. 69–94 and p. 167–184.

Teichert, C 1949, Stratigraphy and palaeontology of Devonian portion of Kimberley Division, Western Australia: Australia, Bureau of Mineral Resources, Geology & Geophysics, Report 2, 50p.

Wade, A 1924, Petroleum prospects, Kimberley District of Western Australia, and Northern Territory: Special publication of the Parliament of the Commonwealth of Australia, p. 1–63.

Wade, A 1938, The geological succession in the West Kimberley District of Western Australia: Australian and New Zealand Association for the Advancement of Science, Report 23, p. 93–96.

Wedekind, R 1908, Die Cephalopodenfauna des höheren Oberdevon am Enkeberge: Neues Jahrbuch für Mineralogie; Geologie und Paläontologie, Beilage-Band, v. 26, p. 565–633, pls 39–45.

Wedekind, R 1913, Die Goniatitenkalke des unteren Oberdevon vom Martenberg bei Adorf: Sitzungsberichte der Gesellschaft naturforschender Freunde zu Berlin, v. 1, p. 1–77.

Wedekind, R 1914, Monographie der Clymenien des Rheinischen Gebirges: Abhandlungen der Königlichen Gesellschaft der Wissenschaften zu Göttingen, mathematisch-physikalische Klasse, neue Folge, v. 10(1), p. 1–73 + pl. 1–7.

Yang, Y 1984, Devonian System and its ammonoid fauna from Baoshan District, Western Yunnan: Journal of the Chengdu College of Geology, v. for 1984, p. 22–36 [in Chinese].

Yatskov, S V 1990, K sistematike semeystva Beloceratidae (Ammonoidea): Trudy Paleontologicheskogo Instituta, v. 243, p. 36–51.

Ziegler, W 1962, Taxionomie und Phylogenie Oberdevonischer Conodonten und ihre stratigraphische Bedeutung: Abhandlungen des Hessischen Landesamtes für Bodenforschung, v. 38, p. 1–66 + 14 pls.

Ziegler, W and Sandberg, C A 1984, *Palmatolepis*-based revision of upper part of standard Late Devonian conodont zonation: Geological Society of America, Special Paper 196, p. 179–194.

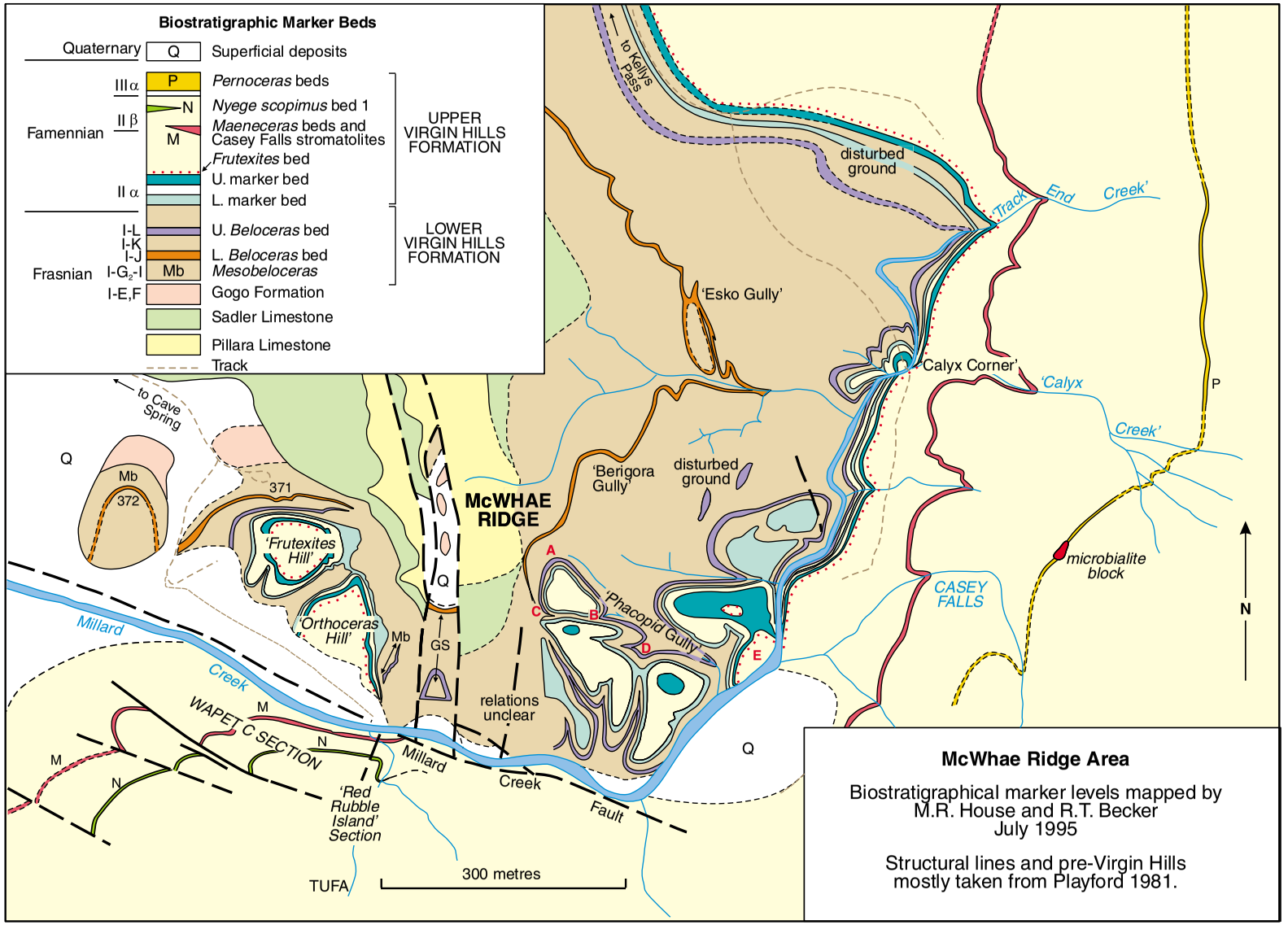

Figure 2.1. Geology of the McWhae Ridge area (based on Playford, 1981, and on updates by Playford and Hocking, 1999) showing the positions of several localities, including WCB sections (371, 372) and informal field names referred to in the text. Biostratigraphic and lithostratigraphic marker units, including the *Maeneceras* (M), *Nyege scopimus* (N) and *Pernoceras* (P) Beds, were mapped by M R House and R T Becker. A–E = sections around 'Phacopid Gully', GS = Graben Section, Mb = *Mesobeloceras* Section.

chrono-stratigraphy			key	goniatite zones	goniatite subzones	conodont zones
FAMENNIAN	Upper	D.	V-A1	*Endosiphonites* n. sp.		Middle *expansa* Zone
		HEMBERGIAN	IV-C	*Protoxyclymenia* sp.		Lower *expansa* Zone
			IV-B			Upper *postera* Zone
			IV-A	*Protactoclymenia eurylobica*		Lower *postera* Zone
	Middle		III-C	*Protactoclymenia euryomphala*		Upper *trachytera* Zone
			III-B3	*Falcitornoceras* n. sp. M [ur]		Lower *trachytera* Zone
			III-B2	*Pseudoclymenia australis*	*Pseudoclymenia australis*	Uppermost *marginifera* Zone
			III-B1		*Sporadoceras angustisellatum*	
			III-A2	*Sporadoceras equale*	*Pernoceras delepinei*	Upper *marginifera* Zone
			III-A1		*Sporadoceras equale*	
		NEHDENIAN	II-I2	*Dimeroceras* n. sp.	*Cycloclymenia* n. sp.	
			II-I1		*Dimeroceras* n. sp.	
			II-H	*Sporadoceras teicherti*		
	Lower		II-G2	*Maeneceras meridionale*	*Maeneceras latilobatum*	Lower *marginifera* Zone
			II-G1		*Maeneceras meridionale*	
			II-F2	*Paratornoceras polonicum*	*Acrimeroceras clarkei*	
			II-F1		*Paratornoceras polonicum*	Upper *rhomboidea* Zone
			II-E2	*Praemeroceras petterae*	*Praemeroceras primaevum*	
			II-E1		*Praemeroceras petterae*	Lower *rhomboidea* Zone
			II-D	*Oxytornoceras* n. sp.		Uppermost *crepida* Zone
			II-C	*"Falcitornoceras"* n. sp. 1		Upper *crepida* Zone
			II-B			Middle *crepida* Zone
			II-A	[no ammonoids]		Lower *crepida* Zone
						triangularis Zones
FRASNIAN	Upper	ADORFIAN	I-L2	*Crickites lindneri*	*Manticoceras cordatum* [ur]	Zone 13c
			I-L1b		*"Manticoceras "* guppyi	Zone 13b
			I-L1a		*Crickites lindneri*	Zone 13a
			I-K	*Manticoceras* n. sp. 5		Zone 12
			I-J3	*Maternoceras retorquatum*	*Clauseniceras* n. sp.	
			I-J2		*Virginoceras erraticum*	
			I-J1		*Maternoceras retorquatum*	
	Middle		I-I2	*Playfordites tripartitus*		Zone 11
			I-I1	*Costamanticoceras koeneni*		
			I-H	*Beloceras tenuistriatum*		Zones 9 - 10
			I-G2b	*Mesobeloceras thomasi*		Zone 8
			I-G2a	*Mesobeloceras housei*		Zone 7
			I-G1	*Naplesites naplense* Gp.		Zone 6
			I-F3	*Sphaeromanticoceras affine*		
			I-F2	*Gogoceras nicolli*		Zone 5
			I-F1	*Prochorites alveolatus*		
			I-E3	*Manticoceras* n. sp. 1		
			I-E2	*Ponticeras discoidale*		
			I-E1	*Probeloceras lutheri lutheri*		
	Lower		I-D	[no ammonoids]		Zone 4
			I-C2	*Timanites angustus*	*Manticoceras* sp.	
			I-C1		*Timanites angustus*	
			I-B3	*Koenenites* n. sp. A		Zone 3
			I-B2	*"Hoeninghausia" pons*		Zone 2
			I-B1	*Koenenites* n. sp. B		
			I-A	[no ammonoids]		Zone 1

PEP326 02.06.09

Figure 2.2. Correlation of ammonoid and conodont zonation in the Canning Basin; [ur] = upper range of index species since the zone is defined by the extinction of other taxa (conodont data supplied by G Klapper, see Klapper, this volume). The zonal key refers to subdivisions of the Upper Devonian (UD).

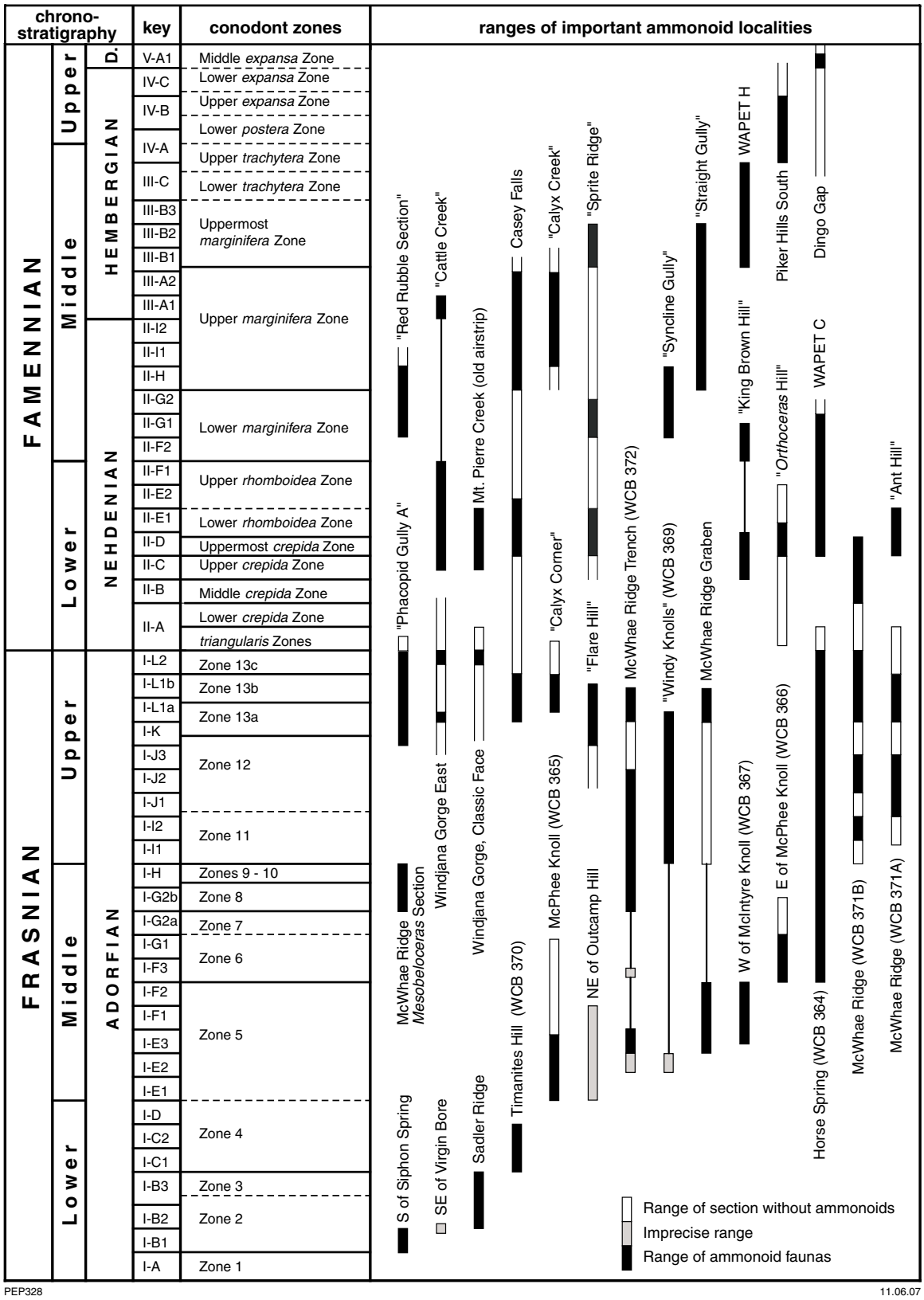

Figure 2.3. Stratigraphic ranges of the main ammonoid localities, plotted against both the regional ammonoid and conodont scales (conodont data supplied by G Klapper). The zonal key refers to subdivisions of the Upper Devonian (UD). Faunas from south of Siphon Spring, southeast of Virgin Bore, and Sadler Ridge are from hypoxic (pyritic) facies of the Sadler Limestone, faunas from Timanites Hill and northeast of Outcamp Hill are from the Gogo Formation. Assemblages at Piker Hills South are from the Piker Hills Formation. Single ammonoids from Dingo Gap are from the Napier Formation. All other sections are in the Virgin Hills Formation but include several middle Frasnian hypoxic tongues (WCB 365–367 and faunas from the base of WCB 372 and 369, and from the floor of the McWhae Ridge graben).

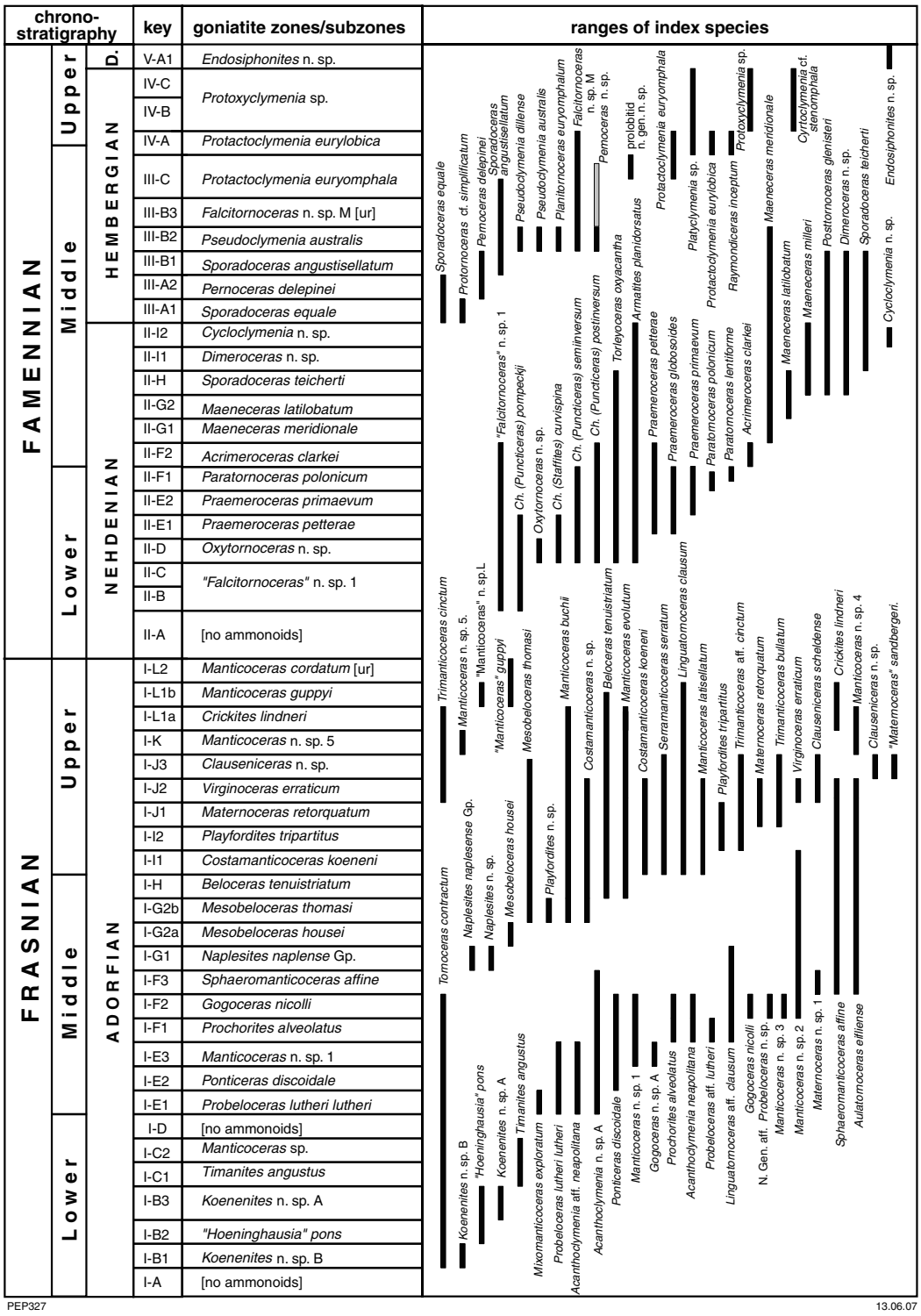

Figure 2.4. Stratigraphic ranges of important Canning Basin marker ammonoids, plotted against the regional ammonoid biozonation. [ur] = low diversity upper range zone, defined by the extinction of many other species. Black bars = range of typical specimens, shaded bar = range of cf. specimens.

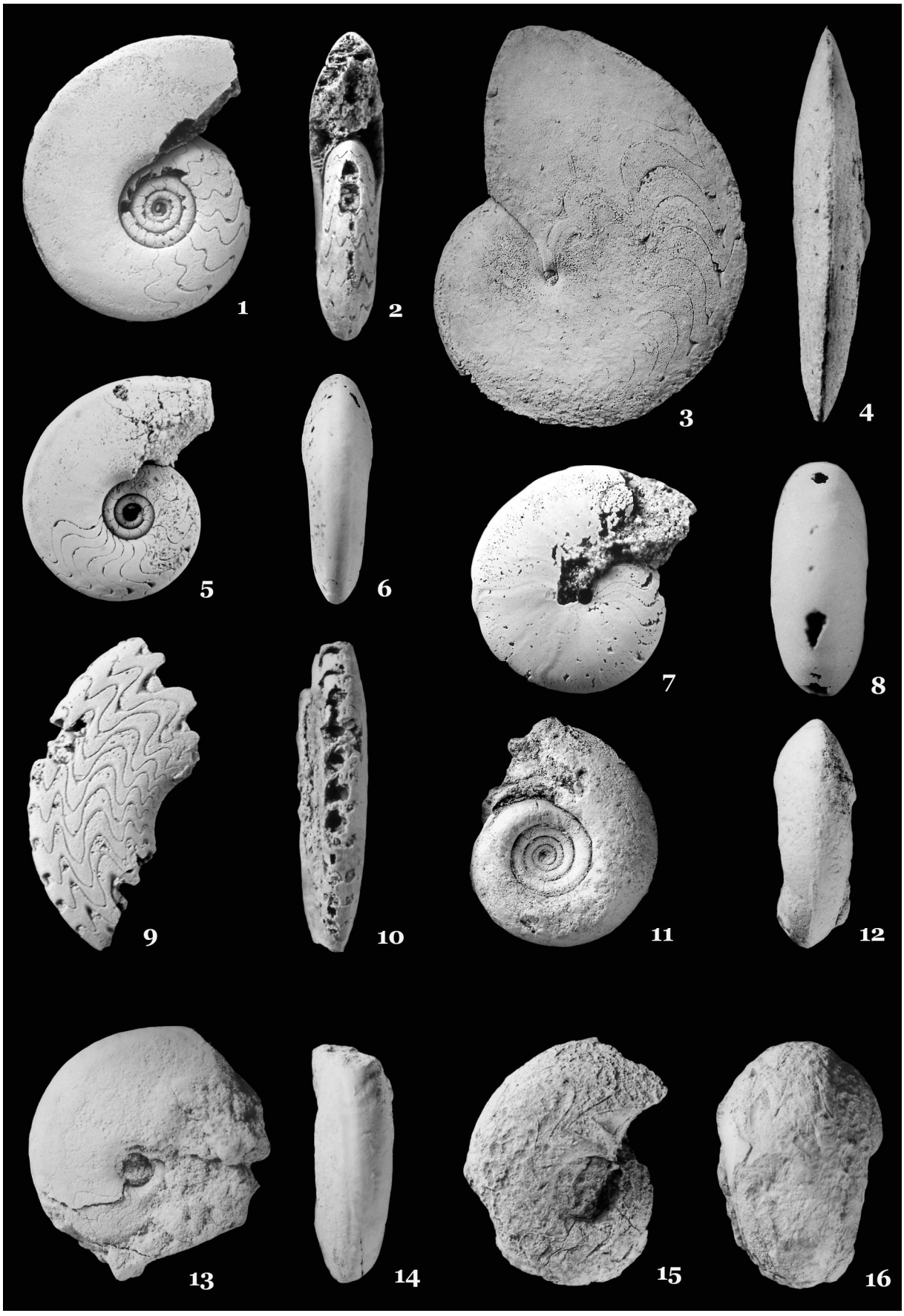
1
2
3
4
5
6
7
8
9
10
11
12
13
14
15
16

Figure 2.5. (facing page) Typical Frasnian ammonoids of the Canning Basin.
1–2. *'Hoeninghausia' pons* Glenister, 1958, GSWA F5247w, Sadler Ridge, index species of UD I-B_2, lateral and adoral views, ×3.
3–4. *Timanites angustus* Glenister, 1958, GSWA F48530, sample GSWA 102902, 'Timanites Hill', ~5.6 m above section base, index species of UD I-C_1, lateral and ventral views, ×1.
5–6. *Ponticeras discoidale* Glenister 1958, GSWA F48531, sample GSWA 102883/E, WCB 367, 110 m west of main section, ~lower part of Bed 10a, from UD I-F_2, lateral and ventral views, ×3.
7–8. *Gogoceras nicolli* Becker, House and Kirchgasser, 1993, paratype, GSWA F48532, sample GSWA 102871/A1, WCB 367, collection area K, ~middle part of Bed 10a, index species of UD I-F_2, lateral and ventral views, ×3.
9–10. *Mesobeloceras housei* Montesinos and Henn, 1986, BMR collection, WCB 366, Bed 6a, index species of UD I-G_{2b}, juvenile specimen, lateral and ventral views, ×4.
11–12. *Costamanticoceras koeneni* (Holzapfel, 1882), GSWA F48533, sample GSWA 115335/B, WCB 369 ('Windy Knolls'), Harpid Bed 200 m east of main section, ~Bed 8, 1.3–1.4 m above basal conglomerate, index species of UD I-I_1, lateral and ventral views, ×2.
13–14. *Playfordites tripartitus* (Sandberger and Sandberger, 1851), GSWA F48534, sample GSWA 102927/A1, WCB 372, trench at McWhae Ridge, 12.1 m above base, index species of UD I-I_2, lateral view and ventral view with asymmetric position of internal spiral groves, ×2.
15–16. *Crickites lindneri* (Glenister, 1958), GSWA F48535, sample GSWA 109381/A, WCB 369 ('Windy Knolls'), top of section (Bed 22b/23), index species of UD I-L_{1a}, juvenile specimen, lateral and ventral views, ×1.

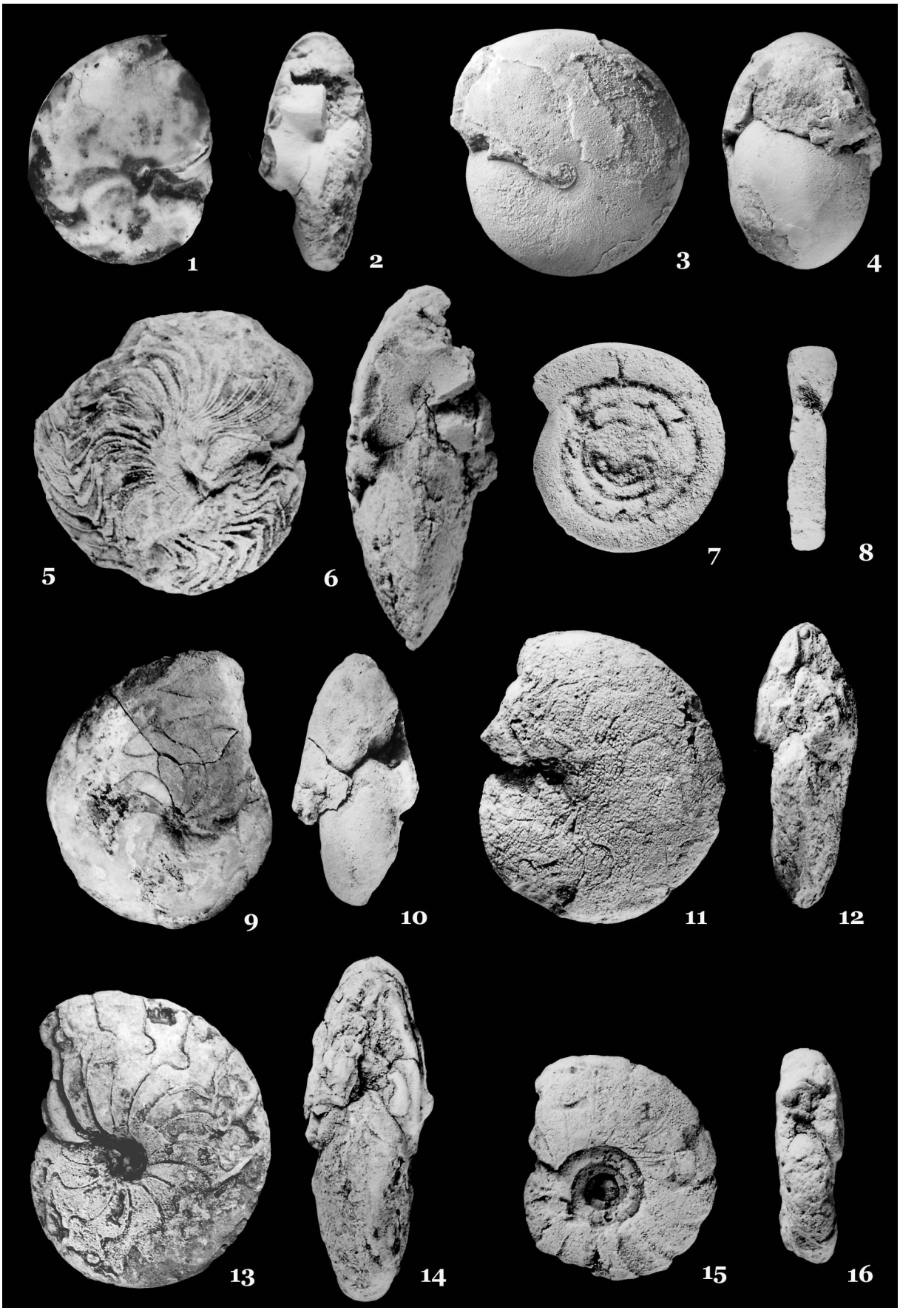
1
2
3
4
5
6
7
8
9
10
11
12
13
14
15
16

Figure 2.6. Typical Famennian ammonoids of the Canning Basin.
1–2. *'Falcitornoceras'* n. sp. 1, GSWA F48536, sample GSWA 102999/A1, McWhae Ridge, WCB 371B´, 40 cm above *Frutexites* Bed, index species of UD II-B/C, lateral view uncoated in order to show sutures, ventral view showing the septal face with its deep internal lobe, ×1.6.
3–4. *Praemeroceras primaevum* (Schindewolf, 1923), GSWA F48537, sample GSWA 109126/1, McWhae Ridge area, WAPET C, Bed 5b, index species of UD II-E2, medium-sized specimen, lateral view with almost closed umbilicus and ventral view showing the subglobose shell form, ×2.
5. *Acrimeroceras clarkei* (Delépine, 1935), GSWA F48538, sample GSWA 109349/A1, WAPET C, lower metre of Bed 18b, index species of UD II-F2, lateral view with sutures, ×1.
6. *Acrimeroceras clarkei* (Delépine, 1935), GSWA F48539, sample GSWA 109349/A3, WAPET C, lower metre of Bed 18b, ventral view showing the deep and undivided internal lobe, ×2.
7–8. *Cycloclymenia* n. sp., future holotype, GSWA F48540, sample GSWA 109326/B1, Casey Falls, Bed 27b, index species of UD II-I_2, lateral and ventral views, ×2.5.
9–10. *Sporadoceras equale* Becker in Becker et al. 2002, GSWA F48541, sample GSWA 109316/A1, Casey Falls, top of Bed 28, index species of UD III-A_1, lateral and adoral views, ×1.
11–12. *Dimeroceras* n. sp., GSWA F48542, sample GSWA 109320, Casey Falls, Bed 29c, from UD III-A_1, lateral and adoral views, ×1.
13–14. *Pernoceras* n. sp., GSWA F48543, sample GSWA 109187/A1, WAPET H, Bed 2a, alternative marker species of UD III-B_2, lateral view showing the lingulate adventitious lobe, ventral view, ×1.3.
15–16. *Protactoclymenia euryomphala* Wedekind, 1914, GSWA F48544, sample GSWA 109176/E1, WAPET H, Bed 14, index species of UD III-C, lateral and ventral views, ×2.5.

Appendix 3

Review of Devonian palynology, Canning Basin

by

Geoffrey Playford[1]

Palynological studies of marine Devonian strata of the Canning Basin began in the late 1950s – early 1960s. Depending on the availability of suitable materials, the studies progressed intermittently thereafter, and a limited number of publications have resulted. As summarized in Table 3.1, these documented the taxonomy and stratigraphic distribution of the land-derived miospores and co-occurring marine organic-walled microphytoplankton (i.e. acritarchs and prasinophyte phycomata), together with a few chitinozoans, from strata datable within the interval of late Middle Devonian (Givetian) – latest Devonian (latest Famennian). Because of the highly weathered nature of much of the Australian continent, and hence the predominantly non-palyniferous nature of outcropping rocks, palynological analyses are necessarily based on subsurface material. Numerous boreholes in the Canning Basin, drilled for petroleum and other mineral exploration and for stratigraphic purposes, have provided core (mainly) and other samples for palynological studies (McGregor and Playford, 1993, figs 3, 5). These investigations have proven very useful in stratigraphic correlation of certain subsurface Devonian successions of the northern Canning Basin and, moreover, in age determination of those successions by reference to the well-dated miospore biozones defined by Richardson and McGregor (1986) in the Euramerican (Old Red Sandstone) region.

Limited information from the pre-reef subsurface strata of the Anna Plains Sandstone and the Dominic Shale suggests that their content of miospores is attributable, respectively, to the Euramerican *devonicus–naumovae* (mid-Eifelian – early Givetian) and the *lemuratua–magnificus* (mid-Givetian) miospore zones (McGregor and Playford, 1993, table 2, fig. 8). The reef complexes of the northern Canning Basin have yielded abundant and diverse suites of trilete miospores (Grey, 1974, 1991, 1992) and microphytoplankton (Colbath, 1990), principally from siltstones and shales in the Gogo Formation, Pillara Limestone, and Sadler Limestone. The miospores include such species as *Ancyrospora langii, A. parva, Apiculatasporites adavalensis, Archaeozonotriletes variabilis, Archaeoperisaccus indistinctus, Convolutispora caementosa, Cristatisporites triangulatus, Dibolisporites turriculatus, Emphanisporites* spp., *Geminospora lemurata, Gneudnaspora divellomedia, Medusaspora dringii, Retusotriletes* spp., *Rhabdosporites langii*, and *Verrucosisporites scurrus*. A selection of characteristic species is illustrated in Figure 3.1, nos 1–12. This palynoflora is clearly correlative with those known from the latest Givetian – early Frasnian Gneudna Formation of the Carnarvon Basin, Western Australia (Balme, 1988); and also from the similarly dated Etonvale Formation of the Adavale Basin, Queensland (de Jersey, 1966; Hashemi and Playford, 2005) and the Parke Siltstone, Amadeus Basin, Northern Territory (Hodgson, 1968). Moreover, it contains a number of age-definitive (late Givetian – early Frasnian) species that characterize the *optivus–triangulatus* and *ovalis–bulliferus* miospore zonal interval of Euramerica (McGregor and Playford, 1993, tables 1, 2, fig. 8).

Grey (1991) considered that elements of the preceding Euramerican *lemurata–magnificus* zone were detectable at the base of the reefal deposits, thus indicating that reef development commenced slightly earlier than had traditionally been concluded; i.e. in the mid- rather than late Givetian. However, by reference to data presented by Richardson and McGregor (1986) and McGregor and Playford (1993, table 1), none of the species identified by Grey (1991, p. 45–46; e.g. *Geminospora lemurata, Ancyrospora langii, Archaeozonotriletes timanicus, A. variabilis*, and *Verrucosisporites scurrus*) can, individually or collectively, be regarded as unequivocally definitive of the *lemurata–magnificus* zone as distinct from the succeeding *optivus–triangulatus* zone. Hence, her claim that reefs were initiated during the mid-Givetian (i.e. predating *optivus–triangulatus* time) is considered unsubstantiated on palynological grounds.

The profuse assemblage of acritarchs and prasinophyte phycomata described by Colbath (1990) from calcareous shales and siltstones of the Limestone Billy Hills reef complex includes such species as *Cymatiosphaera perimembrana*, *C. spicigera, Daillydium pentaster, Dictyotidium venulosa, Lomatolopas cellulosa, Lophosphaeridium deminutum, Papulogabata annulata, Pterospermella tenellula, Synsphaeridium catenarium, Tornacia sarjeantii, Unellium lunatum*, and *U. piriforme*. As with the miospores, this assemblage includes both endemic and cosmopolitan forms and mirrors that of the Gneudna Formation (Playford and Dring, 1981; Playford, 1981). Accordingly, it confirms a late Givetian – early Frasnian age for the host sediments (Gogo Formation; Pillara and Sadler Limestones). Winchester-Seeto and Paris

[1] School of Earth Sciences, The University of Queensland, Qld. 4072.

(1995) examined several 'spot' (core) samples of the latter formations that they obtained from three boreholes drilled in the same general area as those of Colbath's (1990) study. They recorded three species of chitinozoans (one known also from France and Algeria, another from North America). Their chronostratigraphic inferences, related also to conodont data, complemented and were in essential agreement with the accrued miospore and phytoplankton evidence.

Scant palynological data are currently available from the Australian lower to middle Famennian. However, post-reef strata of the northern Canning Basin, belonging to the lower (uppermost Devonian) part of the Fairfield Group, and comprising the Gumhole Formation and much of the succeeding Yellow Drum Sandstone, have been analysed palynologically by Balme and Hassell (1962) and Playford (1976). The most characteristic miospore component recorded by those authors is *Retispora lepidophyta* (Kedo, 1957) Playford, 1976, junior taxonomic synonyms of which include *Leiozonotriletes naumovae* Balme and Hassell, 1962 (see Playford, 1976, p. 45). This highly distinctive pseudosaccate species is well known internationally as a key palynostratigraphic index, on account of its remarkable global distribution and its confinement to the latest Famennian or 'Strunian' (e.g. Richardson and McGregor, 1986; Playford, 1993; Playford and McGregor, 1993). Hence the exit of *R. lepidophyta*, evidently a worldwide event, is a reliable and well-documented marker of the Devonian–Carboniferous (Famennian–Tournaisian) boundary within the Fairfield Group. Associates of *R. lepidophyta* recorded by Balme and Hassell (1962) and Playford (1976) include other cosmopolitan or widely disseminated trilete species such as *Auroraspora macra, Endosporites micromanifestus, Hystricosporites porrectus, Indotriradites explanatus, Tumulispora rarituberculata*, and *Verrucosisporites nitidus*; together with many endemic forms including *Brochotriletes textilis*, *Convolutispora fromensis*, *Diaphanospora depressa, D. riciniata*, *Granulatisporites frustulentus*, *Indotriradites scorpius*, *Leiozonotriletes laurelensis*, and *Reticulatisporites ancoralis*. This miospore suite, selectively illustrated in Figure 3.1, nos 13–20, is clearly consonant with the latest Famennian *pusillites–lepidophyta/lepidophyta–nitidus* zonal interval of Euramerican successions (see McGregor and Playford, 1993, tables 1, 2, fig. 8). Moreover, Playford (1982) recognized the presence of the lower Fairfield assemblage in the Buttons Formation of the Bonaparte Basin; this was corroborated by Jones's (1985, 1987) documentation of a latest Famennian ostracod fauna from that formation.

Judging from the morphological (hence taxonomic) diversity of the plant microfossil assemblages preserved in the Canning Basin's marine Middle and Upper Devonian succession, it is evident that a well-diversified terrestrial vegetation successfully colonized coastal lowlands. However, the precise nature of the vegetation, as it developed during the later Devonian, is mostly speculative. This reflects the general scarcity of plant megafossils in the strata and the fact that botanical affinities of the majority of the dispersed miospores cannot be ascertained in other than fairly general terms. Parental vegetation of the Canning Basin's late Middle – early Late Devonian palynofloras would have included, as elsewhere in Australia, such lower vascular (seedless, free-sporing) plant groups as the zosterophyllophytes, barinophytes, pterophytes (true ferns), and lycophytes (Balme, 1988, 1995; Hashemi and Playford, 2005). Moreover, Balme (1988, p. 151) noted that progymnosperms (likely progenitors of gymnosperms) — in particular, the constituent archeopterids — are signified by often-striking abundances of *Geminospora lemurata* in association with *Rhabdosporites langii*. The arborescent archeopterids are thus envisaged as having constituted major elements of the late Givetian–Frasnian coastal plant communities. The latest Devonian (late Famennian) *lepidophytus* palynoflora was evidently also produced by an appreciable range of lower vascular plants. In particular, *Granulatisporites frustulentus*, which is profusely represented (and ranges into the Lower Carboniferous (Mississippian) of both the Canning and Bonaparte Basins), is considered of lycophytic affinity on morphological grounds. Moreover, and presumably not coincidentally, the only recognizable plant megafossils that have been encountered in the Famennian deposits of those basins are lycophyte stems (Balme, 1988, p. 150).

In summary, the miospore assemblages of the Canning Basin, although including certain clearly endemic forms, do share many species and morphological characters with palynofloras reported from Euramerica (McGregor and Playford, 1993). This is a manifestation of Devonian floral cosmopolitanism (Edwards, 1973) that was followed by the increasing floral provincialism that characterized the later Paleozoic.

As would be anticipated from the global decline in productivity of marine organic-walled microphytoplankton through the Late Devonian (Tappan, 1980; Playford, 2003), the quantitative and qualitative representation of these palynomorphs in the *lepidophyta* assemblage is greatly diminished. Playford (1976) described nine species of acritarchs/prasinophytes, the majority of which (e.g. *Gorgonisphaeridium ohioense*, *G. absitum*, *Stellinium micropolygonale*, and *Tornacia sarjeantii*) are known (Playford, 1993) to be widely distributed geographically in strata contiguous with the Devonian–Carboniferous boundary.

References

Balme, B E 1988, Miospores of Late Devonian (early Frasnian) strata, Carnarvon Basin, Western Australia: Palaeontographica, Abteilung B, v. 209, p. 109–166.

Balme, B E 1995, Fossil in situ spores and pollen grains: an annotated catalogue: Review of Palaeobotany and Palynology, v. 87, p. 85–323.

Balme, B E and Hassell, C W 1962, Upper Devonian spores from the Canning Basin, Western Australia. Micropaleontology, v. 8, p. 1–28.

Colbath, G K 1990, Devonian (Givetian-Frasnian) organic-walled phytoplankton from the Limestone Billy Hills reef complex, Canning Basin, Western Australia: Palaeontographica, Abteilung B, v. 217, p. 87–145.

De Jersey, N J 1966, Devonian spores from the Adavale Basin: Geological Survey of Queensland, Publication 334, Palaeontological Paper 3, 28p.

Edwards, D 1973, Devonian floras, *in* Atlas of palaeobiogeography *edited by* A Hallam: Elsevier, Amsterdam, p. 105–115.

Grey, K 1974, Devonian spores from the Gogo Formation, Canning Basin: Geological Survey of Western Australia, Annual Report 1973, p. 96–99.

Grey, K 1991, A mid-Givetian miospore age for the onset of reef development on the Lennard Shelf, Canning Basin, Western Australia: Review of Palaeobotany and Palynology, v. 68, p. 37–48.

Grey, K 1992, Miospore assemblages from the Devonian reef complexes, Canning Basin, Western Australia: Geological Survey of Western Australia, Bulletin 140, 139p.

Hashemi, H and Playford, G 2005, Devonian miospore assemblages of the Adavale Basin, Queensland (Australia): descriptive systematics and stratigraphic significance: Revista Española de Micropaleontología, v. 37, p. 317–417.

Hodgson, E A 1968, Devonian spores from the Pertnjara Formation, Amadeus Basin, Northern Territory: Australia, Bureau of Mineral Resources, Geology and Geophysics, Bulletin 80, p. 65–82.

Jones, P J 1985, Treposellidae (Beyrichiacea: Ostracoda) from the latest Devonian (Strunian) of the Bonaparte Basin: Australia, BMR Journal of Australian Geology and Geophysics, v. 9, p. 149–162.

Jones, P J 1987, *Rhytiobeyrichia*, a new beyrichiacean ostracod from the Late Devonian of Western Australia: Australia, BMR Journal of Australian Geology and Geophysics, v. 10, p. 287–300.

Kedo, G I 1957, Spores from the supra-salt Devonian deposits of the Pripyat Basin and their stratigraphic importance: Report on palaeontology and stratigraphy of Byelorussian S.S.R., v. 2, p. 3–43. (in Russian)

McGregor, D C and Playford, G 1993, Canadian and Australian Devonian spores: zonation and correlation: Bulletin of the Geological Survey of Canada, v. 438, 125p. (imprinted 1992)

Playford, G 1976, Plant microfossils from the Upper Devonian and Lower Carboniferous of the Canning Basin, Western Australia: Palaeontographica, Abteilung B, v. 158, p. 1–71.

Playford, G 1981, Late Devonian acritarchs from the Gneudna Formation in the western Carnarvon Basin, Western Australia: Géobios, v. 14, p. 145–171.

Playford, G 1982, A latest Devonian palynoflora from the Buttons beds, Bonaparte Gulf Basin, Western Australia: Australia, BMR Journal of Australian Geology and Geophysics, v. 7, p. 149–157.

Playford, G 1993, Miospores and organic-walled microphytoplankton characteristic of strata contiguous with the Devonian-Carboniferous boundary*:* Compte Rendu, Douzième Congrès International de Stratigraphie et de Géologie du Carbonifère-Permien, Buenos Aires, September 1991, v. 1, p. 127–160.

Playford, G 2003, Acritarchs and prasinophyte phycomata: a short course: American Association of Stratigraphic Palynologists, Contributions Series, v. 41, p. 1–39.

Playford, G and Dring, RS 1981, Late Devonian acritarchs from the Carnarvon Basin, Western Australia: Special Papers in Palaeontology, v. 27, 78p.

Playford, G and McGregor, D C 1993, Miospores and organic-walled microphytoplankton of Devonian–Carboniferous boundary beds (Bakken Formation), southern Saskatchewan: a systematic and stratigraphic appraisal: Bulletin of the Geological Survey of Canada, v. 445, 107p.

Richardson, J B and McGregor, D C 1986, Silurian and Devonian spore zones of the Old Red Sandstone Continent and adjacent regions: Bulletin of the Geological Survey of Canada, v. 364, 79p.

Tappan, H 1980, The paleobiology of plant protists: Freeman, San Francisco, 1028p.

Winchester-Seeto, T and Paris, F 1995, Late Givetian and Frasnian chitinozoans from Australia, France and Pakistan in relation to conodont zonation: Courier Forschungsinstitut Senckenberg, v. 182, p. 451–473.

Table 3.1. Publications on the palynology of Devonian strata, Canning Basin.

Author/date	*Borehole*	*Devonian lithostratigraphic units*	*Inferred age*	*Palynomorphs identified*
Balme and Hassell (1962)	Laurel Downs 2, Frome Rocks 1, The Sisters 2,Kimberley Downs 67 Mile, Stumpys Soak	Fairfield Group: Gumhole Formation, Yellow Drum Sandstone	late Famennian	miospores
Grey (1974, 1991, 1992)	numerous boreholes in Napier and Pillara Ranges	Pillara Limestone, Sadler Limestone, Gogo Formation, Virgin Hills Formation	Givetian–Frasnian	miospores
Playford (1976)	Laurel Downs 2, Lennard River 1 and 2, Noonkanbah 4, Pickands-Mather AH 2	Fairfield Group: Gumhole Formation, Yellow Drum Sandstone	late Famennian	miospores, acritarchs, prasinophyte phycomata
Colbath (1990)	18 boreholes in Pillara Range area	Pillara Limestone, Sadler Limestone, Gogo Formation	late Givetian–Frasnian	acritarchs, prasinophyte phycomata
McGregor and Playford (1993)	see McGregor and Playford (1993, p. 77–80; Figs 3, 5)	–	Givetian–Famennian	miospores
Winchester-Seeto and Paris (1995)	3 boreholes: 2 in Pillara Range area, 1 in Prices Hill area	Pillara Limestone, Sadler Limestone, Gogo Formation	late Givetian–Frasnian	chitinozoans

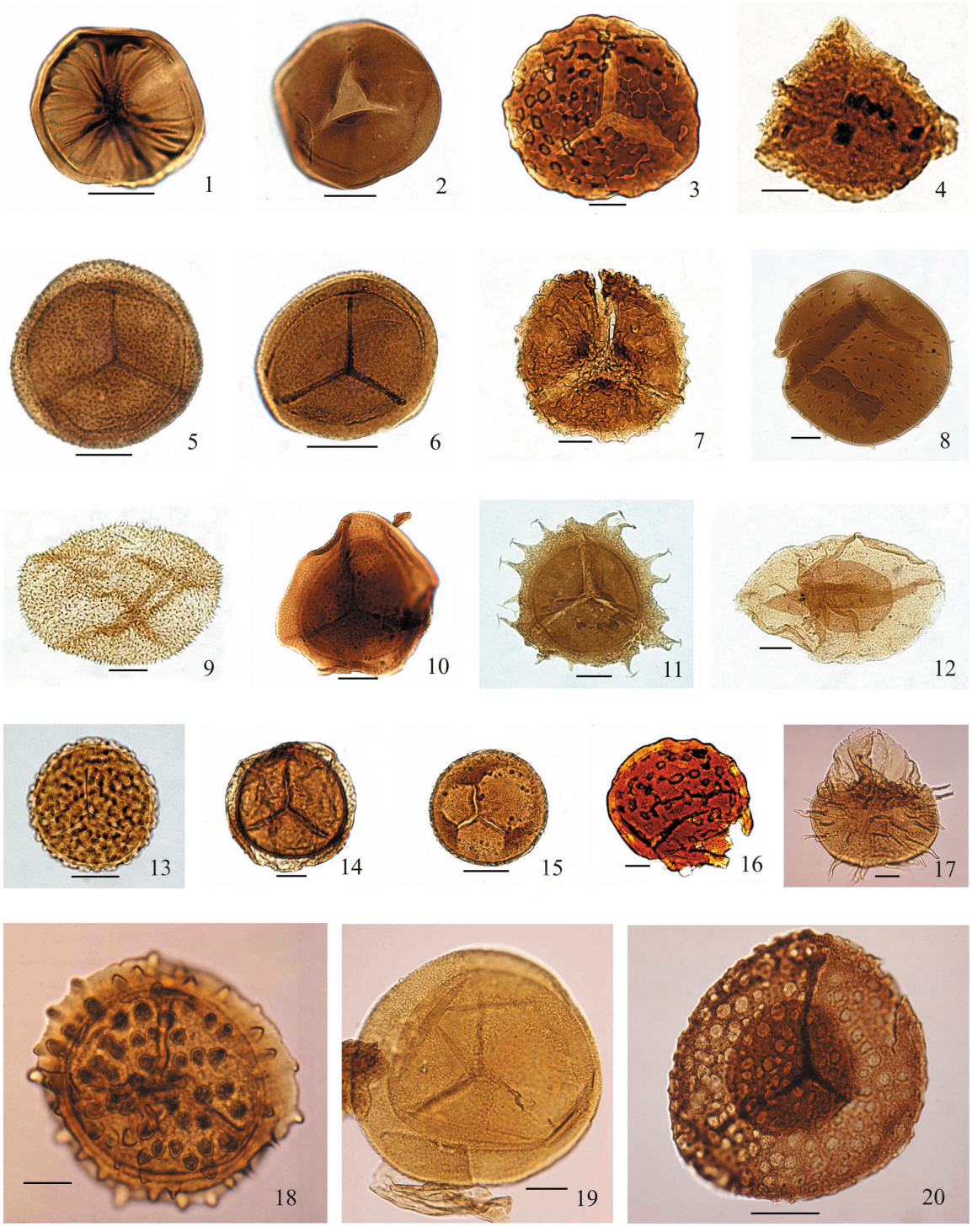

Figure 3.1. Selection of miospores characteristic of the late Givetian– Frasnian Pillara Limestone (nos 1–12) and the latest Famennian lower Fairfield Group (nos 13–20), northern Canning Basin subsurface. Scale bars represent 20 µm.

1. ***Emphanisporites rotatus*** **McGregor, 1961.**
2. ***Retusotriletes*** **sp.**
3. ***Convolutispora*** **sp. cf. *C. caementosa* Balme, 1988.**
4. ***Cristatisporites triangulatus*** **(Allen, 1965) McGregor and Camfield, 1982.**
5, 6. ***Geminospora lemurata*** **Balme, 1962 emend. Playford, 1983.**
7. ***Cristatisporites*** **sp.**
8. ***Dibolisporites turriculatus*** **Balme, 1988.**
9. ***Apiculatasporites adavalensis*** **(de Jersey, 1966) Grey, 1992.**
10. ***Rhabdosporites langii*** **(Eisenack, 1944) Richardson, 1960.**
11. ***Ancyrospora langii*** **(Taugourdeau-Lanz, 1960) Allen, 1965.**
12. ***Archaeoperisaccus indistinctus*** **Lu Lichang, 1988.**
13. ***Convolutispora fromensis*** **Balme and Hassell, 1962.**
14. ***Diaphanospora riciniata*** **Balme and Hassell, 1962.**
15. ***Diaphanospora depressa*** **(Balme and Hassell, 1962) Evans, 1970.**
16. ***Brochotriletes textilis*** **(Balme and Hassell, 1962) Playford, 1976.**
17. ***Hystricosporites porrectus*** **(Balme and Hassell, 1962) Allen, 1965.**
18. ***Indotriradites scorpius*** **(Balme and Hassell, 1962) Higgs, 1996.**
19. ***Leiozonotriletes laurelensis*** **Balme and Hassell, 1962.**
20. ***Retispora lepidophyta*** **(Kedo, 1957) Playford, 1976.**

The Devonian reef complexes of the Canning Basin form a spectacular belt of rugged limestone ranges that extend for some 350 km along the northern margin of the basin. They have become known as the 'Devonian Great Barrier Reef' and constitute what is regarded as one of the world's best examples of an ancient barrier-reef system.

Systematic research on these reefs began in 1956, when West Australian Petroleum Pty Ltd (WAPET) conducted detailed mapping and research of the Oscar Range reef complex, followed in 1958 by a study of Windjana Gorge. The reports on those investigations laid firm foundations for subsequent studies. The first mapping and research by the Geological Survey of Western Australia (GSWA) was undertaken in 1962–63, resulting in Bulletin 118, published in 1966. Field work for the present Bulletin was conducted during 1968, 1972, and several years since 1992. Many staff and students from Australian and overseas universities have worked with GSWA on the project. For its senior author this Bulletin represents the culmination of more than 50 years of his studies of these rocks.

The reefs were constructed during the Middle and Late Devonian by colonial organisms, mainly cyanobacteria, stromatoporoids, and corals. Those reef-building organisms are very well preserved, along with other fossils that once lived in and around the reefs, especially ammonoids, fish, and conodonts. Large masses of conglomerate, eroded from Precambrian rocks of the adjoining Devonian landmass, interfinger with or pass through the reef complexes.

The limestones have been faulted, tilted, and mildly folded in some areas, but are generally little deformed. During the Early Permian they were subjected to subglacial erosion and karstification below a succession of continental ice sheets. This subglacial erosion planed off the limestones, forming a level surface that now approximates the tops of the ranges.

The Devonian reef complexes are highly prospective for zinc-lead deposits, and are also prospective for petroleum where they extend into the subsurface. Several zinc-lead deposits (including Pillara, Goongewa, and Cadjebut) and a small oilfield (Blina) have so far been discovered in these rocks.



SYMBOLS

Geological boundary
- observed
- concealed or gradational facies boundary

Fault
- exposed
- concealed
- normal, tick on downthrown side, showing dip
- thrust, triangle on upthrown side

Fold or bothem, showing axial trace
- anticline or bothem axis, exposed
- synclne, exposed

Bedding
- inclined, showing strike and dip
- trend from aerial photography

Paleocurrent direction

Asphalts treatment

Neptunian dyke or major joint

Formed road, bridge

Track

Aboriginal Community — Windjingoy Community

Homestead — Napier Downs

Aboriginal name — Djalangkarri

Building

Yard

National Park boundary

Horizontal control, mirror

Watercourse

Spring — S

Bore, well — B, W

Windpump — T

Tank — T

Abandoned — (abd)

Petroleum exploration well
- dry, abandoned — Napier 5

Opencut, abandoned — Russell

Quarry or pit

Prospect

Mineral occurrance
- Building stone — Bs
- Garnet — Grt
- Lead — Pb
- Rock material — Rm
- Zinc — Zn

REFERENCE

CAINOZOIC — QUATERNARY

Qa Qb Qk Qs

Qa Alluvial deposits — reddish sand, gravel and clay in channels and floodplains
Qb Black-soil deposits — black clayey gilgai soil
Qk Calcrete and tufa
Qs Sandplain deposits — unconsolidated eolian and residual sands; minor silt and clay; includes low vegetated dunes

TERTIARY — MIOCENE

Czd — Duricrust — siliceous and ferruginous deposits

Ti — **KYCROY VOLCANICS:** lamprolite diatremes and associated pyroclastic rocks, largely or entirely covered by Quaternary soils

PALAEOZOIC — PERMIAN

Pl — **LIVERINGA GROUP:** well-bedded, shallow-marine to fluvial sandstone and siltstone; ferruginous in port

Pg — **GRANT GROUP:** crudely bedded marine sandstone and siltstone; in port glorygene

CARBONIFEROUS — TOURNAISIAN

DCF — **FAIRFIELD GROUP:** shale, sandstone, and fossiliferous limestone

FAMENNIAN

Dw — **WINDJANA LIMESTONE:** *reef-margin subfacies*: massive, microbial reef limestone; locally dolomitized; commonly with many neptunian dykes

+ Dwc — Large allochthonous blocks of **WINDJANA LIMESTONE (reef)** in fore-reef subfacies

Dl — **NULLARA LIMESTONE:** *back-reef subfacies*: well-bedded, fenestral, oolitic, and pelloidal limestone; locally dolomitized, sandy, and conglomeratic

DEVONIAN — FRASNIAN *reef* FAMENNIAN

Dn — **NAPIER FORMATION:** *reefal-slope, fore-reef, and basinemal subfacies*

Dnc — Famennian well-bedded to massive reefal-slope and fore-reef limestone; locally dolomitized and steeply dipping; locally microbial and sponge rich

Dne — Frasnian and Famennian deep-water bioherms: stromatolite and *Receptaculites* sponge limestone; locally dolomitized

Dnr — Frasnian well-bedded to massive reefal-slope and fore-reef limestone, locally dolomitized and steeply dipping; locally microbial and sponge rich; some allochthonous blocks and debris flows; some sandstone and conglomeratic

FRASNIAN

Dp — **PILLARA LIMESTONE:** *platform facies, undivided*; mostly *back-reef* and lesser *reef-flat subfacies*: white to light-grey and yellow, medium-bedded, stromatoporoid and lenestrid limestone; locally dolomitized, sandy and grading into calcareous sandstone; commonly forming shallowing-upward cyclic sequences

Dpr — *Reef-margin and reef-flat subfacies*: white to light-grey and yellow, massive to thick-bedded stromatoporoid and microbial reef limestone; locally dolomitized

+ Dpc — Large allochthonous blocks of **PILLARA LIMESTONE (reef)** in fore-reef subfacies

Devonian reef complexes

FAMENNIAN *reef* FRASNIAN

Dcv — **VAN EMMERICK CONGLOMERATE:** siliciclastic conglomerate and sandstone; alluvial-cone, fan-delta, and submarine-fan deposits. Extends into Gneiss in subsurface

Dcvu — Upper Van Emmerick Conglomerate (probably Famennian)

FRASNIAN *reef* FAMENNIAN

Dcb — **BIDHI CONGLOMERATE:** siliciclastic conglomerate and sandstone; alluvial-cone, fan-delta, and submarine-fan deposits

DEVONIAN — GIVETIAN

Dn — **POULTON FORMATION:** sandstone, shale, and siltstone; minor dolomite; marine (section only)

Devonian conglomerates

PROTEROZOIC — NEOPROTEROZOIC

Pf — Proterozoic rock, undivided (sections and stratigraphic relationships diagram)

PALAEOPROTEROZOIC

Ehu — 810–810 Ma — Sedimentary rock

Ehr — 1635–1790 Ma — Sedimentary rock and diderite

Eg — 1885–1850 Ma — Granitoid rock

Ew — *c.* 1850 Ma — **WHITEWATER VOLCANICS:**

Eh — 1870–1840 Ma — Metamorphic rock

STRATIGRAPHIC RELATIONSHIPS OF THE DEVONIAN REEF COMPLEXES

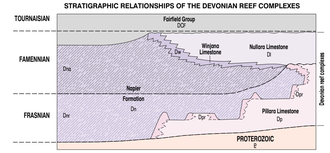

SHEET INDEX

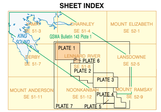



Compiled by R. M. Hocking and P. E. Playford

Devonian geology by P. E. Playford, 1961–1995, R. M. Hocking, 1993–1995, D. C. Lowry, 1961–1962, and M. B. Ward, 1985–1986

Precambrian geology modified from Griffin and Tyler, 1986

Edited by N. Tetlow, D. Ferdinando, F. Apodopoulos, C. Brien, and G. Loon

Cartography by E. Green, S. Cordouil, T. Lemme, and K. Greenberg

Topography from the Department of Land Administration with modifications from geological field survey

Published by the Geological Survey of Western Australia. Copies available from the Information Centre, Department of Minerals and Energy, 100 Plain Street, East Perth, WA, 6004. Phone (08) 9222 3459, Fax (08) 9222 3444

This map is also available in digital form

Printed by the Sands Print Group, Western Australia

GRID / MAGNETIC ANGLE 1.6°

GRID CONVERGENCE 0.7°

True north, grid north and magnetic north are shown diagrammatically for the centre of the map. Magnetic north is correct for 1988 and moves easterly by about 0.1° in 6 years

DIAGRAMMATIC SECTIONS

NATURAL SCALE (MAP SCALE x 2)

SCALE 1:50 000

1000 Metres 0 1 2 3 4 Kilometres

DEPARTMENT OF MINERALS AND ENERGY
L. C. RANFORD, DIRECTOR GENERAL

GOVERNMENT OF WESTERN AUSTRALIA
HON. NORMAN MOORE, M.L.C.
MINISTER FOR MINES

GEOLOGICAL SURVEY OF WESTERN AUSTRALIA
DAVID BLIGHT, DIRECTOR

SCALE 1:100 000

1000 Metres 0 1 2 3 4 5 6 7 8 9 10 Kilometres

TRANSVERSE MERCATOR PROJECTION
HORIZONTAL DATUM: AUSTRALIAN GEODETIC DATUM 1984
VERTICAL DATUM: AUSTRALIAN HEIGHT DATUM
Grid lines indicate 1000 metre interval of the Australia Map Grid Zone 51

NAPIER RANGE AREA

DEVONIAN REEF COMPLEXES OF THE CANNING BASIN

BULLETIN 145 PLATE 1

© Western Australia 1998

SYMBOLS

Geological boundary
- exposed
- concealed or gradational facies boundary

Fault
- observed
- concealed
- normal, tick on downthrown side
- thrust, triangle on upthrown side

Fold or bohemn, showing axial trace
- anticline or bohemn axis; exposed
- syncline; exposed
- overturned anticline; exposed

Bedding
- inclined, showing strike and dip
- horizontal
- trend from aerial photography

Palaeocurrent direction

Arghisto lineament

Neptunian dyke or major joint

Highway with national route marker

Formed road

Track

Aboriginal community — Womoli Community

Homestead — Pilirfield

Aboriginal name — Ibanangmer

Building

Yard

National Park boundary

Conservation Park boundary

Horizontal control, minor

Watercourse

Spring

Bore; well

Windpump

Dam; tank

Abandoned

Position doubtful

Petroleum exploration well
- dry, abandoned — ◇ Chestnut 1

Quarry

Prospect

Mineral occurrence
- Diamond
- Rood metal — Rm

REFERENCE

CAINOZOIC — QUATERNARY

Qc Qh Qk Qs

Alluvial deposits — reddish sand and clay in channels and floodplains
Qh Black-soil deposits — black clayey gilgai soil
Qk Calcrete and tufa
Qs Sand/dune deposits — unconsolidated eolian and residual sands; minor silt and clay; includes low vegetated dunes

Czd Duricrust — siliceous and ferruginous deposits

TERTIARY — MIOCENE

Ti FITZROY VOLCANICS: lamprophyre dolmenites and associated pyroclastic rocks; some diamond bearing; largely or entirely covered by Quaternary soils

PALAEOZOIC — PERMIAN

Pn NOONKANBAH FORMATION: well-bedded detritic to shallow-marine sandstone, siltstone, and shale; minor dolomite

PG GRANT GROUP: crudely bedded marine sandstone and siltstone; in port glocigere

CARBONIFEROUS — TOURNAISIAN

DCF FAIRFIELD GROUP: shale, sandstone, and fossiliferous limestone

Cm LAUREL FORMATION: marine limestone, shale, siltstone, and sandstone

DPy YELLOW DRUM SANDSTONE: fluvial to partolic sandstone and dolomite; minor shale and siltstone

DPg GUNHOLE FORMATION: shallow-marine limestone, siltstone, and shale; minor dolomite

DEVONIAN — FAMENNIAN

Dw WINDJANA LIMESTONE: *reef-margin subfacies* massive, microbial reef limestone; locally dolomitized, commonly with many neptunian dykes

Dwo Large allochthonous blocks of WINDJANA LIMESTONE (reef) in fore-reef subfacies

Dl NULLARA LIMESTONE: *back-reef subfacies* well-bedded lenatrol, oolitic, and pelloidal limestone; locally dolomitized

Dn NAPIER FORMATION: *reef/I-slope, bine-reef, and bioherm/l subfacies*

Dnso Famennian well-bedded to massive reef/d-slope and fore-reef limestone; locally dolomitized, sandy and grading to sandstone and steeply dipping to flat lying, with olliothrorous blocks and debris flows in some horizons

Dns Frasnian and Famennian deep-water bioherms: stromatolite and *Receptaculites* sponge limestone; locally dolomitized

Dor Frasnian well-bedded to massive reef/d-slope and fore-reef limestone; locally dolomitized, steeply dipping, with olliothrorous blocks and debris flows in some horizons

Dnb **Barrer Member:** Famennian well-bedded to massive fins-reef limestone; locally dolomitized, sandy, and grading to sandstone, steeply dipping to flat lying, with large olliothrorous blocks and debris flows in some horizons

Dnt **Terakatu Member:** Famennian well-bedded to massive sandstone grading into sandy limestone; with some olliothrorous blocks of reef limestone

Dnkp **Kidnapp Member:**
Famennian well-bedded to massive reef/d-slope and fore-reef limestone; locally dolomitized, steeply dipping, with olliothrorous blocks and debris flows in some horizons

Dnkr Frasnian well-bedded to massive reef/d-slope and fore-reef limestone; locally dolomitized, steeply dipping, with olliothrorous blocks and debris flows in some horizons

Devonian reef complexes

DEVONIAN — FRASNIAN

Dp PILLARA LIMESTONE: *platform facies undivided, mainly back-reef and lesser reef-flat subfacies* white to light-grey and yellow, medium-bedded, stromatoporoid and lenatrol limestone; locally dolomitized and sandy and grading into calcareous sandstone; may extend into Gneiton in subsurface

Dpr *Reef-margin and reef-flat subfacies* white to light-grey and yellow, massive to thick-bedded stromatoporoid and microbial reef limestone; locally dolomitized, with subordinate coralline limestone

Dpo Large allochthonous blocks of PILLARA LIMESTONE (reef) in fore-reef subfacies

DEVONIAN — GIVETIAN

Dx BIG SPRING FORMATION: sandstone, well-bedded to massive; locally calcareous, with massive siliciclastic conglomerate at the base; fan-delta and alluvial-cone deposits

Dc Conglomerate, siliciclastic, overlying Proterozoic rock of the Oscar Range

Do POULTON FORMATION: sandstone, shale, and siltstone; minor dolomite; marine (section only)

PROTEROZOIC — NEOPROTEROZOIC / PALAEOPROTEROZOIC

Z Proterozoic rock, undivided (sections and stratigraphic relationships diagram)

Bau 800–810 Ma — Sedimentary rock

Eg 1865–1850 Ma — Granitoid rock

Ew c 1855 Ma — WHITEWATER VOLCANICS: volcanic and sedimentary rocks

Bl 1870–1840 Ma — Metamorphic rock

STRATIGRAPHIC RELATIONSHIPS OF THE DEVONIAN REEF COMPLEXES

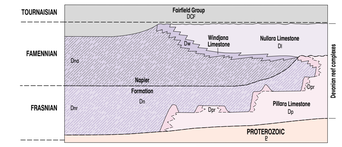

SHEET INDEX

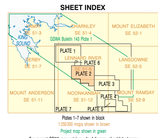

See current GSWA map catalogue for full range of published maps



DIAGRAMMATIC SECTIONS

NATURAL SCALE (MAP SCALE x 2)

SCALE 1:50 000

1000 0 1 2 3 4 Metres Kilometres

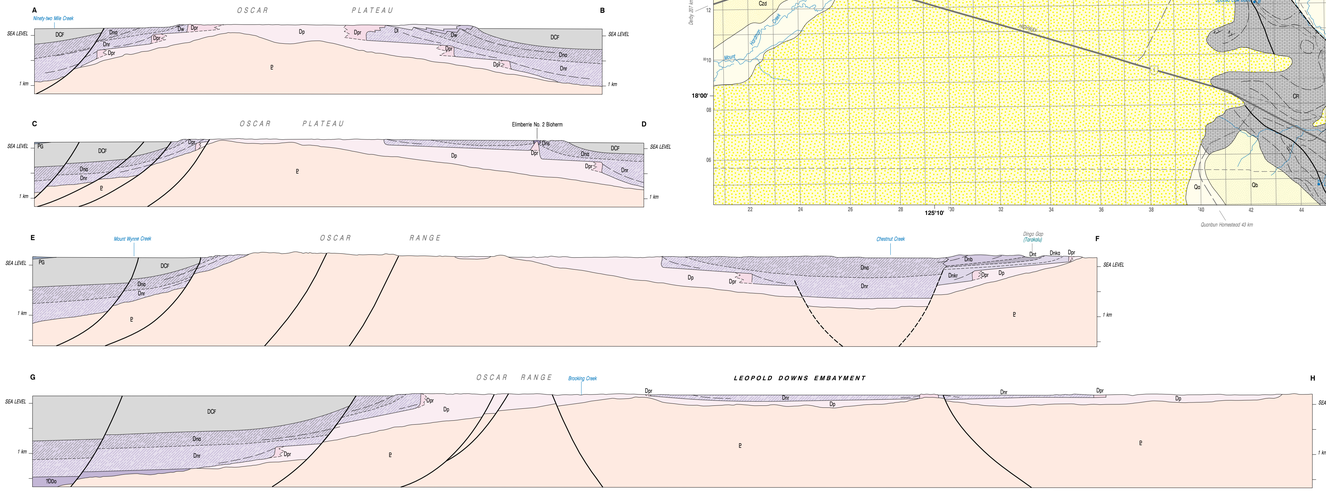

Compiled by R. M. Hocking and P. E. Playford

Devonian geology by P. E. Playford, 1961–1995, R. M. Hocking, 1993–1995, N. F. Hurley 1983–1984, D. C. Lowry, 1961–1962, and W. B. Ward, 1985–1986

Precambrian geology modified from Griffin and Tyler, 1990

Edited by D. Ferdinando, N. Tetlow, F. Apidopoulos, G. Loon, and K. Greenberg

Cartography by E. Green, S. Colcloud, T. Lenane, and B. Williams

Topography from the Department of Land Administration with modifications from geological field survey

Published by the Geological Survey of Western Australia. Copies available from the Information Centre, Department of Minerals and Energy, 100 Plain Street, East Perth, WA, 6004. Phone (08) 9222 3459. Fax (08) 9222 3444

This map is also available in digital form

Printed by the Sands Print Group, Western Australia

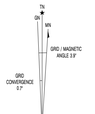

True north, grid north and magnetic north are shown diagrammatically for the centre of the map. Magnetic north is correct for 1996 and moves westerly by about 0.1° in 6 years

DEPARTMENT OF MINERALS AND ENERGY
L. C. RAWLINS, DIRECTOR GENERAL

GOVERNMENT OF WESTERN AUSTRALIA
HON. NORMAN MOORE, M.L.C.
MINISTER FOR MINES

GEOLOGICAL SURVEY OF WESTERN AUSTRALIA
DAVID BLIGHT, DIRECTOR

SCALE 1:100 000

1000 0 1 2 3 4 5 6 7 8 9 10 Metres Kilometres

TRANSVERSE MERCATOR PROJECTION
HORIZONTAL DATUM: AUSTRALIAN GEODETIC DATUM 1984
VERTICAL DATUM: AUSTRALIAN HEIGHT DATUM
Grid lines indicate 1000 metre interval of the Australia Map Grid Zone 51

OSCAR RANGE AREA

DEVONIAN REEF COMPLEXES OF THE CANNING BASIN

BULLETIN 145 PLATE 2

© Western Australia 1998

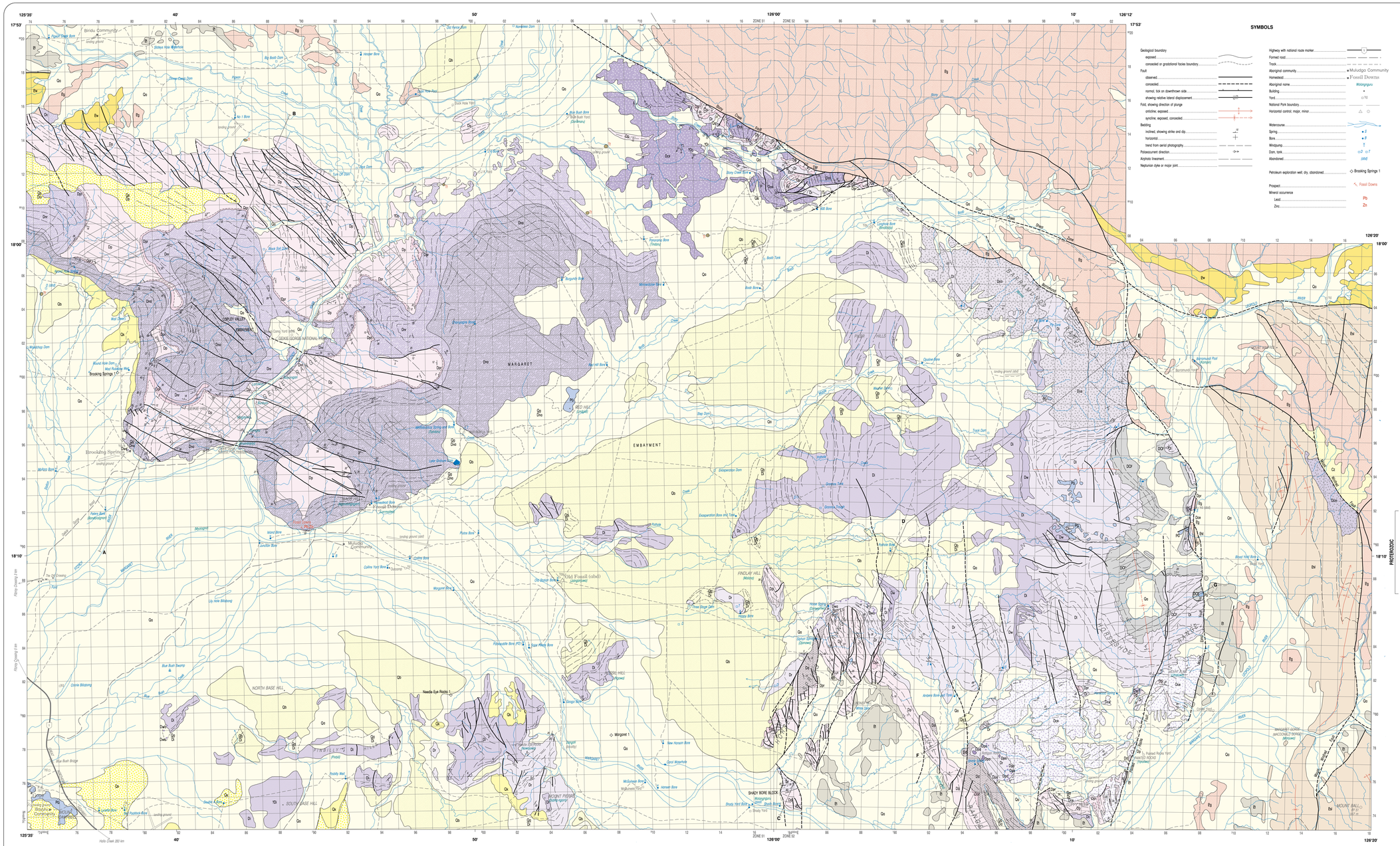
Birdiu Community
Brooking Springs
Brooking Springs TO
Mulugo Community
Fossil Downs
Wolangarra
Brooking Springs 1
Fossil Downs
Old Fossil (dbd)
Longstreet
Old Fossil (obd)
Longstreet
Pb
Zn
COPLEY VALLEY
EMBAYMENT
MARGARET
HORSE SPRING RANGE
BARRAMUNDI RANGE
HULL RANGE
HORSESHOE RANGE
SHADY BORE BLOCK
MOUNT PIERRE
SOUTH BASE HILL
NORTH BASE HILL
FINDLAY HILL
KINDLAY HILL
RED HILL
PIPER HILLS
MOUNT BALL
Barramundi Fault
Mount Elma Fault
Fitzroy River
Gekko Gorge Road
Margaret River
Horse Spring Dome
Barramundi Dome
Mount Ball Dome
Horseshoe Dome
Old Fossil Dome
Old Fossil Syncline
Margaret Syncline
Fossil Downs Syncline
Fossil Downs Fault
Mount Ball Fault
Horseshoe Fault
Barramundi Fault
Fitzroy Crossing 8 km
Halls Creek 383 km
Derby 240 km
Great Northern Highway
Gibb River Road
Mitchell River National Park
Geikie Gorge National Park
Fitzroy River
Margaret River
Bow River
Bluff
Mount Ball
Mount Elma
Mount Pierre
Finbelly Hill
Kindlay Hill
Red Hill
Piper Hills
Mount Anderson
Mount Elizabeth
Mount Channing
Mount Ramsay
Noonkanbah
Ringer Soak
Old Fossil Bore
Margaret 1
Fossil Downs 1
Brooking Springs 1
Old Fossil (obd) Longstreet
Old Fossil (dbd) Longstreet
Bow River Bore
Margaret River Bore
Mount Ball Bore
Mount Elma Bore
Horseshoe Bore
Barramundi Bore
Fossil Downs Bore
Old Fossil Bore
Margaret Bore
Mount Pierre Bore
Shady Bore Bore
Shady Yard Bore
Shady Bore Block
Shady Yard
Fossil Downs Yard
Fossil Downs Yard (dbd)
Longstreet
Mount Ball Yard
Mount Ball

REFERENCE

QUATERNARY

Qa Qb Qk Qs

Qa Alluvial deposits — reddish sand and clay in channels and floodplains
Qb Black-soil deposits — brown clayey gilgai soil
Qk Calcrete and tufa
Qs Sand — unconsolidated eolian and residual sands; minor clay; includes low vegetated dunes

CAINOZOIC

Cz Alluvial and colluvial deposits

TERTIARY — MIOCENE

Ti **LAWFORD FORMATION:** crudely bedded lacustrine siltstone, sandstone, and chalcedonic limestone

PERMIAN

- Pl **LIVERINGA GROUP:** well-bedded shallow-marine to fluvial sandstone and siltstone; ferruginous in part
- Pn **NOONKANBAH FORMATION:** well-bedded deltaic to shallow-marine sandstone, siltstone, and shale; minor dolomite
- Pp **POOLE SANDSTONE:** well-bedded, fine-grained marine sandstone
- PG **GRANT GROUP:** crudely bedded marine sandstone and siltstone; porty glacigene; includes boulder-bearing tillite

CARBONIFEROUS — TOURNAISIAN

DCF **FAIRFIELD GROUP:** shale, sandstone and fossiliferous limestone

DEVONIAN — FAMENNIAN

- Dw **WINDJANA LIMESTONE:** *reef-margin subfacies:* massive dolomite and microbial reef limestone (stratigraphic relationships diagram)
- Dl **NULLARA LIMESTONE:** *back-reef subfacies:* well-bedded fenestral and peloidal limestone; locally sandy, with some interbedded sandstone and siltstone
- Dlx Conglomerate, sandstone, and siltstone, Larrowa area

DEVONIAN — FRASNIAN AND FAMENNIAN

- Du **BUGLE GAP LIMESTONE:** *fore-reef subfacies:* crudely bedded, pale-grey limestone with some allochthonous blocks of reef limestone
- Dr **VIRGIN HILLS FORMATION:** *marginal-slope and basin facies:* grey limestone, thick- to thin-bedded, with scattered allochthonous blocks of reef limestone, some debris-flow deposits, and common silicified fossils
- Dsl **SADLER LIMESTONE:** *marginal-slope and basin facies:* grey limestone, thick- to thin-bedded, with scattered allochthonous blocks of reef limestone, some debris-flow deposits, and common silicified fossils

DEVONIAN — FRASNIAN

- Dg **GOGO FORMATION:** *basin facies and lower fore-reef subfacies:* grey, weathering yellow, siltstone, shale, and silty limestone
- Dgb *Basin facies:* siltstone, shale, and minor silty limestone, includes horizons with abundant cannon-ball concretions
- Dgf *Basin facies and lower fore-reef subfacies:* siltstone and shale, with thin interbeds of silty limestone containing some platform-derived debris

DEVONIAN — GIVETIAN AND FRASNIAN

- Dp **PILLARA LIMESTONE:** *platform facies:* undivided, mostly *back-reef subfacies* with some *reef flat subfacies:* white to light-grey and yellow, medium-bedded, stromatoporoid, coralline, and fenestral limestone; locally sandy and grading into calcareous sandstone
- Dpr *Reef-margin and reef-flat subfacies:* white to light-grey and yellow, massive to thick-bedded stromatoporoid and microbial reef limestone, with subordinate coralline limestone
- Dpo + Allochthonous blocks of **PILLARA LIMESTONE** (reef) in marginal-slope and basin facies

GIVETIAN

Dcs **CADJEBUT FORMATION:** *evaporitic facies:* siltstone, shale, sandstone, dolomite, and evaporites, leached in outcrop; *coastal shoal and hypersaline lagoon deposits*

GIVETIAN — FAMENNIAN

- Dcg **BOBS BORE CONGLOMERATE:** siliciclastic conglomerate and sandstone; submarine-fan deposits
- Dcgs **SPARKE CONGLOMERATE:** siliciclastic conglomerate and sandstone, with minor limestone and dolomite; alluvial-cone, fan-delta, and submarine-fan deposits
- **Golieru Member:** cyclic sequences, coarsening-upwards, commonly from marine siltstone or sandstone at the base to subaerial boulder conglomerate at the top
- Dcgss Sheared conglomerate, limestone, and dolomite

ORDOVICIAN

- OP **PRICES CREEK GROUP:** undivided (section and stratigraphic relationships diagram)
- OPg **GAP CREEK FORMATION:** shallow-marine dolomitic sandstone and siltstone
- OPe **EMANUEL FORMATION:** shallow-marine siltstone, shale, and limestone, with lesser sandstone

PALAEOPROTEROZOIC — PROTEROZOIC

E Proterozoic rock, undivided (section and stratigraphic relationships diagram)

1835–1790 Ma
- Ew Sedimentary rock and dolerite

1885–1852 Ma
- Eg Granitoid rock
- Ew **WHITEWATER VOLCANICS:** volcanic and sedimentary rocks

1870–1840 Ma
- Et Metamorphic rock

SYMBOLS

- Geological boundary: exposed; concealed
- Fault: observed; concealed; normal, tick on downthrow side; showing relative lateral displacement
- Fold, showing direction of plunge: anticline, exposed; syncline, exposed
- Bedding: horizontal; inclined, showing strike and dip; overturned
- trend from aerial photography
- Palaeocurrent direction
- Anphoto lineament
- Napunyan dyke or major joint
- Highway with national route marker, bridge
- Formed road
- Track
- Aboriginal Community
- Homestead

Devonian reef complexes

Devonian conglomerates

- Aboriginal Name; Building; Yard; Microwave repeater station; Horizontal control, major, minor
- Watercourse; Spring, waterhole; Bore, well; Windpump; Dam, tank; Abandoned; Position doubtful
- Petroleum exploration or stratigraphic well: dry, abandoned; Gap Creek 1
- Mine; abandoned; Prospect; Quarry; Treatment plant; Mining area
- Mineral occurrence: Lead; Road metal; Zinc

Lowungu; Gp Creek 1; Gloongewa; Codjebut; Pb; Rm; Zn

STRATIGRAPHIC RELATIONSHIPS OF THE DEVONIAN REEF COMPLEXES

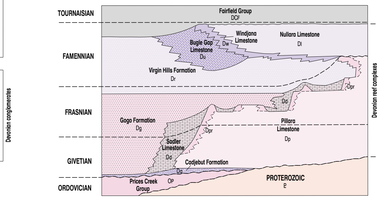

SHEET INDEX

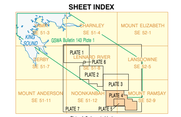

See current GSWA map catalogue for full range of published maps



Compiled by R. M. Hocking and P. E. Playford

Devonian geology by P. E. Playford 1961–1995, R. M. Hocking 1993–1995, A. E. Cockbain 1968, D. C. Lowry 1961–1962, V. A. Pedone 1985–1986

Precambrian geology modified from Tyler, Griffin, Playford, and Hocking, 1998, and Griffin and Tyler, 1995

Edited by N. Tetlow, D. Ferdinando, F. Apidopoulos, and G. Loan

Cartography by S. Craiciuti, E. Green, T. Lemone, and K. Greenberg

Topography from the Department of Land Administration with modifications from geological field survey

Published by the Geological Survey of Western Australia. Copies available from the Information Centre, Department of Minerals and Energy, 100 Plain Street, East Perth, WA 6004. Phone (08) 9222 3459. Fax (08) 9222 3444

This map is also available in digital form

Printed by the Banks Print Group, Western Australia

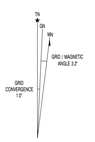

True north, grid north and magnetic north are shown diagrammatically for the centre of the map. Magnetic north is correct for 1998 and moves easterly by about 0.1° in 8 years.

DEPARTMENT OF MINERALS AND ENERGY
L. C. RANFORD, DIRECTOR GENERAL

GOVERNMENT OF WESTERN AUSTRALIA
HON. NORMAN MOORE, M.L.C.
MINISTER FOR MINES

GEOLOGICAL SURVEY OF WESTERN AUSTRALIA
DAVID BLIGHT, DIRECTOR

SCALE 1:100 000

1000 Metres 0 1 2 3 4 5 6 7 8 9 10 Kilometres

TRANSVERSE MERCATOR PROJECTION
HORIZONTAL DATUM: AUSTRALIAN GEODETIC DATUM 1984
VERTICAL DATUM: AUSTRALIAN HEIGHT DATUM

Grid lines indicate 1000 metre interval of the Australia Map Grid Zone 51 and 52

PILLARA RANGE — EMANUEL RANGE SPARKE RANGE AREA

DEVONIAN REEF COMPLEXES OF THE CANNING BASIN

BULLETIN 145 PLATE 4

© Western Australia 1998

DIAGRAMMATIC SECTIONS

NATURAL SCALE (MAP SCALE x 2)

1000 Metres 0 1 2 3 4 Kilometres 1:50 000

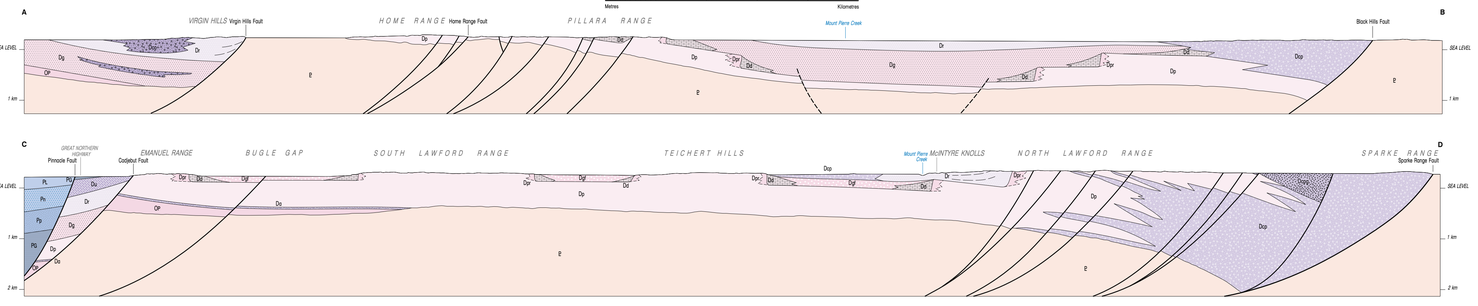

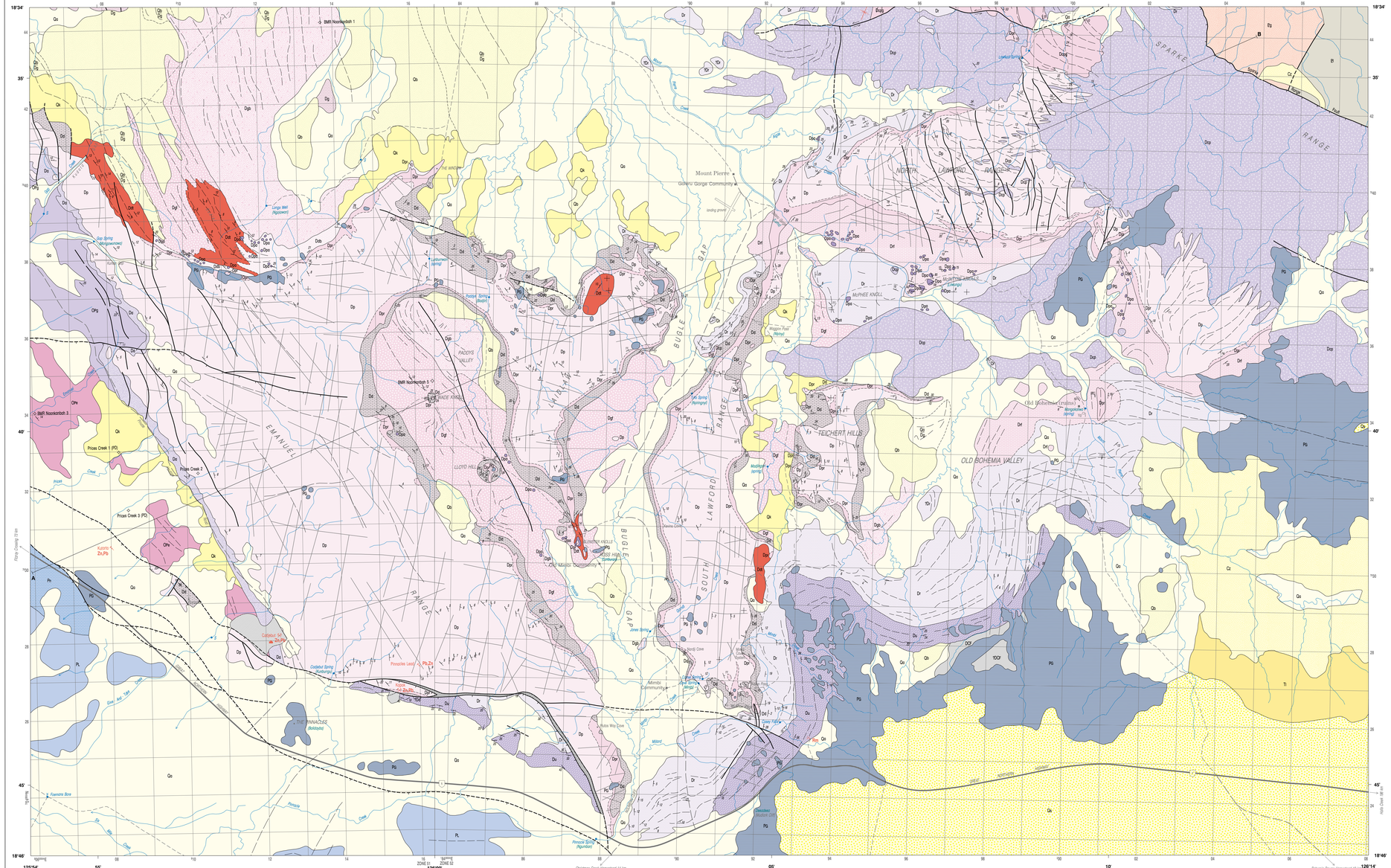
125°54'
55'
126°00'
05'
10'
126°14'
18°34'
35'
40'
45'
18°46'
MGA94 ZONE 51
MGA94 ZONE 52
Mount Pierre
Gulleri Gorge Community
Mimbi Community
Old Bohemia Downs
Old Bohemia (ruins)
Christmas Creek Homestead 14 km
Bohemia Downs Homestead 19 km
EMANUEL RANGE
PADDYS VALLEY
WADE KNOLL
LAIDLAW RANGE
SOUTH LAWFORD RANGE
NORTH LAWFORD RANGE
SPARKE RANGE
BUGLE GAP
TEICHERT HILLS
McPHEE KNOLL
THE PINNACLES
OLD BOHEMIA VALLEY
GREAT NORTHERN HIGHWAY
Pinnacle Fault
Codjebut Fault
Sporke Range Fault
Mount Pierre Creek
Prices Creek 1 (PC)
Prices Creek 2
Prices Creek 3 (PC)
BMR Noonkanbah 1
BMR Noonkanbah 3
BMR Noonkanbah 5
Fossil Spring (Water)
Codjebut Spring (Kurburra)
Jones Spring
Mimbi Community
Sandy Cove
Ruins Way Cove
Lawford Range Spring
Mudhopper Spring
Wagon Pass Spring
Old Bohemia Spring
Fossil Spring (Water)
Francois Bore
Lawford Range Bore
Prices Creek Spring (Agyrdart)
Ord–Victoria Stock Route
Gibb River Road
Great Northern Highway
Fitzroy River
Lennard River
Meda
Mitord
Lloyd Hills
Sandy Cove
Ruins Way Cove
Prices Creek Spring
Jones Spring

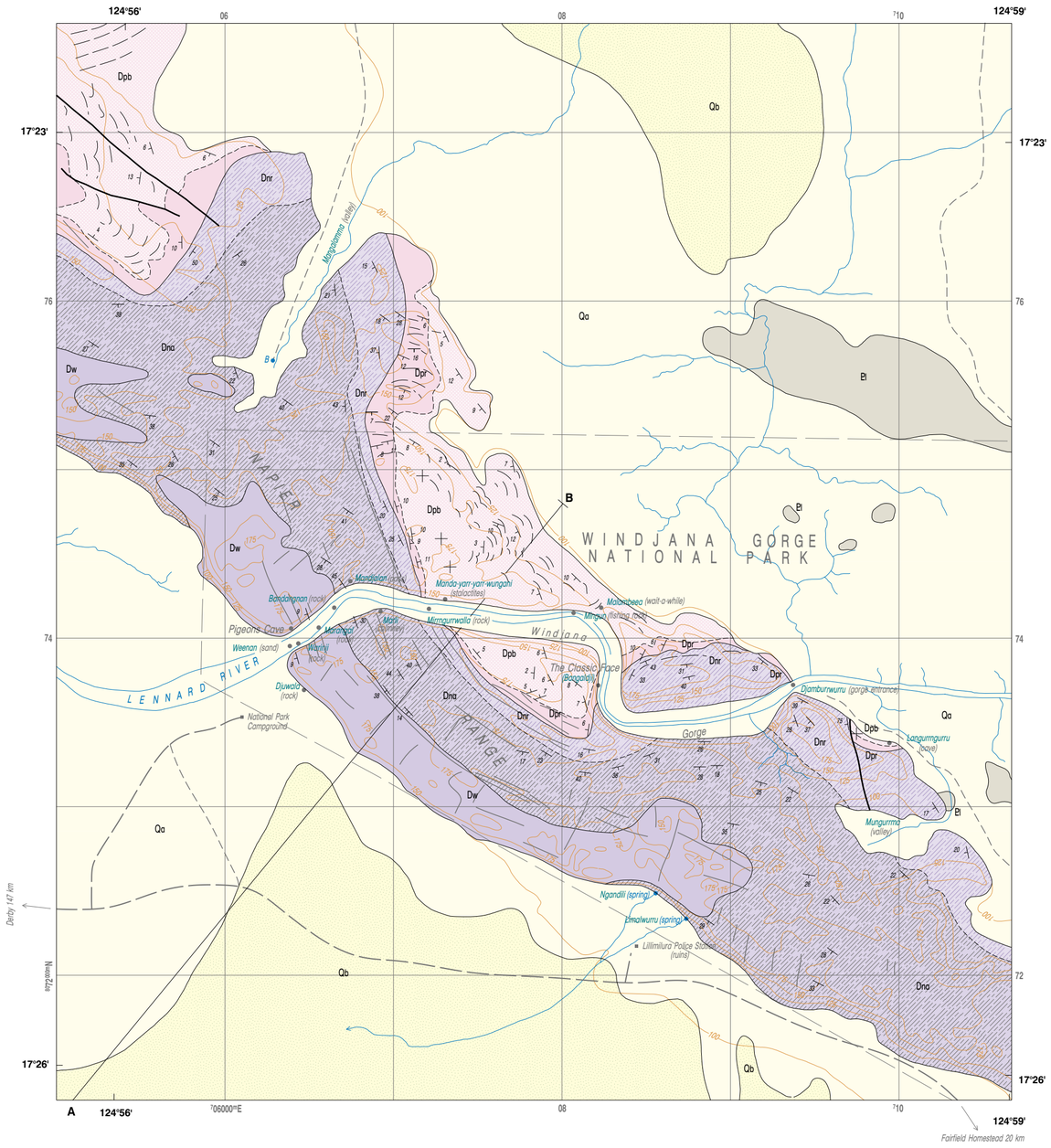

REFERENCE

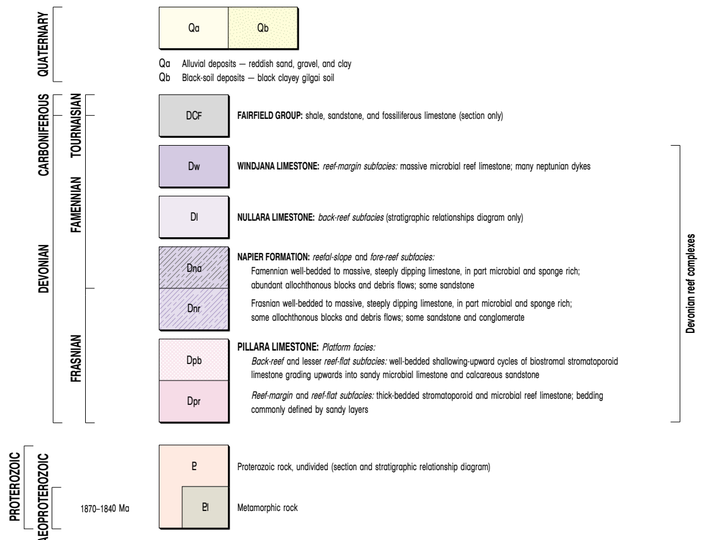

SYMBOLS

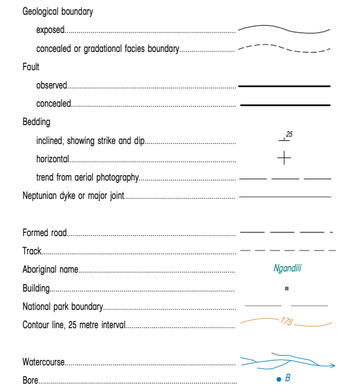

STRATIGRAPHIC RELATIONSHIPS OF THE DEVONIAN REEF COMPLEXES

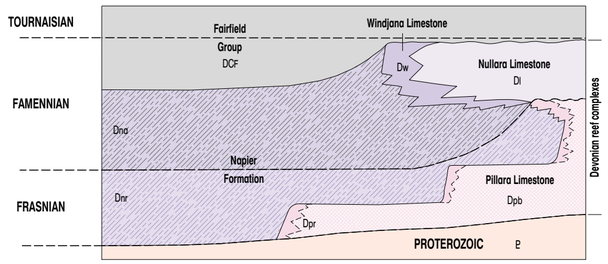



SHEET INDEX

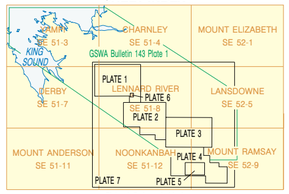

Plates 1–7 shown in black
1:250 000 maps shown in brown
Project map shown in green
See current GSWA map catalogue for full range of published maps



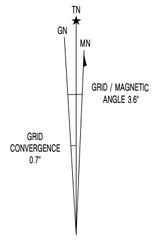

True north, grid north, and magnetic north are shown diagrammatically for the centre of the map. Magnetic north is correct for 1998 and moves easterly by about 0.1° in 9 years.

DIAGRAMMATIC SECTION

NATURAL SCALE

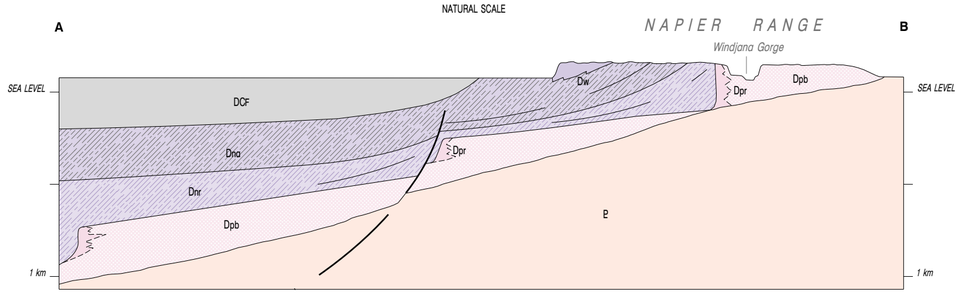

Compiled by P. E. Playford and R. M. Hocking

Geology by P. E. Playford 1971–1995, R. M. Hocking 1993–1995, and A. E. Cockbain 1971

Edited by N. Tetlaw, D. Ferdinando, F. Apidopoulos, and C. Brien

Cartography by E. Green, S. Coldicutt, T. Edwards, and B. Williams

Topography from the Department of Land Administration with modifications from geological field survey

Published by the Geological Survey of Western Australia. Copies available from the Information Centre, Department of Minerals and Energy, 100 Plain Street, East Perth, WA, 6004. Phone (08) 9222 3459, Fax (08) 9222 3444

This map is also available in digital form

Printed by the Sands Print Group, Western Australia

DEPARTMENT OF MINERALS AND ENERGY
L. C. RANFORD, DIRECTOR GENERAL

GOVERNMENT OF WESTERN AUSTRALIA
HON. NORMAN MOORE, M.L.C.
MINISTER FOR MINES

GEOLOGICAL SURVEY OF WESTERN AUSTRALIA
DAVID BLIGHT, DIRECTOR

SCALE 1:25 000

1000 0 1 2
Metres Kilometres

TRANSVERSE MERCATOR PROJECTION
HORIZONTAL DATUM: AUSTRALIAN GEODETIC DATUM OF 1984
VERTICAL DATUM: AUSTRALIAN HEIGHT DATUM

Grid lines indicate 1000 metre interval of the Map Grid Australia Zone 51

WINDJANA GORGE

DEVONIAN REEF COMPLEXES OF THE CANNING BASIN

BULLETIN 145 PLATE 6

© Western Australia 1998

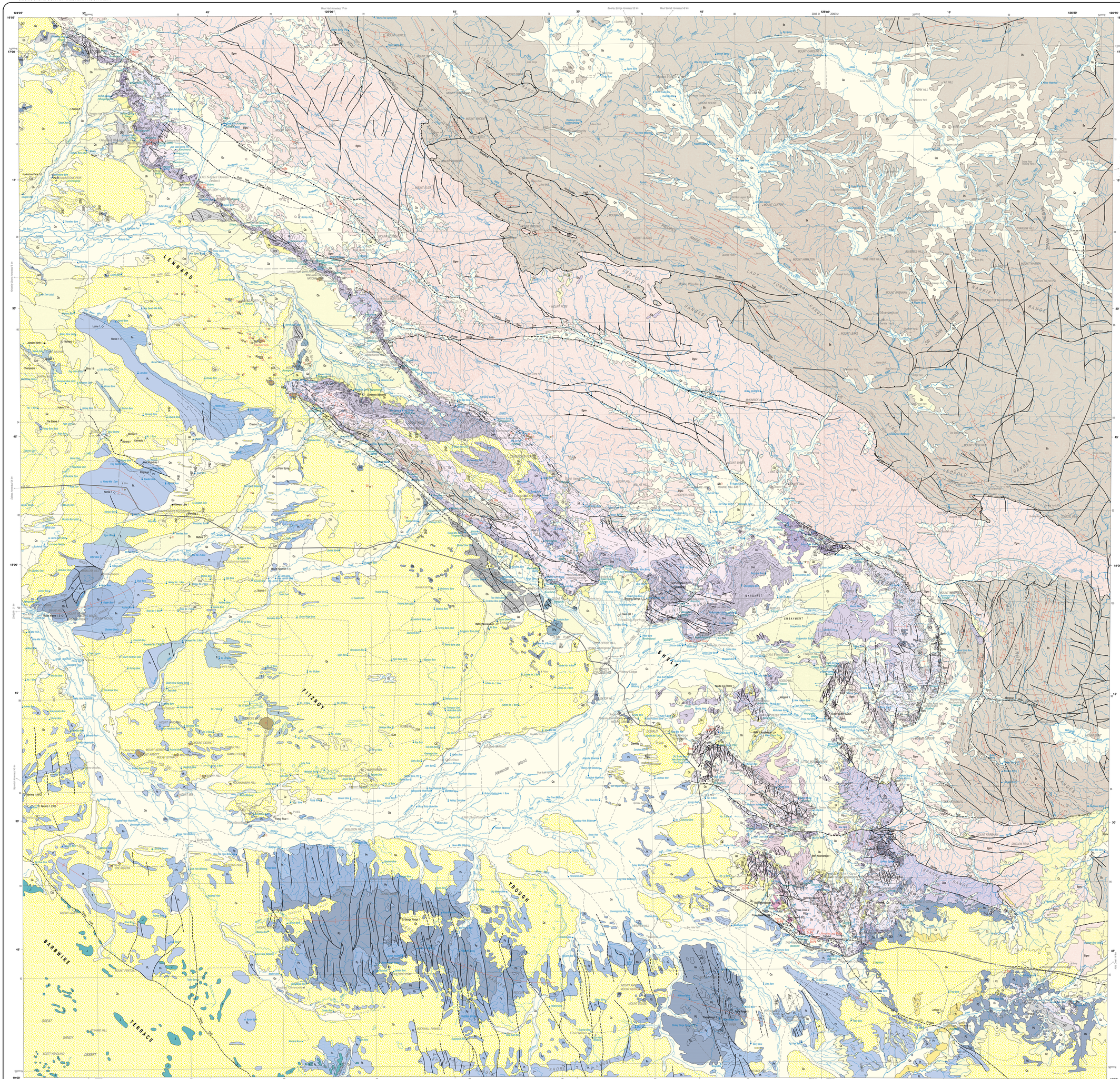
LENNARD
FITZROY
TROUGH
BARBWIRE TERRACE
LENNARD SHELF
FITZROY EMBAYMENT
KING LEOPOLD RANGES
LADY FORREST RANGES
PRECIPICE RANGE
MARIE RANGE
WARBURTON RANGE
ONSLOW PEAK
MOUNT HOUSE
MOUNT CAROLINE
MOUNT ELIZA
MOUNT CLIFTON
MOUNT HAMILTON
MOUNT MARTEN
MOUNT BRENNAN
MOUNT LEAKE
MOUNT PRESTON
MOUNT SHEIL
MOUNT HARRIS
MOUNT VINCENT
MOUNT GLARUS
MOUNT ROE
MOUNT MELVILLE
MOUNT MEREDITH
MOUNT ANDERSON
MOUNT RAMSAY
MOUNT FARRIMOND
MOUNT ORD
MOUNT BARNETT
MOUNT ELLIOTT
MOUNT HOPKINS
MOUNT MARSHALL
MOUNT CHANDLER
MOUNT CHURCHMAN
MOUNT BOWMAN
MOUNT ADAMS
MOUNT BARNETT
MOUNT ELLIOTT
MOUNT HOPKINS
MOUNT MARSHALL
MOUNT CHANDLER
MOUNT CHURCHMAN
MOUNT BOWMAN
MOUNT ADAMS
Old Ngapier Downs
Old Fossil Downs
Old Charnley
Old Theda
Old Mowla
Old Gogo
Old Yeeda
Old Yeda
Old Mount Hardman
Old Mount Elizabeth
Old Mount Barnett
Old Mount Anderson
Old Mount Ramsay
Old Mount Farrimond
Old Mount Ord
Old Mount Barnett
Old Mount Elliott
Old Mount Hopkins
Old Mount Marshall
Old Mount Chandler
Old Mount Churchman
Old Mount Bowman
Old Mount Adams

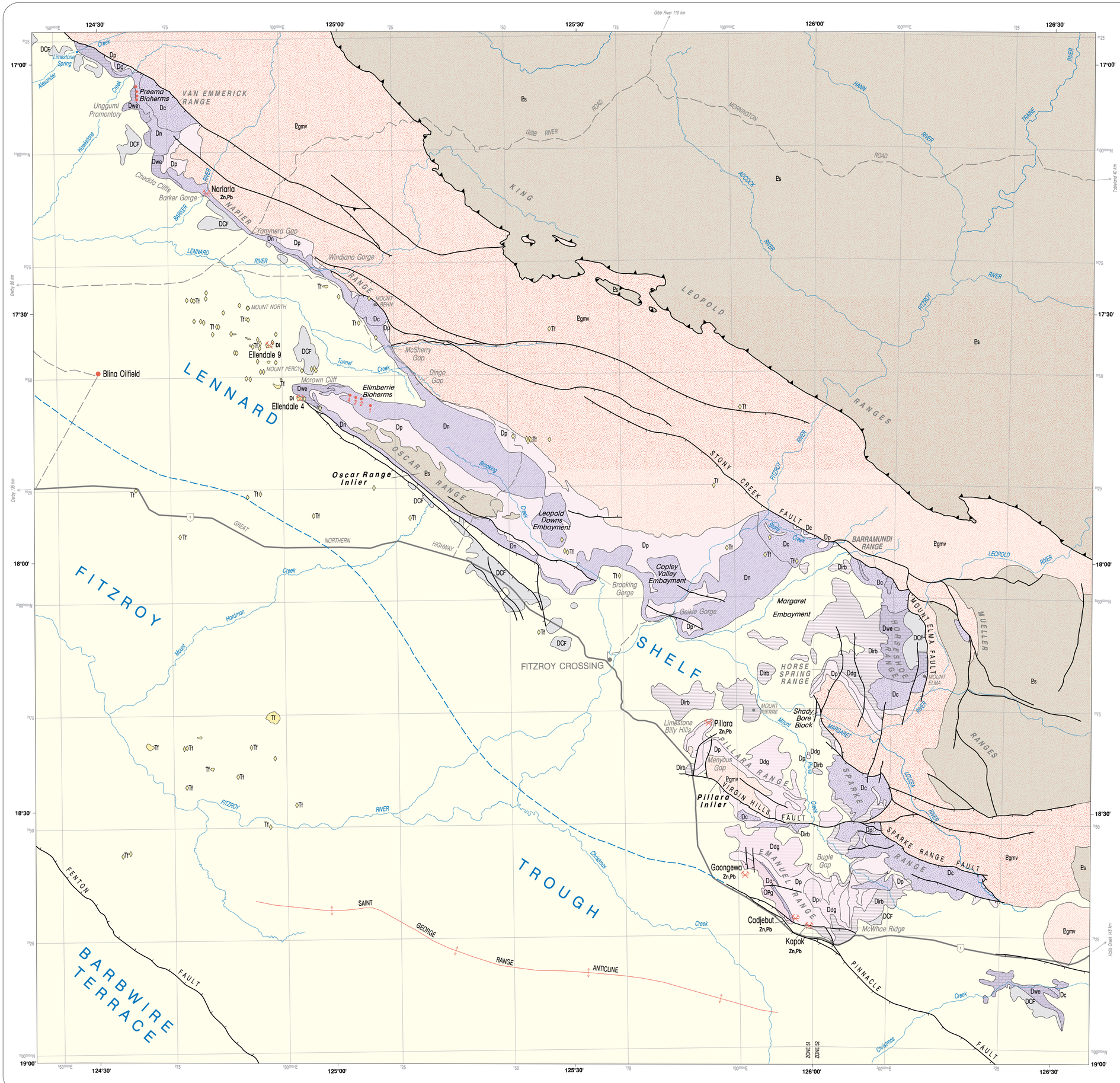

PERMIAN, TRIASSIC, JURASSIC and CENOZOIC

- MIOCENE — Tf — **FITZROY VOLCANICS:** lamprolite diatremes, largely covered by Cenozoic soils
- **PERMIAN, TRIASSIC, JURASSIC, and CENOZOIC:** sedimentary rocks and regolith

DEVONIAN–CARBONIFEROUS

- DCF — **Fairfield Group:** post-reef shale, sandstone, and limestone

DEVONIAN (Reef Complexes)

- FAMENNIAN — Dwe — **WINDJANA and NULLARA LIMESTONES:** reef, back-reef, and bank limestone, dolomite, and sandstone
- FAMENNIAN and FRASNIAN — Dn — **NAPIER FORMATION:** marginal-slope limestone and sandstone, some debris-flow deposits
- FAMENNIAN and FRASNIAN — Dirb — **PIKER HILLS and VIRGIN HILLS FORMATIONS and BUGLE GAP LIMESTONE:** marginal-slope and basin limestone, sandstone, and siltstone
- FRASNIAN and GIVETIAN — Ddg — **SADLER LIMESTONE and GOGO FORMATION:** marginal-slope and basin limestone, siltstone, and shale
- FRASNIAN and GIVETIAN — Dp — **PILLARA LIMESTONE:** reef, back-reef, and bank limestone; some sandstone and dolomite
- GIVETIAN — Dc — **CADJEBUT FORMATION:** dolomite, siltstone, shale, sandstone, and evaporites
- FAMENNIAN, FRASNIAN, and GIVETIAN — Dc — Conglomerate and lesser sandstone, predominantly siliciclastic

ORDOVICIAN

- OPg — **Prices Creek Group:** dolomite, shale, and siltstone

PROTEROZOIC

- 1835–810 Ma — Bs — Paleoproterozoic to Neoproterozoic sedimentary rocks and dolerite
- 1870–1805 Ma — Bgmv — **KING LEOPOLD and HALLS CREEK OROGENS:** granitic, metamorphic, and volcanic rocks

Geological boundary, exposed
Fault
- normal, showing dip direction
- thrust, triangle on upthrown side

Tectonic unit boundary
Fold, anticline, exposed
Highway with national route marker
Road, unsealed
Town
Major hill

Watercourse
Bioherm
Mine
Mine, abandoned
Oilfield
Mineral occurrence
- Diamond — Di
- Lead — Pb
- Zinc — Zn

TN GN MN
GRID / MAGNETIC ANGLE 3.8°
GRID CONVERGENCE 0.7°

True north, grid north and magnetic north are shown diagrammatically for the centre of the map. Magnetic north is correct for 2008 and moves westerly by approx. 7' annually



SHEET INDEX

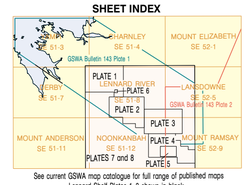

See current GSWA map catalogue for full range of published maps
Lennard Shelf Plates 1–8 shown in black
1:250000 maps shown in brown
Project maps shown in green and red

Government of **Western Australia**
Department of **Mines and Petroleum**

HON. NORMAN MOORE, M.L.C.
MINISTER FOR MINES AND PETROLEUM

Geological Survey of Western Australia

RICK ROGERSON
ACTING EXECUTIVE DIRECTOR

SCALE 1:500 000

5000 0 5 10 15 20 25 30 35 40 45 50
Metres Kilometres

TRANSVERSE MERCATOR PROJECTION
HORIZONTAL DATUM: AUSTRALIAN GEODETIC DATUM 1984
VERTICAL DATUM: AUSTRALIAN HEIGHT DATUM
Grid lines indicate 25 000 metre interval of the Australian Map Grid Zone 51 and 52

Compiled by PE Playford and RM Hocking 2005

Cartography by D Ladbrook

Topography from the Department of Land Information with modifications from geological field surveys

Published by the Geological Survey of Western Australia. Copies available from the Information Centre, Department of Industry and Resources, 100 Plain Street, East Perth, WA, 6004 Phone (08)9222 3444

This map is also available in digital form

LENNARD SHELF

DEVONIAN REEF COMPLEXES OF THE CANNING BASIN

BULLETIN 145 PLATE 8

Version 1.0 — January 2009

© Western Australia 2009